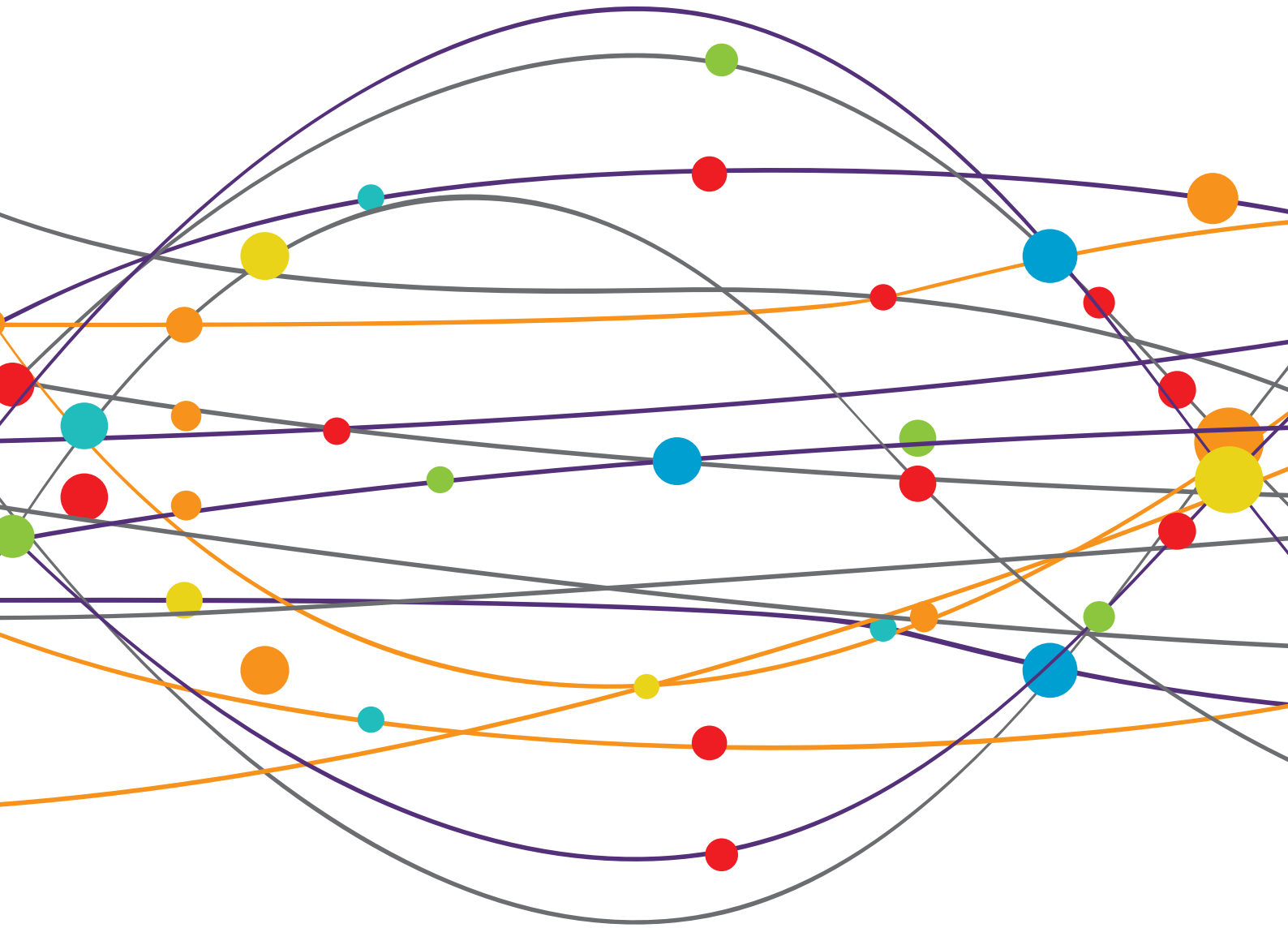
PATHOPHYSIOLOGIC INSIGHTS FROM BIOMARKER STUDIES IN NEUROLOGICAL DISORDERS

EDITED BY: Tobias Ruck, Marcello Moccia, Tobias Warnecke and Stefan Bittner
PUBLISHED IN: Frontiers in Neurology and Frontiers in Immunology



frontiers Research Topics



frontiers

Frontiers eBook Copyright Statement

The copyright in the text of individual articles in this eBook is the property of their respective authors or their respective institutions or funders. The copyright in graphics and images within each article may be subject to copyright of other parties. In both cases this is subject to a license granted to Frontiers.

The compilation of articles constituting this eBook is the property of Frontiers.

Each article within this eBook, and the eBook itself, are published under the most recent version of the Creative Commons CC-BY licence. The version current at the date of publication of this eBook is CC-BY 4.0. If the CC-BY licence is updated, the licence granted by Frontiers is automatically updated to the new version.

When exercising any right under the CC-BY licence, Frontiers must be attributed as the original publisher of the article or eBook, as applicable.

Authors have the responsibility of ensuring that any graphics or other materials which are the property of others may be included in the CC-BY licence, but this should be checked before relying on the CC-BY licence to reproduce those materials. Any copyright notices relating to those materials must be complied with.

Copyright and source acknowledgement notices may not be removed and must be displayed in any copy, derivative work or partial copy which includes the elements in question.

All copyright, and all rights therein, are protected by national and international copyright laws. The above represents a summary only. For further information please read Frontiers' Conditions for Website Use and Copyright Statement, and the applicable CC-BY licence.

ISSN 1664-8714
ISBN 978-2-88963-643-3
DOI 10.3389/978-2-88963-643-3

About Frontiers

Frontiers is more than just an open-access publisher of scholarly articles: it is a pioneering approach to the world of academia, radically improving the way scholarly research is managed. The grand vision of Frontiers is a world where all people have an equal opportunity to seek, share and generate knowledge. Frontiers provides immediate and permanent online open access to all its publications, but this alone is not enough to realize our grand goals.

Frontiers Journal Series

The Frontiers Journal Series is a multi-tier and interdisciplinary set of open-access, online journals, promising a paradigm shift from the current review, selection and dissemination processes in academic publishing. All Frontiers journals are driven by researchers for researchers; therefore, they constitute a service to the scholarly community. At the same time, the Frontiers Journal Series operates on a revolutionary invention, the tiered publishing system, initially addressing specific communities of scholars, and gradually climbing up to broader public understanding, thus serving the interests of the lay society, too.

Dedication to Quality

Each Frontiers article is a landmark of the highest quality, thanks to genuinely collaborative interactions between authors and review editors, who include some of the world's best academicians. Research must be certified by peers before entering a stream of knowledge that may eventually reach the public - and shape society; therefore, Frontiers only applies the most rigorous and unbiased reviews.
Frontiers revolutionizes research publishing by freely delivering the most outstanding research, evaluated with no bias from both the academic and social point of view. By applying the most advanced information technologies, Frontiers is catapulting scholarly publishing into a new generation.

What are Frontiers Research Topics?

Frontiers Research Topics are very popular trademarks of the Frontiers Journals Series: they are collections of at least ten articles, all centered on a particular subject. With their unique mix of varied contributions from Original Research to Review Articles, Frontiers Research Topics unify the most influential researchers, the latest key findings and historical advances in a hot research area! Find out more on how to host your own Frontiers Research Topic or contribute to one as an author by contacting the Frontiers Editorial Office: researchtopics@frontiersin.org

PATHOPHYSIOLOGIC INSIGHTS FROM BIOMARKER STUDIES IN NEUROLOGICAL DISORDERS

Topic Editors:
Tobias Ruck, University of Münster, Germany
Marcello Moccia, University of Naples Federico II, Italy
Tobias Warnecke, University of Münster, Germany
Stefan Bittner, Johannes Gutenberg University Mainz, Germany

Citation: Ruck, T., Moccia, M., Warnecke, T., Bittner, S., eds. (2020). Pathophysiologic Insights From Biomarker Studies in Neurological Disorders. Lausanne: Frontiers Media SA. doi: 10.3389/978-2-88963-643-3

Table of Contents

07 ***Editorial: Pathophysiologic Insights From Biomarker Studies in Neurological Disorders***
Stefan Bittner, Marcello Moccia, Tobias Warnecke and Tobias Ruck

11 ***Brainstem Raphe Alterations in TCS: A Biomarker for Depression and Apathy in Parkinson's Disease Patients***
Daniel Richter, Dirk Woitalla, Siegfried Muhlack, Ralf Gold, Lars Tönges and Christos Krogias

19 ***Biomarkers of Neurodegeneration in Autoimmune-Mediated Encephalitis***
Peter Körtvelyessy, Harald Prüss, Lorenz Thurner, Walter Maetzler, Deborah Vittore-Welliong, Jörg Schultze-Amberger, Hans-Jochen Heinze, Dirk Reinhold, Frank Leypoldt, Stephan Schreiber and Daniel Bittner

29 ***Induction of Osmolyte Pathways in Skeletal Muscle Inflammation: Novel Biomarkers for Myositis***
Boel De Paepe, Jana Zschüntzsch, Tea Šokčević, Joachim Weis, Jens Schmidt and Jan L. De Bleecker

42 ***Real World Lab Data: Patterns of Lymphocyte Counts in Fingolimod Treated Patients***
Maxi Kaufmann, Rocco Haase, Undine Proschmann, Tjalf Ziemssen and Katja Akgün

53 ***Real-World Lab Data in Natalizumab Treated Multiple Sclerosis Patients Up to 6 Years Long-Term Follow Up***
Maxi Kaufmann, Rocco Haase, Undine Proschmann, Tjalf Ziemssen and Katja Akgün

65 ***Moderate Frequency Resistance and Balance Training Do Not Improve Freezing of Gait in Parkinson's Disease: A Pilot Study***
Christian Schlenstedt, Steffen Paschen, Jana Seuthe, Jan Raethjen, Daniela Berg, Walter Maetzler and Günther Deuschl

69 ***Dermal Phospho-Alpha-Synuclein Deposition in Patients With Parkinson's Disease and Mutation of the Glucocerebrosidase Gene***
Kathrin Doppler, Kathrin Brockmann, Annahita Sedghi, Isabel Wurster, Jens Volkmann, Wolfgang H. Oertel and Claudia Sommer

74 ***CSF-Progranulin and Neurofilament Light Chain Levels in Patients With Radiologically Isolated Syndrome—Sign of Inflammation***
Marc Pawlitzki, Catherine M. Sweeney-Reed, Daniel Bittner, Anke Lux, Stefan Vielhaber, Stefanie Schreiber, Friedemann Paul and Jens Neumann

80 ***Serum Inflammatory Profile for the Discrimination of Clinical Subtypes in Parkinson's Disease***
Rezzak Yilmaz, Antonio P. Strafella, Alice Bernard, Claudia Schulte, Lieneke van den Heuvel, Nicole Schneiderhan-Marra, Thomas Knorpp, Thomas O. Joos, Frank Leypoldt, Johanna Geritz, Clint Hansen, Sebastian Heinzel, Anja Apel, Thomas Gasser, Anthony E. Lang, Daniela Berg, Walter Maetzler and Connie Marras

89 ***Quantitative EEG and Verbal Fluency in DBS Patients: Comparison of Stimulator-On and -Off Conditions***
Florian Hatz, Antonia Meyer, Anne Roesch, Ethan Taub, Ute Gschwandtner and Peter Fuhr

96 ***A Smart Device System to Identify New Phenotypical Characteristics in Movement Disorders***
Julian Varghese, Stephan Niewöhner, Iñaki Soto-Rey, Stephanie Schipmann-Miletić, Nils Warneke, Tobias Warnecke and Martin Dugas

102 ***Potential of Sodium MRI as a Biomarker for Neurodegeneration and Neuroinflammation in Multiple Sclerosis***
Konstantin Huhn, Tobias Engelhorn, Ralf A. Linker and Armin M. Nagel

114 ***IL-6 Plasma Levels Correlate With Cerebral Perfusion Deficits and Infarct Sizes in Stroke Patients Without Associated Infections***
Benjamin Hotter, Sarah Hoffmann, Lena Ulm, Christian Meisel, Jochen B. Fiebach and Andreas Meisel

122 ***Predictors for Therapy Response to Intrathecal Corticosteroid Therapy in Multiple Sclerosis***
Katja Vohl, Alexander Duscha, Barbara Gisevius, Johannes Kaisler, Ralf Gold and Aiden Haghikia

128 ***An Assay to Determine Mechanisms of Rapid Autoantibody-Induced Neurotransmitter Receptor Endocytosis and Vesicular Trafficking in Autoimmune Encephalitis***
Elsie Amedonu, Christoph Brenker, Sumanta Barman, Julian A. Schreiber, Sebastian Becker, Stefan Peischard, Nathalie Strutz-Seebohm, Christine Strippel, Andre Dik, Hans-Peter Hartung, Thomas Budde, Heinz Wiendl, Timo Strünker, Bernhard Wünsch, Norbert Goebels, Sven G. Meuth, Guiscard Seebohm and Nico Melzer

137 ***Biomarkers for Dementia, Fatigue, and Depression in Parkinson's Disease***
Tino Prell, Otto W. Witte and Julian Grosskreutz

150 ***Neuronal ICAM-5 Plays a Neuroprotective Role in Progressive Neurodegeneration***
Katharina Birkner, Julia Loos, René Gollan, Falk Steffen, Beatrice Wasser, Tobias Ruck, Sven G. Meuth, Frauke Zipp and Stefan Bittner

161 ***CSF Cytokines in Aging, Multiple Sclerosis, and Dementia***
William T. Hu, Jennifer Christina Howell, Tugba Ozturk, Umesh Gangishetti, Alexander L. Kollhoff, Jaime M. Hatcher-Martin, Albert M. Anderson and William R. Tyor

169 ***Impact of the McDonald Criteria 2017 on Early Diagnosis of Relapsing-Remitting Multiple Sclerosis***
Philipp Schwenkenbecher, Ulrich Wurster, Franz Felix Konen, Stefan Gingele, Kurt-Wolfram Sühs, Mike P. Wattjes, Martin Stangel and Thomas Skripuletz

177 ***The Shaking Palsy of the Larynx—Potential Biomarker for Multiple System Atrophy: A Pilot Study and Literature Review***
Tobias Warnecke, Annemarie Vogel, Sigrid Ahring, Doreen Gruber, Hans-Jochen Heinze, Rainer Dziewas, Georg Ebersbach and Florin Gandor

189 ***Substance P Saliva Reduction Predicts Pharyngeal Dysphagia in Parkinson's Disease***
Jens Burchard Schröder, Thomas Marian, Inga Claus, Paul Muhle, Matthias Pawlowski, Heinz Wiendl, Sonja Suntrup-Krueger, Sven G. Meuth, Rainer Dziewas, Tobias Ruck and Tobias Warnecke

194 ***Identification of Candidate Protein Markers in Skeletal Muscle of Laminin-211-Deficient CMD Type 1A-Patients***
Heike Kölbel, Denisa Hathazi, Matthew Jennings, Rita Horvath, Andreas Roos and Ulrike Schara

210 ***Disease Specific Autoantibodies in Idiopathic Inflammatory Myopathies***
Bruno Stuhlmüller, Udo Schneider, José-B. González-González and Eugen Feist

225 ***α7 Nicotinic Acetylcholine Receptor Signaling Modulates Ovine Fetal Brain Astrocytes Transcriptome in Response to Endotoxin***
Mingju Cao, James W. MacDonald, Hai L. Liu, Molly Weaver, Marina Cortes, Lucien D. Durosier, Patrick Burns, Gilles Fecteau, André Desrochers, Jay Schulkin, Marta C. Antonelli, Raphael A. Bernier, Michael Dorschner, Theo K. Bammler and Martin G. Frasch

238 ***Proteomic Profiling Unravels a Key Role of Specific Macrophage Subtypes in Sporadic Inclusion Body Myositis***
Andreas Roos, Corinna Preusse, Denisa Hathazi, Hans-Hilmar Goebel and Werner Stenzel

249 ***Apolipoprotein E Homozygous ε4 Allele Status: A Deteriorating Effect on Visuospatial Working Memory and Global Brain Structure***
Janik Goltermann, Ronny Redlich, Katharina Dohm, Dario Zaremba, Jonathan Repple, Claas Kaehler, Dominik Grotegerd, Katharina Förster, Susanne Meinert, Verena Enneking, Emily Schlaghecken, Lara Fleischer, Tim Hahn, Harald Kugel, Andreas Jansen, Axel Krug, Katharina Brosch, Igor Nenadic, Simon Schmitt, Frederike Stein, Tina Meller, Dilara Yüksel, Elena Fischer, Marcella Rietschel, Stephanie H. Witt, Andreas J. Forstner, Markus M. Nöthen, Tilo Kircher, Anbupalam Thalamuthu, Bernhard T. Baune, Udo Dannlowski and Nils Opel

260 ***Biomarkers in Vasculitides of the Nervous System***
Daniel Strunk, Antje Schmidt-Pogoda, Carolin Beuker, Lennart S. Milles, Catharina Korsukewitz, Sven G. Meuth and Jens Minnerup

277 ***Psychological and Cognitive Markers of Behavioral Variant Frontotemporal Dementia–A Clinical Neuropsychologist's View on Diagnostic Criteria and Beyond***
Andreas Johnen and Maxime Bertoux

301 ***Identification of Cellular Pathogenicity Markers for SIL1 Mutations Linked to Marinesco-Sjögren Syndrome***
Christian Gatz, Denisa Hathazi, Ute Münchberg, Stephan Buchkremer, Thomas Labisch, Ben Munro, Rita Horvath, Ana Töpf, Joachim Weis and Andreas Roos

316 ***Lymphocyte Count and Body Mass Index as Biomarkers of Early Treatment Response in a Multiple Sclerosis Dimethyl Fumarate-Treated Cohort***
Alessia Manni, Antonio Iaffaldano, Giuseppe Lucisano, Mariangela D'Onghia, Domenico Maria Mezzapesa, Vincenzo Felica, Pietro Iaffaldano, Maria Trojano and Damiano Paolicelli

325 ***Dysphagia as Isolated Manifestation of Jo-1 Associated Myositis?***
Bendix Labeit, Paul Muhle, Sonja Suntrup-Krueger, Sigrid Ahring, Tobias Ruck, Rainer Dziewas and Tobias Warnecke

330 ***Neuro-Sjögren: Peripheral Neuropathy With Limb Weakness in Sjögren's Syndrome***
Tabea Seeliger, Nils K. Prenzler, Stefan Gingele, Benjamin Seeliger, Sonja Körner, Thea Thiele, Lena Bönig, Kurt-Wolfram Sühs, Torsten Witte, Martin Stangel and Thomas Skripuletz

frontiers in Neurology

EDITORIAL
published: 28 February 2020
doi: 10.3389/fneur.2020.00151

Editorial: Pathophysiologic Insights From Biomarker Studies in Neurological Disorders

Stefan Bittner[1], *Marcello Moccia*[2], *Tobias Warnecke*[3] *and Tobias Ruck*[3]*

[1] Department of Neurology, Focus Program Translational Neuroscience (FTN) and Immunotherapy (FZI), Rhine Main Neuroscience Network, University Medical Center of the Johannes Gutenberg University Mainz, Mainz, Germany, [2] Multiple Sclerosis Clinical Care and Research Centre, Department of Neuroscience, Reproductive Science and Odontostomatology, Federico II University, Naples, Italy, [3] Department of Neurology with Institute of Translational Neurology, University of Münster, Münster, Germany

Keywords: biomarker, pathophysiology, neuroimmunology, neurodegeneration, pathomechanism

Editorial on the Research Topic

Pathophysiologic Insights From Biomarker Studies in Neurological Disorders

Neuroimmunological and neurodegenerative disorders are major healthcare issues, associated with high individual and socioeconomic burden. For many neurological disorders an early diagnosis is key for efficient management and therapy. However, neural tissues from brain, spinal cord, or peripheral nerves are difficult to sample, and their extraction is often associated with functional deficits. Therefore, in most cases a combination of biomarkers such as radiologic or biochemical findings are used to define a diagnosis in the clinical practice. The development of pathologically-sensitive and easy-to-measure disease biomarkers is a key factor for investigating new medications in phase II trials aiming to quickly screen their efficacy, and in phase III trials where they are coupled to clinical measures. Moreover, biomarkers are used to predict treatment efficacy and adverse event risk, paving the way for personalized medicine with individual risk assessment and prevention strategies.

In the last few decades the enormous technological progress, especially omics technologies, expanded the definition of biomarkers from biochemical and clinical, to genetic, proteomic, metabolic, or microbial markers. Interestingly, some of the biomarker studies additionally provided important insights into the pathophysiology of neurological disorders. In multiple sclerosis TNF-blocking drugs can promote onset or exacerbation of MS and GWAS (genome-wide association studies) data informed about the underlying mechanisms instructing clinical practice (1). In Parkinson's disease (PD), evaluation of Lewy pathology provided new pathophysiological insights attributing PD pathology progression to a prion-like process starting in the gastrointestinal tract (2). However, many other suggested biomarkers remain solely correlative, often lacking a causative link to the underlying disease mechanisms possibly explaining their lack in sensitivity and specificity.

This Research Topic reviews current knowledge and provides new insights into pathomechanisms of a wide variety of neuroimmunological and neurodegenerative disorders from studies on (novel) risk factors and outcome predicting biomarkers.

INFLAMMATORY DISORDERS OF THE CENTRAL NERVOUS SYSTEM

There is still an unmet need for novel, innovative biomarker approaches in different stages of central nervous system inflammation ranging from first diagnosis to evaluation of inflammatory and

OPEN ACCESS

Edited by:
Hans-Peter Hartung, Heinrich Heine University of Düsseldorf, Germany

Reviewed by:
Roberto Furlan, San Raffaele Hospital (IRCCS), Italy

***Correspondence:**
Tobias Ruck
tobias.ruck@ukmuenster.de

Specialty section:
This article was submitted to Multiple Sclerosis and Neuroimmunology, a section of the journal Frontiers in Neurology

Received: *03 November 2019*
Accepted: *14 February 2020*
Published: *28 February 2020*

Citation:
Bittner S, Moccia M, Warnecke T and Ruck T (2020) Editorial: Pathophysiologic Insights From Biomarker Studies in Neurological Disorders. Front. Neurol. 11:151. doi: 10.3389/fneur.2020.00151

neurodegenerative processes and therapy responses. In this Research Topic, Pawlitzki et al. shows the value of CSF-based biomarker approaches indicating ongoing chronic CNS inflammation even before first clinical sign of symptoms in patients with radiologically isolated syndrome, while Schwenkenbecher et al. demonstrate the importance of oligoclonal bands in the diagnostic algorithm of multiple sclerosis assessing the impact of the newest McDonald criteria. Until now, we have only a limited understanding of inflammatory and neurodegenerative processes within the CNS compartment in multiple sclerosis. Here, Birkner et al. assessed the role of ICAM-5, a CNS-restricted adhesion molecule, in mediating T cell-induced neuronal damage in the animal model of experimental autoimmune encephalomyelitis (EAE), Huhn et al. investigated the use of sodium MRI as a translational approach in MS patients. Another part of this Research Topic section focuses on the value of biomarker approaches in different real-world therapeutic settings, namely blood-based biomarkers in patients treated with fingolimod (Kaufmann et al.), dimethylfumarate (Manni et al.), and in a longitudinal setting in patients treated with natalizumab (Kaufmann et al.). The study by Vohl et al. investigates a cohort of patients treated with intrathecal corticosteroid therapy, a long-established, but sometimes under-appreciated therapeutic approach, in numerous centers specialized on the treatment of MS patients, that so far has suffered from the lack of large studies. In a cohort of 38 patients with autoimmune encephalitis (AE), Körtvelyessy et al. showed that CSF Progranulin levels were elevated during the acute phase, suggesting ongoing neuro-axonal damage, and that total-Tau (t-tau) and neurofilament light chain (NfL) levels were associated with the risk of clinical, laboratory, and radiological progression. Future studies on AE could benefit from the work of Amedonu et al., with the use of a novel assay to study molecular mechanisms of autoantibody-induced receptor internalization and to screen new molecular-based therapies.

NEURODEGENERATION AND STROKE

Neurodegenerative diseases have been conventionally studied in relation to the genetic risk of clinical/cognitive dysfunction and neuronal damage. In line with this, Goltermann et al. showed that apolipoprotein E (APOE) ε4 homozygosity, a well-known risk factor for Alzheimer's disease (AD), was associated with worse visuospatial working memory and global brain structural alterations in 62 non-neurological subjects from the FOR2107 Marburg-Münster Affective Cohort Study.

More recently, an interplay between inflammation and neurodegeneration has been recognized. Looking at conditions that are conventionally unrelated to inflammation, Hu et al. demonstrated an inflammatory component in the normal aging and in AD, by showing an accentuated shift from T-helper (Th)-1 to non-Th1 inflammatory pathways in the cerebrospinal fluid (CSF) (similar to what happens in multiple sclerosis). Hotter et al. evaluated 91 stroke patients not suffering from stroke-associated infections (derived from the PREDICT and 1000 Plus studies), and found that IL-6 was associated with several MRI measures of stroke severity (e.g., acute and final lesion perfusion and size), suggesting that inflammation is related to vascular parenchymal damage. Also, neuroinflammation during the fetal period could be related to neurodevelopmental disorders (e.g., autism spectrum disorder, schizophrenia). Cao et al. studied the role of α7nAChR on fetal sheep astrocytes, a classic model of fetal neurobiology, and further unraveled the complex interactions between inflammation and neurodegeneration at neurodevelopmental stages.

However, our Research Topic did not aim to underestimate clinical examination, which remains of utmost importance in the neurology clinical practice. In particular, in their review, Johnen and Bertoux suggested that the early clinical diagnosis of the behavioral variant frontotemporal dementia (bvFTD) requires an in-depth assessment of clinical signs, behavioral and psychological symptoms as well as cognitive performance. Authors strongly encouraged the design of novel neuropsychological tests covering understudied aspects of dementia (e.g., social and emotional processing, praxis abilities, interoceptive processing), and further expanding the number of clinical and neuropsychological biomarkers for the neurology clinical practice (Johnen and Bertoux).

MOVEMENT DISORDERS, PARKINSON'S DISEASE, AND DYSPHAGIA

Over the last decade increasing scientific efforts have been made to establish biomarkers for early diagnosis of Parkinson's disease (PD) and other movement disorders. These potentially helpful biomarkers include findings from neuroimaging techniques, blood and cerebrospinal fluid (CSF) immune markers, technology-based objective measures (TOMs) provided by wearable devices, results from skin biopsies, and several others. Doppler et al. were now able to show that dermal phospho-alpha-synuclein (p-syn) in PD patients with glucocerebrosidase gene (GBA1) mutations seems to offer a similar distribution and frequency as observed in PD patients without a known mutation. Therefore, skin biopsy may be suitable to study p-syn deposition in these patients or even to identify premotor patients with GBA1 mutations (Doppler et al.). However, a panel of serum immune markers (i.e., cytokines) as analyzed using principal component analysis (PCA) was not found to allow for reliably predicting clinical PD subtypes (Yilmaz et al.). Varghese et al. introduced a technology-based system called Smart Device System (SDS) that was tested over 2 years to train an Artificial Intelligence System; this system will be further implemented for multi-modal high-resolution acceleration measurement of patients with PD or essential tremor (ET). Furthermore, Warnecke et al. used flexible endoscopic evaluation of swallowing (FEES) to detect specific pharyngolaryngeal movement disorders, such as arytenoid tremor that may help to differentiate multiple system atrophy (MSA) from PD.

In addition, biomarkers for detection of specific symptoms related to PD and other movement disorders have been studied throughout the last years. In their narrative review Prell et al. provide an overview of recent developments of bio-fluid and

imaging biomarkers for dementia, depression, and fatigue in PD. They conclude that more research needs to be undertaken to find reliable combinations of predictors of these neuropsychological symptoms in PD on an individual level, and that standardization and harmonization of protocols in particular in CSF handling and neuroimaging has to be further implemented (Prell et al.). Richter et al. assessed the utility of brainstem raphe (BR) alterations evaluated by transcranial sonography (TCS) as a potential biomarker for apathy and depression in PD patients. These BR alterations correlated with depression and apathy scales indicating that a serotonergic signal disturbance might exist for both symptoms in PD (Richter et al.). Beside these neuropsychological symptoms, significant attention has being paid to gastrointestinal dysfunction and particularly swallowing disorders. Clinical research has shown that dysphagia is an often overlooked, but complex syndrome in many patients with neurodegenerative and neuromuscular disorders mainly contributing to disease burden in the majority of cases. Schröder et al. were able to show that reduced saliva substance P (SP) concentrations may predict early pharyngeal swallowing dysfunction in PD patients and may help to identify PD patients with a higher risk of developing clinically relevant dysphagia. Labeit et al. reported the first case of isolated dysphagia due to Jo-1 antibodies associated myositis. They suggest that myositis-focused diagnostics including an autoantibody panel should be done in patients with unclear dysphagia that show typical sings for myositis in the instrumental dysphagia assessment (Labeit et al.).

In the future biomarkers should not only be available for early diagnosis, but also for indicating responses to specific therapeutic interventions that help to guide treatment decisions in PD and other movements disorders. Schlenstedt et al. presented pilot data indirectly supporting the hypothesis that exercises specifically designed to target freezing of gait (FOG) might be more beneficial than non-FOG-specific interventions in PD patients. However, future studies should include larger samples and high frequency interventions to investigate the role of training balance performance to reduce the severity of FOG and to analyze which subgroup of PD patients shows the largest effect size (Schlenstedt et al.). Finally, Hatz et al. were able to demonstrate that deep brain stimulation of the subthalamic nucleus (STN) used to treat motor complications in advanced PD does not alter verbal fluency performance in a systematic way at group level. Nevertheless, when STN stimulation produces an alteration of verbal fluency performance in an individual PD patient, it was inversely correlated with left temporal delta power as measured by quantitative EEG (Hatz et al.).

DISORDERS OF THE PERIPHERAL NERVOUS SYSTEM

The peripheral nervous system (PNS) consists of nervous structures (cranial and spinal nerves, enteric nervous system) and their associated receptors and organs. The diagnosis of PNS disorders is a multi-step process and often complicated by unspecific findings. Instructive cellular and non-cellular biomarkers for diagnosis, prognosis and/or treatment management are largely missing. However, recent years including studies of this Research Topic support the high relevance of biomarkers for an adequate disease management. Correspondingly, Stuhlmüller et al. review the role of myositis-specific and -associated antibodies in idiopathic inflammatory myopathies (IIM). They highlight their value in the diagnostic process and prognosis (organ involvement, risk for malignancies), and elaborate on detection methods and associated clinical phenotypes (Stuhlmüller et al.). De Paepe et al. demonstrate an upregulation of osmolyte accumulators and identify associated inflammatory signaling pathways in skeletal muscle cells upon pro-inflammatory stimuli *in vitro* and in skeletal muscle biopsies of IIM patients. The authors characterize specific osmolyte accumulators as potential biomarkers for regenerating muscle fibers or autoreactive immune cells (De Paepe et al.).

However, biomarker research might not only unravel associations with clinical parameters but also reveal important insights into pathophysiological disease mechanisms. With an unbiased proteomic profiling Roos et al. identified key molecules involved in the pathogenesis of sporadic inclusion body myositis (sIBM), which were further characterized by qPCR, immunostaining, immunofluorescence *in situ* and *in silico* studies. By these means, they were able to demonstrate a key role of specific macrophage subtypes and molecules (CD74, CD163, and STAT1) involved in their activation and type I interferon and interferon gamma associated pathways in sIBM (Roos et al.). With a similar proteomic approach Kölbel et al. identified candidate protein biomarkers in skeletal muscle of laminin-211 deficient type 1 A (MDC1A) congenital muscular dystrophy (CMD), one of the most devastating CMDs characterized by severe muscle weakness, brain abnormalities, and delayed motor milestones. The expression of 86 proteins associated with fibrosis and altered synaptic transmission was specifically linked to MDC1A skeletal muscle. Moreover, the observed alterations in metabolic pathways and mitochondrial function might identify new therapeutic targets (Kölbel et al.).

Changes in protein function, folding or metabolism is a common feature of several degenerative disorders of the PNS. In Marinesco-Sjögren syndrome (MSS) characterized by a clinical triad of bilateral cataracts, ataxia, and myopathy, mutations in the SIL1 gene lead to protein misfolding. However, read-out systems to identify pathogenic variants of SIL1 mutations are missing. Therefore, Gatz et al. introduce an *in vitro* system identifying the pathogenic consequences of different mutations on a cellular level. In the future, these findings can instruct genetic testing of patients with suspected MSS.

Besides disorders primarily affecting structures of the PNS, systemic autoimmune diseases such as Sjögren's syndrome might involve the PNS as well. In this Research Topic, Seeliger et al. provide a cross-sectional study of 144 patients with polyneuropathy of whom 44 were diagnosed with Sjögren's syndrome. They describe clinical findings and discuss potential tools to identify Neuro-Sjögren (Seeliger et al.). Other systemic inflammatory disorders such as vasculitides can also affect structures of the nervous system including the PNS resulting in

a variety of potential symptoms. Strunk et al. review potential biomarkers in the context of nervous system vasculitides with a focus on body fluid derived markers and discuss their diagnostic and prognostic value.

Overall, the current Research Topic provides a deeper understanding of the pathomechanisms underlying neurological disorders and identifies new biomarkers and their pathophysiologic background. Thereby, the Research Topic might initiate hypothesis-driven refinement of current and novel biomarkers.

AUTHOR CONTRIBUTIONS

SB, MM, TW, and TR edited the Research Topic and drafted and revised the editorial manuscript. All authors read and approved the final version of the manuscript.

REFERENCES

1. Gregory AP, Dendrou CA, Attfield KE, Haghikia A, Xifara DK, Butter F, et al. TNF receptor 1 genetic risk mirrors outcome of anti-TNF therapy in multiple sclerosis. *Nature.* (2012) 488:508–11. doi: 10.1038/nature 11307
2. Braak H, Del Tredici K, Rüb U, De Vos RAI, Jansen Steur ENH, Braak E. Staging of brain pathology related to sporadic Parkinson's disease. *Neurobiol Aging.* (2003) 24:197–211. doi: 10.1016/S0197-4580(02) 00065-9

Conflict of Interest: The authors declare that the research was conducted in the absence of any commercial or financial relationships that could be construed as a potential conflict of interest.

Copyright © 2020 Bittner, Moccia, Warnecke and Ruck. This is an open-access article distributed under the terms of the Creative Commons Attribution License (CC BY). The use, distribution or reproduction in other forums is permitted, provided the original author(s) and the copyright owner(s) are credited and that the original publication in this journal is cited, in accordance with accepted academic practice. No use, distribution or reproduction is permitted which does not comply with these terms.

frontiers in Neurology

ORIGINAL RESEARCH
published: 07 August 2018
doi: 10.3389/fneur.2018.00645

Brainstem Raphe Alterations in TCS: A Biomarker for Depression and Apathy in Parkinson's Disease Patients

Daniel Richter[1], *Dirk Woitalla*[1,2], *Siegfried Muhlack*[1], *Ralf Gold*[1,3], *Lars Tönges*[1,3] *and Christos Krogias*[1]*

[1] Department of Neurology, St. Josef-Hospital, Ruhr University Bochum, Bochum, Germany, [2] Department of Neurology, Katholische Kliniken Ruhrhalbinsel, Essen, Germany, [3] Neurodegeneration Research, Protein Research Unit Ruhr (PURE), Ruhr University Bochum, Bochum, Germany

OPEN ACCESS

Edited by:
Tobias Warnecke, University Hospital Muenster, Germany

Reviewed by:
Georgios Tsivgoulis, National and Kapodistrian University of Athens, Greece
Matteo Bologna, Sapienza Università di Roma, Italy

***Correspondence:**
Christos Krogias
christos.krogias@rub.de

Specialty section:
This article was submitted to Movement Disorders, a section of the journal Frontiers in Neurology

Received: 19 May 2018
Accepted: 18 July 2018
Published: 07 August 2018

Citation:
Richter D, Woitalla D, Muhlack S, Gold R, Tönges L and Krogias C (2018) Brainstem Raphe Alterations in TCS: A Biomarker for Depression and Apathy in Parkinson's Disease Patients. Front. Neurol. 9:645. doi: 10.3389/fneur.2018.00645

Depression and apathy can both be present in patients with Parkinson's disease (PD) while e. g., essential tremor (ET) patients mostly only report depressive symptoms. In PD, depression has been linked with brainstem raphe (BR) signal alterations in transcranial sonography (TCS) but apathy has not been evaluated in such terms as a putative biomarker. Furthermore, the BR has only been investigated using a singular axial TCS examination plane, although coronal TCS examination allows a much more accurate evaluation of the craniocaudal formation of serotonergic raphe structures in the midbrain area. The objective of this study was to investigate the value of coronal TCS examination for the detection of BR signal alterations and clinically correlate it to apathy in patients with PD, ET and healthy controls (HC). We prospectively included PD patients ($n = 31$), ET patients ($n = 16$), and HC ($n = 16$). All were examined by TCS in the axial and coronal plane with focus on BR signal alterations. LARS and BDI-II scores were conducted to assess apathic and depressive symptoms in the study population. In a detailed analysis we found that the correlation of coronal and axial TCS alterations of BR was very high (rho = 0.950, $p < 0.001$). BR signal alterations were more frequent in PD patients than in ET patients and HC, while it was not different between ET patients and HC. In the PD patient group, BDI-II and LARS scores were negatively correlated to BR signal changes in TCS in a significant manner (BDI-II and axial BR: $p = 0.019$; BDI-II and coronal BR: $p = 0.011$; LARS and axial BR: $p = 0.017$; LARS and coronal BR: $p = 0.023$). Together in this brainstem ultrasound study we find a significant association of BR signal alterations with clinically evident apathy and depression in patients with PD. Therefore, TCS might enable the identification of a subgroup of PD patients which are at higher risk to suffer from or to develop depression or apathy.

Keywords: sonography, TCS, raphe, apathy, depression

INTRODUCTION

Transcranial sonography (TCS) is increasingly applied for the differential diagnosis of Parkinson's disease (PD) patients. Hyperechogenicity of substantia nigra (SN) has been identified as a biomarker and risk factor for PD patients and thus has been included as a diagnostic item in the new MDS research criteria for prodromal PD (1).

Depression and apathy frequently appear in PD patients and can represent early non-motor symptoms (2–4). Several studies have shown that many PD patients are affected by depression, even in the prodromal state of disease (5). Apathy has been described to appear independently from depression (6) and can severely impact quality of life (7). Brainstem raphe (BR) alterations in TCS have been associated with depressed PD patients (8, 9) but were not observed in patients with essential tremor (ET). So far, BR signal alterations have never been examined in relation to apathy and, furthermore, have only been evaluated using a singular axial TCS plane in spite of an additional coronal examination (10).

In this study, we investigated symptoms of apathy and depression by using the Lille apathy rating scale (LARS) and the Beck Depression Inventory II (BDI-II) in PD patients, ET patients and healthy controls. Recently, a new coronal examination plane has been introduced in the field of TCS by our group in order to study Substantia nigra echogogenicity (10). We applied this methodology of an additional coronal TCS examination now for BR alterations and evaluated this finding as a putative biomarker for depression and apathy in PD.

MATERIALS AND METHODS

Subjects

We prospectively included patients fulfilling the clinical diagnostic criteria of the UK Parkinson's Disease Society Brain Bank for idiopathic PD (11) or patients meeting the diagnostic criteria for ET (12). Participants with an insufficient transtemporal bone window were excluded. All patients received best medical treatment according to international guidelines for the treatment of advanced Parkinson's disease (13) or essential tremor (14). None of the participants of this study received anti-depressive therapy. Additionally, healthy controls (HC) were included to serve as an age-matched control group. The same clinical assessment and TCS imaging was performed for every subject in this study.

All subjects were included after detailed information about the study and gave written informed consent. In accordance to the Helsinki Declaration of 1975, the study was approved by the local university ethics committee of the Ruhr University Bochum, Germany (approval no. 4961-14).

Clinical Assessment

All PD and ET patients as well as the group of HC underwent clinical neurological assessment, done by a trained and experienced interviewer. Demographic and clinical data was assessed including disease duration and comorbidity (**Table 1**).

To evaluate motor symptoms of PD, part III of the Unified Parkinson's Disease Rating Scale (UPDRS) (15) was conducted in the entire study cohort. Definition of depression and apathy was based on established scores: using the Beck Depression Inventory II (16) to investigate severity of depression symptoms. A score of $\geq$19 points was defined as cut-off value for depression (17). Using the Lille Apathy Rating Scale (LARS) (18) to assess apathy, a cut-off-score of $\geq$-16 was chosen for apathy, since this cut-off-value has shown a high sensitivity of 87% and a high specificity of 93% in diagnosing apathy (18).

Transcranial Sonography

Transcranial sonographic (TCS) examination was performed on the same day as clinical assessment, and was performed by two experienced investigators (DR, CK) being blinded to clinical scores using a phased array ultrasound system equipped with a 2.5-MHz transducer (Aplio® XG Ultrasound System, Toshiba Medicals, Tochigi, Japan). A penetration depth of 150 mm and a dynamic range of 45–50 dB were chosen. Image brightness and time gain compensations were adapted as needed for each examination.

The examination protocol of the axial examination plane was based on previous published recommendations for TCS (19). Using the transtemporal approach, the midbrain and diencephalic examination planes were visualized in axial section. To evaluate SN hyperechogenicity, a planimetric measurement of SN was performed. According to previously published studies (20), we used the mean + 1 SD of SN echogenic area in the group of HC for each plane as upper normal value defining SN hyperechogenicty. In general, an enlarged echogenic area of the SN is a predictive biomarker with high sensitivity and specificity for the diagnosis of PD (10).

The echogenicity of brainstem raphe (BR) was classified semi-quantitatively on a three-point scale: 0 = raphe structure not visible, 1 = slight and interrupted echogenic raphe structure, 2 = normal echogenicity (echogenicity of raphe structure is not interrupted) (**Figure 1**). Different to the enlarged echogenic area of the SN in PD, a reduced echogenic signal of the BR is thought to visualize changes in the serotonergic system (9).

Similar to the axial examination plane protocol, the temporal bone window was used to assess also the coronal TCS plane: by rotating the transducer for 90°, the hypoechogenic midbrain is visualized in longitudinal view including SN and BR (**Figure 2**).

The sonographic findings were stored, so that the investigators could perform a second evaluation and classification of the results from the other investigator. In the case of discrepant ratings, a consensus was accomplished, subsequently.

Statistical Analysis

The descriptive statistics are given as median and interquartile range throughout the manuscript. As needed, the range is given additionally. Using appropriate nonparametric tests, the groups were statistically compared and correlation analysis were performed (Kruskal-Wallis H test, Mann-Whitney–U test,

TABLE 1 | Demographic, clinical and sonographic data.

	Parkinson's disease ($n = 31$)	Essential tremor ($n = 16$)	HC ($n = 16$)	*p*-value
Age (years)	69.0 (14.0)	63.5 (21.25)	58.0 (9.25)	0.079[H]
Female (%)/	10 (32.3)/	8 (50)/	10 (62.5)/	0.129[F]
Male (%)	21 (67.7)	8 (50)	6 (37.5)	
Time to first suspected disease	9.0 (6.0)	4.5 (9.75)	–	0.220[U]
Hoehn and Yahr	2.0 (0)	–	–	
MDR-UPDRS III	28.0 (14.0)	7.5 (5.0)	0.5 (2.0)	**<0.001**[H,b]
BDI-II	10.0 (14.0)	12.0 (12.5)	5.0 (8.25)	**0.050**[H,c]
LARS	−24.0 (15.0)	−30.0 (9.0)	−31.0 (4.75)	**<0.001**[H,b]
TCS				
Axial SN echogenicity in cm^2 (Hyperechogen in %)	0.27 (0.10) (90.3)	0.14 (0.04) (12.5)	0.145 (1.0) (18.8)	**<0.001**[H,a] **<0.001**[F,a]
Reduced BR signal axial (%)	32.3	6.7	6.3	**0.044**[F,a]
Reduced BR signal coronal (%)	29.0	6.7	6.7	0.119[F]

Boldface p-values indicate statistical sgnificance. Values are given in median and (interquartile range). MDR-UPDRS, Part 3 of the Movement Disorder Society Unified Parkinson Disease Rating Scale, BDI-II, Becks Depression Inventory II; LARS, Lille Apathy Rating Scale; TCS, Transcranial sonography.
[a] Significant difference between the three groups but not between ET patients and HC; [b] Significant difference between the three groups and also between ET patients and HC; [c] Significant difference between the three groups but not between PD and ET patients; [H] Kruskal-Wallis H test; [U] Mann-Whitney-U test;
[F] Freeman-Halton extension of Fisher's exact test.

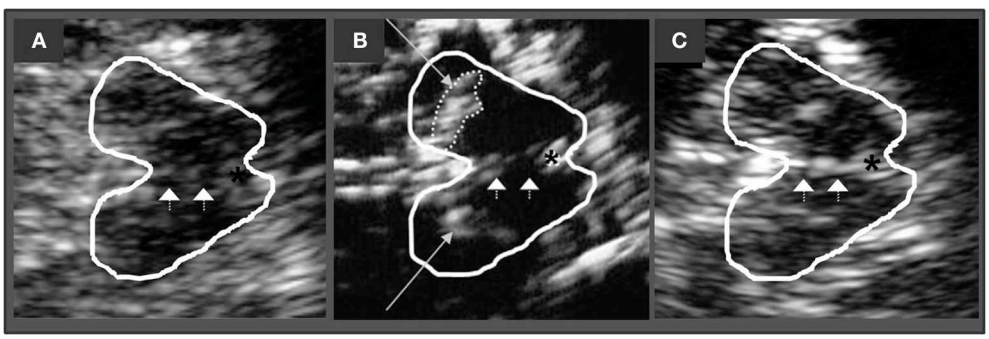


FIGURE 1 | Corresponding mesencephalic axial examination planes. The butterfly-shaped midbrain is outlined for better visualization. The asterisk indicates the aqueduct. Arrowheads indicate the brain stem raphe. **(A)** Raphe structure not visible, grade 0, pathologic finding. **(B)** Echogenic line of the raphe is interrupted, grade 1, pathologic finding. Long arrows indicating the hyperechogenic enlarged area of Substania nigra **(C)** Normal echogenicity, grade 2, normal finding.

Wilcoxon-Test, Fisher's exact test, Freeman-Halton extension of Fisher's exact test, Spearman rho analysis) with SPSS 23.0 for Mac.

RESULTS

Study Population and Clinical Features

We screened 36 patients with Parkinson's disease; four patients (11.1%) were excluded owing to an inadequate temporal bone window and one patient (2.7%) was excluded owing to severe dementia. Thus, 31 PD-patients (21 men, 10 women; age = 69.0 [14.0] years) were included into the study. Furthermore, one of the initially 17 patients with essential Tremor was excluded owing to an inadequate temporal bone window resulting in 16 ET patients (8 men, 8 women; age = 63.5 [21.25] years) being included. As control group, 16 healthy subjects were recruited (6 men, 10 women; age = 58.0 [9.25] years). LARS could be performed in 44 participants of the patient population. Detailed information about the clinical characteristics of all participants is demonstrated in **Table 1**.

Symptoms of Depression and Apathy

Prevalence of depression based on BDI-II definition value differed significantly over the three groups. Owing to the definition, 10 (32.3%) PD patients, 3 (18.8%) ET patients and none of the HC were depressive in our investigation (Freeman-Halton extension of Fisher's exact test, $p = 0.024$). Additionally, there was a strong tendency for difference between PD-patients, ET-patients and HC regarding to the BDI-II Score (Kruskal-Wallis H test, $p = 0.05$). BDI-II scores of PD-patients and

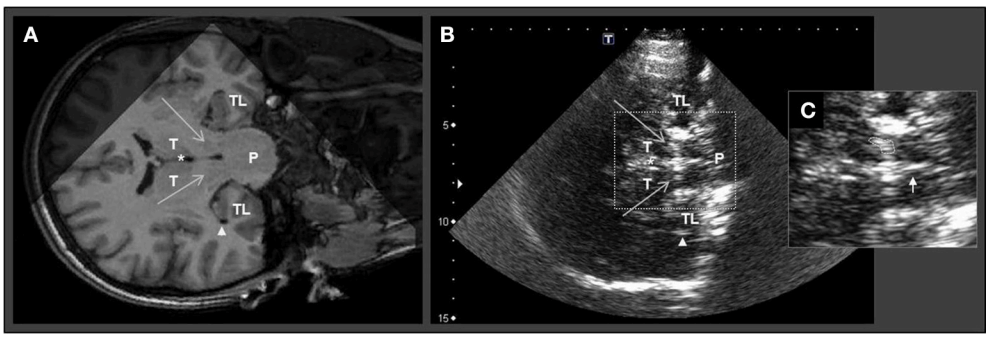


FIGURE 2 | Corresponding MRI and TCS images of coronal examination planes in a patient with idiopathic Parkinson's disease. Coronal MR scanning plane **(A)** and corresponding TCS examination plane **(B)** at brainstem level. **(C)** Zoom in of midbrain structures for planimetric assessment of the echogenic area of substantia nigra and evaluation of brainstem raphe. The large arrows in **(A)** and **(B)** indicate substantia nigra (note that in TCS the SN is displayed echogenic). White asterisks mark the third ventricle. Arrowheads in **(A)** and **(B)** indicate the inferior horn of lateral ventricle. Small arrow in **(C)** indicates the normal appearing brainstem raphe. TL, temporal lobe; P, Pons; T, thalamus.

ET-patients showed comparable results (Mann-Whitney–U test $p = 0.770$). The BDI-II score was significantly different between PD-patients and HC (Mann-Whitney–U test, $p = 0.02$) while the BDI-II scores of ET-patients and HC did not show a substantial difference as the postulated p-value level of statistical significance could not be reached (Mann-Whitney–U test, $p = 0.056$).

Analyzing the appearance of apathy, 12 (38.7%) PD patients, one (7.7%) ET patient and none of the HC were apathic indicating a significant difference in apathy prevalence over the groups (Freeman-Halton extension of Fisher's exact test, $p = 0.002$). Between ET patients and HC no difference in apathy prevalence was found (Fisher's exact test, $p = 1.000$). Regarding to LARS scores, there was also significant difference over the three groups (Kruskal-Wallis H test, $p < 0.001$). This difference in LARS scores appeared significant between PD and ET patients (Mann-Whitney–U test, $p = 0.023$) and significant between ET patients and HC (Mann-Whitney–U test, $p = 0.045$) and PD patients and HC (Mann-Whitney–U test, $p < 0.001$), respectively.

In respect to coexisting apathy and depression, 5 (41.6%) of the apathic PD patients had only apathy and 7 (58.3%) had apathy and depression. Concerning depressive PD patients, 3 (30.0%) had only depression and 7 (70.0%) had both depression and apathy. Interestingly, in these subgroups of PD patients with isolated either depressive (3 patients, 9.7%) or apathic (5 patients, 16.1%) symptoms, only one (3.2%) PD patient with isolated apathy showed an altered BR Signal in TCS.

Correlation of LARS and BDI-II

For each group of the study population BDI-II and LARS scores were correlated. Only for PD patients a significant positive correlation was found (PD: rho = 0.657, $p < 0.001$). In ET patients and in the group of HC, no significant correlation was determined (ET: rho = 0.075, $p = 0.808$; HC: rho = 0.131, $p = 0.630$).

Transcranial Sonography Findings

In one ET patient the BR could not sufficiently be evaluated. In one HC only the axial sonographic BR analyzes could be examined. In both cases there was a partially insufficient bone window. Evaluation of BR echogenicity revealed that 10 (32.3%) of the 31 patients with PD, but only one (6.7%) of the remaining 15 patients with ET and only one (6.3%) of the 16 healthy controls exhibited a reduced BR signal in the axial TCS plane indicating structural alterations in this area (Freeman-Halton extension of Fisher's exact test, $p = 0.044$). Using the coronal TCS plane, almost the same distribution of BR alterations in the groups was found (Freeman-Halton extension of Fisher's exact test, $p = 0.119$). Correlation of axial and coronal TCS results in BR region was very high (rho = 0.950, $p < 0.001$) (**Table 1**).

As BR signal alterations in TCS were very rare in ET patients und HC, correlation analysis of BDI-II, LARS and the sonographic BR results was only performed in the PD group determining a significant negative correlation between BDI-II and BR (rho = −0.420, $p = 0.019$) and LARS and BR (rho = −0.427, $p = 0.017$) using the axial TCS plane. Assessing BR through the coronal TCS plane in the PD population, the negative correlation values between BDI-II and BR (rho = −0.434, $p = 0.015$) and LARS and BR (rho = −0.407, $p = 0.023$) were comparable to the axial TCS assessment. The correlation analysis is also visualized as scatterplots in **Figure 3**.

Comparing BDI-II and LARS scores between PD patients with and without BR signal alterations in TCS, a significant difference was found. PD patients with BR alterations in axial TCS plane had higher scores in BDI-II (Mann-Whitney–U test, $p = 0.025$) and LARS (Mann-Whitney–U test, $p = 0.022$) compared to PD patients without BR signal changes. The same relation was found for coronal TCS plane by comparing the BDI-II and LARS scores in PD patients and without BR signal changes (BDI-II: Mann-Whitney–U test, $p = 0.029$; LARS: Mann-Whitney–U test, $p = 0.018$). Findings are summarized in **Table 2**.

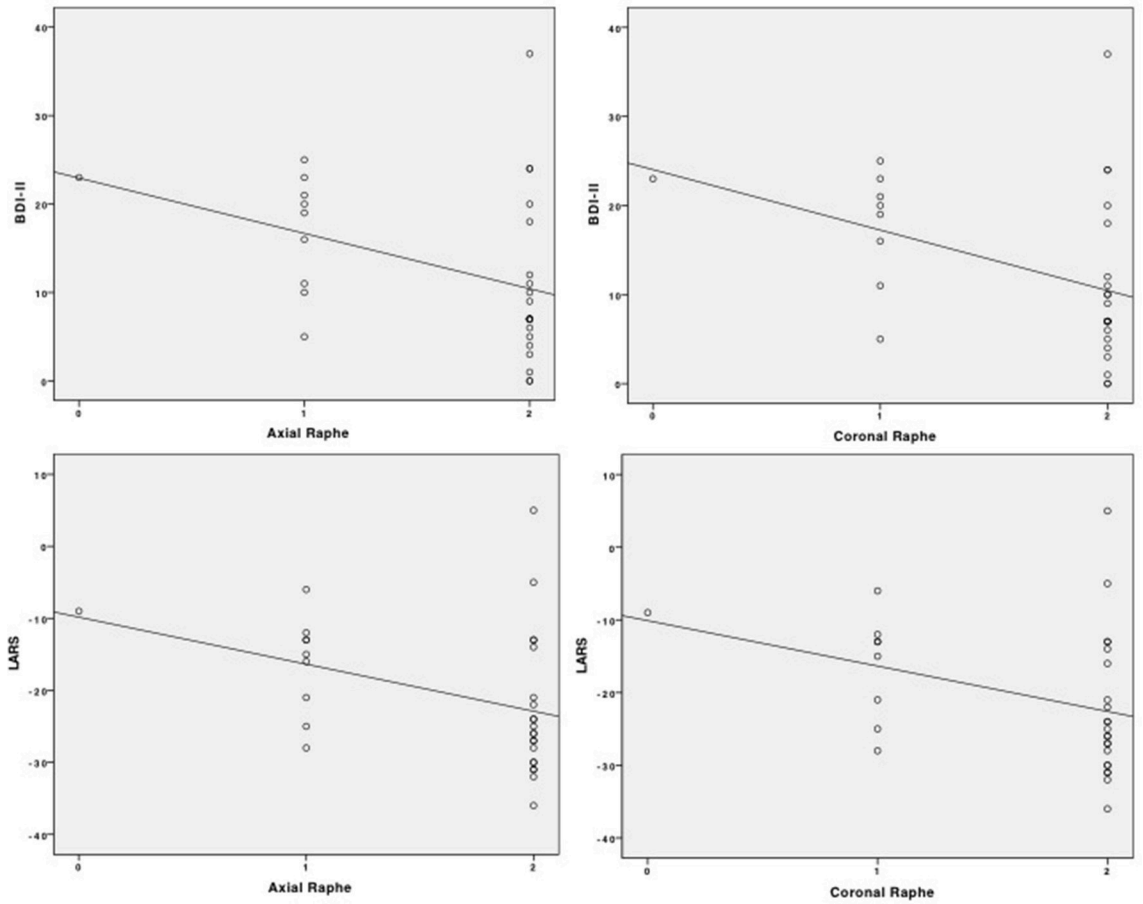


FIGURE 3 | Scatterplots of correlation analysis of BDI-II and LARS with BR signal alteration in the axial and coronal TCS examination.

No differences in BDI-II scores were found if depressive PD patients with and without BR signal alteration in TCS were compared irrespective of applying the axial (Kruskal Wallis H Test, $p = 0.469$) or coronal TCS plane (Mann-Whitney–U test, $p = 0.257$). Moreover, no differences in LARS scores were found, comparing apathic PD patients with and without BR signal alteration in TCS, neither for the axial (Kruskal Wallis H Test, $p = 0.683$) nor for the coronal TCS plane (Mann-Whitney–U test, $p = 0.792$).

Concerning SN hyperechogenicity, the mean ± 1 SD in the group of HC was calculated as 0.19 cm^2 for axial TCS plane resulting in a robust cut-off value for SN hyperechogenicity of unilateral echogenic SN area of at least 0.20 cm^2.

28 PD patients (90.3%), *three* HC (18.8%) and two ET patients (12.5%) showed SN hyperechogenicity (Freemann-Halton extension of Fisher's exact test, $p < 0.001$). Relating to the appearance of axial SN hyperechogenicity in the ET patients compared with the HC, no difference between these groups was found (Fisher's exact test, $p = 1.000$).

In the group of PD patients, the area of the SN in TCS was significantly larger than the SN area of the ET patients and HC (Kruskal-Wallis H test, $p < 0.001$), respectively. No difference in SN areas was found between ET patients and HC (Mann-Whitney–U test, $p = 1.000$).

DISCUSSION

To our knowledge, this is the first study to correlate BR signal alterations with symptoms of apathy in PD patients. Furthermore, this is the first study which detects BR echogenicity additionally in the recently introduced coronal TCS examination plane. We could show, that BR signal alterations detected by axial TCS examination plane appear more frequently in PD patients compared to ET patients and HC. Similarly, concerning the coronal TCS examination plane, we could confirm a higher prevalence of BR signal alterations in PD patients compared to ET patients and HC. With regard to BR signal changes, the correlation of axial and coronal TCS examination planes was very high indicating no superiority of one TCS plane compared to the other. However, as sonographic raphe analysis is based on a three-point scale we did not expect a substantial difference between the results of both TCS planes a priori.

In other studies, there have been discrepancies in the prevalence of apathy and its status as an independent symptom

TABLE 2 | Relation of BR, LARS, and BDI-II.

PD patients ($n = 31$)

	BDI-II		LARS	
	Spearman rho	***p*-value**	**Spearman rho**	***p*-value**
Axial BR evaluation in TCS	−0.420	**0.019**	−0.427	**0.017**
Coronal BR evaluation in TCS	−0.434	**0.011**	−0.407	**0.023**

	Axial BR evaluation in TCS		Coronal BR evaluation in TCS		*p*-value	
	BR-	**BR+**	**BR-**	**BR+**	**Axial**	**Coronal**
BDI-II	19.5 (12.25)	7.0 (11.5)	20.0 (9.5)	7.0 (8.75)	**0.025**^{U}	**0.029**^{U}
LARS	−14 (10.75)	−26.0 (17.5)	−13.0 (12.5)	−25.5 (14.5)	**0.022**^{U}	**0.018**^{U}

Boldface p-values indicate statistical significance. Values are given in median and (interquartile range). BDI-II, Becks Depression Inventory II; LARS, Lille Apathy Rating Scale; TCS, Transcranial sonography; BR, Brainstem raphe; BR–, With brainstem raphe alterations; BR+, Without brainstem raphe alterations; ^{U}*Mann-Whitney-U test.*

of PD. Brok et al. found that about 40% of PD patients are suffering from apathy (21). In our study, we found comparable results by determining apathy in about 38.7% of our PD patient population. We could show that a higher grade of apathy was negatively correlated to BR signal alterations in TCS and that PD patients with BR signal changes in TCS had higher scores in LARS. BR alterations in TCS might appear as a structural correlate to apathic symptoms and thus could serve as a correlating biomarker for apathy in PD. Furthermore, TCS might allow to identify PD patients which are at high risk of developing apathy. To validate these findings, a prospective longitudinal study paradigm is needed.

One of the ET patients and none of the HC were apathic according to the definition. Apathy has been occasionally described to occur independently from depression in ET patients (22). In our study, ET patients had higher overall scores in LARS compared to HC indicating a difference in the magnitude of apathic symptoms between these two groups.

In our study, PD patients with BR signal alterations showed significantly higher scores in BDI-II compared to those without BR signal alterations. Independently of the applied TCS plane, the BR signal alteration in TCS was significantly negatively correlated to the BDI-II scores in the PD patients group. This suggests that a structural change in the BR could be associated with the occurrence of depression as well as the severity of depressive symptoms in PD patients and thus might also have a value as a biomarker for depression in PD. Therefore, BR evaluation by TCS might allow to identify a subpopulation of PD patients which are at higher risk to develop a depressive symptomatology and would benefit from a more frequent follow up or more intensive medical treatment. Additionally, we have found a correlation of BR signal changes and apathic symptoms indicating that BR alterations in PD could serve as a biomarker for both apathy and depression. In most of the PD patients apathy and depression were present simultaneously and BDI-II and LARS scores were significantly positively correlated indicating a coexistence of apathic and depressive symptoms in PD.

A reduced BR signal, seen as absent or interrupted echogenic midline structure, is thought to reflect alterations in the serotonergic system and has been reported to be associated with depression in PD patients and with other extrapyramidal neuropsychiatric disorders like Huntington's disease (8, 9, 23). Anatomically, the echogenic midline in general represents various nuclei and fiber tracts of which the dorsal raphe nucleus is one of the main structures. The raphe nucleus is the major origin for serotonin release in the brain (24). A reduced echogenic signal of the BR could be due to alterations in the micro-architecture of this region (25, 26) and thus reflect a serotonin deficiency which is involved in depression pathophysiology.

The pathophysiological basis of apathy is still unknown. Concerning PD, this study found a correlation between sonographic BR alteration and apathy. As the echogenic raphe midline has much more fine anatomical structures than the raphe nuclei, it is also possible that microanatomical changes in other brain regions involved in the serotonin metabolism exist in addition. To our knowledge, sonographic BR signal alterations in PD have only been associated to mood disorders. Interestingly, a recent study has found a significant correlation between tremor severity in PD and raphe dysfunction measured by 123 ioflupane-fluoropropyl-carbomethoxy-3-beta-4-iodophenyltropane single photon emission computed tomography images (27). Further studies should check if sonographic BR signal changes are also linked to motor symptoms in PD.

Because the current BR evaluation in TCS is limited to a three-point scale, the discrimination of BR assessment might not be precise enough to detect differences in the severity of depression. We could not correlate the severity of depression in depressive PD patients to the extent of BR alterations in our study.

Interestingly, no difference with regard to BR signal alterations was found between ET patients and HC, although depression was present in some cases and BDI-II scores were

higher in ET patients compared to HC as has been shown before (28, 29). This implies that depression in ET in contrast to PD does not seem to be associated with BR alterations in TCS.

In conclusion, BR signal alterations were found more frequently in PD patients compared to ET patients and HC independent of the applied axial or coronal TCS examination plane. BDI-II and LARS scores of PD patients could be correlated to BR signal alterations of both TCS planes. This indicates that a serotonergic signal disturbance might exist for both depression and apathy and that pharmacologic therapy should take these findings into account. In the case of depression, it has been already reported that a reduced BR signal might be associated with better treatment responses to serotonin-reuptake-inhibitors (SSRI) (30). Further prospective and longitudinal studies are urgently needed to validate these study results in PD in order to substantiate this novel tool to more precisely identify PD and ET patients at risk to develop depression and apathy.

AUTHOR CONTRIBUTIONS

DR contributed to conceptualizing, organizing the project, analyzing, acquiring, and interpreting the data and writing of the first draft. DW contributed to conceptualizing and revising the manuscript. SM and RG contributed to conceptualizing, organizing the project and revising the manuscript. LT contributed to organizing the project, analyzing, acquiring and interpreting the data and revising the manuscript. CK contributed to conceptualizing, organizing the project, analyzing, acquiring and interpreting the data and revising the manuscript.

REFERENCES

1. Berg D, Postuma RB, Adler CH, Bloem BR, Chan P, Dubois B, et al. MDS research criteria for prodromal Parkinson's disease. *Mov Disord*. (2015) 12:1600–11. doi: 10.1002/mds.26431
2. Aarsland D, Marsh L, Schrag A. Neuropsychiatric symptoms in Parkinson's disease. *Mov Disord.* (2009) 24:2175–86. doi: 10.1002/mds.22589
3. Reijnders JS, Ehrt U, Weber WE, Aarsland D, Leentjens AF. A systematic review of prevalence studies of depression in Parkinson's disease. *Mov Disord.* (2008) 23:183–9. doi: 10.1002/mds.21803
4. Pedersen KF, Larsen JP, Alves G, Aarsland D. Prevalence and clinical correlates of apathy in Parkinson's disease: a community-based study. *Parkinsonism Relat Disord.* (2009) 15:295–9. doi: 10.1016/j.parkreldis.2008.07.006
5. Gaenslen A, Wurster I, Brockmann K, Huber H, Godau J, Faust B, et al. Prodromal features for Parkinson's disease–baseline data from the TREND study. *Eur J Neurol.* (2014) 21:766–72. doi: 10.1111/ene.12382
6. Oguru M, Tachibana H, Toda K, Okuda B, Oka N. Apathy and depression in Parkinson disease. *J Geriatr Psychiatry Neurol.* (2010) 23:35–41. doi: 10.1177/0891988709351834
7. Prakash KM, Nadkarni NV, Lye WK, Yong MH, Tan EK. The impact of non-motor symptoms on the quality of life of Parkinson's disease patients: a longitudinal study. *Eur J Neurol.* (2016) 23:854–60. doi: 10.1111/ene.12950
8. Walter U, Hoeppner J, Prudente-Morrissey L, Horowski S, Herpertz SC, Benecke R. Parkinson's disease-like midbrain sonography abnormalities are frequent in depressive disorders. *Brain* (2007) 130:1799–807.doi: 10.1093/brain/awm017
9. Krogias C, Walter U. Transcranial sonography findings in depression in association with psychiatric and neurologic diseases: a review. *J Neuroimaging* (2016) 26:257–63. doi: 10.1111/jon.12328
10. Richter D, Woitalla D, Muhlack S, Gold R, Tönges L, Krogias C. Coronal transcranial sonography and m-mode tremor frequency determination in Parkinson's disease and essential tremor. *J Neuroimaging* (2017) 27:524–30. doi: 10.1111/jon.12441
11. Hughes AJ, Daniel SE, Kilford L, Lees AJ. Accuracy of clinical diag- nosis of idiopathic Parkinson's disease: a clinico-pathological study of 100 cases. *J Neurol Neurosurg Psychiatry* (1992) 55:181–4.
12. Deuschl G, Bain P, Brin M. Consensus statement of the movement disorder society on tremor. *ad hoc* scientific committee. *Mov Disord.* (1998) 13:2–23.
13. Horstink M, Tolosa E, Bonuccelli U, Deuschl G, Friedman A, Kanovsky P, et al. European federation of neurological societies; movement disorder society-european section. review of the therapeutic management of Parkinson's disease. report of a joint task force of the european federation of neurological societies and the movement disorder society-european section. *Eur J Neurol.* (2006) 13:1186–202. doi: 10.1111/j.1468-1331.2006.01548.x
14. Zesiewicz TA, Elble RJ, Louis ED, Gronseth GS, Ondo WG, Dewey RB Jr, et al. Evidence-based guideline update: treatment of essential tremor: report of the quality standards subcommittee of the american academy of neurology. *Neurology* (2011) 77:1752–5. doi: 10.1212/WNL.0b013e318236f0fd
15. Movement Disorder Society Task Force on Rating Scales for Parkinson's Disease. The Unified Parkinson's Disease Rating Scale (UPDRS): status and recommendations. *Mov Disord.* (2003) 18:738–50. doi: 10.1002/mds.10473
16. Beck AT, Steer RA, Ball R, Ranieri W. Comparison of beck depression inventories–IA and –II in psychiatric outpatients. *J Personal Assess.* (1996) 67:588–97.
17. Arnau RC, Meagher MW, Norris MP, Bramson R. Psychometric evaluation of the beck depression inventory-II with primary care medical patients. *Health Psychol.* (2001) 20:112–9. doi: 10.1037//0278-6133.20.2.112
18. Sockeel P, Defebvre L, Denève C, Destèe A, Devos D, Dujardin K. The Lille apathy rating scale (LARS), a new instrument for detecting and quantifying apathy: validation in Parkinson's disease. *J Neurol Neurosurg Psychiatry* (2006) 77:579–84. doi: 10.1136/jnnp.2005.075929
19. Walter U, Skoloudik D. Transcranial sonography (TCS) of brain parenchyma in movement disorders: quality standards, diagnostic applications, and novel technologies. *Ultraschall Med.* (2014) 35:322–31. doi: 10.1055/s-0033-1356415
20. Doepp F, Plotkin M, Siegel L, Kivi A, Gruber D, Lobsien E, et al. Brain parenchyma sonography and ^{123}I-FP-CIT SPECT in Parkinson's disease and essential tremor. *Mov Disord.* (2008) 23:405–10. doi: 10.1002/mds.21861
21. den Brok MG, van Dalen JW, van Gool WA, Moll van Charante EP, de Bie RM, Richard E. Apathy in Parkinson's disease: a systematic review and meta-analysis. *Mov Disord.* (2015) 30:759–69. doi: 10.1002/mds.26208
22. Louis ED. Non-motor symptoms in essential tremor: a review of the current data and state of the field. *Parkinsonism Relat Disord.* (2016) 22(Suppl. 1):115–8. doi: 10.1016/j.parkreldis.2015.08.034
23. Krogias C, Strassburger K, Eyding J, Gold R, Norra C, Juckel G, et al. Depression in patients with Huntington disease correlates with alterations of the brain stem raphe depicted by transcranial sonography. *J Psychiatry Neurosci.* (2011) 36:187-94. doi: 10.1503/jpn.100067
24. Carpenter MB, Sutin J. *Human Neuroanatomy*. Baltimore: Williams and Wilkins (1983).
25. Berg D, Supprian T, Hofmann E, Zeiler B, Jäger A, Lange KW, et al. Depression in Parkinson's disease: brainstem midline alteration on transcranial sonography and magnetic resonance imaging. *J Neurol.* (1999) 246:1186–93.

26. Becker G, Berg D, Lesch KP, Becker T. Basal limbic system alteration in major depression: a hypothesis supported by transcranial sonography and MRI findings. *Int J Neuropsychopharmacol.* (2001) 4:21–31. doi: 10.1017/S1461145701002164
27. Pasquini J, Ceravolo R, Qamhawi Z, Lee JY, Deuschl G, Brooks DJ, et al. Progression of tremor in early stages of Parkinson's disease: a clinical and neuroimaging study. *Brain* (2018) doi: 10.1093/brain/awx376)
28. Sengul Y, Sengul HS, Yucekaya SK, Yucel S, Bakim B, Pazarci NK, et al. Cognitive functions, fatigue, depression, anxiety, and sleep disturbances: assessment of nonmotor features in young patients with essential tremor. *Acta Neurol Belg.* (2014) 115:281–7. doi: 10.1007/s13760-014-0396-6
29. Louis ED, Cosentino S, Huey ED. Depressive symptoms can amplify embarrassment in essential tremor. *J Clin Mov Disord.* (2016) 3:11. doi: 10.1186/s40734-016-0039-6
30. Walter U, Prudente-Morrissey L, Herpertz SC, Benecke R, Hoeppner J. Relationship of brainstem raphe echogenicity and clinical findings in depressive states. *Psychiatry Res.* (2007) 155:67–73. doi: 10.1016/j.pscychresns.2006.12.001

Conflict of Interest Statement: RG has received consultation fees and speaker's honoraria from BayerSchering, BiogenIdec, MerckSerono, Novartis, Sanofi-Aventis and TEVA. He also acknowledges grant support from BayerSchering, BiogenIdec, MerckSerono, Sanofi-Aventis and TEVA, none related to this manuscript. LT served as a member of AbbVieParkinson Advisory Board. CK received Honoraria for oral presentations or travel grants for scientific meetings from Bayer Vital, Bristol-Meyer Squidd, and Boehringer Ingelheim, none related to this manuscript.

The remaining authors declare that the research was conducted in the absence of any commercial or financial relationships that could be construed as a potential conflict of interest.

Copyright © 2018 Richter, Woitalla, Muhlack, Gold, Tönges and Krogias. This is an open-access article distributed under the terms of the Creative Commons Attribution License (CC BY). The use, distribution or reproduction in other forums is permitted, provided the original author(s) and the copyright owner(s) are credited and that the original publication in this journal is cited, in accordance with accepted academic practice. No use, distribution or reproduction is permitted which does not comply with these terms.

frontiers in Neurology

ORIGINAL RESEARCH
published: 19 September 2018
doi: 10.3389/fneur.2018.00668

Biomarkers of Neurodegeneration in Autoimmune-Mediated Encephalitis

Peter Körtvelyessy[1,2,3,4], Harald Prüss[3,4], Lorenz Thurner[5], Walter Maetzler[6,7,8], Deborah Vittore-Welliong[9], Jörg Schultze-Amberger[10], Hans-Jochen Heinze[1,2,11], Dirk Reinhold[12], Frank Leypoldt[8], Stephan Schreiber[13] and Daniel Bittner[1,2]*

[1] Department of Neurology, University Hospital Magdeburg, Magdeburg, Germany, [2] German Center for Neurodegenerative Diseases Magdeburg, Magdeburg, Germany, [3] Department of Neurology, Charité-Universitätsmedizin Berlin, Berlin, Germany, [4] German Center for Neurodegenerative Diseases Berlin, Berlin, Germany, [5] José Carreras Center for Immuno- and Gene Therapy and Internal Medicine I, Saarland University Medical School, Homburg, Germany, [6] Department of Neurodegeneration, Hertie Institute for Clinical Brain Research (HIH), University of Tübingen, Tübingen, Germany, [7] German Center for Neurodegenerative Diseases Tübingen, Tübingen, Germany, [8] Department of Neurology, University Hospital Schleswig-Holstein, Kiel, Germany, [9] Department of Neurology and Epileptology, Universitätsklinikum Tübingen, Universität Tübingen, Tübingen, Germany, [10] Department of Neurology, Median Clinic Kladow, Kladow, Germany, [11] Department of Behavioral Neurology, Leibniz Institute for Neurobiology, Magdeburg, Germany, [12] Department of Immunohistopathology, Institute of Molecular and Clinical Immunology, Magdeburg, Germany, [13] Asklepios Department of Neurology, Brandenburg a.d. Havel, Germany

OPEN ACCESS

Edited by:
Stefan Bittner, Johannes Gutenberg-Universität Mainz, Germany

Reviewed by:
Nico Melzer, Universität Münster, Germany
Michael R. Pranzatelli, National Pediatric Neuroinflammation Organization, Inc., United States

***Correspondence:**
Peter Körtvelyessy
peter.koertvelyessy@med.ovgu.de

Specialty section:
This article was submitted to Multiple Sclerosis and Neuroimmunology, a section of the journal Frontiers in Neurology

Received: *12 May 2018*
Accepted: *25 July 2018*
Published: *19 September 2018*

Citation:
Körtvelyessy P, Prüss H, Thurner L, Maetzler W, Vittore-Welliong D, Schultze-Amberger J, Heinze H-J, Reinhold D, Leypoldt F, Schreiber S and Bittner D (2018) Biomarkers of Neurodegeneration in Autoimmune-Mediated Encephalitis. Front. Neurol. 9:668. doi: 10.3389/fneur.2018.00668

Progranulin (PGRN), Total-Tau (t-tau), and Neurofilament light chain (NfL) are well known biomarkers of neurodegeneration. The objective of the present study was to investigate whether these parameters represent also biomarkers in autoimmune-mediated Encephalitis (AE) and may give us insights into the pathomechanisms of AE. We retrospectively examined the concentration of PGRN in the cerebrospinal fluid (CSF) and serum of 38 patients suffering from AE in acute phase and/or under treatment. This AE cohort comprises patients with autoantibodies against: NMDAR ($n = 18$ patients), Caspr2 ($n = 8$), Lgi-1 ($n = 10$), GABAB(R) ($n = 1$), and AMPAR ($n = 1$). Additionally, the concentrations of NfL ($n = 25$) and t-tau ($n = 13$) in CSF were measured when possible. Follow up data including MRI were available in 13 patients. Several age-matched cohorts with neurological diseases besides neuroinflammation or neurodegeneration served as control groups. We observed that PGRN was significantly elevated in the CSF of patients with NMDAR-AE in the acute phase, but normalized at follow up under treatment ($p < 0.01$). In the CSF of other patients with AE PGRN was in the range of the CSF levels of control groups. T-tau was highly elevated in the CSF of patients with temporal FLAIR-signal in the MRI and in patients developing a hippocampal sclerosis. NfL was exceptionally high initially in Patients with AE with a paraneoplastic or parainfectious cause and also normalized under treatment. The normalizations of all biomarkers were mirrored in an improvement on the modified Rankin scale. The data suggest that the concentration of PGRN in CSF might be a biomarker for acute NMDAR-AE. Pathological high t-tau levels may indicate a risk for hippocampal sclerosis. The biomarker properties of NfL remain unclear since the levels decrease under treatment, but it could not predict severity of disease in this small cohort. According to our results, we recommend to measure in clinical practice PGRN and t-tau in the CSF of patients with AE.

Keywords: progranulin, neurofilament light chain, NMDAR encephalitis, Lgi-1 encephalitis, Caspr2 encephalitis, tau, autoimmune encephalitis

INTRODUCTION

Since the appearance of antibody-mediated autoimmune encephalopathy (AE) numerous antibodies (ab) have been linked to different clinical symptoms such as limbic encephalitis, faciobrachial dystonic seizures or dementia-like symptoms (1–3). Biomarkers of neurodegeneration mirror certain pathomechanisms of neuronal or axonal loss. The measurement of these biomarkers should bear the potential to provide useful information in everyday clinical life, e.g., to monitor the immunosuppressive therapy in Patients with AE. CSF antibody titres in e.g., contactin-associated-protein-receptor-2 (Caspr2)-AE or Leucin-rich glioma inactivated ptotein-1 (Lgi-1)-AE do not mirror the disease course in a linear way (4, 5). Furthermore, the clinical course in several patients suggests that an antibody titer independent pathomechanism might take place (6–8). The underlying mechanisms causing this dichotomy of clinical symptoms and antibody titer are largely unknown (8). One possible explanation could be the effect of the long survival of plasma cells in the brain (9). The brain-resident plasma cells itself cannot be measured as yet, but the damage possibly caused by autoantibodies should be detected via biomarkers for neuronal and axonal loss such as t-tau, PGRN, and NfL.

Recently, a direct connection between neurodegenerative mechanisms and AE has been detected in AEs mediated by IgLON5 causing an atypical tauopathy (10). Vice versa a correlation between autoimmune diseases and Tar DNA-binding Protein 43 (TDP-43) mediated neurodegeneration in FTD patients has been reported (11). There is also some debate about IgA-NMDAR-Abs and IgM-NMDAR-Abs (3, 12, 13) causing dementia-like symptoms and mimicking neurodegenerative diseases. Histopathological examinations in patients with AE have been focused on the immunological mechanisms triggered and maintained by the antibodies (8) disregarding a systematic research for markers of neurodegeneration so far. Only one case report of a Lgi-1 antibody positive patient presenting some neurodegenerative markers has been reported at autopsy, without witnessing pathological changes in alpha-synuclein, beta-amyloid, or neurofibrillary tangle (14). MRI findings and long-term neuropsychological data also suggest an involvement of the frontal and temporal lobes in the clinical course of the NMDAR-AE and voltage-gated-potassium channel (VGKC)-complex-mediated AE (15–18). Another group has looked at the glial fibrillary acid, NfL and t-tau levels in patients with suspected AE (19). Their group only encompassed four patients with NMDAR-AE and one Lgi-1 patient with most of them having a status epilepticus (SE) before, as SE is known for confounding the protein levels in the CSF (20, 21). They found higher NfL and t-tau levels in all patients, which is most likely due to the SE before. In pediatric opsoclonus-myoclonus syndrome caused by antibodies with intracellular epitopes, immunosuppressive treatment has shown to decrease the CSF-Neurofilament light chain levels together with a concomitant clinical improvement (22, 23).

Here, we examined concentrations of PGRN, NfL, and t-tau, well-established biomarkers of neurodegeneration, in CSF and serum of 38 patients with antibody positive AE. The aim of this study is to investigate if these proteins are possible biomarkers in Patients with AE. Also, the knowledge about the biomarkers of neurodegeneration CSF-levels may give clues about the pathological mechanisms in these patients.

Abbreviations: Ab, Antibody; AD, Alzheimer's disease; AE, Autoimmune mediated Encephalitis; AMPAR, alpha-amino-3-hydroxy-5-methyl-4-isoxazolepropionic acid receptor; Caspr2, Contactin associated protein 2; CSF, cerebrospinal fluid; FTD, Frontotemporal dementia; GABAB(R), Gabaaminobutyrat-B subunit receptor; Lgi1, Leucin-rich glioma inactivated protein1; NMDAR, N-methyl-D-aspartate receptor; NfL, Neurofilament light chain; PGRN, Progranulin; SE, Status Epilepticus; t-tau, T-tau; VGKC, Voltage-gated potassium channel.

METHODS

Clinical Cohort

This retrospective study was performed according to the local ethical committees in Berlin, Potsdam, Brandenburg, Magdeburg and Bielefeld, respectively. All patients gave written and informed consent (ethics committee approval number 100/16). We included only patients with a proven AE by clinical symptoms as recommended by Graus et al. (24) and detection of pathological antibodies with extracellular epitopes via indirect immunofluorescence tests. The samples of AE-Patients were collected from April 2013 until October 2017 in Berlin, Potsdam, Tübingen, Bielefeld, and Magdeburg where their samples were initially stored at −80°C and sent to Magdeburg. Every sample was stored in Magdeburg at −80°C and all biomarkers were measured in Magdeburg. All samples were run in duplicate with the mean taken as result. Samples were measured over time and not in a batch.

All patients received a lumbar puncture as part of the diagnostical work up when presenting for the first time on the ward and for antibody titre control in follow up depending on each individual disease course. At least 5 ml up to 13 ml CSF was taken and serum was collected in serum separator tubes and centrifuged at site. Every patient ($n = 38$) suffered from a limbic encephalitis including its variants, e.g., limbic encephalitis together with vegetative and/or peripheral neurological symptoms. All patients improved under immunosuppressive therapy. Treatment comprised methylprednisolone (dosage ranges from 3 g up to 18 g during disease course), cyclophosphamid or rituximab (with a minimum dosage of 2g), plasmapheresis or ivIG. We had no patients with a relapse in this cohort. None of the patients had a status epilepticus before lumbar puncture confounding the biomarker levels because of neuronal and axonal death due to the status epilepticus.

Two patients with other antibodies targeting extracellular epitopes [AMPAR and GABAB(R)] were not considered in the statistical analysis but for **Figure 3** to illustrate the biomarker and MRI timeline an AE patients. See **Table 1** for the different AE cohorts used per biomarker. We had follow up data in 13 patients. All other patients (samples) were categorized into either initial/acute phase or under treatment.

TABLE 1 | Epidemiological data.

Biomarker	Antibody	Initial [age/sex]	Follow up [age/sex]
Progranulin	NMDAR	**6** [28.9/6:0]	**17** [27.1/16:1]
	Caspr2	**8** [61.9/2:6]	**5** [67.1/0:5]
	Lgi-1	**7** [69.0/5:2]	**6** [63.2/3:3]
T-Tau	NMDAR	**3** (38.7/3:0]	**3** (38.7/3:0]
	Caspr2	**5** [69.6/0:5]	**5** [69.6/0:5]
	Lgi-1	**3** [63.7/2:1]	**3** [63.7/2:1]
Nfl	NMDAR	**3** (38.7/3:0]*	**13** (30.2/12:0]
VGKC-group	Caspr2	**6** (68.3/1:5]	**5** [67.1/0:5]
	Lgi-1	**3** [63.7/2:1]	**3** [63.7/2:1]
Control group young	None	**24** [29.9/18:6]	*
Control group old	None	**21** [60.0/9:12]	*

*not part of statistics

sex = female:male

Overview of the single groups tested in this study. Number of patients included in bold, sex and mean age are listed.

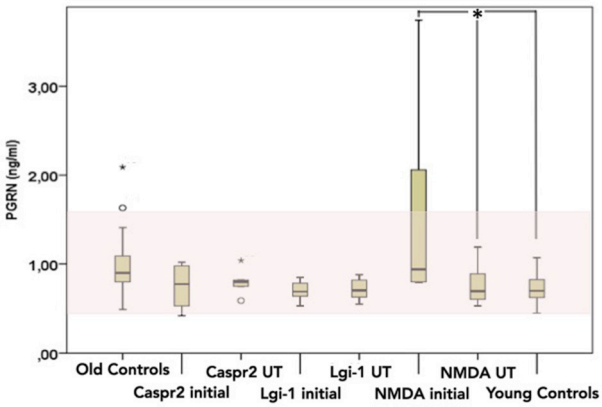


FIGURE 1 | CSF Progranulin levels [pg/ml] in patients with AE ($n = 36$) measured divided by antibody and by phase of disease (initial vs. under treatment). Significant results are marked with a *. Normal range is marked in light red. Line represents the median and the error bars represent the interquartile range. Black points are outliers.

Magdeburg Group

Patients with AE who were identified and treated in Magdeburg ($n = 13$) build a special cohort, because we could e.g., compare serial MRIs to look for AE caused lesions, basic CSF parameters, the outcome with the modified Rankin scale, t-tau, and other biomarker levels in the CSF and ab titer. The modified Rankin scale in this cohort was assessed by two experienced neurologist (PK, DB). Six out of thirteen had a paraneoplastic origin and one patient a postinfectious origin of the AE.

CSF-Neurofilament Light Chain Measurements

We divided the AE cohort into three groups regarding the CSF-NfL measurements in order to be able to perform a sufficient statistical analysis (see **Table 1**). One group with voltage-gated potassium channels (VGKC) mediated AE (comprising the Caspr2 and Lgi-1 patients) subdivided in an "initial" ($n = 9$) and "under treatment," meaning after several immunosuppressive therapies, subgroup ($n = 8$) and one group with NMDA patients under treatment ($n = 13$) (see **Table 1** and **Figure 1**). There were not enough NMDA patients who would fit into an initial/acute phase group ($n = 3$). Therefore, this group could unfortunately not be part of the statistical analysis.

Neurofilament light chain was measured with a commercial ELISA (Umandiagnostics, Sweden, catalogue number 10-7001 CE). The sensitivity of this assay is 31 pg/ml. The cut-off for pathological levels was set at 3523 ng/ml (mean (1823[ng/ml]) + 2 standard deviation (850[ng/ml]) above). Intraessay coefficient of variance is 7.4% and interessay coefficient of variance is 6%. NfL is a stable protein, which can be measured in the CSF even though the sample was on room temperature for up to 8 days (25). Therefore, we could measure NfL in samples not collected at Magdeburg, We used an already established control group at Magdeburg ($n = 34$, mean age = 64.4, CSF-NfL= 1823 ± 850 [ng/ml]) comprising patients with other than neuroinflammatory or neurodegenerative diseases (e.g., headache, suspicion of infection in the CNS etc.).

Total-Tau Measurements

The correct measurement of t-tau due to manufacturer's instructions requires different than standard processing of the CSF samples to create a cell-free sample excluding this parameter from a retrospective study. We yielded t-tau levels only in the Magdeburg group, as t-tau is part of the routine in Magdeburg but not in the other centers involved. Total-Tau levels were determined using a commercially available single-parameter ELISA kit [Innogenetics, Ghent, Belgium, catalogue numbers: 81572 (962-CE) and 81573] established in our routine diagnostical work up. Intraessay coefficient of variance is 13.2% and interessay coefficient of variance is 11.5%. The pathological levels were considered according to the manufacture guidelines.

CSF-Progranulin Measurements

We measured PGRN in CSF and serum of 36 Patients with AE. We divided our AE cohort ($n = 36$) into three groups according to the antibody causing the limbic encephalitis when looking statistically at the CSF-PGRN levels: one Lgi-1 group ($n = 10$, mean age = 69.2), one Caspr2 group ($n = 8$, mean age = 61.9) and a NMDAR group ($n = 18$, mean age = 27.1). These three groups were subdivided into two subgroups respectively one before and one after initiating immunosuppressive therapy (again, called "initial" or "under treatment") (see **Table 1** and **Figure 2**).

A commercial ELISA was performed to determine the levels of PGRN (Human Progranulin ELISA Kit, Mediagnost, Reutlingen, Germany, catalogue number E103) according to the manufacturer's instructions. Intraessay coefficient of variance is 4.4% and interessay coefficient of variance is 8.0%.

We established two control groups for PGRN measurements. Since PRGN levels are age dependent, we build a younger control group ($n = 24$; mean age 29.3 years; 18–40yrs) and one older group ($n = 39$; mean age 66.3 years,

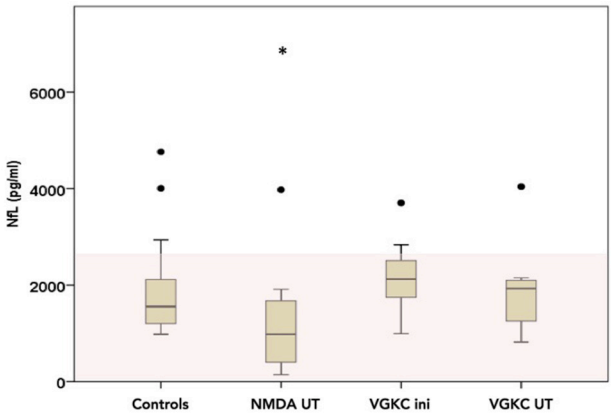


FIGURE 2 | CSF-Neurofilament light chain (NfL) levels divided into three possible groups (NMDA under treatment $n = 14$, VGKC initial $n = 7$ and under treatment $n = 6$) as box plots (number of measurements, $n = 30$). The area in light red marks the normal range. Please note that all levels are inside the normal range. Line represents the median and the error bars represent the interquartile range. White points mean outlier and star extreme outliers.

50–75 years) and correlated it to age. The patients from these control groups had other neurological diseases than neuroinflammatory or neurodegenerative (e.g., acute headache, excluding neuroinflammatory diseases, no epilepsy patients). CSF-PGRN level was considered pathological, when the CSF-PGRN levels per control group were two standard deviation above or below the mean for each control group respectively.

Antibody Detection

Antibody detection was either performed at the antibody laboratory Bielefeld, at the University Hospital Schleswig-Holstein, Department of Neuroimmunology Kiel and Lübeck or at the Institute of Molecular and Clinical Immunology Magdeburg. Standard indirect immunofluorescence tests were performed on antigen-specific transfected Hek293 cells as commercially available and used in clinical routine (EUROIMMUN, Lübeck, Germany, catalogue numbers: FA 112d-1003-6, FA 112d-1003-51, FA 1430-1003-1) for each patient revealing the specific antibody and the titer in CSF and serum.

Statistics

Statistics were calculated by SPSS 21.0 (IBM, Seattle, USA). Since group size and variances were not equal non-parametric tests were applied. For comparison of more than two different groups Kruskal-Wallis test was used with tamhanes *post-hoc* analysis. Group comparison of two groups was analyzed with Mann-Whitney-U test when they were independent and with the Wilcoxon test when the samples were paired to each other. For correlational analysis of serum and CSF PGRN Spearmann-rho correlation was applied. Tests were considered significant when reaching $p < 0.05$. There was no test for outliers applied.

RESULTS

Cohorts

Since the CSF-PGRN level is age-dependent we established a younger control group aged 18–40 years ($n = 24$, CSF-PGRN$= 0.72 \pm 0.17$ ng/ml, Serum-PGRN $= 36.4$ ng/ml, mean age $= 29.3$ years) and a control group 50-75 years ($n = 39$, CSF-PGRN $= 0.94 \pm 0.22$ ng/ml, Serum-PGRN $= 28.5$ ng/ml mean age $= 66.3 \pm 9.8$ years). Spearman correlation statistics revealed a significant correlation between CSF-PGRN and age ($r = 0.275$, $p = 0.02$).

In the Magdeburg group 9/13 had a FLAIR-intense signal in the limbic system on the MRI. Five out of thirteen patients developed a hippocampal sclerosis due to AE (see **Table 2** and **Figure 3**). Every patient with pathologically elevated t-tau levels developed a hippocampal sclerosis. The one patient, who developed a hippocampal sclerosis without elevated t-tau levels but elevated NfL concentrations, was administered after he was already treated and had a hippocampal sclerosis. Therefore the CSF was taken and measured ∼8 months after beginning of the AE and treatment. On the contrary only 4 out of 7 patients with pathological NfL levels developed a hippocampal sclerosis. Every marker of neurodegeneration and the modified Rankin scale (mRS) decreased after initializing the immunosuppressive treatment paralleled by a decrease in antibody titre (see **Figure 3** for examples and **Table 2** for the follow up data).

Neurofilament Light Chain

NfL was pathologically high (>3523 pg/ml) in 7/23 patients at different stages of the AE (see **Figures 2**, **3** and **Table 2**). Out of these seven patients, four had a paraneoplastic origin of the AE and one a postinfectious origin. Furthermore, 5/7 patients had a FLAIR-intense signal in the limbic areas on the MRI, which normalized during immunosuppressive treatment. This decrease in FLAIR signal was mirrored by a decrease in NfL-levels reaching normal NfL levels during disease course (see **Figure 3** and **Table 2**). Three out of five patients who developed hippocampal sclerosis had elevated CSF-NfL levels additionally to the also elevated t-tau. Solely elevated CSF-NfL was found in 4 patients. We correlated the leukocyte count to the NFL levels in the Magdeburg cohort and found no correlation (Spearmans $r = 0.625$).

There was a trend toward a lower NfL in the NMDA under treatment group (CSF-NfL = 1455 [pg/ml], range 142–6841[pg/ml]) compared to the VGKC under treatment group (CSF-NfL = 2164 [pg/ml], range 821–4039 [pg/ml]) (Mann-Whitney U test $p = 0.052$ $Z = -1.941$), while there was no difference comparing the VGKC subgroups initial vs. under treatment (Wilcoxon test $p = 0.735$ and $Z = -0.338$).

Total Tau

Looking at the initial t-tau in our patients (before initiating the treatment) revealed a pathologically high t-tau in 4 patients (see **Table 2**). All 4 patients had MRI-FLAIR intense signals in the temporal lobe/limbic system and subsequently a hippocampal sclerosis. Immunosuppressive treatment did show an effect on

TABLE 2 | Biomarkers in the Magdeburg cohort.

	Antibody	Titer	Age	Year	T-tau	NFlight	CSF-PGRN	Serum-PGRN	Cell count	mRS	Comment
		CSF/Serum	Onset		pg/ml	ng/ml	pg/ml	pg/ml	CSF		
					>370	>3488	<0.54–1.4>	<18–54>	< 4 cells/mm2		
Patient 1	Caspr2	1:128/1:32000	60–65	2013	253	12342	0.76	n.a.	3	5	Temporal FLAIR-intense signal
		none/1:375		2015	133	2152	0.8	32.5	0	3	Paraneoplastic origin
		none /1:128		2015	108	2055	0.61	30.62	1	3	Hippocampal sclerosis
Patient 2	Caspr2	1:64000/1:750000	75–80	2014 #	292	2047	1.02	27.11	13	5	Temporal FLAIR-intense signal
		1:6000/1:96000		2015	213	2123	0.87	30.63	17	1	
Patient 3	Caspr2	1:320/1:3200	70–75	2015 #	367	4536	0.84	21.94	0	1	Normal MRI
		1:320/1:3200		2015 #	328	3580	0.74	22.05	3	1	
Patient 4	Caspr2	1:3200/1:1000	70–75	2016 #	314	3705	0.95	35.18	6	5	Temporal FLAIR-intense signal
		1:10 /1:2000		2016	317	4039	0.82	51.57	2	1	
Patient 5	Caspr2	1:320/1:4000	66–70	2017 #	349	2159	1.01	32.04	5	4	Normal MRI
		1:8/1:1000		2017	375	2586	0.82	43.58	2	0	
Patient 6	Lgi-1	none/1:100	60–65	2015 #	796	2128	0.63	32.97	1	3	Temporal FLAIR-intense signal
		none/1:32		2015	>11	2493	0.54	38.92	0	0	Hippocampal sclerosis
Patient 7	Lg-1	1:2/1:1000	65–70	2017 #	128	993	0.74	19.97	1	3	Paraneoplastic origin
		none/1:320		2017	149	1273	0.73	23	0	0	
Patient 8	Lgi-1	1:2 /1:160	60–65	2017 #	197	1582	0.65	27.33	0	3	Temporal FLAIR-intense signal
		1:20/1:10		2017	161	1233	0.68	30.12	2	0	
Patient 9	NMDA	1:32/1:320	25–30	2010 #	141	n.a.	0.76	29.11	1	5	Paraneoplastic origin
		1:10/1:100		2014	105	390	0.89	33.06	3	1	
		1:1/none		2015	58	553	1.3	n.a.	2	1	
Patient 10	NMDA	1:40/1:80	25–30	2016 #	869	38650	1	23.08	7	5	Temporal FLAIR-intense signal
		1:10/1:5		2016	229	20736	0.71	17.86	6	2	Hippocampal sclerosis
		1:5/1:5		2017	68	6841	0.71	25.43	3	1	Postinfectious origin
Patient 11	NMDA	none/1:10	60–65	2014 #	801	28791	1.53	35.51	96	4	Hippocampal sclerosis
		none/1:10		2014	372	42286	1.19	32.9	43	0	Temporal FLAIR-intense signal
		none/none		2015	192	3975	0.96	35.4	9	0	Paraneoplastic
Patient 12	GABA(B)R	1:320/1:32	50–55	2016 #	135	32029	1.79	37.21	47	5	Paraneoplastic origin
		1:320/1:1		2016	168	21439	1.03	37.5	1	3	Temporal FLAIR-intense signal
		none/1:10		2016	126	3581	0.95	n.a.	1	2	
Patient 13	AMPA	1:32/1:3200	70–75	2014 #	1950	32151	2.47	34.21	43	5	Paraneoplastic origin
		1:8/1:375		2014	1984	20354	1.23	38.22	90	4	Temporal FLAIR-intense signal
		1:1/none		2015	173	2892	0.7	n.a.	3	2	Hippocampal sclerosis
		#	Before treatment								
		n.a.	Not available								

Complete list of all 13 patients in the cohort where follow up data is available including antibody, antibody serum titer, age, year at which the sample has been obtained, Neurofilament light chain (NfL), Total-tau (T-Tau), CSF-Progranulin (PGRN), Serum-Progranulin, cell count, modified Rankin scale (mRS) and comments on MRI abnormalities and putative pathogenesis; n.a., not available; #, timepoint before start of the immunosuppression.

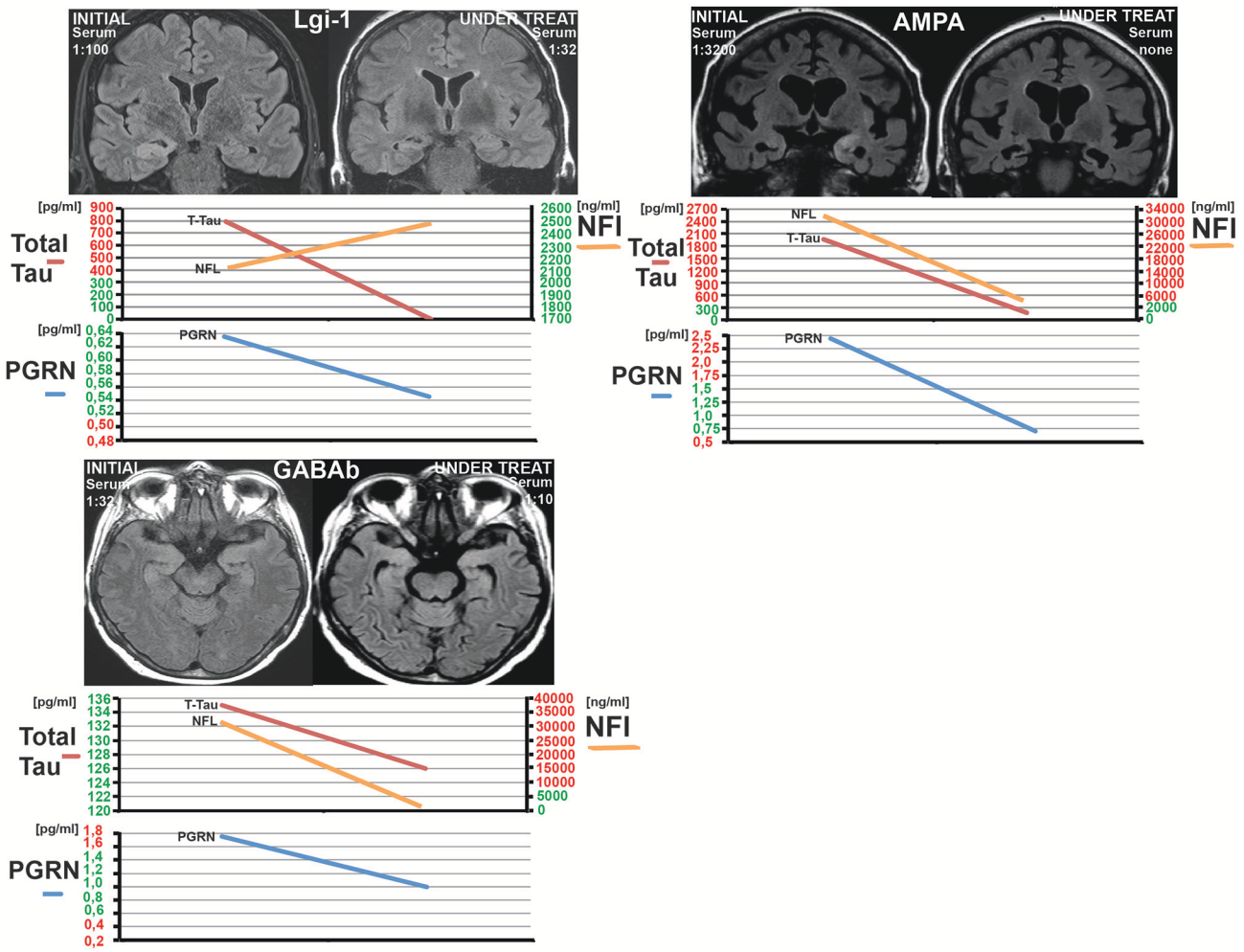


FIGURE 3 | Three examples of patients from the Magdeburg cohort (patient 5, 12, and 13 see **Table 1**) showing the under treatment MRI together with the CSF-Neurofilament light chain (NfL), CSF-Progranulin (PGRN), and Total tau. Normal levels are marked in green at the y-axis and pathological levels are marked in red. Notice the hippocampal sclerosis in the Lgi-1 patient and the complete recovery from the oedema in the GABA(B)R-AE-patient without a clear sign of a hippocampal atrophy. The third patient has a AMPAR-AE. The follow up in this patient shows a severe bilateral hippocampal atrophy. Nevertheless the patient improved over years.

the modified Rankin scale and also resulted in a decrease of t-tau in these patients. The FLAIR signal also decreased in these patients (see **Figure 3**). In the other 8 patients without elevated t-tau levels immunosuppressive therapy had no effect on t-tau levels. A concomitant tumor had no impact at all on the t-tau levels. (see **Table 2**).

Progranulin

The mean CSF-PGRN levels were pathologically high in the initial NMDAR-group (CSF-PGRN=1.55 ± 1.1 ng/ml) reaching significance when compared to the NMDAR under treatment group (Mann-Whitney-U test $Z = -2.5$ and $p = 0.012$) and also when compared to the age-matched healthy group (Mann-Whitney-U test $Z = -2.689$ and $p = 0.007$). Serum PGRN levels were inside normal ranges in every AE patient and did not change after immunosuppression (see **Figure S1**). CSF-PGRN and CSF-Serum ratios ranged from 0.01 to 0.1, still CSF-PGRN is show to originate from the CNS when measured in the CSF (26, 27) We also could not find a correlation between Serum-PGRN and CSF-PGRN in all groups (Spearman-rho coefficient $r = 0.17$, $p = 0.3$) (**Figure S1** in the Supplement).After initiating the immunosuppressive therapy CSF-PGRN dropped to normal levels (CSF-PGRN = 0.75 ± 0.2 ng/ml) in the "under treatment"-group.

Mean CSF-PGRN levels were normal in the Lgi-1 "initial" group (CSF-PGRN = 0.71 ± 0.11 ng/ml) and in the under treatment group (CSF-PGRN = 0.72 ± 0.12 ng/ml) (see **Figure 1**). Comparing these results to the age-matched group revealed significant differences (Kruskal-Wallis test: for "initial" PGRN: $p = 0.009$, $X^2 = 9.4$, for follow-up: $p = 0.04$, $X^2 = 6.3$). There were significantly lower levels in tamhane *post-hoc* in the Patients with AE (Lgi-1 initial vs. control $p = 0.009$ and $p = 0.041$ for the under treatment vs. control) The CSF-PGRN levels in both Caspr2 groups were inside the normal range (mean

CSF-PRGN initially = 0.75 ± 0.23 ng/ml and mean CSF-PGRN under treatment = 0.8 ± 0.16 ng/ml) without significant results when compared to the age-matched controls (Caspr2 initial vs. under treatment $p = 0.35$ and Caspr2 under treatment vs. control $p = 0.92$). There was no difference between the "initial" and the "under treatment" group in the Lgi-1 and Caspr2 cohorts, respectively.

Follow Up Data

In summary, in all cases with an elevated biomarker of neurodegeneration in the CSF a decrease of biomarkers, ab titres, and mRS was observed following immunosuppressive treatment in all patients (see **Table 1** and **Figure 3**) regardless if the origin was postinfectious, paraneoplastic, or cryptogenic. There were two patients with all biomarkers simultaneously elevated. None of these parameters could predict a hippocampal sclerosis for sure on the one hand; on the other hand every patient who developed a sclerosis had either elevated t-tau or NfL levels with t-tau appearing to be more predictive.

DISCUSSION

We could show for the first time that biomarkers of neurodegeneration originating from CNS are mirroring the clinical and probably neuroimmunological course of patients suffering from AE associated with antibodies to extracellular epitopes. CSF-PGRN is elevated in patients with NMDAR-AE during the acute phase. Furthermore, biomarkers of neurodegeneration such as t-tau together with CSF-NfL in Patients with AE might be predictive of the clinical outcome especially for developing a hippocampal sclerosis. The pathologically elevated biomarkers correlated with the mRS, the clinical course and the antibody titre. Besides Progranulin in acute NMDAR-AE, NfL, PGRN and t-tau did not seem to be restricted to one special autoantibody mediated AE. This may be due to the fact that the neuronal and axonal damages in general are mirrored and not the distinct pathomechanisms of each putative pathological autoantibody.

Neurofilament Light Chain

NfL has been proven as an excellent marker of axonal loss (28). It seems very unlikely and there has been no data on whether peripheral tumors such as teratomas nor other neuroendocrine tumors can influence the CSF-NfL levels as possible confounders in our study. The co-occurrence of MRI changes, hippocampal sclerosis, and elevated NfL levels in our Magdeburg cohort is pointing at a pathomechanism causing the edema and subsequently the FLAIR signal resulting in the axonal dysfunction and subsequently increased NfL levels in the CSF. Other than in neurodegenerative diseases such as FTD (29, 30) the axonal loss in AE ceases after initiating sufficient immunosuppressive therapy as seen by the group of Pranzatelli in pediatric patients with opsoclonus-myoclonus syndrome caused by antibodies with intracellular epitopes (22, 23). Constantinescu et al. also measured CSF-NfL in four Patients with NMDAR-AE with AE and one Lgi-1 patient (19). Three NMDA-patients had a status epilepticus and highly pathological CSF-NFL levels, which has been seen in SE for nearly every marker of neuronal death (20, 21). In our cohort none had a status epilepticus confounding the biomarkers. This is possibly the reason why we found normal CSF-NfL levels in all measured Patients with NMDAR-AE except for the one with postinfectious origin. The meningoencephalitis with subsequent neuronal and axonal loss before the AE might be a reason for the elevated NfL levels in this patient since the infection was only 7 weeks apart from the AE. Our results are also much more in line with the known pathomechanism in NMDAR- AE (31, 32) where only marginal neuronal damage occurs and the main reason for the clinical symptoms is most likely the internalization of the NMDA-receptor. The one Lgi-1 patient (without SE) in the cohort of Constantiescu et al had normal NfL levels as our entire Lgi-1 group.

Total-Tau is a better marker for neuronal death as NfL (see below). However, FLAIR intense signals in the hippocampus as a consequence of disturbances of neuronal membrane function did correlate with NfL levels in our small cohort.

Total-Tau

Total-tau is an excellent marker for neuronal death (21, 33) 4/5 patients who developed a hippocampal sclerosis had pathological elevated t-tau levels in our Magdeburg cohort ($n = 13$). This is well in line with the current concept of the pathomechanisms leading to a sclerosis (34). Although, patient 1 (see **Table 2**) with the Caspr2 AE who was already treated months before admission to Magdeburg had only elevated CSF-NfL and normal t-tau levels and a hippocampal sclerosis (see **Table 2**). Sadly, it was not possible to measure NfL and t-tau levels in this patients initial CSF.

In sum, the measurement of t-tau may be a good marker before treatment decision in suspected autoimmune encephalitis or before deciding on the further immunosuppressive treatment but is limited to laboratories with expertise in measuring t-tau.

Progranulin

PGRN is playing a role in autoimmune mediated diseases such as rheuma or bowel disease or status epilepticus or in suppression of neuroinflammation (30, 35–37) Recently, EpiphrinA2 as a part of the Ephrin receptor kinase has been identified as functional receptor of PGRN and the potential of PGRN phosphorylating and activating the EpiphrinB2 receptor (38) linking it to the dysfunction in the EpiphrinB2 pathway known in AE mediated by autoantibodies against the NMDA-receptor (39, 40). The distribution in the fronto-temporal structures (41), the possible common link with the AE mediated by NMDAR via the EpiphrinA2-EpiphrinB2 pathway and the known role as a mediator in neuroinflammation and autoimmunity makes PGRN an interesting protein in AE.

We detected elevated CSF-PGRN levels in our NMDA-patients with a severe ongoing AE. On the other hand, CSF-PGRN was low in patients suffering from Lgi-1-AE sometimes reaching levels of FTD patients (29) in contrast to Patients with NMDAR-AE and controls. The significance of this low

CSF-PGRN is doubtful because none of the CSF-PGRN levels normalized after initiating the immunosuppressive therapy. Also most CSF-PGRN levels in the patients with Lgi-1-AE were still inside the normal range.

When looking at the t-cell or b-cell specific cytokine patterns in the patient's CSF suffering from NMDAR-AE several groups have seen a massive b-cell predominant cytokine pattern in the beginning especially in CXCL-13 levels (42, 43) and then a decrease in follow up. Also, cytokine pattern associated with t-cell activation were detectable throughout the course of AE without relevant changes. This course in cytokine levels could explain the elevated Progranulin levels in patients having acute NMDAR-AE.

PGRN in Serum and CSF was not elevated in patients with AE due to paraneoplastic origin although PGRN is also known as a tumor marker for certain tumors such as Lymphomas (44) The missing correlation between the serum-PGRN and CSF-PGRN is pointing at a cerebral origin of the CSF-PGRN as already seen in other diseases (26, 27). Overall, this result is probably due to an affection of the CSF-PGRN pathway in acute NMDAR-AE but needs more *in vivo* and *in vitro* experiments to be further examined.

One major limitation of the study is the small sample size in every subgroup tested. This fact is due to the very low numbers of patients with AE overall. Although total numbers are too small to draw a final conclusion the t-tau levels together with the CSF-NFL levels seem to best characterize the stage of neuronal death in the brain. The diagnostic value of NFL levels in the CSF should be evaluated in further studies. Another limitation is that we only had follow up data in 13 patients limiting our knowledge about MRI, mRS, and ab titres. Another limitation of the study is that due to the scarcity of the diseases measurements of the biomarkers could not be done in a batch but on demand.

A larger study should be conducted to further elucidate the correlation of these interesting parameters how they could contribute to therapeutic decisions.

CONCLUSION

NfL, t-tau and PGRN could be potential biomarkers of neuronal or axonal loss in patients suffering from AE. Especially, the Patients with NMDAR-AE have elevated PGRN levels at the acute phase of the AE. This fact further strengthens the hypothesis of a pathological change in the Epiphrin receptor metabolism in NMDAR patients. CSF-PGRN may be a marker for acute NMDA-AE.

Furthermore, we strongly recommend measuring NfL and t-tau in the CSF of every patient with AE although one biomarker for itself could not predict all hippocampal sclerosis in this pilot study. Pathological levels of a biomarker of neurodegeneration should be considered as an on-going AE and may be taken into account when planning further therapy.

ETHICS STATEMENT

This study was carried out in accordance with the recommendations of ethics committee of the University hospital Magdeburg (number 100/16). The protocol was approved by the ethics committee of the University hospital Magdeburg. All subjects gave written informed consent in accordance with the Declaration of Helsinki.

AUTHOR CONTRIBUTIONS

PK has access to all the data and takes responsibility for the data, accuracy of the data analysis, and the conduct of the research design or conceptualization of the study and analysis or interpretation of the data and drafting or revising the manuscript for intellectual content; HP and DB: Design and conceptualization of the study; analysis or interpretation of the data; drafting and revising the manuscript for intellectual content; LT: Conceptualization of the study; analysis of the data; drafting the manuscript for intellectual content; DV-W, JS-A, and SS: Conceptualization of the study; drafting the manuscript for intellectual content; WM, DR and FL: Conceptualization of the study; analysis and interpretation of the data; drafting and revising the manuscript for intellectual content; H-JH: Design of the study; drafting the manuscript for intellectual content.

ACKNOWLEDGMENTS

First, we have to thank our patients for the willingness to take part in this study. We have to thank Jeanette Witzke and Kerstin Kaiser at the neurochemical laboratory, Magdeburg for performing the excellent laboratory work. Furthermore, we have to thank Christian Bien at the Mara Epilepsy Center Bielefeld, Germany for laboratory work, samples and comments on the manuscript. We also appreciate the laboratory work of EUROIMMUN, Lübeck, Germany.

SUPPLEMENTARY MATERIAL

The Supplementary Material for this article can be found online at: https://www.frontiersin.org/articles/10.3389/fneur.2018.00668/full#supplementary-material

REFERENCES

1. Dalmau J, Gleichman AJ, Hughes EG, Rossi JE, Peng X, Lai MS, et al. Anti-NMDA-receptor encephalitis: case series and analysis of the effects of antibodies. *Lancet Neurol.* (2008) 7:1091–8. doi: 10.1016/S1474-4422(08)70224-2
2. Irani SR, Stagg CJ, Schott JM, Rosenthal CR, Schneider SA, Pettingill PR, et al. Faciobrachial dystonic seizures: the influence of immunotherapy on seizure control and prevention of cognitive impairment in a broadening phenotype. *Brain* (2013) 136:3151–62. doi: 10.1093/brain/awt212
3. Doss S, Wandinger KP, Hyman BT, Panzer JA, Synofzik M, Dickerson BB, et al. High prevalence of NMDA receptor IgA/IgM antibodies in different dementia types. *Ann Clin Transl Neurol.* (2014) 1:822–32. doi: 10.1002/acn3.120
4. Malter MP, Frisch C, Schoene-Bake JC, Helmstaedter C, Wandinger KP, Stoecker W, et al. Outcome of limbic encephalitis with VGKC-complex

antibodies: relation to antigenic specificity. *J Neurol.* (2014) 261:1695–705. doi: 10.1007/s00415-014-7408-6
5. van Sonderen A, Petit-Pedrol M, Dalmau J, Titulaer MJ. The value of LGI1, Caspr2 and voltage-gated potassium channel antibodies in encephalitis. *Nat Rev Neurol.* (2017) 13:290–301. doi: 10.1038/nrneurol.2017.43
6. Körtvelyessy P, Bauer J, Stoppel CM, Brück W, Gerth I, Vielhaber S, et al. Complement-associated neuronal loss in a patient with CASPR2 antibody-associated encephalitis. *Neurol Neuroimmunol Neuroinflamm.* (2015) 2:e75. doi: 10.1212/NXI.0000000000000075
7. Taguchi Y, Takashima S, Nukui T, Tanaka K. Reversible "brain atrophy" in anti-NMDA receptor encephalitis. *Intern Med.* (2011) 50:2697. doi: 10.1097/MD.0000000000006776
8. Bien CG, Vincent A, Barnett MH, Becker AJ, Blümcke I, Graus FK, et al. Immunopathology of autoantibody-associated encephalitides: clues for pathogenesis. *Brain* (2012) 135:1622–38. doi: 10.1093/brain/aws082
9. Martinez-Hernandez E, Horvath J, Shiloh-Malawsky Y, Sangha N, Martinez-Lage M, Dalmau J. Analysis of complement and plasma cells in the brain of patients with anti-NMDAR encephalitis. *Neurology* (2011) 77:589–93. doi: 10.1212/WNL.0b013e318228c136
10. Sabater L, Gaig C, Gelpi E, Bataller L, Lewerenz J, Torres-Vega E, et al. A novel non-rapid-eye movement and rapid-eye-movement parasomnia with sleep breathing disorder associated with antibodies to IgLON5: a case series, characterisation of the antigen, and post-mortem study. *Lancet Neurol.* (2014) 13:575–86. doi: 10.1016/S1474-4422(14)70051-1
11. Miller ZA, Rankin KP, Graff-Radford NR, Takada LT, Sturm VE, Cleveland CM, et al. TDP-43 frontotemporal lobar degeneration and autoimmune disease. *J Neurol Neurosurg Psychiatry* (2013) 84:956–62. doi: 10.1136/jnnp-2012-304644
12. Dahm L, Ott C, Steiner J, Stepniak B, Teegen B, Saschenbrecker SC, et al. Seroprevalence of autoantibodies against brain antigens in health and disease. *Ann Neurol.* (2014) 76:82–94. doi: 10.1002/ana.24189
13. Hara M, Martinez-Hernandez E, Ariño H, Armangué T, Spatola M, Petit-Pedrol M, et al. Clinical and pathogenic significance of IgG, IgA, and IgM antibodies against the NMDA receptor. *Neurology* (2018) 90:e1386–94. doi: 10.1212/WNL.0000000000005329
14. Schultze-Amberger J, Pehl D, Stenzel W. LGI-1-positive limbic encephalitis: a clinicopathological study. *J Neurol.* (2012) 259:2478–80. doi: 10.1007/s00415-012-6559-6
15. Wagner J, Witt JA, Helmstaedter C, Malter MP, Weber B, Elger CE. Automated volumetry of the mesiotemporal structures in antibody-associated limbic encephalitis. *J Neurol Neurosurg Psychiatry* (2014) 86:735–42. doi: 10.1136/jnnp-2014-307875
16. Wagner J, Weber B, Elger CE. Early and chronic gray matter volume changes in limbic encephalitis revealed by voxel-based morphometry. *Epilepsia* (2015) 56:754–61. doi: 10.1111/epi.12968
17. Finke C, Kopp UA, Prüss H, Dalmau J, Wandinger KP, Ploner CJ. Cognitive deficits following anti-NMDA receptor encephalitis. *J Neurol Neurosurg Psychiatry* (2012) 83:195–8. doi: 10.1136/jnnp-2011-300411
18. Leypoldt F, Gelderblom M, Schöttle D, Hoffmann S, Wandinger KP. Recovery from severe frontotemporal dysfunction at 3years after N-methyl-d-aspartic acid (NMDA) receptor antibody encephalitis. *J Clin Neurosci.* (2013) 20:611–3. doi: 10.1016/j.jocn.2012.03.036
19. Constantinescu R, Krýsl D, Bergquist F, Andrén K, Malmeström C, Asztély F, et al. Cerebrospinal fluid markers of neuronal and glial cell damage to monitor disease activity and predict long-term outcome in patients with autoimmune encephalitis. *Eur J Neurol.* (2016) 23:796–806. doi: 10.1111/ene.12942
20. Huchtemann T, Körtvélyessy P, Feistner H, Heinze HJ, Bittner D. Progranulin levels in status epilepticus as a marker of neuronal recovery and neuroprotection. *Epilepsy Behav.* (2015) 49:170–2. doi: 10.1016/j.yebeh.2015.06.022
21. Monti G, Tondelli M, Giovannini G, Bedin R, Nichelli PF, Trenti T, et al. Cerebrospinal fluid tau proteins in status epilepticus. *Epilepsy Behav.* (2015) 49:150–4. doi: 10.1016/j.yebeh.2015.04.030
22. Pranzatelli MR, Tate ED, McGee NR, Verhulst SJ. CSF neurofilament light chain is elevated in OMS (decreasing with immunotherapy) and other pediatric neuroinflammatory disorders. *J Neuroimmunol.* (2014) 266:75–81. doi: 10.1016/j.jneuroim.2013.11.004
23. Pranzatelli MR, McGee NR. Neuroimmunology of OMS and ANNA-1/anti-Hu paraneoplastic syndromes in a child with neuroblastoma. *Neurol Neuroimmunol Neuroinflamm.* (2018) 5:e433. doi: 10.1212/NXI.0000000000000433
24. Graus F, Titulaer MJ, Balu R, Benseler S, Bien CG, Cellucci T, et al. A clinical approach to diagnosis of autoimmune encephalitis. *Lancet Neurol.* (2016) 15:391–404. doi: 10.1016/S1474-4422(15)00401-9
25. Kuhle J, Plattner K, Bestwick JP, Lindberg RL, Ramagopalan SV, Norgren N, et al. A comparative study of CSF neurofilament light and heavy chain protein in MS. *Mult Scler.* (2013) 19:1597–603. doi: 10.1177/1352458513482374
26. Nicholson AM, Finch NA, Thomas CS, Wojtas A, Rutherford NJ, Mielke MM, et al. Progranulin protein levels are differently regulated in plasma and CSF. *Neurology* (2014) 82:1871–8. doi: 10.1212/WNL.0000000000000445
27. Wilke C, Gillardon F, Deuschle C, Dubois E, Hobert MA, Müller vom Hagen J, et al. Serum levels of progranulin do not reflect cerebrospinal fluid levels in neurodegenerative disease. *Curr Alzheimer Res.* (2016) 13:654–62. doi: 10.2174/1567205013666160314151247
28. Steinacker P, Feneberg E, Weishaupt J, Brettschneider J, Tumani H, Andersen PM, et al. Neurofilaments in the diagnosis of motoneuron diseases: a prospective study on 455 patients. *J Neurol Neurosurg Psychiatry* (2016) 87:12–20. doi: 10.1136/jnnp-2015-311387
29. Körtvélyessy P, Gukasjan A, Sweeny-Reed C, Heinze HJ, Thurner L, Bittner DM. Progranulin and Amyloid-β levels: relationship to neuropsychology in frontotemporal and Alzheimer's Disease. *J Alzheimers Dis* (2015) 46:375–80. doi: 10.3233/JAD-150069
30. Kortvelyessy P, Heinze HJ, Prudlo J, Bittner D. CSF biomarkers of neurodegeneration in progressive non-fluent aphasia and other forms of frontotemporal dementia: clues for pathomechanisms? *Front Neurol.* (2018) 9:504. doi: 10.3389/fneur.2018.00504
31. Planagumà J, Leypoldt F, Mannara F, Gutiérrez-Cuesta J, Martín-García E, Aguilar E, et al. Human N-methyl D-aspartate receptor antibodies alter memory and behaviour in mice. *Brain* (2015) 138:94–109. doi: 10.1093/brain/awu310
32. Kreye J, Wenke NK, Chayka M, Leubner J, Murugan R, Maier NB, et al. Human cerebrospinal fluid monoclonal N-methyl-D-aspartate receptor autoantibodies are sufficient for encephalitis pathogenesis. *Brain* (2016) 139:2641–52. doi: 10.1093/brain/aww208
33. Spillantini MG, Goedert M. Tau pathology and neurodegeneration. *Lancet Neurol.* (2013) 12:609–22. doi: 10.1016/S1474-4422(13)70090-5
34. Thom M, Eriksson S, Martinian L, Caboclo LO, McEvoy AW, Duncan JS, et al. Temporal lobe sclerosis associated with hippocampal sclerosis in temporal lobe epilepsy: neuropathological features. *J Neuropathol Exp Neurol.* (2009) 68:928–38. doi: 10.1097/NEN.0b013e3181b05d67
35. Cenik B, Sephton CF, Kutluk Cenik B, Herz J, Yu G. Progranulin: a proteolytically processed protein at the crossroads of inflammation and neurodegeneration. *J Biol Chem.* (2012) 287:32298–306. doi: 10.1074/jbc.R112.399170
36. De Muynck L, Van Damme P. Cellular effects of progranulin in health and disease. *J Mol Neurosci.* (2011) 45:549–60. doi: 10.1007/s12031-011-9553-z
37. Jian J, Li G, Hettinghouse A, Liu C. Progranulin: A key player in autoimmune diseases. *Cytokine* (2016) 101:48–55. doi: 10.1016/j.cyto.2016.08.007
38. Neill T, Buraschi S, Goyal A, Sharpe C, Natkanski E, Schaefer L, et al. EphA2 is a functional receptor for the growth factor progranulin. *J Cell Biol.* (2016) 215:687–703. doi: 10.1083/jcb.201603079
39. Mikasova L, De Rossi P, Bouchet D, Georges F, Rogemond V, Didelot A, et al. Disrupted surface cross-talk between NMDA and Ephrin-B2 receptors in anti-NMDA encephalitis. *Brain* (2012) 135:1606–21. doi: 10.1093/brain/aws092

40. Planagumà J, Haselmann H, Mannara F, Petit-Pedrol M, Grünewald B, Aguilar E, et al. Ephrin-B2 prevents N-methyl-D-aspartate receptor antibody effects on memory and neuroplasticity. *Ann Neurol.* (2016) 80:388–400. doi: 10.1002/ana.24721
41. Daniel R, He Z, Carmichael KP, Halper J, and Bateman A. Cellular localization of gene expression for progranulin. *J Histochem Cytochem.* (2000) 48:999–1009. doi: 10.1177/00221554000 4800713
42. Liba Z, Kayserova J, Elisak M, Marusic P, Nohejlova H, Hanzalova J, et al. Anti-N-methyl-D-aspartate receptor encephalitis: the clinical course in light of the chemokine and cytokine levels in cerebrospinal fluid. *J Neuroinflammation* (2016) 13:55. doi: 10.1186/s12974-016-0507-9
43. Leypoldt F, Höftberger R, Titulaer MJ, Armangue T, Gresa-Arribas N, Jahn H, et al. Investigations on CXCL13 in Anti-N-Methyl-D-aspartate receptor encephalitis: a potential biomarker of treatment response. *JAMA Neurol* (2014) 72:180–6. doi: 10.1001/jamaneurol.201 4.2956
44. Arechavaleta-Velasco F, Perez-Juarez CE, Gerton GL, Diaz-Cueto L. Progranulin and its biological effects in cancer. *Med Oncol.* (2017) 34:194. doi: 10.1007/s12032-017-1054-7

Conflict of Interest Statement: PK has received consulting fees from Eisai (Germany). JS-A obtained honoraria for speaking engagements from Boehringer Ingelheim (Germany) and Bristol-Myers Squibb (Germany). LT: Saarland University, LT and others filed 61/730,772 which covers means and methods for detecting autoimmune disorders in which progranulin antibodies may be involved. FL runs an antibody detection laboratory in Kiel, Germany where part of the work has been performed.

The remaining authors declare that the research was conducted in the absence of any commercial or financial relationships that could be construed as a potential conflict of interest.

Copyright © 2018 Körtvelyessy, Prüss, Thurner, Maetzler, Vittore-Welliong, Schultze-Amberger, Heinze, Reinhold, Leypoldt, Schreiber and Bittner. This is an open-access article distributed under the terms of the Creative Commons Attribution License (CC BY). The use, distribution or reproduction in other forums is permitted, provided the original author(s) and the copyright owner(s) are credited and that the original publication in this journal is cited, in accordance with accepted academic practice. No use, distribution or reproduction is permitted which does not comply with these terms.

frontiers in Neurology

ORIGINAL RESEARCH
published: 11 October 2018
doi: 10.3389/fneur.2018.00846

Induction of Osmolyte Pathways in Skeletal Muscle Inflammation: Novel Biomarkers for Myositis

Boel De Paepe[1], Jana Zschüntzsch[2], Tea Šokčević[1], Joachim Weis[3], Jens Schmidt[2†] and Jan L. De Bleecker[1†]*

[1] Department of Neurology and Neuromuscular Reference Center, Ghent University Hospital, Ghent, Belgium, [2] Department of Neurology, University Medical Center Göttingen, Göttingen, Germany, [3] Institute for Neuropathology, Reinisch-Westfälische Technische Hochschule Aachen University Hospital, Aachen, Germany

We recently identified osmolyte accumulators as novel biomarkers for chronic skeletal muscle inflammation and weakness, but their precise involvement in inflammatory myopathies remains elusive. In the current study, we demonstrate *in vitro* that, in myoblasts and myotubes exposed to pro-inflammatory cytokines or increased salt concentration, mRNA levels of the osmolyte carriers SLC5A3, SLC6A6, SLC6A12, and AKR1B1 enzyme can be upregulated. Induction of SLC6A12 and AKR1B1 was confirmed at the protein level using immunofluorescence and Western blotting. Gene silencing by specific siRNAs revealed that these factors were vital for muscle cells under hyperosmotic conditions. Pro-inflammatory cytokines activated mitogen-activated protein kinases, nuclear factor κB as well as nuclear factor of activated T-cells 5 mRNA expression. In muscle biopsies from patients with polymyositis or sporadic inclusion body myositis, osmolyte pathway activation was observed in regenerating muscle fibers. In addition, the osmolyte carriers SLC5A3 and SLC6A12 localized to subsets of immune cells, most notably to the endomysial macrophages and T-cells. Collectively, this study unveiled that muscle cells respond to osmotic and inflammatory stress by osmolyte pathway activation, likely orchestrating general protection of the tissue. Moreover, pro-inflammatory properties are attributed to SLC5A3 and SLC6A12 in auto-aggressive macrophages and T-cells in inflamed skeletal muscle.

Keywords: inflammatory myopathy, osmotic stress, inflammatory stress, osmolytes, muscle regeneration

OPEN ACCESS

Edited by:
Tobias Ruck,
Universität Münster, Germany

Reviewed by:
Tim Hagenacker,
Universitätsklinikum Essen, Germany
Corinna Preuße,
Charité Universitätsmedizin Berlin, Germany

****Correspondence:***
Boel De Paepe
boel.depaepe@ugent.be

† These authors have contributed equally to this work

Specialty section:
This article was submitted to Multiple Sclerosis and Neuroimmunology, a section of the journal Frontiers in Neurology

Received: *20 August 2018*
Accepted: *20 September 2018*
Published: *11 October 2018*

Citation:
De Paepe B, Zschüntzsch J, Šokčević T, Weis J, Schmidt J and De Bleecker JL (2018) Induction of Osmolyte Pathways in Skeletal Muscle Inflammation: Novel Biomarkers for Myositis. Front. Neurol. 9:846. doi: 10.3389/fneur.2018.00846

INTRODUCTION

The idiopathic inflammatory myopathies represent a diverse group of autoimmune muscle diseases. The main disease entities recognized today are dermatomyositis (DM), polymyositis (PM), sporadic inclusion body myositis (IBM), immune-mediated necrotizing myopathy (IMNM), anti-synthetase syndrome, and unspecific myositis, each of which possess distinct clinical and myopathological characteristics (1–5). DM patients develop complement-mediated blood vessel destruction, perimysial inflammation and perifascicular muscle fiber atrophy (6). PM and IBM are characterized by invasion of nonnecrotic muscle fibers by auto-aggressive cytotoxic T-cells and macrophages, with inflammation building up mostly at endomysial sites (7). In IBM muscle fibers, additional degenerative phenomena occur, with rimmed vacuoles and inclusions that contain aggregates of ectopic proteins (8), a process that is presumed to follow inflammation (9). IMNM

represents 3 subdivisions according to serologic characteristics: anti-3-hydroxy-3-methylglutaryl-coenzyme A reductase myopathy, signal recognition particle myopathy, and myositis-specific autoantibody negative IMNM (10). Many of the immunopathogenic mechanisms underlying the inflammatory myopathies remain poorly understood, hampering the development of successful therapies that suit the different patient subtypes.

Muscle is a highly adaptive and dynamic tissue capable of increasing its mass in response to exercise and of restoring damage caused by injury via processes that require hypertrophy and regeneration, respectively. In addition, cells possess a universal ability to adapt to changing osmotic conditions, a feature essential for their survival, allowing active anticipation toward perturbations in volume and disrupted cellular homeostasis. A complex intracellular mixture of interacting osmolytes regulates osmotic pressure, which takes shape through the synthesis and/or import of osmo-active compounds in cells (11). The solute carrier family (SLC) contains several salt-dependent membrane transport proteins involved in the selective import of extracellular constituents: (i) the sodium-myoinositol cotransporter SLC5A3, (ii) the high-affinity taurine transporter SLC6A6, and (iii) the betaine and γ-amino-n-butyric acid (GABA) transporter SLC6A12. AKR1B1 is an aldose reductase that catalyzes the intracellular conversion of glucose to sorbitol. In a joint effort, these osmoprotective constituents represent a universal tool for mammalian cells, and their accumulators can be ubiquitously expressed throughout human tissues. The central regulator of osmolyte pathway gene expression is the transcription factor nuclear factor of activated T-cells 5 (NFAT5), also termed tonicity enhancer-binding protein (12).

Several observations allowed us to speculate NFAT5-inducible pathways might be involved in the inflammatory myopathies. Firstly, the NFAT5 pathway participates in muscle development and regeneration, by regulating the differentiation of immature myoblasts to mature multinucleated myotubes (13). NFAT5 levels have been shown to increase in the regenerating fibers of mice exposed to experimental muscle tissue injury (14), attributing the transcription factor a role in countering disease-inflicted muscle tissue damage. Secondly, the NFAT5 pathway has been firmly linked to nuclear factor κB (NFκB) activity (15), the latter a key regulator of inflammatory diseases in general and the inflammatory myopathies in particular (16). NFAT5 and NFκB share multiple molecular targets (17), many of which are involved in the immunopathogeneses of inflammatory myopathy including CCL2, also termed monocyte chemo-attractant protein-1 (MCP-1) (18), lymphotoxin β (LTβ) (19), tumor necrosis factor α (TNFα) (20), inducible nitric oxide synthase (iNOS) (21), and heat shock protein family of 70kd (HSP70) (22). Thirdly, NFAT5-downstream osmolyte pathways are potent activators of cytotoxic activities of immune cells and could therefore be implicated in human autoimmune disease. In addition, dietary salt is determinant to T-cell differentiation, by direct activation of glycogen synthase kinase 1 (GSK-1) and subsequent Interleukin 23 receptor stabilization, which enforces the type 17 helper T-cell (Th17), a T-cell phenotype associated with autoimmune disease (23).

We recently were the first to describe upregulation of the osmolyte accumulators SLC5A3, SLC6A6 and AKR1B1 in muscle tissues from myositis patients (24), and described NFAT5 expression in myoblasts in culture (25), yet the precise role osmolyte pathways play in disease mechanisms remained unexplored. With this study, we aim to substantiate and functionally connect these biomarkers with muscle inflammation. We set up *in vitro* muscle cell models to investigate osmolyte pathway member expression, using both the human rhabdomyosarcoma CCL-136 cell line and normal primary human myotubes. In addition, we investigated their possible signaling routes, which involves the upstream transcription factors NFκB and NFAT5, and the mitogen-activated protein kinases (MAPKs). We confronted this *in vitro* evidence with findings in muscle biopsies from patients diagnosed with inflammatory myopathies.

METHODS

Cell Cultures

Human rhabdomyosarcoma CCL-136 cells (ATCC, Manassas, VA) were kept in Dulbecco's modified Eagle medium (DMEM) supplemented with 10% fetal calf serum (Biochrom, Berlin, Germany) and 1% L-glutamine (ThermoFisher Scientific, Waltham, MA). Human muscle cell cultures originated from muscle biopsies taken from healthy patients needing knee surgery, obtained with patient consent and approved by the local ethics committee. Biopsies were minced and trypsinized. Fragments were seeded in DMEM with pyruvate, high glucose and L-glutamine, supplemented with penicillin, streptomycin and 10% fetal calf serum (ThermoFisher Scientific). Cells were cultured for 2 periods of ∼ 3 weeks during which CD56+ cells were purified twice with magnetic separation MiniMACS columns using the supplier's standard protocol (Miltenyi Biotec, Bergisch Gladbach, Germany). Myotubes were obtained by allowing cells to differentiate for approximately 5 days in DMEM medium supplemented with penicillin, streptomycin and 2% horse serum (ThermoFisher Scientific). **Supplementary Figure S1** illustrates a representative culture of differentiated myotubes, showing aligned multinucleate muscle cells. All cells were kept in culture wells or chamber slides at 37°C in a humified atmosphere containing 5% CO_2. Conditions for cytokine stimulation were as determined earlier (26), being 30 ng/ml TNFα, 300 u/ml Interferon γ (IFNγ), 20 ng/ml Interleukin 1β (IL1β) (R and D Systems, Minneapolis, MN), or

Abbreviations: AKR1B1, aldose reductase; DM, dermatomyositis; dMyHC, developmental myosin heavy chain; ERK, extracellular signal-regulated kinase; GAPDH, glyceraldehyde-3-phosphate dehydrogenase; GSK-3α/β, glycogen synthase kinase 3α/β; HSP70, heat shock protein family of 70kd; IBM, sporadic inclusion body myositis; IFNγ, Interferon γ; IL1β, Interleukin 1β; IMNM, immune-mediated necrotizing myopathy; iNOS, inducible nitric oxide synthase; LTβ, lymphotoxin β; MAPK, mitogen-activated protein kinase; MCP-1, monocyte chemo-attractant protein-1; MSK2, mitogen- and stress-activated kinase 2; NFAT5, nuclear factor of activated T-cells 5; NFκB, nuclear factor κB; PM, polymyositis; siRNA, silencing RNA; SLC5A3, solute carrier sodium-myoinositol cotransporter; SLC6A6, solute carrier taurine transporter; SLC6A12, solute carrier betaine and γ-amino-n-butyric acid (GABA) transporter; Th17, Interleukin 17-producing T-cells; TNFα, tumor necrosis factor α.

double combinations. Hyperosmotic conditions were created by supplementing the culture medium with 25–150 mM of added NaCl. Higher concentrations of NaCl lead to complete cell death within 24 h.

Quantitative Reverse Transcription PCR

RNA was prepared from cells cultured in 12-well culture plates, using the RNeasy Mini kit and according to the manufacturer's specifications (Qiagen, Hilden, Germany). RNA concentration was measured with a Nanodrop 1000 (ThermoFisher Scientific). cDNA was prepared from 200 ng of RNA with SuperScript II reverse transcriptase, 500 ng/μl oligo dTs, 0.1 M DTT, and 10 mM dNTPs each (Invitrogen, Darmstadt, Germany). cDNA was quantified through PCR reaction with Taqman Gene Expression Master mix (Applied Biosystems, Foster City, CA), using 6-carboxy-fluorescein-labeled probes and specific primers for: SLC5A3, Hs00272857_s1; SLC6A6, Hs00161778_m1; SLC6A12, HS00758246_m1; AKR1B1, Hs00739326_m1; NFAT5, Hs00232437_m1; MAPK14, Hs01051152_m1; RELA, Hs00153294_m1; NFKB1, Hs00765730_m1; NFKB2, Hs01028901_g1; glyceraldehyde-3-phosphate dehydrogenase (GAPDH), Hs99999905_m1 (Applied Biosystems). Reactions were run in triplicate, following the standard cycle protocol on a 7500 Real Time PCR System, and analyzed with software version 2.0.6. (Applied Biosystems). Data was presented as ΔΔCt fold-changes compared to the expression levels in untreated cells, with GAPDH as an internal housekeeping gene standard.

Immunofluorescent Cytostaining

Cells cultured on glass chamber slides were fixed with ice-cold acetone and blocked in phosphate buffered saline with 10% bovine serum albumin and 10% goat serum for 1 h at room temperature. Immunofluorescent detection was carried out for 1 h at room temperature with commercially available antibodies: mouse (4 μg/ml, sc-514024, SantaCruz Biotechnology, Santa Cruz, CA) and rabbit (10 μg/ml, nbp188641, Novus Biologicals, Abingdon, UK) anti-SLC6A12; rabbit (2 μg/ml, sc-33219, SantaCruz Biotechnology) and goat (1 μg/ml, sc-17732, SantaCruz Biotechnology) anti-AKR1B1; mouse anti-developmental myosin heavy chain (dMyHC) (40 μg/ml, RMMy2/9D2, Leica Biosystems, Nussloch, Germany). The corresponding Alexa594—and Alexa488-labeled secondary antibodies (ThermoFisher Scientific) were added. After mounting in Fluoromount G (Southern Biotech, Alabama, USA), digital photography was performed on a Zeiss Axiophot microscope (Zeiss, Goettingen, Germany). Pictures were taken by a cooled CCD digital camera (Retiga 1300, Qimaging, Burnaby, BC, Canada) and visualized with ImageProPlus software (MediaCybernetics, Bethesda, MD).

Immunofluorescent Histostaining

For localization studies in muscle tissues, 8 μm cryostat sections were cut from frozen muscle biopsies obtained from patients without muscle abnormalities ($n = 10$), inflammatory myopathies ($n = 28$), and disease controls diagnosed with muscular dystrophy ($n = 8$; for pathological information consult **Supplementary Table S1**). Diagnosis of the disease subgroups PM ($n = 4$), IBM ($n = 9$), DM ($n = 9$), and IMNM ($n = 6$) were based upon clinical and myopathological criteria (27). Diagnosis of PM was reserved to patients with nonnecrotic invaded muscle fibers present in the biopsy that had subsequently responded to immunosuppressive therapy. Sections were fixed in ice-cold acetone and treated with blocking solution containing 5% donkey serum, 10% heat-inactivated human serum and 2% bovine serum albumine in phosphate buffered saline. Incubations with primary antibodies were carried out in the same solution: 4 μg/ml rabbit polyclonal anti-SLC5A3 (NBP1-02399, Novusbio); 4 μg/ml mouse monoclonal anti-SLC6A6 (E10, SantaCruz Biotechnology); 6 μg/ml rabbit polyclonal anti-SLC6A12 (HPA034973; Merck, Kenilworth, NJ); 1 μg/ml goat polyclonal anti-AKR1B1 (N20, SantaCruz Biotechnology). Immune cell subtypes and muscle tissue constituents were visualized through double staining as described (18). Satellite cells were visualized with goat anti-Pax3/7 (1 μg/ml, sc-7748, SantaCruz Biotechnology). To allow double staining of macrophages with mouse monoclonal antibodies, FITC labeled anti-CD68 (Agilent, Santa Clara, CA) was applied. Secondary antibodies were used labeled with CY3 (Jackson ImmunoResearch Laboratories, West Grove, PA) and AlexaFluor488 (ThermoFisher Scientific). Slides were mounted with Fluoromount (Southern Biotech) and visualized with a fluorescence microscope (Zeiss). Conventional semi-quantitative scoring of staining intensity was performed by three non-blinded independent observers. Negative control studies consisted of the omission of primary antibody and the substitution by non-immune IgGs. Positive control tissues for checking immunodetection were cultured Hela cells (SLC6A6), frozen sections containing kidney medulla (SLC5A3, SLC6A12), and Jurkat cells (AKR1B1).

Western Blotting

Cells cultured in 12-well culture plates were lysed in Ripa buffer (50 mM Tris-HCl, 150 mM NaCl, 2.5% Na-deoxycholate, 2.5% NP40, 0.1% sodium dodecyl sulfate pH 7.4) with a protease inhibitor cocktail added (Roche, Indianapolis, IN) and centrifuged for 5 min at 13000 rpm. The supernatant was collected and protein concentrations were determined following a Bradford procedure (Bio-Rad protein assay, Hercules, CA) with bovine serum albumine standard solutions, measured in triplicates on the Infinite M200Pro and analyzed with Magellan 7.2 software (Tecan, Mannedorf, Switzerland). 60 μg protein samples were dissolved in Laemli buffer, boiled for 2 min, separated by 12% sodium dodecyl sulfate-polyacrylamide gelelectrophoresis, and transferred to a nitrocellulose membrane (Schleicher and Schuell, Dassel, Germany). Membranes were blocked with 5% bovine serum albumine for 1 h at 4°C and incubated overnight at 4°C with 2 μg/ml mouse anti-SLC6A12 (sc-514024, SantaCruz Biotechnology), 4 h at room temperature with 2 μg/ml goat anti-AKR1B1 (sc-17732, SantaCruz Biotechnology), and 1 h at room temperature with 0.7 μg/ml mouse anti-GAPDH (Sp210-Ag14; Abcam, Cambridge, UK). All incubations were done in tris-buffered saline buffer containing 0.05% Tween20.

Appropriate horseradish peroxidase-conjugated secondary antibodies (Jackson ImmunoResearch, West Grove, PA) were added for 1 h at room temperature. The chemiluminescent signal was generated with the Pierce Western blotting substrate (ThermoFisher Scientific), visualized with the Fusion FX, and quantified with Vision Capt software, with background noise filtering using a rolling-ball algorithm (Vilber Lourmat, Eberhardzell, Germany).

Protein Phosphorylation Profiling

Protein phosphorylation patterns were determined in extracts obtained from cultured myotubes, using the Proteome Profiler human phosphor-mitogen activated protein kinase (MAPK) antibody array according to the manufacturer's specifications (Bio-Techne, Abingdon, United Kingdom). Briefly, array membranes were incubated overnight at 4°C with lysate containing 200 μg of cellular protein, detection conditions were as described in the western blotting section. Protein densities were quantified, relative to phosphorylated Akt2, as the calculated mean of duplicate spots per protein, using Image Studio 5.2 software (Li-Cor Biosciences, Cambridge, UK).

Knockdown Studies

Pools of three target-specific 19–25 nucleotide silencing RNAs (siRNAs), purchased from SantaCruz Biotechnology, were used: siRNA SLS5A3 (sc-44516), siRNA SLC6A12 (sc-95904), and siRNA AKR1B1 (sc-37119). 50% confluent CCL-136 cells and myotube cultures were changed to 500 μl X-Vivo15 medium (Sartorius, Goettingen, Germany), to which 3 μl of lipofectamine (ThermoFisher) and 100 nM siRNA had been added. After 5 h, an extra 200 μl of X-Vivo15 was added, which in treated cells contained cytokines to a final well concentration of 20 ng/ml IL1β+300 u/ml IFNγ, or 50 mM added NaCl. Cells were assayed 26 h after addition of the siRNAs. Live and dead cells were visualized using the ReadyProbes cell viability imaging blue/green kit (ThermoFisher) according to the manufacturer's specifications. Using a fluorescence microscope, a minimum of 50 cells (blue) was counted per condition, determining the amount of dead cells (green). Afterwards, cell cultures were stained with hematoxylin and eosin according to standard procedures, dehydrated, mounted, and interpreted under a light microscope. Efficiency of knockdown was evaluated at the mRNA level using quantitative reverse transcription PCR, following the method described above. From controls and siRNA-treated CCL-136 cells seeded in 12-well culture plates, protein samples were prepared for electrophoresis by adding lithium dodecyl sulfate sample buffer and reducing agent (Invitrogen, Carlsbad, CA, USA) and boiling for 3 min. Samples were loaded onto 10% bis-tris gels, with prestained markers alongside to determine the molecular weight of protein bands. Proteins were transferred to nitrocellulose membranes by electroblotting, and incubated with 2 μg/ml mouse anti-SLC6A12 (sc-514024), 2 μg/ml goat anti-AKR1B1 (sc-17732), or mouse anti-β actin (sc-47778) (SantaCruz Biotechnology) for 4 h at room temperature on a rocking platform. Immunoreaction was visualized using the chromogenic Western Breeze kit according to the manufacturer's specifications (Invitrogen).

Compliance With Ethical Standards

Human experimentation presented in the study was approved by the Ghent University Hospital Ethics Committee (EC-UZG-#B670201316956) and adhered to privacy regulations (CBPL-BEL-#HM003039095). Written informed consent was obtained from all individual participants included in the study, and all procedrues were in accordance with the Declaration of Helsinki.

RESULTS

mRNA Quantification in Cultured Muscle Cells

In CCL-136 cells, *e*xpression levels of osmolyte pathway members were determined in cells treated with pro-inflammatory cytokines or added NaCl for 24 h (**Table 1**). In general, a moderate increase of expression was shown for SLC5A3, SLC6A6, SLC6A12, and AKR1B1 when cells were treated with cytokines. The strongest response was a 10-fold increase of SLC5A3 mRNA expression in IL1β+TNFα-treated cells. Hyperosmotic conditions also induced osmolyte pathway expression, with 100 mM of added NaCl leading to a 179-fold increase of SLC6A12, and increasing NFAT5 expression 2.5-fold. MAPK14 levels were 2-fold increased in both IFNγ+TNFα– and 50 mM NaCl-treated cells. Highest levels of RelA, NFkB1 and NFkB2 could be achieved with pro-inflammatory cytokine mixtures, though NFkB1 and NFkB2 expression also responded to added NaCl.

Primary human myotubes treated for 24 h with cytokines or added NaCl showed induction of osmolyte pathway mRNA levels (**Table 2**). For SLC5A3 and AKR1B1, the strongest induction could be achieved with added NaCl; SLC6A6 and SLC6A12 were most strongly induced by pro-inflammatory cytokine mixtures. NFAT5 expression was influenced by both cytokines and increased salt concentrations, but reached higher expression levels with IFNγ+IL1β (4,5-fold) than with 125 mM NaCl (3-fold). MAPK14 expression levels were found increased 2-fold in myotubes treated with IL1β and with 125 mM NaCl. The expression of NFκB subunits was most strongly induced by treatment with pro-inflammatory cytokines. Nonetheless, 25 mM added NaCl increased NFkB1 expression 8,5-fold. In myotubes treated for longer periods, added NaCl lead to continuously increasing SLC5A3, SLC6A12 and AKR1B1 expression levels over time, culminating in levels all exceeding 200-fold at time point 72 h (**Table 3**). In addition, prolonged salt treatment lead to a time-dependent increase of NFAT5 and MAPK14 expression levels, reaching a maximum of 9-fold (NFAT5) and 18-fold (MAPK14). In contrast, the single pulse of pro-inflammatory cytokines resulted in highest expression levels after 24 h, with levels nearing normal after 72 h.

Immunofluorescent Protein Localization Studies in Cultured Muscle Cells

Immunofluorescent staining of CCL-136 cells (**Figure 1A**) confirmed the induction of SLC6A12 and AKR1B1 expression after 24 h of treatment with pro-inflammatory cytokines and

TABLE 1 | Messenger RNA levels in cultured CCL-136 cells treated for 24 h.

	Cytokines						Added NaCl			
	IFNγ	IL1β	TNFα	IFNγ+IL1β	IFNγ+TNFα	IL1β+TNFα	25 mM	50 mM	75 mM	100 mM
SLC5A3	1	1.1	1.3	2.1	4.6	10.3	0.6	0.5	1.9	3.4
SLC6A6	0.5	0.7	0.8	1.4	1.5	4.3	0.9	1.1	1.2	1.5
SLC6A12	1.7	2	1	3.4	3.8	1.2	1.6	7.7	9	178.7
AKR1B1	1.4	2.3	1.9	1.9	1.6	1.7	1.4	2.1	2.4	5.6
NFAT5	1.1	0.3	0.5	1.4	1.7	1	1.4	4.1	0.8	2.5
MAPK14	0.7	0.8	0.8	1.4	1.9	1.4	1.1	2	0.9	1.3
RELA	0.9	1.2	0.9	1.8	1.7	0.5	0.9	0.8	0.9	1.2
NFkB1	1	1.2	1	6	0.5	3.8	1.5	2.9	1.2	1.9
NFkB2	1.3	1.5	2.7	3.3	12.9	1	1.2	2.3	1.5	1.1

Fold changes compared to untreated cells, normalized to glyceraldehyde 3-phosphate dehydrogenase expression levels, were obtained through quantitative reverse transcription PCR and calculated as $2^{-\Delta\Delta Ct}$ (mean of three given). Fold changes >2 green; >5 yellow; >10 orange; >100 red.

TABLE 2 | Messenger RNA levels in cultured normal human myotubes treated for 24 h.

	Cytokines						Added NaCl					
	IFNγ	IL1β	TNFα	IFNγ+IL1β	IFNγ+TNFα	IL1β+TNFα	25 mM	50 mM	75 mM	100 mM	125 mM	150 mM
SLC5A3	2.6	5.8	2.5	2.4	1.4	1.9	1.4	2.1	3.6	13	13.9	5
SLC6A6	1.2	1.9	2.9	3.9	2.2	3.1	1.1	1.9	1.8	1.9	1.8	0.4
SLC6A12	21.3	2.1	1.4	177.7	229.2	3.8	2.1	5.9	7.3	32.4	47.9	9.6
AKR1B1	1.5	6.6	3.7	7.5	5.6	4.9	10.7	3.5	4.7	6.9	8.1	2.5
NFAT5	1.4	4.4	1.6	4.5	2.2	2	0.8	1.6	1.3	2.2	3	0.6
MAPK14	1	1.9	1.1	0.6	0.4	0.9	1.4	1.3	1	1.6	1.9	0.6
RELA	2.1	2	1.4	25.3	18.4	4.2	0.8	1.1	1.2	1.1	1.2	0.5
NFkB1	1.5	1.3	0.8	6.8	3.6	2.6	8.7	0.7	0.7	0.6	1.3	0.7
NFkB2	1.2	4.7	2.7	20.5	4	8.4	0.1	1.3	1.2	0.8	1	0.3

Fold changes compared to untreated cells, normalized to glyceraldehyde 3-phosphate dehydrogenase expression levels, were obtained through quantitative reverse transcription PCR and calculated as $2^{-\Delta\Delta Ct}$ (mean of three given). Fold changes >2 green; >5 yellow; >10 orange; >100 red.

added NaCl at the protein level and showed similar staining patterns with the two different sets of primary antibodies.

Myotubes immunostaining (**Figure 1B**) showed increases of SLC6A12 in response to cytokines at the 48 h time point, with levels declining again at time point 72 h. For AKR1B1, high levels were detected following cytokine stimulation from 24 h onward, compared to the low levels observed in untreated myotubes. A growth-inhibitory effect of hyperosmotic conditions was observed in myotubes, which became conspicuous from the 48 h time point on. NaCl-treatment disfavored differentiation into multinucleate elongated muscle cells, as was assayed with dMyHC staining (**Supplementary Figure S1**). Evaluation of hematoxylin&eosin stains confirmed that salt treatment affected cell morphology and growth, reducing cell elongation and disfavoring multinucleate myotubes.

Protein Quantification and Phosphorylation Patterns of Human Myotubes

SLC6A12 protein levels were below the detection limit in untreated normal myotubes, but SLC6A12 protein could readily be shown in myotubes treated with IL1β+TNFα for 48 h and 72 h (**Figure 2A**). SLC6A12 and AKR1B1 protein levels were found to increase in a time- and dose-dependent manner when myotubes were exposed to 25 and 50 mM of added NaCl (**Figure 2B**). The expression levels with the higher doses of NaCl already reached a maximum at the 48 h time-point (**Table 4**).

Protein phosphorylation patterns of MAPKs showed that the strongest signals in the array were the phosphorylated forms of Akt2 (S474) and heat shock protein 27 (HSP27) (S78, S82) (**Supplementary Figure S2**). Akt2 and HSP27 activation was prominent in untreated and cytokine-treated myotubes alike. The most notable influence of 24 h IFNγ+IL1β treatment was an increase in phosphorylation of mitogen- and stress-activated kinase 2 (MSK2) (S360) 3-fold and MAPK3 (T202, Y204) 2.5-fold. In addition, levels of phosphorylated glycogen synthase kinase 3α/β (GSK-3α/β) (S9, S21), MAPK12 (T183, Y185), and MAPK13 (T180, Y182) were increased 2-fold.

Knockdown Studies in Cultured Muscle Cells

Both in CCL-136 cells and in primary healthy myotubes, 50 mM of added NaCl decreased cell densities in both siSCL6A12— and siAKR1B1-treated cells at the 24 h time point, while this regimen did not harm growth of siSLC5A3-treated muscle

TABLE 3 | Messenger RNA levels in cultured normal human myotubes treated with cytokines or added NaCl for up to 3 days.

	IFNγ+IL1β			IFNγ+TNFα			100 mM NaCl		
	24 h	48 h	72 h	24 h	48 h	72 h	24 h	48 h	72 h
SLC5A3	1	0.4	0.2	1	0.6	0.5	10.8	5.8	240.7
SLC6A12	19.1	4.9	1	14.5	13	2.5	43	50.9	2 × 10exp8
AKR1B1	2.4	1.3	0.9	1.7	1.9	1.1	7	27.4	528.8
NFAT5	0.8	0.3	0.04	0.8	0.9	0.3	1.4	3.8	9.4
MAPK14	0.9	0.4	0.3	0.6	0.6	0.6	1.1	1.6	17.8

Fold changes compared to untreated cells, normalized to glyceraldehyde 3-phosphate dehydrogenase expression levels, were obtained through quantitative reverse transcription PCR and calculated as $2^{-\Delta\Delta Ct}$ (mean of three given). Fold changes >2 green; >5 yellow; >10 orange; >100 red.

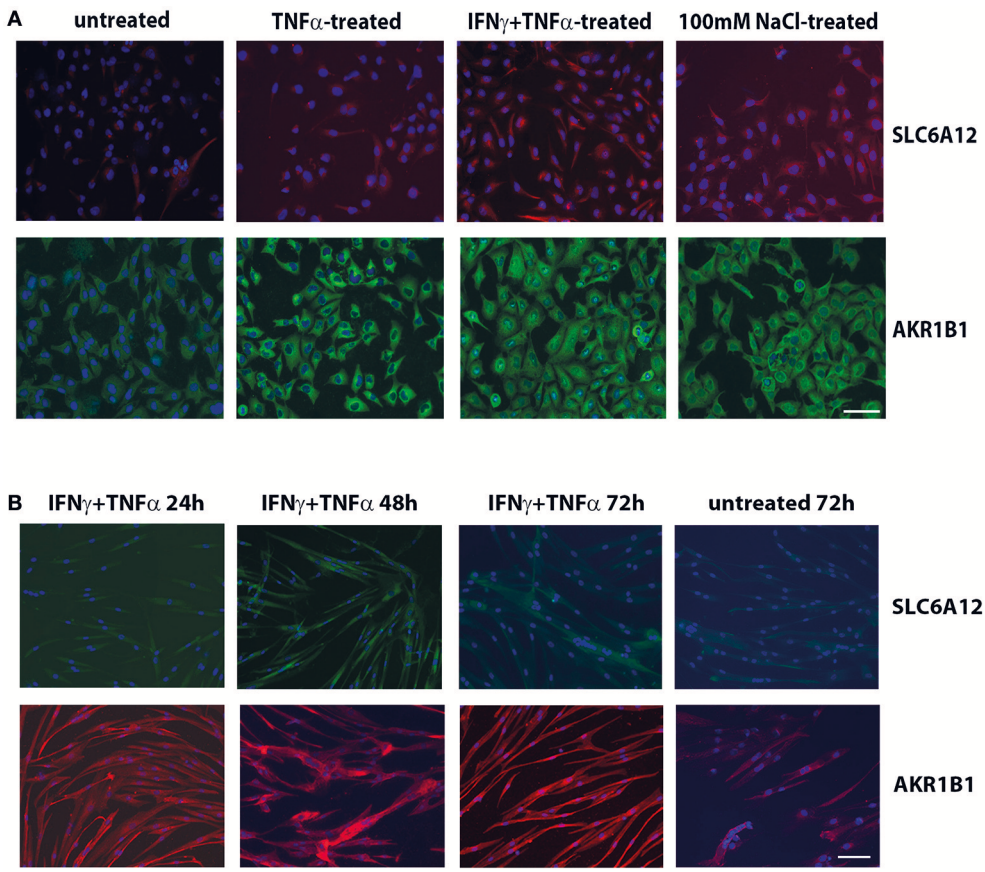


FIGURE 1 | Immunofluorescent cytostaining. **(A)** Staining with mouse anti-SLC6A12 (AlexaFluor 594, red) and rabbit anti-AKR1B1 (AlexaFluor488, green) in CCL-136 cells after 24 h treatment. Untreated control cells shows low levels of SLC6A12 and AKR1B1. Treatment with 30 ng/ml TNFα markedly increases AKR1B1 levels. Treatment with 300 u/ml IFNγ and 30 ng/ml TNFα strongly increases both SLC6A12 levels and AKR1B1 protein levels. Addition of 100 mM NaCl to the medium also increases both SLC6A12 and AKR1B1 protein expression. **(B)** Staining with rabbit anti-SLC6A12 (AlexaFluor 488, green) and goat anti-AKR1B1 (AlexaFluor594, red) in cultured healthy human myotubes at different time points. Myotubes treated with 300 u/ml IFNγ and 30 ng/ml TNFα display low levels of SLC6A12 that is increased at the 48 h time point. Levels return back to constitutive low levels after 72 h, with staining levels similar to those in untreated cells. Staining for AKR1B1 shows continuously high levels between 24 and 72 h. In untreated cells, AKR1B1 expression levels are substantially lower. Scale bar = 50 μm.

cells (**Figure 3A**). Treatment with pro-inflammatory cytokines on the other hand, combined with knockdown of individual osmolyte pathway members, did not cause significant effects on myotube viability, with percentages of dead cells in untreated vs. cytokine-treated cells respectively: 1% vs. 7% (vehicle), 11% vs. 25% (siSLC6A12), 33% vs. 15% (siAKR1B1), and 0% vs. 4% (siSLC5A3). For silencing procedures, efficiency of knockdown was evaluated in CCL-136 cells (calculated as ΔCt siRNA-treated cells minus ΔCt of the vehicle control) detecting 16% (siSLC5A3), 59% (siSLC6A12), and 6% (siAKR1B1) of residual mRNA expression. Western blotting corroborated efficient AKR1B1 knockdown at the protein level but did not show a

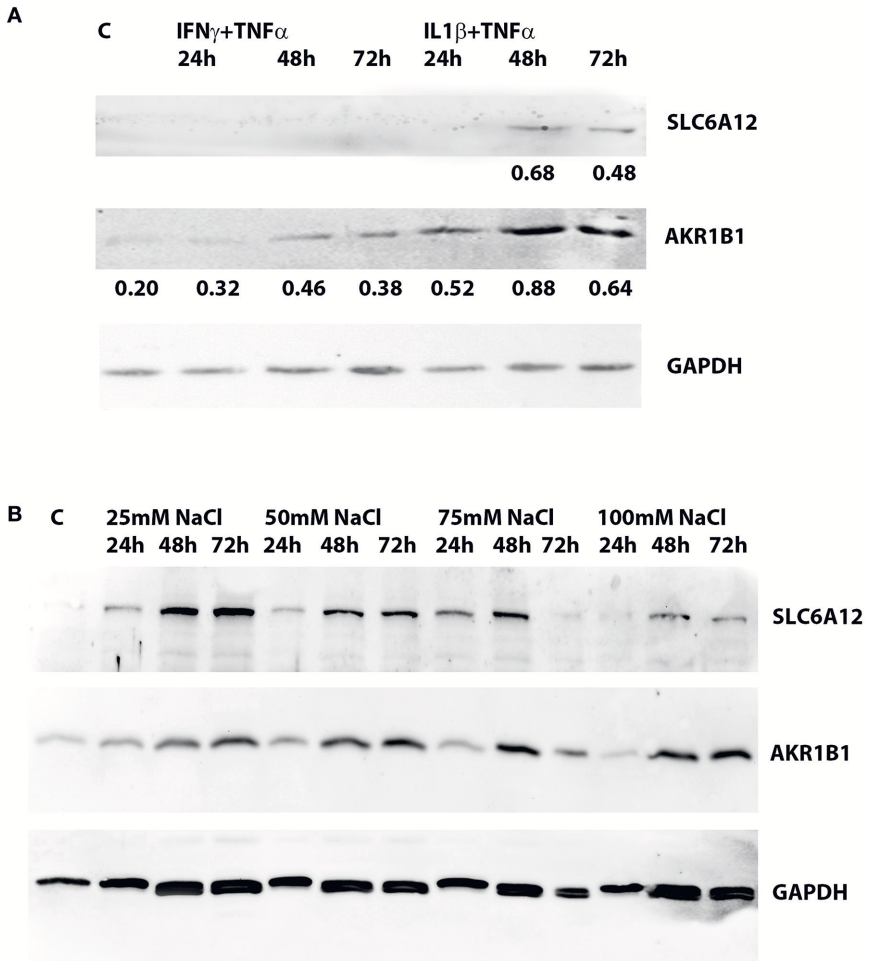


FIGURE 2 | Western blotting of protein extracts preepared from cultured normal human myotubes. **(A)** SLC6A12 and AKR1B1 protein levels in myotubes treated with cytokine mixtures. SLC6A12 and AKR1B1 proteins are visualized in control cells (C) and in cells treated for 24 h-48 h-72 h with either 300 u/ml IFNγ+30 ng/ml TNFα, or 20 ng/ml IL1β+30 ng/ml TNFα. SLC6A12 is undetectable in untreated- and in 300 u/ml IFNγ+30 ng/ml TNFα-treated cells, but is induced by treatment with 20 ng/ml IL1β+30 ng/ml TNFα from the 48 h time point on. Low constitutive levels of AKR1B1 in control cells are increased in myotubes treated with both cytokine mixtures, peaking at the 48 h time point. Relative protein densities of AKR1B1, normalized using glyceraldehyde 3-phosphate dehydrogenase (GAPDH) levels as an internal standard, have been indicated. **(B)** SLC6A12 and AKR1B1 protein levels in myotubes treated with added NaCl. Protein bands for SLC6A12 and AKR1B1, and the internal standard glyceraldehyde 3-phosphate dehydrogenase (GAPDH), are given in an untreated control (C) and in cells treated with different concentrations of added NaCl. A time-dependent increase is observed in cells treated with 25 and 50 mM added NaCl, while more elevated NaCl concentrations show the highest levels at the 48 h timepoint. The corresponding relative protein densities are listed in **Table 4**.

substantial reduction of SLC6A12 protein levels (**Figure 3B**). We could not quantify SLC5A3 protein in muscle samples using western blots, as we were unsuccessful in detecting SLC5A3 in the corresponding positive control samples using rabbit (nbp102399, NovusBiologicals) and goat (sc-23142, SantaCruz Biotechnology) antibodies.

Immunolocalization Studies in Muscle Tissues From Inflammatory Myopathy Patients

Confirming our earlier descriptive myopathological results on SLC5A3, SLC6A6, and AKR1B1 expression (24), we found these factors upregulated in regenerating muscle fibers present in biopsies in this new cohort of inflammatory myopathy patients. We now also add SLC6A12 to the regenerating muscle fiber's repertory of increased osmolyte accumulators (**Figure 4**). High osmolyte pathway member expression contrasted with the low levels present in muscle fibers in biopsies from healthy subjects. In tissues from muscular dystrophy patients, the SLC6A12 muscle fiber staining pattern was similar to inflammatory myopathies, with diffuse staining mostly in small regenerating CD56 positive muscle fibers and discontinuous sarcolemmal staining in subsets of CD56 negative muscle fibers (**Supplementary Figure S3**). We verified that this did not represent adjacent satellite cells and observed no co-localization with Pax3/7 staining.

TABLE 4 | Protein densities in cultured normal human myotubes treated with added NaCl for varying periods of time.

	Untreated	25 mM NaCl			50 mM NaCl			75 mM NaCl			100 mM NaCl		
		24 h	48 h	72 h	24 h	48 h	72 h	24 h	48 h	72 h	24 h	48 h	72 h
SLC6A12	0.001	0.097	0.264	**0.297**	0.139	0.180	**0.198**	0.154	**0.217**	0.131	0.112	**0.115**	0.094
AKR1B1	0.192	0.202	0.210	**0.347**	0.336	0.377	**0.437**	0.281	**0.436**	0.347	0.209	**0.278**	0.263

*Protein densities of western blots (shown in **Figure 2**) were normalized using glyceraldehyde 3-phosphate dehydrogenase levels. Highest protein expression levels per time point have been highlighted.*

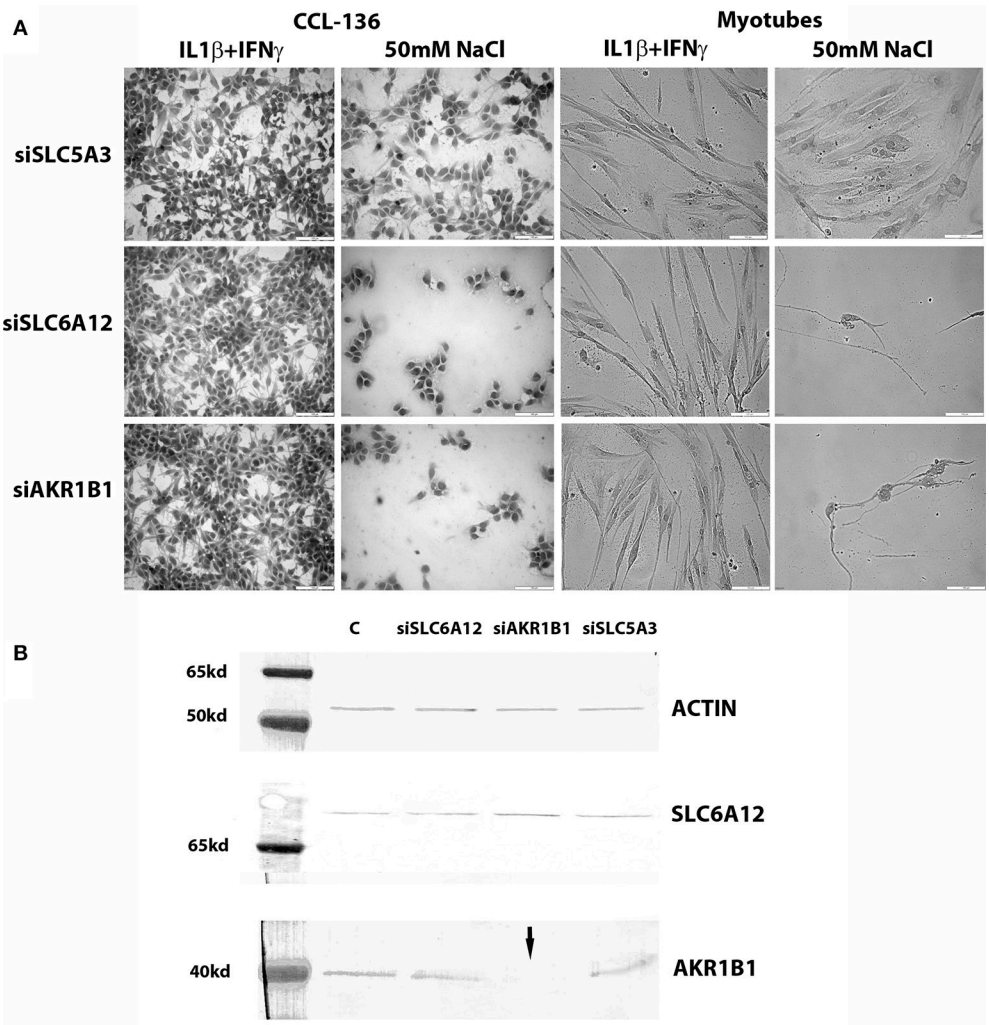


FIGURE 3 | Knockdown studies. **(A)** Hematoxylin&Eosin staining of CCL-136 and healthy human myotube cultures treated with silencing RNAs. Representative images are shown of cell cultures exposed to 300 u/ml IFNγ+20 ng/ml IL1β or to 50 mM of added NaCl. Culture densities decrease substantially in siSLC6A12- and siAKR1B1-treated cultures challenged with 50 mM of added NaCl, both in CCL-136 cells and in normal human myotubes. Addition of siSLC5A3 does not apparently inhibit cell growth, only resulting in mildly reduced densities of CCL-136 cells which could equally be observed in controls treated with 50 mM NaCl.
Scale bar = 100 μm. **(B)** Western blots visualizing SLC6A12 and AKR1B1 protein in CCL-136 cells treated with silencing RNAs. The severe reduction of the AKR1B1 protein band in siAKR1B1-treated cells (arrow) shows the efficiency of expression knockdown. C represents the control sample, and equal loading is shown by β-actin protein bands.

SLC5A3 and SLC6A12 were expressed by inflammatory cells in inflammatory myopathy muscle biopsies (**Figure 4**). SLC6A12 was detected in subsets of the endomysial CD68+ cells surrounding muscle fibers in PM and IBM tissues. In comparison, only a small minority of tissue-infiltrating CD68+ cells in DM and in muscular dystrophy tissues were SLC6A12

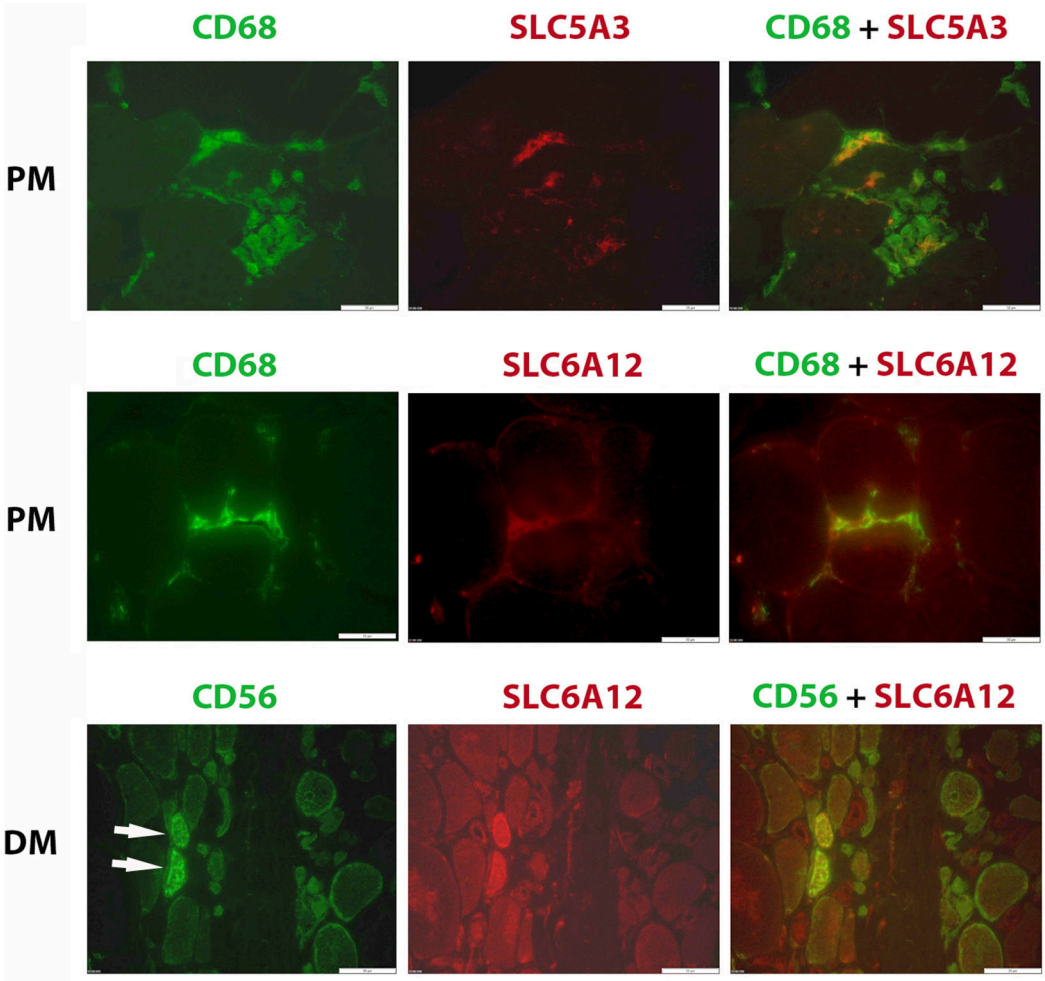


FIGURE 4 | Immunofluorescent histostaining. Staining of SLC6A12 and AKR1B1 in muscle sections from patients diagnosed with inflammatory myopathy. Polymyositis (PM): A subset of CD68+ cells (AlexaFluor488, green), representing mostly M1 phenotype macrophages, express SLC5A3 and SLC6A12 (CY3, red). Dermatomyositis (DM): Two small regenerating muscle fibers (arrows), identified as strongly positive for CD56 (AlexaFluor488, green), express high levels of SLC6A12 protein (CY3, red). Scale bar =50 μm.

positive, and the more sparse inflammatory cells observed in IMNM tissues were SLC6A12 negative. SLC6A12 was rarely observed in the CD8+ T-cells of PM and IBM tissues. SLC5A3 on the other hand, could be detected in a substantial part of CD3+ T-cells, with most non-invading CD8+ T-cells being negative while CD8+ cells actively invading nonnecrotic muscle fibers in PM and IBM were often strongly positive. The majority of CD68+ cells, and part of the CD206+ cells were also SLC5A3 positive. In contrast, inflammatory cells were invariably AKR1B1 and SLC6A6 negative in all muscle tissues tested.

DISCUSSION

Our earlier studies had identified osmolyte pathway members as biomarkers for inflammatory myopathies, yet the pathogenic routes behind their elevated expression remained unknown. The present study offers further context and allows us to speculate on the underlying mechanisms.

Inflammatory Stress Induces Osmolyte Pathways in Muscle Cells

We here report that, in addition to increased NaCl concentrations, pro-inflammatory cytokines can induce osmolyte pathways in muscle cells in an *in vitro* setting. In response to osmotic stress, normal primary myotubes displayed a continuous increase of SLC5A3, SLC6A12, and AKR1B1 mRNA expression levels over time, while single cytokine pulse led to highest mRNA levels after 24 h, steadily decreasing afterwards and returning to near-normal levels at the 72 h time point. Immunocytochemical staining and western blotting experiments confirmed the transient induction pattern of SLC6A12 at the protein level. We cannot rule out fast cytokine degradation in the culture medium, yet this is unlikely as many have

reported prolonged effects by single pulse cytokine treatments over several days (28–30). Using silencing techniques, we showed that compromising osmolyte accumulator expression negatively influenced cell growth only when muscle cells faced hyperosmotic conditions. We produced strongest evidence for AKR1B1, for which the knockdown regimen severely reduced AKR1B1 protein levels, yet did not compromise growth when myoblasts and myotubes were challenged with pro-inflammatory cytokines. Based upon this data, we speculate on different levels of importance of the osmolyte pathway dependent upon the challenges muscle cells face: osmolytes being essential protectors against osmotic stress while having a less vital yet regulatory role in the response to inflammatory stress. Our observations would need to be confirmed and analyzed further with knockdown combinations, as an important additional facet is the degree of redundancy of function displayed by the different osmolyte pathway members. In evidence, only SLC5A3 deficiency represents a lethal murine phenotype (31), with knockout of AKR1B1, SLC6A6, and SLC6A12 resulting in viable mice suffering from limited defects in renal function (32–34). The compensatory role of remaining osmolytes when activity of single pathway members is compromised, has long been confirmed in kidney cells (35).

Transcription factors NFκB and NFAT5 represent key regulators of cell's responses to inflammatory stress on the one hand and osmotic stress on the other hand. Not surprisingly therefore, pro-inflammatory cytokines were the most potent inducers of RelA, NFkB1, NFkB2 expression in muscle cells. However, we did observe some effects of NaCl-treatment on NFκB expression levels and, vice versa, NFAT5 expression responded to pro-inflammatory cytokines. Thus, muscle cells' responses to inflammatory and osmotic stress appear not separately regulated via NFκB and NFAT5, respectively.

The MAP kinases, a large family of Ser/Thr kinases that translate cell surface signals to the nucleus, play a crucial role in inflammation (36), which led us to study their involvement in muscle cells' responses to pro-inflammatory cytokines. We found Akt2 and HSP27 were most heavily phosphorylated in myotube cultures, but their activation was unaltered in response to inflammatory cytokines. Akt signaling influences muscle development and regeneration, affecting either initiation (Akt1) or maturation (Akt2) of myotubes (37). HSP27 is also associated with myotube differentiation and was found absent from myoblasts (38). The strong activation of Akt2 and HSP27 we observed in our *in vitro* model fits with the differentiated stage of the myotubes we studied in our experiments. The MAPKs of the p38 subgroup have been put forward as complex regulators of osmolyte pathways, through their hypertonicity-induced phosphorylation, and have been implicated in inflammatory disease (39). Our study found MAPK14 mRNA expression increased up to 2-fold by pro-inflammatory cytokines, and we observe increased phosphorylation of MAPK12 and MAPK13 in human primary myotubes treated for 24 h with IL1β+IFNγ. Of the extracellular signal-regulated kinases (ERK) on the other hand, we observed increased phosphorylation of MAPK3 (ERK1) in IL-1β+IFN-γ-treated myotubes. This is in line with our recent study that showed cytokines induce ERK1/2 phosphorylation, which subsequently leads to protein deposition and autophagy in muscle cell cultures (40). We propose that the 24 h response of muscle cells to pro-inflammatory cytokines may thus be regulated primarily via such phosphorylation-driven activation of residential MAPKs. Muscle cells exposed to osmotic stress for prolonged periods appear to require extra measures for their protection, culminating in 18-fold (MAPK14) and 9-fold (NFAT5) increases in expression levels.

Osmolyte Pathways Are Activated in Regenerating Muscle Cells

Osmolytes are known regulators of skeletal muscle development, with the involvement of taurine and betaine already described in most detail. Taurine is essential for skeletal muscle buildup, and knockout mice lacking its transporter SLC6A6 display severe structural defects (41) and exercise intolerance (42). The trimethylglycine betaine appears also important for proper muscle functioning, although SLC6A12 knockout mice have been reported to develop only mild myopathy (34). Betaine promotes muscle fiber differentiation and myotube size (43) via stimulation of the mechanistic target of rapamycin pathway (44) and disturbed osmolyte balances have been implicated in muscle disease. Taurine levels were significantly reduced in muscle from myositis patients compared to healthy controls (45), while in urine on the other hand both taurine and betaine levels were increased in patients (46). In the murine Duchenne muscular dystrophy model, taurine content of muscle was low, mostly early in disease progression, and a reduction of its transporter SLC6A6 was observed (47). Yet, in the canine golden retriever muscular dystrophy model, muscle levels of taurine and SLC6A6 were 1.5- and 20-fold increased (48) compared to healthy dogs, pointing to possible differences between species and/or at different disease stages. Our localization studies revealed strong increases of osmolyte accumulators in small regenerating fibers. Possibly, protein replacement and refolding during the regeneration process are chaperoned by osmolytes, the latter aiding protection of functional protein conformations (49).

Subsets of Muscle-Infiltrating Inflammatory Cells Express SLC5A3 and SLC6A12

In addition to the muscle cells' general and dynamic repertory of osmolyte accumulators, we found two osmolyte pathway members, SLC5A3 and SLC6A12, selectively expressed in subsets of macrophages and T-cells infiltrating skeletal muscle. Interestingly, we observed an association with active invasion of nonnecrotic muscle fibers, a phenomenon typically observed in PM and IBM muscle tissues (50), which fits with current notions of how osmolytes behave as potent cytotoxic regulators. Cytotoxic macrophages have been shown to accumulate betaine, myoinositol and taurine as compatible organic osmolytes in response to osmotic stress, via MAPK-regulated upregulation of osmolyte transporters (51, 52). It is well known that macrophages have versatile functionalities, with a spectrum stretching out between the classical inflammatory M1 phenotype, to the alternative anti-inflammatory, tissue repair-oriented

M2 phenotype (53). Significantly higher levels of AKR1B1 mRNA and protein have been reported in M1 macrophages compared with M2-polarized macrophages (54). The upstream transcription factor NFAT5 is enhanced by the M1-promoting pro-inflammatory and hypoxic conditions associated with autoimmune diseases, which is particularly suggested to regulate the chemokine MCP-1 and subsequent synovial macrophage survival in rheumatoid arthritis (55). We found a subset of CD68+ cells, regarded as representing mostly M1 macrophages, to express SLC5A3 and SLC6A12, most prominently in PM and IBM tissues. In addition to macrophages, T-cells have also been shown to engage NFAT5-regulated pathways in their development and activation (56) and, in accordance, we found SLC5A3 and SLC6A12 expression in a minority of T-cells. In helper T-cells (Th-cells), salt-induced NFAT5 activity promotes their differentiation into Interleukin 17-producing Th-cells (Th17-cells) (57). This is relevant to inflammatory myopathy, as IL-17 induces and maintains chronic inflammation, and Th17-cells represent a pathogenic subset of T-cells associated with inflammatory myopathy (58).

CONCLUSIONS

The expression of osmolyte pathway members extends to human tissues that normally are not exposed to hypertonicity, which has led to the assumption that these factors have additional more versatile functions. In this respect, they have been put forward as biomarkers for inflammation (59) and tumor metastasis (60). The data we presented here points to a general role for osmolyte accumulation, via AKR1B1, SLC5A3, SLC6A6, and SLC6A12 upregulation, in muscle cells challenged by inflammatory stress, presumably in an attempt to stabilize protein function in sight of the changed proteome during regeneration. In addition, our data suggest an individual inflammatory role for SLC5A3 and SLC6A12 as potential regulators of the myocytotoxicity displayed by muscle tissue-infiltrating auto-aggressive immune cells. The data we offer further adds to the complexity of inflammatory myopathy immunopathogeneses, broadening our understanding of this heterogeneous group of diseases.

AUTHOR CONTRIBUTIONS

BD conceived, designed, and executed the study. JW and JD analyzed patient data and material. BD, JZ, and TŠ carried out experiments and analyzed the data. BD drafted the manuscript, which was critically revised by JZ, JS, and JD.

FUNDING

BD is recipient of a research grant from the Association Belge contre les Maladies neuro-Musculaires (ABMM), aides à la recherche 2018. JD received confined sponsoring by CAF DCF. The international cooperation this work entailed, was supported by mobility grants from the Research Foundation—Flanders (FWO), German Academic Exchange Service (DAAD), the International Federation of Medical Students' Associations SCORE research exchange program, and the U4 university network OSMYO.

ACKNOWLEDGMENTS

We graciously thank the patients for their participation in this study, and thank Iris Iben and Sophie D'hose for skilful technical support.

SUPPLEMENTARY MATERIAL

The Supplementary Material for this article can be found online at: https://www.frontiersin.org/articles/10.3389/fneur.2018.00846/full#supplementary-material

REFERENCES

1. Dalakas MC. Inflammatory muscle diseases. *N Eng J Med.* (2015) 372:1734–47. doi: 10.1056/NEJMra1402225
2. Mammen AL. Statin-associated autoimmune myopathy. *N Eng J Med.* (2016) 374:664–9. doi: 10.1056/NEJMra1515161
3. Uruha A, Suzuki S, Suzuki N, Nishino I. Perifascicular necrosis in anti-synthetase syndrome beyond anti-Jo-1. *Brain* (2016) 139:e50. doi: 10.1093/brain/aww125
4. Malik A, Hayat G, Kalia JS, Guzman MA. Idiopathic inflammatory myopathies: clinical approach and management. *Front Neurol.* (2016) 7:e64. doi: 10.3389/fneur.2016.00064
5. Allenbach Y, Benveniste O, Goebel HH, Stenzel W. Integrated classification of inflammatory myopathies. *Neuropathol Appl Neurobiol.* (2017) 43:62–81. doi: 10.1111/nan.12380
6. Lahoria R, Selcen D, Engel AG. Microvascular alterations and the role of complement in dermatomyositis. *Brain* (2016) 139:1891–903. doi: 10.1093/brain/aww122
7. Dalakas MC. Pathogenesis and therapies of immune-mediated myopathies. *Autoimm Rev.* (2011) 11:203–6. doi: 10.1016/j.autrev.2011.05.013
8. Askanas V, Engel WK. Molecular pathology and pathogenesis of inclusion-body myositis. *Microsc Res Tech.* (2005) 67:114–20. doi: 10.1002/jemt.20186
9. Benveniste O, Stenzel W, Hilton-Jones D, Sandri M, Boyer O, van Engelen BGM. Amyloid deposits and inflammatory infiltrates in sporadic inclusion body myositis: the inflammatory egg comes before the degenerative chicken. *Acta Neuropathol.* (2015) 129:611–24. doi: 10.1007/s00401-015-1384-5
10. Allenbach Y, Mammen AL, Benveniste O, Stenzel W, on behalf of the Immune-Mediated Necrotizing Myopathies Working Group. 224th ENMC International Workshop: Clinico-sero-pathological classification of immune-mediated necrotizing myopathies Zandvoort, The Netherlands, 14–16 October. *Neuromuscul Disord.* (2017) 28:87–99. doi: 10.1016/j.nmd.2017.09.016
11. Warepam M, Singh LR. Osmolyte mixtures have different effects than individual osmolytes on protein folding and functional activity. *Arch Biochem Biophys.* (2015) 573:77–83. doi: 10.1016/j.abb.2015.03.017
12. Cheung CY, Ko BCB. NFAT5 in cellular adaptation to hypertonic stress-regulations and functional significance. *J Mol Signal.* (2013) 8:5. doi: 10.1186/1750-2187-8-5
13. Abbott KL, Friday BB, Thaloor D, Murphy TJ, Pavlath GK. Activation and cellular localization of the cyclosporine A-sensitive transcription factor NF-AT in skeletal muscle cells. *Mol Biol Cell* (1998) 9:2905–16. doi: 10.1091/mbc.9.10.2905

14. O'Connor RS, Mills ST, Jones KA, Ho SN, Pavlath GK. A combinatorial role for NFAT5 in both myoblast migration and differentiation during skeletal muscle myogenesis. *J Cell Sci.* (2007) 120:149–59. doi: 10.1242/jcs.03307
15. Roth I, Leroy V, Moo Kwon H, Martin PY, Feraille E, Hasler U. Osmoprotective transcription factor NFAT5/TonEBP modulates nuclear factor-kB activity. *Mol Biol Cell* (2010) 21:3459–74. doi: 10.1091/mbc.E10-02-0133
16. Creus KK, De Paepe B, De Bleecker JL. Idiopathic inflammatory myopathies and the classical NF-kappaB complex: current insights and implications for therapy. *Autoimm Rev.* (2009) 8:627–31. doi: 10.1016/j.autrev.2009.02.026
17. De Paepe B. A recipe for myositis: nuclear factor kB and nuclear factor of activated T-cells transcription factor pathways spiced up by cytokines. *AIMS All Immunol.* (2017) 1:31–42. doi: 10.3934/Allergy.2017.1.31
18. De Bleecker J, De Paepe B, Vanwalleghem IE, Schröder JM. Differential expression of chemokines in inflammatory myopathies. *Neurology* (2002) 58:1779–85. doi: 10.1212/WNL.58.12.1779
19. Creus KK, De Paepe B, Weis J, De Bleecker JL. The multifaceted character of lymphotoxin b in inflammatory myopathies and muscular dystrophies. *Neuromuscul Disord.* (2012) 22:712–9. doi: 10.1016/j.nmd.2012.04.012
20. De Bleecker JL, Meire VI, Declercq W, Van Aken EH. Immunolocalization of tumor necrosis factor-alpha and its receptors in inflammatory myopathies. *Neurmuscul Disord.* (1999) 9:239–46. doi: 10.1016/S0960-8966(98)00126-6
21. De Paepe, Racz GZ, Schröder JM, De Bleecker JL. Expression and distribution of the nitric oxide synthases in idiopathic inflammatory myopathies. *Acta Neuropathol.* (2004) 108:37–42. doi: 10.1007/s00401-004-0859-6
22. De Paepe B, Creus KK, Weis J, De Bleecker JL. Heat shock protein families 70 and 90 in Duchenne muscular dystrophy and inflammatory myopathy: Balancing muscle protection and destruction. *Neuromuscul Disord.* (2012) 22:26–33. doi: 10.1016/j.nmd.2011.07.007
23. Van der Meer JW, Netea MG. A salty taste to autoimmunity. *N Engl J Med.* (2013) 368:2520–1. doi: 10.1056/NEJMcibr1303292
24. De Paepe B, Martin JJ, Herbelet S, Jimenez-Mallebrera C, Iglesias E, Jou C, et al. Activation of osmolyte pathways in inflammatory myopathy and Duchenne muscular dystrophy points to osmotic regulation as a contributing pathogenic mechanism. *Lab Invest.* (2016) 96:872–84. doi: 10.1038/labinvest.2016.68
25. Herbelet S, De Vlieghere E, Gonçalves A, De Paepe B, Schmidt K, Nys E, et al. Localization and expression of nuclear factor of activated T-cells 5 in myoblasts exposed to pro-inflammatory cytokines or hyperosmolar stress and in biopsies from myositis patients, *Front Physiol.* (2018) 9:e126. doi: 10.3389/fphys.2018.00126
26. Schmidt J, Barthel K, Zschüntzsch J, Muth IE, Swindle EJ, Hombach A, et al. Nitric oxide stress in sporadic inclusion body myositis muscle fibres: inhibition of inducible nitric oxide synthase prevents interleukin-1β-induced accumulation of β-amyloid and cell death. *Brain* (2012) 135:1102–14. doi: 10.1093/brain/aws046
27. De Bleecker JL, De Paepe B, Aronica E, de Visser M, ENMC Myositis Muscle Biopsy Study Group, Amato A. 205th ENMC International Workshop: Pathology diagnosis of idiopathic inflammatory myopathies Part II 28–30 March 2014, Naarden, The Netherlands. *Neuromuscul Disord.* (2015) 25:268–72. doi: 10.1016/j.nmd.2014.12.001
28. Michaelis D, Goebels N, Hohlfeld R. Constitutive and cytokine-induced expression of human leukocyte antigens and cell adhesion molecules by human myotubes. *Am J Pathol.* (1993) 143:1142–9.
29. Liu CJ, Wang H, Zhao Z, Yu S, Lu YB, Meyer J, et al. MyoD-dependent induction during myoblast differentiation of p204, a protein also inducible by interferon. *Mol Cell Biol.* (2000) 20:7024–36. doi: 10.1128/MCB.20.18.7024-7036.2000
30. Langen RC, Schols AM, Kelders MC, Wouters EF, Janssen-Heininger YM. Inflammatory cytokines inhibit myogenic differentiation through activation of nuclear factor-kappa B. *FASEB J* (2001) 15:1169–80. doi: 10.1096/fj.00-0463
31. Buccafusca R, Venditti CP, Kenyon LC, Johanson RA, Van Bockstaele E, Ren J, et al. Characterization of the null murine sodium/myo-inositol cotransporter 1 (Smit1 or Slc5a3) phenotype: myo-inositol rescue is independent of expression of its cognate mitochondrial ribosomal protein subunit 6 (Mrps6) gene and of phosphatidylinositol levels in neonatal brain. *Mol Genet Metab.* (2008) 95:81–95. doi: 10.1016/j.ymgme.2008.05.008
32. Aida K, Ikegishi Y, Chen J, Tawata M, Ito S, Maeda S, et al. Disruption of aldose reductase gene (Akr1b1) causes defect in urinary concentrating ability and divalent cation homeostasis. *Biochem Biophys Res Commun.* (2000) 277:281–6. doi: 10.1006/bbrc.2000.3648
33. Huang DY, Boini KM, Lang PA, Grahammer F, Duszenko M, Heller-Stilb B, et al. Impaired ability to increase water excretion in mice lacking the taurine transporter gene TAUT. *Eur J Physiol.* (2006) 451:668–77. doi: 10.1007/s00424-005-1499-y
34. Lehre AC, Rowley NM, Zhou Y, Holmseth S, Guo C, Holen T, et al. Deletion of the betaine-GABA transporter (BGT1; slmc6a12) gene does not affect seizure thresholds of adult mice. *Epilepsy Res.* (2011) 95:70–81. doi: 10.1016/j.eplepsyres.2011.02.014
35. Moriyama TA, Garcia-Perez A, Olson A, Burg MB. Intracellular betaine substitutes for sorbitol in protecting renal medullary cells from hypertonicity. *Am J Physiol.* (1991) 260:F494–7. doi: 10.1152/ajprenal.1991.260.4.F494
36. Dong C, Davis RJ, Flavell RA. Map kinases in the immune reponse. *Annu Rev Immunol.* (2002) 20:55–72. doi: 10.1146/annurev.immunol.20.091301.131133
37. Rotwein P, Wilson EM. Distinct actions of Akt1 and Akt2 in skeletal muscle differentiation. *J Cell Physiol.* (2009) 219:503–11. doi: 10.1002/jcp.21692
38. Dubinska-Magiera M, Jablonska J, Saczko J, Kulbacka J, Kagla T, Daczewska M. Contribution of small heat shock proteins to muscle development. *FEBS Lett.* (2014) 588:517–30. doi: 10.1016/j.febslet.2014.01.005
39. Waetzig GH, Seegert D, Rosenstiel P, Nikolaus S, Schreiber S. p38 mitogen-activated protein kinase is activated and linked to TNF-alpha signaling in inflammatory bowel disease. *J Immunol.* (2002) 168:5342–51. doi: 10.4049/jimmunol.168.10.5342
40. Schmidt K, Wienken M, Keller CW, Balcarek P, Munz C, Schmidt J. IL-1β-induced accumulation of amyloid: macrophagy in skeletal muscle depends on ERK. *Mediat Inflamm.* (2017) 2017:e5470831. doi: 10.1155/2017/5470831
41. Ito T, Kimura Y, Uozumi Y, Takai M, Muraoka S, Matsuda T, et al. Taurine depletion caused by knocking out the taurine transporter gene leads to cardiomyopathy with cardiac atrophy. *J Mol Cell Cardiol.* (2008) 44:927–37. doi: 10.1016/j.yjmcc.2008.03.001
42. Warskulat U, Heller-Stilb B, Germann E, Zilles K, Haas H, Lang F, et al. Phenotype of the taurine transporter knockout mouse. *Methods Enzymol.* (2007) 428:439–58. doi: 10.1016/S0076-6879(07)28025-5
43. Senesi P, Luzi L, Montesano A, Mazzocchi N, Terruzzi I. Betaine supplement enhances skeletal muscle differentiation in murine myoblasts via IGF-1 signaling activation. *J Translat Med.* (2013) 11:e174. doi: 10.1186/1479-5876-11-174
44. Huang QC, Xu ZR, Han XY, Li WF. Changes in hormones, growth factor and lipid metabolism in finishing pigs fed betaine. *Livestock Sci.* (2006) 105:78–85. doi: 10.1016/j.livsci.2006.04.031
45. Stuerenburg HJ, Stangneth B, Schoser BG. Age related profiles of free amino acids in human skeletal muscle. *Neuroendocrinol Lett.* (2006) 27:133–6.
46. Chung YL, Wassif WS, Bell JD, Huley M, Scott DL. Urinary levels of creatine and other metabolites in the assessment of polymyositis and dermatomyositis. *Rheumatology* (2003) 42:298–303. doi: 10.1093/rheumatology/keg084
47. Terrill JR, Grounds MD, Arthur PG. Taurine deficiency, synthesis and transport in the mdx mouse model for Duchenne Muscular Dystrophy. *Int J Biochem Cell Biol.* (2015) 66:141–8. doi: 10.1016/j.biocel.2015.07.016
48. Terrill JR, Duong MN, Turner R, Le Guiner C, Boyatzis A, Kettle AJ, et al. Levels of inflammation and oxidative stress, and a role for taurine in dystropathology of the Golden Retriever Muscular Dystrophy dog model for Duchenne Muscular Dystrophy. *Redox Biol.* (2016) 9:276–86. doi: 10.1016/j.redox.2016.08.016
49. Khan SH, Ahmad N, Ahmad F, Kumar R. Naturally occurring organic osmolytes: from cell physiology to disease prevention. *IUBMB Life* (2010) 62:891–5. doi: 10.1002/iub.406
50. De Paepe B, De Bleecker JL. The nonnecrotic invaded muscle fibers of polymyositis and sporadic inclusion body myositis: on the interplay of chemokines and stress proteins. *Neurosci Lett.* (2013) 535:18–23. doi: 10.1016/j.neulet.2012.11.064
51. Warskulat U, Zhang F, Häussinger D. Taurine is an osmolyte in rat liver macrophages (Kupffer cells). *J Hepatol.* (1997) 26:1340–7. doi: 10.1016/S0168-8278(97)80470-9
52. Denkert C, Warskulat U, Hensel F, Häussinger D. Osmolyte strategy in human monocytes and macrophages: involvement of p38MAPK

in hyperosmotic induction of betaine and myoinositol transporters. *Arch Biochem Biophys.* (1998) 354:172–80. doi: 10.1006/abbi.1998.0661

53. Mantovani A, Sica A, Sozzani S, Allavena P, Vecchi A, Locati M. The chemokine system in diverse forms of macrophage activation and polarization. *Trends Immunol.* (2004) 25:677–86. doi: 10.1016/j.it.2004.09.015
54. Erbel C, Rupp G, Domschke G, Linden F, Akhavanpoor M, Doesch AO, et al. Differential regulation of aldose reductase expression during macrophage polarization depends on hyperglycemia. *Innate Immun.* (2016) 22:230–7. doi: 10.1177/1753425916632053
55. Choi S, You S, Kim D, Choi SY, Kwon HM, Kim HS, et al. Transcription factor NFAT5 promotes macrophage survival in rheumatoid arthritis. *J Clin Invest.* (2017) 127:954–69. doi: 10.1172/JCI87880
56. Trama J, Go WY, Ho SN. The osmoprotective function of the NFAT5 transcription factor in T cell development and activation. *J Immunol.* (2002) 169:5477–88. doi: 10.4049/jimmunol.169.10.5477
57. Kleinewietfeld M, Manzel A, Totze J, Kvakan H, Yosef N, Linker RA, et al. Sodium chloride drives autoimmune disease by the induction of pathogenic TH17 cells. *Nature* (2013) 496:518–22. doi: 10.1038/nature11868
58. Tournadre A, Miossec P. Interleukin-17 in inflammatory myopathies. *Curr Rheumatol Rep.* (2012) 14:252–6. doi: 10.1007/s11926-012-0242-x
59. Trama J, Lu Q, Hawley RG, Ho SN. The NFAT-related protein NFATL1 (TonEBP/NFAT5) is induced upon T cell activation in a calcineurin-dependent manner. *J Immunol.* (2000) 165:4884–94. doi: 10.4049/jimmunol.165.9.4884
60. Jauliac S, Lopez-Rodriguez C, Shaw LM, Brown LF, Rao A, Toker A. The role of NFAT transcription factors in integrin-mediated carcinoma invasion. *Nat Cell Biol.* (2002) 4:540–4. doi: 10.1038/ncb816

Conflict of Interest Statement: The authors declare that the research was conducted in the absence of any commercial or financial relationships that could be construed as a potential conflict of interest.

Copyright © 2018 De Paepe, Zschüntzsch, Šokčević, Weis, Schmidt and De Bleecker. This is an open-access article distributed under the terms of the Creative Commons Attribution License (CC BY). The use, distribution or reproduction in other forums is permitted, provided the original author(s) and the copyright owner(s) are credited and that the original publication in this journal is cited, in accordance with accepted academic practice. No use, distribution or reproduction is permitted which does not comply with these terms.

frontiers in Immunology

ORIGINAL RESEARCH
published: 20 November 2018
doi: 10.3389/fimmu.2018.02669

Real World Lab Data: Patterns of Lymphocyte Counts in Fingolimod Treated Patients

Maxi Kaufmann, Rocco Haase, Undine Proschmann, Tjalf Ziemssen† and Katja Akgün†*

MS Center, Center of Clinical Neuroscience, University Hospital Carl Gustav Carus, University of Technology Dresden, Dresden, Germany

Objective: Fingolimod is approved for the treatment of highly active relapsing remitting multiple sclerosis (MS) patients and acts by its unique mechanism of action via sphingosine-1-phosphate receptor-modulation. Although fingolimod-associated lymphopenia is a well-known phenomenon, the exact cause for the intra- and inter-individual differences of the fluctuation of lymphocyte count and its subtypes is still subject of debate. In this analysis, we aim to estimate the significance of the individual variation of distinct lymphocyte subsets for differences in absolute lymphocyte decrease in fingolimod treated patients and discuss how different lymphocyte subset patterns are related to clinical presentation in a long-term real life setting.

Methods/Design: One hundred and thirteen patients with MS were characterized by complete blood cell count and immune cell phentopying of peripheral lymphocyte subsets before, at month 1 and every 3 months up to 36 months of fingolimod treatment. In addition, patients were monitored regarding clinical parameters (relapses, disability, MRI).

Results: There was no significant association of baseline lymphocyte count and lymphocyte subtypes with lymphocyte decrease after fingolimod start. The initial drop of the absolute lymphocyte count could not predict the level of lymphocyte count during steady state on fingolimod. Variable CD8+ T cell and NK cell counts account for the remarkable intra- and inter-individual differences regarding initial drop and steady state level of lymphocyte count during fingolimod treatment, whereas CD4+ T cells and B cells mostly present a quite uniform decrease in all treated patients. Selected patients with lymphocyte count >1.0 GPT/l differed by higher CD8+ T cells and NK cell counts compared to lymphopenic patients but presented comparable clinical effectiveness during treatment.

Conclusion: Monitoring of the absolute lymphocyte count at steady state seems to be a rough estimate of fingolimod induced lymphocyte redistribution. Our results suggest, that evaluation of distinct lymphocyte subsets as CD4+ T cells allow a more detailed evaluation to weigh and interpret degree of lymphopenia and treatment response in fingolimod treated patients.

Keywords: fingolimod, lymphopenia, lymphocyte subsets, real world lab data, monitoring

OPEN ACCESS

Edited by:
Marcello Moccia,
University College London,
United Kingdom

Reviewed by:
Antonio Carotenuto,
Università Degli Studi di Napoli Federico II, Italy
Eva M. Martinez-Caceres,
Hospital Germans Trias i Pujol, Spain

****Correspondence:***
Tjalf Ziemssen
tjalf.ziemssen@uniklinikum-dresden.de

†These authors share senior authorship

Specialty section:
This article was submitted to Multiple Sclerosis and Neuroimmunology, a section of the journal Frontiers in Immunology

Received: *08 August 2018*
Accepted: *29 October 2018*
Published: *20 November 2018*

Citation:
Kaufmann M, Haase R, Proschmann U, Ziemssen T and Akgün K (2018) Real World Lab Data: Patterns of Lymphocyte Counts in Fingolimod Treated Patients. Front. Immunol. 9:2669. doi: 10.3389/fimmu.2018.02669

INTRODUCTION

Multiple sclerosis (MS) is a chronic inflammatory disease of the central nervous system (CNS) initiated and perpetuated by an imbalance in the immune-regulatory network. Different MS specific treatment regimens are available and aim to govern autoimmunity and CNS inflammation (1). For some years cellular anti-migratory strategies have been used to control cell migration and accumulation in the CNS (2). Fingolimod acts as sphingosine-1-phosphate (S1P) receptor modulator that inhibits S1P-mediated lymphocyte egress from lymph nodes impairing peripheral lymphocyte recirculation (3–5). This unique mechanism of action results in reduction of absolute lymphocyte counts including specific subsets as naïve T cells, central memory T and B cells but also pro-inflammatory Th1 and Th17 cell subsets in the peripheral and central compartment (3, 6–9). Natalizumab is a further effective therapy for MS patients also known by its anti-migratory mechanism of action. Compared to fingolimod, natalizumab is effective by the block of the α4-subunit of the very late antigen-4 that impairs transmigration of immune cells across the blood-brain barrier into the CNS. Although immune cell subsets are rapidly decreased in the CNS compartment as well, natalizumab lead to significant lymphocyte increase and distinct changes in CD4/CD8 ratio in peripheral blood of treated patients (10, 11). In contrast to other MS treatment regimens e.g., dimethylfumarate therapy even low levels of absolute lymphocyte count up to 0.2 GPT/l can be tolerated during fingolimod treatment (12–16). Other disease managing regimens e.g., in cancer treatment use scoring systems as the National Cancer Institute Common Terminology Criteria for Adverse Events (NCI-CTAE) for grading degree and severity of adverse events including lymphopenia to define risk of infectious complications (17). Interestingly, even though there is a potential increased risk for severe and opportunistic infections due to persistent decrease of CD4+ T cells, only herpes reactivation and infection is relevantly increased in fingolimod treatment (18). Although the peripheral decreased lymphocyte count is a well-known phenomenon for clinicians who are experienced with fingolimod, the exact details of the intra- and inter-individual differences regarding drop and fluctuation of lymphocyte count as well of its subtypes is still a subject of debate (19–22). Up to now, it is not clear which factors can lead to higher vs. lower lymphocyte counts during fingolimod treatment and whether distinct lymphocyte count patterns can assist to select patients that are at higher risk for infections or non-responsiveness to fingolimod treatment (20, 21, 23).

Real-world evidence (RWE) and observational studies are becoming increasingly popular because they provide longitudinal information on usefulness of drugs in real life and have the ability to discover uncommon or rare adverse drug reactions inclusive lab abnormalities (24, 25). Following this approach of real world lab data, here we aim to estimate the significance of the individual variation of distinct lymphocyte subsets for differences in absolute lymphocyte count decrease in fingolimod treated patients and discuss how different lymphocyte subset patterns are related to clinical presentation.

Abbreviations: BMI, Body Mass Index; CNS, central nervous system; CRP, C-reactive protein; DMT, disease modifying drug; gamma-GT, EDSS, Expanded Disability Status Scale; EDTA, ethylene diamine tetra acetic acid; GLMM, Generalized Linear Mixed Model; MRI, magnet resonance imaging; MS, multiples sclerosis; NCI-CTCAE, National Cancer Institute Common Terminology Criteria for Adverse Events; NK cells, natural killer cells; RR, relapsing remitting; RWD, real-world data; RWE, real-world evidence; S1P, sphingosine-1-phosphate.

METHODS

Patients

In our observational real world cohort, we included 113 RRMS patients that were treated in our MS center in Dresden (65 females/48 males) with highly active disease course (**Supplementary Table 1**). After critical review of all relevant clinical and imaging parameters and available treatment options, fingolimod treatment was initiated at a dose of 0.5 mg fingolimod daily. Before fingolimod start, 80.5% of patients were pre-treated with different DMTs (**Supplementary Table 1**). During a standardized treatment switch procedure, injectables were stopped 2 weeks before fingolimod start, natalizumab was stopped 12 weeks before fingolimod start and other DMTs at least 6 months before fingolimod start. Blood samples were collected before (baseline), at month 1 and every 3 months up to 36 months of fingolimod treatment. Additionally patients were monitored regarding clinical parameters including infections, relapse activity, confirmed disability progression measured by EDSS ($\geq$1.0 point increase if EDSS baseline score was $<$4.0; $\geq$0.5 point increase if EDSS baseline score was $\geq$4.0) and BMI three-monthly and MRI progression every year assessed by an examined neuro-radiologist. MRI progression was defined in case of appearance of new gadolinium enhancing lesions or new T2 lesions in cerebral MRI scan. No serious adverse events appeared in our cohort. Data have been collected from the MSDS3D database. The study was approved by the institutional review board of the University Hospital of Dresden. Patients gave their written informed consent.

Routine Blood Analysis

Standardized blood testing was performed for routine blood parameters at the Institute of Clinical Chemistry and Laboratory Medicine, University Hospital in Dresden, Germany. The institute complies with standards required by DIN-EN-ISO-15189:2014 for medical laboratories. Whole blood samples were collected in ethylene diamine tetra acetic acid (EDTA). Routine blood testing included complete blood cell count.

Immune Cell Phenotyping by Fluorescence-Activated Cell Sorting (FACS)

Whole blood samples were collected in EDTA. After collection blood samples were incubated with fluorescence labeled monoclonal antibodies including anti-CD3, anti-CD4, anti-CD8, anti-CD16, anti-CD19, anti-CD56 (BD Biosciences, Heidelberg, Germany) to define T cell, B cell, and natural killer (NK) cell subpopulations. Afterwards, red blood cells were lysed using BD FACS Lysing Solution (BD Bioscience). After washing with FACS

buffer (phosphate buffered saline, 0.2% fetal bovine serum, 0.02% sodium azide, all Biochrom) cells were evaluated on FACSCanto II flow cytometer.

Evaluations and Definition of the Groups

Different approaches were chosen to discuss our study objectives: (1) the whole cohort was examined to evaluate mean changes in peripheral immune cell subsets on group level. Ten patients out of our cohort presented lymphocyte count >1.0 GPT/L after fingolimod start. In addition, matched groups of patients with lymphocyte count 0.5–1.0 GPT/l and ≤0.5 GPT/l were defined and used for further considerations. Additionally intra-individual variability of lymphocytes and its subsets was evaluated in these subgroups. Intra-individual variability was calculated as the standard deviation of absolute cell counts measured every 3 months between month 1 to month 36 of fingolimod therapy in each patient (2). The impact of initial absolute lymphocyte drop was assessed. Median-split was done for the initial absolute drop of lymphocyte count at 1.40 GPT/l and the whole cohort was divided into a high vs. low lymphocyte drop group (3). For the third approach the relevance of high vs. low steady state lymphopenia during fingolimod treatment was assessed. Median-split for lymphocyte count was calculated for the steady state period after month 6 at 0.48GPT/l and a lower steady state group vs. a higher steady state group was selected out of the whole cohort.

Scoring and grading of the level of lymphopenia was performed using the system of the National Cancer Institute Common Terminology Criteria for Adverse Events (NCI-CTAE). Characterization of levels of lymphopenia using NCI-CTAE grading was defined by lymphopenia grade 1: > 0.8 GPt/L, lymphopenia grade 2: 0.5-0.8 GPt/L, lymphopenia grade 3: 0.2-0.5 GPt/L, and lymphopenia grade 4: < 0.2 GPt/L.

Statistical Analysis

Data were analyzed applying Generalized Linear Mixed Models (GLMM) with Gamma distribution and log link function for evaluations with immune cell populations with skewed distribution. Absolute lymphocyte counts and lymphocyte steady state were skewed distributed and though groups of interest were defined using medians-split to define groups of same and comparable sample size. Although lymphocyte count drop was normal distributed medians-split was applied as well to use comparable methodology. Differences in patient characteristics were defined using Analysis of Variances (ANOVA), Kruskal-Wallis H test, Person's chi-square test or Fischer exact test, and an alpha error level of 5%. Correlation was calculated using

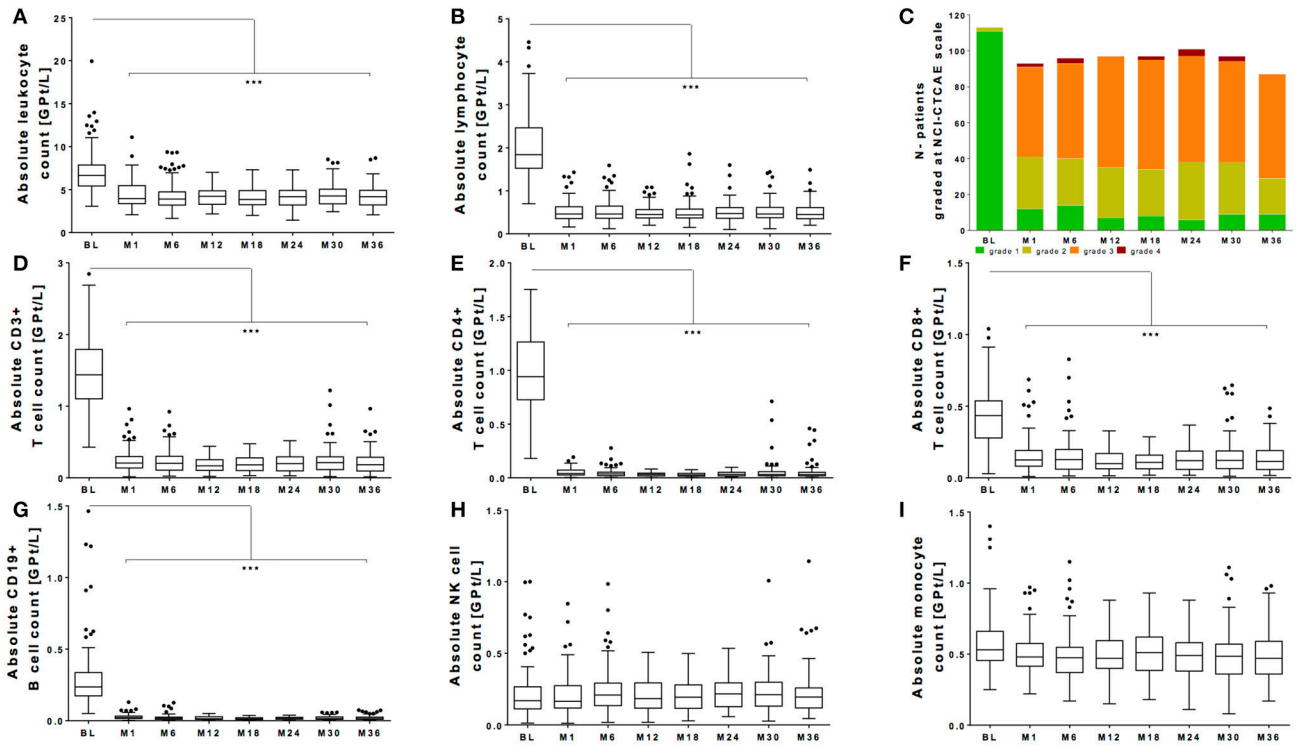


FIGURE 1 | Absolute count of peripheral white blood cells during fingolimod treatment. Absolute cell counts of leukocytes **(A)** lymphocytes **(B)**, CD3+ T cells **(D)**, CD4+ T cells **(E)**, CD8+ T cells **(F)**, CD19+ B cells **(G)** and NK cells **(H)**, and monocytes **(I)** are depicted. Data for the whole cohort are shown as Boxplot Tukey before fingolimod start (baseline, BL), month 1 and every 6 months follow up. **(C)** Distribution of different ranges of lymphocyte count are shown graded with NCI-CTCAE: lymphopenia grade 1 >0.8 GPt/L (green), lymphopenia grade 2 0.5-0.8 GPt/L (yellow), lymphopenia grade 3 0.2-0.5 GPt/L (orange) and lymphopenia grade 4 < 0.2 GPt/L (red). Asterisks indicate level of significance of pairwise comparison (***$p < 0.001$).

Spearman's correlation. In order to control for the familywise error rate of the multiple GLMM analyses, comparable alpha error rates were adjusted via Bonferroni correction as α/k were k is the number of analyses per parameter. Therefore, values of $p < 0.0125$ (0.05/4) were considered significant.

RESULTS

Lymphocyte Decrease and Its Relevance in Lymphocyte Variation During Fingolimod Treatment

All patients of our observational cohort demonstrated the well-known drop of absolute lymphocyte count after fingolimod initiation. There was a significant drop of leukocyte count and lymphocyte count (**Figures 1A,B**). Evaluating grading by NCI-CTAE demonstrated that most of the patients presented lymphopenia grade 2 or 3 after fingolimod start (**Figure 1C**). NCI-CTAE grade 4 was reached only at single time points in selected patients. None of the patients stopped fingolimod treatment due to lymphopenia during the observation period as retest revealed grade 3 lymphopenia. Monocytes and NK cells changed only mildly (**Figures 1H,I**), whereas the most intense decrease was seen on T and B cell subtypes (**Figures 1D–G**).

Within our cohort, 10 of 113 patients presented with lymphocyte counts ≥1.0 GPT/L. This specific high lymphocyte group (HL) was compared with a matched (sex, age) fingolimod treated patient group with lymphocyte counts of 0.5-1.0 GPT/l (median lymphocyte group, ML) respective ≤0.5 GPT/l (low lymphocyte group, LL) (**Table 1**). Although characterized by varying levels in lymphocyte decrease, the patients did not differ regard clinical parameters including relapse activity, confirmed EDSS progression and MRI progression or occurrence of reported infectious events between all three groups (**Table 1**). Distribution of previous DMT use was different in all three groups with a higher proportion of interferon-beta use (30–40%) in the ML and LL group whereas glatiramer acetate was used more frequent in the HL group before fingolimod start (**Table 1**). At baseline, there was a trend to a higher absolute count of leukocytes and lymphocytes in HL group compared to ML and LL group. Nevertheless, this trend was not statistical significant (**Figures 2A,B**). After fingolimod start, all lymphocyte counts significantly decreased (**Table 2**). The HL group presented with the highest lymphocyte count at month 1. Thereafter, lymphocyte count decreased further on but was still higher and different compared to lymphocyte counts of ML and LL group (**Figure 2B**, **Table 2**). Additionally, intra-individual variability was evaluated in all three groups: there was a wide intra-individual variation in lymphocyte count in HL group after month 1 (**Figure 2G**). After the initial drop, ML group and LL group presented with quiet stable levels of lymphocyte count over the whole observation period (**Figure 2B**). Intra-individual variation of lymphocyte count presented at a smaller range compared to HL group (**Figure 2G**).

TABLE 1 | Patient characteristics.

	HL	ML	LL
Age (yr ± SD)	36.6 (9.9)	39.2 (8.6)	39.0 (8.1)
Duration since MS diagnosis (yr ± SD)	4.8 (2.1)	3.6 (4.0)	5.0 (3.6)
Sex (f/m)	3/7	3/7	3/7
Previous DMT use before fingolimod start [no. (%)]	10 (100)	7 (70)	7 (70)
Interferon beta	–	4 (40)	3 (26)
Glatirameracetat	8 (80)	3 (26)	3 (26)
Natalizumab	1 (10)	–	1 (10)
Others	1 (10)	–	–
None previous DMT use [no. (%)]	–	3 (26)	3 (26)
BMI at BL (± SD)	23.8 (2.5)	27.1 (4.0)	25.9 (4.8)
EDSS at BL (± SD)	2.4 (1.0)	2.0 (0.6)	3.6 (1.6)
Relapses during fingolimod (no.)	0	0	0
Confirmed EDSS progression during fingolimod (no.)	0	0	1
MRI progression during fingolimod (no.)	4	2	3
Adverse events—infections (no.)	23	14	15

Baseline characteristics of evaluated patients are depicted. HL (high lymphocyte group) includes patients with lymphocyte count ≥ 1.0 GPT/L after fingolimod start. ML (median lymphocyte group) with lymphocyte count of 0.5–1.0 GPT/l and LL (low lymphocyte group) with lymphocyte count ≤ 0.5 GPT/l. DMT, disease modifying treatment. Other previous treatments included: Laquinimod. Number of relapses, confirmed EDSS progression, MRI progression and infectious events during fingolimod treatment period are presented. Yr, year; SD, standard deviation; f, female; m, male; BL, baseline; no, number.

Lymphocyte subpopulations have been analyzed in all three groups: there were no significant differences at baseline between the three groups for CD4+ T cells and CD19+ B cells (**Figures 3C,E**). In contrast, highest CD8+ T cell and NK cell count was seen in HL group before fingolimod start (**Figures 2D,F**). After fingolimod start, T and B cell subsets significantly dropped in all groups (**Figures 2C–E**, **Table 2**). Interestingly, CD4+ T cells and CD19 B cells dropped similarly and did not differ even at steady state in all three groups (**Figures 2C,E**, **Table 2**), while CD8+ T cells were constantly higher in HL group compared to ML and LL group during fingolimod treatment (**Figure 2D**, **Table 2**). NK cells were not affected by fingolimod treatment but significantly different in absolute count between the HL, ML, and LL group at baseline and follow up (**Figure 2F**, **Table 2**). Evaluation of intra-individual variability of lymphocyte subtypes demonstrated high variability in CD8+ T cells and NK cells especially in HL group whereas ML and LL group presented comparable and lower intra-individual variability (**Figure 2G**). CD4+ T cells and CD19+ B cells were characterized by low variability reflecting constant and stable levels within observation period in all investigated groups (**Figure 2G**). Additional correlation analyses demonstrated that there was a comparable CD4+ T cell decrease irrespective of the lymphocyte count ($r = 0.2849$, n.s.; **Figure 2H**) whereas CD8+ T cell decrease was strongly correlated with lymphocyte decrease in our patients ($r = 0.5998$, $p < 0.001$; **Figure 2I**). These data indicate that variability and occasionally high levels of absolute lymphocyte count are primarily caused by the wide individual variation in CD8+ T cell count, while CD4+ T

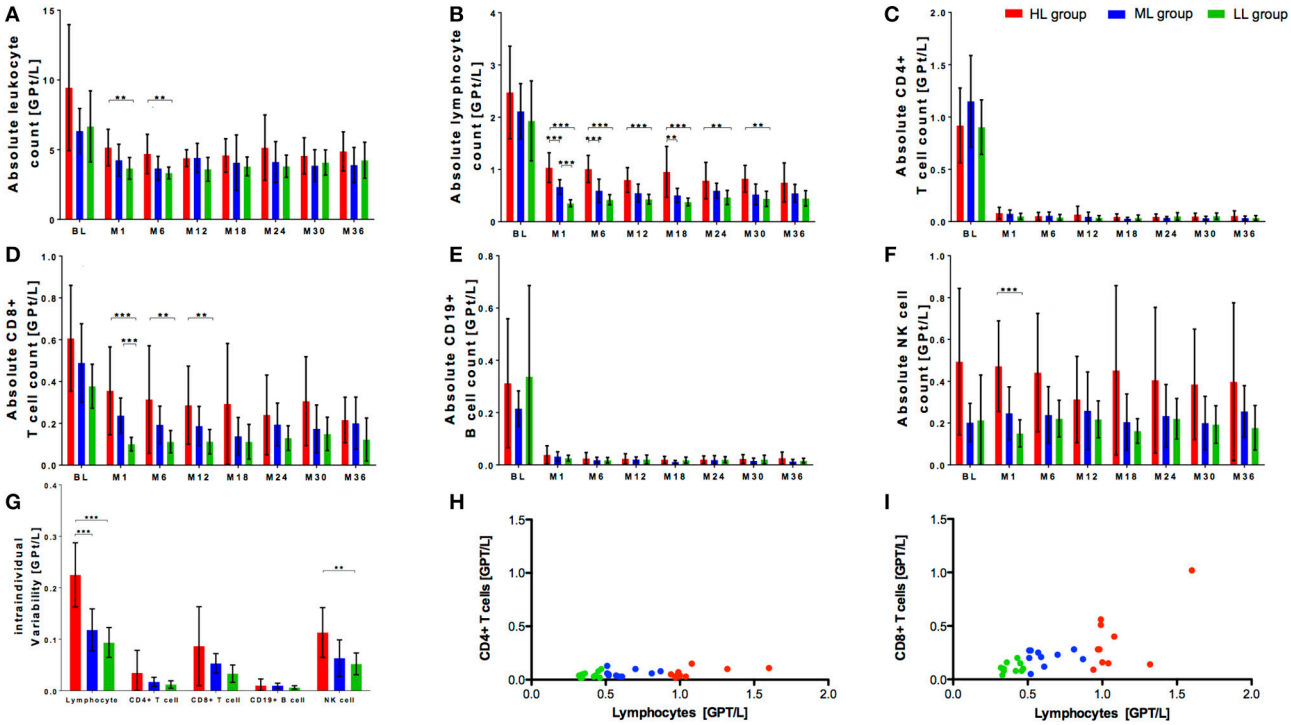


FIGURE 2 | Cell count of selective immune cell subpopulations in cohorts with different initial lymphocyte decrease after fingolimod start. Absolute cell count of leukocytes **(A)**, lymphocytes **(B)**, CD4+ T cells **(C)**, CD8+ T cells **(D)**, CD19+ B cells **(E)**, and NK cells **(F)** are depicted. Three groups of patients during fingolimod treatments are compared: HL group (high lymphocyte count 1 ≥ 1.0 GPt/L, red) ML group (medium lymphocyte count 0.5–1.0 GPt/L, blue) and LL group (low lymphocyte count ≤ 0.5 GPt/L, green). BL, month 1 and 6 months interval of evaluation up to 36 months of fingolimod therapy are depicted. **(G)** Intra-individual variability of lymphocytes, CD4+ T cells and CD8+ T cells, CD19+ B cells and NK cells compared between HL group, ML group and LL group are presented. Intra-individual variability was declared as the standard deviation of absolute cell counts between month 1 to month 36 of fingolimod therapy. Mean ± SD are depicted. Asterisks indicate level of significance of pairwise comparison. (**$p < 0.01$ and ***$p < 0.001$) **(H,I)** Correlation of decrease of CD4+ T cells resp. CD8+ T cells and lymphocytes are presented. Mean of absolute lymphocyte count, CD4+ T cell count and CD8+ T cell count between month 1, month 3, and month 6 after fingolimod start were calculated and depicted. Level of statistical significance was evaluated using Spearman's correlation. **(H)** $r = 0.2849$, n.s. **(I)** $r = 0.5998$, $p < 0.001$.

cells are more robust and less variable to evaluate fingolimod treatment effects.

Initial Drop of Lymphocyte Count Does Not Predict Long-Term Level of Lymphocyte Count

Lymphocyte decrease dependent on individual lymphocyte drop during fingolimod treatment is frequently discussed. Initial drop of lymphocyte count was individually calculated using lymphocyte count at baseline vs. steady state after 6 months for each patient. Median-split was performed for the initial absolute drop of lymphocyte count resulting at 1.40 GPT/l. A lower absolute drop group (LAD group; < 1.40 GPT/l) and a higher absolute drop group (HAD group; ≥ 1.40 GPT/l) were defined. Both groups were not significantly different in age, sex, disease duration, BMI, or EDSS at baseline (**Table 2**). In the HAD there was a significant higher number of patients that were pretreated with natalizumab (21.1% in the HAD vs. 3.6% in the LAD group, $p < 0.01$).

At baseline, absolute lymphocyte count was significantly higher in the HAD group (**Figure 3A**, **Table 2**). Highest baseline lymphocyte counts were seen in previously natalizumab treated patients (treatment stopped 12 weeks before fingolimod initiation), whereas lymphocyte counts in patients with other DMT use or none previous treatments were at comparable range. By definition, the HAD group demonstrated significant higher absolute as well as relative lymphocyte drop compared to LAD group (**Table 3**, $p < 0.001$). Highest drop was found in patients with previous natalizumab treatment (mean absolute drop 2.52 GPT/l ± SD 1.00 GPT/l). During long-term observation, lymphocyte counts were significantly reduced to comparable levels in the LAD group vs. HAD group (**Figure 3A**, **Table 3**). There was no significant correlation between absolute lymphocyte drop and absolute lymphocyte count at steady state ($r = -0.041$, $p = 0.668$). Additional characterization of levels of lymphopenia using NCI-CTAE grading demonstrated that there was a similar distribution of grades of lymphopenia between the LAD group and HAD group threw the whole observation period (**Figures 3H,I**). There was no association between type of previous DMT use and grade of lymphopenia during fingolimod therapy. Independent of degree of lymphocyte drop, disease activity parameters including relapse activity, disability progression and MRI progression were comparable in both groups (**Table 3**).

TABLE 2 | Level of significance for comparing the groups—global effects.

HL/ML/LL group	Group-effect	Time-effect	Time-by-group interaction	HAD/LAD group	Group-effect	Time-effect	Time-by-group interaction	HSS/LSS group	Group-effect	Time-effect	Time-by-group interaction
Leukocyte	$p < 0.001$	$p < 0.001$	$p = 0.747$	Leukocyte	$p < 0.001$	$p < 0.001$	$p = 0.566$	Leukocyte	$p < 0.001$	$p < 0.001$	$p = 0.845$
Lymphocyte	$p < 0.001$	$p < 0.001$	$p = 0.008$	Lymphocyte	$p = 0.120$	$p < 0.001$	$p < 0.001$	Lymphocyte	$p < 0.001$	$p < 0.001$	$p < 0.001$
CD3+ T cell	$p < 0.001$	$p < 0.001$	$p = 0.040$	CD3+ T cell	$p = 0.236$	$p < 0.001$	$p < 0.001$	CD3+ T cell	$p < 0.001$	$p < 0.001$	$p < 0.001$
CD4+ T cell	$p = 0.048$	$p < 0.001$	$p = 0.264$	CD4+ T cell	$p = 0.381$	$p < 0.001$	$p < 0.001$	CD4+ T cell	$p < 0.001$	$p < 0.001$	$p = 0.013$
CD8+ T cell	$p < 0.001$	$p < 0.001$	$p = 0.450$	CD8+ T cell	$p = 0.383$	$p < 0.001$	$p < 0.001$	CD8+ T cell	$p < 0.001$	$p < 0.001$	$p = 0.073$
CD19+ B cell	$p = 0.017$	$p < 0.001$	$p = 0.957$	CD19+ B cell	$p < 0.001$	$p < 0.001$	$p = 0.004$	CD19+ B cell	$p = 0.043$	$p < 0.001$	$p = 0.877$
Monocyte	$p < 0.001$	$p = 0.558$	$p = 0.926$	Monocyte	$p = 0.002$	$p = 0.005$	$p = 0.592$	Monocyte	$p < 0.001$	$p = 0.003$	$p = 0.869$
NK cell	$p < 0.001$	$p = 0.981$	$p = 0.855$	NK cell	$p = 0.220$	$p = 0.955$	$p = 0.165$	NK cell	$p < 0.001$	$p = 0.811$	$p = 0.995$

Values of $p < 0.0125$ were considered significant.

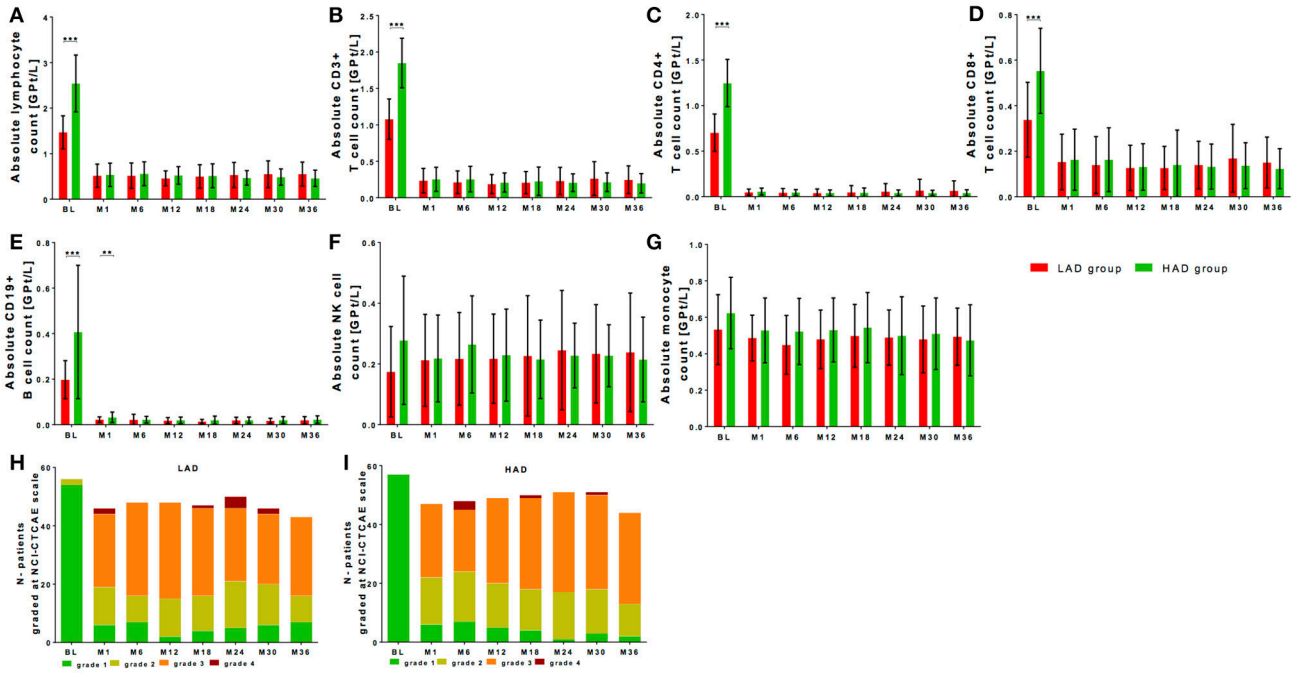


FIGURE 3 | Cell count of selective immune cell subpopulations in patients with high (HAD) vs. low absolute lymphocyte (HAD) drop. Absolute cell counts of lymphocytes **(A)**, CD3+ T cells **(B)**, CD4+ T cells **(C)**, CD8+ T cells **(D)**, CD19+ B cells **(E)**, NK-cells **(F)** and monocytes **(G)** are depicted. Comparison between two groups is presented: LAD group is defined as lower absolute lymphocyte drop group (< 1.40 GPT/l, red) and HAD group defined as higher lymphocyte drop group (≥ 1.40 GPT/l, green) after median-split. Data are shown before fingolimod start (baseline, BL), month 1 and every 6 months follow up. Mean ± SD are depicted. **(H,I)** Distribution of different ranges of lymphocyte count are shown graded with NCI-CTCAE: lymphopenia grade 1 >0.8 GPt/L (green), lymphopenia grade 2 0.5-0.8 GPt/L (yellow), lymphopenia grade 3 0.2-0.5 GPt/L (orange) and lymphopenia grade 4 < 0.2 GPt/L (red). Results are presented for LAD group **(H)** and HAD group **(I)** threw an observation period of 36 months. Asterisks indicate level of significance of pairwise comparison (**$p < 0.01$ and ***$p < 0.001$).

Furthermore, no significant differences in BMI or occurrence of acute infections in the LAD vs. HAD group could be confirmed.

Evaluation of lymphocyte subtypes demonstrated that T and B cells presented with significantly higher absolute cell counts at baseline in the HAD group (**Figures 3B–E**, **Table 3**). After significant drop, T and B cells were at comparable levels in both groups during fingolimod treatment (**Figures 3B–E**, **Table 3**). There were no differences in absolute NK cell at baseline and after treatment initiation between HAD and LAD group (**Figure 3F**, **Table 3**). In monocytes only mild changes were found during fingolimod treatment in both groups (**Figure 3G**, **Table 3**).

Lymphocyte Subtypes Differ in Patients With High-Level vs. Low-Level Steady State Lymphopenia

It is known that lymphocyte count and changes of its subpopulations reach at latest their steady state 6 months after

fingolimod start. Median-split was calculated for the steady state period after month 6 (lymphocyte count of 0.48GPT/l). A lower steady state group (LSS group; < 0.48 GPT/l) and a higher steady state group (HSS group; ≥ 0.48 GPT/l) was defined. There were no significant differences in age, disease duration, previous DMT use, EDSS or BMI at baseline (**Table 3**). In the LSS group a significant higher number of women (LSS group 70.3% vs. HSS group 45.7%) could be identified ($p < 0.05$).

Baseline lymphocyte levels demonstrated only a trend to higher baseline lymphocyte counts in the HSS group that were significantly decreased to different levels of lymphocyte steady state in both groups (**Figure 4A**, **Table 2**). As well after fingolimod start, the absolute lymphocyte drop was not different between LSS group and HSS group in reference to baseline levels; a higher significant relative lymphocyte drop ($p < 0.001$) could be shown for LSS group (**Table 4**). Grading with NCI-CTAE scale demonstrated that LSS group included single patients that presented with lymphocyte counts at grade 2 already before fingolimod start (**Figure 4H**). All of these patients were pretreated with interferon-beta treatment that was stopped two weeks before fingolimod start. During follow up, almost all patients in the LSS group presented with lymphocyte counts lower than grade 2 and up to grade 4 (**Figure 4H**). None of these patients stopped fingolimod treatment due to lymphopenia during the observation period as retest revealed grade 3 lymphopenia. HSS group included only patients with lymphocyte levels in the reference range before fingolimod start and none of the patients presented lymphocyte levels lower than grade 3 during follow up (**Figure 4I**). There was no association between type of previous DMT use and grade of lymphopenia during fingolimod therapy. Patients that presented lymphocyte counts at lower NCI-CTAE grade were not at risk for increased occurrence of infections compared to patients with higher lymphocyte count grade (**Table 4**). We could not find any differences in BMI between the LSS group and HSS group. There were no significant differences in clinical progression or MRI activity over the 36 months observation period in LSS vs. HSS patients (**Table 4**).

There were no significant differences regarding baseline levels of all analyzed T and B cell subpopulations between LSS group and HSS group (**Figures 4B–E**). After fingolimod start, CD4+ T cells and CD19+ B cells significantly decreased to comparable levels, whereas CD8+ T cells were significantly higher in the HSS group vs. LSS group (**Figures 4C–E**, **Table 2**). In addition, NK cells presented with higher counts at baseline and during treatment period in HSS patients (**Figure 4F**, **Table 2**). Interestingly, monocytes were higher at baseline and follow up in the HSS compared to the LSS group (**Figure 4G**, **Table 2**).

TABLE 3 | Patient characteristics.

	LAD group	HAD group
N patients	56	57
Age (yr ± SD)	39.9 (9.6)	39.0 (10.1)
Duration since MS diagnosis (yr ± SD)	6.4 (5.6)	7.1 (6.1)
Sex (f/m)	28/28	37/20
Previous DMT use before fingolimod start [no. (%)]	43 (76.8)	48 (84.2)
Interferon beta	23 (41.1)	22 (38.6)
Glatirameracetat	14 (25.0)	13 (22.8)
Natalizumab	2 (3.6)	12 (21.1)
Others	4 (7.1)	1 (1.8)
None previous DMT use [no. (%)]	13 (23.2)	9 (15.8)
BMI—BL (± SD)	24.1 (4.0)	25.6 (5.1)
EDSS—BL (± SD)	3.0 (1.6)	2.7 (1.3)
Lymphocyte absolute drop [GPT/L] Mean (95% CI)	0.95 (0.87; 1.03)	2.04 (1.88; 2.20)
Lymphocyte relative drop [%] Mean (95% CI)	64.01 (60.80; 67.21)	79.65 (78.03; 81.26)
Lymphocyte steady state [GPT/L] Mean (95% CI)	0.52 (0.46; 0.57)	0.50 (0.46; 0.55)
Relapse during fingolimod (no.)	13	12
Confirmed EDSS progression during fingolimod (no.)	9	11
MR progression during fingolimod (no.)	18	17
Adverse events—infections (no.)	38	40

Patient characteristics of evaluated patients are depicted. LAD group (lower absolute drop group) includes patients with an absolute lymphocyte drop < 1.40 GPT/l. HAD includes patients with an absolute lymphocyte drop ≥ 1.40 GPT/l. DMT, disease modifying treatment. Other previous treatments included: Azathioprin (2), Laquinimod (3). Number of relapses, confirmed EDSS progression, MRI progression and infectious events during fingolimod treatment period are presented. Yr, year; SD, standard deviation; f, female; m, male; BL, baseline; no, number.

DISCUSSION

Lymphopenia is an integral part of fingolimod therapy based on its unique mechanism of action (8). Already initial clinical trials reported a decrease of lymphocyte count about 70% and discussed wide inter-individual differences in lymphocyte drop and fluctuation of total lymphocyte count in treated patients (27–29) There are different hypotheses which try to interpret the variation in levels of lymphopenia in fingolimod treated patients (19, 23, 30). Previous reports already discussed no relevant relation between degree of lymphopenia and clinical efficacy as well as occurrence of side effects (21, 28). Up to date it is unclear whether and why patients appear with less or marked decrease in lymphocyte count after fingolimod start.

Real-world data provide longitudinal information on different outcomes including effects on lab parameters (24). Implementing lab data into a comprehensive real world data approach can complete the fundamental quest of real world evidence for individually improved treatment decisions and balanced therapeutic risk assessment. In our observation, we evaluated individual variation of lymphocytes and its subsets in a long-term real life setting. There was a wide range of baseline lymphocyte levels in our cohort. Differences in baseline lymphocyte count dependent on previous DMT use cannot be excluded based on restricted washout periods. In our evaluation, moderate lymphopenia at baseline was more frequent in interferon-beta treated patients whereas natalizumab pretreatment lead

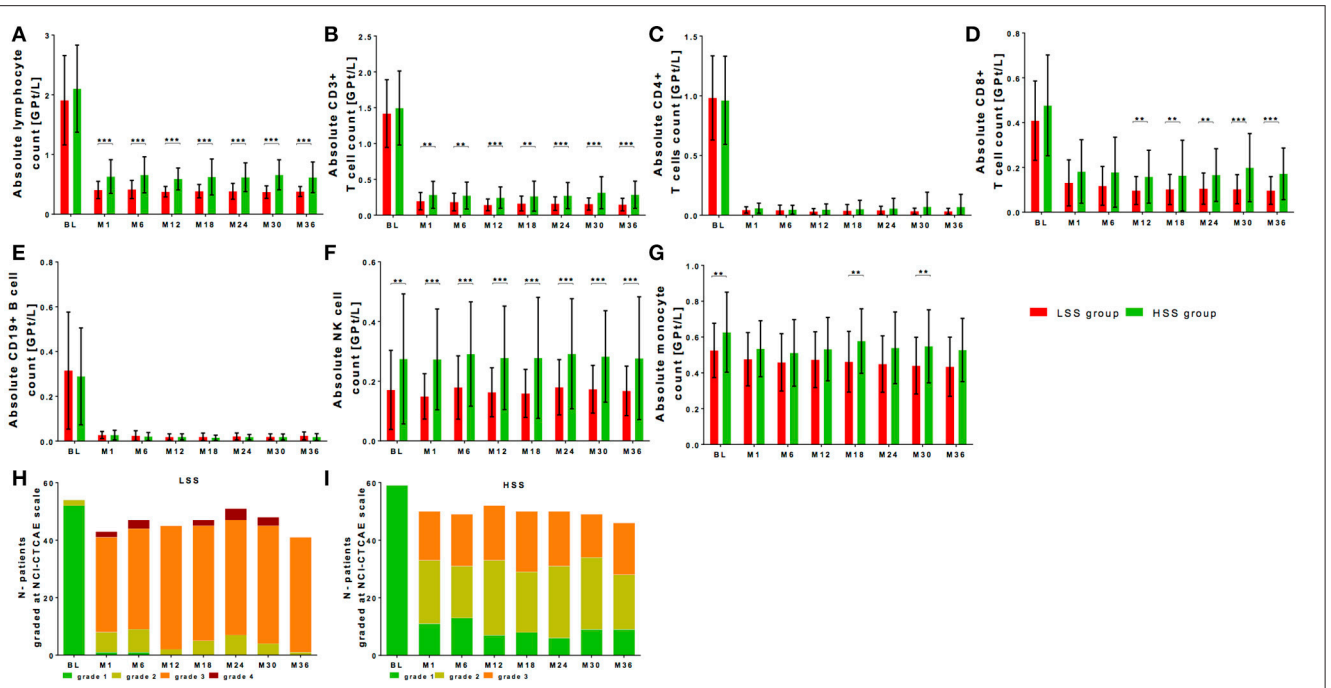


FIGURE 4 | Cell count of selective immune cell subpopulations in patients with high-level vs. low-level steady-state lymphopenia. Absolute cell counts of lymphocytes **(A)**, CD3+ T cells **(B)**, CD4+ T cells **(C)**, CD8+ T cells **(D)**, CD19+ B cells **(E)**, NK cells **(F)**, and monocytes **(G)** are depicted. Comparison between two groups is presented: LSS group defined as lower steady state group (< 0.48 GPT/l; red) and HSS group defined as higher steady state group (≥ 0.48 GPT/l; green) after median split. Data are shown before fingolimod start (baseline, BL), month 1 and every 6 month follow up. Mean ± SD are depicted. **(H,I)** Distribution of different ranges of lymphocyte count are shown graded with NCI-CTCAE: lymphopenia grade 1 >0,8 GPt/L (green), lymphopenia grade 2 0,5-0,8 GPt/L (yellow), lymphopenia grade 3 0,2-0,5 GPt/L (orange) and lymphopenia grade 4 < 0,2 GPt/L (red). Results are presented for LSS group **(H)** and HSS group **(I)** threw an observation period of 36 months. Asterisks indicate level of significance of pairwise comparison (**$p < 0.01$ and ***$p < 0.001$).

to higher levels at fingolimod start. Other reports discussed that higher baseline lymphocyte levels were associated with higher lymphocyte count threw follow up (20, 22). Furthermore, increased risk of fingolinod-associated lymphopenia in patients with interferon-beta pretreatment was suggested (20). In our cohort, we could not statistically prove that higher baseline levels or different pretreatment conditions were associated with the level of lymphocyte count or decrease at steady state during fingolimod therapy. Previous reports discussed an increased risk of lymphopenia in patients with BMI <18.5 kg/m^2 (20). Others presented data that could not confirm correlation between BMI and lymphopenia levels (22). In our observation, we could not define a significant relation between BMI and lymphocyte count, probably because only four patients presented persistent BMI levels <18.5 kg/m^2. Nevertheless, its lymphocyte count was reduced about 0.39–1.13 GPT/l at comparable range in contrast to other treated patients.

Interestingly, the absolute and relative lymphocyte drop after fingolimod start could not predict the level of lymphopenia in our cohort. Although marked differences in lymphocyte drop were present between patients, lymphocyte levels reached comparable levels independent of degree of lymphocyte drop. Most of the recent reports evaluating lymphopenia and its variation in fingolimod treated patients did not analyze specific lymphocyte subtypes. Although absolute lymphocyte count differed in our patients, additional analysis of lymphocyte subtypes confirmed that CD4+ T cells and CD19+ B cells were decreased at a comparable level with narrow intra- and inter-individual variation in all fingolimod treated patients irrespective of the degree of lymphopenia.

In line with previous data, absolute NK cells count was not altered by fingolimod treatment in our cohort (26). NK cell recirculation is mediated by S1PR1 and S1PR5. It is suggested that S1PR5 is less susceptible to fingolimod than S1PR1, which is used by the other lymphocyte subtypes (31). These circulating NK cells maintain their functional capacity and contribute to the immunosurveillance by the innate immune system in fingolimod treated patients (32). In our study, patients with lower lymphocyte count during fingolimod treatment were associated with significant lower NK cell number. Intra-individual fluctuation of NK cell count was highest in patients with higher level of lymphocyte count compared to patients with lower level of lymphocyte count and did significantly differ compared to CD4+ T cells and CD19+ B cells. Main differences in absolute lymphocyte count were induced by variation in NK cell count.

Although initially supposed, degree of lymphopenia could not confirm a correlation with clinical treatment response (21).

TABLE 4 | Patient characteristics.

	LSS group	HSS group
N patients	54	59
Age (yr ± SD)	40.4 (10.0)	38.6 (9.6)
Duration since MS diagnosis (yr ± SD)	7.7 (6.0)	5.7 (5.6)
Sex (f/m)	38/16	27/32
Previous DMT use before fingolimod start [no. (%)]	45 (83.3)	46 (78.0)
Interferon beta	25 (46.3)	20 (33.9)
Glatirameracetat	10 (18.5)	17 (28.8)
Natalizumab	6 (11.1)	8 (13.6)
Others	4 (7.4)	1 (1.7)
None previous DMT use [no. (%)]	9 (16.7)	13 (22.0)
BMI—Baseline (± SD)	24.5 (4.6)	25.3 (4.7)
EDSS—Baseline (± SD)	3.0 (1.5)	2.7 (1.3)
Lymphocyte absolute drop [GPT/L] Mean (95% CI)	1.52 (1.32;1.73)	1.48 (1.29;1.66)
Lymphocyte relative drop [%] Mean (95% CI)	76.86 (74.05;79.68)	67.35 (64.16;70.54)
Lymphocyte steady state [GPT/L] Mean (95% CI)	0.38 (0.37;0.40)	0.63 (0.58;0.68)
Relapse during fingolimod (no.)	15	10
Confirmed EDSS progression during fingolimod (no.)	13	7
MR progression during fingolimod (no.)	15	20
Adverse events—infections (no.)	39	39

Patient characteristics of evaluated patients are depicted. LSS group (lower steady state group) includes patients with a lymphocyte count at steady state < 0.48 GPT/l. HSS group (higher steady state group) includes patients with a lymphocyte count at steady state ≥ 0.48 GPT/l. Number of relapses, confirmed EDSS progression, MRI progression and infectious events during fingolimod treatment period are presented. Yr, year; SD, standard deviation; f, female; m, male; BL, baseline; no, number.

Others discussed increased CD3+ and CD8+ T cell counts and decreased number of NK cells in first 6 months of fingolimod therapy as predictive marker for relapse activity (23). In our cohort, some patients presented with lymphocyte counts above 1.0 GPT/l. In these patients we could not confirm differences of clinical MS disease activity compared to patients with < 1.0 GPT/l or even < 0.5 GPT/l lymphopenia. Differences in lymphocyte count were caused by higher levels and of CD8+ T cell and NK cell count in higher lymphocyte cohort whereas CD4+ T cells and CD19+ B cells were markedly and comparable decreased in all three groups. Though, we suppose that decrease in CD4+ T cell count is associated with fingolimod efficacy and response rather than complete lymphocyte count.

During fingolimod treatment, the degree of lymphopenia and its clinical relevance defined by increased risk of infectious events is critically discussed (18, 30). Grading the level of lymphopenia using the NCI-CTAE is done especially for oncological diseases and treatment to define patients at higher risk for infections (17). Level of lymphopenia displayed in our cohort presented a wide range of distribution from grade 1 to grade 4 of the NCT-CTAE scale. Nevertheless, we could not prove an increased incidence of infectious adverse events in the lower vs. higher-level lymphopenia group. These data are in line with several studies presenting primarily mild to moderate infections during fingolimod (8, 18, 28) The most relevant infectious complication in fingolimod treated patients is defined by varicella-zoster virus (VZV) and herpes simplex virus (HSV) infection or reactivation (8, 18, 33). However, individual variation of VZV specific T cell responses are assumed to be more relevant for upcoming VZV activation rather than absolute lymphocyte counts (34, 35). Up to date, we are not able to confirm that monitoring of absolute lymphocyte count or its subtypes can assist to predict higher infectious risk at lymphocyte counts of 0.2 GPT/l. Instead, cases of severe upcoming disease activity after fingolimod cessation because of lymphopenia (<0.2 GPT/l) are known (35, 36). Though, fingolimod interruption on the basis of lymphopenia of < 0.2 GPT/l has to be critically discussed in the individual context.

In summary, we demonstrate that CD4+ T cells and CD19+ B cells are comparably decreased in all fingolimod treated patients whereas grade of lymphopenia is primarily defined by individual variation of CD8+ T cell and NK cells. Monitoring of absolute lymphocyte drop and absolute lymphocyte count at steady state is only partially helpful as they do not cover distinct changes in the specific immune cell distribution. Our results suggest that monitoring of cellular target populations as CD4+ T cells seems to be more straight forward and probably clinically relevant to weigh and interpret the degree of immunological effects in fingolimod treated patients.

ETHICS STATEMENT

We confirm that any aspect of the work covered in this manuscript that has involved human patients has been conducted with the ethical approval of all relevant bodies (EK 348092014). The study was performed according the Declaration of Helsinki, and the study protocol was approved by the Ethics Committee of the Faculty of Medicine of the Dresden University of Technology. The authors have received consent forms from any participants in the study and have these forms available in case they are requested by the editor.

AVAILABILITY OF THE DATA AND MATERIAL

KA and TZ have full access to all the data in the study and take full responsibility for integrity of the data and the accuracy of the data analysis. Raw data are available on personal demand.

AUTHOR CONTRIBUTIONS

KA and TZ: Study concept and design; MK: Acquisition of data; MK, KA, RH, and UP: Analysis and interpretation of data; MK, KA, and TZ: Drafting of the manuscript; UP and RH: Critical

revision of the manuscript for important intellectual content; MK, and RH: Statistical analysis.

ACKNOWLEDGEMENTS

We are grateful to Prof. Dr. T. Chavakis from the Institute of clinical chemistry and laboratory medicine, University clinic Dresden for performing the analysis and providing the data. We acknowledge support by the Open Access Publication Funds of the SLUB/TU Dresden.

SUPPLEMENTARY MATERIAL

The Supplementary Material for this article can be found online at: https://www.frontiersin.org/articles/10.3389/fimmu.2018.02669/full#supplementary-material

REFERENCES

1. Ziemssen T, De Stefano N, Pia Sormani M, Van Wijmeersch B, Wiendl H, Kieseier BC. Optimizing therapy early in multiple sclerosis: an evidence-based view. *Mult Scler Relat Disord.* (2015) 4:460–9. doi: 10.1016/j.msard.2015.07.007
2. Wiendl H, Kieseier B. Multiple sclerosis: reprogramming the immune repertoire with alemtuzumab in MS. *Nat Rev Neurol.* (2013) 9:125–6. doi: 10.1038/nrneurol.2013.2
3. Brinkmann V, Davis MD, Heise CE, Albert R, Cottens S, Hof R, et al. The immune modulator FTY720 targets sphingosine 1-phosphate receptors. *J Biol Chem.* (2002) 277:21453–7. doi: 10.1074/jbc.C200176200
4. Brinkmann V, Cyster JG, Hla T. FTY720: sphingosine 1-phosphate receptor-1 in the control of lymphocyte egress and endothelial barrier function. *Am J Transplant* (2004) 4:1019–25. doi: 10.1111/j.1600-6143.2004.00476.x
5. Chun J, Hartung HP. Mechanism of action of oral fingolimod (FTY720) in multiple sclerosis. *Clin Neuropharmacol.* (2010) 33:91–101. doi: 10.1097/WNF.0b013e3181cbf825
6. Grutzke B, Hucke S, Gross CC, Herold MV, Posevitz-Fejfar A, Wildemann BT, et al. Fingolimod treatment promotes regulatory phenotype and function of B cells. *Ann Clin Transl Neurol.* (2015) 2:119–30. doi: 10.1002/acn3.155
7. Rudnicka J, Czerwiec M, Grywalska E, Siwicka-Gieroba D, Walankiewicz M, Grafka A, et al. Influence of fingolimod on basic lymphocyte subsets frequencies in the peripheral blood of multiple sclerosis patients - preliminary study. *Cent Eur J Immunol.* (2015) 40:354–9. doi: 10.5114/ceji.2015.54599
8. Thomas K, Proschmann U, Ziemssen T. Fingolimod hydrochloride for the treatment of relapsing remitting multiple sclerosis. *Expert Opin Pharmacother.* (2017) 18:1649–60. doi: 10.1080/14656566.2017.1373093
9. Thomas K, Sehr T, Proschmann U, Rodriguez-Leal FA, Haase R, Ziemssen T. Fingolimod additionally acts as immunomodulator focused on the innate immune system beyond its prominent effects on lymphocyte recirculation. *J Neuroinflammation* (2017) 14:41. doi: 10.1186/s12974-017-0817-6
10. Signoriello E, Lanzillo R, Brescia Morra V, Di Iorio G, Fratta M, Carotenuto A, et al. Lymphocytosis as a response biomarker of natalizumab therapeutic efficacy in multiple sclerosis. *Mult Scler.* (2016) 22:921–5. doi: 10.1177/1352458515604381
11. Carotenuto A, Scalia G, Ausiello F, Moccia M, Russo CV, Sacca F, et al. CD4/CD8 ratio during natalizumab treatment in multiple sclerosis patients. *J Neuroimmunol.* (2017) 309:47–50. doi: 10.1016/j.jneuroim.2017.05.006
12. Fox RJ, Miller DH, Phillips JT, Hutchinson M, Havrdova E, Kita M, et al. Placebo-controlled phase 3 study of oral BG-12 or glatiramer in multiple sclerosis. *N Engl J Med.* (2012) 367:1087–97. doi: 10.1056/NEJMoa1206328
13. Gold R, Kappos L, Arnold DL, Bar-Or A, Giovannoni G, Selmaj K, et al. Placebo-controlled phase 3 study of oral BG-12 for relapsing multiple sclerosis. *N Engl J Med.* (2012) 367:1098–107. doi: 10.1056/NEJMoa1114287
14. Thomas K, Ziemssen T. Management of fingolimod in clinical practice. *Clin Neurol Neurosurg.* (2013) 115(Suppl 1):S60–64. doi: 10.1016/j.clineuro.2013.09.023
15. Giovannoni G, De Jong B, Derfuss T, Izquierdo G, Mazibrada G, Molyneux P, et al. A pragmatic approach to dealing with fingolimod-related lymphopaenia in Europe. *Mult Scler Relat Disord.* (2015) 4:83–4. doi: 10.1016/j.msard.2014.09.215
16. Nakhaei-Nejad M, Barilla D, Lee CH, Blevins G, Giuliani F. Characterization of lymphopenia in patients with MS treated with dimethyl fumarate and fingolimod. *Neurol Neuroimmunol Neuroinflamm.* (2018) 5:e432. doi: 10.1212/NXI.0000000000000432
17. Trotti A, Colevas AD, Setser A, Rusch V, Jaques D, Budach V, et al. CTCAE v3.0: development of a comprehensive grading system for the adverse effects of cancer treatment. *Semin Radiat Oncol* (2003) 13:176–81. doi: 10.1016/S1053-4296(03)00031-6
18. Redelman-Sidi G, Michielin O, Cervera C, Ribi C, Aguado JM, Fernandez-Ruiz M, et al. ESCMID study group for infections in compromised hosts (ESGICH) consensus document on the safety of targeted and biological therapies: an infectious diseases perspective (Immune checkpoint inhibitors, cell adhesion inhibitors, sphingosine-1-phosphate receptor modulators and proteasome inhibitors). *Clin Microbiol Infect.* (2018) 24(Suppl 2):S95–107. doi: 10.1016/j.cmi.2018.01.030
19. Henault D, Galleguillos L, Moore C, Johnson T, Bar-Or A, Antel J. Basis for fluctuations in lymphocyte counts in fingolimod-treated patients with multiple sclerosis. *Neurology* (2013) 81:1768–72. doi: 10.1212/01.wnl.0000435564.92609.2c
20. Warnke C, Dehmel T, Ramanujam R, Holmen C, Nordin N, Wolfram K, et al. Initial lymphocyte count and low BMI may affect fingolimod-induced lymphopenia. *Neurology* (2014) 83:2153–7. doi: 10.1212/WNL.0000000000001049
21. Fragoso YD, Spelman T, Boz C, Alroughani R, Lugaresi A, Vucic S, et al. Lymphocyte count in peripheral blood is not associated with the level of clinical response to treatment with fingolimod. *Mult Scler Relat Disord.* (2018) 19:105–8. doi: 10.1016/j.msard.2017.11.018
22. Ohtani R, Mori M, Uchida T, Uzawa A, Masuda H, Liu J, et al. Risk factors for fingolimod-induced lymphopenia in multiple sclerosis. *Mult Scler J Exp Transl Clin.* (2018) 4:2055217318759692. doi: 10.1177/2055217318759692
23. Paolicelli D, Manni A, D'onghia M, Direnzo V, Iaffaldano P, Zoccolella S, et al. Lymphocyte subsets as biomarkers of therapeutic response in Fingolimod treated relapsing multiple sclerosis patients. *J Neuroimmunol.* (2017) 303:75–80. doi: 10.1016/j.jneuroim.2016.12.012
24. Ziemssen T, Hillert J, Butzkueven H. The importance of collecting structured clinical information on multiple sclerosis. *BMC Med.* (2016) 14:18. doi: 10.1186/s12916-016-0627-1
25. Haase R, Wunderlich M, Dillenseger A, Kern R, Akgun K, Ziemssen T. Improving multiple sclerosis management and collecting safety information in the real world: the MSDS3D software approach. *Expert Opinion on Drug Safety* (2018) 17:369–78. doi: 10.1080/14740338.2018.1437144
26. Vaessen LM, Van Besouw NM, Mol WM, Ijzermans JN, Weimar W. FTY720 treatment of kidney transplant patients: a differential effect on B cells, naive T cells, memory T cells and NK cells. *Transpl Immunol.* (2006) 15:281–8. doi: 10.1016/j.trim.2006.02.002
27. Kappos L, Radue EW, O'connor P, Polman C, Hohlfeld R, Calabresi P, et al. A placebo-controlled trial of oral fingolimod in relapsing multiple sclerosis. *N Engl J Med.* (2010) 362:387–401. doi: 10.1056/NEJMoa0909494
28. Kappos L, Cohen J, Collins W, De Vera A, Zhang-Auberson L, Ritter S, et al. Fingolimod in relapsing multiple sclerosis: An integrated analysis of safety findings. *Mult Scler Relat Disord.* (2014) 3:494–504. doi: 10.1016/j.msard.2014.03.002
29. Teniente-Serra A, Hervas JV, Quirant-Sanchez B, Mansilla MJ, Grau-Lopez L, Ramo-Tello C, et al. Baseline differences in minor lymphocyte subpopulations may predict response to fingolimod in relapsing-remitting multiple sclerosis patients. *CNS Neurosci Ther.* (2016) 22:584–92. doi: 10.1111/cns.12548

30. Francis G, Kappos L, O'connor P, Collins W, Tang D, Mercier F, et al. Temporal profile of lymphocyte counts and relationship with infections with fingolimod therapy. *Mult Scler.* (2014) 20:471–80. doi: 10.1177/1352458513500551
31. Gross CC, Schulte-Mecklenbeck A, Wiendl H, Marcenaro E, Kerlero De Rosbo N, Uccelli A, et al. Regulatory functions of natural killer cells in multiple sclerosis. *Front Immunol.* (2016) 7:606. doi: 10.3389/fimmu.2016.00606
32. Johnson TA, Evans BL, Durafourt BA, Blain M, Lapierre Y, Bar-Or A, et al. Reduction of the peripheral blood CD56(bright) NK lymphocyte subset in FTY720-treated multiple sclerosis patients. *J Immunol.* (2011) 187:570–9. doi: 10.4049/jimmunol.1003823
33. Quirant-Sanchez B, Hervas-Garcia JV, Teniente-Serra A, Brieva L, Moral-Torres E, Cano A, et al. Predicting therapeutic response to fingolimod treatment in multiple sclerosis patients. *CNS Neurosci Ther.* (2018) 24:1175–84. doi: 10.1111/cns.12851
34. Asanuma H, Sharp M, Maecker HT, Maino VC, Arvin AM. Frequencies of memory T cells specific for varicella-zoster virus, herpes simplex virus, and cytomegalovirus by intracellular detection of cytokine expression. *J Infect Dis.* (2000) 181:859–66. doi: 10.1086/315347
35. Avasarala J, Jain S, Urrea-Mendoza E. Approach to Fingolimod-induced lymphopenia in multiple sclerosis patients: do we have a roadmap? *J Clin Pharmacol.* (2017) 57:1415–8. doi: 10.1002/jcph.945
36. Hatcher SE, Waubant E, Nourbakhsh B, Crabtree-Hartman E, Graves JS. Rebound syndrome in patients with multiple sclerosis after cessation of fingolimod treatment. *JAMA Neurol.* (2016) 73:790–4. doi: 10.1001/jamaneurol.2016.0826

Conflict of Interest Statement: KA received personal compensation for from Novartis, Biogen Idec, Roche, Sanofi, and Merck for consulting service. TZ received personal compensation from Biogen Idec, Bayer, Novartis, Sanofi, Teva, and Synthon for consulting services and received additional financial support for research activities from Bayer, Biogen Idec, Novartis, Teva, and Sanofi Aventis. UP speaker fee from Roche. RH received speaker fee from Sanofi.

The remaining author declares that the research was conducted in the absence of any commercial or financial relationships that could be construed as a potential conflict of interest.

Copyright © 2018 Kaufmann, Haase, Proschmann, Ziemssen and Akgün. This is an open-access article distributed under the terms of the Creative Commons Attribution License (CC BY). The use, distribution or reproduction in other forums is permitted, provided the original author(s) and the copyright owner(s) are credited and that the original publication in this journal is cited, in accordance with accepted academic practice. No use, distribution or reproduction is permitted which does not comply with these terms.

frontiers in Neurology

ORIGINAL RESEARCH
published: 07 December 2018
doi: 10.3389/fneur.2018.01071

Real-World Lab Data in Natalizumab Treated Multiple Sclerosis Patients Up to 6 Years Long-Term Follow Up

Maxi Kaufmann, Rocco Haase, Undine Proschmann, Tjalf Ziemssen† and Katja Akgün†*

MS Center Dresden, Center of Clinical Neuroscience, Carl Gustav Carus University Hospital, University of Technology Dresden, Dresden, Germany

Natalizumab inhibits the transmigration of immune cells across the blood-brain barrier thus inhibiting inflammation in the central nervous system. Generally, this blockade at the blood-brain barrier has significant influence on the circulating lymphocytes. Up to date, only short-term data on peripheral blood parameters are available which are mostly from controlled clinical trials and not from real-world experience. Real-world lab data of 120 patients diagnosed with highly active disease course of relapsing-remitting multiple sclerosis (RRMS) were analyzed during natalizumab treatment. Patient sampling was performed by consecutive recruitment in the Multiple Sclerosis Center Dresden. Lab testing was performed before and at every third infusion up to 72 months follow-up. After first natalizumab infusion, absolute numbers of all major lymphocyte populations including CD4+ T-cells, CD8+ T-cells, CD19+ B-cells, and NK-cells significantly increased and remained stable during the whole observation period of 72 months. Upon lymphocyte subsets, CD19+ B-cells presented a disproportionate increase up to levels higher than normal level in most of the treated patients. Neutralizing antibodies to natalizumab abrogated the described changes. Intra-individual variation of lymphocytes and its subsets remained in a narrow range for the whole treatment period. CD4/CD8 ratio did not change compared to baseline measurement up to 6 years of natalizumab treatment. Monocytes, eosinophils, and basophils, but not neutrophils persistently increased during natalizumab treatment. Hematological parameters including erythrocyte, platelet count, hemoglobin, and hematocrit remained unchanged compared to baseline. Interestingly, immature precursor cells including erythroblasts were detectable in 36,8% of the treated patients during natalizumab therapy, but not in the pretreatment period. Asymptomatic elevations of liver enzymes were rare, mostly only transient and lower than 3x upper normal limit. Kidney function parameters remained stable within physiological ranges in most patients. CRP levels >20 mg/dl were recognized only in 10 patients during natalizumab therapy and were mostly linked to respiratory tract infections. In our present analysis, we report persistent, but stable increases of peripheral immune cell subtypes in natalizumab treated patients. Additional serological analyses confirm excellent tolerability and safety even 6 years after natalizumab initiation in post-marketing experience.

Keywords: natalizumab, multiple sclerosis, real-world lab data, peripheral immune cell subtypes, clinical practice

OPEN ACCESS

Edited by:
Tobias Ruck,
Universität Münster, Germany

Reviewed by:
Anne-Katrin Pröbstel,
University of California, San Francisco, United States
Niels Hellings,
University of Hasselt, Belgium

***Correspondence:**
Tjalf Ziemssen
tjalf.ziemssen@uniklinikum-dresden.de

†*These authors have contributed to this work as senior authors*

Specialty section:
This article was submitted to Multiple Sclerosis and Neuroimmunology, a section of the journal Frontiers in Neurology

Received: *24 August 2018*
Accepted: *23 November 2018*
Published: *07 December 2018*

Citation:
Kaufmann M, Haase R, Proschmann U, Ziemssen T and Akgün K (2018) Real-World Lab Data in Natalizumab Treated Multiple Sclerosis Patients Up to 6 Years Long-Term Follow Up. Front. Neurol. 9:1071. doi: 10.3389/fneur.2018.01071

INTRODUCTION

Natalizumab (NAT) is a humanized monoclonal antibody selectively directed against the α4-subunit of the very late antigen-4 (VLA-4) integrin, a specific adhesion molecule on the surface of leukocytes except neutrophils. The α4-integrin interacts with the vascular cell adhesion molecule-1 (VCAM-1) expressed on endothelial cells of blood vessels to mediate extravasation and transmigration of immune cells across the blood-brain barrier into the central nervous system (CNS) (1–3). By its unique mechanism of action, NAT blocks the VLA-4/VCAM-1 mediated leukocyte-endothelial interaction (2, 4). Though, lymphocyte migration into brain tissue is prevented and the CNS inflammation is inhibited (5). NAT is highly effective in relapsing-remitting (RR) multiple sclerosis (MS) proven by marked decrease in relapse rate, MRI activity and disease progression (6, 7). There is a growing experience in selection of appropriated patients and use of NAT in everyday clinical practice since approval. Among disease-modifying treatments (DMT) in MS therapy, NAT is associated with an increased risk of progressive multifocal leukoencephalopathy (PML) especially in John Cunningham virus (JCV) positive and long-term treated patients (8). Since re-approval in 2006, a detailed and standardized management program was established which is now used in everyday clinical practice (8–10). As part of this risk management plan, standardized lab testing is recommended including complete blood count, peripheral immune cell status, and serological parameters to be aware of clinical relevant changes. Especially lymphocytosis has been already described in NAT-treated patients due to impaired lymphocyte extravasation into tissues as well as mobilization of hematopoetic precursor cells from bone marrow (11–16). As part of our NAT management, data from clinical practice are collected providing longitudinal information on different outcomes inclusive adverse affects (17). Such real-world evidence (RWE) and observational studies are becoming increasingly popular because they reflect the usefulness of drugs in real life and have the ability to discover uncommon or rare adverse drug reactions inclusive lab abnormalities (18). Therefore, RWE can assist to evaluate the drug profile in clinical practice and to link it with other clinical outcomes. The MSDS3D software which has been adapted to the NAT management in particular combines documentation of patient data with management of patients with MS implementing treatment-specific modules, to collect data of safety management inclusive lab data with regard to the characteristics of different treatments and populations (19).

Today, NAT has been successfully used in MS patients for more than 11 years. The increase in lymphocyte count was already discussed during the initial clinical trials (6, 20). Further single evaluations followed after approval and in post-marketing experience (21–24). Nevertheless, a systematic and long-term evaluation of real-world routine lab testing data including peripheral cell subtypes and serological parameters is not yet available.

In this study, we present real world laboratory data of a cohort of NAT treated patients up to 72 months follow up. We aim to describe the biological impact of NAT on peripheral blood cell subset distribution during long period treatment observation in the real world. Additional serological analyses allow evaluation of tolerability and safety after NAT initiation in real world experience.

Abbreviations: ALAT, alanine aminotransferase; ASAT, aspartate aminotransferase; CNS, central nervous system; CRP, C-reactive protein; DMT, disease modifying drug; gamma-GT, gamma-glutamyltransferase; EDSS, Expanded Disability Status Scale; i.v., intravenously; JCV, John Cunningham virus; MRI, magnet resonance imaging; MS, multiples sclerosis; NAT, natalizumab; NEDA, no evidence of disease activity; NK cells, natural killer cells; PML, progressive multifocal leukoencephalopathy; RR, relapsing remitting; VCAM-1, vascular cell adhesion molecule-1; VLA-4, very late antigen 4.

METHODS

Patients

We included 120 patients (91 females and 29 males) diagnosed with RRMS according the McDonald criteria and highly active disease course (25). After critical review of clinical and MRI data as well as available treatment options, NAT treatment was initiated. Patient sampling was performed by consecutive recruitment (**Figure 1**) in the MS center, University Hospital Dresden. Expanded Disability Status Scale (EDSS) was performed by an experienced, Neurostatus-certified neurologist (26). Patient baseline characteristics are reported in **Table 1**. Patients starting with NAT presented at an mean age about 33.7 ± 9.6 years, an median EDSS score about 3.5 and median duration since diagnosis of RRMS about 4.0. About 69.2% of patients received at least one DMT before NAT initiation, 30.8% patients were initiated to NAT without previous DMT. During a standardized treatment switch procedure, injectables were stopped 2 weeks before natalizumab start, fingolimod was stopped 8 weeks before natalizumab and other DMTs at least 6 months before natalizumab initiation. The proportion of patients without disease activity and NEDA-3 status defined by no relapses, no confirmed EDSS progression (≥1.0 point increase if EDSS baseline score was <4.0; ≥0.5 point increase if EDSS baseline score was ≥4.0), and no MRI progression (one or more new T2 or gadolinium enhancing lesions) during the 72 months observation period are presented in **Figure 2**. Data have been collected from the MSDS3D database. The study was approved by the institutional review board of the University Hospital of Dresden. Patients gave their written informed consent.

NAT Infusion Protocol and Blood Sampling

NAT infusion protocol used in our MS center was adapted to the standardized infusion protocol described in guidelines of diagnosis and treatment of MS patients of the German association of MS (27). NAT (300 mg) was given every 4 weeks intravenously (i.v.) over the course of 1 h. According to our standard operation procedure, routine blood analysis and EDSS evaluations were realized before NAT start and every 3 months. In this analysis, we evaluated these parameters up to 72 months follow up.

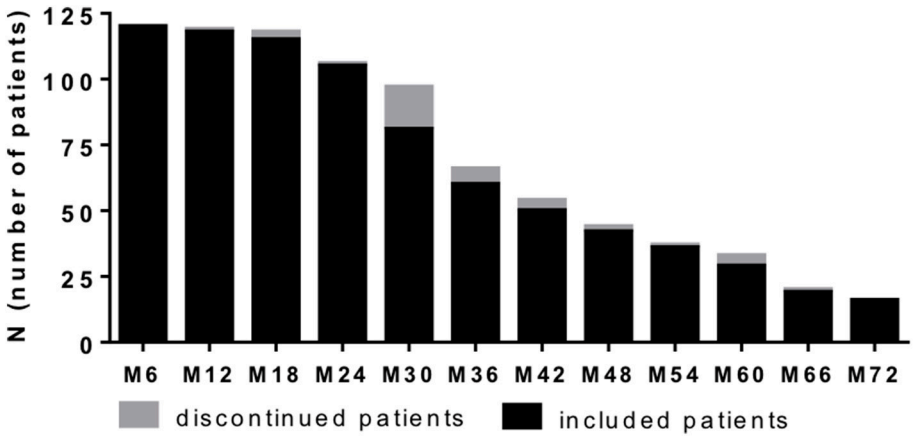


FIGURE 1 | Patient recruitment per 6 months period. One hundred and twenty patients with highly active MS were recruited and evaluated at data analysis. Based on consecutive sampling some of patients already reached 72 month follow up, whereas others did not yet at time point of data analysis. Number of patients included at defined time point are depicted (black bar). Additionally number of patients that discontinued NAT treatment at defined time point are presented (gray bar). Clinical and lab data were evaluated every 3 months.

TABLE 1 | Baseline characteristics.

Age (yr ± SD)	33.7 (9.6)
Male-[no. (%)]	29 (24.2)
Female-[no. (%)]	91 (75.8)
Previous use DMT-[no. (%)]	83 (69.2)
Interferon-beta	51 (42.5)
Glatiramer acetate	21 (17.5)
Fingolimod	4 (3.3)
Other approved medications	7 (5.8)
none-[no. (%)]	37 (30.8)
Duration since MS diagnosis (mean yr ± SD)	5.6 (5.8)
Mean score on EDSS	3.8 (1.8)

Baseline characteristics of evaluated patients. Other approved medications include, Triamcinolon (1), Azathioprin (1), Mitoxantron (4), Laquinimod (1). DMT, disease modifying therapy; yr, years; SD, standard deviation; no, number.

Routine Blood Analysis

Standardized blood testing was performed for routine blood parameters at the Institute of Clinical Chemistry and Laboratory Medicine, University Hospital in Dresden, Germany. The institute complies with standards required by DIN-EN-ISO-15189:2014 for medical laboratories. Routine blood testing included complete blood cell count, liver enzymes, creatinine, sodium, potassium, and C-reactive protein (CRP). Serological testing for JCV antibodies was performed before natalizumab start and every 6 months follow up and was measured at Unilabs, Denmark (Stratify JCV^{TM} Test).

Immune Cell Phenotyping by Fluorescence-Activated Cell Sorting (FACS)

After blood collection, subpopulations of T-cells, B-cells, and natural killer (NK) cells were characterized by surface staining with fluorescence labeled anti-CD3, anti-CD4, anti-CD8, anti-CD16, anti-CD14, anti-CD19, anti-CD56 (BD Biosciences, Heidelberg, Germany) according to the manufacturer's instructions. Negative controls included directly labeled or unlabeled isotype-matched irrelevant antibodies (BD Biosciences). Cells were evaluated on FACSCanto II flow cytometer.

Statistical Analysis

Data were analyzed applying Generalized Linear Mixed Models with Gamma distribution and log link function due to the right-skewed distribution pattern of the data. Bonferroni correction for pairwise tests was used. Correlations were calculated using Spearman's correlation model. At the time, there were no clear variables at hand that should have been treated as confounders. Since we had no determining groups to test for differences, confounders over time were left to be considered. In the graphs (**Figures 3–5**, **7**), data are given as mean ± standard deviation (SD). In **Table 2**, data are additionally presented as mean ±95% confidence interval (CI) providing information about the precision of estimates over the course of the study. Values of $^{*}p < 0.05$, $^{**}p < 0.01$, and $^{***}p < 0.001$ were considered significant.

RESULTS

Complete Blood Cell Count and Its Variation During Long-Term NAT Therapy

In our analysis 120 patients were included starting on NAT therapy. Before NAT initiation, a wide range of leukocyte resp. lymphocyte counts (3.3–13.9 GPT/L, respectively, 0.4–3.7 GPT/L) was seen (**Figures 3A,B**, **Table 2**). Levels of baseline leukocyte resp. lymphocyte count did not significantly differ between patients without or with different previous DMT use in

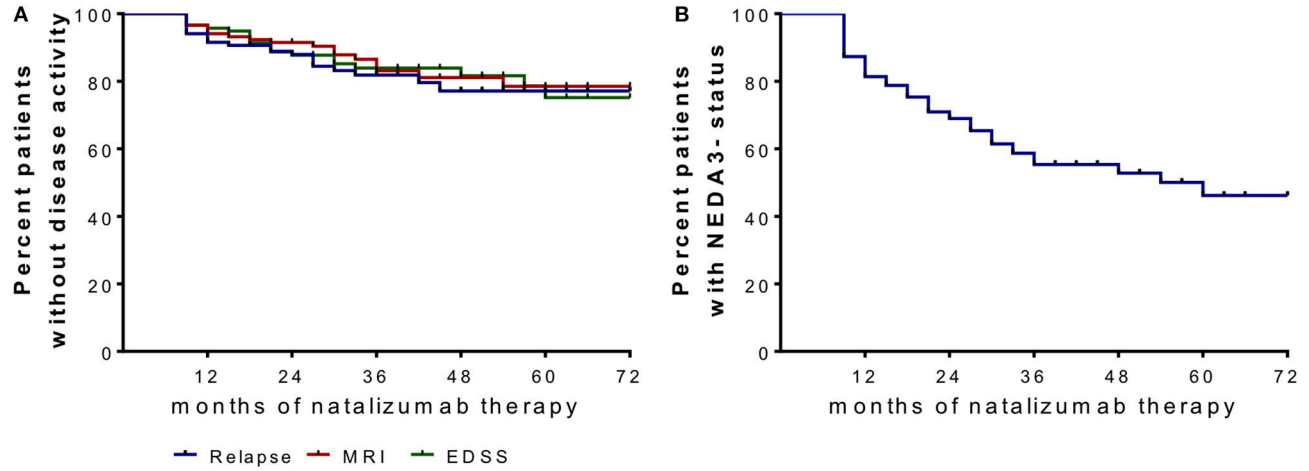


FIGURE 2 | Proportion of patients without disease activity and NEDA-3 status after NAT start. **(A)** Clinical parameters are depicted in a Kaplan–Meier survival curve analysis for relapses, confirmed EDSS progression (≥1.0 point increase if EDSS baseline score was <4.0; ≥0.5 point increase if EDSS baseline score was ≥4.0) and MRI progression (one or more new T2 or gadolinium enhancing lesions) after month 6 and during 72 months follow up. **(B)** No evidence of disease activity (NEDA)-3 status was confirmed when criteria of no relapses, no EDSS progression and no MRI progression were met.

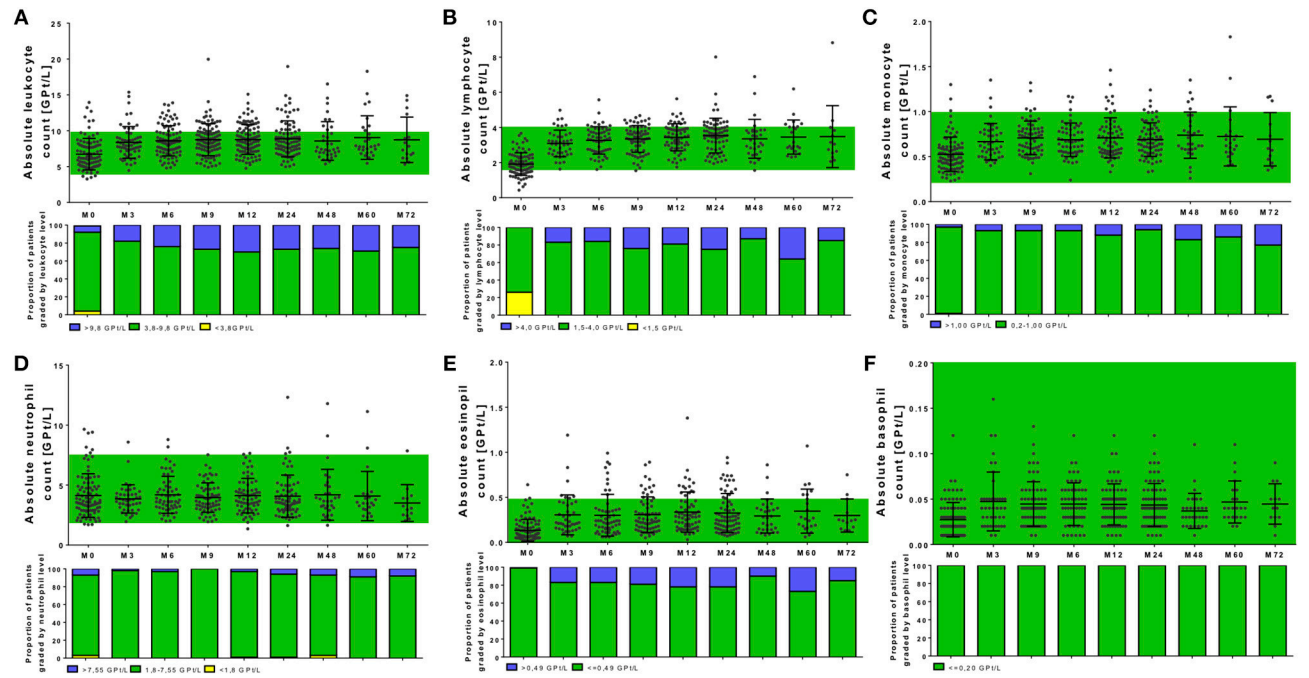


FIGURE 3 | Complete blood analysis during NAT treatment. Blood samples were taken before NAT started (M0) and every 3 months. Blood samples were analyzed in a certified medical laboratory. Analysis of complete blood count as leukocytes **(A)**, lymphocytes **(B)**, monocytes **(C)**, neutrophils **(D)**, eosinophils **(E),** and basophils **(F)** were included. Data are shown for baseline analysis (M0), month 3 (M3), month 6 (M6), month 12 (M12), and every 12 months follow up (M24, M48, M60, M72). Results are depicted as mean ± standard deviation. Green background indicates reference range of depicted parameters. Additionally, proportion of patients graded by white blood cell levels are shown: lower than reference range (yellow), reference range (green), and higher than the reference range (blue). Levels of significance are presented in **Table 2**.

our cohort. At NAT start, 24 patients presented with lymphocyte counts <1.5 GPT/L without a specific pretreatment pattern.

After NAT initiation, leukocyte and lymphocyte counts increased significantly (global time effect $p < 0.001$, **Figures 3A,B**, **Table 2**). On average, leukocyte count increased up to about 2.05 GPT/L absolutely and 37.33% relatively, lymphocytes up to about 1.63 GPT/L in absolute and 99.95% in relatively. The highest increase in leukocyte and lymphocyte

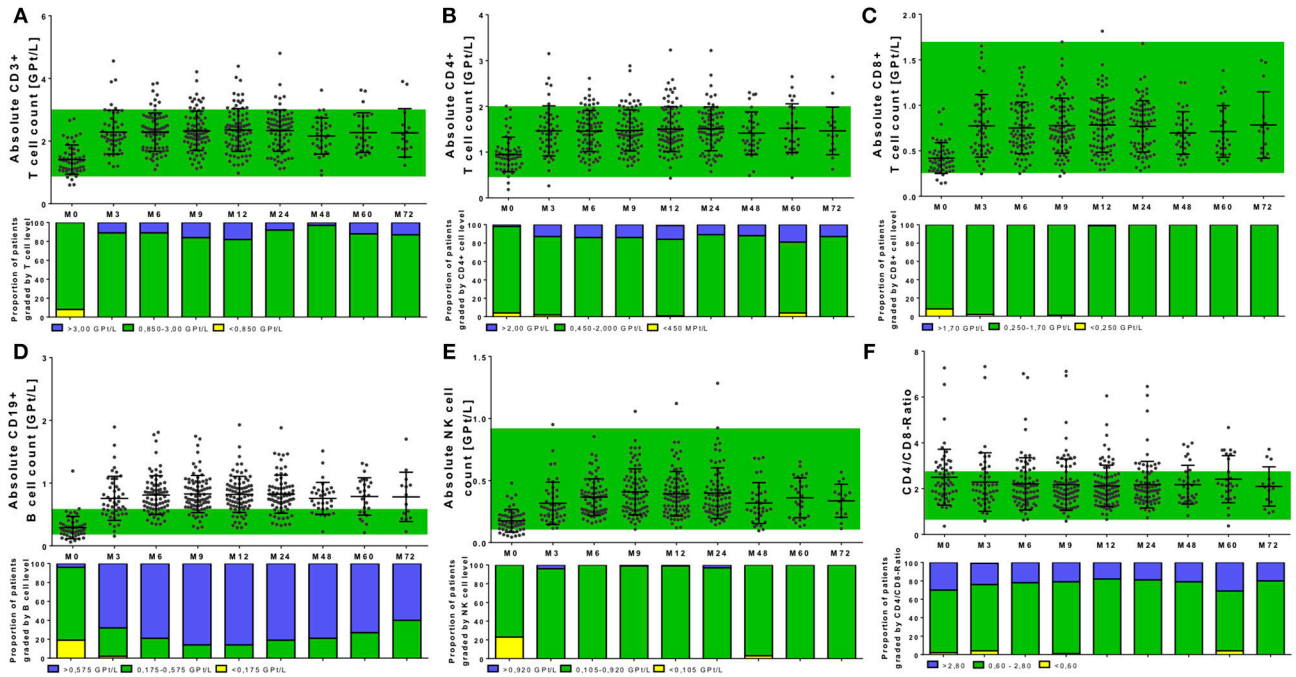


FIGURE 4 | Cell count of selective immune cell subpopulations during NAT treatment. Absolute cell count of $CD3^+$ T cells **(A)**, $CD4^+$ T cells **(B)**, $CD8^+$ T cells **(C)**, $CD19^+$ B cells **(D)**, NK cells **(E)**, and the $CD4^+/CD8^+$-Ratio **(F)** are depicted. Data are shown for baseline analysis (M0), month 3 (M3), month 6 (M6), month 12 (M12), and every 12 months follow up (M24, M48, M60, M72). Mean ± standard deviation are presented. Green background indicates reference range of depicted parameters. Additionally, proportion of patients graded by lymphocyte subtype level are shown: lower than reference range (yellow), reference range (green) and higher than the reference range (blue). Level of significance are presented in **Table 2**.

count was seen in patients pretreated with fingolimod (only 4 patients in our cohort included) before NAT start. Furthermore, there were no significant differences in leukocyte, respectively, lymphocyte increase or distribution during NAT treatment depending on pretreatment use. NAT treatment led to counts even higher than predefined upper normal limit for leukocytes in 28.8% of the treated patients and for lymphocytes in 21.4% of treated patients. Persistent lymphopenia <1.5 GPT/L was not seen during NAT treatment in our cohort.

Other leukocyte subtypes including monocytes, eosinophils, and basophils were significantly elevated and again increased even higher than upper normal level (global time effect $p < 0.001$, **Figures 3C,E,F**, **Table 2**). These effects were persistent without significant fluctuations during the entire observation period in all treated patients. Interestingly, no changes were seen regarding absolute number and distribution of neutrophils during the whole observation period (global time effect $p = 0.863$, **Figure 3D**, **Table 2**). Additional evaluation of blood parameters including hemoglobin, hematocrit, erythrocyte count, and platelets demonstrated stable parameters in normal range during the 72 months evaluation period. Immature precursor cells including erythroblasts were detectable in 36.8% of the treated patients during NAT therapy, whereas none of these patients presented erythroblasts in the pretreatment period.

Effects on Distinct Lymphocyte Subsets and Its Intra-Individual Variation

In addition to complete blood count analysis, distinct lymphocyte subsets were evaluated. Absolute count of T cell subtypes presented in the physiological reference range in most of the patients before NAT start (**Figures 4A–C**). Only in single patients, T cells below lower normal limit could be identified (two patients without pretreatment, one patient with previous fingolimod treatment, one patient with previous interferon-beta treatment). Interestingly, evaluating predefined reference ranges for B cells and NK cells, most of the patients with lower lymphocyte count at baseline were associated with lower B cell and NK cell count at baseline as well (**Figures 4D,F**). All investigated cell subtypes including CD3+ T cells, CD4+ T cells, CD8+ T cells, CD19+ B cells, and NK cells, significantly increased after NAT initiation (global time effect $p < 0.001$, **Figures 4A–E**, **Table 2**). A higher portion of patients with a more intense increase of CD8+ T cells was seen compared to CD4+ T cells (**Figures 4A–C**). For CD4+ T cells, an increase >10% was seen in 94.2% of treated patients, an increase >20% was seen in 88.5% of treated patients, an increase >50% was seen in 61.5% of treated patients, and an increase >100% was seen in 23.1% of treated patients. In contrast for CD8+ T cells, an increase >10% was found in 96.2%, an increase >20% was found on 92.3% of patients, an increase >50% was seen in 80.8% of patients, and an increase >100% was found in

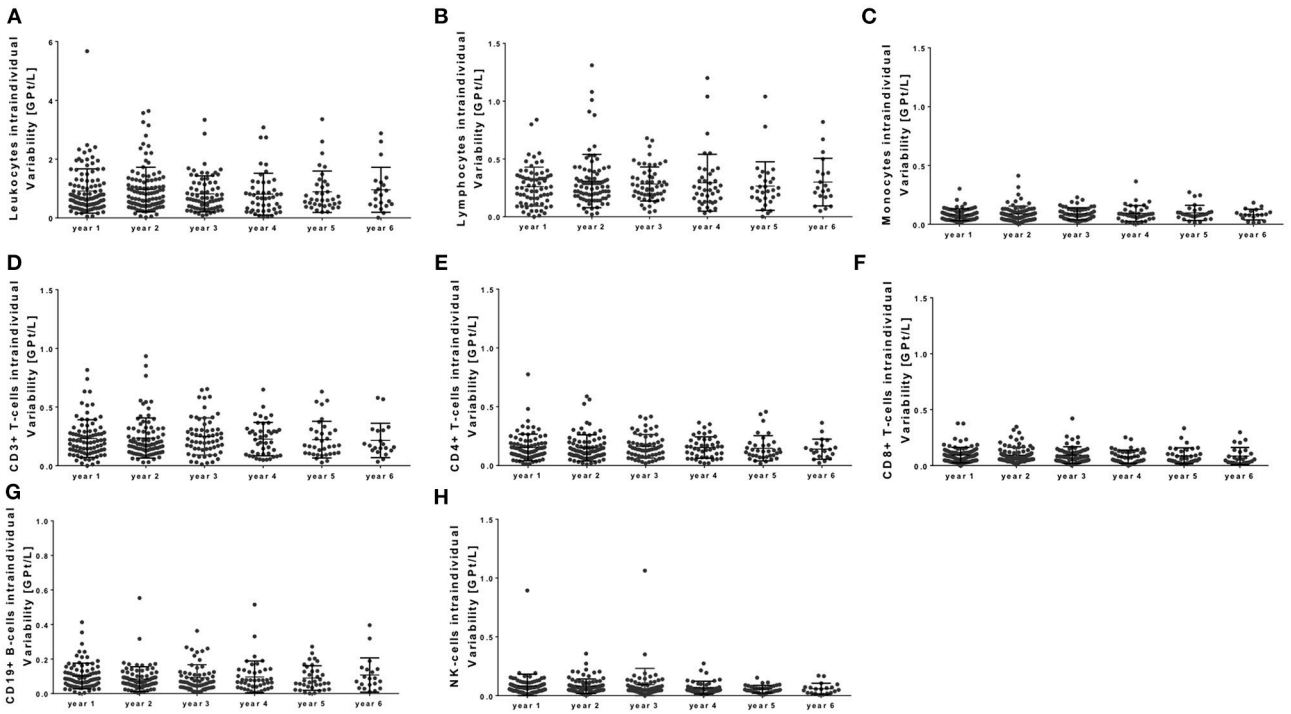


FIGURE 5 | Intra-individual variability of peripheral immune cell subsets during NAT treatment. Intra-individual variation of leukocytes **(A)**, lymphocytes **(B)**, monocytes **(C)**, CD3+ T cells **(D)**, CD4+ T cells **(E)**, CD8+ T cells **(F)**, CD19+ B cells **(G),** and NK cells **(H)** are depicted for each year. Intra-individual variability was defined as the standard deviation of absolute cell counts every 3 months in every year after NAT start (starting at month 3). Mean ± standard deviation.

38.5% of NAT treated patients. Nevertheless, CD4/CD8 ratio was not significantly changed in our cohort during long-term NAT treatment (**Figure 4F**). Patients with increased CD4/CD8 ratio at baseline presented increased CD4/CD8 ratio during follow up as well. CD19+ B cells presented the most pronounced increase in their frequency distribution in almost all treated patients (**Figure 4D**, **Table 2**). Regarding CD19+ B cells, all patients increased more than 20%. An increase >50% was seen in 94.2% of treated patients and an increase >100% was seen in 86.5 % of treated patients. Additionally, NK cells markedly increased, remained in the reference range with stable levels during the whole period of investigation (**Figure 4E**, **Table 2**). An increase >20% was seen in 98.1% of treated patients, an increase >50% was seen in 90.4% of treated patients and an increase >100% was seen in 63.5% of treated patients.

There was a strong correlation between baseline count and relative increase for lymphocytes and its subtypes [r – (0.792 – 0.625); $p < 0.0001$], but no significant correlation between baseline count and absolute increase. Age [r – (0.221 – 0.109); $p > 0.05$] and different pretreatment conditions [r –(0.039 – 0.052); $p > 0.05$] could not predict changes and pattern of immune cell subtypes during NAT therapy. In addition, intra-individual variability of different immune cell subtypes was evaluated during NAT treatment (**Figure 5**). Intra-individual variability was defined as the standard deviation of absolute cell count every 3 months in every year after NAT start. Most pronounced variability was seen for the leukocyte count, whereas lymphocytes and its subtypes varied only in a narrow range (**Figure 5**).

Reference to Clinical Parameters

The proportion of patients with or without disease activity and NEDA-3 status are presented in **Figure 2**. Evaluation of immune cell profiles in NEDA-3 positive patients vs. active patients could not confirm significant differences in the immune cell profile of leukocytes, lymphocytes, monocytes, T cell subsets, B cells, or NK cells during NAT treatment.

At NAT start, JCV antibody status was negative in 75 patients, positive in 19 patients, and unknown in 26 patients. During NAT treatment, 25.4% of JCV antibody negative patients switched to JCV antibody positive status. There were no cases of PML in our cohort. During the observation period, 39 patients stopped NAT treatment: 35 patients stopped because of positive JCV antibody status, three patients because of efficacy reasons and one patient because of the individual patient wish. Immune cell profile in patients that terminated NAT treatment was not statistically different to patients continuing NAT therapy.

Lymphocytes in a NAT Treated Patient With Neutralizing Antibodies Against NAT (nAbs)

This female patient was diagnosed RRMS in 02/2014 at an age of 25 years. In 05/2014 she started on dimethylfumarate treatment (**Figure 6A**). Due to side effects, treatment was changed to glatiramer acetate in 10/2015. In 03/2017 she suffered from a

TABLE 2 | Levels of statistical significance.

Time point	Leukocyte	Lymphocyte	Monocyte	Neutrophile granulocyte	Eosinophile granulocyte	Basophile granulocyte	CD3+ Tcell	CD4+ Tcell	CD8+ Tcell	CD19+ Been	NK cell
MO	6.73 (6.30; 7.18)	1.91 (1.78; 2.05)	0.53 (0.49; 0.57)	4.13 (3.77; 4.52)	0.13 (0.11; 0.16)	0.03 (0.02; 0.03)	1.41 (1.29; 1.54)	0.95 (0.85; 1.06)	0.42 (0.38; 0.47)	0.29 (0.25; 0.34)	0.18 (0.15; 0.20)
M3	8.37 (7.83; 8.95), $p < 0.001$	3.09 (2.87; 3.33), $P < 0.001$	0.67 (0.61; 0.73), $p = 0.005$	3.85 (3.51; 4.22), $P = 1.000$	0.34 (0.26; 0.45), $p = 0.001$	0.05 (0.04; 0.06), $P = 0.007$	2.29 (2.10; 2.50), $p < 0.001$	1.46 (1.32; 1.63), $p < 0.001$	0.77 (0.68; 0.88), $P < 0.001$	0.76 (0.66; 0.86), $p < 0.001$	0.36 (0.27; 0.47), $P = 0.011$
M6	8.56 (8.18; 9.03), $p < 0.001$	3.26 (3.07; 3.47), $P < 0.001$	0.69 (0.64; 0.74), $p < 0.001$	4.19 (3.81; 4.60), $P = 1.000$	0.34 (0.26; 0.44), $p = 0.001$	0.04 (0.04; 0.05), $P < 0.001$	2.29 (2.15; 2.43), $p < 0.001$	1.46 (1.36; 1.57), $p < 0.001$	0.75 (0.69; 0.82), $P < 0.001$	0.81 (0.74; 0.88), $p < 0.001$	0.37 (0.33; 0.40), $P < 0.001$
M9	8.74 (8.33; 9.18), $p < 0.001$	3.35 (3.17; 3.54), $P < 0.001$	0.71 (0.67; 0.75), $p < 0.001$	3.95 (3.67; 4.26), $P = 1.000$	0.34 (0.27; 0.42), $p < 0.001$	0.04 (0.04; 0.05), $p < 0;001$	2.33 (2.19; 2.47), $p < 0.001$	1.47 (1.38; 1.57), $p < 0.001$	0.78 (0.71; 0.85), $P < 0.001$	0.83 (0.76; 0.89), $p < 0.001$	0.41 (0.37; 0.45), $P < 0.001$
M12	8.77 (8.37; 9.18), $p < 0.001$	3.43 (3.25; 3.62), $P < 0.001$	0.71 (0.66; 0.76), $p < 0.001$	4.12 (3.78; 4.48), $P = 1.000$	0.36 (0.30; 0.43), $p < 0.001$	0.04 (0.04; 0.04), $P < 0.001$	2.35 (2.21; 2.51), $p < 0.001$	1.50 (1.40; 1.61), $p < 0.001$	0.78 (0.72; 0.85), $P < 0.001$	0.84 (0.77; 0.92), $p < 0.001$	0.39 (0.36; 0.43), $P < 0.001$
M24	8.86 (8.35; 9.41), $p < 0.001$	3.54 (3.31; 3.77), $P < 0.001$	0.69 (0.65; 0.73), $p < 0.001$	4.08 (3.69; 4.50), $P = 1.000$	0.33 (0.28; 0.38), $p < 0.001$	0.04 (0.04; 0.05), $P < 0.001$	2.33 (2.19; 2.49), $p < 0.001$	1.51 (1.40; 1.62), $p < 0.001$	0.77 (0.71; 0.84), $P < 0.001$	0.82 (0.76; 0.90), $p < 0.001$	0.40 (0.36; 0.45), $P < 0.001$
M48	8.57 (7.72; 9.51), $p = 0.010$	3.35 (2.98; 3.77), $P < 0.001$	0.74 (0.65; 0.84), $p = 0.001$	4.19 (3.49; 5.02), $P = 1.000$	0.29 (0.23; 0.37), $p = 0.001$	0.04 (0.03; 0.04), $p = 0.512$	2.16 (1.97; 2.37), $p < 0.001$	1.41 (1.26; 1.58), $p < 0.001$	0.70 (0.62; 0.78), $P < 0.001$	0.83 (0.68; 1.02), $p < 0.001$	0.32 (0.27; 0.38), $P = 0.001$
M60	9.04 (7.98; 10.24), $p = 0.006$	3.45 (3.07; 3.88), $P < 0.001$	0.73 (0.60; 0.88), $p = 0.193$	4.09 (3.31; 5.04), $P = 1.000$	0.35 (0.26; 0.47), $p = 0.002$	0.05 (0.04; 0.06), $P = 0.009$	2.27 (2.04; 2.53), $p < 0.001$	1.52 (1.33; 1.74), $P < 0.001$	0.71 (0.61; 0.83), $P < 0.001$	0.92 (0.68; 1.25), $p < 0.001$	0.36 (0.30; 0.43), $P < 0.001$
M72	8.73 (7.30; 10.43), $p = 0.448$	3.48 (2.64; 4.58), $p = 0.047$	0.69 (0.55; 0.88), $p = 1.000$	3.50 (2.76; 4.45), $P = 1.000$	0.30 (0.21; 0.42), $p = 0;051$	0.04 (0.03; 0.06), $P = 0.239$	2.26 (1.90; 2.69), $p = 0.002$	1.46 (1.22; 1.75), $p = 0.011$	0.78 (0.62; 0.99), $P = 0.006$	1.04 (0.62; 1.77), $p = 0.226$	0.34 (0.28; 0.412), $P = 0.001$

Mean and 95% confidence interval of each time-point of selected immune cell subsets. Level of significance with respective p-value (change compared to MO).

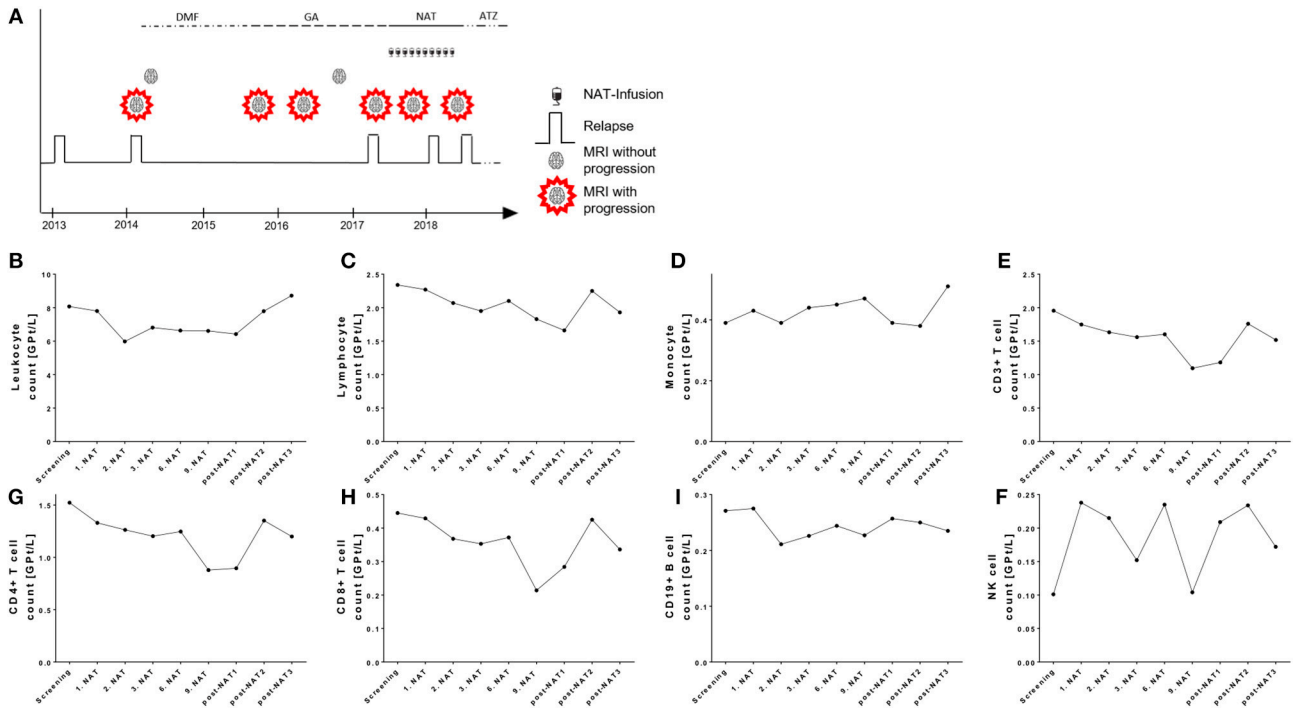


FIGURE 6 | Case presentation and course of peripheral immune cell subset in a NAT treated patient with positive nAbs. **(A)** Clinical data including relapse activity, MRI progression, and treatment conditions are presented. DMF, dimethylfumarate; GA, glatiramer acetate; NAT, natalizumab; ATZ, alemtuzumab. **(B–I)** Absolute cell count of leukocytes **(B)**, lymphocytes **(C)**, monocytes **(D)**, CD3+ T cells **(E)**, CD4+ T cells **(F)**, CD8+ T cells **(G)**, CD19+ B cells **(H),** and NK cells **(I)** are depicted. Data are shown for screening, NAT treatment period (1. NAT, 1st NAT infusion etc), and period after NAT cessation (post-NAT1, post-NAT2, post-NAT3; 1, 2, or 3 months after NAT stop).

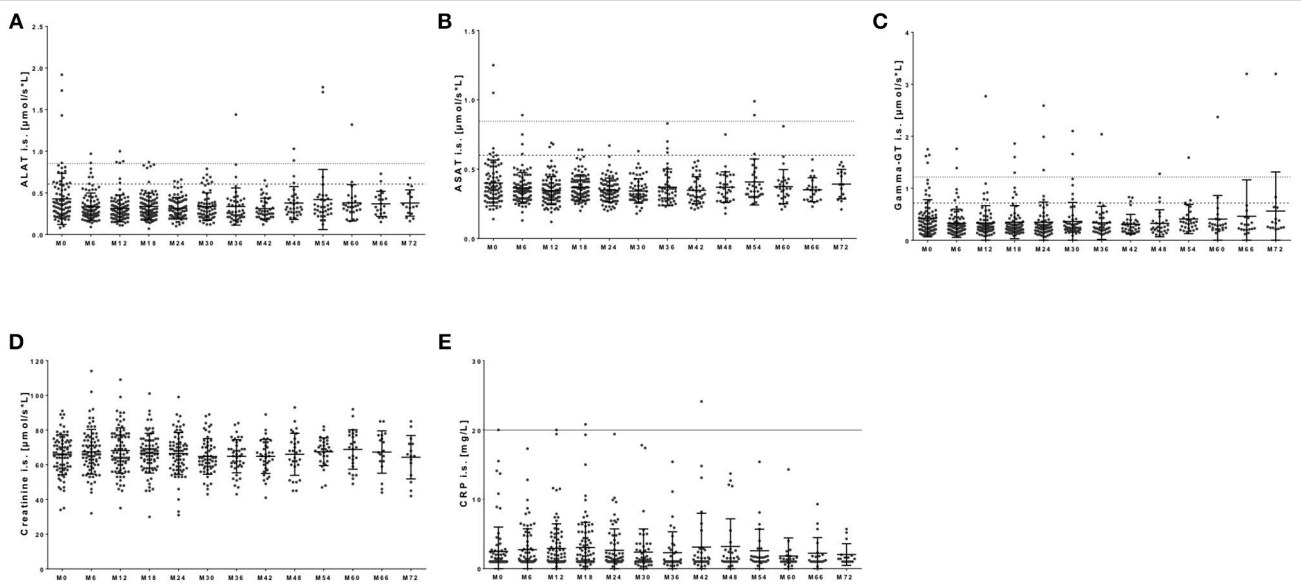


FIGURE 7 | Serological parameters during NAT treatment. Before each infusion started, blood samples were taken and analyzed in a certified medical laboratory. Analysis of serological parameters including ALAT **(A)**, ASAT **(B)**, gamma-GT **(C)**, creatinine **(D),** and CRP **(E)** were included. Data are shown for baseline analysis (M0) and sixth months follow up (M6, M12, […], M72). Data are presented as mean ± standard deviation. Dotted line indicates the reverence range for men for ALAT and ASAT at a value of 0.85 µmol/s*L and for gamma-GT at 1.2 µmol/s*L. Broken line indicates reverence range for women for ALAT and ASAT at a value of 0.6 µmol/s*L and for gamma-GT at 0.7 µmol/s*L. There were no statistical significant changes.

severe relapse and cerebral MRI scan demonstrated new T2 lesions. JCV index was negative and first NAT infusion was performed in 06/2017. After 4 months, cerebral MRI scan presented two new T2 lesions. NAT infusions were continued. In 01/2018 after the 8. NAT infusion, the patient suffered again of an acute relapse that was treated with corticosteroids. Testing and re-testing of antibodies against NAT (nAbs) was done and high titers of nAbs were confirmed in 02/2018 and 03/2018 (testing was performed at the Department of Neurology, University Hospital Bochum, Prof. Dr. R. Gold). Evaluation of JCV index in 11/2017 and 04/2018 presented again negative results. MRI scan presented progress of >10 new T2 lesions in 05/2018. NAT treatment was stopped and treatment with alemtuzumab was started in 06/2018 (**Figure 6**).

Evaluation of blood cell count demonstrated that in contrast to our cohort presented above leukocytes and lymphocytes were not relevantly changed after starting NAT treatment in this patient (**Figures 6B,C**). Lymphocytes and its subsets were not increased during the NAT treatment and did not change in the post-treatment period as well (**Figures 6E,F**). We assume that nAbs developed quite early after NAT start. This case report demonstrates that real world lab data can potentially identify patients with nAbs development to NAT.

Standard Serological Parameters During NAT Treatment

Standard serological parameters were measured every 3 months as well (**Figure 7**). In most of the patients, liver enzymes including alanine aminotransferase (ALAT), aspartate aminotransferase (ASAT), and gamma-Glutamyltransferase (gamma-GT) demonstrated levels in the reference range over the whole observation period (**Figures 7A–C**). Nevertheless, out of our 120 patients few patients presented with transient and asymptomatic increase of ALAT, ASAT or gamma-GT (**Figures 7A–C**). After NAT initiation, ALAT levels were increased once during the whole observation period but reached reference range at re-test in 16 patients. Seven patients presented with repeated increase of ALAT level. In nine patients increased ASAT levels were seen once during NAT treatment with normalized values at re-testing. One patient presented repeated increase of ASAT levels threw observation. None of these patients reached levels >3x upper normal limit for ASAT, and only one patient reached levels >3x upper normal limit for ALAT, but presented with normalized values after re-test. (**Figures 7A,B**). Gamma-GT was elevated in 21 patients during NAT therapy. Elevation of gamma-GT was transient and appeared only once in eight of the investigated patients. In 13 patients, repeated elevations of gamma-GT levels were seen. Only three patients presented with gamma-GT levels >3x upper normal limit. This increase was asymptomatic and without any clinical significance.

Kidney function parameters including creatinine (**Figure 7D**) as well as sodium and potassium levels (data not shown) remained stable within physiological ranges in most of the patients. Only few patients appeared with transient elevation in creatinine levels at least once during NAT therapy in our cohort (**Figure 7D**). Creatinine levels lower than physiological reference ranged appeared primarily in immobilized patients and did not reflect any clinical relevance (**Figure 7D**). CRP levels ≥20 mg/dL were defined as clinical significant. In our observation, almost all patients presented with normal CRP levels during the whole observation period (**Figure 7E**). Nevertheless, 10 patients presented with an increase in CRP up to 144 mg/dL during NAT therapy. Six of these 10 patients showed clinical symptoms of an infection. At onset of CRP increase, six of these 10 patients suffered from respiratory tract infection that resolved during follow up. In four of these patients, CRP increase was paralleled by clinical significant increase of leukocyte but not lymphocyte count.

DISCUSSION

In our longitudinal observational study, we systematically collected real world lab data including specific immune cell subsets and routine laboratory parameters in NAT treated patients during long-term NAT treatment. Upon NAT treated patients, there are a huge amount of reports available discussing long period outcome and clinical parameters including relapse rate, MRI-activity, and disease progression presenting long-term efficacy (28–30), whereas analyses of immune cell subsets and standard lab analyses are restricted only up to 24–48 months follow up (15, 23, 24). Compared to previous studies, we analyzed a representative large number of patients for a treatment period up to 6 years. Our cohort demonstrated the excellent clinical effectiveness of NAT in the real world scenario as well. NAT selectively directs the α4 subunit of VLA-4 on the surface of leukocytes (2). The interplay of VLA-4 on white blood cells and VCAM-1 expressed on endothelial cells enables peripheral immune cells to cross the blood-brain barrier and boosting CNS inflammation as known in MS pathology (1, 31). While NAT treatment, leukocyte extravasation especially into the CNS is inhibited and immune cells are sequestrated in peripheral blood (13, 21). In line with previous data, our results confirm early increase of peripheral lymphocyte subsets in NAT treated patients (21, 22, 24, 32, 33). Additionally we demonstrate an early and persistent biological response of NAT treatment in different leukocyte subsets over the entire period of 6 years evaluation. Interestingly, pretreatment conditions could not predict the course of leukocytes and lymphocytes after NAT start in our cohort, baseline leukocyte and lymphocyte count was correlated with relative but not absolute increase. Regarding lymphocyte subsets, increase of CD8+ and CD19+ lymphocytes was most pronounced and especially CD19+ B cells were higher than normal level in most of the treated patients. These data were also reported by others (24, 33). Previous observations confirmed the relevance of VLA-4 also on B cells for the CNS recruitment and inflammation in MS pathogenesis (34). Though selective inhibition of VLA-4 dependent B cells may contributes to the efficacy during NAT therapy (34). The risk of nAbs development during NAT therapy is a well-known phenomenon and may interfere with NAT efficacy (35). Here we demonstrate that the typical immunological effects in the periphery are missing in a patient with nAbs to NAT. Though, even standard blood count can probably assist to identify insufficient impact of NAT treatment and to consider further testing. Of course, this has to be systematically proven in a larger cohort.

Previous studies presented various expression levels of VLA-4 on different lymphocyte subtypes with higher levels on B lymphocytes than on T lymphocytes and also more pronounced on CD8+ T cells than on CD4+ T cells (21, 32, 36). Though, the VLA-4/VCAM-1 mediated transmigration of immune cells is differently affected among different peripheral immune cells in NAT treated patients that lead to different sequestration in peripheral blood. Additional to peripheral lymphocyte sequestration due to impaired transmigration mechanisms, effects on the lymphocyte release from bone marrow are discussed (11, 12, 14, 16). Different studies presented mobilization of hematopoietic lymphoid precursor cells from the bone marrow by NAT mediated blocking of retention signals (11, 12, 14). In the line with this, an increase in erythroblasts was seen as well in our cohort. This mobilization additionally contributes to increase of circulating B cells especially with naïve and memory phenotype in NAT treated patients (16). Furthermore, NAT-associated but not clinically relevant morphologic changes in lymphocytes have been described defined by enhanced fraction of atypical lymphocytes (37, 38).

During our observation, CD4/CD8 ratio did not change during the entire period of therapy compared to baseline. These findings are comparable with other results of shorter evaluation periods (24), whereas some early reports presented a decrease in CD4/CD8 ratio suggesting increased risk of opportunistic infections including PML in such patients (23, 39). These studies were usually characterized by smaller samples size and shorter period of evaluation compared to our analysis. In our cohort, NAT lead to increase and re-distribution of peripheral immune cell subsets, which happened early and remained constant without relevant variation during the whole period of 6 years evaluation. Although some immune cell subsets increased out of reference range, no serious adverse events including severe infections or opportunistic infections appeared, no malignancies, or hematological abnormalities were detectable.

Additionally to T and B cell subsets, NK cells increased early directly after NAT initiation. In comparison with other lymphocyte subtypes, NK cells presented one of the most pronounced increases in periphery. These data are in line with other observations that additionally discussed a link between increase of NK cells and response during NAT treatment (21, 24, 40, 41). Here we show, that NAT induced changes in NK cell count persist even years after treatment initiation possible additionally contributing to efficacy in long-term treatment.

Monocytes, eosinophils, and basophils showed a lower but significant increase. In contrast to another study in which monocytes steadily increased over the whole observational period (15), in our analysis monocyte cell count increased to a constant level already after 1 month of treatment start and kept stable. Blocking VLA-4 by NAT leads to sequestration of monocytes and granulocyte subsets in peripheral blood, but does not affect migration of myeloid progenitor cells as seen for the lymphoid progenitors described above (42). These aspects may explain the moderate increase in monocytes and granulocyte subsets compared to lymphocytes. No significant changes were seen in cell count and distribution of neutrophils. Neutrophils do not express VLA-4, therefore, NAT does not affect its distribution (15, 43). Furthermore, we confirmed stable hematological parameters including erythrocyte count, hemoglobin, hematocrit, and platelet count during longterm evaluation of NAT treatment (15). In our evaluation, no association between the distribution of peripheral immune cell subsets and clinical disease activity parameters during NAT treatment could be found. The immune cell phenotyping presented in our study is part of the routine lab testing in our treated MS patients and is characterized by limitations in comparison to more detailed immune cell profiling as presented in other immune profiling studies using e.g., high-dimensional cytometry (44). These studies are more complex in immune cell profiling techniques but may elucidate more details in immune cell patterns and clinical response.

Although controlled data regarding peripheral immune cell subsets within first years of NAT treatment are available, reports on standard testing of serological parameters especially in long-term evaluation are missing. Based on the known excellent safety profile of NAT, hepatic, or kidney dysfunction is not common. Nevertheless, frequent testing of routine lab parameters is recommended and part of the monitoring program applied in NAT treated patients (45). During our observation period of 6 years, there were no relevant or long lasting abnormalities in serological testing of liver enzymes or kidney function. In general, patients presented these parameters in physiological ranges with rare, only transient and not clinical significant increases during the whole period of NAT treatment. Evaluation of CRP levels is a helpful tool to define infectious conditions. NAT therapy does not impair variation of CRP levels as seen by other MS treatments e.g., after alemtuzumab initiation (46, 47). In our cohort, only few patients with transient increase of CRP levels were found. In six out of ten patients with increased CRP levels, a clinical relevant infection was apparent. These data are important to demonstrate that evaluation of CRP levels maybe a helpful tool to identify acute infections even in NAT treated patients when changes in peripheral blood cells are a common phenomenon.

Here, we presented real world lab data on NAT demonstrating the consistent and safe impact of NAT on peripheral immune cell subsets and routine lab parameters within real world conditions and everyday clinical practice. We have already shown the value of real world lab data for fingolimod recently (48). Patients included in our investigation have a different clinical profile compared to those included in randomized clinical trials with limiting inclusion criteria allowing the assessment of real world lab data. The broad and unselected patient population is a great advantage of our study, which does represent the common patient in daily clinical practice. Because of the differences in disease duration, previous medication use and various pre-existing conditions, they describe the real world patient population best. Nevertheless, differences in monitoring procedures and data collection in different centers impact the quality and comparability of such real world data (17). Standardized treatment protocols and monitoring tools (e.g., the MSDS3D software approach) can assist to achieve comparable requirements for patient care as well as data

collection even at multiple centers and in every-day clinical practice (18). So NAT real world data on pregnancy are available (49). This standardized collection of real world data and observational studies providing longitudinal information on drug profile and different outcomes in real life are essential to improve decision-making and optimize treatment management.

AVAILABILITY OF THE DATA AND MATERIAL

TZ and KA have full access to all the data in the study and takes full responsibility for integrity of the data and the accuracy of the data analysis. Raw data are available on personal demand.

AUTHOR CONTRIBUTIONS

KA and TZ study concept and design. MK acquisition of data. MK, KA, and RH analysis and interpretation of data. MK, KA, and TZ drafting of the manuscript. UP and RH critical revision of the manuscript for important intellectual content. RH and MK statistical analysis.

ACKNOWLEDGMENTS

We are grateful to Prof. Dr. T. Chavakis from the Institute of Clinical Chemistry and Laboratory Medicine, University Clinic Dresden for performing the analysis and providing the data. We acknowledge support by the Open Access Publication Funds of the SLUB/TU Dresden.

REFERENCES

1. Elices MJ, Osborn L, Takada Y, Crouse C, Luhowskyj S, Hemler ME, et al. VCAM-1 on activated endothelium interacts with the leukocyte integrin VLA-4 at a site distinct from the VLA-4/fibronectin binding site. *Cell* (1990) 60:577–84. doi: 10.1016/0092-8674(90)90661-W
2. Yednock TA, Cannon C, Fritz LC, Sanchez-Madrid F, Steinman L, Karin N. Prevention of experimental autoimmune encephalomyelitis by antibodies against alpha 4 beta 1 integrin. *Nature* (1992) 356:63–6. doi: 10.1038/356063a0
3. Lobb RR, Hemler ME. The pathophysiologic role of alpha 4 integrins *in vivo*. *J Clin Invest.* (1994) 94:1722–8. doi: 10.1172/JCI117519
4. Sehr T, Proschmann U, Thomas K, Marggraf M, Straube E, Reichmann H, et al. New insights into the pharmacokinetics and pharmacodynamics of natalizumab treatment for patients with multiple sclerosis, obtained from clinical and *in vitro* studies. *J Neuroinflammation* (2016) 13:164. doi: 10.1186/s12974-016-0635-2
5. Skarica M, Eckstein C, Whartenby KA, Calabresi PA. Novel mechanisms of immune modulation of natalizumab in multiple sclerosis patients. *J Neuroimmunol.* (2011) 235:70–6. doi: 10.1016/j.jneuroim.2011.02.010
6. Polman CH, O'connor PW, Havrdova E, Hutchinson M, Kappos L, Miller DH, et al. A randomized, placebo-controlled trial of natalizumab for relapsing multiple sclerosis. *N Engl J Med.* (2006) 354:899–910. doi: 10.1056/NEJMoa044397
7. Rudick RA, Stuart WH, Calabresi PA, Confavreux C, Galetta SL, Radue EW, et al. Natalizumab plus interferon beta-1a for relapsing multiple sclerosis. *N Engl J Med* (2006) 354:911–23. doi: 10.1056/NEJMoa044396
8. Bloomgren G, Richman S, Hotermans C, Subramanyam M, Goelz S, Natarajan A, et al. Risk of natalizumab-associated progressive multifocal leukoencephalopathy. *N Engl J Med.* (2012) 366:1870–80. doi: 10.1056/NEJMoa1107829
9. Gorelik L, Lerner M, Bixler S, Crossman M, Schlain B, Simon K, et al. Anti-JC virus antibodies: implications for PML risk stratification. *Ann Neurol.* (2010) 68:295–303. doi: 10.1002/ana.22128
10. Ziemssen T, Gass A, Wuerfel J, Bayas A, Tackenberg B, Limmroth V, et al. Design of TRUST, a non-interventional, multicenter, 3-year prospective study investigating an integrated patient management approach in patients with relapsing-remitting multiple sclerosis treated with natalizumab. *BMC Neurol.* (2016) 16:98. doi: 10.1186/s12883-016-0625-0
11. Bonig H, Wundes A, Chang KH, Lucas S, Papayannopoulou T. Increased numbers of circulating hematopoietic stem/progenitor cells are chronically maintained in patients treated with the CD49d blocking antibody natalizumab. *Blood* (2008) 111:3439–41. doi: 10.1182/blood-2007-09-112052
12. Zohren F, Toutzaris D, Klarner V, Hartung HP, Kieseier B, Haas R. The monoclonal anti-VLA-4 antibody natalizumab mobilizes CD34+ hematopoietic progenitor cells in humans. *Blood* (2008) 111:3893–5. doi: 10.1182/blood-2007-10-120329
13. Kivisakk P, Healy BC, Viglietta V, Quintana FJ, Hootstein MA, Weiner HL, et al. Natalizumab treatment is associated with peripheral sequestration of proinflammatory T cells. *Neurology* (2009) 72:1922–30. doi: 10.1212/WNL.0b013e3181a8266f
14. Jing D, Oelschlaegel U, Ordemann R, Holig K, Ehninger G, Reichmann H, et al. CD49d blockade by natalizumab in patients with multiple sclerosis affects steady-state hematopoiesis and mobilizes progenitors with a distinct phenotype and function. *Bone Marrow Transplant.* (2010) 45:1489–96. doi: 10.1038/bmt.2009.381
15. Bridel C, Beauverd Y, Samii K, Lalive PH. Hematologic modifications in natalizumab-treated multiple sclerosis patients: an 18-month longitudinal study. *Neurol Neuroimmunol Neuroinflamm.* (2015) 2:e123. doi: 10.1212/NXI.0000000000000123
16. Mattoscio M, Nicholas R, Sormani MP, Malik O, Lee JS, Waldman AD, et al. Hematopoietic mobilization: potential biomarker of response to natalizumab in multiple sclerosis. *Neurology* (2015) 84:1473–82. doi: 10.1212/WNL.0000000000001454
17. Ziemssen T, Hillert J, Butzkueven H. The importance of collecting structured clinical information on multiple sclerosis. *BMC Med.* (2016) 14:81. doi: 10.1186/s12916-016-0627-1
18. Haase R, Wunderlich M, Dillenseger A, Kern R, Akgun K, Ziemssen T. Improving multiple sclerosis management and collecting safety information in the real world: the MSDS3D software approach. *Expert Opin Drug Saf.* (2018) 17:369–78. doi: 10.1080/14740338.2018.1437144
19. Ziemssen T, Kempcke R, Eulitz M, Grossmann L, Suhrbier A, Thomas K, et al. Multiple sclerosis documentation system (MSDS): moving from documentation to management of MS patients. *J Neural Transm.* (2013) 120:S61–6. doi: 10.1007/s00702-013-1041-x
20. Miller DH, Khan OA, Sheremata WA, Blumhardt LD, Rice GP, Libonati MA, et al. A controlled trial of natalizumab for relapsing multiple sclerosis. *N Engl J Med.* (2003) 348:15–23. doi: 10.1056/NEJMoa020696
21. Putzki N, Baranwal MK, Tettenborn B, Limmroth V, Kreuzfelder E. Effects of natalizumab on circulating B cells, T regulatory cells and natural killer cells. *Eur Neurol.* (2010) 63:311–7. doi: 10.1159/000302687
22. Zanotti C, Chiarini M, Serana F, Sottini A, Garrafa E, Torri F, et al. Peripheral accumulation of newly produced T and B lymphocytes in natalizumab-treated multiple sclerosis patients. *Clin Immunol.* (2012) 145:19–26. doi: 10.1016/j.clim.2012.07.007
23. Marousi S, Karkanis I, Kalamatas T, Travasarou M, Paterakis G, Karageorgiou CE. Immune cells after prolonged Natalizumab therapy: implications for effectiveness and safety. *Acta Neurol Scand.* (2013) 128:e1–5. doi: 10.1111/ane.12080
24. Koudriavtseva T, Sbardella E, Trento E, Bordignon V, D'agosto G, Cordiali-Fei P. Long-term follow-up of peripheral lymphocyte subsets in a cohort

of multiple sclerosis patients treated with natalizumab. *Clin Exp Immunol.* (2014) 176:320–6. doi: 10.1111/cei.12261
25. Polman CH, Reingold SC, Banwell B, Clanet M, Cohen JA, Filippi M, et al. Diagnostic criteria for multiple sclerosis: 2010 revisions to the McDonald criteria. *Ann Neurol.* (2011) 69:292–302. doi: 10.1002/ana.22366
26. Kurtzke JF. Rating neurologic impairment in multiple sclerosis: an expanded disability status scale (EDSS). *Neurology* (1983) 33:1444–52. doi: 10.1212/WNL.33.11.1444
27. Kknms A. (ed.). *Qualitätshandbuch MS/NMOSD Empfehlungen zur Therapie der Multiple Sklerose Neuro- myelitis-optica-Spektrum- Erkrankungen für Ärzte* (2017).
28. Hoepner R, Faissner S, Salmen A, Gold R, Chan A. Efficacy and side effects of natalizumab therapy in patients with multiple sclerosis. *J Cent Nerv Syst Dis.* (2014) 6:41–9. doi: 10.4137/JCNSD.S14049
29. Van Pesch V, Sindic CJ, Fernandez O. Effectiveness and safety of natalizumab in real-world clinical practice: review of observational studies. *Clin Neurol Neurosurg.* (2016) 149:55–63. doi: 10.1016/j.clineuro.2016.07.001
30. Shirani A, Stuve O. Natalizumab for multiple sclerosis: a case in point for the impact of translational neuroimmunology. *J Immunol.* (2017) 198:1381–6. doi: 10.4049/jimmunol.1601358
31. Hickey WF. Migration of hematogenous cells through the blood-brain barrier and the initiation of CNS inflammation. *Brain Pathol.* (1991) 1:97–105. doi: 10.1111/j.1750-3639.1991.tb00646.x
32. Niino M, Bodner C, Simard ML, Alatab S, Gano D, Kim HJ, et al. Natalizumab effects on immune cell responses in multiple sclerosis. *Ann Neurol.* (2006) 59:748–54. doi: 10.1002/ana.20859
33. Krumbholz M, Meinl I, Kumpfel T, Hohlfeld R, Meinl E. Natalizumab disproportionately increases circulating pre-B and B cells in multiple sclerosis. *Neurology* (2008) 71:1350–4. doi: 10.1212/01.wnl.0000327671.91357.96
34. Lehmann-Horn K, Sagan SA, Bernard CC, Sobel RA, Zamvil SS. B-cell very late antigen-4 deficiency reduces leukocyte recruitment and susceptibility to central nervous system autoimmunity. *Ann Neurol.* (2015) 77:902–8. doi: 10.1002/ana.24387
35. Vennegoor A, Rispens T, Strijbis EM, Seewann A, Uitdehaag BM, Balk LJ, et al. Clinical relevance of serum natalizumab concentration and anti-natalizumab antibodies in multiple sclerosis. *Mult Scler.* (2013) 19:593–600. doi: 10.1177/1352458512460604
36. Ryan DH, Nuccie BL, Abboud CN, Winslow JM. Vascular cell adhesion molecule-1 and the integrin VLA-4 mediate adhesion of human B cell precursors to cultured bone marrow adherent cells. *J Clin Invest.* (1991) 88:995–1004. doi: 10.1172/JCI115403
37. Leclerc M, Lesesve JF, Gaillard B, Troussard X, Tourbah A, Debouverie M, et al. Binucleated lymphocytes in patients with multiple sclerosis treated with natalizumab. *Leuk Lymphoma* (2011) 52:910–2. doi: 10.3109/10428194.2010.551156
38. Robier C, Amouzadeh-Ghadikolai O, Bregant C, Diez J, Melinz K, Quehenberger F, et al. The frequency of occurrence of atypical lymphocytes in peripheral blood smears of natalizumab-treated patients with multiple sclerosis. *Int J Lab Hematol.* (2017) 39:469–74. doi: 10.1111/ijlh.12662
39. Stuve O, Marra CM, Bar-Or A, Niino M, Cravens PD, Cepok S, et al. Altered CD4+/CD8+ T-cell ratios in cerebrospinal fluid of natalizumab-treated patients with multiple sclerosis. *Arch Neurol.* (2006) 63:1383–7. doi: 10.1001/archneur.63.10.1383
40. Mellergard J, Edstrom M, Jenmalm MC, Dahle C, Vrethem M, Ernerudh J. Increased B cell and cytotoxic NK cell proportions and increased T cell responsiveness in blood of natalizumab-treated multiple sclerosis patients. *PLoS ONE* (2013) 8:e81685. doi: 10.1371/journal.pone.0081685
41. Caruana P, Lemmert K, Ribbons K, Lea R, Lechner-Scott J. Natural killer cell subpopulations are associated with MRI activity in a relapsing-remitting multiple sclerosis patient cohort from Australia. *Mult Scler.* (2016) 23:1479–1487. doi: 10.1177/1352458516679267
42. Planas R, Jelcic I, Schippling S, Martin R, Sospedra M. Natalizumab treatment perturbs memory- and marginal zone-like B-cell homing in secondary lymphoid organs in multiple sclerosis. *Eur J Immunol.* (2012) 42:790–8. doi: 10.1002/eji.201142108
43. Bochner BS, Luscinskas FW, Gimbrone MA Jr, Newman W, Sterbinsky SA, Derse-Anthony CP, et al. Adhesion of human basophils, eosinophils, and neutrophils to interleukin 1-activated human vascular endothelial cells: contributions of endothelial cell adhesion molecules. *J Exp Med.* (1991) 173:1553–7. doi: 10.1084/jem.173.6.1553
44. Lohmann L, Janoschka C, Schulte-Mecklenbeck A, Klinsing S, Kirstein L, Hanning U, et al. Immune cell profiling during switching from natalizumab to fingolimod reveals differential effects on systemic immune-regulatory networks and on trafficking of non-t cell populations into the cerebrospinal fluid-results from the tofingo successor study. *Front Immunol.* (2018). 9:1560. doi: 10.3389/fimmu.2018.01560
45. Klotz L, Berthele A, Bruck W, Chan A, Flachenecker P, Gold R, et al. Monitoring of blood parameters under course-modified MS therapy. Substance-specific relevance and current recommendations for action. *Nervenarzt* (2016) 87:645–59. doi: 10.1007/s00115-016-0077-1
46. Targan SR, Feagan BG, Fedorak RN, Lashner BA, Panaccione R, Present DH, et al. Natalizumab for the treatment of active Crohn's disease: results of the ENCORE Trial. *Gastroenterology* (2007) 132:1672–83. doi: 10.1053/j.gastro.2007.03.024
47. Thomas K, Eisele J, Rodriguez-Leal FA, Hainke U, Ziemssen T. Acute effects of alemtuzumab infusion in patients with active relapsing-remitting MS. *Neurol Neuroimmunol Neuroinflamm.* (2016) 3:e228. doi: 10.1212/NXI.0000000000000228
48. Kaufmann M, Haase R, Proschmann U, Ziemssen T, Akgün K. Real world lab data: Patterns of lymphocyte counts in fingolimod treated patients. *Frontiers in Immunology* (2018) 9: 460–11. doi: 10.3389/fimmu.2018.02669
49. Proschmann U, Thomas K, Thiel S, Hellwig K, Ziemssen T. Natalizumab during pregnancy and lactation. *Multiple Sclerosis* (2018) 24:1627–34. doi: 10.1177/1352458517728813

Conflict of Interest Statement: KA received personal compensation for from Novartis, Biogen Idec, Roche, Sanofi, and Merck for consulting service. TZ received personal compensation from Biogen Idec, Bayer, Novartis, Sanofi and Teva for consulting services. TZ received additional financial support for research activities from Bayer, Biogen Idec, Novartis, Teva, and Sanofi Aventis. UP received speaker fee from Roche. RH received fee from Sanofi.

The remaining authors declare that the research was conducted in the absence of any commercial or financial relationships that could be construed as a potential conflict of interest.

Copyright © 2018 Kaufmann, Haase, Proschmann, Ziemssen and Akgün. This is an open-access article distributed under the terms of the Creative Commons Attribution License (CC BY). The use, distribution or reproduction in other forums is permitted, provided the original author(s) and the copyright owner(s) are credited and that the original publication in this journal is cited, in accordance with accepted academic practice. No use, distribution or reproduction is permitted which does not comply with these terms.

frontiers in Neurology

BRIEF RESEARCH REPORT
published: 10 December 2018
doi: 10.3389/fneur.2018.01084

Moderate Frequency Resistance and Balance Training Do Not Improve Freezing of Gait in Parkinson's Disease: A Pilot Study

Christian Schlenstedt, Steffen Paschen, Jana Seuthe, Jan Raethjen, Daniela Berg, Walter Maetzler and Günther Deuschl*

Department of Neurology, University Hospital Schleswig-Holstein, Christian-Albrechts-University, Kiel, Germany

Background and Aim: Individuals with Parkinson's disease (PD) and Freezing of Gait (FOG) have impaired postural control, which relate to the severity of FOG. The aim of this study was to analyze whether a moderate frequency resistance (RT) and balance training (BT), respectively, are effective to diminish FOG.

Methods: This *post-hoc* sub-analysis of a randomized controlled training intervention study of PD patients with and without FOG reports about results from FOG patients. Twelve FOG patients performed RT and 8 BT (training 2x/week, 7 weeks). Testing was performed prior and post intervention. FOG was assessed with the FOG Questionnaire (FOGQ) and with the FOG score of a FOG provoking walking course. Balance performance was evaluated with the Fullerton Advanced Balance (FAB) scale. Tests were conducted by raters blinded to group allocation and assessment time point (only FOG score and FAB scale).

Results: For the FOGQ and FOG score, no significant differences were found within and between the two training groups ($p > 0.05$) and effect sizes for the improvements were small ($r < 0.1$). Groups did not significantly improve in the FAB scale. FOG score changes and FAB scale changes within the RT group showed a trend toward significant negative correlation (Rho $= -0.553$, $p = 0.098$).

Conclusions: Moderate frequency RT and BT was not effective in reducing FOG in this pilot study. The trend toward negative correlation between changes in FOG score and FAB scale suggests an interaction between balance (improvement) and FOG (improvement). Future studies should include larger samples and high frequency interventions to investigate the role of training balance performance to reduce the severity of FOG.

Keywords: freezing, postural control, balance, Parkinson's disease, exercise, training

OPEN ACCESS

Edited by:
Tobias Warnecke, Universitätsklinikum Münster, Germany

Reviewed by:
Simon Steib, Friedrich-Alexander-Universität Erlangen-Nürnberg, Germany
Andres Ceballos-Baumann, Technische Universität München, Germany

****Correspondence:***
Christian Schlenstedt
c.schlenstedt@neurologie.uni-kiel.de

Specialty section:
This article was submitted to Movement Disorders, a section of the journal Frontiers in Neurology

Received: *29 August 2018*
Accepted: *27 November 2018*
Published: *10 December 2018*

Citation:
Schlenstedt C, Paschen S, Seuthe J, Raethjen J, Berg D, Maetzler W and Deuschl G (2018) Moderate Frequency Resistance and Balance Training Do Not Improve Freezing of Gait in Parkinson's Disease: A Pilot Study. Front. Neurol. 9:1084. doi: 10.3389/fneur.2018.01084

INTRODUCTION

Freezing of gait (FOG) in Parkinson's disease (PD) is a disabling symptom which is defined as the "brief, episodic absence or marked reduction of forward progression of the feet despite the intention to walk" (1). It has been shown that FOG-specific training interventions, such as cueing, can reduce FOG (2–4). It is however unclear whether non-FOG-specific exercises which target FOG-related deficits also alleviate FOG.

Individuals with PD with FOG (PD + FOG) have postural control deficits (5, 6) and the severity of FOG relates to the degree of postural instability (5). Recently it has been shown that PD+FOG have smaller anticipatory postural adjustments (APAs) when preparing for step initiation compared to patients without FOG (PD-FOG) and that the size of medio-lateral APAs was positively correlated with FOG severity (7). It has been suggested that reducing the size of APA might be a compensatory strategy addressing postural control deficits (7). Further, Plotnik et al. (8) proposed that FOG might be a result of multiple with FOG associated motor impairments such as dynamic postural control, gait asymmetry, and gait variability. According to this framework, FOG might occur if enough of these features deteriorate. It is unclear, whether an improvement of postural control as one of these FOG related features might diminish FOG.

In a recent study we compared resistance training (RT) with balance training (BT) to improve postural control in PD and we showed that RT was beneficial to improve balance performance. This sub-analysis has two aims: first, to test whether RT or BT is effective to reduce the severity of FOG and second, whether an improvement in FOG is related to improved postural control.

MATERIALS AND METHODS

This study is a sub-analysis (only PD + FOG, $N = 20$) of a randomized controlled trial that investigated the efficacy of RT vs. BT to improve postural control in PD ($N = 40$) (9).

Participants

Inclusion criteria were the diagnosis of idiopathic PD as defined by the UK Brain Bank criteria, FOG based on the FOG Questionnaire (10) (FOGQ) (item 3 > 0) and postural instability [Fullerton Advanced Balance (FAB) scale <26 points (11)]. Details about the exclusion criteria are reported in Schlenstedt et al. (9). Individuals had to be on stable medication during the training and assessment periods.

This study was carried out in accordance with the recommendations of Ethik-Kommission, Universitätsklinikum Schleswig-Holstein, Campus Kiel, Arnold-Heller-Straße 3, 24105 Kiel, Germany, with written informed consent from all subjects. All subjects gave written informed consent in accordance with the Declaration of Helsinki. The protocol was approved by the Ethik-Kommission, Universitätsklinikum Schleswig-Holstein, Campus Kiel, Arnold-Heller-Straße 3, 24105 Kiel, Germany.

Randomization and Intervention

Participants were randomized into either RT or BT (7 weeks, 2x/week, 60 min per session) within the original study. There was no stratification for FOG in the original randomization. Training was conducted in groups of 4–5 people. Each session started with a warm-up (10 min) followed by either RT or BT. In brief, RT consisted of lower limb muscle strength exercises and participants' own weight, cuff weights, and elasticated bands were used as resistance. Squats, knee extensions, toe/calf raises, hip abductions, and other exercises were performed [for details see (9)].

BT consisted of static and dynamic postural control tasks. Participants were asked to train their limits of stability by leaning forward/backward/sideward. Reactive postural control was trained by shoulder pulls. One option to reach training progression was the inclusion of unstable surfaces on which the participants had to stand or walk [see Schlenstedt et al. (9) for further details about training progression].

Testing Procedure and Outcome Measures

Participants were tested 1 week prior (PRE) and 1 week post (POST) intervention. Testing was conducted in the ON state of medication at the same time of a day for each participant. Severity of FOG was assessed with the FOGQ (10) and with the FOG score by Ziegler et al. (12). The FOGQ was conducted by an assessor blinded to group allocation. Trials of the FOG score were video-recorded and videos were rated by an independent rater, also blinded to assessment time point and group allocation.

Furthermore, the following tests were included in the analysis: FAB scale (to assess postural control) (11, 13), Unified Parkinson's Disease Rating Scale (UPDRS), and Mini Mental State Examination.

Statistical Analysis

Demographic and baseline differences between groups were analyzed with a Mann-Whitney-*U*-Test (except for gender: Chi-Square Test). As data were not normally distributed, non-parametric tests were used. A Wilcoxon-Signed-Rank-Test was conducted to analyze the changes from PRE to POST within one group. To compare the different training types, the differences from PRE to POST were calculated and the magnitude of change were compared between the two groups were analyzed with using the Mann-Whitney-*U*-Test. Effect sizes were calculated ($r = z$-score/(n)^1/2). We considered effect sizes to be small with $0.1 < r < 0.3$, medium with $0.3 < r < 0.5$ and large with $r > 0.5$ (14). The magnitude of change in FOG severity was correlated [Spearman's rank correlation coefficient [Rho] with the change

TABLE 1 | Participant characteristics.

Variable	Resistance training ($n = 12$)	Balance training ($n = 8$)	*p*-value*
Age (y)	78.3 (5.8)	81.4 (7.3)	0.41
Gender (M/F)	9/3	6/2	1.00
BMI (kg/m²)	27.3 (6.5)	24.5 (3.5)	0.34
Disease duration (y)	11.2 (6.6)	8.4 (7.3)	0.38
HandY stage	2.8 (0.3)	2.9 (0.5)	1.00
UPDRS	43.2 (13.2)	45.8 (9.8)	0.51
UPDRS III	24.3 (10.0)	25.8 (5.7)	0.61
FAB scale	21.1 (4.7)	22.4 (5.2)	0.61
MMSE	27.4 (3.7)	26.2 (4.0)	0.44
LEDD	765 (448)	652 (286)	0.46
FOGQ	12.5 (4.5)	15.3 (3.1)	0.22
FOG score	6.6 (7.2)	5.9 (4.4)	0.92

*Values represent mean (SD) or number. *p-value of Mann-Whitney-U-Test (and Chi-Square-Test for Gender).*

TABLE 2 | Statistical results of the FOGQ and FOG score.

Test	Group	Value	PRE	POST	Within group comparison from PRE to POST		Between group comparison of changes from PRE to POST	
					p-value*	Effect size r	*p*-value**	Effect size *r*
FOGQ	RT	Mean (SD)	12.5 (4.5)	12.3 (4.8)	0.878	0.031	0.279	0.255
		Median (Range)	12 (5–20)	13.5 (5–19)				
	BT	Mean (SD)	15.3 (3.1)	17.0 (2.4)	0.136	0.430		
		Median (Range)	16 (10–19)	17.5 (13–19)				
FOG score	RT	Mean (SD)	6.6 (7.2)	6.9 (9.1)	0.833	0.047	0.153	0.347
		Median (Range)	5 (0–22)	3.5 (0–29)				
	BT	Mean (SD)	5.9 (4.4)	8.7 (5.1)	0.105	0.433		
		Median (Range)	6 (0–12)	8 (2–15)				
FAB scale	RT	Mean (SD)	21.1 (4.7)	23.2 (5.0)	0.245	0.336	0.534	0.139
		Median (Range)	22 (10–29)	22.5 (15–34)				
	BT	Mean (SD)	22.4 (5.2)	22.4 (5.7)	1.000	0.000		
		Median (Range)	23.5 (15–27)	25.5 (12–27)				

**p-value of Wilcoxon Signed Rank Test. **p-value of Mann-Whitney-U Test. RT, Resistance Training; BT, Balance Training.*

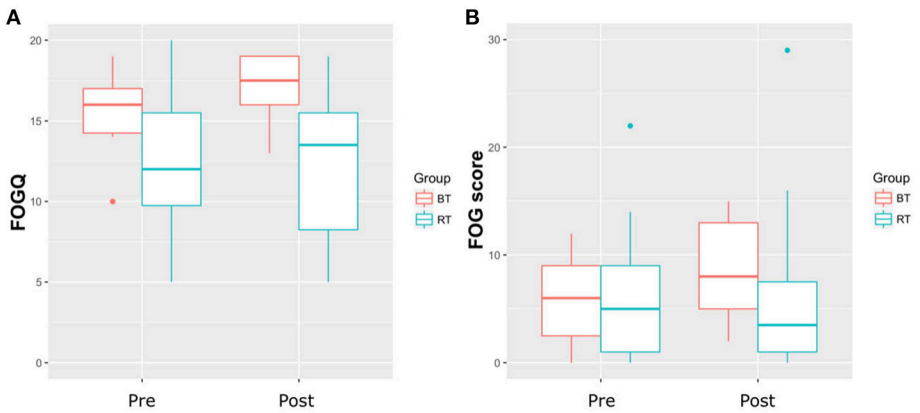


FIGURE 1 | (A) Results of the Freezing of Gait Questionnaire (FOGQ). **(B)** Results of the Freezing of Gait score; BT, Balance Training; RT, Resistance Training.

in balance performance (FAB scale). Level of significance was set at $p < 0.05$. Statistical analysis was performed with R (version 1.1.442) (15).

RESULTS

Table 1 shows the participant characteristics. RT and BT groups neither significantly differed in any demographic variable, nor with regard to severity of FOG. Both training types had no significant effect on FOGQ and FOG score (**Table 2** and **Figure 1**) ($p < 0.05$). The effect sizes for the slight improvements within the RT group were small ($r < 0.1$) (14). Within this sample, the groups did not improve significantly in postural control as measured with the FAB scale ($p < 0.05$). Although statistically not significant within this sample, a large effect was found within the RT group when relating the change in balance performance (FAB scale) with the change in FOG score (Rho $= -0.553$, $p = 0.098$). A similar trend was found when calculating this correlation taken both groups together ($p = 0.11$, Rho $= -0.4$). A medium effect was found within the BT group ($p = 0.426$, Rho $= 0.361$). Changes in FOGQ was not related to the change in FAB scale (RT: $p = 0.948$; BT: $p = 0.612$). The exclusion of outliers did not relevantly affect our results.

DISCUSSION

We could not show that a moderate frequency RT and BT is effective to diminish FOG in people with PD in the present pilot study. As FOG-specific training interventions such as cueing did indeed show statistically significant reduction in FOG severity (2–4), our study might indirectly supports the hypothesis that exercises specifically designed to target FOG might be more beneficial than non-FOG-specific interventions. We acknowledge that our sample was small and results have to be interpreted cautiously; however, due to the low effect sizes we do not expect reaching significant results with this training protocol

even with a larger sample. We rather believe that increasing the intensity and frequency of training is required to see a relevant effect and this has been suggested by other larger trials (16).

As FOG is related to postural control deficits (5, 6) the idea of this project was that improved postural control might lead to a reduction in FOG episodes. In the original study, participants of the RT group significantly improved postural control whereas the group of BT did not. We found a large effect when correlating the change in balance performance with the change in FOG severity within the RT group, indicating that those participants who improved postural control may also benefit with respect to FOG, supporting our hypothesis with respect to study aim II. However, this failed to reach statistical significance within this sample and the subgroup of participants with FOG did not significantly improve their postural control in this sub-analysis. This might be explained by the low training frequency (2x/week) and by the small subsample size, as in the original study on all participants of the RT balance performance improved significantly (9). Thus, the impact of training balance performance on FOG cannot clearly be answered with this study.

The following limitations have to be mentioned: Sample size is small and results therefore have to be interpreted cautiously. This study did not include a non-exercise control group which would give additional information with respect to the training effects.

A moderate frequency RT and BT was not effective to diminish FOG within this small sample. This pilot study might help designing future studies which should include larger samples and higher training frequency to investigate the role of training balance performance to reduce FOG occurrence in PD.

AUTHOR CONTRIBUTIONS

CS: Study design, study conduction, data collection, statistical analysis, and writing of first draft; SP and JS: Data analysis and manuscript critical revision; JR and GD: Study design and manuscript critical revision; DB and WM: Manuscript critical revision.

ACKNOWLEDGMENTS

We thank our participant for donating their time to volunteer. We thank Annika Kruse and Anna Krebs for helping in conducting the training sessions and in data collection. This publication was made possible with support from the Coppenrath-Foundation, Geeste/Groß-Hesepe, Niedersachsen, Germany and Krumme-Stiftung, Eckernförde, Schleswig-Holstein, Germany (Schlenstedt). We acknowledge financial support by Land Schleswig-Holstein within the funding programme Open Access Publikationsfonds.

REFERENCES

1. Giladi N, Nieuwboer A. Understanding and treating freezing of gait in parkinsonism, proposed working definition, and setting the stage. *Mov Disord.* (2008) 23(Suppl. 2):S423–5. doi: 10.1002/mds.21927
2. Fietzek UM, Schroeteler FE, Ziegler K, Zwosta J, Ceballos-Baumann AO. Randomized cross-over trial to investigate the efficacy of a two-week physiotherapy programme with repetitive exercises of cueing to reduce the severity of freezing of gait in patients with Parkinson's disease. *Clin Rehabil.* (2014) 28:902–11. doi: 10.1177/0269215514527299
3. Plotnik M, Shema S, Dorfman M, Gazit E, Brozgol M, Giladi N, et al. A motor learning-based intervention to ameliorate freezing of gait in subjects with Parkinson's disease. *J Neurol.* (2014) 261:1329–39. doi: 10.1007/s00415-014-7347-2
4. Barthel C, Nonnekes J, van Helvert M, Haan R, Janssen A, Delval A, et al. The laser shoes: a new ambulatory device to alleviate freezing of gait in Parkinson disease. *Neurology* (2018) 90:e164–71. doi: 10.1212/WNL.0000000000004795
5. Schlenstedt C, Muthuraman M, Witt K, Weisser B, Fasano A, Deuschl G. Postural control and freezing of gait in Parkinson's disease. *Parkinsonism Relat Disord.* (2016) 24:107–12. doi: 10.1016/j.parkreldis.2015.12.011
6. Bekkers EMJ, Dijkstra BW, Dockx K, Heremans E, Verschueren SMP, Nieuwboer A. Clinical balance scales indicate worse postural control in people with Parkinson's disease who exhibit freezing of gait compared to those who do not: a meta-analysis. *Gait Posture* (2017) 56:134–40. doi: 10.1016/j.gaitpost.2017.05.009
7. Schlenstedt C, Mancini M, Nutt J, Hiller AP, Maetzler W, Deuschl G, et al. Are hypometric anticipatory postural adjustments contributing to freezing of gait in Parkinson's disease? *Front Aging Neurosci.* (2018) 10:36. doi: 10.3389/fnagi.2018.00036
8. Plotnik M, Giladi N, Hausdorff JM. Is freezing of gait in Parkinson's disease a result of multiple gait impairments? Implications for treatment. *Parkinsons Dis.* (2012) 2012:459321. doi: 10.1155/2012/459321
9. Schlenstedt C, Paschen S, Kruse A, Raethjen J, Weisser B, Deuschl G. Resistance versus balance training to improve postural control in Parkinson's disease: a randomized rater blinded controlled study. *PLoS ONE* (2015) 10:e0140584. doi: 10.1371/journal.pone.0140584
10. Giladi N, Tal J, Azulay T, Rascol O, Brooks DJ, Melamed E, et al. Validation of the freezing of gait questionnaire in patients with Parkinson's disease. *Mov Disord.* (2009) 24:655–61. doi: 10.1002/mds.21745
11. Schlenstedt C, Brombacher S, Hartwigsen G, Weisser B, Moller B, Deuschl G. Comparing the fullerton advanced balance scale with the mini-BESTest and Berg Balance Scale to assess postural control in patients with Parkinson disease. *Arch Phys Med Rehabil.* (2015) 96:218–25. doi: 10.1016/j.apmr.2014.09.002
12. Ziegler K, Schroeteler F, Ceballos-Baumann AO, Fietzek UM. A new rating instrument to assess festination and freezing gait in Parkinsonian patients. *Mov Disord.* (2010) 25:1012–8. doi: 10.1002/mds.22993
13. Rose DJ, Lucchese N, Wiersma LD. Development of a multidimensional balance scale for use with functionally independent older adults. *Arch Phys Med Rehabil.* (2006) 87:1478–85. doi: 10.1016/j.apmr.2006.07.263
14. Cohen J. A power primer. *Psychol Bull.* (1992) 112:155–9.
15. Development Core Team. *R: A Language and Environment for Statistical Computing*. Vienna: R Foundation for Statistical Computing (2005).
16. Clarke CE, Patel S, Ives N, Rick CE, Woolley R, Wheatley K, et al. Clinical effectiveness and cost-effectiveness of physiotherapy and occupational therapy versus no therapy in mild to moderate Parkinson's disease: a large pragmatic randomised controlled trial (PD REHAB). *Health Technol Assess.* (2016) 20:1–96. doi: 10.3310/hta20630

Conflict of Interest Statement: The authors declare that the research was conducted in the absence of any commercial or financial relationships that could be construed as a potential conflict of interest.

Copyright © 2018 Schlenstedt, Paschen, Seuthe, Raethjen, Berg, Maetzler and Deuschl. This is an open-access article distributed under the terms of the Creative Commons Attribution License (CC BY). The use, distribution or reproduction in other forums is permitted, provided the original author(s) and the copyright owner(s) are credited and that the original publication in this journal is cited, in accordance with accepted academic practice. No use, distribution or reproduction is permitted which does not comply with these terms.

frontiers in Neurology

BRIEF RESEARCH REPORT
published: 17 December 2018
doi: 10.3389/fneur.2018.01094

Dermal Phospho-Alpha-Synuclein Deposition in Patients With Parkinson's Disease and Mutation of the Glucocerebrosidase Gene

Kathrin Doppler[1*†], *Kathrin Brockmann*[2†], *Annahita Sedghi*[1], *Isabel Wurster*[2], *Jens Volkmann*[1], *Wolfgang H. Oertel*[3] *and Claudia Sommer*[1]

[1] Department of Neurology, University Hospital Würzburg, Würzburg, Germany, [2] Department of Neurology, University Hospital Tübingen, Tubingen, Germany, [3] Department of Neurology, University Hospital Marburg, Marburg, Germany

Heterozygous mutations in the glucocerebrosidase gene (*GBA1*) represent the most common genetic risk factor for Parkinson's disease (PD) and are histopathologically associated with a widespread load of alpha-synuclein in the brain. Therefore, PD patients with *GBA1* mutations are a cohort of high interest for clinical trials on disease-modifying therapies targeting alpha-synuclein. There is evidence that detection of phospho-alpha-synuclein (p-syn) in dermal nerve fibers might be a biomarker for the histopathological identification of PD patients even at premotor or very early stages of disease. It is so far unknown whether dermal p-syn deposition can also be found in PD patients with *GBA1* mutations and may serve as a biomarker for PD in these patients. Skin biopsies of 10 PD patients with different *GBA1* mutations (six N370S, three E326K, one L444P) were analyzed by double-immunofluorescence labeling with anti-p-syn and anti-protein gene product 9.5 (PGP9.5, axonal marker) to detect intraaxonal p-syn deposition. Four biopsy sites (distal, proximal leg, paravertebral Th10, and C7) per patient were studied. P-syn was found in six patients (three N370S, three E326K). P-syn deposition was mainly detected in autonomic nerve fibers, but also in somatosensory fibers and was not restricted to a certain *GBA1* mutation. In summary, dermal p-syn in PD patients with *GBA1* mutations seems to offer a similar distribution and frequency as observed in patients without a known mutation. Skin biopsy may be suitable to study p-syn deposition in these patients or even to identify premotor patients with *GBA1* mutations.

Keywords: Parkinson's disease, glucocerebrosidase mutation, alpha-synuclein, skin biopsy, biomarker

OPEN ACCESS

Edited by:
Tobias Warnecke, Universitätsklinikum Münster, Germany

Reviewed by:
Tino Prell, Friedrich-Schiller-Universität Jena, Germany
Francisco José Pan-Montojo, Ludwig Maximilian University of Munich, Germany

****Correspondence:***
Kathrin Doppler
Doppler_K@ukw.de

† These authors have contributed equally to this work

Specialty section:
This article was submitted to Movement Disorders, a section of the journal Frontiers in Neurology

Received: *06 October 2018*
Accepted: *29 November 2018*
Published: *17 December 2018*

Citation:
Doppler K, Brockmann K, Sedghi A, Wurster I, Volkmann J, Oertel WH and Sommer C (2018) Dermal Phospho-Alpha-Synuclein Deposition in Patients With Parkinson's Disease and Mutation of the Glucocerebrosidase Gene. Front. Neurol. 9:1094. doi: 10.3389/fneur.2018.01094

INTRODUCTION

Pre-mortal diagnosis of Parkinson's disease (PD) is based on its clinical presentation with tremor, rigor, akinesia, and postural instability. Alpha-synuclein aggregates in neurons of the substantia nigra represent the histopathological hallmark of the disease and are not only considered as post-mortem disease marker but also offer insights into the pathogenesis of the disease.

In the last few years, focus has been set on the onset of PD-associated neurodegeneration and it is known that the disease starts many years before the onset of motor symptoms (1). Non-motor symptoms such as obstipation, hyposmia, depression, or rapid eye movement sleep behavior

disorder (RBD) may occur during the prodromal phase of PD when the patients do not show any motor symptoms but alpha-synuclein deposition and neuronal loss can already be found in the brain (2). Major efforts of drug development focus on the deposition of alpha-synuclein as a probable pathogenic key event. Clinical trials of drugs targeting alpha-synuclein deposition require reliable identification of patients with primarily alpha-synuclein-driven neurodegeneration who are in the prodromal stage of the disease and in whom pre-mortem non-invasive monitoring of alpha-synuclein deposition is possible. Within a high-risk cohort for PD, skin biopsy might be a potential tool to identify individuals at the earliest stages of the disease and to monitor progression of alpha-synuclein deposition. One of such a high-risk PD cohort are patients with RBD (3) and it has already been shown that p-syn deposition can be found in skin biopsies of RBD patients, rendering skin biopsy a potential biomarker for prodromal PD (4, 5). Another risk factor for the development of PD are glucocerebrosidase gene (*GBA1)* mutations that are supposed to be found in 4–10% of all PD patients (6–8) and increase the risk of developing PD 20-fold (8). PD patients carrying *GBA1* mutations are of special interest as a first clinical trial with a substrate reduction inhibitor, GZ/SAR402671, has already started in in this subgroup of PD. However, alpha-synuclein deposition in skin biopsy has not yet been tested in PD patients with *GBA1* mutations.

In the present study, we aimed to evaluate the use of skin biopsy for the detection of p- syn in PD patients with *GBA1* mutations and to evaluate potential differences of dermal p-syn deposition in patients with *GBA1* mutation associated PD compared to results from former studies on patients with idiopathic PD.

MATERIALS AND METHODS

Patients

Ten patients with a known *GBA1* mutation were prospectively recruited at the University Hospital Tübingen (mean age 61.7 (±8.1) years. Initially, they had been recruited for the prospective observational MiGAP study (Markers in *GBA1* associated Parkinson) funded by the DZNE (German Centre for Neurodegenerative Diseases, Site Tuebingen)[1] Out of 100 patients of the MIGAP study, we randomly selected and asked 10 PD patients to take part in the present sub-study. Diagnosis of PD was based on the UK brain bank criteria (9). Stage of disease was assessed using the Hoehn&Yahr scale (10), motor function was evaluated by Unified Parkinson's Disease Ranking Scale part III (UPDRS-III) (11). The bradykinesia score and annual UPDRSIII progression were calculated as previously described (12). Ten age and gender matched healthy controls who were recruited for former studies (5) and whose biopsy material was stored at our department were also investigated. All patients and controls gave oral and written informed consent to participate. The study was approved by the Ethic's committee of the University of Würzburg.

Abbreviations: *GBA1*, glucocerebrosidase gene; PD, Parkinson's disease; RBD, REM sleep behavior disorder; PGP9. 5, protein gene product 9.5; p-syn, phospho-alpha-synuclein.

[1]https://www.dzne.de/forschung/studien/klinische-studien/migap/

Demographic data of all patients and controls and the type of mutation are summarized in **Table 1**.

Skin Biopsy

Skin punch biopsies were taken from the distal and proximal leg, back (Th10), and neck (C7), fixed with paraformaldehyde and cryconserved until use as previously described (13). Twenty micrometer serial cryosections were cut. Double-immunofluorescence-labeling was performed using anti-PGP9.5 (axonal marker, Zytomed Systems, Berlin, Germany, 1:200) and anti-p-syn (Biolegend, San Diego, CA, United States, 1:500) and appropriate Cy3 and AlexaFluor488-conjugated secondary antibodies (Dianova, Hamburg, Germany, 1:100/1:400).

Microscopy

Double-immunofluorescence-labeling was assessed in a blinded manner using a fluorescence microscope with CARVII system (Ax10, Zeiss, Oberkochen, Germany/Visitron GmbH, Puchheim, Germany). All slides were scanned for p-syn-positive dermal nerve fibers. Nerve fibers were identified by staining with anti-PGP9.5 and only p-syn deposition within nerve fibers was considered "positive." A biopsy was assessed "positive" if at least one dermal nerve fiber was immunoreactive for p-syn. P-syn-positive nerve fibers were categorized as sudomotor, vasomotor, pilomotor, or somatosensory (subepidermal plexus or intraepidermal) according to their location. Nerve fibers that could not be assigned to a certain skin structure were assessed as dermal nerve bundles. P-syn deposition was quantified as the number of skin structures that contained at least one p-syn-positive nerve fiber.

Statistical Evaluation

Statistical analysis was calculated using SPSS Statistics 23 software (IBM, New York, United States). Two-sided Pearson's correlation test was used for correlation analysis. A significance level of 5% was applied.

RESULTS

P-syn deposition was found in 6/10 PD patients with *GBA1* mutations, not in any healthy control (**Figure 1**). P-syn-positive nerve fibers were found in four biopsies of the distal leg, four of the proximal leg, two of the back, and two of the neck. Autonomic vasomotor fibers were affected in three cases, sudomotor fibers in one patient (**Figure 1C**), pilomotor in two (**Figure 1A**), and dermal nerve bundles in five cases. Somatosensory nerve fibers of the subepidermal plexus were found positive in two patients, in one of them, intraepidermal fibers were positive (**Figure 1B**). P-syn-positive fibers were not restricted to a certain mutation within *GBA1* and were found in 3/6 patients with N370S mutation, 3/3 patients with E326K mutation, and 0/1 patient with L444P mutation. The number of p-syn positive dermal structures correlated with the duration of disease ($p = 0.02$, $r = 0.71$), but not with age at assessment. Correlation analysis between p-syn-positive structures and H&Y stage, bradykinesia score and annual UPDRSIII progression was not significant (H&Y: $p = 0.06$, r = 0.61, bradykinesia score: $p = 0.37$, $r = 0.32$, annual UPDRSIII progression: $p = 0.08$, $r = -0.58$).

TABLE 1 | Demographic data and p-syn deposition of patients with *GBA1* mutation.

Patient no.	Duration of disease (y)	H&Ystage	UPDRS part III	Annual UPDRS III progression	Bradykinesia score	Subtype	*GBA1* mut.	p-syn pos biopsy site	p-syn pos structures	No. of positive struct.
1	14	3	70	5	1.7	Equivalent	N370S	LL	ves, db, ep	3
2	6	2	48	8	1.5	Equivalent	N370S	–		0
3	17	2	34	2	0.6	Equivalent	N370S	LL, Th10	subepi, intraepi,ves, db	4
4	6	2.5	35	5.8	1.7	Equivalent	N370S	–		0
5	5	2	32	6.4	1.1	Equivalent	N370S	UL, Th10	db	2
6	1	2	10	10	0.5	Tremor dominant	L444P	–		0
7	8	3	49	6.1	2.5	Equivalent	E326K	UL, LL, C7	db, ves, ep	4
8	14	2	32	2.3	1.6	Equivalent	E326K	UL	subepi	1
9	14	3	53	3.8	2.6	Equivalent	E326K	UL, LL, C7	db, sg	4
10	2	2	36	18	1.8	Acinetic-rigid	N370S	–		0

No., number; y, years; H&Y, Hoehn&Yahr; GBA1, glucocerebrosidase gene; p-syn, phospho-alpha-synuclein; pos, positive; struct., structures; LL, lower leg; UL, upper leg; ves, vessel; db, dermal nerve bundle; ep, erector pilorum muscle; subepi, subepidermal; intraepi, intraepidermal; sg, sweat gland; UPDRS, Unified Parkinson Disease Rating Scale.

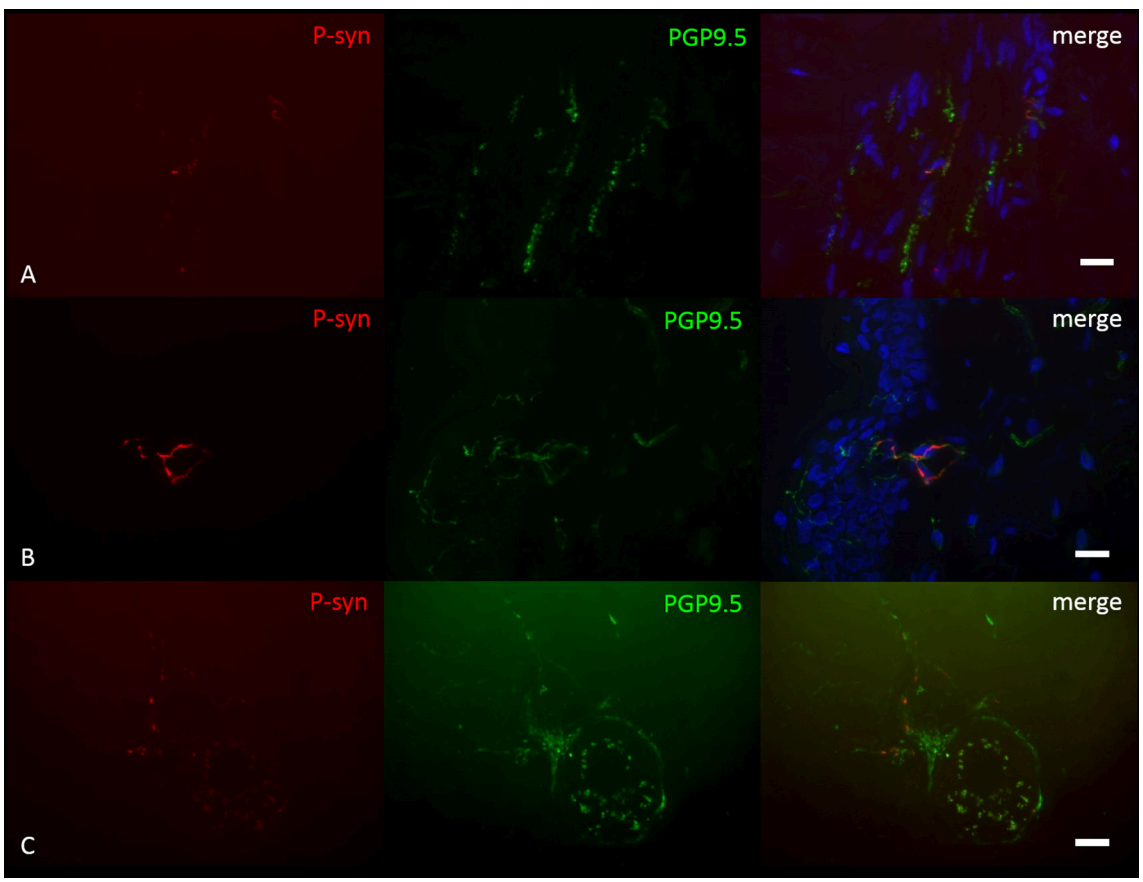


FIGURE 1 | Photomicrographs of a double-immunofluorescence staining with anti-p-syn (red) and anti-PGP9.5 (green). Cell nuclei are stained with DAPI (blue). P-syn deposition is detectable in pilomotor fibers **(A)**, intraepidermal fibers **(B)** and sudomotor fibers **(C)** of patients with *GBA1* mutation-associated PD. Scale Bar = 10 μm.

DISCUSSION

Here, we report p-syn deposition in dermal nerve fibers of PD patients carrying a mutation in *GBA1*.

The frequency of 60% in our study is comparable with former skin biopsy studies in idiopathic PD using similar protocols (5, 13, 14). Predominant autonomic involvement with vasomotor fibers as the mostly affected fibers is also in line with previous

studies (13, 15). Our results indicate that dermal p-syn pathology of patients with *GBA1* mutations does not differ from idiopathic PD. This corresponds to findings from brain autopsy studies that also did not show a clear difference except for some studies describing more extensive diffuse cortical Lewy bodies (6, 16) that could not be confirmed by others (17, 18). Dermal p-syn deposition was not restricted to a certain mutation and was also found in patients with the E326K mutation which is considered a rather "mild" mutation (19). Our results indicate that clinical and neuropathological similarity between patients with *GBA1* mutations and without can be extended to the PNS, rendering skin biopsy a pre-mortem tool to investigate p-syn pathology in this patient group.

In recent studies no correlation between p-syn deposition and stage or duration of disease could be determined for PD (13, 15). Only in RBD, a potential prodromal stage of PD, a correlation between dermal p-syn and disease progression markers could be found, indicating a steady-state of dermal p-syn deposition during motor stages of disease. In the present study, p-syn positive structures correlated with duration of disease. This might indicate progressive p-syn deposition during the course of disease in patients with *GBA1* mutations. This is of special interest as this subgroup of PD patients was shown to present a more rapid disease progression (20). The frequency of p-syn deposition in early or even prodromal stages of *GBA1* associated PD needs to be investigated in future studies.

The exact underlying pathomechanism of p-syn deposition in patients with *GBA1* mutations is still unclear, but there is evidence that impaired lysosomal function and endoplasmatic reticulum stress play a role (21) and that accumulation of alpha synuclein is promoted by glucocerebrosidase deficiency (22). Involvement of dermal nerve fibers in p-syn pathology in *GBA1* mutation associated PD provides the opportunity for the use of skin biopsy as a pre-mortem easily accessible tissue for the investigation of p-syn pathology in this subgroup of PD.

In summary, this pilot study gives evidence that dermal nerve fibers are affected by p-syn pathology in PD with *GBA1* mutations. A major limitation is the small sample size that does not allow a clear conclusion on the frequency and distribution of p-syn deposition in this subgroup compared to idiopathic PD. Detection of p-syn in skin biopsies of *GBA1*-associated PD is a basic prerequisite for future studies on prodromal *GBA1*-associated PD.

AUTHOR CONTRIBUTIONS

KD planned and designed the study, performed, and analyzed skin biopsies and wrote the first draft of the manuscript. KB planned and designed the study, recruited and characterized patients, performed skin biopsies, and revised the manuscript. AS performed and analyzed skin biopsies. IW recruited and characterized patients. JV and WO were involved in the study design. CS was involved in study design and revised the manuscript.

ACKNOWLEDGMENTS

We thank Barbara Dekant and Barbara Reuter for expert technical assistance. The study was funded by Parkinson Fonds Deutschland. WO is Hertie Senior Research Professor supported by the charitable Hertie Foundation, Frankfurt/Main, Germany.

REFERENCES

1. Berg D, Postuma RB, Adler CH, Bloem BR, Chan P, Dubois B, et al. MDS research criteria for prodromal Parkinson's disease. *Mov Disord.* (2015) 30:1600–11. doi: 10.1002/mds.26431
2. Braak H, Del Tredici K, Rub U, de Vos RA, Jansen Steur EN, Braak E. Staging of brain pathology related to sporadic Parkinson's disease. *Neurobiol Aging* (2003) 24:197–211. doi: 10.1016/S0197-4580(02)00065-9
3. Iranzo A, Tolosa E, Gelpi E, Molinuevo JL, Valldeoriola F, Serradell M, et al. Neurodegenerative disease status and post-mortem pathology in idiopathic rapid-eye-movement sleep behaviour disorder: an observational cohort study. *Lancet Neurol.* (2013) 12:443–53. doi: 10.1016/S1474-4422(13)70056-5
4. Antelmi E, Donadio V, Incensi A, Plazzi G, Liguori R. Skin nerve phosphorylated alpha-synuclein deposits in idiopathic REM sleep behavior disorder. *Neurology* (2017) 88:2128–31. doi: 10.1212/WNL.0000000000003989
5. Doppler K, Jentschke HM, Schulmeyer L, Vadasz D, Janzen A, Luster M, et al. Dermal phospho-alpha-synuclein deposits confirm REM sleep behaviour disorder as prodromal Parkinson's disease. *Acta Neuropathol.* (2017) 133:535–45. doi: 10.1007/s00401-017-1684-z
6. Neumann J, Bras J, Deas E, O'Sullivan SS, Parkkinen L, Lachmann RH, et al. Glucocerebrosidase mutations in clinical and pathologically proven Parkinson's disease. *Brain* (2009) 132:1783–94. doi: 10.1093/brain/awp044
7. Sidransky E, Nalls MA, Aasly JO, Aharon-Peretz J, Annesi G, Barbosa ER, et al. Multicenter analysis of glucocerebrosidase mutations in Parkinson's disease. *N Engl J Med.* (2009) 361:1651–61. doi: 10.1056/NEJMoa0901281
8. Schapira AH. Glucocerebrosidase and Parkinson disease: recent advances. *Mol Cell Neurosci.* (2015) 66:37–42. doi: 10.1016/j.mcn.2015.03.013
9. Hughes AJ, Daniel SE, Kilford L, Lees AJ. Accuracy of clinical diagnosis of idiopathic parkinson's disease: a clinico-pathological study of 100 cases. *J Neurol Neurosurg Psychiatr.* (1992) 55:181–4. doi: 10.1136/jnnp.55.3.181
10. Hoehn MM, Yahr MD. Parkinsonism: onset, progression and mortality. *Neurology* (1967) 17:427–42. doi: 10.1212/WNL.17.5.427
11. Goetz CG, Tilley BC, Shaftman SR, Stebbins GT, Fahn S, Martinez-Martin P, et al. Movement disorder society-sponsored revision of the unified parkinson's disease rating scale (MDS-UPDRS): scale presentation and clinimetric testing results. *Mov Disord.* (2008) 23:2129–70. doi: 10.1002/mds.22340
12. Szewczyk-Krolikowski K, Tomlinson P, Nithi K, Wade-Martins R, Talbot K, Ben-Shlomo Y, et al. The influence of age and gender on motor and non-motor features of early Parkinson's disease: initial findings from the Oxford Parkinson Disease Center (OPDC) discovery cohort. *Parkinsonism Relat Disord.* (2014) 20:99–105. doi: 10.1016/j.parkreldis.2013.09.025
13. Doppler K, Ebert S, Uceyler N, Trenkwalder C, Ebentheuer J, Volkmann J, et al. Cutaneous neuropathy in parkinson's disease: a window into brain pathology. *Acta Neuropathol.* (2014) 128:99–109. doi: 10.1007/s00401-014-1284-0
14. Doppler K, Weis J, Karl K, Ebert S, Ebentheuer J, Trenkwalder C, et al. Distinctive distribution of phospho-alpha-synuclein in dermal nerves in multiple system atrophy. *Mov Disord.* (2015) 30:1688–92. doi: 10.1002/mds.26293
15. Donadio V, Incensi A, Leta V, Giannoccaro MP, Scaglione C, Martinelli P, et al. Skin nerve alpha-synuclein deposits: a biomarker for idiopathic Parkinson disease. *Neurology* (2014) 82:1362–9. doi: 10.1212/WNL.0000000000000316

16. Clark LN, Kartsaklis LA, Wolf Gilbert R, Dorado B, Ross BM, Kisselev S, et al. Association of glucocerebrosidase mutations with dementia with lewy bodies. *Arch Neurol.* (2009) 66:578–83. doi: 10.1001/archneurol.2009.54
17. Parkkinen L, Neumann J, O'Sullivan SS, Holton JL, Revesz T, Hardy J, et al. Glucocerebrosidase mutations do not cause increased lewy body pathology in parkinson's disease. *Mol Genet Metab.* (2011) 103:410–2. doi: 10.1016/j.ymgme.2011.04.015
18. Adler CH, Beach TG, Shill HA, Caviness JN, Driver-Dunckley E, Sabbagh MN, et al. GBA mutations in Parkinson disease: earlier death but similar neuropathological features. *Eur J Neurol.* (2017) 24:1363–8. doi: 10.1111/ene.13395
19. Berge-Seidl V, Pihlstrom L, Maple-Grodem J, Forsgren L, Linder J, Larsen JP, et al. The GBA variant E326K is associated with Parkinson's disease and explains a genome-wide association signal. *Neurosci Lett.* (2017) 658:48–52. doi: 10.1016/j.neulet.2017.08.040
20. Brockmann K, Srulijes K, Pflederer S, Hauser AK, Schulte C, Maetzler W, et al. GBA-associated Parkinson's disease: reduced survival and more rapid progression in a prospective longitudinal study. *Mov Disord.* (2015) 30:407–11. doi: 10.1002/mds.26071
21. Beavan MS, Schapira AH. Glucocerebrosidase mutations and the pathogenesis of Parkinson disease. *Ann Med.* (2013) 45:511–21. doi: 10.3109/07853890.2013.849003
22. Bae EJ, Yang NY, Song M, Lee CS, Lee JS, Jung BC, et al. Glucocerebrosidase depletion enhances cell-to-cell transmission of alpha-synuclein. *Nat Commun.* (2014) 5:4755. doi: 10.1038/ncomms5755

Conflict of Interest Statement: The authors declare that the research was conducted in the absence of any commercial or financial relationships that could be construed as a potential conflict of interest.

Copyright © 2018 Doppler, Brockmann, Sedghi, Wurster, Volkmann, Oertel and Sommer. This is an open-access article distributed under the terms of the Creative Commons Attribution License (CC BY). The use, distribution or reproduction in other forums is permitted, provided the original author(s) and the copyright owner(s) are credited and that the original publication in this journal is cited, in accordance with accepted academic practice. No use, distribution or reproduction is permitted which does not comply with these terms.

frontiers in Neurology

ORIGINAL RESEARCH
published: 18 December 2018
doi: 10.3389/fneur.2018.01075

CSF-Progranulin and Neurofilament Light Chain Levels in Patients With Radiologically Isolated Syndrome—Sign of Inflammation

Marc Pawlitzki[1,2], Catherine M. Sweeney-Reed[1], Daniel Bittner[1], Anke Lux[3], Stefan Vielhaber[1], Stefanie Schreiber[1], Friedemann Paul[4,5,6] and Jens Neumann[1]*

[1] Department of Neurology, Otto-von-Guericke University, Magdeburg, Germany, [2] Department of Neurology with Institute of Translational Neurology, University Hospital of Muenster, Münster, Germany, [3] Department for Biometrics and Medical Informatics, Otto-von-Guericke-University, Magdeburg, Germany, [4] Charité – Universitätsmedizin Berlin, Corporate Member of Freie Universität Berlin, Humboldt-Universität zu Berlin, and Berlin Institute of Health, NeuroCure Clinical Research Center, Berlin, Germany, [5] Charité – Universitätsmedizin Berlin, Corporate Member of Freie Universität Berlin, Humboldt-Universität zu Berlin, and Berlin Institute of Health, Department of Neurology, Berlin, Germany, [6] Experimental and Clinical Research Center, Max Delbrueck Center for Molecular Medicine and Charité – Universitätsmedizin Berlin, Corporate Member of Freie Universität Berlin, Humboldt-Universität zu Berlin, and Berlin Institute of Health, Berlin, Germany

OPEN ACCESS

Edited by:
Jorge Matias-Guiu, Complutense University of Madrid, Spain

Reviewed by:
Julián Benito León, Hospital Universitario 12 De Octubre, Spain
Angel Perez Sempere, Hospital General Universitario de Alicante, Spain

***Correspondence:**
Marc Pawlitzki
marc.pawlitzki@ukmuenster.de

Specialty section:
This article was submitted to Multiple Sclerosis and Neuroimmunology, a section of the journal Frontiers in Neurology

Received: *18 October 2018*
Accepted: *26 November 2018*
Published: *18 December 2018*

Citation:
Pawlitzki M, Sweeney-Reed CM, Bittner D, Lux A, Vielhaber S, Schreiber S, Paul F and Neumann J (2018) CSF-Progranulin and Neurofilament Light Chain Levels in Patients With Radiologically Isolated Syndrome—Sign of Inflammation. Front. Neurol. 9:1075. doi: 10.3389/fneur.2018.01075

Background: Cerebrospinal fluid (CSF) markers of disease in patients with radiologically isolated syndrome (RIS) are the subject of intense investigation, because they have the potential to enhance our understanding of the natural disease course and provide insights into similarities and differences between RIS and other multiple sclerosis (MS) disease identities.

Methods: Here we compared neurofilament light chain (NFL) and progranulin (PGRN) levels in the CSF in RIS patients with levels in patients with different subtypes of MS and healthy controls (HC) using Kruskal–Wallis one-way analysis of variance.

Results: Median CSF NFL concentrations in RIS patients did not differ to those in HC and clinically isolated syndrome (CIS) patients, but were significantly lower than in relapsing remitting (RRMS) and primary progressive (PPMS) MS patients. In contrast, RIS patients exhibited higher median CSF PGRN levels than HC and showed no significant differences compared with CIS, RRMS, and PPMS cases.

Conclusion: We postulate that elevated PGRN values in the CSF of RIS patients might indicate inflammatory and repair activity prior to axonal disintegration.

Keywords: multiple sclerosis, radiologically isolated syndrome, cerebrospinal fluid, neurofilament light chain, progranulin

INTRODUCTION

Widespread routine clinical implementation of magnetic resonance imaging (MRI) leads to incidental detection of MRI abnormalities suggestive of multiple sclerosis (MS) in patients undergoing cerebral MRI due to non-specific neurological symptoms (e.g., headache, dizziness) (1). Among these patients, a considerable number, mainly young men, develop radiological and clinical progression to relapsing (RRMS) or primary progressive (PPMS) forms of MS within 5

years (2, 3). This observation led to the establishment of the definition of the radiologically isolated syndrome (RIS) (4) as a probable preclinical variant of MS (5, 6). Additionally, a fraction of these patients exhibit oligoclonal bands (OCBs) in the cerebrospinal fluid (CSF), similar to those found in patients with a clinically isolated syndrome (CIS) (7).

Because early disease-modifying treatment (DMT) could delay the conversion from CIS to clinical MS (8), and repeated MRI examinations have led to early identification of progression to MS from CIS, with the offer of more powerful therapies, the question arises as to whether RIS patients could profit from these procedures as well. To address this question, the understanding of pro- and anti-inflammatory activity, repair mechanisms, and axonal loss, in the absence of noticeable clinical events, needs to be expanded to estimate the clinical relevance of incidentally diagnosed MRI lesions.

We consider CSF progranulin (PGRN) and neurofilament light chain (NFL) to serve as *in vivo* measures of inflammatory activity, tissue repair and neuroaxonal damage. In short, in the central nervous system, PGRN is mainly expressed in neurons and microglia (9). Considering anti-inflammatory and repair activity, progranulin (PRGN) has been identified as a molecule, which could regulate inflammation after axonal injury in the context of MS-associated relapses and continuous inflammation in progressive forms of MS by overexpression in activated microglia (10).

Neurofilaments are structural constituents of the neuroaxonal cytoskeleton and integral components of synapses; they are essential for axonal growth, transport, and signaling pathways (11, 12). White matter and cortical injury is related to elevated CSF NFL that represents a downstream effect of neuroaxonal loss (13), and CSF NFL increase has been found in early MS disease stages with axonal injury as well (14).

In the current study, we assessed the concentrations of CSF PGRN and NFL in RIS patients as potential markers of early repair mechanisms/inflammation and axonal loss, to compare them with the CSF PGRN and NFL concentrations in controls and patients at different MS disease stages and with different MS subtypes.

METHODS

Patients, Controls, and Clinical Assessment

Our cross-sectional study included $n = 23$ RIS patients, diagnosed according to the criteria proposed by Okuda et al. (4) and MAGNIMS (15), and $n = 15$ CIS, $n = 15$ RRMS and $n = 26$ PPMS patients, diagnosed according to the McDonald criteria (2010) (16). All patients were recruited retrospectively at the Department of Neurology, Otto-von-Guericke University Magdeburg, Germany, between 2012 and 2017. Due to the retrospective character of the study, written informant consent was not obtained, but all analyses were taken from diagnostic procedures in clinical routine.

All patients underwent a lumbar puncture (LP) and their clinical disability was assessed applying the Expanded Disability

TABLE 1 | Summary of the clinical and radiologic data of all investigated groups.

	HC (*N* = 30)	RIS (*N* = 23)	CIS (*N* = 15)	RRMS (*N* = 15)	PPMS (*N* = 26)
Age at lumbar puncture (years)	35 (18-49)	37 (18–72)	44 (21–61)	33 (17–55)	52 (25-71)
Male SEX, *N* (%)	12 (33)	8 (35)	3 (16)	6 (30)	15 (60)
Disease duration (months)	–	6 (0–89)	4 (1–78)	19 (2–174)	61 (12–255)
EDSS	–	0 (0–1.5)	1 (0–3.5)	1.5 (0–6)	4.5 (2–7.5)
Presence of Gd+ lesions, *n* (%)	–	0 (0)	0 (0)	4 (29)	3 (11.5)
Presence of periventricular lesions, *n* (%)	–	22 (96)	13 (87)	13 (87)	25 (96)
Presence of infratentorial lesions, *n* (%)	–	9 (39)	3 (20)	7 (46)	16 (62)
Presence of juxtacortical lesions, *n* (%)	–	14 (61)	8 (53)	10 (67)	20 (77)
Presence of spinal cord lesions lesions, *n* (%)	–	4 (17)	5 (33)	8 (53)	20 (77)

N, number of participants; unless otherwise reported median (range) is given. CSF, cerebrospinal fluid; CIS, Clinically isolated syndrome; EDSS, Expanded Disability Status Scale; Gd+, Gadolinium enhancing; HC, healthy controls; PPMS, primary progressive multiple sclerosis; RIS, radiologically isolated syndrome; RRMS, relapsing remitting multiple sclerosis. Disease duration was defined as the timespan between symptom onset and the date of lumbar puncture.

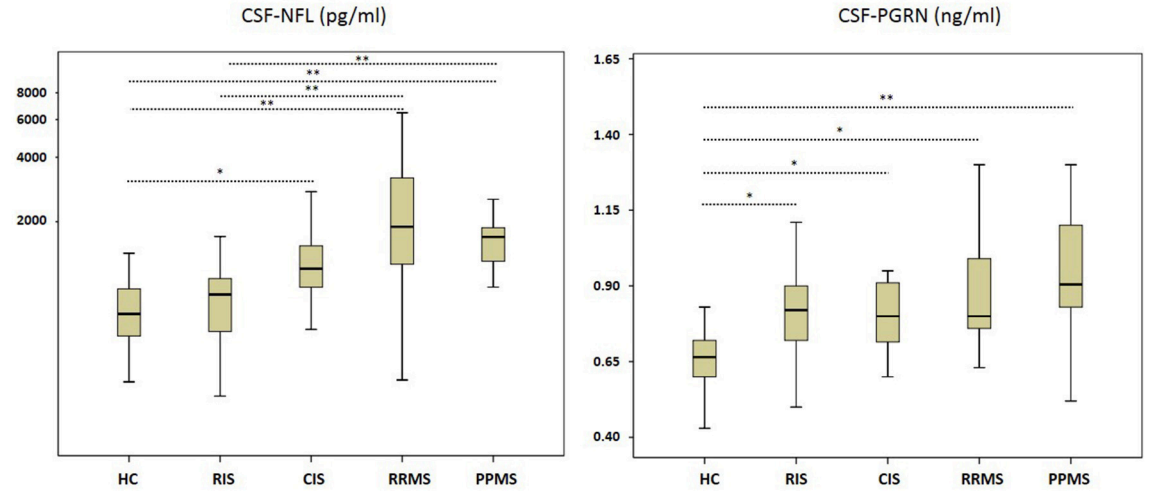


FIGURE 1 | Neurofilament light (NFL) and Progranulin (PGRN) in cerebrospinal fluid (CSF). CIS, clinically isolated syndrome; HC, healthy controls; PPMS, primary progressive multiple sclerosis; RIS, radiologically isolated syndrome; RRMS, relapsing remitting multiple sclerosis. Boxes indicate the interquartile range, bars indicates median CSF-NFL/PGRN values, and Whiskers present the 95% CI. Group comparisons were conducted using a Kruskal–Wallis one way analysis of variance with *post-hoc* Dunn–Bonferroni-testing. $P < 0.05$ were deemed to be statistically significant. RIS, CIS, RRMS, and PPMS showed higher CSF PGRN values than HC, while PPMS and RRMS also differed in contrast to RIS cases. RJS, CIS, RRMS, and PPMS showed higher CSF PGRN values than HC. $^{*}P < 0.005$; $^{**}P < 0.001$.

Status Scale (EDSS) (17). Reasons for performing a MRI examination in RIS patients were non-specific complaints including headache ($n = 7$ [30%]), non-specific dizziness ($n = 5$ [22%]), tinnitus ($n = 3$ [13%]), transitory ischemic attack (5 [22%]), back pain ($n = 2$ [9%]) and idiopathic peripheral facial palsy ($n = 1$ [4%]). In MS patients, disease duration was defined as time in months from symptom onset to the LP, while in RIS cases it was defined as time from the patients' first complaints to the LP. CIS, RRMS and PPMS patients neither presented with a relapse within the last 4 weeks, nor did they received any disease-modifying treatment.

CSF was additionally acquired from a hospital-based cohort of $n = 30$ healthy controls (HC). The CSF from the HC group was obtained from individuals in whom the presence of a neurological disorder had been suspected, but these individuals were deemed to be healthy in retrospect and in particular have normal cerebral MRI scans. In addition to the clinical classification, patients included in the control group also fulfilled the following Reiber laboratory criteria defining a non-inflammatory CSF [<5 cells/µl, >500 mg protein/ml, <2 mmol/l lactate, no disruption of the blood/CSF barrier, no oligoclonal bands (OCB) in the CSF, and no intrathecal immunoglobulin (Ig) G, IgA, or IgM synthesis] (18).

The study was approved by the local ethics committee (No. 07/17).

Neuro-Imaging Investigations

Brain and spinal cord MRI scans from patients originated from non-standardized protocols from differing MRI units and magnetic field strengths (1.5 or 3.0 Tesla) were performed within 6 months or after CSF measurement. All examinations included T1- and T2-weighted spin-echo sequences with the administration of gadolinium (Gd). Abnormalities including T1-hypointesities, T2-hyperintesities, and Gd-enhanced T1-lesions were initially identified by a neuroradiologist and they were subsequently verified by a MS specialist (M.P.). Brain and spinal cord scans of all RIS cases were reviewed to confirm the fulfillment of dissemination in space (DIS) criteria (4).

CSF Measures

Immediately after LP, CSF cells were counted, and total protein, albumin quotient (Q_{alb}), and OCBs were measured. The remaining CSF material was centrifuged at 4°C, aliquoted, and stored at −80°C until PGRN and NFL analysis was performed. PGRN and NFL levels were measured using commercially available ELISA kits (PGRN: Human Progranulin ELISA kit, Mediagnost, Reutlingen, Germany; NFL: UmanDiagnostics NF-light®, Umeå, Sweden) following the instructions provided by the manufacturer. All samples were processed in duplicate, in serial procedures, and the mean was taken for statistical analysis.

Statistical Analysis

Statistical analysis was conducted using SPSS 21 (IBM, Armonk, New York, USA). Comparisons of categorical variables (e.g., sex or OCBs) were performed using a α^2-test. Moreover, a univariate analysis of variance, including the estimated marginal means was performed to evaluate between-subject-effects and the effect of age, sex on PGRN and NFL. For further group comparisons of continuous variables (e.g., age, CSF NFL, CSF PGRN, disease duration, EDSS), a Kruskal–Wallis one-way analysis of variance was conducted with group (HC vs. RIS vs. CIS vs. RRMS vs. PPMS patients) as the independent variable, applying pairwise *post-hoc* testing (Dunn-Bonferroni-test).

TABLE 2 | Summary of the cerebrospinal fluid results of all investigated groups.

HC (*N* = 30)	RIS (*N* = 23)	CIS (*N* = 15)	RRMS (*N* = 15)	PPMS (*N* = 26)	*p*-values								
					HC vs. RIS	HC vs. CIS	HC vs. RRMS	HC vs. PPMS	RIS vs. CIS	RIS vs. RRMS	RIS vs. PPMS	CIS vs. RRMS	CIS vs. PPMS	RRMS vs. PPMS
CSF Cell count /µl	1 (0–4)	3 (0–19)	3(1-25)	4(1-16)	1 (0–14)	**0.001**	0.08	**0.01**	1.0	1.0	1.0	0.09	1.0	1.0	**0.04**
CSF protein (mg/dl)	311 (178–460)	371 (238–909)	321 (226–491)	421 (255–650)	410 (248–1047)	0.2	1.0	**0.04**	**0.001**	1.0	1.0	1.0	1.0	1.0	1.0
Positive OCB, N (%)	0 (0)	19 (83)	15 (100)	15 (100)	25 (96)	–	–	–	–	–	–	–	–	–	–
Qalb	4.3 (2.3–6.4)	4.7 (2.8–11.8)	4.03 (3.0–7.2)	5.5 (2.5–8.9)	5.0 (2.0–18.8)	0.05	0.05	0.05	0.05	0.05	0.05	0.05	0.05	0.05	0.05
CSF NFL (pg/ml)	742 (357–1424)	914 (306–2552)	1206 (628–2762)	1893 (364–6458)	1699 (990–4275)	1.0	**0.03**	**<0.001**	**<0.001**	0.3	**<0.001**	**<0.001**	0.8	0.5	1.0
CSF PGRN (pg/ml)	0.67 (0.43–1.12)	0.82 (0.50–1.20)	0.80 (0.60–1.45)	0.91 (0.63–1.30)	0.91 (0.52–1.59)	**0.004**	**0.04**	**0.004**	**<0.001**	1.0	1.0	0.7	1.0	0.6	1.0

N, number of participants; unless otherwise reported median (range) is given. CIS, clinically isolated syndrome; CSF, cerebrospinal fluid; HC, healthy controls; NFL, neurofilament light chain; PGRN, progranulin; PPMS, primary progressive multiple sclerosis; Qalb, albumin quotient; RIS, radiologically isolated syndrome; RRMS, relapsing remitting multiple sclerosis. Disease duration was defined as the timespan between symptom onset and time of lumbar puncture. For group comparisons a Kruskal–Wallis one-way analysis of variance with post-hoc Dunn-Bonferroni-testing were conducted. Bold value indicates P-values < 0.05 were deemed to be statistically significant.

RESULTS

Cohort Characterization and MRI Examination

The demographics, the clinical and MRI data of the cohorts are provided in **Table 1**. Median age and sex [$\chi^2(4) = 0.07$] did not differ between SC, RIS, CIS, and RRMS patients, whereas PPMS patients were significantly older than SC, RIS ($p < 0.001$, respectively) and RRMS patients ($p = 0.002$). Median disease duration was longer in PPMS compared to RIS and CIS ($p < 0.001$, respectively). Median EDSS at the time of LP differed between RIS compared to RRMS and PPMS ($p = 0.007$; $p < 0.001$), as well as between CIS and PPMS ($p < 0.001$) and RRMS vs. PPMS ($p = 0.02$).

CSF Examination

CSF cell count was significantly higher in RRMS compared with PPMS patients and HC as well as between RIS and HC patients. OCBs were present exclusively in the CSF of 19 (83%) RIS, 25 (96%) PPMS, and all (100%) CIS and RRMS patients (Table 2). Univariate analysis underlined the group difference in particular, and the absence of an effect of age and sex on PGRN and NFL levels.

The concentration of CSF NFL was significantly higher in CIS, RRMS, and PPMS compared to RIS and HC, while there were no significant differences between RIS and HC (**Figure 1** and **Table 2**). The comparison of CSF PRGN between groups revealed significantly higher levels in CIS, RIS, RRMS, and PPMS than detected in HC (**Figure 1** and **Table 2**).

DISCUSSION

Detection and characterization of early biomarkers in RIS patients, in order to investigate whether they could reflect MS disease courses, is an ongoing challenge. We compared the concentrations of CSF PGRN and NFL in RIS patients with the concentrations in healthy controls and in patients at different disease stages and with different subtypes of treatment-naive MS in the absence of an acute clinical relapse. Our analysis revealed similar PGRN concentrations in RIS patients to those found in several MS subtypes. PGRN levels were significantly higher, on the other hand, in RIS patients than in HC, while NFL concentrations did not differ between the RIS and HC cohorts.

To the best of our knowledge, the current study provides the largest comparison of CSF PGRN levels in different subtypes of MS, including RIS patients, to date. Surprisingly, while NFL values in the CSF of RIS patients were comparable with the HC cohort and significant lower compared with those in patients at different MS disease stages, the RIS cohort exhibited significantly higher concentrations of PRGN in comparison with the HC cohort and showed similar concentrations to those found in patients with the different MS subtypes.

Former studies have reported elevated (19) or unchanged CSF PGRN values in MS but included patients who had experienced an acute relapse (20). The absence of differences of CSF PGRN thus seems to be unusual, because acute inflammation is considered to provoke PGRN expression (19). Furthermore, it

has been shown that disease-modifying treatment could decrease PGRN levels (19). In order to exclude heterogeneity, we divided the cohorts into distinct subtypes (RIS, CIS, RRMS, PPMS), comprising only patients without an acute clinical relapse and also without disease-modifying treatments.

The role of PGRN is currently under intense investigation, and microglia cells have been identified as expressing and secreting PGRN after axonal injury (21). CSF PGRN level seems to be largely unaffected by blood PGRN concentration and in turn potential blood-CSF barrier disruption which underline the specificity of intrathecal produced PRGN (22). In addition, PGRN levels correlate with the concentration of the proinflammatory cytokine interleukin 6, which is elevated after acute (19) and chronic axonal injury (10). However, NFL levels were not increased in our RIS cohort, indicating that PGRN could be secreted even before axonal injury is detectable in the CSF via elevated NFL concentrations. This finding leads us to speculate tentatively that PGRN may be upregulated early, at the beginning of disease activity, and that RIS might in turn be a prodromal stage of MS. PGRN may thus shed new light on, clinically silent, disease-related alterations at the earliest MS stages. In line with histological findings that inflammation is the primary hallmark of MS and induces neuronal injury (23, 24), we suggest that PGRN might be more sensitive to detecting early disease-related abnormalities, also in RIS cases, in the face of (still) normal axonal integration, as measured by NFL levels (25).

The finding of missing NFL elevation in RIS patients is surprising, given the early, MRI-detectable neurodegeneration already found in the RIS cohorts (26) and the recognized association between raised CSF NFL and GD-enhancing white matter lesions in RIS patients (27). However, no GD-enhancing white matter lesions were present in our RIS group, suggesting that our cohort is more homogeneous or less severely affected, and acute axonal loss might thus play an insignificant role and be therefore not detectable via the elevated NFL concentrations that are seen in relapsing and progressive MS patients (14, 28, 29).

In addition to the MRI findings resulting in a diagnosis of RIS, we identified CSF abnormalities, e.g., OCBs in the CSF, in almost all of our RIS patients, which is in line with previous studies, in which OCBs were identified as independent predictors for early conversion to MS (27, 30). Our RIS-cohort may thus be characterized as high-risk patients (27) for conversion. However, the prevalence of OCBs is not specific for MS (31), nor does it mirror acute or continuous inflammatory activity (32).

Here we demonstrated significantly elevated CSF PGRN levels in RIS and MS patients during the clinically silent or non-relapsing phase, presumably suggesting ongoing inflammation, while only the later disease stages revealed an increased CSF NFL, thus mirroring axonal injury in addition. We here report the results from a pilot study. The limitations are the relatively small sample size and the higher mean age of PPMS patients. Standardized MRI, in addition, might assist to improve the evaluation of the relationship between white matter lesion volume and CSF-PGRN in MS patients. Hence, longitudinal studies with a larger sample size are needed to overcome these limitations and to determine the prognostic role of PGRN in MS and in particular in RIS patients.

ETHICS STATEMENT

The study was approved by the local ethics committee, Otto-von-Guericke-University, Magdeburg, Germany (No. 07/17).

AUTHOR CONTRIBUTIONS

All authors listed have made a substantial, direct and intellectual contribution to the work, and approved it for publication.

ACKNOWLEDGMENTS

We thank Kerstin Kaiser and Jeanette Witzke, Department of Neurology, Otto-von-Guericke University, Magdeburg, Germany, for excellent technical assistance.

REFERENCES

1. Granberg T, Martola J, Kristoffersen-Wiberg M, Aspelin P, Fredrikson S. Radiologically isolated syndrome–incidental magnetic resonance imaging findings suggestive of multiple sclerosis, a systematic review. *Mult Scler.* (2013) 19:271–80. doi: 10.1177/1352458512451943
2. Okuda DT, Siva A, Kantarci O, Inglese M, Katz I, Tutuncu M, et al. Radiologically isolated syndrome: 5-year risk for an initial clinical event. *PLoS ONE* (2014) 9:e90509. doi: 10.1371/journal.pone.0090509
3. Lebrun C, Bensa C, Debouverie M, De Seze J, Wiertlievski S, Brochet B, et al. Unexpected multiple sclerosis: follow-up of 30 patients with magnetic resonance imaging and clinical conversion profile. *J Neurol Neurosurg Psychiatr.* (2008) 79:195–8. doi: 10.1136/jnnp.2006.108274
4. Okuda DT, Mowry EM, Beheshtian A, Waubant E, Baranzini SE, Goodin DS, et al. Incidental MRI anomalies suggestive of multiple sclerosis: the radiologically isolated syndrome. *Neurology* (2009) 72:800–5. doi: 10.1212/01.wnl.0000335764.14513.1a
5. Makhani N, Lebrun C, Siva A, Brassat D, Carra Dallière C, Seze J, et al. Radiologically isolated syndrome in children: clinical and radiologic outcomes. *Neurol Neuroimmunol Neuroinflamm.* (2017) 4:e395. doi: 10.1212/NXI.0000000000000395
6. Alcaide-Leon P, Cybulsky K, Sankar S, Casserly C, Leung G, Hohol M, et al. Quantitative spinal cord MRI in radiologically isolated syndrome. *Neurol Neuroimmunol Neuroinflamm.* (2018) 5:e436. doi: 10.1212/NXI.0000000000000436
7. Gabelić T, Radmilović M, Posavec V, Skvorc A, Bošković M, Adamec I, et al. Differences in oligoclonal bands and visual evoked potentials in patients with radiologically and clinically isolated syndrome. *Acta Neurol Belg.* (2013) 113:13–7. doi: 10.1007/s13760-012-0106-1
8. Leist TP, Comi G, Cree BA, Coyle PK, Freedman MS, Hartung HP, et al. Effect of oral cladribine on time to conversion to clinically definite multiple sclerosis in patients with a first demyelinating event (ORACLE MS): A phase 3 randomised trial. *Lancet Neurol.* (2014) 13:257–67. doi: 10.1016/S1474-4422(14)70005-5
9. Eriksen JL, Mackenzie IRA. Progranulin: normal function and role in neurodegeneration. *J Neurochem.* (2008) 104:287–97. doi: 10.1111/j.1471-4159.2007.04968.x
10. Vercellino M, Grifoni S, Romagnolo A, Masera S, Mattioda A, Trebini C, et al. Progranulin expression in brain tissue and cerebrospinal

fluid levels in multiple sclerosis. *Mult Scler.* (2011) 17:1194–201. doi: 10.1177/1352458511406164
11. Oberstadt M, Claßen J, Arendt T, Holzer M. TDP-43 and Cytoskeletal Proteins in ALS. *Mol Neurobiol.* (2018) 55:3143–51. doi: 10.1007/s12035-017-0543-1
12. Petzold A, Gveric D, Groves M, Schmierer K, Grant D, Chapman M, et al. Phosphorylation and compactness of neurofilaments in multiple sclerosis: indicators of axonal pathology. *Exp Neurol.* (2008) 213:326–35. doi: 10.1016/j.expneurol.2008.06.008
13. Bergman J, Dring A, Zetterberg H, Blennow K, Norgren N, Gilthorpe J, et al. Neurofilament light in CSF and serum is a sensitive marker for axonal white matter injury in MS. *Neurol Neuroimmunol Neuroinflamm.* (2016) 3:e271. doi: 10.1212/NXI.0000000000000271
14. Kuhle J, Plattner K, Bestwick JP, Lindberg RL, Ramagopalan SV, Norgren N, et al. A comparative study of CSF neurofilament light and heavy chain protein in MS. *Mult Scler.* (2013) 19:1597–603. doi: 10.1177/1352458513482374
15. De Stefano N, Giorgio A, Tintoré M, Pia Amato M, Kappos L, Palace J, et al. Radiologically isolated syndrome or subclinical multiple sclerosis: MAGNIMS consensus recommendations. *Mult Scler.* (2018) 24:214–21. doi: 10.1177/1352458517717808
16. Polman CH, Reingold SC, Banwell B, Clanet M, Cohen JA, Filippi M, et al. Diagnostic criteria for multiple sclerosis: 2010 revisions to the McDonald criteria. *Ann Neurol.* (2011) 69:292–302. doi: 10.1002/ana.22366
17. Kurtzke JF. Rating neurologic impairment in multiple sclerosis: an expanded disability status scale (EDSS). *Neurology* (1983) 33:1444–52. doi: 10.1212/WNL.33.11.1444
18. Reiber H, Lange P. Quantification of virus-specific antibodies in cerebrospinal fluid and serum: sensitive and specific detection of antibody synthesis in brain. *Clin Chem.* (1991) 37:1153–60.
19. Kimura A, Takemura M, Saito K, Serrero G, Yoshikura N, Hayashi Y, et al. Increased cerebrospinal fluid progranulin correlates with interleukin-6 in the acute phase of neuromyelitis optica spectrum disorder. *J Neuroimmunol.* (2017) 305:175–81. doi: 10.1016/j.jneuroim.2017.01.006
20. Riz M, de Galimberti D, Fenoglio C, Piccio LM, Scalabrini D, Venturelli E, et al. Cerebrospinal fluid progranulin levels in patients with different multiple sclerosis subtypes. *Neurosci Lett.* (2010) 469:234–6. doi: 10.1016/j.neulet.2009.12.002
21. Naphade SB, Kigerl KA, Jakeman LB, Kostyk SK, Popovich PG, Kuret J. Progranulin expression is upregulated after spinal contusion in mice. *Acta Neuropathol.* (2010) 119:123–33. doi: 10.1007/s00401-009-0616-y
22. Feneberg E, Steinacker P, Volk AE, Weishaupt JH, Wollmer MA, Boxer A, et al. Progranulin as a candidate biomarker for therapeutic trial in patients with ALS and FTLD. *J Neural Transm.* (2016) 123:289–96. doi: 10.1007/s00702-015-1486-1
23. Bitsch A, Schuchardt J, Bunkowski S, Kuhlmann T, Brück W. Acute axonal injury in multiple sclerosis. Correlation with demyelination and inflammation. *Brain* (2000) 123:1174–83. doi: 10.1093/brain/123.6.1174
24. Brück W. The pathology of multiple sclerosis is the result of focal inflammatory demyelination with axonal damage. *J Neurol.* (2005) 252(Suppl. 5):v3–9. doi: 10.1007/s00415-005-5002-7
25. Giorgio A, Stromillo ML, De Leucio A, Rossi F, Brandes I, Hakiki B, et al. Appraisal of brain connectivity in radiologically isolated syndrome by modeling imaging measures. *J Neurosci.* (2015) 35:550–8. doi: 10.1523/JNEUROSCI.2557-14.2015
26. Azevedo CJ, Overton E, Khadka S, Buckley J, Liu S, Sampat M, et al. Early CNS neurodegeneration in radiologically isolated syndrome. *Neurol Neuroimmunol Neuroinflamm.* (2015) 2:e102. doi: 10.1212/NXI.0000000000000102
27. Matute-Blanch C, Villar LM, Álvarez-Cermeño JC, Rejdak K, Evdoshenko E, Makshakov G, et al. Neurofilament light chain and oligoclonal bands are prognostic biomarkers in radiologically isolated syndrome. *Brain* (2018) 141:1085–93. doi: 10.1093/brain/awy021
28. Lycke JN, Karlsson JE, Andersen O, Rosengren LE. Neurofilament protein in cerebrospinal fluid: a potential marker of activity in multiple sclerosis. *J Neurol Neurosurg Psychiatr.* (1998) 64:402–4. doi: 10.1136/jnnp.64.3.402
29. Semra YK, Seidi OA, Sharief MK. Heightened intrathecal release of axonal cytoskeletal proteins in multiple sclerosis is associated with progressive disease and clinical disability. *J Neuroimmunol.* (2002) 122:132–9. doi: 10.1016/S0165-5728(01)00455-6
30. Thouvenot E, Hinsinger G, Demattei C, Uygunoglu U, Castelnovo G, Pittion-Vouyovitch S, et al. Cerebrospinal fluid chitinase-3-like protein 1 level is not an independent predictive factor for the risk of clinical conversion in radiologically isolated syndrome. *Mult Scler.* (2018). doi: 10.1177/1352458518767043. [Epub ahead of print].
31. Jarius S, Eichhorn P, Franciotta D, Petereit HF, Akman-Demir G, Wick M, et al. The MRZ reaction as a highly specific marker of multiple sclerosis: re-evaluation and structured review of the literature. *J Neurol.* (2017) 264:453–66. doi: 10.1007/s00415-016-8360-4
32. Haertle M, Kallweit U, Weller M, Linnebank M. The presence of oligoclonal IgG bands in human CSF during the course of neurological diseases. *J Neurol.* (2014) 261:554–60. doi: 10.1007/s00415-013-7234-2

Conflict of Interest Statement: MP received speaker honoraria from Roche, Genzyme, and Novartis as well as travel, accommodation, and meeting expenses from Novartis, Biogen Idec, Genzyme, and MERCK Serono. DB has received honoraria from Bristol-Myers Squibb. JP has received honoraria and research support from Alexion, Bayer, Biogen, Chugai, MerckSerono, Novartis, Genyzme, MedImmune, Shire, Teva, and serves on scientific advisory boards for Alexion, MedImmune, and Novartis. He has received funding from Deutsche Forschungsgemeinschaft (DFG Exc 257), Bundesministerium für Bildung und Forschung (Competence Network Multiple Sclerosis), Guthy Jackson Charitable Foundation, EU Framework Program 7, National Multiple Sclerosis Society of the USA.

The remaining authors declare that the research was conducted in the absence of any commercial or financial relationships that could be construed as a potential conflict of interest.

Copyright © 2018 Pawlitzki, Sweeney-Reed, Bittner, Lux, Vielhaber, Schreiber, Paul and Neumann. This is an open-access article distributed under the terms of the Creative Commons Attribution License (CC BY). The use, distribution or reproduction in other forums is permitted, provided the original author(s) and the copyright owner(s) are credited and that the original publication in this journal is cited, in accordance with accepted academic practice. No use, distribution or reproduction is permitted which does not comply with these terms.

frontiers in Neurology

ORIGINAL RESEARCH
published: 21 December 2018
doi: 10.3389/fneur.2018.01123

Serum Inflammatory Profile for the Discrimination of Clinical Subtypes in Parkinson's Disease

Rezzak Yilmaz[1†], Antonio P. Strafella[2,3,4,5,6,7†], Alice Bernard[8†], Claudia Schulte[8,9], Lieneke van den Heuvel[3,4], Nicole Schneiderhan-Marra[10], Thomas Knorpp[10], Thomas O. Joos[10], Frank Leypoldt[1,11], Johanna Geritz[1], Clint Hansen[1], Sebastian Heinzel[1], Anja Apel[8,9], Thomas Gasser[8,9], Anthony E. Lang[2,3,4,7,12], Daniela Berg[1,8,9], Walter Maetzler[1,8,9†] and Connie Marras[3,4†]*

[1] Department of Neurology, Christian-Albrechts-University of Kiel, Kiel, Germany, [2] Institute of Medical Science, University of Toronto, Toronto, ON, Canada, [3] Edmond J Safra Program in Parkinson's Disease and the Morton and Gloria Shulman Movement Disorders Clinic, University of Toronto, Toronto, ON, Canada, [4] Division of Neurology, Department of Medicine, University of Toronto, Toronto, ON, Canada, [5] Research Imaging Centre, Centre for Addiction and Mental Health, Toronto, ON, Canada, [6] Division of Brain, Imaging and Behaviour-Systems Neuroscience, Toronto Western Research Institute, University Hospital Network, University of Toronto, Toronto, ON, Canada, [7] Krembil Brain Institute, University Health Network, Toronto, ON, Canada, [8] Department of Neurodegeneration, Hertie Institute for Clinical Brain Research, University of Tübingen, Tübingen, Germany, [9] German Center for Neurodegenerative Diseases (DZNE), Tübingen, Germany, [10] Natural and Medical Sciences Institute (NMI) at the University of Tübingen, Reutlingen, Germany, [11] Neuroimmunology, Institute of Clinical Chemistry, University Hospital Schleswig-Holstein, Kiel, Germany, [12] Tanz Centre for Research in Neurodegenerative Diseases, University of Toronto, Toronto, ON, Canada

OPEN ACCESS

Edited by:
Tobias Warnecke,
Universitätsklinikum Münster,
Germany

Reviewed by:
Stefan Bittner,
Johannes Gutenberg University
Mainz, Germany
Avner Thaler,
Tel Aviv Sourasky Medical Center,
Israel
Nico Melzer,
Universität Münster, Germany

***Correspondence:**
Johanna Geritz
j.geritz@neurologie.uni-kiel.de

[†] These authors have contributed equally to this work

Specialty section:
This article was submitted to Movement Disorders, a section of the journal Frontiers in Neurology

Received: 08 September 2018
Accepted: 06 December 2018
Published: 21 December 2018

Citation:
Yilmaz R, Strafella AP, Bernard A, Schulte C, van den Heuvel L, Schneiderhan-Marra N, Knorpp T, Joos TO, Leypoldt F, Geritz J, Hansen C, Heinzel S, Apel A, Gasser T, Lang AE, Berg D, Maetzler W and Marras C (2018) Serum Inflammatory Profile for the Discrimination of Clinical Subtypes in Parkinson's Disease. Front. Neurol. 9:1123. doi: 10.3389/fneur.2018.01123

Background: Blood levels of immune markers have been proposed to discriminate patients with Parkinson's disease (PD) from controls. However, differences between clinical PD subgroups regarding these markers still need to be identified.

Objective: To investigate whether clinical phenotypes can be predicted by the assessment of immune marker profiles in the serum of PD patients.

Methods: Phenotypes of clinical PD from Tübingen, Germany ($n = 145$) and Toronto, Canada ($n = 90$) were defined regarding clinical subtype, disease onset, severity, and progression as well as presence of cognitive and/or autonomic dysfunction. A panel of serum immune markers was assessed using principal component analysis (PCA) and regression models to define the marker(s) that were associated with clinical phenotypes after adjusting for potential confounders. Findings of both centers were compared for validation. Further, a [18F] FEPPA-PET was performed in a group of patients with high and low values of candidate markers for the assessment of *in vivo* brain microglial activation.

Results: Overall, serum immune markers did not cluster to define a pro/anti-inflammatory profile in PCA. Out of 25 markers only IL-12p40 showed a trend to discriminate between PD subgroups in both cohorts which could not be replicated by [18F] FEPPA-PET.

Conclusions: Assessment of cytokines in serum does not reliably differentiate clinical PD subtypes. Accompanying subtype-irrelevant inflammation in PD, dual activity, and

lack of specificity of the immune markers, the complex function of microglia, probable effects of treatment, disease stage, and progression on inflammation as well as current technical limitations may limit the usefulness of serum immune markers for the differentiation of subtypes.

Keywords: Parkinson's inflammation, Parkinson subtypes, immune markers, interleukins, cytokines

INTRODUCTION

Parkinson's disease (PD) is one the most frequent movement disorders affecting about 2–3% of the aging population (1). It has been estimated that the number of people with PD will double by 2030, indicating a progressive increase in the socio-economic burden in the near future (1). For this reason, understanding the underlying neurodegeneration is vital and the development of disease modifying therapies is urgently needed.

The pathological process which eventually leads to both a progressive loss of dopaminergic neurons of the substantia nigra and more widespread neurodegeneration in PD has been associated with neuronal inflammation (1, 2). It has been shown that accumulation of extracellular alpha-synuclein (α-syn) facilitates microglia activation, which further promotes production of immune markers, nitric oxide, and reactive oxygen species. It is proposed that this process may lead to nigral cell death. Within this context, pro-inflammatory cytokines produced by the microglia are responsible for the activation of the neighboring inactive glial cells and thus magnify the inflammation. In addition they attach to surface cytokine receptors of the dopaminergic cells and trigger apoptosis (3). This mechanism may provoke protein misfolding and thus create a vicious cycle (1). Evidence for inflammation has been demonstrated in PD animal models (4) as well as in PD patients in genetic (5, 6), imaging (7), CSF (8, 9), and postmortem studies (10, 11).

PD shows considerable variability with regard to age of onset, clinical manifestations, and disease progression which may indicate pathophysiological heterogeneity. The extent that inflammatory processes differ and potentially contribute to clinical PD subtypes has not been elucidated. Detection of a clinical PD phenotype that associates with an inflammatory profile would be critical in terms of outlining the contribution of the immunologic mechanisms to the underlying pathology, understanding the diversity in issues such as drug-response, or disease progression as well as formulating disease modifying strategies. For this reason, we set out to determine the clinical phenotype that correlates with the presence or absence of an inflammatory profile by extensive clinical phenotyping of PD patients and exploratory analysis of inflammatory markers. The results were validated by the assessment of a separate PD cohort and further evaluated by assessing microglial activation *in vivo* using [18F] FEPPA-PET.

MATERIALS AND METHODS

The current study has been designed as a collaborative project between the German Center for Neurodegenerative Diseases (DZNE), Tübingen, Germany and the University Health Network, Toronto, Canada which was supported by the Centers of Excellence in Neurodegeneration (CoEN) initiative.

Study Design

In this cross-sectional study, two separate prospectively assessed cohorts of PD patients from the centers of Tübingen and Toronto were analyzed independently. In each center, patients were grouped according to their clinical phenotypes (see methods below) and then compared with regard to serum inflammatory markers in order to define a clinical PD phenotype associated with inflammation. Then, the findings of both centers were compared for validation. In case of an agreement between two centers regarding the inflammatory markers that differ between clinical phenotypes, [18F] FEPPA-PET imaging was subsequently performed on a subset of patients to further validate the relevance of the inflammatory marker.

The study was approved by the ethics committees of the Medical Faculties of the University of Tübingen and the University Health Network, Toronto. All procedures were in accordance with the Declaration of Helsinki and a written informed consent was obtained from all participants.

Patients and Clinical Assessments

Participants older than 40 years fulfilling the criteria for idiopathic PD according to the UK Brain Bank Criteria were recruited from the neurology department of University Hospital of Tübingen, Germany, and from the Morton and Gloria Shulman Movement Disorders Clinic of Toronto Western Hospital, Toronto, Canada. Demographic data and detailed PD history including disease onset and duration, medication, presence of wearing off or motor fluctuations, and accompanying non-motor symptoms were collected. Motor performance in the "on" medication state and the disease severity were assessed by the Movement Disorders Society-Unified Parkinson's Disease Rating Scale (MDS-UPDRS) part-III and Hoehn and Yahr Scale (H&Y), respectively. Cognitive performance and autonomic dysfunction were assessed using the Montreal Cognitive Assessment (MoCa) and by Scales for Outcomes in Parkinson's disease—Autonomic (SCOPA-AUT), respectively. Patients with a C-reactive protein (CRP) value above 1.0 mg/dl were excluded from the study based on the assumption that these individuals may have an acute infection that could influence

TABLE 1 | Methods of comparison for PD subtypes (n for Tübingen/Toronto cohort).

Method-1[13]	*n*	Method-2	*n*	Method-3[15]	*n*	Method-4[12,14]	*n*
Young onset	31/23	Young onset and slow progression	45/31	Benign motor	37/16	Benign motor	50/35
Non-tremor dominant	44/20	Late onset and fast progression	38/17	Benign motor with cognitive/autonomic impairment	26/22	Benign motor with cognitive impairment	15/14
Tremor dominant	24/19	–		Poor motor with cognitive/autonomic impairment	56/12	Poor motor with cognitive impairment	37/15
Rapid progression	32/8	–		–		–	

the levels of the collected inflammation markers. All included PD patients were categorized into different groups with regard to their disease onset, severity or progression rate, autonomic, and cognitive status. Based on the previously published cluster analyses defining PD subtypes (12–15), four different methods of subtype classification were constructed. Each method resulted in 2–4 groups with each group representing a clinically defined PD subtype (**Table 1**). Within these subtypes, "young onset" was defined by an age of onset of <55 or <60 years in method 1 and 2, respectively. Motor subtyping (tremor dominant or non-tremor dominant) of the groups was selected by evaluating the tremor and postural instability and gait disorder (PIGD) scores of MDS-UPDRS part-III. Disease progression was defined by dividing the MDS-UPDRS part-III scores by disease duration. Cognitive or autonomic impairment were defined by Montreal Cognitive Assessment (MoCA) score lower than 26 and Scales for Outcomes in Parkinson's Disease-Autonomic (SCOPA-AUT) equal to or lower than 16, respectively. The details of the group definitions are explained in the **Supplementary Table 1**.

Biomaterial Collection

The following panel of immune markers composed of pro- or anti-inflammatory cytokines as well as neuroprotective trophic factors were assessed from the blood samples of the PD patients: TNF-α, TNF-β, IL-1α, IL-2, IL-3, IL-4, IL-5, IL-7, IL-8, IL-10, IL-12p40, IL-12p70, IL-13, IL-15, IL-16, IL-18, Brain-derived neurotrophic factor (BDNF), Epithelial Neutrophil Activating Peptide (ENA78), granulocyte-macrophage colony-stimulating factor (GM-CSF), lymphotactin, macrophage-derived chemokine (MDC), macrophage inflammatory protein-1β (MIP-1β), monocyte chemotactic protein-1 (MCP-1), stem cell factor (SCF), thrombopoetin (TPO). In both centers, storing and analyses of biomaterial were performed by means of standard operating procedures using the kit components of the multiplexed immunoassay by Myriad RBM, Austin, TX, USA. Blood samples of Toronto were obtained according to the protocol and were sent frozen to Tübingen for the analyses. The Tübingen samples were also frozen before the analysis in order to allow the comparability. Analysis of the serum inflammatory marker levels was performed using the Luminex 100/200 instrument and data were interpreted using the software developed and provided by Myriad RBM. Details of the serum inflammatory marker analysis are given elsewhere (16).

[18F] FEPPA-PET Imaging

Assessment of the *in vivo* brain microglial activation using a [18F] FEPPA-PET imaging was planned as a further validation step given that immune markers that discriminate PD groups were detected in both cohorts. A subgroup of patients from the Toronto cohort that underwent [18F] FEPPA-PET to assess microglial activation were categorized according to values of the cytokines of interest being lower or higher than the 50th percentile of the entire group undergoing PET imaging. [18F] FEPPA-PET images were preprocessed and region of interests (ROI) were automatically generated using in-house software, ROMI (17). In brief, ROMI fits a standard template of ROIs to an individual proton density (PD)-weighted MR image based on the probability of white matter, gray matter, and cerebrospinal fluid. The individual MR images were then co-registered to each summed [18F] FEPPA-PET image using the normalized mutual information algorithm so that individual refined ROI template can be transferred to the PET image space to generate the time activity curve for each ROI. Our a priori ROIs included cortical as well as subcortical brain regions such as frontal and temporal lobes, cingulate cortex, occipital lobe, insula, cerebellum, thalamus, and striatum. Total distribution volume (V_T), of the radioligand concentration in the ROI was measured taking into consideration rs6791 polymorphism binding affinity. The effect of age on the tissue volume was taken into account by partial volume effect correction (PVEC) method. PET scans were obtained with a high resolution PET/CT, Siemens-Biograph HiRez XVI (Siemens Molecular Imaging, Knoxville, TN, U.S.A.).

Statistics

The collected serum inflammatory markers were compared between the groups of each method with an exploratory approach in both cohorts. Statistical analyses were designed in two steps. First, a principal component analysis (PCA) was performed in the Tübingen (main) cohort with a bigger sample size to identify the cytokines that form a pro- or anti-inflammatory immune profile (factor) that could discriminate groups of PD. As the data could not be reduced to factors which convincingly represent the marker profiles (see results), binomial (for Method-2) and multinomial logistic regression analyses (For Methods-1,3, and 4) were performed for each immune marker in the Tübingen and the Toronto cohort in order to explore the predictive effect of an individual immune marker. Subtype was defined as the dependent variable, and the immune marker as the predictor variable with age, sex, disease duration or levodopa equivalent

TABLE 2 | Demographic characteristics of both cohorts.

	Tübingen ($n = 145$)	Toronto ($n = 90$)
Age [years], mean *(SD)*	67 (9)	62 (9)
Male sex [%]	66	70
Disease duration [years], mean *(SD)*	6.5 (4.0)	7.7 (4.5)
H&Y Stage (0-5), mean	2.3	1.8
LEDD [mg/day], mean *(SD)*	626 (407)	539 (482)
MDS-UPDRS part-III, mean *(SD)*	28.4 (12.5)	21.1 (10.3)
MoCA, mean *(SD)*	26 (3.3)	26.1 (2.6)
SCOPA-AUT, mean *(SD)*	14.3 (7.8)	13.4 (7)

H&Y, Hoehn & Yahr; LEDD, Levodopa equivalent daily dose, MDS-UPDRS, Movement Disorders Society - Unified Parkinson's Disease Rating Scale; MoCA, Montreal Cognitive Assessment; SCOPA-AUT, Scales for Outcomes in Parkinson's Disease - Autonomic.

daily dose (LEDD) as covariates which were added to the model according to the group definition. For example, in Method-2, age, and disease duration were not added to the model since the groups were defined according to these variables. Some cytokines were dichotomized at the median value when the data did not fit into the regression model.

As 13 group comparisons were performed for each immune marker (6 group comparisons for method-1, one for 2, and three for method-3 and 4), alpha value was corrected as $p < 0.05/13 = 0.0038$ for each cytokine (18). A trend in the data was defined as $p < 0.05$. The results from both cohorts were compared in order to see whether the effect from the Tübingen cohort (main cohort with a larger sample size) was verified by the second (Toronto) cohort. Inclusion of a second cohort in the study for the confirmation of the results was performed to reduce the risk of type-1 error, and only significant results from both centers were considered definitive. For the [18F] FEPPA-PET two-group analysis an independent samples *t*-test was performed also corrected for multiple comparison. SPSS Statistics 22.0.0 (SPSS Ltd., Chicago IL) was used for statistical analyses.

RESULTS

A total of 145 PD patients from Tübingen and 90 from Toronto were included in the analysis. 14 patients were excluded due to elevated CRP. Demographic data are shown in **Table 2**. IL-12p70 and GM-CSF from Toronto, and IL-2 and lymphotactin from both cohorts were excluded since more than 95% of patients had cytokine levels below analytical limit.

Principal Component Analysis (PCA)

In the Tübingen cohort, a PCA was conducted on serum inflammatory markers with oblique (related) rotation (oblimin) and elimination of factor loadings <0.4. The Kaiser–Meyer–Olkin measure of sampling adequacy was 0.81, verifying the adequacy of the sample size for the analysis. Bartlett's test of sphericity [chi-square(253) = 2125.5, $p < 0.001$] indicated that correlations between items were sufficiently large for PCA. Six components had eigenvalues over Kaiser's criterion of 1 and in combination explained 67% of the variance (**Supplementary Table 2**). It was found that Factor-1, which has the highest loading (28%), included pro-inflammatory cytokines as well as IL-13 which is an anti-inflammatory cytokine. Likewise, Factor 5 included both pro- (IL-15) and anti-inflammatory (IL-4, IL-10) cytokines. According to the markers that gather on the same factors, a clear separation between pro- and anti-inflammatory marker profiles could not be achieved with PCA (**Figure 1**, **Supplementary Table 2**).

Logistic Regression Analyses

In the Tübingen cohort, IL-1α and IL-3 (at median), and in Toronto cohort IL-1α, IL-12p40 (at median), IL-3 and IL-5 (as >0) were dichotomized to better fit in the model. None of the analyzed cytokines from either cohort reached significance ($p < 0.0038$) with regard to subtype membership prediction except for BDNF in the Toronto cohort ($p < 0.003$), which could not be confirmed in the Tübingen cohort. Some other cytokines showed a tendency ($p < 0.05$) for group separation. In some markers, a significant confounding effect of age or LEDD (not gender and disease duration) was detected which was inconsistent between cohorts. Comparison of the results in both cohorts is presented in **Supplementary Table 3**.

Out of all cytokines analyzed, only IL-12p40 showed a trend toward significance in both cohorts for distinguishing the "Benign motor" from the "Poor motor with cognitive impairment" group (Method-4, **Supplementary Table 3**). In the Tübingen cohort, lower values of IL-12p40 were associated with the "Poor motor with cognitive impairment" group against "Benign motor" group independent from the effects of age, sex, disease duration, and LEDD [Nagelkerke R^2 23%, B = −3.8, $p = 0.03$, Exp(B) = 0.02]. Likewise, the Toronto cohort showed that individuals with a high IL-12p40 value were less likely to be in the "Poor motor with cognitive impairment" group compared to the "Benign motor" group [Nagelkerke R^2=35%, B = −2.16, $p = 0.02$, Exp(B) = 0.12] (**Supplementary Figure 1**). Details of logistic regression results of other cytokines are given in the **Supplementary Table 4**.

[18F] FEPPA-PET Imaging

A [18F] FEPPA-PET imaging from 8 regions of brain was performed for IL12-p40, since it was the only (trend toward an) effect that could be replicated in the second cohort. Eighteen participants from Toronto were divided into two groups according to the lower and upper half of IL-12p40 values. Individuals in both groups showed a mixture of clinical phenotypes. No significant difference was detected between individuals with high or low values of IL-12p40 regarding the microglial activation from different regions of the brain ($p > 0.10$) (**Figure 2**). Details of the statistical analysis of brain regions are shown in **Supplementary Table 5**.

DISCUSSION

In this study, we compared serum immune markers in PD patients with different clinical subtypes in two independent cohorts. The results show that our assessment of serum immune

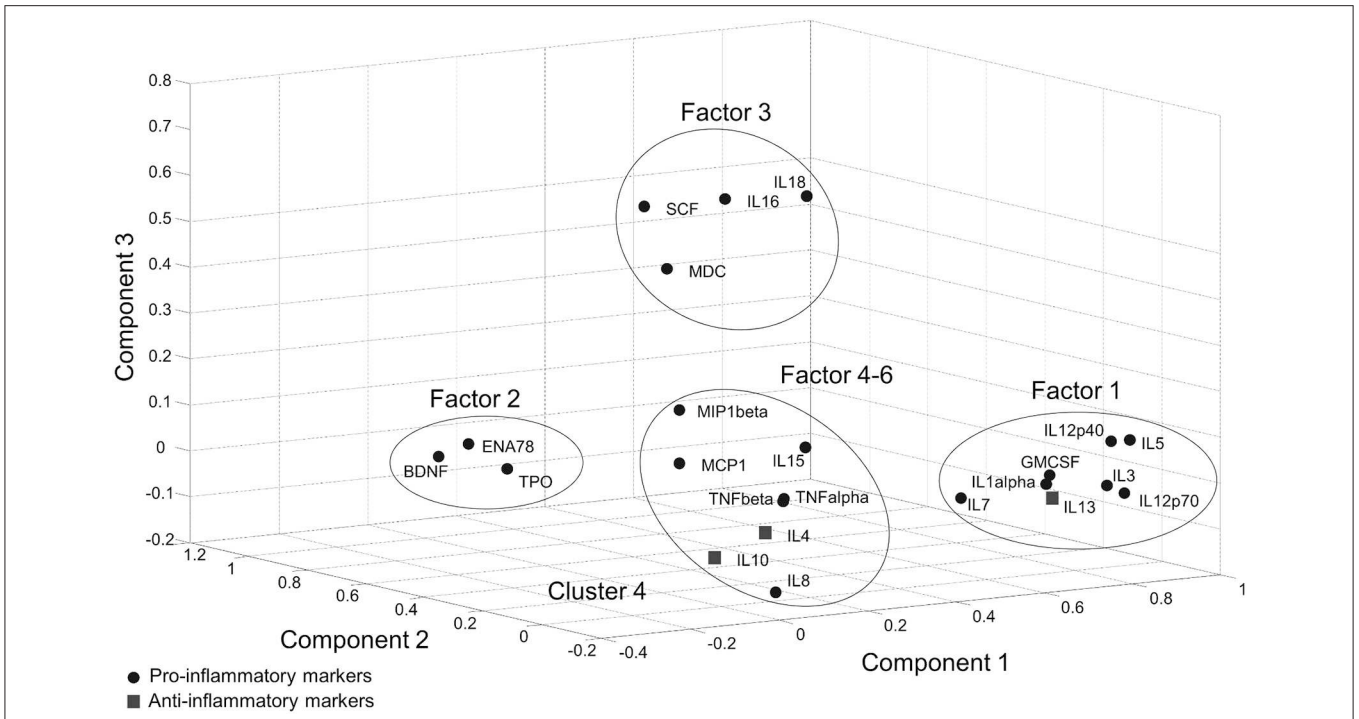


FIGURE 1 | Score plot of the component values of individual inflammatory markers in PCA.

markers, based on the current state of the art of technology, does not sufficiently discriminate clinical subgroups of PD.

Assessing immune marker levels in blood is easily accessible, and therefore has been frequently used to investigate the differences between PD patients and healthy controls. Although there are variations in study design, analysis technology, and findings in these studies (19), peripheral levels of some immune markers seem to be increased in PD patients indicating an ongoing inflammatory process that may trigger or at least accompany neurodegeneration (19). Some of these studies additionally investigated correlations between marker levels and several clinical characteristics such as motor worsening, disease severity, and non-motor status (20–23). Although the results are inconclusive, a further question was raised whether a substantial increase in already existing inflammation may be associated with non-motor features such as autonomic disturbances or dementia. To date, few studies have focused on relationships with non-motor features as the primary outcome. In a 3-year longitudinal study, William-Gray et al. reported that a pro-inflammatory immune marker profile predicted disease progression and correlated with Mini-Mental State Examination scores (24). In another study, Brockmann et al. separated PD patients with LRRK2 mutations according to the presence of non-motor symptoms and found that some pro-inflammatory marker levels were higher in the subgroup with a greater non-motor burden (16).

Contrary to these results, we failed to find an association with these disease specific features. Although some markers showed a trend ($p < 0.05$), no clear finding could be extracted from the results of both cohorts for separating subtypes. On this basis, it can be argued that a direct or linear association between serum marker levels and symptom profile is unlikely in a complex disorder like PD, which is comprised of a variety of motor, autonomic, cognitive, psychiatric, and sensory symptoms from distinct domains with different onset and progression rates. Besides, studies investigating immune markers in blood samples for a relatively regional neurodegeneration of the central nervous system have important limitations. For example, these immune markers are not specific for neuroinflammation and a co-existing systemic inflammation/infection should be taken into account which was considered only in few of the studies (22, 24). Perhaps even a subclinical infection which cannot be easily ruled out could compromise the results. In our study, we have excluded patients with CRP >1.0 mg/dl at least to rule out clinically relevant infections, but we can still not be entirely sure whether the results were biased by an unknown systemic or regional inflammatory process. Therefore, even if an increase in serum immune markers was detected, this increase may not be indicative of neuroinflammation related to the CNS pathogenesis of PD but rather another overlapping comorbidity such as a metabolic syndrome, rheumatic disease, or another accompanying inflammatory process (e.g., via dysphagia and consecutive subtle pulmonary infection, via urinary symptoms with consecutive infection) secondary to PD since these patients are relatively prone to systemic infections (25).

Immune markers may also have both pro- and anti-inflammatory functions according to the stage of inflammation. Accumulating evidence shows that some of the cytokines, even

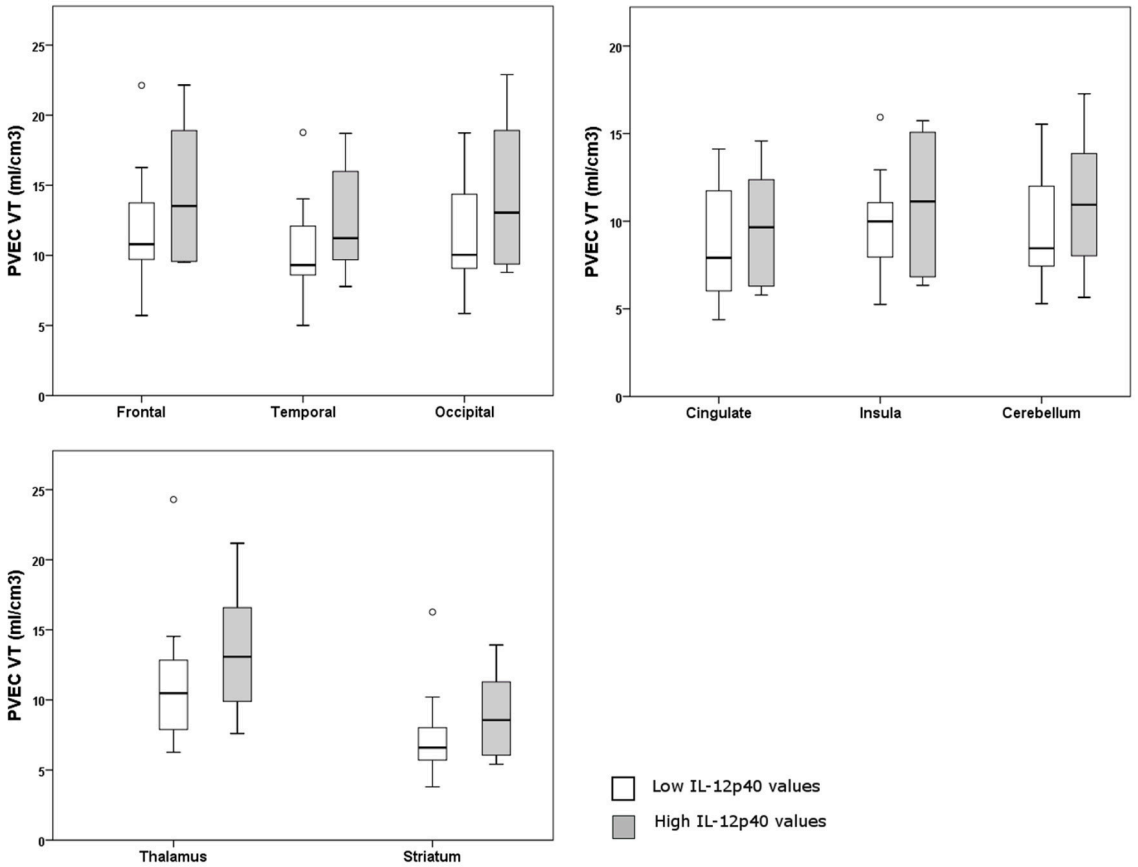


FIGURE 2 | Graphs of partial volume effect corrected (PVEC) total distribution volume (V_T) in different brain regions in individuals with higher or lower IL-12p40 values.

the well-known pro-inflammatory cytokines such as TNF-α, IFN-δ, or IL-6 may have a dual function (26–29), which supports the idea that functional distinction of cytokines as pro- or anti-inflammatory is too simplistic and may not adequately describe the actual inflammatory landscape (30). In our study, we found a trend for IL-12p40 to be decreased in more affected PD patients in both cohorts. This result is in line with recent literature about IL-12p40 in Alzheimer disease (31). Alternatively, although IL-12p40 is primarily a pro-inflammatory marker, it can also stimulate an immunosuppressive response when only slightly increased (32), supporting the dual-function hypothesis. This dual function of the cytokines may have prevented the clear separation of factor loadings in our PCA analysis which was also observed in William-Gray et al. (24). In both studies, the component with a pro-inflammatory profile also included anti-inflammatory cytokines indicating that these immune markers act closely in a complex network and cannot be used to determine a PD subgroup.

The levels of serum immune markers are also affected by a variety of factors such as nutrition (33), body mass index (34), sleep (35), smoking (36), thyroid hormone levels (37), exercise (38, 39), drinking coffee (40, 41), frailty (42), or depression (43, 44), and thus can be considered to be non-specific. These factors could have contributed to the negative outcome of this study. They may also explain the controversial literature that exists for levels of IL-15 (45, 46), IL-6 (47–49), TNF-α (49, 50), IL-10 (32, 51) in association with PD occurrence, TNF-α in association with cognitive scores (20, 52), and IL-6 with UPDRS (24, 53), cognition (20, 54), and depression scores (22, 48) in PD patients. Similarly, results are also conflicting in Alzheimer's disease (55). Considering that all these factors that can hardly be controlled, results from such studies should be interpreted with appropriate caution.

Moreover, intrinsic factors such as treatment and disease progression may contribute to the high variability of immune markers. Little is known about the effect of antiparkinsonian treatment on ongoing inflammation. Several reports have shown that dopamine may have some effect on the immune response (56, 57). Based on these findings, the effect of treatment on immune markers was investigated in some studies (45, 46) or has been taken into account by adding LEDD in the regression model as a confounder (including our study), but not all studies have done this (20, 52). Furthermore, over the course of the progressive disease, the inflammation rate and therefore the blood level of markers may vary since the inflammatory response may modify itself due to the changes in the amount of cells alive, receptor count, or accumulation of α-syn (58). Diversity in the inflammatory response in different brain regions, and

up/downregulations in mRNA expression of pro-inflammatory markers between early and late Braak stages have been demonstrated (59). Besides, activation of microglia by α-syn may result in upregulation of both toxic and neuroprotective activity of the microglia (60), further contributing to the limitations in the interpretation of immune markers in PD.

Limitations of the current study have to be mentioned. Eliminating patients with a serum CRP level >1 may have affected our results i.e., may party explain the non-significant results. The serum levels of other positive or negative acute-phase proteins such as procalcitonin, alpha-1 antitrypsin, albumin, or ferritin could also have been alternatively considered for a better detection of individuals with an acute infection. Moreover, we have only considered age, sex, disease duration, and LEDD as potential confounders. Other above mentioned factors such as body mass index, exercise, sleep, smoking, anti-inflammatory drug usage as well as potential comorbidities such as rheumatic or cardiovascular diseases were not taken into account. The possible distortion of results during the transport of frozen blood samples from Toronto and the cross-sectional study-design are also limitations. On the other hand, comparison of the findings in two independent and prospectively assessed cohorts, and although with a small sample, PET imaging are the strengths of the present study. Considering the lack of convincing associations in either cohort, and considering the ambiguous results from previous literature, we conclude that immune mechanisms in PD are far more complex than previously thought. Future longitudinal studies should include strictly designed grouping and confounder assessments to reveal whether specific inflammatory backgrounds are associated with and potentially account for clinical diversity in PD.

AUTHOR CONTRIBUTIONS

AS, TG, AL, DB, WM, and CM conceived the research project. RY, AB, AA, TG, AL, SH, DB, WM, and CM organized the research project. AS, AB, CS, LvdH, NS-M, TK, TJ, TG, AL, DB, WM, and CM executed the research project. RY, AB, LvdH, FL, JG, WM, and CM designed the statistical analysis. RY, AS, SH, and AA executed the statistical analysis. RY and CH wrote the first draft in the manuscript preparation. All authors reviewed and critiqued the statistical analysis and manuscript preparation.

FUNDING

Funding of this research was provided by the German Center for Neurodegenerative Diseases (DZNE) and the Canadian Institutes of Health Research (INE 117891), through CoEN initiative (www.coen.org). We acknowledge financial support by Land Schleswig-Holstein within the funding programme Open Access Publikationsfonds.

SUPPLEMENTARY MATERIAL

The Supplementary Material for this article can be found online at: https://www.frontiersin.org/articles/10.3389/fneur.2018.01123/full#supplementary-material

REFERENCES

1. Poewe W, Seppi K, Tanner CM, Halliday GM, Brundin P, Volkmann J, et al. Parkinson disease. *Nat Rev Dis Prim*. (2017) 3:17013. doi: 10.1038/nrdp.2017.13
2. Tufekci KU, Meuwissen R, Genc S, Genc K. Inflammation in Parkinson's Disease. In: R. Donev, Editor, *Advances in Protein Chemistry and Structural Biology*. Oxford: Elsevier (2012). p. 69–132.
3. Vila M, Jackson-Lewis V, Guégan C, Wu DC, Teismann P, Choi DK, et al. The role of glial cells in Parkinson's disease. *Curr Opin Neurol.* (2001) 14:483–9.
4. Gao HM, Jiang J, Wilson B, Zhang W, Hong JS, Liu B. Microglial activation-mediated delayed and progressive degeneration of rat nigral dopaminergic neurons: relevance to Parkinson's disease. *J Neurochem.* (2002) 81:1285–97. doi: 10.1046/j.1471-4159.2002.00928.x
5. Saiki M, Baker A, Williams-Gray CH, Foltynie T, Goodman RS, Taylor CJ, et al. Association of the human leucocyte antigen region with susceptibility to Parkinson's disease. *J Neurol Neurosurg Psychiatry* (2010) 81:890–1. doi: 10.1136/jnnp.2008.162883
6. Greggio E, Civiero L, Bisaglia M, Bubacco L. Parkinson's disease and immune system: is the culprit LRRKing in the periphery? *J Neuroinflammation* (2012) 9:94. doi: 10.1186/1742-2094-9-94
7. Ouchi Y, Yoshikawa E, Sekine Y, Futatsubashi M, Kanno T, Ogusu T, et al. Microglial activation and dopamine terminal loss in early Parkinson's disease. *Ann Neurol*. (2005) 57:168–75. doi: 10.1002/ana.20338
8. Zhang J, Sokal I, Peskind ER, Quinn JF, Jankovic J, Kenney C, et al. CSF multianalyte profile distinguishes Alzheimer and Parkinson diseases. *Am J Clin Pathol*. (2008) 129:526–9. doi: 10.1309/W01Y0B80 8EMEH12L
9. Mogi M, Harada M, Narabayashi H, Inagaki H, Minami M, Nagatsu T. Interleukin (IL)-1 beta, IL-2, IL-4, IL-6, and transforming growth factor-alpha levels are elevated in ventricular cerebrospinal fluid in juvenile parkinsonism and Parkinson's disease. *Neurosci Lett*. (1996) 211:13–6. doi: 10.1016/0304-3940(96)12706-3
10. Imamura K, Hishikawa N, Sawada M, Nagatsu T, Yoshida M, Hashizume Y. Distribution of major histocompatibility complex class II-positive microglia and cytokine profile of Parkinson's disease brains. *Acta Neuropathol*. (2003) 106:518–26. doi: 10.1007/s00401-003-0766-2
11. Mogi M, Togari A, Kondo T, Mizuno Y, Komure O, Kuno S, et al. Caspase activities and tumor necrosis factor receptor R1 (p55) level are elevated in the substantia nigra from Parkinsonian brain. *J Neural Transm.* (2000) 107:335–41. doi: 10.1007/s007020050028
12. Graham JM, Sagar HJ. A data-driven approach to the study of heterogeneity in idiopathic Parkinson's disease: identification of three distinct subtypes. *Mov Disord*. (1999) 14:10–20.
13. Lewis SJ, Foltynie T, Blackwell AD, Robbins TW, Owen AM, Barker RA. Heterogeneity of Parkinson's disease in the early clinical stages using a data driven approach. *J Neurol Neurosurg Psychiatry* (2005) 76:343–8. doi: 10.1136/jnnp.2003.033530
14. Dujardin K, Leentjens AF, Langlois C, Moonen AJ, Duits AA, Carette AS, et al. The spectrum of cognitive disorders in Parkinson's disease: a data-driven approach. *Mov Disord*. (2013) 28:183–9. doi: 10.1002/mds.25311
15. Fereshtehnejad SM, Romenets SR, Anang JB, Latreille V, Gagnon JF, Postuma RB. New clinical subtypes of parkinson disease and their longitudinal progression. *JAMA Neurol.* (2015) 72:863–73. doi: 10.1001/jamaneurol.2015.0703
16. Brockmann K, Schulte C, Schneiderhan-Marra N, Apel A, Pont-Sunyer C, Vilas D, et al. Inflammatory profile discriminates clinical subtypes

in LRRK2-associated Parkinson's disease. *Eur J Neurol*. (2017) 24:427–e6. doi: 10.1111/ene.13223
17. Rusjan P, Mamo D, Ginovart N, Hussey D, Vitcu I, Yasuno F, et al. An automated method for the extraction of regional data from PET images. *Psychiatry Res*. (2006) 147:79–89. doi: 10.1016/j.pscychresns.2006.01.011
18. Armstrong RA. When to use the Bonferroni correction. *Ophthalmic Physiol Opt*. (2014) 34:502–8. doi: 10.1111/opo.12131
19. Qin XY, Zhang SP, Cao C, Loh YP, Cheng Y. aberrations in peripheral inflammatory cytokine levels in parkinson disease. *JAMA Neurol*. (2016) 73:1316–24. doi: 10.1001/jamaneurol.2016.2742
20. Menza M, Dobkin RD, Marin H, Mark MH, Gara M, Bienfait K, et al. The role of inflammatory cytokines in cognition and other non-motor symptoms of Parkinson's disease. *Psychosomatics* (2010) 51:474–9. doi: 10.1176/appi.psy.51.6.474
21. Scalzo P, Kümmer A, Bretas TL, Cardoso F, Teixeira AL. Serum levels of brain-derived neurotrophic factor correlate with motor impairment in Parkinson's disease. *J Neurol*. (2010) 257:540–5. doi: 10.1007/s00415-009-5357-2
22. Lindqvist D, Kaufman E, Brundin L, Hall S, Surova Y, Hansson O. Non-motor symptoms in patients with Parkinson's disease - correlations with inflammatory cytokines in serum. *PLoS ONE* (2012) 7:e47387. doi: 10.1371/journal.pone.0047387
23. Wang XM, Zhang YG, Li AL, Long ZH, Wang D, Li XX, et al. Relationship between levels of inflammatory cytokines in the peripheral blood and the severity of depression and anxiety in patients with Parkinson's disease. *Eur Rev Med Pharmacol Sci*. (2016) 20:3853–6.
24. Williams-Gray CH, Wijeyekoon R, Yarnall AJ, Lawson RA, Breen DP, Evans JR, et al. Serum immune markers and disease progression in an incident Parkinson's disease cohort (ICICLE-PD). *Mov Disord*. (2016) 31:995–1003. doi: 10.1002/mds.26563
25. Alcalay RN. Cytokines as potential biomarkers of parkinson disease. *JAMA Neurol*. (2016) 73:1282–4. doi: 10.1001/jamaneurol.2016.3335
26. Liu J, Marino MW, Wong G, Grail D, Dunn A, Bettadapura J, et al. TNF is a potent anti-inflammatory cytokine in autoimmune-mediated demyelination. *Nat Med*. (1998) 4:78–83. doi: 10.1038/nm0198-078
27. Scheller J, Chalaris A, Schmidt-Arras D, Rose-John S. The pro- and anti-inflammatory properties of the cytokine interleukin-6. *Biochim Biophys Acta* (2011) 1813:878–88. doi: 10.1016/j.bbamcr.2011.01.034
28. Wilke CM, Wei S, Wang L, Kryczek I, Kao J, Zou W. Dual biological effects of the cytokines interleukin-10 and interferon-γ. *Cancer Immunol Immunother*. (2011) 60:1529–41. doi: 10.1007/s00262-011-1104-5
29. Shachar I, Karin N. The dual roles of inflammatory cytokines and chemokines in the regulation of autoimmune diseases and their clinical implications. *J Leukoc Biol*. (2013) 93:51–61. doi: 10.1189/jlb.0612293
30. Cavaillon JM. Pro- versus anti-inflammatory cytokines: myth or reality. *Cell Mol Biol (Noisy-le-grand)*. (2001) 47:695–702.
31. Johansson P, Almqvist EG, Wallin A, Johansson JO, Andreasson U, Blennow K, et al. Reduced cerebrospinal fluid concentration of interleukin-12/23 subunit p40 in patients with cognitive impairment. *PLoS ONE* (2017) 12:e0176760. doi: 10.1371/journal.pone.0176760
32. Rentzos M, Nikolaou C, Andreadou E, Paraskevas GP, Rombos A, Zoga M, et al. Circulating interleukin-10 and interleukin-12 in Parkinson's disease. *Acta Neurol Scand*. (2009) 119:332–7. doi: 10.1111/j.1600-0404.2008.01103.x
33. Ampatzoglou A, Williams CL, Atwal KK, Maidens CM, Ross AB, Thielecke F, et al. Effects of increased wholegrain consumption on immune and inflammatory markers in healthy low habitual wholegrain consumers. *Eur J Nutr*. (2016) 55:183–95. doi: 10.1007/s00394-015-0836-y
34. Khaodhiar L, Ling PR, Blackburn GL, Bistrian BR. Serum levels of interleukin-6 and C-reactive protein correlate with body mass index across the broad range of obesity. *J Parenter Enter Nutr*. (2004) 28:410–5. doi: 10.1177/0148607104028006410
35. Irwin MR, Wang M, Campomayor CO, Collado-Hidalgo A, Cole S. Sleep deprivation and activation of morning levels of cellular and genomic markers of inflammation. *Arch Intern Med*. (2006) 166:1756. doi: 10.1001/archinte.166.16.1756
36. Shiels MS, Katki HA, Freedman ND, Purdue MP, Wentzensen N, Trabert B, et al. Cigarette smoking and variations in systemic immune and inflammation markers. *JNCI J Natl Cancer Inst*. (2014) 106:dju294. doi: 10.1093/jnci/dju294
37. Fabris N, Mocchegiani E, Provinciali M. Pituitary-thyroid axis and immune system: a reciprocal neuroendocrine-immune interaction. *Horm Res*. (1995) 43:29–38. doi: 10.1159/000184234
38. Hopps E, Canino B, Caimi G. Effects of exercise on inflammation markers in type 2 diabetic subjects. *Acta Diabetol*. (2011) 48:183–9. doi: 10.1007/s00592-011-0278-9
39. Kasapis C, Thompson PD. The effects of physical activity on serum C-reactive protein and inflammatory markers: a systematic review. *J Am Coll Cardiol*. (2005) 45:1563–9. doi: 10.1016/j.jacc.2004.12.077
40. Zampelas A, Panagiotakos DB, Pitsavos C, Chrysohoou C, Stefanadis C. Associations between coffee consumption and inflammatory markers in healthy persons: the ATTICA study. *Am J Clin Nutr*. (2004) 80:862–7. doi: 10.1093/ajcn/80.4.862
41. Loftfield E, Shiels MS, Graubard BI, Katki HA, Chaturvedi AK, Trabert B, et al. Associations of coffee drinking with systemic immune and inflammatory markers. *Cancer Epidemiol Biomarkers Prev*. (2015) 24:1052–60. doi: 10.1158/1055-9965.EPI-15-0038-T
42. Velissaris D, Pantzaris N, Koniari I, Koutsogiannis N, Karamouzos V, Kotroni I, et al. C-reactive protein and frailty in the elderly: a literature review. *J Clin Med Res*. (2017) 9:461–5. doi: 10.14740/jocmr2959w
43. Dowlati Y, Herrmann N, Swardfager W, Liu H, Sham L, Reim EK, et al. A meta-analysis of cytokines in major depression. *Biol Psychiatry* (2010) 67:446–57. doi: 10.1016/j.biopsych.2009.09.033
44. Birur B, Amrock EM, Shelton RC, Li L. Sex differences in the peripheral immune system in patients with depression. *Front Psychiatry* (2017) 8:108. doi: 10.3389/fpsyt.2017.00108
45. Rentzos M, Nikolaou C, Andreadou E, Paraskevas GP, Rombos A, Zoga M, et al. Circulating interleukin-15 and RANTES chemokine in Parkinson's disease. *Acta Neurol Scand*. (2007) 116:374–9. doi: 10.1111/j.1600-0404.2007.00894.x
46. Gangemi S, Basile G, Merendino RA, Epifanio A, Di Pasquale G, Ferlazzo B, et al. Effect of levodopa on interleukin-15 and RANTES circulating levels in patients affected by Parkinson's disease. *Mediators Inflamm*. (2003) 12:251–3. doi: 10.1080/09629350310001599701
47. Dursun E, Gezen-Ak D, Hanagasi H, Bilgiç B, Lohmann E, Ertan S, et al. The interleukin 1 alpha, interleukin 1 beta, interleukin 6 and alpha-2-macroglobulin serum levels in patients with early or late onset Alzheimer's disease, mild cognitive impairment or Parkinson's disease. *J Neuroimmunol*. (2015) 283:50–7. doi: 10.1016/j.jneuroim.2015.04.014
48. Selikhova MV, Kushlinskii NE, Lyubimova NV, Gusev EI. Impaired production of plasma interleukin-6 in patients with Parkinson's disease. *Bull Exp Biol Med*. (2002) 133:81–3. doi: 10.1023/A:1015120930920
49. Brodacki B, Staszewski J, Toczyłowska B, Kozłowska E, Drela N, Chalimoniuk M, et al. Serum interleukin (IL-2, IL-10, IL-6, IL-4), TNFα, and INFγ concentrations are elevated in patients with atypical and idiopathic parkinsonism. *Neurosci Lett*. (2008) 441:158–62. doi: 10.1016/j.neulet.2008.06.040
50. Dobbs RJ, Charlett A, Purkiss AG, Dobbs SM, Weller C, Peterson DW. Association of circulating TNF-alpha and IL-6 with ageing and parkinsonism. *Acta Neurol Scand*. (1999) 100:34–41. doi: 10.1111/j.1600-0404.1999.tb00721.x
51. Rota E, Bellone G, Rocca P, Bergamasco B, Emanuelli G, Ferrero P. Increased intrathecal TGF-beta1, but not IL-12, IFN-gamma, and IL-10 levels in Alzheimer's disease patients. *Neurol Sci*. (2006) 27:33–9. doi: 10.1007/s10072-006-0562-6
52. Dufek M, Hamanová M, Lokaj J, Goldemund D, Rektorová I, Michálková Z, et al. Serum inflammatory biomarkers in Parkinson's disease. *Parkinsonism Relat Disord*. (2009) 15:318–20. doi: 10.1016/j.parkreldis.2008.05.014
53. Tang P, Chong L, Li X, Liu Y, Liu P, Hou C, et al. Correlation between Serum RANTES Levels and the Severity of Parkinson's Disease. *Oxid Med Cell Longev*. (2014) 2014:208408. doi: 10.1155/2014/208408
54. Scalzo P, Kümmer A, Cardoso F, Teixeira AL. Serum levels of interleukin-6 are elevated in patients with Parkinson's disease and correlate with physical performance. *Neurosci Lett*. (2010) 468:56–8. doi: 10.1016/j.neulet.2009.10.062

55. Brosseron F, Krauthausen M, Kummer M, Heneka MT. Body fluid cytokine levels in mild cognitive impairment and alzheimer's disease: a comparative overview. *Mol Neurobiol*. (2014) 50:534–44. doi: 10.1007/s12035-014-8657-1
56. Basu S, Dasgupta PS. Dopamine, a neurotransmitter, influences the immune system. *J Neuroimmunol*. (2000) 102:113–24. doi: 10.1016/S0165-5728(99)00176-9
57. Carr L, Tucker A, Fernandez-Botran R. The enhancement of T cell proliferation by L-dopa is mediated peripherally and does not involve interleukin-2. *J Neuroimmunol*. (2003) 142:166–9. doi: 10.1016/S0165-5728(03)00270-4
58. Sanchez-Guajardo V, Tentillier N, Romero-Ramos M. The relation between α-synuclein and microglia in Parkinson's disease: Recent developments. Neuroscience. (2015) 302:47–58.
59. Garcia-Esparcia P, Llorens F, Carmona M, Ferrer I. Complex deregulation and expression of cytokines and mediators of the immune response in parkinson's disease brain is region dependent. *Brain Pathol*. (2014) 24:584–98. doi: 10.1111/bpa.12137
60. Reynolds AD, Kadiu I, Garg SK, Glanzer JG, Nordgren T, Ciborowski P, et al. Nitrated alpha-synuclein and microglial neuroregulatory activities. *J Neuroimmune Pharmacol*. (2008) 3:59–74. doi: 10.1007/s11481-008-9100-z

Conflict of Interest Statement: AS received research funding from Canadian Institute of Health Research, Canada Research Chair Program, National Parkinson Foundation, Parkinson Disease Foundation, Parkinson Society Canada, and Weston Brain Institute. TJ serves on the editorial board of Proteomics, Drug Discovery Today. He has received funding for travel or consultancy from Luminex and Myriad RBM. FL reports honoraria by Grifols, Beyer, Roche, Teva, and Biogen, and is an advisory board member for Roche and Biogen. He performs commercial antibody testing in the Institute of Laboratory Medicine, University Hospital Schleswig-Holstein, without personal benefits. TG serves on the editorial boards of *Parkinsonism and Related Disorders, Movement Disorders*, and *Journal of Neurology*; holds a patent re: Kinase Associated with Parkinsonism with Pleiomorphic Pathology (KASPP) (LRRK2) Gene, its Production and Use for the Detection and Treatment of Neurodegenerative Diseases; serves as a consultant for Cephalon, Inc., and Merck Serono; serves on speaker's bureaus of Novartis, Merck Serono, SCHWARZ PHARMA, Boehringer Ingelheim, and Valeant Pharmaceuticals International; and receives research support from Novartis, the European Union, BMBF (the Federal Ministry of Education and Research), and Helmholtz Association. AL has served as an adviser for Abbvie Inc., Allon Therapeutics, Avanir Pharmaceuticals, Biogen Idec, Boerhinger-Ingelheim, Ceregene, Lilly, Medtronic, Merck, Novartis, NeuroPhage Pharmaceuticals, Teva, and UCB; received honoraria from Teva, UCB, AbbVie Inc.; received grants from Brain Canada, Canadian Institutes of Health Research, Edmond J Safra Philanthropic Foundation, Michael J. Fox Foundation, the Ontario Brain Institute, National Parkinson Foundation, Parkinson Society Canada, Tourette Syndrome Association, W. Garfield Weston Foundation; received publishing royalties from Saunders, Wiley-Blackwell, Johns Hopkins Press, and Cambridge University Press; and has served as an expert witness in cases related to the welding industry. DB has served on scientific advisory boards for Novartis, Union chemique belge (UCB)/SCHWARZ PHARMA, Lundbeck, and Teva Pharmaceutical Industries Ltd.; has received funding for travel or speaker honoraria from Boehringer Ingelheim, Lundbeck Inc., Novartis, GlaxoSmithKline, UCB/SCHWARZ PHARMA, Merck Serono, Johnson & Johnson, and Teva Pharmaceutical Industries Ltd.; and has received research support from Janssen, Teva Pharmaceutical Industries Ltd., Solvay Pharmaceuticals, Inc./Abbott, Boehringer, UCB, Michael J Fox Foundation, Bundesministerium für Bildung und Forschung (BMBF), Deutsche Parkinson Vereinigung (dPV) (German Parkinson's disease association), Neuroallianz, DZNE, and Center of Integrative Neurosciences. WM receives or received funding from the European Union, the Michael J. Fox Foundation, Robert Bosch Foundation, Neuroalliance, Lundbeck and Janssen, and holds part of a patent for the assessment of dyskinesias (German patent office, 102015220741.2). He received speaker honoraria from GlaxoSmithKline, Abbvie, UCB, Licher MT and Rölke Pharma, and was invited to Advisory Boards of Market Access & Pricing Strategy GmbH and Abbvie. CM has been consultant for Pfizer, has received honoraria for teaching from EMD Serono, and has received grants from the Michael J Fox Foundation, Canadian Institutes of Health Research, National Parkinson Foundation and the Parkinson Society Canada; Site PI for clinical trial sponsored by Alllon Therapeutics, Physician Services Incorporated, International Parkinson and Movement Disorders Socitety and the Parkinson Disease Foundation. She is employee of the University Health Network and has a contract from Horizon Pharma.

The remaining authors declare that the research was conducted in the absence of any commercial or financial relationships that could be construed as a potential conflict of interest.

Copyright © 2018 Yilmaz, Strafella, Bernard, Schulte, van den Heuvel, Schneiderhan-Marra, Knorpp, Joos, Leypoldt, Geritz, Hansen, Heinzel, Apel, Gasser, Lang, Berg, Maetzler and Marras. This is an open-access article distributed under the terms of the Creative Commons Attribution License (CC BY). The use, distribution or reproduction in other forums is permitted, provided the original author(s) and the copyright owner(s) are credited and that the original publication in this journal is cited, in accordance with accepted academic practice. No use, distribution or reproduction is permitted which does not comply with these terms.

frontiers in Neurology

ORIGINAL RESEARCH
published: 09 January 2019
doi: 10.3389/fneur.2018.01152

Quantitative EEG and Verbal Fluency in DBS Patients: Comparison of Stimulator-On and -Off Conditions

*Florian Hatz[1], Antonia Meyer[1], Anne Roesch[1], Ethan Taub[2], Ute Gschwandtner[1] and Peter Fuhr[1]**

[1] Department of Neurology, Hospitals of University of Basel, Basel, Switzerland, [2] Department of Neurosurgery, Hospitals of University of Basel, Basel, Switzerland

Introduction: Deep brain stimulation of the subthalamic nucleus (STN-DBS) ameliorates motor function in patients with Parkinson's disease and allows reducing dopaminergic therapy. Beside effects on motor function STN-DBS influences many non-motor symptoms, among which decline of verbal fluency test performance is most consistently reported. The surgical procedure itself is the likely cause of this decline, while the influence of the electrical stimulation is still controversial. STN-DBS also produces widespread changes of cortical activity as visualized by quantitative EEG. The present study aims to link an alteration in verbal fluency performance by electrical stimulation of the STN to alterations in quantitative EEG.

Methods: Sixteen patients with STN-DBS were included. All patients had a high density EEG recording (256 channels) while testing verbal fluency in the stimulator on/off situation. The phonemic, semantic, alternating phonemic and semantic fluency was tested (Regensburger Wortflüssigkeits-Test).

Results: On the group level, stimulation of STN did not alter verbal fluency performance. EEG frequency analysis showed an increase of relative alpha2 (10–13 Hz) and beta (13–30 Hz) power in the parieto-occipital region ($p \leq 0.01$). On the individual level, changes of verbal fluency induced by stimulation of the STN were disparate and correlated inversely with delta power in the left temporal lobe ($p < 0.05$).

Conclusion: STN stimulation does not alter verbal fluency performance in a systematic way at group level. However, when in individual patients an alteration of verbal fluency performance is produced by electrical stimulation of the STN, it correlates inversely with left temporal delta power.

Keywords: Parkinson, DBS, quantitative EEG, automated artifact removal, verbal fluency

OPEN ACCESS

Edited by:
Marcello Moccia, University College London, United Kingdom

Reviewed by:
Martijn Beudel, University Medical Center Groningen, Netherlands
Antonio Suppa, Sapienza University of Rome, Italy

***Correspondence:**
Peter Fuhr
peter.fuhr@usb.ch

Specialty section:
This article was submitted to Movement Disorders, a section of the journal Frontiers in Neurology

Received: *15 August 2018*
Accepted: *12 December 2018*
Published: *09 January 2019*

Citation:
Hatz F, Meyer A, Roesch A, Taub E, Gschwandtner U and Fuhr P (2019) Quantitative EEG and Verbal Fluency in DBS Patients: Comparison of Stimulator-On and -Off Conditions. Front. Neurol. 9:1152. doi: 10.3389/fneur.2018.01152

INTRODUCTION

Deep brain stimulation of the subthalamic nucleus (STN-DBS) is widely used in advanced Parkinson's disease (PD) to treat motor complications. The subthalamic nucleus is the preferred target for DBS in most cases (1). STN-DBS improves motor manifestations in the limbs, while axial motor manifestations and language are improved variably, to a lesser extent, or not at all (2).

As for neuropsychological performance, verbal fluency (VF) performance is reportedly impaired by STN-DBS (3–7), while there is less evidence for GPi-DBS causing a decline in VF (8). The pathophysiological reason for this decline is still in debate (8). Chouiter et al. found that lesions by stroke or tumor of the left basal ganglia impair semantic and phonemic VF performance (9). However, to our current knowledge there is no study showing a direct long-term effect of precise microsurgical placement of electrodes on neuropsychological capacity. Interestingly, in a study by Isler et al. (10) reduction in cognitive flexibility after microsurgical penetration of the caudate nucleus recovered after 12 months. Anatomical studies in non-human primates have yielded evidence of a subdivision of the STN into a motor portion, an associative portion, and a smaller limbic portion (11, 12), while the associative portion is highly connected to the dorsolateral prefrontal and lateral orbitofrontal cortex. STN stimulation lessens the amount of language-related basal ganglia output via the thalamus and thus reduces thalamo-cortical drive (13). As striatal dysfunction is thought to induce set-shifting deficits by way of secondary dysfunction of the prefrontal cortex (4), this may partly account for decrease of VF after DBS. While it has been shown that the decline of VF after STN-DBS is an effect of the surgical procedure/perioperative activities (14), the influence of the electrical stimulation on VF performance is still controversial.

Both, the temporal and frontal lobes are involved in semantic and phonemic fluency tests. The left hemisphere is generally more important for VF than the right, and frontal lobes are more relevant for phonemic than for semantic fluency (15, 16).

Reduction of VF performance correlates with a reduction of median frequency or an increase of relative power in lower frequency bands in EEG (17).

In this study we aim to characterize the STN-stimulation-related changes in semantic, phonemic, and alternating fluency tasks and quantitative EEG (QEEG) measures (band powers, median frequency) in a group of PD patients. As VF is reduced by DBS, potentially by the stimulation itself, and as changes in VF performance are linked to frontal and temporal lobes, we expect a reduction of VF performance in the DBS-on compared to the DBS-off condition along with an increase of lower band power in frontal and temporal lobes.

METHODS

Patients

Eighteen patients with STN-DBS were included. Sixteen completed the study protocol and were included in the analysis. Fifteen patients were right-handed and one was ambidextrous. Subjects characteristics are shown in **Table 1**. All of them underwent high-density resting-state EEG recordings (256 channels) and testing of VF in the DBS-on and DBS-off conditions. The phonemic, semantic, alternating phonemic, and alternating semantic fluency was evaluated RWT, Regensburger Wortflüssigkeits-Test, 2 min testing per task, no counting of errors, (18). Median age was 68.0 (IQR 60–71), 9 males and 7 females. Median duration of education was 14 years (IQR 12–16.5). Median years after first symptoms of PD were 12.5 (IQR 10.75–19). Patients were included 32 months (IQR 26–58) after STN-DBS operation and had a median levodopa equivalents dose of 562 (IQR 219–798).

TABLE 1 | Subjects characteristics.

Age (years)	68.0 (59.2–71.8)
Education (years)	14 (12–16.5)
Years since diagnosis of PD (years)	12.5 (10.75–19)
Levodopa-equivalence-dose (mg)	562 (219–798)
Duration since DBS implantation (months)	32 (25.75–58.25)

Median values and lower/upper quartiles are shown.

EEG Recording

After initial testing of VF performance, QEEGs from all patients were initially recorded with the DBS-on. For EEG recordings a 256-channel Geodesic DC-EEG System 300 was used. Sampling rate was set to 1,000 Hz, first high pass filter to 0.01 Hz. Impedances of EEG electrodes were kept below 40 kΩ. Subjects were seated comfortably in a reclining chair in a dimly lit, sound attenuated and electromagnetically shielded room. They were instructed to relax, but to stay awake and to minimize eye and body movements. After 12 min recording DBS was turned off and QEEG was recorded for additional 12 min, followed by VF testing. As for all subjects in the study STN-DBS consisted in a monopolar stimulation.

EEG Post-processing

DBS-stimulation generates an artifact of considerably larger amplitude than the intrinsic brain signal recorded by EEG (19); the latter can only be analyzed once the former has been removed. Different methods of artifact removal have been proposed. The method described by Sun et al. for subtracting a reconstructed artifact is difficult to apply to real-life data (20). Lio et al. applied a combination of low-pass filter and a frequency-domain filter tracking outliers (21). Santillan-Guzman et al. proposed a temporal-frequency-domain filter (22). This method takes advantage of the known frequency characteristics of the artifact but does not exploit the similarity of signal shape at all of the recording electrodes due to the effect of volume conduction. We therefore used principal-component analysis to delete the first component, followed by an independent component analysis. These components were averaged using the DBS artifact as a trigger, and components with remaining signals after averaging were eliminated. Finally a 70 Hz low-pass filter (high-order, least-square filter) was applied (**Figure 1**). All steps for DBS-artifact elimination were integrated and performed in the toolbox "TAPEEG" (23), allowing fully automated artifact removal. Visually, frequency spectra for every patient in the ON- and OFF-condition were compared, showing a convincing reduction/elimination of the DBS artifact (**Supplemental Figure 1**).

Inverse Solution (Frequency Domain)

Using a previously published method (24), resulting EEG data was re-referenced to average reference and bad channels were interpolated with spherical spline method. Power spectra were calculated from epochs of 4 s duration (spectral resolution 0.25 Hz) using Welch's method (20, 25). Source-space data was

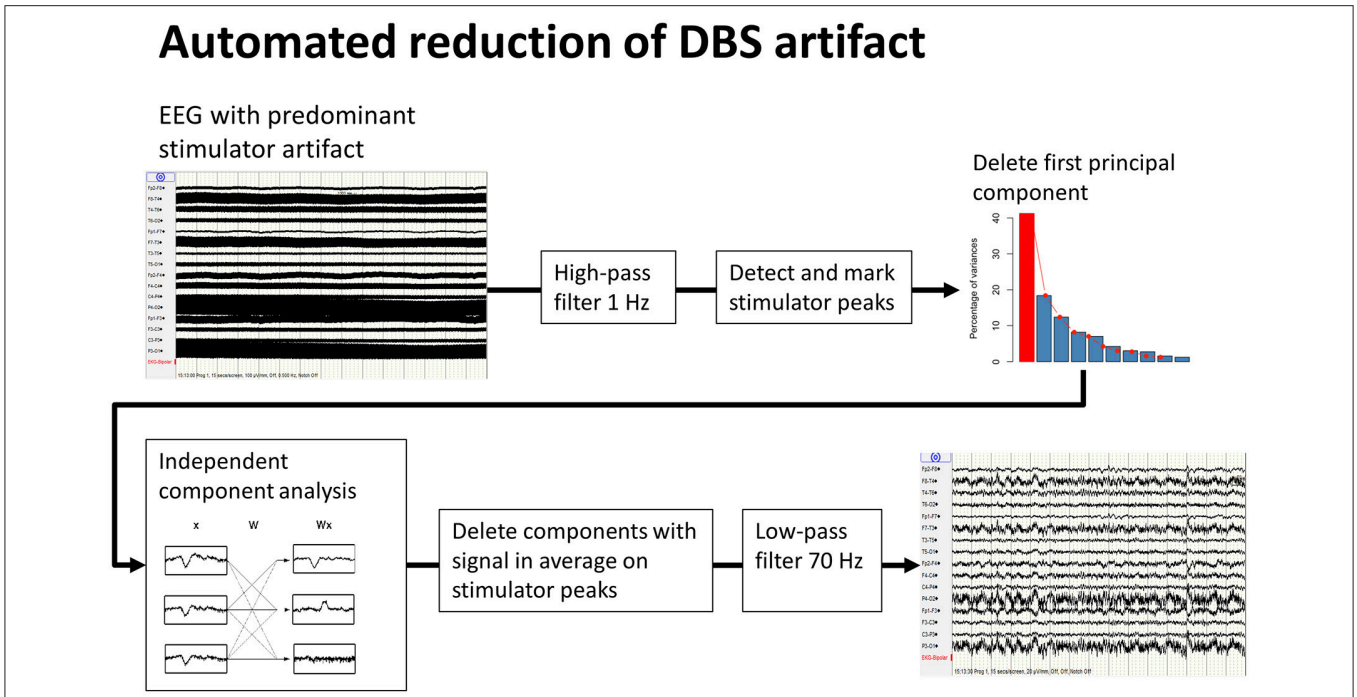


FIGURE 1 | Workflow of automated reduction of DBS artifacts. A high-order least-square filter, high-pass at 1 Hz was applied first, followed by detection of the peaks of the stimulator artifacts. Second, a principal-component analysis was performed. A large part of the stimulator artifact is accounted for by the first principal component. This component was then deleted and the EEG reconstructed. Third, after an independent component analysis, all resulting components were averaged on the previously detected peaks for identification of the components, including DBS artifacts. These components were deleted and, again, the EEG was reconstructed. Finally, a high order least-square filter, low-pass at 70 Hz, was applied.

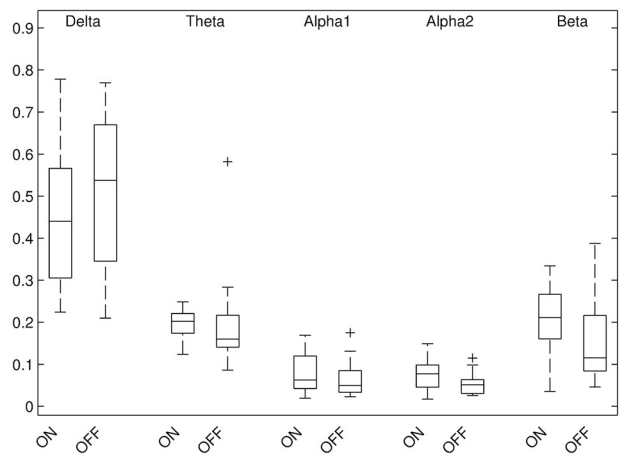


FIGURE 2 | Results of global relative band power, comparison DBS-on vs. DBS-off.

calculated by LORETA inverse solution for spectral data as described by Frei et al. (26), using a vector transposition matrix calculated with the software-package Cartool (27), based on the MNI brain atlas (28) and without using a normalization. The calculation was achieved using 5,011 solution points with subsequent reduction to 78 regions of interest (ROIs) based on the AAL atlas (29). According to previous studies by our group, median frequency and relative power in the delta- (1–4 Hz), theta- (4–8 Hz), alpha1- (8–10 Hz), alpha2- (10–13 Hz) and beta- (13–30 Hz) bands were calculated.

Statistics

The relative band powers, median frequencies, and results of VF testing in the DBS-on and DBS-off conditions were compared with paired *t*-tests. The changes in relative power and VF tests were calculated ("value DBS-on" minus "value DBS-off") and Spearman rank correlations calculated. Due to large intersubject power differences, relative power is the preferred measure for group data, while due to intrasubject stability of the EEG, absolute power is the preferred measure for longitudinal data within subjects. Permutation was used to correct for multiple testing and non-normal distributions of the resulting values.

The study was carried out in accordance with the recommendations of the Ethikkommission beider Basel (EKBB). The protocol was approved by the EKBB. All subjects gave written informed consent in accordance with the Declaration of Helsinki.

RESULTS

Results of relative band power are shown in **Figure 2**. In the DBS-on condition, the relative alpha2 power was higher in parieto-occipital regions bilaterally (**Figure 3**, $p \leq 0.01$) and the relative beta power was higher in the left parieto-occipital region (**Figure 3**, $p \leq 0.05$).

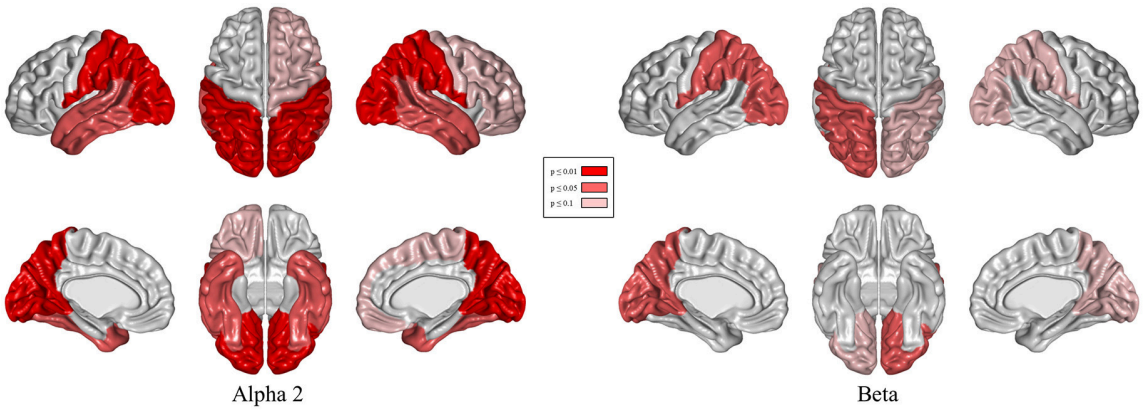


FIGURE 3 | Topographical differences in relative alpha2 and beta power: DBS-on vs. DBS-off. Results of *t*-tests with permutation (red = regions with $p < 0.01$/light red = regions with $p < 0.05$/rose = regions with $p < 0.1$).

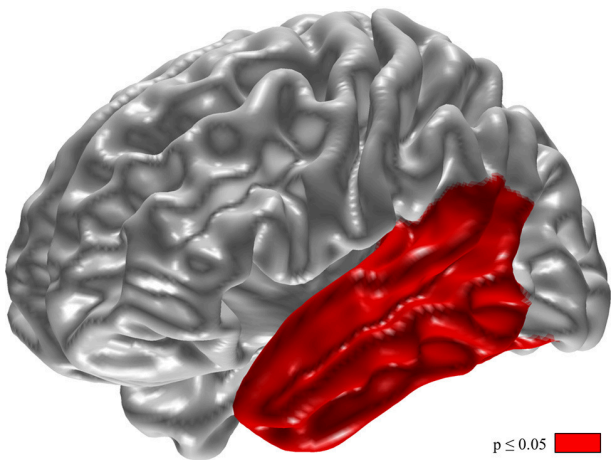


FIGURE 4 | Inverse correlation of changes in phonemic verbal fluency and relative delta power. For calculation the difference of VF (VF with DBS-on minus VF with DBS-off) and relative delta power (delta with DBS-on minus delta with DBS-off). Results of *t*-tests with permutation (red = regions with $p < 0.05$).

Changes of relative delta power in the left temporal lobe and the phonemic VF were inversely correlated (**Figure 4**, $p < 0.05$).

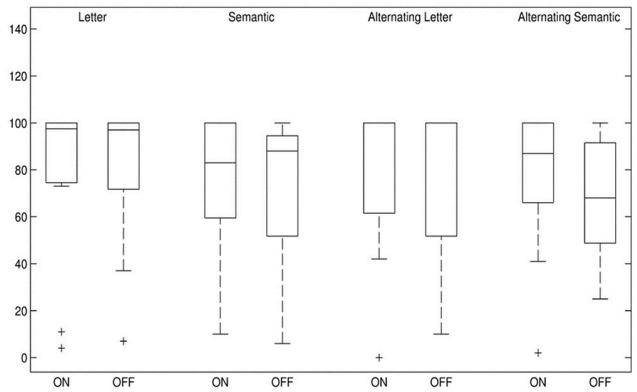
Alternating semantic fluency performance slightly decreased after switching off stimulation, but this result is below statistical significance. For all other VF tests, no difference between the two conditions was found (**Figure 5**).

DISCUSSION

Switching off the STN-DBS did not improve VF performance in the present study in PD patients at least 6 months after operation. This finding accords with that of previous studies (14, 30) and supports the hypothesis that impairment in VF tests after operation is due to STN-DBS procedure rather than to the electrical stimulation. In addition to the surgical microtrauma, STN-DBS procedure includes anesthesia, changes in medication and sometimes post-operative delirium. Especially, the reduction of dopaminergic pharmacotherapy after the STN-DBS procedure may be an important factor, as VF performance is known to be ameliorated by dopaminergic drugs (31).

According to the present results, bilateral STN-DBS stimulation increases alpha2 and beta power in posterior regions in the resting-state EEG compared to the stimulator off condition. High alpha2 power is linked to increased capacity to initiate new tasks (32, 33) and probably facilitates switching between different tasks as tested in alternating VF. Alpha activity requires an intact thalamo-cortical loop (34), and its increase may reflect a partial functional normalization of this loop in the DBS-on condition, contributing to improved motor function and VF. This concept is compatible with the observation of a trend toward ameliorated alternating semantic fluency in the DBS-on state and is further supported by a previous study including 14 patients with PD, showing a slight positive effect of stimulation in the STN on phonemic fluency (30). However, this effect may be not strong enough to compensate for the decline of VF after STN-DBS procedure including a reduction of dopaminergic drugs.

The present result of increased beta power in the DBS-on state seems to contradict previous studies, which showed an improvement of motor function associated with a decrease of beta power over the sensorimotor, premotor and prefrontal cortex during STN stimulation and movement (35). However, in the present study the increase of beta power in the DBS-on situation occurs in resting state EEG and, therefore, the results are not directly comparable to studies analyzing event-related EEG alterations. Two MEG studies recorded also in resting state showed in contrast to the present results a decrease of beta band activity by STN-DBS (36, 37). While recordings in the study by Abbasi et al. took place 1 day after implantation and, therefore, were obtained in a different situation, the study by Luoma et al. with a latency of at least 3 months after implantation is better



	T	p
P - M	-0.04	0.97
VN - NA	0.43	0.67
G/R – H/T	0.11	0.91
S/F – K/B	0.65	0.52

FIGURE 5 | Differences in verbal fluency: DBS-on vs. DBS-off. Percent ranks of test results, boxplots showing median, upper and lower quartiles. P–M, comparison of phonemic fluency with "P" and "M" letters; VN–NA, comparison of semantic fluency with "Names" and "Food"; G/R–H/T, comparison of phonemic fluency with alternating "G" and "R" and alternating "H" and "T" letters; S/F–K/B, comparison of semantic fluency with alternating "Sport" and "Fruits" and alternating "Clothes" and "Flowers".

comparable to our results obtained at a latency of at least 6 months.

However, the present result is in line with the observation of a correlation between beta power in the paracentral region and motor function as well as sensorimotor integration after L-dopa intake (38) and with the results of a study by Cao et al. (39). The reason for these contradictory results is currently unclear; medication may play a role.

Changes of absolute delta power in the left temporal lobe and the phonemic fluency on the individual level correlate inversely. The fact that neither delta power nor phonemic fluency changes significantly between DBS-on and DBS-off conditions on the group level does not contradict such a correlation on the individual level as observed here. However, according to a post-stroke study using voxel-based volumetry phonemic fluency is a dysfunction of the left frontal rather than the left temporal lobe (15).

One limitation of this study is its small sample size. Speculations can be made about the underlying mechanisms of DBS-induced changes in brain rhythms, but no inferences can be drawn about therapeutic language effects in individual patients. For practical and ethical reasons, the time spent in the DBS-off condition was limited, and this necessitated the retesting of VF after only 12 min in off-time. Although this was longer than the 3 min off-time in the study by Yilmaz et al. (14), it may still not have been long enough for the effects of DBS on VF to disappear entirely.

DATA AVAILABILITY

The EEG raw datasets of all patients in the study are not publicly available, as the signed informed consent by all patients does not include the possibility of the publication of these highly subject specific datasets. Raw results of the processed EEG datasets are available on demand. Requests to access the datasets should be directed to Peter Fuhr, peter.fuhr@usb.ch.

AUTHOR CONTRIBUTIONS

FH conceived and conducted the study, processed the EEG data, and drafted the manuscript. AM and AR conducted neuropsychological and linguistical testing of all patients. PF and UG initiated and designed the study, cared for the patients and critically reviewed the manuscript. ET had operated all patients and critically reviewed the manuscript. All authors read and approved the final manuscript.

ACKNOWLEDGMENTS

We thank the participating subjects and caregivers. The financial support of the Freiwillige Akademische Gesellschaft Basel, the Gottfried und Julia Bangerter-Rhyner-Stiftung, the Hedwig Widmer Stiftung, the Swiss National Science Foundation (grants: 33CM30-140338, 33CM30-124115, 326030-128775/1) and the Novartis Research Foundation is gratefully acknowledged.

SUPPLEMENTARY MATERIAL

The Supplementary Material for this article can be found online at: https://www.frontiersin.org/articles/10.3389/fneur.2018.01152/full#supplementary-material

Supplemental Figure 1 | Frequency spectra of single subject in DBS-off, DBS-on without artifact removal, and DBS-on after artifact removal (1 Hz highpass filter was applied before plotting).

REFERENCES

1. Volkmann J. Deep brain stimulation for the treatment of Parkinson's disease. *J Clin Neurophysiol Off Publ Am Electroencephalogr Soc.* (2004) 21:6–17.
2. Fasano A, Aquino CC, Krauss JK, Honey CR, Bloem BR. Axial disability and deep brain stimulation in patients with Parkinson disease. *Nat Rev Neurol.* (2015) 11:98–110. doi: 10.1038/nrneurol.2014.252
3. Combs HL, Folley BS, Berry DTR, Segerstrom SC, Han DY, Anderson-Mooney AJ, et al. Cognition and depression following deep brain stimulation of the subthalamic nucleus and globus pallidus pars internus in Parkinson's disease: a meta-analysis. *Neuropsychol Rev.* (2015) 25:439–54. doi: 10.1007/s11065-015-9302-0
4. Marshall DF, Strutt AM, Williams AE, Simpson RK, Jankovic J, York MK. Alternating verbal fluency performance following bilateral subthalamic nucleus deep brain stimulation for Parkinson's disease. *Eur J Neurol.* (2012) 19:1525–31. doi: 10.1111/j.1468-1331.2012.03759.x
5. Parsons TD, Rogers SA, Braaten AJ, Woods SP, Tröster AI. Cognitive sequelae of subthalamic nucleus deep brain stimulation in Parkinson's disease: a meta-analysis. *Lancet Neurol.* (2006) 5:578–88. doi: 10.1016/S1474-4422(06)70475-6
6. Daniels C, Krack P, Volkmann J, Pinsker MO, Krause M, Tronnier V, et al. Risk factors for executive dysfunction after subthalamic nucleus stimulation in Parkinson's disease. *Mov Disord.* (2010) 25:1583–9. doi: 10.1002/mds.23078
7. Witt K, Granert O, Daniels C, Volkmann J, Falk D, Eimeren T. van, et al. Relation of lead trajectory and electrode position to neuropsychological outcomes of subthalamic neurostimulation in Parkinson's disease: results from a randomized trial. *Brain* (2013) 136:2109–19. doi: 10.1093/brain/awt151
8. Højlund A, Petersen MV, Sridharan KS, Østergaard K. Worsening of verbal fluency after deep brain stimulation in Parkinson's disease: a focused review. *Comput Struct Biotechnol J.* (2016) 15:68–74. doi: 10.1016/j.csbj.2016.11.003
9. Chouiter L, Holmberg J, Manuel AL, Colombo F, Clarke S, Annoni J-M, et al. Partly segregated cortico-subcortical pathways support phonologic and semantic verbal fluency: a lesion study. *Neuroscience* (2016) 329:275–83. doi: 10.1016/j.neuroscience.2016.05.029
10. Isler C, Albi A, Schaper FL, Temel Y, Duits A. Neuropsychological outcome in subthalamic nucleus stimulation surgeries with electrodes passing through the caudate nucleus. *Stereotact Funct Neurosurg.* (2016) 94:413–20. doi: 10.1159/000453278
11. Haynes WIA, Haber SN. The organization of prefrontal-subthalamic inputs in primates provides an anatomical substrate for both functional specificity and integration: implications for basal ganglia models and deep brain stimulation. *J Neurosci Off J Soc Neurosci.* (2013) 33:4804–14. doi: 10.1523/JNEUROSCI.4674-12.2013
12. Wise SP, Murray EA, Gerfen CR. The frontal cortex-basal ganglia system in primates. *Crit Rev Neurobiol.* (1996) 10:317–56.
13. Barbas H, García-Cabezas MÁ, Zikopoulos B. Frontal-thalamic circuits associated with language. *Brain Lang.* (2013) 126:49–61. doi: 10.1016/j.bandl.2012.10.001
14. Yilmaz R, Akbostanci MC, Mercan FN, Sorgun MH, Savas A. No effect of different stimulation conditions on verbal fluency and visuospatial orientation in patients with subthalamic nucleus deep brain stimulation. *Stereotact Funct Neurosurg.* (2015) 93:326–32. doi: 10.1159/000438996
15. Baldo JV, Schwartz S, Wilkins D, Dronkers NF. Role of frontal versus temporal cortex in verbal fluency as revealed by voxel-based lesion symptom mapping. *J Int Neuropsychol Soc.* (2006) 12:896–900. doi: 10.1017/S1355617706061078
16. Metternich B, Buschmann F, Wagner K, Schulze-Bonhage A, Kriston L. Verbal fluency in focal epilepsy: a systematic review and meta-analysis. *Neuropsychol Rev.* (2014) 24:200–18. doi: 10.1007/s11065-014-9255-8
17. Zimmermann R, Gschwandtner U, Hatz F, Schindler C, Bousleiman H, Ahmed S, et al. Correlation of EEG slowing with cognitive domains in nondemented patients with Parkinson's disease. *Dement Geriatr Cogn Disord.* (2015) 39:207–14. doi: 10.1159/000370110
18. Aschenbrenner S. *Regensburger Wortflüssigkeits-Test: RWT* (2000). Hogrefe: Verlag für Psychologie.
19. Frysinger RC, Quigg M, Elias WJ. Bipolar deep brain stimulation permits routine EKG, EEG, and polysomnography. *Neurology* (2006) 66:268–70. doi: 10.1212/01.wnl.0000194272.79084.7e
20. Sun Y, Farzan F, Garcia Dominguez L, Barr MS, Giacobbe P, Lozano AM, et al. A novel method for removal of deep brain stimulation artifact from electroencephalography. *J Neurosci Methods* (2014) 237:33–40. doi: 10.1016/j.jneumeth.2014.09.002
21. Lio G, Thobois S, Ballanger B, Lau B, Boulinguez P. Removing deep brain stimulation artifacts from the electroencephalogram: issues, recommendations and an open-source toolbox. *Clin Neurophysiol.* (2018) 129:2170–85. doi: 10.1016/j.clinph.2018.07.023
22. Santillan-Guzman A, Heute U, Muthuraman M, Stephani U, Galka A. DBS artifact suppression using a time-frequency domain filter. In: *2013 35th Annual International Conference of the IEEE Engineering in Medicine and Biology Society (EMBC)*. Osaka (2013). p. 4815–8. doi: 10.1109/EMBC.2013.6610625
23. Hatz F, Hardmeier M, Bousleiman H, Rüegg S, Schindler C, Fuhr P. Reliability of fully automated versus visually controlled pre- and post-processing of resting-state EEG. *Clin Neurophysiol Off J Int Fed Clin Neurophysiol.* (2015) 126:268–74. doi: 10.1016/j.clinph.2014.05.014
24. Hatz F, Benz N, Hardmeier M, Zimmermann R, Rueegg S, Schindler C, et al. Quantitative EEG and apolipoprotein E-genotype improve classification of patients with suspected Alzheimer's disease. *Clin Neurophysiol Off J Int Fed Clin Neurophysiol.* (2013) 124:2146–52. doi: 10.1016/j.clinph.2013.04.339
25. Welch P. The use of fast Fourier transform for the estimation of power spectra: a method based on time averaging over short, modified periodograms. *IEEE Trans Audio Electroacoust.* (1967) 15:70–3.
26. Frei E, Gamma A, Pascual-Marqui R, Lehmann D, Hell D, Vollenweider FX. Localization of MDMA-induced brain activity in healthy volunteers using low resolution brain electromagnetic tomography (LORETA). *Hum Brain Mapp.* (2001) 14:152–65. doi: 10.1002/hbm.1049
27. Brunet D, Murray MM, Michel CM. Spatiotemporal analysis of multichannel EEG: CARTOOL. *Comput Intell Neurosci.* (2011) 2011:813870. doi: 10.1155/2011/813870
28. Aubert-Broche B, Evans AC, Collins L. A new improved version of the realistic digital brain phantom. *Neuroimage* (2006) 32:138–45. doi: 10.1016/j.neuroimage.2006.03.052
29. Tzourio-Mazoyer N, Landeau B, Papathanassiou D, Crivello F, Etard O, Delcroix N, et al. Automated anatomical labeling of activations in SPM using a macroscopic anatomical parcellation of the MNI MRI single-subject brain. *Neuroimage* (2002) 15:273–89. doi: 10.1006/nimg.2001.0978
30. Ehlen F, Vonberg I, Kühn AA, Klostermann F. Effects of thalamic deep brain stimulation on spontaneous language production. *Neuropsychologia* (2016) 89:74–82. doi: 10.1016/j.neuropsychologia.2016.05.028
31. Herrera E, Cuetos F, Ribacoba R. Verbal fluency in Parkinson's disease patients on/off dopamine medication. *Neuropsychologia* (2012) 50:3636–40. doi: 10.1016/j.neuropsychologia.2012.09.016
32. Klimesch W. EEG alpha and theta oscillations reflect cognitive and memory performance: a review and analysis. *Brain Res Rev.* (1999) 29:169–95. doi: 10.1016/S0165-0173(98)00056-3
33. Sadaghiani S, Scheeringa R, Lehongre K, Morillon B, Giraud A-L, Kleinschmidt A. Intrinsic connectivity networks, alpha oscillations, and tonic alertness: a simultaneous electroencephalography/functional magnetic resonance imaging study. *J Neurosci.* (2010) 30:10243–50. doi: 10.1523/JNEUROSCI.1004-10.2010
34. Schreckenberger M, Lange-Asschenfeld C, Lochmann M, Mann K, Siessmeier T, Buchholz H-G, et al. The thalamus as the generator and modulator of EEG alpha rhythm: a combined PET/EEG study with lorazepam challenge in humans. *Neuroimage* (2004) 22:637–44. doi: 10.1016/j.neuroimage.2004.01.047
35. Brown P, Marsden CD. Bradykinesia and impairment of EEG desynchronization in Parkinson's disease. *Mov Disord.* (1999) 14:423–9. doi: 10.1002/1531-8257(199905)14:3<423::AID-MDS1006>3.0.CO;2-V
36. Abbasi O, Hirschmann J, Storzer L, Özkurt TE, Elben S, Vesper J, et al. Unilateral deep brain stimulation suppresses alpha and beta oscillations in sensorimotor cortices. *Neuroimage* (2018) 174:201–7. doi: 10.1016/j.neuroimage.2018.03.026
37. Luoma J, Pekkonen E, Airaksinen K, Helle L, Nurminen J, Taulu S, et al. Spontaneous sensorimotor cortical activity is suppressed by deep brain

stimulation in patients with advanced Parkinson's disease. *Neurosci Lett.* (2018) 683:48–53. doi: 10.1016/j.neulet.2018.06.041
38. Melgari J-M. Alpha and beta EEG power reflects L-dopa acute administration in parkinsonian patients. *Front Aging Neurosci.* (2014) 6:302. doi: 10.3389/fnagi.2014.00302
39. Cao C, Li D, Jiang T, Ince NF, Zhan S, Zhang J, et al. Resting state cortical oscillations of patients with Parkinson disease and with and without subthalamic deep brain stimulation: a magnetoencephalography study. *J Clin Neurophysiol.* (2015) 32:109–18. doi: 10.1097/WNP.0000000000000137

Conflict of Interest Statement: FH is supported by the Freiwillige Akademische Gesellschaft Basel. AM is supported by the Hedwig Widmer Foundation. UG's research is supported by Mach-Gaensslen-Foundation, Gossweiler Foundation, Parkinson Schweiz, Synapsis Foundation, Botnar Foundation. PF's research is supported by the Swiss National Science Foundation, Mach-Gaensslen-Foundation, Gossweiler Foundation, Parkinson Schweiz, Synapsis Foundation, Botnar Foundation, Freiwillige Akademische Gesellschaft Basel, Novartis Research Foundation, FreeNovation Foundation, as well as by unconditional research grants from Novartis, Roche, AbbVie, and Biogen.

The remaining authors declare that the research was conducted in the absence of any commercial or financial relationships that could be construed as a potential conflict of interest.

Copyright © 2019 Hatz, Meyer, Roesch, Taub, Gschwandtner and Fuhr. This is an open-access article distributed under the terms of the Creative Commons Attribution License (CC BY). The use, distribution or reproduction in other forums is permitted, provided the original author(s) and the copyright owner(s) are credited and that the original publication in this journal is cited, in accordance with accepted academic practice. No use, distribution or reproduction is permitted which does not comply with these terms.

frontiers in Neurology

PROTOCOLS
published: 30 January 2019
doi: 10.3389/fneur.2019.00048

A Smart Device System to Identify New Phenotypical Characteristics in Movement Disorders

Julian Varghese[1]*, *Stephan Niewöhner*[2], *Iñaki Soto-Rey*[1], *Stephanie Schipmann-Miletić*[3], *Nils Warneke*[3], *Tobias Warnecke*[4] and *Martin Dugas*[1]

[1] Institute of Medical Informatics, University of Münster, Münster, Germany, [2] Department of Information Systems, University of Münster, Münster, Germany, [3] Department of Neurosurgery, University Hospital Münster, Münster, Germany, [4] Department of Neurology, University Hospital Münster, Münster, Germany

Parkinson's disease and Essential Tremor are two of the most common movement disorders and are still associated with high rates of misdiagnosis. Collected data by technology-based objective measures (TOMs) has the potential to provide new promising and highly accurate movement data for a better understanding of phenotypical characteristics and diagnostic support. A technology-based system called Smart Device System (SDS) is going to be implemented for multi-modal high-resolution acceleration measurement of patients with PD or ET within a clinical setting. The 2-year prospective observational study is conducted to identify new phenotypical biomarkers and train an Artificial Intelligence System. The SDS is going to be integrated and tested within a 20-min assessment including smartphone-based questionnaires, two smartwatches at both wrists and tablet-based Archimedean spirals drawing for deeper tremor-analyses. The electronic questionnaires will cover data on medication, family history and non-motor symptoms. In this paper, we describe the steps for this novel technology-utilizing examination, the principal steps for data analyses and the targeted performances of the system. Future work considers integration with Deep Brain Stimulation, dissemination into further sites and patient's home setting as well as integration with further data sources as neuroimaging and biobanks. Study Registration ID on ClinicalTrials.gov: NCT03638479.

Keywords: Parkinson's Disease, Essential Tremor, smart wearables, artificial intelligence, neural networks

OPEN ACCESS

Edited by:
Maria Salsone,
Italian National Research Council (CNR), Italy

Reviewed by:
Mattia Volta,
EURAC Research, Italy
Alessia Sarica,
Università degli Studi Magna Graecia, Italy

***Correspondence:**
Julian Varghese
julian.varghese@uni-muenster.de

Specialty section:
This article was submitted to Neurodegeneration, a section of the journal Frontiers in Neurology

Received: *05 October 2018*
Accepted: *14 January 2019*
Published: *30 January 2019*

Citation:
Varghese J, Niewöhner S, Soto-Rey I, Schipmann-Miletić S, Warneke N, Warnecke T and Dugas M (2019) A Smart Device System to Identify New Phenotypical Characteristics in Movement Disorders. Front. Neurol. 10:48. doi: 10.3389/fneur.2019.00048

INTRODUCTION

Tremor-related diseases as Parkinson's Disease (PD) and Essential Tremor (ET) are two of the most common movement disorders (1). Disease classification is primarily based on clinical criteria and remains challenging (2, 3). Smart wearables with multi-sensor technology provide a source of objective movement monitoring allowing for greater precision in recording subtle changes unlike current clinical rating scales in hospital routine (4, 5). A technology-based system—called Smart Device System (SDS)—was implemented to monitor and visualize multi-modal high-resolution data. The project is going to be conducted in close collaboration with the local departments of Neurology and Neurosurgery and the Task Force on Technology by the International Movement Disorder Society. Though there is an increasing number of existent mobile apps from application stores or mature medical devices as the Parkinson's KinetiGraph™ system, there is a low number

of large-scale deployments to capture and analyze the monitored data (6). More importantly, two key barriers—mentioned in a review by the International Movement Disorder Society—hamper integration into routine healthcare and identification of new phenotypical characteristics (7):

- First, there is poor integration of clinically relevant motor and non-motor phenomena. Especially, changes in tremor characteristics in relation to provoking circumstances (e.g., specific motor or cognitive actions) are currently not integrated into electronic tremor analyses. The SDS system utilizes different monitoring settings in one easy-to-follow examination at a health care facility: (A) Movement monitoring using two smartwatches at both patient wrists in a pre-defined neurological examination that provokes different tremor types. (B) Electronic questionnaires regarding medication/drug consumption, family history and non-motor symptoms on a smartphone. (C) Archimedean Spirals drawn by the patient on a tablet. Each of these three settings viewed individually already show high potential to classify or stratify tremor-related diseases (7–9). However, synchronization of these multimodal data (A–C) and advanced pattern recognition analyses such as Deep Learning would unlock a new integrative approach to boost classification performance and to find new phenotypical characteristics. In particular, Deep Learning methods have recently shown high classification performance in pattern recognition in other medical domains if a large amount of expert-tagged training data is available (10, 11).
- Second, there is a lack of open data repositories and data standards to share best practices of existing smart wearable solutions. This project uses the Medical-Data-Models Portal (MDM Portal) that has evolved to the largest European information infrastructure for medical data models (12). This portal will be used to harmonize and enrich developed data models toward established data standards and foster interoperability with other health information systems. Moreover, active collaboration with the Neurology Department and Task Force on Technology will align clinical and technical key requirements with current ongoing developments.

A 2-year prospective exploratory study is going to be conducted in which the SDS system will be applied within a 20-min data capture session for each included participant. The objective is to train a Deep Neural Network that is capable of predicting the disease entity (PD, ET, none of them) and to identify new phenotypical characteristics based on the fully integrated and pseudonymized study data.

MATERIALS AND EQUIPMENT

The project is planned as a 2-year prospective exploratory study at the Movement Disorders outpatient clinic at the University Hospital Münster. Each patient diagnosed with PD (ICD 10-GM: G20.-) or ET (ICD-10-GM G25.0) and visiting the outpatient clinic is going to be a potential study participant. To be included, each patient must receive, fully understand and sign the informed consent form. All requirements of the updated EU data protection regulation from the start of May 2018 will be strictly adhered to. The study design is registered on Clinicaltrial.gov (Identifier: NCT03638479).

Figure 1 provides an overview of the SDS system and its intended processing steps. Three Apple-based mobile devices will be customized for different monitoring settings. Smartwatch-based examination takes 10-min including calibration and putting them on both wrists. The total assessment time including questionnaires (8 min), drawing one spiral (1–2 min) is 20 min.

The examiner smartphone (iPhone at least Series 7) constitutes the first step of examination and provides short questionnaires about non-motor symptoms, family history and medication. Two smartwatches (Series 4.0) constitute the second step and enables high-resolution tremor capture from both wrists in a neurological examination (see **Table 1**). The captured data will be sent via Bluetooth to the smartphone. Since only one smartwatch can be paired with one smartphone at the same time, another smartphone is necessary to forward data from the second smartwatch to the examiner iPhone. The iPad Pro constitutes the final step of the assessment and will enable drawing of Archimedean spirals after protocol-based neurological examination. Captured data will be sent to the examiner smartphone, from which all captured data will be pseudonymized and securely transmitted in JSON format into a European General Data Protection Regulation-compliant research database. This connection to the research database is implemented within a REST-based client-server architecture using HTTPS as encryption. Two exemplary JSON files are attached as **Supplementary Files** that show structure of the transmitted raw data for two subject cases (one healthy subject, one with Parkinson's disease). The raw data from each JSON file will then be imported into a PostgreSQL-based research database. The overview of all data items is listed in the **Table S1**. All data processing, transmission, and storage processes were approved by the local data protection officer.

The software development for smartwatch-based and smartphone-based data capture is already finished. Tablet-based data capture will be included as soon as development and tests are completed. The first 3 months of the study consist of a setting up and testing phase, regardless of the tablet-based component. Only then, patients will be recruited and data capture commences and endures for 21 months. Based on a database report of the local EMR system, we expect 120 patients with ET and 954 patients with PD at our local site. A fixed number of follow up visits is not planned during this study. However, patients that will re-appear at the local site according to the usual treatment plan will be identified as follow-up patients to enable data analysis on disease progression.

STEPWISE PROCEDURES

The following sections describe data capture settings in detail to provide a highly structured and reproducible data basis. Principal steps regarding data processing, analysis and model training are

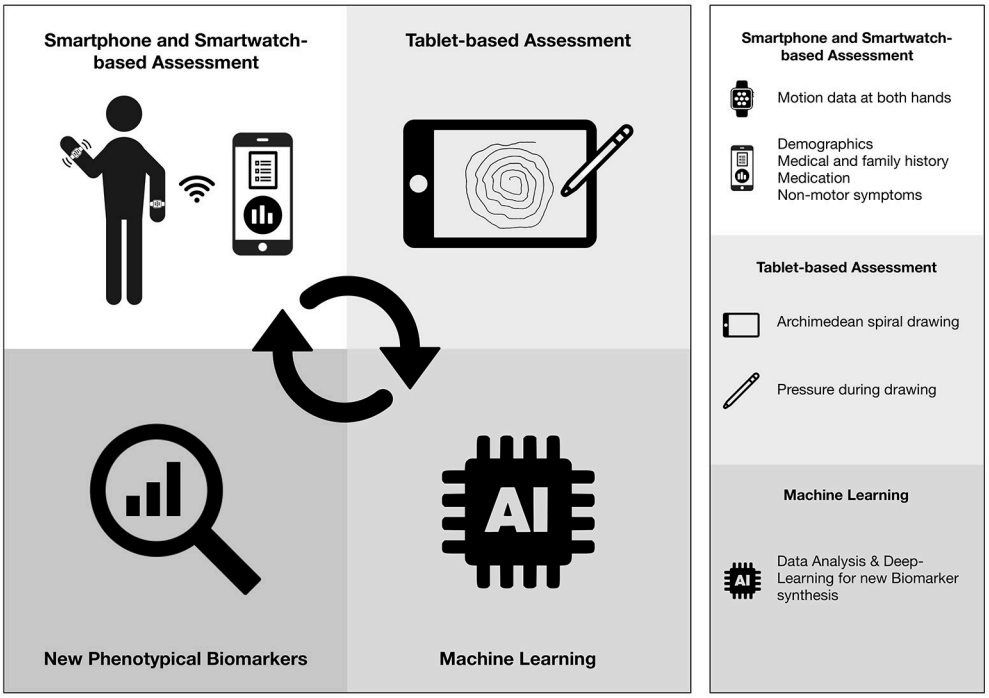


FIGURE 1 | Overview of the Smart Device System.

listed in the *Methods and Anticipated Results* section and will be subject to further refinements once the data is collected and evaluated.

Recruitment

Each patients and his/her accompanying person (e.g., life partner), who visit the movement disorders outpatient clinic at the University Hospital in Münster and fulfill the aforementioned criteria will be asked to participate in the study. In most cases, each patient will be accompanied by a familiar person. These companions represent age-matched healthy controls. Each participant will be informed about the SDS system, the data to be captured, pseudonymized, transferred and stored for data analysis. Study inclusion starts once informed consent form has been signed.

Data Capture and Neurological Examination

Preceded by a literature review of tremor-related medical history, clinical phenomenology and the new tremor classification (8, 13–18) a series of workshops were conducted with neurologists specialized in Movement Disorders. As a result, a set of questionnaire items and a short technology-based examination were designed to capture data features, which were regarded to have highest predictive power for differential diagnoses of ET and PD. The questionnaire items will be captured first and are listed in **Table S1**. Then, neurological examination will start with one smartwatch at each participant's wrist, see **Table 1**. All steps in this examination are illustrated in a video (19) and the examiner initiates the next step or can repeat the current step. Thus, the acceleration data is always labeled with the corresponding examination step, which will provide essential context information for training the Deep-Learning model. The final assessment is to have the participant draw a spiral with a provided stylus and tablet (**Figure 2**), starting with the right hand and then with left hand. All components of the SDS-system (smartphone, smartwatches, and tablet) will only capture, pseudonymize, and submit data to a research database for Deep Learning. No components of the system will apply any analyses that intends to confirm or change any routine diagnostic or therapeutic procedures. Instead, all advanced data analyses will be conducted subsequently on the pseudonymized data at the research database server and none of analyses results will be sent back to the patient-level.

METHODS AND ANTICIPATED RESULTS

Acceleration data by the smartwatches will be analyzed with signal processing methods (including Fast Fourier Transform and band-pass filters) to infer average tremor amplitude and frequency in each examination section. **Figure 3** illustrates a number of readily implemented graphical user interfaces and functioning initial results analyses.

Data captured by spiral drawing will be processed for angular feature detection, direction inversion and pattern deviation from ideal spiral according to Zham et al. (8). The sum of all captured and processed data will train a neural network model to predict the diagnosis label (PD, ET,

TABLE 1 | Smartwatch-based steps of neurological examination.

Step	Duration (s)	Description
1a	20	Rest tremor. Participant is seated in resting position, standardized to Zhang et al. (9)
1b	20	Rest tremor and serial sevens. Participant starts from 100, subtracts 7, and stops after five answers.
2	10	Hold arms lifted.
3	10	Lift and extend arms according to Zhang et al. (9)
4	20	Hold 1 kg weight in every hand for 10 s. Start with the right hand. Then, have the participant's arm rested again as in 1a.
5	20	Finger pointing. Participant should point with his index fingers repetitively to examiner's lifted hand for 10 s. Start with participant's right index, then left.
6	20	Drink from glass. Have the participant grasp an empty glass with his right hand as if he/she would drink from it. Then repeat with his/her left hand.
7	10	Cross and extend both arms.
8	10	Bring both index fingers to each other, repeat until time expires.
9	20	Let participant's both index fingers tap his/her nose. Repetitively with the right (10 s), then with left index (10 s).
10	20	Entrainment. While holding the arms extended, have the participant stamp with his/her right foot according to the stamp frequency of the examiner. Then have him/her repeat with the left foot.

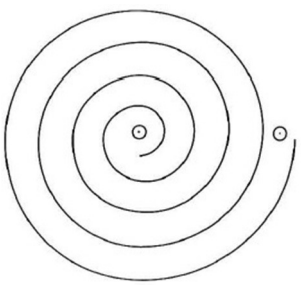


FIGURE 2 | Archimedean spiral to be drawn with a pressure-sensing stylus on a 10.5 inch screen on an Apple iPad Touch, starting from the point in the middle.

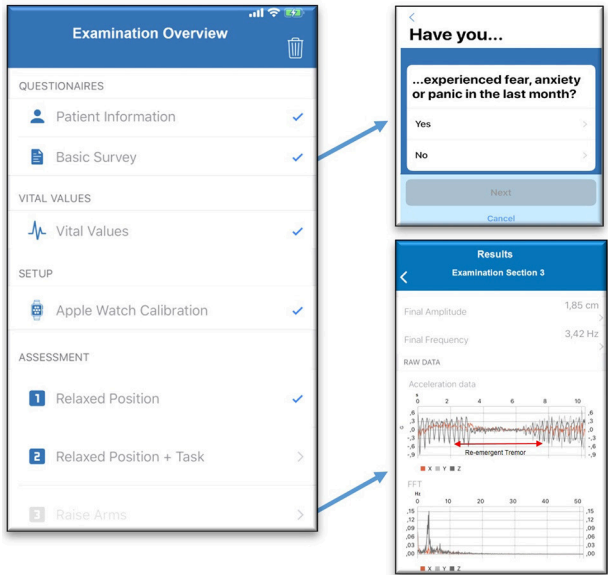


FIGURE 3 | Overview screen **(left)**: the full examination takes approximately 20-min and starts with questionnaires and heart frequency measurement by the smartwatch. Before hand-tremor assessment starts, smart-watch calibration is required. Questionnaire screen **(upper right)**: showing one item of the PD-NMS instrument. Initial signal processing on the smartphone **(bottom right)**: visualization of average amplitude and frequency, raw acceleration data during examination section 3 and frequency spectrum. The acceleration data illustrates a simulated case of re-emergent tremor on the time axis. FFT, Fast Fourier Transform. Data capture and analyses of tablet-based spiral drawing is not implemented yet.

none of them) and identify data patterns that could represent new biomarkers. The model will be trained applying Google Tensor Flow-based Network architectures using Convolutional neural networks (CNN) as they have shown highly promising pattern recognition results in medical images (11). In addition, long short-term memories (LSTM) networks will enable time-series analysis to account for temporal dynamics within the protocol-based examination and tablet-based spiral drawing. Both core methods (CNN + LSTM) will continuously be evaluated separately and in combination (e.g., using LSTM on top of CNN-extracted features). Sensitivity, positive predictive value/precision and accuracy will be calculated based on existent diagnosis labels using nested cross-validation. Statistical significance of classification results will be calculated by permutation tests. Univariate and Multivariate Analyses will be performed based on standard statistical regression analyses (e.g., logistic regression). This is necessary, first, to continuously and critically compare performance of Deep Learning black boxes with classical statistical approaches and second, to get a deeper understanding of the inter-related input features and their predictive power to classification results.

A concrete formulation of hypotheses is limited since we did not find any similar systems that were evaluated in studies from which we can derive a reliable patient sample size calculation based on statistical power analyses. Therefore, following key performance indicators (KPI) are aimed at the end of the study period based on classification performances in other disease domains (11, 20):

- **KPI 1:** >80% of all recruited participant cases will provide complete data as described in data capture **Table S1** in the pseudonymized research database.
- **KPI 2:** >90% accuracy, >90% sensitivity, >90% positive predictive value for classifying ET and PD by the tested model using nested cross validation.

All data items from smartwatch-based data and questionnaires that are relevant for data analysis are specified in the standardized Operational Data Model by the clinical data interchange standards consortium and will be available on the MDM-Portal.

Limitations

A proper sample size calculation was not performed, since it cannot be inferred how many samples the model will require to approach the targeted key performance indicators as—to our knowledge—there was no similar model trained and tested within this domain. However, there are basic assumptions of machine learning principles, stating that the size of training samples should be a multiple of the number input variables and output classes of the model to perform reasonably well (21). The smart-watch-based examination is the most data-consuming procedure capturing acceleration (A) and rotation (R) in 3 axes in 10 different examination sections at 2 different hands. This results in approximately 2 (A+R)* 3 * 10 * 2 = 120 input variables. Three output classes are modeled (PD, ET, control: none of them or healthy). Ideally, we require a multiple of 120 * 3 training samples. Based on the EMR report, we can expect at least 500 patients with PD or ET at our local site, if every second will provide consent. Additionally, most of the patients will attend the ambulance with their spouses or partners, who will also be asked to participate as controls. We are convinced that the required recruitment number is approachable within the study phase, since the data capture is non-obtrusive without any interventional character.

In the case of reaching the targeted key performance indicators, they should still be taken with caution. The predictive capability will never be 100% flawless. This is even more likely to be the case if the system is tested in different environments with different examiners. The study will acquire at least two different regular examiners to train robustness for inter-examiner differences. We believe that this work has established a straight forward and fully-documented examination framework, that can be reproduced in other environments. After study completion, the resulting model, implementation code and execution description will be published as open source and supplied with anonymized training data samples.

INTERPRETATION OF ANTICIPATED RESULTS

Results

Each of the three technology-driven data capture settings is expected to show high potential to classify tremor-related diseases. Synchronization of these multimodal data and integrative pattern recognition analyses are expected to provide deeper insights into tremor characteristics. All of the technical devices used within this study have recently evolved to affordable mass products. Coupled with highly customizable apps, some of these devices already received FDA approval as for instance the Kardiaband app by AliveCor, the first FDA-cleared smartwatch-based ECG reader (22). This demonstrates the qualified use of such smart wearables not only for fitness or wellness purposes but also for valid medical use. A further advantage of the SDS system—compared to commercial and proprietary systems as the KinetiGraph™ system—is that all of its devices can be programmed and adapted by any Apple-based App developer through well-established Software Development kits and therefore preventing vendor lock-in. Once our system has reached the required level of accuracy, sensitivity and precision, regulatory steps will be taken for medical device approval and rollout to further sites. As a consequence, the system will not replace but could decisively extend diagnostic processes, which are currently suffering from high misdiagnoses rates in this domain (2, 3).

Future Work

Deep brain stimulation (DBS) is an effective surgical treatment option and shows significant benefit for tremor and quality of life in patients with PD, ET, and other tremor etiologies (23–26). Intraoperative neurophysiological and clinical testing is important for optimal targeting of the DBS leads. Currently, evaluation of effects and symptoms is performed by an experienced neurologist and might be influenced by individual perception. Methods that enable an objective evaluation of the neurological status might help improving positioning of the DBS leads aiming at more accurate positioning and better results. A major challenge is to obtain medical clearance for the aforementioned devices or to establish sensors which comply with high regulatory requirements for intraoperative usage. In addition, the devices might help detecting minor changes in tremor pre- and post-operatively during the course of the disease and facilitate adjustment of DBS systems.

Extending the hospital-based setting, continuous and longitudinal measurement of movement and patient questionnaire-based input will be captured to provide patient home-based data for detailed monitoring of individual disease courses. This feature will be implemented after this study, because new phenotypical key characteristics from the IMF funded phase will first need to be identified and then captured with highest priority in the home-based setting. Moreover, the timely relations between medication intake and tremor effects will elucidate therapeutic effects in a long-term setting.

Further characteristics from Neuroimaging data are going to be identified and integrated to the research database. To elaborate on a larger patient sample size and ongoing genetic testing approaches of PD and ET, the need of a multi-center study and biobanks for genome-wide association analyses will be discussed.

ETHICS STATEMENT

The ethical board of the University of Münster and the physician's chamber of Westphalia-Lippe approved the study protocol (Reference number: 2018-328-f-S).

AUTHOR CONTRIBUTIONS

JV has written the study design, acquired the funding, supervised the implementation of the system and written the manuscript. SN has implemented the system. IS-R has made significant contributions to the study design, acquisition of funding the project. SS-M and NW provided

significant input to the study design and neurosurgical applications. TW has provided significant input to the study design, system requirements and the neurologic examination. MD has supervised and guided the project. All authors have received, critically revised and approved the manuscript.

FUNDING

The study is funded by Innovative Medizinische Forschung of the University of Münster, Germany (Grant ID: VA111809).

ACKNOWLEDGMENTS

This is a short text to acknowledge the contributions of specific colleagues, institutions, or agencies that aided the efforts of the authors.

SUPPLEMENTARY MATERIAL

The Supplementary Material for this article can be found online at: https://www.frontiersin.org/articles/10.3389/fneur.2019.00048/full#supplementary-material

REFERENCES

1. Louis ED, Ottman R, Hauser WA. How common is the most common adult movement disorder? Estimates of the prevalence of essential tremor throughout the world. *Mov Disord*. (1998) 13:5–10. doi: 10.1002/mds.870130105
2. Newman EJ, Breen K, Patterson J, Hadley DM, Grosset KA, Grosset DG. Accuracy of Parkinson's disease diagnosis in 610 general practice patients in the West of Scotland. *Mov Disord*. (2009) 24:2379–85. doi: 10.1002/mds.22829
3. Jain S, Lo SE, Louis ED. Common misdiagnosis of a common neurological disorder: how are we misdiagnosing essential tremor? *Arch Neurol*. (2006) 63:1100–4. doi: 10.1001/archneur.63.8.1100
4. Heldman DA, Espay AJ, LeWitt PA, Giuffrida JP. Clinician versus machine: reliability and responsiveness of motor endpoints in Parkinson's disease. *Parkinsonism Relat Disord*. (2014) 20:590–5. doi: 10.1016/j.parkreldis.2014.02.022
5. Papapetropoulos S, Mitsi G, Espay AJ. Digital health revolution: is it time for affordable remote monitoring for Parkinson's disease? *Front Neurol*. (2015) 6:34. doi: 10.3389/fneur.2015.00034
6. Silva de Lima AL, Hahn T, Evers LJW, Vries NM de, Cohen E, Afek M, et al. Feasibility of large-scale deployment of multiple wearable sensors in Parkinson's disease. *PLoS ONE* (2017) 12:e0189161. doi: 10.1371/journal.pone.0189161
7. Espay AJ, Bonato P, Nahab FB, Maetzler W, Dean JM, Klucken J, et al. Technology in Parkinson's disease: challenges and opportunities. *Mov Disord*. (2016) 31:1272–82. doi: 10.1002/mds.26642
8. Zham P, Arjunan S, Raghav S, Kumar DK. Efficacy of guided spiral drawing in the classification of Parkinson's disease. *IEEE J Biomed Health Inform*. (2017) 22:1648–52. doi: 10.1109/JBHI.2017.2762008
9. Zhang B, Huang F, Liu J, Zhang D. A novel posture for better differentiation between Parkinson's tremor and essential tremor. *Front Neurosci*. (2018) 12:317. doi: 10.3389/fnins.2018.00317
10. LeCun Y, Bengio Y, Hinton G. Deep learning. *Nature* (2015) 521:436–44. doi: 10.1038/nature14539
11. Esteva A, Kuprel B, Novoa RA, Ko J, Swetter SM, Blau HM, et al. Dermatologist-level classification of skin cancer with deep neural networks. *Nature* (2017) 542:115–8. doi: 10.1038/nature21056
12. Dugas M, Neuhaus P, Meidt A, Doods J, Storck M, Bruland P, et al. Portal of medical data models: Information infrastructure for medical research and healthcare. *Database (Oxford)* (2016) 2016:bav121. doi: 10.1093/database/bav121
13. Deuschl G, Bhatia KP, Elble R, Hallett M. Understanding the new tremor classification. *Mov Disord*. (2018) 33:1267–8. doi: 10.1002/mds.27368
14. Gövert F, Becktepe J, Deuschl G. Die neue Tremorklassifikation der International Parkinson and Movement Disorder Society. *Der Nervenarzt* (2018) 89:376–85. doi: 10.1007/s00115-018-0489-1
15. Hopfner F, Deuschl G. Is essential tremor a single entity? *Eur J Neurol*. (2018) 25:71–82. doi: 10.1111/ene.13454
16. Papengut F, Raethjen J, Binder A, Deuschl G. Rest tremor suppression may separate essential from parkinsonian rest tremor. *Parkinsonism Relat Disord*. (2013) 19:693–7. doi: 10.1016/j.parkreldis.2013.03.013
17. Alty JE, Kempster PA. A practical guide to the differential diagnosis of tremor. *Postgrad Med J*. (2011) 87:623–9. doi: 10.1136/pgmj.2009.089623
18. Bötzel K, Tronnier V, Gasser T. The differential diagnosis and treatment of tremor. *Dtsch Arztebl Int*. (2014) 111:225–35; quiz 236. doi: 10.3238/arztebl.2014.0225
19. Varghese J. *Examination Video and Supplement for Smartwatch-Based Data Capturing*. (2018). Available online at: https://uni-muenster.sciebo.de/s/gLxVcl7mF5mfb4W (Accessed October 5, 2018).
20. Bangor A, Kortum PT, Miller JT. An empirical evaluation of the system usability scale. *Int J Hum Comput Interact*. (2008) 24:574–94. doi: 10.1080/10447310802205776
21. Natarajan P, Frenzel JC, Smaltz DH. *Demystifying Big Data and Machine Learning for Healthcare*. Taylor & Francis (2017). Available online at: https://books.google.de/books?id=omxdDgAAQBAJ
22. Food and Drug Administration. *November 2017 510(k) Clearances, Including Kardia Band System*. (2017). Available online at: https://www.fda.gov/medicaldevices/productsandmedicalprocedures/deviceapprovalsandclearances/510kclearances/ucm587897.htm (Accessed August 29, 2018).
23. Paschen S, Deuschl G. Patient evaluation and selection for movement disorders surgery: the changing spectrum of indications. *Prog Neurol Surg*. (2018) 33:80–93. doi: 10.1159/000480910
24. Deuschl G, Paschen S, Witt K. Clinical outcome of deep brain stimulation for Parkinson's disease. *Handb Clin Neurol*. (2013) 116:107–28. doi: 10.1016/B978-0-444-53497-2.00010-3
25. Fasano A, Romito LM, Daniele A, Piano C, Zinno M, Bentivoglio AR, et al. Motor and cognitive outcome in patients with Parkinson's disease 8 years after subthalamic implants. *Brain* (2010) 133:2664–76. doi: 10.1093/brain/awq221
26. Deuschl G, Raethjen J, Hellriegel H, Elble R. Treatment of patients with essential tremor. *Lancet Neurol*. (2011) 10:148–61. doi: 10.1016/S1474-4422(10)70322-7

Conflict of Interest Statement: The authors declare that the research was conducted in the absence of any commercial or financial relationships that could be construed as a potential conflict of interest.

Copyright © 2019 Varghese, Niewöhner, Soto-Rey, Schipmann-Miletić, Warneke, Warnecke and Dugas. This is an open-access article distributed under the terms of the Creative Commons Attribution License (CC BY). The use, distribution or reproduction in other forums is permitted, provided the original author(s) and the copyright owner(s) are credited and that the original publication in this journal is cited, in accordance with accepted academic practice. No use, distribution or reproduction is permitted which does not comply with these terms.

frontiers in Neurology

REVIEW
published: 11 February 2019
doi: 10.3389/fneur.2019.00084

Potential of Sodium MRI as a Biomarker for Neurodegeneration and Neuroinflammation in Multiple Sclerosis

Konstantin Huhn[1], Tobias Engelhorn[2], Ralf A. Linker[3] and Armin M. Nagel[4,5]*

[1] Department of Neurology, Friedrich-Alexander-University of Erlangen-Nuremberg, Erlangen, Germany, [2] Department of Neuroradiology, Friedrich-Alexander-University of Erlangen-Nuremberg, Erlangen, Germany, [3] Department of Neurology, University of Regensburg, Regensburg, Germany, [4] Department of Radiology, Friedrich-Alexander-University of Erlangen-Nuremberg, Erlangen, Germany, [5] Division of Medical Physics in Radiology, German Cancer Research Center (DKFZ), Heidelberg, Germany

OPEN ACCESS

Edited by:
Tobias Ruck,
University of Münster, Germany

Reviewed by:
Aiden Haghikia,
University Hospitals of the Ruhr-University of Bochum, Germany
Julia Krämer,
University of Münster, Germany
Wafaa Zaaraoui,
UMR7339 Centre de Résonance Magnétique Biologique et Médicale (CRMBM), France

***Correspondence:**
Konstantin Huhn
konstantin.huhn@uk-erlangen.de

Specialty section:
This article was submitted to Multiple Sclerosis and Neuroimmunology, a section of the journal Frontiers in Neurology

Received: *04 October 2018*
Accepted: *22 January 2019*
Published: *11 February 2019*

Citation:
Huhn K, Engelhorn T, Linker RA and Nagel AM (2019) Potential of Sodium MRI as a Biomarker for Neurodegeneration and Neuroinflammation in Multiple Sclerosis. Front. Neurol. 10:84. doi: 10.3389/fneur.2019.00084

In multiple sclerosis (MS), experimental and *ex vivo* studies indicate that pathologic intra- and extracellular sodium accumulation may play a pivotal role in inflammatory as well as neurodegenerative processes. Yet, *in vivo* assessment of sodium in the microenvironment is hard to achieve. Here, sodium magnetic resonance imaging (^{23}NaMRI) with its non-invasive properties offers a unique opportunity to further elucidate the effects of sodium disequilibrium in MS pathology *in vivo* in addition to regular proton based MRI. However, unfavorable physical properties and low *in vivo* concentrations of sodium ions resulting in low signal-to-noise-ratio (SNR) as well as low spatial resolution resulting in partial volume effects limited the application of ^{23}NaMRI. With the recent advent of high-field MRI scanners and more sophisticated sodium MRI acquisition techniques enabling better resolution and higher SNR, ^{23}NaMRI revived. These studies revealed pathologic total sodium concentrations in MS brains now even allowing for the (partial) differentiation of intra- and extracellular sodium accumulation. Within this review we (1) demonstrate the physical basis and imaging techniques of ^{23}NaMRI and (2) analyze the present and future clinical application of ^{23}NaMRI focusing on the field of MS thus highlighting its potential as biomarker for neuroinflammation and -degeneration.

Keywords: multiple sclerosis, magnetic resonance imaging, sodium MRI, ^{23}Na MRI, neurodegeneration, biomarker

SODIUM AND THE PATHOPHYSIOLOGY OF MULTIPLE SCLEROSIS (MS)

As a widely accepted paradigm, the pathology of MS is hallmarked by inflammatory demyelination but also neuro-axonal damage. In fact, neurodegeneration occurs already at the early stages of the disease constituting a primary contributor to sustained or progressive disability in the longer disease course (1, 2). On a cellular level, the maintenance of a transmembrane ion gradient resulting in a negatively charged intracellular and positively charged extracellular space is crucial to enable vital electrochemical signal transduction in humans. This process strongly depends on sodium: the ion gradient is largely created and maintained by the energy consuming Na^+/K^+-ATPase, leading to cellular efflux of 3 Na^+ ions and influx of 2 K^+ ions. Independent of its origin,

loss of ATPase function leads to breakdown of the resting transmembrane potential difference, intracellular sodium accumulation, deficiency of the ATP generating mitochondrial respiratory chain and finally to expiring signal transduction and cell death as well as increase of the extracellular volume fraction (3, 4).

In MS, chronically demyelinated axons are prone to degeneration and trophic failure as consequence of an increased energy demand. Maladaptive repair and neuro-axonal rearrangements as well as a decreased ATP supply may further contribute to this process. Finally, lack of energy may lead to breakdown of the Na^+/K^+-ATPase as a major energy consumer in the CNS (5). In fact, chronically demyelinated MS lesions display a substantially reduced axonal Na^+/K^+-ATPase expression (6).

Additionally, the pivotal role of pathologic sodium accumulation in MS was previously demonstrated in several *ex vivo* and *in vivo* studies (7). These studies point to a compensatory redistribution or over-expression of distinct voltage-gated Na^+ channels (e. g. Nav1.2, Nav1.6) on demyelinated axons in order to compensate for demyelination. This is an energy demanding process that is hardly sustained in already energy deprived axons. Thus, energy failure and toxic sodium accumulation may initiate a vicious cycle. Consecutively, increased intracellular sodium concentrations may provoke reverse action of the Na^+/Ca^{2+} exchanger and thus calcium accumulation, which leads to activation of neurodegenerative signaling cascades (8–11). Hence, application of therapeutic Na^+ channel blockers like amiloride, lamotrigine, phenytoin, or carbamazepine display some neuroprotective properties in experimental MS models (12–16). However, clinical trials with Na^+ channel blockers in MS are few and report conflicting results on potential neuroprotective properties, yet (17–19).

In addition, the so-called fat- and salt- (NaCl) rich "western-diet" has recently been implicated in the etiology of MS (20, 21). In this context, sodium reappeared in the center of (experimental) MS studies as a mediator of pro-inflammatory effects (21, 22). In cell culture, an excess of NaCl up to 40 mM led to enhanced pro-inflammatory Th17 cell differentiation. In experimental autoimmune encephalomyelitis (EAE), an animal model for MS, a high salt diet was associated with increased disease severity mediated by enhanced levels of pro-inflammatory Th17 cells (23). However, transfer from experimental to clinical studies has been difficult and results of clinical studies on the influence of sodium to MS are conflicting: In a first study, high salt intake was partly associated with disease activity (24). Yet, a retrospective analysis of a large interferon-beta treated cohort with clinically isolated syndrome (BENEFIT study) showed no relevant association of further disease activity with blood or urine sodium levels (25). Similarly, a study investigating MS with early onset failed to demonstrate an association of relapse activity and the amount of dietary salt intake (26). However, the retrospective nature of sodium exposure analysis and the lack of standardized sodium load quantification limit the definite validity of these studies.

In consequence of these conflicting study results and with the advance of sodium magnetic resonance imaging (^{23}NaMRI) techniques, sodium MRI drew growing interest for the analysis of pathologic sodium accumulation and its consequences in MS. However, the history of sodium MRI application in the field of MS is short, only comprising about a decade to date. In addition to regular proton based MRI, ^{23}NaMRI with its ability to measure brain sodium *in vivo* along with additional advantages of modern imaging techniques may constitute a promising biomarker for the influence of sodium on neurodegeneration and -inflammation in MS and vice versa. In our review, we aim at (1) demonstrating the physical basis and imaging techniques of sodium MRI and at (2) analyzing previous and future clinical applications of sodium MRI in the field of MS.

PHYSICAL BASICS AND IMAGING TECHNIQUES OF SODIUM MRI

Conventional MRI is based on the signal of protons (hydrogen, H^+). Protons exhibit the best properties for *in vivo* MRI due to their large gyromagnetic ratio and their high abundance in human tissues, predominantly contained in water or fat (27, 28). Besides protons, MR imaging of other so called "X-nuclei" is feasible in principle if they inhere a non-zero nuclear magnetic spin moment, which requires an odd number of protons or neutrons (29). Almost all elements of the periodic table have at least one isotope that fulfills this requirement (30). However, the most limiting issue for X-nuclei MRI is the signal-to-noise ratio (SNR), which is proportional to the *in vivo* concentration, the physical MR sensitivity of the nucleus and the voxel volume. For most isotopes either the physical MR sensitivity or the *in vivo* concentration is too low to achieve sufficient SNR and reasonable

Abbreviations: ADEM, acute disseminated encephalomyelitis; AnaWeTV, anatomically weighted second-order total variation; ATP, adenosine triphosphate; ATPase, adenosine triphosphatase; Ca^{2+}, calcium; CAG, trinucleotide of cytosine, adenine, guanine; cho, choline; ^{35}Cl, chlorine; CNS, central nervous system; CSF, cerebrospinal fluid; CVF, cell volume fraction; DA-3DPR, density-adapted 3D projection reconstruction; DTI, diffusion tensor imaging; EAE, experimental autoimmune encephalomyelitis; EDSS, expanded disability status scale; ESC, extracellular sodium concentration; ^{19}F, fluorine; FLAIR, fluid-attenuated inversion recovery; Glx, glutamate/glutamine; GM, gray matter; H^+, Proton hydrogen; H-EPSI, proton echo planar spectroscopic imaging; IR, inversion recovery; ISC, intracellular sodium concentration; ISVF, intracellular sodium volume fraction; ^{39}K, potassium; K^+, potassium; l, liter; m-Ins, myo-inositol; mM, millimolar; mm, millimeter; MQF, multiple quantum filtering; MRI, magnetic resonance imaging; MRS, magnetic resonance spectroscopy; MS, multiple sclerosis; ms, millisecond; MSFC, multiple sclerosis functional composite; MTR, magnetization transfer ratio; MWI, myelin water imaging; n, number; ^{23}Na, sodium; Na^+, sodium; NAA, N-acetyl aspartate; NaCl, sodium chloride, salt; NAGM, normal-appearing gray matter; Nav, voltage gated sodium channel; NAWM, normal-appearing white matter; NMO-SD, neuromyelitis optica spectrum diseases; ^{17}O, oxygen; OCT, optical coherence tomography; ^{31}P, phosphorous; PET, positron emission tomography; PPMS, primary progressive multiple sclerosis; *r*, correlation coefficient; RF, radiofrequency; ROI, region of interest; RRMS, relapsing remitting multiple sclerosis; SDWA, sampling density weighted apodization; SNR, signal-to-noise ratio; SPMS, secondary progressive multiple sclerosis; SQF, single quantum filtering; T, Tesla; T1, T1-weighted MRI sequence; T2, T2-weighted MRI sequence; tCr, total creatine; Th, T-helper cell; TSC, tissue sodium concentration; TPI, twisted projection imaging; TQF, triple quantum filtering; UTE, ultra-short echo time; WM, white matter.

voxel volumes. Thus, only a few X-nuclei, such as oxygen (^{17}O) (31), fluorine (^{19}F) (32), phosphorous (^{31}P) (33), chlorine (^{35}Cl) (34), potassium (^{39}K) (35, 36) and especially sodium (^{23}Na) (37–39) have been used for MR imaging so far.

Among these, Na^+ exhibits the best properties for *in vivo* MRI (40, 41).

Yet, ^{23}NaMRI is challenged by low tissue sodium concentrations and an approximately 4-fold lower gyromagnetic ratio of sodium as compared to protons. For brain white matter, these shortcomings result in a roughly 5.500 times lower *in vivo* SNR of ^{23}NaMRI vs. ^{1}HMRI, if the similar acquisition times and voxel sizes would be used (41). Furthermore, Na^+ highly interacts with surrounding macromolecules resulting in short biexponential T2 times (fast: 0.5–8 ms; slow: 15–40 ms; T1 time: 30–40 ms) (4, 42–45). To achieve sufficient SNR, only images with low spatial resolution can be acquired, which results in partial volume effects. In addition, longer acquisition times can be used to increase SNR. These effects limit the application of ^{23}NaMRI. Additionally, distinction of different sodium compartments, i.e., intra-/extracellular, is difficult (29, 46–48).

Hence, dedicated acquisition techniques and elaborated post-processing may help to improve ^{23}NaMRI imaging technologies. Above all, application of ultra-short echo-time (UTE) sequences is the common basis of quantitative sodium MRI (29, 49).

Additionally, ^{23}NaMRI requires dedicated hardware, such as an appropriate radiofrequency (RF) amplifier and RF coils. Yet, both hardware components are not standard on routine clinical MRI scanners (50). Optimized scanner hardware may further improve the detection of the weak ^{23}NaMRI signal. In detail, special dual-tuned ^{23}Na/^{1}H head array coils with up to 32 multi-channel receive arrays enable a synchronized registration of proton and sodium images with sufficient SNR (51–53).

As reviewed elsewhere, specialized ^{23}NaMRI acquisition techniques, image reconstruction and post-processing techniques further improve SNR and spatial resolution. At the same time they reduce partial volume effects as well as acquisition time. Such techniques comprise compressed sensing with iterative reconstruction, sampling density weighted apodization (SDWA), twisted projection imaging (TPI), density-adapted 3D projection reconstruction (DA-3DPR), multi-echo radial sequences or different trajectories, i.e., 3D cones (29, 54–62).

In principle, sodium MR imaging is feasible at any magnetic field strength. However, due to the physical properties of Na^+, application of at least 3 Tesla (T) field strength is warranted for a sufficient SNR and resolution. Modern 7 or 9.4 T ultra-high field MRI scanners further reduce the limitation of low signal strength, resulting in higher SNR (**Figure 1**) or improved spatial resolution (63). Nowadays, modern techniques enable sodium MRI of human brain at nominal spatial resolutions of $1 \times 1 \times 5$ mm^3 to $4 \times 4 \times 4$ mm^3 within 10–35 min acquisition time (48, 57, 64–67). Along with the development and advantages of high-field MRI scanners, research in the field of ^{23}NaMRI has been prospering within the last decade without signs of any harm to study participants (51, 66, 68, 69). Comparing ^{23}NaMRI signal intensities of brain tissue regions of interest (ROI) to control tubes containing predefined liquid saline solutions (i.e., 0–150 mM) placed beside the patient's head enables quantification of sodium concentrations (66).

MRI total tissue sodium concentrations (TSC) are the volume-weighted average of respective intracellular (normal: 10–15 mmol/l) and extracellular (normal: 140–150 mmol/l) sodium compartments. Typical intracellular volume fractions are on the order of 80% and extracellular volume fractions are around 20% (70). This leads to a TSC of ∼40 mmol/l, which is close to results of studies directly analyzing the sodium concentration in brain white matter (3, 4, 47, 48, 71).

While classic ^{23}NaMRI sequences only allow for quantification of TSC, differentiation between sodium accumulation in extracellular and intracellular compartments is even more interesting. Yet, the single resonance spectrum of sodium ions limits such discrimination. Use of paramagnetic shift reagents, which cannot pass cell membranes like anionic complexes of dysprosium or thulium, principally enables discrimination of intra- and extracellular sodium. Thus, MRI may detect shift of resonance lines exclusively in the extracellular space. However, clinical application of these compounds is not readily feasible for CNS studies due to their inability to cross the blood brain barrier and possible toxic effects (29, 72–74).

Instead, the application of relaxation-weighted imaging may be better suited for human studies. Preclinical studies showed that intracellular sodium exhibits shorter relaxation times (75). Thus, inversion recovery imaging (IR) can be utilized to suppress signals originating from sodium with a distinct T1 relaxation time. This may enable a weighting of the signal toward the intracellular compartment (29). At the same time, suppression of the CSF sodium signal also reduces disturbing partial volume effects when analyzing brain regions close to the CSF (71, 76–78). Sodium MRI IR sequences with a specific suppression of Na^+ signals are comparable to the established fluid-attenuated-inversion-recovery (FLAIR) sequence of proton based MRI.

Sodium MRI IR sequences may be also the basis for the calculation of (pseudo) intracellular sodium concentrations and extracellular volume fractions (79). If additional anatomical masks from proton MRI are used, these techniques may even discriminate between intracellular sodium of white and gray matter (4). However, IR techniques only enable indirect calculation of compartmental sodium concentrations and are susceptible for confounders. In detail, the required intra- and extracellular relaxation times need to be estimated from preclinical studies and cannot be measured directly in humans, which might introduce a potential bias. In addition, relaxation times in pathologic structures are unknown and altered relaxation times may affect quantification. In consequence, some authors prefer the terms "pseudo-"intracellular sodium and "pseudo-"extracellular sodium for such analyses (79).

Alternatively, the use of two or more excitation pulses along with multiple quantum filtering (MQF; usually triple quantum filters = TQF) may also facilitate sodium compartment differentiation (80–82). In principle, the T2 relaxation based MQF allows for separation of different signals from sodium ions due to their variably restricted mobility within different compartments (81–86). However, MQF are

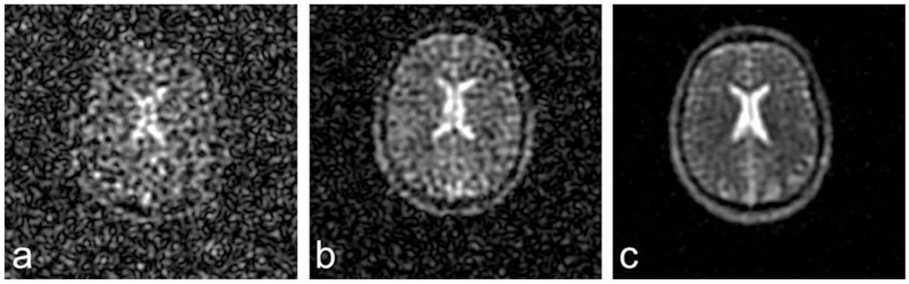


FIGURE 1 | ^{23}NaMRI at 1.5 **(A)**, 3 **(B)**, and 7 T **(C)**. Similar acquisition parameters and a nominal spatial resolution of $(4\,mm)^3$ were applied. SNR increases approximately linearly with magnetic field strengths. Figure reproduced from (63) with permission of John Wiley and Sons, Journal of Magnetic Resonance Imaging.

prone to artifacts caused by field-inhomogeneity, low SNR or long acquisition times and its indirect calculation of sodium concentrations, similar to IR techniques (87). Recent quantitative multicompartment-multipulse techniques aim at exploiting differences in T1 and T2 relaxation times of different sodium compartments. This approach may enable separation of intracellular, extracellular and cerebrospinal fluid (CSF) signals, but is still hampered by low SNR (67).

SODIUM MRI IN NEUROLOGICAL DISORDERS OTHER THAN MS

First *in vivo* investigations using sodium MRI already stem from the 1980's: in an experimental model and in human investigations of stroke, Hilal and colleagues detected temporal changes of sodium levels over time. These studies already indicated the potential of sodium MRI as a biomarker for brain disorders (37, 46). However, technical restrictions limited brain sodium imaging to the investigation of widespread cerebral lesions or CSF (see above).

Yet, with the rapid development in scanner hardware and MRI software, several consecutive sodium MRI studies for stroke were conducted confirming highly elevated TSC in acute stroke due to estimated Na^+/K^+ ATPase breakdown, consecutive sodium accumulation, hypoxic cell death and perifocal edema (88). Furthermore, sodium MRI may represent a biomarker of viable, but hypoxic tissue-at-risk ("penumbra") in stroke (88–90).

In primary brain tumors like low- and high-grade glioma, exaggerated proliferation rates lead to cellular membrane depolarization preceding cell division. Here, ^{23}NaMRI may additionally be useful as a predictive biomarker for the discrimination of therapy responsive tissue (45, 77, 91–95).

Sodium MRI analysis of neurodegenerative diseases revealed whole-brain TSC increase in Huntington's disease independently of structural changes depicted by proton MRI. The caudate nucleus exhibited the highest TSC which correlated with gray matter atrophy and CAG repeat length (96). In addition, a small study in Alzheimer's disease ($n = 5$) reported a 7.5% brain TSC increase with an inverse correlation to hippocampal volume (97). Similarly, 9.4T sodium MRI of subjects with structural brain damage revealed loss of "cell volume fraction" (CVF) indicating a reduced CNS cell density. In contrast, individuals with a constant CVF may represent aging patients without disease. Hence, sodium MRI may evolve as a predictive biomarker for neurodegenerative diseases which are often hallmarked by early regional neuronal loss before the onset of clinical symptoms (98).

SODIUM MRI IN MULTIPLE SCLEROSIS (MS)

Sodium MRI Alterations in Cerebral Lesions, NAWM, and NAGM in MS

In 2010, Inglese and colleagues published the first study applying ^{23}NaMRI in 17 relapsing-remitting MS (RRMS) patients and 13 healthy controls, using a 3D radial gradient-echo UTE sequence at 3T (64). In MS, lesional (**Figure 2**) and gray-matter (GM) TSC was increased as compared to normal appearing white matter (NAWM). Further studies confirmed these findings (65, 99–101). As compared to healthy controls, the NAWM of MS patients exhibited an elevated TSC (mean 19.4 vs. 26.9 mM). This increase was particularly predominant in the cerebellum and splenium, yet without statistical significance. The normal-appearing gray matter (NAGM) displayed even higher sodium levels, but without any regional predominance (64). In this study, MS lesion analysis was restricted to plaques with a diameter >5 mm due to potential partial volume effects. The mean lesion sodium concentration was 35.3 mM, clearly higher than TSC of NAWM.

Gadolinium-enhancing acute MS lesions showed the highest TSC. This finding may be the direct consequence of inflammatory processes in the cell (e.g., mitochondrial failure, ATP deprivation, sodium accumulation) and the extracellular space (e.g., tissue damage, edema, enlarged extracellular space, infiltrating immune cells). However, analyses only comprised a low number of acute MS lesions and did not discriminate between intra- and extracellular sodium compartments. Therefore, it was not possible to determine the exact source of lesional sodium accumulation.

A study of Eisele et al. further analyzed neuroinflammatory aspects and studied the evolution of lesional sodium accumulation by ^{23}Na MRI with a 3D radial sequence and SDWA at 3T. The authors analyzed acute and chronic lesions

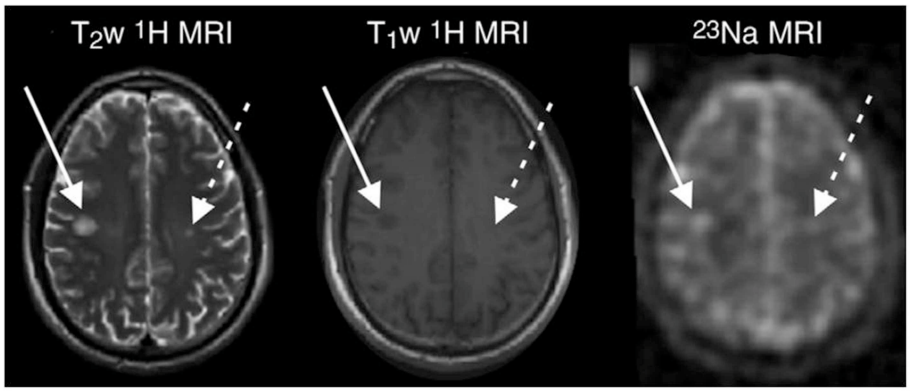


FIGURE 2 | MR images in a 33-years-old man with early RRMS. Examples of substantial sodium accumulation in two macroscopic T2 lesions with two different signal intensity patterns at T1-weighted imaging: one lesion was hypointense (solid arrows) and one was isointense (dashed arrows) to normal-appearing white matter on T1-weighted image. Figure reproduced from (99) with permission of the Radiological Society of North America (RSNA).

in 65 relapsing MS patients as compared to 10 controls (102). Mean TSC was quantified in all MS lesions with a diameter of >5 mm and in the NAWM as well as GM. First, TSC in NAWM and GM were higher in MS patients than in controls. Second, all types of MS lesions displayed a TSC increase. The most pronounced accumulation was seen in contrast-enhancing T1 lesions > T1 hypointense lesions > T1 isointense lesions. Interestingly, non-enhancing, hyperacute lesions with restricted diffusion on proton based diffusion-weighted MRI sequences showed a TSC comparable to the NAWM. Thus, TSC may not only serve as a biomarker for chronic tissue pathology and neurodegeneration, but also allow the detection and monitoring of inflammatory processes. Thus, this study further supported the use of TSC measured by sodium MRI as a potential biomarker for neuroinflammation. ^{23}Na MRI may enable visualization of blood-brain barrier disruption without need for application of contrast-enhancing agents.

Another study used ^{23}NaMRI in a case report on a large open-ring enhancing MS lesion. The authors reported intralesional sodium heterogeneity with declining TSC from the center of the active plaque (TSC: 50 mmol/l) across the enhanced periphery (33 mmol/l) toward the NAWM (26 mmol/l) (103). This gradual and centripetal TSC increase may result from the underlying degree of inflammation and mitochondrial dysfunction within acute MS lesions. Therefore, ^{23}NaMRI may constitute a future biomarker for the extent of neuroinflammation. It may even point to inflammatory "tissue at risk" before persistent neuro-axonal damage occurs.

Our group additionally studied ^{23}NaMRI in a case with an acute, enhancing tumefactive MS lesion over a follow-up of 5 weeks. Sodium accumulation outlasted contrast enhancement after steroid treatment as a potential sign of prolonged metabolic dysfunction and delayed recovery. At the same time, TSC in NAWM remained unaffected by steroid therapy (104).

However, comprehensive longitudinal studies reporting temporal evolution of sodium accumulation in acute MS lesions are still lacking. Upon repeated sodium MRI investigations in five healthy controls, WM and GM areas revealed a coefficient of variation for TSC < 5% and an intra-class correlation coefficient of > 0.9. These data indicate sufficient reproducibility of ^{23}NaMRI as a basis for future longitudinal studies (64).

Zaaroui and colleagues used a DA-3DPR sequence for sodium MRI at 3T to analyze 26 RRMS patients. They compared patients with a disease duration <5 vs. >5 years to healthy controls (99). The authors investigated TSC in three different compartments: GM, NAWM, and T2 lesions. In T2 lesions of all MS patients, TSC was higher than in WM of controls. In contrast, only the RRMS cohort with advanced disease duration exhibited a significantly increased TSC of GM and NAWM. Both MS groups displayed a similar TSC in T2 lesions and NAWM. Yet, GM TSC was higher in the advanced duration RRMS cohort. Nevertheless, this study was able to detect brain sodium accumulation even at the early stages of RRMS. When analyzing for anatomic distribution of TSC, the same study found widespread brain regions with elevated TSC in both MS cohorts. In advanced RRMS, TSC increase was scattered in the splenial, thalamic, cingular, parietal, frontal, and prefrontal cortices. A recent 7T study further complemented these findings of a widespread distribution of increased TSC in various MS GM and WM regions (101).

Sodium MRI and MS Disease Course

Paling and colleagues conducted an investigation of 70 MS patients comprising three MS clinical subtypes (27 RRMS, 23 SPMS, 20 PPMS patients, and 27 controls). They applied a ramp sampled radial UTE sequence at 3 T with additional partial volume correction (65).

The authors analyzed TSC in cortical and deep GM, NAWM and in MS lesions, differentiated in T1 hypo- or isointense lesions. Independent of the disease course, MS patients exhibited an increased TSC of GM and NAWM as compared to controls. Additionally, deep GM and NAWM TSC were higher in the progressive MS subtypes. SPMS patients showed pronounced TSC in GM and NAWM as compared to RRMS. Further testing between MS subgroups was not significant. However, TSC of T1 hypointense lesions was higher in progressive MS subtypes than

in RRMS. In conclusion, the study revealed increased sodium accumulation within MS lesions, NAWM and GM in all clinical MS courses. TSC accumulation was pronounced in SPMS and in patients with increased disability. This finding may serve as a hint for neuro-axonal damage, thus emphasizing the potential of ^{23}NaMRI to provide a biomarker for neurodegeneration.

An investigation of Maarouf and colleagues included 20 progressive MS patients (11 PPMS, 9 SPMS) and 15 controls. The authors applied a DA-3DPR sequence at 3 T analyzing TSC of GM, NAWM and T2 lesions (100). They also found that TSC of T2 lesions and GM were significantly elevated in progressive forms as compared to controls. However, NAWM TSC was not significantly elevated in both progressive forms vs. controls. Independent of the analyzed brain tissue, no differences between PPMS and SPMS were detected. In this study, TSC accumulated to a higher degree in distinct brain areas of SPMS patients than in PPMS: Above all, it involved primary or supplementary locomotor areas consistent with the pronounced disability of patients with a median expanded disability status scale (EDSS) score of 5.5.

Interestingly, early sodium MRI studies and a study performed at 9.4 T did not find relevant age-dependent changes in TSC (64, 65, 98–100). However, a 7 T study described a positive correlation of age with WM and GM TSC as well as with GM intracellular sodium accumulation in healthy controls. In contrast, a negative association of age with intracellular sodium concentration (ISC) but not with extracellular sodium concentration (ESC) or TSC was detected in MS patients. The same study also showed correlations between disease duration, WM TSC and ISC for both, GM and WM as well as between extracellular sodium accumulation in GM and EDSS (101).

Sodium MRI and MS Disability

In the first ever conducted MS sodium MRI study, Inglese and colleagues reported a low correlation of EDSS as a measure of disability with the mean TSC in T1-hypointense lesions ($r = 0.22$) as well as in NAWM and GM ($r = 0.20$). However, they did not find an association between disease duration, age or gender and TSC in lesions, GM or NAWM of RRMS patients (64).

Zaaroui et al. described no correlation of the TSC in T2 lesions or NAWM of RRMS patients with disability as measured by EDSS. However, GM TSC was significantly associated with EDSS as a potential biomarker for the degree of MS disability. In particular, the EDSS showed a positive correlation with the local TSC of the right primary motor area, middle frontal, and bilateral superior gyrus as well as the bilateral cerebellum (99).

In a study including progressive forms of MS, disability was correlated with TSC in deep GM and T1 isointense lesions. In addition, the authors showed independent associations of deep GM TSC with EDSS and features of the clinical assessment tool "Multiple Sclerosis Functional Composite" (MSFC). These data further support sodium MRI as a new method for monitoring disability and neurodegeneration (65).

In contrast, Maarouf et al. reported no significant correlation between TSC in T2 lesions or GM and EDSS or MSFC in their progressive MS study. Solely, the authors found an association between local TSC of the left premotor cortex and EDSS as well as of the left anterior prefrontal cortex and MSFC (100). Further brain regions of the limbic and the frontal areas displayed an increased TSC only in SPMS. Thus, the authors concluded that in PPMS, sodium accumulation was restricted to the motor system. In SPMS, it was more widespread involving regions related to higher cognitive functions.

Sodium MRI and Correlation With Markers of Neurodegeneration

To date, brain atrophy is the "goldstandard" MRI marker. Yet, sodium MRI may provide additional information for imaging clinically relevant neurodegeneration (28, 105). Indeed, in the early 2010 study of Inglese and colleagues, RRMS patients already displayed a significantly lower normalized brain volume and GM volume. They also showed a trend toward lower WM volume as compared to controls.

TSC negatively associated with regional GM volume. However, there was no correlation of TSC with whole brain volume. TSC of NAWM did not correlate with any brain volume. In the respective control cohort, TSC in WM and GM showed an inverse correlation with normalized brain volume. Furthermore, TSC in RRMS associated with total T1 and T2 lesion volume (64).

An additional 3 T study showed an association of TSC in NAWM and GM with T2 lesion load. However, this study did not analyze brain atrophy (99). Application of 7 T ultra-highfield MRI showed no correlation of global and regional TSC, neither of intracellular or extracellular sodium concentrations to measures of brain volumes. In contrast, there was a trend for correlation of extracellular sodium accumulation and GM volume (101).

In 2017, Maarouf and colleagues investigated if brain TSC and GM atrophy were associated with cognitive dysfunction. They analyzed 58 RRMS patients in the early course and 31 controls using DA-3DPR at 3 T (106). The TSC increase in GM and NAWM was associated with cognitive dysfunction and predominantly located in neocortical regions. GM TSC even outmatched GM atrophy as a better predictor of cognitive dysfunction in MS patients. These data further emphasize the potential of sodium MRI for depiction of neurodegeneration, probably even at earlier stages than the "goldstandard" MRI brain atrophy. Hence, sodium MRI may show early neuronal dysfunction even before final neuronal damage occurs. Only the latter can be demonstrated by proton based MRI techniques (106).

To gain complementary information on microstructural pathologies, a recent analysis of 21 RRMS patients and 20 controls applied a DA-3DPR sodium MRI sequence at 3 T in combination with a proton based MR spectroscopy (proton echo planar spectroscopic imaging, 3D ^{1}H-EPSI). Spectroscopy studies included N-acetyl aspartate (NAA; marker for mitochondrial activity), glutamate/glutamine (Glx; marker for neuro-astrocytic metabolism), total creatine (tCr; marker for cellularity), choline (Cho; marker for inflammatory demyelination) and myo-inositol (m-Ins; marker for glial activation) (107). TSC was elevated in all types of brain tissue in MS patients. MR spectroscopy revealed decreased Cho and

Glx in GM, an increase of m-Ins but a decrease of NAA and Glx in NAWM and an increase in m-Ins but decrease in NAA in T2 lesions. In sum, TSC was negatively correlated with NAA as a marker for mitochondrial dysfunction and consecutive neuro-axonal damage. These data are consistent with findings from experimental studies pointing to mitochondrial damage as a consequence of toxic sodium accumulation (3, 108, 109). However, these studies did not correct for the influence of different sodium compartments.

Sodium MRI and Differentiation of Intra- vs. Extracellular Sodium

In the early MS sodium MRI studies, the distinction of different sodium compartments was not possible, mainly due to limited MRI techniques. However, such a differentiation was regarded as highly relevant for a better understanding of MS pathogenesis. Yet, it remained unclear if elevated TSC was the result of rising extracellular fluid sodium due to edema, neuro-axonal damage or demyelination on the one hand, or the result of intracellular sodium accumulation due to inflammatory toxicity on the other (64, 65, 99).

The first study enabling differentiation of cellular compartments in 19 RRMS patients and 17 controls applied a combined single (SQ) and triple quantum filtered (TQF) 3D gradient echo ^{23}NaMRI sequence at 7 T ultra-high field (101). The applied TQF technique used the different relaxation properties and signals of intracellular and extracellular distributed sodium ions. It thus enabled measurement of TSC, but also differentiation of the intracellular sodium concentration (ISC) and the intracellular sodium volume fraction (ISVF). ISVF is an indirect, inversely correlated measure of the extracellular sodium concentration (ESC): ISVF reduction is assumed to be a marker for a diminished intracellular volume and, accordingly, an increase of the extracellular space and ESC. As a limitation discussed by the authors, the applied model is based on the assumption, that the pathology itself does not change the ^{23}Na relaxation times and that the TQF sequence enables a precise and unbiased sodium compartment differentiation. However, the quantitative accuracy of ISC measurements in MS patients is still undefined, since there is no non-invasive "goldstandard" that the ISC measurement can be compared to *in vivo*.

In accordance with previous 3 T studies, TSC of GM and MS lesions was higher than in WM and higher in MS than in healthy controls. ISC did not differ between the respective GM and WM but was higher in MS patients than in controls in GM and WM. In contrast, ISVF was lower in MS patients than in controls and higher in WM than in GM of both groups. In conclusion, TSC accumulation was in part depending on the growth of the extracellular compartment as potential consequence of axonal loss in MS. Nevertheless, it also depended on a distinct intracellular sodium increase. These results support findings of *ex vivo* and experimental studies suggesting a concomitant toxic metabolic dysfunction due to sodium imbalance (101).

Another study aimed at elucidating (1) differences in sodium levels between acute (= contrast enhancing) and chronic MS lesions and (2) differences between intracellular (ISC) and total sodium concentrations. Besides a regular DA-3DPR sequence, the authors also employed a fluid-attenuated sodium signal at 7 T in 29 MS patients (78). The applied fluid-attenuated sequence with a relaxation-weighted sodium signal preferentially depicts sodium ions with short relaxation times as found intracellularly. Thus, the setting enables a weighting toward the intracellular sodium compartment similar to previous approaches (4, 76, 77, 110). The study demonstrated that TSC and ISC were higher in acute as compared to chronic MS lesions. Hence, the fluid-attenuated sequence was useful to differentiate both types of lesions. TSC was positively correlated with T1 and T2 proton based lesion signals. In contrast, ISC only correlated with acute contrast enhancing T1 lesions. Interestingly, TSC and ISC levels were not associated. These data further support the additional biological significance of intracellular sodium accumulation measured by ^{23}NaMRI. Thus, ISC increase may occur independently of extracellular sodium increase due to inflammatory edema or cell loss. This observation renders ISC a useful biomarker of metabolic neuroinflammatory processes.

In addition, this study contributed rare longitudinal sodium MRI data. Three patients were analyzed before and after steroid treatment indicating decrease of both sodium signals after treatment. Besides intracellular sodium accumulation, a distinct inflammatory hyper-cellularity may lead to elevated ISC in acute lesions. A combination of proton (lesion detection) and sodium (lesion differentiation) MRI may yield a neurodegenerative and neuroinflammatory biomarker and potentially an alternative to contrast agent application in the future (78).

Additionally, in the above mentioned case report of an acute enhancing MS lesion with open ring sign, also ISC was analyzed. ISC was reduced in the center of the acute lesion as compared to the periphery and NAWM. The low central ISC may be explained by enhanced cellular necrosis as compared to a more viable periphery. Thus, sodium MRI may constitute a useful biomarker for the degree of acute neuroinflammatory damage in MS (103).

Sodium MRI and Further Fields of Applications in MS

Since low SNR and low spatial resolution is a major issue in sodium MRI, the incorporation of proton based anatomical MRI data in the reconstruction process enables improved image quality (111). A recent study described the application of an anatomically weighted second-order total variation (AnaWeTV) interative construction constraint in a MS patient including anatomical weighted MRI. AnaWeTV resulted in improved sodium MRI quality and less confounding partial volume effects, particularly in tissues or lesions that are visible in sodium and proton base MRI (60).

Another study was particularly engaged in the detection of potential errors of sodium MRI. Here, partial volume effects and spatially correlated noise artifacts impede quantification of sodium in small MS lesions (112). Besides a sodium-phantom analysis with given sodium concentration, sodium MRI signal variation in small lesions of five MS patients was compared to a computed predictive value using twisted projection imaging. Both, theoretical and *in vivo* sodium measurement pointed to

a variation error of 20% in large, and even of 40–50% in small lesions as defined by the investigators. These data suggest underestimation of Na^+ signals especially in small lesions and emphasize the limitations of sodium MRI despite improved imaging techniques.

Regular proton based MRI often requires gadolinium containing contrast agents. At the same time, several previous studies detected distinct MRI signal alterations of the dentate nucleus as a potential consequence of multiple gadolinium applications. Consequently, a recent study aimed at investigation of the dentate nucleus by sodium MRI at 3 T (113): in 12 MS patients and 6 controls, there was no difference in TSC between both groups despite a signal-altered dentate nucleus. These results suggest sustained tissue integrity of dentate nuclei with gadolinium deposition.

Finally, a recent study was able to exclude relevant influences of a preceding gadolinium application to the subsequent sodium MRI measurement. Despite a distinct quantitative influence of gadolinium on sodium relaxation times, this study further emphasized the compatibility and potential of combined proton and sodium MRI (114).

CONCLUSIONS AND PERSPECTIVES

Within the last decade, there was increasing evidence for the value of sodium accumulation measured by ^{23}NaMRI as a biomarker for neurodegeneration and -inflammation in MS. Studies point to a widespread increase of TSC in MS as compared to healthy populations with a pronounced increase in the GM and in MS lesions as well as in progressive disease courses. Furthermore, sodium accumulation partly correlated with disability (as measured by EDSS) and brain atrophy as the proton based MRI "goldstandard" for monitoring neurodegeneration in MS. Moreover, the TSC increase occurs even in "unaffected" NAWM as defined by standard proton based MRI. Thus, TSC as measured by sodium MRI is discussed as an early biomarker of neurodegenerative changes in MS brains.

The value of ^{23}NaMRI as a potential tool for monitoring of neuroinflammation has mainly been restricted to lesional TSC measurements. These studies consistently showed highest TSC in acute contrast-enhancing lesions as compared to NAWM. To date, the investigation of intra- vs. extracellular sodium accumulation in inflammatory lesions is limited to case reports or studies including very few MS patients.

Moreover, the analysis of acute MS lesions still necessitates a large lesion size of roughly >5 mm to minimize partial volume effects. Furthermore, large longitudinal studies to examine the temporal evolution of the sodium content in MS lesions and the correlation to conventional markers of inflammation are still lacking. Meanwhile, novel imaging techniques allowing for discrimination of tissue compartments are in part capable to delineate increased extracellular sodium. These studies analyze the expanded extracellular space as consequence of neuro-axonal damage or inflammatory edema caused by increased intracellular sodium due to intraneuronal/-axonal sodium accumulation with its consecutive toxic intracellular signal cascades (4, 67, 78, 101). Preceding findings indicate that ISC in MS are elevated in different brain regions as compared to healthy controls. However, TSC accumulation in MS was shown to depend on both, ESC and ISC increase. These findings suggest an expanded extracellular compartment i.e., due to axonal loss in MS on the one hand, but also on a distinct intracellular accumulation on the other. However, the precise differentiation of intra- vs. extracellular sodium via ^{23}NaMRI is still limited. In particular, a mutual influence of intra- and extracellular spaces on each other cannot be definitely excluded. Progress in the development of respective imaging techniques will enable a more detailed insight in the diverse origin and effects of intra- vs. extracellular sodium accumulation.

Despite all progress, sodium MRI still has to overcome several limitations: initial studies displayed huge range of TSC quantification of more than 40 mM, mainly due to different scanner hardware, acquisition protocols or quantification models. Novel sodium imaging techniques improved the quantification range to roughly 10 mM but still may vary significantly (39). Thus, comparability of results from different study groups is complicated. Using the intraventricular CSF sodium signal as an intra-individual reference signal for quantification of sodium concentrations was recently discussed to specify sodium measurement. This approach is based in the observation that sodium levels in the CSF may be stable at the levels of extracellular fluid i.e., 140 mM (66, 115).

Yet, as a consequence of the physical properties of Na^+, application of ultra-high field ≥7 T scanners and/or long acquisition times is warranted for "state-of-the-art" sodium MRI. This is of particular relevance when aiming at the precise differentiation of sodium compartments.

In consequence, further development of sodium MRI techniques and hardware is crucial (1) to improve SNR and resolution, (2) to diminish partial volume effects and scanning times, and (3) to enable precise differentiation of sodium compartments.

The future technical improvement together with the demonstrated high potential of brain sodium as a biomarker in neurological disorders may pave the way for the implementation of sodium MRI in clinical routine. The implementation of this ambitious goal may be further supported by affordable sodium MRI head coils and software packages enabling widespread sodium measurement at commercial MRI systems (39).

Since ^{23}NaMRI requires no contrast agents, similar contraindications as for conventional proton MRI apply. Even at ultra-high field strengths, MRI is well-tolerated, thus further supporting an extended application of ^{23}NaMR investigations (29, 68, 116). However, none of the published studies so far comprised an MS collective with $n > 100$ thus in part limiting their significance. In consequence, multi-center studies with strictly defined MS patient cohorts and sodium MRI methods are warranted to improve the validity of future studies.

Furthermore, improved sodium MRI techniques may enable the future investigation of smaller regions of interest i.e., inflammatory brain lesions with a diameter <5 mm or spinal cord sodium concentrations. Analyzing the spinal cord would

add useful information about disability-relevant MS pathology beyond previous *ex vivo* or proton based MRI analyses (117).

As another attractive location for sodium MRI, studies of hypertension, renal and rheumatological diseases displayed elevated sodium deposition in the skin and muscle (118–120). Together with experimental findings of proinflammatory properties of elevated sodium levels in the skin, analysis of dermal and muscular soft tissue sodium could also be interesting in the field of MS. Here, the inflammatory pathogenesis may likely be initiated in the periphery before immune cells enter the CNS (23). Hence, sodium MRI may help to elucidate sodium dependent effects of the yet scarcely characterized origin of inflammatory processes in the periphery of MS patients.

Finally, sodium MRI has not been applied in other acute or chronic inflammatory diseases of the CNS, such as acute disseminated encephalomyelitis (ADEM), vasculitis, granulomatous diseases, or aquaporine-4-antibody associated neuromyelitis optica spectrum diseases (NMO-SD). Here, the technique may add further valuable insights beyond conventional proton MRI which often cannot sufficiently differentiate between these entities (28). In addition, the effects of underlying disease-modifying therapies on MRI brain sodium levels have not been analyzed yet and remain to be demonstrated. Such studies warrant longitudinal investigations of MS patients under immunomodulatory treatment.

Combination of sodium MRI with additional imaging tools beyond standard proton MRI may gain novel information about pathological metabolic processes associated with sodium accumulation. Here, additional MRI techniques [i.e., myelin water imaging (MWI), magnetization transfer ratio (MTR), diffusion tensor imaging (DTI), magnetic resonance spectroscopy (MRS), optical coherence tomography (OCT) or metabolic imaging techniques, such as positron emission tomography (PET)] would be promising candidates (48).

In conclusion, modern sodium MRI has in part overcome its inherent physical limitations, but still is in need for further development. With its capability to give yet unknown insights in the pathology of MS, this imaging technique deserves further investigation aiming at implementation of sodium accumulation as a biomarker for neurodegeneration and -inflammation in the future.

DATA AVAILABILITY STATEMENT

No primary datasets were generated for this study. KH and AN have access to referenced articles and are responsible for all data presented in the manuscript.

AUTHOR CONTRIBUTIONS

KH drafted the work, contributed to the conception and interpretation of the work, and acquired the included data and references. TE contributed to the conception and interpretation of the work and revised it critically for important intellectual content. RL contributed to drafting the work, contributed to the conception and interpretation of the work, and revised it critically for important intellectual content. AN contributed to drafting the work, acquired the included data and references, contributed to the conception and interpretation of the work, and revised it critically for important intellectual content. All authors provide approval for publication of the content.

FUNDING

We acknowledge support by Deutsche Forschungsgemeinschaft and Friedrich-Alexander-Universität Erlangen-Nürnberg (FAU) within the funding programme Open Access Publishing for the publication fee.

REFERENCES

1. Trapp BD, Stys PK. Virtual hypoxia and chronic necrosis of demyelinated axons in multiple sclerosis. *Lancet Neurol.* (2009) 8:280–91. doi: 10.1016/S1474-4422(09)70043-2
2. Haider L, Zrzavy T, Hametner S, Hoftberger R, Bagnato F, Grabner G, et al. The topograpy of demyelination and neurodegeneration in the multiple sclerosis brain. *Brain* (2016) 139(Pt 3):807–15. doi: 10.1093/brain/awv398
3. Murphy E, Eisner DA. Regulation of intracellular and mitochondrial sodium in health and disease. *Circ Res.* (2009) 104:292–303. doi: 10.1161/CIRCRESAHA.108.189050
4. Madelin G, Kline R, Walvick R, Regatte RR. A method for estimating intracellular sodium concentration and extracellular volume fraction in brain *in vivo* using sodium magnetic resonance imaging. *Sci Rep.* (2014) 4:4763. doi: 10.1038/srep04763
5. Paling D, Golay X, Wheeler-Kingshott C, Kapoor R, Miller D. Energy failure in multiple sclerosis and its investigation using MR techniques. *J Neurol.* (2011) 258:2113–27. doi: 10.1007/s00415-011-6117-7
6. Young EA, Fowler CD, Kidd GJ, Chang A, Rudick R, Fisher E, et al. Imaging correlates of decreased axonal Na^+/K^+ ATPase in chronic multiple sclerosis lesions. *Ann Neurol.* (2008) 63:428–35. doi: 10.1002/ana.21381
7. Smith KJ. Sodium channels and multiple sclerosis: roles in symptom production, damage and therapy. *Brain Pathol.* (2007) 17:230–42. doi: 10.1111/j.1750-3639.2007.00066.x
8. Moll C, Mourre C, Lazdunski M, Ulrich J. Increase of sodium channels in demyelinated lesions of multiple sclerosis. *Brain Res.* (1991) 556:311–6.
9. Black JA, Dib-Hajj S, Baker D, Newcombe J, Cuzner ML, Waxman SG. Sensory neuron-specific sodium channel SNS is abnormally expressed in the brains of mice with experimental allergic encephalomyelitis and humans with multiple sclerosis. *Proc Natl Acad Sci USA*. (2000) 97:11598–602. doi: 10.1073/pnas.97.21.11598.
10. Craner MJ, Newcombe J, Black JA, Hartle C, Cuzner ML, Waxman SG. Molecular changes in neurons in multiple sclerosis: altered axonal expression of Nav1.2 and Nav1.6 sodium channels and Na^+/Ca^{2+} exchanger. *Proc Natl Acad Sci USA*. (2004) 101:8168–73. doi: 10.1073/pnas.0402765101
11. Waxman SG. Mechanisms of disease: sodium channels and neuroprotection in multiple sclerosis-current status. *Nat Clin Pract Neurol.* (2008) 4:159–69. doi: 10.1038/ncpneuro0735
12. Stys PK, Ransom BR, Waxman SG. Tertiary and quaternary local anesthetics protect CNS white matter from anoxic injury at concentrations that do not block excitability. *J Neurophysiol.* (1992) 67:236–40. doi: 10.1152/jn.1992.67.1.236
13. Fern R, Ransom BR, Stys PK, Waxman SG. Pharmacological protection of CNS white matter during anoxia: actions of phenytoin, carbamazepine and diazepam. *J Pharmacol Exp Ther.* (1993) 266:1549–55.
14. Bechtold DA, Kapoor R, Smith KJ. Axonal protection using flecainide in experimental autoimmune encephalomyelitis. *Ann Neurol.* (2004) 55:607–16. doi: 10.1002/ana.20045

15. Bechtold DA, Miller SJ, Dawson AC, Sun Y, Kapoor R, Berry D, et al. Axonal protection achieved in a model of multiple sclerosis using lamotrigine. *J Neurol.* (2006) 253:1542–51. doi: 10.1007/s00415-006-0204-1
16. Vergo S, Craner MJ, Etzensperger R, Attfield K, Friese MA, Newcombe J, et al. Acid-sensing ion channel 1 is involved in both axonal injury and demyelination in multiple sclerosis and its animal model. *Brain* (2011) 134(Pt 2):571–84. doi: 10.1093/brain/awq337
17. Kapoor R, Furby J, Hayton T, Smith KJ, Altmann DR, Brenner R, et al. Lamotrigine for neuroprotection in secondary progressive multiple sclerosis: a randomised, double-blind, placebo-controlled, parallel-group trial. *Lancet Neurol.* (2010) 9:681–8. doi: 10.1016/S1474-4422(10)70131-9
18. Arun T, Tomassini V, Sbardella E, de Ruiter MB, Matthews L, Leite MI, et al. Targeting ASIC1 in primary progressive multiple sclerosis: evidence of neuroprotection with amiloride. *Brain* (2013) 136(Pt 1):106–15. doi: 10.1093/brain/aws325
19. Yang C, Hao Z, Zhang L, Zeng L, Wen J. Sodium channel blockers for neuroprotection in multiple sclerosis. *Cochrane Database Syst Rev.* (2015) CD010422. doi: 10.1002/14651858.CD010422.pub2
20. Haghikia A, Jorg S, Duscha A, Berg J, Manzel A, Waschbisch A, et al. Dietary fatty acids directly impact central nervous system autoimmunity via the small intestine. *Immunity* (2015) 43:817–29. doi: 10.1016/j.immuni.2015.09.007
21. Jorg S, Grohme DA, Erzler M, Binsfeld M, Haghikia A, Muller DN, et al. Environmental factors in autoimmune diseases and their role in multiple sclerosis. *Cell Mol Life Sci.* (2016) 73:4611–22. doi: 10.1007/s00018-016-2311-1
22. Hammer A, Schliep A, Jorg S, Haghikia A, Gold R, Kleinewietfeld M, et al. Impact of combined sodium chloride and saturated long-chain fatty acid challenge on the differentiation of T helper cells in neuroinflammation. *J Neuroinflammation* (2017) 14:184. doi: 10.1186/s12974-017-0954-y
23. Kleinewietfeld M, Manzel A, Titze J, Kvakan H, Yosef N, Linker RA, et al. Sodium chloride drives autoimmune disease by the induction of pathogenic TH17 cells. *Nature* (2013) 496:518–22. doi: 10.1038/nature11868
24. Farez MF. Salt intake in multiple sclerosis: friend or foe? *J Neurol Neurosurg Psychiatry* (2016) 87:1276. doi: 10.1136/jnnp-2016-313768
25. Fitzgerald KC, Munger KL, Hartung HP, Freedman MS, Montalban X, Edan G, et al. Sodium intake and multiple sclerosis activity and progression in BENEFIT. *Ann Neurol.* (2017) 82:20–9. doi: 10.1002/ana.24965
26. Nourbakhsh B, Graves J, Casper TC, Lulu S, Waldman A, Belman A, et al. Dietary salt intake and time to relapse in paediatric multiple sclerosis. *J Neurol Neurosurg Psychiatry* (2016) 87:1350–3. doi: 10.1136/jnnp-2016-313410
27. Currie S, Hoggard N, Craven IJ, Hadjivassiliou M, Wilkinson ID. Understanding MRI: basic MR physics for physicians. *Postgrad Med J.* (2013) 89:209–23. doi: 10.1136/postgradmedj-2012-131342
28. Kaunzner UW, Gauthier SA. MRI in the assessment and monitoring of multiple sclerosis: an update on best practice. *Ther Adv Neurol Disord.* (2017) 10:247–61. doi: 10.1177/1756285617708911
29. Konstandin S, Nagel AM. Measurement techniques for magnetic resonance imaging of fast relaxing nuclei. *MAGMA* (2014) 27:5–19. doi: 10.1007/s10334-013-0394-3
30. Harris RK, Becker ED, Cabral de Menezes SM, Goodfellow R, Granger P. NMR nomenclature: nuclear spin properties and conventions for chemical shifts. IUPAC recommendations 2001. *Solid State Nucl Magn Reson.* (2002) 22:458–83. doi: 10.1006/snmr.2002.0063
31. Gordji-Nejad A, Mollenhoff K, Oros-Peusquens AM, Pillai DR, Shah NJ. Characterizing cerebral oxygen metabolism employing oxygen-17 MRI/MRS at high fields. *MAGMA* (2014) 27:81–93. doi: 10.1007/s10334-013-0413-4
32. Chen J, Lanza GM, Wickline SA. Quantitative magnetic resonance fluorine imaging: today and tomorrow. *Wiley Interdiscip Rev Nanomed Nanobiotechnol.* (2010) 2:431–40. doi: 10.1002/wnan.87
33. Lu A, Atkinson IC, Zhou XJ, Thulborn KR. PCr/ATP ratio mapping of the human head by simultaneously imaging of multiple spectral peaks with interleaved excitations and flexible twisted projection imaging readout trajectories at 9.4 T. *Magn Reson Med.* (2013) 69:538–44. doi: 10.1002/mrm.24281
34. Nagel AM, Lehmann-Horn F, Weber MA, Jurkat-Rott K, Wolf MB, Radbruch A, et al. *In vivo* 35Cl MR imaging in humans: a feasibility study. *Radiology* (2014) 271:585–95. doi: 10.1148/radiol.13131725
35. Umathum R, Rosler MB, Nagel AM. *In vivo* 39K MR imaging of human muscle and brain. *Radiology* (2013) 269:569–76. doi: 10.1148/radiol.13130757
36. Atkinson IC, Claiborne TC, Thulborn KR. Feasibility of 39-potassium MR imaging of a human brain at 9.4 Tesla. *Magn Reson Med.* (2014) 71:1819–25. doi: 10.1002/mrm.24821
37. Hilal SK, Maudsley AA, Ra JB, Simon HE, Roschmann P, Wittekoek S, et al. *In vivo* NMR imaging of sodium-23 in the human head. *J Comput Assist Tomogr.* (1985) 9:1–7.
38. Konstandin S, Schad LR. 30 Years of sodium/X-nuclei magnetic resonance imaging. *MAGMA* (2014) 27:1–4. doi: 10.1007/s10334-013-0426-z
39. Thulborn KR. Quantitative sodium MR imaging: a review of its evolving role in medicine. *Neuroimage* (2018) 168:250–68. doi: 10.1016/j.neuroimage.2016.11.056
40. Madelin G, Lee JS, Regatte RR, Jerschow A. Sodium MRI: methods and applications. *Prog Nucl Magn Reson Spectrosc.* (2014) 79:14–47. doi: 10.1016/j.pnmrs.2014.02.001
41. Ladd ME, Bachert P, Meyerspeer M, Moser E, Nagel AM, Norris DG, et al. Pros and cons of ultra-high-field MRI/MRS for human application. *Prog Nucl Magn Reson Spectrosc.* (2018) 109:1–50. doi: 10.1016/j.pnmrs.2018.06.001
42. Maudsley AA, Hilal SK. Biological aspects of sodium-23 imaging. *Br Med Bull.* (1984) 40:165–6.
43. Hirai H, Yamasaki K, Kidena H, Kono M. Quantitative analysis of sodium fast and slow component in *in vivo* human brain tissue using MR Na image. *Kaku Igaku* (1992) 29:1447–54.
44. Constantinides CD, Gillen JS, Boada FE, Pomper MG, Bottomley PA. Human skeletal muscle: sodium MR imaging and quantification-potential applications in exercise and disease. *Radiology* (2000) 216:559–68. doi: 10.1148/radiology.216.2.r00jl46559
45. Ouwerkerk R, Bleich KB, Gillen JS, Pomper MG, Bottomley PA. Tissue sodium concentration in human brain tumors as measured with 23Na MR imaging. *Radiology* (2003) 227:529–37. doi: 10.1148/radiol.2272020483
46. Hilal SK, Maudsley AA, Simon HE, Perman WH, Bonn J, Mawad ME, et al. *In vivo* NMR imaging of tissue sodium in the intact cat before and after acute cerebral stroke. *AJNR Am J Neuroradiol.* (1983) 4:245–9.
47. Petracca M, Fleysher L, Oesingmann N, Inglese M. Sodium MRI of multiple sclerosis. *NMR Biomed.* (2016) 29:153–61. doi: 10.1002/nbm.3289
48. Shah NJ, Worthoff WA, Langen KJ. Imaging of sodium in the brain: a brief review. *NMR Biomed.* (2016) 29:162–74. doi: 10.1002/nbm.3389
49. Boada FE, Christensen JD, Huang-Hellinger FR, Reese TG, Thulborn KR. Quantitative *in vivo* tissue sodium concentration maps: the effects of biexponential relaxation. *Magn Reson Med.* (1994) 32:219–23.
50. Wiggins GC, Brown R, Lakshmanan K. High-performance radiofrequency coils for (23)Na MRI: brain and musculoskeletal applications. *NMR Biomed.* (2016) 29:96–106. doi: 10.1002/nbm.3379
51. Qian Y, Zhao T, Wiggins GC, Wald LL, Zheng H, Weimer J, et al. Sodium imaging of human brain at 7 T with 15-channel array coil. *Magn Reson Med.* (2012) 68:1807–14. doi: 10.1002/mrm.24192
52. Benkhedah N, Hoffmann SH, Biller A, Nagel AM. Evaluation of adaptive combination of 30-channel head receive coil array data in 23Na MR imaging. *Magn Reson Med.* (2016) 75:527–36. doi: 10.1002/mrm.25572
53. Lommen JM, Resmer F, Behl NGR, Sauer M, Benkhedah N, Bitz AK, et al. Comparison of of a 30-channel head array with a birdcage for 23Na MRI at 7 Tesla. *Proc. Intl. Soc. Mag. Reson. Med.* (2016) 24:3974.
54. Irarrazabal P, Nishimura DG. Fast three dimensional magnetic resonance imaging. *Magn Reson Med.* (1995) 33:656–62.
55. Boada FE, Gillen JS, Shen GX, Chang SY, Thulborn KR. Fast three dimensional sodium imaging. *Magn Reson Med.* (1997) 37:706–15.
56. Stobbe R, Beaulieu C. Advantage of sampling density weighted apodization over postacquisition filtering apodization for sodium MRI of the human brain. *Magn Reson Med.* (2008) 60:981–6. doi: 10.1002/mrm.21738
57. Nagel AM, Laun FB, Weber MA, Matthies C, Semmler W, Schad LR. Sodium MRI using a density-adapted 3D radial acquisition technique. *Magn Reson Med.* (2009) 62:1565–73. doi: 10.1002/mrm.22157
58. Madelin G, Chang G, Otazo R, Jerschow A, Regatte RR. Compressed sensing sodium MRI of cartilage at 7T: preliminary study. *J Magn Reson.* (2012) 214:360–5. doi: 10.1016/j.jmr.2011.12.005

59. Gnahm C, Bock M, Bachert P, Semmler W, Behl NG, Nagel AM. Iterative 3D projection reconstruction of (23) Na data with an (1) H MRI constraint. *Magn Reson Med.* (2014) 71:1720–32. doi: 10.1002/mrm.24827
60. Gnahm C, Nagel AM. Anatomically weighted second-order total variation reconstruction of 23Na MRI using prior information from 1H MRI. *Neuroimage* (2015) 105:452–61. doi: 10.1016/j.neuroimage.2014.11.006
61. Behl NG, Gnahm C, Bachert P, Ladd ME, Nagel AM. Three-dimensional dictionary-learning reconstruction of (23)Na MRI data. *Magn Reson Med.* (2016) 75:1605–16. doi: 10.1002/mrm.25759
62. Ridley B, Nagel AM, Bydder M, Maarouf A, Stellmann JP, Gherib S, et al. Distribution of brain sodium long and short relaxation times and concentrations: a multi-echo ultra-high field (23)Na MRI study. *Sci Rep.* (2018) 8:4357. doi: 10.1038/s41598-018-22711-0
63. Kraff O, Fischer A, Nagel AM, Monninghoff C, Ladd ME. MRI at 7 Tesla and above: demonstrated and potential capabilities. *J Magn Reson Imaging* (2015) 41:13–33. doi: 10.1002/jmri.24573
64. Inglese M, Madelin G, Oesingmann N, Babb JS, Wu W, Stoeckel B, et al. Brain tissue sodium concentration in multiple sclerosis: a sodium imaging study at 3 tesla. *Brain* (2010) 133(Pt 3):847–57. doi: 10.1093/brain/awp334
65. Paling D, Solanky BS, Riemer F, Tozer DJ, Wheeler-Kingshott CA, Kapoor R, et al. Sodium accumulation is associated with disability and a progressive course in multiple sclerosis. *Brain* (2013) 136(Pt 7):2305–17. doi: 10.1093/brain/awt149
66. Mirkes CC, Hoffmann J, Shajan G, Pohmann R, Scheffler K. High-resolution quantitative sodium imaging at 9.4 Tesla. *Magn Reson Med.* (2015) 73:342–51. doi: 10.1002/mrm.25096
67. Gilles A, Nagel AM, Madelin G. Multipulse sodium magnetic resonance imaging for multicompartment quantification: proof-of-concept. *Sci Rep.* (2017) 7:17435. doi: 10.1038/s41598-017-17582-w
68. Atkinson IC, Renteria L, Burd H, Pliskin NH, Thulborn KR. Safety of human MRI at static fields above the FDA 8 T guideline: sodium imaging at 9.4 T does not affect vital signs or cognitive ability. *J Magn Reson Imaging* (2007) 26:1222–7. doi: 10.1002/jmri.21150
69. Shah NJ. Multimodal neuroimaging in humans at 9.4 T: a technological breakthrough towards an advanced metabolic imaging scanner. *Brain Struct Funct.* (2015) 220:1867–84. doi: 10.1007/s00429-014-0843-4
70. Madelin G, Regatte RR. Biomedical applications of sodium MRI *in vivo*. *J Magn Reson Imaging* (2013) 38:511–29. doi: 10.1002/jmri.24168
71. Niesporek SC, Hoffmann SH, Berger MC, Benkhedah N, Kujawa A, Bachert P, et al. Partial volume correction for *in vivo* (23)Na-MRI data of the human brain. *Neuroimage* (2015) 112:353–63. doi: 10.1016/j.neuroimage.2015.03.025
72. Naritomi H, Kanashiro M, Sasaki M, Kuribayashi Y, Sawada T. *In vivo* measurements of intra- and extracellular Na^+ and water in the brain and muscle by nuclear magnetic resonance spectroscopy with shift reagent. *Biophys J.* (1987) 52:611–6. doi: 10.1016/S0006-3495(87)83251-4
73. Bansal N, Germann MJ, Lazar I, Malloy CR, Sherry AD. *In vivo* Na-23 MR imaging and spectroscopy of rat brain during TmDOTP5-infusion. *J Magn Reson Imaging* (1992) 2:385–91.
74. Boada FE, LaVerde G, Jungreis C, Nemoto E, Tanase C, Hancu I. Loss of cell ion homeostasis and cell viability in the brain: what sodium MRI can tell us. *Curr Top Dev Biol.* (2005) 70:77–101. doi: 10.1016/S0070-2153(05)70004-1
75. Winter PM, Bansal N. $TmDOTP^{5-}$ as a ^{23}Na shift reagent for the subcutaneously implanted 9L gliosarcoma in rats. *Magn Reson Med.* (2001) 45:436–42. doi: 10.1002/1522-2594(200103)45:3<436::AID-MRM1057>3.0.CO;2-6
76. Stobbe R, Beaulieu C. *In vivo* sodium magnetic resonance imaging of the human brain using soft inversion recovery fluid attenuation. *Magn Reson Med.* (2005) 54:1305–10. doi: 10.1002/mrm.20696
77. Nagel AM, Bock M, Hartmann C, Gerigk L, Neumann JO, Weber MA, et al. The potential of relaxation-weighted sodium magnetic resonance imaging as demonstrated on brain tumors. *Invest Radiol.* (2011) 46:539–47. doi: 10.1097/RLI.0b013e31821ae918
78. Biller A, Pflugmann I, Badde S, Diem R, Wildemann B, Nagel AM, et al. Sodium MRI in multiple sclerosis is compatible with intracellular sodium accumulation and inflammation-induced hyper-cellularity of acute brain lesions. *Sci Rep.* (2016) 6:31269. doi: 10.1038/srep31269
79. Madelin G, Babb J, Xia D, Regatte RR. Repeatability of quantitative sodium magnetic resonance imaging for estimating pseudo-intracellular sodium concentration and pseudo-extracellular volume fraction in brain at 3 T. *PLoS ONE* (2015) 10:e0118692. doi: 10.1371/journal.pone.0118692
80. Pike KJ, Malde RP, Ashbrook SE, McManus J, Wimperis S. Multiple-quantum MAS NMR of quadrupolar nuclei. Do five-, seven- and nine-quantum experiments yield higher resolution than the three-quantum experiment? *Solid State Nucl Magn Reson.* (2000) 16:203–15. doi: 10.1016/S0926-2040(00)00081-3
81. Fleysher L, Oesingmann N, Brown R, Sodickson DK, Wiggins GC, Inglese M. Noninvasive quantification of intracellular sodium in human brain using ultrahigh-field MRI. *NMR Biomed.* (2013) 26:9–19. doi: 10.1002/nbm.2813
82. Worthoff WA, Shymanskaya A, Shah NJ. Relaxometry and quantification in simultaneously acquired single and triple quantum filtered sodium MRI. *Magn Reson Med.* (2018) 81:303–15. doi: 10.1002/mrm.27387
83. Matthies C, Nagel AM, Schad LR, Bachert P. Reduction of B(0) inhomogeneity effects in triple-quantum-filtered sodium imaging. *J Magn Reson.* (2010) 202:239–44. doi: 10.1016/j.jmr.2009.11.004
84. Benkhedah N, Bachert P, Semmler W, Nagel AM. Three-dimensional biexponential weighted (23)Na imaging of the human brain with higher SNR and shorter acquisition time. *Magn Reson Med.* (2013) 70:754–65. doi: 10.1002/mrm.24516
85. Fiege DP, Romanzetti S, Mirkes CC, Brenner D, Shah NJ. Simultaneous single-quantum and triple-quantum-filtered MRI of 23Na (SISTINA). *Magn Reson Med.* (2013) 69:1691–6. doi: 10.1002/mrm.24417
86. Tsang A, Stobbe RW, Beaulieu C. Evaluation of B0-inhomogeneity correction for triple-quantum-filtered sodium MRI of the human brain at 4.7 T. *J Magn Reson.* (2013) 230:134–44. doi: 10.1016/j.jmr.2013.01.017
87. Gast LV, Gerhalter T, Hensel B, Uder M, Nagel AM. Double quantum filtered (23) Na MRI with magic angle excitation of human skeletal muscle in the presence of B0 and B1 inhomogeneities. *NMR Biomed.* (2018) 31:e4010. doi: 10.1002/nbm.4010
88. Thulborn KR, Gindin TS, Davis D, Erb P. Comprehensive MR imaging protocol for stroke management: tissue sodium concentration as a measure of tissue viability in nonhuman primate studies and in clinical studies. *Radiology* (1999) 213:156–66. doi: 10.1148/radiology.213.1.r99se15156
89. Hussain MS, Stobbe RW, Bhagat YA, Emery D, Butcher KS, Manawadu D, et al. Sodium imaging intensity increases with time after human ischemic stroke. *Ann Neurol.* (2009) 66:55–62. doi: 10.1002/ana.21648
90. Tsang A, Stobbe RW, Asdaghi N, Hussain MS, Bhagat YA, Beaulieu C, et al. Relationship between sodium intensity and perfusion deficits in acute ischemic stroke. *J Magn Reson Imaging* (2011) 33:41–7. doi: 10.1002/jmri.22299
91. Thulborn KR, Davis D, Adams H, Gindin T, Zhou J. Quantitative tissue sodium concentration mapping of the growth of focal cerebral tumors with sodium magnetic resonance imaging. *Magn Reson Med.* (1999) 41:351–9.
92. Kline RP, Wu EX, Petrylak DP, Szabolcs M, Alderson PO, Weisfeldt ML, et al. Rapid *in vivo* monitoring of chemotherapeutic response using weighted sodium magnetic resonance imaging. *Clin Cancer Res.* (2000) 6:2146–56.
93. Babsky AM, Zhang H, Hekmatyar SK, Hutchins GD, Bansal N. Monitoring chemotherapeutic response in RIF-1 tumors by single-quantum and triple-quantum-filtered (23)Na MRI, (1)H diffusion-weighted MRI and PET imaging. *Magn Reson Imaging* (2007) 25:1015–23. doi: 10.1016/j.mri.2006.11.004
94. Thulborn KR, Lu A, Atkinson IC, Damen F, Villano JL. Quantitative sodium MR imaging and sodium bioscales for the management of brain tumors. *Neuroimaging Clin N Am.* (2009) 19:615–24. doi: 10.1016/j.nic.2009.09.001
95. Nunes Neto LP, Madelin G, Sood TP, Wu CC, Kondziolka D, Placantonakis D, et al. Quantitative sodium imaging and gliomas: a feasibility study. *Neuroradiology* (2018) 60:795–802. doi: 10.1007/s00234-018-2041-1
96. Reetz K, Romanzetti S, Dogan I, Sass C, Werner CJ, Schiefer J, et al. Increased brain tissue sodium concentration in Huntington's disease–a sodium imaging study at 4 T. *Neuroimage* (2012) 63:517–24. doi: 10.1016/j.neuroimage.2012.07.009
97. Mellon EA, Pilkinton DT, Clark CM, Elliott MA, Witschey WR II, Borthakur A, et al. Sodium MR imaging detection of mild Alzheimer disease: preliminary study. *AJNR Am J Neuroradiol.* (2009) 30:978–84. doi: 10.3174/ajnr.A1495

98. Thulborn K, Lui E, Guntin J, Jamil S, Sun Z, Claiborne TC, et al. Quantitative sodium MRI of the human brain at 9.4 T provides assessment of tissue sodium concentration and cell volume fraction during normal aging. *NMR Biomed.* (2016) 29:137–43. doi: 10.1002/nbm.3312
99. Zaaraoui W, Konstandin S, Audoin B, Nagel AM, Rico A, Malikova I, et al. Distribution of brain sodium accumulation correlates with disability in multiple sclerosis: a cross-sectional 23Na MR imaging study. *Radiology* (2012) 264:859–67. doi: 10.1148/radiol.12112680
100. Maarouf A, Audoin B, Konstandin S, Rico A, Soulier E, Reuter F, et al. Topography of brain sodium accumulation in progressive multiple sclerosis. *MAGMA* (2014) 27:53–62. doi: 10.1007/s10334-013-0396-1
101. Petracca M, Vancea RO, Fleysher L, Jonkman LE, Oesingmann N, Inglese M. Brain intra- and extracellular sodium concentration in multiple sclerosis: a 7 T MRI study. *Brain* (2016) 139(Pt 3):795–806. doi: 10.1093/brain/awv386
102. Eisele P, Konstandin S, Griebe M, Szabo K, Wolf ME, Alonso A, et al. Heterogeneity of acute multiple sclerosis lesions on sodium (23Na) MRI. *Mult Scler.* (2016) 22:1040–7. doi: 10.1177/1352458515609430
103. Grist JT, Riemer F, McLean MA, Matys T, Zaccagna F, Hilborne SF, et al. Imaging intralesional heterogeneity of sodium concentration in multiple sclerosis: initial evidence from (23)Na-MRI. *J Neurol Sci.* (2018) 387:111–4. doi: 10.1016/j.jns.2018.01.027
104. Huhn K, Mennecke A, Linz P, Tschunko F, Kastle N, Nagel AM, et al. (23)Na MRI reveals persistent sodium accumulation in tumefactive MS lesions. *J Neurol Sci.* (2017) 379:163–6. doi: 10.1016/j.jns.2017.06.003
105. Filippi M, Rocca MA, De Stefano N, Enzinger C, Fisher E, Horsfield MA, et al. Magnetic resonance techniques in multiple sclerosis: the present and the future. *Arch Neurol.* (2011) 68:1514–20. doi: 10.1001/archneurol.2011.914
106. Maarouf A, Audoin B, Pariollaud F, Gherib S, Rico A, Soulier E, et al. Increased total sodium concentration in gray matter better explains cognition than atrophy in MS. *Neurology* (2017) 88:289–95. doi: 10.1212/WNL.0000000000003511
107. Donadieu M, Le Fur Y, Maarouf A, Gherib S, Ridley B, Pini L, et al. Metabolic counterparts of sodium accumulation in multiple sclerosis: a whole brain ^{23}Na-MRI and fast ^{1}H-MRSI study. *Mult Scler.* (2017) 25:39–47. doi: 10.1177/1352458517736146
108. Dutta R, McDonough J, Yin X, Peterson J, Chang A, Torres T, et al. Mitochondrial dysfunction as a cause of axonal degeneration in multiple sclerosis patients. *Ann Neurol.* (2006) 59:478–89. doi: 10.1002/ana.20736
109. Campbell GR, Ziabreva I, Reeve AK, Krishnan KJ, Reynolds R, Howell O, et al. Mitochondrial DNA deletions and neurodegeneration in multiple sclerosis. *Ann Neurol.* (2011) 69:481–92. doi: 10.1002/ana.22109
110. Nagel AM, Amarteifio E, Lehmann-Horn F, Jurkat-Rott K, Semmler W, Schad LR, et al. 3 Tesla sodium inversion recovery magnetic resonance imaging allows for improved visualization of intracellular sodium content changes in muscular channelopathies. *Invest Radiol.* (2011) 46:759–66. doi: 10.1097/RLI.0b013e31822836f6
111. Constantinides CD, Weiss RG, Lee R, Bolar D, Bottomley PA. Restoration of low resolution metabolic images with a priori anatomic information: ^{23}Na MRI in myocardial infarction. *Magn Reson Imaging* (2000) 18:461–71. doi: 10.1016/S0730-725X(99)00145-9
112. Stobbe RW, Beaulieu C. Calculating potential error in sodium MRI with respect to the analysis of small objects. *Magn Reson Med.* (2018) 79:2968–77. doi: 10.1002/mrm.26962
113. Eisele P, Konstandin S, Szabo K, Ong M, Zollner F, Schad LR, et al. Sodium MRI of T1 high signal intensity in the dentate nucleus due to gadolinium deposition in multiple sclerosis. *J Neuroimaging* (2017) 27:372–5. doi: 10.1111/jon.12448
114. Paschke NK, Neumann W, Uhrig T, Winkler M, Neumaier-Probst E, Fatar M, et al. Influence of gadolinium-based contrast agents on tissue sodium quantification in sodium magnetic resonance imaging. *Invest Radiol.* (2018) 53:555–62. doi: 10.1097/RLI.0000000000000487
115. Strange K. Regulation of solute and water balance and cell volume in the central nervous system. *J Am Soc Nephrol.* (1992) 3:12–27.
116. Rauschenberg J, Nagel AM, Ladd SC, Theysohn JM, Ladd ME, Moller HE, et al. Multicenter study of subjective acceptance during magnetic resonance imaging at 7 and 9.4 T. *Invest Radiol.* (2014) 49:249–59. doi: 10.1097/RLI.0000000000000035
117. Kearney H, Miller DH, Ciccarelli O. Spinal cord MRI in multiple sclerosis–diagnostic, prognostic and clinical value. *Nat Rev Neurol.* (2015) 11:327–38. doi: 10.1038/nrneurol.2015.80
118. Kopp C, Linz P, Dahlmann A, Hammon M, Jantsch J, Muller DN, et al. 23Na magnetic resonance imaging-determined tissue sodium in healthy subjects and hypertensive patients. *Hypertension* (2013) 61:635–40. doi: 10.1161/HYPERTENSIONAHA.111.00566
119. Titze J. Sodium balance is not just a renal affair. *Curr Opin Nephrol Hypertens.* (2014) 23:101–5. doi: 10.1097/01.mnh.0000441151.55320.c3
120. Wang P, Deger MS, Kang H, Ikizler TA, Titze J, Gore JC. Sex differences in sodium deposition in human muscle and skin. *Magn Reson Imaging* (2017) 36:93–7. doi: 10.1016/j.mri.2016.10.023

Conflict of Interest Statement: The authors declare that the research was conducted in the absence of any commercial or financial relationships that could be construed as a potential conflict of interest.

The reviewer AH declared a past co-authorship with one of the authors RL to the handling Editor.

Copyright © 2019 Huhn, Engelhorn, Linker and Nagel. This is an open-access article distributed under the terms of the Creative Commons Attribution License (CC BY). The use, distribution or reproduction in other forums is permitted, provided the original author(s) and the copyright owner(s) are credited and that the original publication in this journal is cited, in accordance with accepted academic practice. No use, distribution or reproduction is permitted which does not comply with these terms.

frontiers in Neurology

ORIGINAL RESEARCH
published: 15 February 2019
doi: 10.3389/fneur.2019.00083

IL-6 Plasma Levels Correlate With Cerebral Perfusion Deficits and Infarct Sizes in Stroke Patients Without Associated Infections

Benjamin Hotter[1,2]*, *Sarah Hoffmann*[1,2], *Lena Ulm*[3], *Christian Meisel*[4], *Jochen B. Fiebach*[1,2] and *Andreas Meisel*[1,2]

[1] Charité – Universitätsmedizin Berlin, Corporate Member of Freie Universität Berlin, Berlin Institute of Health, Humboldt-Universität zu Berlin, Berlin, Germany, [2] Center for Stroke Research Berlin, NeuroCure Clinical Research Center and Department of Neurology, Charité University Hospital Berlin, Berlin, Germany, [3] Centre for Clinical Research, University of Queensland, Herston, QLD, Australia, [4] Department of Medical Immunology, Charité University Medicine & Labor Berlin - Charité Vivantes, Berlin, Germany

Introduction: We aimed to investigate several blood-based biomarkers related to inflammation, immunity, and stress response in a cohort of patients without stroke-associated infections regarding their predictive abilities for functional outcome and explore whether they correlate with MRI markers, such as infarct size or location.

Methods: We combined the clinical and radiological data of patients participating in two observational acute stroke cohorts: the PREDICT and 1000Plus studies. The following blood-based biomarkers were measured in these patients: monocytic HLA-DR, IL-6, IL-8, IL-10, LBP, MRproANP, MRproADM, CTproET, Copeptin, and PCT. Multiparametric stroke MRI was performed including T2*, DWI, FLAIR, TOF-MRA, and perfusion imaging. Standard descriptive sum statistics were used to describe the sample. Associations were analyzed using Fischer's exact test, independent samples *t*-test and Spearmans correlation, where appropriate.

Results: Demographics and stroke characteristics were as follows: 94 patients without infections, mean age 68 years (SD 10.5), 32.2% of subjects were female, median NIHSS score at admission 3 (IQR 2–5), median mRS 3 months after stroke 1 (IQR 0–2), mean volume of DWI lesion at admission 5.7 ml (SD 12.8), mean FLAIR final infarct volume 10 ml (SD 14.9), cortical affection in 61% of infarctions. Acute DWI lesion volume on admission MRI was moderately correlated to admission/maximum IL-6 as well as maximum LBP. Extent of perfusion deficit and mismatch were moderately correlated to admission/maximum IL-6 levels. Final lesion volume on FLAIR was moderately correlated to admission IL-6 levels.

Conclusion: We found IL-6 to be associated with several parameters from acute stroke MRI (acute DWI lesion, perfusion deficit, final infarct size, and affection of cortex) in a cohort of patients not influenced by infections.

Clinical Trial Registration: www.ClinicalTrials.gov, identifiers NCT01079728 and NCT00715533

Keywords: stroke, biomarker, MRI, IL-6, neuroinflammation

OPEN ACCESS

Edited by:
Tobias Ruck,
University of Münster, Germany

Reviewed by:
Mathias Gelderblom,
University Medical Center Hamburg-Eppendorf, Germany
Ali Maisam Afzali,
Technische Universität München, Germany

***Correspondence:**
Benjamin Hotter
benjamin.hotter@charite.de

Specialty section:
This article was submitted to Multiple Sclerosis and Neuroimmunology, a section of the journal Frontiers in Neurology

Received: *18 September 2018*
Accepted: *21 January 2019*
Published: *15 February 2019*

Citation:
Hotter B, Hoffmann S, Ulm L, Meisel C, Fiebach JB and Meisel A (2019) IL-6 Plasma Levels Correlate With Cerebral Perfusion Deficits and Infarct Sizes in Stroke Patients Without Associated Infections. Front. Neurol. 10:83. doi: 10.3389/fneur.2019.00083

INTRODUCTION

Stroke is globally recognized as a leading cause for mortality and adult disability. While the advent of intravenous thrombolysis and recanalization has significantly improved the outcome of stroke, a significant proportion of patients persist to suffer from deficits and disabilities. This is partly explained by the course of stroke itself, but also depending on neurological and medical complications (1–3). Prognosis and precise prediction of outcome remains challenging, especially during the hyperacute phase of the disease. While demographic and clinical characteristics, such as i.e., age and severity of acute clinical syndrome, allow for an educated guess (4), the accuracy of prediction is limited (5). For the post-acute phase of the disease, recent progress has been made in prediction of motor and cognitive recovery (6, 7).

Development of more accurate scores to predict outcome in the acute setting may benefit from the inclusion of biomarkers. While individual association of sanguine parameters with stroke characteristics and functional outcome has been reported, no single biomarker stands out in the field. Immune parameters including cytokines and other acute phase proteins are indicative to the risk of post-stroke infections but have also been associated to functional outcome after stroke (8).

We aimed to investigate a range of inflammation-, immunity-, and stress-related biomarkers in a cohort of patients without stroke-associated infections regarding their predictive abilities for functional outcome and explore whether they correlate with MRI markers, such as infarct size or location.

METHODS

We combined the clinical and radiological data of patients participating in two observational acute stroke cohorts: the PREDICT and 1000Plus studies (clinicaltrials.gov NCT01079728 and NCT00715533). Both studies received full approval by the institutional ethics' committee, including the pooling of data for combined analysis. All patients (or if necessary, their legal representatives) gave informed consent to participation. Protocol details of both studies have been previously published (9, 10). Briefly, both studies recruited acute ischemic stroke patients to investigate either the prediction of stroke-associated pneumonia (PREDICT) or the natural course of multimodal MRI parameters (1000Plus), especially the evolution of DWI-perfusion imaging-

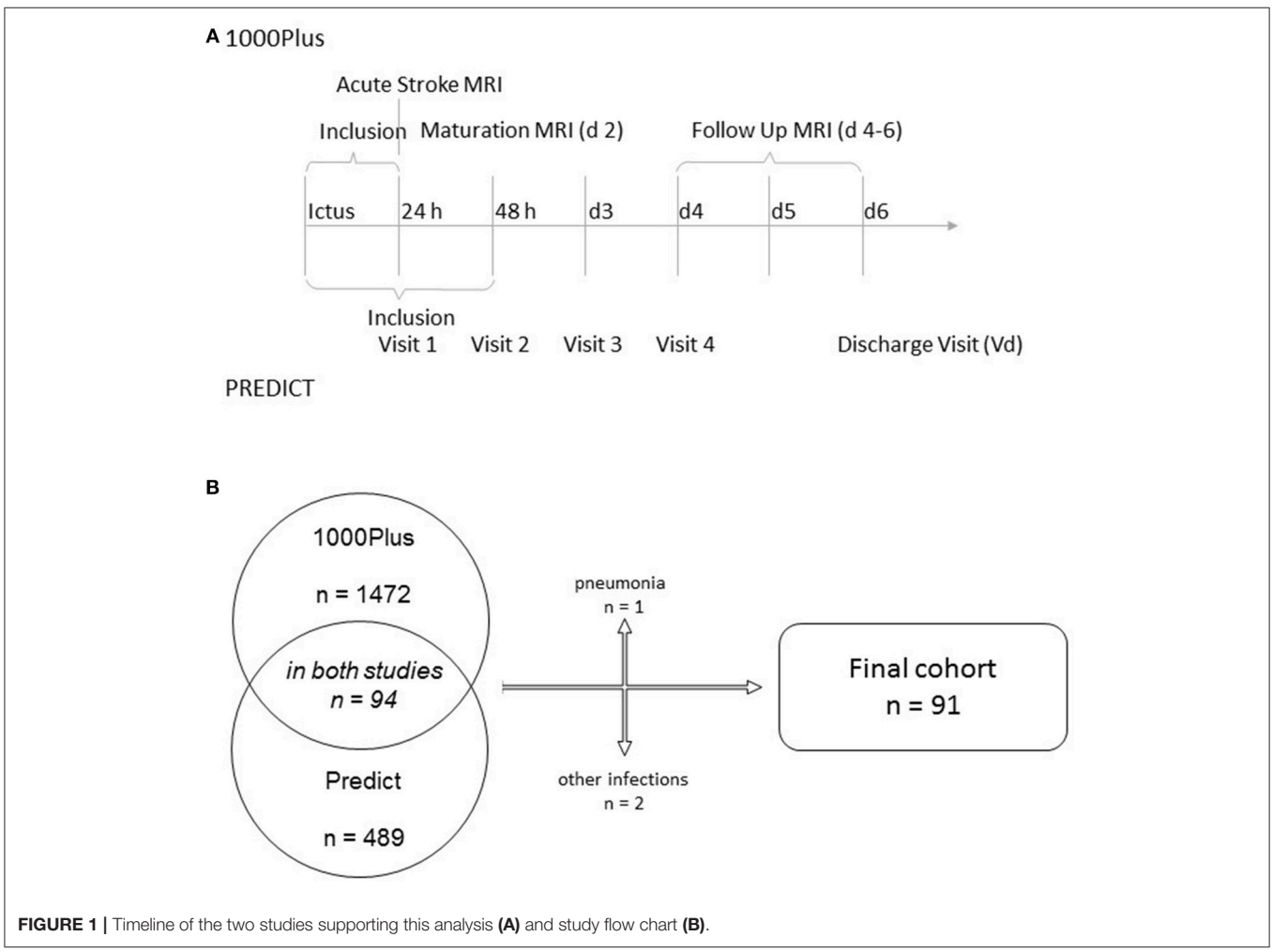


FIGURE 1 | Timeline of the two studies supporting this analysis **(A)** and study flow chart **(B)**.

mismatch. There was significant overlap of visit time points throughout the course of the study (see **Figure 1**). PREDICT was a multicentric study, with one of the participating centers (Charité Campus Benjamin Franklin) being the only study site in the 1000Plus study. PREDICT recruited 189 patients on that common site, 94 of which also participating in the 1000Plus study. We excluded patients suffering from an infection during their time of hospital admission for this analysis.

Blood samples parameters were obtained within the first 4 days of hospital admission. Samples were immediately post-processed and then frozen at −80°C in order to allow for batch analyses at the end of the study. Serum levels of mid-regional pro atrial natriuretic peptide (MRproANP), mid-regional pro adrenomedullin (MRproADM), C-terminal pro endothelin (CTproET), ultrasensitive copeptin (CPus), and ultrasensitive procalcitonin (PCTus) were measured using fluorescent immunoassays on the automated BRAHMS KRYPTOR compact PLUS™ analyzer (BRAHMS GmbH/Thermo Fisher Scientific, Henningsdorf, Germany) according to the manufacturer's protocol. The lower limits of quantitation were 4.5 pmol/l for MRproANP, 0.05 nmol/l for MRproADM, 3 pmol/l for CTproET, 1.9 pmol/l for CPus, and 0,02 μg/l for PCTus. Plasma concentrations of IL-6, IL-8, IL-10, and LBP were determined with the IMMULITE™ semi-automatic chemiluminescent immunoassay (Siemens Medical Solutions, Bad Nauheim, Germany). The detection limit for IL-6 and IL-8 is 2, 1 pg/ml for IL-10 and 0.8 μg/ml for LBP. Expression of human leukocyte antigen-DR (HLA-DR) on monocytes was determined in EDTA whole blood samples by flow cytometry using a highly standardized quantitative assay, as described earlier (9).

Multiparametric stroke MRI was performed on a 3T scanner (Tim Trio; Siemens AG, Erlangen, Germany) at admission (always within 24 h of the event), the following day and lastly 4–6 days after the event. Applied sequences contained T2*, DWI, FLAIR, TOF-MRA, and for the first two imaging time points also perfusion imaging. For further detail please refer to the published protocol (10). Admission MRI was performed as initial imaging upon presentation, or if outside of regular hours as the first examination the next morning. Follow-up MRIs were performed in the morning of the respective days. Blood samples were collected for the first day as soon as the patients and/or their legal representatives consented. The following samples were drawn with the routine laboratory rounds in the morning. Hence, delay between imaging and blood sampling was kept as short as logistically possible.

Standard descriptive sum statistics were used to describe demographics and stroke characteristics as well as biomarker and imaging results. Associations were analyzed by use of Fischer's exact test, independent samples *t*-test and Spearmans correlation, depending on character of variables. Alpha-error level was set at 2-tailed $p = 0.05$. All statistics were performed using SPSS (version 24.0, IBM, Armonk, NY, USA). In view of the small sample size and the explorative nature of the study, we decided against statistical correction such as Bonferroni.

RESULTS

We identified 94 patients participating in both Predict and 1000Plus. Three of them suffered from an infection during the course of their hospital stay and were excluded from this analysis (see **Figure 1B** for further detail). Mean age was 68 years (SD 10.5) and 32.2% of subjects were female. Median NIHSS score at admission was 3 (IQR 2–5). At 3 months, median mRS was 1 (IQR 0–2). Thrombolysis was applied in 23% of patients. For further details on clinical syndrome on admission, risk factors and stroke etiology refer to **Table 1**.

Initial MRI was performed at a median of 549.5 min (IQR 130.25–860) after event. Mean volume of DWI lesion at admission was 5.7 ml (SD 12.8), mean final infarct volume as measured on FLAIR was 10 ml (SD 14.9). The right hemisphere was more frequently affected than the left hemisphere (52 vs. 37%) and cortex was involved in 61% of infarctions. Blood samples were collected during the first 4 days of hospitalization after stroke, and values for day of admission as well as maximum/minimum values are outlined in **Table 2**.

Age of patients was associated with IL-6, MRproANP, MRproADM, and CTproET. Stroke severity at admission as measured by National Institute of Health Stroke Scale

TABLE 1 | Demographics and clinical stroke characteristics.

n	91
Sex, *n* (%) female	29 (32.2)
Age, years, mean (SD)	68.0 (10.5)
Admission NIHSS, median (IQR)	3 (2-5)
Admission mRS, median (IQR)	2 (1-3)
ADMISSION SYMPTOMS	
Aphasia [7]	10 (11.9)
Motor deficit	67 (77.9)
Dysarthria [7]	46 (54.8)
Dysphagia [11]	5 (6.3)
RISK FACTORS	
Diabetes mellitus	25 (28.7)
Atrial fibrillation	14 (16.1)
Previous stroke	16 (18.4)
Arterial hypertension	74 (85.1)
Hyperlipidemia	55 (63.2)
Smoking [61]	5 (16.1)
Thrombolysis	20 (23.0)
TOAST	
Large artery occlusion	56 (64.4)
Cardioembolism	18 (20.7)
Small artery disease	6 (6.9)
Other etiology	3 (3.4)
Unknown etiology	3 (3.4)
Concurring etiology	1 (1.1)
mRS 90 days after event, median (IQR) [17]	1 (0–2)

Values given are n (%) if not explicitly stated otherwise, missing cases reported if >5 as [n]. NIHSS, National Institute of Health Stroke Scale; mRS, modified Rankin Scale; TOAST, Trial of Org10172 in Acute Stroke Treatment.

TABLE 2 | Imaging and blood-based biomarker results.

Hemisphere of DWI lesion	
Right	46 (51.7)
Left	32 (36.0)
Bilateral	11 (12.4)
DWI lesion volume on acute MRI, ml	5.7 (12.8)
PI deficit volume on acute MRI, ml	45.1 (78.0)
DWI-PI mismatch on acute MRI, ml	26.4 (58.5)
TYPE OF INFARCTION	
Territorial	76 (85.4)
Lacunar infarction	12 (13.5)
Borderzone infarction	1 (1.1)
REGIONS AFFECTED	
Any Cortex	54 (60.7)
Caudate	3 (3.3)
Lenticulate	4 (4.4)
Capsula interna	8 (8.8)
Insula	11 (12.1)
ASPECT M1	6 (6.6)
ASPECT M2	17 (18.7)
ASPECT M3	14 (15.4)
ASPECT M4	15 (16.5)
ASPECT M5	34 (37.4)
ASPECT M6	21 (23.1)
FLAIR lesion volume on Follow Up, ml [33]	10.0 (14.9)
HLA-DR, EPITOPES/CELL, MEDIAN (IQR)	
At inclusion [3]	18,387 (14,434–25,788)
Lowest [1]	16,505 (11,386–21,285)
IL-6, PG/ML, MEDIAN (IQR)	
At inclusion [3]	2.8 (2.0–5.2)
Highest [1]	5.2 (2.7–11.0)
IL-8, PG/ML, MEDIAN (IQR)	
At inclusion [3]	5.0 (5.0–5.0)
Highest [1]	5.0 (5.0–5.2)
IL-10, PG/ML, MEDIAN (IQR)	
At inclusion [3]	5.0 (5.0–5.0)
Highest [1]	5.0 (5.0–5.0)
LBP, μG/ML, MEDIAN (IQR)	
At inclusion [3]	7.23 (5.48–9.34)
Highest [1]	8.90 (6.68–11.65)
MPproANP, PG/ML, MEDIAN (IQR)	
At inclusion [29]	111.4 (65.5–180.9)
Highest [23]	122.5 (79.1–195.8)
MPproADM, PG/ML, MEDIAN (IQR)	
At inclusion [29]	0.703 (0.593–0.868)
Highest [22]	0.751 (0.613–0.917)
CTproET, PG/ML, MEDIAN (IQR)	
At inclusion [30]	61.4 (50.7–75.9)
Highest [22]	64.4 (54.6–83.1)
CPus, PG/ML, MEDIAN (IQR)	
At inclusion [29]	8.84 (5.27–14.22)
Highest [22]	10.19 (5.60–17.40)
PCT us, PG/ML, MEDIAN (IQR)	
At inclusion [30]	0.031 (0.024–0.041)
Highest [23]	0.039 (0.028–0.050)

Values given are n (%) if not explicitly stated otherwise, missing cases reported if >5 as [n]. HLA-DR, Human leukocyte antigen expression on monocytes; IL-6, IL-8, IL-10, three interleukins; LBP, lipopolysaccharide-binding protein; MRproANP, mid-regional pro atrial natriuretic peptide; MRproADM, mid-regional pro adrenomedullin; CTproET, C-terminal pro endothelin; CPus, ultrasensitive copeptin; PCTus, ultrasensitive procalcitonin.

(NIHSS) score was associated with IL-6. Functional outcome as measured by modified Rankin Scale (mRS) at day 90 was associated with admission levels of ultrasensitive Copeptin, maximum MRproADM, IL-6, and minimum HLA-DR levels (**Table 3**).

Acute volume of DWI restriction on admission MRI scans was moderately correlated to admission (Spearman's ρ 0.336) and maximum (Spearman's ρ 0.276) IL-6 as well as maximum LBP (Spearman's ρ 0.222) levels. Extent of perfusion imaging (PI) deficit and DWI-PI-Mismatch were moderately correlated to admission (Spearman's ρ 0.306 and 0.231, respectively) and maximum (Spearman's ρ 0.277 and 0.215, respectively) IL-6 levels. Final lesion volume on FLAIR was moderately correlated to admission IL-6 levels (Spearman's ρ 0.364) (**Table 4**). Cortical infarcts were associated with higher IL-6 levels at admission. By use of the ASPECT scoring system we only found inconsistent associations of biomarker levels with infarct location (**Supplementary Table 1**).

DISCUSSION

We examined the relationship of inflammatory, immune, and stress biomarkers with MRI parameters in 91 stroke patients not suffering from stroke-associated infections during the course of the study. Interleukin-6 was associated with infarct size and tissue at risk, as well as final infarct volume. The other studied biomarkers did not show any associations with imaging markers in the absence of infection. Overall, the studied cohort was rather mildly affected by stroke (median admission NIHSS 3 IQR 2–5 and 3 months mRS 1 IQR 0–2).

The biological role of IL-6 in ischemic stroke remains uncertain. Astrocytes and microglia express IL-6, but whether it primarily exerts neurotoxic or—protective effects is a matter of scientific discourse (11, 12). Our study found a significant association of IL-6 levels with NIHSS scores at admission, although Spearman's ρ only showed moderate correlation. Furthermore, we found a significant correlation of IL-6 levels with lesion volume, whether on DWI scans at admission, PI deficit, DWI-PI mismatch or on follow-up FLAIR images, which is in line with the association of IL-6 levels and NIHSS scores at admission. Infarct size has previously been reported to correlate at least with intrathecal levels, but not consistently with serum levels, of IL-6 (13–15). IL-6 was repeatedly associated with poor functional outcome, but whether this is an independent effect or a signal due to infection remains unclear (8). Our data shows a significant association of IL-6 with functional outcome as measured by mRS in a cohort of patients not suffering from infection, further corroborating an association independent of infections. IL-6 has been previously linked to small vessel disease and silent cerebral infarctions (16–18). IL-6 and also IL-10 were associated with the presence of diffusion-perfusion- or clinical-diffusion-mismatch on acute stroke MRI (19–21). Furthermore, cortical infarcts were associated with IL-6. The associations of several other biomarkers with localization of lesions have to be interpreted with caution considering the sample size and plausibility.

TABLE 3 | Association of biomarkers at inclusion and lowest/highest measurement with clinical parameters.

		Aphasia	Motor deficit	Dysarthria	Dysphagia	Sex	NIHSS	mRS d90	Age
HLA-DR	Inclusion	0.405	0.979	0.548	0.757	0.606	0.409	0.052	0.249
	Lowest	0.987	0.436	0.959	0.173	0.340	0.099	**0.030**	0.069
IL-6	Inclusion	0.410	0.478	0.912	0.739	0.824	**0.005**	0.252	**0.001**
	Highest	0.369	0.281	0.983	0.438	0.884	**0.005**	**0.015**	**0.030**
IL-8	Inclusion	0.443	**0.050**	0.640	0.552	0.803	0.073	0.226	0.339
	Highest	0.633	0.393	0.386	0.467	0.597	0.331	0.683	0.566
IL-10	Inclusion	0.416	0.468	0.136	0.611	0.564	0.916	0.248	0.460
	Highest	0.247	0.360	0.257	0.727	0.989	0.683	0.587	0.236
LBP	Inclusion	0.086	0.364	0.958	0.660	0.227	0.291	0.952	0.148
	Highest	0.857	0.861	0.442	0.353	0.621	0.062	0.637	0.152
MPproANP	Inclusion	0.486	0.640	**0.012**	**0.029**	0.914	0.163	0.654	**0.005**
	Highest	0.521	0.287	**0.047**	**0.005**	0.926	0.068	0.911	**0.005**
MPproADM	Inclusion	**0.001**	0.320	0.310	0.915	0.296	0.241	0.264	**<0.001**
	Highest	0.351	0.209	0.618	0.979	0.547	0.158	**0.043**	**0.001**
CTproET	Inclusion	0.398	0.323	0.613	0.994	0.962	0.160	0.344	**0.018**
	Highest	**0.015**	0.330	0.893	0.888	0.933	0.092	0.169	**0.039**
Copeptin us	Inclusion	0.720	0.455	0.548	0.436	0.357	0.768	**0.006**	0.540
	Highest	0.335	0.910	0.354	0.441	0.115	0.918	0.144	0.298
PCT us	Inclusion	0.643	0.381	**0.007**	0.736	0.286	0.254	0.962	0.975
	Highest	0.855	0.560	0.056	0.908	0.362	0.634	0.230	0.711

Values given are two-sided p-values obtained by a students' t-test; Bold text denotes significant associations; HLA-DR, Human leukocyte antigen expression on monocytes; IL-6, IL-8, IL-10, three interleukins; LBP, lipopolysaccharide-binding protein; MRproANP, mid-regional pro atrial natriuretic peptide; MRproADM, mid-regional pro adrenomedullin; CTproET, C-terminal pro endothelin; CPus, ultrasensitive copeptin; PCTus, ultrasensitive procalcitonin.

Interestingly, in our cohort of patients not suffering from infections, plasma levels of IL-8 and IL-10 were mostly not detectable and below the upper limit of normal (5.0 pg/ml). This is in line with previous findings by us and Chamorro et al. showing increased IL-10 levels in patients with stroke-associated infections (22, 23). These cytokines may therefore be mainly triggered by systemic inflammation in the course of infectious complications after stroke, whereas neuroinflammation within the CNS does not seem to trigger their expression.

As previously described, we found functional outcome after 3 months to be inversely correlated to HLA-DR (24), and furthermore correlated to MRproADM and ultrasensitive Copeptin. Expression of monocytic HLA-DR is a marker of monocyte activation and has been shown to be a key marker for stroke-induced immune depression (9, 25). Lower HLA-DR expression is a strong predictor of stroke-associated pneumonia and is associated with worse functional outcome (9, 24). The latter association is further corroborated in our data independent of infection.

Several biomarkers showed an association with age, and while this has previously been reported for CTproET (26) and appears plausible for a vascular stress marker as MRproANP, the relationship for MRproADM and IL-6 is less seemingly obvious. LBP is a marker of bacterial translocation and higher levels are found in patients with post-stroke infection (27). It is also associated with a worse short-term stroke outcome (28). We could not reproduce this finding in stroke patients not suffering from infection or show any association with imaging characteristics. MRproANP is used as a biomarker for hemodynamic stress and was previously shown to indicate higher risk for ischemic stroke (29). There were no significant associations with imaging characteristics or functional outcome in our cohort. MRproADM exerts vasodilating, vasoprotective, and angiogenic effects and is associated with post-stroke infections (30) and functional outcome after stroke (31). MRproADM has been associated with progression of small vessel disease accompanying cognitive decline (32). We could not reproduce the association with poor outcome or find an association with imaging characteristics. The vasopressin surrogate CP has been associated with higher risk of all-cause mortality, poor functional outcome and infections after ischemic stroke (33–36). Furthermore, it has been proposed to improve prediction of recurring cerebrovascular events (37). CTproET is influenced by age, renal function, and hemodynamic parameters of healthy subjects, and is a strong vasoconstrictor (26). While it has not been studied as biomarker in ischemic stroke before, its derivative endothelin has been associated with carotid atherosclerosis and silent cerebral infarctions (38). Both biomarkers were not associated with outcome in our cohort, and did not show any significant correlations with imaging findings. PCT is a blood-based marker for infection in general and was shown to be associated with post-stroke infections and functional outcome (36, 39, 40). Furthermore, higher levels of PCT are associated with extent of small vessel disease and silent infarctions on MRI (41). Our data did not show an association with functional outcome or imaging characteristics.

TABLE 4 | Association of biomarkers at inclusion and lowest/highest measurement with imaging parameters.

		Initial DWI volume	Initial PI deficit	Initial mismatch	Final FLAIR volume
HLA-DR	At Inclusion	0.933	0.936	0.716	0.397
	Lowest	0.678	0.234	0.443	0.300
IL-6	At Inclusion	**0.002**	**0.016**	**0.030**	**0.006**
	Highest	**0.009**	**0.029**	**0.042**	0.383
IL-8	At Inclusion	0.955	0.667	0.928	0.068
	Highest	0.787	0.798	0.099	0.347
IL-10	At Inclusion	0.290	0.555	0.701	0.822
	Highest	0.081	0.101	0.595	0.435
LBP	At Inclusion	0.084	0.877	0.625	0.546
	Highest	**0.037**	0.349	0.431	0.688
MPproANP	At Inclusion	0.949	0.945	0.566	0.830
	Highest	0.853	0.795	0.486	0.941
MPproADM	At Inclusion	0.882	0.901	0.123	0.130
	Highest	0.682	0.801	0.267	0.340
CTproET	At Inclusion	0.923	0.887	0.665	0.827
	Highest	0.834	0.906	0.541	0.849
Copeptin us	At Inclusion	0.144	0.801	0.457	0.701
	Highest	0.487	0.673	0.648	0.815
PCT us	At Inclusion	0.804	0.214	0.224	0.637
	Highest	0.418	0.151	0.381	0.513

Values given are two-sided p-values obtained by a Spearman's correlation; Bold text denotes significant associations; HLA-DR, Human leukocyte antigen expression on monocytes; IL-6, IL-8, IL-10, three interleukins; LBP, lipopolysaccharide-binding protein; MRproANP, mid-regional pro atrial natriuretic peptide; MRproADM, mid-regional pro adrenomedullin; CTproET, C-terminal pro endothelin; CPus, ultrasensitive copeptin; PCTus, ultrasensitive procalcitonin.

Our study suffers from several limitations: the sample size, while average for a study in this field, is limited, especially considering the amount of analyses performed. While multiple testing was a concern for us, the purpose of this study was purely exploratory. Our findings need to be corroborated by further confirmatory studies. Furthermore, our study cohort was overall rather mildly affected by stroke, not necessarily reflecting a cohort of severely impaired patients. Strengths of this report are the prospective collection of data with an in-depth clinical and neuroradiological assessment during the acute course of the disease avoiding recall H bias.

Our data supports the conclusion that IL-6 is an inflammatory marker of cerebral parenchymal damage independent of systemic infections.

DATA AVAILABILITY

The raw data supporting the conclusions of this manuscript will be made available by the authors, without undue reservation, to any qualified researcher.

AUTHOR CONTRIBUTIONS

BH wrote the manuscript and conducted all statistical analyses. SH and LU co-designed the PREDICT study and revised the manuscript. JF designed the 1000Plus study and was a major contributor in writing the manuscript. CM was a major contributor in writing the manuscript. AM designed the trial and was a major contributor in writing and revising the manuscript. All authors read and approved the final manuscript.

FUNDING

This analysis was based on the PREDICT study funded by German Research Foundation (Exc257), German Federal Ministry of Education and Research (01EO0801), European Community FP7 (201024), and Siemens Healthcare Diagnostics, and the 1000Plus study funded by the Federal Ministry of Education and Research (01 EO 0801). Additional funding was received from Thermo Fisher Scientific BRAHMS GmbH, Germany. Design of the study, as well as collection, analysis, and interpretation of data, as well as writing of the manuscript were independent of all funding sources.

SUPPLEMENTARY MATERIAL

The Supplementary Material for this article can be found online at: https://www.frontiersin.org/articles/10.3389/fneur.2019.00083/full#supplementary-material

REFERENCES

1. Kumar S, Selim MH, Caplan LR. Medical complications after stroke. *Lancet Neurol.* (2010) 9:105–18. doi: 10.1016/S1474-4422(09)70266-2
2. Weimar C, Roth MP, Zillessen G, Glahn J, Wimmer MLJ, Busse O, et al. Complications following acute ischemic stroke. *Eur Neurol.* (2002) 48:133–40. doi: 10.1159/000065512
3. Heuschmann PU, Wiedmann S, Wellwood I, Rudd A, Di Carlo A, Bejot Y, et al. Three-month stroke outcome: the European Registers of Stroke (EROS) investigators. *Neurology* (2011) 76:159–65. doi: 10.1212/WNL.0b013e318206ca1e
4. Ntaios G, Faouzi M, Ferrari J, Lang W, Vemmos K, Michel P. An integer-based score to predict functional outcome in acute ischemic stroke: the ASTRAL score. *Neurology* (2012) 78:1916–22. doi: 10.1212/WNL.0b013e318259e221
5. Byblow WD, Stinear CM. It is difficult to make predictions, especially about the future. *Stroke* (2017) 48:3187–8. doi: 10.1161/STROKEAHA.117.019071
6. Scrutinio D, Lanzillo B, Guida P, Mastropasqua F, Monitillo V, Pusineri M, et al. Development and validation of a predictive model for functional outcome after stroke rehabilitation: the maugeri model. *Stroke* (2017) 48:3308–15. doi: 10.1161/STROKEAHA.117.018058
7. Stinear CM. Prediction of motor recovery after stroke: advances in biomarkers. *Lancet Neurol.* (2017) 16:826–36. doi: 10.1016/S1474-4422(17)30283-1
8. Bustamante A, Sobrino T, Giralt D, García-Berrocoso T, Llombart V, Ugarriza I, et al. Prognostic value of blood interleukin-6 in the prediction of functional outcome after stroke: a systematic review and meta-analysis. *J Neuroimmunol.* (2014) 274:215–24. doi: 10.1016/j.jneuroim.2014.07.01
9. Hoffmann S, Harms H, Ulm L, Nabavi DG, Mackert B-M, Schmehl I, et al. Stroke-induced immunodepression and dysphagia independently predict stroke-associated pneumonia - The PREDICT study. *J Cereb Blood Flow Metab.* (2016) 37:3671–82. doi: 10.1177/0271678X16671964
10. Hotter B, Pittl S, Ebinger M, Oepen G, Jegzentis K, Kudo K, et al. Prospective study on the mismatch concept in acute stroke patients within the first 24 h after symptom onset - 1000Plus study. *BMC Neurol.* (2009) 9:60. doi: 10.1186/1471-2377-9-60
11. Van Wagoner NJ, Benveniste EN. Interleukin-6 expression and regulation in astrocytes. *J Neuroimmunol.* (1999) 100:124–39. doi: 10.1016/S0165-5728(99)00187-3
12. Müller B. Cytokine imbalance in non-immunological chronic disease. *Cytokine* (2002) 18:334–9. doi: 10.1006/cyto.2002.0882
13. Tarkowski E, Rosengren L, Blomstrand C, Wikkelso C, Jensen C, Ekholm S, et al. Early intrathecal production of interleukin-6 predicts the size of brain lesion in stroke. *Stroke* (1995) 26:1393–8. doi: 10.1161/01.STR.26.8.1393
14. Ormstad H, Aass HCD, Lund-Sørensen N, Amthor K-F, Sandvik L. Serum levels of cytokines and C-reactive protein in acute ischemic stroke patients, and their relationship to stroke lateralization, type, and infarct volume. *J Neurol.* (2011) 258:677–85. doi: 10.1007/s00415-011-6006-0
15. Waje-Andreassen U, Krakenes J, Ulvestad E, Thomassen L, Myhr KM, Aarseth J, et al. IL-6: an early marker for outcome in acute ischemic stroke. *Acta Neurol Scand.* (2005) 111:360–5. doi: 10.1111/j.1600-0404.2005.00416.x
16. Satizabal CL, Zhu YC, Mazoyer B, Dufouil C, Tzourio C. Circulating IL-6 and CRP are associated with MRI findings in the elderly: the 3C-Dijon Study. *Neurology* (2012) 78:720–7. doi: 10.1212/WNL.0b013e318248e50f
17. Miwa K, Tanaka M, Okazaki S, Furukado S, Sakaguchi M, Kitagawa K. Relations of blood inflammatory marker levels with cerebral microbleeds. *Stroke* (2011) 42:3202–6. doi: 10.1161/STROKEAHA.111.621193
18. Hoshi T, Kitagawa K, Yamagami H, Furukado S, Hougaku H, Hori M. Relations of serum high-sensitivity C-reactive protein and interleukin-6 levels with silent brain infarction. *Stroke* (2005) 36:768–72. doi: 10.1161/01.STR.0000158915.28329.51
19. Montaner J, Rovira A, Molina CA, Arenillas JF, Ribó M, Chacón P, et al. Plasmatic level of neuroinflammatory markers predict the extent of diffusion-weighted image lesions in hyperacute stroke. *J Cereb Blood Flow Metab.* (2003) 23:1403–7. doi: 10.1097/01.WCB.0000100044.07481.97
20. Rodríguez-Yánez M, Sobrino T, Arias S, Vázquez-Herrero F, Brea D, Blanco M, et al. Early biomarkers of clinical-diffusion mismatch in acute ischemic stroke. *Stroke* (2011) 42:2813–8. doi: 10.1161/STROKEAHA.111.614503
21. Rodríguez-Yánez M, Castellanos M, Sobrino T, Brea D, Ramos-Cabrer P, Pedraza S, et al. Interleukin-10 facilitates the selection of patients for systemic thrombolysis. *BMC Neurol.* (2013) 13:62. doi: 10.1186/1471-2377-13-62
22. Chamorro A, Amaro S, Vargas M, Obach V, Cervera A, Torres F, et al. Interleukin 10, monocytes and increased risk of early infection in ischaemic stroke. *J Neurol Neurosurg Psychiatr.* (2006) 77:1279–81. doi: 10.1136/jnnp.2006.100800
23. Klehmet J, Harms H, Richter M, Prass K, Volk HD, Dirnagl U, et al. Stroke-induced immunodepression and post-stroke infections: lessons from the preventive antibacterial therapy in stroke trial. *Neuroscience* (2009) 158:1184–93. doi: 10.1016/j.neuroscience.2008.07.044
24. Urra X, Cervera Á, Obach V, Climent N, Planas AM, Chamorro A. Monocytes are major players in the prognosis and risk of infection after acute stroke. *Stroke* (2009) 40:1262–8. doi: 10.1161/STROKEAHA.108.532085
25. Hug A, Dalpke A, Wieczorek N, Giese T, Lorenz A, Auffarth G, et al. Infarct volume is a major determiner of post-stroke immune cell function and susceptibility to infection. *Stroke* (2009) 40:3226–32. doi: 10.1161/STROKEAHA.109.557967
26. Bhandari SS, Davies JE, Struck J, Ng LL. Plasma C-terminal proEndothelin-1 (CTproET-1) is affected by age, renal function, left atrial size and diastolic blood pressure in healthy subjects. *Peptides* (2014) 52:53–7. doi: 10.1016/j.peptides.2013.12.001
27. Worthmann H, Tryc AB, Dirks M, Schuppner R, Brand K, Klawonn F, et al. Lipopolysaccharide binding protein, interleukin-10, interleukin-6 and C-reactive protein blood levels in acute ischemic stroke patients with post-stroke infection. *J Neuroinflammation* (2015) 12:13. doi: 10.1186/s12974-014-0231-2
28. Klimiec E, Pera J, Chrzanowska-Wasko J, Golenia A, Slowik A, Dziedzic T. Plasma endotoxin activity rises during ischemic stroke and is associated with worse short-term outcome. *J Neuroimmunol.* (2016) 297:76–80. doi: 10.1016/j.jneuroim.2016.05.006
29. Katan M, Moon YP, Paik MC, Mueller B, Huber A, Sacco RL, et al. Procalcitonin and midregional proatrial natriuretic peptide as markers of ischemic stroke: the Northern Manhattan study. *Stroke* (2016) 47:1714–9. doi: 10.1161/STROKEAHA.115.011392
30. Bustamante A, García-Berrocoso T, Penalba A, Giralt D, Simats A, Muchada M, et al. Sepsis biomarkers reprofiling to predict stroke-associated infections. *J Neuroimmunol.* (2017) 312:19–23. doi: 10.1016/j.jneuroim.2017.08.012
31. Seifert-Held T, Pekar T, Gattringer T, Simmet NE, Scharnagl H, Bocksrucker C, et al. Plasma midregional pro-adrenomedullin improves prediction of functional outcome in ischemic stroke. *PLoS ONE* (2013) 8:e68768. doi: 10.1371/journal.pone.0068768
32. Kuriyama N, Ihara M, Mizuno T, Ozaki E, Matsui D, Watanabe I, et al. Association between mid-regional proadrenomedullin levels and progression of deep white matter lesions in the brain accompanying cognitive decline. *J Alzheimers Dis.* (2017) 56:1253–62. doi: 10.3233/JAD-160901
33. Xu Q, Tian Y, Peng H, Li H. Copeptin as a biomarker for prediction of prognosis of acute ischemic stroke and transient ischemic attack: a meta-analysis. *Hypertens Res.* (2017) 40:465–71. doi: 10.1038/hr.2016.165
34. Tu W-J, Ma G-Z, Ni Y, Hu X-S, Luo D-Z, Zeng X-W, et al. Copeptin and NT-proBNP for prediction of all-cause and cardiovascular death in ischemic stroke. *Neurology* (2017) 88:1899–905. doi: 10.1212/WNL.0000000000003937
35. Katan M, Fluri F, Morgenthaler NG, Schuetz P, Zweifel C, Bingisser R, et al. Copeptin: a novel, independent prognostic marker in patients with ischemic stroke. *Ann Neurol.* (2009) 66:799–808. doi: 10.1002/ana.21783
36. Fluri F, Morgenthaler NG, Mueller B, Christ-Crain M, Katan M. Copeptin, procalcitonin and routine inflammatory markers-predictors of infection after stroke. *PLoS ONE* (2012) 7:e48309. doi: 10.1371/journal.pone.0048309
37. De Marchis GM, Weck A, Audebert H, Benik S, Foerch C, Buhl D, et al. Copeptin for the prediction of recurrent cerebrovascular events after transient

ischemic attack: results from the CoRisk study. *Stroke* (2014) 45:2918–23. doi: 10.1161/STROKEAHA.114.005584

38. Minami S, Yamano S, Yamamoto Y, Sasaki R, Nakashima T, Takaoka M, et al. Associations of plasma endothelin concentration with carotid atherosclerosis and asymptomatic cerebrovascular lesions in patients with essential hypertension. *Hypertens Res.* (2001) 24:663–70. doi: 10.1291/hypres.24.663
39. Ulm L, Hoffmann S, Nabavi DG, Hermans M, Mackert B-M, Hamilton F, et al. The Randomized Controlled STRAWINSKI Trial: procalcitonin-guided antibiotic therapy after stroke. *Front Neurol.* (2017) 8:153. doi: 10.3389/fneur.2017.00153
40. Wang C, Gao L, Zhang Z-G, Li Y-Q, Yang Y-L, Chang T, et al. Procalcitonin is a stronger predictor of long-term functional outcome and mortality than high-sensitivity C-reactive protein in patients with ischemic stroke. *Mol Neurobiol.* (2016) 53:1509–17. doi: 10.1007/s12035-015-9112-7
41. Li G, Zhu C, Li J, Wang X, Zhang Q, Zheng H, et al. Increased level of procalcitonin is associated with total MRI burden of cerebral small vessel disease in patients with ischemic stroke. *Neurosci Lett.* (2018) 662:242–6. doi: 10.1016/j.neulet.2017.10.040

Conflict of Interest Statement: The authors declare that the research was conducted in the absence of any commercial or financial relationships that could be construed as a potential conflict of interest.

Copyright © 2019 Hotter, Hoffmann, Ulm, Meisel, Fiebach and Meisel. This is an open-access article distributed under the terms of the Creative Commons Attribution License (CC BY). The use, distribution or reproduction in other forums is permitted, provided the original author(s) and the copyright owner(s) are credited and that the original publication in this journal is cited, in accordance with accepted academic practice. No use, distribution or reproduction is permitted which does not comply with these terms.

frontiers in Neurology

ORIGINAL RESEARCH
published: 22 February 2019
doi: 10.3389/fneur.2019.00132

Predictors for Therapy Response to Intrathecal Corticosteroid Therapy in Multiple Sclerosis

*Katja Vohl, Alexander Duscha, Barbara Gisevius, Johannes Kaisler, Ralf Gold and Aiden Haghikia**

Department of Neurology, Ruhr-University Bochum, St. Josef-Hospital, Bochum, Germany

Objective: The autoimmune disease Multiple Sclerosis (MS) represents a heterogeneous disease pattern with an individual course that may lead to permanent disability. In addition to immuno-modulating therapies patients benefit from symptomatic approaches like intrathecal corticosteroid therapy (ICT), which is frequently applied in a growing number of centers in Germany. ICT reduces spasticity, which elongates patient's walking distance and speed, thus improves quality of life.

Methods: In our study we set out to investigate cerebrospinal fluid (CSF) parameters and clinical predictors for response to ICT. Therefore, we analyzed 811 CSF samples collected from 354 patients over a time period of 12 years. Patients who received ICT were divided in two groups (improving or active group) depending on their EDSS-progress. As control groups we analyzed data of ICT naïve patients, who were divided in the two groups as well. Additionally we observed the clinical progress after receiving ICT by comparison of patients in both groups.

Results: The results showed clinical data had a significant influence on the probability to benefit from ICT. The probability (shown by Odds Ratio of 1.77–2.43) to belong to the improving group in contrast to the active group is significantly ($p < 0.0001$) higher at later stages of disease with early disease onset (<35 years, OR = 2.43) and higher EDSS at timepoint of ICT-initiation (EDSS > 6, OR = 2.06). Additionally, we observed lower CSF cell counts (6.68 ± 1.37 μl) and lower total CSF protein (412 ± 18.25 mg/l) of patients who responded to ICT compared to patients who did not ($p < 0.05$). In the control group no significant differences were revealed. Furthermore analyses of our data revealed patients belonging to the improving group reach an EDSS of 6 after ICT-initiation less often than patients of the active group (after 13 years 39.8% in the improving group, 67.8% in the active group).

Conclusion: Our study implies two relevant messages: (i) although the study was not designed to prospectively assess clinical data, in this cohort no severe side effects were observed under ICT; (ii) disease onset, EDSS, CSF cell count, and total protein may serve as predictive markers for therapy response.

Keywords: multiple sclerosis, disease progression, intrathecal corticosteroid therapy, clinical predictor, cerebrospinal fluid

OPEN ACCESS

Edited by:
Stefan Bittner, Johannes Gutenberg University Mainz, Germany

Reviewed by:
Clemens Warnke, Uniklinik Köln, Germany
Moussa Antoine Chalah, Hôpitaux Universitaires Henri Mondor, France

****Correspondence:***
Aiden Haghikia
aiden.haghikia@rub.de

Specialty section:
This article was submitted to Multiple Sclerosis and Neuroimmunology, a section of the journal Frontiers in Neurology

Received: *07 October 2018*
Accepted: *31 January 2019*
Published: *22 February 2019*

Citation:
Vohl K, Duscha A, Gisevius B, Kaisler J, Gold R and Haghikia A (2019) Predictors for Therapy Response to Intrathecal Corticosteroid Therapy in Multiple Sclerosis. Front. Neurol. 10:132. doi: 10.3389/fneur.2019.00132

INTRODUCTION

Multiple Sclerosis (MS) is one of the most common non-traumatic neurological diseases of young adults (1). Besides the immunological component of MS, axonal damage is a pathological hallmark of disease, which causes permanent disability (2). Despite already existing and approved immunomodulating therapies for MS, chronic disability, and disease progression caused by neurodegeneration still pose a therapeutic challenge. More than 80% of patients afflicted by MS suffer from spasticity during disease, subsequently leading to critical impairment of daily life routine in 30% of these patients (3), i.e., reduced or diminished walking ability. After insufficient response to first-line (oral) antispastic therapies, intrathecal corticosteroid therapy (ICT) is an adjuvant option to reduce permanent disability (3). Several studies have previously shown the efficacy of ICT in various cohorts (3, 4). ICT can reduce the Expanded Disability Status Scale (EDSS), elongates walking distance and increases walking speed (3). Moreover, ICT improves effectively neuropathic pain which is caused by disease activity (5). In summary, ICT is stated as a safe and effective option for the reduction of disability (6). Additionally, ICT has a beneficial impact on bladder function (3) and generally improves quality of life in responsive patients. Thus, ICT is a promising option to slow down disease progression and reduce permanent disability. However, aside from the clinical improvement no stratifying markers for therapy response/non-response are available so far. Hence, the aim of our study was to identify possible CSF markers that may predict the individual response to ICT. CSF, due to its proximity to MS pathomechanism, has been shown to be a suitable biocompartment, e.g., for epigenetic markers (7), that is usually not affected by systemic metabolic processes derived from the peripheral blood (8).

In our department, we have established (4, 5) and performed ICT for decades. Patients usually receive a cumulative dose of 40–200 mg triamcinolone-acetonide (Volon A) via 1–3 injections (every other day) every 3 months on average in an individualized manner (9). With this study we addressed the following questions: (I) Are there any differences in standard CSF parameters to distinguish between response and non-response to ICT?; and (II) which clinical parameters indicate a beneficial response to ICT?

METHODS

Retrospective data from patients assessed during clinical routine at the Department of Neurology of the Ruhr-University Bochum, St. Josef-Hospital since 2005 were considered for analysis. CSF analysis for possible surrogate markers was approved by the ethics committee of the Department of Medicine at the Ruhr-University Bochum (registration number 4493-12). The mean observation period per patient comprised to 2.58 ± 2.51 years. The distribution of the observation intervals is shown in **Table 1**. We analyzed a total of 811 CSF samples from 354 different patients. All study patients had been diagnosed with MS according to the McDonald criteria (10) including all different disease subtypes, i.e., relapsing remitting (RR), secondary progressive (SP), and primary progressive (PP). Only those patients who had been unstable with other MS medication for at least 6 months and showed insufficient response to oral first line antispastic therapies received ICT. Written and informed consent of all patients was obtained before initiation of ICT. We screened 206 patients (with 508 CSF analyzed samples) who had received ICT at least at one time point, and 148 patients (with 303 CSF analyses) who had been ICT naïve. Patients and CSF values were included in this study fulfilling the mentioned criteria. Patients were followed longitudinally for their EDSS as well as their CSF.

CSF assessment and analysis were performed once before the first ICT injection and afterwards as follow up during longitudinal ICT. Lumbar punctures of patients, who did not receive ICT, were part of diagnostic routine, for instance reevaluation of diagnosis or verification of the conversion of oligoclonal bands. Triamcinolon (40–80 mg) was injected directly into the CSF under sterile conditions using an atraumatic needle (4).

Patients were divided into two groups depending on their respective clinical progress mirrored by individual EDSS (11). EDSS was collected routinely in our department, thus it is possible to monitor patient's disability progression retrospectively over a long period of time as it was essential in our study. We defined two groups based on the ratio of first determined EDSS and the mean of all following respective EDSS of the same patient ≥ 1: improving group—patients, whose EDSS remained stable or decreased over time < 1: active group—patients, whose EDSS increased over time.

Due to the retrospective character of our study, the evaluation of the EDSS in standardized time intervals was not possible. However, the EDSS assessment prior to the first ICT-injection was evaluated in a time range of 1.2 ± 0.24 years, the EDSS

TABLE 1 | Observation Interval of ICT patients; number of values and patients of the observation intervals.

Observation interval	Number of patients	Number of CSF values
Less than 1 year	6	26
1–2 years	93	127
2–3 years	50	75
3–4 years	37	50
4–5 years	34	54
5–6 years	31	66
6–7 years	18	51
7–8 years	15	47
8–9 years	22	81
9–10 years	20	72
10–11 years	11	63
11–12 years	10	51
More than 12 years	7	48

Abbreviations: MS, Multiple Sclerosis; ICT, intrathecal corticosteroid therapy; EDSS, Expanded Disability Status Scale; CSF, cerebrospinal fluid; RRMS, relapsing remitting MS; SPMS, secondary progressive MS; PPMS, primary progressive MS.

post ICT-injection was evaluated in a time range of 1.68 ± 0.26 years. By definition we excluded patients of whom only one EDSS value was available during the observation period, which leads to an impediment for a definitive group assignment. Hence, for final assessment we included 157 patients with 446 CSF samples who received ICT, and additionally 103 patients with 213 CSF analyses who were ICT naïve. Detailed demographic information of patients is shown in **Table 2**. We compared these two groups separately for patients who received ICT and patients who were ICT naïve, because of the retrospective vs. cross sectional character of data used for the study. Statistical analysis for CSF parameters of these subgroups was performed by Mann-Whitney-*U*-test, after Kolmogorov–Smirnov-Test had ruled out Gaussian distribution. Therefore, we included all baseline data of CSF of all patients included in the improving or active group to represent the long-term changes. Additionally we analyzed the patients mean cell count to show patient's intrapersonal cell count value dependent on individual disease progress and activity. To examine clinical parameters of patients we used fisher's exact test. For the examination of clinical parameters, we defined specific ranges of these parameters: age range at diagnosis and manifestation were set up to 35 years based on epidemiological data suggesting a transition age of RRMS to SPMS at 33 years (12). We stratified EDSS in below and above EDSS 6 (13, 14).

Kaplan Maier analysis was performed for evaluating risk of disease progression, i.e., disease progression defined as EDSS increase above 6 over time for both ICT receiving groups; statistical analysis was performed by log-rank (Mantel-Cox) test. All statistical data in figures are shown with mean ± SEM, following p were considered as statistically significant: $p < 0.05$, $p < 0.001$, and $p < 0.0001$.

Additionally, we evaluated the effect of patient specific MS medication in combination with or without ICT, i.e., established immuno-modulating therapies used in MS like interferon-beta, glatiramer acetate, fingolimod, dimethylfumarat, azathioprine, mitoxantrone, and natalizumab.

RESULTS

CSF Analyses of ICT Patients

Analyzed data of patients who received ICT showed a significant lower absolute cell count in the CSF in the improving group (6.68 ± 1.37 μl) when compared to the active group (9.206 ± 2.39 μl; $p = 0.04416$; **Figure 1A**). This result was confirmed by observation of the individual patient's mean cell count. Also in this analysis the improving group significantly ($p = 0.0221$) showed a lower cell count mean (7.20 ± 3.41 μl) in comparison to the active group (10.82 ± 3.18 μl; **Figure 1B**). The amount of total protein in the CSF was significantly lower in the improving group ($p = 0.0014$, improving group 412 ± 18.25 mg/l vs. active group 462.4 ± 14.04 mg/l; **Figure 1C**). Separately analyzed data of ICT naïve MS-patients did not display significant differences neither in cell count nor in total protein between improving and active group (**Figures 1A–C**).We detected no significant differences in other standardized CSF parameters including erythrocytes count, glucose, lactate, albumin, and IgG (data not shown).

In addition, we investigated whether patient's individual MS medication had an effect on the specific response to ICT. Therefore, we observed the different immune-modulating therapy options of patients receiving ICT based on their assignment for active and improving group. Since patients only received ICT when they were not stable for at least 6 months with other MS medication, the results confirmed that the effects of ICT were not significantly influenced by the specific MS medication (data not shown).

TABLE 2 | Demographic parameters of MS patients; demographic data separated for patients with or without ICT and for improving and active group; [a]in years (mean ± SD); RRMS, relapsing remitting multiple sclerosis; SPMS, secondary progressive multiple sclerosis; PPMS, primary progressive multiple sclerosis; n, number of patients; f, female; m, male.

			n	Sex	Current age[a]	Age at diagnosis[a]	Disease duration[a]
No intrathecal corticosteroid therapy	Improving group		51	f = 33; m = 18	51.98 ± 11.62	36.18 ± 13.65	15.8 ± 10.48
		RRMS	27	f = 20; m = 7	46.78 ± 11.55	35.7 ± 13.76	11.07 ± 7.67
		SPMS	20	f = 12; m = 8	57.8 ± 8.77	34.65 ± 13.59	23.15 ± 10.69
		PPMS	4	f = 1; m = 3	58 ± 9.42	47 ± 10.89	11 ± 2.16
	Active group		52	f = 30; m = 22	54.13 ± 10.5	37.46 ± 10.16	16.67 ± 8.49
		RRMS	9	f = 3; m = 6	40.11 ± 14.41	29.33 ± 10.56	10.78 ± 6.36
		SPMS	39	f = 26; m = 13	56.85 ± 6.79	38.23 ± 9.19	18.62 ± 8.52
		PPMS	4	f = 1; m = 3	59.25 ± 3.86	48.25 ± 5.19	11 ± 1.41
Intrathecal corticosteroid therapy	Improving group		72	f = 45; m = 27	51.42 ± 10.57	38.42 ± 10.65	13 ± 8.15
		RRMS	35	f = 22: m = 13	46.66 ± 10.19	37.0 ± 11.2	9.66 ± 6.24
		SPMS	31	f = 19; m = 12	57.29 ± 8.2	39.81 ± 10.43	17.48 ± 8.45
		PPMS	6	f = 4; m = 2	48.83 ± 9.83	39.5 ± 8.76	9.33 ± 5.65
	Active group		85	f = 55; m = 30	54.54 ± 10.98	36.52 ± 10.21	18.02 ± 7.86
		RRMS	14	f = 9; m = 5	44.43 ± 12.11	28.14 ± 11.41	16.29 ± 8.79
		SPMS	62	f = 40; m = 22	56.08 ± 8.81	36.85 ± 8.26	19.23 ± 7.13
		PPMS	9	f = 6; m = 3	59.67 ± 14.46	47.22 ± 10.50	12.44 ± 9.15

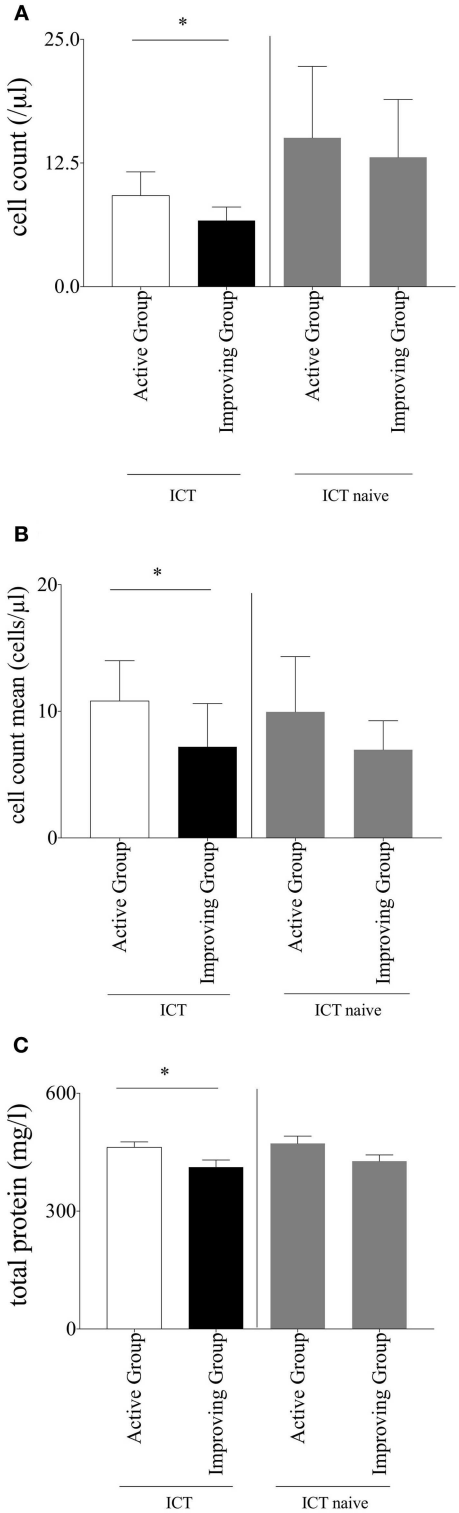


FIGURE 1 | (A) Cell count. Baseline cerebrospinal fluid parameter cell count of multiple sclerosis patients within intrathecal corticosteroid therapy (ICT) compared between the subgroups; separate comparison of multiple sclerosis patients without ICT between the two subgroups; Mann–Whitney-*U*-test, mean with SEM, *n* (improving group ICT) = 172, *n* (active group ICT) = 310, *(Continued)*

FIGURE 1 | *n* (improving group ICT naïve) = 88, *n* (active group ICT naïve) = 137; **p* = 0.0442. **(B)** Cell count mean. Mean of cerebrospinal fluid parameter cell count of multiple sclerosis patients within ICT compared between the subgroups; separate comparison of multiple sclerosis patients without ICT between the two subgroups; Mann–Whitney-*U*-test, mean with SEM, *n* (improving group ICT) = 76, *n* (active group ICT) = 59, *n* (improving group ICT naïve) = 46, *n* (active group ICT naïve) = 47; **p* = 0.0221. **(C)** Total protein. Baseline cerebrospinal fluid parameter total protein of multiple sclerosis patients within ICT compared between the subgroups; separate comparison of multiple sclerosis patients without ICT between the two subgroups; Mann-Whitney-U-test, mean with SEM; *n* (improving group ICT) = 155, *n* (active group ICT) = 282, *n* (improving group ICT naïve) = 88, *n* (active group ICT naïve) = 137; **p* = 0.0014.

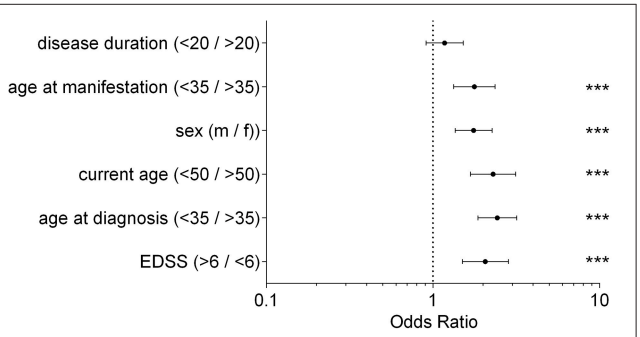


FIGURE 2 | Clinical Parameter; Odds Ratio for each clinical parameter of patients receiving ICT between improving group and active group; fisher's exact test, ****p* < 0.0001; disease duration (*p* = 0.2383); disease duration/current age/age at manifestation/age at diagnosis in years; EDSS, expanded disability status scale; m, male; f, female.

Clinical Parameters for a Response to ICT

The analysis of clinical data revealed that an EDSS > 6 at the first injection of ICT correlated with an increased probability to benefit from ICT (OR = 2.06; 95% CI from 1.5 to 1.75; $p < 0.0001$). Additionally, patients below age of 35 years at first diagnosis of MS benefited most from ICT. In contrast to patients older than 35 years, the probability to belong to the improving group was more than twice as high (OR = 2.43, 95% CI from 1.86 to 3.18, $p < 0.0001$). We found similar results for the individual age at first manifestation of the disease (OR = 1.77, 95% CI from 1.33 to 2.36; $p < 0.0001$).The results showed that an age <50 years currently receiving ICT was accompanied with an increased probability to belong to the improving group (OR = 2.29, 95% CI from 1.68 to 3.14; $p < 0.0001$). Examining the influence of the patients' sex regarding therapy response, male patients responded with a higher probability to ICT than female patients (OR = 1.79, 95% CI from 1.36 to 2.27; $p < 0.0001$). We observed no significant difference between the analyzed groups when assessing disease duration before the start of ICT (OR = 1.18, 95% CI from 0.91 to 1.52; $p < 0.0001$). Results are displayed in **Figure 2**.

Time to Reach EDSS 6

We compared both, the improving and the active group of patients receiving ICT in respect to the time of reaching an EDSS of 6. 13 years after first injection of ICT 39.8% of patients in

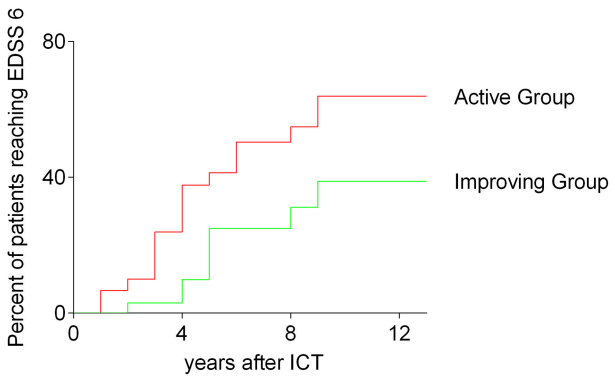


FIGURE 3 | Time to reach EDSS 6; survival curves before reaching an EDSS of 6; all analyzed patients receiving ICT; comparing improving group and active group, Kaplan–Meier survival analysis; log-rank (Mantel-Cox) test, $p = 0.0357$; ICT, intrathecal corticosteroid therapy; EDSS, expanded disability status scale.

the improving group reached an EDSS of 6, whereas 67.8% of patients belonging to the active group reached an EDSS of 6 [$p = 0.0357$; log rank (Mantel-Cox) test]. The results are shown in **Figure 3**.

DISCUSSION

Effective treatment of MS disease progression is one of the major unmet needs in the field of MS therapy. Several studies have demonstrated the safety and efficacy of ICT in MS (3, 4). However, based on its mode of application ICT is not widely used outside German-speaking countries. Also due its invasive nature of application a placebo/sham controlled randomized trial would be un-ethical. The diagnostic value of CSF analysis, however, is being increasingly appreciated even in the age of revised McDonald criteria (10). Our study comprised a cohort of over 200 MS patients with ICT and additionally 148 MS patients without ICT, whose datasets were collected over a time period of 12 years. The weakness of the study is its retrospective nature. However, we could demonstrate a significantly lower level of total protein and cell count in the CSF of patients responding to ICT in a large longitudinally assessed cohort. In accordance with previous studies (3, 15) no severe side effects were observed. Nonetheless, a marker—ideally derived from neurological laboratory routine diagnostic like CSF cell number or total protein—that stratifies responders and non-responders to ICT, may help to assign patients to this therapy. In accordance with previous studies we could stratify clinical data for a positive therapy response to ICT (16).

Our data suggest that patients benefit most from ICT, when (i) diagnosis (and manifestation) was at a younger age (below 35 years of age); (ii) they are younger than 50 years while receiving ICT; (iii) their EDSS is higher than 6 at start of ICT; (iv) when they are male.

CSF analysis is used to exclude differential diagnosis (17) and the standard CSF values are considered as not useful as markers for disease progression or therapy response (8, 18, 19). Among other immunological effects, systemic glucocorticosteroid application has been shown to decrease the number of leucocytes in CSF and to stabilize the blood-brain-barrier (20–22). It is suggested, that low numbers of CSF cells could indicate a beneficial effect on MS progression (20, 23). Furthermore, a dysfunction of the blood-brain-barrier implies a modified expression and secretion of potentially inflammatory mediators in the CSF, e.g., cytokines (24). ICT is an adjuvant option to reduce spasticity and improve patient's motor disabilities, i.e., elongation of walking distance (4). Furthermore, our retrospective data suggest that ICT may have a positive impact on disability progression.

However, the main weakness of this study is its retrospective nature, particularly regarding the clinical data. Hence, the decision whether ICT is used or not is based on an individual risk and benefit assessment. Our data point to a CSF standard assessment, that may serve as a potential tool of predicting therapy response in context of ICT.

AUTHOR CONTRIBUTIONS

KV and AD conducted and analyzed the data and wrote the manuscript. BG and JK assessed CSF and edited the manuscript. RG designed the study and edited the manuscript. AH designed and supervised the study, analyzed the data, and edited the manuscript.

REFERENCES

1. Haghikia A, Hohlfeld R, Gold R, Fugger L. Therapies for multiple sclerosis: translational achievements and outstanding needs. *Trends Mol Med.* (2013) 19:309–19. doi: 10.1016/j.molmed.2013.03.004
2. Duddy M, Haghikia A, Cocco E, Eggers C, Drulovic J, Carmona O, et al. Managing MS in a changing treatment landscape. *J Neurol.* (2011) 258:728–39. doi: 10.1007/s00415-011-6009-x
3. Kamin F, Rommer PS, Abu-Mugheisib M, Koehler W, Hoffmann F, Winkelmann A, et al. Effects of intrathecal triamincinolone-acetonide treatment in MS patients with therapy-resistant spasticity. *Spinal Cord* (2015) 53:109–13. doi: 10.1038/sc.2014.155
4. Hoffmann V, Kuhn W, Schimrigk S, Islamova S, Hellwig K, Lukas C, et al. Repeat intrathecal triamcinolone acetonide application is beneficial in progressive MS patients. *Eur J Neurol.* (2006) 13:72–6. doi: 10.1111/j.1468-1331.2006.01145.x
5. Hellwig K, Lukas C, Brune N, Schimrigk S, Przuntek H, Muller T. Repeat intrathecal triamcinolone acetonide application reduces acute occurring painful dysesthesia in patients with relapsing remitting multiple sclerosis. *Sci World J.* (2006) 6:460–5. doi: 10.1100/tsw.2006.86
6. Muller T. Role of intraspinal steroid application in patients with multiple sclerosis. *Expert Rev Neurother.* (2009) 9:1279–87. doi: 10.1586/ern.09.60
7. Haghikia A, Haghikia A, Hellwig K, Baraniskin A, Holzmann A, Decard BF, et al. Regulated microRNAs in the CSF of patients with multiple sclerosis: a case-control study. *Neurology* (2012) 79:2166–70. doi: 10.1212/WNL.0b013e3182759621
8. Tumani H, Hartung HP, Hemmer B, Teunissen C, Deisenhammer F, Giovannoni G, et al. Cerebrospinal fluid biomarkers in multiple sclerosis. *Neurobiol Dis.* (2009) 35:117–27. doi: 10.1016/j.nbd.2009.04.010

9. Rommer PS, Kamin F, Petzold A, Tumani H, Abu-Mugheisib M, Koehler W, et al. Effects of repeated intrathecal triamcinolone-acetonide application on cerebrospinal fluid biomarkers of axonal damage and glial activity in multiple sclerosis patients. *Mol Diagn Ther.* (2014) 18:631–7. doi: 10.1007/s40291-014-0114-3
10. Thompson AJ, Banwell BL, Barkhof F, Carroll WM, Coetzee T, Comi G, et al. Diagnosis of multiple sclerosis: 2017 revisions of the McDonald criteria. *Lancet Neurol.* (2018) 17:162–73. doi: 10.1016/S1474-4422(17)30470-2
11. Kurtzke JF. Rating neurologic impairment in multiple sclerosis: an expanded disability status scale (EDSS). *Neurology* (1983) 33:1444–52. doi: 10.1212/WNL.33.11.1444
12. Skoog B, Tedeholm H, Runmarker B, Oden A, Andersen O. Continuous prediction of secondary progression in the individual course of multiple sclerosis. *Mult Scler Relat Disord.* (2014) 3:584–92. doi: 10.1016/j.msard.2014.04.004
13. Skoog B, Runmarker B, Winblad S, Ekholm S, Andersen O. A representative cohort of patients with non-progressive multiple sclerosis at the age of normal life expectancy. *Brain* (2012) 135(Pt 3):900–11. doi: 10.1093/brain/awr336
14. Alroughani R, Akhtar S, Ahmed S, Behbehani R, Al-Hashel J. Is time to reach EDSS 6.0 faster in patients with late-onset versus young-onset multiple sclerosis? *PLoS ONE* (2016) 11:e0165846. doi: 10.1371/journal.pone.0165846
15. Hoffmann V, Schimrigk S, Islamova S, Hellwig K, Lukas C, Brune N, et al. Efficacy and safety of repeated intrathecal triamcinolone acetonide application in progressive multiple sclerosis patients. *J Neurol Sci.* (2003) 211:81–4. doi: 10.1016/S0022-510X(03)00060-1
16. Lukas C, Bellenberg B, Hahn HK, Rexilius J, Drescher R, Hellwig K, et al. Benefit of repetitive intrathecal triamcinolone acetonide therapy in predominantly spinal multiple sclerosis: prediction by upper spinal cord atrophy. *Ther Adv Neurol Disord.* (2009) 2:42–9. doi: 10.1177/1756285609343480
17. Deisenhammer F, Bartos A, Egg R, Gilhus NE, Giovannoni G, Rauer S, et al. Guidelines on routine cerebrospinal fluid analysis. Report from an EFNS task force. *Eur J Neurol.* (2006) 13:913–22. doi: 10.1111/j.1468-1331.2006.01493.x
18. Walker RW, Thompson EJ, McDonald WI. Cerebrospinal fluid in multiple sclerosis: relationships between immunoglobulins, leucocytes and clinical features. *J Neurol.* (1985) 232:250–9. doi: 10.1007/BF00313789
19. Awad A, Hemmer B, Hartung HP, Kieseier B, Bennett JL, Stuve O. Analyses of cerebrospinal fluid in the diagnosis and monitoring of multiple sclerosis. *J Neuroimmunol.* (2010) 219:1–7. doi: 10.1016/j.jneuroim.2009.09.002
20. Rocchelli B, Poloni M, Mazzarello P, Piccolo G, Delodovici M, Pinelli P. Intrathecal methylprednisolone acetate in multiple sclerosis treatment: effect on the blood-CSF barrier and on the intrathecal IgG production. *Ital J Neurol Sci.* (1982) 3:119–26. doi: 10.1007/BF02043943
21. Rosenberg GA, Dencoff JE, Correa N Jr, Reiners M, Ford CC. Effect of steroids on CSF matrix metalloproteinases in multiple sclerosis: relation to blood-brain barrier injury. *Neurology* (1996) 46:1626–32. doi: 10.1212/WNL.46.6.1626
22. Salvador E, Shityakov S, Forster C. Glucocorticoids and endothelial cell barrier function. *Cell Tissue Res.* (2014) 355:597–605. doi: 10.1007/s00441-013-1762-z
23. Marinangeli F, Ciccozzi A, Donatelli F, Paladini A, Varrassi G. Clinical use of spinal or epidural steroids. *Minerva Anestesiol.* (2002) 68:613–20.
24. McLean BN, Zeman AZ, Barnes D, Thompson EJ. Patterns of blood-brain barrier impairment and clinical features in multiple sclerosis. *J Neurol Neurosurg Psychiatr.* (1993) 56:356–60. doi: 10.1136/jnnp.56.4.356

Conflict of Interest Statement: The authors declare that the research was conducted in the absence of any commercial or financial relationships that could be construed as a potential conflict of interest.

Copyright © 2019 Vohl, Duscha, Gisevius, Kaisler, Gold and Haghikia. This is an open-access article distributed under the terms of the Creative Commons Attribution License (CC BY). The use, distribution or reproduction in other forums is permitted, provided the original author(s) and the copyright owner(s) are credited and that the original publication in this journal is cited, in accordance with accepted academic practice. No use, distribution or reproduction is permitted which does not comply with these terms.

frontiers in Neurology

ORIGINAL RESEARCH
published: 01 March 2019
doi: 10.3389/fneur.2019.00178

An Assay to Determine Mechanisms of Rapid Autoantibody-Induced Neurotransmitter Receptor Endocytosis and Vesicular Trafficking in Autoimmune Encephalitis

*Elsie Amedonu[1,2], Christoph Brenker[3], Sumanta Barman[4], Julian A. Schreiber[1], Sebastian Becker[1], Stefan Peischard[1], Nathalie Strutz-Seebohm[1], Christine Strippel[2], Andre Dik[2], Hans-Peter Hartung[4], Thomas Budde[5], Heinz Wiendl[2], Timo Strünker[3], Bernhard Wünsch[6], Norbert Goebels[4], Sven G. Meuth[2], Guiscard Seebohm[1] and Nico Melzer[2]**

[1] Myocellular Electrophysiology and Molecular Biology, Institute for Genetics of Heart Diseases, University of Muenster, Muenster, Germany, [2] Department of Neurology, University of Muenster, Muenster, Germany, [3] Centre of Reproductive Medicine and Andrology, University of Muenster, Muenster, Germany, [4] Department of Neurology, Universitätsklinikum and Center for Neurology and Neuropsychiatry LVR Klinikum, Heinrich Heine University Duesseldorf, Duesseldorf, Germany, [5] Institute for Physiology I, University of Muenster, Muenster, Germany, [6] Institute for Pharmaceutical and Medical Chemistry, University of Muenster, Muenster, Germany

OPEN ACCESS

Edited by:
Stefan Bittner,
Johannes Gutenberg University Mainz, Germany

Reviewed by:
Chiara Cordiglieri,
Istituto Nazionale Genetica Molecolare (INGM), Italy
Christoph Kleinschnitz,
Universität Würzburg, Germany
Erhard Wischmeyer,
Universität Würzburg, Germany

***Correspondence:**
Nico Melzer
nico.melzer@ukmuenster.de

Specialty section:
This article was submitted to Multiple Sclerosis and Neuroimmunology, a section of the journal Frontiers in Neurology

Received: 19 September 2018
Accepted: 11 February 2019
Published: 01 March 2019

Citation:
Amedonu E, Brenker C, Barman S, Schreiber JA, Becker S, Peischard S, Strutz-Seebohm N, Strippel C, Dik A, Hartung H-P, Budde T, Wiendl H, Strünker T, Wünsch B, Goebels N, Meuth SG, Seebohm G and Melzer N (2019) An Assay to Determine Mechanisms of Rapid Autoantibody-Induced Neurotransmitter Receptor Endocytosis and Vesicular Trafficking in Autoimmune Encephalitis. Front. Neurol. 10:178. doi: 10.3389/fneur.2019.00178

N-Methyl-D-aspartate (NMDA) receptors (NMDARs) are among the most important excitatory neurotransmitter receptors in the human brain. Autoantibodies to the human NMDAR cause the most frequent form of autoimmune encephalitis involving autoantibody-mediated receptor cross-linking and subsequent internalization of the antibody-receptor complex. This has been deemed to represent the predominant antibody effector mechanism depleting the NMDAR from the synaptic and extra-synaptic neuronal cell membrane. To assess in detail the molecular mechanisms of autoantibody-induced NMDAR endocytosis, vesicular trafficking, and exocytosis we transiently co-expressed rat GluN1-1a-EGFP and GluN2B-ECFP alone or together with scaffolding postsynaptic density protein 95 (PSD-95), wild-type (WT), or dominant-negative (DN) mutant Ras-related in brain (RAB) proteins (RAB5WT, RAB5DN, RAB11WT, RAB11DN) in HEK 293T cells. The cells were incubated with a pH-rhodamine-labeled human recombinant monoclonal GluN1 IgG1 autoantibody (GluN1-aAb$^{pH-rhod}$) genetically engineered from clonally expanded intrathecal plasma cells from a patient with anti-NMDAR encephalitis, and the pH-rhodamine fluorescence was tracked over time. We show that due to the acidic luminal pH, internalization of the NMDAR-autoantibody complex into endosomes and lysosomes increases the pH-rhodamine fluorescence. The increase in fluorescence allows for mechanistic assessment of endocytosis, vesicular trafficking in these vesicular compartments, and exocytosis of the NMDAR-autoantibody complex under steady state conditions. Using this method, we demonstrate a role for PSD-95 in stabilization of NMDARs in the cell membrane in the presence of GluN1-aAb$^{pH-rhod}$, while RAB proteins did not exert a significant effect on vertical trafficking of

the internalized NMDAR autoantibody complex in this heterologous expression system. This novel assay allows to unravel molecular mechanisms of autoantibody-induced receptor internalization and to study novel small-scale specific molecular-based therapies for autoimmune encephalitis syndromes.

Keywords: autoimmune encephalitis, N-Methyl-D-aspartate receptors, cross-linking, endocytosis, vesicular trafficking, exocytosis, autoantibodies

INTRODUCTION

Most of the glutamatergic signaling mechanisms in the central nervous system (CNS) rely on the binding of this neurotransmitter (NT) to specific glutamate receptors (GluRs). Ionotropic ligand-gated ion channels (iGluRs) and metabotropic G protein-coupled receptors (mGluRs) mediate fast and slow glutamatergic excitatory synaptic transmission at synapses between neuronal axons and dendrites (1). The iGluRs include the slow, modulatory N-Methyl-D-aspartate receptors (NMDARs), the fast α-Amino-3-hydroxy-5-methyl-4-isoxazolepropionic acid receptors (AMPARs) (2), and the Kainate receptors (KARs), which typically do not contribute to baseline synaptic transmission.

Functional adult neuronal NMDARs are hetero-tetrameric complexes, formed predominantly by two GluN1 and two GluN2 subunits (3). The subunits share a similar membrane topology, i.e., four transmembrane domains (M1–M4), a reentrant membrane loop between M3 and M4 domains, and long extracellular N- and intracellular C-termini (relatively short for GluN1) (4). Hallmarks of NMDARs include voltage-sensitive block by extracellular Mg^{2+}, slow current kinetics, and high Ca^{2+} permeability (1). Thereby, NMDARs serve a crucial function in synaptic plasticity (expressed as a change in receptor number and functional properties), learning, and memory. These processes start with the release of glutamate from presynaptic axon terminals and the subsequent binding together with the co-agonist glycine mainly to postsynaptic NMDARs. Postsynaptic NMDARs, in turn, are associated with and regulated by several proteins that together constitute the postsynaptic density (PSD), an elaborate complex of interlinked proteins and elements of the cytoskeleton.

Neuronal glutamate receptor trafficking is a multi-step process that involves protein synthesis at the dendritic tree of the postsynaptic neuron, receptor subunit quality control and assemblage in the endoplasmic reticulum (ER), processing in the Golgi apparatus (GA), vesicular packaging in the Golgi complex (GC), subsequent *vertical trafficking* to the neuronal cell surface membrane and anchorage at the PSD, *lateral trafficking* into and out of the PSD, as well as the internalization (endocytosis), subsequent neuronal surface membrane reinsertion (exocytosis) carried out by endosomes (*vertical trafficking*) or degradation carried out by lysosomes (5). At each step of the trafficking process, NMDARs associate with specific partner proteins that allow for their maturation and/or transportation (4).

Glutamate receptors are major targets in autoimmune encephalitis syndromes (6, 7), in which autoantibodies of the immunoglobulin (Ig) G type target iGluRs like NMDARs (8) and AMPARs (9) as well as mGluRs like metabotropic glutamate receptor 1 (mGluR1) (10) and 5 (mGluR5) (11). These autoantibodies disrupt receptor function, cross-link receptors leading to internalization of the antibody-receptor complex (9, 12–15), and activate complement depending on the autoantibody, its IgG subclass, and the complement concentration in the cerebrospinal fluid.

NMDAR autoantibodies are of the IgG 1 or 3 subtypes and can directly affect the gating of the receptor (16). Residues N^{368}/G^{369} in the extracellular domain of the GluN1 subunit of NMDARs may form part of the immunodominant binding region for IgG on the receptor molecule. In single-channel recordings, antibody binding to the receptor instantly caused more frequent openings and prolonged open times of the receptor (16). Moreover, NMDAR autoantibodies caused selective and reversible decrease in postsynaptic surface density and synaptic anchoring of NMDAR in both glutamatergic and GABAergic rat hippocampal neurons by disrupting the interaction of NMDAR with Ephrin-B2 receptors (17), followed by selective NMDAR cross-linking and internalization (13, 14). Consistently, NMDAR antibodies selectively decreased NMDAR-mediated miniature excitatory post-synaptic currents (mEPSCs) without affecting AMPAR-mediated mEPSCs in cultured rat hippocampal neurons (13).

In cultured rat hippocampal neurons, once internalized, antibody-bound NMDAR traffic through recycling endosomes and lysosomes, but do not induce compensatory changes in glutamate receptor gene expression (14). The internalized antibody-receptor complexes co-localize rather with RAB11-positive recycling endosomes than with Lamp1-positive lysosomes suggesting subsequent recycling and exocytosis (14). The process of NMDAR internalization plateaus after 12 h, reaching a steady state that persists throughout the duration of the antibody treatment (14), likely reflecting a state of equilibrium between the rate of receptor internalization and the

Abbreviations: AMPA, α-Amino-3-hydroxy-5-methyl-4-isoxazolepropionic acid; AMPAR, α-Amino-3-hydroxy-5-methyl-4-isoxazolepropionic acid receptor; CNS, central nervous system; DMEM, Dulbecco's modified Eagle's medium; DN, dominant-negative; ECFP, enhanced cyan fluorescent protein; EE, early endosomes; EGFP, enhanced green fluorescent protein; ER, endoplasmic reticulum; FBS, fetal bovine serum; GluN1-$aAb^{pH-rhod}$, pH-rhodamine-labeled human recombinant monoclonal GluN1 IgG1 autoantibody; GA, Golgi apparatus; GC, Golgi complex; GluR, glutamate receptors; Ig, immunoglobulin; iGluR, ionotropic glutamate receptor; KAR, kainate receptor; NEAA, non-essential amino acids; NMDA, N-Methyl-D-aspartate; NMDAR, N-Methyl-D-aspartate receptor; NT, neurotransmitter; mEPSCs, miniature excitatory post-synaptic currents; mGluR, metabotropic G-protein coupled receptor; PSD-95, postsynaptic density protein 95; RAB, Ras-related in brain; RE, recycling endosomes; RV, recycling vesicle; WT, wild-type.

rate of receptor (re-)insertion from different compartments into the surface membrane (14).

Probably due to the lack of blood-brain barrier disruption in NMDAR encephalitis and subsequent lack of relevant complement concentrations in the cerebrospinal fluid, as well as internalization of NMDAR together with the autoantibodies, no complement depositions or major neuronal loss could be detected in biopsy specimens of patients with NMDAR encephalitis, despite large numbers of intracerebral autoantibody-secreting plasma cells (18, 19). Indeed, fully reversible impairment of behavior and memory occurs in mice receiving passive intrathecal transfer of NMDAR autoantibodies (20, 21) that is prevented by co-application of ephrin (22).

The effects on receptor-mediated currents are rather small in heterologous expression systems and do not allow for mechanistic studies on autoantibody-induced neurotransmitter receptor internalization and trafficking in anti-NMDAR encephalitis and other forms of autoimmune encephalitis (21). Thus, the aim of this study was to develop an assay suitable to study in molecular detail the mechanism of autoantibody-induced NMDAR endocytosis, vesicular trafficking, and exocytosis and potentially to study novel small-scale specific molecular-based therapies for autoimmune encephalitis syndromes.

MATERIALS AND METHODS

Construction of NMDAR Expression Vectors

NMDAR constructs were kindly provided by Prof. Michael Hollmann, Receptor Biochemistry, Faculty of Chemistry and Biochemistry, Ruhr University Bochum, Germany. cDNAs encoding the rat GluN1-1a and GluN2B NMDAR subunits were sub-cloned into the pEGFP-N1 and pECFP-N1 mammalian expression vectors, respectively. To allow for the visualization of the subunits, enhanced cyan fluorescent protein (ECFP), and enhanced green fluorescent protein (EGFP) were inserted in-frame at the N-terminus of the subunits. The subunit-containing plasmids were amplified via growth in *E. coli* followed by purification based on a modified alkaline lysis procedure (QIAGEN Miniprep kit).

The generation of PSD-95 as well as WT and DN RAB5 and RAB11 expression vector constructs has been described elsewhere (5, 23).

HEK 293T Cell Co-transfection

HEK 293T cells were cultured in growth media comprising high-glucose Dulbecco's modified Eagle's medium (DMEM) supplemented with 10% fetal bovine serum (FBS), non-essential amino acids (NEAA), Pen-Strep, and 2 mM glutamine. Two days prior to transfection, exponentially growing cells were seeded on poly-D-lysine-coated glass bottom 96-well-plates to a density of approximately 5.0–8.0 $\times$ 10^5/well. Two hours prior to co-transfection, the culture medium was replaced with fresh culture medium. HEK 293T cells were then transiently co-transfected with the cDNAs (0.25 μg GluN1-1a-EGFP and 0.25 μg GluN2B-ECFP) encoding the NMDAR subunits as well as PSD-95, or WT, or DN RAB proteins using the FuGene HD (Promega Corporations) transfection technique according to manufacturer's instructions or left untransfected. 24 h post co-transfection, cells were seeded onto poly-D-lysine-coated glass bottom 96-well-plates. Confocal laser-scanning microscopy was used to quantify cell-surface NMDAR density (×63 glycerol objective; TCS-SP5 Leica- Microsystems, Germany).

pH-rhodamine Labeling of a Human Recombinant Monoclonal GluN1 Autoantibody

Generation of a recombinant human monoclonal GluN1 autoantibody (GluN1-aAb) engineered from clonally expanded intrathecal plasma cells of a patient with anti-NMDAR encephalitis has recently been described (21). Labeling of GluN1-aAb was performed using a pHrodo^{TM} Red Microscale Labeling Kit (Thermofisher Scientific) according to the recommendations of the supplier. Briefly, 100 μL of GluN1-aAb solution (1 mg/mL in PBS) were transferred to a "component D" containing reaction tube and supplemented with 10 μL of 1M sodium bicarbonate. pHrodo red succinimidyl ester was dissolved in 10 μL of DMSO. From the resulting solution, 0.70 μL (as calculated according to the equation 1 of the labeling kit's protocol) was added to the reaction tube containing the pH-adjusted GluN1-aAb. This reaction mixture was incubated for 15 min at RT to allow conjugation. For separation from unbound dye, the reaction mix was spun through a resin-containing column (provided with the kit) at 1,000 g for 5 min. The purified pH-rhodo red labeled GluN1-aAb (GluN1-aAb$^{pH-rhod}$) was recovered from the collection tube and stored aliquoted at −20°C, while unbound dye remained in the resin.

Co-incubation of GluN1-aAb$^{pH\text{-}rhod}$ With HEK 293T Cells Expressing GluN1-1a-EGFP/GluN2B-ECFP NMDARs and Fluorescence Intensity Analysis

The rhodamine fluorophore possesses a well-known pH- and temperature-dependent fluorescence quantum yield (24), which decreases linearly as pH and temperature increases (25). These physicochemical properties needed to be considered in our experimental setting.

Untransfected or co-transfected HEK 293T cells from the same 96-well-plate were incubated with GluN1-aAb$^{pH-rhod}$ at a concentration of 4 μg/ml in phosphate-buffered saline (PBS, pH 7.4) for 2 min. After that, unbound GluN1-aAb$^{pH-rhod}$ was washed-out by superfusing 96-wells with PBS to yield cell-bound GluN1-aAb$^{pH-rhod}$ fluorescence. Wells on the same 96-well-plate without cells incubated with GluN1-aAb$^{pH-rhod}$ at a concentration of 4 μg/ml in PBS without wash-off served as control. All incubations were conducted at 4°C on ice to prevent endocytosis prior to recordings.

Subsequently, fluorescence of GluN1-EGFP and GluN1-aAb$^{pH-rhod}$ was excited at 480 and 520 nm and detected at 510 nm (confocal imaging) and 580 nm (plate reader), respectively, verifying GluN1-1a-EGFP expression and

presence of the GluN1-aAb-bound rhodamine fluorescence (GluN1-aAb$^{pH-rhod}$).

Subsequently, the temperature was increased rapidly from 4 to 30°C to allow for endocytosis, and pH-rhodamine-fluorescence was repetitively excited at 520 nm and the emission was detected at 580 nm. The overall pH-rhodamine fluorescence decreased exponentially with time reaching a steady state after approximately 500 s mainly reflecting the known temperature-dependent fluorescence quantum yield of rhodamine under all experimental conditions.

The steady state pH-rhodamine-fluorescence intensity at 580 nm after 500 s of HEK 293T cells expressing GluN1-1a-EGFP/GluN2B-ECFP NMDARs was significantly higher compared to untransfected HEK 293T cells and served as a cumulative measure of endocytosis of GluN1-aAb$^{pH-rhod}$ bound to the NMDAR with subsequent acidification within endosomes and/or lysosomes and exocytosis. This allowed for mechanistic studies in HEK 293T cells expressing GluN1-1a-EGFP/GluN2B-ECFP NMDARs co-transfected with scaffolding protein PSD-95 as well as RAB5WT and RAB5DN (mediating vesicle endocytosis) and RAB11WT or RAB11DN (mediating vesicle exocytosis).

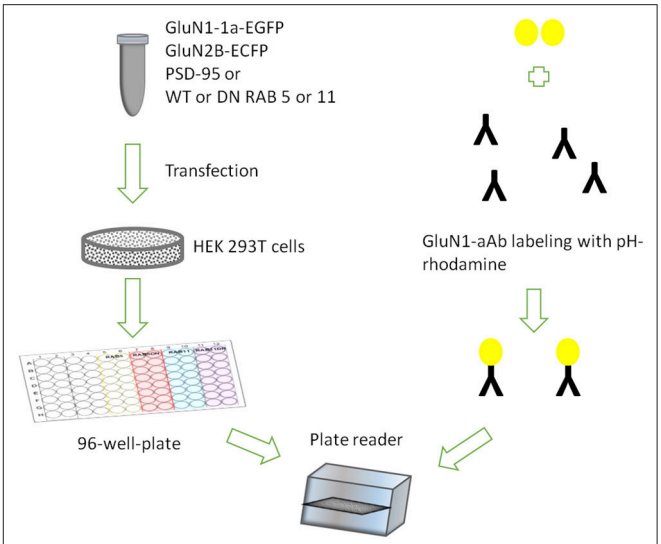


FIGURE 1 | Assay design showing HEK 293T cells transiently expressing rat GluN1-1a-EGFP/GluN2B-ECFP incubated with GluN1-aAb$^{pH-rhod}$ in 96-well-plates under variable conditions in parallel.

Statistical Analysis

Data was analyzed using Origin 9 (OriginLab Corporation). One-way ANOVA followed by multiple pair-wise comparisons with Bonferroni's *post-hoc* correction was used to statistically analyze differences in fluorescence intensity; $p \leq 0.05$ were considered as significant; data in figures were expressed as mean ± SEM. All experiments were performed in triplicates.

RESULTS

To assess in detail the molecular mechanisms of NMDAR autoantibody-induced NMDAR endocytosis, vesicular trafficking, and exocytosis we transiently expressed rat GluN1-1a-EGFP and GluN2B-ECFP alone or together with PSD-95 or with WT- or DN-mutant RAB proteins (RAB5WT, RAB5DN, RAB11WT, RAB11DN) in HEK 293T cells. As a control, HEK 293T cells were left untransfected.

The cells were incubated with a pH-rhodamine-labeled human recombinant monoclonal GluN1 IgG1 autoantibody [GluN1-aAb$^{pH-rhod}$, (21)].

We surmised that the pH-rhodamine fluorescence is increased during the ensuing internalization of the NMDAR-autoantibody complex, due to the acidic luminal pH of endosomes and lysosomes. This might allow for mechanistic assessment of endocytosis, vesicular trafficking in both vesicular compartments and exocytosis of the NMDAR-autoantibody complex (for assay design see **Figure 1**).

In a first set of experiments, HEK 293T cells were transiently co-transfected only with rat GluN1-1a-EGFP and GluN2B-ECFP or left untransfected. After 2 days, expression of fluorescently labeled NMDARs was verified using confocal laser-scanning microscopy. About 70–80% of the cells expressed GluN1-1a-EGFP as subunit putatively targeted by the GluN1-aAb$^{pH-rhod}$ (**Figure 2A**) and GluN2B-ECFP (data not shown). Longer expression times or higher amounts of NMDAR-cDNA for transfections decreased expression levels, supposedly due to cytotoxic effects of pronounced overexpression of NMDARs.

Next, GluN1-1a-EGFP- and GluN2B-ECFP-transfected and untransfected cultured cells were incubated with GluN1-aAb$^{pH-rhod}$. The incubation was performed at 4°C to stop ongoing endocytosis. After that, unbound GluN1-aAb$^{pH-rhod}$ was washed-off. As a control, wells without cells were incubated with GluN1-aAb$^{pH-rhod}$ without wash-off.

Subsequently, GluN1-1a-EGFP and GluN1-aAb$^{pH-rhod}$ fluorescence was excited at 480 nm and 520 nm and measured at 510 and 580 nm, respectively, verifying GluN1-1a-EGFP expression of transfected but not untransfected cells and presence of the GluN1-aAb-bound rhodamine fluorescence (GluN1-aAb$^{pH-rhod}$, **Figure 2B**).

The plate was subsequently transferred to a fluorescence plate reader for time-resolved detection of the pH-rhodamine fluorescence intensity at 30°C. The temperature was increased rapidly from 4–30°C to start endocytosis, and pH-rhodamine-fluorescence was repetitively excited at 520 nm and the emission was detected at 580 nm. The overall rhodamine fluorescence at 580 nm decreased exponentially with time, reaching a steady state after approximately 500 s (**Figure 3B**) mainly reflecting the known temperature-dependent fluorescence quantum yield of rhodamine (24–26) under all experimental conditions.

Of note, the fluorescence-spectrum did not change over time (**Figure 3A**), illustrating that pH-rhodamine fluorescence was detected throughout the experiments. Moreover, steady-state fluorescence intensities of empty wells without wash-off of GluN1-aAb$^{pH-rhod}$ were much larger than those of wells with HEK 293T cells illustrating the known background fluorescence of pH rhodamine at neutral pH of 7.4 in PBS (roughly 1/3 of the maximal fluorescence at acidic pH of 4.0) and thus the necessity of the washing step (**Figure 3B**).

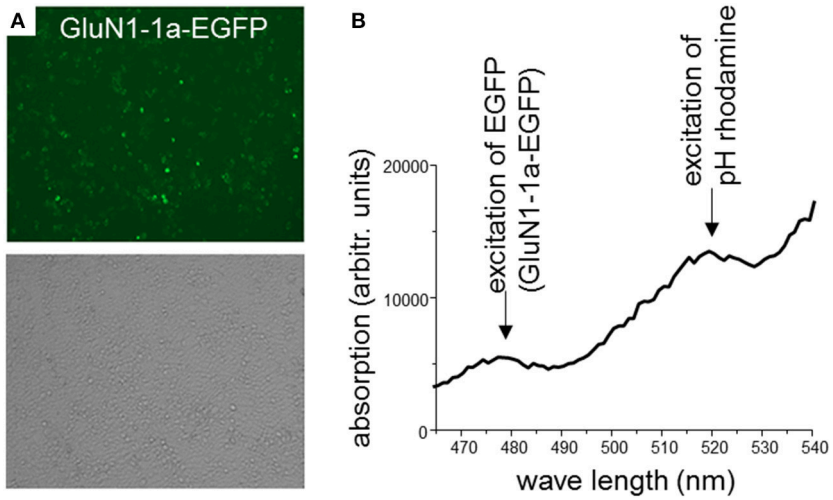


FIGURE 2 | (A) HEK 293T cells co-expressing rat GluN1-1a-EGFP and GluN2B-ECFP. 2 days after transfection, expression of fluorescently labeled NMDARs was verified using confocal laser-scanning microscopy. About 70–80% of the cells expressed GluN1-1a-EGFP as subunit putatively targeted by the GluN1-aAb$^{pH-rhod}$ (upper panel) and GluN2B-ECFP (data not shown). Light microscopy demonstrates typical cell densities (lower panel). **(B)** Binding of GluN1-aAb$^{pH-rhod}$ to the NMDAR subunits as determined by the plate reader experiment. HEK 293T cells expressing GluN1-1a-EGFP/GluN2B-ECFP were incubated with GluN1-aAb$^{pH-rhod}$ on ice in 96-well-plates. GluN1-1a-EGFP and GluN1-aAb$^{pH-rhod}$ fluorescence was excited at wavelengths of 480 nm and 520 nm and emission measured at wavelengths of 510 and 580 nm, respectively, verifying the GluN1-1a-EGFP expression and the binding of GluN1-aAb$^{pH-rhod}$.

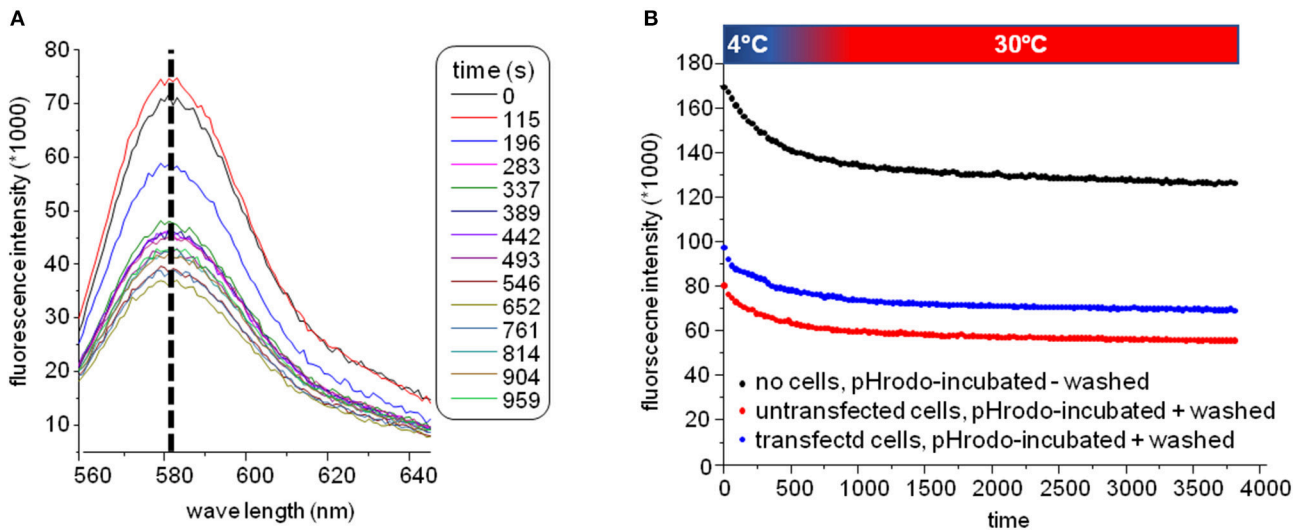


FIGURE 3 | (A) Spectra of the GluN1-aAb$^{pH-rhod}$ fluorescence. The overall fluorescence at 580 nm decreased over time reaching a steady state after approximately 500 s mainly reflecting the known temperature-dependent fluorescence quantum yield of rhodamine (24–26) elicited by elevating the temperature for 4–30°C at the beginning of the experiment under all experimental conditions. During this decay, the excitation spectrum did not shift/change indicating that indeed pH-rhodamine-fluorescence was detected throughout the whole experiment. **(B)** Representative time-dependent traces of the GluN1-aAb$^{pH-rhod}$ fluorescence without wash-off of the unbound GluN1-aAb$^{pH-rhod}$ in PBS at pH 7.4 (black trace) and after wash-off of unbound GluN1-aAb$^{pH-rhod}$ in wells seeded with HEK 293T cells expressing GluN1-1a-EGFP/GluN2B-ECFP (blue trace) or untransfected HEK 293T cells (red trace). The steady state pH-rhodamine-fluorescence intensity at 580 nm after 500 s of HEK 293T cells expressing GluN1-1a-EGFP/GluN2B-ECFP NMDARs was significantly higher compared to the background fluorescence of untransfected HEK 293T cells and served as a cumulative measure of endocytosis of GluN1-aAb$^{pH-rhod}$ bound to the NMDAR with subsequent acidification within endosomes and/or lysosomes and exocytosis.

The steady state pH-rhodamine-fluorescence intensity at 580 nm after 500 s of HEK 293T cells expressing GluN1-1a-EGFP/GluN2B-ECFP NMDARs was significantly higher compared to the background fluorescence of untransfected HEK 293T cells (**Figure 4**) and served as a cumulative measure of endocytosis of GluN1-aAb$^{pH-rhod}$ bound to the NMDAR with

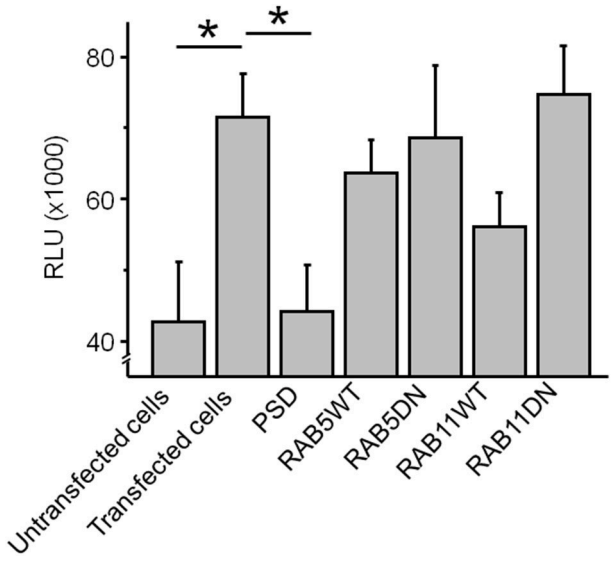


FIGURE 4 | The co-expression of GluN1-1a-EGFP/GluN2B-ECFP NMDARs with the scaffolding protein PSD-95 significantly reduced the cumulative steady state pH-rhodamine-fluorescence intensity at 580 nm after 500 s toward background levels of untransfected HEK 293T cells. In contrast, co-transfection with RAB5WT or RAB5DN (mediating/inhibiting endocytosis) or RAB11 WT or RABDN (mediating/inhibiting exocytosis) did not significantly affect the cumulative steady state pH-rhodamine-fluorescence intensity at 580 nm after 500 s in this heterologous expression system. One-way ANOVA followed by multiple pair-wise comparisons with Bonferroni's *post-hoc* correction was used to statistically analyze differences in fluorescence intensity; $p \leq 0.05$ were considered as significant (*); data are expressed as mean ± SEM. All experiments were performed in triplicates.

subsequent acidification within endosomes and/or lysosomes and exocytosis. This allowed for mechanistic studies in HEK 293T cells expressing GluN1-1a-EGFP/GluN2B-ECFP NMDARs co-transfected with scaffolding protein PSD-95 as well as WT and DN RAB5 (mediating vesicle endocytosis) and RAB11 (mediating vesicle exocytosis).

The co-expression of GluN1-1a-EGFP/GluN2B-ECFP NMDARs with the scaffolding protein PSD-95 significantly reduced the cumulative steady state pH-rhodamine-fluorescence intensity at 580 nm after 500 s toward background levels of untransfected HEK 293T cells (**Figure 4**). In contrast, co-transfection with RAB5WT or RAB5DN (mediating/inhibiting endocytosis) or RAB11 WT or RABDN (mediating/inhibiting exocytosis) did not significantly affect the cumulative steady state pH-rhodamine-fluorescence intensity at 580 nm after 500 s in this heterologous expression system (**Figure 4**).

DISCUSSION

NMDARs are among the most important excitatory receptors in the human brain. NMDAR autoantibodies cause encephalitis by binding to NMDARs, transducing conformational changes and subsequent endocytosis (21, 27). Recently, we showed that pre-incubation for an hour of a recombinant human monoclonal GluN1 autoantibody engineered from clonally expanded intrathecal plasma cells of a patient with anti-NMDAR encephalitis reduced NMDAR-mediated currents recorded from *Xenopus laevis* oocytes by about 20% (21). This result is similar to previous results in *Xenopus laevis* oocytes, showing a time-dependent inhibition of steady-state NMDAR-mediated currents of about 30% within 16 min upon exposure to dialysed sera of patients with anti-NMDAR encephalitis (28). To record NMDAR-mediated currents *in Xenopus laevis* oocytes (and other heterologous expression systems), it is required to use Ca^{2+}-free media to block current inactivation (29). This might explain the rather small antibody-mediated action in oocytes (and probably other heterologous expression systems) compared to the pronounced effects on NMDAR expression on neuronal cell surface *in vitro*, *ex vivo*, and on memory impairment *in vivo* in mice. The Ca^{2+}-free recording conditions may cause conformational changes of the NMDAR induced by binding of the antibody or modulate antibody binding itself and thus diminish subsequent receptor cross-linking and internalization.

These effects on receptor-mediated currents in *Xenopus laevis* oocytes (and other heterologous expression systems) do not allow for further mechanistic studies on autoantibody-induced neurotransmitter receptor internalization and trafficking in anti-NMDAR encephalitis and other forms of autoimmune encephalitis (30). Thus, the aim of this study was to develop an assay suitable for this kind of study.

We used a pH-rhodamine labeled single recombinant human GluN1 IgG1 autoantibody [GluN1-aAb$^{pH-rhod}$, (21)]. This monoclonal autoantibody has previously been shown to evoke all effects of natural NMDAR autoantibodies contained in cerebrospinal fluid of patients with anti-NMDAR encephalitis *in vitro* and *in vivo* (21).

We tested the effects of GluN1-aAb$^{pH-rhod}$ incubation on NMDAR endocytosis, trafficking, and exocytosis mechanisms in HEK 293T cells co-transfected with EGFP-tagged GluN1-1a and ECFP-tagged GluN2B subunits alone or together with PSD-95 or WT- or DN-mutant RAB 5 (mediating endocytosis) and 11 (mediating exocytosis) proteins.

Endocytosis, intracellular trafficking, and exocytosis of the antibody-receptor complex is mediated by transporting vesicles with acidic luminal pH. Thus, we took advantage of this fact, as we found that the use of the steady state GluN1-aAb$^{pH-rhod}$ fluorescence in HEK 293T cells expressing GluN1-1a-EGFP/GluN2B-ECFP NMDARs was significantly higher compared to the background fluorescence of untransfected HEK 293T cells. Thus, this steady state fluorescence served as a cumulative measure of endocytosis of GluN1-aAb$^{pH-rhod}$ bound to the NMDAR with subsequent acidification within endosomes and/or lysosomes and exocytosis.

Using this approach we could demonstrate a role for PSD-95 for stabilization of NMDAR in the cell membrane in the presence of NMDAR autoantibodies. This suggests that autoantibody-induced depletion from the cell membrane predominantly affects extra-synaptic NMDARs not associated with PSD-95 and to a lesser extent synaptic NMDARs. This finding is consistent with the notion that autoantibodies through dissociation from clustering ephrinB2 receptors lead to lateral diffusion of synaptic NMDARs within the neuronal cell membrane out to the synapse where they become cross-linked and internalized as extra-synaptic NMDARs (17, 31). Cell membrane stabilization of

synaptic NMDARs [displaying pro-survival functions (32)] and internalization of extra-synaptic NMDARs [displaying cell-death promoting functions (32)] is further consistent with the lack of overt neurodegeneration in NMDAR encephalitis despite excitotoxic excessive extracellular levels of glutamate (33–35).

Endocytosis, intracellular trafficking and exocytosis are under the guidance of small G-proteins of the RAB type. The use of functional WT and DN mutants has been previously successful in identification of intracellular trafficking pathways of glutamate receptors (36). We found that co-transfection with WT or DN RAB5 (mediating/inhibiting endocytosis) did not affect the cumulative steady state GluN1-aAb$^{pH-rhod}$ fluorescence intensity, whereas the cumulative steady state GluN1-aAb$^{pH-rhod}$ fluorescence intensity was tentatively lowered by co-transfection with WT RAB11 (mediating exocytosis) and tentatively augmented by co-transfection with RAB11DN (inhibiting exocytosis) compared to expression of NMDARs alone. This lack of overt effects of RAB proteins on endocytosis, trafficking and exocytosis of the antibody-receptor complex in our assay is probably due to the overlay by the temperature-dependent fluorescence decrease the amplitude of which is roughly as large as the steady state amplitude of the pH-dependent fluorescence increase upon internalization of the antibody-receptor complex. These opposing effects hinder detailed kinetic analysis of the autoantibody-induced vertical trafficking of the NMDAR performed here.

Hence, given the necessity of washing-off unbound GluN1-aAb$^{pH-rhod}$ and halting trafficking during that time by lowering the temperature due to the residual rhodamie fluorescence at pH 7.4 in PBS, the use of fluorophores (that inevitably are also concordantly temperature-sensitive) with an optimized pH-dependence i.e., no fluorescence at physiological pH of 7.4 might be better suited for our assay. They would enable synchronic adding of the labeled antibody to the cells cultured in PBS at pH 7.4 at constant temperature of 30°C and thus time-resolved tracking of fluorescence increase upon antibody-receptor internalization.

Taken together, we demonstrate a role for PSD-95 for stabilization of NMDAR in the cell membrane of HEK 293T cells in the presence of NMDAR autoantibodies, while RAB proteins did not exert a significant effect on vertical trafficking of the internalized NMDAR autoantibody complex in this heterologous expression system.

Our assay should be sensitive enough to study novel small-scale specific molecular-based therapies for autoimmune encephalitis that may become feasible as follows:

1) Autoantibody binding to the GluN1 subunit and subsequent induction of conformational changes in the NMDAR could be blocked by antibody fragments, for example. However, with existence of a multitude of autoantibody epitopes within the NMDAR, this approach may not be successful.
2) The autoantibody binding-induced conformational changes within the NMDAR. Small molecule allosteric modulators have recently been developed (5, 37, 38). Potentially, these compounds may be used to block the conformational changes induced by GluN1-aAb$^{pH-rhod}$ binding and thus inhibit internalization.
3) Inhibition of the GluN1-aAb$^{pH-rhod}$-induced internalization. To achieve this, general cellular trafficking pathways have to be blocked. It is questionable if such an approach can be tolerated by patients and would not cause severe side effects.

Taking these considerations into account, development and use of small molecule allosteric modulators may represent a group of drug candidates for anti-NMDAR encephalitis and other forms of autoimmune encephalitis. Evidenced by the relatively robust novel assay, they may be used to screen for compounds that block autoantibody-induced NMDAR cross-linking and internalization. This should always be accompanied by NMDAR stabilization within the synapse to avoid accumulation of NMDAR at extra-synaptic sides of the cell membrane potentially promoting excitotoxic cell death in NMDAR encephalitis.

Therefore, screening results obtained with our assay in HEK 293T overexpressing NMDAR should always be validated using super-resolution microscopy in cultured living neurons and brain slices exhibiting physiological expression levels and subcellular localization of NMDARs.

CONCLUSION

This novel assay allows to unravel molecular mechanisms of autoantibody-induced receptor internalization and to study novel small-scale specific molecular-based therapies for autoimmune encephalitis syndromes.

DATA AVAILABILITY

The dataset obtained and analyzed in the current study is available from the corresponding author on a reasonable request.

AUTHOR CONTRIBUTIONS

CS and AD: collected patient samples under the supervision of HW, SM, and NM; SBa and NG: performed the synthesis and pH-rhodamine labeling of GluN1-aAb$^{pH-rhod}$; EA, SBe, SP, and JS: performed the transfection, immunocytochemistry, and confocal microscopy with the HEK 293T cells; EA, CB, and TS: together with TB, NS-S, GS, and NM performed incubation of transfected HEK 293T cells with GluN1-aAb$^{pH-rhod}$ and data analysis; H-PH, BW, SM, GS, and NM: designed and supervised the project; EA, SM, GS, and NM: wrote the first draft of the manuscript. All authors contributed to and approved the final version of the manuscript.

FUNDING

This work was supported by the German Research Foundation (DFG, INST 2105/27-1 to SM), the German Academic Exchange Service (DAAD-MoE postgraduate scholarship to EA), the Walter und Ilse-Rose-Stiftung (to H-PH), the Forschungskommission of the Heinrich-Heine-University Düsseldorf, Germany (to NG) and the Bundesministerium für Bildung und Forschung (BMBF 031A232 to NG).

ACKNOWLEDGMENTS

We thank Prof. Michael Hollmann, Receptor Biochemistry, Faculty of Chemistry and Biochemistry, Ruhr University Bochum, Germany for providing the NMDAR constructs used in this study, and Christina Burhoi, Institute for Genetics of Heart Diseases (IfGH), University of Muenster, Germany, for excellent technical assistance.

REFERENCES

1. Traynelis SF, Wollmuth LP, Mcbain CJ, Menniti FS, Vance KM, Ogden KK, et al. Glutamate receptor ion channels: structure, regulation, and function. *Pharmacol Rev*. (2010) 62:405–96. doi: 10.1124/pr.109.002451
2. Hollmann M, Heinemann S. Cloned glutamate receptors. *Annu Rev Neurosci*. (1994) 17:31–108. doi: 10.1146/annurev.ne.17.030194.000335
3. Dingledine R, Borges K, Bowie D, Traynelis SF. The glutamate receptor ion channels. *Pharmacol Rev*. (1999) 51:7–61.
4. Petralia RS, Al-Hallaq RA, Wenthold RJ. Trafficking and targeting of NMDA receptors. In: Van Dongen AM, editor. *Biology of the NMDA Receptor*. Boca Raton, FL: CRC Press/Taylor & Francis (2009).
5. Seebohm G, Neumann S, Theiss C, Novkovic T, Hill EV, Tavare JM, et al. Identification of a novel signaling pathway and its relevance for GluA1 recycling. *PLoS ONE*. (2012) 7:e33889. doi: 10.1371/journal.pone.0033889
6. Melzer N, Meuth SG, Wiendl H. Paraneoplastic and non-paraneoplastic autoimmunity to neurons in the central nervous system. *J Neurol*. (2013) 260:1215–33. doi: 10.1007/s00415-012-6657-5
7. Graus F, Titulaer MJ, Balu R, Benseler S, Bien CG, Cellucci T, et al. A clinical approach to diagnosis of autoimmune encephalitis. *Lancet Neurol*. (2016) 15:391–404. doi: 10.1016/S1474-4422(15)00401-9
8. Dalmau J, Gleichman AJ, Hughes EG, Rossi JE, Peng X, Lai M, et al. Anti-NMDA-receptor encephalitis: case series and analysis of the effects of antibodies. *Lancet Neurol*. (2008) 7:1091–8. doi: 10.1016/S1474-4422(08)70224-2
9. Lai M, Hughes EG, Peng X, Zhou L, Gleichman AJ, Shu H, et al. AMPA receptor antibodies in limbic encephalitis alter synaptic receptor location. *Ann Neurol*. (2009) 65:424–34. doi: 10.1002/ana.21589
10. Sillevis Smitt P, Kinoshita A, De Leeuw B, Moll W, Coesmans M, Jaarsma D, et al. Paraneoplastic cerebellar ataxia due to autoantibodies against a glutamate receptor. *N Engl J Med*. (2000) 342:21–7. doi: 10.1056/NEJM200001063420104
11. Lancaster E, Martinez-Hernandez E, Titulaer MJ, Boulos M, Weaver S, Antoine JC, et al. Antibodies to metabotropic glutamate receptor 5 in the Ophelia syndrome. *Neurology*. (2011) 77:1698–701. doi: 10.1212/WNL.0b013e3182364a44
12. Coesmans M, Smitt PA, Linden DJ, Shigemoto R, Hirano T, Yamakawa Y, et al. Mechanisms underlying cerebellar motor deficits due to mGluR1-autoantibodies. *Ann Neurol*. (2003) 53:325–36. doi: 10.1002/ana.10451
13. Hughes EG, Peng X, Gleichman AJ, Lai M, Zhou L, Tsou R, et al. Cellular and synaptic mechanisms of anti-NMDA receptor encephalitis. *J Neurosci*. (2010) 30:5866–75. doi: 10.1523/JNEUROSCI.0167-10.2010
14. Moscato EH, Peng X, Jain A, Parsons TD, Dalmau J, Balice-Gordon RJ. Acute mechanisms underlying antibody effects in anti-N-methyl-D-aspartate receptor encephalitis. *Ann Neurol*. (2014) 76:108–19. doi: 10.1002/ana.24195
15. Peng X, Hughes EG, Moscato EH, Parsons TD, Dalmau J, Balice-Gordon RJ. Cellular plasticity induced by anti-alpha-amino-3-hydroxy-5-methyl-4-isoxazolepropionic acid (AMPA) receptor encephalitis antibodies. *Ann Neurol*. (2015) 77:381–98. doi: 10.1002/ana.24293
16. Gleichman AJ, Spruce LA, Dalmau J, Seeholzer SH, Lynch DR. Anti-NMDA receptor encephalitis antibody binding is dependent on amino acid identity of a small region within the GluN1 amino terminal domain. *J Neurosci*. (2012) 32:11082–94. doi: 10.1523/JNEUROSCI.0064-12.2012
17. Mikasova L, De Rossi P, Bouchet D, Georges F, Rogemond V, Didelot A, et al. Disrupted surface cross-talk between NMDA and Ephrin-B2 receptors in anti-NMDA encephalitis. *Brain*. (2012) 135:1606–21. doi: 10.1093/brain/aws092
18. Martinez-Hernandez E, Horvath J, Shiloh-Malawsky Y, Sangha N, Martinez-Lage M, Dalmau J. Analysis of complement and plasma cells in the brain of patients with anti-NMDAR encephalitis. *Neurology*. (2011) 77:589–93. doi: 10.1212/WNL.0b013e318228c136
19. Bien CG, Vincent A, Barnett MH, Becker AJ, Blumcke I, Graus F, et al. Immunopathology of autoantibody-associated encephalitides: clues for pathogenesis. *Brain*. (2012) 135:1622–38. doi: 10.1093/brain/aws082
20. Planaguma J, Leypoldt F, Mannara F, Gutierrez-Cuesta J, Martin-Garcia E, Aguilar E, et al. Human N-methyl D-aspartate receptor antibodies alter memory and behaviour in mice. *Brain*. (2015) 138:94–109. doi: 10.1093/brain/awu310
21. Malviya M, Barman S, Golombeck KS, Planaguma J, Mannara F, Strutz-Seebohm N, et al. NMDAR encephalitis: passive transfer from man to mouse by a recombinant antibody. *Ann Clin Transl Neurol*. (2017) 4:768–83. doi: 10.1002/acn3.444
22. Planaguma J, Haselmann H, Mannara F, Petit-Pedrol M, Grunewald B, Aguilar E, et al. Ephrin-B2 prevents N-methyl-D-aspartate receptor antibody effects on memory and neuroplasticity. *Ann Neurol*. (2016) 80:388–400. doi: 10.1002/ana.24721
23. Seebohm G, Strutz-Seebohm N, Birkin R, Dell G, Bucci C, Spinosa MR, et al. Regulation of endocytic recycling of KCNQ1/KCNE1 potassium channels. *Circ Res*. (2007) 100:686–92. doi: 10.1161/01.RES.0000260250.83824.8f
24. Ferguson J, Mau AWH. Spontaneous and stimulated emission from dyes. Spectroscopy of the neutral molecules of acridine orange, proflavine, and rhodamine B. *Aust J Chem*. (1973) 26:1617–24. doi: 10.1071/CH9731617
25. Kubin RF, Fletcher AN. Fluorescence quantum yields of some rhodamine dyes. *J Lumin*. (1982) 27:455–62. doi: 10.1016/0022-2313(82)90045-X
26. Moreau D, Lefort C, Burke R, Leveque P, O'connor RP. Rhodamine B as an optical thermometer in cells focally exposed to infrared laser light or nanosecond pulsed electric fields. *Biomed Opt Express*. (2015) 6:4105–17. doi: 10.1364/BOE.6.004105
27. Kreye J, Wenke NK, Chayka M, Leubner J, Murugan R, Maier N, et al. Human cerebrospinal fluid monoclonal N-methyl-D-aspartate receptor autoantibodies are sufficient for encephalitis pathogenesis. *Brain*. (2016) 139:2641–52. doi: 10.1093/brain/aww208
28. Castillo-Gomez E, Oliveira B, Tapken D, Bertrand S, Klein-Schmidt C, Pan H, et al. All naturally occurring autoantibodies against the NMDA receptor subunit NR1 have pathogenic potential irrespective of epitope and immunoglobulin class. *Mol Psychiatry*. (2017) 22:1776–84. doi: 10.1038/mp.2016.125
29. Levitan IB. It is calmodulin after all! Mediator of the calcium modulation of multiple ion channels. *Neuron*. (1999) 22:645–8. doi: 10.1016/S0896-6273(00)80722-9
30. Crisp SJ, Kullmann DM, Vincent A. Autoimmune synaptopathies. *Nat Rev Neurosci*. (2016) 17:103–17. doi: 10.1038/nrn.2015.27
31. Jezequel J, Johansson EM, Dupuis JP, Rogemond V, Grea H, Kellermayer B, et al. Dynamic disorganization of synaptic NMDA receptors triggered by autoantibodies from psychotic patients. *Nat Commun*. (2017) 8:1791. doi: 10.1038/s41467-017-01700-3
32. Hardingham GE, Bading H. Synaptic versus extrasynaptic NMDA receptor signalling: implications for neurodegenerative disorders. *Nat Rev Neurosci*. (2010) 11:682–96. doi: 10.1038/nrn2911
33. Melzer N, Biela A, Fahlke C. Glutamate modifies ion conduction and voltage-dependent gating of excitatory amino acid transporter-associated anion channels. *J Biol Chem*. (2003) 278:50112–9. doi: 10.1074/jbc.M307990200
34. Melzer N, Torres-Salazar D, Fahlke C. A dynamic switch between inhibitory and excitatory currents in a neuronal glutamate transporter. *Proc Natl Acad Sci USA*. (2005) 102:19214–8. doi: 10.1073/pnas.0508837103
35. Manto M, Dalmau J, Didelot A, Rogemond V, Honnorat J. *In vivo* effects of antibodies from patients with anti-NMDA receptor encephalitis: further evidence of synaptic glutamatergic dysfunction. *Orphanet J Rare Dis*. (2010) 5:31. doi: 10.1186/1750-1172-5-31

36. Seebohm G, Piccini I, Strutz-Seebohm N. Paving the way to understand autoantibody-mediated epilepsy on the molecular level. *Front Neurol*. (2015) 6:149. doi: 10.3389/fneur.2015.00149
37. Dey S, Temme L, Schreiber JA, Schepmann D, Frehland B, Lehmkuhl K, et al. Deconstruction - reconstruction approach to analyze the essential structural elements of tetrahydro-3-benzazepine-based antagonists of GluN2B subunit containing NMDA receptors. *Eur J Med Chem*. (2017) 138:552–64. doi: 10.1016/j.ejmech.2017.06.068
38. Gawaskar S, Temme L, Schreiber JA, Schepmann D, Bonifazi A, Robaa D, et al. Design, synthesis, pharmacological evaluation and docking studies of GluN2B-selective NMDA receptor antagonists with a Benzo[7]annulen-7-amine Scaffold. *Chem Med Chem*. (2017) 12:1212–22. doi: 10.1002/cmdc.201700311

Conflict of Interest Statement: The authors declare that the research was conducted in the absence of any commercial or financial relationships that could be construed as a potential conflict of interest.

Copyright © 2019 Amedonu, Brenker, Barman, Schreiber, Becker, Peischard, Strutz-Seebohm, Strippel, Dik, Hartung, Budde, Wiendl, Strünker, Wünsch, Goebels, Meuth, Seebohm and Melzer. This is an open-access article distributed under the terms of the Creative Commons Attribution License (CC BY). The use, distribution or reproduction in other forums is permitted, provided the original author(s) and the copyright owner(s) are credited and that the original publication in this journal is cited, in accordance with accepted academic practice. No use, distribution or reproduction is permitted which does not comply with these terms.

frontiers in Neurology

REVIEW
published: 08 March 2019
doi: 10.3389/fneur.2019.00195

Biomarkers for Dementia, Fatigue, and Depression in Parkinson's Disease

Tino Prell[1,2]*, *Otto W. Witte*[1,2] *and Julian Grosskreutz*[1,2]

[1] Department of Neurology, Jena University Hospital, Jena, Germany, [2] Center for Healthy Ageing, Jena University Hospital, Jena, Germany

Parkinson's disease is a common multisystem neurodegenerative disorder characterized by typical motor and non-motor symptoms. There is an urgent need for biomarkers for assessment of disease severity, complications and prognosis. In addition, biomarkers reporting the underlying pathophysiology assist in understanding the disease and developing neuroprotective therapies. Ultimately, biomarkers could be used to develop a more efficient personalized approach for clinical trials and treatment strategies. With the goal to improve quality of life in Parkinson's disease it is essential to understand and objectively monitor non-motor symptoms. This narrative review provides an overview of recent developments of biomarkers (biofluid samples and imaging) for three common neuropsychological syndromes in Parkinson's disease: dementia, fatigue, and depression.

Keywords: Parkinson's disease, biomarker, non-motor syndromes, depression, fatigue, dementia

OPEN ACCESS

Edited by:
Tobias Warnecke,
University Hospital Münster, Germany

Reviewed by:
Walter Maetzler,
University of Kiel, Germany
Gennaro Pagano,
King's College London,
United Kingdom

***Correspondence:**
Tino Prell
tino.prell@med.uni-jena.de

Specialty section:
This article was submitted to Movement Disorders, a section of the journal Frontiers in Neurology

Received: *01 October 2018*
Accepted: *15 February 2019*
Published: *08 March 2019*

Citation:
Prell T, Witte OW and Grosskreutz J (2019) Biomarkers for Dementia, Fatigue, and Depression in Parkinson's Disease. Front. Neurol. 10:195. doi: 10.3389/fneur.2019.00195

INTRODUCTION

Parkinson's disease (PD) is now considered as progressive and multisystem α-synucleinopathy. Therefore, PD is characterized not only by motor symptoms, but also a broad range of non-motor symptoms (NMS) (1). NMS can aggravate disease burden and significantly contribute to worsening of quality of life (2). Biomarkers which are associated with worse motor performance as well as development of NMS are of special importance in PD. A biomarker is "a characteristic that is objectively measured and evaluated as an indicator of normal biological processes, pathogenic processes, or pharmacologic responses to a therapeutic intervention" (3). The ideal PD biomarkers should have a reasonable effect size, are reproducible across different cohorts and are ideally verified in neuropathological proven PD cases. Biomarkers in PD can include (i) biomarker for prodromal stage to identify PD before motor symptoms occur, (ii) biomarkers of susceptibility to identify persons who are at risk for PD, (iii) biomarkers for motor and non-motor burden to assess disease severity and monitor the efficacy of therapies. The last one can help to identify patients who are at risk to develop complications and may lead to individual optimization and prevention in health care. This review provides an update on recent advances in the development of biomarkers (biofluid samples and neuroimaging) for three common neuropsychological syndromes: dementia, fatigue and depression.

COGNITIVE IMPAIRMENT

Cognitive deficits are common in PD and can present as mild dysfunction in the prodromal and early stages, or as dementia (PDD) in advanced stages (4). Approximately 20%

of patients with *de novo* PD have mild cognitive impairment (MCI) (5). The concept of PD-MCI was introduced 2012 (MDS Task Force) and characterizes a cognitive decline that is assessed during neuropsychological testing but does not impair activities of daily living (6). MCI is considered an intermediate state of cognitive dysfunction in PD that may progress to PDD. Up to 75% of patients will develop dementia over the longterm disease course (7). However, the rate to PDD, the cognitive profile and severity of cognitive dysfunction show high interindividual variation. Given its high medical and social impact and its health-related costs, the identification of biomarkers for PDD is of high priority (8). Biomarkers reflecting cognitive decline can facilitate early diagnosis and may indicate response to therapeutic interventions.

Clinical factors, such as higher age, male sex, low level of education, longer disease duration, higher Hoehn & Yahr stage, axial impairment, excessive daytime sleepiness, cardiovascular autonomic dysfunction, REM sleep behavior disorder, hallucinations and PD-MCI were found to strongly predict the development of PDD (9–13). Moreover, impairment of memory and language (posterior-cortical dysfunction) seems to be linked to a higher risk of PDD (14, 15).

Given the neuropathology of PDD several studies aimed to identify biomarkers which reflect proteinopathy, neuronal loss, abnormal neurotransmitters, and structural and functional brain changes. Lewy bodies and amyloid plaques in the neocortex and limbic system are typical neuropathological features of Alzheimer's disease and PDD (16, 17). Hence, the majority of studies investigated amyloid-ß 1–42 (Aß), tau protein, and α-synuclein in the cerebrospinal fluid (CSF) of PD patients (**Table 1**). In many studies the level of Aß was reduced in PDD. Low CSF levels of Aß were found to be related to deterioration in attention, executive function, semantic fluency and memory (21, 38, 40, 45). One-half of PDD patients had the CSF biomarker signature of Alzheimer's disease (46) suggestive of an overlap with Alzheimer's disease pathology (47). Low baseline CSF Aβ was associated with more rapid cognitive decline later in disease. By contrast, the levels of total (t-tau) and phosphorylated tau (p-tau) were found to be increased or unchanged in PDD (**Table 1**). For clinicians it is highly relevant to know which biomarkers accurately predict the progression from MCI to PDD. Therefore, based on the data from cross-sectional and longitudinal studies one can assume that reduced Aß predicts cognitive decline in PD (40, 42, 48).

Several studies assessed the CSF levels of α-synuclein in PD. Meta-analyses demonstrated that total α-synuclein levels are lower in PD compared to controls (49, 50). However, in terms of α-synuclein and cognitive decline there are conflicting results with both low and high levels in the presence of cognitive impairment (29, 41, 48). In the DATATOP study with up to 8 years of follow-up, lower α-synuclein levels predicted better preservation of cognitive function (verbal learning and memory, visuospatial working memory) in early disease. Thus, α-synuclein may reflect changes in multiple cognitive domains and may predict cognitive decline in PD (29, 41, 48). On the other hand most studies of non-demented PD failed to find any association between α-synuclein levels and cognition (51, 52). It seems that CSF α-synuclein levels may increase with disease stage. This could explain why cognitive deficits in connection with high levels of α- synuclein were found in more advanced disease stages (53). Isoforms of α-synuclein (e.g., phosphorylated, ubiquitinated, oligomeric) are potentially more sensitive to cognitive decline than the total α-synuclein level (24, 30). Another study examining plasma levels of α-synuclein found higher levels in PDD and a correlation with mini mental state examination scores (54). This finding, however, requires further investigations.

In another longitudinal study, high neurofilament light chain protein, low Aβ and high heart fatty acid–binding protein at baseline were related to future PDD with a relatively high diagnostic accuracy (19). Also several serum proteins, such as C-reactive protein, interleukins, interferon-γ, tumor necrosis factor α, uric acid, and cystatin C were found to be associated with cognition in PD (55). In particular, low uric acid concentrations, low levels of epidermal growth factor (EGF) and insulin-like growth factor (ILGF) seems to have predictive value for deterioration of cognitive function in PD (56–61). In combination with clinical markers, a study of 390 patients from the Progression Markers Initiative study with newly diagnosed PD, the occurrence of cognitive impairment at 2 years follow-up could be predicted with good accuracy using a model combining information on age, non-motor assessments, DAT imaging, and CSF biomarkers. Here, the Montreal Cognitive Assessment (MoCA) scores and low CSF Aβ to t-tau ratio and DAT imaging results were the best predictors of cognitive impairment (39). Using data from the Parkinson's Progression Markers Initiative, Fereshtehnejad et al., identified distinct subgroups via a cluster analysis of a comprehensive dataset consisting of clinical characteristics, neuroimaging, biospecimen and genetic information. Here, the CSF biomarkers differed between these PD subtypes. Patients with diffuse malignant disease course and fast cognitive decline, showed an Alzheimer's disease-like CSF profile (low Aβ, low Aβ/t-tau ratio) (62).

Applying computerized neuroimaging analyses several MRI studies have found gray matter atrophy and disruptions of white matter integrity in PDD, although findings in non-demented PD and PD-MCI remain inconsistent (63) (**Tables 2**, **3**). A longitudinal study using voxel-based morphometry (VBM) found neocortical volume reduction (temporo-occipital region, hippocampal and parahippocampal) as the most relevant finding in patients who develop PDD (97). Another study has identified a validated Alzheimer's disease pattern of brain atrophy as an independent predictor of cognitive impairment in PD (64). More specifically cortical thinning in the right precentral, frontal, and in the anterior cingulate cortex as well as gray matter atrophy (prefrontal, insula, caudate nucleus, hippocampal) predicted cognitive decline in PD (23, 66, 70, 76, 98). Cognitive impairment was also found to be associated with lower gray matter volume and increased mean diffusivity in the nucleus basalis of Meynert, compared to non-demented patients. Moreover, these changes were predictive for developing cognitive impairment in cognitively intact patients with PD, independent of other clinical and non-clinical markers of the disease (99). The nucleus basalis of Meynert and the pedunculopontine nucleus

TABLE 1 | Cerebrospinal-fluid (CSF) biomarkers of cognitive impairment and dementia in Parkinson's disease.

Study	CSF biomarker						Participants	Methods	Result
	Aß1-42	t- tau	p-tau	t-α-syn	o-α-syn	other			
Alves et al. (18)*	+	+	+				PDND 104	MDS Task Force	Low Aβ predicted early dementia
Bäckström et al. (19)*	+	+	+	+		+	PDND 104 C 30 PSP 13 MSA 11	NFL H-FABP	Low Aβ, NFL and H-FABP predicted PDD
Brockmann et al. (20)	+					+	PDND 353 PDD 103	Genetic variants known to be involved in Aβ clearance	Risk variants in *APOE* and cystatin C genes were associated with lower Aβ
Compta et al. (21)	+	+					PDND 20 PDD 20 C 30	MMSE DSM-IV-R MDS Task Force	PDD: ↑ t-tau PDND: ↓ Aβ positively correlated with phonemic fluency
Compta et al. (22)	+	+	+				PDND 19 PDD 29 C 9	MMSE MDS Task Force	PDD: ↓ Aβ ↑ t-tau and p-tau in a subgroup
Compta et al. (23)*	+	+	+				PDND 27	MMSE MDS Task Force	Low Aβ predicted PDD
Compta et al. (24)	+	+		+	+		PDND 21 PDD 20 C 13	MMSE/PDD by MDS Task Force	PDD: ↓ Aβ, ↑ t-tau, ↑ o-α-syn
Ffytche et al. (25)	+						PD 423 3-4 years of follow-up	Compare baseline structural imaging and CSF data in patients who go on to develop illusions or hallucinations in newly diagnosed PD	Patients with early onset PD psychosis: Aβ ↓
Gmitterová et al. (26)	+	+	+			+	PDND 22 PDD 31 DLB 51 C 32	Discriminatory potential of tau, p-tau, Aβ, NSE and S100B across the spectrum of LBD	PDD Aβ ↓, tau ↑ Rapid disease course not associated with decrease of Aβ
Halbgebauer et al. (27)						+	PDND 22 PDD 29 C 36	Modified serpinA1	PDD: acidic serpinA1 isoform ↑
Hall et al. (28)	+	+	+	+			PDND 90 PDD 33 C 107	MMSE MDS Task Force	PDD: ↑ p-tau, Aβ or t-α-syn no differences
Hall et al. (29)*	+	+	+	+		+	PDND 42 C 69		Low Aβ predicted memory decline, high α-syn predicted reduced cognitive speed
Hansson et al. (30)				+	+		PDND 30 C 98	MMSE MDS Task Force	PDD: ↑ o-α-syn
Janssens et al. (31)	+	+	+			+	probable AD 52 FTD 59 DLB 39 PDD 14 C 88 young C 32	3-methoxy-4-hydroxyphenylglycol (MHPG)	Aβ young C > C > FTD > PDD, DLB > AD tau AD > FTD > PDD, DLB > C > young C p-tau AD > FTD = PDD,DLB = C> young C MHPG PDD, DLB > AD > C

(Continued)

TABLE 1 | Continued

Study	CSF biomarker						Participants	Methods	Result
	Aß1-42	t- tau	p-tau	t-α-syn	o-α-syn	other			
Lindqvist et al. (32)						+	PDND 71 PDD 16 C 33	MMSE	PDD: C-reactive protein ↑ IL6 ↑ TNF-Alpha → Eotaxin→ MCP-1→ MIP-1beta→ IP-10→
Maetzler et al. (33)	+						PDND 14 PDD 12	MMSE	PDD: Aβ ↓
Maetzler et al. (34)	+	+					PDND 21 PDD 10 C 39	MMSE	No difference
Maetzler et al. (35)	+	+					PDND 77 PDD 26 C 72	MMSE MDS Task Force	No difference
Modreanu et al. (36)	+	+	+				PD 37 PDD 21 PDD at 18-months 35	Spatial disorientation, memory complaints over disease course	PDD: Aβ ↓ tau and p-tau no difference 'PDD -converters' had significantly lower Aβ at baseline
Parnetti et al. (37)		+	+				PDND 67 PDD 48 C 41	MMSE	No difference
Parnetti et al. (38)*	+	+	+	+	+		PDND 44 Disease C 25	MMSE MoCa	Low Aβ predicted more rapid decline
Schrag et al. (39)*	+	+					PDND 390 C 178	MoCa over 2 years	Low Aβ/t-tau ratio predicts cognitive decline
Siderowf et al. (40)*	+	+	+				PDND: 45	Dementia rating scale	Low Aβ predicted rapid decline in Dementia rating scale
Stewart et al. (41)*	+	+	+	+			PDND 350	Verbal memory, cognitive processing speed, and visuospatial working memory	Lower α-synuclein predicted better preservation of cognitive function
Terrelonge et al. (42)*	+	+	+	+			PDND 341	Memory, visuospatial, working memory–executive function, and attention processing speed	Low Aβ predicted cognitive impairment
Vranová et al. (43)	+	+					PDND 27 PDD 14 C 14	MMSE MDS Task Force	PDD: ↑ t-tau/ Aβ index Aβ or t-tau no differences
Wennström et al. (44)				+			PDND 38 PDD 22 C 52	MMSE MDS Task Force	No difference

*PD, Patients with Parkinson's disease; PD-MCI, Parkinson's disease patients with mild cognitive impairment; PDD, Parkinson's disease patients with dementia; PDND, non-demented PD; MSA, multiple system atrophy; PSP, progressive supranuclear palsy; AD, Patients with Alzheimer's disease; DLB, Dementia with Lewy body; C, Controls; MoCA, Montreal Cognitive Assessment; MMSE, Mini Mental Status Examination; Aβ, $A\beta_{1-42}$ amyloid; NFL, neurofilament light chain protein; H-FABP, heart fatty acid-binding protein; ***longitudinal studies.***

in the brainstem are important cholinergic projections in and post-mortem studies have shown that neuronal loss in in the nucleus basalis is an early phenomenon in PD (100, 101). Combining many modalities, Compta et al. (23) performed a longitudinal study in non-demented PD patients including CSF, neuropsychological and MRI studies at baseline and 18 months follow up. Here, a combination of lower CSF Aβ, reduced verbal learning, semantic fluency and visuoperceptual scores, as well

TABLE 2 | Cortical and subcortical structural changes related to cognitive impairment and dementia in Parkinson's disease.

Study	Participants	Methods	Result
Weintraub et al. (64)	PDND 60	VBM*	In PD-MCI hippocampal and temporal gray matter atrophy.
Melzer et al. (65)	PDND 57 PD-MCI 23 PDD 16 C 34	VBM	In PD-MCI gray matter atrophy in temporal, parietal, frontal cortex, amygdala, right putamen, and hippocampus. In PDD additional atrophy in medial temporal lobe, lingual gyrus, posterior cingulate gyrus, and bilateral caudate.
Lee et al. (66)	PD-MCI 51 C 25	VBM*	PD-MCI to PDD converters had lower GM density in the left prefrontal areas, left insular cortex and bilateral caudate nucleus compared with that in PD-MCI non-converters.
Borroni et al. (67)	PDND11 PDD 10 LBD 13 C 10	VBM	In PDD bilateral frontal and subcortical (caudate nucleus) gray matter atrophy.
Duncan et al. (68)	PDND 125 C 50	VBM DTI	Frontal and parietal gray matter volume reductions were associated with reduced executive function. Increased mean diffusivity was associated with performance on the semantic fluency and Tower of London tasks in frontal and parietal white matter tracts.
Hattori et al. (69)	PDND 32 PD-MCI 28 PDD 25 DLB 29 C 40	VBM TBSS	In PDD more atrophy in the cerebellum, thalami, insula, parietal cortex and occipital cortex.
Kandiah et al. (70)	PDND 97	Hippocampal volume White matter hyperintensities*	Hippocampal volume predicts PD-MCI and PDD.
Rektorova et al. (71)	PDND 75 PD-MCI 29 PDD 22	Spatial Independent Component Analysis	In PDD gray matter volume reductions in the hippocampus and temporal lobes, fronto-parietal regions and increases in the midbrain/cerebellum correlated with visuospatial deficits and letter verbal fluency, respectively.
Biundo et al. (72)	PDND 15 PD-MCI 14 HC 21	Cortical thickness	In PD-MCI cortical thinning in right supramarginal, dorsolateral prefrontal cortex, hippocampus, orbito-frontal, fusiform, superior parietal, and cuneus.
Pereira et al. (73)	PDND 90 PD-MCI 33 H 56	Cortical thickness	In PD-MCI cortical thinning in left precuneus, inferior temporal precentral, superior parietal, and lingual regions.
Hanganu et al. (74)	PDND 15 PD-MCI 17 H 18	Cortical thickness *	In PD-MCI thinning in temporal and medial occipital lobe, nucleus accumbens and amygdala correlate with cognitive decline.
Ibarretxe-Bilbao et al. (75)	PDND 16 C 15	Cortical thickness*	In PD cortical thinning in bilateral fronto-temporal regions and reduced amygdala volume.
Mak et al. (76)	PDND 66 PD-MCI 39 H 37	Cortical thickness*	PD-MCI converters showed bilateral temporal cortex thinning at baseline.
Hwang et al. (77)	PDND 12 PDD 11 C 14	Cortical pattern matching Cortical thickness	PDD showed thinning bilateral sensorimotor, lateral parietal, right posterior cingulate, parieto-occipital, inferior temporal and lateral frontal relative to C and PDND.
Zarei et al. (78)	Early PD 24 moderate PD 18 PDD 15 C 39	Cortical thickness	MMSE correlated positively with cortical thickness in the anterior temporal, dorsolateral prefrontal, posterior cingulate, temporal fusiform and occipitotemporal cortex.
Pagonabarraga et al. (79)	PDND 26 PD-MCI 26 PDD 20 C 18	Cortical thickness	From PDND to PDD a linear and progressive cortical thinning was observed in areas functionally specialized in declarative memory (entorhinal cortex, anterior temporal pole), semantic knowledge (parahippocampus, fusiform gyrus), and visuoperceptive integration (banks of the superior temporal sulcus, lingual gyrus, cuneus and precuneus).
Carlesimo et al. (80)	PDND 25 C 25	DTI	Increased mean diffusivity in the PD hippocampi; high hippocampal mean diffusivity values obtained low memory scores.
Chen et al. (81)	PDND 19 PDD 11 C 21	DTI	In PDD lower fractional anisotropy in the left hippocampus, higher mean diffusivity in widespread white matter regions. In PD positive correlation between MoCA score and fractional anisotropy of left inferior longitudinal and hippocampus, and bilateral superior longitudinal fasciculus.

*PD, Patients with Parkinson's disease; PD-MCI, Parkinson's disease patients with mild cognitive impairment; PDD, Parkinson's disease patients with dementia; PDND, non-demented PD; DLB, Dementia with Lewy body; C, Controls; MoCA, Montreal Cognitive Assessment; MMSE, Mini Mental Status Examination; * **longitudinal studies.***

TABLE 3 | Changes of function and connectivity related to cognitive impairment and dementia in Parkinson's disease.

Study	Participants	Methods	Result
Gorges et al. (82)	PDND 14 PDD 17 C 22	Resting-state fMRI	In PDND hyperconnectivity (network expansions) in cortical, limbic, and basal ganglia-thalamic areas. In PDD decreased intrinsic functional connectivity compared with controls (predominantly between major nodes of the default mode network).
Baggio et al. (83)	PDND 32 PD-MCI 23 C 36	Resting-state fMRI	In PD-MCI reduced connectivity between dorsal attention network and right fronto-insular regions (worse performance in executive functions) and increased connectivity between default mode network and medial and lateral occipito-parietal regions (worse visuo-spatial performance).
Amboni et al. (84)	PDND 21 PD-MCI 21 C 20	Resting-state fMRI	In PD-MCI patients decreased functional connectivity in bilateral prefrontal cortex (fronto-parietal network).
Tessitore et al. (85)	PDNT 16 C 16	Resting-state fMRI	In PDND decreased default mode network connectivity correlated with cognitive parameters.
Rektorova et al. (86)	PDND 18 PDD 14 C 18	Resting-state fMRI	In PDD decreased connectivity in the right inferior frontal gyrus compared to PDND and C (using posterior cingulate cortex/precuneus as seed for analysis).
Borroni et al. (67)	PDND11 PDD 10 LBD 13 C 10	Resting-state fMRI	Reduced local coherence of frontal regions in PD and in PDD.
Olde et al. (87)	PDND 55 C 15	Resting-state fMRI	In PDND longitudinally decreases in functional connectivity most prominent for posterior brain regions correlated with disease progression and cognitive decline.
Seibert et al. (88)	C 19 PDND 19 PDD 18	Resting-state fMRI	In PDD corticostriatal functional correlations were decreased in bilateral prefrontal regions.
Lin et al. (89)	PDND 17 PDD 17 C 17	Arterial spin labeling (ASL) magnetic resonance imaging (ASL-MRI)	In PDND and PDD progressive widespread cortical hypoperfusion.
Le Heron et al. (90)	PDD 20 AD 17 C 37	Arterial spin labeling (ASL) magnetic resonance imaging (ASL-MRI)	In AD and PDD posterior hypoperfusion (including posterior cingulate gyrus, precuneus, occipital regions). Perfusion in medial temporal lobes (AD<PDD) and right frontal cortex (PDD<AD) differed between PDD and AD.
Vander Borght et al. (91)	PDD 9 AD 9 C 9	[18F]fluorodeoxyglucose-PET	In PDD and AD hypometabolism with similar regional accentuation (lateral parietal, lateral temporal and lateral frontal association cortices and posterior cingulate cortex). In contrast to AD PDD showed greater metabolic reduction in the visual cortex and relatively preserved metabolism in the medial temporal cortex.
Gonzalez-Redondo et al. (92)	PDND 14 PD-MCI 17 PDD 15 C 19	[18F]fluorodeoxyglucose-PET	In PD-MCI the hypometabolism exceeded atrophy in the angular gyrus, occipital, orbital and anterior frontal lobes. In PDD these areas were atrophic and surrounded by extensive hypometabolism.
Shinotoh et al. (93)	PDND 14 PDD 2 PSP 12 C 13	Acetylcholinesterase activity using N-methyl-4-[11C]piperidyl acetate PET	In PDD higher reduction of choline acetyltransferase and acetylcholinesterase than in PDND.
Bohnen et al. (94)	PDND 11 PDD 14 AD 12 C 10	Acetylcholinesterase activity using [^{11}C]Methylpiperidin-4-ylpropionate PET	Mean cortical acetylcholinesterase activity was lowest in PDD.
Hiraoka et al. (95)	PDD 12 C 13	[5-(11)C-methoxy]donepezil-PET	In PDD density of acetylcholinesterase in the cerebral cortices correlated with improvements in visuoperceptual function after 3 months of donepezil therapy.
Kotagal et al. (96)	PDND 11 PDD 6 DLB 6 C 14	Acetylcholinesterase activity using [^{11}C]Methylpiperidin-4-ylpropionate PET	Thalamic cholinergic denervation is present in PD, PDD, and DLB but not in AD.

PD, Patients with Parkinson's disease; PD-MCI, Parkinson's disease patients with mild cognitive impairment; PDD, Parkinson's disease patients with dementia; PDND, non-demented PD; DLB, Dementia with Lewy body; AD, Patients with Alzheimer's disease; C, Controls; MoCA, Montreal Cognitive Assessment; MMSE, Mini Mental Status Examination; PET, positron emission tomography.

as cortical thinning in superior-frontal/anterior cingulate and precentral regions were found to be predictive for PDD.

For the assessment of white matter pathology using DTI and imaging of metabolites (Proton magnetic resonance spectroscopy) there is currently not enough longitudinal data available and the value of these techniques to predict cognitive decline has to be further explored. The existing studies indicate that microstructural changes, such as increased mean diffusivity or reduced fractional anisotropy in the hippocampus, the frontal and parietal white matter tracts are associated with cognitive decline in PD (68, 80, 81, 102–104). In particular, an increased mean diffusivity may be predictive for cognitive decline before fractional anisotropy decreases. However, these findings need further validation in longitudinal studies.

FATIGUE

Fatigue is a common symptom that includes both mental and physical aspects. Up to 70% of individuals with PD experience fatigue every day (105). Fatigue dramatically impairs quality of life (106). It is a complex syndrome emerging from dysfunction in the nervous, endocrine and immune system (107). From a clinical point of view fatigue is frequently associated with other non-motor syndromes, like sleepiness, apathy, depression and autonomic dysfunction (105, 108). However, fatigue can also occur as an isolated syndrome; it is therefore important to understand that fatigue and sleepiness or depression is not the same condition (109, 110). Central fatigue is commonly measured through questionnaires, such as the Fatigue Severity Scale (111) which is recommended by the Movement Disorder Society (MDS) task force (112). Central fatigue can be described as a feeling of constant exhaustion and can occur in various chronic disorders. Peripheral fatigue is characterized by failure to sustain the force of muscle contraction and is more readily accessible to quantification (106, 113).

A key mechanism underlying fatigue is the activation of the inflammatory cytokine network (107, 114). Therefore, inflammatory markers serve as potential biomarkers of fatigue. In particular, higher serum levels of IL-6, IL1-Ra, sIL-2R, and VCAM-1 were associated with higher fatigue levels in patients with newly diagnosed, drug-naïve PD (115, 116). This neuroinflammatory processes may promote glutamate dysregulation and further influence neuronal activity and neuroplasticity, and impact neuronal circuits mediating distress and motivation in PD (117–119). Interestingly, higher serum uric acid levels were significantly associated with less fatigue (120).

In addition, dysfunction of the endocrine system, such as hypothalamic-pituitary-adrenal system which is connected to basal ganglia, amygdala, thalamus and frontal cortex, seems to contribute to the pathophysiology of fatigue (113). Although there are no neuropathological studies of PD-fatigue supporting this model so far, several neuroimaging studies showed that multiple brain areas are involved in fatigue in PD. These include frontal, temporal and parietal regions indicative of emotion, motivation and cognitive functions (121–126). In SPECT imaging with technetium-99 hexamethyl-propylene-amine-oxime PD-fatigue was associated with reduced perfusion in the frontal lobe (125). Others used PET with dopaminergic and serotonergic markers in fatigued vs. non-fatigued PD patients. Less serotonergic marker binding was found in striatal and limbic regions (thalamus, anterior cingulate, amygdala, insula) in PD-fatigue. The striatal ^{18}F-dopa uptake was similar in fatigued and non-fatigued groups, but voxel-based analysis localized the reduced dopamine uptake to the caudate and insula in PD-fatigue (127). In addition the serotonin transporter (SERT) availability was significantly reduced in the striatum and thalamus of fatigued PD patients, suggesting that increasing the brain level of serotonin may improve PD-fatigue (127). The reduced serotonergic transmission suggests that a disturbed neurotransmitter balance within the basal ganglia and associated regions changes the integration of emotional and motor information in limbic regions, thus resulting in fatigue symptoms (128). With regard to striatal dopamine transporter uptake, results are conflicting. Two studies found no difference between fatigued and non-fatigued PD (127, 129). In the study by Chou et al., striatal dopamine transporter uptake was a significant predictor of fatigue in mild but not moderate-to-severe PD. They postulated that the lack of association between fatigue and nigrostriatal loss in advanced PD may reflect a denervation "floor" effect (130). Many of these studies have assessed advanced disease stages and patients on dopaminergic treatment. In contrast, Tessitore et al. studied fatigue in drug-naïve early PD using resting-state functional MRI (fMRI). Fatigue itself, and fatigue severity were associated with a decreased connectivity within the supplementary motor area and an increased connectivity within the default mode network (121). Importantly, these functional abnormalities occur independently from both dopamine-induced connectivity and structural changes. This study is in line with earlier neurophysiological studies suggesting that abnormal premotor and primary motor cortices connectivity correlate with fatigue (131, 132). Tessitore et al. hypothesized that the increased connectivity of the default mode network represents an initial cognitive compensatory response to the fatigue-related motor connectivity changes. In this sense fatigued PD-patients, when internally oriented, have to increase mental expenditure to maintain the same level of motor planning performance in order to switch more easily to externally oriented processing (121).

In summary, abnormalities in motivation of self-initiated tasks and motor function may play a significant role in the pathophysiology of fatigue (133). While non-dopaminergic basal ganglia pathways seem to be involved in PD-fatigue, the dopaminergic dysfunction may only play a role through extrastriatal projections.

DEPRESSION

PD patients are twice as likely to develop depression compared to healthy individuals (134). Depressive symptoms affect 40–50%

of PD patients and significantly impact quality of life in PD (2). In particular, patients with cognitive impairment, longer disease duration, motor fluctuations, female gender, and higher doses of levodopa are at risk to develop depression (9).

Like other NMS, depression seems to be linked to inflammatory signaling. Increased inflammatory responses have been described both in the brain and peripheral blood of PD patients (135). Depression correlated with a high serum level of IL-10 (136) and IL-6 (137). High levels of both sIL-2R and TNF-α in blood samples from PD patients were significantly associated with more severe depression and anxiety (119). As reflection of CNS involvement, high CRP levels in CSF of PD patients were associated with more severe symptoms of depression (32). However, these findings are not specific for PD. Chronic inflammation in physically ill patients is often associated with symptoms of depression and also occurs in normal aging (138–140). Moreover, PD in general is characterized by elevated levels of inflammatory cytokines, such as IL-6, tumor necrosis factor, IL-1β, IL-2, IL-10, C-reactive protein, and RANTES (141).

Depression in PD is associated with several structural and functional changes in the limbic system. In particular, changes in the amygdala, hippocampus and orbitofrontal cortex were frequently reported in PD depression (142–151). The involvement of the serotonergic system was demonstrated in post-mortem tissue and validated *in vivo* by several PET imaging studies (152–155). Compared to controls the serotonin transporter binding in non-depressed PD was lower in the striatal region, the orbitofrontal cortex, and the dorsolateral pre-frontal cortex which is an area known to be involved in major depression (155). Using dopaminergic and serotonergic presynaptic transporter radioligands a prominent role of serotonergic degeneration in limbic regions such as the anterior cingulate cortex was demonstrated (156, 157). Other PET studies observed a higher availability of the serotonin transporter in the raphe nuclei and limbic regions of depressed PD patients (152, 153). Likewise, decreased plasma levels of serotonin were found to be correlated with severity of depression (158). However, studies of the serotonin metabolite 5-hydroxyindoleacetic acid (5-HIAA) in CSF from depressed and non-depressed PD patients, have yielded contradictory results (159), and serotonergic dysfunction alone may only explain vulnerability to depression in PD. Yet, symptoms of depression are also linked to mesolimbic dopaminergic degeneration (160, 161) which is in line with the clinical observation of improvement of depression by dopaminergic treatment (162).

CONCLUSION

From this overview emerges a comprehensive picture of recent fluid and imaging biomarkers which have been studied in a number of clearly defined and sizable cohorts of PD patients with PD. Especially longitudinal studies are necessary to make the biomarkers potentially useful for therapeutic or even clinical trial evaluation. A number of recent studies have provided ample evidence for specific predictive biomarkers across multiple domains combining clinical, biochemical, and neuroimaging information. Yet, at this stage a lack of standardized and comparable methods preclude clinical everyday use of these biomarkers beyond their value as diagnostic or prognostic tools in cohorts of patients. Thus, more research needs to be undertaken into finding reliable combinations of predictors of NMS in PD on an individual level, and standardization and harmonization of protocols in particular in CSF handling and neuroimaging has to be taken further.

AUTHOR CONTRIBUTIONS

TP and JG: conception, collection of data, interpretation of data, drafting the work; OW: revising the work critically for important intellectual content.

ACKNOWLEDGMENTS

We thank Elena Huß for assistance of data collection.

REFERENCES

1. Schapira AHV, Chaudhuri KR, Jenner P. Non-motor features of Parkinson disease. *Nat Rev Neurosci*. (2017) 18:509. doi: 10.1038/nrn.2017.91
2. van Uem JM, Marinus J, Canning C, van Lummel R, Dodel R, Liepelt-Scarfone I, et al. Health-related quality of life in patients with parkinson's disease–a systematic review based on the ICF model. *Neurosci Biobehav Rev*. (2016) 61:26–34. doi: 10.1016/j.neubiorev.2015.11.014
3. Biomarkers Definitions Working Group. Biomarkers and surrogate endpoints: preferred definitions and conceptual framework. *Clin Pharmacol Ther*. (2001) 69:89–95. doi: 10.1067/mcp.2001.113989
4. Fengler S, Liepelt-Scarfone I, Brockmann K, Schäffer E, Berg D, Kalbe E. Cognitive changes in prodromal Parkinson's disease: a review. *Mov Disord*. (2017) 32:1655–66. doi: 10.1002/mds.27135
5. Aarsland D, Brønnick K, Larsen JP, Tysnes OB, Alves G, Norwegian ParkWest Study Group. Cognitive impairment in incident, untreated Parkinson disease: the Norwegian ParkWest study. *Neurology*. (2009) 72:1121–6. doi: 10.1212/01.wnl.0000338632.00552.cb
6. Litvan I, Goldman JG, Tröster AI, Schmand BA, Weintraub D, Petersen RC, et al. Diagnostic criteria for mild cognitive impairment in Parkinson's disease: movement disorder society task force guidelines. *Mov Disord*. (2012) 27:349–56. doi: 10.1002/mds.24893
7. Aarsland D, Andersen K, Larsen JP, Lolk A, Kragh-Sørensen P. Prevalence and characteristics of dementia in Parkinson disease: an 8-year prospective study. *Arch Neurol*. (2003) 60:387–92. doi: 10.1001/archneur.60.3.387
8. Svenningsson P, Westman E, Ballard C, Aarsland D. Cognitive impairment in patients with Parkinson's disease: diagnosis, biomarkers, and treatment. *Lancet Neurol*. (2012) 11:697–707. doi: 10.1016/S1474-4422(12)70152-7
9. Marinus J, Zhu K, Marras C, Aarsland D, van Hilten JJ. Risk factors for non-motor symptoms in Parkinson's disease. *Lancet Neurol*. (2018) 17:559–68. doi: 10.1016/S1474-4422(18)30127-3
10. Anang JB, Gagnon JF, Bertrand JA, Romenets SR, Latreille V, Panisset M, et al. Predictors of dementia in Parkinson disease: a prospective cohort study. *Neurology*. (2014) 83:1253–60. doi: 10.1212/WNL.0000000000000842
11. Zhu K, van Hilten JJ, Marinus J. Predictors of dementia in Parkinson's dise findings from a 5-year prospective study using

the SCOPA-COG. *Parkinsonism Relat Disord*. (2014) 20:980–5. doi: 10.1016/j.parkreldis.2014.06.006
12. Litvan I, Aarsland D, Adler CH, Goldman JG, Kulisevsky J, Mollenhauer B, et al. MDS Task Force on mild cognitive impairment in Parkinson's disease: critical review of PD-MCI. *Mov Disord*. (2011) 26:1814–24. doi: 10.1002/mds.23823
13. Pagano G, De Micco R, Yousaf T, Wilson H, Chandra A, Politis M. REM behavior disorder predicts motor progression and cognitive decline in Parkinson disease. *Neurology*. (2018) 91:e894–e905. doi: 10.1212/WNL.0000000000006134
14. Williams-Gray CH, Foltynie T, Brayne CE, Robbins TW, Barker RA. Evolution of cognitive dysfunction in an incident Parkinson's disease cohort. *Brain*. (2007) 130(Pt 7):1787–98. doi: 10.1093/brain/awm111
15. Kehagia AA, Barker RA, Robbins TW. Cognitive impairment in Parkinson's disease: the dual syndrome hypothesis. *Neurodegener Dis*. (2013) 11:79–92. doi: 10.1159/000341998
16. Braak H, Rüb U, Jansen Steur EN, Del Tredici K, de Vos RA. Cognitive status correlates with neuropathologic stage in Parkinson disease. *Neurology*. (2005) 64:1404–10. doi: 10.1212/01.WNL.0000158422.41380.82
17. Aarsland D, Perry R, Brown A, Larsen JP, Ballard C. Neuropathology of dementia in Parkinson's disease: a prospective, community-based study. *Ann Neurol*. (2005) 58:773–6. doi: 10.1002/ana.20635
18. Alves G, Lange J, Blennow K, Zetterberg H, Andreasson U, Førland MG, et al. CSF $A\beta_{42}$ predicts early-onset dementia in Parkinson disease. *Neurology*. (2014) 82:1784–90. doi: 10.1212/WNL.0000000000000425
19. Bäckström DC, Eriksson Domellöf M, Linder J, Olsson B, Öhrfelt A, Trupp M, et al. Cerebrospinal fluid patterns and the risk of future dementia in early, incident Parkinson disease. *JAMA Neurol*. (2015) 72:1175–82. doi: 10.1001/jamaneurol.2015.1449
20. Brockmann K, Lerche S, Dilger SS, Stirnkorb JG, Apel A, Hauser AK, et al. SNPs in Aβ clearance proteins: lower CSF $A\beta_{1-42}$ levels and earlier onset of dementia in PD. *Neurology*. (2017) 89:2335–40. doi: 10.1212/WNL.0000000000004705
21. Compta Y, Martí MJ, Ibarretxe-Bilbao N, Junqué C, Valldeoriola F, Mu-oz E, et al. Cerebrospinal tau, phospho-tau, and beta-amyloid and neuropsychological functions in Parkinson's disease. *Mov Disord*. (2009) 24:2203–10. doi: 10.1002/mds.22594
22. Compta Y, Ezquerra M, Mu-oz E, Tolosa E, Valldeoriola F, Rios J, et al. High cerebrospinal tau levels are associated with the rs57 tau gene variant and low cerebrospinal β-amyloid in Parkinson disease. *Neurosci Lett*. (2011) 487:169–73. doi: 10.1016/j.neulet.2010.10.015
23. Compta Y, Pereira JB, Ríos J, Ibarretxe-Bilbao N, Junqué C, Bargalló N, et al. Combined dementia-risk biomarkers in Parkinson's disease: a prospective longitudinal study. *Parkinsonism Relat Disord*. (2013) 19:717–24. doi: 10.1016/j.parkreldis.2013.03.009
24. Compta Y, Valente T, Saura J, Segura B, Iranzo Á, Serradell M, et al. Correlates of cerebrospinal fluid levels of oligomeric- and total-α-synuclein in premotor, motor and dementia stages of Parkinson's disease. *J Neurol*. (2015) 262:294–306. doi: 10.1007/s00415-014-7560-z
25. Ffytche DH, Pereira JB, Ballard C, Chaudhuri KR, Weintraub D, Aarsland D. Risk factors for early psychosis in PD: insights from the Parkinson's progression markers initiative. *J Neurol Neurosurg Psychiatry*. (2017) 88:325–31. doi: 10.1136/jnnp-2016-314832
26. Gmitterov,á K, Gawinecka J, Llorens F, Varges D, Valkovič P, Zerr I. Cerebrospinal fluid markers analysis in the differential diagnosis of dementia with Lewy bodies and Parkinson's disease dementia. *Eur Arch Psychiatry Clin Neurosci*. (2018). doi: 10.1007/s00406-018-0928-9
27. Halbgebauer S, Nagl M, Klafki H, Haußmann U, Steinacker P, Oeckl P, et al. Modified serpinA1 as risk marker for Parkinson's disease dementia: analysis of baseline data. *Sci Rep*. (2016) 6:26145. doi: 10.1038/srep26145
28. Hall S, Öhrfelt A, Constantinescu R, Andreasson U, Surova Y, Bostrom F, et al. Accuracy of a panel of 5 cerebrospinal fluid biomarkers in the differential diagnosis of patients with dementia and/or parkinsonian disorders. *Arch Neurol*. (2012) 69:1445–52. doi: 10.1001/archneurol.2012.1654
29. Hall S, Surova Y, Öhrfelt A, Zetterberg H, Lindqvist D, Hansson O. CSF biomarkers and clinical progression of Parkinson disease. *Neurology*. (2015) 84:57–63. doi: 10.1212/WNL.0000000000001098
30. Hansson O, Hall S, Ohrfelt A, Zetterberg H, Blennow K, Minthon L, et al. Levels of cerebrospinal fluid α-synuclein oligomers are increased in Parkinson's disease with dementia and dementia with Lewy bodies compared to Alzheimer's disease. *Alzheimers Res Ther*. (2014) 6:25. doi: 10.1186/alzrt255
31. Janssens J, Vermeiren Y, Fransen E, Aerts T, Van Dam D, Engelborghs S, et al. Cerebrospinal fluid and serum MHPG improve Alzheimer's disease versus dementia with Lewy bodies differential diagnosis. *Alzheimers Dement*. (2018) 10:172–81. doi: 10.1016/j.dadm.2018.01.002
32. Lindqvist D, Hall S, Surova Y, Nielsen HM, Janelidze S, Brundin L, et al. Cerebrospinal fluid inflammatory markers in Parkinson's disease: associations with depression, fatigue, and cognitive impairment. *Brain Behav Immun*. (2013) 33:183–9. doi: 10.1016/j.bbi.2013.07.007
33. Maetzler W, Liepelt I, Reimold M, Reischl G, Solbach C, Becker C, et al. Cortical PIB binding in Lewy body disease is associated with Alzheimer-like characteristics. *Neurobiol Dis*. (2009) 34:107–12. doi: 10.1016/j.nbd.2008.12.008
34. Maetzler W, Stapf AK, Schulte C, Hauser AK, Lerche S, Wurster I, et al. Serum and cerebrospinal fluid uric acid levels in lewy body disorders: associations with disease occurrence and amyloid-β pathway. *J Alzheimers Dis*. (2011) 27:119–26. doi: 10.3233/JAD-2011-110587
35. Maetzler W, Tian Y, Baur SM, Gauger T, Odoj B, Schmid B, et al. Serum and cerebrospinal fluid levels of transthyretin in Lewy body disorders with and without dementia. *PLoS ONE*. (2012) 7:e48042. doi: 10.1371/journal.pone.0048042
36. Modreanu R, Cerquera SC, Martí MJ, Ríos J, Sánchez-Gómez A, Cámara A, et al. *Cross*-sectional and longitudinal associations of motor fluctuations and non-motor predominance with cerebrospinal τ and Aβ as well as dementia-risk in Parkinson's disease. *J Neurol Sci*. (2017) 373:223–9. doi: 10.1016/j.jns.2016.12.064
37. Parnetti L, Tiraboschi P, Lanari A, Peducci M, Padiglioni C, D'Amore C, et al. Cerebrospinal fluid biomarkers in Parkinson's disease with dementia and dementia with Lewy bodies. *Biol Psychiatry*. (2008) 64:850–5. doi: 10.1016/j.biopsych.2008.02.016
38. Parnetti L, Farotti L, Eusebi P, Chiasserini D, De Carlo C, Giannandrea D, et al. Differential role of CSF alpha-synuclein species, tau, and Aβ42 in Parkinson's Disease. *Front Aging Neurosci*. (2014) 6:53. doi: 10.3389/fnagi.2014.00053
39. Schrag A, Siddiqui UF, Anastasiou Z, Weintraub D, Schott JM. Clinical variables and biomarkers in prediction of cognitive impairment in patients with newly diagnosed Parkinson's disease: a cohort study. *Lancet Neurol*. (2017) 16:66–75. doi: 10.1016/S1474-4422(16)30328-3
40. Siderowf A, Xie SX, Hurtig H, Weintraub D, Duda J, Chen-Plotkin A, et al. CSF amyloid β 1-42 predicts cognitive decline in Parkinson disease. *Neurology*. (2010) 75:1055–61. doi: 10.1212/WNL.0b013e3181f39a78
41. Stewart T, Liu C, Ginghina C, Cain KC, Auinger P, Cholerton B, et al. Parkinson Study Group DATATOP Investigators. Cerebrospinal fluid α-synuclein predicts cognitive decline in Parkinson disease progression in the DATATOP cohort. *Am J Pathol*. (2014) 184:966–75. doi: 10.1016/j.ajpath.2013.12.007
42. Terrelonge M Jr, Marder KS, Weintraub D, Alcalay RN. CSF β-amyloid 1-42 predicts progression to cognitive impairment in newly diagnosed parkinson disease. *J Mol Neurosci*. (2016) 58:88–92. doi: 10.1007/s12031-015-0647-x
43. Vranová HP, Hényková E, Kaiserová M, Menšíková K, Vaštík M, Mareš J, et al. Tau protein, beta-amyloid$_{1-42}$and clusterin CSF levels in the differential diagnosis of Parkinsonian syndrome with dementia. *J Neurol Sci*. (2014). 343:120–4. doi: 10.1016/j.jns.2014.05.052
44. Wennström M, Surova Y, Hall S, Nilsson C, Minthon L, Boström F, et al. Low CSF levels of both α-synuclein and the α-synuclein cleaving enzyme neurosin in patients with synucleinopathy. *PLoS ONE*. (2013) 8:e53250. doi: 10.1371/journal.pone.0053250
45. Liu C, Cholerton B, Shi M, Ginghina C, Cain KC, Auinger P, et al. CSF tau and tau/$A\beta_{42}$ predict cognitive decline in Parkinson's disease. *Parkinson Relat Disord*. (2015). 21:271–6. doi: 10.1016/j.parkreldis.2014.12.027
46. Montine TJ, Shi M, Quinn JF, Peskind ER, Craft S, Ginghina C, et al. CSF $A\beta_{42}$ and tau in Parkinson's disease with cognitive impairment. *Mov Disord*. (2010) 25:2682–5. doi: 10.1002/mds.23287

47. Palmqvist S, Zetterberg H, Blennow K, Vestberg S, Andreasson U, Brooks DJ, et al. Accuracy of brain amyloid detection in clinical practice using cerebrospinal fluid β-amyloid 42: a cross-validation study against amyloid positron emission tomography. *JAMA Neurol.* (2014) 71:1282–9. doi: 10.1001/jamaneurol.2014.1358
48. Skogseth RE, Bronnick K, Pereira JB, Mollenhauer B, Weintraub D, Fladby T, et al. Associations between cerebrospinal fluid biomarkers and cognition in early untreated Parkinson's disease. *J Parkinsons Dis.* (2015) 5:783–92. doi: 10.3233/JPD-150682
49. Zhou B, Wen M, Yu WF, Zhang CL, Jiao L. The diagnostic and differential diagnosis utility of cerebrospinal fluid α-synuclein levels in Parkinson's disease: a meta-analysis. *Parkinsons Dis*. (2015) 2015:567386 doi: 10.1155/2015/567386
50. Gao L, Tang H, Nie K, Wang L, Zhao J, Gan R, et al. Cerebrospinal fluid alpha-synuclein as a biomarker for Parkinson's disease diagnosis: a systematic review and meta-analysis. *Int J Neurosci.* (2015) 125:645–54. doi: 10.3109/00207454.2014.961454
51. Stav AL, Aarsland D, Johansen KK, Hessen E, Auning E, Fladby T. Amyloid-β and α-synuclein cerebrospinal fluid biomarkers and cognition in early Parkinson's disease. *Parkinsonism Relat Disord*. (2015) 21:758–64. doi: 10.1016/j.parkreldis.2015.04.027
52. Buddhala C, Campbell MC, Perlmutter JS, Kotzbauer PT. Correlation between decreased CSF α-synuclein and $A\beta_{1-42}$ in Parkinson disease*Neurobiol Aging.* (2015) 36:476–84. doi: 10.1016/j.neurobiolaging.2014.07.043
53. Hall S, Surova Y, Öhrfelt A, Swedish BioFINDER Study, Blennow K, Zetterberg H, et al. Longitudinal measurements of cerebrospinal fluid biomarkers in Parkinson's Disease. *Mov Disord.* (2016) 31:898–905. doi: 10.1002/mds.26578
54. Lin CH, Yang SY, Horng HE, Yang CC, Chieh JJ, Chen HH, et al. Plasma α-synuclein predicts cognitive decline in Parkinson's disease. *J Neurol Neurosurg Psychiatry*. (2017) 88:818–24. doi: 10.1136/jnnp-2016-314857
55. Delgado-Alvarado M, Gago B, Navalpotro-Gomez I, Jiménez-Urbieta H, Rodriguez-Oroz MC. Biomarkers for dementia and mild cognitive impairment in Parkinson's disease. *Mov Disord*. (2016) 31:861–81. doi: 10.1002/mds.26662
56. Annanmaki T, Pessala-Driver A, Hokkanen L, Murros K. Uric acid associates with cognition in Parkinson's disease. *Parkinsonism Relat Disord*. (2008) 14:576–8. doi: 10.1016/j.parkreldis.2007.11.001
57. Moccia M, Picillo M, Erro R, Vitale C, Longo K, Amboni M, et al. Is serum uric acid related to non-motor symptoms in de-novo Parkinson's disease patients? *Parkinsonism Relat Disord*. (2014) 20:772–5. doi: 10.1016/j.parkreldis.2014.03.016
58. Moccia M, Picillo M, Erro R, Vitale C, Longo K, Amboni M, et al. Presence and progression of non-motor symptoms in relation to uric acid in *de novo* Parkinson's disease. *Eur J Neurol.* (2015) 22:93–8. doi: 10.1111/ene.12533
59. Pellecchia MT, Santangelo G, Picillo M, Pivonello R, Longo K, Pivonello C, et al. Serum epidermal growth factor predicts cognitive functions in early, drug-naive Parkinson's disease patients. *J Neurol.* (2013) 260:438–44. doi: 10.1007/s00415-012-6648-6
60. Chen-Plotkin AS, Hu WT, Siderowf A, Weintraub D, Goldmann Gross R, Hurtig HI, et al. Plasma epidermal growth factor levels predict cognitive decline in Parkinson disease. *Ann Neurol.* (2011) 69:655–63. doi: 10.1002/ana.22271
61. Pellecchia MT, Santangelo G, Picillo M, Pivonello R, Longo K, Pivonello C, et al. Insulin-like growth factor-1 predicts cognitive functions at 2-year follow-up in early, drug-naïve Parkinson's disease. *Eur J Neurol.* (2014) 21:802–7. doi: 10.1111/ene.12137
62. Fereshtehnejad SM, Zeighami Y, Dagher A, Postuma RB. Clinical criteria for subtyping Parkinson's disease: biomarkers and longitudinal progression. *Brain.* (2017) 140:1959–76. doi: 10.1093/brain/awx118
63. Prell T. Structural and functional brain patterns of non-motor syndromes in Parkinson's Disease. *Front Neurol.* (2018) 9:138. doi: 10.3389/fneur.2018.00138
64. Weintraub D, Dietz N, Duda JE, Wolk DA, Doshi J, Xie SX, et al. Alzheimer's disease pattern of brain atrophy predicts cognitive decline in Parkinson's disease. *Brain.* (2012) 135(Pt 1):170–180. doi: 10.1093/brain/awr277
65. Melzer TR, Watts R, MacAskill MR, Pitcher TL, Livingston L, Keenan RJ, et al. Grey matter atrophy in cognitively impaired Parkinson's disease. *J Neurol Neurosurg Psychiatry.* (2012) 83:188–94. doi: 10.1136/jnnp-2011-300828
66. Lee JE, Cho KH, Song SK, Kim HJ, Lee HS, Sohn YH, et al. Exploratory analysis of neuropsychological and neuroanatomical correlates of progressive mild cognitive impairment in Parkinson's disease. *J Neurol Neurosurg Psychiatry*. (2014) 85:7–16. doi: 10.1136/jnnp-2013-305062
67. Borroni B, Premi E, Formenti A, Turrone R, Alberici A, Cottini E, et al. Structural and functional imaging study in dementia with Lewy bodies and Parkinson's disease dementia. *Parkinsonism Relat Disord*. (2015) 21:1049–55. doi: 10.1016/j.parkreldis.2015.06.013
68. Duncan GW, Firbank MJ, Yarnall AJ, Khoo TK, Brooks DJ, Barker RA, et al. Gray and white matter imaging: a biomarker for cognitive impairment in early Parkinson's disease? *Mov Disord*. (2016) 31:103–10. doi: 10.1002/mds.26312
69. Hattori T, Orimo S, Aoki S, Ito K, Abe O, Amano A, et al. Cognitive status correlates with white matter alteration in Parkinson's disease. *Hum Brain Mapp*. (2012) 33:727–39. doi: 10.1002/hbm.21245
70. Kandiah N, Zainal NH, Narasimhalu K, Chander RJ, Ng A, Mak E, et al. Hippocampal volume and white matter disease in the prediction of dementia in Parkinson's disease. *Parkinsonism Relat Disord*. (2014) 20:1203–8. doi: 10.1016/j.parkreldis.2014.08.024
71. Rektorova I, Biundo R, Marecek R, Weis L, Aarsland D, Antonini A. Grey matter changes in cognitively impaired Parkinson's disease patients. *PLoS ONE.* (2014) 9:e85595. doi: 10.1371/journal.pone.0085595
72. Biundo R, Calabrese M, Weis L, Facchini S, Ricchieri G, Gallo P, et al. Anatomical correlates of cognitive functions in early Parkinson's disease patients. *PLoS ONE.* (2013) 8:e64222. doi: 10.1371/journal.pone.0064222
73. Pereira JB, Svenningsson P, Weintraub D, Brønnick K, Lebedev A, Westman E, et al. Initial cognitive decline is associated with cortical thinning in early Parkinson disease. *Neurology*. (2014) 82:2017–25. doi: 10.1212/WNL.0000000000000483
74. Hanganu A, Bedetti C, Degroot C, Mejia-Constain B, Lafontaine AL, Soland V, et al. Mild cognitive impairment is linked with faster rate of cortical thinning in patients with Parkinson's disease longitudinally. *Brain.* (2014) 137(Pt 4):1120–9. doi: 10.1093/brain/awu036
75. Ibarretxe-Bilbao N, Junque C, Segura B, Baggio HC, Marti MJ, Valldeoriola F, et al. Progression of cortical thinning in early Parkinson's disease. *Mov Disord*. (2012) 27:1746–53. doi: 10.1002/mds.25240
76. Mak E, Su L, Williams GB, Firbank MJ, Lawson RA, Yarnall AJ, et al. Baseline and longitudinal grey matter changes in newly diagnosed Parkinson's disease: ICICLE-PD study. *Brain.* (2015) 138(Pt 10):2974–86. doi: 10.1093/brain/awv211
77. Hwang KS, Beyer MK, Green AE, Chung C, Thompson PM, Janvin C, et al. Mapping cortical atrophy in Parkinson's disease patients with dementia. *J Parkinsons Dis.* (2013) 3:69–76. doi: 10.3233/JPD-120151
78. Zarei M, Ibarretxe-Bilbao N, Compta Y, Hough M, Junque C, Bargallo N, et al. Cortical thinning is associated with disease stages and dementia in Parkinson's disease. *J Neurol Neurosurg Psychiatry*. (2013) 84:875–81. doi: 10.1136/jnnp-2012-304126
79. Pagonabarraga J, Corcuera-Solano I, Vives-Gilabert Y, Llebaria G, García-Sánchez C, Pascual-Sedano B, et al. Pattern of regional cortical thinning associated with cognitive deterioration in Parkinson's disease. *PLoS ONE.* (2013) 8:e54980. doi: 10.1371/journal.pone.0054980
80. Carlesimo GA, Piras F, Assogna F, Pontieri FE, Caltagirone C, Spalletta G. Hippocampal abnormalities and memory deficits in Parkinson disease: a multimodal imaging study. *Neurology.* (2012) 78:1939–45. doi: 10.1212/WNL.0b013e318259e1c5
81. Chen B, Fan GG, Liu H, Wang S. Changes in anatomical and functional connectivity of Parkinson's disease patients according to cognitive status. *Eur J Radiol.* (2015) 84:1318–24. doi: 10.1016/j.ejrad.2015.04.014
82. Gorges M, Müller HP, Lulé D; LANDSCAPE Consortium, Pinkhardt EH, Ludolph AC,et al. To rise and to fall: functional connectivity in cognitively normal and cognitively impaired patients with Parkinson's disease. *Neurobiol Aging.* (2015) 36:1727–35. doi: 10.1016/j.neurobiolaging.2014.12.026
83. Baggio HC, Segura B, Sala-Llonch R, Marti MJ, Valldeoriola F, Compta Y, et al. Cognitive impairment and resting-state network

connectivity in Parkinson's disease. *Hum Brain Mapp*. (2015) 36:199–212. doi: 10.1002/hbm.22622
84. Amboni M, Tessitore A, Esposito F, Santangelo G, Picillo M, Vitale C, et al. Resting-state functional connectivity associated with mild cognitive impairment in Parkinson's disease. *J Neurol*. (2015) 262:425–34. doi: 10.1007/s00415-014-7591-5
85. Tessitore A, Esposito F, Vitale C, Santangelo G, Amboni M, Russo A, et al. Default-mode network connectivity in cognitively unimpaired patients with Parkinson disease. *Neurology*. (2012) 79:2226–32. doi: 10.1212/WNL.0b013e31827689d6
86. Rektorova I, Krajcovicova L, Marecek R, Mikl M. Default mode network and extrastriate visual resting state network in patients with Parkinson's disease dementia. *Neurodegener Dis*. (2012) 10:232–7. doi: 10.1159/000334765
87. Olde Dubbelink KT, Schoonheim MM, Deijen JB, Twisk JW, Barkhof F, Berendse HW. Functional connectivity and cognitive decline over 3 years in Parkinson disease. *Neurology*. (2014) 83:2046–53. doi: 10.1212/WNL.0000000000001020
88. Seibert TM, Murphy EA, Kaestner EJ, Brewer JB. Interregional correlations in Parkinson disease and Parkinson-related dementia with resting functional MR imaging. *Radiology*. (2012) 263:226–34. doi: 10.1148/radiol.12111280
89. Lin WC, Chen PC, Huang YC, Tsai NW, Chen HL, Wang HC, et al. Dopaminergic therapy modulates cortical perfusion in parkinson disease with and without dementia according to arterial spin labeled perfusion magnetic resonance imaging. *Medicine*. (2016) 95:e2206. doi: 10.1097/MD.0000000000002206
90. Le Heron CJ, Wright SL, Melzer TR, Myall DJ, MacAskill MR, Livingston L, et al. Comparing cerebral perfusion in Alzheimer's disease and Parkinson's disease dementia: an ASL-MRI study. *J Cereb Blood Flow Metab*. (2014) 34:964–70. doi: 10.1038/jcbfm.2014.40
91. Vander Borght T, Minoshima S, Giordani B, Foster NL, Frey KA, Berent S, et al. Cerebral metabolic differences in Parkinson's and Alzheimer's diseases matched for dementia severity. *J Nucl Med*. (1997) 38:797–802.
92. González-Redondo R, García-García D, Clavero P, Gasca-Salas C, García-Eulate R, Zubieta JL, et al. Grey matter hypometabolism and atrophy in Parkinson's disease with cognitive impairment: a two-step process. *Brain*. (2014) 137(Pt 8):2356–67. doi: 10.1093/brain/awu159
93. Shinotoh H, Namba H, Yamaguchi M, Fukushi K, Nagatsuka S, Iyo M, et al. Positron emission tomographic measurement of acetylcholinesterase activity reveals differential loss of ascending cholinergic systems in Parkinson's disease and progressive supranuclear palsy. *Ann Neurol*. (1999) 46:62–9. doi: 10.1002/1531-8249(199907)46:1<62::AID-ANA10>3.0.CO;2-P
94. Bohnen NI, Kaufer DI, Ivanco LS, Lopresti B, Koeppe RA, Davis JG, et al. Cortical cholinergic function is more severely affected in parkinsonian dementia than in Alzheimer disease: an *in vivo* positron emission tomographic study. *Arch Neurol*. (2003) 60:1745–8. doi: 10.1001/archneur.60.12.1745
95. Hiraoka K, Okamura N, Funaki Y, Hayashi A, Tashiro M, Hisanaga K, et al. Cholinergic deficit and response to donepezil therapy in Parkinson's disease with dementia. *Eur Neurol*. (2012) 68:137–143. doi: 10.1159/000338774
96. Kotagal V, Müller ML, Kaufer DI, Koeppe RA, Bohnen NI. Thalamic cholinergic innervation is spared in Alzheimer disease compared to parkinsonian disorders. *Neurosci Lett*. (2012) 514:169–72. doi: 10.1016/j.neulet.2012.02.083
97. Ramírez-Ruiz B, Mart,í MJ, Tolosa E, Bartrés-Faz D, Summerfield C, Salgado-Pineda P, et al. Longitudinal evaluation of cerebral morphological changes in Parkinson's disease with and without dementia. *J Neurol*. (2005) 252:1345–52. doi: 10.1007/s00415-005-0864-2
98. Morales DA, Vives-Gilabert Y, Gómez-Ansón B, Bengoetxea E, Larraaga P, Bielza C, et al. Predicting dementia development in Parkinson's disease using bayesian network classifiers. *Psychiatry Res*. (2013) 213:92–8. doi: 10.1016/j.pscychresns.2012.06.001
99. Schulz J, Pagano G, Fernández Bonfante JA, Wilson H, Politis M. Nucleus basalis of Meynert degeneration precedes and predicts cognitive impairment in Parkinson's disease. *Brain*. (2018) 141:1501–16. doi: 10.1093/brain/awy072
100. Arendt T, Bigl V, Arendt A, Tennstedt A. Loss of neurons in the nucleus basalis of Meynert in Alzheimer's disease, paralysis agitans and Korsakoff's Disease. *Acta Neuropathol*. (1983) 61:101–8. doi: 10.1007/BF00697388
101. Candy JM, Perry RH, Perry EK, Irving D, Blessed G, Fairbairn AF, et al. Pathological changes in the nucleus of meynert in Alzheimer's and Parkinson's diseases. *J Neurol Sci*. (1983) 59:277–89. doi: 10.1016/0022-510X(83)90045-X
102. Agosta F, Canu E, Stefanova E, Sarro L, Tomić A, Špica V, et al. Mild cognitive impairment in Parkinson's disease is associated with a distributed pattern of brain white matter damage. *Hum Brain Mapp*. (2014) 35:1921–9. doi: 10.1002/hbm.22302
103. Theilmann RJ, Reed JD, Song DD, Huang MX, Lee RR, Litvan I, et al. White-matter changes correlate with cognitive functioning in Parkinson's disease. *Front Neurol*. (2013) 4:37. doi: 10.3389/fneur.2013.00037
104. Zheng Z, Shemmassian S, Wijekoon C, Kim W, Bookheimer SY, Pouratian N. DTI correlates of distinct cognitive impairments in Parkinson's disease. *Hum Brain Mapp*. (2014) 35:1325–33. doi: 10.1002/hbm.22256
105. Friedman JH, Brown RG, Comella C, Garber CE, Krupp LB, Lou JS, et al. (2007). Working Group on Fatigue in Parkinson's Disease.Fatigue in Parkinson's disease: a review. *Mov Disord*. 22:297–308. doi: 10.1002/mds.21240
106. Friedman JH, Beck JC, Chou KL, Clark G, Fagundes CP, Goetz CG, et al. Fatigue in Parkinson's disease: report from a mutidisciplinary symposium. *NPJ Parkinsons Dis*. (2016) 2:15025. doi: 10.1038/npjparkd.2015.25
107. Klimas NG, Broderick G, Fletcher MA. Biomarkers for chronic fatigue. *Brain Behav Immun*. (2012) 26:1202–10. doi: 10.1016/j.bbi.2012.06.006
108. Chou KL, Gilman S, Bohnen NI. Association between autonomic dysfunction and fatigue in Parkinson disease. *J Neurol Sci*. (2017) 377:190–2. doi: 10.1016/j.jns.2017.04.023
109. Alves G, Wentzel-Larsen T, Larsen JP. Is fatigue an independent and persistent symptom in patients with Parkinson disease? *Neurology*. (2004) 63:1908–11. doi: 10.1212/01.WNL.0000144277.06917.CC
110. van Hilten JJ, Weggeman M, van der Velde EA, Kerkhof GA, van Dijk JG, Roos RA. Sleep, excessive daytime sleepiness and fatigue in Parkinson's disease. *J Neural Transm Park Dis Dement Sect*. (1993) 5:235–44. doi: 10.1007/BF02257678
111. Krupp LB, LaRocca NG, Muir-Nash J, Steinberg AD. The fatigue severity scale. Application to patients with multiple sclerosis and systemic lupus erythematosus. *Arch Neurol*. (1989) 46:1121–3. doi: 10.1001/archneur.1989.00520460115022
112. Kluger BM, Herlofson K, Chou KL, Lou JS, Goetz CG, Lang AE, et al. Parkinson's disease-related fatigue: A case definition and recommendations for clinical research. *Mov Disord*. (2016) 31:625–31. doi: 10.1002/mds.26511
113. Chaudhuri A, Behan PO. Fatigue in neurological disorders. *Lancet*. (2004) 363:978–88. doi: 10.1016/S0140-6736(04)15794-2
114. Bower JE. Cancer-related fatigue: links with inflammation in cancer patients and survivors. *Brain Behav Immun*. (2007) 21:863–71. doi: 10.1016/j.bbi.2007.03.013
115. Herlofson K, Heijnen CJ, Lange J, Alves G, Tysnes OB, Friedman JH, et al. Inflammation and fatigue in early, untreated Parkinson's disease. *Acta Neurol Scand*. (2018) 138:394–9. doi: 10.1111/ane.12977
116. Pereira JR, Santos LVD, Santos RMS, Campos ALF, Pimenta AL, de Oliveira MS, et al. IL-6 serum levels are elevated in Parkinson's disease patients with fatigue compared to patients without fatigue. *J Neurol Sci*. (2016) 370:153–6. doi: 10.1016/j.jns.2016.09.030
117. Eyre H, Baune BT. Neuroplastic changes in depression: a role for the immune system. *Psychoneuroendocrinology*. (2012) 37:1397–416. doi: 10.1016/j.psyneuen.2012.03.019
118. Miller AH, Haroon E, Raison CL, Felger JC. Cytokine targets in the brain: impact on neurotransmitters and neurocircuits. *Depress Anxiety*. (2013) 30:297–306. doi: 10.1002/da.22084
119. Lindqvist D, Kaufman E, Brundin L, Hall S, Surova Y, Hansson O. Non-motor symptoms in patients with Parkinson's disease - correlations with inflammatory cytokines in serum. *PLoS ONE*. (2012) 7:e47387. doi: 10.1371/journal.pone.0047387

120. Huang X, Ng SY, Chia NS, Acharyya S, Setiawan F, Lu ZH, et al. Serum uric acid level and its association with motor subtypes and non-motor symptoms in early Parkinson's disease: PALS study. *Parkinsonism Relat Disord.* (2018) 55:50–54. doi: 10.1016/j.parkreldis.2018.05.010
121. Tessitore A, Giordano A, De Micco R, Caiazzo G, Russo A, Cirillo M, et al. Functional connectivity underpinnings of fatigue in "Drug-Naïve" patients with Parkinson's disease. *Mov Disord.* (2016) 31:1497–505. doi: 10.1002/mds.26650
122. Zhang JJ, Ding J, Li JY, Wang M, Yuan YS, Zhang L, et al. Abnormal resting-state neural activity and connectivity of fatigue in Parkinson's disease. *CNS Neurosci Ther*. (2017) 23:241–7. doi: 10.1111/cns.12666
123. Li J, Yuan Y, Wang M, Zhang J, Zhang L, Jiang S, et al. Alterations in regional homogeneity of resting-state brain activity in fatigue of Parkinson's disease. *J Neural Transm.* (2017) 124:1187–95. doi: 10.1007/s00702-017-1748-1
124. Cho SS, Aminian K, Li C, Lang AE, Houle S, Strafella AP. Fatigue in Parkinson's disease: The contribution of cerebral metabolic changes. *Hum Brain Mapp*. (2017) 38:283–92. doi: 10.1002/hbm.23360
125. Abe K, Takanashi M, Yanagihara T. Fatigue in patients with Parkinson's disease. *Behav Neurol.* (2000) 12:103–6. doi: 10.1155/2000/580683
126. Zhang L, Li T, Yuan Y, Tong Q, Jiang S, Wang M, et al. Brain metabolic correlates of fatigue in Parkinson's disease: a PET study. *Int J Neurosci.* (2018) 128:330–6. doi: 10.1080/00207454.2017.1381093
127. Pavese N, Metta V, Bose SK, Chaudhuri KR, Brooks DJ. Fatigue in Parkinson's disease is linked to striatal and limbic serotonergic dysfunction. *Brain.* (2010) 133:3434–43. doi: 10.1093/brain/awq268
128. Politis M, Loane C. Serotonergic dysfunction in Parkinson's disease and its relevance to disability. *Scientific World Journal.* (2011) 11:1726–34. doi: 10.1100/2011/172893
129. Schifitto G, Friedman JH, Oakes D, Shulman L, Comella CL, Marek K, et al. Investigators. Fatigue in levodopa-naive subjects with Parkinson disease. *Neurology.* (2008) 71:481–5. doi: 10.1212/01.wnl.0000324862.29733.69
130. Chou KL, Kotagal V, Bohnen NI. Neuroimaging and clinical predictors of fatigue in Parkinson disease. *Parkinsonism Relat Disord.* (2016) 23:45–9. doi: 10.1016/j.parkreldis.2015.11.029
131. Lou JS, Benice T, Kearns G, Sexton G, Nutt J. Levodopa normalizes exercise related cortico-motoneuron excitability abnormalities in Parkinson's disease. *Clin Neurophysiol.* (2003) 114:930–7. doi: 10.1016/S1388-2457(03)00040-3
132. Berardelli A, Rothwell JC, Thompson PD, Hallett M. Pathophysiology of bradykinesia in Parkinson's disease. *Brain.* (2001) 124(Pt 11):2131–46. doi: 10.1093/brain/124.11.2131
133. Fabbrini G, Latorre A, Suppa A, Bloise M, Frontoni M, Berardelli A. Fatigue in Parkinson's disease: motor or non-motor symptom? *Parkinsonism Relat Disord.* (2013) 19:148–52. doi: 10.1016/j.parkreldis.2012.10.009
134. Becker C, Brobert GP, Johansson S, Jick SS, Meier CR. Risk of incident depression in patients with Parkinson disease in the UK. *Eur J Neurol.* (2011) 18:448–53. doi: 10.1111/j.1468-1331.2010.03176.x
135. Pessoa Rocha N, Reis HJ, Vanden Berghe P, Cirillo C. Depression and cognitive impairment in Parkinson's disease: a role for inflammation and immunomodulation? *Neuroimmunomodulation.* (2014) 21:88–94. doi: 10.1159/000356531
136. Karpenko MN, Vasilishina AA, Gromova EA, Muruzheva ZM, Bernadotte A. Interleukin-1β, interleukin-1 receptor antagonist, interleukin-6, interleukin-10, and tumor necrosis factor-α levels in CSF and serum in relation to the clinical diversity of Parkinson's disease. *Cell Immunol.* (2018) 327:77–82. doi: 10.1016/j.cellimm.2018.02.011
137. Veselý B, Dufek M, Thon V, Brozman M, Králová S, Halászová T, et al. Interleukin 6 and complement serum level study in Parkinson's disease. *J Neural Transm.* (2018). 125:875–81. doi: 10.1007/s00702-018-1857-5
138. Bruunsgaard H, Pedersen M, Pedersen BK. Aging and proinflammatory cytokines. *Curr Opin Hematol.* (2001) 8:131–6. doi: 10.1097/00062752-200105000-00001
139. Chen WW, Zhang X, Huang WJ. Role of neuroinflammation in neurodegenerative diseases (Review). *Mol Med Rep*. (2016) 13:3391–6. doi: 10.3892/mmr.2016.4948
140. Brites D, Fernandes A. Neuroinflammation and depression: microglia activation, extracellular microvesicles and microRNA dysregulation. *Front Cell Neurosci*. (2015) 9:476. doi: 10.3389/fncel.2015.00476
141. Qin XY, Zhang SP, Cao C, Loh YP, Cheng Y. Aberrations in peripheral inflammatory cytokine levels in Parkinson disease: a systematic review and meta-analysis. *JAMA Neurol*. (2016) 73:1316–24. doi: 10.1001/jamaneurol.2016.2742
142. Matsui H, Nishinaka K, Oda M, Niikawa H, Komatsu K, Kubori T, et al. Depression in Parkinson's disease. Diffusion tensor imaging study. *J Neurol*. (2007) 254:1170–3. doi: 10.1007/s00415-006-0236-6
143. Feldmann A, Illes Z, Kosztolanyi P, Illes E, Mike A, Kover F, et al. Morphometric changes of gray matter in Parkinson's disease with depression: a voxel-based morphometry study. *Mov Disord*. (2008) 23:42–6. doi: 10.1002/mds.21765
144. Kostić VS, Agosta F, Petrović I, Galantucci S, Spica V, Jecmenica-Lukic M, et al. Regional patterns of brain tissue loss associated with depression in Parkinson disease. *Neurology*. (2010) 75:857–63. doi: 10.1212/WNL.0b013e3181f11c1d
145. Surdhar I, Gee M, Bouchard T, Coupland N, Malykhin N, Camicioli R. Intact limbic-prefrontal connections and reduced amygdala volumes in Parkinson's disease with mild depressive symptoms. *Parkinsonism Relat Disord*. (2012) 18:809–13. doi: 10.1016/j.parkreldis.2012.03.008
146. van Mierlo TJ, Chung C, Foncke EM, Berendse HW, van den Heuvel OA. Depressive symptoms in Parkinson's disease are related to decreased hippocampus and amygdala volume. *Mov Disord*. (2015) 30:245–52. doi: 10.1002/mds.26112
147. Huang C, Ravdin LD, Nirenberg MJ, Piboolnurak P, Severt L, Maniscalco JS, et al. Neuroimaging markers of motor and nonmotor features of Parkinson's disease: an 18f fluorodeoxyglucose positron emission computed tomography study. *Dement Geriatr Cogn Disord.* (2013) 35:183–96. doi: 10.1159/000345987
148. O'Callaghan C, Shine JM, Lewis SJ, Hornberger M. Neuropsychiatric symptoms in Parkinson's disease: fronto-striatal atrophy contributions. *Parkinsonism Relat Disord*. (2014) 20:867–72. doi: 10.1016/j.parkreldis.2014.04.027
149. Huang P, Lou Y, Xuan M, Gu Q, Guan X, Xu X, et al. Cortical abnormalities in Parkinson's disease patients and relationship to depression: A surface-based morphometry study. *Psychiatry Res Neuroimag.* (2016) 250:24–8. doi: 10.1016/j.pscychresns.2016.03.002
150. Cardoso EF, Maia FM, Fregni F, Myczkowski ML, Melo LM, Sato JR, et al. Depression in Parkinson's disease: convergence from voxel-based morphometry and functional magnetic resonance imaging in the limbic thalamus. *Neuroimage.* (2009) 47:467–72. doi: 10.1016/j.neuroimage.2009.04.059
151. Lou Y, Huang P, Li D, Cen Z, Wang B, Gao J, et al. Altered brain network centrality in depressed Parkinson's disease patients. *Mov Disord*. (2015) 30:1777–84. doi: 10.1002/mds.26321
152. Boileau I, Warsh JJ, Guttman M, Saint-Cyr JA, McCluskey T, Rusjan P, et al. Elevated serotonin transporter binding in depressed patients with Parkinson's disease: a preliminary PET study with [11C]DASB. *Mov Disord*. (2008) 23:1776–80. doi: 10.1002/mds.22212
153. Politis M, Wu K, Loane C, Turkheimer FE, Molloy S, Brooks DJ, et al. Depressive symptoms in PD correlate with higher 5-HTT binding in raphe and limbic structures. *Neurology.* (2010) 75:1920–7. doi: 10.1212/WNL.0b013e3181feb2ab
154. Ballanger B, Klinger H, Eche J, Lerond J, Vallet AE, Le Bars D, et al. Role of serotonergic 1A receptor dysfunction in depression associated with Parkinson's disease. *Mov Disord*. (2012) 27:84–9. doi: 10.1002/mds.23895
155. Guttman M, Boileau I, Warsh J, Saint-Cyr JA, Ginovart N, McCluskey T, et al. Brain serotonin transporter binding in non-depressed patients with Parkinson's disease. *Eur J Neurol*. (2007) 14:523–8. doi: 10.1111/j.1468-1331.2007.01727.x
156. Maillet A, Krack P, Lhommée E, Météreau E, Klinger H, Favre E, et al. The prominent role of serotonergic degeneration in apathy, anxiety and depression in *de novo* Parkinson's disease. *Brain.* (2016) 139(Pt 9):2486–502. doi: 10.1093/brain/aww162
157. Skidmore FM, Yang M, Baxter L, von Deneen K, Collingwood J, He G, et al. Apathy, depression, and motor symptoms have distinct and separable resting activity patterns in idiopathic Parkinson disease. *Neuroimage.* (2013) 81:484–95. doi: 10.1016/j.neuroimage.2011.07.012

158. Tong Q, Zhang L, Yuan Y, Jiang S, Zhang R, Xu Q, et al. Reduced plasma serotonin and 5-hydroxyindoleacetic acid levels in Parkinson's disease are associated with nonmotor symptoms. *Parkinsonism Relat Disord*. (2015) 21:882–7. doi: 10.1016/j.parkreldis.2015.05.016
159. Svenningsson P, Pålhagen S, Mathé AA. Neuropeptide Y and calcitonin gene-related peptide in cerebrospinal fluid in parkinson's disease with comorbid depression versus patients with major depressive disorder. *Front Psychiatry*. (2017) 8:102. doi: 10.3389/fpsyt.2017.00102
160. Thobois S, Ardouin C, Lhommée E, Klinger H, Lagrange C, Xie J, et al. Non-motor dopamine withdrawal syndrome after surgery for Parkinson's disease: predictors and underlying mesolimbic denervation. *Brain*. (2010) 133(Pt 4):1111–27. doi: 10.1093/brain/awq032
161. Koerts J, Leenders KL, Koning M, Portman AT, van Beilen M. Striatal dopaminergic activity (FDOPA-PET) associated with cognitive items of a depression scale (MADRS) in Parkinson's disease. *Eur J Neurosci*. (2007) 25:3132–6. doi: 10.1111/j.1460-9568.2007.05580.x
162. Barone P, Poewe W, Albrecht S, Debieuvre C, Massey D, Rascol O, et al. Pramipexole for the treatment of depressive symptoms in patients with Parkinson's disease: a randomised, double-blind, placebo-controlled trial. *Lancet Neurol*. (2010) 9:573–80. doi: 10.1016/S1474-4422(10)70106-X

Conflict of Interest Statement: The authors declare that the research was conducted in the absence of any commercial or financial relationships that could be construed as a potential conflict of interest.

Copyright © 2019 Prell, Witte and Grosskreutz. This is an open-access article distributed under the terms of the Creative Commons Attribution License (CC BY). The use, distribution or reproduction in other forums is permitted, provided the original author(s) and the copyright owner(s) are credited and that the original publication in this journal is cited, in accordance with accepted academic practice. No use, distribution or reproduction is permitted which does not comply with these terms.

frontiers in Neurology

ORIGINAL RESEARCH
published: 12 March 2019
doi: 10.3389/fneur.2019.00205

Neuronal ICAM-5 Plays a Neuroprotective Role in Progressive Neurodegeneration

Katharina Birkner[1†], Julia Loos[1†], René Gollan[1], Falk Steffen[1], Beatrice Wasser[1], Tobias Ruck[2], Sven G. Meuth[2], Frauke Zipp[1] and Stefan Bittner[1]*

[1] Department of Neurology, Focus Program Translational Neuroscience (FTN) and Immunotherapy (FZI), Rhine Main Neuroscience Network (rmn2), University Medical Center of the Johannes Gutenberg University Mainz, Mainz, Germany, [2] Department of Neurology, University of Muenster, Muenster, Germany

Multiple sclerosis (MS) is a chronic autoimmune disease of the central nervous system (CNS) leading to CNS inflammation and neurodegeneration. Current anti-inflammatory drugs have only limited efficacy on progressive neurodegenerative processes underlining the need to understand immune-mediated neuronal injury. Cell adhesion molecules play an important role for immune cell migration over the blood-brain barrier whereas their role in mediating potentially harmful contacts between invading immune cells and neurons is incompletely understood. Here, we assess the role of the CNS-specific neuronal adhesion molecule ICAM-5 using experimental autoimmune encephalomyelitis (EAE), an animal model of MS. ICAM-5 knockout mice show a more severe EAE disease course in the chronic phase indicating a neuroprotective function of ICAM-5 in progressive neurodegeneration. In agreement with the predominant CNS-specific function of ICAM-5, lymphocyte function-associated antigen 1 (LFA-1)/ICAM-1 contact between antigen-presenting cells and T helper (Th)17 cells in EAE is not affected by ICAM-5. Strikingly, intrathecal application of the shed soluble form, sICAM-5, ameliorates EAE disease symptoms and thus might serve locally as an endogenous neuronal defense mechanism which is activated upon neuroinflammation in the CNS. In humans, cerebrospinal fluid from patients suffering from progressive forms of MS shows decreased sICAM-5 levels, suggesting a lack of this endogenous protective pathway in these patient groups. Overall, our study points toward a novel role of ICAM-5 in CNS autoinflammation in progressive EAE/MS.

Keywords: T cells, experimental autoimmune encephalomyelitis, multiple sclerosis, neuroinflammation, adhesion molecules

OPEN ACCESS

Edited by:
V. Wee Yong,
University of Calgary, Canada

Reviewed by:
Fabrizio Giuliani,
University of Alberta, Canada
Fred Lühder,
University of Göttingen, Germany

****Correspondence:***
Stefan Bittner
stefan.bittner@unimedizin-mainz.de

[†] These authors have contributed equally to this work and share first authorship

Specialty section:
This article was submitted to Multiple Sclerosis and Neuroimmunology, a section of the journal Frontiers in Neurology

Received: *07 November 2018*
Accepted: *18 February 2019*
Published: *12 March 2019*

Citation:
Birkner K, Loos J, Gollan R, Steffen F, Wasser B, Ruck T, Meuth SG, Zipp F and Bittner S (2019) Neuronal ICAM-5 Plays a Neuroprotective Role in Progressive Neurodegeneration. Front. Neurol. 10:205. doi: 10.3389/fneur.2019.00205

INTRODUCTION

Multiple sclerosis (MS) is an inflammatory neurodegenerative disease which is characterized by T cells infiltrating the central nervous system (CNS), thereby initiating autoimmune neuroinflammation (1–3). Subsequent to destabilization of the blood-brain barrier (BBB), proinflammatory cytokines are secreted by lymphocytes (4) thus orchestrating a proinflammatory environment via recruitment of other immune cells into the CNS (5). Throughout the pathogenesis of MS or in its animal model experimental autoimmune encephalomyelitis (EAE), adhesion molecules are not only involved in the migration process of lymphocytes into the CNS parenchyma

via the BBB (6–8), they also contribute to reactivation of these immune cells via antigen-presenting cells (APCs). Recently, adhesion molecules have been shown to be involved in direct T cell interactions with neurons *in vivo*, thus inducing cell-cell contact-mediated neuronal calcium elevations (6, 9, 10).

Adhesion molecules play an important role for the regulation of peripheral immune processes. One prominent example is the intercellular adhesion molecule 1 (ICAM-1), which is typically expressed on endothelial and immune cells, and which can be induced by inflammatory cytokines such as interleukin-1 (IL-1) and tumor necrosis factor (TNF). Upon activation, leukocytes can bind to endothelial cells via lymphocyte function-associated antigen 1 (LFA-1)/ ICAM-1 and transmigrate into CNS tissue (11). In contrast, the related CNS-specific intercellular adhesion molecule 5 (ICAM-5, also called telencephalin (TLN) was first described as a regulator for brain development and the formation of synapses and is exclusively expressed on neurons in the telencephalon (12). A putative role of ICAM-5 in neuroinflammation is of high interest as pharmacological targeting might specifically address T cell-neuron contacts leading to T cell-mediated neuronal cell death. The binding partner of ICAM-5 is the β2-integrin LFA-1, which is expressed by invading leukocytes. LFA-1/ICAM-5 binding has therefore been proposed as a possible target to investigate neuroinflammatory processes in the CNS (13, 14). Additionally, ICAM-5 can be cleaved by matrix metalloproteinase (MMP)-2 and 9 from the neuronal surface (15) and the soluble form (sICAM-5) has been proposed to act as an inhibitor of ICAM-1–LFA-1 interactions between $CD4^+$ T cells and APCs (16); the involvement of pathogenic Th17 cells has not been addressed so far. Interestingly, encephalitis patients show elevated concentrations of sICAM-5 in the cerebrospinal fluid (CSF); however its pathological relevance is still unclear (17).

Here, we examined the role of ICAM-5 as a direct binding partner between neurons and T helper 17 (Th17) cells in MS pathology, and investigated whether the interaction of its soluble form, sICAM-5, influences the interactions between Th17 cells and APCs thereby serving as an immunosuppressive molecule (**Figure 1**). The functional expression of ICAM-5 in the CNS and secretion levels of protective sICAM-5 proteins in the CSF of MS patients was assessed to provide insights into the relevance of ICAM-5 for the human system. Our results contribute to a deeper understanding of immune cell-driven neuronal injury which may influence future therapeutic approaches.

MATERIAL AND METHODS

Experimental Autoimmune Encephalomyelitis

ICAM-5 knockout (KO) mice were originally provided by the Gahmberg laboratory, University of Helsinki (Finland); C57BL/6 mice were purchased from Janvier laboratory (France). All animal experiments were approved by local authorities and conducted according to the German Animal Protection Law. Active EAE in C57BL/6, ICAM5-KO mice and littermates was induced using the Hooke Kit™ MOG_{35-55}/CFA Emulsion + PTX following the manufacturer's protocol. Thus, mice were actively immunized by subcutaneous injection of 200 μg emulsion of MOG_{35-55} in complete Freund's adjuvant (CFA), followed by the administration of two intraperitoneal doses of 400 ng of pertussis toxin (PTX) in PBS, at the time of immunization and 48 h later. Clinical signs of EAE were monitored daily and translated into clinical scores as follows: 0, no detectable signs of EAE; 0.5, tail weakness; 1, complete tail paralysis; 1.5, impaired righting reflex; 2, partial hind limb paralysis; 2.5, unilateral complete hind limb paralysis; 3, complete bilateral hind limb paralysis; 3.5, complete hind limb paralysis and partial forelimb paralysis; 4, total paralysis of forelimbs and hind limbs; and 5, death. EAE mice were treated with steroid pulses of 16 μg/g Urbason (Methylprednisolone) given via intraperitoneal injections on five consecutive days as soon as a clinical score of 2 was reached, supporting the development of a chronic progressive EAE disease course in this model. The 16 μg/g dose was based on the clinical human dose of 1,000 mg per day and a median weight of 63 kg (human) vs. 20 g (mouse).

Intrathecal Injection of ICAM-5 D1-2-Fc by Lumbar Injection

Recombinant mouse ICAM-5 Fc chimera protein (ICAM-5 D1-2-Fc, R&D Systems, USA) was delivered intrathecally by lumbar puncture in awake mice as described elsewhere (18, 19). In short, the mouse was grasped at the iliac crest, so that both hind legs move outward and downward. Then the Hamilton syringe/needle was inserted at about a 45° angle between the L5 and L6 spinous process and 5 μl injection solution was applied. A reflexive flick of the tail indicated puncture of the dura. After reaching a clinical score of 2, EAE mice received 0.2 μg of ICAM-5 D1-2-Fc in this manner seven times at 48-h intervals to induce an ICAM-5 D1-2-Fc concentration in the CSF of 5 μg/ml. The control group was treated with IgG peptide.

Murine Cell Culture

Naïve $CD4^+CD62L^+$ cells were isolated and MACS-sorted from spleens and lymph nodes of B6.2D2 and B6.RFP.2D2 mice (6–10 weeks old) with a purity of >95% of total cells. Murine Th17 cell differentiation was achieved by the addition of 2 μg/ml anti-CD3, 3 ng/ml TGF-β, 20 ng/ml mrIL-6, 20 ng/ml IL-23, 10 μg/ml anti-IL-4, and 10 μg/ml anti-IFNγ. Irradiated APCs were used for initial stimulation of the T lymphocytes in a ratio 1:10. Cells were kept in cell culture medium and were split with 50 U/ml IL-2 and 10 ng/ml IL-23. Cells that produced >30% of IL-17 were used for *in vitro* assays. Cytokine production was assessed using intracellular cytokine staining following standard protocols (CD4-PeCy7 (clone: RM4-5, BD Bioscience), IL-17A-AF647 (clone: 17B7, Affimetrix), IFNγ-Horizon (clone: XMG1.2, BD Bioscience), TNFα-AF700 (clone: MP6-XT22BD, Bioscience)). Surface stainings were performed with CD44-AF700 (clone: IM7, eBioscience), CD49d-FITC (clone: R1-2, eBioscience), CD54-APC (clone: YN1/1.7.4, Biolegend) and MHCII-PerCP (clone: AF6-120.1, BD), CD62L-APC (clone: MEL-14, BD Biosciences), CD69-PE (clone: H1-2F3, BD Biosciences), CD40L-PECy7 (clone: MR1, Biolegend), and CD25-PECy7 (clone: PC61, BD Biosciences). ICAM-5 treatment was performed by adding

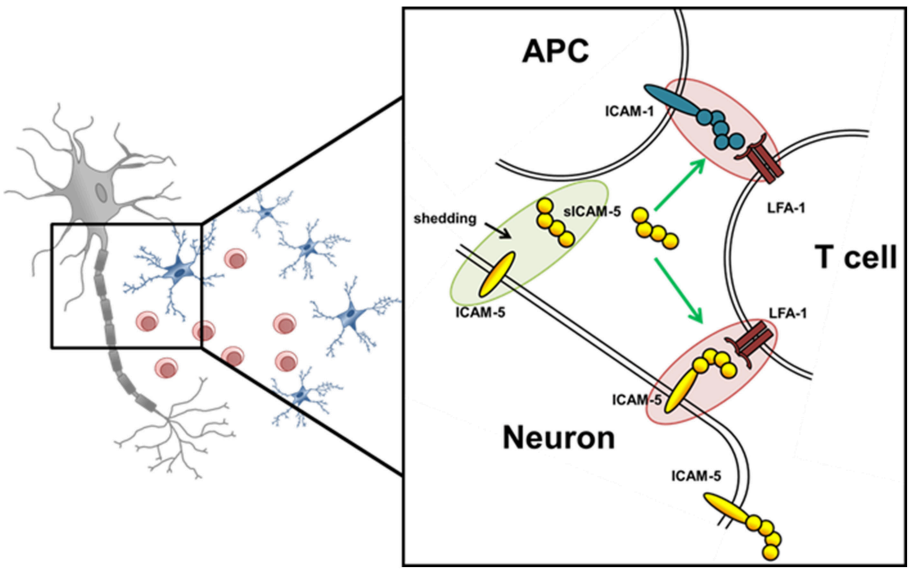


FIGURE 1 | Schematic overview of potential ICAM-5 dependent T cell—neuron and T cell—APC interactions in the CNS. Schematic illustration of the interplay of neurons, T cells, and APCs in the CNS. The adhesion molecule ICAM-5 (yellow) is exclusively expressed by neurons and can be cleaved by MMP-2 and 9 from the neuronal surface (also called shedding). The soluble form (sICAM-5) has been proposed to act as an inhibitor of ICAM1–LFA-1 interactions between T cells and APCs and T cells and neurons therefore displaying a protective function. Green highlights and arrows represent anti-inflammatory/ protective function and red highlights represent proinflammatory properties.

10 μg/ml ICAM-5 D1-2-Fc (R&D Systems, USA) either during the whole time of Th17 cell differentiation or after restimulation of differentiated Th17 cells.

Proliferation Assay

Carboxyfluorescein succinimidyl ester (CFSE) proliferation assay was performed by incubating naïve T cells in mouse-medium at 37°C for 30 min, then cells were washed twice with pre-warmed RPMI+1% HEPES (RH) and then dissolved in CFSE in pre-warmed RH at a concentration of 2.5 μM. After quenching the stained cells with cold mouse-medium, cells were incubated for at least 72 h and evaluated by flow cytometric measurements.

Cortical Neuronal Cell Culture

For neuronal cultures, p0-p1 pups were beheaded and brains were removed from the skull. The brains were prepared in ice-cold Hank's balanced salt solution (HBSS). The olfactory bulbs and the meninges were removed from the cortex. The hippocampus was stripped from the cortex and all cortices were collected in ice-cold HBSS. Cortices from up to three animals were pooled into one falcon tube. The tissue was washed once with ice-cold HBSS and digested in HBSS with 1% DNAse and 0.5% trypsin for 20 min at 37°C. For homogenizing, tissue was sucked through two small glass pipettes and finally poured over a 70 μm cell sieve. 500,000−750,000 cells were seeded in each well of the 6-well plate in plating medium. After 3 h cells were washed with neuro basal medium. The cultures were washed every 2–3 days. Neuronal cultures were inflamed between d7 and d8 with LPS (10 μg/ml), IFNγ (100 ng/ml) or splenocyte supernatant. Cultures were harvested 24 h later, between d8 and d9. Cells were harvested with 3% trypsin for 5 min at 37°C, washed from the plates and collected on ice. The cells were centrifuged for 5 min at 550 g at 4°C and washed once with ice-cold phosphate-buffered saline (PBS). Pellets for mRNA analysis were frozen at −80°C.

Quantitative Real-Time PCR

For analysis of ICAM-5 and MMP-9 expression, RNA was isolated using the RNeasy Mini Kit© (Quiagen) according to the manufacturer's protocol; quality and integrity of total RNA preparation was confirmed using a NanoDropTM 2000c Spectrophotometer (Thermo Scientific). Complementary DNA (cDNA) synthesis was performed by reverse transcription of total RNA using the SuperScript©III First Strand Synthesis System and random hexamer primers (Invitrogen) following the manufacturer's instructions. Amplification primers for real-time PCR analysis were designed using Beacon Designer 8 Software (PREMIER Biosoft International) according to the manufacturer's guidelines and subsequently tested for amplification efficiency and specificity. Real-time PCR was performed using iQ SYBR Green supermix (BioRad Laboratories) in an CFX Connect TM Real Time Detection System (BioRad). Primer sequence as given: ICAM-5 (forward: CGT ATG TAT TGT TCG CTC TC; reverse: TTA TTG AAG GGA ATG GGT AGA) and MMP-9 (forward: AAG TCT CAG AAG GTG GAT; reverse: AAT AGG CTT TGT CTT GGTA). Relative changes in gene expression were determined using the Ct method (20) with β-actin as the reference gene.

Immunohistochemistry

Immunohistochemistry was performed with neuronal cortical cultures of B6.2D2 mice. Neurons were stained for ICAM-5

(TubIII, Covance), NeuN (Millipore, Billerica), MAP2 (HM-2, Sigma), and Tuj1 (Covance); cell nuclei were stained with DAPI (Invitrogen). Pictures were obtained using a confocal laser scanning microscope (Leica TCS-SP8; Leica Microsystems Heidelberg, Mannheim, Germany).

Human ICAM-5 ELISA

CSF samples were collected at the time of first diagnosis from 48 patients fulfilling the revised McDonald criteria for MS (21) which included 17 with relapsing-remitting MS (RRMS, age: 38.6 ± 1 years, range: 21–78 years, EDSS: 1.7 ± 0.1, range: 0–3.5, disease duration: 15.6 ± 1.7 months, range: 0–84 months), 19 with primary progressive MS (PPMS, age 56.7 ± 0.5 years, range: 42–70 years, EDSS 3.7 ± 0.1, range: 1–6.5, disease duration 45.2 ± 2.5 months, range: 1–156 months), and 12 with secondary progressive MS (SPMS, age 48.5 ± 0.7 years, range: 34–67 years, EDSS 4.5 ± 0.2, range: 2–7.5, disease duration 99.5 ± 8.3 months, range: 18–300 months). Samples from 35 patients with non-inflammatory neurological disease (NIND, mean (± SEM) age: 42.3 ± 0.5 years, range: 17–79 years) served as controls. CSF was collected and kept frozen at −80°C until assayed. ICAM-5 levels were measured using a human ICAM-5 ELISA kit (DY1950-05, R&D Systems) with an ancillary reagent pack according to the manufacturers' protocol (DY008, R&D Systems). Fluorescence was determined using an Infinite M200 pro reader (Tecan). This study was approved by the local ethical committee (Landesaerztekammer Rheinland-Pfalz) and performed according to the Helsinki Declaration; all patients provided written informed consent.

Histology

Cryosections of EAE mouse brains were stained for hematoxylin and eosin (HE), luxol fast blue stain with periodic acid-Schiff's (LFB-PAS), amyloid precursor protein (APP), and neurofilament (NF). Pictures were obtained using an Olympus microscope equipped with a cellSense camera and analyzed with ImageJ software.

NfL Measurements

Briefly, blood or CSF samples were spun at 2,000 g at room temperature for 10 min within 2 h after withdrawal and stored in polypropylene tubes at −80°C. Neurofilament levels in serum and CSF were measured by SiMoA HD-1 (Quanterix, USA) using the NF-Light Advantage Kit (Quanterix) according to manufacturer's instructions. Samples were measured in duplicates; the intra-assay coefficient of variation (CV) of all samples was below 20%. sNfL measurements were performed in a blinded fashion without information about clinical data.

Statistics

Statistical analyses were performed with Graphpad Prism 6. We used a K-S test for normality, followed by Mann-Whitney test, unpaired two-tailed Student's *t*-test or one-way ANOVA followed by Tukey's multiple comparison test, as appropriate. Data are presented as the mean ± standard error of the mean (SEM) unless otherwise indicated. *P*-values <0.05 were considered statistically significant.

RESULTS

sICAM-5 Has No Impact on Th17 Cell—APC Interaction

LFA-1 is a central binding partner of both ICAM-5 and ICAM-1 (16). Since Th17 cells play a major role in the immunopathology of both EAE and MS (22, 23), we first aimed to elucidate the influence of sICAM-5 on the interactions of this pathogenic T cell type with APCs. There were no significant differences in the expression levels of LFA-1 on either cell type (**Figure 2A**) indicating that T-cell differentiation and stimulation are independent of LFA-1 expression. Next, we analyzed the influence of sICAM-5 on the APC-dependent proliferation of Th17 cells and found no differences in the proliferation between the sICAM-5-treated T cells and control conditions (**Figure 2B**). Furthermore, we did not see any significant differences in the expression of CD44, CD49d, CD54, MHC class II, CD62L, IL-17, or TNFα after 4 or 24 h of stimulation with CD3/CD28 and sICAM5 on differentiated Th17 cells (**Figure 2C**). We moreover assessed the differentiation of naïve T cells into Th17 cells in the presence of sICAM-5 and did not find significant differences in the expression of surface markers CD69, CD25, CD40L, or intracellular cytokine levels for IL-17 and IFNγ (**Figures 2D,E**). Overall, these results indicate that sICAM-5 does not directly alter the differentiation and function of murine Th17 cells themselves. Both species differences between mouse and human and our focus on the Th17 cell subtype of T cells might explain a different outcome compared to previous reports on human naïve $CD4^+$ T cells (24).

Absence of ICAM-5 Worsens Disease Progression in Active EAE Which Can be Reversed by sICAM-5 Application

Despite its potential to regulate T cell restimulation as well as function as an adhesion molecule for lymphocytes *in vitro*, the relevance of ICAM-5 in neuroinflammation has not been investigated *in vivo*. To this end, we first cultured dissociated cortical neurons and stained them for NeuN and ICAM-5 (**Figure 3A**). Indeed, ICAM-5 is highly expressed by neurons. We found a further upregulation of both ICAM-5 and the matrix metalloproteinase 9 (MMP-9), a protein able to cleave ICAM-5 from the neuronal surface, after inflammatory stimulation with LPS and splenocyte supernatant, but not with IFNγ (**Figure 3B**). Additional neuronal markers MAP-2 or beta-III tubulin (Tuj1) were used to stain cortical neurons and to validate that ICAM-5 is preferentially expressed on soma and dendrites (**Figure 3C**) (16). Next, we induced EAE in mice deficient for ICAM-5 and significant differences were observed between the two groups exclusively in the chronic phase of disease (**Figure 3D**). Taking into account possible pro- and anti-inflammatory effects of ICAM-5 in the context of EAE (see also **Figure 1**), this indicates that the biologically relevant function of ICAM-5 *in vivo* is to serve as an endogenous neuroprotective pathway in chronic neurodegeneration, most likely via sICAM-5-mediated effects. Further, histopathological stainings were performed for inflammation (HE staining), demyelination (LFB-PAS), and

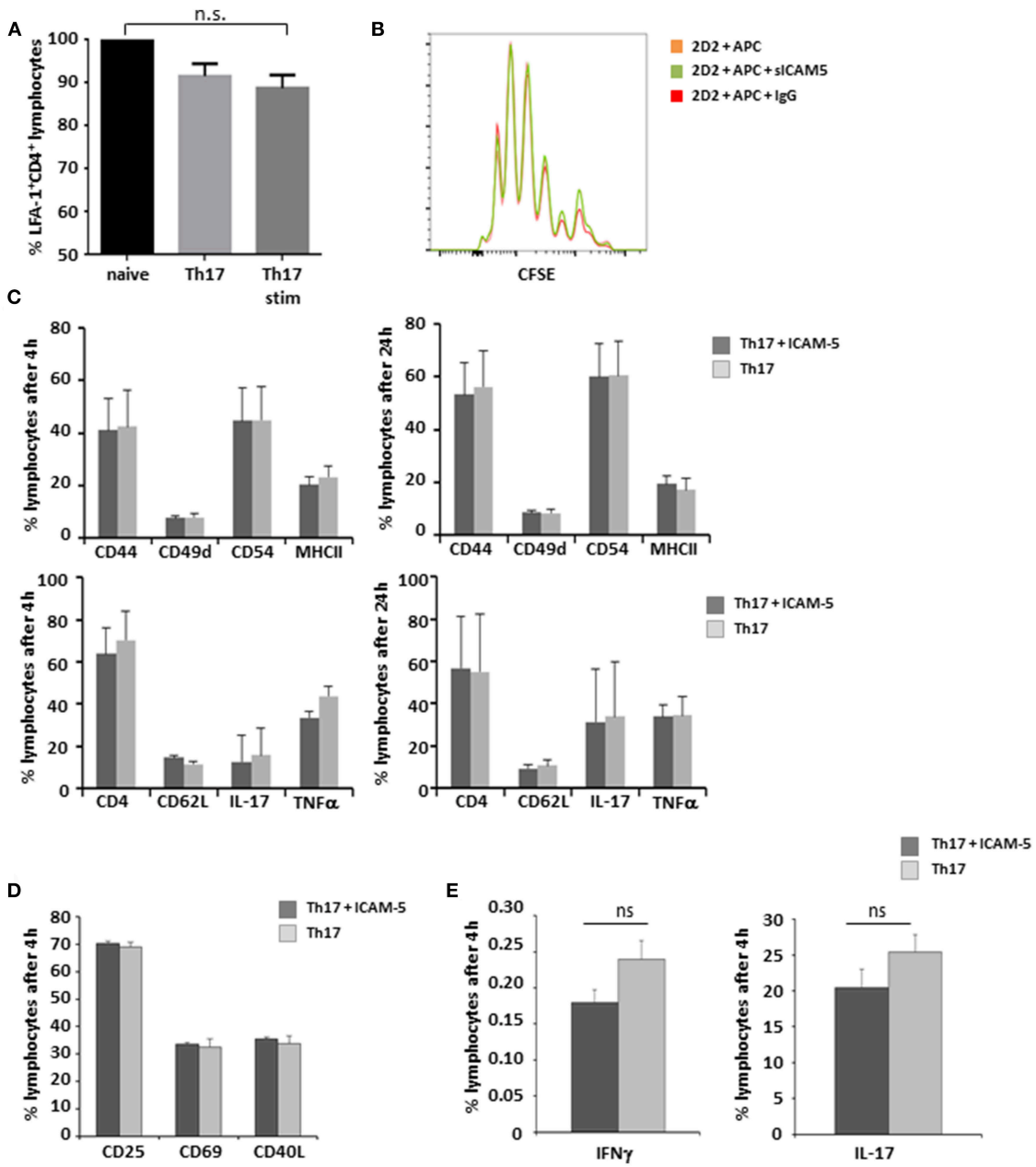


FIGURE 2 | sICAM-5 does not affect Th17—APC interactions. **(A)** FACS staining for LFA-1 of naïve T-cells, Th17 cells, and Th17 cells after 24 h of stimulation with anti-CD3/CD28 ($n = 3$ for each condition). **(B)** Representative depiction of CFSE stainings of naïve 2d2 T cells cocultured with APCs and sICAM-5 (10 μg/ml) or IgG (10 μg/ml) for 72 h. **(C)** FACS staining of Th17 cells stimulated for 4 and 24 h with anti-CD3/CD28 and with or without ICAM-5 treatment (10 μg/ml). **(D,E)** Naïve T cells were differentiated into Th17 cells in the presence of or without sICAM-5 treatment (10 μg/ml) and stained for extracellular **(D)** and intracellular **(E)** markers. Data shown are mean ± SEM. **(A)** One-way ANOVA followed by Tukey's multiple comparison test, n.s. no significance; **(C–E)** Student's *t*-test.

axonal loss (APP) in the lesions of these EAE mice. Neither inflammation nor demyelination was reduced in ICAM5-KO mice, though axonal loss was significantly elevated (**Figure 3E**), arguing in favor of predominating axonal pathology. To examine the impact of sICAM-5 in ongoing neuroinflammation, we applied sICAM-5 locally via intrathecal injection by lumbar puncture during EAE. Indeed, sICAM-5-treated mice displayed a more pronounced recovery after the peak of disease as compared to the control group which was injected with a control IgG peptide (**Figure 3F**).

Patients Suffering From Progressive Forms of MS Show Low Levels of sICAM-5 in CSF

Based on our EAE findings indicating an endogenous protective role of sICAM-5, we assessed the role of sICAM-5 in the CSF of patients with MS. CSF samples from RRMS, SPMS, and PPMS

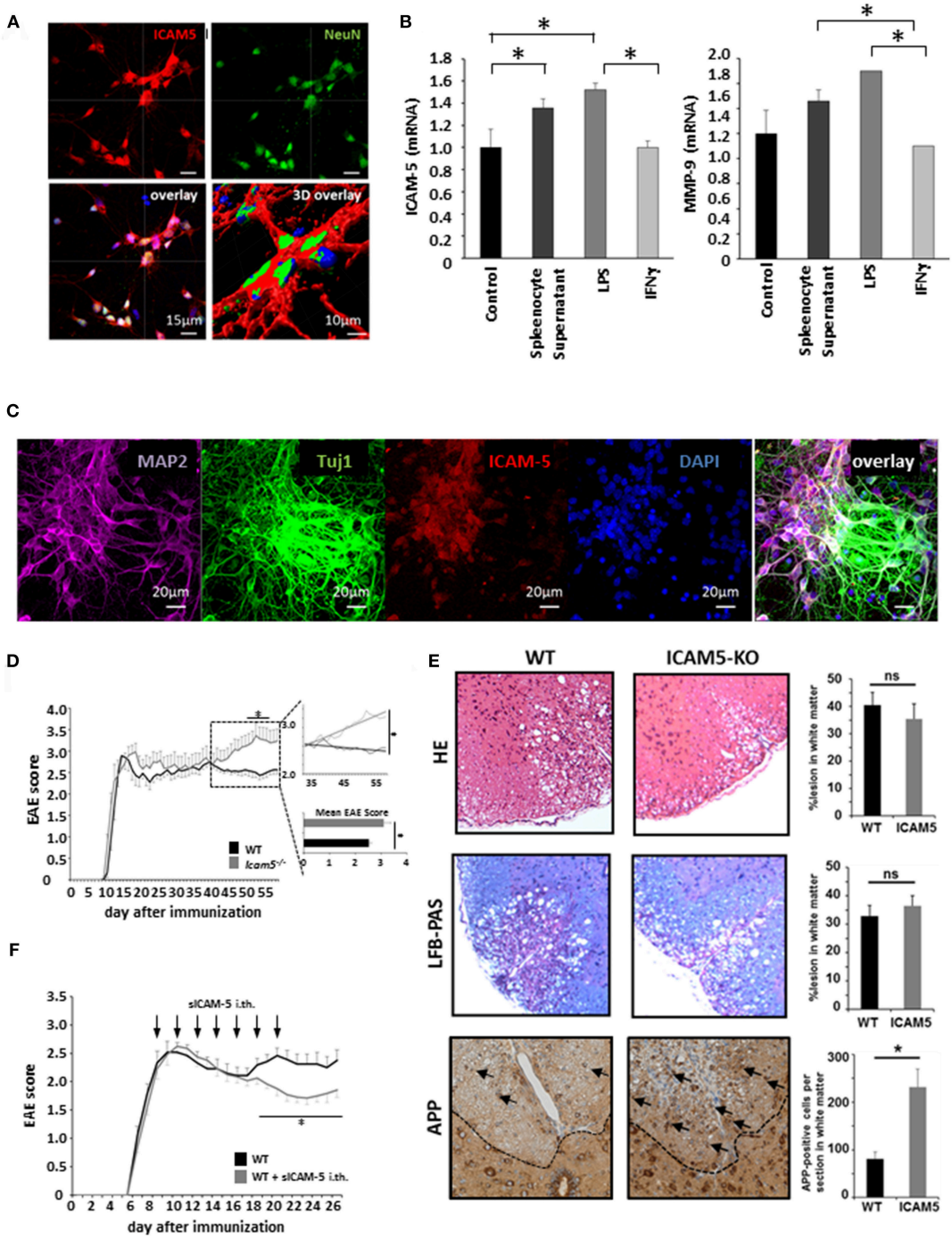


FIGURE 3 | Absence of ICAM-5 worsens disease progression which can be reversed by application of sICAM-5. **(A)** Immunohistochemical staining of ICAM-5-AF647 on cortical neurons (scale bar = 15 µm, 3D overlay scale bar = 10 µm). Co-staining was performed with NeuN-AF488 and DAPI (blue). **(B)** mRNA analysis of ICAM-5 and MMP-9 were performed with cortical neurons after stimulation with LPS, IFNγ, and splenocyte supernatant ($n = 6$ for each condition). Unstimulated cortical neurons served as a control. **(C)** Immunohistochemical staining of MAP2- AF647, Tuj1-FITC, ICAM-5-AF568, and DAPI on cortical neurons (scale bar = 20 µm. **(D)** EAE was induced actively in ICAM-5-KO mice and WT littermates via the injection of MOG_{35-55} (two independent EAEs, untreated; WT $n = 12$, KO $n = 12$). The dotted box on the plot provides a closer look at the chronic phase of the EAE but does not agree with the x axis of the upper plot. The lower plot shows only the mean disease score of the period from day 40 after immunization. **(E)** EAE lesions were stained from wt ($n = 9$) and ICAM5 KO mice ($n = 6$) for inflammation (HE staining), demyelination (LFB-PAS), and axonal loss (APP) and were quantified accordingly. **(F)** EAE was induced actively in B6 mice via the injection of MOG_{35-55} and mice were treated with Methylprednisolone for 5 days as soon as the mice reached a clinical score of 2. Additionally, once animals reached a clinical score of 2, 0.2 µg ICAM-5 D1-2 Fc or human IgG was applied via intrathecal (i.th) injection by lumbar puncture seven times on every second day (WT $n = 7$, KO $n = 7$). Data shown are mean ± SEM. **(C, D)** Mann-Whitney *U*-test; $^*p < 0.05$.

patients as well as from a control group (NIND) with normal CSF findings were analyzed using a human ICAM-5 ELISA. While RRMS and control patients showed comparable levels of sICAM-5, sICAM-5 levels in PPMS, and SPMS patients were significantly lower (**Figure 4A**). This suggests that a reduction in ICAM-5 shedding in humans may play a role specifically in chronic forms of MS. This might either indicate a loss-of-function of an endogenous protective pathway driving neurodegeneration or a secondary effect due to a higher neuronal loss in progressive phases of MS and therefore a lower availability of sICAM-5. We moreover correlated sICAM-5 concentration in CSF with the EDSS score and disease duration (**Figure 4B**) for each MS patient subtype. In RRMS, we found a moderate correlation between EDSS and sICAM-5 concentration in the CSF with higher EDSS scores being associated with a lower concentration of sICAM-5 in the CSF. In SPMS and PPMS, we found a correlation between disease duration and sICAM-5 concentration with higher sICAM-5 concentrations correlating with longer disease duration. We found no correlation between age and sICAM-5 levels (**Supplementary Figure 1**).

No Significant Correlation Between Neurofilament Light Chain Levels and sICAM-5

Neurofilament light chain (NfL) is emerging as a biomarker assessing neuroaxonal damage in patients with multiple sclerosis while knowledge about its relevance in patients with progressive MS is still limited. We measured NfL serum and CSF concentration in the PPMS and SPMS group and correlated these values with ICAM-5 levels (**Figures 5A–C**). Of note, although reflecting neurodegeneration in MS patients NfL is sensitive to almost every type of neuronal damage including inflammatory causes (25). SPMS patients showed higher NfL levels than observed in PPMS patients, confirming previous results derived from larger cohorts [SPMS $n = 1452$ and PPMS $n = 378$; retrospective analysis of INFORMS and EXPAND trials presented by Kuhle et al. (26) ECTRIMS 2018] and CSF levels were highly correlated with serum concentration (Spearman rho = 0.684; $p = 0.007$). In the SPMS subgroup, CSF NfL significantly correlated with the EDSS scores and disease duration (Spearman rho = 0.843, $p = 0.009$ and Spearman rho = 0.838, $p = 0.009$, respectively). Notably, the correlation between NfL and EDSS score is still depicted in the literature by contrary results (27–30). We observed only trends regarding the association between NfL and ICAM-5 in this study but NfL values are drastically different between individuals. There is therefore a need for large cohorts to show significant cross-sectional differences between groups, and we should be aware of our small study population size when interpreting these results. In addition, a more powerful interpretation of sNfL might be achieved by using the individual rate of change of NfL rather than cross-sectional absolute NfL levels (31). The comparison of NfL and ICAM-5 in this study is aggravated by the fact that ICAM-5 is not only released in the extracellular space upon cell damage but, as we showed, its expression is changed upon different stimuli and its concentration in CSF depends on MMP9 activity. In conclusion, combining ICAM-5 with NfL levels in future studies will certainly help to decipher the role of ICAM-5 in neurodegeneration in more detail, but in this study is limited by the small cohort size and different release dynamics.

DISCUSSION

In MS, T cells directly interact with neurons *in vivo* inducing neuronal calcium elevations thus leading to neuronal damage. Here, we investigated the role of ICAM-5 in mediating T cell-neuron contacts. ICAM-5 is exclusively expressed on neurons where it can serve as a binding partner to LFA-1 on invading leukocytes. Soluble ICAM-5 might act as an endogenous regulator of neuronal damage as it has anti-inflammatory effects after binding to LFA-1. Thus, neuronally released sICAM5 can modulate immune cell-neuron as well as T cell-APC interactions. Indeed, ICAM-5 expression was detected on neuronal cell cultures *in vitro*, but not on other cell types. Induction of MOG_{35-55} peptide-induced EAE in wildtype (WT) and ICAM-$5^{-/-}$ mice led to an unchanged phenotype in the inflammatory phase, followed by a significant deterioration in the progressive phase. For the interpretation of results from the ICAM-$5^{-/-}$ mouse, it has to be kept in mind that the full knockout of ICAM-5 might have both beneficial effects (via deletion of T cell-neuron binding capacity) and detrimental effects (since the beneficial effects of sICAM-5 would also be abrogated). The EAE phenotype underlines that the protective effect of sICAM-5 is of major biological importance, especially in the chronic phase of EAE. To further address the therapeutic potential of ICAM-5 modulation, sICAM-5 was applied intrathecally into WT mice, to address only the CNS milieu, leading to a subsequent amelioration of clinical disease symptoms. Although it cannot be excluded that the recombinant ICAM-5 chimera used in these experiments may behave differently to the endogenously shed sICAM-5, the improvement in EAE disease symptoms suggests that sICAM-5 serves locally as an endogenous neuronal defense mechanism which might be activated upon neuroinflammation in the CNS.

Comparing the so far known effects of ICAM-5 to its related molecule ICAM-1 is interesting since ICAM-1 mostly localizes to glia and endothelial cells while ICAM-5 is restricted to telencephalic neurons (24). ICAM-1 was shown to have proinflammatory effects on macrophages (32) but to also influence T cell receptor signaling by slowing the actin flows in primary $CD4^+$ T cells especially with regard to T cell interactions with dendritic cells (33). Contrary to ICAM-1, ICAM-5 was shown to have a rather immune-suppressive function in T cells (24). Neurons which were stimulated with LPS or splenocyte supernatant upregulated ICAM-5 and MMP-9 mimicking the situation of inflammation. Since we were able to exclude a direct effect of ICAM-5 on Th17 cell pathology we hypothesize that ICAM-5 might also play an important role in the interaction of neurons with APCs such as dendritic cells and microglia in EAE. Interestingly, LFA-1 is highly expressed by microglia in chronic active lesions (34) and can be bound by ICAM-5, again

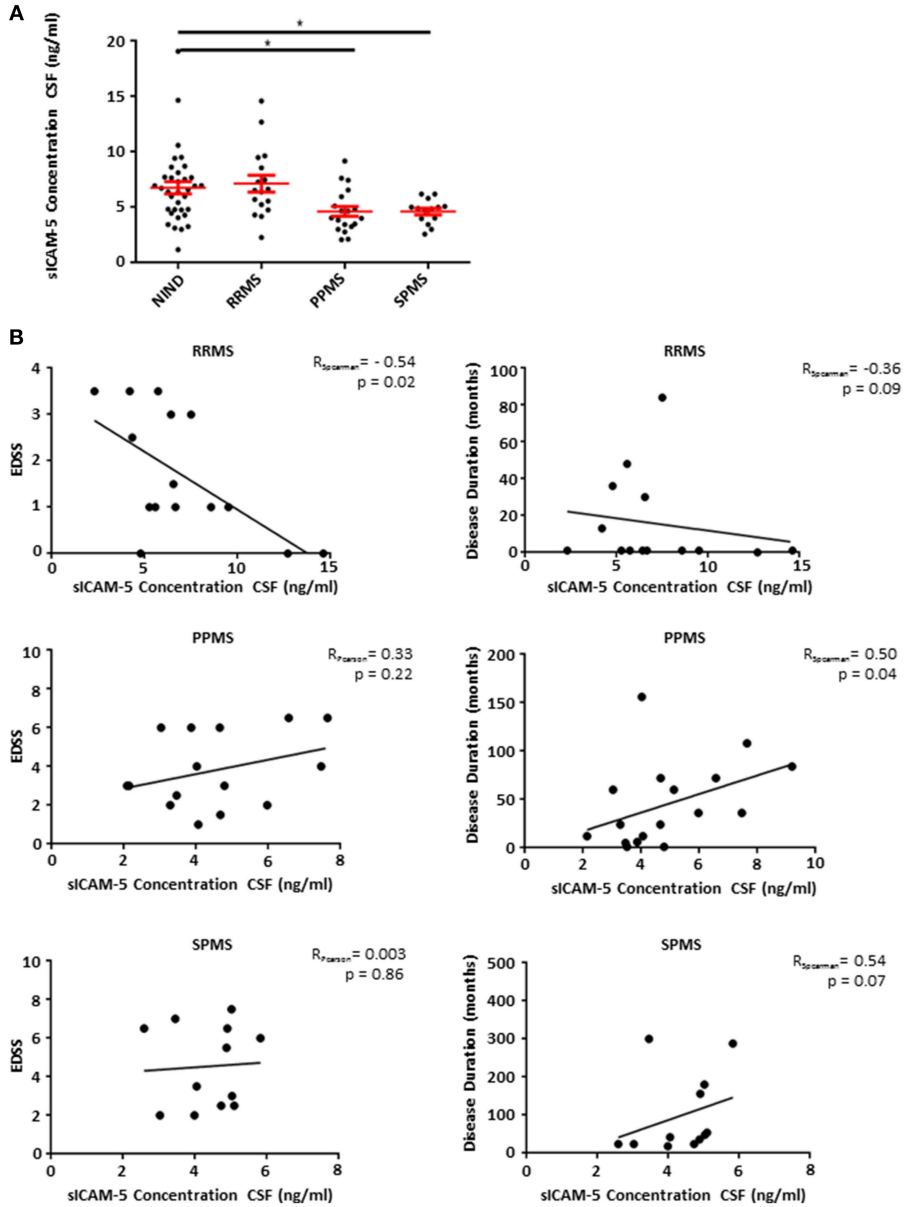


FIGURE 4 | Patients suffering from progressive forms of MS show lower levels of sICAM-5 in CSF. **(A)** ICAM-5 concentration in ng/ml in the cerebrospinal fluid of NIND patients (NIND, $n = 35$), RRMS ($n = 17$), PPMS ($n = 19$), and SPMS ($n = 12$) patients. Data shown are mean ± SEM. One-way ANOVA followed by Tukey's multiple comparison test, $^*p < 0.05$. **(B)** Correlation between EDSS or disease duration in months and ICAM-5 concentration in CSF (ng/ml). Data was tested for normality using Shapiro-Wilk normality test and Pearson's or Spearman's r and *p*-values were determined accordingly.

indicating a potential neuroprotective role of ICAM-5 especially in the chronic phase of MS.

Furthermore, it is known that ICAM-5 regulates neuronal development in several ways and is highly expressed on the dendrites and soma of neurons (35) and during the initial contact between the pre- and the postsynaptic terminals, ICAM-5 stabilizes postsynaptic connections by binding to β1 integrins (36). β1 integrins are also expressed by APCs such as microglia (37). Interestingly, there is direct proof that endogenous ICAM-5 from neurons is bound by microglia and induces clustering and weak adhesion of microglia (38). Additionally, ICAM-5 downregulates phagocytosis in unchallenged microglia and promotes IL-10 production in LPS-stimulated microglia (38) thus further suggesting a potential role of ICAM-5 in the regulation of microglia in the chronic phase of disease. These microglia-related ICAM-5 pathways merit further investigation.

Importantly, CSF from patients suffering from a progressive form of MS show decreased ICAM-5 levels. This is in accordance with our murine data showing a neuroprotective

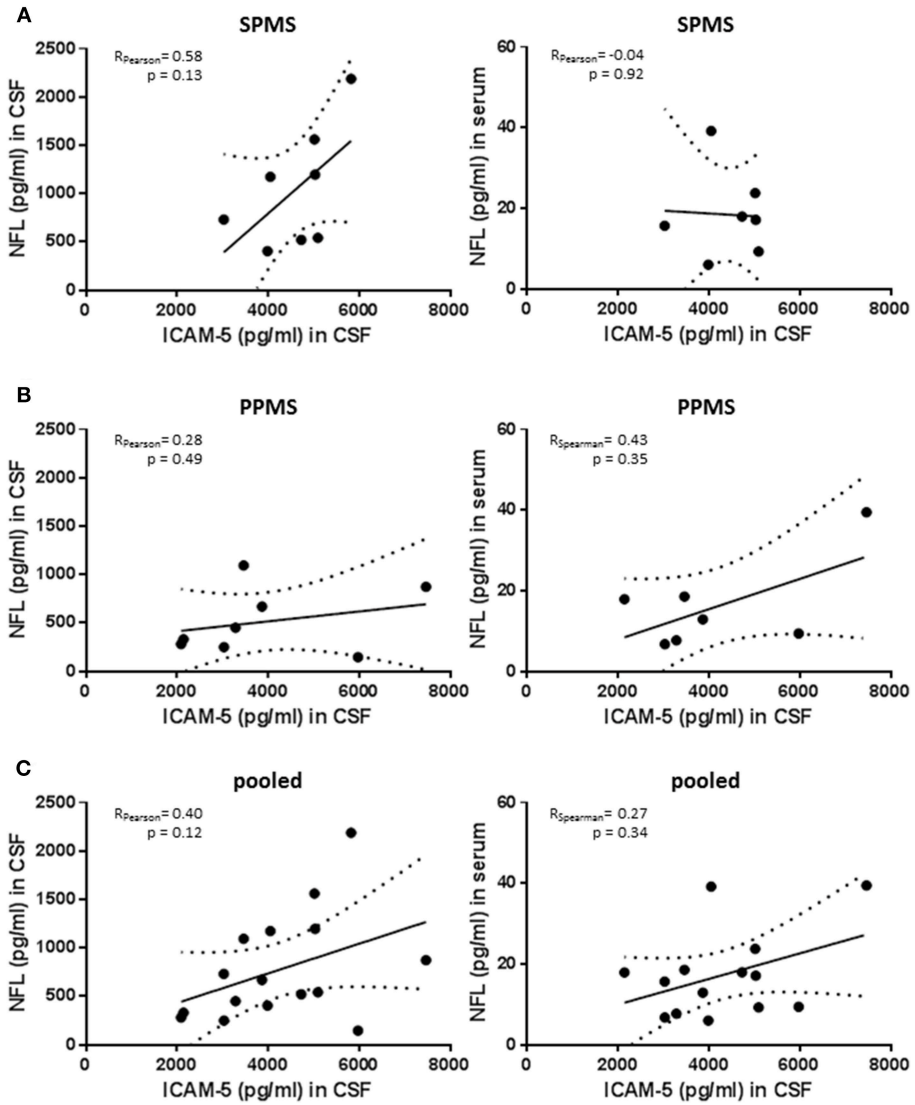


FIGURE 5 | No significant correlation between neurofilament light chain levels and sICAM-5. **(A)** ICAM-5 was correlated with NfL concentrations (pg/ml) in the cerebrospinal fluid and the serum of SPMS patients (n = 7–8). **(B)** ICAM-5 was correlated to NfL concentrations (pg/ml) in the cerebrospinal fluid and the serum of PPMS patients (n = 7–8). **(C)** ICAM-5 was correlated to NfL concentrations (pg/ml) in the cerebrospinal fluid and the serum of pooled SPMS and PPMS patients (n = 14–16). For all figures: Data was tested for normality using Shapiro-Wilk normality test and Pearson's or Spearman's r and p-values was determined accordingly.

effect in the chronic phase of the disease, underlining the importance of ICAM-5 in the human system. Moreover, ICAM-5 concentrations in the CSF correlate with disease duration in patients with progressive forms of MS. It has previously been shown that sICAM-5 is cleaved and released into the CSF also in other neurological diseases such as acute encephalitis (17). Although our study could not classify the exact pathophysiological role of sICAM-5 release into the CSF in progressive MS patients, interesting possibilities are raised. ICAM-5 has been discussed as a marker of neuronal death in traumatic brain injury (39). Increased levels of sICAM-5 in the CSF could therefore be caused by an increase in neuronal death and thereby caused release of ICAM-5. As there is a link between chronic disease, microglia activation and neuronal ICAM-5 (38), the positive correlation between sICAM-5 and disease duration could also point toward other involved pathways which are not addressed in the current study. Interestingly, although there was no significant difference in ICAM-5 levels between NIND and RRMS patients, there was a strong negative correlation between EDSS and ICAM-5 concentration in the CSF of RRMS patients, which supports our hypothesis.

DATA AVAILABILITY

The datasets generated for this study are available on request to the corresponding author.

AUTHOR CONTRIBUTIONS

KB, JL, and SB conceived the study. KB, JL, RG, FS, BW, TR, and SM performed experiments and analyzed data. KB, JL, FZ, and SB wrote and edited the manuscript. This work contains part of the doctoral thesis of JL.

FUNDING

This study was supported by the German Research Foundation (DFG, SFB CRC-TR-128 to FZ and SB) and the Hertie foundation (mylab, SB).

ACKNOWLEDGMENTS

The authors thank Ilse Graevenitz, Silke Fregin, Christin Liefländer, and Shibajee Mandal for excellent technical assistance and Cheryl Ernest for editing the manuscript.

SUPPLEMENTARY MATERIAL

The Supplementary Material for this article can be found online at: https://www.frontiersin.org/articles/10.3389/fneur.2019.00205/full#supplementary-material

REFERENCES

1. Cua DJ, Sherlock J, Chen Y, Murphy CA, Joyce B, Seymour B, et al. Interleukin-23 rather than interleukin-12 is the critical cytokine for autoimmune inflammation of the brain. *Nature.* (2003) 421:744–8. doi: 10.1038/nature01355
2. Langrish CL, Chen Y, Blumenschein WM, Mattson J, Basham B, Sedgwick JD, et al. IL-23 drives a pathogenic T cell population that induces autoimmune inflammation. *J Exp Med.* (2005) 201:233–40. doi: 10.1084/jem.20041257
3. Komiyama Y, Nakae S, Matsuki T, Nambu A, Ishigame H, Kakuta S, et al. IL-17 plays an important role in the development of experimental autoimmune encephalomyelitis. *J Immunol.* (2006) 177:566–73.
4. Bittner S, Wiendl H. Neuroimmunotherapies Targeting T Cells: from pathophysiology to therapeutic applications. *Neurotherapeutics*. (2016) 13:4–19. doi: 10.1007/s13311-015-0405-3
5. Ellwardt E, Walsh JT, Kipnis J, Zipp F. Understanding the Role of T Cells in CNS Homeostasis. *Trends Immunol.* (2016) 37:154–65. doi: 10.1016/j.it.2015.12.008
6. Larochelle C, Alvarez JI, Prat A. How do immune cells overcome the blood-brain barrier in multiple sclerosis? *FEBS Lett.* (2011) 585:3770–80. doi: 10.1016/j.febslet.2011.04.066
7. Engelhardt B. Cluster: barriers of the central nervous system. *Acta Neuropathol.* (2018) 135:307–10. doi: 10.1007/s00401-018-1816-0
8. Lopes Pinheiro MA, Kooij G, Mizee MR, Kamermans A, Enzmann G, Lyck R, et al. Immune cell trafficking across the barriers of the central nervous system in multiple sclerosis and stroke. *Biochim Biophys Acta*. (2016) 1862:461–71. doi: 10.1016/j.bbadis.2015.10.018
9. Paterka M, Siffrin V, Voss JO, Werr J, Hoppmann N, Gollan R, et al. Gatekeeper role of brain antigen-presenting CD11c+ cells in neuroinflammation. *Embo J.* (2016) 35:89–101. doi: 10.15252/embj.201591488
10. Siffrin V, Radbruch H, Glumm R, Niesner R, Paterka M, Herz J, et al. *In vivo* imaging of partially reversible th17 cell-induced neuronal dysfunction in the course of encephalomyelitis. *Immunity.* (2010) 33:424–36. doi: 10.1016/j.immuni.2010.08.018
11. Rothlein R, Dustin ML, Marlin SD, Springer TA. A human intercellular adhesion molecule (ICAM-1) distinct from LFA-1. *J Immunol.* (1986) 137:1270–4.
12. Mori K, Fujita SC, Watanabe Y, Obata K, Hayaishi O. Telencephalon-specific antigen identified by monoclonal antibody. *Proc Natl Acad Sci USA*. (1987) 84:3921–5.
13. Tian L, Yoshihara Y, Mizuno T, Mori K, Gahmberg CG. The neuronal glycoprotein telencephalin is a cellular ligand for the CD11a/CD18 leukocyte integrin. *J Immunol.* (1997) 158:928–36.
14. Tian L, Kilgannon P, Yoshihara Y, Mori K, Gallatin WM, Carpen O, et al. Binding of T lymphocytes to hippocampal neurons through ICAM-5 (telencephalin) and characterization of its interaction with the leukocyte integrin CD11a/CD18. *Eur J Immunol.* (2000) 30:810–8. doi: 10.1002/1521-4141(200003)30:3<810::aid-immu810>3.0.co;2-x
15. Tian L, Stefanidakis M, Ning L, Van Lint P, Nyman-Huttunen H, Libert C, et al. Activation of NMDA receptors promotes dendritic spine development through MMP-mediated ICAM-5 cleavage. *J Cell Biol.* (2007) 178:687–700. doi: 10.1083/jcb.200612097
16. Gahmberg CG, Tian L, Ning L, Nyman-Huttunen H. ICAM-5–a novel two-facetted adhesion molecule in the mammalian brain. *Immunol Lett.* (2008) 117:131–5. doi: 10.1016/j.imlet.2008.02.004
17. Lindsberg PJ, Launes J, Tian L, Valimaa H, Subramanian V, Siren J, et al. Release of soluble ICAM-5, a neuronal adhesion molecule, in acute encephalitis. *Neurology.* (2002) 58:446–51. doi: 10.1212/WNL.58.3.446
18. Lu R, Schmidtko A. Direct intrathecal drug delivery in mice for detecting *in vivo* effects of cGMP on pain processing. *Methods Mol Biol.* (2013) 1020:215–21. doi: 10.1007/978-1-62703-459-3_14
19. Vulchanova L, Schuster DJ, Belur LR, Riedl MS, Podetz-Pedersen KM, Kitto KF, et al. Differential adeno-associated virus mediated gene transfer to sensory neurons following intrathecal delivery by direct lumbar puncture. *Mol Pain.* (2010) 6:31. doi: 10.1186/1744-8069-6-31
20. Livak KJ, Schmittgen TD. Analysis of relative gene expression data using real-time quantitative PCR and the 2(-Delta Delta C(T)) Method. *Methods.* (2001) 25:402–8. doi: 10.1006/meth.2001.1262
21. Polman CH, Reingold SC, Banwell B, Clanet M, Cohen JA, Filippi M, et al. Diagnostic criteria for multiple sclerosis: 2010 revisions to the McDonald criteria. *Ann Neurol.* (2011) 69:292–302. doi: 10.1002/ana.22366
22. Sie C, Korn T, Mitsdoerffer M. Th17 cells in central nervous system autoimmunity. *Exp Neurol.* (2014) 262 (Pt A):18–27. doi: 10.1016/j.expneurol.2014.03.009
23. Luchtman DW, Ellwardt E, Larochelle C, Zipp F. IL-17 and related cytokines involved in the pathology and immunotherapy of multiple sclerosis: current and future developments. *Cytokine Growth Factor Rev.* (2014) 25:403–13. doi: 10.1016/j.cytogfr.2014.07.013
24. Tian L, Lappalainen J, Autero M, Hanninen S, Rauvala H, Gahmberg CG. Shedded neuronal ICAM-5 suppresses T-cell activation. *Blood.* (2008) 111:3615–25. doi: 10.1182/blood-2007-09-111179
25. Khalil M, Teunissen CE, Otto M, Piehl F, Sormani MP, Gattringer T, et al. Neurofilaments as biomarkers in neurological disorders. *Nat Rev Neurol.* (2018) 14:577–89. doi: 10.1038/s41582-018-0058-z
26. Kuhle J, Kropshofer H, Haering DA, Kundu U, Meinert R, Barro C, et al. Blood neurofilament light chain as a biomarker of MS disease activity and treatment response. *Neurol Mar.* (2019) 92:e1007–15. doi: 10.1212/WNL.0000000000007032
27. Varhaug KN, Barro C, Bjornevik K, Myhr KM, Torkildsen O, Wergeland S, et al. Neurofilament light chain predicts disease activity in relapsing-remitting MS. *Neurology Neuroimmunol Neuroinflamm.* (2018) 5:e422. doi: 10.1212/nxi.0000000000000422
28. Disanto G, Barro C, Benkert P, Naegelin Y, Schadelin S, Giardiello A, et al. Serum neurofilament light: a biomarker of neuronal damage in multiple sclerosis. *Ann Neurol.* (2017) 81:857–70. doi: 10.1002/ana.24954
29. Kuhle J, Barro C, Disanto G, Mathias A, Soneson C, Bonnier G, et al. Serum neurofilament light chain in early relapsing remitting MS is increased and correlates with CSF levels and with MRI measures of disease severity. *Multi Scler.* (2016) 22:1550–9. doi: 10.1177/1352458515623365

30. Siller N, Kuhle J, Muthuraman M, Barro C, Uphaus T, Groppa S, et al. Serum neurofilament light chain is a biomarker of acute and chronic neuronal damage in early multiple sclerosis. *Multi Scler.* (2018) doi: 10.1177/1352458518765666. [Epubh ahead of print].
31. Preische O, Schultz SA, Apel A, Kuhle J, Kaeser SA, Barro C, et al. Serum neurofilament dynamics predicts neurodegeneration and clinical progression in presymptomatic Alzheimer's disease. *Nat Med.* (2019) 25:277–83. doi: 10.1038/s41591-018-0304-3
32. Schmal H, Czermak BJ, Lentsch AB, Bless NM, Beck-Schimmer B, Friedl HP, et al. Soluble ICAM-1 activates lung macrophages and enhances lung injury. *J Immunol.* (1998) 161:3685–93.
33. Jankowska KI, Williamson EK, Roy NH, Blumenthal D, Chandra V, Baumgart T, et al. Integrins modulate T cell receptor signaling by constraining actin flow at the immunological synapse. *Front Immunol.* (2018) 9:25. doi: 10.3389/fimmu.2018.00025
34. Brosnan CF, Cannella B, Battistini L, Raine CS. Cytokine localization in multiple sclerosis lesions: correlation with adhesion molecule expression and reactive nitrogen species. *Neurology.* (1995) 45(6 Suppl. 6):S16–21.
35. Yoshihara Y, Oka S, Nemoto Y, Watanabe Y, Nagata S, Kagamiyama H, et al. An ICAM-related neuronal glycoprotein, telencephalin, with brain segment-specific expression. *Neuron.* (1994) 12:541–53.
36. Ning L, Tian L, Smirnov S, Vihinen H, Llano O, Vick K, et al. Interactions between ICAM-5 and beta1 integrins regulate neuronal synapse formation. *J Cell Sci.* (2013) 126 (Pt 1):77–89. doi: 10.1242/jcs.106674
37. Nutile-McMenemy N, Elfenbein A, Deleo JA. Minocycline decreases *in vitro* microglial motility, beta1-integrin, and Kv1.3 channel expression. *J Neurochem.* (2007) 103:2035–46. doi: 10.1111/j.1471-4159.2007.04889.x
38. Paetau S, Rolova T, Ning L, Gahmberg CG. Neuronal ICAM-5 inhibits microglia adhesion and phagocytosis and promotes an anti-inflammatory response in LPS stimulated microglia. *Front Mol Neurosci.* (2017) 10:431. doi: 10.3389/fnmol.2017.00431
39. Di Battista AP, Buonora JE, Rhind SG, Hutchison MG, Baker AJ, Rizoli SB, et al. Blood biomarkers in moderate-to-severe traumatic brain injury: potential utility of a multi-marker approach in characterizing outcome. *Front Neurol.* (2015) 6:110. doi: 10.3389/fneur.2015.00110

Conflict of Interest Statement: The authors declare that the research was conducted in the absence of any commercial or financial relationships that could be construed as a potential conflict of interest.

Copyright © 2019 Birkner, Loos, Gollan, Steffen, Wasser, Ruck, Meuth, Zipp and Bittner. This is an open-access article distributed under the terms of the Creative Commons Attribution License (CC BY). The use, distribution or reproduction in other forums is permitted, provided the original author(s) and the copyright owner(s) are credited and that the original publication in this journal is cited, in accordance with accepted academic practice. No use, distribution or reproduction is permitted which does not comply with these terms.

frontiers in Immunology

ORIGINAL RESEARCH
published: 15 March 2019
doi: 10.3389/fimmu.2019.00480

CSF Cytokines in Aging, Multiple Sclerosis, and Dementia

William T. Hu[1,2*], *Jennifer Christina Howell*[1,3], *Tugba Ozturk*[1], *Umesh Gangishetti*[1], *Alexander L. Kollhoff*[1], *Jaime M. Hatcher-Martin*[4], *Albert M. Anderson*[5] *and William R. Tyor*[1,6]

[1] Department of Neurology, Emory University, Atlanta, GA, United States, [2] Center for Neurodegenerative Disease, Emory University, Atlanta, GA, United States, [3] Alzheimer's Disease Research Center, Emory University, Atlanta, GA, United States, [4] Jean and Paul Amos Parkinson's Disease and Movement Disorders Program, Emory University, Atlanta, GA, United States, [5] Department of Internal Medicine, Emory University, Atlanta, GA, United States, [6] Atlanta VA Medical Center, Decatur, GA, United States

OPEN ACCESS

Edited by:
Stefan Bittner,
Johannes Gutenberg University
Mainz, Germany

Reviewed by:
Anna Fogdell-Hahn,
Karolinska Institute (KI), Sweden
Olaf Stuve,
University of Texas
Southwestern Medical Center,
United States

***Correspondence:**
William T. Hu
wthu@emory.edu;
william.hu@emory.edu

Specialty section:
This article was submitted to
Multiple Sclerosis and
Neuroimmunology,
a section of the journal
Frontiers in Immunology

Received: 15 October 2018
Accepted: 21 February 2019
Published: 15 March 2019

Citation:
Hu WT, Howell JC, Ozturk T,
Gangishetti U, Kollhoff AL,
Hatcher-Martin JM, Anderson AM and
Tyor WR (2019) CSF Cytokines in
Aging, Multiple Sclerosis, and
Dementia. Front. Immunol. 10:480.
doi: 10.3389/fimmu.2019.00480

Inflammation is a common process involved in aging, multiple sclerosis (MS), and age-related neurodegenerative disorders such as Alzheimer's disease (AD) and Parkinson's disease (PD), but there is limited evidence for the effects of aging on inflammation in the central nervous system. We collected cerebrospinal fluid (CSF) from 105 healthy control subjects representing a wide age range (23–86), and analyzed levels of cytokines associated innate immunity (TNF-α) and different T-helper subtypes: interferon–gamma induced protein 10 (IP-10) for Th1, interleukin-10 (IL-10) for Th2, and interleukin 8 (IL-8/CXCL8) for Th17. We show that CSF levels of TNF-α, IP-10, and IL-8 all increased linearly with age, but levels of IL-10 demonstrated a U-shaped relationship with age. We further found greater age-related increases in TNF-α, IL-10, and IL-8 relative to increases in IP-10 levels, consistent with a shift from Th1 to other inflammatory phenotypes. Finally, when we analyzed the same four cytokines in people with neurological disorders, we found that MS and AD, but not PD or dementia with Lewy bodies, further accentuated the age-related shift from Th1- to non-Th1-related cytokines. We propose that CSF cytokine levels represent powerful surrogates of brain inflammation and aging, and some, but not all, neurological disorders accelerate the shift away from Th1 phenotypes.

Keywords: inflammaging, neuroinflammation and neurodegeneration, IP10, IL10, IL8, Alzheimer's disease, Parkinsons disease (PD), dementia with Lewy bodies (DLB)

INTRODUCTION

Neuro-inflammation is increasingly implicated in age-related neurodegenerative diseases such as Alzheimer's disease (AD) and Parkinson's disease (PD) (1, 2). Following examples in multiple sclerosis (MS) and other demyelinating conditions, many recent human neurodegenerative studies have analyzed soluble cytokine levels in the blood or cerebrospinal fluid (CSF) to generate hypotheses testable in other cohorts or animal models (3–5). However, factors such as age can

themselves bias the immune system and therefore cytokine levels, including aging-associated pro-inflammatory bias and a shift from Th1 to Th2/innate immunity dominance (6, 7). These patterns, usually sterile (free of symptomatic infection), independent of organ- or system-based disease, and involving the innate and adaptive immune systems, have been together referred to as inflamm-aging (8, 9). Potential drivers for inflamm-aging include persistent low-grade viral and bacterial infection, changing gut microbiome (10), and clearance of accumulating self-proteins. Because of inflamm-aging, it is not always straightforward to distinguish between the effects of disease and non-disease factors on absolute cytokine levels. A thorough evaluation of disease-associated cytokine alterations thus requires an adequate number of healthy subjects across a wide age range to detect not only cytokine level differences but also multi-cytokine profiles, which inform about disease specific changes that also reflect complex immune pathways.

Because recruiting healthy subjects to undergo CSF collection can be difficult, multiple smaller cohorts may need to be combined to generate a larger cohort. This process is not without its own challenges, including the need for standardized CSF collection across multiple research centers with disease-specific protocols (11, 12), reproducible cytokine quantitation, and data-sharing. Over the past 4 years, we have recruited 105 healthy control (HC) subjects over a wide age-range (22–86) to participate in multiple disease-oriented studies using a modified but standardized Alzheimer's Disease Neuro-Imaging (ADNI) protocol (12). This cohort provides a unique opportunity to simultaneously interrogate CSF cytokines from different functional pathways across seven decades of life. Here we measured four cytokines associated with innate immunity and helper T cell subtypes (Th1, Th2, Th17) in these HC subjects, and present a new framework to assess imbalance between cytokine pairs in central nervous system (CNS) disorders including MS, AD, PD, and dementia with Lewy bodies (DLB).

MATERIALS AND METHODS

Standard Protocol Approvals and Patient Consents

This study was carried out in accordance to US Code of Federal Regulations Title 45 Part 46 Protection of Human Subjects, and Emory University and Emory School of Medicine policies. The protocols were approved by the Emory University Institutional Review Board. Banked CSF samples were used for this study, and all subjects had previously given written informed consent according to the Declaration of Helsinki for long-term sample storage and future analysis.

Subject Characterization

Older HC and AD subjects ($n = 52$, median age 69, range 48–89) were recruited during a previous study on CSF and MRI biomarkers of aging and dementia in Caucasian and African Americans (13). Younger HC subjects were recruited from the Emory Cognitive Neurology Clinic, Emory Alzheimer's Disease Research Center, and Emory University in an on-going study of pre-symptomatic carriers for dominantly-inherited frontotemporal lobar degeneration, and a separate study examining CSF biomarkers of HIV. All HC subjects underwent detailed neuropsychological testing (14) to confirm normal cognition. Older and younger HC subjects were then combined to form a continuum (median age 60; range 22–105), with 52/105 (50%) HC subjects younger than 60 years of age. MS ($n = 18$, median age 48, range 28–74), PD ($n = 37$, median age 69, range 41–81), and DLB ($n = 23$, median age 68, range 47–80) were recruited from the Emory Neuroimmunology, Movement Disorders, and Cognitive Neurology Clinics. Because recruitment was completed prior to the latest revisions in diagnostic criteria for MS and DLB in 2017, all MS patients were diagnosed according to the 2010 revised McDonald criteria (15), and all DLB patients were diagnosed according to the 2005 McKeith criteria (16). PD patients had clinical features and findings consistent with the Movement Disorders Society Parkinson's disease criteria (17).

CSF Collection

CSF samples were all previously collected using a modified Alzheimer's Disease Neuroimaging Initiative protocol at Emory University (18). Briefly, CSF was collected into 15 mL polypropylene tubes via a 24-gauge atraumatic needle and syringe aspiration without overnight fasting. CSF in polypropylene tubes was immediately inverted several times, aliquotted (500 μL), labeled, and frozen at −80°C until analysis. CSF samples from 13 young HC subjects (mean age 37.0, range 23–54) were centrifuged at 2,500 rpm after collection before freezing. We previously carried out a prospective experiment centrifuging in this condition half of freshly collected CSF in 16 subjects, and compared levels of eight CSF cytokines (including the four included in the current study) in the supernatant with levels from the uncentrifuged halves. We showed that centrifugation did not influence measured cytokine levels (19), and these samples can be analyzed together. We have also determined the stability of each analyte through freeze-thawing following a pre-established protocol such that the measured levels from frozen samples most closely reflect *in vivo* levels (18).

CSF Cytokine Analysis

Four inflammatory proteins were selected for their preferential association with innate immunity or different immune cell populations, including tumor necrosis alpha (TNF-α) (20), Th-2 related interleukin 10 (IL-10) (21), and Th17-related interleukin 8 (IL-8/CXCL8) (22). Levels of Th1-associated interferon gamma were not consistently detectable, and a downstream marker interferon gamma-induced protein (IP-10/CXCL10, Th1) (23) was used instead as a surrogate. Assays were performed in a Luminex 200 platform using the Merck-Milliplex MAP Human Cytokine Panel (HCYTOMAG-60K, Merck-Millipore, Burlington, MA) following the manufacturer's protocol except two 100 μL aliquots of CSF were used for duplicates instead of what was stated in the protocol. IL-9 is also associated with Th17 pathways but its CSF alterations are challenging to interpret because of influence from race and potentially other factors

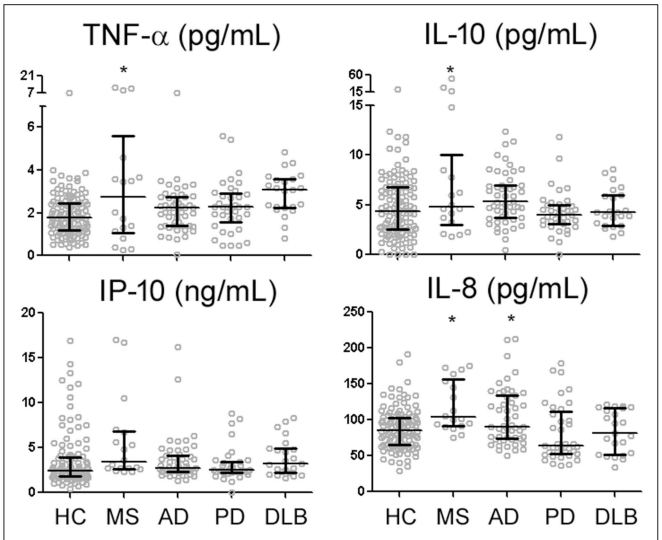


FIGURE 1 | CSF levels of four reliably-measured cytokines in healthy control subjects (HC), multiple sclerosis (MS), Alzheimer's disease (AD), Parkinson's disease (PD), and dementia with Lewy bodies (DLB). *$p < 0.05$ compared to HC.

(Wharton and Hu, unpublished data). Analysis involving IL-9 was thus deferred here. IL-6 was also not measured because its CSF levels were found to be normal in multiple previous studies including in aging, AD (5, 24, 25), and MS (26–29), potentially confounded by the large inter-individual variability (30). Intermediate precision achieved in our laboratory using thirteen biological replicates (different aliquots from the same lumbar puncture for thirteen subjects) over 9 weeks was 4.8% for IP-10, 9.4% for TNF-α, 16.5% for IL-10, and 12.0% for IL-8.

Statistical Analysis

HC subjects were analyzed with age as a continuous variable or according to categories each spanning two decades of life: 20–39, 40–59, and 60–79. Six subjects older than 80 (range 81–86) were combined with the last group to form the category of ≥60. For basic demographic comparison, Chi-squared tests and analysis of variance were used to determine categorical and continuous baseline variables across the five diagnostic categories (HC, MS, AD, PD, DLB). CSF IP-10 levels did not have a normal distribution, and were thus $\log_{10}$-transformed. Analysis of co-variance (ANCOVA) was used to analyze the main effect of diagnosis on CSF cytokine levels, adjusting for age and sex. Pearson's correlational analysis was used to determine the association between cytokines. Regression analysis was used to determine the impact of inflamm-aging in HC subjects with $\log_{10}$-transformed IP-10, age, and gender, and the interaction between age and $\log_{10}$(IP-10) as variables.

To determine impact of neurological disorders on inflamm-aging, levels of $\log_{10}$(IP-10), TNF-α, IL-10, and IL-8 were Z-transformed to adjust for absolute level and distribution differences between the cytokines. Specifically, mean and standard deviation values were calculated for each cytokine from all HC subjects, and all subjects' cytokine levels were then converted to Z-scores. Regression analysis was then used to determine the impact of disease on inflamm-aging, with $\log_{10}$(IP-10), age, gender, age X $\log_{10}$(IP-10), and diagnosis X $\log_{10}$(IP-10) as variables.

RESULTS

Among 105 HC subjects, CSF levels of TNF-α, IL-10, and IP-10 all strongly correlated with one another (R range of 0.354–0.449, $p < 0.001$), while IL-8 only correlated with IP-10 levels ($R = 0.469$, $p < 0.001$). Univariate analysis showed higher levels of TNF-α, IP-10, IL-10, and IL-8 in MS than HC (**Figure 1**). In contrast, univariate analysis identified AD as the only non-MS disorder associated with higher levels of a single cytokine (IL-8) than HC (**Figure 1**). Regression analysis including HC and MS patients taking into account age, gender, MS diagnosis, and MS treatment showed MS treatment to be associated with relative decrease in IL-10 levels ($p = 0.014$).

Because inflamm-aging can potentially complicate the interpretation of group-level comparisons, we next explored the effects of age on CSF cytokine levels in HC subjects using regression analysis. Consistent with a pro-inflammatory bias, TNF-α ($R = 0.250$, $p = 0.010$), IP-10 ($R = 0.453$ for $\log_{10}$-transformed values, $p < 0.001$) and IL-8 ($R = 0.439$, $p < 0.001$) levels all increased with age (**Table 1**, **Figure 2**) while controlling for gender. Interestingly, instead of a linear or step-wise increase, we observed a trend of lower CSF IL-10 levels in the middle-aged group (40–59) than the older and younger groups (**Table 1**). This led us to model this U-shaped relationship between age and IL-10 levels using a quadratic equation (**Figure 2**, $R = 0.495$, $p < 0.001$), with the inflection point (lowest levels) at 50 years of age. ANCOVA showed that MS was associated with greater IP-10 [$F_{(2,123)} = 14.537$, $p < 0.001$], TNF-α [$F = 19.321$, $p < 0.001$], IL-10 [$F = 18.921$, $p < 0.001$], and IL-8 [$F = 23.358$, $p < 0.001$] levels (**Figure 2**), but only IP-10 and IL-8 increased with age in MS ($p < 0.001$ for both).

Beyond paralleled increases in cytokine levels beyond the age of 50, we further analyzed if age modified the relationship between Th1-associated IP-10 and other cytokines by examining the interaction between age and IP-10. This showed that, not only is there an age-associated increase in these CSF cytokines, age further accentuated the positive correlation between IP-10 and TNF-α, IL-10, and IL-8 levels ($p < 0.001$ for the interaction terms, **Table 2**) after controlling for gender. These findings suggest relatively greater increases in these three cytokines for each standard unit of age-associated increase in IP-10, in keeping with a consistent phenotype switch from Th1 to innate immunity (31) and Th2 (7) phenotypes.

While inflammatory changes are either pathogenic (e.g., MS) or commonly observed in neurodegenerative disorders (e.g., AD, PD), it is not clear if each neurological disorder can specifically alter the balance between cytokines linked to inflamm-aging. We thus analyzed if IP-10 levels interacted with disease status in addition to its interaction with age (**Figure 3**) by examining if each disease alters the slope linking IP-10 and the three other cytokines. We found that, for each standard deviation increase

TABLE 1 | Basic demographic and CSF cytokine levels of people with healthy control (HC) with normal cognition according to age group as well as multiple sclerosis (MS).

	MS ($n = 18$)	NC, 20–39 year ($n = 23$)	NC, 40–59 year ($n = 29$)	NC, ≥60 year ($n = 53$)
Male	4 (22%)	16 (70%)	11 (38%)	24 (45%)
Age (SD), year	50.0 (12.8)	31.9 (4.2)	52.8 (5.8)	69.5 (6.6)
Disease duration (SD), yr	11.0 (12.9)	–	–	–
MS Type				
RRMS	15			
PPMS	2			
SPMS	1			
Current MS therapy	8			
Interferon β-1a	2			
Glatiramer acetate	2			
Fingolimod	2			
Dimethyl fumarate	1			
Natalizumab	1			
TNF-α (SD), pg/mL	4.55 (5.78)*	1.51 (0.76)	1.75 (1.28)	2.11 (0.89)
IP-10 (SD), pg/mL	5.61 (4.64)**	2.46 (2.71)	3.09 (3.38)	4.07 (2.65)
IL-10 (SD), pg/mL	9.51 (12.20)*	4.57 (2.48)	2.82 (1.87)	5.30 (2.93)
IL-8 (SD), pg/mL	119.1 (35.2)*	67.5 (22.9)†	88.4 (21.3)	96.4 (31.5)

RRMS, relapsing-remitting MS; PPMS, primary progressive MS; SPMS, secondary progressive MS.
**Higher in MS than other groups.*
***Higher in MS than 22–39 and 40–59 year old groups.*
†Lower in the youngest group than the other two.

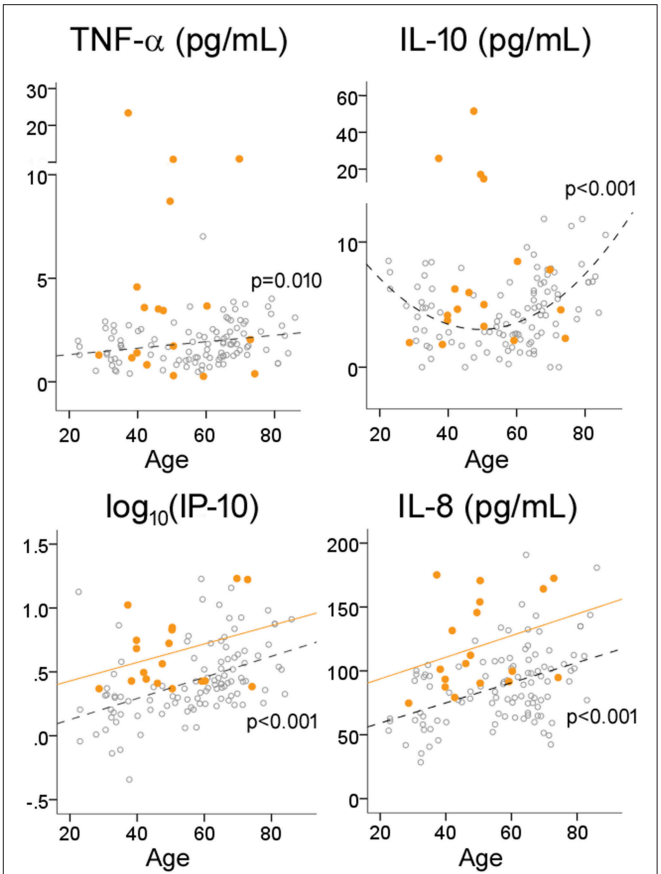


FIGURE 2 | Effects of age on cytokine levels in HC and MS. Open circles and dotted lines (with associated *p*-values) represent individual values and best fit lines for HC subjects; orange circles and orange lines represent individual values and best fit lines for MS subjects.

in IP-10 beyond the age-associated effect on IP-10, both MS ($p < 0.001$) and AD ($p = 0.026$) were associated with greater change in TNF-α than HC, AD was associated with greater change in IL-10 levels ($p = 0.018$) than HC, and MS was associated with greater change in IL-8 levels ($p = 0.013$) than HC. Importantly, these interactions were independent of the age-associated shift. While PD and DLB were associated with greater TNF-α levels and lower IL-8 levels than NC, these disorders did not modify the inflamm-aging relationships between IP-10 and other cytokines. Combining subjects with PD and DLB as Lewy body disease did not change the outcomes.

TABLE 2 | Age modifies the relationship between IP-10 and other cytokines in HC (coefficients and *p*-values are shown).

	TNF-α	IL-10	IL-8
Age, year	−0.007 ($p = 0.357$)	−0.052 ($p = 0.053$)	−6.259 ($p = 0.207$)
Male gender	0.133 ($p = 0.456$)	0.955 ($p = 0.047$)	−6.838 ($p = 0.161$)
$\log_{10}$(IP-10)	0.287 ($p = 0.780$)	−3.985 ($p = 0.146$)	−4.000 ($p = 0.888$)
Age X $\log_{10}$ (IP-10)	0.023 ($p < 0.001$)	0.146 ($p = 0.003$)	0.759 ($p < 0.001$)

DISCUSSION

Inflamm-aging is known to occur in the blood (32, 33) and bone marrow (34), but only limited evidence exists in the human CNS (35, 36). Here we show in a cross-sectional cohort spanning seven decades of life that CSF levels of cytokines associated with innate immunity, Th1, Th2, and Th17 all increased with age. We further show that these cytokines did not increase according to age at the same rates, and aging was associated with greater relative increases in cytokines levels linked to innate immunity, Th2, and Th17 than Th1. Finally, we show that MS and AD further accentuate the age-associated phenotype shift from Th1 to non-Th1 pathways independent of inflamm-aging. Altogether, these CSF findings provide evidence for inflamm-aging in the CNS, and put forth the hypothesis that some–but not all–neurological disorders mimic key features of inflamm-aging.

Inflamm-aging is thought to result from chronic unresolved infection and immunosenesence among other factors (37). There is a general paucity of evidence for inflamm-aging in the human CNS due to limited availability of *normal* post-mortem brain tissue across the life span (36, 38, 39). Using brains from 57 neuropathologically and cognitively normal people from seven

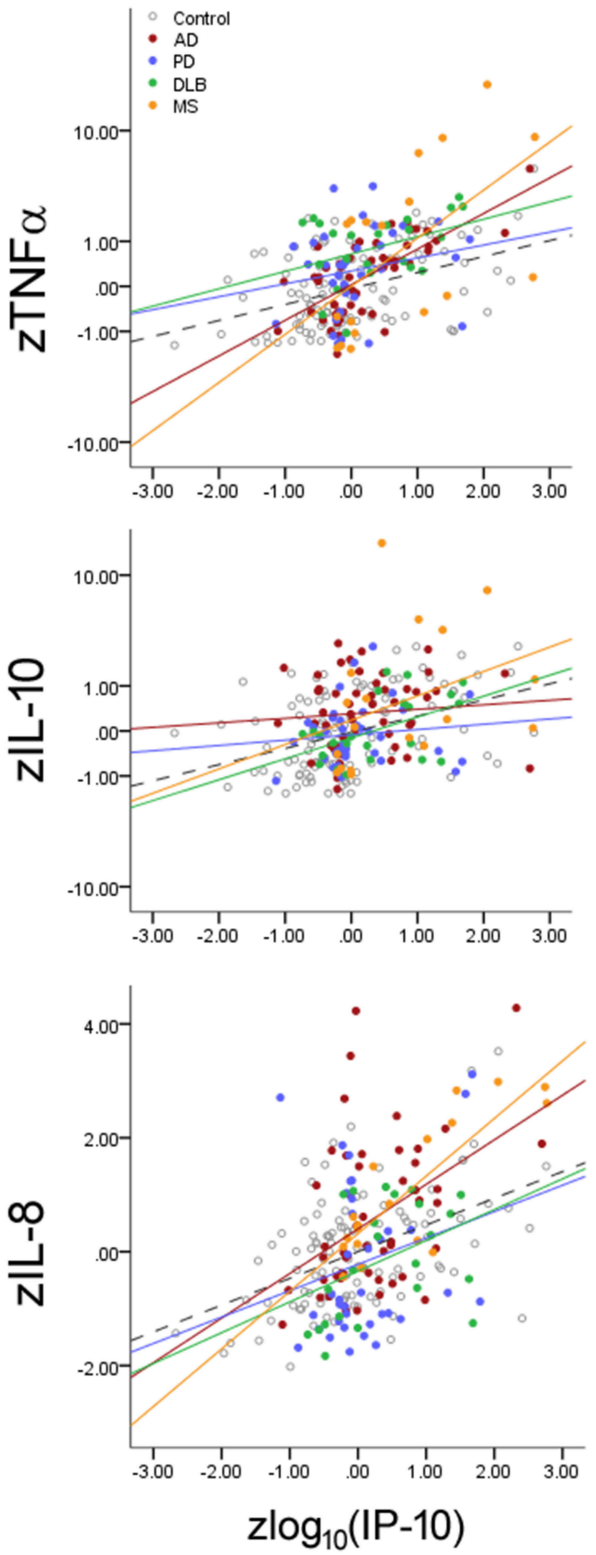


FIGURE 3 | Effects of neurological diseases on the relationship between Th1-associated IP-10 and cytokines associated with innate immunity (TNF-α), Th2 (IL-10), and Th17 (IL-8). Cytokine levels were normalized according to HC *(Continued)*

FIGURE 3 | mean and standard deviation values for illustrative purposes. Accounting for inflamm-aging showed that MS and AD enhanced the relationship between these cytokines, while PD and DLB changed the absolute cytokine levels without altering the relationships. Dotted lines represent best fit line for HC subjects.

brain banks, an expression analysis showed aging and AD to each upregulate genes associated the complement pathway and the toll-like receptors (39). They also identified brain IL-10 as a cytokine implicated in inflamm-aging, in keeping with our findings of age- and AD-associated increase in IL-10 relative to IP-10 elevations. However, a difference in brain IL-10 expression was not reported by a subsequent RNA-Seq study examining 79 subjects when cases were analyzed according to age (under 60 or over 60) (36), possibly due to the U-shaped distribution of CSF IL-10 levels according to age. This age-dependent U-shaped curve can also potentially account for inconsistent findings of normal (28, 40, 41) or elevated (29, 42). CSF IL-10 levels in MS patients from cross-sectional studies. At the same time, the aging-associated trough for CSF IL-10 levels in the fifth decade may identify a window during which the brain is susceptible to immune-mediated processes. Because the peak age at onset for MS precedes this natural IL-10 decline by one to two decades, it is conceivable that patients with MS may experience this IL-10 trough–and the associated unopposed increase in TNF-α, IP-10, and IL-8–earlier in life. Indeed, age at onset has prognostic roles in initial phenotype, progression, and disability (43–45), and the CSF cytokine milieu at onset may better represent biological age with respects to neuroinflammation than chronological age. While definitive testing of this hypothesis would require pre-symptomatic identification of MS patients, healthy young adults at increased risks for MS through family history or a GWAS-based polygenic risk score (46) may determine candidate genes associated with premature IL-10 decline.

Increased CSF TNF-α, IP-10, and IL-8 levels have been previously reported in untreated and treated MS (29, 47–51). A treatment-associated decrease in IL-10 levels in MS may seem contradictory at first especially if premature IL-10 decline may be a risk factor for MS. Previous studies have shown coupled increase of CSF TNF-α and IL-10 during MS flare-ups (52) as well as their coupled normalization after interferon-β or natalizumab treatment (53, 54). Therefore, lower IL-10 levels in treated vs. untreated MS patients likely reflect generalized reduction in immune activation, and MS-treatment does not attenuate the bias toward IL-10 from IP-10. It remains to be determined whether individual cytokine levels or the relative balance between cytokines better predict disease progression or response to therapy.

The exact mechanisms underlying inflamm-aging are not clear. Relevant to the CNS, aging is associated with dendritic remodeling (55), reduced CSF outflow (56), increasing risks of tau-related pathology (57), premature immunosenescense (58), and often white matter hyperintensity associated with cerebrovascular disease on MRI. While we cannot clearly distinguish between CSF cytokine changes due to chronological

aging, immunosenescence, and cumulative subclinical injury common in aging (e.g., ischemia, hypoxia), our work–to the best of our knowledge–provides the first CSF-based evidence for CNS inflamm-aging. Major strengths of the current study include the pooling of subjects with HC and neurological disorders based on standardized collection protocols across multiple sites, and the joint analysis of cytokine levels with age-adjusted balance between cytokines. At the expense of scope, we restricted our analysis to four CSF analytes for their readily detectable levels (e.g., CSF IFN-γ and IL-4 are not easily detected in most CSF samples), measurement accuracy (e.g., some commercial assays fail to validate when non-kit protein standards are used), high intermediate precision (reproducibility between assays run on different days), stability during processing (e.g., freeze-thawing), and invariance across racial groups. Omitting cytokine measures that fall short on specificity or reproducibility allowed for more consistent statistical analysis to address inflamm-aging and to detect linear as well as the U-shaped trends. It is important to note that the cross-sectional nature of our study is suggestive–not confirmatory–of an age-related change over time. An independent validation cohort and longitudinal analysis within the same individuals are necessary to confirm these findings. We also did not quantify different cell types in the CSF, and immunophenotyping will be necessary to test whether cytokine level changes are due to cell type switch, hyperactivity, or both. Because of our focus on CNS inflamm-aging, we did not measure plasma cytokines because we have previously found little correlation between plasma and CSF cytokine levels in HC or people with neurological diseases. In keeping with this, prior studies reported dissociated patterns of plasma and CSF cytokine alterations in MS, but a comparative study of peripheral and CNS inflamm-aging may bring about additional insight. Nevertheless, we present a new framework for simultaneously evaluating CSF cytokines related to inflamm-aging and neurological disorders that goes beyond up- or down-regulation, and extends the Th1 to non-Th1 shift associated with aging to AD.

DATA AVAILABILITY

The raw data supporting the conclusions of this manuscript will be made available by the authors, without undue reservation, to any qualified researcher.

AUTHOR CONTRIBUTIONS

WH, JH, and UG contributed to conception and design of the study. WH, JH, TO, UG, AK, JH-M, AA, and WT organized the dataset. WH performed the statistical analysis. WH and JH wrote sections of the manuscript. TO, UG, JH-M, AA, and WT contributed to the revision of the manuscript. All authors read and approved the submitted version.

FUNDING

This study was sponsored by the NIH K23AG042856 (WH), R21AG043885 (WH), R01AG054046 (WH), K23MH095679 (AA), R01MH116695 (WT), I01BX01506 (WT), the Patterson Family Foundation, and the Bumpus Foundation (JH-M).

ACKNOWLEDGMENTS

We would like to thank Drs. Jonathan D. Glass, Stewart A. Factor, and Neil S. Lava for their assistance in recruitment.

REFERENCES

1. Lapenna A, De Palma M, Lewis CE. Perivascular macrophages in health and disease. *Nat Rev Immunol.* (2018) 18:689–702. doi: 10.1038/s41577-018-0056-9
2. Skaper SD, Facci L, Zusso M, Giusti P. An Inflammation-centric view of neurological disease: beyond the neuron. *Front Cell Neurosci.* (2018) 12:72. doi: 10.3389/fncel.2018.00072
3. Ray S, Britschgi M, Herbert C, Takeda-Uchimura Y, Boxer A, Blennow K, et al. Classification and prediction of clinical Alzheimer's diagnosis based on plasma signaling proteins. *Nat Med.* (2007) 13:1359–62. doi: 10.1038/nm1653
4. Craig-Schapiro R, Perrin RJ, Roe CM, Xiong C, Carter D, Cairns NJ, et al. YKL-40: a novel prognostic fluid biomarker for preclinical Alzheimer's disease. *Biol Psychiatry.* (2010) 68:903–12. doi: 10.1016/j.biopsych.2010.08.025
5. Hu WT, Chen-Plotkin A, Arnold SE, Grossman M, Clark CM, Shaw LM, et al. Novel CSF biomarkers for Alzheimer's disease and mild cognitive impairment. *Acta Neuropathol.* (2010) 119:669–78. doi: 10.1007/s00401-010-0667-0
6. Franceschi C, Bonafe M, Valensin S, Olivieri F, De Luca M, Ottaviani E, et al. Inflamm-aging. An evolutionary perspective on immunosenescence. *Ann N Y Acad Sci.* (2000) 908:244–54. doi: 10.1111/j.1749-6632.2000.tb06651.x
7. Sandmand M, Bruunsgaard H, Kemp K, Andersen-Ranberg K, Pedersen AN, Skinhoj P, et al. Is ageing associated with a shift in the balance between Type 1 and Type 2 cytokines in humans? *Clin Exp Immunol.* (2002) 127:107–14.
8. Franceschi C, Garagnani P, Parini P, Giuliani C, Santoro A. Inflammaging: a new immune-metabolic viewpoint for age-related diseases. *Nat Rev Endocrinol.* (2018) 14:576–90. doi: 10.1038/s41574-018-0059-4
9. Rea IM, Gibson DS, McGilligan V, McNerlan SE, Alexander HD, Ross OA. Age and age-related diseases: role of inflammation triggers and cytokines. *Front Immunol.* (2018) 9:586. doi: 10.3389/fimmu.2018.00586
10. Biagi E, Nylund L, Candela M, Ostan R, Bucci L, Pini E, et al. Through ageing, and beyond: gut microbiota and inflammatory status in seniors and centenarians. *PLoS ONE.* (2010) 5:e10667. doi: 10.1371/journal.pone.0010667
11. Freedman MS, Thompson EJ, Deisenhammer F, Giovannoni G, Grimsley G, Keir G, et al. Recommended standard of cerebrospinal fluid analysis in the diagnosis of multiple sclerosis: a consensus statement. *Arch Neurol.* (2005) 62:865–70. doi: 10.1001/archneur.62.6.865
12. Hu WT, Watts KD, Shaw LM, Howell JC, Trojanowski JQ, Basra S, et al. CSF beta-amyloid 1-42 - what are we measuring in Alzheimer's disease? *Ann Clin Transl Neurol.* (2015) 2:131–9. doi: 10.1002/acn3.160
13. Howell JC, Parker MW, Watts KD, Kollhoff A, Tsvetkova DZ, Hu WT. Research lumbar punctures among African Americans and Caucasians: perception predicts experience. *Front Aging Neurosci.* (2016) 8:296. doi: 10.3389/fnagi.2016.00296
14. Howell JC, Watts KD, Parker MW, Wu J, Kollhoff A, Wingo TS, et al. Race modifies the relationship between cognition and Alzheimer's disease cerebrospinal fluid biomarkers. *Alzheimers Res Ther.* (2017) 9:88. doi: 10.1186/s13195-017-0315-1
15. Polman CH, Reingold SC, Banwell B, Clanet M, Cohen JA, Filippi M, et al. Diagnostic criteria for multiple sclerosis: 2010 revisions to the McDonald criteria. *Ann Neurol.* (2011) 69:292–302. doi: 10.1002/ana.22366
16. McKeith IG, Dickson DW, Lowe J, Emre M, O'Brien JT, Feldman H, et al. Diagnosis and management of dementia with Lewy bodies:

third report of the DLB Consortium. *Neurology.* (2005) 65:1863–72. doi: 10.1212/01.wnl.0000187889.17253.b1
17. Postuma RB, Berg D, Stern M, Poewe W, Olanow CW, Oertel W, et al. MDS clinical diagnostic criteria for Parkinson's disease. *Mov Disord.* (2015) 30:1591–601. doi: 10.1002/mds.26424
18. Hu WT, Watts K, Grossman M, Glass J, Lah JJ, Hales C, et al. Reduced CSF p-Tau181 to Tau ratio is a biomarker for FTLD-TDP. *Neurology.* (2013) 81:1945–52. doi: 10.1212/01.wnl.0000436625.63650.27
19. Gangishetti U, Christina Howell J, Perrin RJ, Louneva N, Watts KD, Kollhoff A, et al. Non-beta-amyloid/tau cerebrospinal fluid markers inform staging and progression in Alzheimer's disease. *Alzheimers Res Ther.* (2018) 10:98. doi: 10.1186/s13195-018-0426-3
20. Clark IA. How TNF was recognized as a key mechanism of disease. *Cytokine Growth Factor Rev.* (2007) 18:335–43. doi: 10.1016/j.cytogfr.2007.04.002
21. Hunt NH, Grau GE. Cytokines: accelerators and brakes in the pathogenesis of cerebral malaria. *Trends Immunol.* (2003) 24:491–9. doi: 10.1016/S1471-4906(03)00229-1
22. Pelletier M, Maggi L, Micheletti A, Lazzeri E, Tamassia N, Costantini C, et al. Evidence for a cross-talk between human neutrophils and Th17 cells. *Blood.* (2010) 115:335–43. doi: 10.1182/blood-2009-04-216085
23. Haabeth OA, Lorvik KB, Hammarstrom C, Donaldson IM, Haraldsen G, Bogen B, et al. Inflammation driven by tumour-specific Th1 cells protects against B-cell cancer. *Nat Commun.* (2011) 2:240. doi: 10.1038/ncomms1239
24. Schuitemaker A, Dik MG, Veerhuis R, Scheltens P, Schoonenboom NS, Hack CE, et al. Inflammatory markers in AD and MCI patients with different biomarker profiles. *Neurobiol Aging.* (2009) 30:1885–9. doi: 10.1016/j.neurobiolaging.2008.01.014
25. Craig-Schapiro R, Kuhn M, Xiong C, Pickering EH, Liu J, Misko TP, et al. Multiplexed immunoassay panel identifies novel CSF biomarkers for Alzheimer's disease diagnosis and prognosis. *PLoS ONE.* (2011) 6:e18850. doi: 10.1371/journal.pone.0018850
26. Uzawa A, Mori M, Ito M, Uchida T, Hayakawa S, Masuda S, et al. Markedly increased CSF interleukin-6 levels in neuromyelitis optica, but not in multiple sclerosis. *J Neurol.* (2009) 256:2082–4. doi: 10.1007/s00415-009-5274-4
27. Horellou P, Wang M, Keo V, Chretien P, Serguera C, Waters P, et al. Increased interleukin-6 correlates with myelin oligodendrocyte glycoprotein antibodies in pediatric monophasic demyelinating diseases and multiple sclerosis. *J Neuroimmunol.* (2015) 289:1–7. doi: 10.1016/j.jneuroim.2015.10.002
28. Matejcikova Z, Mares J, Prikrylova Vranova H, Klosova J, Sladkova V, Dolakova J, et al. Cerebrospinal fluid inflammatory markers in patients with multiple sclerosis: a pilot study. *J Neural Transm.* (2015) 122:273–7. doi: 10.1007/s00702-014-1244-9
29. Sosvorova L, Kanceva R, Vcelak J, Kancheva L, Mohapl M, Starka L, et al. The comparison of selected cerebrospinal fluid and serum cytokine levels in patients with multiple sclerosis and normal pressure hydrocephalus. *Neuro Endocrinol Lett.* (2015) 36:564–71. doi: 10.1046/j.1365-2249.2002.01736.x
30. Brosseron F, Krauthausen M, Kummer M, Heneka MT. Body fluid cytokine levels in mild cognitive impairment and Alzheimer's disease: a comparative overview. *Mol Neurobiol.* (2014) 50:534–44. doi: 10.1007/s12035-014-8657-1
31. Panda A, Arjona A, Sapey E, Bai F, Fikrig E, Montgomery RR, et al. Human innate immunosenescence: causes and consequences for immunity in old age. *Trends Immunol.* (2009) 30:325–33. doi: 10.1016/j.it.2009.05.004
32. Bartlett DB, Firth CM, Phillips AC, Moss P, Baylis D, Syddall H, et al. The age-related increase in low-grade systemic inflammation (Inflammaging) is not driven by cytomegalovirus infection. *Aging Cell.* (2012) 11:912–5. doi: 10.1111/j.1474-9726.2012.00849.x
33. Nevalainen T, Kananen L, Marttila S, Jylha M, Hervonen A, Hurme M, et al. Transcriptomic and epigenetic analyses reveal a gender difference in aging-associated inflammation: the vitality 90+ study. *Age.* (2015) 37:9814. doi: 10.1007/s11357-015-9814-9
34. Pangrazzi L, Meryk A, Naismith E, Koziel R, Lair J, Krismer M, et al. Inflamm-aging influences immune cell survival factors in human bone marrow. *Eur J Immunol.* (2017) 47:481–92. doi: 10.1002/eji.201646570
35. Rhinn H, Abeliovich A. Differential aging analysis in human cerebral cortex identifies variants in TMEM106B and GRN that regulate aging phenotypes. *Cell Syst.* (2017) 4:404–15.e405. doi: 10.1016/j.cels.2017.02.009
36. Cheng H, Xuan H, Green CD, Han Y, Sun N, Shen H, et al. Repression of human and mouse brain inflammaging transcriptome by broad gene-body histone hyperacetylation. *Proc Natl Acad Sci USA.* (2018) 115:7611–6. doi: 10.1073/pnas.1800656115
37. Franceschi C, Campisi J. Chronic inflammation (inflammaging) and its potential contribution to age-associated diseases. *J Gerontol A Biol Sci Med Sci.* (2014) 69(Suppl. 1):S4–9. doi: 10.1093/gerona/glu057
38. Berchtold NC, Cribbs DH, Coleman PD, Rogers J, Head E, Kim R, et al. Gene expression changes in the course of normal brain aging are sexually dimorphic. *Proc Natl Acad Sci USA.* (2008) 105:15605–10. doi: 10.1073/pnas.0806883105
39. Cribbs DH, Berchtold NC, Perreau V, Coleman PD, Rogers J, Tenner AJ, et al. Extensive innate immune gene activation accompanies brain aging, increasing vulnerability to cognitive decline and neurodegeneration: a microarray study. *J Neuroinflammation.* (2012) 9:179. doi: 10.1186/1742-2094-9-179
40. Fainardi E, Rizzo R, Melchiorri L, Vaghi L, Castellazzi M, Marzola A, et al. Presence of detectable levels of soluble HLA-G molecules in CSF of relapsing-remitting multiple sclerosis: relationship with CSF soluble HLA-I and IL-10 concentrations and MRI findings. *J Neuroimmunol.* (2003) 142:149–58. doi: 10.1016/S0165-5728(03)00266-2
41. Braitch M, Nunan R, Niepel G, Edwards LJ, Constantinescu CS. Increased osteopontin levels in the cerebrospinal fluid of patients with multiple sclerosis. *Arch Neurol.* (2008) 65:633–5. doi: 10.1001/archneur.65.5.633
42. Maxeiner HG, Marion Schneider E, Kurfiss ST, Brettschneider J, Tumani H, Bechter K. Cerebrospinal fluid and serum cytokine profiling to detect immune control of infectious and inflammatory neurological and psychiatric diseases. *Cytokine.* (2014) 69:62–7. doi: 10.1016/j.cyto.2014.05.008
43. Scalfari A, Neuhaus A, Daumer M, Ebers GC, Muraro PA. Age and disability accumulation in multiple sclerosis. *Neurology.* (2011) 77:1246–52. doi: 10.1212/WNL.0b013e318230a17d
44. Cossburn M, Ingram G, Hirst C, Ben-Shlomo Y, Pickersgill TP, Robertson NP. Age at onset as a determinant of presenting phenotype and initial relapse recovery in multiple sclerosis. *Mult Scler.* (2012) 18:45–54. doi: 10.1177/1352458511417479
45. Roy S, Frndak S, Drake AS, Irwin L, Zivadinov R, Weinstock-Guttman B, et al. Differential effects of aging on motor and cognitive functioning in multiple sclerosis. *Mult Scler.* (2017) 23:1385–93. doi: 10.1177/1352458516679036
46. Sawcer S. The major cause of multiple sclerosis is environmental: genetics has a minor role–no. *Mult Scler.* (2011) 17:1174–5. doi: 10.1177/1352458511421106
47. Maimone D, Gregory S, Arnason BG, Reder AT. Cytokine levels in the cerebrospinal fluid and serum of patients with multiple sclerosis. *J Neuroimmunol.* (1991) 32:67–74. doi: 10.1016/0165-5728(91)90073-G
48. Sorensen TL, Tani M, Jensen J, Pierce V, Lucchinetti C, Folcik VA, et al. Expression of specific chemokines and chemokine receptors in the central nervous system of multiple sclerosis patients. *J Clin Invest.* (1999) 103:807–15. doi: 10.1172/JCI5150
49. Narikawa K, Misu T, Fujihara K, Nakashima I, Sato S, Itoyama Y. CSF chemokine levels in relapsing neuromyelitis optica and multiple sclerosis. *J Neuroimmunol.* (2004) 149:182–6. doi: 10.1016/j.jneuroim.2003.12.010
50. Rossi S, Motta C, Studer V, Barbieri F, Buttari F, Bergami A, et al. Tumor necrosis factor is elevated in progressive multiple sclerosis and causes excitotoxic neurodegeneration. *Mult Scler.* (2014) 20:304–12. doi: 10.1177/1352458513498128
51. de Flon P, Soderstrom L, Laurell K, Dring A, Sundstrom P, Gunnarsson M, et al. Immunological profile in cerebrospinal fluid of patients with multiple sclerosis after treatment switch to rituximab and compared with healthy controls. *PLoS ONE.* (2018) 13:e0192516. doi: 10.1371/journal.pone.0192516
52. Rodriguez-Sainz Mdel C, Sanchez-Ramon S, de Andres C, Rodriguez-Mahou M, Munoz-Fernandez MA. Th1/Th2 cytokine balance and nitric oxide in cerebrospinal fluid and serum from patients with multiple sclerosis. *Eur Cytokine Netw.* (2002) 13:110–4.
53. Khademi M, Wallstrom E, Andersson M, Piehl F, Di Marco R, Olsson T. Reduction of both pro- and anti-inflammatory cytokines after 6 months of interferon beta-1a treatment of multiple sclerosis. *J Neuroimmunol.* (2000) 103:202–10. doi: 10.1016/S0165-5728(99)00184-8

54. Mellergard J, Edstrom M, Vrethem M, Ernerudh J, Dahle C. Natalizumab treatment in multiple sclerosis: marked decline of chemokines and cytokines in cerebrospinal fluid. *Mult Scler.* (2010) 16:208–17. doi: 10.1177/1352458509355068
55. Mrak RE, Griffin ST, Graham DI. Aging-associated changes in human brain. *J Neuropathol Exp Neurol.* (1997) 56:1269–75. doi: 10.1097/00005072-199712000-00001
56. Ma Q, Ineichen BV, Detmar M, Proulx ST. Outflow of cerebrospinal fluid is predominantly through lymphatic vessels and is reduced in aged mice. *Nat Commun.* (2017) 8:1434. doi: 10.1038/s41467-017-01484-6
57. Crary JF, Trojanowski JQ, Schneider JA, Abisambra JF, Abner EL, Alafuzoff I, et al. Primary age-related tauopathy (PART): a common pathology associated with human aging. *Acta Neuropathol.* (2014) 128:755–66. doi: 10.1007/s00401-014-1349-0
58. Thewissen M, Linsen L, Somers V, Geusens P, Raus J, Stinissen P. Premature immunosenescence in rheumatoid arthritis and multiple sclerosis patients. *Ann N Y Acad Sci.* (2005) 1051:255–62. doi: 10.1196/annals.1361.066

Conflict of Interest Statement: WH has a patent on the use of CSF biomarkers to diagnose FTLD-TDP (US 9,618,522); has received research support from Avid Radiopharmaceuticals (Philadelphia, PA) and Fujirebio US (Malvern, PA); serves as a consultant to AARP, Inc, Locks Law Firm, Interpleader Law, and Roche Diagnostics USA, ViveBio LLC; has received travel support from Hoffman-LaRoche and Abbvie. The funder played no role in the study design, the collection, analysis or interpretation of data, the writing of this paper or the decision to submit it for publication.

The remaining authors declare that the research was conducted in the absence of any commercial or financial relationships that could be construed as a potential conflict of interest.

Copyright © 2019 Hu, Howell, Ozturk, Gangishetti, Kollhoff, Hatcher-Martin, Anderson and Tyor. This is an open-access article distributed under the terms of the Creative Commons Attribution License (CC BY). The use, distribution or reproduction in other forums is permitted, provided the original author(s) and the copyright owner(s) are credited and that the original publication in this journal is cited, in accordance with accepted academic practice. No use, distribution or reproduction is permitted which does not comply with these terms.

frontiers in Neurology

MINI REVIEW
published: 15 March 2019
doi: 10.3389/fneur.2019.00188

Impact of the McDonald Criteria 2017 on Early Diagnosis of Relapsing-Remitting Multiple Sclerosis

*Philipp Schwenkenbecher[1], Ulrich Wurster[1], Franz Felix Konen[1], Stefan Gingele[1], Kurt-Wolfram Sühs[1], Mike P. Wattjes[2], Martin Stangel[1] and Thomas Skripuletz[1]**

[1] Clinical Neuroimmunology and Neurochemistry, Department of Neurology, Hannover Medical School, Hannover, Germany, [2] Department of Diagnostic and Interventional Neuroradiology, Hannover Medical School, Hannover, Germany

OPEN ACCESS

Edited by:
Tobias Ruck, University of Münster, Germany

Reviewed by:
Mario Habek, University of Zagreb, Croatia
Massimiliano Di Filippo, University of Perugia, Italy

***Correspondence:**
Thomas Skripuletz
skripuletz.thomas@mh-hannover.de

Specialty section:
This article was submitted to Multiple Sclerosis and Neuroimmunology, a section of the journal Frontiers in Neurology

Received: *03 January 2019*
Accepted: *14 February 2019*
Published: *15 March 2019*

Citation:
Schwenkenbecher P, Wurster U, Konen FF, Gingele S, Sühs K-W, Wattjes MP, Stangel M and Skripuletz T (2019) Impact of the McDonald Criteria 2017 on Early Diagnosis of Relapsing-Remitting Multiple Sclerosis. Front. Neurol. 10:188. doi: 10.3389/fneur.2019.00188

Multiple sclerosis is a chronic immune mediated demyelinating disease leading to neurological disabilities that need to be diagnosed and treated early. Guidelines on multiple sclerosis diagnosis and monitoring experienced comprehensive changes over the last decades. The first McDonald criteria published in 2001 emphasized the importance of MR imaging but also recognized the role of cerebrospinal fluid diagnostics. The demonstration of an intrathecal immunoglobulin G synthesis is a well-established additional component and has a long tradition in the diagnosis of relapsing-remitting multiple sclerosis. However, the role of cerebrospinal fluid for diagnostic purposes was rather diminished in each revision of the McDonald criteria. In the latest revision of the McDonald criteria of 2017, the detection of an intrathecal immunoglobulin G synthesis as oligoclonal bands experienced a revival. Patients with the first clinical event suggesting multiple sclerosis who fulfill the criteria for dissemination in space can be diagnosed with relapsing-remitting multiple sclerosis when oligoclonal bands in cerebrospinal fluid are detected. The diagnostic sensitivity of these novel criteria with a focus on dissemination in time and oligoclonal bands as a substitute for dissemination in time was published in different cohorts in the last year and is of special interest in this review. Recently published data show that by applying the 2017 McDonald criteria, multiple sclerosis can be diagnosed more frequently at the time of first clinical event as compared to the 2010 McDonald criteria. The main effect was due to the implementation of oligoclonal bands as a substitute for dissemination in time. However, careful differential diagnosis is essential in patients with atypical clinical manifestations to avoid misdiagnoses.

Keywords: multiple sclerosis, clinically isolated syndrome, McDonald criteria, MRI, oligoclonal bands, cerebrospinal fluid

INTRODUCTION

Multiple sclerosis is the most frequent chronic inflammatory demyelinating disease in young adult leading to long term disability (1). Multiple sclerosis is characterized by inflammation in different regions of the central nervous system which is called dissemination in space (DIS) (2–6). Furthermore, inflammation of the central nervous system has to be recurring which is called dissemination in time (DIT) (2–6). Both criteria DIS and DIT have to be fulfilled either by clinical disease course with relapses and different neurological symptoms or by magnetic resonance imaging (MRI) demonstrating inflammatory lesions in different regions and different activity stages to diagnose multiple sclerosis (3–6). Since disease-modifying therapies administered in an early stage of multiple sclerosis have the potential to prevent relapses and future disabilities, an early diagnosis is essential (7–10). The McDonald diagnostic criteria for relapsing-remitting multiple sclerosis facilitated an early and accurate diagnosis in clinical practice (4, 6, 10, 11). In 85% of multiple sclerosis patients, the clinical manifestations start with a clinically isolated syndrome, the first clinical episode of the chronic inflammatory demyelinating disease (10, 12). Multiple sclerosis can be diagnosed when a typical clinically isolated syndrome is followed by a new clinical event with new symptoms which would be then considered as the second relapse. Alternatively, one or more new T2 and/or contrast enhancing lesions on a follow-up MRI scan could also demonstrate DIT allowing the diagnosis of multiple sclerosis in these patients when lesions in different regions of the central nervous system have also be found in one of the MRI scans or when the patient experienced symptoms related to different regions (4–6, 10). Since the introduction of the McDonald criteria of 2010 multiple sclerosis can be diagnosed based on a single baseline MRI scan showing at least one asymptomatic contrast enhancing lesion and non-enhancing lesions (5). The revised McDonald criteria of 2017 contain several novelties in the diagnosis of multiple sclerosis (2, 13). The criteria are easier to apply than the 2010 McDonald criteria, since it is no longer necessary to differentiate between cortical and juxtacortical MRI lesions and between symptomatic and asymptomatic contrast enhanced MRI lesions to fulfill the criterion for DIS (2). Further changes are that cortical lesions and symptomatic brainstem and spinal lesions can be used to demonstrate DIS (2). DIT can be demonstrated by contrast enhanced lesions independently whether they are asymptomatic or symptomatic, which has been shown to increase the sensitivity of MRI criteria for diagnosing multiple sclerosis without compromising specificity (2, 14). However, the presence of oligoclonal bands in cerebrospinal fluid can also be used to substitute for DIT, which has been supported by the observation that oligoclonal bands are an independent risk factor for further clinical episodes in patients with clinically isolated syndrome (3, 9, 15). Thus, cerebrospinal fluid diagnostics with the detection of oligoclonal bands is essential for patients who experienced a clinically isolated syndrome, allowing the diagnosis of multiple sclerosis when MRI scan meets criteria for DIS (2). The impact of the new McDonald criteria for the diagnosis of multiple sclerosis was in the focus of several investigations during the past year. The objective of this review is to review and to summarize these data from different cohorts and to verify if the diagnosis of multiple sclerosis has been improved using the McDonald criteria of 2017.

OLIGOCLONAL BANDS IN MULTIPLE SCLEROSIS

The significance of cerebrospinal fluid examination for multiple sclerosis diagnosis decreased successively in each revision of the McDonald criteria until 2010 but still remained an important diagnostic test (2). The qualitative demonstration of two or more cerebrospinal fluid specific oligoclonal bands is the most sensitive method to show an intrathecal IgG antibody synthesis (16–18). The highest sensitivity and specificity of oligoclonal band testing can be achieved with the method of isoelectric focusing (16–18). To confirm that oligoclonal bands are exclusive to cerebrospinal fluid, paired cerebrospinal fluid and serum samples have to be analyzed in parallel and equal amounts of IgG have to be applied (2). Visualization of oligoclonal bands is preferentially performed by IgG specific antibody staining or by a general protein staining (16). Five isoelectric focusing patterns of oligoclonal bands are differentiated following the recommendations of the first European consensus on cerebrospinal fluid analysis in multiple sclerosis (16). Isoelectric focusing pattern type 1 are defined as absence of oligoclonal bands in the cerebrospinal fluid. Type 2 represents oligoclonal bands restricted to the cerebrospinal fluid (local synthesis). Type 3 means oligoclonal bands restricted to the cerebrospinal fluid and additional identical oligoclonal bands in cerebrospinal fluid and serum (local and systemic synthesis). Type 4 represents identical oligoclonal bands in cerebrospinal fluid and serum (systemic synthesis, no local synthesis). Type 5 demonstrates monoclonal bands in cerebrospinal fluid and serum (paraproteinemia, no local synthesis).

In recent studies, about 70% of patients with clinically isolated syndrome and more than 90% of patients with multiple sclerosis were tested oligoclonal bands positive (19–27). It has been demonstrated that the presence of oligoclonal bands has a positive predictive value of 97%, a negative predictive value of 84%, a sensitivity of 91%, and a specificity of 94% for developing relapsing-remitting multiple sclerosis after clinically isolated syndrome (28). Oligoclonal bands can also serve as biomarker to predict conversion from clinically isolated syndrome to multiple sclerosis (29). Studies applying older McDonald criteria to diagnose multiple sclerosis showed that the presence of oligoclonal bands in clinically isolated syndrome patients doubled the risk to develop multiple sclerosis independent of the MRI findings (3). Furthermore, two recent studies demonstrated that clinically isolated syndrome patients with oligoclonal bands were twice as likely to convert to multiple sclerosis according to McDonald criteria of 2010 as oligoclonal bands negative patients (29, 30). The probability to develop multiple sclerosis was even more pronounced when referred to quantitative intrathecal IgG synthesis (Reiber graphs) (29). On the other side, it should be noted that the finding of oligoclonal bands by isoelectric focusing is not specific for

multiple sclerosis. The differential diagnosis for the presence of oligoclonal bands comprises various other autoimmune diseases such as autoimmune encephalitis, cerebral vasculitis, and neurosarcoidosis and numerous infectious diseases such as viral encephalitis, neuroborreliosis, and neurosyphilis (31–37). The exclusion of alternative diagnoses is fundamental in patients with a clinically isolated syndrome and in general in patients with suspected CNS inflammatory disease (19, 20).

McDONALD CRITERIA

McDonald Criteria 2001

In 1983, the Poser criteria originally incorporated oligoclonal bands into multiple sclerosis diagnostic criteria to stress paraclinical evidence of inflammatory damage in the central nervous system (11, 38). The subsequent McDonald criteria of 2001 replaced the Poser criteria and established the use of MRI as a central tool in the diagnosis of multiple sclerosis (4, 38). The 2001 McDonald criteria demanded evidence of dissemination of lesions in both space and time which could be demonstrated clinically or by MRI supported by other paraclinical diagnostic methods like cerebrospinal fluid examination to enable the diagnosis of multiple sclerosis in patients with different clinical presentations (4, 38). DIS was defined according to the Barkhof–Tintoré MRI criteria for brain abnormalities in multiple sclerosis (three of the four: $\geq$1 Gd-enhancing or $\geq$9 T2-hyperintense lesions, $\geq$1 infratentorial, $\geq$1 juxtacortical, and $\geq$3 periventricular lesions), or the presence of 2 silent T2-weighted brain lesions and oligoclonal bands (4, 38–40). DIT could be demonstrated by evidence of a new contrast enhanced lesion 3 months or by a new T2-hyperintensive lesion 6 months after the initial clinical event (4, 38–40). According to the McDonald criteria of 2001 multiple sclerosis could be diagnosed in an earlier stage in patients with clinically isolated syndrome and showed high specificity (83%), sensitivity (83%), positive predictive value (75%), negative predictive value (89%), and accuracy (83%) for the risk to develop multiple sclerosis after clinically isolated syndrome (38, 41).

McDonald Criteria 2005

In the 2005 revisions of the McDonald criteria of 2001, DIT was evident when a MRI scan, which was performed at least 30 days (instead of 90 days in the 2001 criteria) after the initial clinical event showed a new T2 lesion or a new contrast enhanced lesion was found 3 month after (6, 38). Changes of DIS criteria affected MRI spinal cord lesions, which were considered equivalent to a infratentorial brain lesion or counted as one brain lesion to reach the required number of T2 lesions (6, 38). Furthermore, enhancing spinal cord and brain lesions were equated (6, 38).

The detection of oligoclonal bands remained an additional parameter to demonstrate DIS together with at least 2 multiple sclerosis typical MRI lesions in relapsing-remitting multiple sclerosis (6, 38). The revision resulted in higher sensitivity (77%) and accuracy (86%) in the diagnosis of multiple sclerosis after clinically isolated syndrome with maintaining the high specificity (90%) of the original McDonald criteria (38, 42).

McDonald Criteria 2010

The major achievement of the 2010 revision of the McDonald criteria was that multiple sclerosis can already be diagnosed with a single baseline MRI at the time of first clinical manifestation (5, 38, 43). DIT could be demonstrated when on MRI scan at any time asymptomatic gadolinium enhancing and non-enhancing lesions were simultaneously present or when any T2 or gadolinium enhancing lesion(s) could be found on follow up scan any time after the baseline scan (5, 38, 43). Furthermore, DIS was easier to achieve by demonstration of at least one T2 lesion in at least two of four central nervous system locations: juxtacortical, periventricular, infratentorial, and spinal cord (5, 38, 43). However, symptomatic brainstem and spinal cord lesions could neither be used for DIT nor DIS (5, 38, 43). On the other side, cerebrospinal fluid diagnostic including presentation of oligoclonal bands lost its role in supporting the diagnosis of relapsing-remitting multiple sclerosis (5, 38, 43).

The revision of the McDonald criteria of 2010 was intended to make diagnostic work-up easier and more efficient by reducing the number of MRI scans but contained pitfalls for neuroradiologist who had to differentiate between symptomatic and asymptomatic lesions (5, 38). It has also led to an earlier definite diagnosis of multiple sclerosis (25, 38). Nevertheless, clinicians were cautioned not to overemphasize MRI findings without making a thorough clinical evaluation and careful differential diagnosis, as the MRI criteria do not distinguish between multiple sclerosis and other disorders that can cause similar changes in the central nervous system (44, 45). This concern has been demonstrated in a recent study which included 168 patients with headache who presented with T2 white matter hyperintensities on brain MRI. In 2.4% of these patients MRI lesions were in contact with cortical and ventricular surfaces thus fulfilling the Barkhof-Tintoré criteria for multiple sclerosis and in 7.1% of these patients MRI lesions were at least close with having an edge within 3 mm of the surfaces (38, 46). When applying the McDonald criteria of 2010, numbers even increased to 24.4% of patients who met the imaging criteria for multiple sclerosis and 34.5% of patients whose lesions were close to cortical and ventricular surfaces (38, 46).

McDonald Criteria 2017

One of the most important changes in the 2017 revised McDonald criteria is that oligoclonal bands can be taken as a substitute for DIT, and thus, can be used to establish the diagnosis of multiple sclerosis after the first clinical event and a single brain MRI (2, 45). These new implications based on observations demonstrating that in patients who fulfilled the criteria of DIS, the additional presence of oligoclonal bands increased the specificity and has a high positive predictive value for diagnosis of multiple sclerosis (2, 25, 30, 45, 47). Cerebrospinal fluid analysis is not only important to determine oligoclonal bands but also to exclude differential diagnosis by assessing atypical parameters such as an elevated protein concentration, pleocytosis with $>$50 cells/μl, or the presence of neutrophils, eosinophils, atypical cells (18, 25). Furthermore, the distinction from neuromyelitis optica spectrum disease, a demyelinating disease with overlapping

TABLE 1 | Demographic characteristics of patients diagnosed with multiple sclerosis according to the McDonald criteria of 2010 and 2017 in different studies.

Authors	Country	Study inclusion criteria	Patient numbers	Mean age (years)	Females/males	Multiple sclerosis		Additional multiple sclerosis diagnoses based on new DIT criteria	
						McDonald 2010	McDonald 2017	Oligoclonal bands in CSF	Symptomatic MRI lesions
Schwenkenbecher et al. (56)	Germany	First clinical event	325	34.2	1.8	136/325 (42%)	214/325 (66%)	76/78 (97%)	16/78 (21%)
Hyun et al. (54)	Korea	First clinical event	163	31	2.1	72/163 (44%)	124/163 (76%)	n.a. for all patients	n.a. for all patients
Habek et al. (53)	Croatia	First clinical event	113	32.1	0.4	39/113 (35%)	83/113 (74%)	43/44 (98%)	15/44 (34%)
van der Vuurst de Vries et al. (10)	Netherlands	First clinical event	229	33.5	2.7	46/180* (26%)	97/180* (54%)	32/51 (63%)	19/51 (37%)
Lee et al. (55)	Germany	First clinical event + DIS in MRI	290	36.4	2.1	152/290 (52%)	273/290 (94%)	121/121 (100%)	10/121 (8%)
McNicholas et al. (57)	Ireland	First clinical event + conversion to multiple sclerosis** during follow up	250	33	2.6	40/250 (16%)	110/250 (44%)	61/71 (86%)	10/71 (14%)
Gobbin et al. (58)	Italy	First clinical event with follow up investigations***	55	30****	1.5	49/55 (89%)	54/55 (98%)	4/5 (80%)	1/5 (20%)
Gaetani et al. (52)	Italy	Clinically isolated syndrome***** + DIS in MRI	137	31.4	2.9	0/137	113/137 (82%)	105/137 (77%)	58/137 (42%)

Whether additional multiple sclerosis diagnoses according to McDonald 2017 based on new DIT criteria by symptomatic MRI lesions or oligoclonal bands is enlisted.

**MRI data available for 180/229 patients.*

***McDonald 2010.*

****The McDonald criteria were compared in patients with follow up investigations.*

*****Mean age was not described, Median age was 30 years.*

******Multiple sclerosis patients diagnosed according to McDonald 2010 were not included.*

clinical, imaging, and cerebrospinal fluid features, is in particular important due to the different treatment (2).

Further changes in the 2017 McDonald criteria apply to MRI activity. The 2010 McDonald criteria did not allow symptomatic brainstem or spinal cord lesions to demonstrate DIT or DIS to avoid so-called double counting. Since several studies indicated that the inclusion of symptomatic lesions increased the diagnostic sensitivity with slight affection on specificity (2, 14, 48) the 2017 McDonald criteria allow now including symptomatic and asymptomatic MRI lesions in the determination of DIS and DIT. Furthermore, in the new McDonald criteria cortical lesions are equivalent to juxtacortical lesions. Since histopathological studies have shown that cortical lesions and juxtacortical lesions are typical of multiple sclerosis and MRI techniques improved to identify these lesions, cortical lesions can now be used to fulfill MRI criteria for DIS (2, 49, 50). However, cortical lesions have to be considered carefully, since standard MRI has limited ability to detect and distinguish cortical lesions from other causes and artifacts (2).

Recently published data show that by applying the 2017 McDonald criteria, multiple sclerosis can be diagnosed more frequently at the time of first clinical event (10, 51–56). We previously investigated the diagnostic sensitivity in 325 patients with a clinical event suggestive of multiple sclerosis and found that 70 patients (22%) were diagnosed with multiple sclerosis when the 2005 criteria were applied (25). The McDonald criteria of 2010 allowed already a higher number of 136 patients (42%) to be designated as having multiple sclerosis (25). Application of the new McDonald criteria of 2017 on the same cohort allowed the diagnosis of definite multiple sclerosis in 78 additional patients (in total 214 patients; 66%) (56). Seventy-six of the 78 newly diagnosed patients with multiple sclerosis presented oligoclonal bands (56). These effects of the new McDonald criteria on earlier diagnosis of multiple sclerosis results were confirmed by additional recently published studies (summarized in **Table 1**).

Habek and colleagues investigated 113 patients with clinically isolated syndrome and found that 83 patients (74%) could be diagnosed with multiple sclerosis by applying the McDonald criteria of 2017, whereas the McDonald criteria of 2010 allowed only 39 patients (35%) to be designated as having multiple sclerosis (53). The sensitivity was higher for the new McDonald criteria (85%) as compared to the McDonald criteria of 2010 (41%), however, the specificity dropped from 85% in the criteria of 2010 to 63% with the criteria of 2017 (53). In the study of van der Vuurst de Vries and colleagues 97 of 180 patients (54%) fulfilled the McDonald criteria of 2017 in contrast to only 46 of 180 patients (26%) by applying the McDonald criteria of 2010 (10). The sensitivity was higher for the 2017 criteria than for the 2010 criteria (68 vs. 36%), but the specificity was lower (61 vs. 85%) (10). Hyun and colleagues found similar results when applying the McDonald criteria of 2017 in Korean clinically isolated syndrome patients and described higher sensitivity (88.8%) and accuracy (70.6%) but lower specificity (43.1%) compared with the 2010 McDonald criteria (sensitivity: 53.1%, accuracy 69.2%, specificity 59.5%) for prediction of conversion (54). Again, more clinically isolated syndrome patients could be diagnosed with multiple sclerosis by using the new criteria (76%) as compared to 2010 criteria (44%) (54). Lee and colleagues investigated a large cohort of 290 clinically isolated syndrome patients and identified 52% of patients with the diagnosis of multiple sclerosis according to the McDonald criteria of 2010 (55). The application of the McDonald criteria of 2017 increased the number of multiple sclerosis patients to 94%, thus leaving only 6% of patients with the diagnosis of clinically isolated syndrome (55). The high number of multiple sclerosis patients differs from the other described cohorts and might be explained by the fact that Lee and colleagues included only patients with clinically isolated syndrome who fulfilled MRI criteria for DIS in their cohort (55). In contrast, in the cohort of van der Vuurst de Vries and colleagues only 54% of clinically isolated syndrome patients fulfilled DIS criteria (10). Similar results to Lee and colleagues were found by Gaetani and colleagues who investigated clinically isolated syndrome patients only (excluding patients diagnosed with multiple sclerosis according to the McDonald criteria of 2010) in combination with fulfilled DIS (52). Eighty-two percent of these clinically isolated syndrome patients could be diagnosed with multiple sclerosis by applying the McDonald criteria of 2017 (52). McNicholas and colleagues compared the time to diagnosis when applying the 2017 McDonald criteria in a cohort of patients who had been diagnosed with multiple sclerosis according to the McDonald criteria of 2010 and found a significant improvement (57). The median time to diagnosis could be reduced from 7.4 months (McDonald 2010) to 2.3 months (McDonald 2017) (57). In total, the 2017 McDonald criteria allowed 142/250 patients (57%) to receive an earlier diagnosis. CSF data were available in 200/250 patients and the authors found that the presence of oligoclonal bands allowed an earlier diagnosis in 127/200 patients. The authors describe that 40 of 250 patients (16%) initially fulfilled the 2010 McDonald criteria for multiple sclerosis in an outpatient setting. The 2017 McDonald criteria would have allowed 110 patients (44%) to be diagnosed with multiple sclerosis. However, the authors describe that the extent of investigations carried out prior to first review in this group varied greatly according to the referral source.

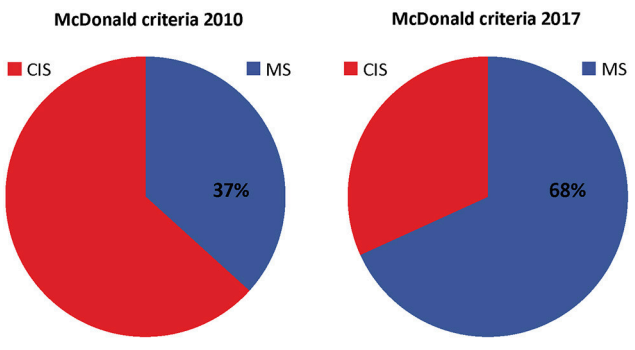


FIGURE 1 | Distribution of patients diagnosed with clinically isolated syndrome (CIS) and multiple sclerosis (MS) according to McDonald criteria of 2010 and 2017. Distribution was created with pooled data from Schwenkenbecher et al. (56); Hyun et al. (54), Habek et al. (53), van der Vuurst de Vries et al. (10), Lee et al. (55), and McNicholas et al. (57).

Gobbin and colleagues investigated a cohort of 55 patients with a first demyelinating event. Forty-nine of these 55 patients fulfilled the multiple sclerosis diagnostic criteria according to McDonald 2010 after a follow-up of 7 months (0–73) (58). A higher number of 54 of these patients were diagnosed with multiple sclerosis after 1 month (0–64) when the 2017 McDonald criteria were applied.

Five studies calculated the sensitivity for conversion to multiple sclerosis by applying the 2017 McDonald criteria which ranged from 68 to 100% (10, 53–55, 58). The specificity was low in these studies and ranged from 13.8 to 63% for the new criteria. However, a low specificity is expected when retrospectively testing newer and more inclusive criteria compared to older and less inclusive diagnostic criteria. Furthermore, there are several bias due to limitations that need to be critically discussed: the studies included a low number of patients and short time of follow-up; the exposure to disease-modifying drugs during follow-up needs to be considered since it could lead to a delay in the second clinical manifestation or in the appearance of new MRI T2 or contrast enhancing lesions. These limitations within a short time period might be a reason for a reduced disease activity limiting the frequency of conversion rates to definitive multiple sclerosis. Thus, future prospective studies with larger cohorts are needed to evaluate the specificity of the new McDonald criteria.

Pitfalls by Applying McDonald Criteria 2017

While the McDonald criteria were developed to establish a consensus for multiple sclerosis diagnosis, limitations are related to alternative inflammatory central nervous system disorders (2, 45). It is challenging to diagnose multiple sclerosis in patients who indeed fulfill the diagnostic criteria but present with uncommon clinical syndromes. Since the McDonald criteria are primarily to be applied in patients with a typical clinically isolated syndrome, cases of an atypical clinical presentation are challenging and require expertise in multiple sclerosis in order to make a reliable diagnosis or an alternative diagnosis (2, 45). MRI findings and clinical presentations can be misleading in patients with migraine and vascular risk comorbidities (45). The specificity for multiple sclerosis diagnosis may also be improved by considering the perivascular distribution pattern of multiple sclerosis lesions including the so called "central vein sign" to differentiate vascular pathology and other inflammatory CNS lesions from multiple sclerosis, the identification of callosal lesions, thorough assessment of spinal cord lesions and at least two different MRI sequences to confirm lesions (39, 45, 59). Furthermore, the detection of oligoclonal bands can support the diagnosis of multiple sclerosis or when absent should lead to a thorough re-evaluation (45). On the other hand, it could also be shown that initially oligoclonal bands negative multiple sclerosis patients were eventually tested positive in a follow-up spinal tap (60, 61). Therefore, a second lumbar puncture is desirable in patients with a questionable multiple sclerosis diagnosis and in patients with clinically isolated syndrome at high risk to develop multiple sclerosis (25). However, although highly prevalent, oligoclonal bands are not specific for multiple sclerosis and can be also detected in numerous other autoimmune and infectious central nervous system diseases (31–37).

CONCLUSION

The 2017 McDonald criteria were developed to allow a more rapid diagnosis of multiple sclerosis and achieved their goal at an impressive extent (**Figure 1**). The main effect was due to the implementation of oligoclonal bands as a substitute for dissemination in time. Alternative less technically demanding and cost saving biomarker to oligoclonal bands might play a role in a future revision of the McDonald criteria. However, limitations of the 2017 McDonald criteria when applied on atypical clinical manifestations and misleading MRI findings should be carefully considered.

DATA AVAILABILITY

All datasets generated for this study are included in the manuscript and/or the supplementary files.

AUTHOR CONTRIBUTIONS

PS, UW, FK, SG, K-WS, MW, MS, and TS provided expertise for the conception and design of the study, contributed to the drafting and approved the final version of this manuscript.

REFERENCES

1. Reich DS, Lucchinetti CF, Calabresi PA. Multiple sclerosis. *N Engl J Med.* (2018) 378:169–80. doi: 10.1056/NEJMra1401483
2. Thompson AJ, Banwell BL, Barkhof F, Carroll WM, Coetzee T, Comi G, et al. Diagnosis of multiple sclerosis: 2017 revisions of the McDonald criteria. *Lancet Neurol.* (2017) 17:162–73. doi: 10.1016/S1474-4422(17)30470-2
3. Kuhle J, Disanto G, Dobson R, Adiutori R, Bianchi L, Topping J, et al. Conversion from clinically isolated syndrome to multiple sclerosis: a large multicentre study. *Mult Scler.* (2015) 21:1013–24. doi: 10.1177/1352458514568827
4. McDonald WI, Compston A, Edan G, Goodkin D, Hartung HP, Lublin FD, et al. Recommended diagnostic criteria for multiple sclerosis: guidelines from the International Panel on the diagnosis of multiple sclerosis. *Ann Neurol.* (2001) 50:121–7. doi: 10.1002/ana.1032
5. Polman CH, Reingold SC, Banwell B, Clanet M, Cohen JA, Filippi M, et al. Diagnostic criteria for multiple sclerosis: 2010 revisions to the McDonald criteria. *Ann Neurol.* (2011) 69:292–302. doi: 10.1002/ana.22366
6. Polman CH, Reingold SC, Edan G, Filippi M, Hartung HP, Kappos L, et al. Diagnostic criteria for multiple sclerosis: 2005 revisions to the "McDonald Criteria". *Ann Neurol.* (2005) 58:840–6. doi: 10.1002/ana.20703
7. Comi G, Martinelli V, Rodegher M, Moiola L, Bajenaru O, Carra A, et al. Effect of glatiramer acetate on conversion to clinically definite multiple sclerosis in patients with clinically isolated syndrome (PreCISe study): a randomised, double-blind, placebo-controlled trial. *Lancet.* (2009) 374:1503–11. doi: 10.1016/S0140-6736(09)61259-9
8. Kappos L, Polman CH, Freedman MS, Edan G, Hartung HP, Miller DH, et al. Treatment with interferon beta-1b delays conversion to clinically definite and McDonald MS in patients with clinically isolated syndromes. *Neurology.* (2006) 67:1242–9. doi: 10.1212/01.wnl.0000237641.33768.8d

9. Tintore M, Rovira A, Rio J, Otero-Romero S, Arrambide G, Tur C, et al. Defining high, medium and low impact prognostic factors for developing multiple sclerosis. *Brain.* (2015) 138(Pt 7):1863–74. doi: 10.1093/brain/awv105
10. van der Vuurst de Vries RM, Mescheriakova JY, Wong YYM, Runia TF, Jafari N, Samijn JP, et al. Application of the 2017 revised McDonald criteria for multiple sclerosis to patients with a typical clinically isolated syndrome. *JAMA Neurol.* (2018) 75:1392–8. doi: 10.1001/jamaneurol.2018.2160
11. Poser CM, Paty DW, Scheinberg L, McDonald WI, Davis FA, Ebers GC, et al. New diagnostic criteria for multiple sclerosis: guidelines for research protocols. *Ann Neurol.* (1983) 13:227–31. doi: 10.1002/ana.410130302
12. Miller DH, Chard DT, Ciccarelli O. Clinically isolated syndromes. *Lancet Neurol.* (2012) 11:157–69. doi: 10.1016/S1474-4422(11)70274-5
13. Schwenkenbecher P, Konen FF, Wurster U, Jendretzky KF, Gingele S, Suhs KW, et al. The persisting significance of oligoclonal bands in the dawning era of kappa free light chains for the diagnosis of multiple sclerosis. *Int J Mol Sci.* (2018) 19:E3796. doi: 10.3390/ijms19123796
14. Brownlee WJ, Swanton JK, Miszkiel KA, Miller DH, Ciccarelli O. Should the symptomatic region be included in dissemination in space in MRI criteria for MS? *Neurology.* (2016) 87:680–3. doi: 10.1212/WNL.0000000000002975
15. Franciotta D, Salvetti M, Lolli F, Serafini B, Aloisi F. B cells and multiple sclerosis. *Lancet Neurol.* (2008) 7:852–8. doi: 10.1016/S1474-4422(08)70192-3
16. Andersson M, Alvarez-Cermeno J, Bernardi G, Cogato I, Fredman P, Frederiksen J, et al. Cerebrospinal fluid in the diagnosis of multiple sclerosis: a consensus report. *J Neurol Neurosurg Psychiatry.* (1994) 57:897–902. doi: 10.1136/jnnp.57.8.897
17. Freedman MS, Thompson EJ, Deisenhammer F, Giovannoni G, Grimsley G, Keir G, et al. Recommended standard of cerebrospinal fluid analysis in the diagnosis of multiple sclerosis: a consensus statement. *Arch Neurol.* (2005) 62:865–70. doi: 10.1001/archneur.62.6.865
18. Stangel M, Fredrikson S, Meinl E, Petzold A, Stuve O, Tumani H. The utility of cerebrospinal fluid analysis in patients with multiple sclerosis. *Nat Rev Neurol.* (2013) 9:267–76. doi: 10.1038/nrneurol.2013.41
19. Awad A, Hemmer B, Hartung HP, Kieseier B, Bennett JL, Stuve O. Analyses of cerebrospinal fluid in the diagnosis and monitoring of multiple sclerosis. *J Neuroimmunol.* (2010) 219:1–7. doi: 10.1016/j.jneuroim.2009.09.002
20. Karussis D. The diagnosis of multiple sclerosis and the various related demyelinating syndromes: a critical review. *J Autoimmun.* (2014) 48-49:134–42. doi: 10.1016/j.jaut.2014.01.022
21. Miller D, Barkhof F, Montalban X, Thompson A, Filippi M. Clinically isolated syndromes suggestive of multiple sclerosis, part 2: non-conventional MRI, recovery processes, and management. *Lancet Neurol.* (2005) 4:341–8. doi: 10.1016/S1474-4422(05)70095-8
22. Paolino E, Fainardi E, Ruppi P, Tola MR, Govoni V, Casetta I, et al. A prospective study on the predictive value of CSF oligoclonal bands and MRI in acute isolated neurological syndromes for subsequent progression to multiple sclerosis. *J Neurol Neurosurg Psychiatry.* (1996) 60:572–5. doi: 10.1136/jnnp.60.5.572
23. Polman C, Kappos L, Freedman MS, Edan G, Hartung HP, Miller DH, et al. Subgroups of the BENEFIT study: risk of developing MS and treatment effect of interferon beta-1b. *J Neurol.* (2008) 255:480–7. doi: 10.1007/s00415-007-0733-2
24. Sastre-Garriga J, Tintore M, Rovira A, Grive E, Pericot I, Comabella M, et al. Conversion to multiple sclerosis after a clinically isolated syndrome of the brainstem: cranial magnetic resonance imaging, cerebrospinal fluid and neurophysiological findings. *Mult Scler.* (2003) 9:39–43. doi: 10.1191/1352458503ms847oa
25. Schwenkenbecher P, Sarikidi A, Wurster U, Bronzlik P, Suhs KW, Raab P, et al. McDonald criteria 2010 and 2005 compared: persistence of high oligoclonal band prevalence despite almost doubled diagnostic sensitivity. *Int J Mol Sci.* (2016) 17:1592. doi: 10.3390/ijms17091592
26. Tintore M, Rovira A, Brieva L, Grive E, Jardi R, Borras C, et al. Isolated demyelinating syndromes: comparison of CSF oligoclonal bands and different MR imaging criteria to predict conversion to CDMS. *Mult Scler.* (2001) 7:359–63. doi: 10.1177/135245850100700603
27. Zipoli V, Hakiki B, Portaccio E, Lolli F, Siracusa G, Giannini M, et al. The contribution of cerebrospinal fluid oligoclonal bands to the early diagnosis of multiple sclerosis. *Mult Scler.* (2009) 15:472–8. doi: 10.1177/1352458508100502
28. Masjuan J, Alvarez-Cermeno JC, Garcia-Barragan N, Diaz-Sanchez M, Espino M, Sadaba MC, et al. Clinically isolated syndromes: a new oligoclonal band test accurately predicts conversion to MS. *Neurology.* (2006) 66:576–8. doi: 10.1212/01.wnl.0000198253.35119.83
29. Schwenkenbecher P, Sarikidi A, Bonig L, Wurster U, Bronzlik P, Suhs KW, et al. Clinically isolated syndrome according to McDonald 2010: intrathecal IgG synthesis still predictive for conversion to multiple sclerosis. *Int J Mol Sci.* (2017) 18:E2061. doi: 10.3390/ijms18102061
30. Huss AM, Halbgebauer S, Ockl P, Trebst C, Spreer A, Borisow N, et al. Importance of cerebrospinal fluid analysis in the era of McDonald 2010 criteria: a German-Austrian retrospective multicenter study in patients with a clinically isolated syndrome. *J Neurol.* (2016) 263:2499–504. doi: 10.1007/s00415-016-8302-1
31. Tumani H, Nolker G, Reiber H. Relevance of cerebrospinal fluid variables for early diagnosis of neuroborreliosis. *Neurology.* (1995) 45:1663–70. doi: 10.1212/WNL.45.9.1663
32. Caudie C, Garel F, Bancel J, Lombard C, Vandenberghe N. [Diagnosis and biological monitoring of 6 neurosyphilis cases: value of cerebrospinal fluid analysis]. *Ann Biol clin.* (2003) 61:563–9.
33. Dalmau J, Gleichman AJ, Hughes EG, Rossi JE, Peng X, Lai M, et al. Anti-NMDA-receptor encephalitis: case series and analysis of the effects of antibodies. *Lancet Neurol.* (2008) 7:1091–8. doi: 10.1016/S1474-4422(08)70224-2
34. Wengert O, Rothenfusser-Korber E, Vollrath B, Bohner G, Scheibe F, Otto C, et al. Neurosarcoidosis: correlation of cerebrospinal fluid findings with diffuse leptomeningeal gadolinium enhancement on MRI and clinical disease activity. *J Neurol Sci.* (2013) 335:124–30. doi: 10.1016/j.jns.2013.09.008
35. Spreer A, Nau R. [Cerebrospinal fluid diagnostics for neuroinfectious diseases]. *Fortschritte Neurol-Psychiatrie.* (2015) 83:109–22. doi: 10.1055/s-0034-1398932
36. Pars K, Pul R, Schwenkenbecher P, Suhs KW, Wurster U, Witte T, et al. Cerebrospinal fluid findings in neurological diseases associated with Sjogren's syndrome. *Eur Neurol.* (2017) 77:91–102. doi: 10.1159/000454765
37. Schwenkenbecher P, Pul R, Wurster U, Conzen J, Pars K, Hartmann H, et al. Common and uncommon neurological manifestations of neuroborreliosis leading to hospitalization. *BMC Infect Dis.* (2017) 17:90. doi: 10.1186/s12879-016-2112-z
38. Milo R, Miller A. Revised diagnostic criteria of multiple sclerosis. *Autoimmun Rev.* (2014) 13:518–24. doi: 10.1016/j.autrev.2014.01.012
39. Barkhof F, Filippi M, Miller DH, Scheltens P, Campi A, Polman CH, et al. Comparison of MRI criteria at first presentation to predict conversion to clinically definite multiple sclerosis. *Brain.* (1997) 120 (Pt 11):2059–69.
40. Tintore M, Rovira A, Martinez MJ, Rio J, Diaz-Villoslada P, Brieva L, et al. Isolated demyelinating syndromes: comparison of different MR imaging criteria to predict conversion to clinically definite multiple sclerosis. *Am J Neuroradiol.* (2000) 21:702–6.
41. Dalton CM, Brex PA, Miszkiel KA, Hickman SJ, MacManus DG, Plant GT, et al. Application of the new McDonald criteria to patients with clinically isolated syndromes suggestive of multiple sclerosis. *Ann Neurol.* (2002) 52:47–53. doi: 10.1002/ana.10240
42. Swanton JK, Fernando K, Dalton CM, Miszkiel KA, Thompson AJ, Plant GT, et al. Modification of MRI criteria for multiple sclerosis in patients with clinically isolated syndromes. *J Neurol Neurosurg Psychiatry.* (2006) 77:830–3. doi: 10.1136/jnnp.2005.073247
43. Montalban X, Tintore M, Swanton J, Barkhof F, Fazekas F, Filippi M, et al. MRI criteria for MS in patients with clinically isolated syndromes. *Neurology.* (2010) 74:427–34. doi: 10.1212/WNL.0b013e3181cec45c
44. Miller DH, Weinshenker BG, Filippi M, Banwell BL, Cohen JA, Freedman MS, et al. Differential diagnosis of suspected multiple sclerosis: a consensus approach. *Mult Scler.* (2008) 14:1157–74. doi: 10.1177/1352458508096878
45. Solomon AJ, Naismith RT, Cross AH. Misdiagnosis of multiple sclerosis: impact of the 2017 McDonald criteria on clinical practice. *Neurology.* (2019) 92:26–33. doi: 10.1212/WNL.0000000000006583
46. Liu S, Kullnat J, Bourdette D, Simon J, Kraemer DF, Murchison C, et al. Prevalence of brain magnetic resonance imaging meeting Barkhof and

McDonald criteria for dissemination in space among headache patients. *Mult Scler.* (2013) 19:1101–5. doi: 10.1177/1352458512471874
47. Arrambide G, Tintore M, Espejo C, Auger C, Castillo M, Rio J, et al. The value of oligoclonal bands in the multiple sclerosis diagnostic criteria. *Brain.* (2018) 141:1075–84. doi: 10.1093/brain/awy006
48. Tintore M, Otero-Romero S, Rio J, Arrambide G, Pujal B, Tur C, et al. Contribution of the symptomatic lesion in establishing MS diagnosis and prognosis. *Neurology.* (2016) 87:1368–74. doi: 10.1212/WNL.0000000000003144
49. Geurts JJ, Stys PK, Minagar A, Amor S, Zivadinov R. Gray matter pathology in (chronic) MS: modern views on an early observation. *J Neurol Sci.* (2009) 282:12–20. doi: 10.1016/j.jns.2009.01.018
50. Peterson JW, Bo L, Mork S, Chang A, Trapp BD. Transected neurites, apoptotic neurons, and reduced inflammation in cortical multiple sclerosis lesions. *Ann Neurol.* (2001) 50:389–400. doi: 10.1002/ana.1123
51. Beesley R, Anderson V, Harding KE, Joseph F, Tomassini V, Pickersgill TP, et al. Impact of the 2017 revisions to McDonald criteria on the diagnosis of multiple sclerosis. *Mult Scler.* (2018) 24:1786–7. doi: 10.1177/1352458518778007
52. Gaetani L, Prosperini L, Mancini A, Eusebi P, Cerri MC, Pozzilli C, et al. 2017 revisions of McDonald criteria shorten the time to diagnosis of multiple sclerosis in clinically isolated syndromes. *J Neurol.* (2018) 265:2684–7. doi: 10.1007/s00415-018-9048-8
53. Habek M, Pavicic T, Ruska B, Pavlovic I, Gabelic T, Barun B, et al. Establishing the diagnosis of multiple sclerosis in Croatian patients with clinically isolated syndrome: 2010 versus 2017 McDonald criteria. *Mult Scler Relat Disord.* (2018) 25:99–103. doi: 10.1016/j.msard.2018.07.035
54. Hyun JW, Kim W, Huh SY, Park MS, Ahn SW, Cho JY, et al. Application of the 2017 McDonald diagnostic criteria for multiple sclerosis in Korean patients with clinically isolated syndrome. *Mult Scler.* (2018) 1352458518790702. doi: 10.1177/1352458518790702. [Epub ahead of print].
55. Lee DH, Peschke M, Utz KS, Linker RA. Diagnostic value of the 2017 McDonald criteria in patients with a first demyelinating event suggestive of relapsing-remitting multiple sclerosis. *Eur J Neurol.* (2018) 26:540–5. doi: 10.1111/ene.13853
56. Schwenkenbecher P, Wurster U, Suhs KW, Stangel M, Skripuletz T. Applying the 2017 McDonald diagnostic criteria for multiple sclerosis. *Lancet Neurol.* (2018) 17:498. doi: 10.1016/S1474-4422(18)30160-1
57. McNicholas N, Lockhart A, Yap SM, O'Connell K, Tubridy N, Hutchinson M, et al. New versus old: implications of evolving diagnostic criteria for relapsing-remitting multiple sclerosis. *Mult Scler.* (2018) 1352458518770088. doi: 10.1177/1352458518770088. [Epub ahead of print].
58. Gobbin F, Zanoni M, Marangi A, Orlandi R, Crestani L, Benedetti MD, et al. 2017 McDonald criteria for multiple sclerosis: earlier diagnosis with reduced specificity? *Mult Scler Relat Disord.* (2019) 29:23–5. doi: 10.1016/j.msard.2019.01.008
59. Maggi P, Absinta M, Grammatico M, Vuolo L, Emmi G, Carlucci G, et al. Central vein sign differentiates Multiple Sclerosis from central nervous system inflammatory vasculopathies. *Ann Neurol.* (2018) 83:283–94. doi: 10.1002/ana.25146
60. Davies G, Keir G, Thompson EJ, Giovannoni G. The clinical significance of an intrathecal monoclonal immunoglobulin band: a follow-up study. *Neurology.* (2003) 60:1163–6. doi: 10.1212/01.WNL.0000055864.08740.CB
61. Zeman AZ, Kidd D, McLean BN, Kelly MA, Francis DA, Miller DH, et al. A study of oligoclonal band negative multiple sclerosis. *J Neurol Neurosurg Psychiatry.* (1996) 60:27–30. doi: 10.1136/jnnp.60.1.27

Conflict of Interest Statement: The authors declare that the research was conducted in the absence of any commercial or financial relationships that could be construed as a potential conflict of interest.

Copyright © 2019 Schwenkenbecher, Wurster, Konen, Gingele, Sühs, Wattjes, Stangel and Skripuletz. This is an open-access article distributed under the terms of the Creative Commons Attribution License (CC BY). The use, distribution or reproduction in other forums is permitted, provided the original author(s) and the copyright owner(s) are credited and that the original publication in this journal is cited, in accordance with accepted academic practice. No use, distribution or reproduction is permitted which does not comply with these terms.

frontiers in Neurology

ORIGINAL RESEARCH
published: 26 March 2019
doi: 10.3389/fneur.2019.00241

The Shaking Palsy of the Larynx—Potential Biomarker for Multiple System Atrophy: A Pilot Study and Literature Review

*Tobias Warnecke[1†], Annemarie Vogel[2†], Sigrid Ahring[1], Doreen Gruber[2,3], Hans-Jochen Heinze[3], Rainer Dziewas[1], Georg Ebersbach[2] and Florin Gandor[2,3]**

[1] Department of Neurology, University of Münster, Münster, Germany, [2] Hospital for Movement Disorders/Parkinson's Disease, Beelitz-Heilstätten, Germany, [3] Department of Neurology, Otto-von-Guericke University, Magdeburg, Germany

OPEN ACCESS

Edited by:
Rou-Shayn Chen,
Chang Gung Memorial Hospital,
Taiwan

Reviewed by:
Emilia Mabel Gatto,
Sanatorio de la Trinidad Mitre,
Argentina
Roland Dominic Jamora,
University of the Philippines Manila,
Philippines

***Correspondence:**
Florin Gandor
gandor@kliniken-beelitz.de

[†]These authors have contributed equally to this work

Specialty section:
This article was submitted to Movement Disorders, a section of the journal Frontiers in Neurology

Received: 26 November 2018
Accepted: 25 February 2019
Published: 26 March 2019

Citation:
Warnecke T, Vogel A, Ahring S, Gruber D, Heinze H-J, Dziewas R, Ebersbach G and Gandor F (2019) The Shaking Palsy of the Larynx—Potential Biomarker for Multiple System Atrophy: A Pilot Study and Literature Review. Front. Neurol. 10:241. doi: 10.3389/fneur.2019.00241

In its early stages multiple system atrophy (MSA), a neurodegenerative movement disorder, can be difficult to differentiate from idiopathic Parkinson's disease (PD), and emphasis has been put on identifying premotor symptoms to allow for its early identification. The occurrence of vegetative symptoms in addition to motor impairment, such as orthostatic hypotension and neurogenic bladder dysfunction, enable the clinical diagnosis in the advanced stages of the disease. Usually with further disease progression, laryngeal abnormalities become clinically evident and can manifest in laryngeal stridor due to impaired vocal fold motion, such as vocal fold abduction restriction, mostly referred to as vocal fold paresis, or paradoxical vocal fold adduction during inspiration. While the pathogenesis of laryngeal stridor is discussed controversially, its occurrence is clearly associated with reduced life expectancy. Before the clinical manifestation of laryngeal dysfunction however, abnormal vocal fold motion can already be seen in patients that might not yet fulfill the diagnostic criteria of MSA. In this article we summarize the current literature on pharyngolaryngeal findings in MSA and report preliminary findings from a pilot study investigating eight consecutive MSA patients. Patients showed varying speech abnormalities. Only 2/8 patients exhibited laryngeal stridor. However, during FEES, all patients presented with irregular arytenoid cartilages movements and vocal fold abduction restriction. 3/8 showed vocal fold fixation and 1/8 paradoxical vocal fold motion. All patients presented with oropharyngeal dysphagia, 5/8 with penetration or aspiration events. We suggest that specific abnormal vocal fold motion can help identifying MSA patients and may allow for delimiting this disorder from idiopathic PD. These findings therefore may serve as a novel clinical biomarker for MSA. Based on the available data and our preliminary clinical experience we developed a standardized easy-to-implement task-protocol to be performed during

flexible endoscopic evaluation of swallowing (FEES) for detection of MSA-related pharyngolaryngeal movement disorders. Furthermore, we initiated a prospective study to evaluate the diagnostic utility of this protocol.

Keywords: multiple system atrophy, laryngeal dysfunction, pharyngeal dysfunction, irregular arytenoid cartilage movements, FEES, dysphagia, tremulous arytenoid movements, biomarker

INTRODUCTION

Multiple system atrophy (MSA) is a sporadic progressive neurodegenerative disorder characterized by Parkinsonian and cerebellar symptoms of varying severity and autonomic dysfunction. Similar to Parkinson's disease (PD), its age of onset is in the 6th decade with both sexes equally affected (1, 2). In contrast, MSA is a rapidly progressing disease, and mean survival after diagnosis is 6–10 years (3, 4). Depending on the leading presentation of the motor impairment, the disease is divided into a Parkinsonian (MSA-P) and a cerebellar sub-type (MSA-C). In a ratio of 2:1 to 4:1, MSA-P is more prevalent in the Americas, Europe and Korea (5–7). In Japan however, MSA-C is the more common (2). Currently, only symptomatic pharmacological and non-pharmacological treatments are available (1, 8).

Despite its faster progression, MSA in its early stages can be misinterpreted as PD or late-onset cerebellar ataxia and therefore poses a major diagnostic challenge (1). It is usually not until the advanced stages of the disease that autonomic failure and urogenital dysfunction become apparent (9, 10), which then, in addition to poor levodopa response, allow for the diagnosis of probable or possible MSA according to the current diagnostic criteria (11). Due to the diagnostic challenges in the early phase of the disease, emphasis has been put on identifying premotor symptoms to improve diagnostic accuracy on one hand and delineate MSA from PD or other lookalikes on the other (6, 12, 13). The European MSA study group (EMSA-SG) developed a red flag check list and analyzed the prevalence of 22 clinical features in 74 MSA and 116 PD patients (14). Of these 22, 13 showed a specifity of >95% for MSA and where grouped into six categories: early instability, rapid progression, abnormal postures (including Pisa syndrome, disproportionate antecollis and/or contractures of hand or feet), respiratory dysfunction (including diurnal or nocturnal inspiratory stridor and/or inspiratory sighs) and emotional incontinence. With two or more of six red flag categories present specificity was 98.3% and sensitivity was 84.2% in that cohort. When applying these criteria to patients with possible MSA-P, 76.5% of them would have been correctly diagnosed as probable MSA-P 15.9 ± 7.0 months earlier than with the consensus criteria alone (14). Interestingly, with 5 of these 13, nearly half of the red flag symptoms affected laryngopharyngeal functions including bulbar abnormalities such as severe dysphonia, dysarthria or dysphagia, and respiratory dysfunction including diurnal or nocturnal inspiratory stridor. This underlines the importance of assessing the laryngopharynx when suspecting MSA (15). It becomes even more significant when the clinical presentation does not yet allow for the diagnosis of MSA according to the consensus criteria. Examination of the laryngopharynx may reveal subclinical abnormalities associated with MSA and thereby allow for an earlier diagnosis. Williams stated already in 1979 that MSA patients "…should be examined routinely for laryngeal dysfunction and the examination repeated if suggestive symptoms develop…." (15). To date however, there is no standardized examination protocol for easy to implement diagnostic procedures such as flexible endoscopic laryngoscopy and examination of the swallowing (FEES) to systematically assess laryngopharyngeal symptoms in patients with suspected MSA.

This article gives an overview of the current literature on laryngeal abnormalities in MSA (summary of publications in **Table 1**) and pharyngeal symptoms in MSA and their potential pathophysiological mechanisms. We present a pilot study in 8 MSA patients and highlight the laryngopharyngeal findings. Based on the current data and our preliminary findings we suggest a simple structured diagnostic task-protocol to be performed during FEES for detection of MSA-related laryngopharyngeal symptoms. We furthermore suggest that irregular arytenoid cartilage movements (ACM) are specific for MSA and can serve as a clinical biomarker for the disease that may allow for differentiation of MSA from PD.

LARYNGEAL FINDINGS IN MSA

Inspiratory Stridor

Typically in the advanced disease stages, inspiratory stridor becomes evident (16, 17) but may manifest at any stage of the disease (18–20), with few reports of stridor being the initial (21, 22) or even the sole symptom of MSA (23, 24). Inspiratory stridor is found in up to one third of MSA patients (17–19), is therefore considered a red flag (14) and consequently was included in the updated consensus diagnostic criteria as a supportive feature (11). It can manifest as a diurnal or nocturnal symptom (14), and its occurrence is associated with reduced life expectancy (25). Furthermore, inspiratory stridor might be a predictor for sudden nocturnal death (10, 26). However, the exact underlying mechanism of sudden nocturnal death in MSA remains unresolved and considered of multifactorial origin (27).

Paradoxical Vocal Fold Motion

Aragane (28) first described paradoxical vocal fold motion (PVFM) during respiration in MSA patients, with adduction during inspiration and abduction during expiration (**Figure 1**). Isono and colleagues presented tonic thyroarytenoid muscle (TA) activation during inspiration in MSA patients (29). The TA muscle ceases activity under physiological conditions since it serves as a vocal fold adductor. Umeno described one MSA patient with normal vocal fold motion and normal EMG activity

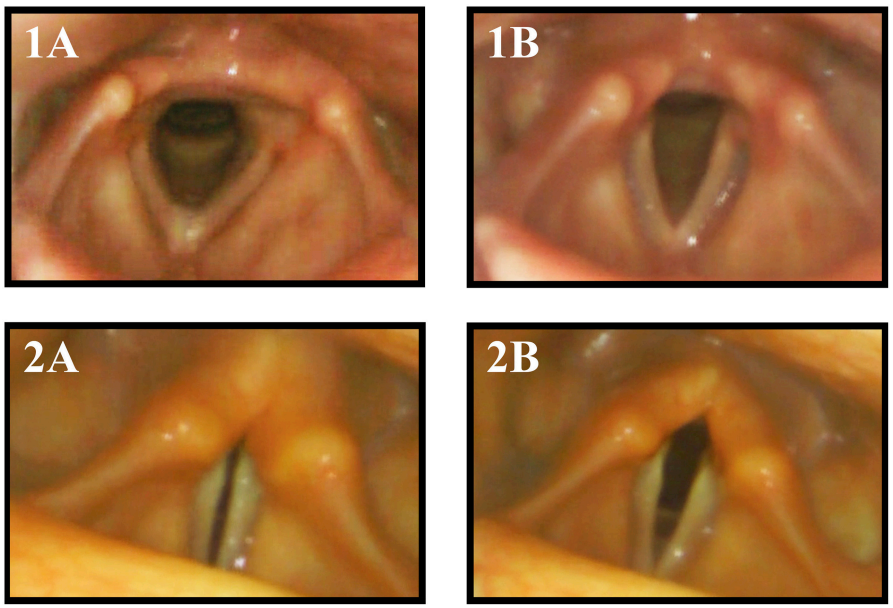


FIGURE 1 | Vocal fold motion during breathing with inspiration **(A)** and expiration **(B)** in a healthy control subject (1) and MSA patient (2). The MSA patient exhibited paradoxical vocal fold motion with inspiratory stridor.

of laryngeal muscles in the wake state but paradoxical vocal fold motion during sleep with inspiratory vocal fold adduction and abduction during expiration, resulting in nocturnal stridor (30). Shiba initiated several studies presenting activation of laryngeal adductor muscles during inspiration (31–33).

Vocal Fold Motion Impairment

A retrospective review of 38 MSA patients that underwent otolaryngologic examination revealed a bilateral vocal fold motion impairment (VFMI) in 32 patients and a unilateral VFMI in 6 patients (34). Higo and colleagues (35) performed laryngoscopy on 38 MSA patients to assess laryngeal function and found VFMI in 17 patients (**Figure 2**). Fourteen of these had moderate to severe bilateral vocal fold abductor restriction, two showed unilateral vocal fold fixation, one patient a bilateral vocal fold fixation in the paramedian position.

Irregular Arytenoid Cartilage Movement

Ward was the first to describe irregular and involuntary adduction/abduction movements of the vocal folds in two MSA patients that underwent laryngoscopy and described "…quivering tonicity, pseudomyoclonic motions of the aryepiglottic folds with irregular involuntary adduction or abduction of the cords…" and "… fine quivering, tremorous motions of both arytenoids and aryepiglottic folds.…" (36). Simpson and colleagues described "…flickering movements of the vocal folds…" in 3 of 6 MSA patients during laryngoscopy (37). Shimohata and colleagues observed bilateral tremulous movements of the arytenoid cartilages in 6 of 21 MSA patients during fiberoptic laryngoscopy at rest (27). Ozawa and colleagues performed fiberendoscopic laryngoscopy on 28 MSA patients and 14 healthy controls. In 18 (64.3%) MSA patients irregular tremulous movement of the arytenoid cartilages was detected, none in the healthy control group (38).

Pathophysiological Insights Into Laryngeal Findings in MSA

Initial reports supported the hypothesis that inspiratory stridor is the clinical manifestation of vocal fold abductor paralysis (15, 39–45) in addition to the Bernoulli effect, when a sudden drop of air pressure narrows the glottic gap resulting in the characteristic acoustic phenomenon (31), similar to infantile laryngomalacia (46).

Early laryngeal EMG studies using surface electrodes supported the findings of primary denervation of the laryngeal abductor muscle. Williams observed a bilateral abduction paralysis in 8 of 12 MSA patients (15). Banister described marked atrophy of the posterior cricoarytenoid muscle (PCA) on histology in three MSA patients with significant inspiratory stridor requiring tracheostomy (43). Surface EMG recording of laryngeal muscles in five MSA patients revealed evidence for denervation of the PCA (42). Furthermore, Deguchi described two patients with reduced laryngeal abduction and attributed the finding to potential peripheral palsy of the laryngeal nerve (44). These findings were supported by one autopsy study that found loss of large myelinated fibers of the laryngeal nerve in MSA patients with abductor palsy (45). The only other autopsy study focusing on the recurrent laryngeal nerve did however not find gross abnormalities or focal changes of the recurrent laryngeal nerve (43). But why is there, next to the selective weakness of the laryngeal abductor muscle, an overactivation of adductor muscles as seen in PVFM?

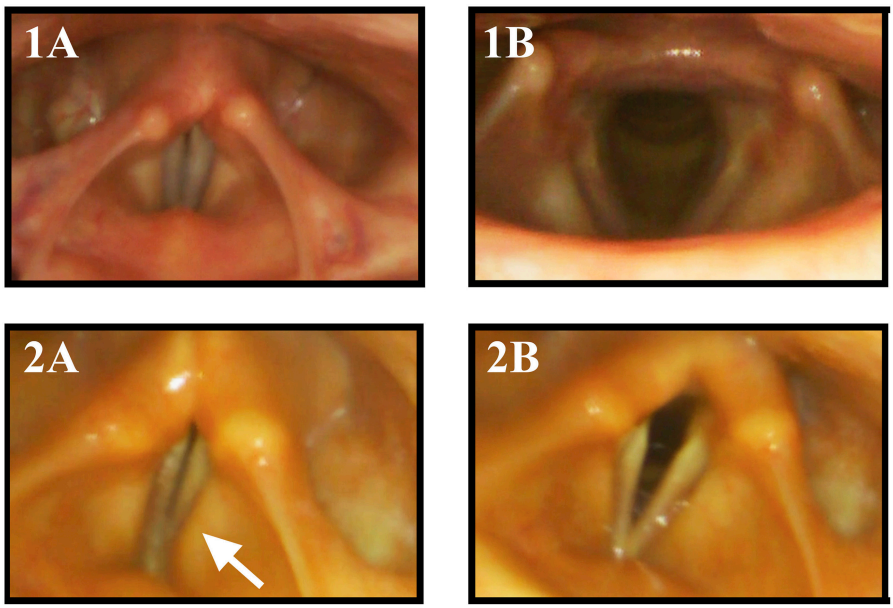


FIGURE 2 | Vocal fold motion during laryngeal tasks in a healthy control subject and a MSA patient: 1 healthy control, 2 MSA patient, **(1A)** phonation "eeee," **(1B)** sniff. The MSA patient exhibits VFMI with insufficient vocal fold adduction and activation of the vestibular folds (arrow) during phonation **(2A)** and incomplete VF abduction during sniffing maneuver **(2B)**.

An airway reflex was recently discovered that activates the adductor muscles during inspiration when inspiratory effort against a narrowed glottic gap increases (33, 47). This was shown in a study on five non-MSA-patients, four of which suffered from traumatic glottic narrowing, one from a laryngeal nerve palsy post thyroidectomy. All patients exhibited inspiratory stridor, and tonic activation of the adductor muscles was recorded during inspiration. Two patients therefore received a tracheostomy. Interestingly, when breathing through the open tracheostoma, the tonic activity of the adductor muscles during inspiration ceased but reoccurred when the tracheostoma was closed and air flow had to pass through the narrow glottic gap again (33). Similar findings were shown in one MSA patient (32). Hence, bypassing the glottic gap via tracheostomy abolishes the paradoxical activation of laryngeal adductor muscles during inspiration. In addition, several authors showed that in MSA patients exhibiting inspiratory nocturnal stridor, CPAP could abolish the tonic laryngeal adductor activation (29, 48–50). This effect might be explained by reducing the intratracheal negative pressure, thereby reducing the transglottic pressure gradient through the glottic stenosis during inspiration and the likelihood of the airway reflex to be triggered (31).

The theory of a pure peripheral nerve palsy resulting in reduced vocal fold motion is opposed by findings of simultaneous co-activation of laryngeal abductor and adductor muscles during inspiration (51, 52). The posterior cricoarytenoid (PCA) muscle, the only laryngeal abductor, is by far outnumbered by the laryngeal adductors. This dysbalance and the lack of the physiological agonistic/antagonistic play contributes to the restriction of vocal fold motion in MSA (29, 39). It is likely that co-activation of laryngeal abductor and adductor muscles results in a vocal fold abduction restriction and reduced vocal fold motion on one hand and irregular arytenoid cartilages movements (ACM) on the other.

Treatment Options for Laryngeal Findings in MSA

CPAP

Several studies could show the efficacy of CPAP in abolishing laryngeal stridor in MSA patients (29, 49, 50, 53). Since CPAP is a non-invasive treatment, it should be first choice when approaching laryngeal inspiratory stridor in MSA patients. Iranzo found inspiratory pressure levels of 5–10 mbar to suffice. However, he also mentioned that only few MSA patients profit from CPAP ventilation longer than 20 weeks (49). When CPAP fails to reduce laryngeal inspiratory stridor, biPAP should be considered (48).

Botulinum Toxin Injection

A minimal-invasive option to treat laryngeal inspiratory stridor in MSA is botulinum toxin injection into the adductor muscle complex (TA/LCA complex). Merlo showed improvement of laryngeal stridor and of vocal fold abduction in 3 of 4 MSA patients (52). Botulinum toxin injection should however be restricted to patients without dysphagia.

Tracheostomy

When non-invasive measures to treat laryngeal inspiratory stridor are not able to abolish the symptom, tracheostomy

should be considered (15, 25). Tracheostomy is furthermore recommended when, in addition to stridor, vocal fold motion is significantly restricted and the vocal folds fixed in a paramedian position (49). In contrast, tracheostomy could potentiate dysphagia, with aspiration necessitating the use of a cuffed cannula, resulting in cessation of speech. The additional requirement of PEG-tube feeding might significantly lower the quality of life in MSA patients (31).

Surgery

With vocal fold laterofixation, arytenoidectomy, and partial cordectomy, three surgical options to enlarge the glottic gap are at hand. Kenyon and Umeno reported MSA patients whose nocturnal stridor improved after laterofixation of the vocal fold (30, 54). The authors emphasized however that this method should be evaluated carefully because of the significantly increased risk of aspiration due to potential worsening of the swallowing function. In addition, the intervention itself poses risks with unexpected postoperative respiratory failure, such as laryngeal edema after cordectomy and slipping of ligature after laterofixation of the vocal fold (31). This intervention is usually performed in patients with denervation palsy of the vocal fold. In MSA patients however, it must be taken into account that the adductor muscles are still activated and exhibit force on the suture providing the laterofixation (31). Some MSA patients underwent arytenoidectomy with conflicting outcomes (30, 55).

Laryngeal Findings in Related Movement Disorders

Parkinson's Disease

Vocal fold bowing is a typical cinelaryngoscopy finding in 80–93% of PD patients, which can also be identified with stroboscopic laryngoscopy (56–58). Furthermore, vocal tremor can be clinically present in about 50% of PD patients and is caused by vertical laryngeal tremor during phonatory tasks (56, 57). One case study presenting rare laryngeal findings report seven patients identified over 14 years with non-paralytic vocal fold abductor paralysis exhibiting PVFM with diurnal and nocturnal inspiratory stridor (59).

Spinocerebellar Ataxia

Spinocerebellar ataxia (SCA) can present with cerebellar, pyramidal, extrapyramidal and autonomic symptoms similar MSA. One study compared laryngeal findings in MSA, SCA1, and SCA3 patients and found vocal fold paralysis to be less prevalent in SCA1 and SCA3 in comparison to MSA (in 29% in SCA1 and 16% in SCA3 in contrast to 82% in MSA) (39). Furthermore, SCA patients did not present with sleep-related exacerbation of VFMI, and neurogenic atrophy occurred in all intrinsic laryngeal muscles, not solely the laryngeal abductor. In addition, none of the patients exhibited irregular ACM.

PHARYNGEAL FINDINGS IN MSA

Dysphagia in MSA

Although dysphagia is a common symptom of MSA and seems to be closely related to the disease prognosis (60), only a limited number of studies have investigated the specific characteristics of dysphagia in MSA patients in detail. It should be taken into account that most of these studies were performed in Japan, a noteworthy fact when considering the higher prevalence of MSA-C in comparison to MSA-P (2). Similar to laryngeal abnormalities, swallowing is often impaired early in the disease (61, 62). There are varying reports about time of onset of dysphagia during the course of MSA. Isono and colleagues reported dysphagia in MSA-C patients to begin 4.6 $\pm$ 3.5 years after disease onset (61). Petrovic in contrast described a much later onset of dysphagia in MSA-P patients at 9.0 $\pm$ 3.7 years (63). A recent study in 59 Korean MSA patients showed a much earlier dysphagia onset in both MSA sub-types (MSA-P: 2.94 $\pm$ 1.43 years, MSA-C: 3.05 $\pm$1.24 years) (64).

Since the act of swallowing consists of four phases (65), one might raise the question whether a certain phase is typically impaired in MSA. Taniguchi investigated 13 MSA-C and 3 MSA-P patients. All patients showed an impaired esophageal phase presenting with intraesophageal food stagnation, which potentially entails aspiration leading to pneumonia or even bolus regurgitation with bolus aspiration (66). Higo performed videofluoroscopy on 22 MSA-C and 7 MSA-P patients assessing the swallowing performance (67). The evaluation revealed a disturbed oral phase with delayed bolus transport in 73%, reduced tongue base movement in 55% and impaired oral bolus control in 49% of patients. Abnormalities in the pharyngeal phase however were detected in only 20% of the patients. 25% of these patients had a history of aspiration pneumonia. Interestingly, disease severity rather than age or disease duration were identified as risk factors for aspiration pneumonia (67). These results are in line with the findings by Isono who showed that pharyngeal dysphagia severity did not correlate with disease duration (61). An analysis of videofluoroscopic examinations in 59 MSA patients showed pharyngeal symptoms to be more often disturbed than oral symptoms. 89.8% of the patients presented with vallecular residue. Penetration or aspiration occurred in 67.8%, delayed pharyngeal swallow was observed in 57.6%. In addition, pharyngeal apraxia and vallecular residue were observed more frequently in the MSA-P sub-type and were more severe in comparison to MSA-C patients. Frequency of oral phase symptoms did not differ between MSA sub-types, with inadequate mastication in 32% and premature spillage in 23.7%.

Treatment of Dysphagia in MSA

To date there are no treatment guidelines for MSA-related dysphagia. Furthermore, there are very few clinical studies addressing treatment strategies of dysphagia in MSA.

Firstly, levodopa response of dysphagia should be evaluated, despite the fact that levodopa responsiveness on motor symptoms is usually considered poor in MSA. However, up to 31.2% of MSA

TABLE 1 | Overview and frequency of typical laryngeal findings in MSA.

Symptom	Frequency n/total (%)	References
Stridor	34/100 (34%) MSA-P: 30/82 (37%) MSA-C: 4/18 (22%)	(18)
	36/104 (34.6%)	(17)
PVFM	1/1 (100%)	(30)
	9/10 (90%)	(29)
	1/1 (100%)	(32)
VFMI	38/38 (100%) Bilateral: 32/38 (84,2%) Unilateral: 6/38 (15.8%)	(34)
	17/36 (47.2%)	(35)
Irregular ACM	3/6 (50%)	(37)
	6/21 (28.6%)	(27)
	18/28 (64.3%)	(38)

PVFM, paradoxical vocal fold motion; VFMI, vocal fold motion impairment; ACM, arytenoid cartilage movement.

patients show a beneficial levodopa response of symptoms for a mean duration of 3.5 years (3) and might even exhibit motor fluctuations (68–70). Since adjusting dopaminergic therapy is the least invasive treatment option, a structured FEES-levodopa test should be performed to evaluate swallowing in the ON- and OFF-state (71, 72). When levodopa responsiveness has been ruled out, treatment of mild or moderate dysphagia should encompass postural maneuvers to facilitate swallowing, such as the chin tuck maneuver (71). Moreover, behavioral changes with slowing of eating, reduction of meal volumes or changing food consistencies should be considered (73). When intraesophageal bolus transport is disturbed and overactivation of the distal esophagus sphincter suspected, botulinum toxin injection into the distal esophagus has proven to alleviate dysphagia severity in PD patients (74). With the results of Taniguchi who reported intraesophageal food stagnation (66), botulinum toxin injection could be considered. When severe dysphagia with repetitive aspiration and aspiration pneumonia is present, avoidance of the oral route with a PEG-tube should be discussed with the patient to guarantee adequate nutrition and hydration (75).

PILOT STUDY

Standardized Task Protocol for Pharyngolaryngeal Abnormalities in MSA

To date, no structured protocol has been suggested to evaluate MSA specific findings in the laryngopharynx (35). Especially in diseases that pose diagnostic challenges, structured examination procedures are necessary (71). We developed a simple FEES-MSA-protocol that allows for assessing laryngeal functions and oropharyngeal performance (**Table 2**).

Methods

This study was approved by the local Ethics Committee of the Brandenburg Medical Board (S21(a)/2017) and is conducted in accordance with the Declaration of Helsinki (76). After written informed consent was obtained, eight consecutive patients with possible or probable MSA according to the Gilman criteria (11) underwent examination. Speech characteristics were assessed by auditive analysis. All patients underwent flexible endoscopic evaluation of the swallowing (FEES). FEES equipment consisted of a 3.9-mm-diameter flexible fiberoptic rhinolaryngoscope (Olympus ENF-VH), a video processor (Olympus CV-170), and processing software (rpSzene 10 on Panel-PC-226/227) or a 2.9 mm-diameter flexible fiberoptic rhinolaryngoscope (Storz CMOS) with a portable video processor (Storz CMAC) linked to a 19″ flat screen monitor (Storz 9519NB). FEES was performed as previously described (72).

Specific FEES-MSA-Protocol

To assess MSA specific impairment of the laryngopharynx, patients underwent the FEES-MSA-protocol allowing for a standardized endoscopic evaluation of the pharyngolaryngeal and swallowing function. The protocol is divided into an examination of the laryngeal function at rest and in action, followed by an evaluation of the swallowing.

Evaluation of the Larynx at Rest

After insertion of the rhinolaryngoscope, the tip of the endoscope is placed into the mid pharyngeal cavity to allow for full inspection of laryngeal structures. Firstly, the larynx is examined at rest during normal breathing for at least 2 min. Mobility of the vocal folds and arytenoid cartilages in relation to the breathing cycle is recorded. Notion is taken of any uni- or bilateral abnormal desynchronized movement. Vocal fold motion impairment (VFMI) is noted either in the inspiratory, expiratory or both phases. The position of the vocal folds and degree of maximum opening (median, paramedian, intermediate, prelateral, lateral position) is recorded. Paradoxical vocal fold motion (PVFM) with e.g., vocal fold adduction during inspiration, and irregular ACM at any time of the examination are recorded. Vocal fold fixation and its configuration is captured.

Evaluation of the Larynx in Action

To examine the degree of glottic opening, the patient is asked to repeatedly 1) inhale deeply and 2) sniff thereby performing vocal fold abduction tasks. To evaluate glottic closure, the patient is asked to phonate a prolonged "eee", thereby performing a vocal fold adduction task. To examine the maximum amplitude of the vocal fold motion, the patient is then asked to perform these two tasks alternately. Furthermore, these tasks can initiate or aggravate irregular ACM.

Next, the patient is asked to perform a postural action of the vocal folds by imagining vocalizing an "eeee". In our experience this postural task can initiate or aggravate irregular ACM.

Evaluation of the Swallowing

The third part comprises a supplemented standardized FEES protocol performing one dry swallow, 11 consecutive

TABLE 2 | Tasks of the FEES-MSA-protocol, assessed functions, and possible findings.

	Task	Physiological function	Possible findings
Laryngeal tasks	Normal breathing	Inspiration: mild VF abduction Expiration: VF relaxation with Mild VF adduction	VFMI Uni- or bilaterally reduced VF movement during inspiration and/or expiration with maximal amplitude to median, paramedian or intermediate position VF fixation Uni- or bilateral lack of respiration-linked VF motion with fixed position in median, paramedian, intermediate, prelateral or lateral PVFM Inspiratory VF adduction with glottic narrowing Irregular ACM Uni- or bilateral irregular movements of the arytenoid cartilages
	Fast and deep inhale	VF abduction	VFMI PVFM Irregular ACM pre and post maneuver
	Sniff through nose	VF abduction	VFMI PVFM Irregular ACM pre and post maneuver
	Phonation of "eee"	VF adduction	VFMI irregular ACM pre and post maneuver
	Imagined non-voiced "eee" ("Prepair youself or imagine to say "eee" without really saying it.")	VF adduction	Irregular ACM pre, during and post maneuver
	sniff - "eee"- sniff – "eee"	VF adduction/ abduction and VF diadochokinesis	VFMI PVFM Irregular ACM pre, during and post maneuver
Swallowing tasks	Dry swallow	Clearing of secretion	Pharyngeal residue Penetration/aspiration
	Oral bolus control ("Keep the water in your mouth until I say to swallow.")	Bolus control without spillage	Premature spillage
	Swallowing of (1) Pudding (2) Liquid (3) Solid consistencies (4) Placebo tablet	Swallowing function for different consistencies	Piecemeal deglutition Premature spillage Pharyngeal residue Penetration/aspiration
	Therapeutic maneuver e.g., Chin tuck maneuver ("Swallow the bolus keeping your neck upright and your chin down.")	Potential improvement of impaired swallowing	Improvement of/unchanged swallowing function

VFMI, vocal fold motion impairment; VF, vocal fold; PVFM, paradoxical vocal fold motion; ACM arytenoid cartilage movement.

standardized test boli and a minimum of one swallow performing an individual therapeutic maneuver. Consistencies are applied in the following order: (1) three teaspoonful of green jelly (appr. 8 mls each), (2) one teaspoonful of blue-dyed liquid (appr. 5 mls) to test for oral bolus control, (3) three teaspoonful of blue-dyed liquid, (4) one sip of blue-dyed liquid from a glass, (5) three pieces of bread with butter (about 1 inch square), (6) one swallow of a placebo tablet ingested with either blue-dyed liquid or green jelly. Depending on the individual findings, a specific therapeutic swallow maneuver is performed at the end.

Swallowing function was evaluated as previously described (**Table 3**) (71) with the addition of documentation of fragmented swallows, i.e., piecemeal deglutition (more than one swallow needed to clear bolus from the oral cavity). To score dysphagia severity we applied the endoscopic severity of dysphagia scale, utilized in Parkinson's disease (**Table 4**) (72).

Results

Four female and 4 male MSA patients underwent the FEES-MSA-protocol. Duration of performing the FEES-MSA-protocol varied from 15-20 min.

Seven patients suffered from MSA-P, one patient from MSA-C. Mean age was 59.9 ± 6.9 years, mean disease duration 3.0 ± 1.2 years, mean Hoehn and Yahr stage 3.75 ± 1.04 (**Table 5**). Patients exhibited a broad variety of speech pathology. Four (50%) patients showed fluctuating pitch when phonating, only one patient presented with high-pitched voice. 5/8 patients showed hypokinetic-rigid dysarthria of varying severity. The patient presenting with MSA-C showed an ataxic type of dysarthria. One patient exhibited a mixed type of dysarthria (**Table 5**). Only two (25%) patients exhibited diurnal inspiratory laryngeal stridor as a clinical sign of laryngeal pathology.

TABLE 3 | Scores of swallowing function parameters (71).

Score	Premature spillage	Pharyngeal residue	Penetration/aspiration
0	Bolus behind tongue	No residue	No penetration/aspiration event
1	Bolus at the base of tongue or valleculae	Coating, no pooling	Penetration with protective reflex
2	Bolus moves to lateral channels or tip of epiglottis	Mild pooling, fills less than half of the cavities	Penetration without protective reflex
3	Bolus is in the piriform sinus or touches laryngeal rim	Moderate pooling, fills the cavities	Aspiration with protective reflex
4	Bolus falls into laryngeal vestibule	Severe pooling, overflows the cavities	Aspiration without protective reflex

TABLE 4 | Endoscopic severity of dysphagia scale (72).

Score	Classification of dysphagia severity
0	No relevant dysphagia
1	Mild dysphagia (premature spillage and/or residues, but no penetration/aspiration events)
2	Moderate dysphagia (penetration/aspiration events with one consistency)
3	Severe dysphagia (penetration/aspiration events with two or more consistencies)

However, during flexible endoscopic evaluation of the laryngeal and swallowing function, all patients showed irregular ACM. In 6 (75%) patients, irregular ACM was present at rest (**Supplementary Video 1**). The remaining 2 (25%) showed irregular ACM during provoking maneuvers (sniff, deep inhale, phonation "eee" and imagined non-voiced "eee") (**Supplementary Video 2**). In 2 (25%) patients with irregular ACM at rest, the movements were enhanced during provoking maneuvers (**Supplementary Video 2**). Furthermore, all patients exhibited vocal fold abduction restriction (**Figure 2**). Three (37.5%) patients showed a vocal fold fixation in the paramedian position and one patient presented paradoxical vocal fold motion (**Figure 1**).

When evaluating the swallowing, 5 (62.5%) patients presented with piecemeal deglutition for all consistencies. Seven (87.5%) patients showed premature spillage with 6 events for pudding, 5 for liquids and 2 for solids. All patients showed pharyngeal phase dysfunction. Six patients showed pharyngeal residues in the valleculae with four events for solids, 3 for pudding and 1 for liquids. Five (62.5%) patients showed penetration/aspiration events. The first of these patients presented with penetration/aspiration score 1 for pudding and score 3 for liquids, the second showed score 1 for pudding and liquids, the third showed score 1 for all consistencies, the fourth presented with score 3 for liquids and the fifth showed score 2 for liquids. Characteristics of laryngeal findings and swallowing function did not differ between the MSA subtypes (**Table 6**).

DISCUSSION

The structured FEES-MSA-protocol was well tolerated by all patients. With a duration of about 20 min, the examination was easy to implement into the diagnostic routine.

Patients presented with MSA typical speech characteristics of varying severity (77). However, in our cohort, all MSA patients exhibited laryngeal and pharyngeal abnormalities on flexible endoscopic evaluation, regardless of the severity of clinical speech pathology. More so, the severity of clinical speech impairment did not correlate with the laryngeal abnormalities detected while performing the FEES-MSA-protocol. Irregular ACM at rest were present in 75% of patients. These findings are in line with previous results from laryngoscopy studies that found irregular ACM in 50–100% of cases (27, 36–38). Irregular involuntary movements have been described in MSA patients to occur predominantly in hands and fingers. Some authors stated that these involuntary jerky movements are underrecognized in MSA patients (78–80). Similar to these irregular jerky and tremulous movements of the limbs, these movements might not be present at rest but can be observed during postural action. Salazar investigated 11 patients with MSA. Only one patient showed Parkinsonian pill-rolling tremor of the hand at rest. However, during postural maneuvers, irregular jerky movements of the hands were present in 9 (82%) patients (80). With this clinical observation in mind we designed a "postural" task for the larynx and could show that in those two patients without irregular ACM at rest, ACM could be provoked during this "postural" maneuver.

In addition, all patients showed vocal fold abduction restriction. Despite this laryngoscopic finding, only two patients demonstrated diurnal inspiratory stridor on clinical examination. This finding of vocal fold motion impairment resulting in a narrow glottic gap is in line with previous results reported by Lalich, who investigated 38 MSA patients and found 32 to present with a bilateral VFMI, the remaining 6 with a unilateral VFMI (34).

Since the prevalence of irregular ACM in our MSA cohort was 100% we do believe that ACM might serve as clinical biomarker for MSA, potentially allowing for differentiating MSA from other disorders. This finding is even more relevant when bearing the young mean age and short disease duration of our cohort in mind. Irregular ACM was found as early as 1 year after disease onset and was present in both MSA-P and MSA-C subtypes. In contrast to PVFM or inspiratory stridor (59), irregular ACM have not been described in other movement disorders. There are numerous publications on tremor affecting the larynx [for review see: (81–83)]. However, these tremor forms show rhythmic and regular movements of laryngeal structures as opposed to the findings we observed in this pilot study.

TABLE 5 | Patients' demographic data and speech characteristics.

	Patients' characteristics				Speech characteristics			
#	Age, sex	Disease duration in years	MSA sub-type	Hoehn-Yahr stage	Hypophonia	Pitch	Diurnal stridor	Dysarthria
1	51, f	4	MSA-P	4	+	Fluctuating	–	Severe Hypokinetic-rigid
2	61, f	4	MSA-P	2	+	Fluctuating	+	Normal
3	58, f	3	MSA-P	5	+	Normal	–	Severe Mixed
4	63, f	2	MSA-P	5	+	Fluctuating	–	Moderate Hypokinetic-rigid
5	54, m	4	MSA-P	4	+	Fluctuating	+	Moderate Hypokinetic-rigid
6	57, m	1	MSA-C	3	+	High	–	Severe Ataxic
7	74, m	2	MSA-P	4	+	Normal	–	Moderate hypokinetic-rigid
8	61, m	4	MSA-P	3	+	Normal	–	Severe Hypokinetic-rigid

TABLE 6 | Endoscopic pharyngolaryngeal findings performing the MSA-FEES-protocol in 8 MSA patients.

	Flexible endoscopic evaluation of the larynx						Flexible endoscopic evaluation of swallowing (FEES)		
#	VF abduction restriction	VF fixation	PVFM	Irregular ACM	Irregular ACM provoked	Premature spillage score	Pharyngeal residue score	Penetration/ aspiration score	Dysphagia severity score
1	+	–	+	+	–	3	0	0	1
2	+	–	–	–	+	3	2	1	2
3	+	–	–	+	–	4	2	3	2
4	+	–	–	+	–	3	0	3	2
5	+	+	–	–	+	0	0	0	1
6	+	+	–	+	–	4	0	1	2
7	+	–	–	+	+	2	2	2	3
8	+	+	–	+	+	2	2	0	1

VF, vocal fold; PVFM, paradoxical focal fold motion; ACM, arytenoid cartilage movements.

Dysphagia was present in all patients, regardless of disease duration or MSA sub-type. These findings are in line with previous results (61, 66, 67). Although not useful as a specific biomarker, dysphagia however remains a clinically relevant symptom associated with survival in MSA patients (60, 63). Since dysphagia is preclinically detectable by instrumental assessment tools (67), an early diagnosis is vital for preventing dysphagia-related complications.

We here present results from a pilot study. Despite the small sample size and lack of a control group, we propose an interesting hypothesis. We are currently conducting a trial in a larger cohort of MSA patients and compare findings to PD patients to further support the theory that irregular ACM might serve as a clinical biomarker allowing for differentiating MSA from PD.

CONCLUSION

Pharyngolaryngeal abnormalities have a high prevalence in MSA. Our findings suggest that characteristic pathologic findings can be revealed on flexible endoscopy before becoming evident clinically when implementing the FEES-MSA-protocol. Irregular arytenoid cartilages movement (ACM) at rest or with provoking maneuvers might serve as a diagnostic clinical biomarker and facilitate identification of MSA patients. Since FEES is now widely established in many Neurology departments we strongly suggest that all patients with suspected MSA should undergo this procedure to look for disease specific findings that support the diagnosis and enable adequate treatment as early as possible (84). Utilizing a structured FEES-MSA-protocol will help assessing relevant functions and identify MSA-specific abnormalities such as irregular ACM, PVFM, VFMI, premature

spillage, or pharyngeal residue. A prospective study is under way to evaluate the diagnostic utility of this protocol.

DATA AVAILABILITY

All datasets generated for this study are included in the manuscript and/or the **Supplementary Files**.

AUTHOR CONTRIBUTIONS

FG: ethics application. FG, AV, and TW: conception and design, acquisition, analysis, and interpretation of data, retrieving review data, manuscript writing, and editing. SA: acquisition, analysis and interpretation of data. DG: acquisition, analysis, and interpretation of data, editing manuscript. H-JH, RD, and GE: conception and design, review data, editing manuscript.

SUPPLEMENTARY MATERIAL

The Supplementary Material for this article can be found online at: https://www.frontiersin.org/articles/10.3389/fneur.2019.00241/full#supplementary-material

Supplementary Video 1 | Irregular arytenoid cartilages movements at rest in MSA patient.

Supplementary Video 2 | Irregular arytenoid cartilages movements during postural maneuver in MSA patient.

REFERENCES

1. Fanciulli A, Wenning GK. Multiple-system atrophy. *N Engl J Med*. (2015) 372:249–63. doi: 10.1056/NEJMra1311488
2. Watanabe H, Saito Y, Terao S, Ando T, Kachi T, Mukai E, et al. Progression and prognosis in multiple system atrophy. *Brain*. (2002) 125:1070–83. doi: 10.1093/brain/awf117
3. Wenning GK, Geser F, Krismer F, Seppi K, Duerr S, Boesch S, et al. The natural history of multiple system atrophy: a prospective European cohort study. *Lancet Neurol*. (2013) 12:264–74. doi: 10.1016/S1474-4422(12)70327-7
4. Ben-Shlomo Y, Wenning GK, Tison F, Quinn NP. Survival of patients with pathologically proven multiple system atrophy: a meta-analysis. *Neurology*. (1997) 48:384–93.
5. Kim H-J, Jeon BS, Lee J-Y, Yun JY. Survival of Korean patients with multiple system atrophy. *Mov Disord*. (2011) 26:909–12. doi: 10.1002/mds.23580
6. Köllensperger M, Geser F, Ndayisaba J-P, Boesch S, Seppi K, Ostergaard K, et al. Presentation, diagnosis, and management of multiple system atrophy in Europe: final analysis of the European multiple system atrophy registry. *Mov Disord*. (2010) 25:2604–12. doi: 10.1002/mds.23192
7. Gilman S, May SJ, Shults CW, Tanner CM, Kukull W, Lee VM-Y, et al. The North American Multiple System Atrophy Study Group. *J Neural Transm*. (2005) 112:1687–94. doi: 10.1007/s00702-005-0381-6
8. Levin J, Kurz A, Arzberger T, Giese A, Höglinger GU. The differential diagnosis and treatment of atypical Parkinsonism. *Dtsch Arztebl Int*. (2016) 5:61–9. doi: 10.3238/arztebl.2016.0061
9. Coon EA, Sletten DM, Suarez MD, Mandrekar JN, Ahlskog JE, Bower JH, et al. Clinical features and autonomic testing predict survival in multiple system atrophy. *Brain*. (2015) 138:3623–31. doi: 10.1093/brain/awv303
10. Wenning GK, Tison F, Ben Shlomo Y, Daniel SE, Quinn NP. Multiple system atrophy: a review of 203 pathologically proven cases. *Mov Disord*. (1997) 12:133–47. doi: 10.1002/mds.870120203
11. Gilman S, Wenning GK, Low PA, Brooks DJ, Mathias CJ, Trojanowski JQ, et al. Second consensus statement on the diagnosis of multiple system atrophy. *Neurology*. (2008) 71:670–6. doi: 10.1212/01.wnl.0000324625.00404.15
12. Jecmenica-Lukic M, Poewe W, Tolosa E, Wenning GK. Premotor signs and symptoms of multiple system atrophy. *Lancet Neurol*. (2012) 11:361–8. doi: 10.1016/S1474-4422(12)70022-4
13. Walsh RR, Krismer F, Galpern WR, Wenning GK, Low PA, Halliday G, et al. Recommendations of the global multiple system atrophy research roadmap meeting. *Neurology*. (2018) 90:74–82. doi: 10.1212/WNL.0000000000004798
14. Köllensperger M, Geser F, Seppi K, Stampfer-Kountchev M, Sawires M, Scherfler C, et al. Red flags for multiple system atrophy. *Mov Disord*. (2008) 23:1093–9. doi: 10.1002/mds.21992
15. Williams A, Hanson D, Calne DB. Vocal cord paralysis in the Shy-Drager syndrome. *J Neurol Neurosurg Psychiatry*. (1979) 42:151–3. doi: 10.1111/j.1600-0404.1982.tb06873.x
16. Ozawa T, Sekiya K, Aizawa N, Terajima K, Nishizawa M. Laryngeal stridor in multiple system atrophy: Clinicopathological features and causal hypotheses. *J Neurol Sci*. (2016) 361:243–9. doi: 10.1016/j.jns.2016.01.007
17. Yamaguchi M, Arai K, Asahina M, Hattori T. Laryngeal Stridor in Multiple System Atrophy. *Eur Neurol*. (2003) 49:154–9. doi: 10.1159/000069077
18. Wenning GK, Ben Shlomo Y, Magalhães M, Danie SE, Quinn NP. Clinical features and natural history of multiple system atrophy: an analysis of 100 cases. *Brain*. (1994) 117:835–45. doi: 10.1093/brain/117.4.835
19. Wenning GK, Ben-Shlomo Y, Hughes A, Daniel SE, Lees A, Quinn NP. What clinical features are most useful to distinguish definite multiple system atrophy from Parkinson's disease? *J Neurol Neurosurg Psychiatry*. (2000) 68:434–40. doi: 10.1136/jnnp.68.4.434
20. Giannini G, Calandra-Buonaura G, Mastrolilli F, Righini M, Bacchi-Reggiani ML, Cecere A, et al. Early stridor onset and stridor treatment predict survival in 136 patients with MSA. *Neurology*. (2016) 87:1375–83. doi: 10.1212/WNL.0000000000003156
21. Martinovits G, Leventon G, Goldhammer Y, Sadeh M. Vocal cord paralysis as a presenting sign in the Shy-Drager syndrome. *J Laryngol Otol*. (1988) 102:280–1. doi: 10.1017/S0022215100104724
22. Glass GA, Josephs KA, Ahlskog JE. Respiratory insufficiency as the primary presenting symptom of multiple-system atrophy. *Arch Neurol*. (2006) 63:978–81. doi: 10.1001/archneur.63.7.978
23. Uzawa A, Sakakibara R, Tamura N, Asahina M, Yamanaka Y, Uchiyama T, et al. Laryngeal abductor paralysis can be a solitary manifestation of multiple system atrophy. *J Neurol Neurosurg Psychiatry*. (2005) 76:1739. doi: 10.1136/jnnp.2005.068023
24. Kew J, Gross M, Chapman P. Shy-Drager syndrome presenting as isolated paralysis of vocal cord abductors. *Br Med J*. (1990) 300:1441.
25. Silber MH, Levine S. Stridor and death in multiple system atrophy. *Mov Disord Off J Mov Disord Soc*. (2000) 15:699–704. doi: 10.1002/1531-8257(200007)15:4<699::AID-MDS1015>3.0.CO;2-L
26. Papapetropoulos S, Tuchman A, Laufer D, Papatsoris AG, Papapetropoulos N, Mash DC. Causes of death in multiple system atrophy. *J Neurol Neurosurg Psychiatry*. (2006) 78:327–9. doi: 10.1136/jnnp.2006.103929
27. Shimohata T, Shinoda H, Nakayama H, Ozawa T, Terajima K, Yoshizawa H, et al. Daytime hypoxemia, sleep-disordered breathing, and laryngopharyngeal findings in multiple system atrophy. *Arch Neurol*. (2007) 64:856–61. doi: 10.1001/archneur.64.6.856
28. Aragane N, Katoh O, Yamada H, Kuroda Y, Maeyama T. Respiratory failure due to vocal cord dyskinesia in olivo-ponto-cerebellar atrophy. *Chest*. (1989) 96:1212–4.
29. Isono S, Shiba K, Yamaguchi M, Tanaka A, Hattori T, Konno A, Nishino T. Pathogenesis of laryngeal narrowing in patients with multiple system atrophy. *J Physiol*. (2001) 536:237–49. doi: 10.1111/j.1469-7793.2001.t01-1-00237.x
30. Umeno H, Ueda Y, Mori K, Chijiwa K, Nakashima T, Kotby NM. Management of impaired vocal fold movement during sleep in a patient with Shy-Drager syndrome. *Am J Otolaryngol - Head Neck Med Surg*. (2000) 21:344–8. doi: 10.1053/ajot.2000.16174

31. Shiba K, Isono S, Nakazawa K. Paradoxical vocal cord motion: a review focused on multiple system atrophy. *Auris Nasus Larynx*. (2007) 34:443–52. doi: 10.1016/j.anl.2007.03.006
32. Shiba K, Isono S. Tracheostomy abolishes paradoxical activation of the vocal cord adductor in multiple system atrophy. *Auris Nasus Larynx*. (2006) 33:295–8. doi: 10.1016/j.anl.2005.11.018
33. Shiba K, Isono S, Sekita Y, Tanaka A. Inspiratory activation of the vocal cord adductor, part i: human study in patients with restricted abduction of the vocal cords. *Laryngoscope*. (2004) 114:372–5. doi: 10.1097/00005537-200402000-00036
34. Lalich IJ, Ekbom DC, Starkman SJ, Orbelo DM, Morgenthaler TI. Vocal fold motion impairment in multiple system atrophy. *Laryngoscope*. (2014) 124:730–5. doi: 10.1002/lary.24402
35. Higo R, Tayama N, Watanabe T, Nitou T. Vocal fold motion impairment in patients with multiple system atrophy: evaluation of its relationship with swallowing function. *J Neurol Neurosurg Psychiatry*. (2003) 74:982–4. doi: 10.1136/jnnp.74.7.982
36. Ward PH, Hanson DG, Berci G. Observations on central neurologic etiology for laryngeal dysfunction. *Ann Otol Rhinol Laryngol*. (1981) 90:430–41. doi: 10.1177/000348948109000504
37. Simpson D, Kaufman H, Sanders I, Wolfe D. Laryngeal dystonia in multiple system atrophy. *Muscle Nerve*. (1992) 15:1213–5.
38. Ozawa T, Shinoda H, Tomita M, Shimohata T, Nakayama H, Nishizawa M. Tremulous arytenoid movements predict severity of glottic stenosis in multiple system atrophy. *Mov Disord*. (2010) 25:1418–23. doi: 10.1002/mds.23090
39. Isozaki E, Naito R, Kanda T, Mizutani T, Hirai S. Different mechanism of vocal cord paralysis between spinocerebellar ataxia (SCA 1 and SCA 3) and multiple system atrophy. *J Neurol Sci*. (2002) 197:37–43. doi: 10.1016/S0022-510X(02)00046-1
40. Hughes RG, Gibbin KP, Lowe J. Vocal fold abductor paralysis as a solitary and fatal manifestation of multiple system atrophy. *J Laryngol Otol*. (1998) 112:177–8.
41. Hanson DG, Ludlow CL, Bassich CJ. Vocal Fold Paresis in Shy-Drager Syndrome. *Ann Otol Rhinol Laryngol*. (1983) 92:85–90. doi: 10.1177/000348948309200121
42. Guindi GM, Bannister R, Gibson WPR, Payne JK. Laryngeal electromyography in multiple system atrophy with autonomic failure. *J Neurol Neurosurg Psychiatry*. (1981) 44:49–53. doi: 10.1136/jnnp.44.1.49
43. Bannister R, Gibson W, Michaels L, Oppenheimer D. Laryngeal abductor paralysis in multiple system atrophy. A report on three necropsied cases, with observations on the laryngeal muscles and the nuclei ambigui. *Brain*. (1981) 104:351–68.
44. Deguchi K, Ikeda K, Shimamura M, Urai Y, Tsukaguchi M, Touge T, et al. Assessment of autonomic dysfunction of multiple system atrophy with laryngeal abductor paralysis as an early manifestation. *Clin Neurol Neurosurg*. (2007) 109:892–5. doi: 10.1016/j.clineuro.2007.07.020
45. Hayashi M, Isozaki E, Oda M, Tanabe H, Kimura J. Loss of large myelinated nerve fibres of the recurrent laryngeal nerve in patients with multiple system atrophy and vocal cord palsy. *J Neurol Neurosurg Psychiatry*. (1997) 62:234–8.
46. Dion GR, Eller RL, Thomas RF. Diagnosing aerodynamic supraglottic collapse with rest and exercise flexible laryngoscopy. *J Voice*. (2012) 26:779–84. doi: 10.1016/j.jvoice.2012.01.004
47. Sekita Y, Shiba K, Nakazawa K, Numasawa T, Isono S. Inspiratory activation of the vocal cord adductor, part II: Animal study in the cat. *Laryngoscope*. (2004) 114:376–80. doi: 10.1097/00005537-200402000-00037
48. Nonaka M, Imai T, Shintani T, Kawamata M, Chiba S, Matsumoto H. Non-invasive positive pressure ventilation for laryngeal contraction disorder during sleep in multiple system atrophy. *J Neurol Sci*. (2006) 247:53–8. doi: 10.1016/j.jns.2006.03.008
49. Iranzo A, Santamaria J, Tolosa E, Vilaseca I, Valldeoriola F, Martí MJ, et al. Long-term effect of CPAP in the treatment of nocturnal stridor in multiple system atrophy. *Neurology*. (2004) 63:930–2. doi: 10.1212/01.WNL.0000137043.76383.A4
50. Iranzo A, Santamaria J, Tolosa E. Continuous positive air pressure eliminates nocturnal stridor in multiple system atrophy. Barcelona Multiple System Atrophy Study Group. *Lancet*. (2000) 356:1329–30. doi: 10.1016/S0140-6736(00)02824-5
51. Alfonsi E, Terzaghi M, Cosentino G, Tassorelli C, Manni R, Pozzi N, et al. Specific patterns of laryngeal electromyography during wakefulness are associated to sleep disordered breathing and nocturnal stridor in multiple system atrophy. *Parkinsonism Relat Disord*. (2016) 31:104–9. doi: 10.1016/j.parkreldis.2016.07.017
52. Merlo IM, Occhini A, Pacchetti C, Alfonsi E. Not paralysis, but dystonia causes stridor in multiple system atrophy. *Neurology*. (2002) 58:649–52. doi: 10.1212/WNL.58.4.649
53. Ghorayeb I, Yekhlef F, Bioulac B, Tison F. Continuous positive airway pressure for sleep-related breathing disorders in multiple system atrophy: long-term acceptance. *Sleep Med*. (2005) 6:359–62. doi: 10.1016/j.sleep.2004.10.002
54. Kenyon GS, Apps MC, Traub M. Stridor and obstructive sleep apnea in Shy-Drager syndrome treated by laryngofissure and cord lateralization. *Laryngoscope*. (1984) 94:1106–8.
55. Chitose SI, Kikuchi A, Ikezono K, Umeno H, Nakashima T. Effect of laser arytenoidectomy on respiratory stridor caused by multiple system atrophy. *J Clin Sleep Med*. (2012) 8:713–5. doi: 10.5664/jcsm.2272
56. Perez KS, Ramig LO, Smith ME, Dromey C. The parkinson larynx: tremor and videostroboscopic findings. *J Voice*. (1996) 10:354–61. doi: 10.1016/S0892-1997(96)80027-0
57. Blumin JH, Pcolinsky DE, Atkins JP. Laryngeal findings in advanced Parkinson's disease. *Ann Otol Rhinol Laryngol*. (2004) 113:253–8. doi: 10.1177/000348940411300401
58. Hanson DG, Gerratt BR, Ward PH. Cinegraphic observations of laryngeal function in Parkinson's disease. *Laryngoscope*. (1984) 94:348–53.
59. Isozaki E, Shimizu T, Takamoto K, Horiguchi S, Hayashida T, Oda M, Tanabe H. Vocal cord abductor paralysis (VCAP) in Parkinson's disease: difference from VCAP in multiple system atrophy. *J Neurol Sci*. (1995) 130:197–202. doi: 10.1016/0022-510X(95)00030-6
60. Müller J, Wenning GK, Verny M, McKee A, Chaudhuri KR, Jellinger K, et al. Progression of Dysarthria and Dysphagia in Postmortem-Confirmed Parkinsonian Disorders. *Arch Neurol*. (2001) 58:259. doi: 10.1001/archneur.58.2.259
61. Isono C, Hirano M, Sakamoto H, Ueno S, Kusunoki S, Nakamura Y. Differential progression of dysphagia in heredity and sporadic ataxias involving multiple systems. *Eur Neurol*. (2015) 74:237–42. doi: 10.1159/000442252
62. O'Sullivan SS, Massey LA, Williams DR, Silveira-Moriyama L, Kempster PA, Holton JL, et al. Clinical outcomes of progressive supranuclear palsy and multiple system atrophy. *Brain*. (2008) 131:1362–72. doi: 10.1093/brain/awn065
63. Petrovic IN, Ling H, Asi Y, Ahmed Z, Kukkle PL, Hazrati L-N, et al. Multiple system atrophy-parkinsonism with slow progression and prolonged survival: a diagnostic catch. *Mov Disord*. (2012) 27:1186–90. doi: 10.1002/mds.25115
64. Lee HH, Seo HG, Kim K, Lee SH, Lee WH, Oh B-M, et al. Characteristics of early oropharyngeal dysphagia in patients with multiple system atrophy. *Neurodegener Dis*. (2018) 18:84–90. doi: 10.1159/000487800
65. Lang IM. Brain stem control of the phases of swallowing. *Dysphagia*. (2009) 24:333–48. doi: 10.1007/s00455-009-9211-6
66. Taniguchi H, Nakayama H, Hori K, Nishizawa M, Inoue M, Shimohata T. Esophageal involvement in multiple system atrophy. *Dysphagia*. (2015) 30:669–73. doi: 10.1007/s00455-015-9641-2
67. Higo R, Tayama N, Watanabe T, Nitou T, Ugawa Y. Videofluoroscopic and manometric evaluation of swallowing function in patients with multiple system atrophy. *Ann Otol Rhinol Laryngol*. (2003) 112:630–6. doi: 10.1177/000348940311200710
68. Aoyagi R, Fujioka S, Mishima T, Tsuboi Y. Probable multiple system atrophy presenting motor fluctuation: clinical characteristics in three cases. *J Neurol Sci*. (2017) 381:215. doi: 10.1016/j.jns.2017.08.614
69. Hedera P, Claassen D. Deep brain stimulation therapy of levodopa-responsive motor fluctuations in patients with multiple system atrophy. *Parkinsonism Relat Disord*. (2018) 46:e91. doi: 10.1016/J.PARKRELDIS.2017.11.319
70. Meissner WG, Laurencin C, Tranchant C, Witjas T, Viallet F, Guehl D, Damier P, et al. Outcome of deep brain stimulation in slowly progressive multiple system atrophy: a clinico-pathological series and review of the literature. *Parkinsonism Relat Disord*. (2016) 24:69–75. doi: 10.1016/j.parkreldis.2016.01.005

71. Warnecke T, Suttrup I, Schröder JB, Osada N, Oelenberg S, Hamacher C, Suntrup S, Dziewas R. Levodopa responsiveness of dysphagia in advanced Parkinson's disease and reliability testing of the FEES-Levodopa-test. *Parkinsonism Relat Disord*. (2016) 28:100–6. doi: 10.1016/j.parkreldis.2016.04.034
72. Warnecke T, Oelenberg S, Teismann I, Hamacher C, Lohmann H, Ringelstein EB, et al. Endoscopic characteristics and levodopa responsiveness of swallowing function in progressive supranuclear palsy. *Mov Disord*. (2010) 25:1239–45. doi: 10.1002/mds.23060
73. Suttrup I, Warnecke T. Dysphagia in Parkinson's Disease. *Dysphagia*. (2016) 31:24–32. doi: 10.1007/s00455-015-9671-9
74. Triadafilopoulos G, Gandhy R, Barlow C. Pilot cohort study of endoscopic botulinum neurotoxin injection in Parkinson's disease. *Parkinsonism Relat Disord*. (2017) 44:33–7. doi: 10.1016/j.parkreldis.2017.08.020
75. Palma JA, Kaufmann H. Treatment of autonomic dysfunction in Parkinson disease and other synucleinopathies. *Mov Disord*. (2018) 33:372–90. doi: 10.1002/mds.27344
76. World Medical Association. World Medical Association Declaration of Helsinki. Ethical principles for medical research involving human subjects. *J Am Med Assoc*. (2013) 310:2191–4. doi: 10.1001/jama.2013.281053
77. Rusz J, Bonnet C, Klempír J, Tykalová T, Baborová E, Novotný M, et al. Speech disorders reflect differing pathophysiology in Parkinson's disease, progressive supranuclear palsy and multiple system atrophy. *J Neurol*. (2015) 262:992–1001. doi: 10.1007/s00415-015-7671-1
78. Okuma Y, Fujishima K, Miwa H, Mori H, Mizuno Y. Myoclonic tremulous movements in multiple system atrophy are a form of cortical myoclonus. *Mov Disord*. (2005) 20:451–456. doi: 10.1002/mds.20346
79. Kaindlstorfer C, Granata R, Wenning GK. Tremor in Multiple System Atrophy - a review. *Tremor Other Hyperkinet Mov*. (2013) 3:1–9. doi: 10.7916/D8NV9GZ9
80. Salazar G, Valls-Solé J, Martí MJ, Chang H, Tolosa ES. Postural and action myoclonus in patients with parkinsonian type multiple system atrophy. *Mov Disord*. (2000) 15:77–83. doi: 10.1002/1531-8257(200001)15:1<77::AID-MDS1013>3.0.CO;2-N
81. Merati AL, Heman-Ackah YD, Abaza M, Altman KW, Sulica L, Belamowicz S. Common movement disorders affecting the larynx: a report from the neurolaryngology committee of the AAO-HNS. *Otolaryngol - Head Neck Surg*. (2005) 133:654–65. doi: 10.1016/j.otohns.2005.05.003
82. Richards AL. Vocal tremor: where are we at? *Curr Opin Otolaryngol Head Neck Surg*. (2017) 25:475–9. doi: 10.1097/MOO.0000000000000412
83. Woodson G. Management of neurologic disorders of the larynx. *Ann Otol Rhinol Laryngol*. (2008) 117:317–26. doi: 10.1177/000348940811700501
84. Dziewas R, Glahn J, Helfer C, Ickenstein G, Keller J, Ledl C, et al. Flexible endoscopic evaluation of swallowing (FEES) for neurogenic dysphagia: training curriculum of the German Society of Neurology and the German stroke society. *BMC Med Educ*. (2016) 16:70. doi: 10.1186/s12909-016-0587-3

Conflict of Interest Statement: The authors declare that the research was conducted in the absence of any commercial or financial relationships that could be construed as a potential conflict of interest.

Copyright © 2019 Warnecke, Vogel, Ahring, Gruber, Heinze, Dziewas, Ebersbach and Gandor. This is an open-access article distributed under the terms of the Creative Commons Attribution License (CC BY). The use, distribution or reproduction in other forums is permitted, provided the original author(s) and the copyright owner(s) are credited and that the original publication in this journal is cited, in accordance with accepted academic practice. No use, distribution or reproduction is permitted which does not comply with these terms.

frontiers in Neurology

ORIGINAL RESEARCH
published: 16 April 2019
doi: 10.3389/fneur.2019.00386

Substance P Saliva Reduction Predicts Pharyngeal Dysphagia in Parkinson's Disease

Jens Burchard Schröder, Thomas Marian, Inga Claus, Paul Muhle, Matthias Pawlowski, Heinz Wiendl, Sonja Suntrup-Krueger, Sven G. Meuth, Rainer Dziewas, Tobias Ruck and Tobias Warnecke*

Department of Neurology, University Hospital Münster, Münster, Germany

Introduction: Although patients with Parkinson's disease (PD) often suffer from oropharyngeal dysphagia, knowledge about the underlying pathophysiological mechanisms is limited. Substance P (SP) is a localization-independent neurotransmitter of the entire nervous system. Reduced levels of SP were found in saliva of patients with impaired cough reflex and in advanced stages of PD. The aim of the study was to investigate SP in PD patients in order to gain further insights into the underlying pathophysiology of PD-related dysphagia and to evaluate the potential of SP as a biomarker for early dysphagia.

Methods: Flexible endoscopic evaluation of swallowing (FEES) was used to objectively assess pharyngeal swallowing function. From a cohort of 105 consecutive PD patients 20 subjects were recruited: in 10 of them pharyngeal dysphagia was excluded by FEES, the other 10 subjects showed signs of early pharyngeal dysphagia defined as hypopharyngeal sensory deficit with mild to moderate vallecular residues after swallowing solid consistencies. Analysis of the Substance P level in saliva of the 20 included PD patients was performed in the clinical on state condition by ELISA-type immunoassay. Significant differences were calculated by using the Mann-Whitney test.

Results: Twenty PD patients with a mean age of 69.5 ± 12.5 years (8 female) were included in the study. No significant differences were found regarding gender, age, UPDRS III, Hoehn and Yahr stage, disease duration, and Levodopa equivalent dose between the non-dysphagic and dysphagic subjects. Dysphagia was mainly characterized by unrecognized residues in the valleculae without any aspiration risk for all of the tested consistencies in FEES and was thereby scored as mild in all cases. Saliva SP concentrations were significantly lower in PD patients with pharyngeal dysphagia compared to those with a normal pharyngeal swallowing function (9,644 vs. 17,591 pg/mL; $p = 0.001$).

Conclusion: Reduced saliva SP concentrations may predict early pharyngeal swallowing dysfunction in PD patients. This finding supports the hypothesis that an impaired SP mediated neurotransmission has a significant impact for the development of dysphagia in PD patients. Larger studies are needed to confirm SP as a clinical useful biomarker for early detection of PD-related dysphagia.

Keywords: Parkinson's disease, substance P, dysphagia, biomarker, neurodegeneration

OPEN ACCESS

Edited by:
Muthuraman Muthuraman, Johannes Gutenberg University Mainz, Germany

Reviewed by:
Haralampos Gouveris, Johannes Gutenberg University Mainz, Germany
Panagiotis Bargiotas, University of Bern, Switzerland

****Correspondence:***
Jens Burchard Schröder
jensburchard.schroeder@ukmuenster.de

Specialty section:
This article was submitted to Movement Disorders, a section of the journal Frontiers in Neurology

Received: *28 October 2018*
Accepted: *29 March 2019*
Published: *16 April 2019*

Citation:
Schröder JB, Marian T, Claus I, Muhle P, Pawlowski M, Wiendl H, Suntrup-Krueger S, Meuth SG, Dziewas R, Ruck T and Warnecke T (2019) Substance P Saliva Reduction Predicts Pharyngeal Dysphagia in Parkinson's Disease. Front. Neurol. 10:386. doi: 10.3389/fneur.2019.00386

INTRODUCTION

Following Alzheimer's disease, Parkinson's disease (PD) is the second most common neurodegenerative disorder (1, 2). Oropharyngeal dysphagia is a clinically relevant symptom in affected patients as the majority of PD patients will suffer from neurogenic dysphagia during the course of their disease (3–6). In addition to consecutive malnutrition, dehydration and insufficient medication intake, neurogenic dysphagia leads to loss of quality of life for affected patients and aspiration pneumonia, which is the leading cause of death in Parkinson's patients (4, 7–9).

However, clinical diagnosis of dysphagia in PD remains challenging. Particularly in early disease stages affected patients are usually unaware of their swallowing dysfunction and therefore do not report spontaneously about swallowing problems (10, 11). Furthermore, pharyngeal swallowing function cannot be assessed sufficiently by clinical neurological examination resulting in a significant delay of uncovering dysphagia in these patients (11–13). When more elaborate instrumental tools for swallowing evaluation like flexible endoscopic evaluation of swallowing (FEES) or videofluoroscopic swallowing study (VFSS) are systematically applied, dysphagia was found to be present in more than 50% of subjectively asymptomatic PD patients (14). However, access to FEES and VFSS is limited in many institutions.

Furthermore, the underlying pathophysiology of dysphagia in PD and particularly the role of substance P (SP) is still barely understood (15). SP is an ubiquitary neuropeptide in the nervous system (16). It mediates the response to local stimuli in the pharyngeal mucosa and thereby enhances the swallow and cough reflex (17–19). In a cohort of elderly patients with aspiration pneumonia, sputum levels of SP were found to be reduced (20). Probably due to a reduced concentration of SP in the saliva of patients in advanced stages of PD, protective reflexes with consecutive silent aspiration were observed (21, 22). However, it is so far unknown if substance P reduction is already present in PD patients with early pharyngeal dysphagia not showing any risk of aspiration.

The purpose of the present study was to investigate Substance P as a potential biomarker for early detection of pharyngeal dysphagia in PD and thereby gain further insights into pathophysiology.

MATERIAL AND METHODS

Protocol Approval, Registration, and Patient Consent

All patients were prospectively recruited from the movement disorder unit at the Department of Neurology, University Hospital Münster, Germany. Written informed consent was obtained from each subject after the nature of the study was explained in accordance to the principles of the declaration of Helsinki. The local ethics committee of the medical faculty at the University of Muenster approved the protocol of the study (2014-624-f-S).

Participants

From a cohort of 105 consecutive PD patients, who did not have subjective swallowing impairment and were evaluated for dysphagia with FEES, as part of the baseline dysphagia assessment in our clinic, 20 subjects were recruited between January 2017 and March 2018. Participants had to be on stable medication regimen and all examinations were done in the clinical "ON" phase. Exclusion criteria for this study were concomitant diseases that may cause neurogenic dysphagia, autoimmune diseases, anti-inflammatory co-medication (e.g., cytotoxic agents, steroids, non-steroid analgesia), sedatives, or evidence of an acute systemic inflammatory process at the time of Substance P measurement (elevated erythrocyte sedimentation rate above 25 mm/h, C-reactive protein above 0.5 mg/dL, or leukocytes above 11 × 103/μL). Patient characteristics are described in detail in **Table 1**.

Dysphagia Assessment

In all participants, Dysphagia was examined with fiberoptic endoscopic evaluation of swallowing in the on-state condition. FEES was performed in accordance with the standard protocol proposed by Langmore et al. as described in detail elsewhere (23).

Equipment consisted of a 3.1 mm-diameter flexible fiberoptic rhinolaryngoscope (11101RP2, Karl Storz, Tuttlingen, Germany), a light source and camera (rpCam-X, rpSzene®, Rehder/Partner, Hamburg, Germany), a color monitor (WMP-226, Wincomm, Taiwan) and a video recorder (AUCC2WV3F, Computar, CBC Group, Japan).

All PD patients were given nine test boluses in a standardized order. First, they received 8 ml of pudding (green jelly), second 5 ml blue-dyed liquid and finally three trials of white bread with the size of approximately 3 × 3 × 0.5 cm. During all swallowing tasks, the following parameters of swallowing function were assessed: premature spillage, material that enters the hypopharynx unintentionally from the oral cavity before the pharyngeal swallow was initiated, penetration-aspiration events or residues. When residues in FEES were observed, patients were asked explicitly if they perceived any foreign body sensation in their throat.

Swallowing dysfunction was classified with a FEES-based 4-grade dysphagia severity scale that has previously been developed and published: 0 = no relevant dysphagia, 1 = mild dysphagia (premature spillage and/or residues, but no penetration/aspiration events), 2 = moderate dysphagia (penetration/aspiration events with one consistency), 3 = severe dysphagia (penetration/aspiration events with two or more consistencies) (24–26). Substance P was collected from patients with either no signs of pharyngeal dysphagia (group 1), or endoscopic signs of early pharyngeal dysphagia (group 2). Dysphagia was defined as mild to moderate vallecular residues being present after swallowing solid consistencies (27). Patients showing an increased aspiration risk for any of the tested consistencies were excluded.

Sample Collection and Analysis:

Between 09 and 11 a.m., about 2 h after the intake of their regular dopaminergic medication, sputum was collected. Two

TABLE 1 | Subject characteristics and clinical features.

	All	Dysphagia +	Dysphagia –	*p*-value
Number of patients (M/F)	20 (12/8)	10 (8/2)	10 (4/6)	0.068
Mean age (year)	69.5 ± 12.5	71.7 ± 11.8	67.2 ± 13.3	0.172
Disease duration (year)	8.35 ± 5.8	10.9 ± 6.5	5.8 ± 3.7	0.403
Hoehn and Yahr stage[a]	2.4 ± 0.8	2.8 ± 0.6	2.0 ± 0.7	0.698
UPDRS III, points[a]	16.5 ± 4.7	18.2 ± 4.8	14.8 ± 4.1	0.120
L-Dopa-Dose-Equivalent, mg	768.8 ± 276.4	849.2 ± 264.7	688.3 ± 277.1	0.199
Saliva quantity, microliters	792.9 ± 122.5	752.1 ± 108.1	833.8 ± 127.5	0.287
PPI intake (*n*)	7	4	3	0.180

UPDRS, Unified Parkinson Disease Rating Scale.
[a]*At clinical "On"-stage.*

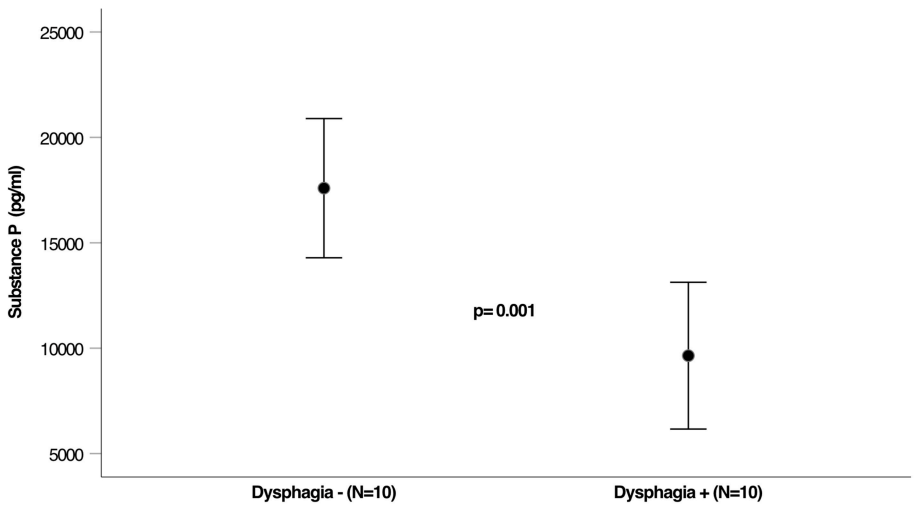


FIGURE 1 | Levels of Substance P in saliva of dysphagic and not dysphagic PD patients.

salivettes were placed into the patient's oral cavity for 1–3 min. Directly after collecting the saliva, the salivettes were centrifuged at 4,110 g for 5 min. Supernatants were stored in a deep freezer at −20°C until further analysis. Substance P levels were assessed by a commercially available competitive ELISA-type immunoassay according to the manufacturer's instructions (SP Immnunoassay, catalog no. KGE007; R&D Systems, Minneapolis, MN, USA).

Statistics

Statistical analysis was performed using SPSS Version 25.0. All data are reported as mean ± standard deviation, and the pre-chosen significance level for all confirmatory tests was $p < 0.05$. Substance P-Level was analyzed by using the Mann-Whitney test, presuming a non-Gaussian distribution.

RESULTS

FEES was successfully performed in all 20 subjects (12 male, 8 female, mean age 68.6 ± 12.5 years), presenting with either no ($n = 10$) or early pharyngeal dysphagia ($n = 10$). No adverse events occurred during the FEES examinations. **Table 1** summarizes patient's characteristics and clinical features of included patients. Gender and age were equally distributed in both study groups. In addition, no statistically significant differences were found regarding disease duration, L-Dopa equivalent doses, UPDRS III, and Hoehn & Yahr stages. PPI-intake was equally distributed between both groups.

Unnoticed pharyngeal residues were present in 10 patients (Group 2). They were located in the vallecular space in all subjects and, to a lesser extent in the pyriform sinuses (30%). Premature spillage and penetration/aspiration events were not observed for any consistency, i.e., liquid, semisolids, solids.

Figure 1 shows the concentration of SP in sputum among the 2 groups. Sputum SP concentrations were significantly lower in patients with dysphagia compared to those in control subjects (9,644 vs. 17,591 pg/mL; $p = 0.001$; see **Figure 1**).

DISCUSSION

This prospective study analyzed the saliva concentrations of SP in PD patients with early pharyngeal dysphagia compared to PD patients without any pharyngeal swallowing impairment.

The study's main finding is that early pharyngeal dysphagia in PD patients is associated with reduced levels of Substance P in patient's saliva.

PD-related dysphagia affects the oral, pharyngeal and the esophageal phase of swallowing and occurs in all stages of the disease (11, 28). Former studies have demonstrated a selective loss of vagal SP neurons in PD, potentially contributing to the emergence of esophageal motility disorders (29). In our study, also in patients with early pharyngeal dysphagia, as indicated by unnoticed significant pharyngeal residues, was associated with reduced SP concentrations. This finding broadens the results of a previous study, where significantly reduced levels of Substance P were found in PD patients with an impaired cough reflex sensitivity in a much more advanced stage of PD-related dysphagia. In early disease stages with by trend slightly lower Substance P levels cough sensitivity was not found to be impaired in this study (21). SP-immunoreactive fibers have been detected in the epithelium and basal membrane of pharyngeal mucosa, especially on the surface of the epiglottis (30). In this context, our findings could be another indication, that in early stages, loss of SP containing neurons in the pharyngeal mucosa may lead to pharyngeal hyposensitivity and merely incipient pharyngeal dysphagia.

Current diagnostic workup of suspected PD related dysphagia usually consists of questionnaires, swallowing assessment by speech language therapists and, in unclear cases, by using instrumental tools such as FEES or videofluoroscopic swallowing study (VFSS). Still, reliable screening methods are lacking (3, 27). FEES and VFSS are both considered to be the gold standard, but availability of instrumental assessment, especially in the outpatient setting, is often limited. In this context, the measurement of SP in saliva may have the potential to serve as a biomarker for the presence of clinically unrecognized pharyngeal dysphagia in early disease stages and thereby lead to earlier comprehensive dysphagia diagnosis and treatment.

Our study has several limitations that need to be addressed. First of all, PD patients were only assessed in one specific stage of their disease. Therefore, the results cannot be generalized over the entire PD population. For a possible use of substance P as a biomarker, in particular the establishment of reference values is necessary, which do not exist today. Furthermore, no follow-up of included patients was performed and, keeping in mind the basic experimental approach in the here presented pilot study, the sample size was rather low and no healthy controls were investigated. Any concomitant medication not excluded might have interfered with SP concentration. Impairment of motor function might as well have contributed to the emergence of dysphagia in our cohort. Furthermore, PD-related dysphagia is a complex symptom probably resulting from several central and peripheral mechanisms and thereby not being linked to one neurotransmitter system alone, and the exact localization of neurodegeneration, that leads to reduced SP release, cannot be identified in the clinical setting here (31).

In conclusion, this study showed for the first time, that reduced levels of SP occur in PD patients with signs of early pharyngeal dysphagia. Future studies should confirm this finding in larger cohorts. Moreover, agents like capsaicin, known to stimulate SP-release, should be investigated to assess their therapeutic potential by targeting the afferent sensory system within the swallowing network (32).

ETHICS STATEMENT

Informed consent was obtained from each subject after the nature of the study was explained in accordance to the principles of the declaration of Helsinki. The local ethics committee of the medical faculty at the University of Muenster approved the protocol of the study (2014-624-f-S).

AUTHOR CONTRIBUTIONS

JS conceived, organized, executed the research project, and wrote the manuscript. TM reviewed the manuscript. PM reviewed the manuscript. IC reviewed the manuscript. MP reviewed the manuscript. HW helped to conceive the study and reviewed the manuscript. SS-K reviewed the manuscript. SM helped to conceive the study and reviewed the manuscript. RD reviewed the manuscript. TR conceived the research project, performed data analysis, and reviewed the manuscript. TW conceived and supervised the research project and reviewed the manuscript.

REFERENCES

1. Kalia LV, Lang AE. Evolving basic, pathological and clinical concepts in PD: Parkinson disease in 2015. *Nat Rev Neurol.* (2016) 12:65–6. doi: 10.1038/nrneurol.2015.249
2. de Lau LM, Breteler MM. Epidemiology of Parkinson's disease. *Lancet Neurol.* (2006) 5:525–35. doi: 10.1016/S1474-4422(06)70471-9
3. Kalf JG, de Swart BJM, Bloem BR, Munneke M. Prevalence of oropharyngeal dysphagia in Parkinson's disease: a meta-analysis. *Parkinsonism Relat Disord.* (2012) 18:311–5. doi: 10.1016/j.parkreldis.2011.11.006
4. Miller N, Allcock L, Hildreth AJ, Jones D, Noble E, Burn DJ. Swallowing problems in Parkinson disease: frequency and clinical correlates. *J Neurol Neurosurg Psychiatry.* (2009) 80:1047–9. doi: 10.1136/jnnp.2008.157701
5. Sapir S, Ramig L, Fox C. Speech and swallowing disorders in Parkinson disease. *Curr Opin Otolaryngol Head Neck Surg.* (2008) 16:205–10. doi: 10.1097/MOO.0b013e3282febd3a
6. Edwards L, Quigley EMM, Hofman R, Pfeiffer RF. Gastrointestinal symptoms in Parkinson disease: 18-month follow-up study. *Mov Disord.* (1993) 8:83–6. doi: 10.1002/mds.870080115
7. Plowman-Prine EK, Sapienza CM, Okun MS, Pollock SL, Jacobson C, Wu SS, et al. The relationship between quality of life and swallowing in Parkinson's disease. *Mov Disord Off J Mov Disord Soc.* (2009) 24:1352–8. doi: 10.1002/mds.22617
8. Morgante L, Salemi G, Meneghini F, Di Rosa AE, Epifanio A, Grigoletto F, et al. Parkinson disease survival: a population-based study. *Arch Neurol.* (2000) 57:507. doi: 10.1001/archneur.57.4.507
9. Lin J-H, Tu K-H, Chang C-H, Chen Y-C, Tian Y-C, Yu C-C, et al. Prognostic factors and complication rates for double-filtration plasmapheresis

in patients with Guillain-Barré syndrome. *Transfus Apher Sci*. (2015) 52:78–83. doi: 10.1016/j.transci.2014.12.005
10. Coelho M, Marti MJ, Tolosa E, Ferreira JJ, Valldeoriola F, Rosa M, et al. Late-stage Parkinson's disease: the Barcelona and Lisbon cohort. *J Neurol*. (2010) 257:1524–32. doi: 10.1007/s00415-010-5566-8
11. Pflug C, Bihler M, Emich K, Niessen A, Nienstedt JC, Flügel T, et al. Critical dysphagia is common in Parkinson disease and occurs even in early stages: a prospective cohort study. *Dysphagia*. (2018) 33:41–50. doi: 10.1007/s00455-017-9831-1
12. Bird MR, Woodward MC, Gibson EM, Phyland DJ, Fonda D. Asymptomatic swallowing disorders in elderly patients with Parkinson's disease: a description of findings on clinical examination and videofluoroscopy in sixteen patients. *Age Ageing*. (1994) 23:251–4.
13. Bushmann M, Dobmeyer SM, Leeker L, Perlmutter JS. Swallowing abnormalities and their response to treatment in Parkinson's disease. *Neurology*. (1989) 39:1309–14.
14. Fuh J-L, Lee R-C, Wang S-J, Lin C-H, Wang P-N, Chiang J-H, et al. Swallowing difficulty in Parkinson's disease. *Clin Neurol Neurosurg*. (1997) 99:106–12.
15. Michou E, Hamdy S. Dysphagia in Parkinson's disease: a therapeutic challenge? *Expert Rev Neurother*. (2010) 10:875–8. doi: 10.1586/ern.10.60
16. Niel JP. Role of substance P in the nervous system control of digestive motility. *Arch Int Physiol Biochim Biophys*. (1991) 99:A65–76.
17. Renner B, Ahne G, Grosan E, Kettenmann B, Kobal G, Shephard A. Tonic stimulation of the pharyngeal mucosa causes pain and a reversible increase of inflammatory mediators. *Inflamm Res*. (2013) 62:1045–51. doi: 10.1007/s00011-013-0663-7
18. Imoto Y, Kojima A, Osawa Y, Sunaga H, Fujieda S. Cough reflex induced by capsaicin inhalation in patients with dysphagia. *Acta Otolaryngol*. (2011) 131:96–100. doi: 10.3109/00016489.2010.516013
19. Jin Y, Sekizawa K, Fukushima T, Morikawa M, Nakazawa H, Sasaki H. Capsaicin desensitization inhibits swallowing reflex in guinea pigs. *Am J Respir Crit Care Med*. (1994) 149:261–3.
20. Nakagawa T, Ohrui T, Sekizawa K, Sasaki H. Sputum substance P in aspiration pneumonia. *Lancet*. (1995) 345:1447. doi: 10.1016/S0140-6736(95)92638-0
21. Ebihara S, Saito H, Kanda A, Nakajoh M, Takahashi H, Arai H, et al. Impaired efficacy of cough in patients with Parkinson disease. *Chest*. (2003) 124:1009–15. doi: 10.1378/chest.124.3.1009
22. Troche MS, Brandimore AE, Okun MS, Davenport PW, Hegland KW. Decreased cough sensitivity and aspiration in Parkinson disease. *Chest*. (2014) 146:1294–9. doi: 10.1378/chest.14-0066
23. Langmore SE. Scoring a FEES examination. *Endosc Eval Treat Swallowing Disord N Y Thieme*. (2001) 101–43.
24. Warnecke T, Oelenberg S, Teismann I, Hamacher C, Lohmann H, Ringelstein EB, et al. Endoscopic characteristics and levodopa responsiveness of swallowing function in progressive supranuclear palsy. *Mov Disord Off J Mov Disord Soc*. (2010) 25:1239–45. doi: 10.1002/mds.23060
25. Warnecke T, Dziewas R. Chapter 106—swallowing in progressive supranuclear palsy and implications for nutrition. In: Martin CR, Preedy VR, editors. *Diet and Nutrition in Dementia and Cognitive Decline*. San Diego, CA: Academic Press. (2014) p. 1135–41.
26. Warnecke T, Suttrup I, Schroder JB, Osada N, Oelenberg S, Hamacher C, et al. Levodopa responsiveness of dysphagia in advanced Parkinson's disease and reliability testing of the FEES-Levodopa-test. *Parkinsonism Relat Disord*. (2016) 28:100–6. doi: 10.1016/j.parkreldis.2016.04.034
27. Suttrup I, Warnecke T. Dysphagia in Parkinson's Disease. *Dysphagia*. (2016) 31:24–32. doi: 10.1007/s00455-015-9671-9
28. Suttrup I, Suttrup J, Suntrup-Krueger S, Siemer M-L, Bauer J, Hamacher C, et al. Esophageal dysfunction in different stages of Parkinson's disease. *Neurogastroenterol Motil*. (2017) 29:e12915. doi: 10.1111/nmo.12915
29. Halliday GM, Li YW, Blumbergs PC, Joh TH, Cotton RG, Howe PR, et al. Neuropathology of immunohistochemically identified brainstem neurons in Parkinson's disease. *Ann Neurol*. (1990) 27:373–85.
30. Yoshida Y, Tanaka Y, Hirano M, Nakashima T. Sensory innervation of the pharynx and larynx. *Am J Med*. (2000) 108:51–61. doi: 10.1016/S0002-9343(99)00342-3
31. Mu L, Sobotka S, Chen J, Su H, Sanders I, Adler CH, et al. Altered pharyngeal muscles in Parkinson disease. *J Neuropathol Exp Neurol*. (2012) 71:520–30. doi: 10.1097/NEN.0b013e318258381b
32. Gamse R, Molnar A, Lembeck F. Substance P release from spinal cord slices by capsaicin. *Life Sci*. (1979) 25:629–36. doi: 10.1016/0024-3205(79)90558-7

Conflict of Interest Statement: The authors declare that the research was conducted in the absence of any commercial or financial relationships that could be construed as a potential conflict of interest.

Copyright © 2019 Schröder, Marian, Claus, Muhle, Pawlowski, Wiendl, Suntrup-Krueger, Meuth, Dziewas, Ruck and Warnecke. This is an open-access article distributed under the terms of the Creative Commons Attribution License (CC BY). The use, distribution or reproduction in other forums is permitted, provided the original author(s) and the copyright owner(s) are credited and that the original publication in this journal is cited, in accordance with accepted academic practice. No use, distribution or reproduction is permitted which does not comply with these terms.

frontiers in Neurology

ORIGINAL RESEARCH
published: 07 May 2019
doi: 10.3389/fneur.2019.00470

Identification of Candidate Protein Markers in Skeletal Muscle of Laminin-211-Deficient CMD Type 1A-Patients

Heike Kölbel[1], Denisa Hathazi[2,3], Matthew Jennings[3], Rita Horvath[3], Andreas Roos[1,2] and Ulrike Schara[1]*

[1] Department of Pediatric Neurology, Developmental Neurology and Social Pediatrics, University of Duisburg-Essen, Essen, Germany, [2] Leibniz-Institut für Analytische Wissenschaften -ISAS- e.V., Dortmund, Germany, [3] Department of Clinical Neuroscience, University of Cambridge, Cambridge, United Kingdom

Laminin-211 deficiency leads to the most common form of congenital muscular dystrophy in childhood, MDC1A. The clinical picture is characterized by severe muscle weakness, brain abnormalities and delayed motor milestones defining MDC1A as one of the most severe forms of congenital muscular diseases. Although the molecular genetic basis of this neurological disease is well-known and molecular studies of mouse muscle and human cultured muscle cells allowed first insights into the underlying pathophysiology, the definition of marker proteins in human vulnerable tissue such as skeletal muscle is still lacking. To systematically address this need, we analyzed the proteomic signature of laminin-211-deficient vastus muscle derived from four patients and identified 86 proteins (35 were increased and 51 decreased) as skeletal muscle markers and verified paradigmatic findings in a total of two further MDC1A muscle biopsies. Functions of proteins suggests fibrosis but also hints at altered synaptic transmission and accords with central nervous system alterations as part of the clinical spectrum of MDC1A. In addition, a profound mitochondrial vulnerability of the laminin-211-deficient muscle is indicated and also altered abundances of other proteins support the concept that metabolic alterations could be novel mechanisms that underline MDC1A and might constitute therapeutic targets. Intersection of our data with the proteomic signature of murine laminin-211-deficient gastrocnemius and diaphragm allowed the definition of nine common vulnerable proteins representing potential tissue markers.

Keywords: laminin-211, laminin-α2, congenital muscular dystrophy, agrin, NudC domain-containing protein 2, muscle proteomics

OPEN ACCESS

Edited by:
Stefan Bittner, Johannes Gutenberg University Mainz, Germany

Reviewed by:
Michele H. Jacob, Tufts University, United States
Dione Kobayashi, Independent Researcher, MA, Cambridge, United States

***Correspondence:**
Andreas Roos
Andreas.Roos@uk-essen.de; andreas.roos@isas.de

Specialty section:
This article was submitted to Movement Disorders, a section of the journal Frontiers in Neurology

Received: *11 October 2018*
Accepted: *17 April 2019*
Published: *07 May 2019*

Citation:
Kölbel H, Hathazi D, Jennings M, Horvath R, Roos A and Schara U (2019) Identification of Candidate Protein Markers in Skeletal Muscle of Laminin-211-Deficient CMD Type 1A-Patients. Front. Neurol. 10:470. doi: 10.3389/fneur.2019.00470

INTRODUCTION

Congenital muscular dystrophies (CMD) comprise a heterogenous group of genetically caused neuromuscular diseases with muscle weakness apparent at birth or in the first 6 months of life. Most of the different subtypes are of autosomal recessive inheritance (1). Laminin-211 (formerly merosin) -deficient CMD type 1A (MDC1A) is caused by recessive mutations in the *LAMA2* gene (encoding for the α2 subunit of laminin-211) and constitutes approximately 10–30% of total CMD cases in the European population. Laminin-211 is expressed in the brain vasculature,

the skeletal muscle basal lamina as well as in the myotendinous and neuromuscular junctions (2). White matter T2 signal hyperintensity as reflection of increased interstitial water content occurs in almost all patients after 6 months of age (3, 4). MDC1A-patients suffer from muscular weakness associated with elevated serum creatine kinase (CK) levels, poor suck and cry, multiple joint contractures and delayed motor development. Most of the MDC1A-patients never achieve independent ambulation (5–7). Extramuscular manifestations include seizures in 30% of patients, demyelinating neuropathy and CNS abnormalities such as polymicrogyria and cortical bandlike heterotopia. Mental retardation rarely occurs (8). Whereas patients with a complete deficiency of laminin-211 present with a severe clinical spectrum of the disease, a partial deficiency of the protein leads to milder phenotypes (6). In 2011, Gawlik and Durbeej speculated that the pathogenicity of *LAMA2* mutations, which disrupt the assembly of the corresponding laminin-211 protein with other basal lamina components, explains the full penetrance of the phenotype (9).

Laminin is a cell-adhesion molecule localized to the basement membrane of skeletal muscle. The biological functions of laminins such as modulation of cytoskeleton and intracellular signaling pathways are accomplished via the interaction with transmembrane receptors which—in skeletal muscle—are represented by dystroglycan and integrin α7β1 as the two major receptors for laminin-211 (10, 11). In this context, laminin has also been postulated to protect the muscle fibers from damage under the constant stress of contractions (9). Notably, while laminin-211 (composed of α2, β1, and γ1 chains) was first isolated from placenta and originally called merosin (12), it is now well established that laminin-211 is the main laminin isoform in skeletal muscle (12–14). In this context, it is important to note that laminin-211 function has been linked to muscle development and through the formation of laminin networks also to cytoskeleton and intracellular signaling pathways. Moreover, it is believed that laminin-211 influences signal transmission events and muscle innervation via modulation of NMJ-integrity and function (9).

Although clinical features of *LAMA2*-patients, especially regarding the manifestation in skeletal muscle are well described, molecular signatures of muscle pathology defining protein markers of the effect of loss of functional laminin-211 remain elusive. Utilizing label free mass spectrometry-based protein quantification, we here systematically address laminin-211-deficiency-related protein changes to define tissue biomarkers in skeletal muscle of MDC1A-patients from the severe disease spectrum. This in turn can provide potential insights into the underlying pathophysiology and thus represent valuable outcome measures for therapeutic intervention concepts such as the emerging gene therapy (15). Hence, data presented in this article provides important molecular insights into MDC1A-related pathophysiology due to alterations in protein composition beyond the extra-cellular matrix, an important aspect for the definition of further or alternative therapeutic intervention concepts.

TABLE 1 | List of antibodies used for the immunofluorescence studies.

Primary antibody	Company	Number	Dilution	Secondary antibody
GPI	Abcam	66340	1:200	Mouse anti-goat 488
Lama α5	Millipore	MAB 1924	1:500	Mouse anti-goat 488
Glypican-1	Abcam	55971	1:100	Donkey anti-rabbit 488
Agrin	Millipore	MAB 5204	1:20	Mouse anti-goat 488
Spectrin	Leica	SPEC 1-CE	1:100	Mouse anti-goat 594
Lama α2C	Millipore	MAB1922	1:500	Mouse anti-goat 488
Lama α2N	Leica	MEROSIN-CE	1:50	Mouse anti-goat 488
Mouse anti goat IgG 488		Alexa A-11029	1:500	
Mouse anti goat IgG 594		Alexa A-11032	1:500	
Donkey anti rabbit IgG 594		Alexa A-2106	1:500	

MATERIALS AND METHODS

The muscle biopsy specimen investigated in this study have been initially collected for diagnostic purposes. Written informed consent was obtained from the participants (or rather their legal guardians) for the participation into the subsequent research as well as for publication of the findings (including any potentially-identifying information). Ethical approval was not required as per the local legislation.

Immunofluorescence-Based Studies in Muscle Biopsies

Five micrometer cryosections of muscle biopsy specimen were generated, dried and afterwards re-hydrated in phosphate-buffered saline (PBS) followed by exposure to primary antibodies (**Table 1**) diluted in 1% bovine serum albumin (BSA). After incubation of the sections in a wet-chamber for one hour at 25°C (incubator), those were washed three times in PBS. Next, the secondary antibodies (Alexa 488-conjugated) 1:500 diluted in 1% BSA were added and sections were again incubated in a wet-chamber for one hour at 25°C. Prior sections were finally covered in mounting medium (Dako), three washing steps in PBS were performed.

Immunoblot-Based Studies on Whole Muscle Protein Extracts

Twenty micrograms of patient skeletal muscle protein lysates were prepared using NuPAGE LDS sample buffer (Thermo) and NuPAGE reducing agent, denatured at room temperature for 10 minutes and loaded into 4–12% gradient SDS-PAGE gels (Thermo, NP0322). Proteins were separated and transferred to a PVDF membrane using an iBlot2 dry transfer system (Thermo). PVDF membranes were blocked using 5% milk in Tris buffer-saline with 1% tween-20 (TBS-T) at room temperature for 1 hour

before probing using monoclonal antibodies targeting NDUFB8, SDHB, UQCRC2, COX2, and ATP5A (Abcam, ab110411) as well as antibodies targeting GAPDH (Abcam, ab8245) and VDAC1 (Abcam, ab14734). Membranes were washed in TBS-T and probed again for 1 h with HRP-conjugated anti-Mouse IgG (Abcam, ab97023) prior to chemiluminescent imaging. Quantification was performed using ImageJ.

Proteomic Profiling in Human Skeletal Muscle

Ammonium hydrogen carbonate (NH_4HCO_3), anhydrous magnesium chloride ($MgCl_2$), guanidine hydrochloride (GuHCl), iodoacetamide (IAA), and urea were purchased from Sigma-Aldrich, Steinheim, Germany. Tris base was obtained from Applichem Biochemica, Darmstadt, Germany and Sodium dodecyl sulfate (SDS) was purchased from Carl Roth, Karlsruhe, Germany. Dithiothreitol (DTT), EDTA-free protease inhibitor (Complete Mini) tablets were obtained from Roche Diagnostics, Mannheim, Germany. Sodium chloride (NaCl) and calcium chloride ($CaCl_2$) were from Merck, Darmstadt. Sequencing grade modified trypsin was from Promega, Madison, WI USA. Benzonase® Nuclease was purchased from Novagen. Bicinchoninic acid assay (BCA) kit was acquired from Thermo Fisher Scientific, Dreieich, Germany. All chemicals for ultra-pure HPLC solvents such as formic acid (FA), trifluoroacetic acid (TFA) and acetonitrile (ACN) were obtained from Biosolve, Valkenswaard, The Netherlands.

Cell Lysis, Sample Preparation and Trypsin Digestion

In total eight samples derived from four healthy controls (gender- and age-matched) and four MDC1A-patients were processes independently. All muscle samples were collected from the mid portion of vastus lateralis. Approximately 10 slices of 10 µm of muscle were lysed in 50 µL of lysis buffer (50 mM Tris-HCl (pH 7.8) 150 mM NaCl, 1% SDS, and Complete Mini) using a manual glass grinder. Then samples were centrifuged for 5 min at 4°C and 5.000 g. Protein concentration of the supernatant was determined by BCA assay (according to the manufacturer's protocol). In order to reduce the cysteines 10 mM of DTT were added to the samples followed by incubation at 56°C for 30 min. Next, the free thiol groups were alkylated with 30 mM IAA at room temperature (RT) in the dark for 30.

Sample digestion and cleanup were performed using filter-aided sample preparation (FASP) as described previously (16, 17) with some minor changes. Briefly, 100 µg of protein lysate was diluted 10-fold with freshly prepared 8 M urea/100 mM Tris-HCl (pH 8.5) buffer (18) and placed on a Microcon centrifugal device (30 KDa cutoff). Afterwards, the filter was centrifuged at 13,500 g at RT for 15 min (all the following centrifugation steps were performed under the same conditions). Three washing steps were carried out with 100 µL of 8 M urea/100 mM Tris-HCl (pH 8.5). For buffer exchange, the device was washed thrice with 100 µL of 50 mM NH_4HCO_3 (pH 7.8). Next, 100 µL of the digestion buffer (trypsin (Promega), 1:25 w/w, protease to substrate, (0.2 M GuHCl and 2 mM $CaCl_2$ in 50 mM NH_4HCO_3 pH 7.8), was added to the filter which contains the bound proteins and the samples were incubated at 37°C for 14 h. Resulting tryptic peptides were recovered by centrifugation with 50 µL of 50 mM NH_4HCO_3 followed by 50 µL of ultra-pure water. In the final step, tryptic peptides were acidified by adding 5 µl of 10 % TFA (v/v). The digests were quality controlled as described previously (19).

LC-MS/MS Analysis

Samples (technical duplicates) were measured using an Ultimate 3000 nano RSLC system coupled to an Orbitrap Fusion Lumos mass spectrometer (both Thermo Scientific) and analyzed in a randomized order to minimize systematic errors. Firstly, peptides were preconcentrated on a 100 µm × 2 cm C18 trapping column for 10 min using 0.1 % TFA (v/v) at a flow rate of 20 µL/min. Next the separation of the peptides was performed on a 75 µm × 50 cm C18 main column (both Pepmap, Thermo Scientific) with a 120 min LC gradient ranging from 3 to 35 % of 84 % ACN, 0.1 % FA (v/v) at a flow rate of 230 nL/min. MS^1 spectra was acquired in the Orbitrap from 300 to 1,500 m/z at a resolution of 120,000 using the polysiloxane ion at *m/z* 445.12003 as lock mass (20),with maximum injection times of 50 ms. Next, top 10 most intense signals were selected for fragmentation by HCD with a collision energy of 30%. MS^2 spectra were acquired in the ion trap at a resolution of 120,000, with maximum injection times of 300 ms and a dynamic exclusion of 15 s. The ACG target was set at 2.0×10^3 ions for MS^2 and 2.0×10^5 for MS^2.

Label Free Data Analysis

Data analysis of the acquired label free quantitative MS data was performed using the Progenesis LC-MS software from Non-linear Dynamics (Newcastle upon Tyne, U.K.). Alignment of MS raw data was conducted by Progenesis, which automatically selected one of the LC-MS files as reference. Next, peak picking was performed and only features within retention time and *m/z* windows from 0 to 120 min and 300–1,500 m/z, with charge states +2, +3, and +4 were considered for peptide statistics, analysis of variance (ANOVA). The MS/MS spectra were exported as peak lists which were searched against a concatenated target/decoy version of the mouse Uniprot database (Homo sapiens with 20273 entries, downloaded 22.07.2017) using Mascot 2.4 (Matrix Science), MS-GF+, and X!Tandem Jackhammer (2013.06.15) with the help of searchGUI 1.14.4 (21). Trypsin with a maximum of two missed cleavages was selected as enzyme. Carbamidomethylation of Cys was set as fixed and oxidation of Met was selected as variable modification. MS and MS/MS tolerances were set to 10 ppm and 0.5 Da, respectively. Combined search results were filtered at a false discovery rate (FDR) of 1 % on the protein level and exported using PeptideShaker 0.28.0 (http://code.google.com/p/peptide-shaker/). Data was reimported into Progenesis and peptide sequences containing oxidized Met were excluded for further analysis. Only proteins that were quantified with unique peptides were exported. For each protein, the average of the normalized abundances (obtained from Progenesis) was calculated and used to determine the ratios between patients and control. Only proteins which were (*i*) commonly quantified in all the replicates with (*ii*) one unique peptides, (*iii*) an ANOVA *p*-value of ≤ 0.05

(Progenesis) and (*iv*) an average ratio $\leq \log_2 0.99$or $\geq \log_2 -0.9$ were considered as up respectively down regulated.

Data Plotting and Pathway Analysis

All data was plotted using Origin 6.0 and Adobe Illustrator. For pathway analysis, the GO ontology, KEGG and Reactome were used and data manually filtered for relevant pathways. The Proteomap was the online tool available (https://www.proteomaps.net/). The annotation of these proteomaps is based on the KEGG database platform, each protein is shown by a polygon, and functionally relevant proteins are arranged as neighbors. Additionally, polygon areas represent protein abundances weighted by protein size.

RESULTS

Clinical and Genetic Findings

We followed six patients diagnosed with CMD type 1A in the Department of Neuropediatrics of the University Children's Hospital, University Duisburg-Essen, in a tertiary care setting. Mutations in *LAMA2* were found in all patients; however, one patient, who was severely affected, was lost of follow-up at the age of 2 years (patient 1).

Table 2 summarizes the molecular genetic, clinical and neuroradiologic findings. All six patients presented with symptoms within the first 4 months of life: poor head control, generalized muscular hypotonia and muscular weakness, poor spontaneous movements, delayed motor milestones, and high levels of creatine kinase (CK). The highest measured CK levels are listed in **Table 2**. The six children never achieved ambulation. Patient 5 was able to walk with support, but after a febrile virus infection with rhabdomyolysis at the age of 20 months she had a dramatic loss of motor function. Currently, at the age of 35 months, she showed a recovery with the ability to stand with support. All patients had dysphagia, recurrent chest infections and need varying levels of pulmonal support (i.e., cough assist). Additionally, joint contractures were present in all six patients. In patients 2–6, the underlying genetic mutations segregate with the phenotypes.

Four of our six patients underwent brain MRI, and three of the four showed white matter lesions (WMLs) on T2-weighted brain MRI images. The WMLs were characterized by a diffuse symmetrical distribution in cerebral areas that are normally myelinated in the developing brain (**Figure 1**) without involvement of thalamus or brainstem in both cases. Lissencephaly could not be detected in our patients. Patient 1 had a brain MRI performed at the age 4 months, which might be too early to detect WML in laminin-211-deficiency. All patients had normal cognitive development with no seizures being reported.

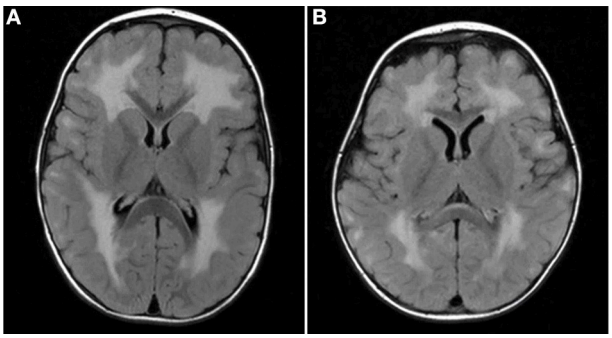


FIGURE 1 | MRI findings in MDC1A-patients included in the study. Brain MRI TIRM (Turbo-Inversion Recovery-Magnitude, axial) show diffuse symmetrical white matter lesions predominantly in the periventricular regions and no involvement of thalamus or brainstem in both cases. **(A)** Patient 3 with expanded supratentorial leukencephalopathy at two years of age. **(B)** Patient 4 diffuse leukencephalopathy.

Muscle Biopsy Findings

Frozen biopsied muscle tissue samples from all six patients were analyzed and showed severe features of muscular dystrophy including increased extracellular connective tissue with fibrosis, cell necrosis, numerous central nuclei, and high fiber size variability (**Figure 2A**). All patients presented total absence of laminin-211 in our immunofluorescence-based microscopic examinations (**Figure 2A**). Moreover, laminin-511 was mild do moderately increased in the muscle biopsy specimen of the six patients as shown for two representative cases in **Figure 2B**. As controls, we selected subjects who had underwent a muscle biopsy, but who were found not to have any signs of a skeletal muscle disease.

Loss of LAMA2 Induces Changes in General Protein Composition in Human Skeletal Muscle

Proteomic profiling is a useful approach to obtain unbiased insights into the molecular etiology of diseases such as muscular disorders (24, 25). To identify, molecular marker proteins for muscle fiber vulnerability due to the loss of functional laminin-211 (protein encoded by *LAMA2*), the proteomic signature of muscle biopsy specimen of four MDC1A-patients (patients 1–4; see **Table 2**) from the severe spectrum of the disease was compared to the signature in four controls. Using liquid chromatography coupled to tandem mass spectrometry (LC-MS/MS) (label free protein quantification) (**Figure 3**), we quantified 1977 proteins out of which 86 proteins presented (4.3%) with statistically significant altered abundances (35 were increased and 51 decreased; **Table 3**). The considerable decrease of laminin-211 (-3.84; $\log_2$) in the patient-derived samples hereby reflects the sensitivity of our proteomic profiling approach as well as the reliability of the data. To obtain insights into the molecular etiopathology of MDC1A, pathway analyses were performed utilizing DAVID (https://david.ncifcrf.gov/), KEGG (www.genome.jp/kegg/pathway.html), Reactome (www.reactome.org) and Proteomap (www.proteomaps.net). In addition, information concerning subcellular localization and function has been extracted from uniport (www.uniprot.org) for each protein altered in abundance to provide a complete picture of the molecular basis of MDC1A manifestation in skeletal muscle (**Table 3**). Data analysis via diverse pathway analysis tools revealed potential changes in axon guidance,

TABLE 2 | Clinical findings in MDC1A patients included in the overall study.

Patient	Age at last visit	Mutation	Achieved motor milestone	Onset of symptoms	Age at biopsy	Inheritance	CK	Cardial function	Pulmonal function	cMRI
1 (female)	2 y		Free sitting after being placed at 14 months of age	Reduced child movements during pregnancy. pp: muscular weakness	2 m	Unknown	4,000	Normal	Normal	At 4m of age normal
2 (male)	7 y	Homozygous: c.5134_5153del (leading to a premature stop-codon; p.Arg1712Glufs*4)	Free sitting at 18 months of age, able to scoot on his bottom	At the 3 months of age not able to lift the head and poor head control	9 m	Recessive	3,434	Normal	Normal	Not done
3 (male)	6 y	Homozygous: c.7898+2T>G (presumably leading to skipping of exon 56; pathogenicity of an adjacent mutation) (c.7898+1G>T) has already been reported (22)	Free sitting at 10 months of age after being placed	pp: muscular weakness	14 m	Recessive	1,584	Corrected QT interval of 451 m/sec (<440) ECHO normal	Normal	Leuko-encephalo-pathy
4 (male)	4 y	Compound heterozygous: c.397_397delG & c.1884+2T>C	Free sitting at 30 months of age after being placed sitting after being placed	pp: muscular weakness	4 m	Recessive	7,400	Normal	Normal	Leuko-encephalo-pathy
5 (female)	3y	Homozygous: c.8244+1G>A (rs749522728); (23)	Walking at 18 months of age with support	At the 4 months of age not able to lift the head and muscular weakness. Rhabdomyolysis at the age of 20 months	26m	Recessive	2,7000	Normal	Normal	Not done
6 (female)	2y	Homozygous: deletion of exons 31-40 (diagnosed via MLPA)	Free sitting at 14 months of age after being placed sitting after being placed	At the 3 months of age not able to lift the head and muscular weakness.	14m	Recessive	5,200	Normal	Normal	Leuko-encephalo-pathy

Y, years; m, month; pp, post-partal; CK, creatine kinase; cMRI, cranial magnetic resonance imaging.

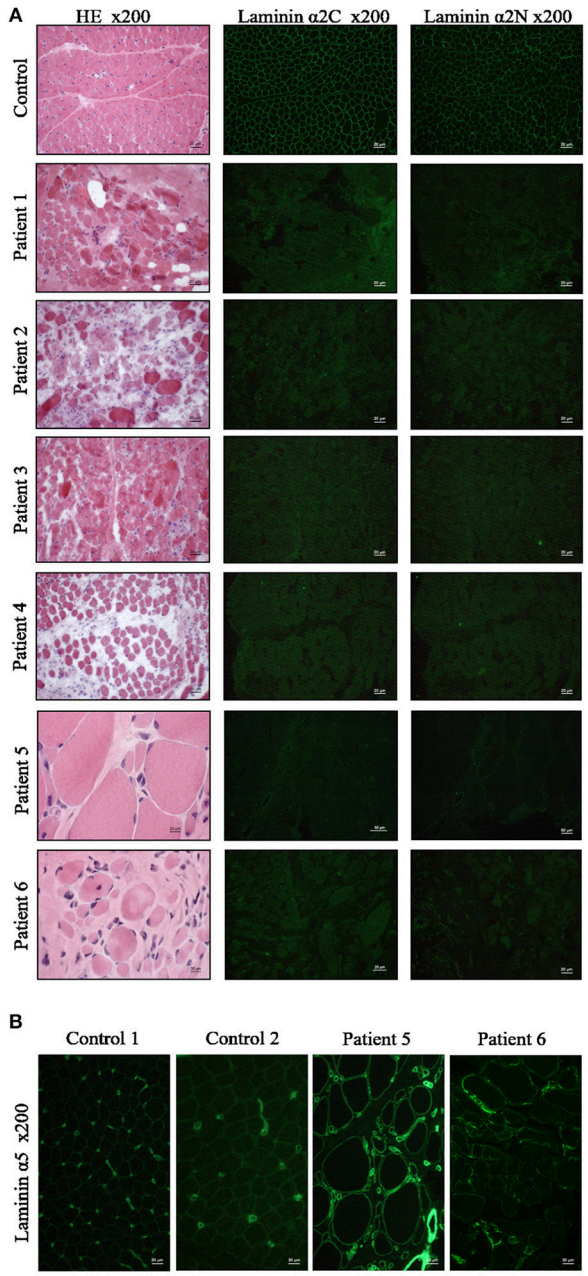


FIGURE 2 | Muscle biopsy findings in MDC1A-patients included in the study. **(A)** Muscle biopsy cryostat sections stained with hematoxylin and eosin (HE) and immunofluorescence staining with anti-laminin-211 antibodies reveals absent immunoreactivity in the patient-derived sections. **(B)** Immunofluorescence staining of muscle cryostat sections with anti-laminin-511 antibody reveals in increased immunoreactivity in muscle biopsies of MDC1A-patients as indicated for two representative cases shown here. Ctrl, control muscle; numbers 1, 2, 3, 4, 5, and 6 refer to muscle biopsies derived from MDC1A-patients with the corresponding patient numbers listed in **Table 2**.

cell cycle and DNA-repair, extracellular matrix organization, metabolism of fatty acids, sugar, lipids and proteins. In addition, protein changes seem to impact on vesicular transport machinery, TCA and respiratory electron transport as well as proper muscle contraction (**Figure 3C**). Data analysis via Proteomap confirmed the impact of detected protein changes on cell cycle, cellular metabolism, muscle contraction as well as on the composition of the extracellular matrix. Based on the functional properties of some of the proteoglycans with altered abundances such as COL1A1 and -A2, LAMA4 and ITGA6, changes in PI3K/Akt-signaling as a pathway involved in a variety of cellular functions has been highlighted by the Proteomaps-representation (**Figure 3D**). This molecular observation accords with a postulated function of laminin-211 in signal transmission (9).

Perturbed proteins represent tissue markers for *LAMA2*-related congenital myopathy and—based on information available in uniport—mainly localize to the sarcoplasm, to nuclei, the SR and to mitochondria thus suggesting a global unified organelle vulnerability in LAMA2-mutant skeletal muscle with a predominance to mitochondria. In addition, functions of several of the accord proteins accord with the known involvement of laminin-211 in ECM-composition, signal transduction, cytoskeleton, mitochondrial homeostasis and muscle cell development. Interestingly, functions of a variety of proteins increased in abundance hint toward the activation of neuroprotective mechanisms including neuromuscular transmission.

Altered Abundance of Paradigmatic Proteins and Mitochondrial Vulnerability Can Be Confirmed in Independent Muscle Biopsies Derived From MDC1A-Patients

To study the potential of altered proteins as tissue markers and reliability of our proteomic findings further immunofluorescence studies were performed on the muscle biopsies derived from the four patients included in the proteomic profiling (patients 1–4) as well as on biopsies derived from two further MDC1A-cases (patients 5 and 6). Doing so, we focused on abundances and distribution of agrin, glypican-1, and glucose-6-phosphate isomerase as paradigmatic proteins. Immunofluorescence-based studies of agrin showed occasionally focal sarcoplasmic accumulations most likely leading to the detected increase of overall agrin protein level (**Table 3**) as shown for two representative cases in **Figure 4A**. In comparison to the controls which show an enrichment of glypican-1 at the sarcolemma, in MDC1A-patient derived biopsies, small sarcoplasmic dots immunoreactive for the protein as well as an enrichment of these dots at the (sub-)sarcolemmal region could be observed. This irregular protein-distribution is shown for two representative cases in **Figure 4A** and most likely causes the 3.25-fold (log2 ratio) increase detected by proteomic profiling. Moreover, immunofluorescence studies confirmed the decreased expression of glucose-6-phosphate isomerase in muscle biopsies derived from four MDC1A-cases (shown for two representative cases in **Figure 4A**).

Given that our proteomic data revealed a profound vulnerability of NADH dehydrogenases, NADH muscle histology (NADH-TR to highlight the oxidative enzyme

TABLE 3 | List of proteomic findings.

Accession	Pep. count/ uniq. Pep.	Anova (p)	Description	Localization	Fold of regu-lation	Log2	Function
P15502	1/1	0.02	Elastin (*ELN*)	ECM	112.37	6.81	Extracellular matrix structural constituent
Q9GZT8	2/1	0.00	NIF3-like protein 1 (*NIF3L1*)	Nucleus	70.76	6.14	Negatively regulating the expression of genes involved in neuronal differentiation
P09486	2/2	0.00	SPARC (*SPARC*)	ECM	32.77	5.03	Regulates cell growth through interactions with the extracellular matrix and cytokines
P20472	7/5	0.00	Parvalbumin alpha (*PVALB*)	Nucleus	15.34	3.94	Involved in muscle-relaxation after contraction
P35052	1/1	0.00	Glypican-1 (*GPC1*)	ECM	9.51	3.25	Binds collagen and participates in Schwann cell myelination
Q8N414	1/1	0.04	PiggyBac transposable element-derived protein 5 (*PGBD5*)	Nucleus	7.63	2.93	Targets regulatory elements and tumor suppressor genes and promotes cell transformation
Q16363	18/17	0.02	Laminin subunit alpha-4 (*LAMA4*)	ECM	5.42	2.44	Mediates attachment, migration and organization of cells into tissues during embryonic development by interacting with other extracellular matrix components
P02452	34/31	0.04	Collagen alpha-1(I) chain (*COL1A1*)	ECM	5.06	2.34	Extracellular matrix structural constituent
P08123	15/15	0.04	Collagen alpha-2(I) chain (*COL1A2*)	ECM	4.93	2.30	Extracellular matrix structural constituent
O00468	5/5	0.02	Agrin (*AGRN*)	Synaptic cleft	4.77	2.25	Formation and the maintenance of the NMJ and postsynaptic differentiation
Q8WVJ2	2/2	0.00	NudC domain-containing protein 2 (*NUDCD2*)	Cyto-skeleton	4.66	2.22	Regulates the LIS1/dynein pathway by stabilizing LIS1 with Hsp90 chaperone
Q04917	10/5	0.04	14-3-3 protein eta (*YWHAH*)	Cytosol	4.17	2.06	Promotes myosin II turnover in the cell cortex and modulates cortical tension, cell shape, and cytokinesis (doi: 10.1074/jbc.M117.819391)
P62888	4/4	0.05	60S ribosomal protein L30 (*RPL30*)	Cytosol	4.14	2.05	Protein synthesis
P29400	2/1	0.05	Collagen alpha-5(IV) chain (*COL4A5*)	ECM	3.90	1.96	Extracellular matrix structural constituent
P12829	14/11	0.02	Myosin light chain 4 (*MYL4*)	Cyto-skeleton	3.75	1.91	Regulatory light chain of myosin
Q14314	2/2	0.02	Fibroleukin (*FGL2*)	ECM	3.38	1.75	Playa a role in physiologic lymphocyte functions
P02766	9/8	0.03	Transthyretin (TTR)	ECM	2.98	1.58	Protects against misfolding and the formation of amyloid fibrils
Q14247	2/2	0.01	Src substrate cortactin (SRC8_HUMAN)	Plasma membrane	2.92	1.55	Plays a role in the regulation of neuron morphology, axon growth and formation of neuronal growth cones
P08697	5/5	0.05	Alpha-2-antiplasmin (*SERPINF2*)	ECM	2.91	1.54	Serine protease inhibitor
P23229	2/2	0.04	Integrin alpha-6 (*ITGA6*)	Plasma membrane	2.90	1.54	Integrin alpha-6/beta-1 is a receptor for laminin
P50454	14/14	0.03	Serpin H1 (*SERPINH1*)	Endoplas-mic Reticulum	2.80	1.48	Chaperone in the biosynthetic pathway of collagen
Q9BZQ8	5/5	0.02	Protein Niban (*FAM129A*)	Endoplas-mic Reticulum	2.75	1.46	Involved in the Endoplasmic Reticulum stress response
Q15417	5/5	0.05	Calponin-3 (*CNN3*)	Cyto-skeleton	2.66	1.41	Thin filament-associated protein that is implicated in the regulation and modulation of muscle contraction
P04003	12/10	0.04	C4b-binding protein alpha chain (*C4BPA*)	ECM	2.62	1.39	Controls the classical pathway of complement activation
P50895	10/10	0.01	Basal cell adhesion molecule (*BCAM*)	Plasma membrane	2.62	1.39	Laminin alpha-5 receptor
P40261	8/8	0.04	Nicotinamide N-methyltransferase (*NNMT*)	Cytoplasm	2.54	1.35	Catalyzes the N-methylation of nicotinamide and other pyridines to form pyridinium ions

(Continued)

TABLE 2 | Continued

Accession	Pep. count/ uniq. Pep.	Anova (p)	Description	Localization	Fold of regu-lation	Log2	Function
Q15651	3/1	0.02	High mobility group nucleosome-binding domain-containing protein 3 (*HMGN3*)	Nucleus	2.45	1.29	Regulates chromatin-dependent processes such as transcription, DNA-replication and -repair
Q8N3D4	3/3	0.04	EH domain-binding protein 1-like protein 1 (*EHBP1L1*)	Endosome	2.39	1.26	Rab effector protein playing a role in vesicle trafficking
Q9UEY8	3/3	0.03	Gamma-adducin (*ADD3*)	Plasma membrane	2.35	1.23	Membrane-cytoskeleton-associated protein that promotes the assembly of the spectrin-actin network and plays a role in actin filament capping
Q8NC56	1/1	0.05	LEM domain-containing protein 2 (*LEMD2*)	Nucleus	2.34	1.22	Involved in nuclear structure organization
P02760	10/10	0.04	Protein AMBP (*AMBP*)	ECM	2.24	1.16	Elastase inhibitor
Q96AQ6	19/18	0.01	Pre-B-cell leukemia transcription factor-interacting protein 1 (*PBXIP1*)	Nucleus	2.20	1.14	Tethers estrogen receptor-alpha (ESR1) to microtubules and allows them to influence estrogen receptors-alpha signaling
Q14BN4	5/5	0.03	Sarcolemmal membrane-associated protein (*SLMAP*)	Plasma membrane	2.10	1.07	Plays a role during myoblast fusion
O43488	4/4	0.05	Aflatoxin B1 aldehyde reductase member 2 (*AKR7A2*)	Golgi apparatus	2.09	1.07	Plays an important role in producing the neuromodulator gamma-hydroxybutyrate (GHB)
P14649	25/22	0.03	Myosin light chain 6B (*MYL6B*)	Cytoskeleton	2.08	1.05	Regulatory light chain of myosin
P09960	11/10	0.03	Leukotriene A-4 hydrolase (*LTA4H*)	Cytoplasm	0.53	−0.92	Biosynthesis of proinflammatory mediator leukotriene B4
Q16775	6/6	0.04	Hydroxyacylglutathione hydrolase, mitochondrial (*HAGH*)	Mito-chondria	0.53	−0.92	Catalyzes the hydrolysis of S-D-lactoyl-glutathione to form glutathione and D-lactic acid
O43598	2/2	0.03	2′-deoxynucleoside 5′-phosphate N-hydrolase 1 (*DNPH1*)	Nucleus	0.53	−0.93	Catalyzes the cleavage of the N-glycosidic bond of deoxyribonucleoside 5′-monophosphates
Q3L8U1	1/1	0.05	Chromodomain-helicase-DNA-binding protein 9 (*CHD9*)	Nucleus	0.52	−0.95	Transcriptional coactivator for PPARA and possibly other nuclear receptors
Q9H0R4	1/1	0.03	Haloacid dehalogenase-like hydrolase domain-containing protein 2 (*HDHD2*)	ECM	0.52	−0.95	Phosphotase activity
P06744	24/24	0.02	Glucose-6-phosphate isomerase (*GPI*)	ECM	0.52	−0.95	Neurotrophic factor for spinal and sensory neurons
P10515	11/11	0.03	Dihydrolipoyllysine-residue acetyltransferase component of pyruvate dehydrogenase complex (*DLAT*)	Mito-chondria	0.51	−0.96	Catalyzes the overall conversion of pyruvate to acetyl-CoA and CO_2
P30086	21/20	0.01	Phosphatidylethanolamine-binding protein 1 (*PEBP1*)	Cytoplasm	0.51	−0.96	Involved in the function of the presynaptic cholinergic neurons of the central nervous system; increases the production of choline acetyltransferase but not acetylcholinesterase
Q9UI09	3/2	0.05	NADH dehydrogenase [ubiquinone] 1 alpha subcomplex subunit 12 (*NDUFA12*)	Mito-chondria	0.51	−0.96	Accessory subunit of the mitochondrial membrane respiratory chain NADH dehydrogenase (complex I)
Q02218	29/26	0.04	2-oxoglutarate dehydrogenase, mitochondrial (*OGDH*)	Mito-chondria	0.51	−0.96	2-oxoglutarate dehydrogenase (E1) component of the 2-oxoglutarate dehydrogenase complex
P09972	11/2	0.02	Fructose-bisphosphate aldolase C (*ALDOC*)	Cytoplasm	0.51	−0.97	Glycolysis
P49821	18/16	0.03	NADH dehydrogenase [ubiquinone] flavoprotein 1 (*NDUFV1*)	Mito-chondria	0.50	−0.99	Core subunit of the mitochondrial membrane respiratory chain NADH dehydrogenase (Complex I)
O95298	2/2	0.05	NADH dehydrogenase [ubiquinone] 1 subunit C2 (*NDUFC2*)	Mito-chondria	0.50	−0.99	Accessory subunit of the mitochondrial membrane respiratory chain NADH dehydrogenase (Complex I)

(Continued)

TABLE 2 | Continued

Accession	Pep. count/ uniq. Pep.	Anova (p)	Description	Localization	Fold of regu-lation	Log2	Function
P21796	22/20	0.05	Voltage-dependent anion-selective channel protein 1 (*VDAC1*)	Mito-chondria	0.50	−0.99	Forms a channel through the mitochondrial outer membrane; allows diffusion of small hydrophilic molecules
P00918	15/12	0.05	Carbonic anhydrase 2 (*CA2*)	Plasma membrane	0.50	−0.99	Contributes to intracellular pH regulation
Q16718	6/6	0.03	NADH dehydrogenase [ubiquinone] 1 alpha subcomplex subunit 5 (*NDUFA5*)	Mito-chondria	0.49	−1.00	Accessory subunit of the mitochondrial membrane respiratory chain NADH dehydrogenase (Complex I)
P83111	6/6	0.04	Serine beta-lactamase-like protein LACTB, (*LACTB*)	Mito-chondria	0.49	−1.01	Serine protease that acts as a regulator of mitochondrial lipid metabolism
Q8TCA0	6/6	0.05	Leucine-rich repeat-containing protein 20 (*LRRC20*)	Information not available	0.49	−1.01	Information not available
P20674	8/8	0.04	Cytochrome c oxidase subunit 5A, (*COX5A*)	Mito-chondria	0.49	−1.02	This is the heme A-containing chain of cytochrome c oxidase
Q96A26	4/4	0.04	Protein FAM162A (*F162A*)	Mito-chondria	0.48	−1.04	Involved in hypoxia-induced cell death of neuronal cells
Q16555	18/13	0.01	Dihydropyrimidinase-related protein 2 (*DPYSL2*)	Cytoplasm	0.48	−1.04	Plays a role in neuronal development and polarity, as well as in axon growth and guidance, neuronal growth cone collapse and cell migration
P04179	9/8	0.00	Superoxide dismutase [Mn], (*SOD2*)	Mito-chondria	0.48	−1.05	Destroys superoxide anion radicals
O96000	7/7	0.03	NADH dehydrogenase [ubiquinone] 1 beta subcomplex subunit 10 (*NDUFB10*)	Mito-chondria	0.48	−1.05	Accessory subunit of the mitochondrial membrane respiratory chain NADH dehydrogenase (Complex I)
P51649	12/12	0.03	Succinate-semialdehyde dehydrogenase, (*ALDH5A1*)	Mito-chondria	0.48	−1.05	Catalyzes one step in the degradation of the inhibitory neurotransmitter gamma-aminobutyric acid (GABA)
P23458	1/1	0.05	Tyrosine-protein kinase JAK1 (*JAK1*)	Cytoplasm	0.48	−1.06	Tyrosine kinase of the non-receptor type, involved in the IFN-alpha/beta/gamma signal pathway
P06732	69/41	0.03	Creatine kinase M-type (*CKM*)	Cytoplasm	0.48	−1.07	Reversibly catalyzes the transfer of phosphate between ATP and various phosphogens
O95139	3/3	0.04	NADH dehydrogenase [ubiquinone] 1 beta subcomplex subunit 6 (*NDUFB6*)	Mito-chondria	048	−1.07	Accessory subunit of the mitochondrial membrane respiratory chain NADH dehydrogenase (Complex I)
P40925	18/18	0.02	Malate dehydrogenase, cytoplasmic (*MDH1*)	Cytoplasm	0.47	−1.08	Malic enzyme activit
A8MU46	9/7	0.04	Smoothelin-like protein 1 (*SMTNL1*)	Nucleus	0.47	−1.09	Regulation of contractile properties of muscles
O95169	4/4	0.03	NADH dehydrogenase [ubiquinone] 1 beta subcomplex subunit 8, (*NDUFB8*)	Mito-chondria	0.46	−1.10	Accessory subunit of the mitochondrial membrane respiratory chain NADH dehydrogenase (Complex I)
P36957	14/12	0.03	Dihydrolipoyllysine-residue succinyltransferase component of 2-oxoglutarate dehydrogenase complex, (*DLST*)	Mito-chondria	0.46	−1.11	Dihydrolipoamide succinyltransferase (E2) component of the 2-oxoglutarate dehydrogenase complex
Q9NVS9	2/2	0.01	Pyridoxine-5′-phosphate oxidase (*PNPO*)	Cytoplasm	0.46	−1.12	Catalyzes the oxidation of either pyridoxine 5′-phosphate (PNP) or pyridoxamine 5′-phosphate (PMP) into pyridoxal 5′-phosphate (PLP)
Q9NPJ3	3/3	0.00	Acyl-coenzyme A thioesterase 13 (*ACOT13*)	Cytoplasm	0.46	−1.12	Catalyzes the hydrolysis of acyl-CoAs to the free fatty acid and coenzyme A
Q9P0J0	7/7	0.05	NADH dehydrogenase [ubiquinone] 1 alpha subcomplex subunit 13 (*NDUFA13*)	Mito-chondria	0.46	−1.13	Accessory subunit of the mitochondrial membrane respiratory chain NADH dehydrogenase (Complex I)

(Continued)

TABLE 2 | Continued

Accession	Pep. count/ uniq. Pep.	Anova (p)	Description	Localization	Fold of regu-lation	Log2	Function
P51970	8/8	0.04	NADH dehydrogenase [ubiquinone] 1 alpha subcomplex subunit 8 (*NDUFA8*)	Mito-chondria	0.46	−1.13	Accessory subunit of the mitochondrial membrane respiratory chain NADH dehydrogenase (Complex I)
P00395	4/4	0.05	Cytochrome c oxidase subunit 1 (*MT-CO1*)	Mito-chondria	0.45	−1.17	Component of the respiratory chain that catalyzes the reduction of oxygen to water
P61019	4/4	0.00	Ras-related protein Rab-2A (*RAB2A*)	Endoplas-mic Reticulum	0.44	−1.19	Protein transport from the endoplasmic reticulum to the Golgi complex
O00217	3/3	0.04	NADH dehydrogenase [ubiquinone] iron-sulfur protein 8, (*NDUFS8*)	Mito-chondria	0.43	−1.20	Core subunit of the mitochondrial membrane respiratory chain NADH dehydrogenase (Complex I)
Q9UKU7	4/4	0.05	Isobutyryl-CoA dehydrogenase, (*ACAD8*)	Mito-chondria	0.43	−1.21	Plays a role in transcriptional coactivation within the ARC complex
P13798	8/8	0.00	Acylamino-acid-releasing enzyme (*APEH*)	Cytoplasm	0.43	−1.21	Catalyzes the hydrolysis of the N-terminal peptide bond of an N-acetylated peptide to generate an N-acetylated amino acid
P53778	3/2	0.05	Mitogen-activated protein kinase 12 (*MAPK12*)	Cytoplasm	0.42	−1.23	Essential component of the MAP kinase signal transduction pathway; In skeletal muscle colocalizes with SNTA1 at the neuromuscular junction and throughout the sarcolemma
O43676	1/1	0.03	NADH dehydrogenase [ubiquinone] 1 beta subcomplex subunit 3 (*NDUFB3*)	Mito-chondria	0.41	−1.26	Accessory subunit of the mitochondrial membrane respiratory chain NADH dehydrogenase (Complex I)
Q9NUU6	1/1	0.02	Inactive ubiquitin thioesterase FAM105A (*FAM105A*)	Information not available	0.40	−1.29	Information not available
Q93100	4/3	0.05	Phosphorylase b kinase regulatory subunit beta (*PHKB*)	Plasma membrane	0.36	−1.45	Catalyzes the phosphorylation of serine in certain substrates, including troponin I
Q8TAT6	3/3	0.01	Nuclear protein localization protein 4 homolog (*NPLOC4*)	Endoplas-mic Reticulum	0.36	−1.45	Binds ubiquitinated proteins and is necessary for the export of misfolded proteins from the ER to the cytoplasm, where they are degraded by the proteasome
Q9H7C9	4/4	0.02	Mth938 domain-containing protein (*AAMDC*)	Cytoplasm	0.36	−1.47	Plays a role in preadipocyte differentiation and adipogenesis
Q8N8N7	5/5	0.02	Prostaglandin reductase 2 (*PTGR2*)	Cytoplasm	0.29	−1.81	Functions as 15-oxo-prostaglandin 13-reductase; overexpression represses transcriptional activity of PPARG and inhibits adipocyte differentiation
P02792	4/4	0.01	Ferritin light chain (*FTL*)	Cytoplasm	0.27	−1.86	Stores iron in a soluble, non-toxic, readily available form
Q14558	1/1	0.01	Phosphoribosyl pyrophosphate synthase-associated protein 1 (*PRPSAP1*)	Cytoplasm	0.17	−2.57	Negative regulatory role in 5-phosphoribose 1-diphosphate synthesis
P29350	2/2	0.04	Tyrosine-protein phosphatase non-receptor type 6 (*PTPN6*)	Nucleus	0.15	−2.73	Modulates signaling by tyrosine phosphorylated cell surface receptors such as KIT and the EGF receptor/EGFR
Q8NDH3	1/1	0.00	Probable aminopeptidase NPEPL1 (*NPEPL1*)	Nucleus	0.13	−2.90	Catalyzes the removal of unsubstituted N-terminal amino acids from various peptides
P24043	50/48	0.00	Laminin subunit alpha-2 (*LAMA2*)	ECM	0.07	−3.84	Binding to cells via a high affinity receptor, laminin; mediates the attachment, migration, and organization of cells into tissues during embryonic development by interacting with other extracellular matrix components

Pep, peptides; uniq, unique. Information concerning subcellular localization and protein function were obtained from uniprot. ECM, extra cellular matrix.

activity) has been investigated in biopsies of six MDC1A-cases and revealed no structural abnormalities like cores, whorles or lobulated fibers but reduced staining and even gaps in some muscle fibers indicative for reduced enzyme activity (shown for four representative cases in **Figure 4B**). Modified Gomori Trichrome staining has additionally been performed in these patients to study mitochondrial abnormalities and occasionally revealed both, focal accumulations and reduced staining suggesting irregular mitochondrial distribution (shown for four representative cases in **Figure 4B**). Immunofluorescence studies of Glucose-6-phosphate isomerase (GPI), glypican-1 and agrin have been carried out twice with similar results. Prompted by the proteomic results suggestive for vulnerability of the respiratory chain, respective complexes have been investigated by immunoblotting utilizing antibodies targeting proteins localized to the respective complexes and muscle protein extracts derived from two controls and three MDC1A-patients. Results of these studies confirm a vulnerability of the respiratory chain complexes (**Figure 4C**) and thus support our proteomic findings which were indicative for mitochondrial vulnerability. Immunoblot studies have been carried out twice with similar results.

DISCUSSION

A complete loss of laminin-211, which is encoded by *LAMA2*, causes a severe congenital muscular dystrophy with onset of symptoms in the first few months of life. Partial laminin-211 deficiency can be caused not only by primarily *LAMA2* mutations, but also secondarily by other muscular dystrophies, including dystroglycanopathy (26, 27). This in turn suggests the need to define tissue marker proteins for patients with classical MDC1A based on *LAMA2* mutations leading to laminin-211 deficiency. To systematically address this need, proteomic profiling has been carried out using muscle biopsy specimens derived from MDC1A patients with myopathy and brain malformations. Results not only confirm laminin-211 deficiency but also accord with elevated CK level in the patients as intramuscular CK was significantly decreased in the patient-derived muscle. In addition, decrease of Mth938 domain-containing protein (involved in preadipocyte differentiation and adipogenesis) as well as of prostaglandin reductase 2 (involved in inhibition of adipocyte differentiation) might provide a molecular link to a replacement of degenerating muscle fibers by fatty tissue. Based on the considerable increase of proteins localized to the extracellular matrix (**Table 3**) our data moreover confirm proliferation of connective tissue as a pathophysiological hallmark of fibrosis observed in the muscle biopsy specimen of our patients (**Figure 1**). The increase of LAMA4 (laminin subunit α4/ Lm-411) as well as of LAMA5 (laminin subunit α5/ Lm-511; identified by our routine diagnostic staining (**Figure 2B**) and 1.7-fold (log2 ratio) increased with a p-Anova of 0.19 in our proteomic findings; data not shown) most likely reflects a cellular attempt to (partially) compensate the loss of laminin-211 and to avoid a complete breakdown of muscle fibers. This assumption is not only supported by the results of a previous study showing that laminin-111 protein therapy reduces muscle pathology and improves viability of a MDC1A mouse model (28) but also by the known important role of LAMA4 for NMJ-integrity (29), the concomitant increase of integrin alpha-6/beta-1, a receptor for laminin and the increase of the basal cell adhesion molecule/ laminin alpha-5 receptor (**Table 3**) to optimize laminin binding to laminin-211-deficient muscle fibers. However, despite the increase of LAMA4 in MDC1A, the resultant laminin-protein complex is known to bind merely poorly to integrins and α-dystroglycan (30).

Given that subtle neuromuscular junction (NMJ) defects have been reported in laminin α2 chain-deficient mice (31), the detected abnormal sarcoplasmic accumulation and thus decreased release to the synaptic cleft of muscle agrin, a basal lamina glycoprotein crucial for the formation and the maintenance of NMJs, might contribute to impaired neuromuscular transmission as part of the MDC1A-pathophysiology. Along this line, increase of glypican-1, might indicate activation of a compensatory mechanism to avoid NMJ-breakdown resulting from profound de-innervation. Notably, mini-agrin has been shown to bind to the basement membrane and the DGC via α-dystroglycan and thus ameliorate muscle pathology *in vivo* (32) and transgenic expression of mini-agrin (contains binding sites for laminins and α-dystroglycan) and αLNNd (recombinant protein linking LAMA4 to α-dystroglycan) in a mouse model for MDC1A fully restored basement membrane stability. This effect resulted in recovery of muscle force and size leading to increased overall body weight, and extended life span (33). Moreover, glypican-1 has recently been linked to the pathophysiology of a muscular dystrophy complicated by a myasthenic syndrome (34) as well as of laminin α4, which has an important role in NMJ-integrity (29). However, the conclusion of endogenous activation of compensatory mechanisms in muscle of MDC1A-patients is further supported by the increase of C4b-binding protein alpha chain belonging to the complement system that deposits its activation products on innervated motor end-plates in ALS-patients (35).These combined findings in turn underline the significance our proteomic profiling data aiding the identification of marker proteins with pathophysiological relevance as well as impacts for attempts to develop new treatment strategies for MDC1A.

However, as the NMJ represents a paradigmatic synapse, altered abundance of a variety of other proteins including 14-3-3F, AKR7A2, protein FAM162A, GTPC1, NIBAN, PRVA, SRC8, Succinate-semialdehyde dehydrogenase, TTHY (**Table 3**), might correlate with the broad activation of neuroprotective mechanisms in the etiopathology of MDC1A and thus also link to the CNS alterations of the children. NudC domain-containing protein 2 modulates the LIS1/dynein pathway via stabilization of lissencephaly protein 1 (LIS1) with Hsp90, a cellular chaperone. Importantly, the p.L279P of NudC domain-containing protein 2 influences LIS1 stability (36). Given that lissencephaly has been described in MDC1A-patients (37) increase of this protein not only accords with the concept

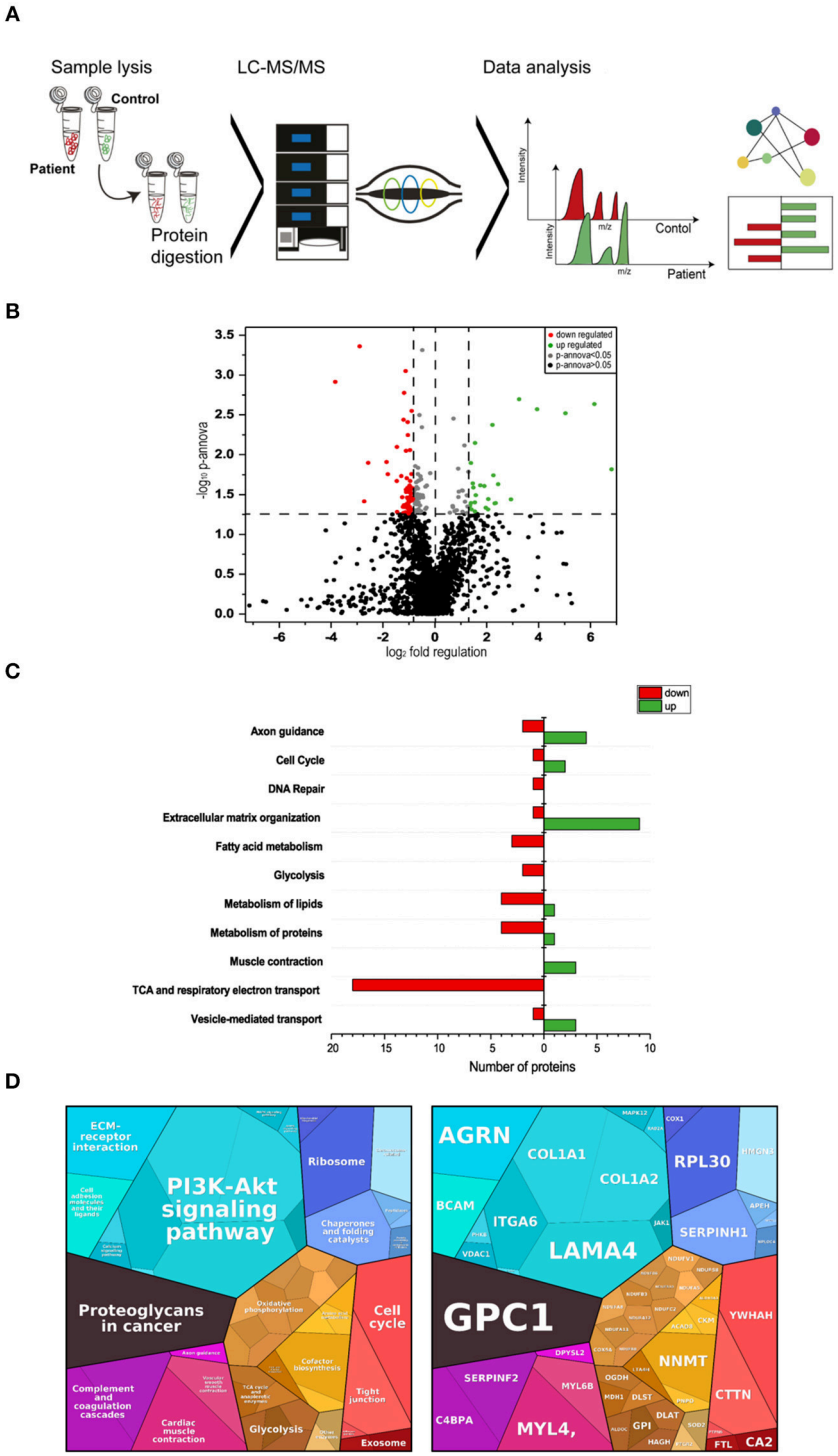


FIGURE 3 | Proteomic profiling of four MDC1A-patient derived muscles. **(A)** Methodological workflow applied in the study. **(B)** Results of our label-free proteomic profiling are shown as a volcano plot. All points (each one represents a protein) over the horizontal line have a statistically significant p-ANOVA of ≤0.05. In total, 51 proteins are decreased (red points) and 35 proteins are increased in abundance (green points) in laminin-211-deficient skeletal muscle. **(C)** Results of an *in silico* pathway analysis of proteins altered in abundance utilizing DAVID, KEGG, and Reactome platforms indicating alterations of ECM protein composition, cellular metabolism, axon guidance, cell cycle, and DNA repair, muscle contraction and of vesicular protein transport. **(D)** Results of an *in silico* pathway analysis of proteins altered in abundance utilizing Proteomap platform confirming the perturbed cellular functions indicated by the results of the previous pathway analysis and moreover indicating perturbed function of cellular signaling cascades such as PI3K-Akt signaling.

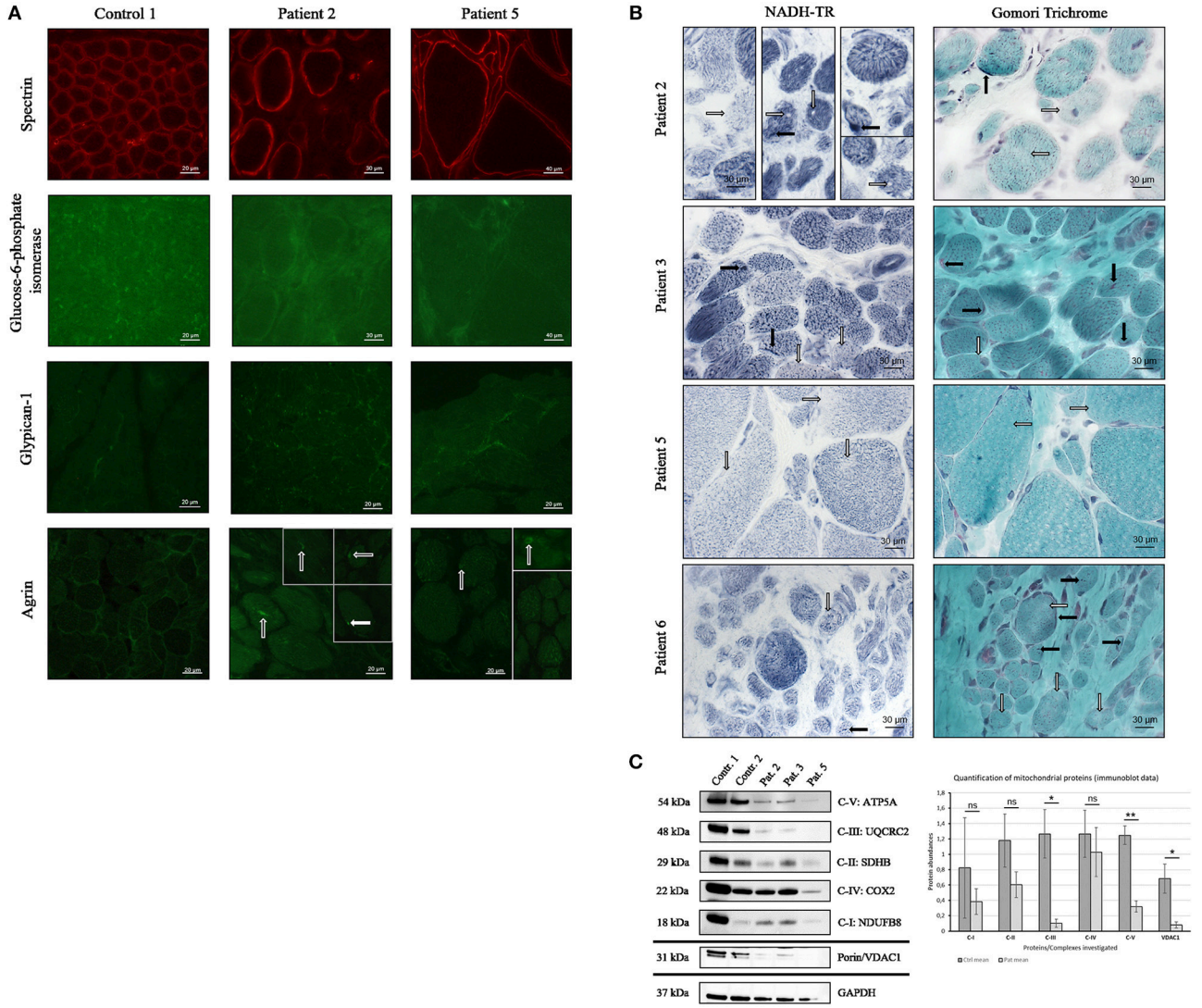


FIGURE 4 | Confirmation study of proteomic findings in independent MDC1A-patient derived muscle biopsies. **(A)** Immunofluorescence studies of spectrin have been carried out to visualize sarcolemma in muscle cryostat sections of control and patient-derived muscles and to show similar abundance and localization of the protein. Further immunofluorescence studies of glucose-6-phosphate isomerase reveal a focal dot-like sarcoplasmic staining/ enrichment in muscle biopsy specimen derived of controls (one representative control is shown here) but show a decrease in the biopsies of two representative MDC1A-patients. Immunofluorescence studies of glypican-1 showed focal enrichment at the sarcolemma of control muscle (one representative control is shown). However, in the LAMA2-diseased muscle fibers, small dots sarcoplasmic, and (sub-)sarcolemmal dots immunoreactive for glypican-1 were detected. Immunofluorescence studies of agrin revealed of a sarcoplasmic enrichment/ aggregation in MDC1A-patient derived muscle fibers (white arrows) compared to control muscle fibers. **(B)** Histological NADH-TR staining revealed "sarcoplasmic gaps" (white arrows in patient 2; second and third column) and reduced enzyme activity (white arrows in patient 2, 3, 5, and 6) as well as focal enrichment in some myofibers (black arrows in patient 2, 3, and 6). Modified Gomori Trichrome staining revealed sarcoplasmic areas with minor staining (white arrows in patient 2, 3, 5, and 6) as well as areas of sarcoplasmic and subsarcolemmal enrichment (black arrows in patient 2,3, and 5). **(C)** Immunoblot analysis of proteins representative for the respiratory chain complexes I-V and of VDAC1 (porin) revealed a statistically significant decrease of complexes III and V as well as of VDAC1 in MDC1A-patient derived protein muscle extracts compared to controls (diagram). GAPDH has been used as loading control and proteins have been quantified against GAPDH (ns, not significant; *statistically significant, **statistically very significant).

of activation of proteins involved in neuroprotection (in none of our patients lissencephaly was found via MRI) but also provides a first molecular hint to the manifestation of lissencephaly in the etiopathology of MDC1A. Neuronal vulnerability associated with altered synaptic transmission—as one pathophysiological cascade among others—is indicated by the decrease of glucose-6-phosphate isomerase, acting as a neurotrophic factor for spinal and sensory neurons (38), of phosphatidylethanolamine-binding protein 1 involved in the function of the presynaptic cholinergic neurons of the central nervous system, of dihydropyrimidinase-related protein 2 involved in neuronal development and polarity and in

axon growth and guidance (**Table 3**). Activation of protective mechanisms toward maintenance of muscle contraction is for instance indicated by increase of ADDG, CNN3 and myosin light chain 4 as well as MYL6B (**Table 3**). Increased abundance of sarcolemmal membrane-associated protein involved in myoblast fusion (**Table 3**) might hint to activation or muscle fiber regeneration.

Interestingly, the results of our proteomic profiling indicate a profound vulnerability of mitochondria in laminin-211-deficient muscle based on the downregulation of a variety of mitochondrial proteins (**Table 3** and **Figure 4C**) and reduced mitochondrial respiration and ATP production in MDC1A-patient derived muscle cells has been reported as the result of changes in abundances of transcripts encoding for mitochondrial key players (39). Among the dysregulated expression of genes related to energy production in myotubes, Fontes-Oliveira and colleagues described reduced level of *NDUFA8* and decrease of NADH dehydrogenase [ubiquinone] 1 alpha subcomplex subunit 8 encoded by this transcript has been identified in our study (**Table 3**). Thus, our proteomic data confirm an impairment of the mitochondrial bioenergetic status on the protein level in human MDC1A muscle cells also in complex laminin-211-deficient muscle progressed in the etiopathology. Clincally, one of our patients (patient 5) presented with rhabdomylosis and loss of the ability to stand and walk with support after a febrile infection. One might speculate that this unusual disease course also hints toward severe metabolic impairment.

As our study is based on the utilization of material derived from patients with progressed status of the disease, it is not possible to clearly differentiate between primary pathophysiological events and molecular changes occurring as a phenomenon secondary to the primary cascades. However, intersection with data obtained from skeletal muscle derived from murine animal models with early (and unified) manifestation of the disease might harbor some limitations regrading general validity of data comparison but still allows to define candidate marker proteins of general significance involved in the initiate pathophysiology. De Oliveira and co-workers studied the proteomic signature of diaphragm and gastrocnemius muscle derived from dy^{3K}/dy^{3K} mice (MDC1A mouse model). Out of the approximately 700 identified proteins, 113 and 101 respectively, were differentially expressed in the investigated tissues (40). Notably, there was no overlap between the proteins increased in the muscle of the mouse model and the patients although few proteins with elevated levels in murine laminin-211-deficient muscle are related to extracellular matrix composition and might hint to early stages of fibrosis. Interestingly, parvalbumin alpha has been identified as decreased in their study but as increased in our proteomic profiling of MDC1A-patient derived quadriceps muscle. As in skeletal muscle, parvalbumin is thought to be involved in relaxation after contraction, its increase might accord with the activation of compensatory mechanisms upon disease progression. However, on a general note, one might speculate that either the differences in the investigated muscles (diaphragm and gastrocnemius in mice and vastus in human) or the progressed disease in our patients compared to the young-aged animals (four weeks) might explain the missing overlap between increased proteins in mice and human. Nevertheless, when focussing on the decreased proteins, a variety of different ones are downregulated in both, human and mice thus representing promising tissue markers for MDC1A across species. These proteins include creatine kinase M-type, voltage-dependent anion-selective channel protein 1, glucose-6-phosphate isomerase, cytoplasmic malate dehydrogenase, cytochrome C oxidase subunit 5A, mitochondrial NADH-dehydrogenase [ubiquinone] flavoprotein 1 and dihydrolipollysine-residue succinyltransferase component of 2-oxoglutarate dehydrogenase complex as well as NADH dehydrogenase [ubiquinone] 1β subcomplex subunit 10 and 2-oxoglutarate dehydrogenase.

The intersected data is indeed indicative of defective metabolism—especially mitochondrial function—in laminin-211-deficient muscle cells of MDC1A patients and hence confirm the findings of Fontes-Oliveira and colleagues in mice (39). This is moreover underlined by the results of our histological NADH-TR and Gomori Trichome staining supporting the concept of impaired mitochondrial activity. Along this line, the findings of both studies support the hypothesis that skeletal muscle metabolism might be a promising pharmacological target to improve muscle function, energy efficiency and tissue maintenance of MDC1A (39). Notably, in a pre-clinical study utilizing Lama2-deficient mice, mitochondria have been proven to represent a promising therapeutic target (41).

CONCLUSION

Analysis of the proteomic signature of proximal muscle derived from four children suffering from MDC1A allowed the identification of 86 proteins with altered abundance and potential pathophysiological impact. Focussing on molecular changes in skeletal muscle, a variety of affected proteins are linked to the vulnerability of the central nervous system, especially to altered synaptic transmission in the disease caused by MDC1A. Moreover, this suggests that therapeutic intervention targeting the synaptic dysfunction might represent a promising element of the overall concept in the treatment of MDC1A as already shown in mice treated with agrin. Although our patients do not present with lissencephaly, increased NudC domain-containing protein 2 might represent a potential protein modifier of the central nervous system phenotype of MDC1A. Proteomic signature of laminin-211-deficient muscle moreover indicated a profound mitochondrial vulnerability with predominant decrease of proteins belonging to complex 1. A comparison of our data with the proteomic signature of laminin-211-deficient distal muscle and diaphragm from mice allowed the identification of nine decreased proteins representing potential markers for MDC1A. However, more comprehensive studies utilizing skeletal muscle derived from MDC1A-patients (sub-cohorts at different stages of the disease) are needed to ultimately define vulnerable proteins as definite MDC1A tissue markers.

CONTRIBUTION TO THE FIELD STATEMENT

MDC1A is the most common form of congenital muscular dystrophies. The disease is caused by mutations in the *LAMA2* gene and molecular studies of mouse muscle and human cultured muscle cells already allowed first insights into the underlying pathophysiology. However, the definition of (candidate) marker proteins in human skeletal muscle is still lacking. To address this gap of knowledge, we conducted a study to investigate the proteomic signature of laminin-211-deficient vastus muscle obtained from four MDC1A-patients. Results of our unbiased screening allowed the identification of potential tissue marker proteins which might also be involved in the pathophysiology of the disease.

ETHICS STATEMENT

Ethics commitee of Duisburg-Essen University.

AUTHOR CONTRIBUTIONS

HK conceptualized and designed the study, drafted the first version of the manuscript, interpreted results, and was principally responsible for the final content. DH carried out the initial analysis and interpretation of results, contributed to the discussion. AR carried out the initial analysis, conceptualized, and designed the study, reviewed and revised the manuscript for important intellectual content. RH and MJ performed the analysis of mitochondrial proteins. US reviewed and revised the manuscript for important intellectual content.

FUNDING

This work was supported by a grant from the French Muscular Dystrophy Association (AFM-Téléthon; #21644; grant to AR). Financial support was moreover obtained from the Ministerium für Innovation, Wissenschaft und Forschung des Landes Nordrhein-Westfalen, from the Senatsverwaltung für Wirtschaft, Technologie und Forschung des Landes Berlin and from the Bundesministerium für Bildung und Forschung.

REFERENCES

1. Philpot J, Sewry C, Pennock J, Dubowitz V. Clinical phenotype in congenital muscular dystrophy: correlation with expression of merosin in skeletal muscle. *Neuromuscul Disord.* (1995) 5:301–5. doi: 10.1016/0960-8966(94)00069-L
2. Mohassel P, Reghan Foley A, Bonnemann CG. Extracellular matrix-driven congenital muscular dystrophies. *Matrix Biol.* (2018) 71–72:188–204. doi: 10.1016/j.matbio.2018.06.005
3. Tan E, Topaloglu H, Sewry C, Zorlu Y, Naom I, Erdem S, et al. Late onset muscular dystrophy with cerebral white matter changes due to partial merosin deficiency. *Neuromuscul Disord.* (1997) 7:85–9. doi: 10.1016/S0960-8966(96)00421-X
4. Buttery PC, Ffrench-Constant C. Laminin-2/integrin interactions enhance myelin membrane formation by oligodendrocytes. *Mol Cell Neurosci.* (1999) 14:199–212. doi: 10.1006/mcne.1999.0781
5. Herrmann R, Straub V, Meyer K, Kahn T, Wagner M, Voit T. Congenital muscular dystrophy with laminin alpha 2 chain deficiency: identification of a new intermediate phenotype and correlation of clinical findings to muscle immunohistochemistry. *Eur J Pediatr.* (1996) 155:968–76. doi: 10.1007/BF02282889
6. Cohn RD, Herrmann R, Sorokin L, Wewer UM, Voit T. Laminin alpha2 chain-deficient congenital muscular dystrophy: variable epitope expression in severe and mild cases. *Neurology.* (1998) 51:94–100. doi: 10.1212/WNL.51.1.94
7. Pegoraro E, Marks H, Garcia CA, Crawford T, Mancias P, Connolly AM, et al. Laminin alpha2 muscular dystrophy: genotype/phenotype studies of 22 patients. *Neurology.* (1998) 51:101–10. doi: 10.1212/WNL.51.1.101
8. Xiong H, Tan D, Wang S, Song S, Yang H, Gao K, et al. Genotype/phenotype analysis in Chinese laminin-alpha2 deficient congenital muscular dystrophy patients. *Clin Genet.* (2015) 87:233–43. doi: 10.1111/cge.12366
9. Gawlik KI, Durbeej M. Skeletal muscle laminin and MDC1A: pathogenesis and treatment strategies. *Skelet Muscle.* (2011) 1:9. doi: 10.1186/2044-5040-1-9
10. Campbell KP, Kahl SD. Association of dystrophin and an integral membrane glycoprotein. *Nature.* (1989) 338:259–62. doi: 10.1038/338259a0
11. Ervasti JM, Campbell KP. A role for the dystrophin-glycoprotein complex as a transmembrane linker between laminin and actin. *J Cell Biol.* (1993) 122:809–23. doi: 10.1083/jcb.122.4.809
12. Ehrig K, Leivo I, Argraves WS, Ruoslahti E, Engvall E. Merosin, a tissue-specific basement membrane protein, is a laminin-like protein. *Proc Natl Acad Sci USA.* (1990) 87:3264–8. doi: 10.1073/pnas.87.9.3264
13. Leivo I, Engvall E. Merosin, a protein specific for basement membranes of Schwann cells, striated muscle, and trophoblast, is expressed late in nerve and muscle development. *Proc Natl Acad Sci USA.* (1988) 85:1544–8. doi: 10.1073/pnas.85.5.1544
14. Patton BL, Miner JH, Chiu AY, Sanes JR. Distribution and function of laminins in the neuromuscular system of developing, adult, and mutant mice. *J Cell Biol.* (1997) 139:1507–21. doi: 10.1083/jcb.139.6.1507
15. Kemaladewi DU, Maino E, Hyatt E, Hou H, Ding M, Place KM, et al. Correction of a splicing defect in a mouse model of congenital muscular dystrophy type 1A using a homology-directed-repair-independent mechanism. *Nat Med.* (2017) 23:984–9. doi: 10.1038/nm.4367
16. Manza LL, Stamer SL, Ham A-JL, Codreanu SG, Liebler DC. Sample preparation and digestion for proteomic analyses using spin filters. *Proteomics.* (2005) 5:1742–5. doi: 10.1002/pmic.200401063
17. Wisniewski JR, Zougman A, Nagaraj N, Mann M. Universal sample preparation method for proteome analysis. *Nat Methods.* (2009) 6:359–62. doi: 10.1038/nmeth.1322
18. Kollipara L, Zahedi RP. Protein carbamylation: *in vivo* modification or *in vitro* artefact? *Proteomics.* (2013) 13:941–4. doi: 10.1002/pmic.201200452
19. Burkhart JM, Schumbrutzki C, Wortelkamp S, Sickmann A, Zahedi RP. Systematic and quantitative comparison of digest efficiency and specificity reveals the impact of trypsin quality on MS-based proteomics. *J Proteomics.* (2012) 75:1454–62. doi: 10.1016/j.jprot.2011.11.016
20. Olsen JV, De Godoy LMF, Li G, Macek B, Mortensen P, Pesch R, et al. Parts per million mass accuracy on an orbitrap mass spectrometer via lock mass injection into a C-trap. *Mol Cell Proteomics.* (2005) 4:2010–21. doi: 10.1074/mcp.T500030-MCP200
21. Vaudel M, Barsnes H, Berven FS, Sickmann A, Martens L. SearchGUI: an open-source graphical user interface for simultaneous OMSSA and X!Tandem searches. *Proteomics.* (2011) 11:996–9. doi: 10.1002/pmic.201000595
22. Geranmayeh F, Clement E, Feng LH, Sewry C, Pagan J, Mein R, et al. Genotype-phenotype correlation in a large population of muscular dystrophy patients with LAMA2 mutations. *Neuromuscul Disord.* (2010) 20:241–50. doi: 10.1016/j.nmd.2010.02.001
23. Siala O, Louhichi N, Triki C, Moriniere M, Rebai A, Richard P, et al. Severe MDC1A congenital muscular dystrophy due to a splicing mutation in the LAMA2 gene resulting in exon skipping and significant decrease of mRNA level. *Genet Test.* (2007) 11:199–207. doi: 10.1089/gte.2006.0517
24. Gonzalez Coraspe JA, Weis J, Anderson ME, Munchberg U, Lorenz K, Buchkremer S, et al. Biochemical and pathological changes result

from mutated Caveolin-3 in muscle. *Skelet Muscle.* (2018) 8:28. doi: 10.1186/s13395-018-0173-y
25. Roos A, Thompson R, Horvath R, Lochmuller H, Sickmann A. Intersection of proteomics and genomics to "solve the unsolved" in rare disorders such as neurodegenerative and neuromuscular diseases. *Proteomics Clin Appl.* (2018) 12. doi: 10.1002/prca.201700073
26. Hayashi YK, Engvall E, Arikawa-Hirasawa E, Goto K, Koga R, Nonaka I, et al. Abnormal localization of laminin subunits in muscular dystrophies. *J Neurol Sci.* (1993) 119:53–64. doi: 10.1016/0022-510X(93)90191-Z
27. Chan SH, Foley AR, Phadke R, Mathew AA, Pitt M, Sewry C, et al. Limb girdle muscular dystrophy due to LAMA2 mutations: diagnostic difficulties due to associated peripheral neuropathy. *Neuromuscul Disord.* (2014) 24:677–83. doi: 10.1016/j.nmd.2014.05.008
28. Rooney JE, Knapp JR, Hodges BL, Wuebbles RD, Burkin DJ. Laminin-111 protein therapy reduces muscle pathology and improves viability of a mouse model of merosin-deficient congenital muscular dystrophy. *Am J Pathol.* (2012) 180:1593–602. doi: 10.1016/j.ajpath.2011.12.019
29. Patton BL, Cunningham JM, Thyboll J, Kortesmaa J, Westerblad H, Edstrom L, et al. Properly formed but improperly localized synaptic specializations in the absence of laminin alpha4. *Nat Neurosci.* (2001) 4:597–604. doi: 10.1038/88414
30. Talts JF, Sasaki T, Miosge N, Gohring W, Mann K, Mayne R, et al. Structural and functional analysis of the recombinant G domain of the laminin alpha4 chain and its proteolytic processing in tissues. *J Biol Chem.* (2000) 275:35192–9. doi: 10.1074/jbc.M003261200
31. Desaki J, Matsuda S, Sakanaka M. Morphological changes of neuromuscular junctions in the dystrophic (dy) mouse: a scanning and transmission electron microscopic study. *J Electron Microsc.* (1995) 44:59–65.
32. Moll J, Barzaghi P, Lin S, Bezakova G, Lochmuller H, Engvall E, et al. An agrin minigene rescues dystrophic symptoms in a mouse model for congenital muscular dystrophy. *Nature.* (2001) 413:302–7. doi: 10.1038/35095054
33. Reinhard JR, Lin S, Mckee KK, Meinen S, Crosson SC, Sury M, et al. Linker proteins restore basement membrane and correct LAMA2-related muscular dystrophy in mice. *Sci Transl Med.* (2017) 9:eaal4649. doi: 10.1126/scitranslmed.aal4649
34. Issop Y, Hathazi D, Khan MM, Rudolf R, Weis J, Spendiff S, et al. GFPT1 deficiency in muscle leads to myasthenia and myopathy in mice. *Hum Mol Genet.* (2018) 27:3218–32. doi: 10.1093/hmg/ddy225
35. Bahia El Idrissi N, Bosch S, Ramaglia V, Aronica E, Baas F, Troost D. Complement activation at the motor end-plates in amyotrophic lateral sclerosis. *J Neuroinflammation.* (2016) 13:72. doi: 10.1186/s12974-016-0538-2
36. Zhu XJ, Liu X, Jin Q, Cai Y, Yang Y, Zhou T. The L279P mutation of nuclear distribution gene C (NudC) influences its chaperone activity and lissencephaly protein 1 (LIS1) stability. *J Biol Chem.* (2010) 285:29903–10. doi: 10.1074/jbc.M110.105494
37. Kubota A, Ishiura H, Mitsui J, Sakuishi K, Iwata A, Yamamoto T, et al. A homozygous LAMA2 mutation of c.818G>A caused partial merosin deficiency in a Japanese patient. *Intern Med.* (2018) 57:877–82. doi: 10.2169/internalmedicine.9588-17
38. Haga A, Niinaka Y, Raz A. Phosphohexose isomerase/autocrine motility factor/neuroleukin/maturation factor is a multifunctional phosphoprotein. *Biochim Biophys Acta.* (2000) 1480:235–44. doi: 10.1016/S0167-4838(00)00075-3
39. Fontes-Oliveira CC, Steinz M, Schneiderat P, Mulder H, Durbeej M. Bioenergetic impairment in congenital muscular dystrophy type 1A and leigh syndrome muscle cells. *Sci Rep.* (2017) 7:45272. doi: 10.1038/srep45272
40. De Oliveira BM, Matsumura CY, Fontes-Oliveira CC, Gawlik KI, Acosta H, Wernhoff P, et al. Quantitative proteomic analysis reveals metabolic alterations, calcium dysregulation, and increased expression of extracellular matrix proteins in laminin alpha2 chain-deficient muscle. *Mol Cell Proteomics.* (2014) 13:3001–13. doi: 10.1074/mcp.M113.032276
41. Millay DP, Sargent MA, Osinska H, Baines CP, Barton ER, Vuagniaux G, et al. Genetic and pharmacologic inhibition of mitochondrial-dependent necrosis attenuates muscular dystrophy. *Nat Med.* (2008) 14:442–7. doi: 10.1038/nm1736

Conflict of Interest Statement: The authors declare that the research was conducted in the absence of any commercial or financial relationships that could be construed as a potential conflict of interest.

Copyright © 2019 Kölbel, Hathazi, Jennings, Horvath, Roos and Schara. This is an open-access article distributed under the terms of the Creative Commons Attribution License (CC BY). The use, distribution or reproduction in other forums is permitted, provided the original author(s) and the copyright owner(s) are credited and that the original publication in this journal is cited, in accordance with accepted academic practice. No use, distribution or reproduction is permitted which does not comply with these terms.

frontiers in Neurology

REVIEW
published: 08 May 2019
doi: 10.3389/fneur.2019.00438

Disease Specific Autoantibodies in Idiopathic Inflammatory Myopathies

Bruno Stuhlmüller[1], *Udo Schneider*[1], *José-B. González-González*[1,2] *and Eugen Feist*[1]*

[1] *Department of Rheumatology and Clinical Immunology, Charité-Universitätsmedizin, Berlin, Germany,* [2] *Labor Berlin-Charité Vivantes GmbH, Berlin, Germany*

Idiopathic inflammatory myopathies represent still a diagnostic and therapeutic challenge in different disciplines including neurology, rheumatology, and dermatology. In recent years, the spectrum of idiopathic inflammatory myopathies has been significantly extended and the different manifestations were described in more detail leading to new classification criteria. A major breakthrough has also occurred with respect to new biomarkers especially with the characterization of new autoantibody-antigen systems, which can be separated in myositis specific antibodies and myositis associated antibodies. These markers are detectable in approximately 80% of patients and facilitate not only the diagnostic procedures, but provide also important information on stratification of patients with respect to organ involvement, risk of cancer and overall prognosis of disease. Therefore, it is not only of importance to know the significance of these markers and to be familiar with the optimal diagnostic tests, but also with potential limitations in detection. This article focuses mainly on antibodies which are specific for myositis providing an overview on the targeted antigens, the available detection procedures and clinical association. As major tasks for the near future, the need of an international standardization is discussed for detection methods of autoantibodies in idiopathic inflammatory myopathies. Furthermore, additional investigations are required to improve stratification of patients with idiopathic inflammatory myopathies according to their antibody profile with respect to response to different treatment options.

Keywords: myositis, inflammation, autoantibodies, antigens, biomarker

OPEN ACCESS

Edited by:
Stefan Bittner,
Johannes Gutenberg University Mainz, Germany

Reviewed by:
Reinhild Klein,
University of Tübingen, Germany
Patrick Joseph Waters,
University of Oxford, United Kingdom

***Correspondence:**
Eugen Feist
eugen.feist@charite.de

Specialty section:
This article was submitted to Multiple Sclerosis and Neuroimmunology, a section of the journal Frontiers in Neurology

Received: *03 December 2018*
Accepted: *10 April 2019*
Published: *08 May 2019*

Citation:
Stuhlmüller B, Schneider U, González-González J-B and Feist E (2019) Disease Specific Autoantibodies in Idiopathic Inflammatory Myopathies. Front. Neurol. 10:438. doi: 10.3389/fneur.2019.00438

INTRODUCTION

Idiopathic inflammatory myopathies (IIM) represent a heterogeneous group of acquired muscle diseases with so far unclear etiology. The different entities are associated with diverse clinical symptoms ranging from amyopathic to necrotic inflammatory muscle involvement, typical skin and internal organ involvement. In addition to the clinical picture, histological and serological findings are especially supportive in differentiation and stratification of disease (1). Based on this characteristics, IIM can be classified into different major sub-types: (i) polymyositis (PM), (ii) sporadic inclusion body myositis (sIBM), (iii) dermatomyositis (DM), (iv) immune-mediated necrotizing myopathy (IMNM), and (v) overlap syndromes with myositis (2, 3). Within the spectrum of antibodies two classes have been proposed (4), designated as myositis specific antibodies (MSAs) due to their exclusive association with IIM or as myositis-associated antibodies (MAAs) due to their prevalence in different other connective tissue disorders. This article focuses on an overview on so far identified specific autoantibody-antigen systems in IIM. Furthermore, we discuss the available methods, strategies and pitfalls of autoantibody detection in IIM as well as their diagnostic performance and clinical association.

CHARACTERIZATION OF DISEASE SPECIFIC ANTIGEN-ANTIBODY SYSTEMS IN IIM

As with many other systemic autoimmune diseases, it is unclear so far, whether and how the observed autoantibody formation is directly associated with the pathogenesis of disease or is just an epiphenomenon. However, the striking association between certain autoantibodies with a distinct clinical phenotype, their high disease specificity and their value for stratification and prognosis of disease suggests that they may play a role in disease induction and propagation (5). This section describes in detail the nature and function of so far identified IIM specific antigens. A complete overview on so far identified antigens and the corresponding autoantibodies in adult and in juvenile patients with IIM is given in **Table 1**.

The best-known autoantigen-autoantibody system in IIM is directed against **transport ribonucleoacid (t-RNA) synthetases** and represents a specific finding in patients with so named anti-synthetase syndrome (ASS). The targeted synthetases catalyze the binding of a specific aminoacid to their t-RNA in the cytoplasm of each eukaryotic cell for transportation to the ribosome and subsequent protein synthesis. At least eight t-RNA synthetases have been identified as autoantigens. Anti-Jo1 antibodies are the most common ones and received their designation after the initials of the index patients (44). It is unclear, why not all t-RNA synthetases are targeted by the immune system in ASS, but only the tRNA synthetase for threonyl (PL-7), alanyl (PL-12), isoleucyl (OJ), glycyl (EJ), asparaginyl (KS), phenylalanyl (Zo), tyrosil (Ha), and finally the histidyl synthetase (Jo-1). Even more of interest is the question, whether the antibodies can interfere with the function of the respective t-RNA synthetase as it has been shown for anti-Jo1 antibodies by *in-vitro* experiments (45, 46). This particular antibody specificity belongs mainly to the IgG1 isotype and binds to common epitopes (47).

For the anti-Jo1 antibodies, it was shown that the formation of the major autoepitope is strongly dependent on proper folding of the molecule (46). As a shared risk factor for anti–Jo-1 autoantibody positivity, the HLA–DRB1*0301 allele was identified in European as well as African Americans (48). In the Japanese population, HLA–DRB1*0405 was associated with the formation of an anti-tRNA antibody response (49).

Another specific antigen is **the transcription intermediary factor-1 gamma** (TIF-1γ). This multi-functional protein with a molecular weight (MW) of 140/155 kilo-Dalton (kDa) is mainly involved in gene transcription (27, 50–53). The TIF-1 family is composed of tripartite motif-containing (TRIM) proteins, which are all implicated in cell proliferation, development, apoptosis, and innate immunity (54). All TIF1 proteins share a C-terminal chromatin reading unit consisting of a plant homeodomain finger and a bromo-domain (BROMO) that is highly conserved among TIF1 family members, but which is not present in any of the other TRIM proteins (55, 56). Of note, while the most common target in anti-TIF1-positive CAM (cancer-associated myositis) is TIF1γ, other proteins of the TIF1 family (TIF1α and β) may also be simultaneously targeted by the immune system (53).

The tripartite containing motif (TRIM) allows these proteins also to function as E3-ligases in the ubiquitination pathway to control protein degradation, localization, and function. In this context, it is interesting to mention that TIF1-γ is involved in the regulation of TGF-β signaling via mono-ubiquitination of SMAD-4 leading to suppression of TGF- β. Thus, by stimulating cell growth and differentiation, TIF1-γ could play a pivotal role in promoting or suppressing malignant cell growth and differentiation (57). The known association of anti-TIF1-γ antibodies with a high risk of cancer development in DM suggest that this link could be not random. Of note, anti-TIF antibodies were only rarely detectable in patients with solid cancer (3.1%) or paraneoplastic rheumatic syndrome (3.3%) without DM (58).

Recently, it was recognized that tumors from paraneoplastic anti-TIF1-γ positive patients showed an increased number of genetic alterations, such as mutations and loss of heterozygosity (LOH) in TIF1 genes (59). Compared with type-matched control tumors from non-myositis patients, TIF1-γ staining was also significantly more intense in tumors as well as muscle tissue from anti-TIF1-γ positive patients. This finding could indicate that the co-occurrence of mutations in peptide regions of TIF1 with high affinity for HLA class I and tumors with high-level TIF1 protein expression may initiate a strong adaptive immune response against neoplastic cells with the mutation. Interestingly, LOH is the most frequent way to lose a mutant allele in human cancer and this is key to tumor immune-editing, since tumor cells with mutations producing a neo-antigen may be eliminated by the immune system and replaced by tumor cells with LOH in that region (without the antigenic mutation) (60, 61). Thus, these modifications can induce an immune response, but also cause an escape of the tumor cell from clearance.

It has been described that DM disease increases toward the equator and strongly associate with latitude. Recently, this observation was confirmed by another study showing that relative prevalence of DM and frequency of anti-TIF1-γ autoantibodies were found to be significantly negatively associated with latitude in adult myositis. Furthermore, HLA alleles HLA-DRB1* 07:01 and HLA-DQB1*02 were strongly associated with the DM-specific autoantibodies anti-Mi-2 as well as anti-TIF1-γ (62).

The component of **the nucleosome remodeling deacetylase complex, Mi-2**, is an autoantigen of 240 kDa MW and exists in two isoforms Mi-2α (CHD3) and Mi-2β (CHD4). Mi-2 is responsible for the remodeling of chromatin by de-acetylating histones and plays a role as transcription repressor (63). The role of anti-Mi-2 autoantibodies in the pathogenesis of DM is unclear. However, the autoantigen Mi-2 is found to be up-regulated in the muscle tissue of DM patients. Of note, exposure of keratinocytes to UV radiation has been shown to increase the expression of Mi-2 protein supporting the hypothesis that UV radiation may be associated with the induction of anti-Mi-2 autoantibodies (64). However, a reported increase in the presence of anti-Mi-2 autoantibodies toward the equator was not confirmed by a current study (62, 65). A preferential expression was described in the nucleus of myofibers within fascicles affected by perifascicular atrophy, particularly in the centralized nuclei of small perifascicular muscle fibers expressing

TABLE 1 | Characterization of myositis specific and myositis associated autoantibodies and their respective antigens.

	Autoantigen name and function	Molecular weight in kilodalton	Cellular localization	Disease and associated manifestations	Frequency in adult (A) and juvenile (J) IIM	Conventional and commercial (*) detection systems	References
ANTI-SYNTHETASE SYNDROME (ASS)							
EJ	Glycyl-tRNA synthetase	79	Cy	ASS with mechanic hands, associated with increased risk of interstitial lung disease	(A) <5%	ELISA, IP & WB, *IIFT *Strip test	(6)
Jo-1	Histidyl-tRNA synthetase	60	Cy	ASS with interstitial lung involvement, mechanic hands, Raynaud, arthritis	(A) 20–30%	ELISA, ID, IP & WB, *IIFT, *Strip test	(7–10)
OJ	Isoleucyl-tRNA synthetase	145	Cy	ASS with interstitial lung disease, sometimes also found in RA	(A) 3%	ELISA, IP & WB, IF, *IIFT, *Strip test	(6, 11)
PI-7	Threonyl-tRNA synthetase	83	Cy	ASS with increased risk of interstitial lung disease, Raynaud syndrome,	(A) < 5%	ELISA, ID, IP & WB, *IIFT, *Strip test	(8)
PI-12	Alanyl-tRNA synthetase	108	Cy	ASS associated in 90% with interstitial lung disease	(A) 2–3%	ELISA, ID, IP & WB, *IIFT, *Strip test	(12)
KS	Asparaginyl-tRNA synthetase	51	Cy	ASS	(A) <5%	ELISA, IP & WB	(13, 14)
Ha	Thyrosyl-tRNA synthetase	59	Cy	ASS	(A) < 1%	ELISA, IP & WB	(15)
Zo	Phenylalanyl-t-RNA synthetase	52	Mi	ASS frequently with fever	(A) < 1%	ELISA, IP & WB	(15, 16)
DERMATOMYOSITIS (DM), POLYMYOSITIS (PM) AND IMMUNE MEDIATED NECROTIZING MYOPATHY (IMNM)							
SRP	Signal recognizing particle	72/52	Cy	IMNM, acute und subacute	(A) 5–10% (J) < 3%	WB, IF, *IIFT *Strip test	(7, 17, 18)
MDA-5 / CADM-140	Melanoma differentiation associated Gene 5	140	Cy	Amyopathic dermatomyositis, mostly in relation with progressive interstitial pneumonia	(A) 50–73% in Asian populations	WB, IF, *IIFT	(19, 20)
Mi-2α and β	Nucleosome deacetylase complex; helicase binding protein	240	Nu	DM mild forms	(A) 15–30% (J) 10–15%	WB, IF, *IIFT, *Strip test	(21, 22)
NXP-2 (MJ)	Nuclear matrix protein 2	140	Nu	DM und juvenile DM/PM, mostly associated with calcinosis, in juvenile DM involved with ischemia and in adult PM with cancer	(A) 18–25% (J) 60%	WB, IF, *IIFT, *Strip test	(23, 24)
SAE1/2	Small ubiquitin like modifying and activating enzyme	90/40	Nu	DM, often also found in patients with amyopathic DM	(A) < 5% (J) < 1%	WB, IF, *IIFT, *Strip test	(23, 25, 26)
TIF-1γ	E3-Ligase, transcriptional factor-1γ hetero complex	155/140	Nu	Cancer associated DM in adults, skin ulcerations in juvenile DM	(A) 13–21% (J) 22–29%	IF, WB, *IIFT, *Strip test	(23, 27)
p200/100 HMGCR (HMG-CoA)	3-hydroxy-3-methylglutaryl-CoA reductase	200/100	ER membrane	IMNM frequently associated with prior statin use	(A) 6-10 %	IP and WB	(28–31)
MYOSITIS ASSOCIATED ANTIBODIES (MAA)							
Ku70 / Ku80	DNA-binding protein kinase complex, involved in DNA double strand repair	70/88	Nu	Overlap-Syndrome frequently with pulmonary fibrosis, arthralgia, gastrointestinal involvement,	(A) 7%	WB, IF, *IIFT, *Strip test	(32)

(Continued)

TABLE 1 | Continued

	Autoantigen name and function	Molecular weight in kilodalton	Cellular localization	Disease and associated manifestations	Frequency in adult (A) and juvenile (J) IIM	Conventional and commercial (*) detection systems	References
cN-1A	Enzyme, Cytosolic 5′-nucleotidase	43	Nu	High frequency in sporadic inclusion body myositis (sIBM), but also in Sjogren's syndrome, infrequent in other forms of IIM	(A-) s-IBM 33–44%, PM/DM 5%	ELISA, IF, *IIFT, *Strip test	(33–36)
U1-RNP	U1-ribonuclear Protein	70	Nu	Associated with mixed connective tissue diseases (MCTD)	(A) up to 12%	WB, IF	(32, 37)
SS-B (La)	RNA-metabolism and processing of pre-tRNA; viral RNA binding protein, RNA-chaperone	50	Nu	Associated with Sjogren's syndrome and systemic lupus erythematosus (SLE)	(A) 10%	WB, IF	(38, 39)
SS-A (Ro)	E3-ubiquitine ligase	60/52	Nu / Cy	Associated with Sjogren's syndrome and SLE	(A) 50% (J) 10%	WB, IF, *IIFT, *Strip test	(40–42)
PM/Scl	Exo-ribonuclease	100/75	Nu / Cy	Overlap syndrome with myositis and scleroderma	(A) 5%	IF, WB, *IIFT *Strip test	(7, 43)

ID, Immunodiffusion; IIFT, Indirect Immunofluorescence test; IF, Immunofluorescence; WB, Immunoblotting; IP, Immunoprecipitation; Mi, mitochondrium; Cy, cytoplasm; Nu, nucleus; (A), adult IIM; (J), juvenile IIM.

markers of regeneration (66). In a mouse model of muscle injury and repair, Mi-2 levels were dramatically and persistently up-regulated during muscle regeneration *in-vivo*. Of note, premature silencing of Mi-2 with RNA interference *in vitro* resulted in accelerated myoblast differentiation. In summary, these results indicate that this protein may play a role in modulating the kinetics of myoblast differentiation. European and American anti–Mi-2 antibody positive DM patients have a common genetic risk factor DRB1*0701 (67). Furthermore, HLA-DRB1*0302 was identified to be associated with anti–Mi-2 autoantibody positive African American patients (48). Of note, all HLA molecules were found to share a 4–amino-acid sequence motif, which was predicted by comparative homology analyses to have identical 3-dimensional orientations within the peptide-binding groove.

The target antigen of antibodies against **small ubiquitin-like modifier activating enzyme (SAE1/2)** is the SUMO-1 activating enzyme heterodimer with a MW of 40 and 90 kDa, respectively. This antigen is involved in the posttranslational modification of proteins, the so called "sumoylation" (68, 69). Of note, a strong association with the HLA-DRB1*04-DQA1*03-DQB1*03 haplotype has been reported (25). This is another example in IIM, where the association between genotype, serotype and clinical picture suggest a link to the pathogenesis of disease.

Immune reactivity against the **signal recognizing protein hetero-complex (SRP)** is associated with immune-mediated necrotizing myopathy (IMNM). This 72/52 kDa antigen is expressed in the cytoplasm and responsible for transport proteins to the endoplasmic reticulum. SRP consists of six polypeptides (including SRP19 and MIM 182175) as well as seven SL-RNA molecules with partial homology to Alu-DNA (70, 71). Although antibodies against SRP can target each of the different SRP components, a signal peptide-binding 54 kDa subunit (SRP54) represents a major epitope recognized by almost every sera and is, therefore, preferentially used in immunoassays (72–76). Although it is not clear, how the antibodies can interact with the SRP1/2 autoantigen, it was shown that anti-SRP antibodies can inhibit the translocation of secretory proteins into the endoplasmic reticulum *in-vitro* and that a passive transfer of IgG from anti-SRP+ patients with IMNM provoked muscle deficiency through a complement-mediated mechanism in mice model. Interestingly, also active immunization with SRP was able to induce an immune response and provoked disease (76, 77). A correlation between anti-SRP54 antibody titers and disease activity was also shown in a longitudinal follow-up study suggesting a pathogenic role of this antibody entity (78). As a genetic risk factor, HLA- DQA1*0102 was identified in anti–SRP autoantibody positive African American patients (48).

The **melanoma differentiation antigen 5 (MDA-5**, synonym CADM-140) with a MW of 140 kDa belongs to the family of RIG-I-like receptors of adhesion molecules and represents a resistance factor against double stranded RNA viruses (49, 79). The MDA-5 molecule plays an important role in the regulation of the immune response by the innate system. In this context, it was shown that MDA-5 bind virus particles, e.g., picornaviruses such as coxsackievirus, and induce an antiviral responses by producing type-I interferons and tumor necrosis factor (80). It was also reported that hyperferritinemia

could be a marker for rapidly progressive ILD in anti–MDA-5 antibody positive DM patients (81, 82). In this context many cytokines regulate the ferritin synthesis, including IL-1β, IL-18, TNF, IFN-γ, and IL-6 and several of these cytokines are considered to be involved in IIM pathogenesis. HLA–DRB1*0101/*0405 was found to be associated with susceptibility to anti–MDA-5 antibody positive DM in the Japanese population (49). Interestingly the same alleles are well-known to play a role in the susceptibility to autoantibody induction in rheumatoid arthritis (83).

Autoantibodies against the **nuclear protein 2 (NXP-2)**, also known as MJ or p140 antibodies, are directed against a nuclear matrix protein complex named NXP2/MORC3, which is involved in regulation of p53-induced cell senescence in the context of oncogenic signals (23). NXP-2 is associated with the small ubiquitin modifier SUMO-2 and represses its expression (84).

The **enzyme 3-hydroxy-3-methylglutaryl-CoA reductase (HMGCR)** was recently identified as a target of autoantibodies induced under treatment with statins. The antigen is expressed in the ER membrane and has a MW of 200/100 kDa. HMGCR catalyzes the conversion of HMG-CoA to mevalonic acid, which is an important step in cholesterol biosynthesis. So far, reports about HMGCR in myositis are rare, however in animal studies it was demonstrated that loss of HMGCR function disrupts vascular stability during developmental processes (4).

DIAGNOSTIC TESTING FOR AUTOANTIBODIES IN IIM

To assess disease activity and as indicators for muscle injury in IIM, basic laboratory diagnostics are used, such as measurements of levels of inflammatory markers as well as serum activity and/or concentration of muscle specific proteins including creatine phosphokinase (CPK) or myoglobin. However, these markers are unspecific and not helpful to distinguish between the different forms of inflammatory muscle damage. In contrast, the reactivity of the described autoantibodies does not sufficiently correlate with disease activity in IIM, but can rather serve for stratification of the disease process and outcome (85). This section focuses on helpful information with respect to routine procedures of autoantibody detection and the recommended diagnostic approaches, since it is of enormous importance to know these basics for appropriate interpretation of results.

Serum is usually used for the detection of autoantibodies, and test procedures are performed according to the manufacturer's validation. From a preanalytical point of view, time point of venepuncture and fasting status of the patient are not relevant. However, hemolytic, lipemic or contaminated blood samples should not be used, since the released proteins and proteinases can interfere with the immunologic method of detection. Especially in case of a prolonged transportation of the blood sample, serum should be separated in advance by centrifugation at 1,300 g. Subsequently, the serum samples can be stored at 2–8°C for up-to 2 weeks before analysis. A longer period requires freezing at minus 20°C, which presumably allows conservation of the autoantibody reactivity for years (86, 87). Furthermore, some treatment procedures including administration of strong immunosuppressive drugs such as B-cell directed therapies as well as plasmapheresis or administration of intravenous immunoglobulins can influence the result of detection by decreasing the concentration of the autoantibodies.

From the methodical point of few, detection of autoantibodies in IIM is not well-standardized and no international reference samples are available so far. In general, immunoprecipitation of radio-labeled proteins or RNA molecules is still considered to represent the "gold standard" (68). However, due to the time-consuming procedure, high amount of required antigens and low sensitivity, this method is not a routine procedure in most clinical laboratories. Therefore, for the detection of IIM specific and/or associated autoantibodies several, more efficient approaches such as immunofluorescence, ELISA and western blotting are widely used (88–90). In general, immunofluorescence requires large experience to interpret patterns and may not be sensitive enough to detect all MSAs/MAA. On the other hand, ELISA methods using recombinant antigens or immunoblotting with denaturated antigens can probably not detect antibodies to certain conformational epitopes. Line-blot assays allow a qualitative detection of many antibodies in one run. In contrast, and in accordance to the manufacturer specification only a limited number of MSAs/MAAs can be detected by commercial available ELISAs so far.

Indirect immunofluorescence (IIF) on HEp-2 cells, a human epithelioma cell line, is commonly be used for detection of anti-nuclear antibodies (ANA), but also enables detection of antibodies against cytoplasmatic antigens. This method allows a screening for a wide range of autoantibodies especially in connective tissue disorders by describing the staining pattern (e.g., nuclear, nucleolar, cytoplamatic), as well as the reactivity titer starting with a serum dilution of usually 1:80. Although no agreement has still been reached on the interpretation and reporting of the ANA titres, results can be considered as weak positive in antibody titer of $\geq$1:160 and as strong positive in a titres of $\geq$1:640. In this context, it is important to mention that measured titers often do not correspond with the significance of the results. In other words, a low reactivity should not be considered as irrelevant. Furthermore, it is also important to pay attention to the described pattern of immunofluorescence in the nucleus, but also the cytoplasm. It is helpful to know that IIF on HEp-2 cells shows characteristic patterns of some MSA or MAA antibodies such as those against PM/Scl with prominent homogeneous staining of the nucleous, U1-RNP with coarse speckled staining of the nucleus, Jo-1 or SRP with fine speckled stainings of the cytoplasm (**Figure 1**), but is not sufficiently accurate to be used as the only screening tool for myositis antibodies.

Although most of the targeted antigens in IMM are expressed within HEp-2 cells, their detection by IIF is clearly limited. The reasons for frequent false negative results is diverse including e.g., low expression level of the antigen or low affinity of the antibodies causing a weak staining signal. Furthermore, the intracellular distribution of relevant antigens in IIM is usually diffuse generating an unspecific staining pattern. Thus, week

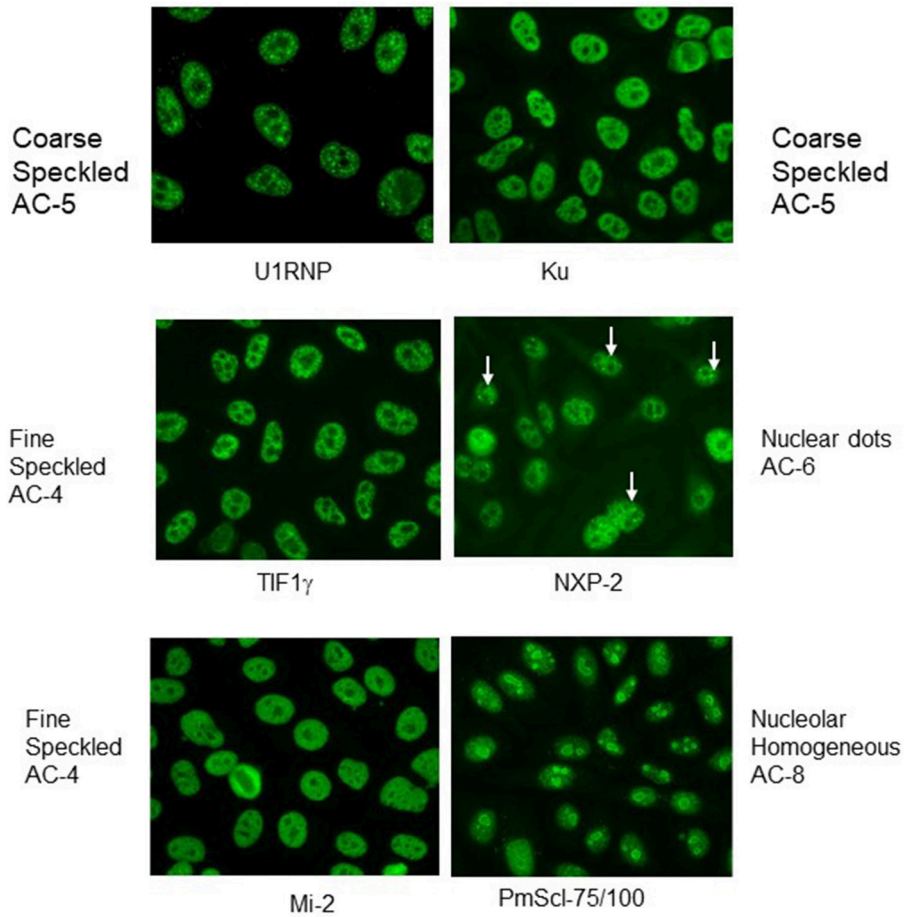


FIGURE 1 | Indirect immunofluorescence with typical nuclear patterns of MSA and MAA. Immunofluorescence patterns are indicated with the terminology of the International Consensus on ANA Patterns (ICAP).

positive results are often not recognized, as it frequently occurs even with anti-tRNA synthetase antibodies. Nevertheless, IIF on HEp-2 cells is an important diagnostic procedure. **Table 1** summarizes frequent staining patterns in conjunction with the respective antibody and, **Figures 1**, **2** show representative IIF staining patterns indicating the respective nomenclature for the most frequent MSAs and MAAs by International Consensus on Autoantibody Patterns (ICAP).

For the detection of classical and new myositis antibodies, multi-analyte line blot assays and ELISA are the current routine methods of choice. In contrast to IIF, commercial ELISAs and line-blot assays use purified or recombinant expressed antigens for detection of antibodies. These methods allow the targeted detection or confirmation of respective antibodies in serum samples, which are usually diluted 1:100. In contrast to semi-quantitative results provided by line-blot assays (with negative, weak or strong positive signals, see **Figure 3**), ELISA based methods allow a better quantification of antibody reactivity, especially if international standards will be available. However, the majority of ELISA methods published hitherto to detect novel myositis antibodies are in-house made and most of the commercial ELISAs only report negative or positive results by using a cut-off level of reactivity defined by the providing manufacturer. A multiplex-approach for detection of several antibodies in one immunoassay has also limitations and pitfalls due to the difficult optimization of the cut-off for all investigated antibodies. Therefore, it is always important to check the plausibility of the obtained results, not only in cases of weak or borderline reactivity, but also in case of discordance between the different immunoassays (e.g., negative ANA staining pattern but positive anti-PM/Scl antibodies in ELISA or line-asays). On the solid phase of an immunoassay, the antigen structure can be altered yielding a false positive antibody reactivity, which is not directed against the native antigen. Therefore, it is important, that involved diagnostic laboratories are be informed about the clinical suspected diagnosis and provide high quality assays proven by regular internal and external quality controls.

The major advantage of ELISA and line blot test assays is the option of automation test fastness. In this context, the development of commercial quantitative immunoassays including ELISA, chemiluminescence and immunofluorometry has facilitated the use at large scale in routine laboratories and provided interesting

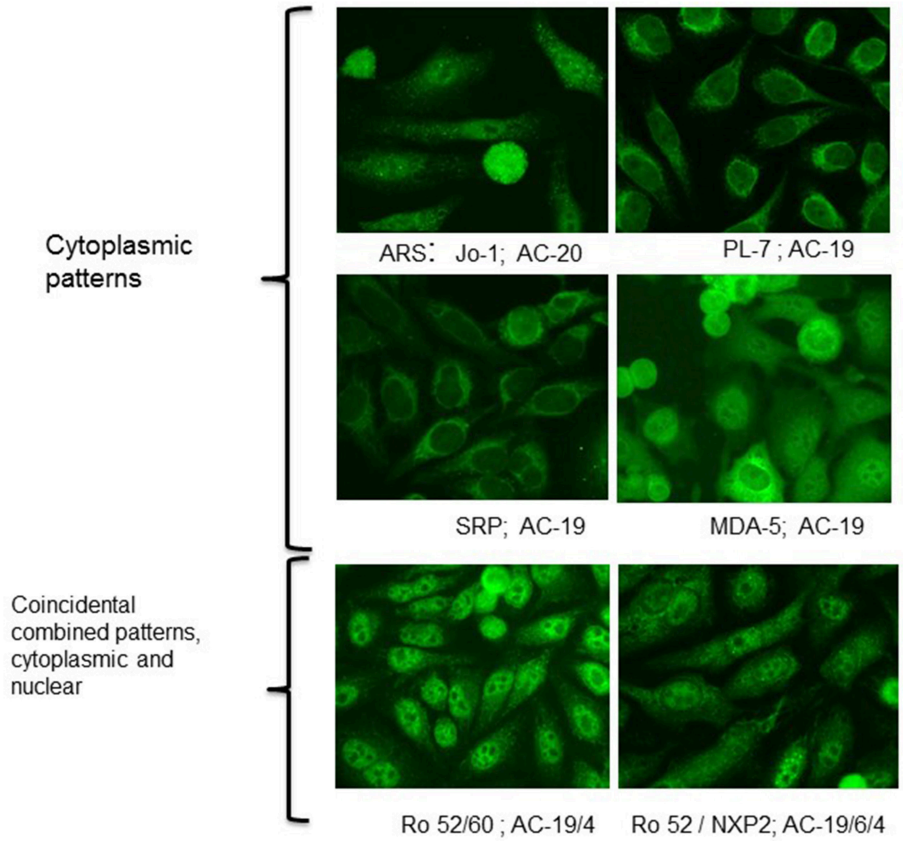
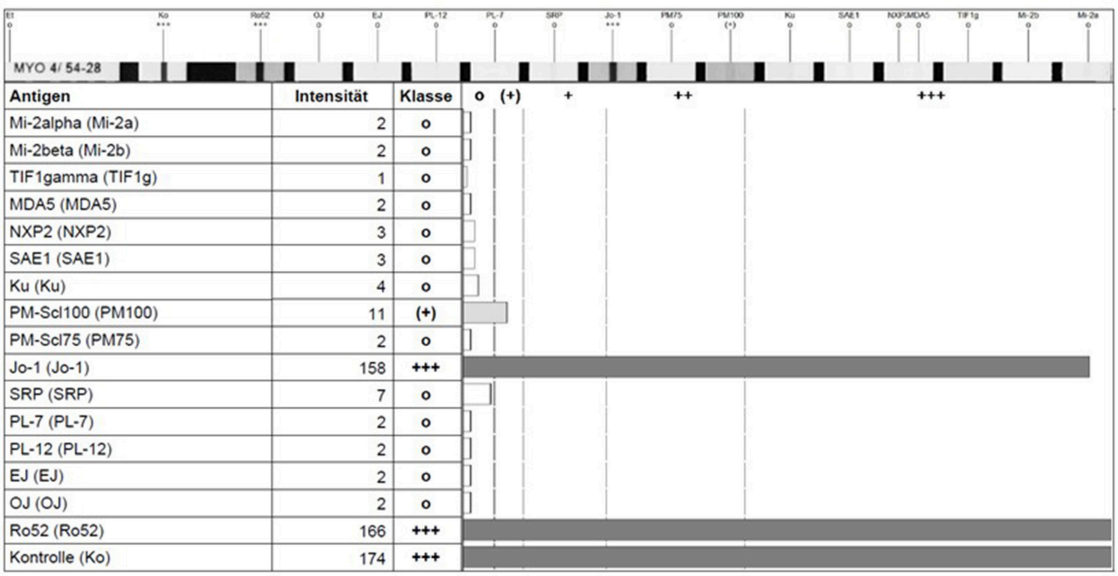


FIGURE 2 | Indirect immunofluorescence with typical cytoplasmic patterns of MSA and MAA. Immunofluorescence patterns are indicated with the terminology of the International Consensus on ANA Patterns (ICAP). AC-19-cytoplasmic dense fine speckled, AC-20-cytoplasmic fine speckled.



Antigen	Intensität	Klasse
Mi-2alpha (Mi-2a)	2	o
Mi-2beta (Mi-2b)	2	o
TIF1gamma (TIF1g)	1	o
MDA5 (MDA5)	2	o
NXP2 (NXP2)	3	o
SAE1 (SAE1)	3	o
Ku (Ku)	4	o
PM-Scl100 (PM100)	11	(+)
PM-Scl75 (PM75)	2	o
Jo-1 (Jo-1)	158	+++
SRP (SRP)	7	o
PL-7 (PL-7)	2	o
PL-12 (PL-12)	2	o
EJ (EJ)	2	o
OJ (OJ)	2	o
Ro52 (Ro52)	166	+++
Kontrolle (Ko)	174	+++

FIGURE 3 | Detection of anti-Jo-1 and anti Ro-52 antibody reactivity in a line-blot assay showing the reaction intensity by a scan-software of the fabricant (EUROLINE, Euroimmune, Germany).

information on correlation of clinical and serological findings in IIM.

CORRELATION OF MSA WITH CLINICAL FINDINGS

In addition to inflammatory lesions of skeletal muscles, involvement of other organs such as skin, joint, lung and heart is frequent in IIM. Extra-muscular involvement, especially interstitial lung disease (ILD) and underlying malignancy in cancer-associated myositis (CAM) are the two dominating factors contributing to increased mortality in IIM-patients (91, 92). This section gives an overview on the association of MSA with clinical findings and their diagnostic performance. The incidence of most of the so far identified autoantibody activities of European patients is in agreement with similar studies of Japanese and American patients (7).

ANTIBODIES AGAINST T-RNA SYNTHETASES

Patients with antibodies against t-RNA synthetases are prone to develop the so called anti-synthetase syndrome (ASS) characterized by myopathy, interstitial lung disease (ILD), non-erosive arthritis, fever, Raynaud's phenomenon and mechanic's hands. Since not all symptoms are present at disease onset, ASS should be carefully considered in patients presenting with isolated arthritis, even in those with erosive manifestation and RF as well as ACPA-positivity (93, 94). The presence of anti-synthetase antibodies can be suspected if a characteristic cytoplasmic pattern on HEp2 cells is evident (**Figure 1**). However, confirmation is needed using ELISA, immunoblot or line-assays with the isolated antigens. Depending on the diagnostic method anti-Jo-1 antibodies are the most frequent autoantibodies in IIM, they can be detected in 20–30% of patients (7, 95). Titers of Jo-1 antibodies were shown to correlate with disease activity in adults (95). In muscle biopsies of anti-Jo-1 positive myositis patients a specific histologic pattern with peri-fascicular necrosis has been described (96).

The CT- and histomorphologic pattern of ILD in anti-synthetase syndrome can vary between non-specific interstitial and organizing pneumonia (97). Antibodies against PL-7 and PL-12 are positive in up to 5% of IIM patients. Clinically they are associated with less muscle involvement but with a higher proportion of ILD, which might have an acute onset (98). Furthermore, pericarditis was observed in up to 50% of anti-PL7 positive patients (99). Antibodies against OJ, EJ, KS, Zo, and Ha are rare and only present in 1–3% of patients with ARS. The coincidence of anti-Ro52/TRIM21with anti-ASS antibodies was described to be associated with severe myositis and arthropathy as well as with an increased risk of cancer (7, 99, 100). The onset of ILD and myositis, as leading symptoms in ASS, can be subsequently or in parallel, while the course of ILD must not necessarily be progressive.

DM-Specific Antibodies

Anti-Mi-2 antibodies have a high specificity for both adult and juvenile DM (JDM). Mi-2-antibodies produce a fine speckled nuclear pattern in IIF on HEp-2 cells (AC-4 of the ICAP nomenclature) and are detectable in approximately 30% in adult and 10% in juvenile DM (JDM) patients, respectively. Patients with positive anti-Mi-2 antibodies have usually a milder myopathy, lower risk of interstitial lung disease (ILD) and malignancy (101). Skin manifestations, such as Gottron's sign and heliotrope rash, as well, rashes in neck (V rash) and upperback (shawl rash) or cuticular overgrowth are typical. Patients respond well to steroid therapy and have a good prognosis. Furthermore, levels of Mi-2 antibodies were shown to correlate with clinical response to B-cell depletion therapy (102). Although DM with antibodies against Mi2-β can be associated with neoplasia (e.g., colon or mama-carcinoma), anti-Mi-2 antibodies are in general associated with a lower risk of paraneoplastic myositis and hence considered to be a good prognostic factor.

Anti-TIF1γ (anti-155/140) antibodies are detectable in 13–21% of patients with tumor associated adult DM and in approximately 30% of severe juvenile DM patients (23, 27). In fact, these antibodies are the most frequent marker in juvenile IIM (JIIM) and are primarily associated with JDM. They were originally found almost exclusively in JDM, in about of 23–29% of cases using immunoprecipitation and immunoblotting. Interestingly, in recent studies including a total of 374 cases with JIIM, 131 cases (35%) were found to be positive for these antibodies. In detail, the antibodies were detectable in 38% of patients with JDM (123/320) and in 26% of patients with an overlap syndrome with myositis (8/31) (103, 104). TIF-γ-antibodies are known to be very frequently associated with malignancy in adults with a specificity of 89%, sensitivity of 78%, and positive and negative predictive values of 58 and 95%, respectively (105). In contrast to adults, there is no paraneoplastic association in JIIM (106). Skin manifestations are characterized by a usually slowly progressive onset, but are more extensive than in other JDM groups. In fact, skin ulcerations and lipodystrophy were reported to be particularly associated with these antibodies. However, this was not reported uniformly, since recent studies did not observe ulceration or V-rashes significantly more frequent in this group than in others (104). Of note, it has been shown that levels of TIF-γ-antibodies correlate with response to B-cell depletion therapy in pediatric patients (102).

Anti-NXP2 antibodies (MJ or p140) cause a fine speckled ANA pattern on IIF, but this pattern is often misinterpreted as variable nuclear dots (**Figure 1**). These antibodies have been originally described in children with JDM in about 25% of cases (107, 108). In a cohort of 436 patients with JIIM, their prevalence was reported to be approximately 21% in JDM, 9% in JPM and 15% in overlap syndromes (juvenile connective tissue myositis, JCTM) (104). Subsequently, anti-NXP2 antibodies have been also detected in approximately 30% of patients with DM and 8% with PM in a cohort of 58 adult Italian patients (109), but in only 1.6% of 507 adult Japanese patients (110). In the Italian cohort, a good response to therapy was reported for muscle involvement (109). In juvenile

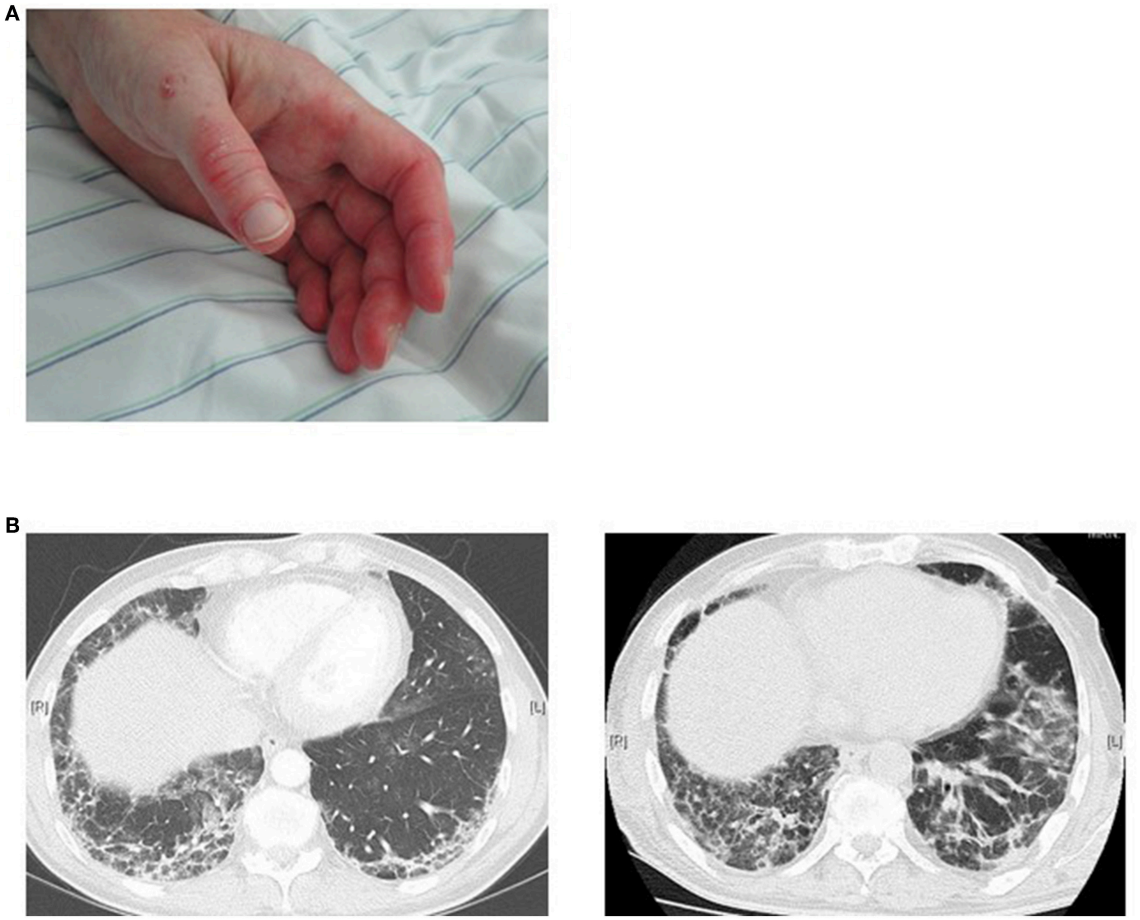


FIGURE 4 | MDA5 positive patient with an amyopathic dermatomyositis **(A)** maculopapular palmar rash and hyperkeratosis, **(B)** rapid progression of ILD manifestations within 5 weeks.

DM, the autoantibodies directed against NXP-2 are frequently associated with calcinosis and ischemic muscle involvement in up to 60% of cases (111). In adults, a possible association was reported with malignancies such as mamma-, uterus- and pancreas-carcinomas.

The ANA pattern of **anti-MDA5 antibodies** on HEp-2 cells in IIF is usually negative. These antibodies were identified for the first time in East-Asian populations. They are more frequently observed in adult DM and were reported in a prevalence of 19–35% (19, 81). In a study with 285 patients with JDM (112), anti-MDA5 antibodies were detectable in 7.4% of patients (21/285) and a recent review reports a prevalence of 0–13% in Europe and USA (113). The typical clinical manifestations of adult IIM patients with anti-MDA5 antibodies were amyopathic myositis with rapidly progressive interstitial lung disease (ILD), which in turn determines a high mortality rate in these patients (**Figure 4**). However, ILD must not be rapidly progressive in every case. In contrast to Asian patients, Caucasian patients often show skin ulcerations and painful palmar papules (114, 115). Furthermore, differences were also reported for Asian compared to Caucasian JDM associated with MDA-5 antibodies. In this context, Japanese patients showed a pulmonary involvement in nearly 50% of patients, whereas the incidence of ILD was much lower in Caucasians. JDM patients with anti-MDA5 antibodies show frequent skin as well as oral ulceration, but no calcinosis and had less severe muscle weakness compared other JDM subtypes. Of note, ILD was found in 4 of 12 cases (19%) on chest X-ray. None of these anti-MDA5 antibodies positive ILD patients was positive for anti-synthetase antibodies suggesting that anti-MDA5 antibodies represent an own subtype of IIM. This study also revealed that more patients with anti-MDA5-antibodies were in remission after 2 years compared to patients without these antibodies. In the follow-up, patients in remission showed a decline in the titer of MDA5 antibodies. These results resemble those of prior studies in which antibodies were shown to disappear during disease remission (20).

The **anti-SAE-antibodies** were originally described in adults with DM exhibiting an amyopathic onset with skin manifestations, but who may develop myositis several months later. Lung involvement was infrequent reported. The antibodies were detected in approximately 7–8% of adult Caucasian patients with DM (25, 116). In a study with 110 Japanese patients with

DM including 13 with JDM, only 2 patients with DM (1,8%) were shown to have SAE-antibodies (117). In a large study with 436 patients with JIIM, only one patient with JDM was positive for **anti-SAE-antibodies** (118). Therefore, the presence of SAE-antibodies in patients with JIIM seems to be extremely rare.

Immune Mediated Necrotizing Myositis (IMNM)

Anti-SRP-Antibodies were detected in about 3 to 7% of adults with IIM (73, 119). In JIIM, these antibodies are even more infrequently observed in only 1.6% of patients exclusively with juvenile polymyositis (JPM) (103, 120). The presence of SRP-antibodies can be suspected by detection of a cytoplasmic staining pattern in ANA IIF (**Figure 1**). Adults with anti-SRP-antibodies develop typically an acute necrotizing myopathy with prominent muscle impairment without skin manifestations. Compared to other myositis forms, a satisfactory response to medicament treatment is difficult to achieve. Pulmonary involvement, Raynaud-symptoms, arthritis or overlap syndromes are infrequent. Similar to adults, juvenile patients have very high levels of CPK as well as often cardiac involvement detectable e.g., by ECG or echocardiography. Of note, adult patients show frequently Raynaud-symptoms, dysphonia and dyspnea under exertion (107). Compared to other forms of JIIM, onset of symptoms is late in patients with anti-SRP-antibodies. However, two unusual cases have been published recently with onset in the first decade of life showing muscular dystrophy and a low degree of inflammation in muscle biopsy (107). The antibody titer against SRP seems to correlate with clinical activity as well as with levels of CPK in adults as well as in JIMM and can be used for monitoring of therapy (78, 121).

Antibodies against the enzyme **3-hydroxy-3-methylglutaryl-CoA reductase** (HMGCR) have been identified initially in patients with immune mediated necrotizing myositis (IMNM) in association with statin treatment. Overall, autoantibodies against HMGCR are detectable in 6–7% of patients with IIM (28–30). Myalgias, as a common side effects under statins, are not associated with this form of myositis and positive HMGCR-antibodies. In fact, only a minority of patients under statin treatment develops myopathy with anti-HMGCR-antibodies (122). Furthermore, even patients without statin treatment can develop necrotizing myositis with positive anti-HMGCR-antibodies (123). Results of a multicenter study show that the majority of patients with anti-HMGCR antibodies have IMNM. In this study, the prevalence of anti-HMGCR antibodies in different subpopulations of IMNM exposed to statins was approximately 70%, and even 75% in patients above the age of 50 years. However, approximately 45% of INMN patients had no exposure to statins and in 5% of cases did not show muscle necrosis (124). In contrast to non-immune statin myopathy, which resolves after stopping statin therapy, patients with anti-HMGCR antibodies have a persistent autoimmune response despite cancelation of treatment with the inducing agent. Similar to SRP antibodies, the titer of anti-HMGCR antibodies correlates with the clinical activity of necrotizing myositis. However, in contrast to SRP antibodies it is not known, whether antibody titres can normalize under effective therapy (125–127). Of note, these antibodies have also been detected in children after statin therapy recently, however, the experience with these cases is very limited (128, 129).

The detection of anti-HMGCR antibodies was performed by only few laboratories using immunoprecipitation so far, since no standardized commercial assay was available. An introduction of other methods such as ELISA or chemiluminescence for the detection of anti-HMGCR antibodies could make this test widely available to facilitate the diagnostic possibilities (130). However, since such immunoassays can yield false positive results due to detection of low avidity antibodies, a confirmatory analysis by immunoprecipitation can be recommended (131). Interestingly, usage of rat hepatocytes in indirect immunofluorescence was proposed (132). However, although some laboratories have adopted this strategy, there are not yet available data from an extended use of this approach (133). Of note, in a French cohort study HMGCR positive IMNM-patients were found to be at higher risk for malignancy (134).

AUTOANTIBODIES IN DM AND THE RISK OF CANCER

A high risk of cancer development is well-described and has led to the sub-categorization of cancer associated myositis (CAM) (135). The overall risk of cancer in myositis is significantly higher than in the age-matched population and approximately 10% of IIM are associated with malignancies (134–138). In DM, the risk is especially increased in the first 5 years after diagnosis (139–144). The most common cancers among the reported cases associated with DM are nasopharyngeal carcinoma and adenocarcinoma of the ovary, lung, pancreas, stomach and colon (139–145). Many studies have claimed the presence or absence of certain antibodies as markers for the risk of cancer in myositis. The autoantibody profile is considered a useful tool to identify patients at risk for CAM (32). In this context, the best established antibodies are directed against TIF1-γ with a high sensitivity and specificity for cancer associated DM in adult patients (27, 52, 53, 105, 146, 147), but not in JDM (50). Furthermore, also NXP-2 positivity in DM patients has been identified as a risk factor for malignancy (148). The association of anti-synthetase and anti-HMGCR antibodies with cancer is less clear and needs further confirmation. To exclude an associated malignancy in clinical practice repetitive examinations can be recommended in DM patients at risk, whereas clear guidelines on the frequency and extension of such diagnostic procedures are missing so far.

SUMMARY

Autoantibodies in IIM are very important diagnostic and prognostic markers, which can help to facilitate our approach to these rare and divers diseases. They correlate closely with the clinical manifestation of disease and allow stratification of patients. However, a laboratory result provides always only a piece of the diagnostic puzzle and should always be questioned if not plausible. For this purpose, a better knowledge on the

limitations of the laboratory procedures is necessary and tests should only be performed if indicated according to the clinical picture. To allow comparison and improve reproducibility, the existing assays require uniform standards on an international level, and optimized methods for a broader distribution. If these issues can be solved, antibodies in IIM will play a more prominent role in the classification of disease. Another interesting and important tasks for the future will be to investigate the treatment response in IIM patients according to their antibody profile in more detail. This includes the question, whether different antibodies correlate with disease activity, but can be also used for an individualized approach to predict the response and outcome. Finally, the interaction of the antibodies with the targeted antigens is of major interest especially for the IIM specific entities. A deeper understanding on the mechanisms behind the induction of the respective immune response as well as on the potential role of the targeted antigens in IIM can improve our insight into the pathogenesis of disease.

AUTHOR CONTRIBUTIONS

BS reviewed published articles and contributed to the manuscript on antigen-antibody systems. US reviewed published articles and contributed to the manuscript on clinical aspects. J-BG-G reviewed published articles and contributed to the manuscript on laboratory diagnostic aspects. EF reviewed published articles and contributed to all parts of the manuscript.

REFERENCES

1. Mantegazza R, Bernasconi P, Confalonieri P, Cornelio F. Inflammatory myopathies and systemic disorders: a review of immunopathogenetic mechanisms and clinical features. *J Neurol*. (1997) 244:277–87. doi: 10.1007/s004150050087
2. Nagaraju K, Casciola-Rosen L, Lundberg I, Rawat R, Cutting S, Thapliyal R, et al. Activation of the endoplasmic reticulum stress response in autoimmune myositis: potential role in muscle fiber damage and dysfunction. *Arthritis Rheum*. (2005) 52:1824–35. doi: 10.1002/art.21103
3. Preuße C, Goebel HH, Held J, Wengert O, Scheibe F, Irlbacher K, et al. Immune-mediated necrotizing myopathy is characterized by a specific Th1-M1 polarized immune profile. *Am J Pathol*. (2012) 181:2161–71. doi: 10.1016/j.ajpath.2012.08.033
4. Eisa-Beygi S, Hatch G, Noble S, Ekker M, Moon TW. The 3-hydroxy-3-methylglutaryl-CoA reductase (HMGCR) pathway regulates developmental cerebral-vascular stability via prenylation-dependent signalling pathway. *Dev Biol*. (2013) 373:258–66. doi: 10.1016/j.ydbio.2012.11.024
5. Gunawardena H, Betteridge ZE, McHugh NJ. Myositis-specific autoantibodies: their clinical and pathogenic significance in disease expression. *Rheumatology*. (2009) 48:607–12. doi: 10.1093/rheumatology/kep078
6. Targoff IN. Autoantibodies to aminoacyl-transfer RNA synthetases for isoleucine and glycine. Two additional synthetases are antigenic in myositis. *J Immunol*. (1990) 144:1737–43.
7. Brouwer R, Hengstman GJ, Vree Egberts W, Ehrfeld H, Bozic B, Ghirardello A, et al. Autoantibody profiles in the sera of European patients with myositis. *Ann Rheum Dis*. (2001) 60:116–23. doi: 10.1136/ard.60.2.116
8. Mathews MB, Reichlin M, Hughes GR, Bernstein RM. Anti-threonyl-tRNA synthetase, a second myositis-related autoantibody. *J Exp Med*. (1984) 160:420–34. doi: 10.1084/jem.160.2.420
9. Rutjes SA, Vree Egberts WT, Jongen P, Van Den Hoogen F, Pruijn GJ, Van Venrooij WJ. Anti-Ro52 antibodies frequently co-occur with anti-Jo-1 antibodies in sera from patients with idiopathic inflammatory myopathy. *Clin Exp Immunol*. (1997) 109:32–40. doi: 10.1046/j.1365-2249.1997.4081308.x
10. Mileti LM, Strek ME, Niewold TB, Curran JJ, Sweiss NJ. Clinical characteristics of patients with anti-Jo-1 antibodies: a single center experience. *J Clin Rheumatol*. (2009) 15:254–5. doi: 10.1097/RHU.0b013e3181b0e910
11. Targoff IN, Trieu EP, Miller FW. Reaction of anti-OJ autoantibodies with components of the multi-enzyme complex of aminoacyl-tRNA synthetases in addition to isoleucyl-tRNA synthetase. *J Clin Invest*. (1993) 91:2556–64. doi: 10.1172/JCI116493
12. Bunn CC, Bernstein RM, Mathews MB. Autoantibodies against alanyl-tRNA synthetase and tRNAAla coexist and are associated with myositis. *J Exp Med*. (1986) 163:1281–91. doi: 10.1084/jem.163.5.1281
13. Hirakata M, Suwa A, Nagai S, Kron MA, Trieu EP, Mimori T, et al. Anti-KS: identification of autoantibodies to asparaginyl-transfer RNA synthetase associated with interstitial lung disease. *J Immunol*. (1999) 162:2315–20.
14. Hirakata M, Suwa A, Takada T, Sato S, Nagai S, Genth E, et al. Clinical and immunogenetic features of patients with autoantibodies to asparaginyl-transfer RNA synthetase. *Arthritis Rheum*. (2007) 56:1295–303. doi: 10.1002/art.22506
15. Vartanian OA. Detection of autoantibodies against phenylalanyl-, tyrosyl-, and tryptophanyl-tRNA-synthetase and anti-idiotypic antibodies to it in serum from patients with autoimmune diseases. *Mol Biol*. (1991) 25:1033–9.
16. Betteridge Z, Gunawardena H, North J, Slinn J, McHugh N. Anti-synthetase syndrome: a new autoantibody to phenylalanyl transfer RNA synthetase (anti-Zo) associated with polymyositis and interstitial pneumonia. *Rheumatology*. (2007) 46:1005–8. doi: 10.1093/rheumatology/kem045
17. Vincze M, Molnár PA, Tumpek J, Szollosi L, Gyetvai A, Kapitány A, et al. An unusual association: anti-Jo1 and anti-SRP antibodies in the serum of a patient with polymyositis. *Clin Rheumatol*. (2010) 29:811–4. doi: 10.1007/s10067-010-1394-6
18. Genth E, Mierau R. Diagnostic significance of scleroderma and myositis-associated autoantibodies. *Z Rheumatol*. (1995) 54:39–49.
19. Sato S, Hoshino K, Satoh T, Fujita T, Kawakami Y, Fujita T, et al. RNA helicase encoded by melanoma differentiation-associated gene 5 is a major autoantigen in patients with clinically amyopathic dermatomyositis: association with rapidly progressive interstitial lung disease. *Arthritis Rheum*. (2009) 60:2193–200. doi: 10.1002/art.24621
20. Muro Y, Sugiura K, Hoshino K, Akiyama M. Disappearance of anti-MDA-5 autoantibodies in clinically amyopathic DM/interstitial lung disease during disease remission. *Rheumatology*. (2012) 51:800–4. doi: 10.1093/rheumatology/ker408
21. Targoff IN, Reichlin M. The association between Mi-2 antibodies and dermatomyositis. *Arthritis Rheum*. (1985) 28:796–803. doi: 10.1002/art.1780280711
22. Hirakata M. Autoantibodies and their clinical significance in idiopathic inflammatory myopathies; polymyositis/dermatomyositis and related conditions. *Nihon Rinsho Meneki Gakkai Kaishi*. (2007) 30:444–54. doi: 10.2177/jsci.30.444
23. Gunawardena H, Betteridge ZE, McHugh NJ. Newly identified autoantibodies: relationship to idiopathic inflammatory myopathy subsets and pathogenesis. *Curr Opin Rheumatol*. (2008) 20:675–80. doi: 10.1097/BOR.0b013e328313bff4
24. Aouizerate J, De Antonio M, Bader-Meunier B, Barnerias C, Bodemer C, Isapof A, et al. Muscle ischaemia associated with NXP2 autoantibodies: a severe subtype of juvenile dermatomyositis. *Rheumatology*. (2018) 57:873–9. doi: 10.1093/rheumatology/kex516
25. Betteridge ZE, Gunawardena H, Chinoy H, North J, Ollier WE, Cooper RG, et al. Clinical and human leucocyte antigen class II haplotype associations of

autoantibodies to small ubiquitin-like modifier enzyme, a dermatomyositis-specific autoantigen target, in UK Caucasian adult-onset myositis. *Ann Rheum Dis*. (2009) 68:1621–5. doi: 10.1136/ard.2008.097162
26. Betteridge ZE, Gunawardena H, McHugh NJ. Novel autoantibodies and clinical phenotypes in adult and juvenile myositis. *Arthritis Res Ther*. (2011) 13:209. doi: 10.1186/ar3275
27. Targoff IN, Mamyrova G, Trieu EP, Perurena O, Koneru B, O'Hanlon TP, et al. A novel autoantibody to a 155-kd protein is associated with dermatomyositis. *Arthritis Rheum*. (2006) 54:3682–9. doi: 10.1002/art.22164
28. Mohassel P, Mammen AL. Anti-HMGCR myopathy. *J Neuromuscul Dis*. (2018) 5:11–20. doi: 10.3233/JND-170282
29. Mammen AL, Chung T, Christopher-Stine L, Rosen P, Rosen A, Doering KR, et al. Autoantibodies against 3-hydroxy-3-methylglutaryl-coenzyme A reductase in patients with statin-associated autoimmune myopathy. *Arthritis Rheum*. (2011) 63:713–21. doi: 10.1002/art.30156
30. Padala S, Thompson PD. Statins as a possible cause of inflammatory and necrotizing myopathies. *Atherosclerosis*. (2012) 222:15–21. doi: 10.1016/j.atherosclerosis.2011.11.005
31. Christopher-Stine L, Casciola-Rosen LA, Hong G, Chung T, Corse AM, Mammen AL. A novel autoantibody recognizing 200-kd and 100-kd proteins is associated with an immune-mediated necrotizing myopathy. *Arthritis Rheum*. (2010) 62:2757–66. doi: 10.1002/art.27572
32. Chinoy H, Fertig N, Oddis CV, Ollier WE, Cooper RG. The diagnostic utility of myositis autoantibody testing for predicting the risk of cancer-associated myositis. *Ann Rheum Dis*. (2007) 66:1345–9. doi: 10.1136/ard.2006.068502
33. Ghirardello A, Doria A. New insights in myositis-specific autoantibodies. *Curr Opin Rheumatol*. (2018) 30:614–22. doi: 10.1097/BOR.0000000000000548
34. Tawara N, Yamashita S, Zhang X, Korogi M, Zhang Z, Doki T, et al. Pathomechanisms of anti-cytosolic 5'-nucleotidase 1A autoantibodies in sporadic inclusion body myositis. *Ann Neurol*. (2017) 81:512–25. doi: 10.1002/ana.24919
35. Lilleker JB, Rietveld A, Pye SR, Mariampillai K, Benveniste O, Peeters MT, et al. Cytosolic 5'-nucleotidase 1A autoantibody profile and clinical characteristics in inclusion body myositis. *Ann Rheum Dis*. (2017) 76:862–8. doi: 10.1136/annrheumdis-2016-210282
36. Herbert MK, Stammen-Vogelzangs J, Verbeek MM, Rietveld A, Lundberg IE, Chinoy H, et al. Disease specificity of autoantibodies to cytosolic 5'-nucleotidase 1A in sporadic inclusion body myositis versus known autoimmune diseases. *Ann Rheum Dis*. (2016) 75:696–701. doi: 10.1136/annrheumdis-2014-206691
37. Mimori T, Hinterberger M, Pettersson I, Steitz JA. Autoantibodies to the U2 small nuclear ribonucleoprotein in a patient with scleroderma-polymyositis overlap syndrome. *J Biol Chem*. (1984) 259:560–5.
38. Hilker M, Tröster H, Grölz D, Hake U, Bachmann M. The autoantigen La/SS-B: analysis of the expression of alternatively spliced La mRNA isoforms. *Cell Tissue Res*. (1996) 284:383–9. doi: 10.1007/s004410050599
39. Teppo AM, Gripenberg M, Kurki P, Baklien K, Helve T, Wegelius O. Purification and characterization of a nuclear SS-B antigen. *Scand J Immunol*. (1982) 15:1–7. doi: 10.1111/j.1365-3083.1982.tb00615.x
40. Pakozdi A, Nihtyanova S, Moinzadeh P, Ong VH, Black CM, Denton CP. Clinical and serological hallmarks of systemic sclerosis overlap syndromes. *J Rheumatol*. (2011) 38:2406–9. doi: 10.3899/jrheum.101248
41. Váncsa A, Gergely L, Ponyi A, Lakos G, Németh J, Szodoray P, et al. Myositis-specific and myositis-associated antibodies in overlap myositis in comparison to primary dermatopolymyositis: Relevance for clinical classification: retrospective study of 169 patients. *Joint Bone Spine*. (2010) 77:125–30. doi: 10.1016/j.jbspin.2009.08.008
42. Limaye VS, Cassidy J, Scott G, Roberts-Thomson PJ, Gillis D. Anti-Ro52 antibodies, antisynthetase antibodies, and antisynthetase syndrome. *Clin Rheumatol*. (2008) 27:521–3. doi: 10.1007/s10067-007-0762-3
43. Ghirardello A, Zampieri S, Tarricone E, Iaccarino L, Bendo R, Briani C, et al. Clinical implications of autoantibody screening in patients with autoimmune myositis. *Autoimmunity*. (2006) 39:217–21. doi: 10.1080/08916930600622645
44. Wasicek CA, Reichlin M, Montes M, Raghu G. Polymyositis and interstitial lung disease in a patient with anti-Jo1 prototype. *Am J Med*. (1984) 76:538–44. doi: 10.1016/0002-9343(84)90677-6
45. Yang DC, Dang CV, Arnett FC. Rat liver histidyl-tRNA synthetase. Purification and inhibition by the myositis-specific anti-Jo-1 autoantibody. *Biochem Biophys Res Commun*. (1984) 120:15–21. doi: 10.1016/0006-291X(84)91407-4
46. Brouwer R, Vree Egberts W, Jongen PH, van Engelen BG, van Venrooij WJ. Frequent occurrence of anti-tRNA(His) autoantibodies that recognize a conformational epitope in sera of patients with myositis. *Arthritis Rheum*. (1998) 41:1428–37. doi: 10.1002/1529-0131(199808)41:8<1428::AID-ART12>3.0.CO;2-J
47. Miller FW, Twitty SA, Biswas T, Plotz PH. Origin and regulation of a disease-specific autoantibody response. Antigenic epitopes, spectrotype stability, and isotype restriction of anti-Jo-1 autoantibodies. *J Clin Invest*. (1990) 85:468–75. doi: 10.1172/JCI114461
48. O'Hanlon TP, Rider LG, Mamyrova G, Targoff IN, Arnett FC, Reveille JD, et al. HLA polymorphisms in African Americans with idiopathic inflammatory myopathy: allelic profiles distinguish patients with different clinical phenotypes and myositis autoantibodies. *Arthritis Rheum*. (2006) 54:3670–81. doi: 10.1002/art.22205
49. Gono T, Kawaguchi Y, Kuwana M, Sugiura T, Furuya T, Takagi K, et al. Brief report: association of HLA-DRB1*0101/*0405 with susceptibility to anti-melanoma differentiation-associated gene 5 antibody-positive dermatomyositis in the Japanese population. *Arthritis Rheum*. (2012) 64:3736–40. doi: 10.1002/art.34657
50. Gunawardena H, Wedderburn LR, North J, Betteridge Z, Dunphy J, Chinoy H, et al. Clinical associations of autoantibodies to a p155/140 kDa doublet protein in juvenile dermatomyositis. *Rheumatology*. (2008) 47:324–8. doi: 10.1093/rheumatology/kem359
51. Kaji K, Fujimoto M, Hasegawa M, Kondo M, Saito Y, Komura K, et al. Identification of a novel autoantibody reactive with 155 and 140 kDa nuclear proteins in patients with dermatomyositis: an association with malignancy. *Rheumatology*. (2007) 46:25–8. doi: 10.1093/rheumatology/kel161
52. Fiorentino D, Casciola-Rosen L. TIF1 autoantibodies in dermatomyositis shed insight into the cancer-myositis connection. *Arthritis Rheum*. (2012) 64:346–9. doi: 10.1002/art.33402
53. Fujimoto M, Hamaguchi Y, Kaji K, Matsushita T, Ichimura Y, Kodera M, et al. Myositis-specific anti-155/140 autoantibodies target transcription intermediary factor 1 family proteins. *Arthritis Rheum*. (2012) 64:513–22. doi: 10.1002/art.33403
54. Kawai T, Akira S. Regulation of innate immune signalling pathways by the tripartite motif (TRIM) family proteins. *EMBO Mol Med*. (2011) 3:513–27. doi: 10.1002/emmm.201100160
55. Khetchoumian K, Teletin M, Mark M, Lerouge T, Cerviño M, Oulad-Abdelghani M, et al. TIF1delta, a novel HP1-interacting member of the transcriptional intermediary factor 1 (TIF1) family expressed by elongating spermatids. *J Biol Chem*. (2004) 279:48329–41. doi: 10.1074/jbc.M404779200
56. Venturini L, You J, Stadler M, Galien R, Lallemand V, Koken MH, et al. TIF1gamma, a novel member of the transcriptional intermediary factor 1 family. *Oncogene*. (1999) 18:1209–17. doi: 10.1038/sj.onc.1202655
57. Agricola E, Randall RA, Gaarenstroom T, Dupont S, Hill CS. Recruitment of TIF1γ to chromatin via its PHD finger-bromodomain activates its ubiquitin ligase and transcriptional repressor activities. *Mol Cell*. (2011) 43:85–96. doi: 10.1016/j.molcel.2011.05.020
58. Venalis P, Selickaja S, Lundberg K, Rugiene R, Lundberg IE. Association of anti-transcription intermediary factor 1gamma antibodies with paraneoplastic rheumatic syndromes other than dermatomyositis. *Arthritis Care Res*. (2018) 70:648–51. doi: 10.1002/acr.23325
59. Pinal-Fernandez I, Ferrer-Fabregas B, Trallero-Araguas E, Balada E, Martínez MA, Milisenda JC, et al. Tumour TIF1 mutations and loss of heterozygosity related to cancer-associated myositis. *Rheumatology*. (2018) 57:388–96. doi: 10.1093/rheumatology/kex413
60. Joseph CG, Darrah E, Shah AA, Skora AD, Casciola-Rosen LA, Wigley FM, et al. Association of the autoimmune disease scleroderma with an immunologic response to cancer. *Science*. (2014) 343:152–7. doi: 10.1126/science.1246886

61. Schreiber RD, Old LJ, Smyth MJ. Cancer immunoediting: integrating immunity's roles in cancer suppression and promotion. *Science*. (2011) 331:1565–70. doi: 10.1126/science.1203486
62. Parkes JE, Rothwell S, Oldroyd A, Chinoy H, Lamb JA, Myositis Genetics Consortium (MYOGEN). Genetic background may contribute to the latitude-dependent prevalence of dermatomyositis and anti-TIF1-gamma autoantibodies in adult patients with myositis. *Arthritis Res Ther*. (2018) 20:117. doi: 10.1186/s13075-018-1617-9
63. Wang HB, Zhang Y. Mi2, an auto-antigen for dermatomyositis, is an ATP-dependent nucleosome remodeling factor. *Nucleic Acids Res*. (2001) 29:2517–21. doi: 10.1093/nar/29.12.2517
64. Burd CJ, Kinyamu HK, Miller FW, Archer TK. UV radiation regulates Mi-2 through protein translation and stability. *J Biol Chem*. (2008) 283:34976–82. doi: 10.1074/jbc.M805383200
65. Okada S, Weatherhead E, Targoff IN, Wesley R, Miller FW. Global surface ultraviolet radiation intensity may modulate the clinical and immunologic expression of autoimmune muscle disease. *Arthritis Rheum*. (2003) 48:2285–93. doi: 10.1002/art.11090
66. Mammen AL, Casciola-Rosen LA, Hall JC, Christopher-Stine L, Corse AM, Rosen A. Expression of the dermatomyositis autoantigen Mi-2 in regenerating muscle. *Arthritis Rheum*. (2009) 60:3784–93. doi: 10.1002/art.24977
67. O'Hanlon TP, Carrick DM, Targoff IN, Arnett FC, Reveille JD, Carrington M, et al. Immunogenetic risk and protective factors for the idiopathic inflammatory myopathies: distinct HLA-A, -B, -Cw, -DRB1, and -DQA1 allelic profiles distinguish European American patients with different myositis autoantibodies. *Medicine*. (2006) 85:111–27. doi: 10.1097/01.md.0000217525.82287.eb
68. Ghirardello A, Bassi N, Palma L, Borella E, Domeneghetti M, Punzi L, et al. Autoantibodies in polymyositis and dermatomyositis. *Curr Rheumatol Rep*. (2013) 15:335. doi: 10.1007/s11926-013-0335-1
69. Betteridge Z, Gunawardena H, North J, Slinn J, McHugh N. Identification of a novel autoantibody directed against small ubiquitin-like modifier activating enzyme in dermatomyositis. *Arthritis Rheum*. (2007) 56:3132–7. doi: 10.1002/art.22862
70. Ullu E, Weiner AM. Human genes and pseudogenes for the 7SL RNA component of signal recognition particle. *EMBO J*. (1984) 3:3303–10. doi: 10.1002/j.1460-2075.1984.tb02294.x
71. Targoff IN, Johnson AE, Miller FW. Antibody to signal recognition particle in polymyositis. *Arthritis Rheum*. (1990) 33:1361–70. doi: 10.1002/art.1780330908
72. Janda CY, Li J, Oubridge C, Hernández H, Robinson CV, Nagai K. Recognition of a signal peptide by the signal recognition particle. *Nature*. (2010) 465:507–10. doi: 10.1038/nature08870
73. Satoh T, Okano T, Matsui T, Watabe H, Ogasawara T, Kubo K, et al. Novel autoantibodies against 7SL RNA in patients with polymyositis/dermatomyositis. *J Rheumatol*. (2005) 32:1727–33.
74. Okada N, Mimori T, Mukai R, Kashiwagi H, Hardin JA. Characterization of human autoantibodies that selectively precipitate the 7SL RNA component of the signal recognition particle. *J Immunol*. (1987) 138:3219–23.
75. Reeves WH, Nigam SK, Blobel G. Human autoantibodies reactive with the signal-recognition particle. *Proc Natl Acad Sci USA*. (1986) 83:9507–11. doi: 10.1073/pnas.83.24.9507
76. Römisch K, Miller FW, Dobberstein B, High S. Human autoantibodies against the 54 kDa protein of the signal recognition particle block function at multiple stages. *Arthritis Res Ther*. (2006) 8:R39. doi: 10.1186/ar1895
77. Bergua C, Chiavelli H, Allenbach Y, Arouche-Delaperche L, Arnoult C, Bourdenet G, et al. *In vivo* pathogenicity of IgG from patients with anti-SRP or anti-HMGCR autoantibodies in immune-mediated necrotising myopathy. *Ann Rheum Dis*. (2018) 78:131–9. doi: 10.1136/annrheumdis-2018-213518
78. Benveniste O, Drouot L, Jouen F, Charuel JL, Bloch-Queyrat C, Behin A, et al. Correlation of anti-signal recognition particle autoantibody levels with creatine kinase activity in patients with necrotizing myopathy. *Arthritis Rheum*. (2011) 63:1961–71. doi: 10.1002/art.30344
79. Betteridge ZE, Gunawardena H, McHugh NJ. Pathogenic mechanisms of disease in myositis: autoantigens as clues. *Curr Opin Rheumatol*. (2009) 21:604–9. doi: 10.1097/BOR.0b013e328331638a
80. Takeuchi O, Akira S. MDA5/RIG-I and virus recognition. *Curr Opin Immunol*. (2008) 20:17–22. doi: 10.1016/j.coi.2008.01.002
81. Nakashima R, Imura Y, Kobayashi S, Yukawa N, Yoshifuji H, Nojima T, et al. The RIG-I-like receptor IFIH1/MDA5 is a dermatomyositis-specific autoantigen identified by the anti-CADM-140 antibody. *Rheumatology*. (2010) 49:433–40. doi: 10.1093/rheumatology/kep375
82. Gono T, Kawaguchi Y, Satoh T, Kuwana M, Katsumata Y, Takagi K, et al. Clinical manifestation and prognostic factor in anti-melanoma differentiation-associated gene 5 antibody-associated interstitial lung disease as a complication of dermatomyositis. *Rheumatology*. (2010) 49:1713–9. doi: 10.1093/rheumatology/keq149
83. Szodoray P, Szabó Z, Kapitány A, Gyetvai A, Lakos G, Szántó S, et al. Anti-citrullinated protein/peptide autoantibodies in association with genetic and environmental factors as indicators of disease outcome in rheumatoid arthritis. *Autoimmun Rev*. (2010) 9:140–3. doi: 10.1016/j.autrev.2009.04.006
84. Rosendorff A, Sakakibara S, Lu S, Kieff E, Xuan Y, DiBacco A, et al. NXP-2 association with SUMO-2 depends on lysines required for transcriptional repression. *Proc Natl Acad Sci USA*. (2006) 103:5308–13. doi: 10.1073/pnas.0601066103
85. Targoff IN. Laboratory testing in the diagnosis and management of idiopathic inflammatory myopathies. *Rheum Dis Clin North Am*. (2002) 28:859–90. doi: 10.1016/S0889-857X(02)00032-7
86. Männistö T, Surcel HM, Bloigu A, Ruokonen A, Hartikainen AL, Järvelin MR, et al. The effect of freezing, thawing, and short- and long-term storage on serum thyrotropin, thyroid hormones, and thyroid autoantibodies: implications for analyzing samples stored in serum banks. *Clin Chem*. (2007) 53:1986–7. doi: 10.1373/clinchem.2007.091371
87. Gislefoss RE, Grimsrud TK, Morkrid L. Stability of selected serum proteins after long-term storage in the Janus Serum Bank. *Clin Chem Lab Med*. (2009) 47:596–603. doi: 10.1515/CCLM.2009.121
88. Nakashima R, Hosono Y, Mimori T. Clinical significance and new detection system of autoantibodies in myositis with interstitial lung disease. *Lupus*. (2016) 25:925–33. doi: 10.1177/0961203316651748
89. Aggarwal R, Oddis CV, Goudeau D, Fertig N, Metes I, Stephens C, et al. Anti-transcription intermediary factor 1-gamma autoantibody ELISA development and validation. *Rheumatology*. (2014) 53:433–7. doi: 10.1093/rheumatology/ket383
90. Fujimoto M, Murakami A, Kurei S, Okiyama N, Kawakami A, Mishima M, et al. Enzyme-linked immunosorbent assays for detection of anti-transcriptional intermediary factor-1 gamma and anti-Mi-2 autoantibodies in dermatomyositis. *J Dermatol Sci*. (2016) 84:272–81. doi: 10.1016/j.jdermsci.2016.09.013
91. Johnson C, Pinal-Fernandez I, Parikh R, Paik J, Albayda J, Mammen AL, et al. Assessment of mortality in autoimmune myositis with and without associated interstitial lung disease. *Lung*. (2016) 194:733–7. doi: 10.1007/s00408-016-9896-x
92. Qiang JK, Kim WB, Baibergenova A, Alhusayen R. Risk of malignancy in dermatomyositis and polymyositis. *J Cutan Med Surg*. (2017) 21:131–6. doi: 10.1177/1203475416665601
93. Cavagna L, Nuño L, Scirè CA, Govoni M, Longo FJ, Franceschini F, et al. Serum Jo-1 autoantibody and isolated arthritis in the antisynthetase syndrome: review of the literature and report of the experience of AENEAS collaborative group. *Clin Rev Allergy Immunol*. (2017) 52:71–80. doi: 10.1007/s12016-016-8528-9
94. Klein M, Mann H, Pleštilová L, Betteridge Z, McHugh N, Remáková M, et al. Arthritis in idiopathic inflammatory myopathy: clinical features and autoantibody associations. *J Rheumatol*. (2014) 41:1133–9. doi: 10.3899/jrheum.131223
95. Stone KB, Oddis CV, Fertig N, Katsumata Y, Lucas M, Vogt M, et al. Anti-Jo-1 antibody levels correlate with disease activity in idiopathic inflammatory myopathy. *Arthritis Rheum*. (2007) 56:3125–31. doi: 10.1002/art.22865
96. Mescam-Mancini L, Allenbach Y, Hervier B, Devilliers H, Mariampillay K, Dubourg O, et al. Anti-Jo-1 antibody-positive patients show a characteristic necrotizing perifascicular myositis. *Brain*. (2015) 138:2485–92. doi: 10.1093/brain/awv192
97. Maturu VN, Lakshman A, Bal A, Dhir V, Sharma A, Garg M, et al. Antisynthetase syndrome: an under-recognized cause of interstitial lung disease. *Lung India*. (2016) 33:20–6. doi: 10.4103/0970-2113.173055

98. Shi J, Li S, Yang H, Zhang Y, Peng Q, Lu X, et al. Clinical profiles and prognosis of patients with distinct antisynthetase autoantibodies. *J Rheumatol*. (2017) 44:1051–7. doi: 10.3899/jrheum.161480
99. Labirua-Iturburu A, Selva-O'Callaghan A, Vincze M, Dankó K, Vencovsky J, Fisher B, et al. Anti-PL-7 (anti-threonyl-tRNA synthetase) antisynthetase syndrome: clinical manifestations in a series of patients from a European multicenter study (EUMYONET) and review of the literature. *Medicine*. (2012) 91:206–11. doi: 10.1097/MD.0b013e318260977c
100. Marie I, Hatron PY, Dominique S, Cherin P, Mouthon L, Menard JF, et al. Short-term and long-term outcome of anti-Jo1-positive patients with anti-Ro52 antibody. *Semin Arthritis Rheum*. (2012) 41:890–9. doi: 10.1016/j.semarthrit.2011.09.008
101. Madan V, Chinoy H, Griffiths CEM, Cooper RG. Defining cancer-risk, and assessing diagnostic usefulness of myositis serology, in dermatomyositis- Part 2. *Clin Exp Dermatol*. (2009) 34:561–5. doi: 10.1111/j.1365-2230.2009.03227.x
102. Aggarwal R, Oddis CV, Goudeau D, Koontz D, Qi Z, Reed AM, et al. Autoantibody levels in myositis patients correlate with clinical response during B cell depletion with rituximab. *Rheumatology*. (2016) 55:1710. doi: 10.1093/rheumatology/kew275
103. Rider LG, Shah M, Mamyrova G, Huber AM, Rice MM, Targoff IN, et al. The myositis autoantibody phenotypes of the juvenile idiopathic inflammatory myopathies. *Medicine*. (2013) 92:223–43. doi: 10.1097/MD.0b013e31829d08f9
104. Shah M, Mamyrova G, Targoff IN, Huber AM, Malley JD, Rice MM, et al. The clinical phenotypes of the juvenile idiopathic inflammatory myopathies. *Medicine*. (2013) 92:25–41. doi: 10.1097/MD.0b013e31827f264d
105. Trallero-Araguás E, Rodrigo-Pendás JÁ, Selva-O'Callaghan A, Martínez-Gómez X, Bosch X, Labrador-Horrillo M, et al. Usefulness of anti-p155 autoantibody for diagnosing cancer-associated dermatomyositis: a systematic review and meta-analysis. *Arthritis Rheum*. (2012) 64:523–32. doi: 10.1002/art.33379
106. Chiu YE, Co DO. Juvenile dermatomyositis: immunopathogenesis, role of myositis-specific autoantibodies, and review of rituximab use. *Pediatr Dermatol*. (2011) 28:357–67. doi: 10.1111/j.1525-1470.2011.01501.x
107. Casciola-Rosen L, Mammen AL. Myositis autoantibodies. *Curr Opin Rheumatol*. (2012) 24:602–8. doi: 10.1097/BOR.0b013e328358bd85
108. Espada G, Maldonado Cocco JA, Fertig N, Oddis CV. Clinical and serologic characterization of an Argentine pediatric myositis cohort: identification of a novel autoantibody (anti-MJ) to a 142-kDa protein. *J Rheumatol*. (2009) 36:2547–51. doi: 10.3899/jrheum.090461
109. Ceribelli A, Fredi M, Taraborelli M, Cavazzana I, Franceschini F, Quinzanini M, et al. Anti-MJ/NXP-2 autoantibody specificity in a cohort of adult Italian patients with polymyositis/dermatomyositis. *Arthritis Res Ther*. (2012) 14:R97. doi: 10.1186/ar3822
110. Ichimura Y, Matsushita T, Hamaguchi Y, Kaji K, Hasegawa M, Tanino Y, et al. Anti-NXP2 autoantibodies in adult patients with idiopathic inflammatory myopathies: possible association with malignancy. *Ann Rheum Dis*. (2012) 71:710–3. doi: 10.1136/annrheumdis-2011-200697
111. Chance B, Younkin DP, Kelley R, Bank WJ, Berkowitz HD, Argov Z, et al. Magnetic resonance spectroscopy of normal and diseased muscles. *Am J Med Genet*. (1986) 25:659–79. doi: 10.1002/ajmg.1320250408
112. Tansley SL, Betteridge ZE, Gunawardena H, Jacques TS, Owens CM, Pilkington C, et al. Anti-MDA5 autoantibodies in juvenile dermatomyositis identify a distinct clinical phenotype: a prospective cohort study. *Arthritis Res Ther*. (2014) 16:R138. doi: 10.1186/ar4600
113. Palterer B, Vitiello G, Carraresi A, Giudizi MG, Cammelli D, Parronchi P. Bench to bedside review of myositis autoantibodies. *Clin Mol Allergy*. (2018) 16:5. doi: 10.1186/s12948-018-0084-9
114. Fiorentino D, Chung L, Zwerner J, Rosen A, Casciola-Rosen L. The mucocutaneous and systemic phenotype of dermatomyositis patients with antibodies to MDA5 (CADM-140): a retrospective study. *J Am Acad Dermatol*. (2011) 65:25–34. doi: 10.1016/j.jaad.2010.09.016
115. Hall JC, Casciola-Rosen L, Samedy LA, Werner J, Owoyemi K, Danoff SK, et al. Anti-melanoma differentiation-associated protein 5-associated dermatomyositis: expanding the clinical spectrum. *Arthritis Care Res*. (2013) 65:1307–15. doi: 10.1002/acr.21992
116. Tarricone E, Ghirardello A, Rampudda M, Bassi N, Punzi L, Doria A. Anti-SAE antibodies in autoimmune myositis: identification by unlabelled protein immunoprecipitation in an Italian patient cohort. *J Immunol Methods*. (2012) 384:128–34. doi: 10.1016/j.jim.2012.07.019
117. Muro Y, Sugiura K, Akiyama M. Low prevalence of anti-small ubiquitin-like modifier activating enzyme antibodies in dermatomyositis patients. *Autoimmunity*. (2013) 46:279–84. doi: 10.3109/08916934.2012.755958
118. Rider LG, Katz JD, Jones OY. Developments in the classification and treatment of the juvenile idiopathic inflammatory myopathies. *Rheum Dis Clin North Am*. (2013) 39:877–904. doi: 10.1016/j.rdc.2013.06.001
119. Hamaguchi Y, Kuwana M, Hoshino K, Hasegawa M, Kaji K, Matsushita T, et al. Clinical correlations with dermatomyositis-specific autoantibodies in adult Japanese patients with dermatomyositis: a multicenter cross-sectional study. *Arch Dermatol*. (2011) 147:391–8. doi: 10.1001/archdermatol.2011.52
120. Rouster-Stevens KA, Pachman LM. Autoantibody to signal recognition particle in African American girls with juvenile polymyositis. *J Rheumatol*. (2008) 35:927–9.
121. Momomura M, Miyamae T, Nozawa T, Kikuchi M, Kizawa T, Imagawa T, et al. Serum levels of anti-SRP54 antibodies reflect disease activity of necrotizing myopathy in a child treated effectively with combinatorial methylprednisolone pulses and plasma exchanges followed by intravenous cyclophosphamide. *Mod Rheumatol*. (2014) 24:529–31. doi: 10.3109/14397595.2013.852852
122. Mammen AL, Pak K, Williams EK, Brisson D, Coresh J, Selvin E, et al. Rarity of anti-3-hydroxy-3-methylglutaryl-coenzyme A reductase antibodies in statin users, including those with self-limited musculoskeletal side effects. *Arthritis Care Res*. (2012) 64:269–72. doi: 10.1002/acr.20662
123. Allenbach Y, Drouot L, Rigolet A, Charuel JL, Jouen F, Romero NB, et al. Anti-HMGCR autoantibodies in European patients with autoimmune necrotizing myopathies: inconstant exposure to statin. *Medicine*. (2014) 93:150–7. doi: 10.1097/MD.0000000000000028
124. Musset L, Allenbach Y, Benveniste O, Boyer O, Bossuyt X, Bentow C, et al. Anti-HMGCR antibodies as a biomarker for immune-mediated necrotizing myopathies: a history of statins and experience from a large international multi-center study. *Autoimmun Rev*. (2016) 15:983–93. doi: 10.1016/j.autrev.2016.07.023
125. Werner JL, Christopher-Stine L, Ghazarian SR, Pak KS, Kus JE, Daya NR, et al. Antibody levels correlate with creatine kinase levels and strength in anti-3-hydroxy-3-methylglutaryl-coenzyme A reductase-associated autoimmune myopathy. *Arthritis Rheum*. (2012) 64:4087–93. doi: 10.1002/art.34673
126. Mohassel P, Mammen AL. Statin-associated autoimmune myopathy and anti-HMGCR autoantibodies. *Muscle Nerve*. (2013) 48:477–83. doi: 10.1002/mus.23854
127. Waters MJ, Limaye V. Clinico-serologic features of statin-induced necrotising autoimmune myopathy in a single-centre cohort. *Clin Rheumatol*. (2018) 37:543–7. doi: 10.1007/s10067-017-3831-2
128. Kishi T, Rider LG, Pak K, Barillas-Arias L, Henrickson M, McCarthy PL, et al. Association of Anti-3-Hydroxy-3-Methylglutaryl-Coenzyme A reductase autoantibodies with DRB1*07:01 and severe myositis in Juvenile myositis patients. *Arthritis Care Res*. (2017) 69:1088–94. doi: 10.1002/acr.23113
129. Liang WC, Uruha A, Suzuki S, Murakami N, Takeshita E, Chen WZ, et al. Pediatric necrotizing myopathy associated with anti-3-hydroxy-3-methylglutaryl-coenzyme A reductase antibodies. *Rheumatology*. (2017) 56:287–93. doi: 10.1093/rheumatology/kew386
130. Shovman O, Gilburd B, Chayat C, Lazar AD, Amital H, Blank M, et al. Anti-HMGCR antibodies demonstrate high diagnostic value in the diagnosis of immune-mediated necrotizing myopathy following statin exposure. *Immunol Res*. (2017) 65:276–81. doi: 10.1007/s12026-016-8867-x
131. Droney L, Gillis D, Wong R. New immunoassays for anti-HMG-CoA reductase antibodies may lead to incorrect diagnosis in inflammatory myositis. *Pathology*. (2017) 49:638–9. doi: 10.1016/j.pathol.2017.04.013
132. Alvarado-Cardenas M, Marin-Sánchez A, Martínez MA, Martínez-Martínez L, Pinal-Fernandez I, Labrador-Horrillo M, et al. Statin-associated autoimmune myopathy: a distinct new IFL pattern can increase the rate of HMGCR antibody detection by clinical laboratories. *Autoimmun Rev*. (2016) 15:1161–6. doi: 10.1016/j.autrev.2016.09.005

133. Palterer B, Cammelli D, Vitiello G, Giudizi MG. Anti-HMGCR and anti-DFS70 antibodies immunofluorescence patterns. *Autoimmun Rev*. (2017) 16:321–2. doi: 10.1016/j.autrev.2017.01.002
134. Allenbach Y, Keraen J, Bouvier AM, Jooste V, Champtiaux N, Hervier B, et al. High risk of cancer in autoimmune necrotizing myopathies: usefulness of myositis specific antibody. *Brain*. (2016) 139:2131–5. doi: 10.1093/brain/aww054
135. Zampieri S, Valente M, Adami N, Biral D, Ghirardello A, Rampudda ME, et al. Polymyositis, dermatomyositis and malignancy: a further intriguing link. *Autoimmun Rev*. (2010) 9:449–53. doi: 10.1016/j.autrev.2009.12.005
136. Buchbinder R, Hill CL. Malignancy in patients with inflammatory myopathy. *Curr Rheumatol Rep*. 4:415–26. doi: 10.1007/s11926-002-0087-9
137. Hill CL, Zhang Y, Sigurgeirsson B, Pukkala E, Mellemkjaer L, Airio A, et al. Frequency of specific cancer types in dermatomyositis and polymyositis: a population-based study. *Lancet*. 357:96–100. doi: 10.1016/S0140-6736(00)03540-6
138. Buchbinder R, Forbes A, Hall S, Dennett X, Giles G. Incidence of malignant disease in biopsy-proven inflammatory myopathy: a population-based Cohort study. *Ann Intern Med*. (2001) 134:1087–95. doi: 10.7326/0003-4819-134-12-200106190-00008
139. Airio A, Pukkala E, Isomäki H. Elevated cancer incidence in patients with dermatomyositis: a population based study. *J Rheumatol*. (1995) 22:1300–3.
140. Barnes BE. Dermatomyositis and malignancya review of the literature. *Ann Intern Med*. (1976) 84:68–76. doi: 10.7326/0003-4819-84-1-68
141. Bonnetblanc JM, Bernard P, Fayol J. Dermatomyositis and malignancy. A multicenter cooperative study. *Dermatologica*. (1990) 180:212–6. doi: 10.1159/000248032
142. Chen YJ, Wu CY, Huang YL, Wang CB, Shen JL, Chang YT. Cancer risks of dermatomyositis and polymyositis: a nationwide cohort study in Taiwan. *Arthritis Res Ther*. (2010) 12:R70. doi: 10.1186/ar2987
143. Chow WH, Gridley G, Mellemkjaer L, McLaughlin JK, Olsen JH, Fraumeni JF. Cancer risk following polymyositis and dermatomyositis: a nationwide cohort study in Denmark. *Cancer Causes Control*. (1995) 6:9–13. doi: 10.1007/BF00051675
144. Maoz CR, Langevitz P, Livneh A, Blumstein Z, Sadeh M, Bank I, et al. High incidence of malignancies in patients with dermatomyositis and polymyositis: an 11-year analysis. *Semin Arthritis Rheum*. (1998) 27:319–24. doi: 10.1016/S0049-0172(98)80052-8
145. Zahr ZA, Baer AN. Malignancy in myositis. *Curr Rheumatol Rep*. (2011) 13:208–15. doi: 10.1007/s11926-011-0169-7
146. Hoshino K, Muro Y, Sugiura K, Tomita Y, Nakashima R, Mimori T. Anti-MDA5 and anti-TIF1-γ antibodies have clinical significance for patients with dermatomyositis. *Rheumatology*. (2010) 49:1726–33. doi: 10.1093/rheumatology/keq153
147. Selva-O'Callaghan A, Trallero-Araguás E, Grau-Junyent JM, Labrador-Horrillo M. Malignancy and myositis: novel autoantibodies and new insights. *Curr Opin Rheumatol*. (2010) 22:627–32. doi: 10.1097/BOR.0b013e32833f1075
148. Fiorentino DF, Chung LS, Christopher-Stine L, Zaba L, Li S, Mammen AL, et al. Most patients with cancer-associated dermatomyositis have antibodies to nuclear matrix protein NXP-2 or transcription intermediary factor 1gamma. *Arthritis Rheum*. (2013) 65:2954–62. doi: 10.1002/art.38093

Conflict of Interest Statement: The authors declare that the research was conducted in the absence of any commercial or financial relationships that could be construed as a potential conflict of interest.

Copyright © 2019 Stuhlmüller, Schneider, González-González and Feist. This is an open-access article distributed under the terms of the Creative Commons Attribution License (CC BY). The use, distribution or reproduction in other forums is permitted, provided the original author(s) and the copyright owner(s) are credited and that the original publication in this journal is cited, in accordance with accepted academic practice. No use, distribution or reproduction is permitted which does not comply with these terms.

frontiers in Immunology

ORIGINAL RESEARCH
published: 09 May 2019
doi: 10.3389/fimmu.2019.01063

α7 Nicotinic Acetylcholine Receptor Signaling Modulates Ovine Fetal Brain Astrocytes Transcriptome in Response to Endotoxin

Mingju Cao[1†], James W. MacDonald[2†], Hai L. Liu[1], Molly Weaver[3], Marina Cortes[4], Lucien D. Durosier[1], Patrick Burns[5], Gilles Fecteau[5], André Desrochers[5], Jay Schulkin[6], Marta C. Antonelli[7], Raphael A. Bernier[8], Michael Dorschner[3], Theo K. Bammler[2] and Martin G. Frasch[1,4,6,9]*

[1] Department of Obstetrics and Gynaecology and Department of Neurosciences, CHU Ste-Justine Research Centre, Faculty of Medicine, Université de Montréal, Montréal, QC, Canada, [2] Department of Environmental and Occupational Health Sciences, University of Washington, Seattle, WA, United States, [3] UW Medicine Center for Precision Diagnostics, University of Washington, Seattle, WA, United States, [4] Animal Reproduction Research Centre (CRRA), Faculty of Veterinary Medicine, Université de Montréal, Montréal, QC, Canada, [5] Department of Clinical Sciences, Faculty of Veterinary Medicine, Université de Montréal, Montréal, QC, Canada, [6] Department of Obstetrics and Gynecology, University of Washington, Seattle, WA, United States, [7] Instituto de Biología Celular y Neurociencia "Prof. Eduardo De Robertis", Facultad de Medicina, Universidad de Buenos Aires, Buenos Aires, Argentina, [8] Department of Psychiatry and Behavioral Sciences, University of Washington, Seattle, WA, United States, [9] Center on Human Development and Disability, University of Washington, Seattle, WA, United States

Neuroinflammation *in utero* may result in lifelong neurological disabilities. Astrocytes play a pivotal role in this process, but the mechanisms are poorly understood. No early postnatal treatment strategies exist to enhance neuroprotective potential of astrocytes. We hypothesized that agonism on α7 nicotinic acetylcholine receptor (α7nAChR) in fetal astrocytes will augment their neuroprotective transcriptome profile, while the inhibition of α7nAChR will achieve the opposite. Using an *in vivo–in vitro* model of developmental programming of neuroinflammation induced by lipopolysaccharide (LPS), we validated this hypothesis in primary fetal sheep astrocytes cultures re-exposed to LPS in the presence of a selective α7nAChR agonist or antagonist. Our RNAseq findings show that a pro-inflammatory astrocyte transcriptome phenotype acquired *in vitro* by LPS stimulation is reversed with α7nAChR agonistic stimulation. Conversely, α7nAChR inhibition potentiates the pro-inflammatory astrocytic transcriptome phenotype. Furthermore, we conducted a secondary transcriptome analysis against the identical α7nAChR experiments in fetal sheep primary microglia cultures. Similar to findings in fetal microglia, in fetal astrocytes we observed a memory effect of *in vivo* exposure to inflammation, expressed in a perturbation of the iron homeostasis signaling pathway (hemoxygenase 1, HMOX1), which persisted under pre-treatment with α7nAChR antagonist but was reversed with α7nAChR agonist. For both glia cell types, common pathways activated due to LPS included neuroinflammation signaling and NF-κB signaling in some, but not all comparisons. However, overall, the overlap on the level of signaling pathways was

OPEN ACCESS

Edited by:
Marcello Moccia,
University College London,
United Kingdom

Reviewed by:
Hua Su,
University of California, San Francisco,
United States
Hans O. Kalkman,
Novartis Pharma AG, Switzerland

***Correspondence:**
Martin G. Frasch
mfrasch@uw.edu

[†]These authors have contributed equally to this work

Specialty section:
This article was submitted to Multiple Sclerosis and Neuroimmunology, a section of the journal Frontiers in Immunology

Received: *19 December 2018*
Accepted: *25 April 2019*
Published: *09 May 2019*

Citation:
Cao M, MacDonald JW, Liu HL, Weaver M, Cortes M, Durosier LD, Burns P, Fecteau G, Desrochers A, Schulkin J, Antonelli MC, Bernier RA, Dorschner M, Bammler TK and Frasch MG (2019) α7 Nicotinic Acetylcholine Receptor Signaling Modulates Ovine Fetal Brain Astrocytes Transcriptome in Response to Endotoxin. Front. Immunol. 10:1063. doi: 10.3389/fimmu.2019.01063

rather minimal. Astrocytes, not microglia—the primary immune cells of the brain, were characterized by unique inhibition patterns of STAT3 pathway due to agonistic stimulation of α7nAChR prior to LPS exposure. Lastly, we discuss the implications of our findings for fetal and postnatal brain development.

Keywords: neuroinflammation, LPS, CHRNA7, RNAseq, astrocyte, microglia, infection, fetal programming

INTRODUCTION

Glial cells (astrocytes and microglia) play a role in neuroinflammation and both cell types acquire a specific reactive phenotype when stimulated by lipopolysaccharide (LPS) (1). Activation of glial cells may lead to neuronal cell death. Activation of nicotinic α7 receptors (α7nAChR) suppresses the LPS-induced reactive phenotype of microglia and astrocytes and thus counteracts the deleterious effect regarding neuronal viability (2–8).

In the periphery the efferent fibers of the Vagus nerve activate α7nAChR on effector cells and inhibit inflammation (9). In the brain, fibers arising from the Nucleus tractus solitarii spread into both hemispheres and their activation may lead to a widespread central anti-inflammatory effect (5, 10, 11). It is currently insufficiently tested if this is also true for the fetal brain.

In a previous experiment we investigated the effect of α7nAChR stimulation on LPS-induced microglia-activation in a double hit model of sheep fetal microglia. In the current experiment, we extended this investigation to study the role of α7nAChR in fetal sheep astrocytes. These experiments may help to shed light on neurodevelopmental disorders such as autism spectrum disorder (ASD) or schizophrenia, that are thought to involve neuroinflammation during the fetal period (12, 13).

We hypothesized that (1) under exposure to LPS, α7nAChR agonist stimulation in fetal astrocytes augments their neuroprotective profile, while the inhibition reduces it; (2) a LPS double-hit (first *in vivo*, then *in vitro*) on astrocytes exacerbates these effects similar to microglia as demonstrated before. Using an *in vivo—in vitro* fetal sheep model (14), we validate these hypotheses via RNASeq analysis in primary fetal astrocyte cultures exposed to LPS in the presence of a selective α7nAChR agonist or antagonist. We compare these findings to the previously published results in identically conducted microglia experiments (3, 15).

METHODS

Study Approval

This study was carried out in strict accordance with the recommendations in the Guide for the Care and Use of Laboratory Animals of the National Institutes of Health. The respective *in vivo* and *in vitro* protocols were approved by the Committee on the Ethics of Animal Experiments of the Université de Montréal (Permit Number: 10-Rech-1560).

Anesthesia and Surgical Procedure

The detailed protocol has been presented elsewhere (3). Briefly, we instrumented pregnant time-dated ewes at 126 days of gestation (dGA, ∼0.86 gestation) with arterial, venous and amniotic catheters and ECG electrodes. Ovine singleton fetuses of mixed breed were surgically instrumented with sterile technique under general anesthesia (both ewe and fetus). In case of twin pregnancy the larger fetus was chosen based on palpating and estimating the intertemporal diameter. The total duration of the procedure was approximately 2 h. Antibiotics were administered to the mother intravenously (trimethoprim sulfadoxine 5 mg/kg body weight) as well as to the fetus intravenously and into the amniotic cavity (ampicillin 250 mg). Amniotic fluid lost during surgery was replaced with warm saline. The catheters exteriorized through the maternal flank were secured to the back of the ewe in a plastic pouch. For the duration of the experiment the ewe was returned to a metabolic cage, where she could stand, lie and eat *ad libitum* while we monitored the non-anesthetized fetus without sedating the mother. During postoperative recovery antibiotic administration was continued for 3 days. Arterial blood was sampled for evaluation of maternal and fetal condition and catheters were flushed with heparinized saline to maintain patency.

In vivo Experimental Protocol

Postoperatively, all animals were allowed 3 days to recover before starting the experiments. On these 3 days, at 9.00 am 3 mL arterial plasma sample were taken for blood gasses and cytokine analysis. Each experiment commenced at 9.00 am with a 1 h baseline measurement followed by the respective intervention as outlined below. FHR and arterial blood pressure were monitored continuously (CED, Cambridge, UK, and NeuroLog, Digitimer, Hertfordshire, UK). Blood samples (3 mL) were taken for arterial blood gases, lactate, glucose, and base excess (ABL800Flex, Radiometer) and cytokines at the time points 0 (baseline), +1 (i.e., after LPS administration), +3, +6, +24, +48, and +54 h (i.e., before sacrifice at day 3). For the cytokine analysis, plasma was spun at 4°C (4 min, 4,000 g, Eppendorf 5804R, Mississauga, ON), decanted and stored at −80°C for subsequent ELISAs. After the +54 h (Day 3) sampling, the animals were sacrificed with an overdose of barbiturate (30 mg pentobarbital sodium, Fatal-Plus; Vortech Pharmaceuticals, Dearborn, MI) and a post mortem was carried out during which fetal gender and weight were determined. The fetal brain was then perfusion-fixed with 250 mL of cold saline followed by 250 mL of 4% paraformaldehyde and processed for histochemical analysis or dissected for cell culture (details see *in vitro* astrocytes culture

paragraph). Fetal growth was assessed by body, brain, liver, and maternal weights.

Astrocytes Isolation and Purification

Briefly, fetal sheep brain tissues were obtained during sheep necropsy after completion of the *in vivo* experiment to conduct the *in vitro* study (**Figure 1**). In the *in vivo* experiments, three *in utero* instrumented fetal sheep were treated intravenously with LPS (400 ng/fetus/day) derived from *E. coli* (Sigma Cat. no L5293, *E. coli* O111:B4, ready-made stock solution at a concentration of 1 mg/ml) on experimental days 1 and 2 at 10:00 am to mimic high levels of endotoxin in fetal circulation (so-called first LPS exposure or first hit). Three *in utero* instrumented fetal sheep were used as control receiving sterile saline. The instrumented fetuses were referred to as primary fetuses. In case of twins, twin fetuses were not instrumented, and their brains directly used for subsequent cell culture. Fetuses not exposed to LPS, either primary or twins, were designated "naïve" (no LPS exposure *in vivo*). Instrumented animals that received LPS *in vivo* were used for second hit LPS exposure *in vitro*.

Astrocytes are the major adherent cell population in flask. Astrocytes were purified by passage into a new T75 flask for 4–5 times before any manipulations and treatments. After floating microglia collection, the adherent cells were detached by trypsinization (Trypsine 0.25% + EDTA 0.1%, Wisent Cat. No 325-043-EL) and re-plated into a new flask. Cells were cultured for another 7 days with 10% ready-to-use medium [DMEM plus 1% penicillin/streptomycin, 1% glutamine, in addition with 10% heat-inactivated fetal bovine serum (Gibco, Canada Origin)]. The cell passage procedure took 4–5 weeks until purified astrocytes could be used for the *in vitro* experiment. The cell culture conditions were 37°C, 5% CO_2.

Pure astrocytes were plated into a 24-well plate at 1×10^5 cells/mL with 10% DMEM for another 7 days, and then treated with LPS or saline for 6 h.

Cell-conditioned media were collected for cytokine analysis. To verify astrocytes purity, a portion of cells was plated into Lab-Tek 8 well chamber glass slide (Thermo Scientific) for immunocytochemistry (ICC) analysis. Glial fibrillary acidic protein (GFAP) was used as an astrocyte marker; cells were counterstained with Hoechst (15).

Astrocyte Cell Culture and Treatment

Prior to exposure to LPS (Sigma Cat. no L5024, *E. coli* O127:B8) at a concentration of 100 ng/ul, cells were pretreated for 1 h with either 10 nM AR-R17779 hydrochloride (Tocris Bioscience Cat# 3964), a selective α7nAChR agonist, or 100 nM α-Bungarotoxin (Tocris Bioscience Cat# 2133), a selective α7nAChR antagonist. Optimal dose of AR-R17779 (A) or α-Bungarotoxin (B) was chosen based on a dose-response experiment with LPS. We have tested 0, 10, 100, and 1,000 nM of α-Bungarotoxin and 0, 1, 10, and 100 nM of AR-R17779 in the absence or presence of 100 ng/ul LPS, and measured IL-1β concentrations in cultured media as the endpoint. The 100 nM α-Bungarotoxin and 10 nM AR-R17779 were chosen because the cells responded in a linear range as indicated by IL-1β production.

AR-R17779 was reconstituted in DMSO as stock solution, serial dilutions were made to prepare the working stock; to obtain 10 nM AR-R17779 in concentration per well, 5 ul working stock was added well by well containing 500 ul media; only DMSO was added in control well, therefore, the DMSO concentration per well was 1%. α-Bungarotoxin was reconstituted with culture media into a stock solution and underwent serial dilutions.

In a complete cell culture experiment, we had four experimental groups: Control (naïve control), LPS100 (naïve LPS), LPS100+B100 (naïve LPS+B) and LPS100+A10 (naïve LPS+A). Second hit cell cultures were designed with the same pattern and divided into four experimental groups: Control (SHC), LPS100, LPS100+B100 and LPS100+A10.

Measurement of the Cytokine IL-1β in Cell Culture Media

The approach is described elsewhere (14, 16). Briefly, IL-1β concentrations in cell culture media was determined by using an ovine-specific sandwich ELISA. Ninety-six-well plates were pre-coated with the mouse anti sheep monoclonal antibodies (IL-1β, MCA1658, Bio Rad AbD Serotec) at a concentration of 4 μg/ml on an ELISA plate at 4°C overnight. After 3 times wash with washing buffer (0.05% Tween 20 in PBS, PBST), plates were blocked for 1h with 1% BSA in PBST for plasma samples or 10% FBS for cell culture media. Recombinant sheep proteins (IL-1β, Protein Express Cat. no 968-405) were used as ELISA standard. All standards and samples were run in duplicate (50μl per well). Rabbit anti-sheep polyclonal antibodies (IL-1β, AHP423, Bio Rad AbD Serotec) at a concentration of 4 μg/ml were applied in wells and incubated for 30 min at room temperature. Plates were washed with washing buffer for 5–7 times between each step. Detection was accomplished by assessing the conjugated enzyme activity (goat anti-rabbit IgG-HRP, dilution 1:5000, Jackson ImmunoResearch, Cat. No 111-035-144) via incubation with TMB substrate solution (BD OptEIA TMB substrate Reagent Set, BD Biosciences Cat. No 555214); color development reaction was stopped with 2N sulphuric acid. Plates were read on an ELISA plate reader at 450 nm, with 570 nm wavelength correction (EnVision 2104 Multilabel Reader, Perkin Elmer). The sensitivity of IL-1β ELISA was 41.3 pg/ml. The intra-assay and inter-assay coefficients of variance were <5 and <10%, respectively.

RNAseq Approach

Nine replicates of astrocyte culture were studied, with one control and three treatment groups (Ctrl, LPS100, LPS+A10, LPS+B100) per replicate. Four replicates were used for RNAseq based on the RNA quality, of which 3 replicates of naive, one replicate of second-hit, with one treatment missing in this second-hit replicate (agonist treatment), fifteen samples in total were assessed with RNAseq in this study (**Table 1**).

RNA Extraction and Quantification

We used Qiagen RNeasy Mini Kit (Cat no 74104) for RNA extraction. RNA quantity and quality (RNA integrity number, RIN) was established by using a RNA Nano Chip (Agilent

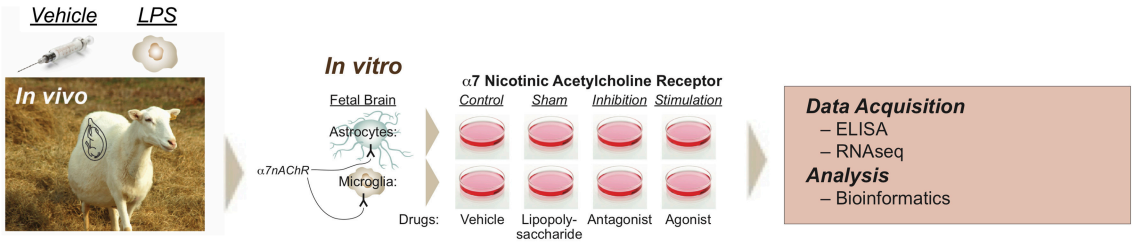


FIGURE 1 | Experimental design of modulating glial α7nAChR signaling in a double-hit fetal sheep model. *In vivo*, *in vitro*, and RNAseq experiments are illustrated. *In vivo* study includes Control (saline) or LPS-exposed sheep fetuses. LPS was administered intravenously to the instrumented fetus at 400 ng/fetus/day for two consecutive days 24 h apart, so-called first hit, inducing fetal inflammatory response with rising IL-6, but without cardiovascular component. For the *in vitro* study, cultured cells (microglia or astrocytes) were derived from an *in vivo* Control animal, named Naïve, or from an *in vivo* LPS-exposed animal, named second hit (SH). There were 8 experimental groups: naïve Control (NC, vehicle *in vivo*, vehicle *in vitro*), naïve LPS (NL, sham in reference to α7nAChR manipulation), naïve exposed to α-Bungarotoxin (NB, i.e., α7nAChR inhibition, preincubated followed by LPS exposure), naïve exposed to AR-R17779 (NA, i.e., α7nAChR stimulation, preincubated followed by LPS exposure), and each respective second-hit groups (SH, LPS *in vivo*). Reproduced with permission (16).

TABLE 1 | Sample inventory for RNAseq study in astrocytes samples.

Biological replicates	Serial#	Sample	Treatment	LPS hit number
Naïve R1	1	4414T1	Ctrl	0
	2	4414T1	LPS100	1
	3	4414T1	LPS100+B100	1
	4	4414T1	LPS100+A10	1
Naïve R2	5	4414T2	Ctrl	0
	6	4414T2	LPS100	1
	7	4414T2	LPS100+B100	1
	8	4414T2	LPS100+A10	1
Naïve R3	9	4502P	Ctrl	0
	10	4502P	LPS100	1
	11	4502P	LPS100+B100	1
	12	4502P	LPS100+A10	1
Second hit R1	13	711P	Ctrl	1
	14	711P	LPS100	2
	15	711P	LPS100+B100	2

Four replicates were used for RNAseq, with one control and three treatment groups (Ctrl, LPS100, LPS100+A10, LPS100+B100) per replicate. There were 3 replicates of naïve, one replicate of second-hit, with one treatment missing in this second-hit replicate (second-hit + Agonist), fifteen samples in total were assessed with RNAseq in this study. The instrumented fetuses were designated as primary fetus, identified as animal ID+P (stands for primary), whereas animal ID+T stands for non-instrumented twins.

RNA 6000 Nano Chips) with Agilent 2,100 BioAnalyzer. All samples had an acceptable RIN value ranging from 8.4 to 9.6. A total of 12 naïve astrocyte cultures from four sets of replicates was selected for RNA sequencing at high throughput, as well as three second hit astrocyte cultures (**Table 1**).

RNAseq libraries were prepared using the TruSeq stranded mRNA kit (Illumina cat #20020594) and quality control was performed on the Agilent TapeStation and using the KAPA SYBRFAST qPCR kit (Kapa Biosystems, Roche). Single read 100-bp sequencing was performed in rapid mode on a HiSeq 2,500 (Illumina Inc.) at the University of Washington Northwest Clinical Genomics Lab (Department of Pathology).

RNAseq Data Analyses

Astrocytes

The goal for this analysis was to compare the single hit LPS treated samples to Control, as well as making comparisons between the LPS treated samples (e.g., testing for changes due to the additional agonist or antagonist pre-treatment). The second hit samples had no replicates, so we could only make the directed comparisons between the single and second hit samples. For example, comparing the single and second hit LPS treated samples, as before (3).

We aligned the reads to the Oar_v3.1 transcriptome using the salmon aligner (17), which infers the most likely transcript for each read using a quasi-mapping algorithm. We then "collapsed" the transcript read counts to the gene level by summing up the reads for each gene's transcripts, using the Bioconductor tximport package (18). In the end, we had a set of read counts per gene, for each sample.

Four replicates were used for RNAseq, with one control and three treatment groups Ctrl, LPS, LPS+A10, LPS+B100) per replicate. There were 3 replicates of naïve, one replicate of second-hit, with one treatment missing in this second-hit replicate (second-hit + agonist, SHA), fifteen samples in total were assessed with RNAseq in this study (**Table 1**). The instrumented fetuses were designated as primary fetus, identified as animal ID+P (stands for primary), whereas animal ID+T stands for non-instrumented twins.

To compare astrocytes transcriptomes, we used the Bioconductor edgeR package (19), to fit a generalized linear model with a negative binomial link function, and made comparisons between groups using quasi-likelihood F-tests.

We fitted the model described above, including the treatment effect for each animal, and made the comparisons, incorporating a fold change criterion into the test. In other words, the conventional test for a difference is between the null hypothesis $H_0: \beta = 0$ vs. the alternative hypothesis $H_A: \beta \neq 0$, but this may include very small changes that are likely to be biologically meaningless. One alternative to exclude such genes is to use a *post hoc* fold change adjustment, where we select genes based on the observed fold change between groups. This is problematic because we ignore the imprecision in our estimate of fold change.

A better method is to incorporate the fold change into our inference, where we test $H_0 : \beta \leq |c|$ against the alternative $H_A : \beta \geq |c|$, for some constant fold change. By doing this, we are testing to see if we have evidence that the underlying population differences are larger than a given fold change, rather than simply testing that our sample data fulfill those criteria. We used a 1.5-fold change, and a false discovery rate (FDR) of 0.05 as criteria to define significantly differentially expressed genes, meaning that we expect that there are, at most, 5% false positives in our set of significant genes.

Microglia—Astrocytes Transcriptome Comparisons

We also made comparisons to the existing RNAseq data that our lab generated using primary cultures of fetal sheep microglia from the identical experimental design in three biological replicates. This data has been published and the data set is accessible online (14).

We downloaded the FASTQ data from SRA and processed using the same salmon/tximport pipeline we used for the astrocyte samples. The only difference was in the modeling step, where we converted the count data to log counts/million and estimated observation-level weights using the limma voom function. We also computed sample-specific weights that are intended to down-weight any samples that are not very similar to other samples of the same type. We then fit a conventional weighted linear model and made empirical Bayes adjusted contrasts between various groups. By incorporating sample-specific weights we were able to account for a single sample (LPS100 treated animal 4414T), which had significantly fewer reads, perhaps due to some technical problems.

Venn Diagrams

We sought to learn which genes are unique to a given comparison, and which are shared between two or more of those comparisons. Thus, we generated Venn diagrams for three sets of comparisons. We made a Venn diagram for the three comparisons of treated vs. control, a two-way Venn diagram of the agonist + LPS vs. either LPS alone or LPS plus antagonist (this shows that there is very little difference between LPS and LPS plus antagonist), and finally we made a Venn diagram of the one-hit vs. two-hit for all three treatments. The genes in any intersection between comparisons had to be significantly differentially expressed in both (or all three, depending on the intersection) of the comparisons. In addition, the direction of change had to be the same as well. For example, if a given gene was differentially expressed in LPS100 vs. control and LPS100+A10 vs. control, and it is either up or down-regulated in both comparisons as well, then it was listed in the intersection between those two comparisons. If it was significant in both comparisons, but was up-regulated in one comparison, but down-regulated in the other, then it was listed in the unique portion of the Venn diagram for each comparison.

Statistical Analyses and Data Repository

Generalized estimating equations (GEE) modeling approach was used to assess the effects of LPS and drug treatments on IL-1β. We used a linear scale response model with LPS/drug treatment group (main term "treatment") and presence or absence of second hit exposure (main term "hit") as predicting factors to assess their interactions using maximum likelihood estimate and Type III analysis with Wald Chi-square statistic. SPSS Version 25 was used for these analyses (IBM SPSS Statistics, IBM Corporation, Armonk, NY). Significance was assumed for $p < 0.05$. Results are provided as median {25–75} percentiles. Not all measurements were obtained for each animal studied, as indicated.

Ingenuity Pathway Analysis (IPA, Qiagen, 2019) was used for identification of signaling pathways unique to each treatment.

The raw RNAseq data has been deposited under GEO accession number *GSE123713*. The analytical pipeline to allow reproduction of this analysis, in the form of a Rmarkdown document, will be made available upon request. Statistics from all comparisons (t-statistics, log fold changes, FDR values, dynamically linked Venn diagrams) can be found in supplemental document under the doi: 10.5281/zenodo.2609202.

TABLE 2 | Astrocytes IL-1β secretion expressed as absolute values* in pg/ml (median and 25–75%).

LPS exposure	Ctrl	LPS	B100	A10
Single hit	1 (1,25)	429 (358,1034)	336 (285,928)	750 (439,1495)
Second hit	1 (1,1)	16 (15,16)	20 (17,22)	99 (95, 103)

Values set to 1 where no signal was detected by the cytokine assay to compute fold-changes for **Figure 2.*

RESULTS AND DISCUSSION

Cytokine Secretion Profile

The fetal *in vivo* exposure to LPS resulted in a rise of IL-6 as reported (14, 16).

The absolute values of IL-1β produced by naive (first hit) and second hit astrocytes at baseline, under LPS exposure and with preceding agonist or antagonist incubation are presented in **Table 2**. As reported, LPS treatment induced IL-1β increase in astrocytes (14). There was no difference in first and second hit astrocytes at baseline or when exposed to LPS alone. Our focus here was on the effect of α7nAChR modulation on LPS-triggered IL-1β production. Consequently, we expressed the data as fold-changes compared to sham treatment (LPS, **Figure 2**, LEFT). We present the response of primary microglia cultures side-by-side (**Figure 2**, RIGHT) in form of re-analysis of previously published data (3).

For astrocytes, the main terms "hit" and "treatment" as well as their interaction were significant (all $p<0.001$). Agonistic stimulation of the α7nAChR appeared, surprisingly, to result in a relative increase of IL-1β concentration, further potentiated in second hit astrocytes. This effect was absent in first hit astrocytes cultures treated with the α7nAChR antagonist and less pronounced but present in the second hit cultures.

For microglia, the main terms "hit" and "treatment" were not significant ($p = 0.716$ and $p = 0.666$, respectively), but their interaction was significant [$p = 0.026$, cf. Figure 1 in (3)].

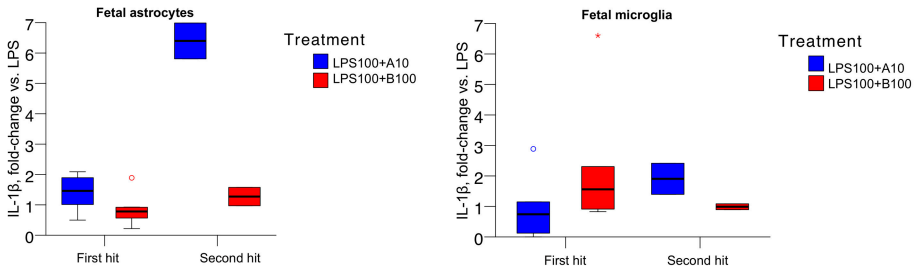


FIGURE 2 | (Left) IL-1β secretion in ovine primary astrocyte cultures in response to 6 h LPS exposure without or with pre-incubation with α7nAChR antagonist (B100) or agonist (A10) for 1 h. Single hit, *in vitro* only LPS exposure; second hit, *in vivo* systemic and subsequent *in vitro* LPS exposure 4 to 5 weeks later. Y axis shows fold changes in IL-1β in relation to the levels of sham treatment (LPS). Generalized estimating equations (GEE) modeling results are presented in text and no significance marks are provided in the figure. For both box plots, an asterisk represents an extreme outlier (a value more than 3 times the interquartile range from a quartile). A circle marks outlier with values between 1.5 and 3 box lengths from the upper or lower edge of the box. Briefly, we found significant main term effects ($p = 0.019$) "treatment" (LPS and α7nAChR drug) as well as main term "hit" ($p = 0.010$), i.e., the contribution of *in vivo* LPS exposure, the second hit effect on the IL-1β secretion profile. Results are provided as median {25–75} percentiles. **(Right)** Identical experimental results from microglia studies are presented for comparison. The main terms "hit" and "treatment" were not significant ($p = 0.716$ and $p = 0.666$, respectively), but their interaction was significant ($p = 0.026$, cf. Figure 1 in (3) where the original results have been published.

The overall pattern of IL-1β levels in response to LPS exposure with prior α7nAChR stimulation was inverted in astrocytes compared to microglia. In astrocytes, both first hit and second hit cell cultures responded under inhibition of α7nAChR with relative decrease of IL-1β production. In microglia, in contrast, first hit (naive) cultures behaved intuitively under the same conditions, showing a rise in IL-1β production. However, second hit microglia cultures, similar to second hit astrocytes, showed a drop in IL-1β production with α7nAChR inhibition. In contrast again, agonistic α7nAChR stimulation in both second hit glia cultures resulted in higher than first hit IL-1β production, albeit, the magnitude of this rise was ∼3.5-fold larger in astrocytes suggesting differences in sensitization of these glia cells to previous LPS exposure *in utero*. These counter-intuitive findings of α7nAChR stimulation in astrocytes on the individual IL-1β secretion stand in contrast to the transcriptome-level findings we discuss below. We attempt to tie together these results in the general discussion section.

Whole Transcriptome Analysis

Mapped reads aligned to any transcript from the Oar_v3.1 transcriptome at 66% which is good. Principal component analysis (PCA) showed large differences between the different treatment groups, and much smaller differences within each group, indicating that we have a good signal with likely many differentially expressed genes (DEG) to be found (**Figure 3**).

We present in **Table 3** the number of genes for each comparison as well as the top ten signaling pathways IPA identified. The results of the analysis on the entire data set are also accessible with search function via this repository.

PCA showed two transcriptome clusters (**Figure 3**):

1) Control, LPS single-hit and second-hit astrocytes pre-treated with α7nAChR agonist and

2) LPS single-hit and second-hit astrocytes pre-treated with α7nAChR antagonist.

That is, a pro-inflammatory transcriptome astrocyte phenotype acquired *in vivo* or *in vitro* by LPS stimulation is reversed with α7nAChR agonistic stimulation. Conversely, α7nAChR inhibition potentiates the pro-inflammatory astrocytic phenotype. The PCA level observations are substantiated further by the IPA analysis of key signaling pathways presented in **Table 3**. The visualization of the up or down regulation of the implicated pathways can be accessed on GitHub in its entirety. Here we focus on some key findings in top 10 signaling pathways.

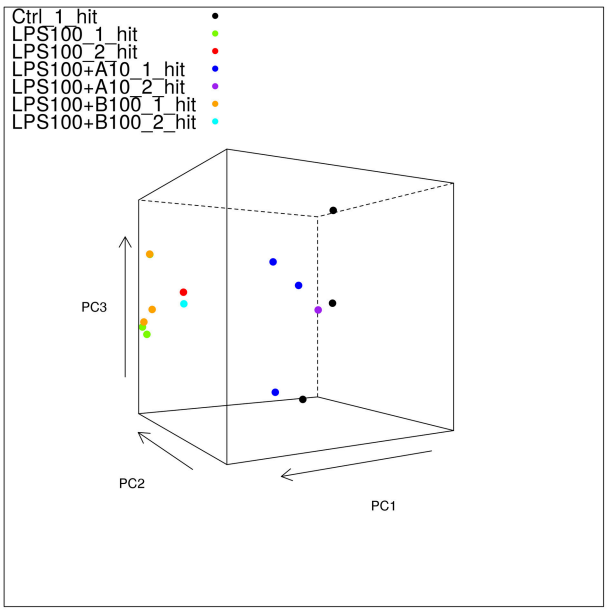


FIGURE 3 | Static 3D plot of the astrocyte RNAseq data with single and double-hit LPS treatment. The angle of the plot was chosen to give the best viewpoint to show differences between the sample types. Note that controls and α7nAChR agonistically pre-treated astrocytes cluster together and separately from those exposed to LPS w/o or with antagonistic α7nAChR pre-treatment. Note here that there are three of the LPS_100_1_hit samples in the plot shown in this figure; it just so happens that the third sample is obscured by the uppermost LPS+B100_1_hit sample.

TABLE 3 | Ingenuity Pathway Analysis of differentially expressed genes from the fetal sheep astrocytes whole transcriptome analysis: naïve and second hit astrocytes after modulation of α7nAChR signaling.

comparison	# genes	Top 10 signaling pathways	-log(*p*-value)
Single hit: LPS100 vs. Control	1835	NF-κB Signaling	15.8
		Role of Pattern Recognition Receptors in Recognition of Bacteria & Viruses	14
		Role of Macrophages, Fibroblasts and Endothelial Cells in Rheumatoid Arthritis	13.7
		Dendritic Cell Maturation	13
		Neuroinflammation Signaling Pathway	12.8
		Role of IL-17A in Arthritis	12.2
		Activation of IRF by Cytosolic Pattern Recognition Receptors	11.6
		Death Receptor Signaling	11.3
		Th1 and Th2 Activation Pathway	10.7
		TREM1 Signaling	10.5
Single hit: LPS100+A10 vs. Control	1725	**NF-κB Signaling**	14.7
		Role of Macrophages, Fibroblasts and Endothelial Cells in Rheumatoid Arthritis	13.7
		Role of Osteoblasts, Osteoclasts and Chondrocytes in Rheumatoid Arthritis	13.1
		Granulocyte Adhesion and Diapedesis	12.7
		Role of Pattern Recognition Receptors in Recognition of Bacteria and Viruses	12.5
		Hepatic Cholestasis	12.5
		Toll-like Receptor Signaling	11.7
		Axonal Guidance Signaling	11.5
		IL-10 Signaling	11.1
		Neuroinflammation Signaling Pathway	10.7
Single hit: LPS100+B100 vs. Control	1744	NF-κB Signaling	16.8
		Role of Macrophages, Fibroblasts and Endothelial Cells in Rheumatoid Arthritis	16
		Dendritic Cell Maturation	15.9
		Neuroinflammation Signaling Pathway	15
		Role of Pattern Recognition Receptors in Recognition of Bacteria & Viruses	14.8
		TREM1 Signaling	12.8
		Role of IL-17A in Arthritis	12.7
		T Cell Exhaustion Signaling Pathway	11.9
		Toll-like Receptor Signaling	11.8
		PI3K Signaling in B Lymphocytes	11.6
Single hit: LPS100+A10 vs. LPS100	273	Granulocyte Adhesion and Diapedesis	6.23
		Pathogenesis of Multiple Sclerosis	5.81
		Agranulocyte Adhesion and Diapedesis	5.12
		Th1 and Th2 Activation Pathway	4.45
		Th2 Pathway	4.4
		LPS/IL-1 Mediated Inhibition of RXR Function	3.81
		NF-κB Signaling	3.71
		Role of Osteoblasts, Osteoclasts and Chondrocytes in Rheumatoid Arthritis	3.63
		Inhibition of Angiogenesis by TSP1	3.33
		STAT3 Pathway	3.25
Single hit: LPS100+B100 vs. LPS100	0		
Single hit:	292	Granulocyte Adhesion and Diapedesis	5.25
LPS100+A10 vs. LPS100+B100		Agranulocyte Adhesion and Diapedesis	4.99
		LPS/IL-1 Mediated Inhibition of RXR Function	4.38
		Hepatic Fibrosis / Hepatic Stellate Cell Activation	4.35
		NF-κB Signaling	4.33
		Role of Osteoblasts, Osteoclasts and Chondrocytes in Rheumatoid Arthritis	4.18
		Pathogenesis of Multiple Sclerosis	3.97
		STAT3 Pathway	3.94
		p53 Signaling	3.57
		Sirtuin Signaling Pathway	3.36

(Continued)

TABLE 3 | Continued

comparison	# genes	Top 10 signaling pathways	-log(*p*-value)
LPS100: single hit vs. second hit	3761	Hepatic Fibrosis / Hepatic Stellate Cell Activation	10.7
		Fcγ Receptor-mediated Phagocytosis in Macrophages and Monocytes	7.69
		Leukocyte Extravasation Signaling	6.82
		Signaling by Rho Family GTPases	6.16
		Iron homeostasis signaling pathway	6.02
		LXR/RXR Activation	5.36
		Epithelial Adherens Junction Signaling	4.99
		Role of Osteoblasts, Osteoclasts and Chondrocytes in Rheumatoid Arthritis	4.96
		Axonal Guidance Signaling	4.91
		Tec Kinase Signaling	4.82
LPS100+A10: single hit vs. second hit	3307	Hepatic Fibrosis / Hepatic Stellate Cell Activation	13
		Leukocyte Extravasation Signaling	8.79
		Neuroinflammation Signaling Pathway	7.18
		Fcγ Receptor-mediated Phagocytosis in Macrophages and Monocytes	6.99
		Axonal Guidance Signaling	6.93
		Phagosome Formation	6.85
		Role of Pattern Recognition Receptors in Recognition of Bacteria and Viruses	6.67
		Agranulocyte Adhesion and Diapedesis	6.24
		GP6 Signaling Pathway	6.1
		Granulocyte Adhesion and Diapedesis	5.92
LPS100+B100: single hit vs. second hit	3860	Hepatic Fibrosis / Hepatic Stellate Cell Activation	8.89
		Fcγ Receptor-mediated Phagocytosis in Macrophages and Monocytes	8.03
		Leukocyte Extravasation Signaling	7.26
		Epithelial Adherens Junction Signaling	5.94
		Iron homeostasis signaling pathway	5.78
		Signaling by Rho Family GTPases	5.51
		Axonal Guidance Signaling	5.18
		Endothelin-1 Signaling	5.04
		Role of Macrophages, Fibroblasts and Endothelial Cells in Rheumatoid Arthritis	5.01
		Phagosome Formation	4.99

Differential analysis of count data was done with the Bioconductor limma package. Differentially expressed genes were selected, based on a 1.5-fold change and an FDR < 0.05. Up regulation and down regulation represent positive and negative log2 fold changes, respectively. For details on "raw gene" level, see our GitHub repository or directly here. Bold font highlights pathways common with microglia.
Orange: positive z-score; blue: negative z-score. For further details as raw data and visualized activity patterns see GitHub.
Significant genes in astrocytes cultures at an FDR < 0.05 and a 1.5-fold change sorted on log(p-value).

LPS treatment triggered activation of pro-inflammatory signaling pathways NF-κB and neuroinflammation. Compared to LPS exposure alone, pretreatment with α7nAChR agonist reversed both signaling pathways activation. Conversely, pretreatment with α7nAChR antagonist up regulated these pro-inflammatory pathways. Albeit the pattern overall was similar to the effect of LPS alone, activation of these signaling pathways under α7nAChR blockade stood out: Toll-like receptor signaling and PI3K signaling. Direct comparison of α7nAChR agonistic stimulation or inhibition yielded reduced activity of NF-κB and STAT3 pathways due to activation of α7nAChR, consistent with the expected intracellular anti-inflammatory effect of α7nAChR agonism. Another notable pathway activated in α7nAChR agonistically treated astrocytes was the Sirtuin signaling. Activation of this pathway in neurons and astrocytes has been implicated in AMPK-dependent neuroprotection from ischemic stroke (20, 21). Adenosine monophosphate kinase (AMPK) is a rapid key regulator of neuronal energy homeostasis implicated in fetal neuroinflammation (22).

The second half of **Table 3** documents some effects of astrocytes memory of LPS exposure *in vivo* when re-exposed *in vitro* (second hit effect). For comparison to microglial activity, see **Table 4**. Notably, we found a perturbation of the iron homeostasis signaling pathway in second hit LPS treated astrocytes which persisted under pre-treatment with α7nAChR antagonist but was reversed with α7nAChR agonist. Similar to our finding of second hit signature in microglia, here we observed hemoxygenase (HMOX)1 gene down regulation in second hit astrocytes compared to first hit cultures (3, 15). HMOX1 is a key gene of iron homeostasis. We observed a similar phenomenon in second hit fetal microglia compared to single hit microglia (15).

Together, observations on Sirtuin and iron homeostasis signaling reinforce the previously reported dual role of energy

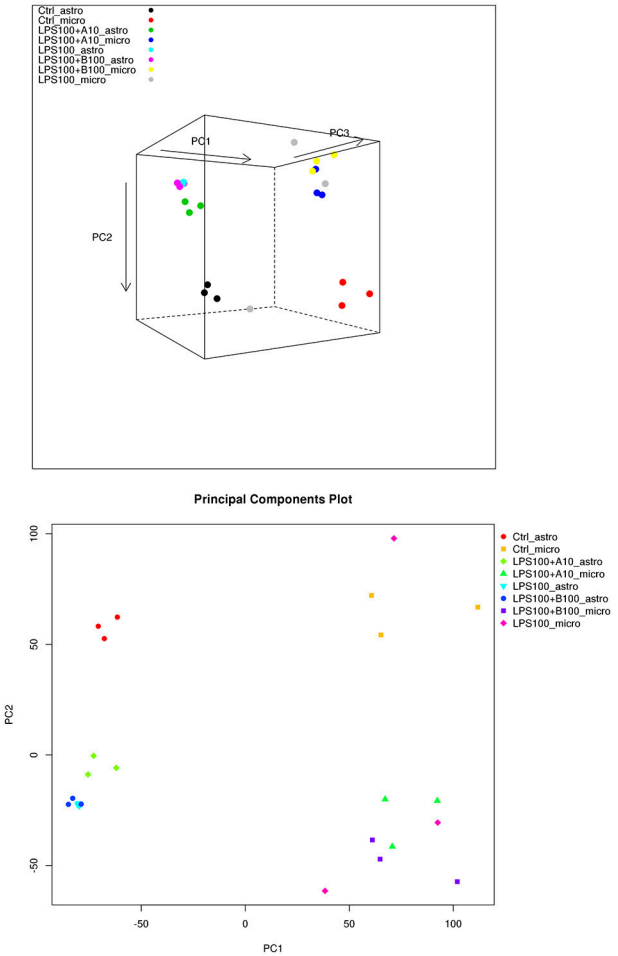


FIGURE 4 | (Top) PCA plot of microglia and astrocyte samples. Here we can see that astrocytes and microglia separate on the first principal component, and the second principal component captures the LPS treatment differences. The third principal component captures some intra-treatment variability for the microglia samples, particularly for one of the LPS treated microglia samples. **(Bottom)** PCA plot of microglia and astrocyte samples, showing just the first two principal components. The largest differences appear to be between the cell types.

metabolism in determining inflammatory phenotype in glia cells (3, 15).

Based on the IPA analysis within the *Ve*nn diagrams, the top down-regulated signaling pathway unique to LPS treatment was Ephrin A signaling [log(*p*-value) 3.21, **Table 5**]. Analysis of genes unique to α7nAChR agonist treatment showed a reduction of this down-regulation [log(*p*-value)1.58, **Table 5**]. Analysis of genes unique to α7nAChR antagonist treatment had no significant effect on this signaling pathway (**Table 5**). Ephrin signaling has been implicated in neuroprotective astrocyte phenotype (23). Our findings suggest a neuroprotective effect of α7nAChR agonism on ephrin signaling pathway.

Consistent with the notion of cholinergic signaling involved in stress axis regulation (3), POMC was the second (by IPA ranking) highest up-regulated gene under cholinergic agonist treatment, with a log ratio of 3.388 (Cf. GitHub repository).

Comparison to Fetal Sheep Microglial Transcriptome

PCA in **Figure 4** (top) shows that the main differences between astrocytes and microglia RNAseq data are captured on the first two principal components, so a 2D plot may be more useful (**Figure 4**, bottom). The intra-group variability is smaller for the astrocytes compared to the microglia. This may have to do with the total library sizes: there were several microglia samples with very few reads that aligned to any known transcript.

We compared the IPA-identified top signaling pathways in microglia and astrocytes under the LPS and α7nAChR signaling manipulation. **Table 4** presents the number of genes for each comparison and the corresponding findings of the IPA signaling pathway analysis. Overall, the response patterns to LPS and modulation of α7nAChR signaling were similar between the two glia cell types. The signaling pathways common to both astrocytes and microglia are bolded in **Tables 3**, **4**. Intuitively, common pathways activated due to LPS included neuroinflammation signaling and NF-κB signaling in some, but not all comparisons. However, overall, the overlap on the level of signaling pathway was rather minimal which may explain the strong separation by cell type on PCA. It is remarkable that astrocytes, not microglia—the primary immune cells of the brain, were characterized by unique inhibition patterns of STAT3 pathway due to agonistic stimulation of α7nAChR prior to LPS exposure.

The presented astrocytes—microglia comparison has limitations. The differences between the two cell types may be exaggerated by the inevitable technical differences (e.g., reagents). However, all these experiments were run from the same cohort, same animals (in some cases), at adjacent times and by the same people.

Do Fetal Neuroinflammation and Stress Mediate an Increased Risk for Autism Spectrum Disorder?

LPS effects on key genes involved in stress axis activity raised the question about the poorly understood role of astrocytes in the signaling pathways of neuroinflammation and prenatal stress (PS) (24).

Indeed, PS is accompanied by inflammation in the mother and offspring (24–29). Both, PS and fetal neuroinflammation have been implicated in the etiology of ASD (30, 31). PS increases expression of glutamate (Glu) transporter vGluT1 (SLC17A7) resulting in higher levels of GLT1 (32, 33).

Here, we sought to verify if the exposure of fetal astrocytes to LPS induces upregulation of Glu transporters in glia akin to PS (32, 33).

Given the known relationship between PS and VGLUT1 expression, we used IPA to annotate VGLUT1 gene network with our findings to test for evidence that the network is being perturbed by LPS treatment. Across all treatment comparisons, two DEGs were identified in astrocytes (common to all comparisons): JAK2 (2.732 (log ratio) upregulated, FDR

TABLE 4 | Ingenuity Pathway Analysis of differentially expressed genes from the fetal sheep microglia whole transcriptomes analysis.

Comparison	# genes	Top 10 signaling pathways	-log(p-value)
LPS100 vs. Control	1779	**Role of Macrophages, Fibroblasts and Endothelial Cells in Rheumatoid Arthritis**	16.7
		Dendritic Cell Maturation	12.9
		iNOS Signaling	12.6
		Role of IL-17A in Arthritis	12.5
		IL-10 Signaling	11.8
		Role of Tissue Factor in Cancer	11.6
		Production of Nitric Oxide and Reactive Oxygen Species in Macrophages	11.1
		Neuroinflammation Signaling Pathway	10.9
		Toll-like Receptor Signaling	10.7
		CD40 Signaling	10
LPS100+A10 vs. Control	4721	Molecular Mechanisms of Cancer	14.1
		Colorectal Cancer Metastasis Signaling	11.2
		Toll-like Receptor Signaling	11
		NF-κB Signaling	10.6
		Role of Macrophages, Fibroblasts and Endothelial Cells in Rheumatoid Arthritis	10.4
		PI3K Signaling in B Lymphocytes	10.4
		Role of Tissue Factor in Cancer	10.3
		B Cell Receptor Signaling	9.83
		TREM1 Signaling	7.83
		Protein Kinase A Signaling	7.81
LPS100+B100 vs. Control	4049	**Role of Macrophages, Fibroblasts and Endothelial Cells in Rheumatoid Arthritis**	13.6
		PI3K Signaling in B Lymphocytes	11.4
		Production of Nitric Oxide and Reactive Oxygen Species in Macrophages	10.2
		Molecular Mechanisms of Cancer	10.2
		Activation of IRF by Cytosolic Pattern Recognition Receptors	10.2
		IL-10 Signaling	9.63
		B Cell Receptor Signaling	9.55
		iNOS Signaling	9.21
		Role of Tissue Factor in Cancer	9.06
		Toll-like Receptor Signaling	8.93
LPS100+A10 vs. LPS100	8		
LPS100+B100 vs. LPS100	0		
LPS100+A10 vs. LPS100+B100	1132	T Cell Exhaustion Signaling Pathway	5.46
		Dendritic Cell Maturation	5.43
		Role of Macrophages, Fibroblasts and Endothelial Cells in Rheumatoid Arthritis	5.42
		Altered T Cell and B Cell Signaling in Rheumatoid Arthritis	5.22
		Th17 Activation Pathway	5.16
		Leukocyte Extravasation Signaling	4.81
		Superpathway of Cholesterol Biosynthesis	4.8
		IL-10 Signaling	4.49
		Role of Tissue Factor in Cancer	4.31
		Th1 and Th2 Activation Pathway	4.26

Differential analysis of count data was done with the Bioconductor limma package. Differentially expressed genes were selected, based on a 1.5-fold change and an FDR < 0.05. Up regulation and down regulation represent positive and negative log2 fold changes, respectively. For details on "raw gene" level, see our GitHub repository or directly here. Bold font highlights signaling pathways common with astrocytes. Orange: positive z-score; blue: negative z-score. For further details as raw data and visualized activity patterns see GitHub. Significant genes in microglia cultures at an FDR < 0.05 and a 1.5-fold change sorted on log(p-value).

3.91E-05) and SLC1A2 (2.350 upregulated, FDR 1.80E-04). JAK1 signaling is involved in glucocorticoid receptor signaling (34) and JAK1/2 signaling is involved in iron homeostasis signaling pathways(35), whereas JAK/Stat is involved in IL-6 signaling pathways. SLC1A2 is also known as GLT-1 or glial high affinity glutamate transporter; it is implicated in glutamate receptor signaling and neuroinflammation signaling pathways (36). Upregulation of glial GLT-1 in the hippocampus has been reported after chronic stress due to its control by glucocorticoids (37–39).

TABLE 5 | Genes unique to LPS, agonistic stimulation or inhibition of α7nAChR in single hit astrocytes cultures.

	Top 10 signaling pathways	-log(*p*-value)
Genes unique to LPS100	Ephrin A Signaling	3.21
	P2Y Purigenic Receptor Signaling Pathway	2.72
	Role of p14/p19ARF in Tumor Suppression	2.55
	Thiamin Salvage III	2.2
	Melanoma Signaling	2.14
	Lymphotoxin β Receptor Signaling	2.03
	CCR3 Signaling in Eosinophils	1.96
	CD40 Signaling	1.84
Genes unique to A10	Germ Cell-Sertoli Cell Junction Signaling	9.13
	Integrin Signaling	7.4
	Actin Cytoskeleton Signaling	5.84
	Leukocyte Extravasation Signaling	5.81
	Sertoli Cell-Sertoli Cell Junction Signaling	5.58
	GDP-glucose Biosynthesis	5.49
	Glucose and Glucose-1-phosphate Degradation	5.24
	Phagosome Formation	4.84
	Signaling by Rho Family GTPases	4.71
	HGF Signaling	4.6
Genes unique to B100	Apelin Cardiomyocyte Signaling Pathway	5.54
	Adrenomedullin signaling pathway	4.09
	Dendritic Cell Maturation	3.23
	Endothelin-1 Signaling	3.2
	UVA-Induced MAPK Signaling	3.2
	Renin-Angiotensin Signaling	2.97
	Role of NFAT in Cardiac Hypertrophy	2.95
	Phagosome Formation	2.95
	GP6 Signaling Pathway	2.91
	Wnt/Ca+ pathway	2.89

Again assessing the present findings together with the previously published RNAseq data from the identical experiment in ovine fetal microglia (3), we found GLT-1 to be upregulated in microglia and astrocytes regardless cholinergic manipulation (for details see GitHub repository). Albeit both pure primary cultures were exposed to LPS, we found the up regulation of JAK2 to be unique to astrocytes. This finding is conceptually in line with studies reporting brain cell-specific signaling pathways behavior in response to IL-1β (40). Much remains to be learned about the differences between second messenger signaling cascades involved in astrocytes, microglia and neurons in the developing fetal brain exposed to inflammatory stimuli. Furthermore, there is still a paucity of data about differences across the species for these signaling pathways.

General Discussion

Fetal sheep is the classic model of fetal physiology and neuroscience (41). It has been used successfully for both integrative physiological as well as genomic studies. In the present study, we expand the recently published series of experiments in the same animal model using primary microglia cultures to now include primary astrocytes cultures (3, 14–16).

Acetylcholine is synthesized by cultured microglia and astrocyte in mouse and rat (42, 43), however, there is no information from other species. It is plausible that the fetal sheep brain astrocytes in culture produce acetylcholine, because they appear to respond to α7nAChR stimulation. However, we do not know how much acetylcholine is produced, and whether or not the speculated endogenous acetylcholine can activate the α7nAChR. This remains worthwhile to investigate in future studies.

The antagonist drug for α7nAChR we used, α-bungarotoxin, is a selective inhibitor for α7 receptors acting by preventing the opening of nicotinic receptor-associated ion channels (Tocris α-bungarotoxin datasheet). By using optimized dose, we treated our astrocyte cells with α-bungarotoxin 1 h prior to LPS exposure, which would block LPS-induced cytokine production in the cells.

LPS exposure had the anticipated effect of increasing IL-1β production in astrocytes and we observed this consistently on the transcriptome level. However, our findings on protein level following pre-incubation with α7nAChR antagonist or agonist do not align with those on the transcriptome level: present results on protein level do not show a clear hypothesized effect of α7nAChR agonism or antagonism on LPS secretion in ovine fetal astrocytes. Such discordant behavior on protein and transcriptome levels has been reported and studied systematically to represent the rule rather than an exception to cellular biology in general (44).

Future studies will need to explore the protein responses in more depth and in different species to further delineate astrocytic behavior under α7nAChR stimulation, especially the peculiarly opposite effect of endotoxin memory in astrocytes and microglia on IL-1β secretion.

Microglia—astrocyte ensemble interactions need to be studied to bridge the methodological gap between *in vitro* experimental design and the *in situ* physiology. This can be done in co-cultures, feasible in ovine species, for example (14). Recent study in mice highlighted the importance of microglia—astrocyte interactions for understanding the polarization dynamics of astrocytes (45).

In an adult rodent model, cholinergic signaling reduced stress responsiveness via cortisol releasing hormone (CRH) receptor 1 with positive behavioral changes (46). We identified POMC as up regulated under α7nAChR stimulation. Considering that CRH is an upstream regulator of POMC, another question for future studies is whether we can implicate a direct interaction with the CRH receptor 1 in the developing brain.

We found that within its interaction network, GLT-1 was upregulated in microglia and astrocytes regardless of cholinergic manipulation, while the up-regulation of JAK1/2 was unique to astrocytes. This is in line with studies showing brain region specific overexpression of vGluT-1 (SLC17A7) both due to endotoxin stress and due to PS and puts the LPS exposure in the context of a more general brain stress exposure paradigm presenting with shared response patterns of neuroinflammation and metabolic adaptations in astrocytes (13, 47, 48). PS has long lasting consequences on α7nACh-ergic signaling in frontal cortex and hippocampus reducing the expression of α7nAChR protein expression in the brain of adult rats (47).

It is plausible to conclude that low grade neuroinflammation results in changes similar to those induced by PS with regard

to reprogramming astrocytes to a higher glutamate uptake. As shown elsewhere (49), PS and exposure to endotoxin may act synergistically to exacerbate the impairment of neuron-glial glutamatergic interaction. For endotoxin exposure, this process is not subject to cholinergic modulation. Whether or not PS effects alone on astrocytes glutamate uptake can be ameliorated or reversed by α7nAChR agonism remains to be investigated.

The phylogenetically conserved interaction between neuroinflammation and chronic stress has been the subject of multiple studies (24), yet we are only beginning to unravel the complex web of interactions, across developmental stages, organs, cell types and species-specific differences, which connect these two phenomena. While the role of microglia in this context has been appreciated, the response of astrocytes we report here and their behavior on protein level under second hit scenario are novel observations warranting further studies in different species.

In summary, we show that genes involved in stress memory of the offspring are also impacted by LPS stress, this impact is further altered by a second hit (memory) and that such memory of LPS stress is amenable to cholinergic treatment via α7nAChR. It remains to be validated in future studies whether, when and which stimulation of the α7nAChR is favorable.

ETHICS STATEMENT

This study was carried out in strict accordance with the recommendations in the Guide for the Care and Use of Laboratory Animals of the National Institutes of Health. The respective *in vivo* and *in vitro* protocols were approved by the Committee on the Ethics of Animal Experiments of the Université de Montréal (Permit Number: 10-Rech-1560).

AUTHOR CONTRIBUTIONS

MCa, PB, GF, AD, and MF are responsible for conception and design. MCa, HL, MW, LD, PB, GF, AD, and MF acquired data. MCa, HL, MW, JM, MCo, MD, TB, JS, and MF did the analysis and interpretation of data. MCa, JM, MCo, TB, and MF drafted the manuscript. MCa, JM, MW, MCo, JS, MA, TB, and MF are responsible for revising it for intellectual content. MCa, JM, HL, MW, MCo, LD, PB, GF, AD, JS, MA, RB, MD, TB, and MF gave final approval of the completed manuscript.

FUNDING

Supported by grants from the Canadian Institute of Health Research (CIHR) (MF); Fonds de la recherche en santé du Québec (FRSQ) (MF) and Molly Towell Perinatal Research Foundation (MF); QTNPR (by CIHR) (LD). Supported in part by Illumina Inc.

ACKNOWLEDGMENTS

The authors thank Dr. Jack Antel lab, especially Manon Blain, and Dr. Craig Moore for invaluable assistance with the cell culture protocol, St-Hyacinthe CHUV team for technical assistance and Jan Hamanishi for graphical design. We also thank MD lab for skilful assistance with RNA samples pipeline on the Illumina platform and Lu Wang for assistance in RNAseq bioinformatics pipeline.

REFERENCES

1. Jassam YN, Izzy S, Whalen M, McGavern DB, El Khoury J. Neuroimmunology of traumatic brain injury: time for a paradigm shift. *Neuron.* (2017) 95:1246–65. doi: 10.1016/j.neuron.2017.07.010
2. Kalkman HO, Feuerbach D. Modulatory effects of α7 nAChRs on the immune system and its relevance for CNS disorders. *Cell Mol Life Sci.* (2016) 73:2511–30. doi: 10.1007/s00018-016-2175-4
3. Cortes M, Cao M, Liu HL, Moore CS, Durosier LD, Burns P, Fecteau G, et al. α7 nicotinic acetylcholine receptor signaling modulates the inflammatory phenotype of fetal brain microglia: first evidence of interference by iron homeostasis. *Sci Rep*. (2017) 7:10645. doi: 10.1038/s41598-017-09439-z
4. Kiguchi N, Kobayashi D, Saika F, Matsuzaki S, Kishioka S. Inhibition of peripheral macrophages by nicotinic acetylcholine receptor agonists suppresses spinal microglial activation and neuropathic pain in mice with peripheral nerve injury. *J Neuroinflamm.* (2018) 15:96. doi: 10.1186/s12974-018-1133-5
5. Frasch MG, Szynkaruk M, Prout AP, Nygard K, Cao M, Veldhuizen R, et al. Decreased neuroinflammation correlates to higher vagus nerve activity fluctuations in near-term ovine fetuses: a case for the afferent cholinergic anti-inflammatory pathway? *J Neuroinflamm.* (2016) 13:103. doi: 10.1186/s12974-016-0567-x
6. Han Z, Li L, Wang L, Degos V, Maze M, Su H. Alpha-7 nicotinic acetylcholine receptor agonist treatment reduces neuroinflammation, oxidative stress, and brain injury in mice with ischemic stroke and bone fracture. *J Neurochem*. (2014) 131:498–508. doi: 10.1111/jnc.12817
7. de Jonge WJ, Ulloa L. The alpha7 nicotinic acetylcholine receptor as a pharmacological target for inflammation. *Br J Pharmacol.* (2007) 151:915–29. doi: 10.1038/sj.bjp.0707264
8. Shytle RD, Mori T, Townsend K, Vendrame M, Sun N, Zeng J, Ehrhart J,et al. Cholinergic modulation of microglial activation by alpha 7 nicotinic receptors. *J Neurochem*. (2004) 89:337–43. doi: 10.1046/j.1471-4159.2004.02347.x
9. Rosas-Ballina M, Olofsson PS, Ochani M, Valdes-Ferrer SI, Levine YA, Reardon C, et al. Acetylcholine-synthesizing T cells relay neural signals in a vagus nerve circuit. *Science*. (2011) 334:98–101. doi: 10.1126/science.1209985
10. Cheyuo C, Jacob A, Wu R, Zhou M, Coppa GF, Wang P. The parasympathetic nervous system in the quest for stroke therapeutics. *J Cereb Blood Flow Metab*. (2011) 31:1187–95. doi: 10.1038/jcbfm.2011.24
11. Cao J, Lu K-H, Powley TL, Liu Z. Vagal nerve stimulation triggers widespread responses and alters large-scale functional connectivity in the rat brain. *PLoS ONE.* (2017) 12:e0189518. doi: 10.1371/journal.pone.0189518
12. al-Haddad BJS, Jacobsson B, Chabra S, Modzelewska D, Olson EM, Bernier R, et al. Long-term risk of neuropsychiatric disease after exposure to infection in utero. *JAMA Psychiatry.* (2019) doi: 10.1001/jamapsychiatry.2019.0029. [Epub ahead of print].
13. Elovitz MA, Brown AG, Breen K, Anton L, Maubert M, Burd I. Intrauterine inflammation, insufficient to induce parturition, still evokes fetal and neonatal brain injury. *Int J Dev Neurosci.* (2011) 29:663–71. doi: 10.1016/j.ijdevneu.2011.02.011
14. Cortes M, Cao M, Liu HL, Burns P, Moore C, Fecteau G, et al. RNAseq profiling of primary microglia and astrocyte cultures in near-term ovine fetus: a glial *in vivo-in vitro* multi-hit paradigm in large mammalian brain. *J Neurosci Methods.* (2017) 276:23–32. doi: 10.1016/j.jneumeth.2016.11.008

15. Cao M, Cortes M, Moore CS, Leong SY, Durosier LD, Burns P, et al. Fetal microglial phenotype in vitro carries memory of prior in vivo exposure to inflammation. *Front Cell Neurosci.* (2015) 9:294. doi: 10.3389/fncel.2015.00294
16. Frasch MG, Burns P, Benito J, Cortes M, Cao M, Fecteau G, et al. Sculpting the sculptors: methods for studying the fetal cholinergic signaling on systems and cellular scales. *Methods Mol Biol.* (2018) 1781:341–52. doi: 10.1007/978-1-4939-7828-1_18
17. Patro R, Duggal G, Kingsford C. Salmon: accurate, versatile and ultrafast quantification from rna-seq data using lightweight-alignment. *bioRxiv.* (2015) 021592. doi: 10.1101/021592
18. Soneson C, Love MI, Robinson MD. Differential analyses for RNA-seq: transcript-level estimates improve gene-level inferences. *F1000Res.* (2015) 4:1521. doi: 10.12688/f1000research.7563.2
19. Smyth GK. Linear models and empirical bayes methods for assessing differential expression in microarray experiments. *Stat Appl Genet Mol Biol.* (2004) 3:Article3. doi: 10.2202/1544-6115.1027
20. Wang P, Xu T-Y, Guan Y-F, Tian W-W, Viollet B, Rui Y-C, et al. Nicotinamide phosphoribosyltransferase protects against ischemic stroke through SIRT1-dependent adenosine monophosphate-activated kinase pathway. *Ann Neurol.* (2011) 69:360–74. doi: 10.1002/ana.22236
21. Li D, Liu N, Zhao H-H, Zhang X, Kawano H, Liu L, et al. Interactions between Sirt1 and MAPKs regulate astrocyte activation induced by brain injury *in vitro* and *in vivo*. *J Neuroinflamm.* (2017) 14:67. doi: 10.1186/s12974-017-0841-6
22. Frasch MG. Putative role of AMPK in fetal adaptive brain shut-down: linking metabolism and inflammation in the brain. *Front Neurol.* (2014) 5:150. doi: 10.3389/fneur.2014.00150
23. Tyzack GE, Hall CE, Sibley CR, Cymes T, Forostyak S, Carlino G, et al. A neuroprotective astrocyte state is induced by neuronal signal EphB1 but fails in ALS models. *Nat Commun.* (2017) 8:1164. doi: 10.1038/s41467-017-01283-z
24. Deak T, Kudinova A, Lovelock DF, Gibb BE, Hennessy MB. A multispecies approach for understanding neuroimmune mechanisms of stress. *Dialogues Clin Neurosci.* (2017) 19:37–53. Available online at: https://www.dialogues-cns.org/contents-19-1/dialoguesclinneurosci-19-37/
25. Diz-Chaves Y, Astiz M, Bellini MJ, Garcia-Segura LM. Prenatal stress increases the expression of proinflammatory cytokines and exacerbates the inflammatory response to LPS in the hippocampal formation of adult male mice. *Brain Behav Immun.* (2013) 28:196–206. doi: 10.1016/j.bbi.2012.11.013
26. Bronson SL, Bale TL. Prenatal stress-induced increases in placental inflammation and offspring hyperactivity are male-specific and ameliorated by maternal antiinflammatory treatment. *Endocrinology.* (2014) 155:2635–46. doi: 10.1210/en.2014-1040
27. Wu S, Gennings C, Wright RJ, Wilson A, Burris HH, Just AC, et al. Prenatal stress, methylation in inflammation-related genes, and adiposity measures in early childhood: the programming research in obesity, growth environment and social stress cohort study. *Psychosom Med.* (2018) 80:34–41. doi: 10.1097/PSY.0000000000000517
28. Shapiro GD, Fraser WD, Frasch MG, Séguin JR. Psychosocial stress in pregnancy and preterm birth: associations and mechanisms. *J Perinat Med.* (2013) 41:631–645. doi: 10.1515/jpm-2012-0295
29. Christian LM, Franco A, Glaser R, Iams JD. Depressive symptoms are associated with elevated serum proinflammatory cytokines among pregnant women. *Brain Behav Immun.* (2009) 23:750–4. doi: 10.1016/j.bbi.2009.02.012
30. El-Ansary A, Al-Ayadhi L. Neuroinflammation in autism spectrum disorders. *J Neuroinflamm.* (2012) 9:265. doi: 10.1186/1742-2094-9-265
31. Kinney DK, Munir KM, Crowley DJ, Miller AM. Prenatal stress and risk for autism. *Neurosci Biobehav Rev.* (2008) 32:1519–32. doi: 10.1016/j.neubiorev.2008.06.004
32. Barros VG, Duhalde-Vega M, Caltana L, Brusco A, Antonelli MC. Astrocyte-neuron vulnerability to prenatal stress in the adult rat brain. *J Neurosci Res.* (2006) 83:787–800. doi: 10.1002/jnr.20758
33. Barros VG, Berger MA, Martijena ID, Sarchi MI, Perez AA, Molina VA, et al. Early adoption modifies the effects of prenatal stress on dopamine and glutamate receptors in adult rat brain. *J Neurosci Res.* (2004) 76:488–96. doi: 10.1002/jnr.20119
34. Pace TWW, Miller AH. Cytokines and glucocorticoid receptor signaling. Relevance to major depression. *Ann N Y Acad Sci.* (2009) 1179:86–105. doi: 10.1111/j.1749-6632.2009.04984.x
35. Schmidt PJ. Regulation of iron metabolism by hepcidin under conditions of inflammation. *J Biol Chem.* (2015) 290:18975–83. doi: 10.1074/jbc.R115.650150
36. Jauregui-Huerta F, Ruvalcaba-Delgadillo Y, Gonzalez-Castañeda R, Garcia-Estrada J, Gonzalez-Perez O, Luquin S. Responses of glial cells to stress and glucocorticoids. *Curr Immunol Rev.* (2010) 6:195–204. doi: 10.2174/157339510791823790
37. Autry AE, Grillo CA, Piroli GG, Rothstein JD, McEwen BS, Reagan LP. Glucocorticoid regulation of GLT-1 glutamate transporter isoform expression in the rat hippocampus. *Neuroendocrinology.* (2006) 83:371–9. doi: 10.1159/000096092
38. Reagan LP, Rosell DR, Wood GE, Spedding M, Muñoz C, Rothstein J, et al. Chronic restraint stress up-regulates GLT-1 mRNA and protein expression in the rat hippocampus: reversal by tianeptine. *Proc Natl Acad Sci USA.* (2004) 101:2179–2184. doi: 10.1073/pnas.0307294101
39. Zschocke J, Bayatti N, Clement AM, Witan H, Figiel M, Engele J, Behl C. Differential promotion of glutamate transporter expression and function by glucocorticoids in astrocytes from various brain regions. *J Biol Chem.* (2005) 280:34924–32. doi: 10.1074/jbc.M502581200
40. Srinivasan D, Yen J-H, Joseph DJ, Friedman W. Cell Type-Specific Interleukin-1β Signaling in the CNS. *J Neurosci.* (2004) 24:6482–8. doi: 10.1523/JNEUROSCI.5712-03.2004
41. Morrison JL, Berry MJ, Botting KJ, Darby JRT, Frasch MG, Gatford KL, et al. Improving pregnancy outcomes in humans through studies in sheep. *Am J Physiol Regul Integr Comp Physiol.* (2018) 315:R1123–53. doi: 10.1152/ajpregu.00391.2017
42. Wessler I, Kirkpatrick CJ, Racké K. The cholinergic "pitfall": acetylcholine, a universal cell molecule in biological systems, including humans. *Clin Exp Pharmacol Physiol.* (1999) 26:198–205.
43. Wessler I, Reinheimer T, Klapproth H, Schneider FJ, Racké K, Hammer R. Mammalian glial cells in culture synthesize acetylcholine. *Naunyn Schmiedebergs Arch Pharmacol.* (1997) 356:694–7.
44. Ghazalpour A, Bennett B, Petyuk VA, Orozco L, Hagopian R, Mungrue IN, et al. Comparative analysis of proteome and transcriptome variation in mouse. *PLoS Genet.* (2011) 7:e1001393. doi: 10.1371/journal.pgen.1001393
45. Rothhammer V, Borucki DM, Tjon EC, Takenaka MC, Chao C-C, Ardura-Fabregat A, et al. Microglial control of astrocytes in response to microbial metabolites. *Nature.* (2018) 557:724–8. doi: 10.1038/s41586-018-0119-x
46. Farrokhi CB, Tovote P, Blanchard RJ, Blanchard DC, Litvin Y, Spiess J. Cortagine: behavioral and autonomic function of the selective CRF receptor subtype 1 agonist. *CNS Drug Rev.* (2007) 13:423–43. doi: 10.1111/j.1527-3458.2007.00027.x
47. Baier CJ, Pallares ME, Adrover E, Monteleone MC, Brocco MA, Barrantes FJ, et al. Prenatal restraint stress decreases the expression of alpha-7 nicotinic receptor in the brain of adult rat offspring. *Stress.* (2015) 18:435–45. doi: 10.3109/10253890.2015.1022148
48. Adrover E, Pallarés ME, Baier CJ, Monteleone MC, Giuliani FA, Waagepetersen HS, et al. Glutamate neurotransmission is affected in prenatally stressed offspring. *Neurochem Int.* (2015) 88:73–87. doi: 10.1016/j.neuint.2015.05.005
49. Cumberland AL, Palliser HK, Rani P, Walker DW, Hirst JJ. Effects of combined IUGR and prenatal stress on the development of the hippocampus in a fetal guinea pig model. *J Dev Orig Health Dis.* (2017) 8:584–96. doi: 10.1017/s2040174417000307

Conflict of Interest Statement: The authors declare that the research was conducted in the absence of any commercial or financial relationships that could be construed as a potential conflict of interest.

Copyright © 2019 Cao, MacDonald, Liu, Weaver, Cortes, Durosier, Burns, Fecteau, Desrochers, Schulkin, Antonelli, Bernier, Dorschner, Bammler and Frasch. This is an open-access article distributed under the terms of the Creative Commons Attribution License (CC BY). The use, distribution or reproduction in other forums is permitted, provided the original author(s) and the copyright owner(s) are credited and that the original publication in this journal is cited, in accordance with accepted academic practice. No use, distribution or reproduction is permitted which does not comply with these terms.

frontiers in Immunology

ORIGINAL RESEARCH
published: 09 May 2019
doi: 10.3389/fimmu.2019.01040

Proteomic Profiling Unravels a Key Role of Specific Macrophage Subtypes in Sporadic Inclusion Body Myositis

Andreas Roos[1,2†], *Corinna Preusse*[3†], *Denisa Hathazi*[2], *Hans-Hilmar Goebel*[3] and *Werner Stenzel*[3,4*]

[1] Department of Neuropediatrics, Developmental Neurology and Social Pediatrics, Centre for Neuromuscular Disorders in Children, University Children's Hospital Essen, University of Duisburg-Essen, Essen, Germany, [2] Leibniz-Institut für Analytische Wissenschaften -ISAS- e.V., Dortmund, Germany, [3] Department of Neuropathology, Charité -Universitätsmedizin Berlin, Corporate Member of Freie Universität Berlin, Humboldt-Universität zu Berlin, and Berlin Institute of Health, Berlin, Germany, [4] Leibniz Science Campus Chronic Inflammation, Berlin, Germany

OPEN ACCESS

Edited by:
Stefan Bittner,
Johannes Gutenberg University
Mainz, Germany

Reviewed by:
Janine Adele Lamb,
University of Manchester,
United Kingdom
Ann Marie Reed,
Duke University, United States

***Correspondence:**
Werner Stenzel
werner.stenzel@charite.de

[†]These authors share first authorship

Specialty section:
This article was submitted to Multiple Sclerosis and Neuroimmunology, a section of the journal Frontiers in Immunology

Received: 30 December 2018
Accepted: 23 April 2019
Published: 09 May 2019

Citation:
Roos A, Preusse C, Hathazi D, Goebel H-H and Stenzel W (2019) Proteomic Profiling Unravels a Key Role of Specific Macrophage Subtypes in Sporadic Inclusion Body Myositis. Front. Immunol. 10:1040. doi: 10.3389/fimmu.2019.01040

Unbiased proteomic profiling was performed toward the identification of biological parameters relevant in sIBM, thus giving hints about the pathophysiological processes and the existence of new reliable markers. For that purpose, skeletal muscle biopsies from 13 sIBM and 7 non-diseased control patients were analyzed with various methods, including liquid chromatography coupled to tandem mass spectrometry (four patients). Subsequent data analysis identified key molecules further studied in a larger cohort by *q*PCR, immunostaining, and immunofluorescence *in situ*. Proteomic signature of muscle biopsies derived from sIBM patients revealed the chaperone and cell surface marker CD74, the macrophage scavenger molecule CD163 and the transcription activator STAT1 to be among the highly and relevantly expressed proteins suggesting a significant contribution of immune cells among the myofibers expressing these markers. Moreover, *in silico* studies showed that 39% of upregulated proteins were involved in type I or mixed type I and type II interferon immunity. Indeed, further studies via immunohistochemistry clearly confirmed the prominent involvement of the key type I interferon signature-related molecules, ISG15 as well as IRF8 with MHC class II$^+$ myofibers. Siglec1 colocalized with CD163$^+$ macrophages and MHC class II molecules also co-localized with CD74 on macrophages. STAT1 co-localized with Siglec1$^+$ macrophages in active myofibre myophagocytosis while STAT6 colocalized with endomysial macrophages. These combined results show involvement of CD74, CD163, and STAT1 as key molecules of macrophage activation being crucially involved in mixed and specific type I interferon, and interferon gamma associated-pathways in sIBM. On a more general note, these results also highlight the type of immune-interaction between macrophages and myofibers in the etiopathology of sIBM.

Keywords: CD74, SIGLEC1, CD163, STAT1, STAT6, type I interferon (IFN), muscle proteomics

INTRODUCTION

Inclusion body myositis is a chronic muscle-specific disease of adulthood leading to progressive and very characteristic hip flexor and quadriceps paresis, long finger flexor paresis, and swallowing difficulties (1–4). Muscle biopsy reveals a severe myopathic/dystrophic process with the characteristic complex inflammatory infiltrate composed of different types of T cells, macrophages and other mononuclear cells. Additional degenerative changes with the presence of amyloidogenic protein deposits, disturbed autophagy, and mitochondrial abnormalities are present. Clinical and muscle biopsy characteristics are the basis of a precise diagnosis of sIBM (1, 3, 5, 6). The autoantibody cN1A can be used as a marker of severity in sIBM, however, its role in the pathogenicity of this disease has not been fully elucidated (7–9). Despite the characteristic clinical picture and well-known biopsy findings, the pathogenesis of sIBM is still elusive and not fully understood. So far, therapeutic approaches have not been broadly successful, questioning the (auto)-immune pathogenesis. Moreover, these therapeutic interventions present attempts to address the degenerative autophagic dysfunction (10).

Proteomics and subsequent specific data analysis of diseased tissue such as skeletal muscle can help to identify key pathogenic molecules or groups of molecules involved in certain processes, which may be of relevance in inflammatory or genetic diseases affecting muscle fiber integrity [exemplified in (11)].

In this study, we applied unbiased proteomic profiling and identified CD74, CD163, and STAT1 among the highly expressed proteins in muscle biopsies of sIBM patients. Notably, these proteins were found to localize to macrophages and partially to the sarcolemma of myofibers. Further analyses were performed in the larger context of associated immune responses in skeletal muscle tissue. These approaches revealed a specific and key role of the cellular interaction of specifically activated macrophages with myofibers.

MATERIALS AND METHODS

Patients

Clinical data of all IBM patients enrolled in this study are listed in **Table 1**. We included patients with clinical, and morphological signs and symptoms consistent with sIBM, according to present criteria (12), as well as sex- and age-matched patients defined as non-diseased controls (NDCs). We chose as controls subjects who had undergone a muscle biopsy, but who were found not to have any inflammatory muscle disease. They had suffered from non-specific complaints like myalgia, but objective muscle weakness and morphological abnormalities on skeletal muscle biopsy were absent. CK levels were normal and no signs of systemic inflammation and no myositis-specific antibodies (MSA) or myositis-associated antibodies (MAA) were detectable. sIBM patients had moderate illness (still ambulatory) and homogeneous muscle biopsy findings (not severely atrophic muscle bulk). Informed consent was obtained from all patients and the Charité ethics committee (EA2/163/17), had granted ethical approval.

Skeletal Muscle Specimens

In this study, we analyzed skeletal muscle biopsies derived from sIBM patients (clinically and morphologically definite sIBM) (12). Skeletal muscle biopsies from sIBM patients were used to produce proteomic results (four biopsies) and qualitative morphological characteristics *in situ* (whole cohort). In addition, four control muscle biopsies were included for the proteomic profiling and additional nine biopsies for subsequent immunohistochemical and *q*PCR studies. All skeletal muscle specimens were cryopreserved at −80°C prior to analysis.

Morphological Analysis

All stains were performed on 7 μm cryomicrotome sections, according to standard procedures. Immunohistochemical and double immunofluorescence reactions were carried out as described previously (13). The following antibodies were used for staining procedures:

Mouse anti-human CD163, 1:50, St. John's Lab/polyclonal; rabbit anti-human CD74, 1:100 St. John's Lab/polyclonal; mouse anti-human CD68, 1:100 Dako/EBM1; rabbit anti-human iNOS, ready-to-use, Genetex/polyclonal; rabbit anti-human ISG15, 1:100, abcam/polyclonal; MHCI, 1:1.000, Dako/W6/32; mouse anti-human MHC class II, 1:100, DAKO/ CR3/43; rat anti-human STAT1, 1:50, R&D Systems/246523; mouse anti-human STAT6, 1:50, R&D Systems/253906; mouse anti-human Siglec1, 1:100, Novus Biologicals/HSn7D2; IRF8, 1:100 Abcam/polyclonal.

Proteomics

Proteomic profiling of four sIBM-patient derived and four control quadriceps muscles was carried out as described previously (14).

In Silico Studies

Further *in silico* studies included "Proteomaps" (www.proteomaps.net), "Interferome" (www.interferome.org), "Cytoscape" (www.cytoscape.org) and "STRING" (www.string-db.org) and have been carried out to unravel functional connections and interdependences between the proteins vulnerable in sIBM with a special focus on such involved in the interferon-mediated immune response. All regulated proteins (24 down, 119 up-regulated) were used for the analyses.

"Proteomaps" enables us to obtain a picture of the quantitative composition of vulnerable pathways and cellular processes with a focus on individual protein functions controlling these pathways and processes. The visualization of affected pathways (and responsible proteins) is built automatically from the computerized proteome data and based on the "KEGG Pathways" gene classification. Hereby, individual proteins are shown as polygons and to emphasize the fold of regulation, polygon-sizes reflect fold of changes abundances. Functionally related proteins are arranged in proximity. This *in silico* tool has been applied

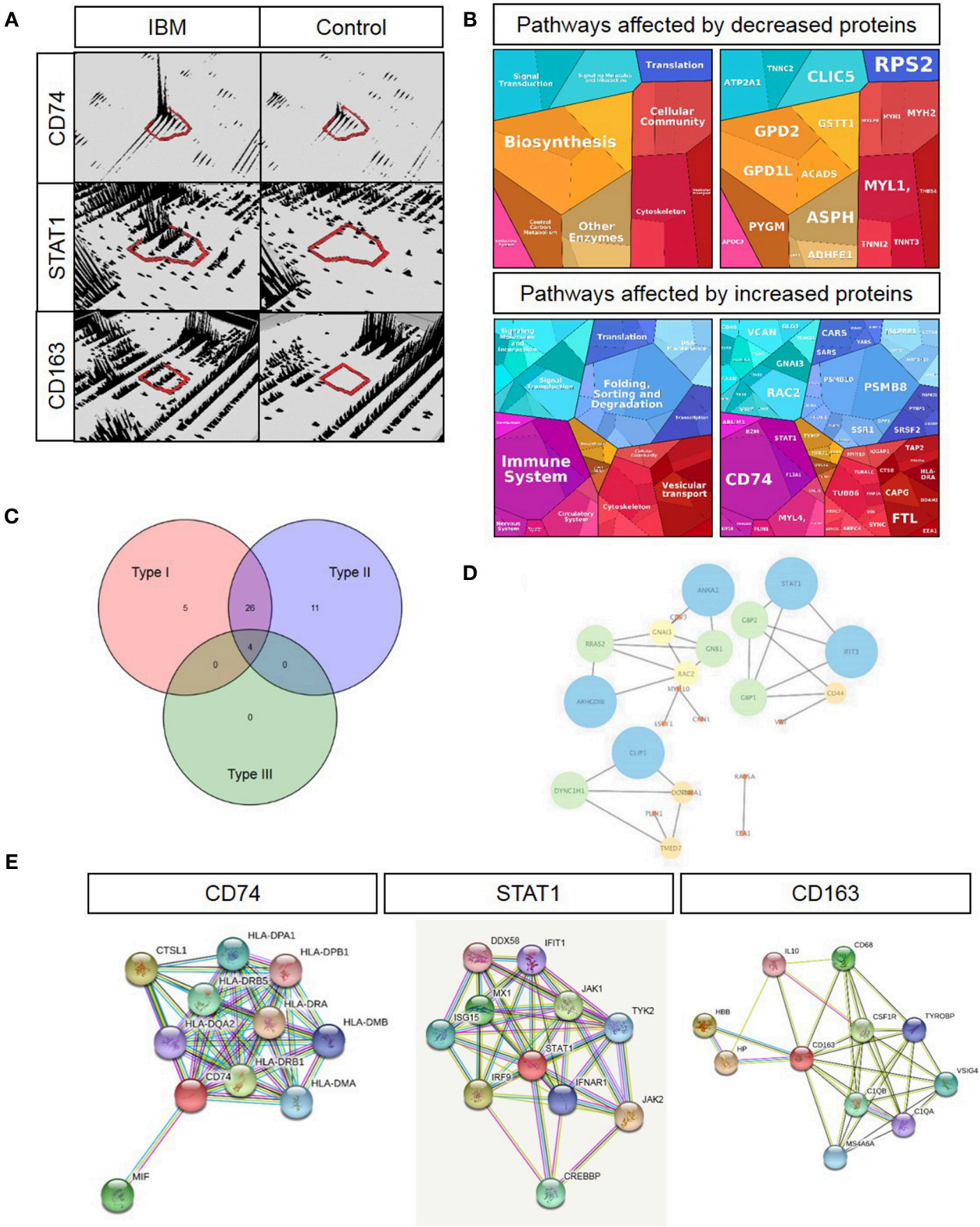


FIGURE 1 | Key proteomic findings and subsequent *in silico* analyses. **(A)** 3-D montages of representative tryptic peptides highlighting the increased abundance of the corresponding proteins, CD47, STAT1, and CD163. **(B)** Proteomaps-based analysis of cellular processes addressed by up- and down-regulated proteins in sIBM-patient-derived muscle (left figures) as well as of proteins predominating the respective cellular processes by taking their relative abundance/fold of regulation

(Continued)

FIGURE 1 | into consideration (right figures). **(C)** Venn diagram-based categorization of proteins increased in sIBM-patient-derived muscle and modulated by the three different interferon types (detailed list of increased proteins controlled by interferons is provided in **Table 2**). **(D)** Cytoscape-based visualization of functional networks of upregulated proteins controlled by interferons. **(E)** STRING-based analysis of functional protein networks of CD74 (left figure), STAT1 (figure in the middle) and CD163 (right figure) toward the identification of further interferon-modulated and macrophage-expressed proteins with pathophysiological significance in sIBM.

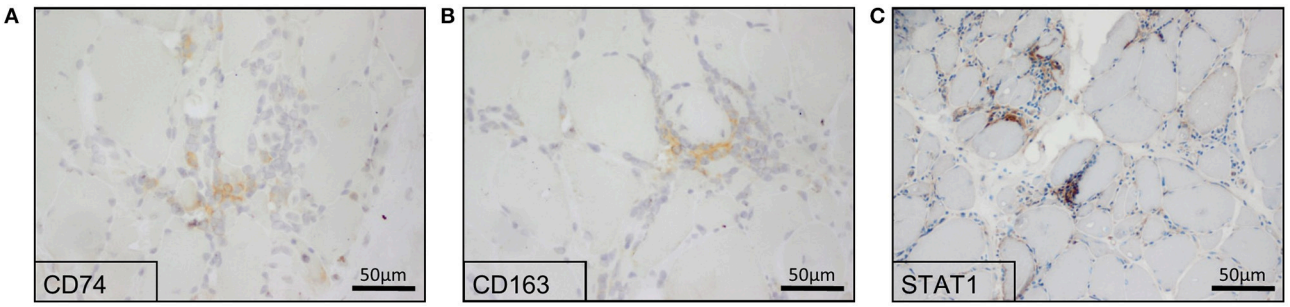


FIGURE 2 | Immunohistochemical reactions of potential key players in the skeletal muscle biopsies from sIBM patients. Proteomics-based identified key players showed a positive staining in sIBM patients' skeletal muscle biopsies, where CD74 **(A)**, as well as CD163 **(B)** highlighted macrophages. STAT1 **(C)** was expressed in macrophages in active myophagocytosis, while it was not present at the sarcolemma of myofibers.

to proteins showing a statistically significant altered abundance and thus vulnerability in sIBM-diseased muscle. "Interferome" enables the reliable identification of individual interferon-regulated genes or respective molecular signatures. Here, "Ensembl IDs" have been utilized to filter for interferon-regulated genes (or rather corresponding proteins) based on our proteomic findings. "Cytoscape" as an additional open source *in silico* tool enabling the visualization of molecular and functional protein-protein interaction networks. Here, we applied "Cytoscape" to proteins modulated by the interferon-response (based on the results of our "Interferome"-based data analysis). "STRING" (Search Tool for the Retrieval of Interacting Genes/Proteins) represents an *in silico* tool enabling the delineation of (direct and functionally related) protein-protein interactions and thus allows to identify functional interdependences of proteins with altered abundances in diseased tissues such as sIBM muscle. Here, we applied "STRING" to decipher proteins interacting with CD74, STAT1, and CD63.

Quantitative Reverse Transcription PCR (*q*RT-PCR)

Total RNA was extracted from muscle specimens using the technique described previously (13). Briefly, cDNA was synthesized using the High-Capacity cDNA Archive Kit (Applied Biosystems, Foster City, CA). For qPCR reactions, 2 ng of cDNA were used and for subsequent analysis, the 7900HT Fast Real-Time PCR System (Applied Biosystems, Foster City, CA) was utilized with the following, running conditions: 95°C 0:20, 95°C 0:01, 60°C 0:20, 45 cycles (values above 40 cycles were defined as not expressed). All targeted transcripts were run as triplicates. For each of these runs, the reference gene *PGK1* has been included as internal control to normalize the relative expression of the targeted transcripts. The qPCR assay identification numbers, TaqMan® Gene Exp Assay from Life Technologies/ThermoFisher are listed as follows: STAT1 Hs01013989_m1, STAT6 Hs00598625_m1, PGK1 Hs99999906_m1. The ΔCT of non-diseased controls was subtracted from the ΔCT of sIBM patients muscles to determine the differences (ΔΔCT) and fold change ($2^{\wedge} - \Delta\Delta CT$) of gene expression. Gene expression was illustrated by the log10 of fold change values compared to NDCs.

Statistical Analysis

Statistical analysis of proteomic data has been carried out as described previously (14). Kruskal-Wallis one-way ANOVA followed by Bonferroni-Dunn correction of the *post hoc* tests was used to analyze quantitative differences of mRNA transcripts. Data are presented as mean ± SEM. The level of significance was set at $P < 0.05$. GraphPad Prism 5.02 software (GraphPad Software, Inc., La Jolla, CA, USA) was used for statistical analysis.

RESULTS

Proteomic Signature: CD74, CD163, and STAT1 Are Highly Expressed in Skeletal Muscle Biopsies of sIBM Patients

Since the precise pathogenesis of IBM is still unclear, we aimed to analyze the proteomic signature via label-free profiling as an unbiased approach to gather new relevant molecules that might play decisive roles in the disease pathogenesis. The proteomic analysis unraveled that CD74 (6.7-fold; $\log_2$-ratio), STAT1 (5-fold; $\log_2$-ratio), and CD163 (4.8-fold; $\log_2$-ratio) are among the highly expressed proteins in skeletal muscle specimens derived from sIBM patients (**Figure 1A**). *In silico* studies (proteomap: https://www.proteomaps.net/) of all proteins altered in abundance (out of 1375 quantified proteins, 24 are statistically significantly decreased and 119 are increased; vulnerability of 10.4% of the investigated proteome) in sIBM-patient derived skeletal muscles, revealed alteration

of biosynthesis, cellular composition, cytoskeleton and altered protein processing (folding, sorting, and degradation) along with vesicular transport. Moreover, the activation of the immune response is a predominating mechanism mirrored by an increase in specific proteins (**Figure 1B**). Remarkably, proteomap-based linking of altered cellular processes to key proteins (taking their fold of regulation into consideration) revealed that CD74 and STAT1 hereby seem to be major molecular "determinators" of modulation of the immune response. Prompted by this finding and by the fact that CD74, STAT1, and CD163 are well-known modulators of interferon-mediated processes (15–21), all up-regulated proteins (total of 119 proteins) were additionally analyzed *in silico* using the "interferome" platform (http://www.interferome.org). This resulted in the identification of a total 46 transcripts corresponding to the proteins up-regulated in the muscle of sIBM patients which are controlled by interferon-modulated processes (**Figure 1C**). Hereby 26 out of the 46 up-regulated transcripts are controlled by both types I and II interferon and four proteins by types I, II, and III. Five transcripts are controlled either by type 1 interferons while eleven are by type 2 interferons (**Figure 1C**). An additional analysis of the interferon-pathway controlled proteins via the "cytoscape" platform (https://cytoscape.org/) confirmed a functional interdependence of these proteins (**Figure 1D**), thus suggesting a functional relevance in sIBM-pathogenesis.

A further STRING analysis (https://string-db.org) toward the identification of functional protein-protein networks confirmed the functional interplay of the proteins encoded by these transcripts (**Figure 1D**), suggesting a fundamental role of interferon-modulated processes in the etiopathology of sIBM. An individual STRING analysis of CD74, STAT1, and CD163 confirmed a functional link of these immune-response proteins to a variety of interferon-induced proteins (**Figure 1E**).

Based on the dense networks of predicted functional protein-protein interplays, we evaluated the potential reaction partners and hence decided to focus on some key players for further studies. The selected key players are MIF—Macrophage migration inhibitory factor, involved in the interferon type response and showing a functional interplay with CD74 (**Figure 1E**) as well as ISG15, which was not upregulated in our analyses, but represents a well-known partner (22) for e.g., STATs, JAKs and IL-6, which are all found in our STRING analysis (**Figure 1E**). Both of these molecules showed an increased immunoreactivity within macrophages in sIBM-patient derived muscle biopsy specimens, thus supporting the concept of the involvement of different types of interferon-mediated downstream intracellular activation programs in macrophages. The concept of a particular role of macrophage-mediated interferon response in sIBM is not only further supported by increased abundance of Macrophage-capping protein (CAPG; identified via proteomic profiling; **Table 2**), but also by the identification of increased immunoreactivity of additional key players such as Siglec1 and CD68 within macrophages in sIBM muscle (see below), adding additional markers to the subsequent analyses.

TABLE 1 | Summarized clinical information of all IBM patients included in the study.

Patient No.	Age	Sex	Duration of disease (years)	Muscle symptoms
sIBM1	72	M	?	Symmetric LL prox. and distal paresis, CK 3-fold elevated
sIBM2	78	F	3	Prox. LL and paresis of finger flexors, CK 2-fold elevated
sIBM3	64	M	2	Prox. tetraparesis and paresis of distal forearms, CK 2-fold elevated
sIBM4	68	F	3	Chronic progressive tetraparesis, significant muscle atrophy
sIBM5	66	M	5	Prox. paresis LL, significant atrophy of vastus lateralis
sIBM6	75	F	?	Prox. paresis LL and distal paresis UL, CK 6-fold elevated
sIBM7	64	M	?	Prox. paresis and distal paresis of fingers
sIBM8	75	M	2	Prox. progressive paresis LL and exercise induced pain, CK 3-fold elevated
sIBM9	66	M	?	Dysphagia, distal and proximal tetraparesis, CK 1.5-fold elevated
sIBM10	79	F	11	Prox. tetraparesis, progressive muscle atrophy
sIBM11	76	M	>2	Muscle pain, proximal weakness, muscle atrophy, CK normal
sIBM12	72	F	7	Prox. tetraparesis, muscle atrophy
sIBM13	71	M	?	Prox. tetraparesis

Cellular Localization of CD74, CD163, and STAT1 in Skeletal Muscle Biopsies From sIBM Patients

To verify the *in silico* results and the respective increased expression of CD74, CD163, and STAT1 in sIBM muscle biopsies, we stained sections of muscle biopsy specimens in a larger cohort of sIBM patients ($n = 13$). In sIBM patients' skeletal muscle biopsies, CD74 mostly stained endomysial macrophages (**Figure 2A**). CD163 highlighted macrophages in the endomysium but was not positive on the sarcolemma of the myofibres (**Figure 2B**). STAT1 was expressed in macrophages in active myophagocytosis but not in the endo- and perimysium, independently of macrophages. STAT1 antibodies did not stain the sarcolemma of myofibers (**Figure 2C**). In summary and on a descriptive first approach, all three molecules are detectable on a variety of macrophages in the endomysium or in myophagocytosis.

Significance of CD74, CD163, and STAT1 to Immunological Processes in Skeletal Muscle of sIBM Patients

To expand these descriptive findings and to further implement functional association of the above-mentioned quantitatively and qualitatively highly relevant proteins, we analyzed

additional proteins which are predicted to interact with those *in situ* and studied co-expression of several markers by immunofluorescence. CD74 stained some muscle fibers sarcolemmaly and co-localized with $CD68^+$ macrophages (**Figure 3A**), as well as with sarcolemmal MHC class II immunoreactivity (**Figure 3B**). On the contrary, the macrophage migration inhibitory factor MIF did not co-stain with CD74 (**Figure 3C**). Furthermore, our immunostaining studies revealed that many $CD163^+$ macrophages co-stained with Siglec1 (CD169) in the endomysium (**Figure 3D**).

In addition, $Siglec1^+$ macrophages expressed the transcription factor STAT1 in active myophagocytic clusters (**Figure 4A**), while STAT6 was expressed endomysially (**Figure 4B**), demonstrating the involvement of different yet complementary immune mechanisms in the course of sIBM-associated muscle inflammation. Importantly, both markers were also significantly elevated on the transcript level in skeletal muscle biopsies of sIBM patients as compared to NDCs (**Figure 4E**), with gene expression of *STAT1* being elevated around 15-fold, and of *STAT6* around 4,5-fold. Of note, activated MHC class II^+ macrophages strongly co-stained with key proteins of the type I interferon pathway such as IRG8 and ISG15 (**Figures 4C,D** and **Table 2**).

DISCUSSION

In the present study, data from unbiased proteomic analysis highlighted the presence of certain proteins playing decisive roles in immune response to be highly abundant in sIBM patients' skeletal muscle biopsies. *In silico* analyses and subsequent morphological studies in skeletal muscle revealed their key characteristics in pathways driving specific macrophage responses. Along this line, $Siglec1^+$ $CD163^+$ and $Siglec1^+$ $STAT1^+$ macrophages were identified. Furthermore, MHC class II^+ macrophages co-expressed ISG15 and IRF8 in patient-derived muscles highlighting a tight bond between these activated macrophages and the type I and type II interferon responses. Additionally, MHC class II^+ macrophages and the sarcoplasm of adjacent muscle fibers expressed CD74.

These findings have important implications for the current understanding of the role of specifically activated macrophages in the pathogenesis of sIBM. Several ways of addressing the activation of macrophages *in vivo* and *in vitro* by using targeted and unbiased approaches notoriously exist (13, 23–27). Flexible states of macrophage activation have been found to occur according to their vast duties in physiology and pathophysiology of different diseases, specifically in chronic inflammatory and fibrotic diseases (24, 28–31). In sIBM, the vast majority of studies focusing on the immune-system have addressed the adverse effects of systemic T cell function and dysfunction or T cell dysfunction within the muscle itself (1, 5, 32–38). In contrast, only few studies have had a broader approach in tackling additional aspects of the immune response (48, 49) or genetic factors influencing the pathogenesis such as the *SQSTM1* or *VCP* variants (39). Proteomic analysis has recently helped to decipher new and unexpected molecules involved in the pathophysiology of sIBM such as FYCO1 and its role in autophagy or the composition of protein aggregates in rimmed vacuoles (40). While the latter studies have focused on the elucidation of vacuole pathophysiology, in the present study we have used the whole protein extracts of skeletal muscle biopsies to obtain molecular information about the entire tissue, and thus, to gain a better and unbiased understanding of the etiology of the disease. This approach revealed that CD74, CD163 and STAT1, driving inflammatory responses, were at the forefront of the highly expressed proteins within the diseased skeletal muscle tissue. This finding accords with our hypothesis of a major role for molecules driving macrophage polarization since sIBM biopsies feature very strong immunity-related aspects over all with macrophages being by far the most abundant cell type in the lesion. Hence, we were able to characterize the immunity of these macrophages in more detail and found molecules identified by proteomic analysis and subsequently verified by immunohistochemistry in biopsies which are strongly related to type I/II interferon responses, specifically IRF8, ISG15, GBP1, GBP1P1, HLA-DOB, IFIT3, STAT1, TAP2. Since macrophages can adopt a great variety of functional states (24, 31, 41, 42), it was not surprising to identify a further important subgroup consisting of $STAT1^+Siglec1^+$ macrophages in active myophagocytosis. This type of macrophages is implicated in acute clearance of necrotic muscle fibers, a process which, despite the explicitly chronic character of the disease (active over decades), is a constant muscle biopsy feature. Of note, we also identified $STAT6^+Siglec1^+$ macrophages in the endomysium at distance of myophagocytic and necrotic fibers, highlighting that both downstream transcription factors may become activated in certain macrophages, which have then different duties and fates. A specific immune phenotype of Caucasian sIBM patients with HLA-A3 suggesting MHC class I activation has been described (43), MHC class II staining patterns were recently described for sIBM patients in comparison to dermatomyositis and anti-synthetase syndrome-associated myositis (44). This finding is in keeping with our proteomic identification of elevated CD74, as a protein regularly interacting with MHC class II molecules. Our findings also indicate that macrophages (which are mentioned as being the most abundant mononuclear inflammatory cells in skeletal muscle biopsies of sIBM patients) have been underestimated as cellular key players in the etiopathology of sIBM. The second relevant finding of this study, is the type I and type II interferon response identified both by proteomic profiling, subsequent *in silico* studies, and immunohistochemistry, expanding previous data where the interferon signature genes have been addressed by transcriptomics (45). Notably, the signatures of type I and type II Interferons, identified here, differ from the ones that have been described to be crucial in dermatomyositis (45–47). Herewith, the relevant role of macrophages as versatile multifunctional immune cells playing a decisive role in the etiopathology of sIBM was shown. These findings may define a molecular starting

TABLE 2 | List of proteins altered in abundance and controlled by interferon-mediated processes (based on "Interferome" database).

Acces-sion #	Peptide count/unique peptides	Anova (p)	Description	Gene Symbol	Ensembl ID	Fold of regu-lation [log2]
UPREGULATED PROTEINS						
Q99972	1/1	0.04	Myocilin	*MYOC*	ENSG00000034971	6.49
P15153	1/1	<0.0005	Ras-related C3 botulinum toxin substrate 2	*RAC2*	ENSG00000128340	5.21
P42224	9/9	0.01	Signal transducer and activator of transcription 1-alpha/beta	*STAT1*	ENSG00000115415	4.99
Q14764	8/8	<0.0005	Major vault protein	*MVP*	ENSG00000013364	4.66
Q9UJU6	1/1	<0.0005	Drebrin-like protein	*DBNL*	ENSG00000136279	4.60
P08754	1/1	0.01	Guanine nucleotide-binding protein G(k) subunit alpha	*GNAI3*	ENSG00000065135	4.44
P33241	1/1	0.02	Lymphocyte-specific protein 1	*LSP1*	ENSG00000130592	4.29
Q03519	1/1	0.01	Antigen peptide transporter 2	*TAP2*	ENSG00000204267 ENSG00000250264	3.95
O95865	2/2	<0.0005	N(G),N(G)-dimethylarginine dimethylaminohydro-lase 2	*DDAH2*	ENSG00000213722	3.89
P32455	4/3	0.03	Interferon-induced guanylate-binding protein 1	*GBP1*	ENSG00000117228 ENSG00000225492	3.72
Q9UKY7	1/1	<0.0005	Protein CDV3 homolog	*CDV3*	ENSG00000091527	3.65
O14879	1/1	0.03	Interferon-induced protein with tetratricopeptide repeats 3	*IFIT3*	ENSG00000119917	3.58
Q9UHD8	4/3	<0.0005	Septin-9	*SEPT9*	ENSG00000184640 ENSG00000261843	3.58
Q14203	3/3	<0.0005	Dynactin subunit 1	*DCTN1*	ENSG00000204843	3.46
P49756	1/1	<0.0005	RNA-binding protein 25	*RBM25*	ENSG00000119707	3.32
Q9Y3B3	1/1	0.01	Transmembrane emp24 domain-containing protein 7	*TMED7*	ENSG00000134970	3.19
P78559	1/1	0.02	Microtubule-associated protein 1A	*MAP1A*	ENSG00000166963	3.16
Q14980	1/1	0.02	Nuclear mitotic apparatus protein 1	*NUMA1*	ENSG00000137497	3.12
P35580	9/4	0.04	Myosin-10	*MYH10*	ENSG00000133026	2.91
P23142	3/3	0.02	Fibulin-1	*FBLN1*	ENSG00000077942	2.87
Q13033	1/1	0.01	Striatin-3	*STRN3*	ENSG00000196792	2.79
O75534	1/1	0.03	Cold shock domain-containing protein E1	*CSDE1*	ENSG00000009307	2.77
Q99536	4/4	<0.0005	Synaptic vesicle membrane protein VAT-1 homolog	*VAT1*	ENSG00000108828	2.77
Q9BSJ8	6/6	<0.0005	Extended synaptotagmin-1	*ESYT1*	ENSG00000139641	2.76
P62070	1/1	<0.0005	Ras-related protein R-Ras2	*RRAS2*	ENSG00000133818	2.75
Q07065	2/2	0.01	Cytoskeleton-associated protein 4	*CKAP4*	ENSG00000136026	2.75
Q9Y696	4/4	0.01	Chloride intracellular channel protein 4	*CLIC4*	ENSG00000169504	2.75
O60240	9/8	0.05	Perilipin-1	*PLIN1*	ENSG00000166819	2.73
P32456	3/2	0.01	Interferon-induced guanylate-binding protein 2	*GBP2*	ENSG00000162645	2.72
Q15075	4/3	0.02	Early endosome antigen 1	*EEA1*	ENSG00000102189	2.72
P04275	5/5	<0.0005	von Willebrand factor	*VWF*	ENSG00000110799	2.71
P04083	9/8	<0.0005	Annexin A1	*ANXA1*	ENSG00000135046	2.70
P51911	2/2	0.01	Calponin-1	*CNN1*	ENSG00000130176	2.66
Q9Y4L1	2/2	0.04	Hypoxia up-regulated protein 1	*HYOU1*	ENSG00000149428	2.61
P09936	5/4	0.02	Ubiquitin carboxyl-terminal hydrolase isozyme L1	*UCHL1*	ENSG00000154277	2.57
P16070	1/1	<0.0005	CD44 antigen	*CD44*	ENSG00000026508	2.52

(Continued)

TABLE 2 | Continued

Acces-sion #	Peptide count/unique peptides	Anova (p)	Description	Gene Symbol	Ensembl ID	Fold of regu-lation [log2]
DOWNREGULATED PROTEINS						
P02585	9/9	0.01	Troponin C, skeletal muscle	*TNNC2*	ENSG00000101470	−2.25
P48788	12/12	0.01	Troponin I, fast skeletal muscle	*TNNI2*	ENSG00000130598	−2.21
P45378	21/20	0.01	Troponin T, fast skeletal muscle	*TNNT3*	ENSG00000130595	−2.19
P16219	5/5	0.02	Short-chain specific acyl-CoA dehydrogenase, mitochondrial	*ACADS*	ENSG00000122971	−1.83
P30711	3/2	0.01	Glutathione S-transferase theta-1	*GSTT1*	ENSG00000184674	−1.37
Q12797	1/1	0.01	Aspartyl/asparaginyl beta-hydroxylase	*ASPH*	ENSG00000198363	−1.11
P11217	55/42	0.01	Glycogen phosphorylase, muscle form	*PYGM*	ENSG00000068976	−1.10
Q8N335	8/7	0.01	Glycerol-3-phosphate dehydrogenase 1-like protein	*GPD1L*	ENSG00000152642	−1.10

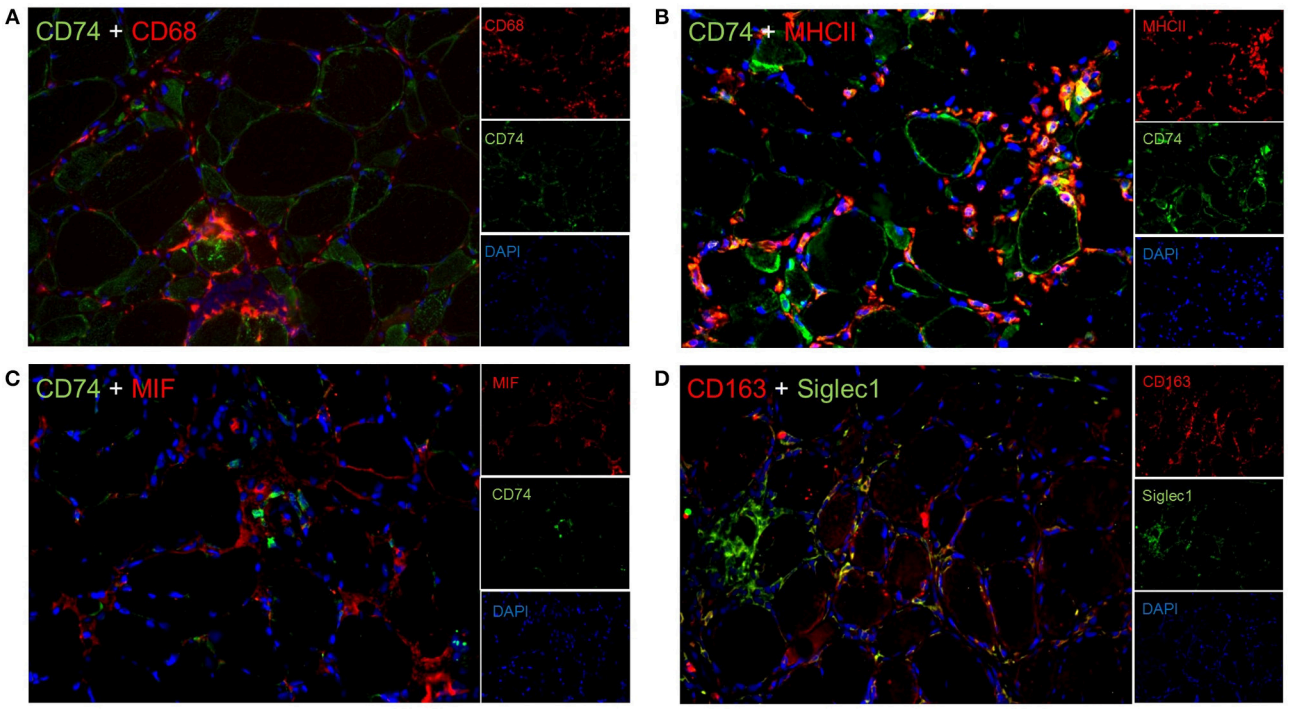


FIGURE 3 | Double immunflorescent staining reveal functional interactions in sIBM patients' muscle tissue. Co-staining of various proteins revealed that CD74 co-labels with CD68+ macrophages **(A)**, and MHC class II **(B)**, but not with the macrophage migration inhibitory factor MIF **(C)**. In addition, $CD163^{+}$ macrophages partially co-express Siglec1 **(D)**.

point for future therapeutic approaches in sIBM utilizing JAK-STAT inhibitors.

SUMMARY

In summary, we demonstrate that unbiased proteomic profiling of skeletal muscle biopsies provides important insights into the molecular etiology of a disease and more precisely in the context of sIBM revealed proteins prominently involved in immunity and characterizing a pattern of macrophage activation. Application of immunohistochemical verification and analysis of these cells in the context of the type I and type II interferon signature *in situ* allowed the attribution of these proteins to specific functional states of

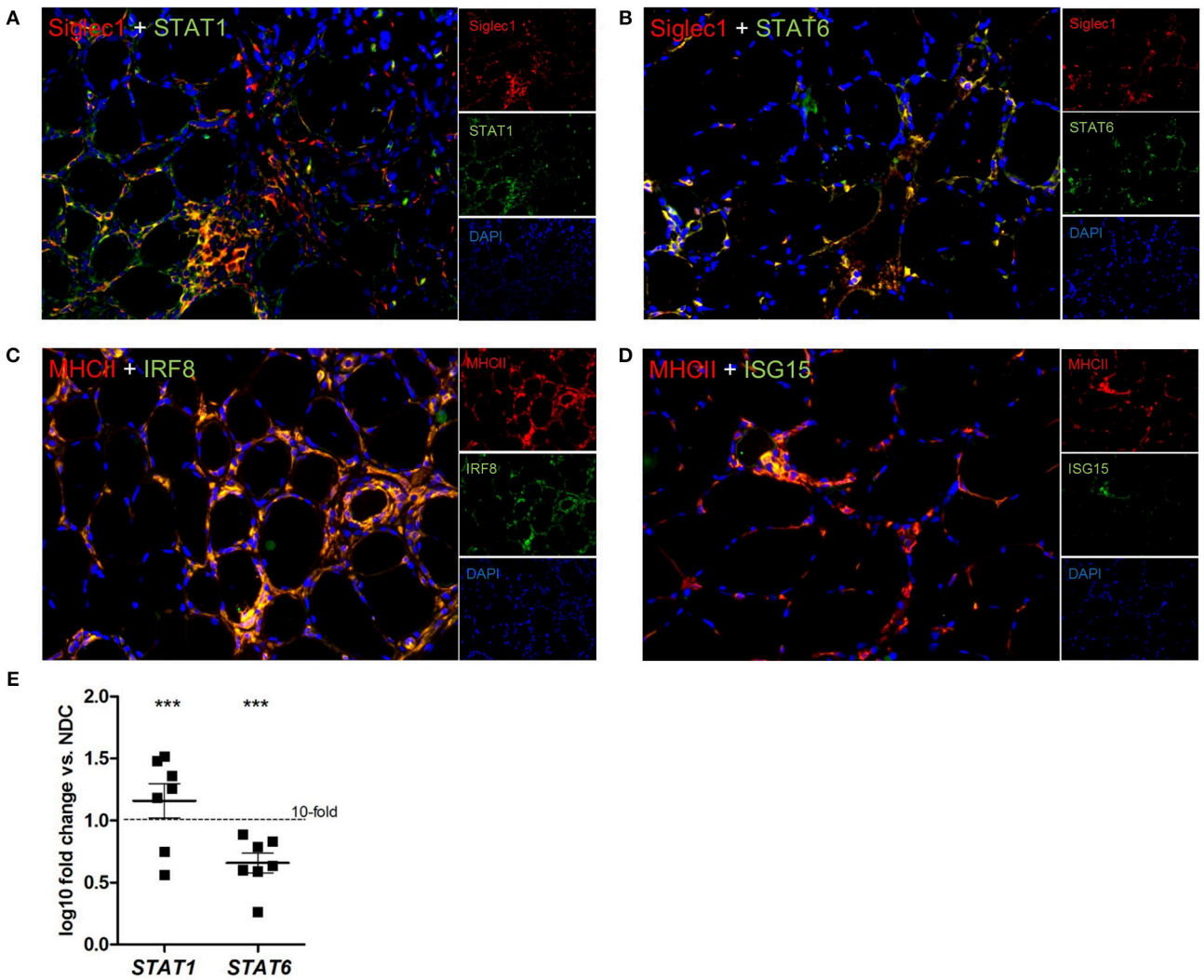


FIGURE 4 | different subforms of macrophages, as well as type I interferon pathways are found in sIBM. We could demonstrate Siglec1+ macrophages, which express STAT1 **(A)**, or STAT6 **(B)**, hinting at involvement of different macrophage subtypes in sIBM muscle inflammation. The activation of STAT1 and STAT6 could also be demonstrated by significantly elevated gene expression levels **(E)**, $p < 0.01$. MHC class II+ macrophages also clearly co-stained with key proteins of the type I interferon pathway like IRF8 **(C)** and ISG15 **(D)**.

macrophage activation. Hence, we show that several different types of macrophages are actively affecting the immune response in sIBM, via a prominent type I interferon signature among others.

ETHICS STATEMENT

This study was carried out in accordance with the recommendations of Charité ethics committee with written informed consent from all subjects. All subjects gave written informed consent in accordance with the Declaration of Helsinki. The protocol was approved by the Charité ethics committee. No. EA2/163/17.

AUTHOR CONTRIBUTIONS

AR and CP: design of the study, acquisition, analysis and interpretation of data, as well as drafting the manuscript. DH: acquisition and analysis of data, as well as revising the manuscript. H-HG: design of the study and revising the manuscript. WS: design of the study, interpretation of data, as well as drafting the manuscript.

ACKNOWLEDGMENTS

The authors thank Petra Matylewski for technical assistance. This work was supported by a grant from the Deutsche

Gesellschaft für Muskelkranke (to AR). Moreover, financial support by the French Muscular Dystrophy Association (AFM-Téléthon; grant 21466 to AR) and the Ministerium für Innovation, Wissenschaft und Forschung des Landes Nordrhein-Westfalen, the Senatsverwaltung für Wirtschaft, Technologie und Forschung des Landes Berlin and the Bundesministerium für Bildung und Forschung is gratefully acknowledged.

REFERENCES

1. Benveniste O, Stenzel W, Hilton-Jones D, Sandri M, Boyer O, Van Engelen BGM. Amyloid deposits and inflammatory infiltrates in sporadic inclusion body myositis: the inflammatory egg comes before the degenerative chicken. *Acta Neuropathol.* (2015) 611–24. doi: 10.1007/s00401-015-1384-5
2. De Bleecker JL, Lundberg IE, De Visser M. 193rd ENMC international workshop pathology diagnosis of idiopathic inflammatory myopathies 30 November - 2 December 2012, Naarden, The Netherlands. *Neuromusc Dis.* (2013) 23:945–51. doi: 10.1016/j.nmd.2013.07.007
3. Brady S, Squier W, Hilton-Jones D. Clinical assessment determines the diagnosis of inclusion body myositis independently of pathological features. *J Neurol Neurosurg Psychiatry*. (2013) 84:1240–6. doi: 10.1136/jnnp-2013-305690
4. Dimachkie MM. Idiopathic inflammatory myopathies. *J Neuroimmunol.* (2011) 231:32–42. doi: 10.1016/j.jneuroim.2010.10.013
5. Benveniste O, Guiguet M, Freebody J, Dubourg O, Squier W, Maisonobe T, et al. Long-term observational study of sporadic inclusion body myositis. *Brain*. (2011) 134:3176–84. doi: 10.1093/brain/awr213
6. Lloyd TE, Mammen AL, Amato AA, Weiss MD, Needham M, Greenberg SA. Evaluation and construction of diagnostic criteria for inclusion body myositis. *Neurology*. (2014) 83:426–33. doi: 10.1212/WNL.0000000000000642
7. Larman HB, Salajegheh M, Nazareno R, Lam T, Sauld J, Steen H, et al. Cytosolic 5′-nucleotidase 1A autoimmunity in sporadic inclusion body myositis. *Ann Neurol.* (2013) 73:408–18. doi: 10.1002/ana.23840
8. Pluk H, van Hoeve BJ, van Dooren SH, Stammen-Vogelzangs J, van der Heijden A, Schelhaas HJ, et al. Autoantibodies to cytosolic 5′-nucleotidase 1A in inclusion body myositis. *Ann Neurol.* (2013) 73:397–407. doi: 10.1002/ana.23822
9. Goyal NA, Cash TM, Alam U, Enam S, Tierney P, Araujo N, et al. Seropositivity for NT5c1A antibody in sporadic inclusion body myositis predicts more severe motor, bulbar and respiratory involvement. *J Neurol Neurosurg Psychiatry*. (2016) 87:373–8. doi: 10.1136/jnnp-2014-310008
10. Benveniste O, Hogrel JY, Annoussamy M, Bachasson D, Rigolet A, Servais L, et al. Rapamycin vs. placebo for the treatment of inclusion body myositis: improvement of the 6 min walking distance, a functional scale, the FVC and muscle quantitative, M. R. I. *Arthr Rheumatol.* (2017) 58:375–6. doi: 10.1093/rheumatology/key043
11. González Coraspe JA, Weis J, Anderson ME, Münchberg U, Lorenz K, Buchkremer S, et al. Biochemical and pathological changes result from mutated caveolin-3 in muscle. *Skeletal Muscle.* (2018) 8:28. doi: 10.1186/s13395-018-0173-y
12. Rose MR, ENMC IBM Working Group. 188th ENMC international workshop: inclusion body myositis, 2-4 December 2011, Naarden, The Netherlands. *Neuromuscul Disord.* (2013) 23:1044–55. doi: 10.1016/j.nmd.2013.08.007
13. Preuße C, Allenbach Y, Hoffmann O, Goebel HH, Pehl D, Radke J, et al. Differential roles of hypoxia and innate immunity in juvenile and adult dermatomyositis. *Acta Neuropathol Commun.* (2016) 4:45. doi: 10.1186/s40478-016-0308-5
14. Ladislau L, Suárez-Calvet X, Toquet S, Landon-Cardinal O, Amelin D, Depp M, et al. JAK inhibitor improves type i interferon induced damage: proof of concept in dermatomyositis. *Brain.* (2018) 141:1609–21. doi: 10.1093/brain/awy105
15. Moeller JB, Nielsen MJ, Reichhardt MP, Schlosser A, Sorensen GL, Nielsen O, et al. CD163-L1 is an endocytic macrophage protein strongly regulated by mediators in the inflammatory response. *J Immunol.* (2012) 188:2399–409. doi: 10.4049/jimmunol.1103150
16. van de Garde MD, Martinez FO, Melgert BN, Hylkema MN, Jonkers RE, Hamann J. Chronic Exposure to glucocorticoids shapes gene expression and modulates innate and adaptive activation pathways in macrophages with distinct changes in leukocyte attraction. *J Immunol.* (2014) 192:1196–208. doi: 10.4049/jimmunol.1302138
17. Gutiérrez-González A, Martínez-Moreno M, Samaniego R, Arellano-Sánchez N, Salinas-Muñoz L, Relloso M, et al. Evaluation of the potential therapeutic benefits of macrophage reprogramming in multiple myeloma. *Blood*. (2016) 128:2241–52. doi: 10.1182/blood-2016-01-695395
18. Court M, Petre G, Atifi MEL, Millet A. Proteomic signature reveals modulation of human macrophage polarization and functions under differing environmental oxygen conditions. *Mol Cell Proteom.* (2017) 16:2153–68. doi: 10.1074/mcp.RA117.000082
19. Tanese K, Hashimoto Y, Berkova Z, Wang Y, Samaniego F, Lee JE, et al. Erratum: cell surface CD74-MIF interactions drive melanoma survival in response to interferon-γ. *J Invest Dermatol.* (2015) 135:2775–84. doi: 10.1038/jid.2015.204
20. Chmielewski S, Olejnik A, Sikorski K, Pelisek J, Błaszczyk K, Aoqui C, et al. STAT1-Dependent signal integration between IFNγ and TLR4 in vascular cells reflect pro-atherogenic responses in human atherosclerosis. *PLoS ONE.* (2014) 9:e113318. doi: 10.1371/journal.pone.0113318
21. Buechler C, Ritter M, Orsó E, Langmann T, Klucken J, Schmitz G. Regulation of scavenger receptor CD163 expression in human monocytes and macrophages by pro- and antiinflammatory stimuli. *J Leukocyte Biol.* (2000) 67:97–103. doi: 10.1002/jlb.67.1.97
22. Chairatvit K, Wongnoppavich A, Choonate, S. Up-regulation of interferon-stimulated gene15 and its conjugates by tumor necrosis factor-α via type I interferon-dependent and -independent pathways. *Mol Cell Biochem.* (2012) 368:195–201. doi: 10.1007/s11010-012-1360-5
23. Pesce JT, Ramalingam TR, Mentink-Kane MM, Wilson MS, El Kasmi KC, Smith AM, et al. Arginase-1-expressing macrophages suppress Th2 cytokine-driven inflammation and fibrosis. *PLoS Pathogens*. (2009) 5:e1000371. doi: 10.1371/journal.ppat.1000371
24. Ginhoux F, Schultze JL, Murray PJ, Ochando J, Biswas SK. New insights into the multidimensional concept of macrophage ontogeny, activation and function. *Nat Immunol.* (2015) 17:34–40. doi: 10.1038/ni.3324
25. Preuße C, Goebel HH, Held J, Wengert O, Scheibe F, Irlbacher K, et al. Immune-mediated necrotizing myopathy is characterized by a specific th1-m1 polarized immune profile. *Am J Pathol.* (2012) 181:2161–71. doi: 10.1016/j.ajpath.2012.08.033
26. Stenzel W, Preuße C, Allenbach Y, Pehl D, Junckerstorff R, Heppner FL, et al. Nuclear actin aggregation is a hallmark of anti-synthetase syndrome-induced dysimmune myopathy. *Neurology*. (2015) 84:1346–54. doi: 10.1212/WNL.0000000000001422
27. Schultze JL, Schmieder A, Goerdt S. Macrophage activation in human diseases. *Sem Immunol.* (2015) 27:249–56. doi: 10.1016/j.smim.2015.07.003
28. Villalta SA, Nguyen HX, Deng B, Gotoh T, Tidball JG. Shifts in macrophage phenotypes and macrophage competition for arginine metabolism affect the severity of muscle pathology in muscular dystrophy. *Hum Mol Genet.* (2009) 18:482–96. doi: 10.1093/hmg/ddn376
29. Tidball JG, Villalta SA. Regulatory interactions between muscle and the immune system during muscle regeneration. *Am J Physiol Regul Integr Comp Physiol.* (2010) 298:R1173–87. doi: 10.1152/ajpregu.00735.2009
30. Wynn TA. Fibrotic disease and the T(H)1/T(H)2 Paradigm. *Nat Rev Immunol.* (2004) 4:583–94. doi: 10.1038/nri1412
31. Murray PJ, Wynn TA. Obstacles and opportunities for understanding macrophage polarization. *J Leukocyte Biol.* (2011) 89:557–63. doi: 10.1189/jlb.0710409
32. Zajac AJ, Blattman JN, Murali-Krishna K, Sourdive DJ, Suresh M, Altman JD, et al. Viral immune evasion due to persistence of activated

T cells without effector function. *J Exp Med.* (1998) 188:2205–13. doi: 10.1084/jem.188.12.2205
33. Crespo J, Sun H, Welling TH, Tian T, Zou W. T cell anergy, exhaustion, senescence and stemness in the tumor microenvironment. *Curr Opin Immunol.* (2013) 25:214–21. doi: 10.1016/j.dcn.2011.01.002
34. Wherry EJ. T cell exhaustion. *Nat Immunol.* (2017) 12:492–9. doi: 10.1038/ni.2035
35. Ivanidze J, Hoffmann R, Lochmüller H, Engel AG, Hohlfeld R, Dornmair K. inclusion body myositis: laser microdissection reveals differential up-regulation of IFN-γ signaling cascade in attacked versus nonattacked myofibers. *Am J Pathol.* (2011) 179:1347–59. doi: 10.1016/j.ajpath.2011.05.055
36. Allenbach Y, Solly S, Grégoire S, Dubourg O, Salomon B, Butler-Browne G, et al. Role of regulatory T cells in a new mouse model of experimental autoimmune myositis. *Am J Pathol.* (2009) 174:989–98. doi: 10.2353/ajpath.2009.080422
37. Dalakas MC. Polymyoisits, dermatomyositis, and inclusion-body-myositis. *N Engl J Med*. (1991) 325:1487–98.
38. Muth IE, Barthel K, Bähr M, Dalakas MC, Schmidt J. Proinflammatory cell stress in sporadic inclusion body myositis muscle: overexpression of alphab-crystallin is associated with amyloid precursor protein and accumulation of beta-amyloid. *J Neurol Neurosurg Psychiatry*. (2009) 80:1344–9. doi: 10.1136/jnnp.2009.174276
39. Gang Q, Bettencourt C, Machado PM, Brady S, Holton JL, Pittman AM, et al. Rare variants in SQSTM1 and VCP genes and risk of sporadic inclusion body myositis. *Neurobiol Aging.* (2016) 47:218.e1–218.e9. doi: 10.1016/j.neurobiolaging.2016.07.024
40. Güttsches AK, Brady S, Krause K, Maerkens A, Uszkoreit J, Eisenacher M, et al. Proteomics of rimmed vacuoles define new risk allele in inclusion body myositis. *Ann Neurol.* (2017) 81:227–39. doi: 10.1002/ana.24847.
41. Murray PJ, Wynn TA. Protective and pathogenic functions of macrophage subsets. *Nat Rev Immunol.* (2011) 11:723–37. doi: 10.1038/nri3073
42. Schultze JL, Freeman T, Hume DA, Latz E. A transcriptional perspective on human macrophage biology. *Sem Immunol.* (2015) 27:44–50. doi: 10.1016/j.smim.2015.02.001
43. Price P, Santoso L, Mastaglia F, Garlepp M, Kok CC, Allcock R, et al. Two major histocompatibility complex haplotypes influence susceptibility to sporadic inclusion body myositis: critical evaluation of an association with HLA-DR3. *Tissue Antigens*. (2014) 64:575–80. doi: 10.1111/j.1399-0039.2004.00310.x
44. Rigolet M, Hou C, Amer YB, Aouizerate J, Periou B, Gherardi RK, et al. Distinct interferon signatures stratify inflammatory and dysimmune myopathies. *RMD Open*. (2019) 5:10–4. doi: 10.1136/rmdopen-2018-000811
45. Greenberg SA. Dermatomyositis and type 1 interferons. *Curr Rheumatol Rep*. (2011) 12:198–203. doi: 10.1007/s11926-010-0101-6.Dermatomyositis
46. Suárez-Calvet X, Gallardo E, Nogales-Gadea G, Querol L, Navas M, Díaz-Manera J, et al. Altered RIG-I/DDX58-mediated innate immunity in dermatomyositis. *J Pathol.* (2014) 233:258–68. doi: 10.1002/path.4346
47. Greenberg SA, Pinkus JL, Pinkus GS, Burleson T, Sanoudou D, Tawil R, et al. Interferon-alpha/beta-mediated innate immune mechanisms in dermatomyositis. *Ann Neurol.* (2005) 57:664–78. doi: 10.1002/ana.20464
48. De Bleecker JL, De Paepe B, Aronica E, de Visser M, Amato A, Benveniste O, et al. 205th ENMC international workshop: pathology diagnosis of idiopathic inflammatory myopathies part II 28-30 March 2014, Naarden, The Netherlands. *Neuromuscul Disord.* (2015) 25:268–72. doi: 10.1016/j.nmd.2014.12.001
49. Paepe BD, Creus KK, De Bleecker JL. Role of cytokines and chemokines in idiopathic inflammatory myopathies. *Curr Opin Rheumatol.* (2009) 21:610–6. doi: 10.1097/BOR.0b013e3283317b31

Conflict of Interest Statement: The authors declare that the research was conducted in the absence of any commercial or financial relationships that could be construed as a potential conflict of interest.

Copyright © 2019 Roos, Preusse, Hathazi, Goebel and Stenzel. This is an open-access article distributed under the terms of the Creative Commons Attribution License (CC BY). The use, distribution or reproduction in other forums is permitted, provided the original author(s) and the copyright owner(s) are credited and that the original publication in this journal is cited, in accordance with accepted academic practice. No use, distribution or reproduction is permitted which does not comply with these terms.

frontiers in Neurology

ORIGINAL RESEARCH
published: 27 May 2019
doi: 10.3389/fneur.2019.00552

Apolipoprotein E Homozygous ε4 Allele Status: A Deteriorating Effect on Visuospatial Working Memory and Global Brain Structure

Janik Goltermann[1], Ronny Redlich[1], Katharina Dohm[1], Dario Zaremba[1], Jonathan Repple[1], Claas Kaehler[1,2], Dominik Grotegerd[1], Katharina Förster[1], Susanne Meinert[1], Verena Enneking[1], Emily Schlaghecken[1], Lara Fleischer[1], Tim Hahn[1], Harald Kugel[3], Andreas Jansen[4,5,6], Axel Krug[4], Katharina Brosch[4], Igor Nenadic[4], Simon Schmitt[4], Frederike Stein[4], Tina Meller[4], Dilara Yüksel[4], Elena Fischer[4], Marcella Rietschel[7], Stephanie H. Witt[7], Andreas J. Forstner[8,9,10], Markus M. Nöthen[8], Tilo Kircher[4], Anbupalam Thalamuthu[11], Bernhard T. Baune[1,12,13], Udo Dannlowski[1†] and Nils Opel[1†]*

[1] Department of Psychiatry, University of Münster, Münster, Germany, [2] Department of Mathematics and Computer Science, University of Münster, Münster, Germany, [3] Institute of Clinical Radiology, University of Münster, Münster, Germany, [4] Department of Psychiatry, University of Marburg, Marburg, Germany, [5] Core-Facility BrainImaging, Faculty of Medicine, University of Marburg, Marburg, Germany, [6] Center for Mind, Brain and Behavior, University of Marburg, Marburg, Germany, [7] Department of Genetic Epidemiology, Central Institute of Mental Health, University of Heidelberg, Mannheim, Germany, [8] School of Medicine & University Hospital Bonn, Institute of Human Genetics, University of Bonn, Bonn, Germany, [9] Centre for Human Genetics, University of Marburg, Marburg, Germany, [10] Department of Biomedicine, University of Basel, Basel, Switzerland, [11] Centre for Healthy Brain Ageing, School of Psychiatry, University of New South Wales Sydney, Sydney, NSW, Australia, [12] Department of Psychiatry, Melbourne Medical School, The University of Melbourne, Melbourne, VIC, Australia, [13] The Florey Institute of Neuroscience and Mental Health, The University of Melbourne, Parkville, VIC, Australia

OPEN ACCESS

Edited by:
Iliya Lefterov, University of Pittsburgh, United States

Reviewed by:
Dimitrios Kapogiannis, National Institute on Aging (NIA), United States
Jacob Raber, Oregon Health & Science University, United States

***Correspondence:**
Udo Dannlowski
dannlow@uni-muenster.de

†These authors have contributed equally to this work and are senior authors

Specialty section:
This article was submitted to Neurodegeneration, a section of the journal Frontiers in Neurology

Received: 19 November 2018
Accepted: 08 May 2019
Published: 27 May 2019

Citation:
Goltermann J, Redlich R, Dohm K, Zaremba D, Repple J, Kaehler C, Grotegerd D, Förster K, Meinert S, Enneking V, Schlaghecken E, Fleischer L, Hahn T, Kugel H, Jansen A, Krug A, Brosch K, Nenadic I, Schmitt S, Stein F, Meller T, Yüksel D, Fischer E, Rietschel M, Witt SH, Forstner AJ, Nöthen MM, Kircher T, Thalamuthu A, Baune BT, Dannlowski U and Opel N (2019) Apolipoprotein E Homozygous ε4 Allele Status: A Deteriorating Effect on Visuospatial Working Memory and Global Brain Structure. Front. Neurol. 10:552. doi: 10.3389/fneur.2019.00552

Theoretical background: The Apolipoprotein E (APOE) ε4 genotype is known to be one of the strongest single-gene predictors for Alzheimer disease, which is characterized by widespread brain structural degeneration progressing along with cognitive impairment. The ε4 allele status has been associated with brain structural alterations and lower cognitive ability in non-demented subjects. However, it remains unclear to what extent the visuospatial cognitive domain is affected, from what age onward changes are detectable and if alterations may interact with cognitive deficits in major depressive disorder (MDD). The current work investigated the effect of APOE ε4 homozygosity on visuospatial working memory (vWM) capacity, and on hippocampal morphometry. Furthermore, potential moderating roles of age and MDD were assessed.

Methods: A sample of $n = 31$ homozygous ε4 carriers was contrasted with $n = 31$ non-ε4 carriers in a cross-sectional design. The sample consisted of non-demented, young to mid-age participants (mean age = 34.47; $SD = 13.48$; 51.6% female). Among them were $n = 12$ homozygous ε4 carriers and $n = 12$ non-ε4 carriers suffering from MDD (39%). VWM was assessed using the Corsi block-tapping task. Region of interest analyses of hippocampal gray matter density and volume were conducted using voxel-based morphometry (CAT12), and Freesurfer, respectively.

Results: Homozygous ε4 carriers showed significantly lower Corsi span capacity than non-ε4 carriers did, and Corsi span capacity was associated with higher gray matter density of the hippocampus. APOE group differences in hippocampal volume could

be detected but were no longer present when controlling for total intracranial volume. Hippocampal gray matter density did not differ between APOE groups. We did not find any interaction effects of age and MDD diagnosis on hippocampal morphometry.

Conclusion: Our results point toward a negative association of homozygous ε4 allele status with vWM capacity already during mid-adulthood, which emerges independently of MDD diagnosis and age. APOE genotype seems to be associated with global brain structural rather than hippocampus specific alterations in young- to mid-age participants.

Keywords: apolipoprotein E, visuospatial working memory, cognitive deficits, hippocampus, structural MRI, Alzheimer, major depression

INTRODUCTION

Alzheimer disease (AD) is a leading cause of dementia and associated with major cognitive and daily life impairments as well as psychiatric symptoms, such as depressed affect, agitation, and delusions (1). AD is a neurodegenerative disease that can be linked to extensive cerebral atrophy typically affecting structures involved in memory and cognition (2–4). Degenerations caused by AD are typically progressive, and mild cognitive impairment (MCI) can be found years before the outbreak of clinically relevant symptoms and constitutes a risk factor for AD (3). Both MCI and AD have been repeatedly associated with a deterioration of the hippocampus and the entorhinal cortex (4). Evidence from longitudinal studies suggests that these regions are the first to be affected by observable structural alterations in the course of AD (5, 6). Cerebral atrophies in these areas are accompanied by neurocognitive decline in several domains (7) as associative verbal memory (8), visuospatial memory (9, 10), and reasoning (11).

Brain structural changes associated with AD have also been shown to play a role in major depressive disorder (MDD) (12). Furthermore, a lifetime history of MDD poses a risk factor for developing AD later in life (13). However, the exact interplay between AD, MDD and brain structural alterations remains unclear.

The Apolipoprotein E (APOE) genotype is the strongest known single predictor of AD. APOE ε4 allele dose has been associated with higher risk and earlier onset of AD (14, 15). Heterozygous ε4 allele carriers are estimated to have a three-fold, and ε4 homozygotes an eight- to fifteen-fold increased risk to develop AD compared to subjects without an ε4 allele (14, 15). The risk effect of the APOE genotype has been replicated numerous times (16) and there is evidence that it is stronger in female compared to male (17).

The APOE genotype has further been associated with cognitive ability in elderly, non-demented samples. Evidence from studies contrasting healthy ε4 allele carriers with non-ε4 carriers suggests better performance in episodic memory (18, 19), working memory (20) and global cognitive functioning (21) in favor of non-ε4 carriers. However, empirical evidence is inconclusive with a considerable number of contradicting findings (21). Heterogeneity of findings may reflect methodological differences in ε4 allele status categorization (coding of zygosity), in the selection and operationalization of cognitive domains, as well as varying sample characteristics regarding age (21). Strongest effects of the APOE genotype have been found in elderly samples above 60 years and for APOE ε4 homozygotes (21). The role of the APOE status for the visuospatial domain has been discussed particularly controversially. There is some evidence for a visuospatial deficit in non-demented ε4 carriers that are mid-adult age (22) and elderly (23), however with no deficit found in a subgroup of age 80 and older (24). Although most studies investigating the APOE effect on cognition examine elderly samples deteriorating genotype effects on visuospatial performance can also be found in children (25) with some evidence for stronger deficits in girls (26). Contrasting findings exist (19) and a meta-analysis concluded that there is little evidence for group differences for the visuospatial domain between ε4 carriers and non-carriers (21). However, due to insufficient available sample sizes this meta-analysis did not carry out analyses comparing homozygous ε4 carriers with non-ε4 carriers, which might be an important biasing factor.

The effect of APOE status on cognitive ability appears to come along with functional and structural brain alterations. Evidence from an early PET study suggests inhibited glucose metabolism in ε4 homozygotes in temporal, frontal, and parietal regions, as well as the posterior cingulum already in a non-demented mid-elderly sample with normal cognitive functioning (27). Further, findings of hippocampal volume reductions are reported in healthy elderly ε4 homozygotes (28) as well as structural alterations in the temporal lobe in heterozygous ε4 carriers in a sample of healthy adults with a wide range of age (29).

A review (30) and a meta-analysis (31) further support these findings of structural alterations particularly in the hippocampal region in healthy elderly subjects as a function of the APOE genotype. However, evidence seems to be inconclusive regarding the role of heterozygous ε4 carriers as some studies find an ε4 dose effect, some find a similar degree and rate of cerebral atrophy for heterozygotes as for homozygotes while other studies find heterozygotes to be indifferent from non-ε4 carriers in respect to brain structural alterations (30). The degree to which studies differentiate the APOE genotype, and what genotypes are categorized as ε4 carriers vary. This has direct implications for methodological considerations of studies investigating APOE effects in that designs should differentiate ε4 allele dosage.

The evidence for a detrimental effect of the APOE ε4 allele on hippocampal structure as well as on vWM task performance raises the question if the hippocampal region might be the neuronal locus of the APOE genotype affecting the vWM. Although the visuospatial cognitive domain is commonly associated with the frontoparietal network (32) there are also studies linking it to the hippocampus. Performance in the Corsi block tapping task has been shown to be impaired in subjects with lesions in the right temporal lobe (33), and to be associated with augmented activation in the hippocampus in addition to frontoparietal regions (34). Other studies report that lower vWM capacity is associated with structural characteristics of the hippocampus, as lesions (35) and atrophy (36).

Brain structures and cognitive domains affected by the APOE genotype (as outlined above) are also closely related to detrimental processes involved in MDD (37, 38). There are studies linking MDD to a two-fold increased risk of AD (13) as well as at least one study suggesting that APOE genotype moderates this risk (39) and evidence linking APOE genotype to an increased risk for depressive symptoms (40). However, the exact interplay between the APOE gene, MDD, cognitive decline, and AD remain largely unresolved. Taylor et al. (41) investigated a sample containing MDD and healthy subjects and found no differences in various cognitive domains and structural MRI in function of ε4 presence (not differentiating between ε4 zygosities) regardless of diagnosis.

Small sample sizes of homozygous ε4 carriers are a common problem in APOE research due to the rare co-occurrence of two ε4 alleles [prevalence 2.9% (42)]. Only few studies exist that include sufficient sample sizes of ε4 homozygotes and further provide structural brain imaging data, and behavioral cognition measures. Despite the potential importance of MDD for APOE effects even fewer studies include mid-age subjects with MDD subsamples. Most studies including these aspects investigate elderly samples, while not differentiating ε4 zygosity (43, 44). To our knowledge only one study exists that included mid-age MDD subjects, however also not differentiating ε4 zygosity (41). We know of no study that has been published combining structural MRI data, and neuropsychological data in mid-age subjects, that includes homozygous ε4, and MDD subsamples.

The goal of the current work was to investigate the relationship of the APOE genotype with visuospatial working memory (vWM) and brain structural alterations first and foremost in the hippocampus in a young- to mid-age, non-demented sample. Further objectives were to identify potential moderators of these relationships, namely age and MDD diagnosis. Importantly homozygous ε4 carriers were operationalized as the genetic risk group and contrasted with a sample without ε4 allele as the literature outlined above suggests effects of the APOE genotype to be most pronounced for homozygotes. We hypothesized that 1) ε4 homozygotes show on average lower vWM performance compared to non-ε4 carriers, 2) vWM performance correlates positively

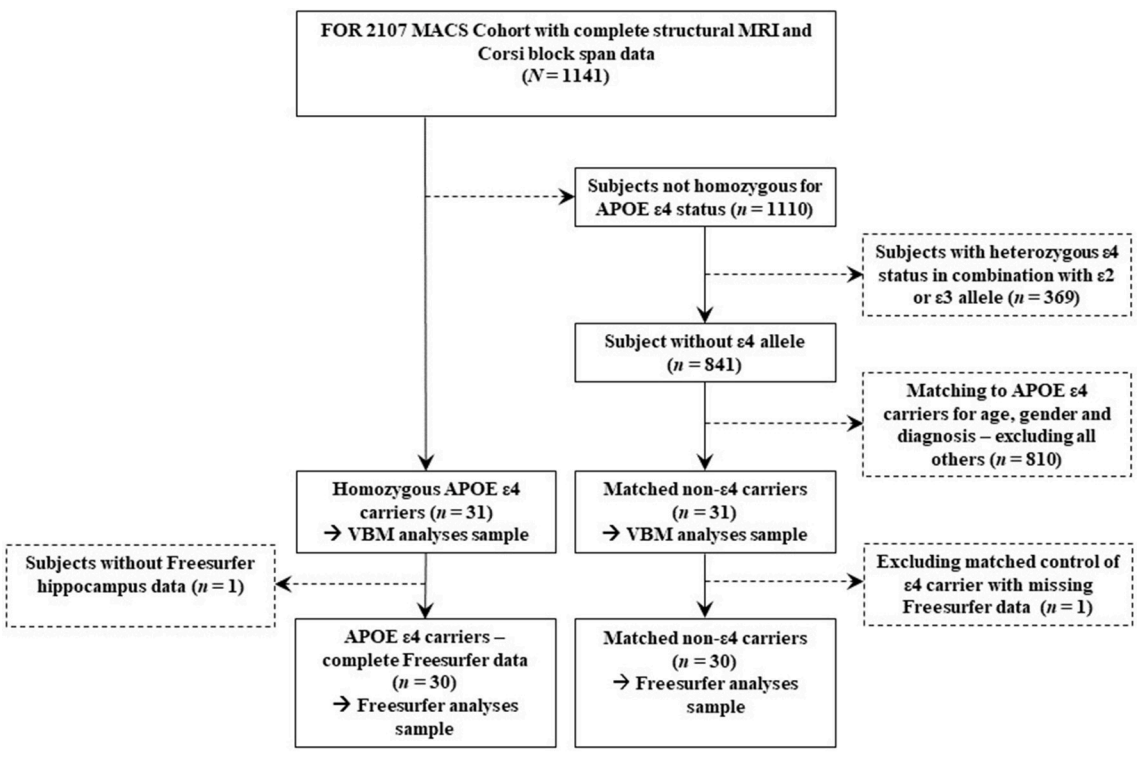


FIGURE 1 | Sample flowchart showing all data exclusion steps for both genotype groups.

with hippocampal volume and gray matter density, and 3) homozygous ε4 carriers exhibit smaller volume and gray matter density in the hippocampal area compared to non-ε4 carriers.

METHODS

Participants

A sample of $N = 1{,}141$ adult subjects with complete cross-sectional MRI and neuropsychological data was available from the FOR2107 Marburg-Münster Affective Cohort Study (MACS) (45) which includes subjects with MDD and healthy control (HC) subjects. Exclusion criteria were any history of neurological (e.g., concussion, stroke, tumor, neuro-inflammatory diseases) and medical (e.g., cancer, chronic inflammatory or autoimmune diseases, heart diseases) conditions as well as substance-related addiction, and MRI contraindications. The study sample was selected based on the genotype of the APOE gene. Within the FOR2107 MACS cohort a study sample of $n = 31$ homozygous ε4 carriers was available which was contrasted with $n = 31$ non-ε4 carriers that were matched for age, sex, and diagnosis. For Freesurfer (FS) analyses a sample of $N = 60$ ($n = 30$ ε4 homozygotes; $n = 30$ matched controls) was available due to missing data for one of the ε4 homozygotes. The sample selection process is depicted in **Figure 1**.

The final sample of $N = 62$ included $n = 24$ MDD patients and $n = 38$ HC subjects. The mean age of the sample was 34.47 ($SD = 13.48$), ranging from 19 to 63 with 51.6% of the sample being female. A more detailed description of the distribution of demographic characteristics can be found in **Table 1**.

Subjects from the MACS cohort were recruited using advertisement in psychiatric hospitals, and outpatient therapeutic offices as well as advertisement in other public places and newspapers. Data were collected at the Departments of Psychiatry either at the University of Marburg or at the University of Münster. Before study participation, all subjects gave written and informed consent. All participants received a financial compensation.

TABLE 1 | Demographic characteristics of the final study sample.

	ε4 homozygotes		Non-ε4 carriers	
	n	Mean age (*SD*)	*n*	Mean age (*SD*)
MDD				
Male	7	41.86 (15.25)	7	41.71 (15.13)
Female	5	35.40 (18.12)	5	35.40 (18.12)
Total	12	39.17 (16.03)	12	39.08 (15.96)
HC				
Male	8	24.50 (2.78)	8	24.50 (2.78)
Female	11	36.64 (12.49)	11	36.64 (12.49)
Total	19	31.53 (11.30)	19	31.53 (11.30)

Materials and Procedure

Neuropsychological Assessment

The Corsi block tapping task (33) was administered in a forward and a backward version. This task is a well-established measure of vWM that has shown to be sensitive for cognitive decline associated with AD (46–48). A mean individual block span capacity was calculated over both version scores regarding a lack of evidence for conceptual differences between both version performances (49).

Clinical Assessment

A structured clinical interview for DSM-IV (SCID-I) was conducted with each participant in order to assess current and lifetime psychopathological diagnoses (50). All subjects allocated to the MDD group in this study either fulfilled the DSM-IV criteria for an acute major depressive episode or had a lifetime history of a major depressive episode. All HC subjects were ensured to be free from presence or any history of psychiatric disorders according to DSM-IV criteria.

Structural Image Acquisition and Processing

T1-weighted high-resolution anatomical images were acquired for all participants. Two MRI scanners were used for data acquisition located at the sites in Marburg and Münster with different hardware and software configurations. In Marburg, a 3T MRI scanner (Tim Trio, Siemens, Erlangen, Germany) was used combined with a 12-channel head matrix Rx-coil. In Münster, data were acquired at a 3T MRI scanner (Prisma, Siemens, Erlangen, Germany) using a 20-channel head matrix Rx-coil. Pulse sequence parameters were standardized across both sites to the extent permitted by each platform. Further details of the imaging procedures and implemented quality assurance protocol have been extensively described elsewhere (51).

Image preprocessing has been conducted using two complementary approaches that have frequently been described in our previous work: voxel-based morphometry (VBM) (52–54) using CAT12 (http://dbm.neuro.uni-jena.de/cat/) and FS (53, 55) based automatic segmentation (Version 5.3) with default parameters (https://surfer.nmr.mgh.harvard.edu/).

CAT12 preprocessing was done using default parameters: Briefly, images were bias-corrected, tissue classified, and normalized to MNI-space using linear (12-parameter affine) and non-linear transformations, within a unified model including high-dimensional DARTEL-normalization. The modulated gray matter images were smoothed with a Gaussian kernel of 8 mm FWHM. Absolute threshold masking with a threshold value of 0.1 was used for all second level analyses as recommended for VBM analyses (http://www.neuro.uni-jena.de/cat/). Image quality was assessed by visual inspection as well as by using the check for homogeneity function implemented in the CAT12 toolbox.

For all analyses using FS based segmentations, volumetric measures of the hippocampal region were used (56). Quality checks of segmentations were done visually and based on a statistical outlier analysis following a standardized protocol provided by the ENIGMA consortium (http://enigma.ini.usc.edu/protocols/imaging-protocols).

Genotyping and Quality Control

DNA was extracted from EDTA blood samples using the chemagic 360 instrument (PerkinElmer, Waltham, MA, USA). Individuals were genotyped using the Infinium PsychArray BeadChip (Illumina, San Diego, CA, USA) and standard protocols. Genotyping was performed at the Institute of Human Genetics, University Hospital Bonn, Germany. Clustering and initial quality control were conducted using GenomeStudio v.2011.1 (Illumina, San Diego, CA, USA) and the Genotyping Module v.1.9.4. Quality control procedures were implemented using PLINK (57) on the FOR2107 dataset. Samples with low genotype rates <95%, sex inconsistencies (X-chromosome heterozygosity), and genetically related individuals were not included in the present study. We also excluded SNPs that had a poor genotyping rate (<95%), strand ambiguity (A/T and C/G SNPs), a minor allele frequency (MAF) <1%, or that showed deviation from Hardy-Weinberg Equilibrium ($p < 10^{-6}$). The quality controlled genotype data was imputed in the Michigan imputation server (https://imputationserver.sph.umich.edu) (58) using the Haplotype Reference Consortium reference panel (v3.20101123). The hard called genotypes for the single nucleotide polymorphisms (SNPs) rs7412 and rs429358 in APOE were extracted from the imputed dosage using PLINK. Both the SNPs were imputed with high accuracy ($R^2 > 0.99$). Participants homozygous for the ε4 allele (ε4/ε4) were contrasted with subjects without an ε4 allele (genotypes ε2/ε2, ε2/ε3, or ε3/ε3).

Statistical Analyses

APOE Status and Visuospatial Working Memory

In order to test our first hypothesis (expecting reduced vWM performance in ε4 homozygotes), APOE genotype was entered as a predicting factor for Corsi block span in a general linear model. Age, sex, and presence of MDD diagnosis were included as covariates in the model.

Visuospatial Working Memory and Hippocampus

The second hypothesis (positive correlation between vWM performance and hippocampus morphometry) was similarly tested using a general linear model. Total intracranial volume (TIV) and scanner site were used as covariates in addition to the covariates age, sex, and MDD diagnosis, while Corsi block span was used as the predictor variable. For this analysis step both (a) FS based analysis using hippocampal volumes as dependent variable (including hippocampal laterality as a within-subject factor in the model) and (b) VBM region of interest analysis of the hippocampus were conducted.

APOE Status and Hippocampus

Identical analyses as for the second hypothesis were used for the investigation of our third hypothesis (negative relationship between homozygous ε4 status and hippocampal morphometry), except that APOE status was used as a predictor instead of Corsi block span. Again the model was used for the prediction of (a) hippocampal volume, and (b) gray matter density (VBM) in two separate analyses in accordance with analyses testing the second hypothesis.

General Aspects and Exploratory Analyses

Generally, all analyses were based on a significance threshold of $p < 0.05$, unless noted differently. However, as all hypotheses were clearly one-sided, halved p-values are reported regarding the main hypotheses (effect of APOE status on vWM, effect of vWM on hippocampal morphometry, and effect of APOE status on hippocampal morphometry) if not specified otherwise. Any interaction terms, and whole brain effects tested for significance were regarded as exploratory and thereby tested two-sided.

VBM analyses were carried out using SPM12 (https://www.fil.ion.ucl.ac.uk/spm/). The hippocampal mask for VBM analyses was created by means of the WFU PickAtlas (59) according to the AAL-Atlas (60) and dilated 2 mm.

To control for multiple comparisons, threshold-free cluster enhancement (TFCE) corrections were applied for all VBM analyses using $N = 1{,}000$ permutations and a cluster size weighting of $E = 0.5$.

All further analyses were conducted with SPSS (version 25.0). Partial η^2 values are reported as effect size measure for significant effects. Reported effect sizes of VBM analyses are based on extracted eigenvariates on cluster level.

RESULTS

APOE Status and Visuospatial Working Memory

In order to test our first hypothesis vWM was predicted with APOE genotype in the above described model. Results yielded a significant main effect of APOE status [$F_{[1,57]} = 6.21$, $p = 0.02$, $\eta^2 = 0.10$] with lower Corsi block span in APOE ε4 carriers. Further, a main effect of diagnosis emerged [$F_{[1,57]} = 4.21$, $p = 0.05$, $\eta^2 = 0.07$] with lower mean block span in MDD subjects. The model yielded no further main effects (all other $p > 0.53$).

When adding an interaction term between APOE status and age it turned out non-significant [$F_{[1,56]} = 0.21$, $p = 0.65$], as was the interaction effect between APOE genotype and sex [$F_{[1,56]} = 2.22$, $p = 0.14$]. Descriptively mean differences as a function of APOE status were more pronounced for MDD compared to HC subjects. However, testing an interaction term between APOE status and diagnosis also yielded a non-significant effect [$F_{[1,5]} = 0.93$, $p = 0.34$]. Mean differences in Corsi span over APOE and diagnosis groups are depicted in **Figure 2**.

Visuospatial Working Memory and Hippocampus

For our second hypothesis the general linear model described above was fitted with Corsi block span predicting hippocampal volume. Results yielded a non-significant effect of block span on FS derived hippocampal volume [$F_{[1,53]} = 0.34$, $p = 0.56$]. The main effect of diagnosis was significant [$F_{[1,53]} = 6.63$, $p = 0.01$, $\eta^2 = 0.11$], with lower hippocampal volume in MDD compared to HC subjects. No significant effect of hippocampal laterality [$F_{[1,53]} = 0.01$, $p = 0.94$], and no other significant main effect of interest was found (all other $p > 0.47$).

When interaction terms were added to the model, results yielded a non-significant interaction effects between Corsi block

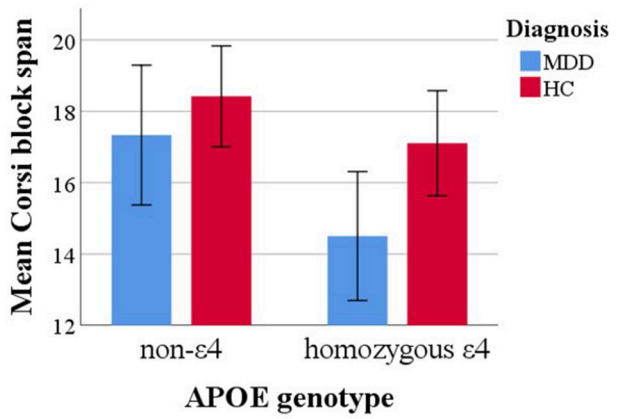


FIGURE 2 | Mean Corsi block span capacity over APOE genotype and diagnosis groups. Error bars represent 95% confidence intervals.

span and age [$F_{[1,52]} = 0.03$, $p = 0.86$], and between Corsi block span and sex [$F_{[1,52]} = 0.69$, $p = 0.41$]. Testing an interaction term between Corsi block span and MDD diagnosis also yielded a non-significant interaction effect [$F_{[1,52]} = 1.76$, $p = 0.19$]. Exploratory analyses revealed that when removing TIV from the model, the main effect of Corsi block span on hippocampal volume becomes significant [$F_{[1,52]} = 3.49$, $p = 0.03$, $\eta^2 = 0.06$]. Further, when substituting hippocampal volume with TIV as the criterion variable the main effect of Corsi block span was significant [$F_{[1,54]} = 5.49$, $p = 0.02$, $\eta^2 = 0.09$], with higher Corsi block span being associated with higher TIV.

In order to further investigate our second hypothesis, model estimation was repeated within a VBM analysis. For the hypothesized main effect of vWM on hippocampal gray matter density the analysis yielded two marginally significant clusters just above a TFCE-corrected significance threshold of $p < 0.05$ (left: $k = 132$, $p = 0.05$, $x = -38$, $y = -28$, $z = -15$, TFCE = 203.05, $\eta^2_{cluster} = 0.18$; right: $k = 50$, $p = 0.07$, $x = 38$, $y = -24$, $z = -18$, TFCE = 181.78, $\eta^2_{cluster} = 0.23$).

Exploratory whole brain analysis for the main effect of vWM revealed three clusters below the exploratory uncorrected threshold of $p < 0.001$ with a minimum cluster size of 20 voxels ($k = 31$, $p < 0.001$, $x = 36$, $y = -14$, $z = -28$; $k = 21$, $p < 0.001$, $x = 38$, $y = -22$, $z = -20$; $k = 20$, $p < 0.001$, $x = -38$, $y = -28$, $z = -15$). Clusters were located in the right parahippocampus, fusiform gyrus, and hippocampus, as well as left temporal inferior and fusiform gyrus, and left hippocampus but not in any other region (see **Figure 3**).

APOE Status and Hippocampus

No significant main effect of APOE status on hippocampal volume using the general linear model outlined above could be detected [$F_{[1,53]} = 0.67$, $p = 0.42$]. However, a significant main effect of MDD diagnosis [$F_{[1,53]} = 7.87$, $p = 0.01$, $\eta^2 = 0.13$] was found, with smaller hippocampal volume in the MDD group compared to the HC group. No within-subject effect of hippocampus laterality [$F_{[1,53]} = 0.33$, $p = 0.57$], and no other main effects of interest emerged (all other $p > 0.41$).

When adding an interaction term between APOE status and age to the model this yielded a non-significant interaction effect [$F_{[1,52]} = 0.12$, $p = 0.73$]. Adding an interaction term between APOE status and sex also yielded a non-significant effect [$F_{[1,52]} = 0.03$, $p = 0.86$]. The interaction between APOE status and diagnosis was also non-significant [$F_{[1,53]} = 0.05$, $p = 0.82$]. Exploratory analyses revealed that when removing TIV from the model, hippocampal volume was significantly predicted by APOE genotype [$F_{[1,54]} = 11.64$, $p = 0.001$, $\eta^2 = 0.18$]. In order to further explore the role of TIV, the same model as described above was applied to predict TIV instead of hippocampal volume in a subsequent analysis. This yielded a significant main effect of APOE status [$F_{[1,54]} = 25.59$, $p < 0.001$, $\eta^2 = 0.32$], with lower mean TIV in ε4 homozygotes. Mean TIV and hippocampal volume over APOE genotype is depicted in **Figure 4**.

VBM model estimation yielded no clusters beyond significance threshold for the APOE genotype contrast at a TFCE-corrected significance level of $p < 0.05$. Exploratory whole brain VBM analysis using the same model yielded eight clusters beyond an exploratory uncorrected threshold of $p < 0.001$ and a minimum cluster size of 20 voxels (see **Table 2**). No clusters remained significant when applying TFCE corrections on whole brain level. When using the exploratory uncorrected threshold at $p < 0.001$ with a minimum cluster size of 20 voxels no clusters emerged for the inverted contrast of greater gray matter density in the ε4 homozygotes on whole brain level.

DISCUSSION

The main finding of the present study is that APOE ε4 homozygosity is associated with lower vWM ability already in young to mid-age, non-demented subjects. Effect size estimates indicate a medium sized effect. This effect seems to be age-independent within the age range of our sample (19–63 years) and is of comparable magnitude in the MDD subsample as in the HC sample. Similarly, we found lower vWM capacity in people with MDD diagnosis compared to HC subjects. Although some evidence was found that hippocampal gray matter density was associated with vWM, no specific relationship was detected between vWM and hippocampal volume when including TIV as a covariate. Furthermore, both measures of hippocampal structure (gray matter density and volume) did not significantly differ between genotypes in our sample when controlling for global brain structural measures. In addition, a specific effect of MDD diagnosis on hippocampal volume was found which appeared to be independent from APOE genotype.

Previous work investigating the influence of APOE genotype on cognitive abilities present a general trend of lower abilities in various cognitive domains for ε4 carriers (18, 20, 21, 24, 41, 61). Although some studies also find differences regarding the visuospatial domain (24, 25) the evidence is more inconsistent in this field and a meta-analysis even concluded that there is little evidence for an impact on the visuospatial domain by the APOE gene (21). This may hold true for heterozygous ε4 carriers compared to non-ε4 carriers (as most studies compare these groups). However, little research exists including valid sample sizes of ε4 homozygotes. The current study provides a comparatively large sample size of ε4 homozygotes. It revealed

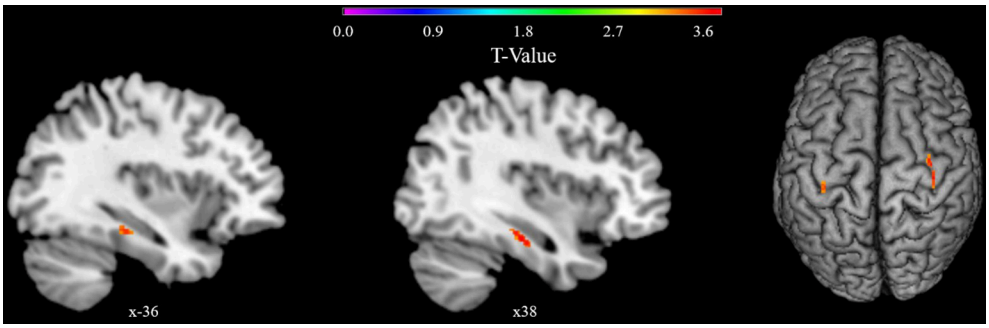


FIGURE 3 | VBM whole brain results showing clusters with a positive correlation of gray matter density with Corsi span in the general linear model. Results are presented below an exploratory uncorrected significance threshold of $p < 0.001$ with a minimum cluster size of 20 voxels. Clusters are located in the left temporal inferior and fusiform gyrus and left hippocampus, and in the right parahippocampus, hippocampus, and fusiform gyrus.

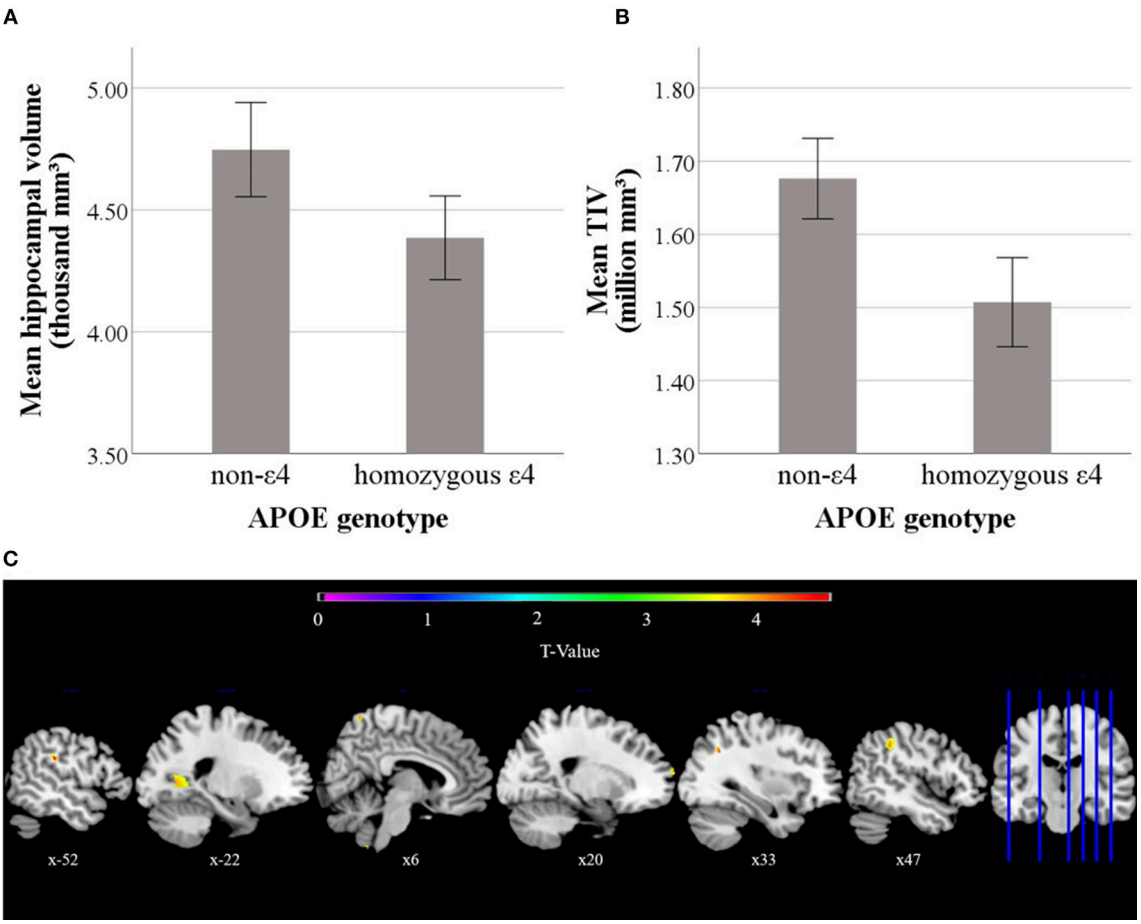


FIGURE 4 | Mean hippocampal volume **(A)**, and mean total intracranial volume (TIV) volume **(B)** differences over APOE genotypes. Depicted hippocampal volumes were calculated as mean volumes between left and right laterality. Error bars represent 95% confidence intervals. VBM results of the contrast that ε4 homozygotes have lower gray matter density than non-ε4 carriers are depicted at the bottom **(C)**. Presented clusters correspond to the clusters described in **Table 2**.

medium sized group differences for the Corsi block-tapping task performance. As measures of visuospatial ability vary between studies it cannot be ruled out that the effect shows more in the Corsi task than other tasks of visuospatial performance that might tax domain components differently (for example more or less taxing of executive components of working memory).

The findings of the current study suggest that both APOE status and MDD diagnosis have deteriorating effects on vWM,

TABLE 2 | Clusters above exploratory uncorrected significance threshold $p < 0.001$ with minimum voxel number of 20 for the contrast of lower gray matter density in homozygous APOE ε4 carriers.

Main area	k_E	Peak voxel coordinates			Peak voxel coefficients	
		x	*y*	*z*	*t*	*p*
Supramarginal gyrus	51	−52	−30	30	4.62	0.000
Angular gyrus	26	33	−57	34	4.24	0.000
Supramarginal gyrus	119	48	−40	42	3.74	0.000
Precuneus	20	6	−58	68	3.70	0.000
Superior frontal gyrus	31	20	69	15	3.66	0.000
Calcarine	311	−24	−62	8	3.64	0.000
Cerebellum	46	2	−50	−58	3.40	0.000
Middle temporal gyrus	26	−63	−22	0	3.24	0.001

Uncorrected p-values of peak voxel differences are reported.

which appear to be of an additive nature. In contrast a longitudinal study investigating the interplay between depression and APOE status on AD risk, proposes an interactional relationship, as that depression constitutes a risk factor only in ε4 carriers (39). Regarding cross-sectional effects in mid-life, our results are in line with other evidence proposing that MDD and ε4 effects on cognitive ability are rather additive (41, 62) suggesting that interactional effects might only show later in life and/or in combination with demential processes.

The literature addressing interaction effects between APOE genotype and age on cognitive ability is very heterogeneous depending on cognitive measures and age span under investigation. Most studies finding cognitive decline effects in APOE ε4 carriers have investigated elderly samples from 60 years upwards (63). Evidence is mixed for mid-age samples (61) while a meta-analysis regarding children and young adults suggest no cognitive differences dependent on APOE status (64). For the sample investigated in the current study no moderating influence of age on APOE effects on cognition became evident. Genotype effects were further not found to be moderated by sex.

Regarding the relationship between vWM and brain structural measures the results found here hold several important insights. Two measures of hippocampal morphometry were used in the current study and findings varied depending on the measure. While hippocampal volume was not associated with vWM capacity, gray matter density was marginally significantly increased in higher vWM capacity individuals. Furthermore, exploratory additional analyses indicated that the effect on hippocampal volume was masked by the covariate TIV (possibly suggesting a more unspecific, global association), while the exploratory whole brain VBM analysis suggested a specific effect located in the hippocampal and parahippocampal area (as no other areas were associated with vWM capacity). Findings suggest a global correlate of vWM regarding volumetric measures, while gray matter density seems to be associated with vWM specifically in the hippocampal and parahippocampal regions. Other findings suggesting a local link between the hippocampus and vWM capacity have used different measures of brain function (9, 34) and structure, as lesions (10, 35), gray matter density (9), and volume (36).

The pattern of results found in the current study suggests that although the ε4 allele may be associated with lower vWM capacity, the neuronal locus of this effect is not the hippocampal region specifically. Previous findings suggest a robust deteriorating APOE ε4 effect on hippocampal structure that supposedly is most pronounced for ε4 homozygotes (30, 31). However, in the current study we were unable to replicate group differences of hippocampal morphometry in dependence of APOE status (neither for a volumetric, nor for a gray matter density measure) after controlling for global brain measures. This finding is particularly surprising since we contrasted ε4 homozygotes with non-ε4 carriers. One possible explanation is given by Cherbuin et al. (30): the authors reviewed studies showing an effect and studies with contradicting findings, and propose that a potential effect of APOE genotype on hippocampal alterations may show only in a narrow age range around ∼70 years. It is suggested that samples below the age of 60 years may not be affected yet, while an APOE effect may be masked by more general age-related alterations in samples over 80 years (30). This interpretation would be in line with our findings as most participants of our sample are considerably younger. A different explanatory approach arises from our exploratory analyses that revealed that the relationship between APOE status and hippocampus is covered by the covariate TIV that may have too much explanatory variance in common with the hippocampal volume. One interpretation of this finding is that the APOE genotype affects the cerebral morphometry on a more global level. This interpretation is in line with a brain reserve hypothesis that implies that a globally increased brain volume serves as a protective factor regarding demential processes (65). Although this hypothesis has been discussed controversially (66, 67) our findings suggest that a protective effect of the APOE genotype (not having an ε4 allele) regarding AD might be mediated by global TIV. Further, it is also possible that the smaller TIV of ε4 homozygotes does not constitute a causal link between genotype and AD risk but is a byproduct of other neuronal processes. Either way, although the rational of controlling for TIV in brain morphology analyses seems straight forward, one should be aware that controlling for TIV variance might also covert morphometric effects of interest (68).

Causality of a genotype on an associated present phenotype cannot be definitely concluded as linkage disequilibrium with other causal factors cannot be ruled out (69). However, there is some evidence for a causal effect of the APOE genotype on visuospatial ability coming from animal models showing a reduced performance in a water maze task in APOE knockout mice with synthetic human APOE ε4 compared to APOE ε3 (70). Even though the translation to humans is not certain this finding supports the notion of a causal effect of APOE genotype on cognition in the current study. Owing to the cross-sectional nature of our data the reported link between brain structure and vWM cannot be interpreted regarding to its causal direction.

Major strengths of the current work comprise the relatively large sample of ε4 homozygotes compared to previous studies (bearing in mind that this cohort was obtained from a total of *N*

= 1,141). Another major strength lies in the inclusion of cognitive as well as brain structural data.

The results of the current study underlie several limitations which have been addressed in part. Firstly, only homozygous ε4 carriers were compared to non-ε4 carriers. Consequently, no conclusions can be derived regarding a potential dose effect of the ε4 allele status, and also no differential conclusions can be made about subgroups of different non-ε4 genotypes. Further, despite the availability of a large initial sample only a relatively small study sample of ε4 homozygotes could be included due to a naturally low occurrence rate of the ε4 allele. Thus, small effects are more difficult to detect and it cannot be ruled out that associations with small effect sizes can be found in higher-powered studies that were not significant in the current study. This could for example concern a potential interaction effect of MDD diagnosis and APOE status that was descriptively looming in the current study but did not become significant. A potential interaction of age and APOE status could particularly be affected by small sample sizes because samples have to be sufficiently powered across the whole age-range under investigation. The current study does not allow conclusions about age effects below the age of 19 and above the age of 63. Further, interactions of small effect sizes may be present within this range.

Furthermore, conclusions derived regarding the vWM capacity are to be interpreted with caution as the concept of vWM is rather heterogeneous and results may vary over different measures of vWM.

CONCLUSIONS

Combined results suggest that a detrimental effect of APOE genotype on vWM capacity exists and might be mediated by global volumetric measures rather than by region-specific volumetric or gray matter density measures. More specific hippocampus alterations as a function of APOE status may occur later in life but do not become evident in our young- to mid-age sample.

More longitudinal high-powered studies investigating the interplay between the APOE genotype, MDD and cognitive deficits, as well as neuronal processes involved are needed. It is important that future studies include sufficient sample sizes of ε4 homozygotes. Large multi-centered studies constitute a promising approach for achieving this goal.

ETHICS STATEMENT

This study was carried out in accordance with the recommendations of the Medical Faculty of the University Münster with written informed consent from all subjects. All subjects gave written informed consent in accordance with the Declaration of Helsinki. The protocol was approved by the Medical Faculty of the University Münster.

AUTHOR CONTRIBUTIONS

JG, RR, NO, UD, BB, TK, MN, MR, IN, AK, and AJ: study concept and design. JG, NO, RR, UD, KD, KF, DZ, SM, VE, ES, LF, KB, DG, AT, SS, FS, TM, DY, and EF: acquisition, analysis, or interpretation of data. JG, NO, and UD: drafting of the manuscript. RR, TK, AJ, BB, AF, VE, SW, AK, TH, KF, JR, DZ, KD, CK, DG, SM, ES, LF, TH, AK, IN, SM, FS, TM, DY, EF and MR: critical revision of the manuscript for important intellectual content. JG, NO, RR, and UD: statistical analysis. UD, NO, RR, and TK: obtained funding. RR, KF, KD, DZ, SM, VE, ES, LF, KB, JG, CK, HK, DG, TH, AT, SS, FS, TM, DY and EF: administrative, technical, or material support. UD, NO, BB, TK, MN, MR, IN, AK, and AJ: study supervision. All authors read and approved the submitted version of the manuscript.

FUNDING

The FOR 2107 consortium is supported by the German Research Council (Deutsche Forschungsgemeinschaft, DFG, Grant nos. KI 588/14-1, KI 588/14-2, KR 3822/7-1, KR 3822/7-2, NE 2254/1-2, DA 1151/5-1, DA 1151/5-2, SCHW 559/14-1, 545/7-2, RI 908/11-2, WI 3439/3-2, NO 246/10-2, DE 1614/3-2, HA 7070/2-2, JA 1890/7-1, JA 1890/7-2, MU 1315/8-2, RE 737/20-2, KI 588/17-1).

This work was furthermore funded by the German Research Foundation (DFG, grant FOR2107 DA1151/5-1 and DA1151/5-2 to UD; SFB-TRR58, Projects C09 and Z02 to UD) and the Interdisciplinary Center for Clinical Research (IZKF) of the Medical Faculty of Münster (grant Dan3/012/17 to UD).

We further acknowledge support from the Open Access Publication Fund of the University of Münster.

ACKNOWLEDGMENTS

We are deeply indebted to all participants of this study, the recruitment sites, and their staff.

REFERENCES

1. Burns A, Iliffe S. Alzheimer's disease. *Br Med J*. (2009) 338:471. doi: 10.1136/bmj.b158
2. Nestor PJ, Scheltens P, Hodges JR. Advances in the early detection of Alzheimer's disease. *Nat Med*. (2004) 10:34–41. doi: 10.1038/nm1433
3. Ries ML, Carlsson CM, Rowley HA, Sager MA, Gleason CE, Asthana S, et al. Magnetic resonance imaging characterization of brain structure and function in mild cognitive impairment: a review. *J Am Geriatr Soc*. (2008) 56:920–34. doi: 10.1111/j.1532-5415.2008.01684.x
4. Chandra A, Dervenoulas G, Politis M. Magnetic resonance imaging in Alzheimer's disease and mild cognitive impairment. *J Neurol*. (2019). 266:1293–302. doi: 10.1007/s00415-018-9016-3
5. Li X, Coyle D, Maguire L, Watson DR, McGinnity TM. Gray matter concentration and effective connectivity changes in Alzheimer's disease: a longitudinal structural MRI study. *Neuroradiology*. (2011) 53:733–48. doi: 10.1007/s00234-010-0795-1
6. Thompson PM, Hayashi KM, Zubicaray G, Janke AL, Rose SE, Semple J. Dynamics of gray matter loss in Alzheimer's disease. *J Neurosci*. (2003) 23:994–1005. doi: 10.1523/JNEUROSCI.23-03-00994.2003

7. Jack CR Jr., Shiung MM, Gunter JL, O'Brien PC, Weigand SD, Knopman DS, et al. Comparison of different MRI brain atrophy rate measures with clinical disease progression in AD. *Neurology*. (2004) 62:591–600. doi: 10.1021/nl061786n
8. Giovanello KS, Schnyer DM, Verfaellie M. A critical role of the anterior hippocampus in relational memory: evidence from an fMRI study comparing associative and item recognition. *Hippocampus*. (2004) 14:5–8. doi: 10.1002/hipo.10182
9. De Rover M, Pironti VA, McCabe JA, Acosta-Cabronero J, Arana FS, Morein-Zamir S, et al. Hippocampal dysfunction in patients with mild cognitive impairment: a functional neuroimaging study of a visuospatial paired associates learning task. *Neuropsychologia*. (2011) 49:2060–70. doi: 10.1016/j.neuropsychologia.2011.03.037
10. Moses SN, Cole C, Ryan JD. Relational memory for object identity and spatial location in rats with lesions of perirhinal cortex, amygdala and hippocampus. *Brain Res Bull*. (2005) 65:501–12. doi: 10.1016/j.brainresbull.2005.02.029
11. Schott JM, Crutch SJ, Frost C, Warrington EK, Rossor MN, Fox NC. Neuropsychological correlates of whole brain atrophy in Alzheimer's disease. *Neuropsychologia*. (2008) 46:1732–7. doi: 10.1016/j.neuropsychologia.2008.02.015
12. Dohm K, Redlich R, Zwitserlood P, Dannlowski U. Trajectories of major depression disorders: a systematic review of longitudinal neuroimaging findings. *Aust N Z J Psychiatry*. (2017) 51:441–54. doi: 10.1177/0004867416661426
13. Ownby RL, Crocco E, Acevedo A, John V, Loewenstein D. Depression and risk for Alzheimer disease: systematic review, meta-analysis, and metaregression analysis. *Arch Gen Psychiatry*. (2006) 63:530–8. doi: 10.1111/j.1743-6109.2008.01122.x.Endothelial
14. Corder E, Saunders A, Strittmatter W, Schmechel D, Gaskell P, Small G, et al. Gene dose of apolipoprotein E type 4 Allele and the risk of Alzheimer's disease in late onset families. *Science*. (1993) 261:921–3.
15. Farrer LA. Effects of age, sex, and ethnicity on the association between apolipoprotein E genotype and Alzheimer disease. *J Am Med Assoc*. (1997) 278:1349. doi: 10.1001/jama.1997.03550160069041
16. Bu G. Apolipoprotein E and its receptors in Alzheimer's disease: pathways, pathogenesis and therapy. *Nat Rev Neurosci*. (2009) 10:333–44. doi: 10.1038/nrn2620
17. Altmann A, Tian L, Victor WH, Greicius MD. Sex modifies the APOE-related risk of developing Alzheimer's disease. *Ann Neurol*. (2014) 75:563–73. doi: 10.1016/j.asieco.2008.09.006.EAST
18. Baxter LC, Caselli RJ, Johnson SC, Reiman E, Osborne D. Apolipoprotein E ε4 affects new learning in cognitively normal individuals at risk for Alzheimer's disease. *Neurobiol Aging*. (2003) 24:947–52. doi: 10.1016/S0197-4580(03)00006-X
19. Caselli RJ, Reiman EM, Osborne D, Hentz JG, Baxter LC, Hernandez JL, et al. Longitudinal changes in cognition and behavior in asymptomatic carriers of the APOE e4 allele. *Neurology*. (2004) 62:1990–5. doi: 10.1212/01.WNL.0000129533.26544.BF
20. Reinvang I, Winjevoll IL, Rootwelt H, Espeseth T. Working memory deficits in healthy APOE epsilon 4 carriers. *Neuropsychologia*. (2010) 48:566–73. doi: 10.1016/j.neuropsychologia.2009.10.018
21. Small BJ, Rosnick CB, Fratiglioni L, Bäckman L. Apolipoprotein E and cognitive performance: a meta-analysis. *Psychol Aging*. (2004) 19:592–600. doi: 10.1037/0882-7974.19.4.592
22. Flory JD, Manuck SB, Ferrell RE, Ryan CM, Muldoon MF. Memory performance and the apolipoprotein E polymorphism in a community sample of middle-aged adults. *Am J Med Genet*. (2000) 96:707–11. doi: 10.1002/1096-8628(20001204)96:6<707::AID-AJMG1>3.0.CO;2-V
23. Berteau-Pavy F, Park B, Raber J. Effects of sex and APOE ε4 on object recognition and spatial navigation in the elderly. *Neuroscience*. (2007) 147:6–17. doi: 10.1016/j.neuroscience.2007.03.005
24. Negash S, Greenwood PM, Sunderland T, Parasuraman R, Geda YE, Knopman DS, et al. The influence of apolipoprotein E genotype on visuospatial attention dissipates after age 80. *Neuropsychology*. (2009) 23:81–9. doi: 10.1037/a0014014.The
25. Bloss CS, Delis DC, Salmon DP, Bondi MW. Decreased cognition in children with risk factors for Alzheimer's disease. *Biol Psychiatry*. (2008) 64:904–6. doi: 10.1016/j.biopsych.2008.07.004
26. Acevedo SF, Piper BJ, Craytor MJ, Benice TEDS, Raber J, Neuroscience B, et al. Apolipoprotein E4 and sex affect neurobehavioral performance in primary school children. *Pediatr Res*. (2010) 67:293–9. doi: 10.1203/PDR.0b013e3181cb8e68
27. Reiman EM, Caselli RJ, Yun LS, Chen K, Bandy D, Minoshima S, et al. Preclinical evidence of Alzheimer's disease in persons homozygous for the ε4 Allele for apolipoprotein E. *N Engl J Med*. (1996) 334:752–8. doi: 10.1056/NEJM199603213341202
28. Lemaître H, Crivello F, Dufouil C, Grassiot B, Tzourio C, Alpérovitch A, et al. No ε4 gene dose effect on hippocampal atrophy in a large MRI database of healthy elderly subjects. *Neuroimage*. (2005) 24:1205–13. doi: 10.1016/j.neuroimage.2004.10.016
29. Wishart HA, Saykin AJ, McAllister TW, Rabin LA, McDonald BC, Flashman LA, et al. Regional brain atrophy in cognitively intact adults with a single APOE epsilon 4 allele. *Neurology*. (2006) 67:1221–4. doi: 10.1212/01.wnl.0000238079.00472.3a
30. Cherbuin N, Leach LS, Christensen H, Anstey KJ. Neuroimaging and APOE genotype: a systematic qualitative review. *Dement Geriatr Cogn Disord*. (2007) 24:348–62. doi: 10.1159/000109150
31. Liu Y, Yu J-T, Wang H-F, Han P-R, Tan C-C, Wang C, et al. APOE genotype and neuroimaging markers of Alzheimer's disease: systematic review and meta-analysis. *J Neurol Neurosurg Psychiatry*. (2015) 86:127–34. doi: 10.1136/jnnp-2014-307719
32. Owen AM, McMillan KM, Laird AR, Bullmore E. N-back working memory paradigm: a meta-analysis of normative functional neuroimaging studies. *Hum Brain Mapp*. (2005) 25:46–59. doi: 10.1002/hbm.20131
33. Corsi PM. *Human Memory and the Medial Temporal Region of the Brain*. Montreal, QC: McGill University (1972).
34. Toepper M, Markowitsch HJ, Gebhardt H, Beblo T, Thomas C, Gallhofer B, et al. Hippocampal involvement in working memory encoding of changing locations: an fMRI study. *Brain Res*. (2010) 1354:91–9. doi: 10.1016/j.brainres.2010.07.065
35. Piekema C, Fernández G, Postma A, Hendriks MPH, Wester AJ, Kessels RPC. Spatial and non-spatial contextual working memory in patients with diencephalic or hippocampal dysfunction. *Brain Res*. (2007) 1172:103–9. doi: 10.1016/j.brainres.2007.07.066
36. Longoni G, Rocca MA, Pagani E, Riccitelli GC, Colombo B, Rodegher M, et al. Deficits in memory and visuospatial learning correlate with regional hippocampal atrophy in MS. *Brain Struct Funct*. (2015) 220:435–44. doi: 10.1007/s00429-013-0665-9
37. Arnone D, McIntosh AM, Ebmeier KP, Munafò MR, Anderson IM. Magnetic resonance imaging studies in unipolar depression: systematic review and meta-regression analyses. *Eur Neuropsychopharmacol*. (2012) 22:1–16. doi: 10.1016/j.euroneuro.2011.05.003
38. Lee RSC, Hermens DF, Porter MA, Redoblado-Hodge MA. A meta-analysis of cognitive deficits in first-episode major depressive disorder. *J Affect Disord*. (2012) 140:113–24. doi: 10.1016/j.jad.2011.10.023
39. Karlsson IK, Bennet AM, Ploner A, Andersson TM-L, Reynolds CA, Gatzc M, et al. Apolipoprotein E ε4 genotype and the temporal relationship between depression and dementia. *Neurobiol Aging*. (2015) 36:1751–6. doi: 10.1016/j.neurobiolaging.2015.01.008
40. Lavretsky H, Ercoli L, Siddarth P, Bookheimer S, Miller K, Small G. Apolipoprotein ε4 Allele status, depressive symptoms, and cognitive decline in middle-aged and elderly persons without dementia. *Am J Geriatr Psychiatry*. (2003) 11:667–73. doi: 10.2217/nnm.12.167
41. Taylor WD, Boyd B, Turner R, McQuoid DR, Ashley-Koch A, MacFall JR, et al. APOE ε4 associated with preserved executive function performance and maintenance of temporal and cingulate brain volumes in younger adults. *Brain Imaging Behav*. (2017) 11:194–204. doi: 10.1007/s11682-016-9522-9
42. Meyer MR, Tschanz JT, Norton MC, Welsh-Bohmer KA, Steffens DC, Wyse BW, et al. APOE genotype predicts when — not whether — one is predisposed to develop Alzheimer disease. *Nat Genet*. (1998) 19:321–2.
43. O'Brien JT, Lloyd A, McKeith I, Gholkar A, Ferrier N. A longitudinal study of hippocampal volume, cortisol levels, and cognition in older depressed subjects. *Am J Psychiatry*. (2004) 161:2081–90. doi: 10.1176/appi.ajp.161.11.2081

44. Egger K, Schocke M, Weiss E, Auffinger S, Esterhammer R, Goebel G, et al. Pattern of brain atrophy in elderly patients with depression revealed by voxel-based morphometry. *Psychiatry Res*. (2008) 164:237–44. doi: 10.1016/j.pscychresns.2007.12.018
45. Kircher T, Wöhr M, Nenadić I, Schwarting R, Schratt G, Alferink J, et al. Neurobiology of the major psychoses. A translational perspective on brain structure and function: the FOR2107 consortium. *Eur Arch Psychiatry Clin Neurosci*. (2018). doi: 10.1007/s00406-018-0943-x. [Epub ahead of print].
46. Carlesimo GA, Fadda L, Lorusso S, Caltagirone C. Verbal and spatial memory spans in Alzheimer's and multi-infarct dementia. *Acta Neurol Scand*. (1994) 89:132–8. doi: 10.1111/j.1600-0404.1994.tb01648.x
47. Trojano L, Chiacchio L, De Luca G, Fragassi NA, Grossi D. Effect of testing procedure on Corsi's block-tapping task in normal subjects and Alzheimer-type dementia. *PerceptMotSkills*. (1994) 78:859–63. doi: 10.2466/pms.1994.78.3.859
48. Grossi D, Becker JT, Smith C, Trojano L. Memory for visuospatial patterns in Alzheimer's disease. *Psychol Med*. (1993) 23:65–70. doi: 10.1017/S003329170003885X
49. Donolato E, Giofrè D, Mammarella IC. Differences in verbal and visuospatial forward and backward order recall: a review of the literature. *Front Psychol*. (2017) 8:663. doi: 10.3389/fpsyg.2017.00663
50. Wittchen H-U, Wunderlich U, Gruschwitz S, Zaudig M. *SKID-I. Strukturiertes Klinisches Interview für DSM-IV*. Göttingen: Hogrefe (1997).
51. Vogelbacher C, Möbius TWD, Sommer J, Schuster V, Dannlowski U, Kircher T, et al. The Marburg-Münster Affective Disorders Cohort Study (MACS): a quality assurance protocol for MR neuroimaging data. *Neuroimage*. (2018) 172:450–60. doi: 10.1016/j.neuroimage.2018.01.079
52. Dannlowski U, Grabe HJ, Wittfeld K, Klaus J, Konrad C, Grotegerd D, et al. Multimodal imaging of a tescalcin (TESC)-regulating polymorphism (rs7294919)-specific effects on hippocampal gray matter structure. *Mol Psychiatry*. (2015) 20:398–404. doi: 10.1038/mp.2014.39
53. Opel N, Amare AT, Redlich R, Repple J, Kaehler C, Grotegerd D, et al. Cortical surface area alterations shaped by genetic load for neuroticism. *Mol Psychiatry*. (2018). doi: 10.1038/s41380-018-0236-9. [Epub ahead of print].
54. Redlich R, Opel N, Grotegerd D, Dohm K, Zaremba D, Burger C, et al. Prediction of individual response to electroconvulsive therapy via machine learning on structural magnetic resonance imaging data. *JAMA Psychiatry*. (2016) 73:557–64. doi: 10.1001/jamapsychiatry.2016.0316
55. Opel N, Redlich R, Repple J, Kaehler C, Grotegerd D, Dohm K, et al. Childhood maltreatment moderates the influence of genetic load for obesity on reward related brain structure and function in major depression. *Psychoneuroendocrinology*. (2019) 100:18–26. doi: 10.1016/j.psyneuen.2018.09.027
56. Fischl B, Salat DH, Busa E, Albert M, Dieterich M, Haselgrove C, et al. Whole brain segmentation: automated labeling of neuroanatomical structures in the human brain. *Neuron*. (2002) 33:341–55. doi: 10.1016/S0896-6273(02)00569-X
57. Chang CC, Chow CC, Tellier LC, Vattikuti S, Purcell SM, Lee JJ. Second-generation PLINK: rising to the challenge of larger and richer datasets. *Gigascience*. (2015) 4:7. doi: 10.1186/s13742-015-0047-8
58. Das S, Forer L, Schönherr S, Sidore C, Locke AE, Kwong A, et al. Next-generation genotype imputation service and methods. *Nat Genet*. (2016) 48:1284–7. doi: 10.1038/ng.3656
59. Maldjian JA, Laurienti PJ, Kraft RA, Burdette JH. An automated method for neuroanatomic and cytoarchitectonic atlas-based interrogation of fMRI data sets. *Neuroimage*. (2003) 19:1233–9. doi: 10.1016/S1053-8119(03)00169-1
60. Tzourio-Mazoyer N, Landeau B, Papathanassiou D, Crivello F, Etard O, Delcroix N, et al. Automated anatomical labeling of activations in SPM using a macroscopic anatomical parcellation of the MNI MRI single-subject brain. *Neuroimage*. (2002) 15:273–89. doi: 10.1006/nimg.2001.0978
61. Greenwood PM, Espesetz T, Lin M-K, Reinvang I, Prasuraman R. Longitudinal change in working memory as a function of APOE genotype in midlife and old age. *Scand J Psychol*. (2014) 55:268–77. doi: 10.1111/j.1743-6109.2008.01122.x
62. Luciano M, Pujals AMF, Marioni RE, Campbell A, Hayward C, MacIntyre DJ, et al. Current versus lifetime depression, APOE variation, and their interaction on cognitive performance in younger and older adults. *Psychosom Med*. (2015) 77:480–92. doi: 10.1097/PSY.0000000000000190
63. Wisdom NM, Callahan JL, Hawkins KA. The effects of apolipoprotein E on non-impaired cognitive functioning: a meta-analysis. *Neurobiol Aging*. (2011) 32:63–74. doi: 10.1016/j.neurobiolaging.2009.02.003
64. Ihle A, Bunce D, Kliegel M. APOE epsilon 4 and cognitive function in early life: a meta-analysis. *Neuropsychology*. (2012) 26:267–77. doi: 10.1037/a0026769
65. Perneczky R, Wagenpfeil S, Lunetta KL, Cupples LA, Green RC, Decarli C, et al. Head circumference, atrophy, and cognition: Implications for brain reserve in Alzheimer disease. *Neurology*. (2010) 75:137–42. doi: 10.1212/WNL.0b013e3181e7ca97
66. Jenkins R, Fox NC, Rossor AM, Harvey RJ, Rossor MN. Intracranial volume and Alzheimer disease. *Arch Neurol*. (2014) 57:220–4. doi: 10.1001/archneur.57.2.220
67. Christensen H, Anstey KJ, Parslow RA, Maller J, Mackinnon A, Sachdev P. The brain reserve hypothesis, brain atrophy and aging. *Gerontology*. (2007) 53:82–95. doi: 10.1159/000096482
68. Voevodskaya O. The effects of intracranial volume adjustment approaches on multiple regional MRI volumes in healthy aging and Alzheimer's disease. *Front Aging Neurosci*. (2014) 6:264. doi: 10.3389/fnagi.2014.00264
69. Marian AJ. Causality in genetics: the gradient of genetic effects and back to Koch's postulates of causality. *Circ Res*. (2014) 114:e18–21. doi: 10.1161/CIRCRESAHA.114.302904
70. Raber J, Wong D, Buttini M, Orth M, Bellosta S, Pitas RE, et al. Isoform-specific effects of human apolipoprotein E on brain function revealed in ApoE knockout mice: increased susceptibility of females. *PNAS*. (1998) 95:10914–9.

Conflict of Interest Statement: The authors declare that the research was conducted in the absence of any commercial or financial relationships that could be construed as a potential conflict of interest.

Copyright © 2019 Goltermann, Redlich, Dohm, Zaremba, Repple, Kaehler, Grotegerd, Förster, Meinert, Enneking, Schlaghecken, Fleischer, Hahn, Kugel, Jansen, Krug, Brosch, Nenadic, Schmitt, Stein, Meller, Yüksel, Fischer, Rietschel, Witt, Forstner, Nöthen, Kircher, Thalamuthu, Baune, Dannlowski and Opel. This is an open-access article distributed under the terms of the Creative Commons Attribution License (CC BY). The use, distribution or reproduction in other forums is permitted, provided the original author(s) and the copyright owner(s) are credited and that the original publication in this journal is cited, in accordance with accepted academic practice. No use, distribution or reproduction is permitted which does not comply with these terms.

frontiers in Neurology

REVIEW
published: 06 June 2019
doi: 10.3389/fneur.2019.00591

Biomarkers in Vasculitides of the Nervous System

*Daniel Strunk, Antje Schmidt-Pogoda, Carolin Beuker, Lennart S. Milles, Catharina Korsukewitz, Sven G. Meuth and Jens Minnerup**

Department of Neurology, Institute for Translational Neurology, University of Münster, Münster, Germany

Besides being affected by the rare and severe primary angiitis of the central nervous system (PACNS) the nervous system is also affected by primary systemic vasculitides (PSV). In contrast to PACNS, PSV affect not only the central but also the peripheral nervous system, resulting in a large array of potential symptoms. Given the high burden of disease, difficulties in distinguishing between differential diagnoses, and incomplete pathophysiological insights, there is an urgent need for additional precise diagnostic tools to enable an earlier diagnosis and initiation of effective treatments. Methods available to date, such as inflammatory markers, antibodies, cerebrospinal fluid (CSF) analysis, imaging, and biopsy, turn out to be insufficient to meet all current challenges. We highlight the use of biomarkers as an approach to extend current knowledge and, ultimately, improve patient management. Biomarkers are considered to be useful for disease diagnosis and monitoring, for predicting response to treatment, and for prognosis in clinical practice, as well as for establishing outcome parameters in clinical trials. In this article, we review the recent literature on biomarkers which have been applied in the context of different types of nervous system vasculitides including PACNS, giant-cell arteritis, Takayasu's arteritis, polyarteritis nodosa, ANCA (anti-neutrophil cytoplasm antibody)-associated vasculitides, cryoglobulinemic vasculitis, IgA vasculitis, and Behçet's disease. Overall, the majority of biomarkers is not specific for vasculitides of the nervous system.

Keywords: PACNS, Primary systemic vasculitides, biomarkers, inflammation, differential diagnoses

OPEN ACCESS

Edited by:
Marcello Moccia,
University College London,
United Kingdom

Reviewed by:
Antonio Carotenuto,
University of Naples Federico II, Italy
Tom Ejnar Pettersson,
University of Helsinki, Finland

****Correspondence:***
Jens Minnerup
jens.minnerup@ukmuenster.de

Specialty section:
This article was submitted to Multiple Sclerosis and Neuroimmunology, a section of the journal Frontiers in Neurology

Received: *30 December 2018*
Accepted: *20 May 2019*
Published: *06 June 2019*

Citation:
Strunk D, Schmidt-Pogoda A, Beuker C, Milles LS, Korsukewitz C, Meuth SG and Minnerup J (2019) Biomarkers in Vasculitides of the Nervous System. Front. Neurol. 10:591. doi: 10.3389/fneur.2019.00591

INTRODUCTION

Primary angiitis of the central nervous system (PACNS) is a rare and often devastating disease with high morbidity and mortality. Major clinical manifestations include ischemic and hemorrhagic stroke, headache and encephalopathy (1). In addition to PACNS, the nervous system may be also affected by primary systemic vasculitides (PSV), which manifest primarily in the context of vasculitides of small and medium sized vessels, e.g., in ANCA-associated vasculitides and polyarteritis nodosa. Due to the severity of nervous system involvement, aggressive immunosuppressive treatments, e.g., high-dose glucocorticoids and cyclophosphamide, are frequently required for remission induction in both, PACNS and PSV. Nonetheless, chronic neuronal damage and persisting symptoms are frequent, even after early immunosuppressive treatment initiation (1).

With respect to the high disease burden there is an urgent need for additional precise diagnostic tools enabling an early diagnosis and treatment initiation. The use of biomarkers may emerge as a valuable approach to overcome these problems. The term "biomarker" is based on the two words "biological" and "marker." Biomarkers can be extracted from different kinds of body fluids and tissues, and are applied as surrogate parameters for various medical conditions (2, 3).

This review aims to give a concise overview of current areas of application for biomarkers with regard to pathogenesis, clinical manifestation, and management of PACNS and those PSV with nervous system involvement. Although biomarkers derived from biopsy specimens are of unquestionable value, this review puts special emphasis on biomarkers derived from body fluids, because biomarkers that can be isolated from body fluids are more likely to be integrated in daily clinical practice (3).

BIOMARKERS IN PRIMARY ANGIITIS OF THE CENTRAL NERVOUS SYSTEM (PACNS)

PACNS is an important cause of stroke and is difficult to differentiate from other conditions that also result in stroke (4). Men are affected twice as often as women. The mean age at disease onset is 50 years (5). Symptoms of PACNS are diverse and not specific. Among them are, in particular, headache, altered cognition, and focal neurologic deficits such as hemiparesis, hemihypesthesia, ataxia, aphasia, dysarthria, and visual disturbances (6). Further typical clinical manifestations are seizures and encephalopathy. The gold standard for the diagnosis of PACNS is a biopsy of brain parenchyma and leptomeninges. Due to possible sampling errors, a negative result does not necessarily mean that PACNS can be ruled out, though (7). Further examinations, including magnetic resonance imaging (MRI), magnetic resonance angiography (MRA), digital subtraction angiography (DSA), or cerebrospinal fluid (CSF) analysis exhibit a rather high degree of sensitivity whereas specificity assumes low values (8). Well-known markers of inflammation and autoimmunity, such as C-reactive protein (CRP), erythrocyte sedimentation rate (ESR), rheumatic antibodies (ANA, dsDNA, ENA, ANCA), and oligoclonal bands do not play a decisive role in PACNS (9).

Our own group retrospectively analyzed the composition of CSF immune cells in patients with PACNS in comparison with sex- and age-matched patients with ischemic stroke, multiple sclerosis, and somatoform disorders by means of multi-parameter flow cytometry (10). PACNS patients were shown to have higher CSF leukocyte counts than controls (10). Some individuals exhibited a shift toward NK (natural killer) or B cells while proportions of T cell subsets remained unmodified. In other patients, we detected higher numbers of plasma cells and an immunoglobulin synthesis within the central nervous system (10). Altogether, characteristics of the intrathecal immune-cell profile were heterogenous in PACNS patients in this study (10).

Ruland et al. employed ion mobility mass spectrometry for unbiased proteomic profiling to further elucidate the pathophysiologic principles and potential biomarkers of PACNS, and identified fourteen proteins from neuronal structures that might be of importance, among others amyloid—beta A4 protein (APP) (11). Amyloid-beta proteins are metal chelators which reduce metal. They are said to activate mononuclear cells in the central nervous systems and evoke inflammatory processes. Both, APP or its fission product beta-amyloid, respectively, are known to be involved in other diseases of the vasculature of the central nervous system, e.g., Amyloid Beta-Related Angiitis (ABRA) (9, 11). This is why the authors highlight the possibility of inflammatory and degenerative processes being intertwined in PACNS (11).

Thom et al. evaluated the potential role of the proinflammatory cytokine interleukin-17 (IL-17), measured in the CSF by flow cytometry, as a biomarker for cerebral vasculitis in patients with stroke. As a major finding, Thom et al. found a marked and persisting increase in IL-17 production in individuals with PACNS compared to patients with non-inflammatory neurological diseases (12). Another study supports the concept of $CD4^+$ T cells being of major importance in vasculitic conditions by detecting an elevated percentage of this cell type in the CSF of individuals with amyloid-ß related cerebral angiitis (13), thus suggesting intrathecal $CD4^+$ T cells as a possible biomarker in PACNS.

The amount of circulating von Willebrand factor antigen (vWF) seems to correlate with a clinical global assessment of disease activity in childhood PACNS (14). vWF is a glycoprotein important for platelet aggregation and the protection of coagulation factor VIII from proteolysis (15). vWF is released by endothelial cells after vascular injury. Consequently an increase in vFW levels may indicate inflammatory processes of the vasculature (14). vWF seems to be an informative indicator of active inflammation in infants but not in adults due to increasing vWF levels with age (14). In Cellucci's study, increased vWF antigen levels were detected at the timepoint of diagnosis in 65% of children with PACNS and showed a significant decrease after treatment initiation (14). The authors found that elevated values of vWF antigen at the timepoint of diagnosis might be indicative of a less active cPACNS after 12 months of course of disease (14). Therefore, vWF antigen represents a promising biomarker of disease activity in children. One of the study's limitations is that results have been derived from experiences at a single medical center in Canada. Consequently its findings cannot be generalized, the more so as adult patients were not examined (14). To overcome these limitations, further investigations in children and adults should be carried out.

In contrast to vWF, the acute phase reactants C-reactive protein (CRP) and erythrocyte sedimentation rate (ESR) did not show a correlation with disease activity, which is not surprising, given that their levels are known to increase in response to many kinds of inflammatory states not necessarily linked to the vasculature (14).

Taking the above mentioned limitations into consideration, none of these potential biomarkers is sufficiently tested and

validated in adult patients with PACNS. For a summary of biomarkers, see **Tables 1**, **2**.

BIOMARKERS IN PRIMARY SYSTEMIC VASCULITIDES

The biomarkers currently used for PSV are well-known and were established before the use of the term "biomarker." The majority of such markers are highly useful for diagnosing systemic vasculitis. Among others, antibodies to proteinase-3 (PR3) and myeloperoxidase (MPO) are highly specific for ANCA (anti-neutrophil cytoplasm antibody)-associated vasculitides. ANCA is an autoantibody against endogenous neutrophilic leukocytes. According to their target antigen they can be divided into c- (anti-PR3, elevated in tuberculosis, HIV infection, uveitis, amoebiasis, and cystic fibrosis with superinfection), p- (anti-MPO, of importance to microscopic polyangiitis, eosinophilic granulomatosis with polyangiitis, and pauci-immunen glomerulonephritis), and a-ANCA (Crohn's disease, autoimmune hepatitis) (16). The identification of ANCA is not essential for the diagnosis: About 10–20% of patients with granulomatosis with polyangiitis or microscopic polyangiitis and about 60% of patients with eosinophilic granulomatosis with polyangiitis (EPGA), previously known as Churg-Strauss syndrome, are ANCA negative (17). Erythrocyte sedimentation rate (ESR) and C-reactive protein (CRP), the most common laboratory signs of inflammation in general, are usually considered being helpful in identifying active vasculitis, especially in untreated patients, or ruling out this kind of disease. Nonetheless, all of these markers are much less useful for assessing disease activity in patients with established diagnoses. In the following, this and other aspects will be addressed in the context of the most relevant vasculitides, introducing each section with a brief engram of the respective disease.

TABLE 1 | Summary of traditional and already sufficiently tested biomarkers and their meaning in vasculitides with neurological manifestations.

Type of vasculitis	Biomarker	Meaning
Primary angiitis of the central nervous system	–	–
Giant-cell arteritis	CRP, ESR	Inflammatory markers, diagnosis, monitoring disease activity
	IL-6	Disease activity
Takayasu's arteritis	IL-6	Disease state and activity
Polyarteritis nodosa	–	–
ANCA (anti-neutrophil cytoplasm antibody)-associated vasculitides	CRP to serum albumin ratio	All-cause mortality
	Delta neutrophil index	Correlation with Birmingham vasculitis activity score; Predicting course of disease/relapses
	PR3-ANCA, MPO-ANCA	Diagnosis, Monitoring and predicting course of disease
Granulomatosis with polyangiitis	CRP, ESR, anti-PR3, and anti-MPO titers	Disease activity; Predicting flares
	B cell reconstitution and ANCA-PR3 level	Predicting relapse in patients treated with rituximab
Microscopic polyangiitis	–	–
Eosinophilic granulomatosis with polyangiitis	–	–
Cryoglobulinemic vasculitis	–	–
Henoch-Schönlein purpura	Serum biomarker index	Diagnosis
Behçet's disease	HLA B51	Diagnosis

vWF, Von Willebrand factor; CSF, Cerebrospinal fluid; IL, Interleukin; CD, Cluster of differentiation; NK cells, Natural killer cells; CRP, C-reactive protein; ESR, Erythrocyte sedimentation rate; SGTB, Small Glutamine Rich Tetratricopeptide Repeat Containing Beta; FCGR3A, Fc Fragment Of IgG Receptor IIIa; CCL, chemokine (C-C motif) ligand; sIL-6R, soluble IL-6 receptor; MMP, Matrix-metalloprotease; FCGR2A/FCGR3A and RPS9/LILRB3 and PSMG1, Gene loci; HLA, Human leukocyte antigen; MPO, myeloperoxidase; PR3, Proteinase-3; CXCL, C-X-C motif chemokine; Ig, Immunoglobulin; TARC, Chemokine (C-C motif) ligand 17 (CCL17); TNF, tumor necrosis factor; HCV, Hepatitis C virus; RNA, Ribonucleic acid.

LARGE VESSEL VASCULITIS

Giant-Cell Arteritis (GCA)

Giant-cell arteritis (GCA) most commonly involves vessels of large and medium size and is characterized by a granulomatous inflammatory process affecting the aorta and its main branches, predominantly the extracranial branches of the carotid artery, first of all the temporal artery (18). It is the most frequent type of vasculitis in the Western world, with women being affected more often than men. The annual incidence of GCA amounts to 20–40 per million. The disease rather affects older people, which is also reflected by the classification criteria defined by the American College of Rheumatology (19). The disorder may coexist with polymyalgia rheumatica, whose hallmarks are pain and stiffness in muscles of the pelvis and/or shoulder. Clinical manifestation of GCA comprises visual disturbances that can be temporary (Amaurosis fugax) or permanent in form of a persisting loss of vision, usually in one eye first (20, 21). Further symptoms may consist of headache, pain over the temples, jaw claudication, and a high degree of sensitivity of the temporal artery, which is prominent in many cases. Not only because of increased stroke risk, especially in the vertebrobasilar circulatory system, GCA is considered a serious disease.

Pentraxin proteins (PTX), which are involved in acute immunological responses, are under investigation as potential biomarkers of GCA. Pentraxin-3 (PTX-3), for instance, which originates from endothelial cells, smooth muscle cells and leukocytes, was found to be markedly increased in GCA patients with acute ischemia of the optic nerve compared to both, GCA cases without ischemic signs and healthy controls (22). Most interestingly, PTX-3 showed poor correlation with ESR and CRP, hinting at the potential benefit of using a combination of markers for a laboratory assessment of GCA. Generally speaking, the production of PTX3 is said to be a characteristic

TABLE 2 | Summary of biomarkers of potential clinical value in the future and their area of application in vasculitides with neurological manifestations.

Type of vasculitis	Biomarker	Meaning
Primary angiitis of the central nervous system	Circulating vWF antigen	Disease activity in children
	CSF IL-17; Increased CD 4 T cells in the CSF	Diagnosis
	CSF pleocytosis; Shift toward NK or B cells; Intrathecal immunoglobulin synthesis; Plasma cells	Diagnosis; Differentiating subtypes of PACNS
Giant-cell arteritis	Pentraxin 3	Acute ischemia of the optic nerve; Disease duration <6 months
	Anti-ferritin antibodies	Diagnosis in untreated patients
	Expression of SGTB and FCGR3A	Confirmation of diagnosis; Predicting course of disease
	Serum Osteopontin	Disease activity and relapse; Disease activity in tocilizumab-treated patients
Takayasu's arteritis	Anti-ferritin antibodies	Diagnosis
	IL-8, IL-18, CCL 2, CCL 5	Diagnosis; Disease activity
	sIL-6R, MMP-1,−3, and−9, soluble receptor for advanced glycation and products, Pentraxin 3	Disease activity; Surrogate parameter of arterial inflammation and progression of vascular involvement, i.e., marker of actual arteritis (PTX-3)
	Metabolites N-acetyl glycoprotein and glutamate	Disease activity; Guide to therapy
	Plasma ghrelin level; Leptin/Ghrelin ratio	Monitoring disease activity and creating treatment strategies
	Neutrophil gelatinase-associated lipocalin	Response to treatment with glucocorticoids and tumor necrosis factor-alpha inhibitors
	Anti-endothelial cell antibodies; Antibodies against Annexin V	Disease activity; Management of TA
	Circulating endothelial progenitor cells; Vascular endothelial growth factor	Disease activity
	Serum myeloid-related protein 8/14	Diagnosis; Disease activity; Prognostic biomarker
	FCGR2A/FCGR3A, IL12B, IL6, RPS9/LILRB3, and a locus on chromosome 21 near PSMG1	Non-HLA susceptibility loci
	Serum amyloid A	Disease activity; Treatment response
Polyarteritis nodosa	Vascular endothelial growth factor	Vasculitic neuropathy
ANCA (anti-neutrophil cytoplasm antibody)-associated vasculitides	Level of activated (CD19+/CD38+) B cells; CD 25+ regulatory B cells	Disease activity
	CD8+ T cell expression	Prognosis
	Tissue inhibitor of metalloproteinase 1	Distinguishing between mildly active AAV and remission; Distinguishing active AAV and infectious disease
	Epigenetic modifications of gene loci Proteinase 3 and MPO	Correlation with disease activity, PR 3 and MPO expression
Granulomatosis with polyangiitis	MMP-3, Tissue inhibitor of metalloproteinase 1, CXCL 13	Inflammation, angiogenesis, tissue damage and repair
	Soluble receptor for advanced glycation end products	Cumulative burden of granulomatous inflammation/Disease activity
Microscopic polyangiitis	Carbonic anhydrase III antibodies	Diagnosis in patients without ANCA; Disease activity
Eosinophilic granulomatosis with polyangiitis	Eotaxin-3, IgG4, CCL17/TARC	Diagnosis; Disease activity; Differentiating from other diseases characterized by vasculitis or eosinophilia
Cryoglobulinemic vasculitis	WA B cells	Marker for the development of CV in asymptomatic patients with HCV infection
	IL-6, CXCL10, TNF-alpha serum levels	Distinguishing HCV hepatitis with or without cryoglobulinemia; Active vasculitis (Increase of CXCL10 levels)
Henoch-Schönlein purpura	White blood cells, CRP, IL-6, serum amyloid A, serum biomarker index	Diagnosis
	Fecal secondary colonic bile acids, deoxycholic acid and lithocholic acid	Diagnosis
Behçet's disease	Tyrosine-protein phosphatase non-receptor type 4, threonine synthase-like 2, and ß-actin	Diagnosis
	Serum Amyloid A	Predicting major organ involvement/ ocular disease relapse; Disease activity
	Anti-Tubulin-α-1c antibodies	Diagnosis; Degree of inflammation; Disease activity; Predicting the course/certain manifestations of BD
	Urine and serum derived metabolites	Diagnosis
	Platelet to lymphocyte ratio, Lymphocytes to monocytes ratio	Disease activity; Differentiating BD from differential diagnoses
	Tissue factor-expressing microparticles	Diagnosis; Estimating the risk of thrombosis

vWF, Von Willebrand factor; CSF, Cerebrospinal fluid; IL, Interleukin; CD, Cluster of differentiation; NK cells, Natural killer cells; CRP, C-reactive protein; ESR, Erythrocyte sedimentation rate; SGTB, Small Glutamine Rich Tetratricopeptide Repeat Containing Beta; FCGR3A, Fc Fragment Of IgG Receptor IIIa; CCL, chemokine (C-C motif) ligand; sIL-6R, soluble IL-6 receptor; MMP, Matrix-metalloprotease; FCGR2A/FCGR3A and RPS9/LILRB3 and PSMG1, Gene loci; HLA, Human leukocyte antigen; MPO, myeloperoxidase; PR3, Proteinase-3; CXCL, C-X-C motif chemokine; Ig, Immunoglobulin; TARC, Chemokine (C-C motif) ligand 17 (CCL17); TNF, tumor necrosis factor; HCV, Hepatitis C virus; RNA, Ribonucleic acid.

of damages of the vasculature (23, 24). Being synthesized at the site of vascular injury, its physiological role consists in averting further damage of the affected vessels (23, 25–27). Additional investigations are required to elucidate in how far structural modifications of affected vessels are due to the locally synthesized PTX-3 (23, 28). In the past, diagnosing GCA was sometimes hampered by low values of ESR, especially when glucocorticoids had already been administered. The informative value of biopsies is known to be significantly reduced in this constellation as well. Given that no dependency of PTX-3 levels on the respective glucocorticoid dosage was found, elevated PTX-3 values might facilitate diagnosing GCA in this context (29). A prospective study would be helpful to proof the assumption that PTX-3 levels might be of use in evaluating different types of optic nerve ischemia, i.e., distinguishing (non-) vasculitic forms (23, 30).

In addition to PTX-3, levels of IL-6 and soluble IL-6 receptor (sIL-6R) were shown to be elevated in patients with GCA (31). Il-6 is a pro-inflammatory cytokine of importance in innate immunity serving as a link between innate and specific immune response. IL-6 binds to IL-6-receptors on hepatocytes and leukocytes and soluble IL-6-receptors resulting in the initiation of immunological pathways. Finally acute-phase-reactants are activated. In particular, IL-6 levels were significantly elevated in patients with active disease, whereas sIL-6R levels turned out to be significantly higher irrespective of disease activity. Therefore, IL-6 is considered as potential biomarker for monitoring disease activity. Most importantly, the IL-6 pathway has also emerged as a promising therapeutic target in GCA patients (32). The therapeutic efficacy of IL-6 receptor alpha inhibitor Tocilizumab in the treatment of GCA patients highlights the importance of IL-6 in GCA pathophysiology.

Baerlecken et al. analyzed anti-ferritin antibodies in GCA patients in various stages of the disease. The highest levels of anti-ferritin antibodies were found in untreated individuals with a concomittant polymyalgia rheumatica, whereas treated patients and patients with inactive stages of the disease had lower levels of anti-ferritin antibodies (33, 34). Therefore, these antibodies could be useful as a diagnostic marker.

De Smit et al. suggest new ways to confirm the diagnosis of GCA and to predict the course of disease (35). By means of transcriptional profiling of T-lymphocytes, 4,031 genes in $CD4^+$ and $CD8^+$ cells were identified that show distinct expression patterns in GCA patients with an active disease (35). Four transcripts in $CD8^+$ cells and 179 in $CD4^+$ cells were identified which were characterized by alternating expression characteristics over 12 months (35). In $CD8^+$ cells transcripts of SGTB [Small glutamine-rich tetratricopeptide repeat (TPR)-containing, β], playing a role in neuronal apoptosis, and FCGR (Fc gamma receptor) 3A, linked to Takayasu's arteritis maintained their altered expression pattern (35). The authors report a connection between genes and clinical aspects in the acute phase, offering the potential to predict prospective disease activity and tailor further therapies (35). The underlying mechanisms linking gene expression to actual symptoms and course of disease and the definite informative values of the aforementioned aspects in terms of a potential biomarker is to be further elucidated (35).

Prieto-González et al. reported that serum osteopontin (sOPN) might be useful in assessing and predicting disease activity in GCA (36). The glycoprotein osteopontin is of importance in the development and specialization of immune cells, inflammatory processes and remodeling in different kinds of tissues (36). Serum osteopontin concentration was significantly elevated in individuals with active disease compared to controls, whereas a significant decline was found as soon as patients entered disease remission (37). Serum osteopontin turned out to correlate with serum IL-6. Additionally, baseline serum osteopontin concentrations were significantly higher in relapsing patients than in non-relapsing patients (37).

Burja et al. investigated existing evidence on the usefulness of already known (potential) biomarkers in GCA by means of a meta-analysis. The results of this meta-analysis highlight the fact that the majority of potential biomarkers in GCA might add valuable information in understanding, diagnosing or treating the disease, but are still not suitable to be integrated in routine clinical use (38). IL-6, CRP, and ESR should, not only because of the meta-analysis by Burja et al., be considered as the best available biomarkers in GCA (for a summary of biomarkers, see **Tables 1**, **2**).

Takayasu's Arteritis (TA)

The prevalence of Takayasu's arteritis (TA) is lower than the prevalence of GCA. Pathophysiologically, the aorta and its main branches are affected by a granulomatous inflammatory process with massive intimal fibrosis and vascular narrowing. Takayasu's arteriitis most commonly affects young or middle-aged women of Asian descent (39). Clinical signs may be rather unspecific for several years, comprising fever, fatigue, and joint pains. Circulatory disturbances may lead to complaints in different regions of the body, e.g., in form of Raynaud's phenomenon or angina pectoris. Frequent symptoms of TA include intermittent claudication of the arms or legs, as well as a difference in pulse or blood pressure between the right and left arms or right and left legs (40). Possible neurological symptoms are transitory ischemic attacks (TIA), stroke, syncope, and posterior reversible encephalopathy syndrome (PRES) (41). Stenosis of the renal arteries is capable of causing arterial hypertension with subsequent blood pressure crises and diverse neurological consequences. Furthermore, seizures as a result of stroke or blood pressure crisis, headache, vertigo, and visual disturbances represent additional symptoms of TA. A well-known genetic susceptibility locus for TA is the human leukocyte antigen (HLA) allele HLA-B 52 (4).

Patients with TA usually exhibit an elevation of ESR and CRP. The presence of anti-ferritin antibodies has been described by Große et al. in 62% of patients with TA, compared to 0% in healthy controls and up to 92% in GCA (42). In so far there is a similarity to patients with GCA/PMR (42). Alibaz-Oner et al. found a stronger increase of IL-6, IL-8, and IL-18 in TA patients in comparison with controls, and an association of IL-18 levels with disease activity (43–46). Interleukin-8 (IL-8) is an inflammatory mediator which attracts neutrophils to the site of inflammation. Interleukin-18 (IL-18), a proinflammatory

cytokine, induces the release of Interferon (IFN) γ that, in turn, plays a role in the stimulation of macrophages. It is assumed that these cytokines contribute to the emergence of vasculitic lesions in TA (45). The role of IL-6 and also sIL-6R was confirmed by Pulsatelli et al., who reported that the levels of these markers were significantly altered in TA patients compared to healthy controls (47). IL-6 levels were markedly elevated in patients with TA irrespective of disease phase, whereas a significant increase in sIL-6R levels was only detected in individuals with active disease. Longitudinal analysis demonstrated that a significant increase in sIL-6R levels was only apparent at baseline (47). Consequently, sIL-6R is suggested to mirror disease activity in TA (48). Additional research on cytokines and chemokines in TA showed that serum/plasma levels of IL-8, and chemokine (C-C motif) ligands (CCL) 2 and (CCL) 5, cytokines which guide immune cells to the site of inflammation by means of chemotaxis, were increased in TA patients in comparison with healthy controls, and were also elevated when comparing individuals with active TA to those in remission. Consequently, elevated values of pro-inflammatory cytokines, among others CCL2 and 5, in this context may serve as a surrogate parameter for the persisting migration of immune cells to the site of inflammation in affected arteries (37).

Serum IL-6 is considered to be particularly important for assessing disease state and disease activity in TA (37). A presumable significance of IL-6 in the development of TA could be shown by analyzing peripheral blood mononuclear cells (PBMC) from TA patients which produced more IL-6 upon stimulation than their counterparts from individuals with Behçet's disease (37). Apart from that IL-6 was found to be upregulated in inflammatory infiltrates of affected vessels from patients with active TA (37). Monitoring IL-6, which is broadly available and can be performed at relatively low cost, could thus help tailoring therapies to individual patients.

Matrix-metalloproteases might be further suitable markers for distinguishing active and inactive TA (49). Matrix-metalloproteases (MMPs) are enzymes capable of tissue remodeling by modifying the extracellular matrix. Matrix-metalloproteases (MMPs) are found on the surface of immune cells. Consequently, higher MMP levels are required in active inflammatory diseases, since the internal elastic lamina of affected vessels needs to be surmounted in order to allow leukocytes to proceed toward the lamina intima (38).

In addition, low values of the soluble receptor for advanced glycation end products (sRAGE) were suggested as an indicator of active TA (50). sRAGE are membrane spanning receptors and belong to the entity of immunoglobulins (51). Activated cells, e.g., macrophages, release ligands which bind to RAGE, which results in low levels of sRAGE. There are limitations of the mentioned studies: All examinations were performed with specimens from the aorta, limiting potential findings to this part of the vasculature (46). Therefore, a broader range of vessels and cell types should be investigated in future studies.

Similar to GCA, PTX-3 was also found to be involved in TA and might help to distinguish active patients with TA from those in remission (52). One noteworthy point is that an elevation of PTX-3 is not necessarily accompanied by increased CRP levels (53). The concentration of PTX-3 but not that of CRP was, according to Tombetti et al., significantly increased in TA patients who suffered from worsening arterial lesions detected by conventional and computed tomography (CT) angiography. Consequently, plasma PTX-3 levels could serve as a surrogate parameter of disease activity in arteries (48, 52, 54, 55). The reasons for an increase in PTX-3 in TA are similar to those mentioned in the context of GCA. Some authors suggest a local production of PTX-3 in affected vessels by those cells contributing to forming an inflammatory infiltrate (49, 52, 53)).

If these findings can be confirmed in larger cohorts, plasma levels of PTX-3 may in future help to differentiate between active and inactive disease (52).

Nuclear Magnetic Resonance Spectroscopy (NMR) based serum metabolomics has identified distinct profiles in individuals suffering from TA in comparison to age- and sex-matched controls (56). The best discriminatory potential was found for N-acetyl glycoprotein (NAG), an anti-inflammatory metabolite, and glutamate, a neurotransmitter often associated with inflammation (56–58). Upon follow up, changes in metabolic spectra evolved with a change in disease activity. Thus, certain metabolic profiles allow the distinction between clinically active and inactive TA patients, representing potential biomarkers for disease activity and delivering additional information which can serve as a guide to therapy (56). Future studies should further investigate these findings in larger cohorts with a longer follow up duration.

Yilmaz et al. found that plasma levels of unacylated and acylated ghrelin (growth hormone release inducing), a peptide hormone which regulates appetite and energy use, could be of use for intermittently evaluating the activity of TA and identifying the best possible way to treat TA patients. Furthermore, serum leptin levels, with leptin diminishing the feeling of hunger, and the leptin/ghrelin ratio might help to assess disease activity (59). Other studies confirm a bidirectional relationship between Ghrelin, Leptin, and inflammation. (60).

A potential biomarker which is supposed to be informative with regard to the effects of therapy on patients with TA treated with glucocorticoids and tumor necrosis factor-alpha inhibitors was identified by Serra et al. in the form of neutrophil gelatinase-associated lipocalin (NGAL) that modulates the activity of MMP-9 (61). NGAL plasma concentration has been shown to be associated with diseases of the vasculature (62). Furthermore, as mentioned above, MMP levels are known to be increased in inflammation so that changes in NGAL levels can be expected. Apart from the low number of patients an important limitation of the studies is the lack of prospective data.

Further possible biomarkers for TA comprise certain autoantibodies, e.g., anti-ferritin antibodies and anti-endothelial cell antibodies (AECA) (63). Antibodies against Annexin V (AA5A), a factor which contributes to the regulation of (endothelial) cell apoptosis, were identified in a certain percentage of individuals with TA and were associated with AECA, so that AA5A represents another potential biomarker for the management of TA (48, 64). Further data suggest that AECA, which are capable of initiating apoptosis of endothelial cells, are

crucially involved in vascular damage observed in TA patients (65–67). The majority of AA5A associated disorders, e.g., systemic lupus erythematosus, and rheumatoid arthritis exhibit AECA as well (64, 68–73). Therefore, AA5A has been proposed as one of the antigen targets of AECA (64). Nonetheless, the actual antigens of AECA have not yet been identified. The differences between isotypes of AECA need to be elucidated in the future. Furthermore, studies on the factors triggering the formation of AA5A and their role under physiological and pathological conditions are required (64).

Dogan et al. focused on markers of destructive and reconstructive processes of the endothelium, such as circulating endothelial cells (CEC), circulating endothelial progenitor cells (CEPC) and vascular endothelial growth factor (VEGF) (49). According to the corresponding study, elevated levels of CEC were detected in patients with TA. Besides, CEC levels showed a slightly positive correlation with CRP levels. Only CEPC and VEGF levels turned out to assume higher values in active compared to inactive patients. Thus, these two markers may correlate with disease activity (74). These findings are based on the following considerations: Systemic vasculitis is, among others, due to endothelial injury (75, 76). This injury causes the detachment of mature endothelial cells, called CEC (74). CEPCs are required for tissue repair in response to various cytokines and growth factors, e.g., VEGF (74).

A limitation of the presented study is that treatment effects on these parameters have not been evaluated. Further larger and prospective studies are required to verify the generated data.

Further promising findings were reported by Goel et al. (77). At the baseline assessment of a longitudinal single center study, median serum myeloid-related protein 8/14 (MRP 8/14) levels, also known as calprotectin, was found to be increased in subjects suffering from TA compared to healthy subjects. In addition, active disease states were characterized by higher MRP 8/14 levels when compared to stable disease states or healthy controls. MRP 8/14 is part of a group of cytosolic calcium-binding protein family called S100 (78). During the course of disease, changes in serial MRP 8/14 levels were linked to disease activity, no matter what the administered glucocorticoid dose has been (77), so that MRP 8/14 has been proposed as another prognostic biomarker in TA (77).

Finally, Nair et al. identified serum amyloid A (SAA), an apolipoprotein which belongs to the group of acute phase proteins, as a biomarker to evaluate disease activity and treatment response in TA (79). At baseline, there were higher SAA levels in individuals with TA than in healthy controls, and also higher values in patients with active disease compared to those with stable disease. SAA exhibited a decreasing trend during follow-up in treatment responders, whereas these changes were not observed in non-responders (79). The study was limited by small sample size and a short duration of follow up (79).

Taking all the above considerations into account, we conclude that IL-6 is particularly valuable for assessing disease state and disease activity in TA. For a summary of biomarkers see **Tables 1**, **2**.

MEDIUM VESSEL VASCULITIS

Polyarteritis Nodosa (PAN)

Polyarteritis nodosa exclusively affects medium-sized vessels and is potentially associated with Hepatitis B and C virus (4). In contrast to the aforementioned vasculitides of large vessels PAN is the scarcest type of vasculitis in central Europe. General symptoms include fever, stomach, muscle, and joint pains, and myocardial infarction even in young patients. With regard to neurological complaints, peripheral neuropathy belongs to the most frequent organ manifestations, mostly in the form of mononeuritis multiplex. Also, symmetrical sensorimotor polyneuropathies or an affection of nerve plexi may occur (80). A combination of polyneuropathy in conjunction with Livedo reticularis is highly suspicious of PAN. CNS manifestations in PAN include ischemic stroke, intracerebral and subarachnoid hemorrhage and seizures (4). It has been demonstrated that recessive loss-of-function mutations affecting the gene which encodes adenosine deaminase 2 (ADA2) might lead to polyarteritis nodosa vasculopathy (81).

As far as the pathogenesis of the disease is concerned Shimojima et al. showed an expansion of T-helper cells and an impaired function of regulatory T cells (82). These findings suggest that PAN results, among others, from defects in T-cell-mediated immunity (82). The changes might be due to insufficient suppressive abilities of regulatory T cells with regard to $CD4^+$ T cells and an impaired cytotoxic T-lymphocyte-associated Protein 4- (CTLA-4-) expression of regulatory T cells. CTLA-4 is essential for the inhibition of the proliferation of $CD4^+$ T cells, i.e., T-helper cells. In order to better understand the underlying pathomechanisms, larger cohorts need to be examined.

Manolov et al. found higher levels of plasma VEGF (see remarks on TA) in subjects with vasculitic neuropathy compared to healthy controls (65). This is why plasma VEGF levels could be of use in predicting vasculitic neuropathy (65). However, this finding does not only apply to PAN and the number of included patients was extremely low so that the current practical benefit of this biomarker is very limited.

In PAN patients with cutaneous manifestations, Okano et al. suggested that anti-phosphatidylserine-prothrombin complex (anti-PSPT) antibodies could be regarded as a biomarker for the existence of PAN and therefore support making an early diagnosis (83). These antibodies turned out to decrease to lower levels after treatment with cyclophosphamide and glucocorticoids in comparison with the pre-treatment levels (83). Mechanistically, it is assumed that prothrombin binds to apoptotic endothelial cells and phosphatidylserine (83). The resulting complexes are thought to trigger the production of anti-PSPT antibodies resulting in the development of PAN (83). Apart from that, deteriorations of the clinical disease course might be associated with higher levels of anti-moesin-antibodies. Moesin is an intracellular protein connecting cell membrane and cytoskeleton (83). Anti-moesin antibodies have been suspected to exacerbate PAN via antiphospholipid antibodies, such as anti-PSPT antibodies (83). However, these findings need to be validated in a prospective study.

There have been few studies on biomarkers in polyarteritis nodosa. Autoantibodies against lysosomal-associated membrane protein-2 (LAMP-2) showed an association with dermatological signs of the disease, but in the end there was no significant difference when compared to values measured in healthy controls (66). LAMP-2 is a component of the lysosomal membrane. It has been assumed that LAMP-2 plays a role in the pathogenesis of vasculitis (66). Mechanistically, Takeuchi et al. hypothesize that anti-LAMP-2-antibodies bind to neutrophils, which then infiltrate small vessels of the skin (66). The main limitation of the study consists in the fact that the association with LAMP-2-antibodies seems to exclusively refer to cutaneous manifestation.

To sum up, the tested biomarkers either refer to cutaneous manifestations or bear the potential to predict vasculitic neuropathy, not only in PAN. With regard to the latter aspect, the corresponding study design does not allow to call VEGF an established biomarker. For a summary of biomarkers see **Tables 1**, **2**.

SMALL VESSEL VASCULITIS

Granulomatosis with polyangiitis (GPA), Microscopic polyangiitis (MPA), and eosinophilic granulomatosis with polyangiitis (EGPA), previously known as Churg-Strauss syndrome, form the group of ANCA (anti-neutrophil cytoplasm antibody)-associated vasculitides (AAV). The AAV, as well as cryoglobulinemic vasculitis, Ig A vasculitis, and Behçet's disease, potentially affecting all types of blood vessels, will be considered in this chapter.

Before focusing on certain subtypes, biomarkers relevant for AAV in general are reviewed: GPA and MPA patients in remission were shown to have higher levels of $CD25^+$ regulatory B cells in proportion to individuals with active vasculitis (67). CD25 is the α-subunit of the Interleukin-2-receptor, which influences the binding process between receptor and ligand. $CD25^+$ B cells are therefore supposed to have regulatory functions in the mentioned vasculitides (67). To confirm or disprove the role of regulatory B cells as a marker of AAV these shortcomings should be overcome in future investigations.

Effective ways to predict relapse rates have been discovered in both GPA and microscopic polyangiitis. First, anti-MPO positive patients showed lower relapse rates than anti-PR3 positive subjects (84–86). Second, a specific gene expression signature in $CD8^+$ cells was identified, which seems to predict relapses (87): Transcriptional profiling analysis has revealed that $CD8^+$ T cell expression may represent a tool to divide patients into two distinct subgroups (relapse/active disease vs. remission/stable disease) (87, 88). The group of patients with a poor prognosis was characterized by a subset of genes playing a role in the IL-7 receptor pathway and T cell receptor signaling. The $CD8^+$ T cell memory cell population, which has been suspected to promote disease relapses, was also expanded in this group. A possible explanation of these observations could be that altered gene expression in naïve CD 8^+ T cells might be the result of genetic modifications in the phase of T cell maturation in the thymus (87, 89–91). As a reaction to antigen exposure, this could lead to T cell proliferation, at least in part via signaling cascades involving IL-7 receptor and T cell receptor, resulting in an increasing number of memory cells (92, 93). In order to use this information to individualize the therapy in AAV depending on a patient's classification as "active" or "stable," a prospective clinical study is required.

Moon et al. identified the CRP to serum albumin ratio (CAR) as an independent predictor of all-cause mortality in patients suffering from AAV with a similar potency as diabetes mellitus (94). Notably, the combined occurrence of CAR $\geq$ 10.35 and diabetes mellitus had a higher mortality, regardless of the actual reason, than the lack of these characteristics (94). These observations might have the following reasons: Chronic inflammation leads to increased IL-6 release, which increases the levels of CRP in the peripheral circulation" (94, 95). Given that IL-6 also diminishes the hepatic albumin production, the CAR is altered in a specific manner (94). The limitations of this study consist in the small sample size derived from a single center, its retrospective character, and the lack of a clear cut-off value of CAR to predict all-cause mortality in patients with AAV (94).

In AAV patients, myeloperoxidase-(MPO-)ANCA levels returned to values within normal limits during a period of 6 months after the initiation of remission induction therapy. A reappearance of MPO-ANCA could be detected in 40% of these individuals and occurred more often in relapsing subjects than in age- and sex-matched non-relapsing controls (96). Therefore, the reappearance of MPO-ANCA might be a biomarker which bears the potential to predict a relapse in individuals "with MPO-ANCA-positive AAV in" remission (96). Becoming ANCA-negative before maintenance therapy has been initiated was connected to a reduced risk of relapse (96). The frequency of relapses in general is much higher in PR3-ANCA- than in MPO-ANCA-positive disease, whereas there is a reverse relation with regard to mortality.

The so called delta neutrophil index (DNI), a simultaneous view at the number of immature granulocytes and the consumption of neutrophil granulocytes, correlates with the Birmingham vasculitis activity score at diagnosis—an instrument which helps assessing disease activity in patients with PSV (97). DNI values $\geq$0.65% were shown to be a surrogate parameter for a difficult progression of AAV and relapse in GPA and MPA during the observation period (97). This connection may be the result of the following considerations: T cells and macrophages release inflammatory cytokines that prime neutrophils and cause an increase in adhesion molecules on neutrophils and endothelial cells. ANCA promote the interaction of neutrophils and endothelial cells, which results in the diapedesis of neutrophils through the vascular cell layers. Finally, activated neutrophils induce vasculitis by reactive oxygen radicals and degranulation (97–104).

Another potential biomarker for disease activity is the tissue inhibitor of metalloproteinase 1 (TIMP1). TIMP1 is responsible for the regulation of MMPs (105–107). In accordance with MMPs, TIMP1-levels increase in inflammatory states. Additionally, unlike CRP, TIMP1-levels were significantly higher in individuals suffering from active AAV than in infected subjects

without disease activity (108). Therefore, TIMP1 can be used to distinguish between AAV with mild activity and remission.

Autoantigen gene loci in ANCA-associated vasculitis Proteinase 3 (PRTN3) and MPO were found to undergo epigenetic modifications, which correlated with disease activity and with PR3 and MPO expression. Epigenetic changes in general may comprise DNA methylation, histone modifications, and non-coding RNA (109–111). Thus, it appears that not only mutations, i.e., changes in the DNA sequence, may have far-reaching consequences for the manifestation of certain diseases. It still has to be elucidated which factors cause certain epigenetic modifications resulting in AAV and, maybe, how they can be avoided or prevented.

Further biomarkers for different types of AAV are, among others, distinct cytokine profiles of PR3-AAV, i.e., IL-6, granulocyte-macrophage colony-stimulating factor (GM-CSF), IL-15, IL-18, CXCL (C-X-C motif chemokine) 8/IL-8, CCL-17/thymus and activation-regulated chemokine, IL-18 binding protein, soluble IL-2 receptor α (sIL-2Rα), and nerve growth factor ß" (NGF-ß). Cytokine profiles of MPO-AAV comprise soluble IL-6 receptor, soluble tumor necrosis factor receptor type II (sTNFRII), neutrophil gelatinase-associated lipocalin (NGAL), and soluble intercellular adhesion molecule 1. Osteopontin, sTNFRII, and NGAL can be attributed to MPA, whereas IL-6, GM-CSF, IL-15, IL-18, sIL-2Rα, and NGF-ß can be attributed to GPA (112). Although these biomarkers bear the potential to improve the handling of ANCA-associated vasculitides, not all of them are suitable for everyday use.

Data derived from the RAVE (Rituximab in ANCA-Associated Vasculitis) trial allow the following conclusions: Patients treated with rituximab, who were anti-PR3 positive and exhibited an increase of calprotectin serum levels between the start of data collection and month 2 or month 6, exhibited a higher risk of relapse at 18 months. Hence, serum calprotectin might guide more intensive or prolonged treatment (113).

Furthermore, anti-PTX3 antibodies were frequently detected in AAV patients and antibody levels were increased in comparison to healthy controls. Comparing the states of remission and active disease, anti-PTX3 antibody values turned out to be higher in the latter case (114). In summary, anti-PTX3 antibody levels allow to distinguish between differential diagnoses and to evaluate disease activity.

Simon et al. hypothesize that Anti-PTX3 autoantibodies attract PTX3-expressing apoptotic neutrophils and enhance their phagocytosis (114). The interaction of PR3- and MPO-expressing neutrophils and ANCA induces phagocytosis and the synthesis of pro-inflammatory cytokines (114–116). Additionally, PTX3 can also be found on the surface of endothelial cells, which, in case of endothelial cell injury, may attract immune cells (114). It still remains to be examined whether the immunogenic capacity of apoptotic cells depends on anti-PTX3 and in how far there is an effect on disease duration (114).

Among others, DNI and CAR seem to be promising, but further studies are required to validate existing findings. For a summary of biomarkers see **Tables 1**, **2**.

Granulomatosis With Polyangiitis (GPA)

GPA is a rare form of small vessel vasculitis with an incidence rate of 0.9/100,000/year that affects both sexes equally (4). In the early stage, local inflammatory processes accompanied by granuloma formation take place in the respiratory tract and later on the disease spreads in terms of a generalization into small vessel vasculitis (117, 118). Leading symptoms in the early stadium of GPA is a bloody and barky nasal discharge. As soon as GPA generalizes, the spectrum of potential manifestations includes general symptoms and an affection of the lungs (therapy-resistant pneumonia with coughing, dyspnea, and hemoptysis), the kidneys in terms of glomerulonephritis, the skin in the form of various efflorescences, the eyes (conjunctivitis, episcleritis), the heart (pericarditis, vasculitis of the coronary arteries, cardiomyopathy), and the nervous system. Furthermore, a saddle nose is a symptom of advanced GPA. The latter can be affected by peripheral neuropathies, polyneuropathies, as well as mononeuritis multiplex. These peripheral neuropathies can be the initial disease manifestation of GPA and of other AAV (119). Therefore, neuropathies of unknown etiology should be inspected for signs of AAV, especially when typical stigmata of AAV are present. In AAV patients, peripheral neuropathy manifestation is associated with a higher number of affected organs, an increased ANCA-titer and a more severe disease course compared to individuals without peripheral neuropathy (120, 121). Cerebral small vessel vasculitis is a rather scarce phenomenon in these patients. Additionally, GPA patients might suffer from pachymeningitis and granulomas of the pituitary gland. GPA is associated with ANCA, above all PR3-ANCA, in 50% of cases in the early, local stadium, and in at least 90% of cases in a later, more generalized stage (122–124).

Biomarkers already in use for assessing disease activity and predicting flares are ESR, CRP, anti-PR3, and anti-MPO titers but, as already mentioned, their informative value is limited, since they are much less useful in evaluating the activity of GPA in individuals, in whom a diagnosis has already been made (3). So far, useful markers of inflammation, angiogenesis, tissue damage, and repair have been identified. Observing MMP-3, TIMP-1, and CXCL13 indicated significant differences between groups of patients. Nonetheless, due to the poor correlation of the markers among each other it has been suggested that a combination of these biomarkers might be the most promising approach (125–127). CXCL13 is a chemokine that attracts immune cells to the site of inflammation. The reasons for increased CXCL13 levels are not fully understood, but high CXCL13 levels have been linked to B cell malfunction (127). Furthermore, sRAGE are considered to mirror the cumulative burden of granulomatous inflammation in GPA, so that sRAGE may in future be established as a mean of assessing disease activity (128).

Further studies are required to detect the changes of sRAGE over time with treatment and exacerbations of the disease.

In patients who receive rituximab, the simultaneous consideration of B cell reconstitution after depletion due to the therapy and ANCA-PR3 levels could fulfill the function of a biomarker for a GPA relapse, given that Cartin-Ceba et al. observed that all occurring relapses in the cohort under

investigation were accompanied by an increase in B cells, preceded by an increase in ANCA-PR3 levels (129) (for a summary of biomarkers, see **Tables 1**, **2**).

Hitherto there are no directly applicable biomarkers in GPA.

Microscopic Polyangiitis (MPA)

Microscopic polyangiitis (MPA) shares some characteristics with GPA regarding the clinical manifestations. Being a necrotizing inflammatory process of small vessels it mostly affects the kidneys and, less often, the lungs, the skin, and the nervous system (4). The latter is mainly affected by peripheral neuropathy, mostly mononeuritis multiplex, by intracranial hemorrhage, seizures, headache and cerebral vasculitis. MPA is strongly associated with ANCA, especially (myeloperoxidase) MPO-ANCA, in 75% of all cases.

Saito et al. demonstrated that carbonic anhydrase III (CAIII) antibodies had a significantly higher prevalence in MPA patients in comparison to healthy controls. Additionally, the authors report, especially in proportion to antibody-negative subjects, elevated values of activity scores for vasculitic disorders in those cases of MPA which came along with anti-CAIII antibodies (130). Therefore, these antibodies might facilitate diagnosing MPA in ANCA-negative patients (70% of MPA patients are pANCA positive) and for assessing disease activity (130). Carbonic anhydrases are zink metalloenzymes that catalyze the hydration of carbondioxide and are present in red skeletal muscle. It is suggested that CA III plays a role in intracellular signaling, particularly in response to oxidative stress (131, 132). Possibly, anti-CAIII-antibodies protect cells from oxidative damage during inflammation (130). The informative value of the results is limited to the low number of patients, highlighting the necessity of future studies involving a higher number of patients.

Hitherto there are no directly applicable biomarkers in MPA.

Eosinophilic Granulomatosis With Polyangiitis (EGPA)

Eosinophilic granulomatosis with polyangiitis (EGPA), previously known as Churg-Strauss syndrome, can be briefly characterized as a granulomatous, necrotizing vasculitis with eosinophilia that is accompanied by pulmonary manifestation with severe asthma attacks as the leading symptom. An ANCA-association, usually MPO-ANCA, is given in 40% of all cases (133). Nervous system manifestations comprise vasculitis of the central nervous system with impaired consciousness as well as sensorimotor deficits. Moreover, EGPA may result in allergic rhinitis/sinusitis, myocarditis, and purpura.

After the initiation of treatment, eosinophilia, the hallmark of EGPA, is not an appropriate biomarker for disease activity, since the eosinophilic cell count tends to drop rapidly as soon as glucocorticoids are administered (134). It has been demonstrated that proteins related to eosinophilia, first of all eoxtaxin-3, and to Th2 immune response in general, particularly IgG4 and CCL17/TARC, were elevated in active EGPA. This elevation was also found when EGPA was compared to inactive disease, other diseases characterized by vasculitis or hypereosinophilia, and healthy controls (135–138). Eotaxins are chemokines which contribute to the accumulation and maturation of eosinophils (136). CCL17/TARC is a chemokine that is released by dendritic and endothelial cells. It is involved in the targeted attraction of activated Th2 lymphocytes to affected foci (135). Further investigations are necessary to increase knowledge on additional characteristics of eotaxin-producing cells in EGPA (136). Higher IgG4 levels might be caused by activated Th2 lymphocytes but the actual pathological role of IgG4 in EGPA is still unclear.

In a cohort of refractory and relapsing EGPA patients treated with rituximab, individuals exhibiting ANCA had a better chance to reach the state of remission (139).

Eotaxin-3, IgG4, and CCL17/TARC are promising future biomarkers, but they are not completely understood yet. For a summary of biomarkers, see **Tables 1**, **2**.

Cryoglobulinemic Vasculitis (CV)

Cryoglobulinemic vasculitis (CV) is a rare disease affecting primarily small vessels due to the formation of immune-complexes, and is accompanied by Hepatitis C virus infection in the large majority of all cases. The main symptoms are purpura, ulcerations, arthritis, and, as a late symptom or in severe courses, glomerulonephritis. With regard to neurological affliction, patients have polyneuropathy and less frequently focal neurological signs resulting from cerebral manifestations (140). Cryoglobulinemic vasculitis is mainly characterized by the combination of arthritis, purpura, and polyneuropathy, in conjunction with complement consumption (low C4 levels) and the evidence of rheumatoid factor (141).

Monoclonal rheumatoid factors (mRF) carrying the WA cross-idiotype (Xid) are of major importance in the pathogenesis of cryoglobulinemic vasculitis in individuals with hepatitis C virus (HCV) infection (142). When the WA Xid is found, individuals without symptoms but with HCV infection can be shown to exhibit WA B cells (142). Consequently, WA B cells in asymptomatic individuals with HCV infection might represent a marker for the development of CV (142). Furthermore, B-cells expressing VH1-69 were considered to be the target of treatment of infectious CV. Therefore, using this cell population as a biomarker might provide information on the activity of CV and response to treatment. A possible future perspective consists in the development of an anti-WA Xid antibody as a method for everyday medical use (142). Maybe novel treatment strategies can be derived from such antibodies.

A further study showed that patients with HCV-related mixed cryoglobulinemia (HCV-MC) exhibited significantly higher mean IL-6 values compared to healthy controls and individuals suffering from HCV chronic hepatitis without concomitant cryoglobulinemia (HCV^+). IL-6 was also elevated in cryoglobulinemic subjects with active vasculitis, thus representing potential indicator for this state (143). A hallmark of HCV-MC is the synthesis of immune-complexes, primarily cryoglobulins incorporating HCV, evoking vasculitis (143). As a consequence, IL-6 levels rise and enhance inflammation (143). However, the prognostic significance of IL-6 in HCV-MC needs to be examined in larger prospective studies (143).

Moreover, increased values of CXCL10 and TNF-alpha were measured in individuals with HCV-associated cryoglobulinemia (144). In HCV-MC patients, active vasculitis was associated with

increased CXCL10 values (144). C-X-C motif chemokine 10 (CXCL10), also known as Interferon gamma-induced protein 10 (IP-10) or small inducible cytokine B10, is a chemokine relevant for chemoattraction of immune cells (144). It is hypothesized that HCV induces the production of CXCL10, which in turn contributes to the development of chronic hepatitis C (144, 145). Further investigations comprising higher numbers of patients will have to test the potential of CXCL10 to predict the disease course of HCV-MC patients and guide the treatment (144).

Hitherto there are no clinically proven biomarkers. For a summary of biomarkers see **Tables 1**, **2**.

Ig A vasculitis

Ig A vasculitis, a vasculitis of small vessels driven by immune complexes, represents the most common vasculitis in childhood (4). Immunoglobulin A (IgA) plays a pivotal role in the disease. Typical clinical manifestations are IgA-nephritis, gastrointestinal symptoms such as stomach pain and hematochezia, purpura, and nephritis. The disease can be associated with cerebral ischemia, intracranial hemorrhage, diffuse cerebral edema, peripheral neuropathies, facial nerve paresis, and Guillain-Barré syndrome (146). Neurological complaints, however, are a rather scarce manifestation of Ig A vasculitis (147).

In pediatric patients with Ig A vasculitis, white blood cells (WBC), serum levels of CRP, IL-6, and SAA (amyloid A) showed a significant increase compared to healthy individuals (148). In addition, a complex serum biomarker index (SAA+IgA/4000+IgM/4000x0.4CRPmeanvalueCRPi) is significantly higher in HSP patients compared to healthy controls (148). The discrimination of these states is enabled by the integration of biomarkers specific and sensitive for Ig A vasculitis, such as SAA, and other biomarkers also connected to inflammatory processes in general, i.e., CRP. The biomarker index can be easily calculated and the number of patients exceeded 100 individuals so that it seems ready for use in discriminating patients with Ig A vasculitis and septicemia or the absence of one of these disorders.

High performance liquid mass spectrometry (HPLC-MS) revealed that levels of fecal secondary colonic bile acids, deoxycholic acid, and lithocholic acid are significantly lower in children with Ig A vasculitis in the acute stage and in remission than in healthy controls (149) (for a summary of biomarkers, see **Table 1**).

The biomarker index is an already available tool that can be used in the treatment of patients with IgA vasculitis.

Behçet's Disease (BD)

Behçet's disease (BD) differs from the aforementioned vasculitides, since both arterial and venous blood vessels of any diameter can be affected. There is a strong association with human leukocyte antigen (HLA) B51 and the leading symptom consists of oral and genital aphthae (4). The peripheral nervous system is rarely affected by polyneuropathies. Manifestations in the central nervous system are divided into a parenchymatic and a non-parenchymatic neurovascular type. The parenchymatic type is characterized by bihemispheric lesions which can cause hemiparesis, hemihypesthesia, vision field losses, seizures, movement disorders, speech disorder, and Parkinson-like symptoms. Furthermore, aseptic meningitis and affections of the brain stem with cranial nerve paralysis, sensorimotor disturbances, and cerebellar symptoms may occur (150–153). The neurovascular type of BD comprises sinus vein thrombosis and increased cerebral pressure, resulting in headache, focal neurological signs, seizures, papilledema, impaired consciousness, and paralysis of the sixth cranial nerve. The affection of arteries may lead to aneurysms, dissections, and consecutive intracranial hemorrhage or cerebral infarction. Peripheral neurological manifestation may consist of Guillain-Barré syndrome, polyneuropathy, autonomous neuropathy, and mononeuritis multiplex (150–153).

In a genome wide association study, the central role of HLA-B51 in regard to BD susceptibility has been confirmed (154). Apart from the connection to HLA-A and HLA-C, BD susceptibility was also associated with cytokines and danger signals IL-10, IL-23R, CCR1, STAT4, KLRC4, GIMAP2/GIMAP4, and UBAC2 genes. These findings hint at an impaired response to danger signals of the human organism and impaired immunological processes in BD patients (154). The presence of HLA-B51 is known to be accompanied by a marked increase in the risk of developing Behcet's disease, but the underlying pathophysiologic mechanisms have not been fully elaborated (154). Case-control studies with higher number of participants could help to elucidate connections between genetic attributes and certain phenotypes of BD (154).

The fact that not only blood but also other body fluids can contribute to the development of new biomarkers was underlined by Ahn et al, who distinguished BD patients from healthy individuals by employing a group of 10 urine derived metabolites, i.e., guanine, pyrrole-2-carboxylate, 3-hydroxypyridine, mannose, l-citrulline, galactonate, isothreonate, sedoheptulose, hypoxanthine, and gluconic acid lactone (155). Similarly, a panel of five metabolic markers derived from serum, i.e., decanoic acid, fructose, tagatose, linoleic acid, and oleic acid, were found to be potential biomarkers of BD with a sensitivity of 100% and a specificity of 97.1% (156). Future studies should include larger sample sizes in order to confirm the results. Apart from that, future studies should take the circadian rhythm of certain metabolites and their dependence on other factors, such as physical activity, into consideration (156).

The expression of Tissue Factor (TF) by microparticles was experimentally shown to contribute to the development of thrombosis (157). Using flow cytometry, it has been demonstrated that the total number of plasma microparticles was elevated in BD patients compared to healthy controls, as were microparticles characterized by TF and Tissue Factor Pathway Inhibitor (TFPI) (157). BD patients who had already presented with thrombosis in the past exhibited elevated counts of total and TF positive microparticles in comparison to individuals without thrombosis, but showed a lower percentage of TFPI positive microparticles. In conclusion, microparticles characterized by TF are elevated in BD and a discrepancy or impaired balance between TF and TFPI could represent a risk factor for thrombosis (157). In order to improve the knowledge about the usefulness

of these markers, larger and prospective studies, e.g., in endemic regions, are required.

Yoshioka et al. analyzed protein profiles of peripheral blood mononuclear cells (PBMCs) and compared them to profiles from patients with rheumatoid arthritis (RA) and Crohn's disease (CD), and to healthy controls (HC) (158). Tyrosine-protein phosphatase non-receptor type 4, threonine synthase-like 2, and ß-actin were identified as possible biomarker candidates for BD, since they can be applied to discriminate inflammatory bowel disease from BD and other diseases (158). Tyrosine-protein phosphatase non-receptor type 4 binds to cytoskeletal proteins and is involved in cellular responses to cytokines. Threonine synthase-like 2 exacerbates inflammation, can act as a cytokine and can promote the production of IL-6 in osteoblasts (158, 159). ß-actin is a structural protein which represents a part of the sarcomere of muscle fibers. The changes in ß-actin levels may be due to structural changes in the actin cytoskeleton as soon as T cells are activated in BD (158). In order to learn more about the significance of the identified proteins, the analysis of the protein expression of different kinds of immune cells may be of interest with regard to the pathophysiological mechanisms underlying BD. By doing so, novel biomarkers for everyday use could be developed.

Sota et al. reported that serum amyloid-A (SAA) levels can be useful to predict the affection of organs and repetitive affections of the eyes, but they also found that SAA cannot serve as a surrogate parameter for disease activity (160). SAA plays a role in the acute phase reaction and is frequently elevated in autoimmune disorders. Some authors suggest that SAA interacts with certain cytokines promoting inflammation, e.g., IL-1ß, which might be involved in the development of BD (161, 162). Future studies should be designed as prospective investigations, including a control group because these features are lacking in Sota's study.

A further study identified potential antigens in circulating immune complexes of BD patients but not in those of healthy subjects. Tubulin-α-1c is such an antigen and antibodies directed against it were increased in individuals with BD in comparison to healthy controls and disease controls (systemic lupus erythematosus, recurrent aphthous ulcers, AAV, and TA). In diagnosing BD, the tubulin-α-1c antibody had a sensitivity of 61.4% and a specificity of 88.4% (163). Additionally, an association of anti-tubulin-α-1c with deep venous thrombosis and erythema nodosum, and a significant correlation with the extent of inflammatory processes in BD and indicators of disease activity, such as ESR, CRP and BVAS (Birmingham Vasculitis Activity Score) were found (163). As part of the cytoskeleton, tubulins maintain the shape and structure of cells, GTPase activity and intracellular movement (163). Tubulin-α-1c was moreover shown to increase VEGF levels and cause endothelial damage under vasculitic conditions and in cases of thrombosis (163). However, precise mechanisms have not been elaborated.

As far as the assessment of disease activity in BD is concerned, a substantial gain in information resulted from the analysis of the platelet to lymphocyte ratio (PLR) and the lymphocyte to monocyte ratio (LMR). The PLR was remarkably higher in BD patients, whereas the LMR assumed lower values in subjects with BD compared to controls (164). When comparing active and inactive BD, active BD was characterized by significantly higher PLR, ESR and highly sensitive CRP. Furthermore, PLR and LMR were demonstrated to be independent factors for BD (164). To sum up, PLR may be useful as a novel biomarker to evaluate disease activity in BD which is not expensive but can be easily used. Current data derives from a cross-sectional analysis in a single center. Future studies should be performed in multiple centers over a longer period of time. Beyond, treatment effects should also be evaluated (164).

In summary, there are not no sufficiently tested and established biomarkers for BD apart from HLA B51. For a summary of biomarkers see **Tables 1**, **2**.

CONCLUSION

Biomarkers are of importance in improving the diagnostic process, the treatment, and the prognosis for patients suffering from various forms of vasculitis. Nonetheless, the majority of the findings reviewed in this article do not exclusively apply to neurological manifestations of vasculitides. Further studies that employ appropriate control groups, use precise definitions for disease states such as "active" and "remission," and clearly outline the type of neurological manifestation involved are needed to guide our use of biomarkers in vasculitides of the nervous system.

AUTHOR CONTRIBUTIONS

DS conceptualized and wrote the manuscript. AS-P contributed to writing the manuscript. CB, LM, CK, and SM gave valuable suggestions for improving the manuscript. JM conceptualized the manuscript and contributed to writing the manuscript.

REFERENCES

1. Beuker C, Schmidt A, Strunk D, Sporns PB, Wiendl H, Meuth SG, et al. Primary angiitis of the central nervous system: diagnosis and treatment. *Ther Adv Neurol Disord*. (2018) 11:1–16. doi: 10.1177/1756286418785071
2. Strimbu K, Tavel JA. What are biomarkers? *Curr Opin HIV AIDS*. (2010) 5:463–6. doi: 10.1097/COH.0b013e32833ed177
3. Monach PA. Biomarkers in vasculitis. *Curr Opin Rheumatol*. (2014) 26:24–30. doi: 10.1097/BOR.0000000000000009
4. Magnus T, Melms A, Kötter I, Holle JU. Neurological manifestations of vasculitis and primary central nervous system vasculitis. *Zeitschr Rheumatol*. (2012) 71:551–63. doi: 10.1007/s00393-012-0957-0
5. Birnbaum J, Hellmann DB. Primary angiitis of the central nervous system. *Arch Neurol*. (2009) 66:704–9. doi: 10.1001/archneurol.2009.76
6. Berlit P, Kraemer M. Cerebral vasculitis in adults: what are the steps in order to establish the diagnosis? Red flags and pitfalls. *Clin Exp Immunol*. (2014) 175:419–24. doi: 10.1111/cei.12221
7. Mandal J, Chung SA. Primary angiitis of the central nervous system. *Rheum Dis Clin North Am*. (2017) 43:503–18. doi: 10.1016/j.rdc.2017.06.001

8. Hajj-Ali RA, Calabrese LH. Diagnosis and classification of central nervous system vasculitis. *J Autoimmun*. (2014) 48:149–52. doi: 10.1016/j.jaut.2014.01.007
9. Smith EE, Greenberg SM. β-Amyloid, blood vessels, and brain function. *Stroke*. (2009) 40:2601–6. doi: 10.1161/STROKEAHA.108.536839
10. Strunk D, Schulte-Mecklenbeck A, Golombeck KS, zu Hörste GM, Melzer N, Beuker C, et al. Immune cell profiling in the cerebrospinal fluid of patients with primary angiitis of the central nervous system reflects the heterogeneity of the disease. *J Neuroimmunol*. (2018) 321:109–16. doi: 10.1016/j.jneuroim.2018.06.004
11. Ruland T, Wolbert J, Gottschalk MG, König S, Schulte-Mecklenbeck A, Minnerup J, et al. Cerebrospinal fluid concentrations of neuronal proteins are reduced in primary angiitis of the central nervous system. *Front Neurol*. (2018) 9:407. doi: 10.3389/fneur.2018.00407
12. Thom V, Schmid S, Gelderblom M, Hackbusch R, Kolster M, Schuster S, et al. IL-17 production by CSF lymphocytes as a biomarker for cerebral vasculitis. *Neurol Neuroimmunol Neuroinflamm*. (2016) 3:e214. doi: 10.1212/NXI.0000000000000214
13. Melzer N, Harder A, Gross CC, Wölfer J, Stummer W, Niederstadt T, et al. CD4+ T cells predominate in cerebrospinal fluid and leptomeningeal and parenchymal infiltrates in cerebral amyloid β-related angiitis. *Arch Neurol*. (2012) 69:773–7. doi: 10.1001/archneurol.2011.2441
14. Cellucci T, Tyrrell PN, Pullenayegum E, Benseler SM. von Willebrand factor antigen-a possible biomarker of disease activity in childhood central nervous system vasculitis? *Rheumatology*. (2012) 51:1838–45. doi: 10.1093/rheumatology/kes156
15. Sadler JE. Biochemistry and genetics of Von Willebrand factor. *Ann Rev Biochem*. (1998) 67:395–424. doi: 10.1146/annurev.biochem.67.1.395
16. de Lind van Wijngaarden RA, van Rijn L, Hagen EC, Watts RA, Gregorini G, Tervaert JWC, et al. Hypotheses on the etiology of antineutrophil cytoplasmic autoantibody-associated vasculitis: the cause is hidden, but the result is known. *Clin J Am Soc Nephrol*. (2008) 3:237–52. doi: 10.2215/CJN.03550807
17. Falk RJ, Hoffman GS. Controversies in small vessel vasculitis-comparing the rheumatology and nephrology views. *Curr Opin Rheumatol*. (2007) 19:1–9. doi: 10.1097/BOR.0b013e328011cb80
18. Hunder GG, Bloch DA, Michel BA, Stevens MB, Arend WP, Calabrese LH, et al. The American College of Rheumatology 1990 criteria for the classification of giant cell arteritis. *Arthritis Rheumat*. (1990) 33:1122–8. doi: 10.1002/art.1780330810
19. Reinhold-Keller E, Herlyn K, Wagner-Bastmeyer R, Gross WL. Stable incidence of primary systemic vasculitides over five years: results from the German vasculitis register. *Arthritis Care Res*. (2005) 53:93–9. doi: 10.1002/art.20928
20. González-Gay MA, Blanco R, Rodríguez-Valverde V, Martínez-Taboada VM, Delgado-Rodriguez M, Figueroa M, Uriarte E. Permanent visual loss and cerebrovascular accidents in giant cell arteritis: predictors and response to treatment. *Arthritis Rheumat*. (1998) 41:1497–504.
21. González-Gay MA, García-Porrúa C, Llorca J, Hajeer AH, Brañas F, Dababneh A, et al. Visual manifestations of giant cell arteritis. Trends and clinical spectrum in 161 patients. *Medicine*. (2000) 79:283–92. doi: 10.1097/00005792-200009000-00001
22. Bottazzi B, Garlanda C, Cotena A, Moalli F, Jaillon S, Deban L, et al. The long pentraxin PTX3 as a prototypic humoral pattern recognition receptor: interplay with cellular innate immunity. *Immunol Rev*. (2009) 227:9–18. doi: 10.1111/j.1600-065X.2008.00719.x
23. Baldini M, Maugeri N, Ramirez GA, Giacomassi C, Castiglioni A, Prieto-González S, et al. Selective up-regulation of the soluble pattern-recognition receptor pentraxin 3 and of vascular endothelial growth factor in giant cell arteritis: relevance for recent optic nerve ischemia. *Arthritis Rheumat*. (2012) 64:854–65. doi: 10.1002/art.33411
24. Maugeri N, Rovere-Querini P, Baldini M, Sabbadini MG, Manfredi AA. Translational mini-review series on immunology of vascular disease: mechanisms of vascular inflammation and remodelling in systemic vasculitis. *Clin Exp Immunol*. (2009) 156:395–404. doi: 10.1111/j.1365-2249.2009.03921.x
25. Manfredi AA, Rovere-Querini P, Bottazzi B, Garlanda C, Mantovani A. Pentraxins, humoral innate immunity and tissue injury. *Curr Opin Immunol*. (2008) 20:538–44. doi: 10.1016/j.coi.2008.05.004
26. Norata GD, Marchesi P, Venu VKP, Pasqualini F, Anselmo A, Moalli F, et al. Deficiency of the long pentraxin PTX3 promotes vascular inflammation and atherosclerosis. *Circulation*. (2009) 120:699–708. doi: 10.1161/CIRCULATIONAHA.108.806547
27. Salio M, Chimenti S, De Angelis N, Molla F, Maina V, Nebuloni M, et al. Cardioprotective function of the long pentraxin PTX3 in acute myocardial infarction. *Circulation*. (2008) 117:1055–64. doi: 10.1161/CIRCULATIONAHA.107.749234
28. Lozano E, Segarra M, Corbera-Bellalta M, García-Martínez A, Espígol-Frigolé G, Plà-Campo A, et al. Increased expression of the endothelin system in arterial lesions from patients with giant-cell arteritis: association between elevated plasma endothelin levels and the development of ischaemic events. *Ann Rheum Dis*. (2010) 69:434–42. doi: 10.1136/ard.2008.105692
29. Doni A, Mantovani G, Porta C, Tuckermann J, Reichardt HM, Kleiman A, et al. Cell-specific regulation of PTX3 by glucocorticoid hormones in hematopoietic and nonhematopoietic cells. *J Biol Chem*. (2008) 283:29983–92. doi: 10.1074/jbc.M805631200
30. Hayreh SS. Ischemic optic neuropathy. *Prog Retin Eye Res*. (2009) 28:34–62. doi: 10.1016/j.preteyeres.2008.11.002
31. Roche NE, Fulbright JW, Wagner AD, Hunder GG, Goronzy JJ, Weyand CM. Correlation of interleukin-6 production and disease activity in polymyalgia rheumatica and giant cell arteritis. *Arthritis Rheumat*. (1993) 36:1286–94. doi: 10.1002/art.1780360913
32. Stone JH, Tuckwell K, Dimonaco S, Klearman M, Aringer M, Blockmans D, et al. Trial of tocilizumab in giant-cell arteritis. *N Engl J Med*. (2017) 377:317–28. doi: 10.1056/NEJMoa1613849
33. Perez-Alamino R, Maldonado-Ficco H. New insights on biomarkers in systemic vasculitis. *Curr Rheumatol Rep*. (2015) 17:12. doi: 10.1007/s11926-015-0497-0
34. Baerlecken NT, Linnemann A, Gross WL, Moosig F, Vazquez-Rodriguez TR, Gonzalez-Gay MA, et al. Association of ferritin autoantibodies with giant cell arteritis/polymyalgia rheumatica. *Ann Rheum Dis*. (2012) 71:943–7. doi: 10.1136/annrheumdis-2011-200413
35. De Smit E, Lukowski SW, Anderson L, Senabouth A, Dauyey K, Song S, et al. Longitudinal expression profiling of CD4+ and CD8+ cells in patients with active to quiescent giant cell arteritis. *BMC Med Genomics*. (2018) 11:61. doi: 10.1186/s12920-018-0376-4
36. Prieto-González S, Terrades-García N, Corbera-Bellalta M, Planas-Rigol E, Miyabe C, Alba MA, et al. Serum osteopontin: a biomarker of disease activity and predictor of relapsing course in patients with giant cell arteritis. Potential clinical usefulness in tocilizumab-treated patients. *RMD Open*. (2017) 3:e000570. doi: 10.1136/rmdopen-2017-000570
37. Savioli B, Abdulahad WH, Brouwer E, Kallenberg CG, de Souza AWS. Are cytokines and chemokines suitable biomarkers for Takayasu arteritis? *Autoimmun Rev*. (2017) 16:1071–8. doi: 10.1016/j.autrev.2017.07.023
38. Burja B, Kuret T, Sodin-Semrl S, Lakota K, Rotar Ž, Ješe R, et al. A concise review of significantly modified serological biomarkers in giant cell arteritis, as detected by different methods. *Autoimmun Rev*. (2018) 17:188–94. doi: 10.1016/j.autrev.2017.11.022
39. Arend WP, Michel BA, Bloch DA, Hunder GG, Calabrese LH, Edworthy SM, et al. The American College of Rheumatology 1990 criteria for the classification of Takayasu arteritis. *Arthritis Rheumat*. (1990) 33:1129–34. doi: 10.1002/art.1780330811
40. de Souza AWS, de Carvalho JF. Diagnostic and classification criteria of Takayasu arteritis. *J Autoimmun*. (2014) 48:79–83. doi: 10.1016/j.jaut.2014.01.012
41. Ringleb PA, Strittmatter EI, Loewer M, Hartmann M, Fiebach JB, Lichy C, et al. Cerebrovascular manifestations of Takayasu arteritis in Europe. *Rheumatology*. (2005) 44:1012–15. doi: 10.1093/rheumatology/keh664
42. Große K, Witte T, Moosig F, Hoyer BF, Lansche C, Schmidt RE, et al. Association of ferritin antibodies with Takayasu arteritis. *Clin Rheumatol*. (2014) 33:1523–6. doi: 10.1007/s10067-014-2764-2
43. Alibaz-Oner F, Yentür SP, Saruhan-Direskeneli G, Direskeneli H. Serum cytokine profiles in Takayasu's arteritis: search for biomarkers. *Clin Exp Rheumatol*. (2015) 33:32–5.

44. Noguchi S, Numano F, Gravanis MB, Wilcox JN. Increased levels of soluble forms of adhesion molecules in Takayasu arteritis1. *Int J Cardiol*. (1998) 66:S23–33. doi: 10.1016/S0167-5273(98)00145-4
45. Noris M, Daina E, Gamba S, Bonazzola S, Remuzzi G. Interleukin-6 and RANTES in Takayasu arteritis: a guide for therapeutic decisions? *Circulation*. (1999) 100:55–60. doi: 10.1161/01.CIR.100.1.55
46. Sun Y, Ma L, Yan F, Liu H, Ding Y, Hou J, et al. MMP-9 and IL-6 are potential biomarkers for disease activity in Takayasu's arteritis. *Int J Cardiol*. (2012) 156:236–8. doi: 10.1016/j.ijcard.2012.01.035
47. Pulsatelli L, Boiardi L, Assirelli E, Pazzola G, Muratore F, Addimanda O, et al. Interleukin-6 and soluble interleukin-6 receptor are elevated in large-vessel vasculitis: a cross-sectional and longitudinal study. *Clin Exp Rheumatol*. (2017) 35:102–10.
48. Sun Y, Huang Q, Jiang L. Radiology and biomarkers in assessing disease activity in Takayasu arteritis. *Int J Rheum Dis*. (2019) 22:53–9. doi: 10.1111/1756-185X.13286
49. Ishihara T, Haraguchi G, Tezuka D, Kamiishi T, Inagaki H, Isobe M. Diagnosis and assessment of Takayasu arteritis by multiple biomarkers. *Circul J*. (2013) 77:477–83. doi: 10.1253/circj.CJ-12-0131
50. Mahajan N, Dhawan V, Malik S, Jain S. Serum levels of soluble receptor for advanced glycation end products (sRAGE) in Takayasu's arteritis. *Int J Cardiol*. (2010) 145:589–91. doi: 10.1016/j.ijcard.2010.05.075
51. Neeper M, Schmidt AM, Brett J, Yan SD, Wang F, Pan YC, et al. Cloning and expression of a cell surface receptor for advanced glycosylation end products of proteins. *J Biol Chem*. (1992) 267:14998–5004.
52. Dagna L, Salvo F, Tiraboschi M, Bozzolo EP, Franchini S, Doglioni C, et al. Pentraxin-3 as a marker of disease activity in Takayasu arteritis. *Ann Intern Med*. (2011) 155:425–33. doi: 10.7326/0003-4819-155-7-201110040-00005
53. Ishihara T, Haraguchi G, Kamiishi T, Tezuka D, Inagaki H, Isobe M. Sensitive assessment of activity of Takayasu's arteritis by pentraxin3, a new biomarker. *J Am Coll Cardiol*. (2011) 57:1712–13. doi: 10.1016/j.jacc.2010.10.058
54. Park JH. Conventional and CT angiographic diagnosis of Takayasu arteritis. *Int J Cardiol*. (1996) 54:S16571. doi: 10.1016/S0167-5273(96)88785-7
55. Tombetti E, Di Chio MC, Sartorelli S, Papa M, Salerno A, Bottazzi B, et al. Systemic pentraxin-3 levels reflect vascular enhancement and progression in Takayasu arteritis. *Arthritis Res Ther*. (2014) 16:479. doi: 10.1186/s13075-014-0479-z
56. Jain A, Kumar D, Guleria A, Misra DP, Zanwar A, Chaurasia S, et al. NMR-based serum metabolomics of patients with Takayasu arteritis: relationship with disease activity. *J Proteome Res*. (2018) 17:3317–24. doi: 10.1021/acs.jproteome.8b00456
57. Haroon E, Felger JC, Jung JM, Wommack EC, Woolwine BJ, Chen X, Hu XP, et al. Increased inflammation is associated with increased glutamate in the basal ganglia of depressed patients. *Brain Behav Immun*. (2015) 49:e24. doi: 10.1016/j.bbi.2015.06.100
58. Haroon E, Miller AH, Sanacora G. Inflammation, glutamate, and glia: a trio of trouble in mood disorders. *Neuropsychopharmacology*. (2017) 42:193–215. doi: 10.1038/npp.2016.199
59. Yilmaz H, Gerdan V, Kozaci D, Solmaz D, Akar S, Can G, et al. Ghrelin and adipokines as circulating markers of disease activity in patients with Takayasu arteritis. *Arthritis Res Ther*. (2012) 14:R272. doi: 10.1186/ar4120
60. Dixit VD, Schaffer EM, Pyle RS, Collins GD, Sakthivel SK, Palaniappan R, et al. Ghrelin inhibits leptin- and activation-induced proinflammatory cytokine expression by human monocytes and T cells. *J Clin Invest*. (2004) 114:57–66. doi: 10.1172/JCI21134
61. Serra R, Grande R, Buffone G, Scarcello E, Tripodi F, Rende P, et al. Effects of glucocorticoids and tumor necrosis factor-alpha inhibitors on both clinical and molecular parameters in patients with Takayasu arteritis. *J Pharmacol Pharmacother*. (2014) 5:193. doi: 10.4103/0976-500X.136101
62. Ramos-Mozo P, Madrigal-Matute J, Vega de Ceniga M, Blanco-Colio LM, Meilhac O, Feldman L, et al. Increased plasma levels of NGAL, a marker of neutrophil activation, in patients with abdominal aortic aneurysm. *Atherosclerosis*. (2012) 220:552–6. doi: 10.1016/j.atherosclerosis.2011.11.023
63. Park M, Park Y, Jung SY, Lee KH, Lee S. Anti-endothelial cell antibodies and antiphospholipid antibodies in Takayasu's arteritis: correlations of their titers and isotype distributions with disease activity. *Clin Exp Rheumatol*. (2006) 24:S10–16.
64. Tripathy NK, Sinha N, Nityanand S. Anti-annexin V antibodies in Takayasu's arteritis: prevalence and relationship with disease activity. *Clin Exp Immunol*. (2003) 134:360–4. doi: 10.1046/j.1365-2249.2003.02282.x
65. Manolov V, Petrova I, Vasilev V. VEGF levels in diagnosis of vasculitic neuropathy. *Clin Lab*. (2014) 60:1573–7. doi: 10.7754/Clin.Lab.2013.130622
66. Takeuchi S, Kimura S, Soma Y, Waki M, Yamaguchi M, Nakazawa D,et al. Lysosomal-associated membrane protein-2 plays an important role in the pathogenesis of primary cutaneous vasculitis. *Rheumatology*. (2013) 52:1592–8. doi: 10.1093/rheumatology/ket159
67. Eriksson P, Sandell C, Backteman K, Ernerudh J. B cell abnormalities in Wegener's granulomatosis and microscopic polyangiitis: role of CD25+-expressing B cells. *J Rheumatol*. (2010) 37:2086–95. doi: 10.3899/jrheum.100074
68. Matsuda J, Saitoh N, Gohchi K, Gotoh M, Tsukamoto AM. Anti-annexin V antibody in systemic lupus erythematosus patients with lupus anticoagulant and/or anticardiolipin antibody. *Am J Hematol*. (1994) 47:56–8. doi: 10.1002/ajh.2830470112
69. Kaburaki J, Kuwana M, Yamamoto M, Kawai S, Ikeda Y. Clinical significance of anti-annexin V antibodies in patients with systemic lupus erythematosus. *Am J Hematol*. (1997) 54:209–13.
70. Nojima J, Kuratsune H, Suehisa E, Futsukaichi Y, Yamanishi H, Machii T, et al. Association between the prevalence of antibodies to β2-glycoprotein I, prothrombin, protein C, protein S, and annexin V in patients with systemic lupus erythematosus and thrombotic and thrombocytopenic complications. *Clin Chem*. (2001) 47:1008–15.
71. Satoh A, Suzuki K, Takayama E, Kojima K, Hidaka T, Kawakami M, et al. Detection of anti-annexin IV and V antibodies in patients with antiphospholipid syndrome and systemic lupus erythematosus. *J Rheumatol*. (1999) 26:1715–20.
72. Rodríguez-García MI, Fernández JA, Rodríguez A, Fernández MP, Gutierrez C, Torre-Alonso JC. Annexin V autoantibodies in rheumatoid arthritis. *Ann Rheum Dis*. (1996) 55:895–900. doi: 10.1136/ard.55.12.895
73. Sugiura K, Muro Y. Anti-annexin V antibodies and digital ischemia in patients with scleroderma. *J Rheumatol*. (1999) 26:2168–72.
74. Dogan S, Piskin O, Solmaz D, Akar S, Gulcu A, Yuksel F, et al. Markers of endothelial damage and repair in Takayasu arteritis: are they associated with disease activity? *Rheumatol Int*. (2014) 34:1129–38. doi: 10.1007/s00296-013-2937-3
75. Blake DR, Winyard P, Scott DG, Brailsford S, Blann A, Lunec J. Endothelial cell cytotoxicity in inflammatory vascular diseases–the possible role of oxidised lipoproteins. *Ann Rheum Dis*. (1985) 44:176–82. doi: 10.1136/ard.44.3.176
76. Brogan PA, Shah V, Brachet C, Harnden A, Mant D, Klein N, et al. Endothelial and platelet microparticles in vasculitis of the young. *Arthritis Rheumat*. (2004) 50:927–36. doi: 10.1002/art.20199
77. Goel R, Nair A, Kabeerdoss J, Mohan H, Jeyaseelan V, Joseph G, et al. Study of serial serum myeloid-related protein 8/14 as a sensitive biomarker in Takayasu arteritis: a single centre study. *Rheumatol Int*. (2018) 38:623–30. doi: 10.1007/s00296-017-3881-4
78. Renauer P, Sawalha AH. The genetics of Takayasu arteritis. *La Presse Méd*. (2017) 46:e179–87. doi: 10.1016/j.lpm.2016.11.031
79. Nair AM, Goel R, Hindhumati M, Jayakanthan K, Visalakshi J, Joseph G, et al. Serum amyloid A as a marker of disease activity and treatment response in Takayasu arteritis. *Rheumatol Int*. (2017) 37:1643–9. doi: 10.1007/s00296-017-3786-2
80. Jennette JC, Falk RJ, Andrassy K, Bacon PA, Churg J, Gross WL, et al. Nomenclature of systemic vasculitides. *Arthritis Rheumat*. (1994) 37:187–92. doi: 10.1002/art.1780370206
81. Navon Elkan P, Pierce SB, Segel R, Walsh T, Barash J, Padeh S, et al. Mutant adenosine deaminase 2 in a polyarteritis nodosa vasculopathy. *N Engl J Med*. (2014) 370:921–31. doi: 10.1056/NEJMoa1307362
82. Shimojima Y, Ishii W, Kishida D, Fukushima K, Ikeda S. Imbalanced expression of dysfunctional regulatory T cells and T-helper cells relates to immunopathogenesis in polyarteritis nodosa. *Modern Rheumatol*. (2017) 27:102–9. doi: 10.3109/14397595.2016.1172999
83. Okano T, Takeuchi S, Soma Y, Suzuki K, Tsukita S, Ishizu A, et al. Presence of anti-phosphatidylserine-prothrombin complex antibodies and anti-moesin

antibodies in patients with polyarteritis nodosa. *J Dermatol*. (2017) 44:18–22. doi: 10.1111/1346-8138.13491
84. Harper L, Morgan MD, Walsh M, Hoglund P, Westman K, Flossmann O, et al. Pulse versus daily oral cyclophosphamide for induction of remission in ANCA-associated vasculitis: long-term follow-up. *Ann Rheum Dis*. (2012) 71:955–60. doi: 10.1136/annrheumdis-2011-200477
85. Pagnoux C, Hogan SL, Chin H, Jennette JC, Falk RJ, Guillevin L, et al. Predictors of treatment resistance and relapse in antineutrophil cytoplasmic antibody-associated small-vessel vasculitis: comparison of two independent cohorts. *Arthritis Rheumat*. (2008) 58:2908–18. doi: 10.1002/art.23800
86. Pierrot-Deseilligny Despujol C, Pouchot J, Pagnoux C, Coste J, Guillevin L. Predictors at diagnosis of a first Wegener's granulomatosis relapse after obtaining complete remission. *Rheumatology*. (2010) 49:2181–90. doi: 10.1093/rheumatology/keq244
87. McKinney EF, Lyons PA, Carr EJ, Hollis JL, Jayne DR, Willcocks LC, et al. A CD8+ T cell transcription signature predicts prognosis in autoimmune disease. *Nat Med*. (2010) 16:586. doi: 10.1038/nm.2130
88. Lally L, Spiera R. Current therapies for ANCA-associated vasculitis. *Ann Rev Med*. (2015) 66:227–40. doi: 10.1146/annurev-med-011514-023051
89. Morley M, Molony CM, Weber TM, Devlin JL, Ewens KG, Spielman RS, et al. Genetic analysis of genome-wide variation in human gene expression. *Nature*. (2004) 430:743–7. doi: 10.1038/nature02797
90. Vezys V, Yates A, Casey KA, Lanier G, Ahmed R, Antia R, et al. Memory CD8 T-cell compartment grows in size with immunological experience. *Nature*. (2009) 457:196–9. doi: 10.1038/nature07486
91. Bevan MJ. Helping the CD8+ T-cell response. *Nat Rev Immunol*. (2004) 4:595–602. doi: 10.1038/nri1413
92. Williams MA, Bevan MJ. Effector and memory CTL differentiation. *Ann Rev Immunol*. (2007) 25:171–92. doi: 10.1146/annurev.immunol.25.022106.141548
93. Hou S, Hyland L, Ryan KW, Portner A, Doherty PC. Virus-specific CD8 + T-cell memory determined by clonal burst size. *Nature*. (1994) 369:652–4. doi: 10.1038/369652a0
94. Moon J-S, Ahn SS, Park Y-B, Lee S-K, Lee S-W. C-Reactive protein to serum albumin ratio is an independent predictor of all-cause mortality in patients with ANCA-associated vasculitis. *Yonsei Med J*. (2018) 59:865–71. doi: 10.3349/ymj.2018.59.7.865
95. Rhodes B, Fürnrohr BG, Vyse TJ. C-reactive protein in rheumatology: biology and genetics. *Nat Rev Rheumatol*. (2011) 7:282–9. doi: 10.1038/nrrheum.2011.37
96. Watanabe H, Sada K-E, Matsumoto Y, Harigai M, Amano K, Dobashi H, et al. Association between reappearance of myeloperoxidase-antineutrophil cytoplasmic antibody and relapse in antineutrophil cytoplasmic antibody-associated vasculitis: subgroup analysis of nationwide prospective cohort studies. Arthritis Rheumatol. (2018) 70:1626–33. doi: 10.1002/art.40538
97. Yoo J, Ahn SS, Jung SM, Song JJ, Park Y-B, Lee S-W. Delta neutrophil index is associated with vasculitis activity and risk of relapse in ANCA-associated vasculitis. *Yonsei Med J*. (2018) 59:397–405. doi: 10.3349/ymj.2018.59.3.397
98. Nakazawa D, Tomaru U, Suzuki A, Masuda S, Hasegawa R, Kobayashi T, et al. Abnormal conformation and impaired degradation of propylthiouracil-induced neutrophil extracellular traps: implications of disordered neutrophil extracellular traps in a rat model of myeloperoxidase antineutrophil cytoplasmic antibody-associated vasculitis. *Arthritis Rheumat*. (2012) 64:3779–87. doi: 10.1002/art.34619
99. Schreiber A, Kettritz R. The neutrophil in antineutrophil cytoplasmic autoantibody-associated vasculitis. *J Leukoc Biol*. (2013) 94:623–31. doi: 10.1189/jlb.1012525
100. Kettritz R. How anti-neutrophil cytoplasmic autoantibodies activate neutrophils. *Clin Exp Immunol*. (2012) 169:220–8. doi: 10.1111/j.1365-2249.2012.04615.x
101. Ooi JD, Chang J, Hickey MJ, Borza D-B, Fugger L, Holdsworth SR, et al. The immunodominant myeloperoxidase T-cell epitope induces local cell-mediated injury in antimyeloperoxidase glomerulonephritis. *PNAS*. (2012) 109:E2615–24. doi: 10.1073/pnas.1210147109
102. Furuta S, Jayne DRW. Antineutrophil cytoplasm antibody-associated vasculitis: recent developments. *Kidney Int*. (2013) 84:244–9. doi: 10.1038/ki.2013.24
103. Xiao H, Dairaghi DJ, Powers JP, Ertl LS, Baumgart T, Wang Y, Seitz LC, et al. C5a receptor (CD88) blockade protects against MPO-ANCA GN. *JASN*. (2014) 25:225–31. doi: 10.1681/ASN.2013020143
104. Charles Jennette J, Xiao H, Hu P. Complement in ANCA-associated vasculitis. *Semin Nephrol*. (2013) 33:557–64. doi: 10.1016/j.semnephrol.2013.08.006
105. Brew K, Nagase H. The tissue inhibitors of metalloproteinases (TIMPs): an ancient family with structural and functional diversity. *Biochim Biophys Acta*. (2010) 1803:55–71. doi: 10.1016/j.bbamcr.2010.01.003
106. Graham CH, Lala PK. Mechanism of control of trophoblast invasion *in situ*. *J Cell Physiol*. (1991) 148:228–34. doi: 10.1002/jcp.1041480207
107. Nothnick WB, Soloway P, Curry TE. Assessment of the Role of tissue inhibitor of metalloproteinase-1 (TIMP-1) during the periovulatory period in female mice lacking a functional TIMP-1 gene. *Biol Reprod*. (1997) 56:1181–8. doi: 10.1095/biolreprod56.5.1181
108. Ishizaki J, Takemori A, Suemori K, Matsumoto T, Akita Y, Sada K, et al. Targeted proteomics reveals promising biomarkers of disease activity and organ involvement in antineutrophil cytoplasmic antibody-associated vasculitis. *Arthritis Res Ther*. (2017) 19:218. doi: 10.1186/s13075-017-1429-3
109. Ciavatta DJ, Yang J, Preston GA, Badhwar AK, Xiao H, Hewins P, et al. Epigenetic basis for aberrant upregulation of autoantigen genes in humans with ANCA vasculitis. *J Clin Investig*. (2010) 120:3209–19. doi: 10.1172/JCI40034
110. Jones BE, Yang J, Muthigi A, Hogan SL, Hu Y, Starmer J, et al. Gene-specific DNA methylation changes predict remission in patients with ANCA-associated vasculitis. *J Am Soc Nephrol*. (2017) 28:1175–87. doi: 10.1681/ASN.2016050548
111. Yang J, Ge H, Poulton CJ, Hogan SL, Hu Y, Jones BE, et al. Histone modification signature at myeloperoxidase and proteinase 3 in patients with anti-neutrophil cytoplasmic autoantibody-associated vasculitis. *Clin Epigenet*. (2016) 8:85. doi: 10.1186/s13148-016-0251-0
112. Berti A, Warner R, Johnson K, Cornec D, Schroeder D, Kabat B, et al. Circulating cytokine profiles and antineutrophil cytoplasmic antibody specificity in patients with antineutrophil cytoplasmic antibody-associated vasculitis. *Arthritis Rheumatol*. (2018) 70:1114–21. doi: 10.1002/art.40471
113. Pepper RJ, Draibe JB, Caplin B, Fervenza FC, Hoffman GS, Kallenberg CGM, et al. Association of serum calprotectin (S100A8/A9) level with disease relapse in proteinase 3-antineutrophil cytoplasmic antibody-associated vasculitis. *Arthritis Rheumatol*. (2017) 69:185–93. doi: 10.1002/art.39814
114. Simon A, Subra J-F, Guilpain P, Jeannin P, Pignon P, Blanchard S, et al. Detection of anti-pentraxin-3 autoantibodies in ANCA-associated vasculitis. *PLoS ONE*. (2016) 11:e0147091. doi: 10.1371/journal.pone.0147091
115. Gilligan HM, Bredy B, Brady HR, Hébert M-J, Slayter HS, Xu Y, et al. Antineutrophil cytoplasmic autoantibodies interact with primary granule constituents on the surface of apoptotic neutrophils in the absence of neutrophil priming. *J Exp Med*. (1996) 184:2231–42. doi: 10.1084/jem.184.6.2231
116. Harper L, Cockwell P, Adu D, Savage COS. Neutrophil priming and apoptosis in anti-neutrophil cytoplasmic autoantibody-associated vasculitis1. *Kidney Int*. (2001) 59:1729–38. doi: 10.1046/j.1523-1755.2001.0590051729.x
117. Mueller A, Holl-Ulrich K, Lamprecht P, Gross WL. Germinal centre-like structures in Wegener's granuloma: the morphological basis for autoimmunity? *Rheumatology*. (2008) 47:1111–3. doi: 10.1093/rheumatology/ken202
118. Soukiasian SH, Foster CS, Niles JL, Raizman MB. Diagnostic value of anti-neutrophil cytoplasmic antibodies in scleritis associated with Wegener's granulomatosis. *Ophthalmology*. (1992) 99:125–32. doi: 10.1016/S0161-6420(92)32027-5
119. Cattaneo L, Chierici E, Pavone L, Grasselli C, Manganelli P, Buzio C, et al. Peripheral neuropathy in Wegener's granulomatosis, Churg-Strauss syndrome and microscopic polyangiitis. *J Neurol Neurosurg Psychiatry*. (2007) 78:1119–23. doi: 10.1136/jnnp.2006.111013
120. de Groot K, Schmidt DK, Arlt AC, Gross WL, Reinhold-Keller E. Standardized neurologic evaluations of 128 patients

with Wegener granulomatosis. *Arch Neurol*. (2001) 58:1215–21. doi: 10.1001/archneur.58.8.1215
121. Suppiah R, Hadden RD, Batra R, Arden NK, Collins MP, Guillevin L, et al. Peripheral neuropathy in ANCA-associated vasculitis: outcomes from the European Vasculitis Study Group trials. *Rheumatology*. (2011) 50:2214–22. doi: 10.1093/rheumatology/ker266
122. Falk RJ, Jennette JC. ANCA small-vessel vasculitis. *J Am Soc Nephrol*. (1997) 8:314–22.
123. Hagen EC, Daha MR, Hermans J, Andrassy K, Csernok E, Gaskin G, et al. Diagnostic value of standardized assays for anti-neutrophil cytoplasmic antibodies in idiopathic systemic vasculitis. EC/BCR Project for ANCA Assay Standardization. *Kidney Int*. (1998) 53:743–53. doi: 10.1046/j.1523-1755.1998.00807.x
124. Savige J, Pollock W, Trevisin M. What do antineutrophil cytoplasmic antibodies (ANCA) tell us? *Best Pract Res Clin Rheumatol*. (2005) 19:263–76. doi: 10.1016/j.berh.2004.10.003
125. Monach PA, Kümpers P, Lukasz A, Tomasson G, Specks U, Stone JH, et al. Circulating angiopoietin-2 as a biomarker in ANCA-associated vasculitis. *PLoS ONE*. (2012) 7:e30197. doi: 10.1371/journal.pone.0030197
126. Monach PA, Tomasson G, Specks U, Stone JH, Cuthbertson D, Krischer J, et al. Circulating markers of vascular injury and angiogenesis in antineutrophil cytoplasmic antibody-associated vasculitis. *Arthritis Rheumat*. (2011) 63:3988–97. doi: 10.1002/art.30615
127. Monach PA, Warner RL, Tomasson G, Specks U, Stone JH, Ding L, et al. Serum proteins reflecting inflammation, injury and repair as biomarkers of disease activity in ANCA-associated vasculitis. *Ann Rheum Dis*. (2013) 72:1342–50. doi: 10.1136/annrheumdis-2012-201981
128. Henes FO, Chen Y, Bley TA, Fabel M, Both M, Herrmann K, et al. Correlation of serum level of high mobility group box 1 with the burden of granulomatous inflammation in granulomatosis with polyangiitis (Wegener's). *Ann Rheum Dis*. (2011) 70:1926–9. doi: 10.1136/ard.2010.146456
129. Cartin-Ceba R, Golbin JM, Keogh KA, Peikert T, Sánchez-Menéndez M, Ytterberg SR, et al. Rituximab for remission induction and maintenance in refractory granulomatosis with polyangiitis (Wegener's): ten-year experience at a single center. *Arthritis Rheumat*. (2012) 64:3770–8. doi: 10.1002/art.34584
130. Saito R, Watanabe H, Asano T, Suzuki E, Iwadate H, Kobayashi H, et al. Anti-carbonic anhydrase III autoantibodies in vasculitis syndrome. *Int J Rheumat Dis*. (2013) 16:339–46. doi: 10.1111/1756-185X.12089
131. Cabiscol E, Levine RL. The phosphatase activity of carbonic anhydrase III is reversibly regulated by glutathiolation. *PNAS*. (1996) 93:4170–4. doi: 10.1073/pnas.93.9.4170
132. Räisänen SR, Lehenkari P, Tasanen M, Rahkila P, Härkönen PL, Väänänen HK. Carbonic anhydrase III protects cells from hydrogen peroxide-induced apoptosis. *The FASEB J*. (1999) 13:513–22. doi: 10.1096/fasebj.13.3.513
133. Moosig F, Bremer JP, Hellmich B, Holle JU, Holl-Ulrich K, Laudien M, et al. A vasculitis centre based management strategy leads to improved outcome in eosinophilic granulomatosis and polyangiitis (Churg-Strauss, EGPA): monocentric experiences in 150 patients. *Ann Rheumat Dis*. (2013) 72:1011–17. doi: 10.1136/annrheumdis-2012-201531
134. Schleimer RP, Bochner BS. The effects of glucocorticoids on human eosinophils. *J Allergy Clin Immunol*. (1994) 94:1202–13. doi: 10.1016/0091-6749(94)90333-6
135. Dallos T, Heiland GR, Strehl J, Karonitsch T, Gross WL, Moosig F, et al. CCL17/thymus and activation-related chemokine in Churg-Strauss syndrome. *Arthritis Rheumat*. (2010) 62:3496–503. doi: 10.1002/art.27678
136. Polzer K, Karonitsch T, Neumann T, Eger G, Haberler C, Soleiman A, et al. Eotaxin-3 is involved in Churg-Strauss syndrome-a serum marker closely correlating with disease activity. *Rheumatology*. (2008) 47:804–8. doi: 10.1093/rheumatology/ken033
137. Vaglio A, Strehl JD, Manger B, Maritati F, Alberici F, Beyer C, et al. IgG4 immune response in Churg-Strauss syndrome. *Ann Rheumat Dis*. (2012) 71:390–3. doi: 10.1136/ard.2011.155382
138. Zwerina J, Bach C, Martorana D, Jatzwauk M, Hegasy G, Moosig F, et al. Eotaxin-3 in Churg-Strauss syndrome: a clinical and immunogenetic study. *Rheumatology*. (2011) 50:1823–7. doi: 10.1093/rheumatology/keq445
139. Cornec D, Cornec-Le Gall E, Fervenza FC, Specks U. ANCA-associated vasculitis-clinical utility of using ANCA specificity to classify patients. *Nat Rev Rheumatol*. (2016) 12:570. doi: 10.1038/nrrheum.2016.123
140. Ferri C, Mascia MT. Cryoglobulinemic vasculitis. *Curr Opin Rheumatol*. (2006) 18:54–63.
141. Ferri C. Mixed cryoglobulinemia. *Orphanet J Rare Dis*. (2008) 3:25. doi: 10.1186/1750-1172-3-25
142. Knight GB, Gao L, Gragnani L, Elfahal MM, De Rosa FG, Gordon FD, et al. Detection of WA B cells in hepatitis C virus infection: a potential prognostic marker for cryoglobulinemic vasculitis and B cell malignancies. *Arthritis Rheumat*. (2010) 62:2152–9. doi: 10.1002/art.27490
143. Antonelli A, Ferri C, Ferrari SM, Ghiri E, Marchi S, Colaci M, et al. High interleukin-6 and tumor necrosis factor-alpha serum levels in hepatitis C infection associated or not with mixed cryoglobulinemia. *Clin Rheumatol*. (2009) 28:1179–85. doi: 10.1007/s10067-009-1218-8
144. Antonelli A, Ferri C, Fallahi P, Ferrari SM, Sebastiani M, Ferrari D, et al. High values of CXCL10 serum levels in mixed cryoglobulinemia associated with hepatitis C infection. *Am J Gastroenterol*. (2008) 103:2488. doi: 10.1111/j.1572-0241.2008.02040.x
145. Apolinario A, Majano PL, Lorente R, Núñez O, Clemente G, García-Monzón C. Gene expression profile of T-cell-specific chemokines in human hepatocyte-derived cells: evidence for a synergistic inducer effect of cytokines and hepatitis C virus proteins. *J Viral Hepatitis*. (2005) 12:27–37. doi: 10.1111/j.1365-2893.2005.00540.x
146. Garzoni L, Vanoni F, Rizzi M, Simonetti GD, Simonetti BG, Ramelli GP, et al. Nervous system dysfunction in Henoch-Schönlein syndrome: systematic review of the literature. *Rheumatology*. (2009) 48:1524–9. doi: 10.1093/rheumatology/kep282
147. Saulsbury FT. Clinical update: Henoch-Schönlein purpura. *Lancet*. (2007) 369:976–8. doi: 10.1016/S0140-6736(07)60474-7
148. Purevdorj N, Mu Y, Gu Y, Zheng F, Wang R, Yu J, et al. Clinical significance of the serum biomarker index detection in children with Henoch-Schonlein purpura. *Clin Biochem*. (2018) 52:167–70. doi: 10.1016/j.clinbiochem.2017.11.006
149. Hu HW, Duan J, Zhao B, Xiong JJ, Liu M, Cui JJ, et al. Significance of detection of biomarker fecal bile acids in the diagnosis and treatment of childhood Henoch-Schönlein purpura. *Zhongguo Dang Dai Er Ke Za Zhi*. (2016) 18:517–21.
150. Akman-Demir G, Serdaroglu P, Tasçi B, Group* N-BS. Clinical patterns of neurological involvement in Behçet's disease: evaluation of 200 patients. *Brain*. (1999) 122:2171–82. doi: 10.1093/brain/122.11.2171
151. Serdaroglu P. Behçet's disease and the nervous system. *J Neurol*. (1998) 245:197–205. doi: 10.1007/s004150050205
152. Siva A, Saip S. The spectrum of nervous system involvement in Behçet's syndrome and its differential diagnosis. *J Neurol*. (2009) 256:513. doi: 10.1007/s00415-009-0145-6
153. Al-Araji A, Kidd DP. Neuro-Behçet's disease: epidemiology, clinical characteristics, and management. *Lancet Neurol*. (2009) 8:192–204. doi: 10.1016/S1474-4422(09)70015-8
154. Gül A. Genetics of Behçet's disease: lessons learned from genomewide association studies. *Curr Opin Rheumatol*. (2014) 26:56–63. doi: 10.1097/BOR.0000000000000003
155. Ahn JK, Kim J, Hwang J, Song J, Kim KH, Cha H-S. Urinary metabolomic profiling to identify potential biomarkers for the diagnosis of Behcet's disease by gas chromatography/time-of-flight- mass spectrometry. *Int J Mol Sci*. (2017) 18:2309. doi: 10.3390/ijms18112309
156. Ahn JK, Kim J, Hwang J, Song J, Kim KH, Cha H-S. Potential metabolomic biomarkers for reliable diagnosis of Behcet's disease using gas chromatography/time-of-flight-mass spectrometry. *Joint Bone Spine*. (2018) 85:337–43. doi: 10.1016/j.jbspin.2017.05.019
157. Khan E, Ambrose NL, Ahnström J, Kiprianos AP, Stanford MR, Eleftheriou D, et al. A low balance between microparticles expressing tissue factor pathway inhibitor and tissue factor is associated with thrombosis in Behçet's Syndrome. *Sci Rep*. (2016) 6:38104. doi: 10.1038/srep38104
158. Yoshioka T, Kurokawa MS, Sato T, Nagai K, Iizuka N, Arito M, et al. Protein profiles of peripheral blood mononuclear cells as a candidate biomarker for Behçet's disease. *Clin Exp Rheumatol*. (2014) 32:S9–19.

159. Rifas L, Weitzmann MN. A novel T cell cytokine, secreted osteoclastogenic factor of activated T cells, induces osteoclast formation in a RANKL-independent manner. *Arthritis Rheumat*. (2009) 60:3324–35. doi: 10.1002/art.24877
160. Sota J, Vitale A, Rigante D, Orlando I, Lucherini OM, Simpatico A, et al. Correlation of serum amyloid-a levels, clinical manifestations, treatment, and disease activity in patients with Behçet's disease. *Israel Med Assoc J*. (2018) 20:517–21.
161. Vitale A, Rigante D, Lopalco G, Selmi C, Galeazzi M, Iannone F, et al. Interleukin-1 inhibition in Behçet's disease. *Isr Med Assoc J*. (2016) 18:171–6.
162. Lopalco G, Lucherini OM, Vitale A, Talarico R, Lopalco A, Galeazzi M, et al. Putative role of serum amyloid-A and proinflammatory cytokines as biomarkers for Behcet's disease. *Medicine*. (2015) 94:e1858. doi: 10.1097/MD.0000000000001858
163. Cheng Y, Zhao X, Chen Y, Li Y, Jia R, Zhu L, et al. Circulating immune complexome analysis identified anti-tubulin-α-1c as an inflammation associated autoantibody with promising diagnostic value for Behcet's disease. *PloS ONE*. (2018) 13:e0199047. doi: 10.1371/journal.pone.0199047
164. Jiang Y, Zang M, Li S. Serum PLR and LMR in Behçet's disease: can they show the disease activity? *Medicine*. (2017) 96:e6981. doi: 10.1097/MD.0000000000006981

Conflict of Interest Statement: SM has received honoraria for lecturing, travel expenses for attending meetings and financial research support from Almirall, Bayer Health Care, Biogen, Diamed, Genzyme, MedDay Pharmaceuticals, Merck Serono, Novartis, Novo Nordisk, ONO Pharma, Roche, Sanofi-Aventis, Chugai Pharma, QuintilesIMS and Teva. JM has received grants from Deutsche Forschungsgemeinschaft, Bundesministerium für Bildung und Forschung (BMBF), Else Kröner-Fresenius-Stiftung, EVER Pharma Jena GmbH, Ferrer International, travel grants from Boehringer Ingelheim and speaking fees from Bayer Vital.

The remaining authors declare that the research was conducted in the absence of any commercial or financial relationships that could be construed as a potential conflict of interest.

Copyright © 2019 Strunk, Schmidt-Pogoda, Beuker, Milles, Korsukewitz, Meuth and Minnerup. This is an open-access article distributed under the terms of the Creative Commons Attribution License (CC BY). The use, distribution or reproduction in other forums is permitted, provided the original author(s) and the copyright owner(s) are credited and that the original publication in this journal is cited, in accordance with accepted academic practice. No use, distribution or reproduction is permitted which does not comply with these terms.

frontiers in Neurology

REVIEW
published: 07 June 2019
doi: 10.3389/fneur.2019.00594

Psychological and Cognitive Markers of Behavioral Variant Frontotemporal Dementia–A Clinical Neuropsychologist's View on Diagnostic Criteria and Beyond

Andreas Johnen[1]* *and Maxime Bertoux*[2]*

[1] Section for Neuropsychology, Department of Neurology, University Hospital Münster, Münster, Germany, [2] Univ Lille, Inserm UMR 1171 Degenerative and Vascular Cognitive Disorders, CHU Lille, Lille, France

OPEN ACCESS

Edited by:
Stefan Bittner,
Johannes Gutenberg University Mainz, Germany

Reviewed by:
Muireann Irish,
Brain and Mind Centre, University of Sydney, Australia
Claire O'Callaghan,
University of Cambridge, United Kingdom

***Correspondence:**
Andreas Johnen
a.johnen@uni-muenster.de
Maxime Bertoux
maxime.bertoux@inserm.fr

Specialty section:
This article was submitted to Neurodegeneration, a section of the journal Frontiers in Neurology

Received: *31 October 2018*
Accepted: *20 May 2019*
Published: *07 June 2019*

Citation:
Johnen A and Bertoux M (2019) Psychological and Cognitive Markers of Behavioral Variant Frontotemporal Dementia–A Clinical Neuropsychologist's View on Diagnostic Criteria and Beyond. Front. Neurol. 10:594. doi: 10.3389/fneur.2019.00594

Behavioral variant frontotemporal dementia (bvFTD) is the second leading cognitive disorder caused by neurodegeneration in patients under 65 years of age. Characterized by frontal, insular, and/or temporal brain atrophy, patients present with heterogeneous constellations of behavioral and psychological symptoms among which progressive changes in social conduct, lack of empathy, apathy, disinhibited behaviors, and cognitive impairments are frequently observed. Since the histopathology of the disease is heterogeneous and identified genetic mutations only account for ∼30% of cases, there are no reliable biomarkers for the diagnosis of bvFTD available in clinical routine as yet. Early detection of bvFTD thus relies on correct application of clinical diagnostic criteria. Their evaluation however, requires expertise and in-depth assessments of cognitive functions, history taking, clinical observations as well as caregiver reports on behavioral and psychological symptoms and their respective changes. With this review, we aim for a critical appraisal of common methods to access the behavioral and psychological symptoms as well as the cognitive alterations presented in the diagnostic criteria for bvFTD. We highlight both, practical difficulties as well as current controversies regarding an overlap of symptoms and particularly cognitive impairments with other neurodegenerative and primary psychiatric diseases. We then review more recent developments and evidence on cognitive, behavioral and psychological symptoms of bvFTD beyond the diagnostic criteria which may prospectively enhance the early detection and differential diagnosis in clinical routine. In particular, evidence on specific impairments in social and emotional processing, praxis abilities as well as interoceptive processing in bvFTD is summarized and potential links with behavior and classic cognitive domains are discussed. We finally outline both, future opportunities and major challenges with regard to the role of clinical neuropsychology in detecting bvFTD and related neurocognitive disorders.

Keywords: bvFTD, cognition, diagnosis, apraxia, social cognition, neuropsychological assessment, interoception, behavior

INTRODUCTION

Behavioral variant frontotemporal dementia (bvFTD) is a neurodegenerative disease characterized by early progressive changes in behavior, social conduct, emotional processing as well as specific cognitive impairments (1, 2). Accounting for this symptomatology is a pronounced and relatively focused neural loss in bilateral frontal, insular, and/or anterior temporal cortices that can typically be found in patients early in the disease.

bvFTD is the most frequent clinical syndrome of FTD (which also includes two other clinical dementia syndromes with predominant language dysfunctions). Fronto-Temporal Lobar Degeneration (FTLD) is the broader pathological disease spectrum also encompassing FTD, motoneuron disease (MND), progressive supranuclear palsy (PSP), and corticobasal degeneration (CBD). Estimated prevalence rates highly vary depending on the employed diagnostic criteria which have been considerably refined during the last two decades (1–3). Prevalence rates are further clouded because bvFTD, FTD, or FTLD patients are not systematically considered separately across studies. The average disease onset of bvFTD is estimated within the early sixth decade of life although patients can also be substantially younger or older as some cases with a disease onset in the 20s and after 85 years of age have been described (4–6). Within the most relevant age range of 45 to 65 years, 10–30 in 100,000 people are estimated to be affected by FTLD (4, 7). Converging evidence then suggests that bvFTD is the second most frequent young-onset (<65 years old) cognitive neurodegenerative disorder following Alzheimer's disease (AD) (4, 7, 8). Due to relatively large symptomatic overlap and the lack of established biomarkers, the prevalence of bvFTD may well be underestimated because of frequent misdiagnoses with either a different neurodegenerative cognitive disorder or a primary psychiatric disorder (9–11). Half of bvFTD patients indeed received a prior primary-psychiatric diagnosis (9, 12).

As FTLD is a heterogenous pathophysiological entity, bvFTD can be caused by different underlying pathologies (13–15). Most of the cases include the abnormal intraneuronal depositions of aberrant forms of specific proteins such as tau (FTLD-tau) and TAR-DNA binding protein 43 (TDP-43; FTLD-TDP) in equal proportion, and less frequently, fused-in-sarcoma (FUS; FTLD-FUS) (16, 17). Currently, no methods allow the detection or prediction of FTLD pathologies during the life of patients and no reliable biomarker exists for the diagnosis of bvFTD, although some associations between genetics and post-mortem histopathological findings have been established (13, 18). While the majority of cases with FTLD are estimated to have a sporadic form, a positive familial history may be found in up to 40% of cases (19, 20), with a suspected autosomal dominant pattern of inheritance found in at least 10% of patients (21, 22). Although other rare genetic variants have been found, mutations in either the MAPT, GRN, or C9orf72 genes account for the vast majority of genetic variants of FTLD. Interestingly, the hexamino acid expansion on the C9orf72 gene is also very frequently associated with families presenting with MND or a combination of FTD and MND (23, 24), suggesting a continuum between both syndromes. Overall, this underlines the importance of a detailed family history during the clinical interview.

On the anatomical level, meta-analyses of the atrophy profile of patients with bvFTD found significant clusters of reduced brain volume in frontomedian areas, in the superior frontal sulcus, parts of the thalamus and insula as well as in striatal regions (25–27). Focal frontal atrophy is a positive marker of bvFTD but can nevertheless be absent or very subtle during the earliest stages of the disease. In those cases, 18-Fluorodeoxyglucose-Positron Emission Tomography (FDG-PET) has shown to enhance diagnostic certainty, by evidencing a regional hypometabolism in similar frontal and anterior temporal brain areas (28, 29). Multimodal imaging approaches simultaneously combining hypometabolism and brain volume loss also showed promising results while being usually not available in clinical routine (30). Interestingly, differential patterns of early brain atrophy have been observed in the genetic forms of bvFTD as well as in asymptomatic mutation carriers, sometimes up to 15 years before the onset of clinical symptoms (31, 32). An atrophy of the hippocampus and amygdala may be observed 15 years before the onset of the disease in asymptomatic MAPT carriers for example (32).

Aims of This Review

As a result of the heterogeneity regarding the underlying pathology of bvFTD, there are currently no reliable, specific, and established biomarkers available to clinicians. A correct and early diagnosis is nevertheless crucial for disease management, initiation of treatment as well as support of the usually highly distressed caregivers (33). Differential diagnosis strongly relies on the correct application of the current FTD Consortium (FTDC) clinical criteria and exclusion of other causes for the symptoms. Recently, however, critics have been raised toward some parts of these criteria, particularly toward their ability to guide the differential diagnosis with AD or primary psychiatric disorders (34, 35). Here, we thus aim for a critical appraisal of the current clinical criteria for the diagnosis of bvFTD. We will highlight strengths, practical difficulties as well as controversies of these criteria, give real-world examples and provide suggestions for their practical evaluation in clinical settings. We then aim to review more recent developments regarding early clinical detection of bvFTD beyond the established diagnostic criteria with an emphasis on in-depth neuropsychological assessment of specific cognitive domains (i.e., social and affective cognition and praxis abilities), physiological alterations (i.e., interoception) and potential links with "classic" behavioral and cognitive symptoms of bvFTD. Finally, we outline current challenges and opportunities for the field of clinical neuropsychology regarding its crucial tasks to develop and establish novel and clinically meaningful "cognitive markers" in order to use them for (i) staging of disease severity, (ii) validating future biomarkers, and (iii) identifying the precise cognitive dysfunctions that will need to be remediated in future disease-modifying strategies for bvFTD.

THE CLINICAL DIAGNOSTIC CRITERIA FOR BVFTD

After an initial paper in 1994, the first comprehensive consensus criteria for bvFTD from the FTDC, an international group of experts on FTD, were released in 1998 (2). These criteria enabled clinicians and researchers to focus on a set of four key criteria for clinical diagnosis, namely a decline in social interpersonal conduct, impairment in regulation of personal conduct, emotional blunting, and loss of insight. Each of these criteria had been standardized by a brief text definition. Key symptoms and definitions have since been consecutively revised and refined and the current set of criteria (1) now reaches high sensitivities and specificities when tested against competing neurodegenerative diseases (by post-mortem pathological confirmation of either of the known underlying FTLD pathologies) as well as good inter-rater reliability (36, 37).

Despite consensus text definitions of the FTDC clinical criteria, clinicians today still face the problem that the criteria have not been standardized by means of "tests" or clinical scales and even the methods of their assessment (e.g., patient anamnesis, clinical judgement, clinical observations, caregiver anamnesis, standardized questionnaires, cognitive performance tests) are not consistently specified and likely differ considerably across centers. In addition, some studies have underlined a substantial overlap between symptoms of specific primary psychiatric diseases (e.g., late-onset unipolar or bipolar affective disorders, schizo-affective disorders) and symptoms of bvFTD. These shared symptoms may explain why bvFTD patients are frequently misdiagnosed with psychiatric disorders as outlined before (9, 12), but they also explain why, on the basis of the FTDC criteria, a significant proportion of psychiatric patients could be misdiagnosed as possible bvFTD (10, 11, 38, 39). Related to the issue of clinical misdiagnoses based on the FTDC criteria and further complicating the picture, a condition mimicking bvFTD has been been described and labeled "bvFTD phenocopy syndrome," implying that patients may display the typical behavioral symptoms of bvFTD but show no progression and no evidence of atrophy or hypometabolism [for a recent systematic review on features of individuals with phenocopy bvFTD, see (40)].

Another important criticism toward the current FTDC criteria for bvFTD is that some exclusion criteria (e.g., the proposed cognitive profile of major executive dysfunction and spared memory functions) seem overly restrictive and may lead to false exclusions (34). In the following, we will first provide an overview on the different sources of information available to clinicians and their respective importance in the process of diagnosing bvFTD. We will then give practical suggestions to assess the proposed behavioral and psychological (section The Clinical Diagnostic Criteria for bvFTD) as well as cognitive (section Cognitive Dysfunctions in bvFTD) criteria (see also **Table 1**).

Sources of Information to Evaluate the FTDC Criteria in a Clinical Setting

Clinical-Neurological Examination

A standardized clinical-neurological examination is critical when an initial suspicion of bvFTD is raised, mainly to exclude alternative causes for the symptoms. For example, ∼10% of patients with FTD develop MND and 10–15% of patients with MND also meet criteria for bvFTD (41, 42). Because bvFTD symptomatology may also overlap with CBD and PSP, a standardized neurological assessment of (extrapyramidal) motor functions is particularly important. In most cases of early stage bvFTD, the neurological examination reveals few obvious abnormalities. In particular, reflexes and motor functions are usually not pathological, although primitive "frontal" reflexes (utilization, gripping reflexes) may sometimes be observed (43). Although originally described as a classic sign for PSP, a positive applause sign may also be observed in bvFTD and may be correlated to overall disease severity (44). Another frequently described cognitive-neurological sign of patients with bvFTD is difficulty or failure to perform anti-saccades, most likely reflecting an inability to inhibit the overlearned motor response of a saccade toward a stimulus as compared to its opposing direction (anti-saccade) (45–47). Other clinical signs frequently seen in patients with AD like the "head turning sign," are not particularly indicative of bvFTD (48).

Patient Anamnesis and Clinical Observations of Patients

Patients with bvFTD usually have a diminished or absent sense for the behavioral, cognitive, or psychological changes that are reported by their relatives or co-workers (sometimes referred to as anosognosia). Unlike the lead symptoms of other early neurocognitive disorders, cognitive, or behavioral symptoms are thus rarely spontaneously reported by patients with bvFTD. If they are, reports are usually brief or shallow, in a stereotypical manner and without showing a coherent sense of either suffering from the symptoms or being overly worried about them. During anamnesis, patients with early bvFTD may even remain to be affectively indifferent when directly confronted with reports of negative consequences of their pathological behaviors (e.g., on their family well-being) or with negative feedback (e.g., regarding their poor cognitive test performances). Although an anosognosia or lack of insight into cognitive and behavioral symptoms may sometimes also be observed in patients with AD, a striking difference in patients with bvFTD is a frequent lack of appropriate emotional participation or affective involvement during the clinical assessment and diagnostic procedure (sometimes specifically referred to as anosodiaphoria or in a wider sense as a sign of "emotional blunting"). Such typical clinical observations during anamnesis may be used to develop an initial suspicion of bvFTD but are highly subjective and require clinical expertise. Only few attempts on the other hand have been published to standardize behavioral observations of patients with bvFTD in clinical contexts (49) or in home settings (50). Preliminary validation studies of these scales have shown that

TABLE 1 | Clinical, behavioral, psychological, and cognitive diagnostic domains for bvFTD.

Domain	Suggested method of assessment (scale/test)	Typical results/observation in early bvFTD
Anamnesis/clinical and neurological examination		
Motor-disinhibition	Saccade and anti-saccade test	Fails to perform anti-saccades as compared to saccades.
Speech and language	Clinical observation	Monotonous speech with little tonal modulation, stereotypic utterances, use of "foul" language.
Emotional blunting	Clinical observation	Seems indifferent and without adequate affect toward diagnostic process or toward the suffering of caregivers.
Anosognosia/Lack of insight	Clinical observation and confrontation with deficits	Spontaneously reports little complaints or only in a stereotypic, shallow way. Reacts indifferent toward cognitive deficits or caregiver reports of behavioral changes.
Behavioral and psychological symptoms		
Behavioral disinhibition	Clinical observation, standardized multiple-domain caregiver interview or questionnaire (e.g., FBI, FrSBE)	High total appearance of disinhibited behaviors compared to healthy subjects and compared to premorbid levels. Possible inappropriate comments or actions during the examination, favored by a lack of rigidity in the clinical setting.
Impulsive, disinhibited eating	Caregiver interview, standardized caregiver questionnaire (e.g., APEHQ)	Shows a disinhibited eating pattern and prefers sweets and candy ("sweet tooth"), sometimes increased, impulsive consumption of alcohol or cigarettes.
Apathy	Clinical observation, standardized caregiver questionnaire (e.g., ACL)	High levels of apathy and inertia, few interests, usually little suffering or complaints about affective/mood disturbances. Sometimes there is a need of frequent incentives from the clinicians during non-directive examination and a possible over compliance to the clinician's instructions.
Loss of empathy	Caregiver interview or standardized caregiver questionnaire (e.g., IRI)	Lacks empathy for others, seems irresponsible for others; significant changes in caring compared to premorbid behaviors.
Change of humor or music preference	Clinical observation, caregiver interview	Prefers simple humor (e.g., "slapstick") and less complex types of music as compared to former preferences; sometimes excessive and repetitive consumption of television programs or music.
Rituals and obsessive-compulsive behaviors	Clinical observation, caregiver interview	Excessive collecting or hoarding, sometimes accompanied by deficits in self-care and hygiene (Diogenes syndrome).
Cognitive performance		
Executive Functions	Standardized neuropsychological tests	Subnormal performance specifically in tasks for behavioral inhibition (e.g., Hayling-task) and cognitive flexibility (e.g., letter fluency). Multiple subtest screenings (e.g., FAB, INECO, FRONTIERS) cannot reliably discriminate bvFTD from other neurodegenerative disorders.
Episodic (verbal) memory	Standardized neuropsychological tests (e.g., FCSRT, RAVLT, CVLT-II)	Often subnormal learning curve and deficient free recall compared to healthy controls/normative data. Possible total (cued) recall deficit as well as (free and cued) delayed recall decrease.
Visuospatial processing and navigation	Standardized neuropsychological tests (e.g., RCFT)	Visuoconstruction and drawing usually spared but may nevertheless appear deficient due to planning deficits and visual organization deficits. Use of qualitative strategy scores are recommended
Social Cognition	Standardized neuropsychological tests (e.g., Mini-SEA)	Reduced ability to recognize facial emotions, particularly those with negative valence. Reduced ability to detect and analyse social norms violations and to infer other's intention and feelings (Theory-of-mind abilities).
Reward processing	Standardized neuropsychological tests	Deficit in reward valuation, reinforcement learning, reversal-learning, decreased sensitivity to losses or delayed reward, diminution of normal cognitive/affective bias.
Apraxia	Standardized neuropsychological tests (e.g., DATE)	Deficits in posture/gesture imitation and pantomime of object-use compared to healthy subjects. Relatively more deficits in "buccofacial" praxis tasks (particularly face imitation) as compared to limb imitation.
Staging of disease severity and progression	Standardized interviews with patient and caregiver (e.g., FTLD-CDR, FRS)	Scales are sensitive for clinical disease progression and may guide clinical observations.

bvFTD, behavioral variant frontotemporal dementia; FBI, Frontal Behavioral Inventory; FrSBe, Frontal Systems Behavioral scale; ACL, apathy checklist; IRI, Interpersonal Reactivity Index; FCSRT, free and cued selective reminding test; RAVLT, Rey auditory Verbal Learning test; CVLT-II, California Verbal Learning Test second edition; RCFT, Rey Complex Figure test; Mini-SEA, Mini Social Emotional Assessment; DATE, Dementia Apraxia Test; FTLD-CDR, Clinical Dementia Rating scale for Frontotemporal Lobar Degeneration; FRS, Frontotemporal rating scale.

standardized observations of behavior are a valid method to delineate patients with bvFTD from other diagnoses, however their application require a rigid and time-consuming assessment that is often not feasible in clinical contexts.

Caregiver Interviews and Standardized Questionnaires

Caregiver reports are so far the main source of information for clinicians to detect and diagnose bvFTD in early disease stages. As psychological and behavioral changes are the lead clinical symptoms of patients with bvFTD they should be assessed extensively through caregiver interviewing, as these information principally allow for a diagnostic differentiation against other common neurodegenerative dementia syndromes like AD (51). As pointed out however, patients with bvFTD frequently present with recent diagnoses of depression, bipolar, schizo-affective disorders, or "burn out" syndromes due to an overlap of similar symptoms e.g., reduced activity, apathy, loss of interest, and in some cases euphoria, agitation, and restlessness (52). To enhance diagnostic accuracy for early bvFTD, it is thus particularly crucial to delineate suspicious behavior and psychological alterations from premorbid personality traits or episodic primary psychiatric disorders. Psychological and behavioral symptoms need to be clearly identified as novel, qualitatively different compared to previous behavior and most important, progressively increasing.

Standardized clinical rating scales that aim at staging symptoms severity in patients with FTLD may thus help clinicians to guide and structure the caregiver anamnesis as well as quantify longitudinal changes of symptoms. The well-known Clinical Dementia Rating scale (CDR) is available in a modified version in order to include behavioral and language dysfunctions geared toward patients with FTD (53). The scale and associated structured interview is available in several languages and has proven successful in staging disease progression in bvFTD. An alternative measurement that focuses more on specific symptoms of bvFTD is the semi-standardized interview Frontotemporal dementia Rating Scale (FRS), which allows a fine-grained clinical severity staging (54).

Several other standardized scales to specifically assess behavioral changes in patients with frontal lobe syndromes are also available (see e.g., **Table 1**). These scales differ in terms of administration (e.g., interview, standardized, or semi-standardized questionnaires) and the included sets or domains of behavioral symptoms. In general, standardized scales on behavioral symptoms that focus on the core features of patients with "frontal lobe syndromes" (e.g., behavioral disinhibition, apathy, irritability, emotional blunting etc.) have been found to be more sensitive for the early detection of bvFTD (55) than more general scales that are geared more toward other features (e.g., hallucinations, delusions) commonly seen in specific primary psychiatric disorders [e.g., the Neuropsychiatric Inventory; NPI (56)]. Psychotic symptoms like delusions and (auditory or visual) hallucinations are rarely seen or reported in patients with early bvFTD although particularly bodily delusions (e.g., altered sense of bodily perceptions) might be more frequent in patients that later develop MND and/or have a C9orf72 mutation (57–59). Among the recommendable caregiver scales on specific frontal behavioral changes are the Frontal Behavioral Inventory [FBI (60), also available in a shortened, modified version that may be used as a questionnaire (61)] and the Frontal Systems Behavioral scale [FrSBe (62), similarly available in a shortened, modified questionnaire version (63)]. The DAPHNE scale, specifically adapted from the current FTDC diagnostic criteria for behavioral and psychological symptoms has also demonstrated good psychometric properties (64). Of note, extensive normative data stratified for age and education are usually not provided for any of these scales and translations into languages other than their original ones are rarely available or unofficial. In addition, only a few studies have been conducted to compare caregiver assessments to patients' self-reports or clinicians' evaluations and it is likely that high levels of caregiver distress impact the reporting of symptoms. In that perspective, more education and caregiver interventions are needed in order to both, alleviate the stress/burden and to reduce bias regarding caregiver reports of symptom severity, especially in longitudinal assessments (65). Finally, it seems important to highlight that behavioral symptoms, or the way patients' relatives react to them, may be subject to large variations due to distinct cultural differences (66). Currently however, the field lacks studies that have assessed how such variations may impact behavior in bvFTD or its inception by caregivers.

Behavioral and Psychological Symptoms of the Current FTDC Criteria

Regarding behavioral and psychological symptoms of bvFTD, the FTDC criteria present five core domains of symptoms, which we will briefly summarize in the following, before we will turn to the currently more heavily discussed "neuropsychology item" of the criteria (in section Cognitive Dysfunctions in bvFTD). Importantly, for a new clinical diagnosis of "possible bvFTD," it is sufficient that any three of the following criteria (e.g., two of the five behavioral/psychological criteria plus the cognition item) are fulfilled (i.e., a functional decline in this domain compared to former level of functioning is seen). Moreover, the criteria require that these symptoms are new and develop "early" i.e., within the first three years of the suspected disease onset. For a higher diagnostic level of evidence ("probable bvFTD"), the criteria require focal atrophy on MRI and/or hypometabolism on PET in frontal or anterior temporal cortices or alternatively, a documented decline of behavioral or cognitive symptoms over time (1).

Behavioral Disinhibition

Socially inappropriate behaviors like inappropriate familiarity or a lack of distance (e.g., staring at or touching the clinician, making inappropriate comments or jokes, being inappropriately jovial) during the anamnesis or during the cognitive assessment (e.g., walking out of the room, smiling, shrugging of shoulders) are often subtle signs of early behavioral disinhibition in bvFTD. Difficulties to inhibit irrelevant stimuli from the environment is often considered as a key feature of bvFTD and patients often struggle to focus on a task because of distractors [e.g., (67)], a symptom that has been linked to "environmental dependency" (68) and to increased stimulus-bound thought and behavior

(69). Pathological gambling and personal neglect or reduced self-care (Diogenes syndrome) have been well-described (70, 71), as well as utilization or imitation behaviors (43, 72). Anecdotal evidence also suggests that patients with bvFTD may have early changes regarding their preferred type of humor that may be viewed as a "loss of manners" by others (i.e., patients tend to make crass jokes or prefer "slapstick" humor) (73). In some cases, patients present with more obvious dissocial behavior (e.g., sexists comments, overt aggression) or criminal actions even in early disease stages (74, 75). Law violations as a potential correlate of increased behavioral disinhibition are indeed frequently observed in bvFTD, as indicated by studies conducted in USA, Japan, and Europe. Patients with bvFTD for example commit law violation up to five times more often than AD patients. These could manifest as theft, traffic violations, physical violence, sexual harassment, trespassing, and public urination, thus reflecting mainly disruptive, impulsive actions (74–76). Patients may also exhibit changes in sexual behavior, but usually show diminished sexual drive, intimacy, and display of affection whereas only rarely hypersexual or inappropriate/disinhibited sexual behaviors are reported (77–79). Importantly disruptive symptoms subsumed under early behavioral disinhibition are major predictors for caregiver distress in bvFTD (80).

Apathy and Inertia

As a behavioral syndrome, apathy could manifest itself as a range of concepts, such as emotional blunting, poor initiation or persistence, indifference to choices, reduced curiosity, lack of interest, and activities, difficulties in implementing actions and social withdrawal. Diminished goal-directed behaviors and intellectual activities (such as reading) as well as diminished responsiveness to emotion are however consensually considered as central to apathy and are among the most frequent symptoms of bvFTD (81–83). Along with cognitive impairments, apathy is also fundamentally related to functional disability in terms of impaired instrumental activities of daily-living and it has a profound impact on patients' relatives (83–85). Immobility and reduced levels of daytime activity for example are seen in almost all patients with bvFTD and are a major source of caregiver distress (85). Along with cognitive impairments, apathy is also closely related to functional disability in terms of impaired instrumental activities of daily-living (86). Excessive TV watching, which may be observed more often in bvFTD than in AD may be perceived as a typical symptom of apathy (87), as well as a general reduction of interest toward pre-morbid activities. Importantly, apathy/inertia (i.e., "negative" symptoms) as well as disinhibited, agitated, or impulsive behaviors (i.e., "positive" symptoms) are no contradiction, but are often concomitantly present in patients with bvFTD and may be differentially triggered by certain situational cues (88). Also potentially related to overall levels of apathy, during anamnesis, patients may show a monotonous speech pattern that lacks modulation and prosody (89, 90). To assess specific symptoms in more detail, the Apathy Evaluation Scale [AES (91)] is available to clinicians.

Loss of Empathy or Sympathy

A diminution or lack of empathy is frequently observed in bvFTD in everyday social contexts and often has considerable negative consequences on caregivers (92). Lack of empathy relies on the interaction of several cognitive and sensorimotor processes (93, 94) and thus is a multifaceted symptom (95) that may be grossly defined as a deficit to share other's affective states (e.g., fear, sadness) leading to an absence of affective concern (and subsequently prosocial behaviors like comforting, helping or caring) for them. In its consensual definition, sympathy does not require one to share a specific affective state with someone else but would rather consist in an emotional reaction, such as sorrow or concern, to other's affective experiences (96). These symptoms could manifest as a diminution of projections into fictional situations such as in movies or books but more frequently, caregivers report a decreased spontaneous tendency to react to other's feelings (97). For example, patients could state their thoughts without considering the feelings of their colleagues or relatives (98). This detachment from friends and family go beyond what could be considered as social withdrawal—as observed in depression or apathy—because it also involves an "emotional blunting" about other's feelings, or, more generally, an overall lack of affective involvement. These deficits often lead to unmoderated, tactless, rough, and sometimes aggressive remarks from patients toward others, including their closest family, leading to what is often perceived as a very selfish and egocentric behavior (67). For instance, patients could be disinterested in spending time with their kids (99), they can be indifferent when their next-of-kin are hospitalized due to illness (98) or they may appear unimpressed when their partners cry during anamnesis. Empathy deficits often have a considerable impact on the family environment and are potentially dramatic for relatives and caregivers, especially as patients with bvFTD could overestimate their own empathic abilities (100). Overall, although empathy decrease can be observed in AD as well, it is substantially higher in bvFTD and plays a more important role in caregiver distress (33, 101). For a standardized clinical assessment of empathy deficits, the Interpersonal Reactivity Index [IRI, (102)], a caregiver questionnaire may be used.

Perserverative, Stereotyped, or Compulsive/ Ritualistic Behaviors

Patients with bvFTD frequently become rigid and inflexible regarding daily routines, which they want to preserve, and a substantial proportion develops unusual rituals or behaviors such as hoarding or collecting, similarly to what is observed in obsessive-compulsive disorders (103). Other anecdotally reported ritualistic behaviors are inflexible grooming or walking routines, counting and strict timekeeping as well as checking or sorting behaviors (14). However, in contrast to obsessive-compulsive disorder, these rituals are not due to compulsions in bvFTD as neither their expression nor their disruption are related to feelings of anxiety (104). Utterances during anamnesis may thus also appear stereotypic and repetitive and some patients present with additional verbal and/or simple repetitive motor tics (105). A proportion of patients develop a disinhibited drive to

listen to music, and some may change their preferred music-style toward less complex music which they may consume in a preserverative manner (106). Creativity abilities have been shown to change during the disease, with patients exhibiting more naïve, stereotypic, and repetitive form of creation (107, 108).

Eating Behavior and Dietary Changes

Patients with bvFTD show significantly stronger changes in stereotypic/altered eating behaviors compared to AD patients (109). A marked hyperphagia (i.e., higher calory intake) has been found as quite specific for bvFTD when compared with other forms of neurodegenerative dementia syndromes, although patients with semantic dementia may also present with similar symptoms (110, 111). A craving for sweet food ("sweet tooth") and a disinhibited, impulsive pattern of eating has been also frequently described as an early and specific sign of bvFTD, with sometimes patients stuffing aliments into their mouth and eating very quickly (binge eating). Patients with bvFTD may also be affected by hyperorality (e.g., Pica-syndrome, i.e., trying to eat inedible things or increased cigarette consumption) and various other dietary changes (112). While this section suggests that cognitive impairments are closely associated with changes in eating beahviors, it is important to highlight that elevated levels of leptin and insulin in bvFTD (as a direct consequence of hypothalamus atrophy) have also been linked to these symptoms (113, 114). The Appetite And Eating Habits Questionnaire [APEHQ (115)] may be used by clinicians to assess specific information on eating habits in a standardized way.

COGNITIVE DYSFUNCTIONS IN BVFTD

Although cognitive dysfunctions are numerically less weighted in the FTDC criteria for bvFTD, representing only 1 out of 6 criteria, the assessment of cognitive performance remains crucial for clinical diagnosis and patient management. Given that the previously described behavioral and psychological changes are often more visible in bvFTD, substantial cognitive impairments (that may account for some of the behavioral symptoms) may easily be overlooked. Recent studies have shown that the vast majority of patients with bvFTD already present with major cognitive dysfunctions in early disease stages when compared with normative data stratified for age and education (116, 117). Presymptomatic mutation carriers (with MAPT mutation) even present with specific (i.e., social cognition and memory) impairments respectively, 2 and 4 years before the diagnosis of bvFTD (118). Critically, commonly used multiple domain screening tests for dementia like the Mini Mental State Examination [MMSE (119)], the Montreal Cognitive Assessment [MoCA (120)] or even the more extensive Addenbrooke's Cognitive Examination [ACE-III (121)] may lack sensitivity to detect bvFTD in early stages and/or specificity to delineate the disease from other conditions, thus clearly warranting a more detailed neuropsychological assessment.

The neuropsychology item in the current criteria requires a cognitive profile of "executive/generation deficits with relative sparing of memory and visuospatial functions" which primarily aims at delineating the cognitive profile of patients with bvFTD from patients with AD (1). An array of recent studies however, revealed a large overlap between early bvFTD and other neurodegenerative diseases (including AD) regarding cognitive performances when using standard neuropsychological test batteries and when examining standard cognitive domains only (117, 122–125). We will thus now summarize the current evidence regarding the cognitive domains mentioned in the criteria (section Cognitive Dysfunctions in bvFTD) and subsequently review newer evidence regarding other cognitive domains (namely social cognition and praxis abilities) that are currently not represented in the criteria (section Promising Cognitive and Psychological Markers for bvFTD Beyond Current Diagnostic Criteria). We finally summarize evidence on impaired processing of interoceptive signals which may constitute a link between a range of cognitive and behavioral deficits in bvFTD.

Executive Functions

Executive functions is an umbrella term for cognitive processes that rely on higher-order cognitive control mechanisms that are proposed to be mainly subserved by a large fronto-parietal network (126, 127). Although the proposed cognitive core deficits in bvFTD are executive dysfunctions, mixed results have been found when evaluating the (differential-) diagnostic properties of performance in neuropsychological tests for executive functions typically used in clinics (116). Executive dysfunction is a common symptom in a range of other neurodegenerative cognitive disorders including Parkinson's disease dementia (128), AD (129), dementia with Lewy-Bodies (130) as well as vascular cognitive impairment (131). When patients reach at least moderate disease severity stages, performances in tests for executive performance becomes strikingly similar across these diagnoses. But even in early stages, assessment of executive functions could not allow to always differentiate bvFTD from AD (116, 122, 125, 129, 132). In addition, executive impairments could be similarly present—or more severe—in a wide range of psychiatric disorders (133–135) and may thus provide only little help for differential diagnosis of bvFTD. Brief screening tools commonly used in clinics and specifically designed to rapidly assess a range of executive functions through a set of commonly employed single tasks [e.g., Frontal Assessment Battery (FAB) (136), INECO Frontal Screening (IFS) (137), FRONTIER Executive Screen (FES) (138)] have shown to effectively detect patients with bvFTD in the general population but have failed to consistently show sharp dissociations between different neurodegenerative dementia syndromes (139). Looking at standard single neuropsychological tasks for executive functions, performances of patients with bvFTD were frequently not unequivocally distinguishable from patients with other neurodegenerative dementia syndromes, including AD (117, 122, 125). This observation remains valid even with the use of more comprehensive evaluation relying on specific neuropsychological batteries such as the Executive Abilities: Measures and Instruments for Neurobehavioral Evaluation and Research (EXAMINER) (129) or the Delis-Kaplan Executive Function System (D-KEFS) (127, 140). When possible, the following part will address the different discriminatory ability

of tasks related to classically defined executive domain in the differential diagnosis mainly of bvFTD and AD in early stages.

Response Inhibition and Cognitive Flexibility

Disappointing results in terms of clear discriminative abilities have been shown for the Stroop tests (117, 141, 142), the Wisconsin-Card-Sorting test (143) and graphical sequences (142). Another commonly used test, the Trail-Making-Test part B (TMT-B) may even be more impaired in patients with AD compared to bvFTD (144) although bvFTD patients may be more insensitive to errors in this task (145). Environmental dependency symptoms such as imitation or utilization behavior have been described as more frequently observed in bvFTD than in AD (43, 72) but the variability of their assessment procedures and the probable multidimensionality of these symptoms (68) may have limited the investigations about their clinical relevancy and applicability. Even though saccade or anti-saccade abnormalities are sometimes reported as typical of bvFTD (46, 146), executive-related oculomotor function have been found to be impaired in AD as well (147), although they may be preserved in early disease stages (148). A range of studies have shown that the Hayling test may be a good candidate to more reliably distinguish patients between bvFTD and early AD on the level of individual cases (116, 149) but more research is needed to safely recommend the use of this test in this context test as some contradictory findings have also been reported (142, 150).

Abstract Reasoning

Verbal abstraction deficit as evaluated by categorization/similarities tasks is observed in bvFTD as opposed to AD, during the early stages of the disease (151, 152). These findings are in line with reported increased deficit in proverb interpretation in bvFTD compared to AD (153), although the semantic load of both tasks could also critically impact the performance due to polar temporal involvement (154). On the contrary, clock hand placement in the clock drawing test, hypothesized as involving the ability of abstracting the concept of time and its specific indication, have been shown to be altered preferentially in early AD as compared to bvFTD (155).

Initiation

Design/figural fluency tasks (e.g., 5-point test) are not differentially impaired in bvFTD compared to AD (144) although one study has found a higher number of qualitative repetition errors (156). Patients with bvFTD may score lower compared to AD patients in lexical fluency tasks (129, 157) and may also display a distinct ratio of semantic fluency vs. letter fluency with relatively less impairment in semantic fluency (158, 159).

Strategic Reasoning (Multitasking, Planning Abilities)

The Brixton test did not show any dissociation between bvFTD and AD (160, 161). This is also the case for the Tower of London test (162) although the use of qualitative information has been showed to have the potential to help the discrimination between both diseases (163). The Multiple Errands Test, the Zoo Map (from the Behavioral Assessment of the Dysexecutive Syndrome; BADS) and the Hotel task have all been found to be impaired in bvFTD (149, 164) but the lack of data in AD does not support their use in the context of clinical differential diagnosis. Cognitive estimation has been shown to be impaired in bvFTD as compared to amnestic MCI only (165).

Working Memory and Attentional Control

Auditory attention and verbal working memory deficits have been retrieved through digit span forward and digit span backward tasks respectively, (129, 143, 144) and were neither exclusively nor specifically impaired in bvFTD when compared with AD. Selective attention could be more impaired in bvFTD than in AD as well (141).

Memory, Episodic Future Thinking, and Spatial/Topographical Navigation

Relative sparing of episodic memory remains a diagnostic feature in the neuropsychological criterion for bvFTD and has been historically heralded as one of the clinical gold standards to distinguish bvFTD from AD. However, this notion has been challenged by a study showing that bvFTD could present with severe amnesia, similarly to what is observed in AD (166). The critics that were made to this study (i.e., patients included only received clinical diagnoses and memory storage was only assessed through free recall testing) were addressed in an independent study with diagnoses supported by AD/non-AD biomarkers and memory assessment based on free and cued recall testing that showed similar results and proposed the existence of an amnestic variant of bvFTD following the observation of a bimodal distribution of patients (167). In the next years, several studies showed similar results and helped to further characterize the memory dysfunctions in bvFTD (168–170). A recent meta-analytic review confirmed a 37–62% overlap between bvFTD and AD in learning and recall test performance (171). Independent of the memory test used, the classic profile of bvFTD, i.e., a decreased spontaneous/free recall that can be normalized using recall cues could still be observed in about half of patients with bvFTD, however vast deficits in encoding, storage, and consolidation are present at a similar frequency. Likewise, recognition deficits have been observed in bvFTD (172, 173) further complicating differential diagnosis against AD. Interestingly, longitudinal studies have shown that early bvFTD could already present with severe amnesia (116, 132), in line with a neuropathological study of early FTD (174). While these two longitudinal studies showed a comparable rate of memory decline in bvFTD and AD, another one showed an even faster decline in bvFTD (175). Episodic future thinking, assumed to rely on the same neural mechanisms, has shown to be impaired in bvFTD (176) as well as the emotional enhancement of memory (177), in contrast to mild AD. Prospective memory is also impaired in bvFTD, similarly to AD, in both time-based (the ability to remember and execute an intended action at a future time) and event-based (when a specific event occurs) dimensions (178, 179). Both, recent and remote autobiographical memory were also shown to be impaired in bvFTD as well (180) but only in later stages of the disease (181). The only domain related to memory

that seems to be robustly preserved in bvFTD as compared to AD is navigation ability. Topographical short-term memory has been found to be preserved in FTD (182), a finding which has been corroborated by recent studies showing that spatial orientation performance and particularly egocentric orientation (representation of spatial relationships in relation to separate objects) seems better preserved in early bvFTD and could thus allow an effective discrimination against early AD (183–185).

Visuo-Spatial and Visuo-Construction Abilities

Drawing or copying of spatially complex (e.g., three-dimensional) figures and abstract forms (sometimes also referred to as constructional praxis) is a multifactorial process relying on a widespread bilateral neural network from temporo-occipital to parietal and lateral frontal areas (186, 187). From a cognitive stance, visual-perceptual abilities, planning abilities, and more general cognitive control processes are involved in figure-copy performance. Performance in tasks for visuoconstruction, such as drawing and figure copy abilities, has consistently found to be significantly more impaired in patients with AD as compared to bvFTD, and some studies suggest that visuoconstruction and visuoperception may be a specific and unique cognitive marker for preclinical AD (185, 188–191). In two samples (one of which included autopsy-proven FTD patients), patients with FTD had higher scores in the clock drawing test (192, 193). The domain of figure-copy abilities and visuoconstruction has further been shown to be particularly well-preserved in bvFTD over time in comparison to AD and other conditions (175). However, C9orf72 mutation carriers may be more likely to present with visuoconstructional deficits than non-carriers (61, 194). An in-depth assessment of visuospatial processing and visuoconstructional abilities e.g., using tests like the Rey-Osterrieth complex figure test (RCFT) is nevertheless highly recommended for the clinical differentiation between bvFTD and AD (195). Although some patients with bvFTD may still perform bad in some figure copy tasks, this is usually due to a deficit in perceptual organization and planning abilities and not due to a genuine visual-perceptual impairment (196, 197). It is thus recommended to qualitatively take into account the type of errors (e.g., planning deficits vs. spatial deficits) as spatial errors are particularly indicative of AD (198). There are several coding systems available to qualitatively study the types of errors in a visuoconstructive task like the Rey Complex Figure Test (199). Another specific qualitative error in figure-copy tasks that has previously been linked to executive dysfunction in patients with dementia is the phenomenon of "closing in," in which the patient draws the copy very near to the model (200). It will be of particular interest whether qualitative assessment of this and other drawing errors may further enhance differential diagnostic efficiency for bvFTD.

Summary of Cognitive Dysfunctions in bvFTD as Stated in the FTDC Criteria

Taken together, although the majority of studies have confirmed patients with bvFTD to show executive impairment, the proposed prototypical "profile" of pronounced executive dysfunction in bvFTD seems to be of low specificity and the cognitive dysfunctions displayed by patients with bvFTD are more heterogeneous than previously assumed. Although studies conducted in pre-diagnosed genetic bvFTD patients show that attention and executive functions could be early markers of MAPT or GRN mutations (118, 201, 202), they do not seem to precede other early cognitive impairments such as facial emotion recognition deficit or even memory storage impairments (118, 203). Furthermore, not all executive subdomains seem to be impaired in early bvFTD, questioning the notion of a general executive core deficit in bvFTD irrespective of disease stage (116). Small series of cases reports have indeed shown that in the earliest stages of bvFTD, executive functions may be normal (204). Overall, converging evidence rather suggests that only a subset of executive tasks that heavily rely on basic behavioral and motor inhibition abilities are robustly impaired in bvFTD, mostly irrespective of disease stage (116, 139, 142, 205).

PROMISING COGNITIVE AND PSYCHOLOGICAL MARKERS FOR BVFTD BEYOND CURRENT DIAGNOSTIC CRITERIA

In the following section we aim to review newer developments regarding the early detection of bvFTD mainly through cognitive domains currently not mentioned in the FTDC criteria and to give practical suggestions regarding their assessment in clinical routine.

Social and Affective Cognition

Social cognition refers to a set of cognitive processes devoted to, or at least critically involved in, normal social interactions. This conceptual and somewhat arbitrary definition allows disentangling some mechanisms quite specific to the social dimension of cognition from others that may not be considered as specifically "social" despite their importance in interpersonal relationships such as language (206). Affective cognition may be defined as the mechanisms involved in emotional mediation of decision making and judgments, such as valence and reward processing, reinforcement, motivation etc. Both domains overlap widely as in one hand, mechanisms related to affective cognition often underlie social adjustment and in another, group, society, and culture could define or modulate the valence of behaviors. While this field of neurosciences is still emerging, studies that were focused on social and affective cognitive processing in bvFTD have flourished early in the 2000s and have contributed to develop our knowledge on the cognitive domain of social cognition besides helping the characterization of the disease (207, 208). In particular, these early studies showed that bvFTD patients could present a severe and early deficit in facial emotion recognition and theory of mind (or mentalizing), a cognitive ability allowing to infer other people's state of mind, such as what they want, think or feel. These pioneering works were followed by studies aiming to characterize the impairments in bvFTD in contrast to its most frequent differential diagnoses (209–214), to

identify the neural correlates of these deficits (215, 216) and to finally enhance the accuracy and earliness of the clinical diagnosis (164, 212). In parallel, the exploration of social and affective cognition in bvFTD also enriched the computational modeling of cognition (217, 218), increased our understanding of the cognitive architecture (219, 220) and provided new theoretical models of social functioning (221). The prototypical social impairments observed in bvFTD have led many to explore social cognition functions in this disease, maybe more than in any other brain disease or neuroatypical functioning, except autism.

Theory of Mind, Mental State-Inference

An impairment in theory of mind abilities has been extensively described in bvFTD (222, 223). Deficits have been observed using different paradigms based on false-belief (224–226), detection of sarcasm (210, 227) or insincere communication (228), agency attribution (229), as well as emotional inference or attribution (209, 230, 231), emotional movement-based inference (232) and social faux pas detection and understanding (207, 209, 212, 213). While similar deficits may be observed in AD as well [e.g., (225, 229) for a review, see (233)], they seem to be variable and to depend on the severity of the disease. In contrast to AD, theory of mind deficits in bvFTD were only sparsely or not associated with other cognitive dysfunctions(209, 225, 232) and only little associations with other cognitive dimensions in bvFTD have been found when cluster-based or regression analyses specifically investing these relationships were employed (219, 220). Considering cases of selective impairment of theory of mind in bvFTD [e.g., (204)], and the vast evidence for theory of mind processing deficits across a wide range of different tasks (i.e., from simple first-order false belief task to more complex test requiring context and social norms processing such as in faux pas detection tasks), a primary deficit of theory of mind in bvFTD, somewhat independent of other cognitive dysfunctions becomes likely. In contrast to that, in AD, a secondary deficit (i.e., impacted by memory or executive dysfunctions) may be assumed (220, 223, 232, 234). However, the primary vs. secondary opposition needs to be refined and may lack of clinical relevancy for single case diagnoses until more reliable measures of theory of mind are available for clinical routine.

Emotion Recognition, Responding, and Expressiveness

Emotion recognition deficits in bvFTD have also been very well described since the earliest studies. Static (208, 235) as well as dynamic (236) facial expression of emotion have been particularly found to be under recognized in bvFTD despite increased eye fixation time being reported (237), with patients over-relying on external contextual information to decode the emotion (238). Emotion responding is also disturbed, with patients showing a diminished self-conscious emotional behavior (embarrassment and amusement) as well as a diminished associated physiological response, particularly toward negative emotional stimuli (239, 240). Similarly, blunted expressiveness in response to emotional stimuli, especially in low-intensity context and decreased autonomic responses such as skin conductance have been observed in bvFTD (241–244). Finally, recent investigations have showed that patients with bvFTD could have difficulties to imitate facial emotion expressions (245). In contrast, independent from the test considered, a systematic review recently conducted has shown that impairment in facial emotion recognition is not a consistent finding in AD and depends on disease severity (246–248).

Self-Related Representations and Agency

Self-related representations are impaired in bvFTD which is sometimes considered as a "prototypical disorder of the self" (249). Patients tend to overestimate their functioning in daily living activities, cognitive, emotional or motivational control, empathic, and social/interpersonal domains (100, 214, 250). As a consequence, they also underestimate their cognitive difficulties and have poor insight about their brain condition and its related management (214, 251). Patients could show inaccurate self-awareness of their current personality (252) and have diminished monitoring abilities and autonomic and emotional reactivity to errors in objective tasks (253, 254). There is also a diminution of the self-reference effect in bvFTD, known to increase performance in controls during memory processing (249).

Social Norms and Rules Processing Deficits

While social norms and rules processing deficits have never been assessed through objective testing in bvFTD unlike in other conditions [e.g., (255)], converging evidence suggest a global deficit in this domain. The differentiation within a culture between proper and improper behaviors that is made through morality mostly provided the most frequent context to assess this domain in the past 20 years. Findings from these studies reported no differences with controls on the evaluation (in terms of right or wrong) of conventional rules such as "how wrong is it if you keep money found on the ground" or in standard moral dilemma such as the Trolley Car Dilemma, in which patients have to adopt a utilitarian choice by deciding between causing the death of either one or five workmen (256). In addition, ratings of responsibility, blameworthiness and punishment were similar between bvFTD, AD and controls in a task involving moral transgressions in low (e.g., cheating for taxes) or high (e.g., murdering one own family) emotional context (257) in a deterministic context (i.e., without free will). However, differences between bvFTD and controls and AD were retrieved in the Footbridge Dilemma that is supposed to illicit empathic concern with a character of the story, as well as in evaluations of social and moral rules that have been considered as being grounded in mutuality and others' respect (256, 258, 259). Interestingly, patients were reported to verbalize less discomfort and also have reduced autonomic response during moral dilemma (256, 260) compared to controls. Lack of empathy, emotional blunting, and cognitive flexibility deficits have been considered as potential explanation for such deficits, as well as an impairment regarding the integration of social contextual information. More recently, the use of more sophisticated tasks to assess moral judgments showed that bvFTD over-rely on outcomes rather than intentions to consider attempted or accidental harms as permissible or not, therefore

judging attempted harm as more permissible and accidental harm as less permissible than controls (261).

Reward Processing Deficit and Affective Decision Making

Only a few objective tasks have been used to assess reward processing in bvFTD but they showed that reward processing deficits are also very commonly observed in this disease. Patients could present a general deficit in reward valuation (262, 263) and thus, stimulus-reinforcement learning impairment (264). In patients in earlier stages of the disease who were not impaired in reinforcement learning, difficulties to suppress a previously rewarded behavior when it becomes punishing were observed (215), a lack of "reversal learning" that could prevent the quick adjustments that are needed on a daily basis in the social life. Although social rewards processing itself has been only rarely investigated in bvFTD, one study suggest that patients could be more indifferent to reward in comparison to AD and controls (265). Patients also showed a decreased sensitivity to negative stimuli (266) and delayed reward (267) as well as an absence of some natural decision-making bias such as the certainty effect, leading to a pathologically, albeit more rational, decision-making behavior (268). An innovative, laboratory-based, free-feeding study suggested that binge eating could be partially mediated by reward processing deficit as well, a result coherent with the fact that food is processed as a primary reward in the brain (269). In most of these different tasks, an AD group was included as a pathological control group and showed normal or subnormal performance in comparison to bvFTD. Reward processing deficits could thus be considered as an interesting cognitive marker of bvFTD but more reliable tasks are needed for clinical assessment.

Although the aforementioned tasks could be considered as assessing "decision-making" because they frequently involve binary choices between two items that are modulated by reward or punishment, the concept of decision making has mostly been retained to describe choices based on more complex information processing. In this context, apart from one exception (270), the Iowa Gambling Task has been employed, but revealed controversial results for the diagnosis of bvFTD. While early studies showed a good sensitivity (164) and specificity (209), others reported less clear results (213, 271), revealing a large intra-group variance in patients with bvFTD and AD as well as in controls that was dependent on levels of explicit knowledge individual participants had developed during the task [for a discussion, see (213)].

Symptomatic Behaviors of bvFTD and Social/Affective Cognition Impairments

While direct relationships between specific dysfunctions of social and affective cognition and abnormal behavior in bvFTD still have to be investigated in depth, social cognition assessment offers an objective evaluation of abilities that may drive many aspects of behavior. For example, a deficit in emotion recognition may prevent patients to recognize sadness, fear or anger in others' faces and to adapt their behavior accordingly. An impairment of theory of mind abilities would prevent patients to grasp others' mental states or feelings and thus to predict others' perspectives or actions, leading to behaviors that might appear egocentric or selfish. Similarly, a pathological theory of mind or empathy deficit could lead to commit abuses (223), or to be victim of one. The disintegration of social norms knowledge could also interfere with day-to-day adaptations in new social groups or contexts and may be associated with law violations in bvFTD (272). Alterations in reward processing may have an impact on the motivational aspects of what drives or regulates day-to-day behaviors, and could thus lead to apathy and lack of interest toward others, activities or things (83) and to a decrease of prosocial behavior (273). Likewise disinhibited eating patterns and binge eating has been associated with particular brain circuits involved in reward processing (269). Describing and delineating the different cognitive processes that drive or regulate behavior and that allow a smooth social life is thus among the biggest challenge in modern social and affective neurosciences [e.g., see the recent attempts to delineate apathy into distinct cognitive mechanisms (274, 275)].

Clinical Assessment of Social and Affective Cognition

The identification of social and affective cognition as a distinct cognitive domain [as in the current edition of the Diagnostic And Statistical Manual For Mental Disorders, DSM-5 (276)] allows researchers and clinicians to specifically target its mechanisms for research and clinical assessment. By contrast to behavioral scales or questionnaires such as the IRI, the Social Behavior Observer Checklist or the Social Norms Questionnaire (277), neuropsychological tests of social and affective cognition abilities offer an objective assessment, less impacted by inter-rater variability and by caregivers or clinicians' subjectivity. Thus, although the assessment of social and affective cognition is not mentioned in neuropsychological criteria of bvFTD, we recommend assessing at least one of the aforementioned functions when a social and/or affective cognitive impairment is suspected. Clinically suitable assessment tools differ widely in their length, reliability and norms availability. Clinical validity, i.e., an appropriate sensitivity and specificity for bvFTD is also a key criterion to guide the choice of a clinical tool. Although comparative validity studies are rare, some meta-analyses have been conducted to explore the ability of functions or tests to distinguish bvFTD from AD. For Facial emotion recognition, Ekman faces (278) or dynamic stimuli from the first part of The Awareness of Social Inference Test [TASIT (279)] are among the recommendable assessments in this perspective (280), while the later may not be available in languages other than English. A novel approach to assess emotion processing, which might be more sensitive to slight or subtle impairments is the rating of facial emotion intensity instead of labeling facial emotional expressions (281). For the assessment of theory of mind, Faux pas recognition tests and, to a lesser extent, sarcasm detection appear to be particularly useful to distinguish bvFTD from AD (233). However, particularly faux pas recognition tests are dependent on intact language comprehension, abstract reasoning and patient motivation, limiting their use to early stages of neurodegenerative cognitive disorders (231). Among validated batteries allowing the assessment of both functions (emotion recognition and theory of mind), the TASIT and the mini Social cognition and

Emotional Assessment [mini-SEA; (212)] offer good clinical sensitivity and specificity. Beyond these tools mostly developed for or with patients in neurodegenerative diseases, the Wechsler Advanced Clinical Solutions Social Perception subtest (282), the Edinburgh Social Cognition Test (283) and the EMOTICOM [for Emotion, Motivation, Impulsivity, and Social Cognition (284)] could offer alternative multi-dimensional assessments of social cognitive functions with less language load, but their applicability in neurodegenerative syndromes has not yet been assessed.

Apraxia

Still relatively poorly understood, apraxia is a multifactorial cognitive disorder affecting skilled movement, tool-use and/or gesturing on command despite intact task comprehension and basic sensorimotor functions (285). Impairments in praxis abilities can differentially involve imitation of limb gestures or face postures, the performance of communicative gestures (e.g., pantomiming the use of a common tool) or actual tool-use on command (286). Apraxic movements are qualitatively characterized by slow, insecure, and inaccurate movements which are performed in a halting and erroneous manner including frequent self-corrections (287). Historically, apraxia has been almost exclusively identified and studied in patients with left hemispheric stroke and comorbid aphasia (286, 288, 289). Nonetheless apraxia can also occur in the absence of aphasia, after e.g., right-brain lesions and also in a range of neurodegenerative disorders of which AD has been most extensively studied (290–295).

Apraxia and Impairment of Praxis Domains in Neurodegenerative Diseases

Despite explicit recommendations in consensus diagnostic guidelines for early neurodegenerative dementia syndromes (296) as well as its mentioning as a cognitive subdomain of the visual-perceptual abilities in the DSM-5 (276), the assessment of praxis disorders is currently widely neglected in clinical and neuropsychological diagnostic routine for patients with suspected dementia. Only recently, apraxia has gotten into the focus of clinical research on the early detection and differential diagnosis of neurodegenerative dementia syndromes such as bvFTD and AD (122, 297–300). Although results highly depend on the employed assessment methods and the tested praxis domains, an array of studies has now shown that patients with bvFTD show overall poorer performance in quantitative praxis tasks as well as clinical evaluations of praxis performance (297–301). Regarding the affected dimensions of praxis dysfunction, evidence suggests that performance in the domains imitation of meaningless hand or limb postures, pantomime of common object-use, and particularly imitation of face-postures are each significantly reduced in early stages of bvFTD compared to healthy age-matched controls (299, 302). These results are particularly intriguing as patients with bvFTD show no or only minor comorbid language symptoms in clear contrast to the prototypical apraxic and aphasic patients after left-hemispheric stroke. When compared to patients with AD, bvFTD patients present with a praxis profile of similar or less severe limb apraxia (i.e., imitation of meaningless gestures and pantomime of object-use) but relatively more pronounced buccofacial [or "orofacial," sometimes used synonymously (303)] praxis deficits with a particular impairment regarding the imitation of face postures (122, 297, 299, 301, 302). Across different samples and using diverse apraxia tests such a relative "buccofacial apraxia profile" robustly showed high diagnostic accuracy for the diagnosis of bvFTD and also stood out among several established standard neurocognitive tests and domains (including standard memory and executive tasks) regarding diagnostic accuracy for the discrimination between AD and bvFTD (122, 301). Conversely, a praxis profile that is more indicative of AD (i.e., relatively more deficits in imitation of spatially complex, semantically meaningless limb gestures as compared to facial imitation) successfully predicted ß-amyloid levels (a core biomarker for AD) in the CSF of patients with a wide range of different clinical dementia syndromes (304). Although more research is needed, these results suggest that disease-specific praxis profiles may be related to underlying pathology beyond clinical presentations of neurodegenerative diseases.

Neural Substrates of Praxis Impairments

Regarding neural correlates of praxis impairments, large-scaled lesion studies in patients with stroke imply that limb praxis skills are subserved by densely interconnected but also segregated functional neuroanatomical networks involving parietal, temporal and frontal cortices mainly within the left hemisphere (305–308). More specifically, converging evidence point toward the involvement of at least two segregated neural "streams" for limb praxis [dual-stream model for action (309)]. A "dorsal stream" (leading from occipital visual areas via the parietal cortex into pre-motor areas) is suggested to be involved in gross visuospatial analysis of postures, online-sensorimotor control (e.g., important for the grasping of objects) as well as holding representations of learned skilled movements. For the latter function, neural correlates have been found primarily in the inferior parietal lobe (IPL) so that some authors subdivide this part of the dorsal stream into a "ventro-dorsal stream" (309). The ventral stream (leading from occipital visual areas via the temporo-parietal junction into the anterior temporal lobe) may be more involved with analysis of semantic aspects of gestures and movements including object identification and knowledge about the use and function of tools (307).

To our knowledge, only one study specifically investigated correlations between praxis performance and brain volume in patients with early stage bvFTD and AD so far (310). The authors found significant correlations between performance on the imitation of meaningless limb gestures and volumes of parietal cortices (primarily the IPL and the precuneus), mostly compatible with neural models of limb apraxia derived from patients with stroke. For object-pantomime, the results pointed toward a distinct involvement of the right hemisphere (correlation with middle right temporal gyrus and angular gyrus).

The neural correlates of deficits in buccofacial praxis abilities (as previously mentioned, a domain that is often specifically impaired in bvFTD) are however, mostly unknown regardless of whether investigating patients with stroke or

neurodegenerative diseases. Anecdotal evidence however, points toward involvement of (medial) frontal areas and the frontal operculum in buccofacial praxis abilities and/or imitation of face postures (245, 311–313). Interestingly, buccofacial apraxia has also been reported in patients with MND (303).

Clinical Assessment of Praxis Impairments

Praxis dysfunction in bvFTD and other neurodegenerative dementia syndromes may well be tested with standardized assessment tools designed for stroke patients [e.g., Cologne Apraxia Screening (CAS) (314), Test of Upper Limp Apraxia (TULIA-AST) (315)]. However, these tests have not been validated in neurodegenerative dementia samples thus far and it has also not been addressed whether the praxis subdomains included in these tests are similarly relevant or important in neurodegenerative diseases. An exception with that regard is the Dementia Apraxia Test (DATE) (302), which has been constructed using a data-driven approach in order to maximize its utility for the early detection of patients with neurodegenerative dementia and particularly for differential diagnosis between AD and patients with FTD. The test is freely available, offers clinical cut-off scores for dementia (vs. healthy age-matched controls) and has been initially validated in patients with early AD, bvFTD and healthy elderly participants. The test has since also proven valuable for the differential diagnosis of language variants of FTD, showing evidence of disease-specific "apraxia profiles" (301). Data on praxis impairments in other early neurodegenerative patient groups (e.g., Parkinson's disease) as well as more extensive normative data for the DATE involving healthy controls from diverse cultural backgrounds is currently collected.

Interoception and its Potential Links With Social Cognition, Apraxia, and Behavioral Symptoms of bvFTD

Interoception refers to the mechanism allowing us to perceive, infer, and predict our own physiological state through the integration of multimodal sensory input arising from the current state of the body (316). This sense of the body's internal states involves a large-scale brain system among which the insula, the thalamus, the anterior cingulate and the somatosensory cortices play a critical role (317). In bvFTD, interoceptive accuracy, and awareness have been shown to be decreased, notably in relation to fronto-insular gray matter and connectivity decrease (i.e., alterations in functional network connectivity). For example the so-called salience network, functionally connecting the main structures that were identified to be involved in interoceptive processing, has found to be attenuated in bvFTD (318, 319). Deficient processing of internal somatosensory signals in bvFTD has been shown across an array of different modalities including pain, temperature, and heartbeat perception, strengthening the hypothesis that the interoceptive function is a domain-general system supporting or at least strongly overlapping with emotion, motivation/reward processing and affective mental state inference (i.e., theory of mind abilities) (318, 320–324). Compared with healthy subjects, patients with bvFTD for example showed a lower autonomic response toward emotional stimuli (243, 244, 325), even when accuracy of detection was similar (326). Another recent study suggests that interoceptive impairment in different variants of FTD may be related to lower autonomic responses as well as to cognitive aspects of correctly analyzing body state representations (327). Because of the importance of emotion and theory of mind deficits in bvFTD as well as the increasing evidence pointing to interoception deficits and the associations of these deficits with insular damage, bvFTD may represent a prototype to investigate the relationship between these functions and could bring clinical data to understand the generative and predictive nature of the embodied mind.

With regard to links between apraxia, social and affective cognition, and interoception, preliminary data suggest that deficits in the imitation of facial postures may be correlated with facial emotion recognition performance and to a lesser degree also with caregiver reports of social-behavioral abnormalities in bvFTD (301). One reason for these associations and a potential common mechanism for both, facial affect recognition and face imitation may be that an accurate interpretation of internal somatosensory signals (and interoceptive changes) is required to (a) correctly decode and label a facial expression (or a body posture) and (b) to correctly imitate it (328). The broader idea of an "embodied cognition framework" for the perception of action stresses that interoceptive signals (e.g., muscle tonus, perception of spatial body postures) need to be correctly interpreted by the brain in order to then form accurate representations via internal motor simulations [e.g., motor imagery (329, 330)] and subsequently to accurately perform a gesture or posture (331–333). In other words, both accurate interoceptive signals and internal mental simulations (in terms of an accurate interpretation of these signals) may be a necessary and shared prerequisite for the ability to identify and correctly label face postures as well as to imitate them (334). Future research will eventually shed light on the precise associations between (facial) imitation abilities in praxis tasks, facial emotion recognition and processing of interoceptive signals as well as their biological and neural underpinnings in bvFTD and other neurodegenerative syndromes that share an early atrophy of brain regions crucial for interoceptive signal processing (e.g., semantic dementia).

CONCLUSION, CHALLENGES, AND OUTLOOK

Despite refined clinical diagnostic criteria, the early clinical diagnosis of bvFTD is still challenging and requires an in-depth assessment of clinical signs, behavioral and psychological symptoms as well as cognitive performance. Given the typically present anognosia in patients with bvFTD, caregivers are currently the main source of information for the evaluation of disease-typical behavioral and psychological changes. However, a standardized and focused neurocognitive assessment including memory, visuospatial abilities, social cognition, and praxis is crucial for an early differential diagnosis. Although executive dysfunction and preserved episodic memory are required to fulfill the "neuropsychology item" in the current criteria, we have highlighted that a range of studies have shown ambiguous results

with more heterogeneous and complex cognitive performance deficits in patients with bvFTD. Neuropsychological assessments of a range of specific functions including aspects of social and affective cognition and praxis abilities have shown to potentially enhance the diagnostic accuracy but are not yet represented in the diagnostic criteria. It is however highly likely that behavioral symptoms e.g., a lack of empathy in bvFTD is mostly a behavioral expression of a social and affective cognitive deficit. Whether behavioral symptoms presented in e.g., psychiatric syndromes or in the phenocopy syndrome of bvFTD could also be captured by specific social and affective cognitive testing remains an open question and a challenge for the field.

In parallel of summarizing behavioral, psychological, and cognitive symptoms of bvFTD, we also presented and critically evaluated common methods of assessment for an early clinical diagnosis of this disease. We came to the conclusion that one of the major challenges of clinical neuropsychology in the coming years will be to fill the current gap of reliable and effective methods to assess cognitive alterations and access the behavioral and psychological symptoms as laid out in the criteria through performance-based testing. Neuropsychologists have to design novel tests that better fit the clinical practice and its requirements. Tools centered on diagnosis, evaluation, and follow-up are critically needed to replace some paper-pencil tests that are in use since several decades. Clinical neuropsychologists need to foster on new theoretical advances (e.g., psychological or neuroscientific models) and concrete (e.g., anatomical or biological) knowledge available in order to design novel ways of assessing cognitive functions and subsequently relate these to the typical behavioral symptoms. The development of new performance-based tasks is necessary to expand our evaluation to the currently over-looked domains of cognition in clinical routine, such as social cognition—a vast domains in itself, as well as reward processing, interoception, decision-making, and praxis abilities. However, in our opinion, there is also a vivid challenge to develop new ways of clinical assessment of the "classic," well-known cognitive functions, such as memory, language, visuospatial processing, or executive functions. Despite the relevance they might have had at a certain time, it is surprising that tests such as the WCST (or its subsequent modified versions), originally published in 1948 (335) and developed to assess abstract reasoning and set-shifting in the normal population, are still used on a daily basis as a clinical test for prefrontal cortex function, despite knowledge about its numerous limits and shortcomings (336) including a lack of validity in non-western cultures (337). Similarly, the typical assessment of "episodic" verbal memory in clinical routine mostly relies on word-list that patients have to remember and recall, despite the lack of ecological value and autonoetic consciousness of this paradigm and the known confounding factor of semantic processing in cue-based recall tests (34). In particular, we believe that the social dimensions of cognitive key domains such as memory need to be taken into account in order to design more ecologically valid tests from which conclusions relevant for both clinical diagnosis and patients' activities of daily living may be drawn. In this perspective, individualized tests that use items specifically relevant to one patient [e.g., presenting faces from colleagues or friends to assess face familiarity (338)] are interesting, although certainly difficult to implement in clinical routine. Digital assessment technologies including computer-games or virtual reality are promising for clinical neuropsychology, however available apps frequently lack data on convergent validity with standard paper-pencil tests and normative data crucial for the interpretation of individual performance is rarely provided. Nevertheless, app-based cognitive research offers promising new opportunities by potentially increasing caregiver's and patient's motivation to participate in cognitive assessments, for example at home and thus with a maximum of comfort. Apps may also provide enormously large data-sets from which normative data and also very early abnormalities may be extracted using statistical "big-data" methods [for a successful example see a recent data analysis involving the app "Sea Hero Quest" (339)].

In the specific case of bvFTD, we believe that a major limitation to include some already well-described novel cognitive markers in the diagnostic criteria is the lack of availability of many current cognitive performance tests and behavioral scales. One of the potential reasons for this is an overall lack of research regarding cross-validation of the existing instruments as well as establishing adequate normative data and evidence of psychometric quality. These approaches require a lot of time and energy while being commonly disregarded in academia and research, as the former often leads to replications or negative-findings and the later will only be published in neuropsychology-specific, often national journals. This might be especially true for neuropsychological tools that are developed within a medical context (such as in neurodegeneration) as the difficulty to convince about the importance of psychometric studies and to conduct such studies in medicine may be higher than in the field of psychology. These shortcomings however, frequently impede a standardized interpretation of a patient's test result (by means of an evaluation of its abnormality) even when standardized performance tests or clinical scales are available for certain symptoms of bvFTD. Particularly, official translations into different languages are rarely provided or have usually not been independently validated in other cultures. In the case of diagnosing bvFTD, this is especially problematic as for example, perceived abnormality of social behaviors is highly culture-dependent. Such cultural variations may directly impact performance-tests as well as, for example, in the commonly used faux pas test: to mistake a young girl for a boy because she has short hair or a man for a waiter because he stands near the checkout in a restaurant may have been considered as rude and as a social faux pas in 1999 in the context of upper-class cantabrigian population in which the test has been originally developed, but may be perceived as simple mistakes without any negative social consequences for a lot of people 20 years later. Although cultural and socio-economical variability may appear as more important for the domain of social cognition, its influence may also be observed in a wide range of neuropsychological measures and "classic" cognitive domains [e.g., (340, 341)]. Finally, the vast majority of the presented standardized performance-tests and scales to differentiate between bvFTD and competing diagnoses (e.g., AD, affective disorders, other neurodegenerative diseases) have so far mainly been shown to function in usually small

samples (with specific demographic and cultural characteristics), highlighting the importance of collaborative research and cross-cultural validation studies. Replications and cross-validation studies of tests and scales in larger and more diverse samples including extensive collection of data from healthy controls are needed in order to extrapolate from individual test results onto specific diagnostic decisions (e.g., Which cognitive performance profile or which set of behaviors are both pathological/abnormal and specific for an early diagnosis of bvFTD in a certain age-group, for a specific level of education, and in a certain culture?). In our view, this is currently one of the major challenges in the field of clinical neuropsychology but also a crucial prerequisite for the future establishment of valid and meaningful biomarkers for FTLD. In this perspective, the Social cognition and FTLD network (https://sites.google.com/view/soccogftld) has been created in order to share data on healthy controls and patients allowing large-scale clinical validity and cross-cultural studies—so far using the mini-SEA. If multiplicated, such initiatives may bring important data on both cognitive functions and the tests used to assess them and could later fasten the inclusion of specific cognitive dysfunction into the diagnostic criteria for neurodegenerative diseases.

An important future role of clinical neuropsychology will emerge with the evaluation and comparison of newly developed biomarkers by means of employing the complex assessment methods for behavioral, psychological symptoms as well as cognitive functions in patients with suspected bvFTD and competing diagnoses. Besides its role in cognitive rehabilitation, expertise in clinical neuropsychology will thus continue to play an important role in the detection and diagnosis of early bvFTD even and particularly in the light of emerging biomarkers for the disease.

AUTHOR CONTRIBUTIONS

All authors listed have made a substantial, direct and intellectual contribution to the work, and approved it for publication.

FUNDING

We acknowledge support from the Open Access Publication Fund of the University of Muenster.

REFERENCES

1. Rascovsky K, Hodges JR, Knopman D, Mendez MF, Kramer JH, Neuhaus J, et al. Sensitivity of revised diagnostic criteria for the behavioural variant of frontotemporal dementia. *Brain*. (2011) 134:2456–77. doi: 10.1093/brain/awr179
2. Neary D, Snowden J, Gustafson L. Frontotemporal lobar degeneration A consensus on clinical diagnostic criteria. *Neurology*. (1998) 51:1546–54. doi: 10.1212/WNL.51.6.1546
3. Pressman PS, Miller BL. Diagnosis and management of behavioral variant frontotemporal dementia. *Biol Psychiatry*. (2014) 75:574–81. doi: 10.1016/j.biopsych.2013.11.006
4. Hogan DB, Jetté N, Fiest KM, Roberts JI, Pearson D, Smith EE, et al. The prevalence and incidence of frontotemporal dementia: a systematic review. *Can J Neurol Sci*. (2016) 43:S96–109. doi: 10.1017/cjn.2016.25
5. Onyike CU, Diehl-Schmid J. The epidemiology of frontotemporal dementia. *Int Rev Psychiatry*. (2013) 25:130–7. doi: 10.3109/09540261.2013.776523
6. Gislason TB, Sjögren M, Larsson L, Skoog I. The prevalence of frontal variant frontotemporal dementia and the frontal lobe syndrome in a population based sample of 85 year olds. *J Neurol Neurosurg Psychiatry*. (2003) 74:867–71. doi: 10.1136/jnnp.74.7.867
7. Johnson JK, Diehl J, Mendez MF, Neuhaus J, Shapira JS, Forman M, et al. Frontotemporal lobar degeneration: demographic characteristics of 353 patients. *Arch Neurol*. (2005) 62:925–30. doi: 10.1001/archneur.62.6.925
8. Rosso SM, Kaat LD, Baks T, Joosse M, De Koning I, Pijnenburg Y, et al. Frontotemporal dementia in The Netherlands: patient characteristics and prevalence estimates from a population-based study. *Brain*. (2003) 126:2016–22. doi: 10.1093/brain/awg204
9. Lanata SC, Miller BL. The behavioural variant frontotemporal dementia (bvFTD) syndrome in psychiatry. *J Neurol Neurosurg Psychiatry*. (2016) 87:501–11. doi: 10.1136/jnnp-2015-310697
10. Vijverberg EGB, Dols A, Krudop WA, Peters A, Kerssens CJ, Van Berckel BNM, et al. Diagnostic accuracy of the frontotemporal dementia consensus criteria in the late-onset frontal lobe syndrome. *Dement Geriatr Cogn Disord*. (2016) 41:210–9. doi: 10.1159/000444849
11. Gossink FT, Dols A, Kerssens CJ, Krudop WA, Kerklaan BJ, Scheltens P, et al. Psychiatric diagnoses underlying the phenocopy syndrome of behavioural variant frontotemporal dementia. *J Neurol Neurosurg Psychiatry*. (2016) 87:64–8. doi: 10.1136/jnnp-2014-308284
12. Wooley JD, Khan BK, Murthy NK, Miller BL, Rankin katherine P. The diagnostic challenge of psychiatric symtpoms in neurodegenerative disease; rates of and risk factors for prior psychiatric disgnosis in patients with early neurodegenerative disease. *J Clin Psych*. (2011) 72:126–33. doi: 10.4088/JCP.10m06382oli
13. Perry DC, Brown JA, Possin KL, Datta S, Trujillo A, Radke A, et al. Clinicopathological correlations in behavioural variant frontotemporal dementia. *Brain*. (2017) 2017:1–17. doi: 10.1093/brain/awx254
14. Woollacott IO, Rohrer JD. The clinical spectrum of sporadic and familial forms of frontotemporal dementia. *J Neurochem*. (2016) 138:6–31. doi: 10.1111/jnc.13654
15. Snowden JS, Thompson JC, Stopford CL, Richardson AMT, Gerhard A, Neary D, et al. The clinical diagnosis of early-onset dementias: diagnostic accuracy and clinicopathological relationships. *Brain*. (2011) 134:2478–92. doi: 10.1093/brain/awr189
16. Mackenzie IRA, Neumann M. Molecular neuropathology of frontotemporal dementia: insights into disease mechanisms from postmortem studies. *J Neurochem*. (2016) 138:54–70. doi: 10.1111/jnc.13588
17. Mackenzie IRA, Neumann M, Bigio EH, Cairns NJ, Alafuzoff I, Kril J, et al. Nomenclature for neuropathologic subtypes of frontotemporal lobar degeneration: consensus recommendations. *Acta Neuropathol*. (2009) 117:15–8. doi: 10.1007/s00401-008-0460-5
18. Rohrer JD, Warren JD. Phenotypic signatures of genetic frontotemporal dementia. *Curr Opin Neurol*. (2011) 24:542–9. doi: 10.1097/WCO.0b013e32834cd442
19. Goldman JS, Farmer JM, Van Deerlin VM, Wilhelmsen KC, Miller BL, Grossman M. Frontotemporal dementia: genetics and genetic counseling dilemmas. *Neurologist*. (2004) 10:227–34. doi: 10.1097/01.nrl.0000138735.48533.26
20. Quaid KA. Genetic counseling for frontotemporal dementias. *J Mol Neurosci*. (2011) 45:706–9. doi: 10.1007/s12031-011-9557-8
21. Pottier C, Ravenscroft TA, Sanchez-Contreras M, Rademakers R. Genetics of FTLD: overview and what else we can expect from genetic studies. *J Neurochem*. (2016) 138:32–53. doi: 10.1111/jnc.13622
22. Seelaar H, Rohrer JD, Pijnenburg YL, Fox NC, van Swieten JC. Clinical, genetic and pathological heterogeneity of frontotemporal

dementia: a review. *J Neurol Neurosurg Psychiatry*. (2011) 82:476–86. doi: 10.1136/jnnp.2010.212225
23. Renton AE, Majounie E, Waite A, Simón-Sánchez J, Rollinson S, Gibbs JR, et al. A hexanucleotide repeat expansion in C9ORF72 is the cause of chromosome 9p21-linked ALS-FTD. *Neuron*. (2011) 72:257–68. doi: 10.1016/j.neuron.2011.09.010
24. DeJesus-Hernandez M, Mackenzie IR, Boeve BF, Boxer AL, Baker M, Rutherford NJ, et al. Expanded GGGGCC hexanucleotide repeat in noncoding region of C9ORF72 causes chromosome 9p-linked FTD and ALS. *Neuron*. (2011) 72:245–56. doi: 10.1016/j.neuron.2011.09.011
25. Gordon E, Rohrer JD, Fox NC. Advances in neuroimaging in frontotemporal dementia. *J Neurochem*. (2016) 138:193–210. doi: 10.1111/jnc.13656
26. Pan P, Song W, Yang J. Gray matter atrophy in behavioral variant frontotemporal dementia: a meta-analysis of voxel-based morphometry studies. *Dement Geriatr Cogn Disord*. (2012) 33:141–8. doi: 10.1159/000338176
27. Schroeter ML, Raczka K, Neumann J, Yves von Cramon D. Towards a nosology for frontotemporal lobar degenerations-a meta-analysis involving 267 subjects. *Neuroimage*. (2007) 36:497–510. doi: 10.1016/j.neuroimage.2007.03.024
28. Krämer J, Lueg G, Schiffler P, Vrachimis A, Weckesser M, Wenning C, et al. Diagnostic value of diffusion tensor imaging and positron emission tomography in early stages of frontotemporal dementia. *J Alzheimer's Dis*. (2018) 63:239–53. doi: 10.3233/JAD-170224
29. Kerklaan BJ, van Berckel BNM, Herholz K, Dols A, van der Flier WM, Scheltens P, et al. The added value of 18-fluorodeoxyglucose-positron emission tomography in the diagnosis of the behavioral variant of frontotemporal dementia. *Am J Alzheimer's Dis Other Dementias*. (2014) 29:607–13. doi: 10.1177/1533317514524811
30. Schroeter ML, Laird AR, Chwiesko C, Deuschl C, Schneider E, Bzdok D, et al. Conceptualizing neuropsychiatric diseases with multimodal data-driven meta-analyses - The case of behavioral variant frontotemporal dementia. *Cortex*. (2014) 57:22–37. doi: 10.1016/j.cortex.2014.02.022
31. Whitwell J, Josephs K. Recent advances in the imaging of frontotemporal dementia. *Curr Neurol Neurosci Rep*. (2012) 12:715–23. doi: 10.1007/s11910-012-0317-0
32. Rohrer JD, Nicholas JM, Cash DM, van Swieten J, Dopper E, Jiskoot L, et al. Presymptomatic cognitive and neuroanatomical changes in genetic frontotemporal dementia in the Genetic Frontotemporal dementia Initiative (GENFI) study: a cross-sectional analysis. *Lancet Neurol*. (2015) 14:253–62. doi: 10.1016/S1474-4422(14)70324-2
33. Uflacker A, Edmondson MC, Onyike CU, Appleby BS. Caregiver burden in atypical dementias: comparing frontotemporal dementia, Creutzfeldt-Jakob disease, and Alzheimer's disease. *Int Psychogeriatr*. (2016) 28:269–73. doi: 10.1017/S1041610215001647
34. Hornberger M, Piguet O. Episodic memory in frontotemporal dementia: a critical review. *Brain*. (2012) 135:678–92. doi: 10.1093/brain/aws011
35. Krudop WA, Dols A, Kerssens CJ, Eikelenboom P, Prins ND, Moller C, et al. The pitfall of behavioral variant frontotemporal dementia mimics despite multidisciplinary application of the FTDC criteria. *J Alzheimers Dis*. (2017) 60:959–75. doi: 10.3233/JAD-170608
36. Harris JM, Gall C, Thompson JC, Richardson AMT, Neary D, du Plessis D, et al. Sensitivity and specificity of FTDC criteria for behavioral variant frontotemporal dementia. *Neurology*. (2013) 80:1881–7. doi: 10.1212/WNL.0b013e318292a342
37. La Marre AK, Rascovsky K, Bostrom A, Toofanian P, Wilkins S, Sha SJ, et al. Interrater reliability of the new criteria for behavioral variant frontotemporal dementia. *Neurology*. (2013) 80:1973–7. doi: 10.1212/WNL.0b013e318293e368
38. Dols A, Van Liempt S, Gossink F, Krudop WA, Sikkes S, Pijnenburg YAL, et al. Identifying specific clinical symptoms of behavioral variant frontotemporal dementia versus differential psychiatric disorders in patients presenting with a late-onset frontal lobe syndrome. *J Clin Psychiatry*. (2016) 2016:1391–5. doi: 10.4088/JCP.15m09844
39. Manes F. Psychiatric conditions that can mimic early behavioral variant frontotemporal dementia: the importance of the new diagnostic criteria. *Curr Psychiatry Rep*. (2012) 14:450–2. doi: 10.1007/s11920-012-0294-7
40. Valente ES, Caramelli P, Gambogi LB, Mariano LI, Guimarães HC, Teixeira AL, et al. Phenocopy syndrome of behavioral variant frontotemporal dementia: a systematic review. *Alzheimers Res Ther*. (2019) 2019:11:30. doi: 10.1186/s13195-019-0483-2
41. Lillo P, Mioshi E, Zoing MC, Kiernan MC, Hodges JR. How common are behavioural changes in amyotrophic lateral sclerosis? *Amyotroph Lateral Scler*. (2011) 12:45–51. doi: 10.3109/17482968.2010.520718
42. Burrell JR, Halliday GM, Kril JJ, Ittner LM, Götz J, Kiernan MC, et al. The frontotemporal dementia-motor neuron disease continuum. *Lancet*. (2016) 388:919–31. doi: 10.1016/S0140-6736(16)00737-6
43. Ghosh A, Dutt A, Bhargava P, Snowden J. Environmental dependency behaviours in frontotemporal dementia: have we been underrating them? *J Neurol*. (2013) 260:861–8. doi: 10.1007/s00415-012-6722-0
44. Schönecker S, Hell F, Bötzel K, Wlasich E, Ackl N, Süßmair C, et al. The applause sign in frontotemporal lobar degeneration and related conditions. *J Neurol*. (2019) 266:330–8. doi: 10.1007/s00415-018-9134-y
45. Hellmuth J, Mirsky J, Heuer HW, Matlin A, Jafari A, Garbutt S, et al. Multicenter validation of a bedside antisaccade task as a measure of executive function. *Neurology*. (2012) 78:1824–31. doi: 10.1212/WNL.0b013e318258f785
46. Douglass A, Walterfang M, Velakoulis D, Abel L. Behavioral variant frontotemporal dementia performance on a range of saccadic tasks. *J Alzheimers Dis*. (2018) 65:231–42. doi: 10.3233/JAD-170797
47. Coe BC, Munoz DP. Mechanisms of saccade suppression revealed in the anti-saccade task. *Philos Trans R Soc B Biol Sci*. (2017) 372:192. doi: 10.1098/rstb.2016.0192
48. Durães J, Tábuas-Pereira M, Araújo R, Duro D, Baldeiras I, Santiago B, et al. The head turning sign in dementia and mild cognitive impairment: its relationship to cognition, behavior, and cerebrospinal fluid biomarkers. *Dement Geriatr Cogn Disord*. (2018) 46:42–9. doi: 10.1159/000486531
49. Rankin KP, Santos-Modesitt W, Kramer JH, Pavlic D, Beckman V, Miller BL. Spontaneous social behaviors discriminate behavioral dementias from psychiatric disorders and other dementias. *J Clin Psychiatry*. (2008) 69:60–73. doi: 10.4088/JCP.v69n0109
50. Mendez MF, Fong SS, Shapira JS, Jimenez EE, Kaiser NC, Kremen SA, et al. Observation of social behavior in frontotemporal dementia. *Am J Alzheimers Dis Other Demen*. (2014) 29:215–21. doi: 10.1177/1533317513517035
51. Mathias JL, Morphett K. Neurobehavioral differences between Alzheimer's disease and frontotemporal dementia : a meta-analysis. *J Clin Exp Neuropsychol*. (2010) 32:682–98. doi: 10.1080/13803390903427414
52. Dols A, Pijnenburg YAL, Wa K, Gossink FT, Stek ML. Late life bipolar disorders evolving into frontotemporal dementia mimic. *Bipolar Disord*. (2015) 17:66–67. doi: 10.2147/NDT.S99229
53. Borroni B, Agosti C, Premi E, Cerini C, Cosseddu M, Paghera B, et al. The FTLD-modified clinical dementia rating scale is a reliable tool for defining disease severity in frontotemporal lobar degeneration: evidence from a brain spect study. *Eur J Neurol*. (2010) 17:703–7. doi: 10.1111/j.1468-1331.2009.02911.x
54. Mioshi E, Hsieh S, Savage S, Hornberger M, Hodges JR. Clinical staging and disease progression in frontotemporal dementia. *Neurology*. (2010) 74:1591–7. doi: 10.1212/WNL.0b013e3181e04070
55. Malloy P, Grace J. A review of rating scales for measuring behavior change due to frontal systems damage background: changes in cognition due to frontal disease or damage. *Cogn Behav Neurol*. (2005) 18:18–27. doi: 10.1097/01.wnn.0000152232.47901.88
56. Cummings JL. The Neuropsychiatric Inventory: assessing psychopathology in dementia patients. *Neurology*. (1997) 48:10–6. doi: 10.1212/WNL.48.5_Suppl_6.10S
57. Snowden JS, Rollinson S, Thompson JC, Harris JM, Stopford CL, Richardson AMT, et al. Distinct clinical and pathological characteristics of frontotemporal dementia associated with C9ORF72 mutations. *Brain*. (2012) 135:693–708. doi: 10.1093/brain/awr355
58. Devenney E, Hornberger M, Irish M, Mioshi E, Burrell J, Tan R, et al. Frontotemporal dementia associated with the C9ORF72 mutation: a unique clinical profile. *JAMA Neurol*. (2014) 71:331–9. doi: 10.1001/jamaneurol.2013.6002

59. Devenney EM, Ahmed RM, Halliday G, Piguet O, Kiernan MC, Hodges JR. Psychiatric disorders in C9orf72 kindreds. *Neurology*. (2018) 91:6344. doi: 10.1212/WNL.0000000000006344
60. Kertesz A, Davidson W, Fox H. Frontal behavioral inventory: diagnostic criteria for frontal lobe dementia. *Can J Neurol Sci*. (1997) 24:29–36. doi: 10.1017/S0317167100021053
61. Suhonen N-M, Hallikainen I, Hanninen T, Jokelainen J, Kruger J, Hall A, et al. The modified frontal behavioral inventory (FBI-mod) for patients with frontotemporal lobar degeneration, alzheimer's disease, and mild cognitive impairment. *J Alzheimer's Dis*. (2017) 56:1241–51. doi: 10.3233/JAD-160983
62. Malloy P, Tremont G, Grace J, Frakey L. The frontal systems behavior scale discriminates frontotemporal dementia from Alzheimer's disease. *Alzheimer's Dement*. (2007) 3:200–3. doi: 10.1016/j.jalz.2007.04.374
63. Duff K, Paulsen JS, Beglinger LJ, Langbehn DR, Wang C, Stout JC, et al. "Frontal" behaviors before the diagnosis of huntington's disease and their relationship to markers of disease progression: evidence of early lack of awareness. *J Neuropsychiatry Clin Neurosci*. (2010) 22:196–207. doi: 10.1176/appi.neuropsych.22.2.196
64. Boutoleau-Bretonnière C, Evrard C, Hardouin JB, Rocher L, Charriau T, Etcharry-Bouyx F, et al. DAPHNE: a new tool for the assessment of the behavioral variant of frontotemporal dementia. *Dement Geriatr Cogn Disord*. (2015) 5:503–16. doi: 10.1159/000440859
65. Wawrziczny E, Larochette C, Papo D, Constant E, Ducharme F, Kergoat MJ, et al. A customized intervention for dementia caregivers: a quasi-experimental design. *J Aging Health*. (2018) 2018:0898264318770056. doi: 10.1177/0898264318770056
66. Ye S, Rosenbohm A, Böhm S, Uttner I, Ji Y, Ludolph AC, et al. Cognitive and behavioral impairments in German and Chinese ALS populations - a *post-hoc* comparison of national study data. *Amyotroph Lateral Scler Frontotemporal Degener*. (2018) 2018:1–9. doi: 10.1080/21678421.2018.1542535
67. Hamdy RC, Kinser A, Kendall-Wilson T, Depelteau A, Whalen K. Impulsive, disinhibited behavior-dining in a restaurant. *Gerontol Geriatr Med*. (2018) 4:2333721418756994. doi: 10.1177/2333721418756994
68. Flanagan EC, Lagarde J, Hahn V, Guichart-Gomez E, Sarazin M, Hornberger M, et al. Executive and social-cognitive determinants of environmental dependency syndrome in behavioral frontotemporal dementia. *Neuropsychology*. (2018) 32:377–84. doi: 10.1037/neu0000433
69. O'Callaghan C, Shine JM, Hodges JR, Andrews-Hanna JR, Irish M. Hippocampal atrophy and intrinsic brain network dysfunction relate to alterations in mind wandering in neurodegeneration. *Proc Natl Acad Sci USA*. (2019) 116:3316–21. doi: 10.1073/pnas.1818523116
70. Finney CM, Mendez MF. Diogenes syndrome in frontotemporal dementia. *Am J Alzheimers Dis Other Demen*. (2017) 32:438–43. doi: 10.1177/1533317517717012
71. Tondo G, De Marchi F, Terazzi E, Sacchetti M, Cantello R. Frontotemporal dementia presenting as gambling disorder: when a psychiatric condition is the clue to a neurodegenerative disease. *Cogn Behav Neurol*. (2017) 30:62–7. doi: 10.1097/WNN.0000000000000122
72. Ghosh A, Dutt A. Utilisation behaviour in frontotemporal dementia. *J Neurol Neurosurg Psychiatry*. (2010) 81:154–6. doi: 10.1136/jnnp.2008.160416
73. Clark CN, Nicholas JM, Gordon E, Golden HL, Cohen MH, Woodward FJ, et al. Altered sense of humor in dementia. *J Alzheimer's Dis*. (2015) 49:111–9. doi: 10.3233/JAD-150413
74. Diehl-Schmid J, Perneczky R, Koch J, Nedopil N, Kurz A. Guilty by suspicion? Criminal behavior in frontotemporal lobar degeneration. *Cogn Behav Neurol*. (2013) 26:73–7. doi: 10.1097/WNN.0b013e31829cff11
75. Liljegren M, Naasan G, Temlett J, Perry DC, Rankin KP, Merrilees J, et al. Criminal behavior in frontotemporal dementia and Alzheimer disease. *JAMA Neurol*. (2015) 72:295–300. doi: 10.1001/jamaneurol.2014.3781
76. Shinagawa S, Shigenobu K, Tagai K, Fukuhara R, Kamimura N, Mori T, et al. Violation of laws in frontotemporal dementia: a multicenter study in Japan. *J Alzheimer's Dis*. (2017) 57:1221–7. doi: 10.3233/JAD-170028
77. Ahmed RM, Goldberg Z, Kaizik C, Kiernan MC, Hodges JR, Piguet O, et al. Neural correlates of changes in sexual function in frontotemporal dementia: implications for reward and physiological functioning. *J Neurol*. (2018) 265:2562–72. doi: 10.1007/s00415-018-9024-3
78. Mendez MF, Shapira JS. Kissing or 'osculation' in frontotemporal dementia. *J Neuropsychiatry Clin Neurosci*. (2014) 26:258–61. doi: 10.1176/appi.neuropsych.13060139
79. Mendez MF, Shapira JS. Hypersexual behavior in frontotemporal dementia: a comparison with early-onset Alzheimer's disease. *Arch Sex Behav*. (2013) 42:501–9. doi: 10.1007/s10508-012-0042-4
80. Cheng ST. Dementia caregiver burden: a research update and critical analysis. *Curr Psychiatry Rep*. (2017) 19:2. doi: 10.1007/s11920-017-0818-2
81. Levy R, Dubois B. Apathy and the functional anatomy of the prefrontal cortex-basal ganglia circuits. *Cereb Cortex*. (2006) 16:916–28. doi: 10.1093/cercor/bhj043
82. Robert P, Onyike CU, Leentjens AFG, Dujardin K, Aalten P, Starkstein S, et al. Proposed diagnostic criteria for apathy in Alzheimer's disease and other neuropsychiatric disorders. *Eur Psychiatry*. (2009) 24:98–104. doi: 10.1016/j.eurpsy.2008.09.001
83. Massimo L, Kales HC, Kolanowski A. State of the science: apathy as a model for investigating behavioral and psychological symptoms in dementia. *J Am Geriatr Soc*. (2018) 66(Suppl 1):S4–12. doi: 10.1111/jgs.15343
84. Massimo L, Powers C, Moore P, Vesely L, Avants B, Gee J, et al. Neuroanatomy of apathy and disinhibition in frontotemporal lobar degeneration. *Dement Geriatr Cogn Disord*. (2009) 27:96–104. doi: 10.1159/000194658
85. Merrilees J, Dowling GA, Hubbard E, Mastick J, Ketelle R, Miller BL. Characterization of apathy in persons with frontotemporal dementia and the impact on family caregivers. *Alzheimer Dis Assoc Disord*. (2013) 27:62–7. doi: 10.1097/WAD.0b013e3182471c54
86. Yassuda MS, Lima da Silva TB, O'Connor CM, Mekala S, Alladi S, Bahia VS, et al. Apathy and functional disability in behavioral variant frontotemporal dementia. *Neurol Clin Pract*. (2018) 8:120–8. doi: 10.1212/CPJ.0000000000000429
87. Shin JS, Kim MS, Kim NS, Kim GH, Seo SW, Kim E-J, et al. Excessive TV watching in patients with frontotemporal dementia. *Neurocase*. (2013) 19:489–96. doi: 10.1080/13554794.2012.701638
88. Lansdall CJ, Coyle-Gilchrist ITS, Jones PS, Rodríguez PV, Wilcox A, Wehmann E, et al. Apathy and impulsivity in frontotemporal lobar degeneration syndromes. *Brain*. (2017) 140:1792–807. doi: 10.1093/brain/awx101
89. Misiewicz S, Brickman AM, Tosto G. Prosodic impairment in dementia: review of the literature. *Curr Alzheimer Res*. (2018) 15:157–63. doi: 10.2174/1567205014666171030115624
90. Nevler N, Ash S, Jester C, Irwin DJ, Liberman M, Grossman M. Automatic measurement of prosody in behavioral variant FTD. *Neurology*. (2017) 89:650–6. doi: 10.1212/WNL.0000000000004236
91. Marin RS, Biedrzycki RC, Firinciogullari S. Reliability and validity of the apathy evaluation scale. *Psychiatry Res*. (1991) 38:143–62. doi: 10.1016/0165-1781(91)90040-V
92. Bartochowski Z, Gatla S, Khoury R, Al-Dahhak R, Grossberg GT. Empathy changes in neurocognitive disorders: a review. *Ann Clin Psychiatry*. (2018) 30:220–32.
93. Shdo SM, Ranasinghe KG, Gola KA, Mielke CJ, Sukhanov P V, Miller BL, et al. Deconstructing empathy: neuroanatomical dissociations between affect sharing and prosocial motivation using a patient lesion model. *Neuropsychologia*. (2018) 116:126–35. doi: 10.1016/j.neuropsychologia.2017.02.010
94. Sturm VE, Sible IJ, Datta S, Hua AY, Perry DC, Kramer JH, et al. Resting parasympathetic dysfunction predicts prosocial helping deficits in behavioral variant frontotemporal dementia. *Cortex*. (2018) 109:141–55. doi: 10.1016/j.cortex.2018.09.006
95. Batson CD. These things called empathy: eight related but distinct phenomena. In: Decety J, William I, editors. *The Social Neuroscience of Empathy*. Cambridge, MA: The MIT Press (2009). doi: 10.7551/mitpress/9780262012973.003.0002
96. Eisenberg N, Eggum ND. Empathic responding: sympathy and personal distress. In: Decety J, William I, editors. *The Social Neuroscience of Empathy*. Cambridge, MA: The MIT Press (2009). doi: 10.7551/mitpress/9780262012973.003.0007

97. Narvid J, Gorno-Tempini ML, Slavotinek A, Dearmond SJ, Cha YH, Miller BL, et al. Of brain and bone: the unusual case of Dr. A. *Neurocase*. (2009) 15:190–205. doi: 10.1080/13554790802632967
98. Cho H, Chin J, Suh MK, Kim HJ, Kim YJ, Ye BS, et al. Postmorbid learning of saxophone playing in a patient with frontotemporal dementia. *Neurocase*. (2015) 21:767–72. doi: 10.1080/13554794.2014.992915
99. Miller BL, Dickerson BC, Lucente DE, Larvie M, Frosch MP. Case records of the Massachusetts General Hospital. Case 9-2015. A 31-year-old man with personality changes and progressive neurologic decline. *N Engl J Med*. (2015) 372:1151–62. doi: 10.1056/NEJMcpc1409839
100. Sollberger M, Rosen HJ, Shany-Ur T, Ullah J, Stanley CM, Laluz V, et al. Neural substrates of socioemotional self-awareness in neurodegenerative disease. *Brain Behav*. (2014) 4:201–14. doi: 10.1002/brb3.211
101. Mioshi E, Foxe D, Leslie F, MClinNeuro SS, Hsieh S, Miller L, et al. The impact of dementia severity on caregiver burden in frontotemporal dementia and alzheimer disease. *Alzheimer Dis Assoc Disord*. (2013) 27:1. doi: 10.1097/WAD.0b013e318247a0bc
102. Davis MH. Measuring individual differences in empathy: evidence for a multidimensional approach. *J Pers Soc Psychol*. (1983) 44:113–26. doi: 10.1037//0022-3514.44.1.113
103. Perry DC, Whitwell JL, Boeve BF, Pankratz VS, Knopman DS, Petersen RC, et al. Voxel-based morphometry in patients with obsessive-compulsive behaviors in behavioral variant frontotemporal dementia. *Eur J Neurol*. (2012) 19:911–7. doi: 10.1111/j.1468-1331.2011.03656.x
104. Moheb N, Charuworn K, Ashla MM, Desarzant R, Chavez D, Mendez MF. Repetitive behaviors in frontotemporal dementia: compulsions or impulsions? *J Neuropsychiatry Clin Neurosci*. (2018) 2018:8060148. doi: 10.1176/appi.neuropsych.18060148
105. Maltete D. Adult-onset stereotypical motor behaviors. *Rev Neurol*. (2016) 172:477–82. doi: 10.1016/j.neurol.2016.07.002
106. Fletcher PD, Downey LE, Witoonpanich P, Warren JD. The brain basis of musicophilia: evidence from frontotemporal lobar degeneration. *Front Psychol*. (2013) 4:1–8. doi: 10.3389/fpsyg.2013.00347
107. De Souza LC, Volle E, Bertoux M, Czernecki V, Funkiewiez A, Allali G, et al. Poor creativity in frontotemporal dementia: a window into the neural bases of the creative mind. *Neuropsychologia*. (2010) 48:3733–42. doi: 10.1016/j.neuropsychologia.2010.09.010
108. de Souza LC, Guimarães HC, Teixeira AL, Caramelli P, Levy R, Dubois B, et al. Frontal lobe neurology and the creative mind. *Front Psychol*. (2014) 5:761. doi: 10.3389/fpsyg.2014.00761
109. Bozeat S, Gregory C, Lambon Ralph MA, Hodges JR. Which neuropsychiatric and behavioural features distinguish frontal and temporal variants of frontotemporal dementia from Alzheimer's disease? *J Neurol Neurosurg Psychiatry*. (2000) 69:178–86. doi: 10.1136/jnnp.69.2.178
110. Ahmed RM, Irish M, Henning E, Dermody N, Bartley L, Kiernan MC, et al. Assessment of eating behavior disturbance and associated neural networks in frontotemporal dementia. *JAMA Neurol*. (2016) 73:282–90. doi: 10.1001/jamaneurol.2015.4478
111. Aiello M, Silani V, Rumiati RI. You stole my food! Eating alterations in frontotemporal dementia. *Neurocase*. (2016) 22:400–9. doi: 10.1080/13554794.2016.1197952
112. Ikeda M, Brown J, Holland AJ, Fukuhara R, Hodges JR. Changes in appetite, food preference, and eating habits in frontotemporal dementia and Alzheimer's disease. *J Neurol Neurosurg Psychiatry*. (2002) 73:371–6. doi: 10.1136/jnnp.73.4.371
113. Woolley JD, Khan BK, Natesan A, Karydas A, Dallman M, Havel P, et al. Satiety-related hormonal dysregulation in behavioral variant frontotemporal dementia. *Neurology*. (2014) 82:512–20. doi: 10.1212/WNL.0000000000000106
114. Ahmed RM, Phan K, Highton-Williamson E, Strikwerda-Brown C, Caga J, Ramsey E, et al. Eating peptides: biomarkers of neurodegeneration in amyotrophic lateral sclerosis and frontotemporal dementia. *Ann Clin Transl Neurol*. (2019) 6:486–95. doi: 10.1002/acn3.721
115. Ahmed RM, Irish M, Kam J, Van Keizerswaard J, Bartley L, Samaras K, et al. Quantifying the eating abnormalities in frontotemporal dementia. *JAMA Neurol*. (2014) 71:1540–6. doi: 10.1001/jamaneurol.2014.1931
116. Ramanan S, Bertoux M, Flanagan E, Irish M, Piguet O, Hodges JR, et al. Longitudinal executive function and episodic memory profiles in behavioral-variant frontotemporal dementia and alzheimer's disease. *J Int Neuropsychol Soc*. (2017) 23:34–43. doi: 10.1017/S1355617716000837
117. Hutchinson AD, Mathias JL. Neuropsychological deficits in frontotemporal dementia and Alzheimer's disease: a meta-analytic review. *J Neurol Neurosurg Psychiatry*. (2007) 78:917–28. doi: 10.1136/jnnp.2006.100669
118. Jiskoot LC, Panman JL, van Asseldonk L, Franzen S, Meeter LHH, Donker Kaat L, et al. Longitudinal cognitive biomarkers predicting symptom onset in presymptomatic frontotemporal dementia. *J Neurol*. (2018) 265:1381–92. doi: 10.1007/s00415-018-8850-7
119. Folstein MF, Folstein SE, McHugh PR, Ingles J. 'Mini-mental state'. A practical method for grading the cognitive state of patients for the clinician. *J Psychiatr Res*. (1975) 12:189–98. doi: 10.1016/0022-3956(75)90026-6
120. Nasreddine ZS, Phillips NA, Bédirian V, Charbonneau S, Whitehead V, Collin I, et al. The montreal cognitive assessment, MoCA: a brief screening tool for mild cognitive impairment. *J Am Geriatr Soc*. (2005) 53:695–9. doi: 10.1111/j.1532-5415.2005.53221.x
121. Hsieh S, Schubert S, Hoon C, Mioshi E, Hodges JR. Validation of the Addenbrooke's cognitive examination III in frontotemporal dementia and alzheimer's disease. *Dement Geriatr Cogn Disord*. (2013) 36:242–50. doi: 10.1159/000351671
122. Reul S, Lohmann H, Wiendl H, Duning T, Johnen A. Can cognitive assessment really discriminate early stages of Alzheimer's and behavioural variant frontotemporal dementia at initial clinical presentation? *Alzheimers Res Ther*. (2017) 9:1–12. doi: 10.1186/s13195-017-0287-1
123. Lagarde J, Valabrègue R, Corvol JC, Pineau F, Le Ber I, Vidailhet M, et al. Are frontal cognitive and atrophy patterns different in PSP and bvFTD? A comparative neuropsychological and VBM study. *PLoS ONE*. (2013) 8:e0080353. doi: 10.1371/journal.pone.0080353
124. Porto CS, Bahia VS, Brucki SMD, Caramelli P, Nitrini R. Neuropsychological differences between frontotemporal lobar degeneration and Alzheimer's disease. *Dement Neuropsychol*. (2008) 2:223–7. doi: 10.1590/S1980-57642009DN20300011
125. Dodich A, Cerami C, Cappa SF, Marcone A, Golzi V, Zamboni M, et al. Combined socio-behavioral evaluation improves the differential diagnosis between the behavioral variant of frontotemporal dementia and Alzheimer's disease: in search of neuropsychological markers. *J Alzheimer's Dis*. (2018) 61:761–72. doi: 10.3233/JAD-170650
126. Stuss DT. Functions of the frontal lobes: relation to executive functions. *J Int Neuropsychol Soc*. (2011) 17:759–65. doi: 10.1017/S1355617711000695
127. Gansler DA, Huey ED, Pan JJ, Wasserman E, Grafman JH. Assessing the dysexecutive syndrome in dementia. *J Neurol Neurosurg Psychiatry*. (2017) 88:254–61. doi: 10.1136/jnnp-2016-313576
128. Kudlicka A, Clare L, Hindle J V. Executive functions in Parkinson's disease: systematic review and meta-analysis. *Mov Disord*. (2011) 26:2305–15. doi: 10.1002/mds.23868
129. Possin KL, Feigenbaum D, Rankin KP, Smith GE, Boxer AL, Wood K, et al. Dissociable executive functions in behavioral variant frontotemporal and Alzheimer dementias. *Neurology*. (2013) 80:2180–5. doi: 10.1212/WNL.0b013e318296e940
130. Gurnani AS, Gavett BE. The differential effects of alzheimer's disease and lewy body pathology on cognitive performance: a meta-analysis. *Neuropsychol Rev*. (2017) 27:9334. doi: 10.1007/s11065-016-9334-0
131. Vasquez BP, Zakzanis KK. The neuropsychological profile of vascular cognitive impairment not demented: a meta-analysis. *J Neuropsychol*. (2015) 9:109–36. doi: 10.1111/jnp.12039
132. Schubert S, Leyton CE, Hodges JR, Piguet O. Longitudinal memory profiles in behavioral-variant frontotemporal dementia and alzheimer's disease. *J Alzheimer's Dis*. (2016) 51:775–82. doi: 10.3233/JAD-150802
133. Fossati P, Ergis AM, Allilaire JF. Problem-solving abilities in unipolar depressed patients: comparison of performance on the modified version of the Wisconsin and the California sorting tests. *Psychiatry Res*. (2001) 104:145–56. doi: 10.1016/S0165-1781(01)00307-9
134. Elderkin-Thompson V, Mintz J, Haroon E, Lavretsky H, Kumar A. Executive dysfunction and memory in older patients with major and minor depression. *Arch Clin Neuropsychol*. (2007) 22:261–70. doi: 10.1016/j.acn.2007.01.021
135. Vijverberg EGB, Schouws S, Meesters PD, Verwijk E, Comijs H, Koene T, et al. Cognitive deficits in patients with neuropsychiatric symptoms:

a comparative study between behavioral variant frontotemporal dementia and primary psychiatric disorders. *J Clin Psychiatry*. (2017) 78:e940–6. doi: 10.4088/JCP.16m11019
136. Dubois B, Slachevsky A, Litvan I, Pillon B. The FAB: a Frontal Assessment Battery at bedside. *Neurology*. (2000) 55:1621–6. doi: 10.1212/WNL.55.11.1621
137. Torralva T, Roca M, Gleichgerrcht E, López P, Manes F. INECO Frontal Screening (IFS): a brief, sensitive, and specific tool to assess executive functions in dementia. *J Int Neuropsychol Soc*. (2009) 15:777–86. doi: 10.1017/S1355617709990415
138. Leslie FVC, Foxe D, Daveson N, Flannagan E, Hodges JR, Piguet O. FRONTIER executive screen: a brief executive battery to differentiate frontotemporal dementia and Alzheimer's disease. *J Neurol Neurosurg Psychiatry*. (2016) 87:831–5. doi: 10.1136/jnnp-2015-311917
139. Moreira HS, Costa AS, Castro SL, Lima CF, Vicente SG. Assessing executive dysfunction in neurodegenerative disorders: a critical review of brief neuropsychological tools. *Front Aging Neurosci*. (2017) 9:369. doi: 10.3389/fnagi.2017.00369
140. Delis D. *Delis-Kaplan Executive Function System (D-KEFS)*. The Psychological Corporation: San Antonio, USA, 2001. doi: 10.1037/t15082-000
141. Perry RJ, Hodges JR. Differentiating frontal and temporal variant frontotemporal dementia from Alzheimer's disease. *Neurology*. (2000) 54:2277–84. doi: 10.1212/WNL.54.12.2277
142. Matías-Guiu JA, Cabrera-Martín MN, Valles-Salgado M, Rognoni T, Galán L, Moreno-Ramos T, et al. Inhibition impairment in frontotemporal dementia, amyotrophic lateral sclerosis, and Alzheimer's disease: clinical assessment and metabolic correlates. *Brain Imaging Behav*. (2018) 2018:1–9. doi: 10.1007/s11682-018-9891-3
143. Stopford CL, Thompson JC, Neary D, Richardson AMT, Snowden JS. Working memory, attention, and executive function in Alzheimer's disease and frontotemporal dementia. *Cortex*. (2012) 48:429–46. doi: 10.1016/j.cortex.2010.12.002
144. Ranasinghe KG, Rankin KP, Lobach I V., Kramer JH, Sturm VE, Bettcher BM, et al. Cognition and neuropsychiatry in behavioral variant frontotemporal dementia by disease stage. *Neurology*. (2016) 86:600–10. doi: 10.1212/WNL.0000000000002373
145. Libon DJ, Xie SX, Moore P, Farmer J, Antani S, McCawley G, et al. Patterns of neuropsychological impairment in frontotemporal dementia. *Neurology*. (2007) 68:369–75. doi: 10.1212/01.wnl.0000252820.81313.9b
146. Burrell JR, Hornberger M, Carpenter RHS, Kiernan MC, Hodges JR. Saccadic abnormalities in frontotemporal dementia. *Neurology*. (2012) 78:1816–23. doi: 10.1212/WNL.0b013e318258f75c
147. Garbutt S, Matlin A, Hellmuth J, Schenk AK, Johnson JK, Rosen H, et al. Oculomotor function in frontotemporal lobar degeneration, related disorders and Alzheimer's disease. *Brain*. (2008) 131:1268–81. doi: 10.1093/brain/awn047
148. Heuer WH, Mirsky BJ, Kong LE, Dickerson CB, Miller LB, Kramer HJ, et al. Antisaccade task reflects cortical involvement in mild cognitive impairment. *Neurology*. (2013) 81:1235–43. doi: 10.1212/WNL.0b013e3182a6cbfe
149. Hornberger M, Piguet O, Kipps C, Hodges JR. Executive function in progressive and nonprogressive behavioral variant frontotemporal dementia. *Neurology*. (2008) 71:1481–8. doi: 10.1212/01.wnl.0000334299.72023.c8
150. Buhl C, Stokholm J, Gade A. Clinical utility of short social cognitive tests in early differentiation of behavioral variant frontotemporal dementia from Alzheimer's disease. *Dement Geriatr Cogn Disord*. (2013) 3:376–85. doi: 10.1159/000355123
151. Lagarde J, Valabrégue R, Corvol JC, Garcin B, Volle E, Le Ber I, et al. Why do patients with neurodegenerative frontal syndrome fail to answer: 'in what way are an orange and a banana alike?' *Brain*. (2015) 138:456–71. doi: 10.1093/brain/awu359
152. Garcin B, Volle E, Funkiewiez A, Miller BL, Dubois B, Levy R. A mosquito bites and a butterfly flies: a specific response type of frontal patients in a similarity task. *Neuropsychologia*. (2018) 117:371–8. doi: 10.1016/j.neuropsychologia.2018.06.022
153. Kaiser NC, Lee GJ, Lu PH, Mather MJ, Shapira J, Jimenez E, et al. What dementia reveals about proverb interpretation and its neuroanatomical correlates. *Neuropsychologia*. (2013) 51:1726–33. doi: 10.1016/j.neuropsychologia.2013.05.021
154. Garcin B, Urbanski M, Thiebaut de Schotten M, Levy R, Volle E. Anterior temporal lobe morphometry predicts categorization ability. *Front Hum Neurosci*. (2018) 12:1–12. doi: 10.3389/fnhum.2018.00036
155. Barrows RJ, Barsuglia J, Paholpak P, Eknoyan D, Sabodash V, Lee GJ, et al. Executive abilities as reflected by clock hand placement: frontotemporal dementia versus early-onset alzheimer disease. *J Geriatr Psychiatry Neurol*. (2015) 28:239–48. doi: 10.1177/0891988715598228
156. Possin KL, Chester SK, Laluz V, Bostrom A, Rosen HJ, Miller BL, et al. The frontal-anatomic specificity of design fluency repetitions and their diagnostic relevance for behavioral variant frontotemporal dementia. *J Int Neuropsychol Soc*. (2012) 18:834–44. doi: 10.1017/S1355617712000604
157. Diehl J, Monsch AU, Aebi C, Wagenpfeil S, Krapp S, Grimmer T, et al. Frontotemporal dementia, semantic dementia, and Alzheimer's disease: the contribution of standard neuropsychological tests to differential diagnosis. *J Geriatr Psychiatry Neurol*. (2005) 18:39–44. doi: 10.1177/0891988704272309
158. Rascovsky K, Salmon DP, Hansen LA, Thal LJ, Galasko D. Disparate letter and semantic category fluency deficits in autopsy-confirmed frontotemporal dementia and Alzheimer's disease. *Neuropsychology*. (2007) 21:20–30. doi: 10.1037/0894-4105.21.1.20
159. Libon DJ, McMillan C, Gunawardena D, Powers C, Massimo L, Khan A, et al. Neurocognitive contributions to verbal fluency deficits in frontotemporal lobar degeneration. *Neurology*. (2009) 73:535–42. doi: 10.1212/WNL.0b013e3181b2a4f5
160. Wong S, Flanagan E, Savage G, Hodges JR, Hornberger M. Contrasting prefrontal cortex contributions to episodic memory dysfunction in behavioural variant frontotemporal dementia and Alzheimer's disease. *PLoS ONE*. (2014) 9:e87778. doi: 10.1371/journal.pone.0087778
161. Hornberger M, Savage S, Hsieh S, Mioshi E, Piguet O, Hodges JR. Orbitofrontal dysfunction discriminates behavioral variant frontotemporal dementia from Alzheimer's disease. *Dement Geriatr Cogn Disord*. (2011) 30:547–52. doi: 10.1159/000321670
162. Carey CL, Woods SP, Damon J, Halabi C, Dean D, Delis DC, et al. Discriminant validity and neuroanatomical correlates of rule monitoring in frontotemporal dementia and Alzheimer's disease. *Neuropsychologia*. (2008) 46:1081–7. doi: 10.1016/j.neuropsychologia.2007.11.001
163. Franceschi M, Caffarra P, Savarè R, Cerutti R, Grossi E, Padovani A, et al. Tower of London test: a comparison between conventional statistic approach and modelling based on artificial neural network in differentiating frontotemporal dementia from Alzheimer's disease. *Behav Neurol*. (2011) 24:149–58. doi: 10.1155/2011/754659
164. Torralva T, Roca M, Gleichgerrcht E, Bekinschtein T, Manes F. A neuropsychological battery to detect specific executive and social cognitive impairments in early frontotemporal dementia. *Brain*. (2009) 132:1299–309. doi: 10.1093/brain/awp041
165. Bisbing TA, Olm CA, McMillan CT, Rascovsky K, Baehr L, Ternes K, et al. Estimating frontal and parietal involvement in cognitive estimation: a study of focal neurodegenerative diseases. *Front Hum Neurosci*. (2015) 9:1–11. doi: 10.3389/fnhum.2015.00317
166. Hornberger M, Piguet O, Graham AJ, Nestor PJ, Hodges JR. How preserved is episodic memory in behavioral variant frontotemporal dementia? *Neurology*. (2010) 74:472–9. doi: 10.1212/WNL.0b013e3181cef85d
167. Bertoux M, De Souza LC, Corlier F, Lamari F, Bottlaender M, Dubois B, et al. Two distinct amnesic profiles in behavioral variant frontotemporal dementia. *Biol Psychiatry*. (2014) 75:582–8. doi: 10.1016/j.biopsych.2013.08.017
168. Fernandez-Matarrubia M, Matias-Guiu JA, Cabrera-Martin MN, Moreno-Ramos T, Valles-Salgado M, Carreras JL, et al. Episodic memory dysfunction in behavioral variant frontotemporal dementia: a clinical and FDG-PET study. *J Alzheimer's Dis*. (2017) 57:1251–64. doi: 10.3233/JAD-160874
169. Wong S, Bertoux M, Savage G, Hodges JR, Piguet O, Hornberger M. Comparison of prefrontal atrophy and episodic memory performance in dysexecutive alzheimer's disease and behavioral-variant frontotemporal dementia. *J Alzheimer's Dis*. (2016) 51:889–903. doi: 10.3233/JAD-151016
170. Bertoux M, Flanagan EC, Hobbs M, Ruiz-Tagle A, Delgado C, Miranda M, et al. Structural anatomical investigation of long-term memory deficit in behavioral frontotemporal dementia. *J Alzheimer's Dis*. (2018) 62:1887–900. doi: 10.3233/JAD-170771

171. Poos JM, Jiskoot LC, Papma JM, van Swieten JC, van den Berg E. Meta-analytic review of memory impairment in behavioral variant frontotemporal dementia. *J Int Neuropsychol Soc*. (2018) 24:593–605. doi: 10.1017/S1355617718000115
172. St. Jacques PL, Grady C, Davidson PSR, Chow TW. Emotional evaluation and memory in behavioral variant frontotemporal dementia. *Neurocase*. (2015) 21:429–37. doi: 10.1080/13554794.2014.917681
173. Flanagan EC, Wong S, Dutt A, Tu S, Bertoux M, Irish M, et al. False recognition in behavioral variant frontotemporal dementia and Alzheimer's disease-disinhibition or amnesia? *Front Aging Neurosci*. (2016) 8:1–11. doi: 10.3389/fnagi.2016.00177
174. Graham A, Davies R, Xuereb J, Halliday G, Kril J, Creasey H, et al. Pathologically proven frontotemporal dementia presenting with severe amnesia. *Brain*. (2005) 128:597–605. doi: 10.1093/brain/awh348
175. Smits LL, Van Harten AC, Pijnenburg YAL, Koedam ELGE, Bouwman FH, Sistermans N, et al. Trajectories of cognitive decline in different types of dementia. *Psychol Med*. (2015) 45:1051–9. doi: 10.1017/S0033291714002153
176. Irish M, Piguet O, Hodges JR, Hornberger M. Common and unique gray matter correlates of episodic memory dysfunction in frontotemporal dementia and alzheimer's disease. *Hum Brain Mapp*. (2014) 35:1422–35. doi: 10.1002/hbm.22263
177. Kumfor F, Irish M, Hodges JR, Piguet O. The orbitofrontal cortex is involved in emotional enhancement of memory: evidence from the dementias. *Brain*. (2013) 136:2992–3003. doi: 10.1093/brain/awt185
178. Kamminga J, Kumfor F, Burrell JR, Piguet O, Hodges JR, Irish M. Differentiating between right-lateralised semantic dementia and behavioural-variant frontotemporal dementia: an examination of clinical characteristics and emotion processing. *J Neurol Neurosurg Psychiatry*. (2015) 86:1082–8. doi: 10.1136/jnnp-2014-309120
179. Dermody N, Hornberger M, Piguet O, Hodges JR, Irish M. Prospective memory impairments in alzheimer's disease and behavioral variant frontotemporal dementia: clinical and neural correlates. *J Alzheimer's Dis*. (2016) 50:425–41. doi: 10.3233/JAD-150871
180. Irish M, Hornberger M, El Wahsh S, Lam BYK, Lah S, Miller L, et al. Grey and white matter correlates of recent and remote autobiographical memory retrieval–insights from the dementias. *PLoS ONE*. (2014) 9:e113081. doi: 10.1371/journal.pone.0113081
181. Irish M, Landin-Romero R, Mothakunnel A, Ramanan S, Hsieh S, Hodges JR, et al. Evolution of autobiographical memory impairments in Alzheimer's disease and frontotemporal dementia - a longitudinal neuroimaging study. *Neuropsychologia*. (2018) 110:14–25. doi: 10.1016/j.neuropsychologia.2017.03.014
182. Bird CM, Chan D, Hartley T, Pijnenburg YA, Rossor MN, Burgess N. Topographical short-term memory differentiates Alzheimer's disease from frontotemporal lobar degeneration. *Hippocampus*. (2010) 20:1154–69. doi: 10.1002/hipo.20715
183. Tu S, Wong S, Hodges JR, Irish M, Piguet O, Hornberger M. Lost in spatial translation - a novel tool to objectively assess spatial disorientation in Alzheimer's disease and frontotemporal dementia. *Cortex*. (2015) 67:83–94. doi: 10.1016/j.cortex.2015.03.016
184. Tu S, Spiers HJ, Hodges JR, Piguet O, Hornberger M. Egocentric versus allocentric spatial memory in behavioral variant frontotemporal dementia and alzheimer's disease. *J Alzheimer's Dis*. (2017) 59:883–92. doi: 10.3233/JAD-160592
185. Coughlan G, Laczó J, Hort J, Minihane AM, Hornberger M. Spatial navigation deficits — overlooked cognitive marker for preclinical Alzheimer disease? *Nat Rev Neurol*. (2018) 14:1–11. doi: 10.1038/s41582-018-0031-x
186. Trojano L, Gainotti G. Drawing disorders in alzheimer's disease and other forms of dementia. *J Alzheimer's Dis*. (2016) 53:31–52. doi: 10.3233/JAD-160009
187. Miall RC, Nam SH, Tchalenko J. The influence of stimulus format on drawing-a functional imaging study of decision making in portrait drawing. *Neuroimage*. (2014) 102:608–19. doi: 10.1016/j.neuroimage.2014.08.015
188. Serra L, Fadda L, Perri R, Spanò B, Marra C, Castelli D, et al. Constructional apraxia as a distinctive cognitive and structural brain feature of pre-senile Alzheimer's disease. *J Alzheimers Dis*. (2014) 38:391–402. doi: 10.3233/JAD-130656
189. Perri R, Koch G, Carlesimo GA, Serra L, Fadda L, Pasqualetti P, et al. Alzheimer's disease and frontal variant of frontotemporal dementia - a very brief battery for cognitive and behavioural distinction. *J Neurol*. (2005) 252:1238–44. doi: 10.1007/s00415-005-0849-1
190. Grossi D, Fragassi NA, Chiacchio L, Valoroso L, Tuccillo R, Perrotta C, et al. Do visuospatial and constructional disturbances differentiate frontal variant of frontotemporal dementia and Alzheimer's disease? An experimental study of a clinical belief. *Int J Geriatr Psychiatry*. (2002) 17:641–8. doi: 10.1002/gps.654
191. Salimi S, Irish M, Foxe D, Hodges JR, Piguet O, Burrell JR. Can visuospatial measures improve the diagnosis of Alzheimer's disease? *Alzheimer's Dement Diagnosis, Assess Dis Monit*. (2018) 10:66–74. doi: 10.1016/j.dadm.2017.10.004
192. Rascovsky K, Salmon DP, Ho GJ, Galasko D, Peavy GM, Hansen LA, et al. Cognitive profiles differ in autopsy-confirmed frontotemporal dementia and AD. *Neurology*. (2002) 58:1801–8. doi: 10.1212/WNL.58.12.1801
193. Blair M, Kertesz A, McMonagle P, Davidson W, Bodi N. Quantitative and qualitative analyses of clock drawing in frontotemporal dementia and Alzheimer's disease. *J Int Neuropsychol Soc*. (2006) 12:159–65. doi: 10.1017/S1355617706060255
194. Floris G, Borghero G, Cannas A, Di Stefano F, Ruiu E, Murru MR, et al. Constructional apraxia in frontotemporal dementia associated with the C9orf72 mutation: broadening the clinical and neuropsychological phenotype. *Amyotroph Lateral Scler Front Degener*. (2015) 16:8–15. doi: 10.3109/21678421.2014.959450
195. Meyers JE, Bayless JD, Meyers KR. Rey complex figure: memory error patterns and functional abilities. *Appl Neuropsychol*. (1996) 3:89–92. doi: 10.1207/s15324826an0302_8
196. Roth HL, Bauer RM, Crucian GP, Heilman KM. Frontal-executive constructional apraxia: when delayed recall is better than copying. *Neurocase*. (2013) 2013:37–41. doi: 10.1080/13554794.2013.770879
197. Possin KL, Laluz VR, Alcantar OZ, Miller BL, Kramer JH. Distinct neuroanatomical substrates and cognitive mechanisms of figure copy performance in Alzheimer's disease and behavioral variant frontotemporal dementia. *Neuropsychologia*. (2011) 49:43–8. doi: 10.1016/j.neuropsychologia.2010.10.026
198. Thompson JC, Stopford CL, Snowden JS, Neary D. Qualitative neuropsychological performance characteristics in frontotemporal dementia and Alzheimer's disease. *J Neurol Neurosurg Psychiatry*. (2005) 76:920–7. doi: 10.1136/jnnp.2003.033779
199. Lezak M, Howieson D, Bigler E, Tranel D. *Neuropsychological Assessment*. New York, NY: Oxford University Press (2012).
200. De Lucia N, Grossi D, Maria Fasanaro A, Carpi S, Trojano L. Frontal defects contribute to the genesis of closing-in in Alzheimer's disease patients. *J Int Neuropsychol Soc*. (2013) 19:802–8. doi: 10.1017/S1355617713000568
201. Hallam BJ, Jacova C, Hsiung GYR, Wittenberg D, Sengdy P, Bouchard-Kerr P, et al. Early neuropsychological characteristics of progranulin mutation carriers. *J Int Neuropsychol Soc*. (2014) 20:694–703. doi: 10.1017/S1355617714000551
202. Cheran G, Wu L, Lee S, Manoochehri M, Cines S, Fallon E, et al. Cognitive indicators of preclinical behavioral variant frontotemporal dementia in MAPT carriers. *J Int Neuropsychol Soc*. (2018) 2018:1–11. doi: 10.1017/S1355617718001005
203. Barandiaran M, Moreno F, de Arriba M, Indakoetxea B, Boda I, Gabilondo A, et al. Longitudinal neuropsychological study of presymptomatic c.709-1G>A progranulin mutation carriers. *J Int Neuropsychol Soc*. (2018) 2018:1–9. doi: 10.1017/S1355617718000735
204. Lough S, Gregory C, Hodges JR. Dissociation of social cognition and executive function in frontal variant frontotemporal dementia. *Neurocase*. (2001) 7:123–30. doi: 10.1093/neucas/7.2.123
205. O'Callaghan C, Hodges JR, Hornberger M. Inhibitory dysfunction in frontotemporal dementia: a review. *Alzheimer Dis Assoc Disord*. (2012) 27:102–8. doi: 10.1097/WAD.0b013e318265bbc9
206. Kennedy DP, Adolphs R. The social brain in psychiatric and neurological disorders. *Trends Cogn Sci*. (2012) 16:559–72. doi: 10.1016/j.tics.2012.09.006
207. Gregory C, Lough S, Stone V, Erzinclioglu S, Martin L, Baron-Cohen S, et al. Theory of mind in patients with frontal variant frontotemporal dementia

and Alzheimer's disease: theoretical and practical implications. *Brain*. (2002) 125:752–64. doi: 10.1093/brain/awf079
208. Lavenu I, Pasquier F, Lebert F, Petit H, Van der Linden M. Perception of emotion in frontotemporal dementia and Alzheimer disease. *Alzheimer Dis Assoc Disord*. (1999) 13:96–101. doi: 10.1097/00002093-199904000-00007
209. Torralva T, Kipps CM, Hodges JR, Clark L, Bekinschtein T, Roca M, et al. The relationship between affective decision-making and theory of mind in the frontal variant of fronto-temporal dementia. *Neuropsychologia*. (2007) 45:342–9. doi: 10.1016/j.neuropsychologia.2006.05.031
210. Rankin KP, Salazar A, Gorno-Tempini ML, Sollberger M, Wilson SM, Pavlic D, et al. Detecting sarcasm from paralinguistic cues: anatomic and cognitive correlates in neurodegenerative disease. *Neuroimage*. (2009) 47:2005–15. doi: 10.1016/j.neuroimage.2009.05.077
211. Kumfor F, Miller L, Lah S, Hsieh S, Savage S, Hodges JR, et al. Are you really angry? The effect of intensity on facial emotion recognition in frontotemporal dementia. *Soc Neurosci*. (2011) 6:502–14. doi: 10.1080/17470919.2011.620779
212. Bertoux M, Delavest M, Cruz De Souza L, Funkiewiez A, Lépine J-P, Fossati P, et al. Social cognition and emotional assessment differentiates frontotemporal dementia from depression. *J Neurol Neurosurg Psychiatry*. (2012) 83:411–6. doi: 10.1136/jnnp-2011-301849
213. Bertoux M, Funkiewiez A, O'Callaghan C, Dubois B, Hornberger M. Sensitivity and specificity of ventromedial prefrontal cortex tests in behavioral variant frontotemporal dementia. *Alzheimer's Dement*. (2012) 9:84–94. doi: 10.1016/j.jalz.2012.09.010
214. Hornberger M, Yew B, Gilardoni S, Mioshi E, Gleichgerrcht E, Manes F, et al. Ventromedial-frontopolar prefrontal cortex atrophy correlates with insight loss in frontotemporal dementia and Alzheimer's disease. *Hum Brain Mapp*. (2014) 35:616–26. doi: 10.1002/hbm.22200
215. Bertoux M, Volle E, Funkiewiez A, de Souza LC, Leclercq D, Dubois B. Social cognition and emotional assessment (SEA) is a marker of medial and orbital frontal functions: a voxel-based morphometry study in behavioral variant of frontotemporal degeneration. *J Int Neuropsychol Soc*. (2012) 18:972–85. doi: 10.1017/S1355617712001300
216. Kumfor F, Irish M, Hodges JR, Piguet O. Discrete neural correlates for the recognition of negative emotions: insights from frontotemporal dementia. *PLoS ONE*. (2013) 8:e67457. doi: 10.1371/journal.pone.0067457
217. O'Callaghan C, Bertoux M, Irish M, Shine JM, Wong S, Spiliopoulos L, et al. Fair play: social norm compliance failures in behavioural variant frontotemporal dementia. *Brain*. (2016) 139:204–16. doi: 10.1093/brain/awv315
218. Melloni M, Billeke P, Baez S, Hesse E, de la Fuente L, Forno G, et al. Your perspective and my benefit: multiple lesion models of self-other integration strategies during social bargaining. *Brain*. (2016) 139:3022–40. doi: 10.1093/brain/aww231
219. Bertoux M, O'Callaghan C, Dubois B, Hornberger M. In two minds: executive functioning versus theory of mind in behavioural variant frontotemporal dementia. *J Neurol Neurosurg Psychiatry*. (2016) 87:231–4. doi: 10.1136/jnnp-2015-311643
220. Ramanan S, de Souza LC, Moreau N, Sarazin M, Teixeira ALL, Allen Z, et al. Determinants of theory of mind performance in Alzheimer's disease: a data-mining study. *Cortex*. (2017) 88:8–18. doi: 10.1016/j.cortex.2016.11.014
221. Ibanez A, Manes F. Contextual social cognition and the behavioral variant of frontotemporal dementia. *Neurology*. (2012) 78:1354–62. doi: 10.1212/WNL.0b013e3182518375
222. Henry JD, Phillips LH, Von Hippel C. A meta-analytic review of theory of mind difficulties in behavioural-variant frontotemporal dementia. *Neuropsychologia*. (2014) 56:53–62. doi: 10.1016/j.neuropsychologia.2013.12.024
223. Strikwerda-Brown C, Ramanan S, Irish M. Neurocognitive mechanisms of theory of mind impairment in neurodegeneration: a transdiagnostic approach. *Neuropsychiatr Dis Treat*. (2019) 15:557–73. doi: 10.2147/NDT.S158996
224. Fernandez-Duque D, Baird JA, Black SE. False-belief understanding in frontotemporal dementia and Alzheimer's disease. *J Clin Exp Neuropsychol*. (2009) 31:489–97. doi: 10.1080/13803390802282688
225. Le Bouc R, Lenfant P, Delbeuck X, Ravasi L, Lebert F, Semah F, et al. My belief or yours? Differential theory of mind deficits in frontotemporal dementia and Alzheimer's disease. *Brain*. (2012) 135:3026–38. doi: 10.1093/brain/aws237
226. Eslinger PJ, Moore P, Troiani V, Antani S, Cross K, Kwok S, et al. Oops! resolving social dilemmas in frontotemporal dementia. *J Neurol Neurosurg Psychiatry*. (2007) 78:457–60. doi: 10.1136/jnnp.2006.098228
227. Kipps CM, Nestor PJ, Acosta-Cabronero J, Arnold R, Hodges JR. Understanding social dysfunction in the behavioural variant of frontotemporal dementia: the role of emotion and sarcasm processing. *Brain*. (2009) 132:592–603. doi: 10.1093/brain/awn314
228. Shany-Ur T, Poorzand P, Grossman SN, Growdon ME, Jang JY, Ketelle RS, et al. Comprehension of insincere communication in neurodegenerative disease: Lies, sarcasm, and theory of mind. *Cortex*. (2012) 48:1329–41. doi: 10.1016/j.cortex.2011.08.003
229. Fong SS, Paholpak P, Daianu M, Deutsch MB, Riedel BC, Carr AR, et al. The attribution of animacy and agency in frontotemporal dementia versus Alzheimer's disease. *Cortex*. (2017) 92:81–94. doi: 10.1016/j.cortex.2017.03.019
230. Schroeter ML, Pawelke S, Bisenius S, Kynast J, Schuemberg K, Polyakova M, et al. A modified reading the mind in the eyes test predicts behavioral variant frontotemporal dementia better than executive function tests. *Front Aging Neurosci*. (2018) 10:1–11. doi: 10.3389/fnagi.2018.00011
231. Dodich A, Cerami C, Crespi C, Canessa N, Lettieri G, Iannaccone S, et al. Differential impairment of cognitive and affective mentalizing abilities in neurodegenerative dementias: evidence from behavioral variant of frontotemporal dementia, alzheimer's disease, and mild cognitive impairment. *J Alzheimer's Dis*. (2016) 50:1011–22. doi: 10.3233/JAD-150605
232. Synn A, Mothakunnel A, Kumfor F, Chen Y, Piguet O, Hodges JR, et al. Mental states in moving shapes: distinct cortical and subcortical contributions to theory of mind impairments in dementia. *J Alzheimers Dis*. (2018) 61:521–35. doi: 10.3233/JAD-170809
233. Bora E, Walterfang M, Velakoulis D. Theory of mind in behavioural-variant frontotemporal dementia and Alzheimer's disease: a meta-analysis. *J Neurol Neurosurg Psychiatry*. (2015) 86:714–9. doi: 10.1136/jnnp-2014-309445
234. Strikwerda-Brown C, Mothakunnel A, Hodges JR, Piguet O, Irish M. External details revisited - a new taxonomy for coding 'non-episodic' content during autobiographical memory retrieval. *J Neuropsychol*. (2018) 2018:12160. doi: 10.1111/jnp.12160
235. Rosen HJ, Pace-Savitsky K, Perry RJ, Kramer JH, Miller BL, Levenson RW. Recognition of emotion in the frontal and temporal variants of frontotemporal dementia. *Dement Geriatr Cogn Disord*. (2004) 17:277–81. doi: 10.1159/000077154
236. Goodkind MS, Sturm VE, Ascher EA, Shdo SM, Miller BL, Rankin KP, et al. Emotion recognition in frontotemporal dementia and Alzheimer's disease: a new film-based assessment. *Emotion*. (2015) 15:416–27. doi: 10.1037/a0039261
237. Hutchings R, Palermo R, Bruggemann J, Hodges JR, Piguet O, Kumfor F. Looking but not seeing: increased eye fixations in behavioural-variant frontotemporal dementia. *Cortex*. (2018) 103:71–81. doi: 10.1016/j.cortex.2018.02.011
238. Kumfor F, Ibanez A, Hutchings R, Hazelton JL, Hodges JR, Piguet O. Beyond the face: how context modulates emotion processing in frontotemporal dementia subtypes. *Brain*. (2018) 141:1172–85. doi: 10.1093/brain/aw y002
239. Sturm VE, Ascher EA, Miller BL, Levenson RW. Diminished self-conscious emotional responding in frontotemporal lobar degeneration patients. *Emotion*. (2008) 8:861–9. doi: 10.1037/a0013765
240. Verstaen A, Eckart JA, Muhtadie L, Otero MC, Sturm VE, Haase CM, et al. Insular atrophy and diminished disgust reactivity. *Emotion*. (2016) 16:903–12. doi: 10.1037/emo0000195
241. Carr AR, Ashla MM, Jimenez EE, Mendez MF. Screening for emotional expression in frontotemporal dementia: a pilot study. *Behav Neurol*. (2018) 2018:1–6. doi: 10.1155/2018/8187457
242. Joshi A, Barsuglia J, Mather M, Jimenez E, Shapira J, Mendez M. Evaluation of emotional blunting in behavioral variant frontotemporal dementia compared to alzheimer's disease. *Dement Geriatr Cogn Disord*. (2011) 193:79–88. doi: 10.1159/000357838
243. Mendez MF, Fong SS, Ashla MM, Jimenez EE, Carr AR. Skin conduction levels differentiate frontotemporal dementia from

alzheimer's disease. *J Neuropsychiatry Clin Neurosci*. (2018) 30:208–13. doi: 10.1176/appi.neuropsych.17080168
244. Kumfor F, Hazelton JL, Rushby JA, Hodges JR, Piguet O. Facial expressiveness and physiological arousal in frontotemporal dementia: phenotypic clinical profiles and neural correlates. *Cogn Affect Behav Neurosci*. (2019) 19:197–210. doi: 10.3758/s13415-018-00658-z
245. Gola KA, Shany-Ur T, Pressman P, Sulman I, Galeana E, Paulsen H, et al. A neural network underlying intentional emotional facial expression in neurodegenerative disease. *NeuroImage Clin*. (2017) 14:672–8. doi: 10.1016/j.nicl.2017.01.016
246. Torres B, Santos RL, Sousa MFBD, Simões Neto JP, Nogueira MML, Belfort TT, et al. Facial expression recognition in Alzheimer's disease: a longitudinal study. *Arq Neuropsiquiatr*. (2015) 73:383–9. doi: 10.1590/0004-282X20150009
247. Lavenu I, Pasquier F. Perception of emotion on faces in frontotemporal dementia and Alzheimer's disease: a longitudinal study. *Dement Geriatr Cogn Disord*. (2005) 19:37–41. doi: 10.1159/000080969
248. Bertoux M, De Souza LC, Sarazin M, Funkiewiez A, Dubois B, Hornberger M. How preserved is emotion recognition in Alzheimer disease compared with behavioral variant frontotemporal dementia? *Alzheimer Dis Assoc Disord*. (2015) 29:154–7. doi: 10.1097/WAD.0000000000000023
249. Wong S, Irish M, Leshikar ED, Duarte A, Bertoux M, Savage G, et al. The self-reference effect in dementia: differential involvement of cortical midline structures in Alzheimer's disease and behavioural-variant frontotemporal dementia. *Cortex*. (2017) 91:169–85. doi: 10.1016/j.cortex.2016.09.013
250. Shany-Ur T, Lin N, Rosen HJ, Sollberger M, Miller BL, Rankin KP. Self-awareness in neurodegenerative disease relies on neural structures mediating reward-driven attention. *Brain*. (2014) 137:2368–81. doi: 10.1093/brain/awu161
251. Arroyo-Anllo EM, Bouston AT, Fargeau M-N, Orgaz Baz B, Gil R. Self-consciousness deficits in alzheimer's disease and frontotemporal dementia. *J Alzheimers Dis*. (2017) 55:1437–43. doi: 10.3233/JAD-160770
252. Rankin KP, Baldwin E, Pace-Savitsky C, Kramer JH, Miller BL. Self awareness and personality change in dementia. *J Neurol Neurosurg Psychiatry*. (2005) 76:632–9. doi: 10.1136/jnnp.2004.042879
253. O'Keeffe FM, Murray B, Coen RF, Dockree PM, Bellgrove MA, Garavan H, et al. Loss of insight in frontotemporal dementia, corticobasal degeneration and progressive supranuclear palsy. *Brain*. (2007) 130:753–64. doi: 10.1093/brain/awl367
254. Scherling CS, Zakrzewski J, Datta S, Levenson RW, Shimamura AP, Sturm VE, et al. Mistakes, too few to mention? Impaired self-conscious emotional processing of errors in the behavioral variant of frontotemporal dementia. *Front Behav Neurosci*. (2017) 11:1–11. doi: 10.3389/fnbeh.2017.00189
255. Duclos H, de La Sayette V, Bonnet A-L, Viard A, Eustache F, Desgranges B, et al. Social cognition in the frontal variant of alzheimer's disease: a case study. *J Alzheimers Dis*. (2017) 55:459–63. doi: 10.3233/JAD-160690
256. Mendez MF, Anderson E, Shapira JS. An investigation of moral judgement in frontotemporal dementia. *Cogn Behav Neurol*. (2005) 18:193–7. doi: 10.1097/01.wnn.0000191292.17964.bb
257. Cova F, Bertoux M, Bourgeois-Gironde S, Dubois B. Judgments about moral responsibility and determinism in patients with behavioural variant of frontotemporal dementia: still compatibilists. *Conscious Cogn*. (2012) 21:851–64. doi: 10.1016/j.concog.2012.02.004
258. Carr AR, Paholpak P, Daianu M, Fong SS, Mather M, Jimenez EE, et al. An investigation of care-based vs. rule-based morality in frontotemporal dementia, Alzheimer's disease, and healthy controls. *Neuropsychologia*. (2015) 78:73–9. doi: 10.1016/j.neuropsychologia.2015.09.033
259. Gleichgerrcht E, Torralva T, Roca M, Pose M, Manes F. The role of social cognition in moral judgment in frontotemporal dementia. *Soc Neurosci*. (2011) 6:113–22. doi: 10.1080/17470919.2010.506751
260. Fong SS, Navarrete CD, Perfecto SE, Carr AR, Jimenez EE, Mendez MF. Behavioral and autonomic reactivity to moral dilemmas in frontotemporal dementia versus Alzheimer's disease. *Soc Neurosci*. (2017) 12:409–18. doi: 10.1080/17470919.2016.1186111
261. Baez S, Couto B, Torralva T, Sposato LA, Huepe D, Montañes P, et al. Comparing moral judgments of patients with frontotemporal dementia and frontal stroke. *JAMA Neurol*. (2014) 71:1172–6. doi: 10.1001/jamaneurol.2014.347
262. Clark CN, Golden HL, McCallion O, Nicholas JM, Cohen MH, Slattery CF, et al. Music models aberrant rule decoding and reward valuation in dementia. *Soc Cogn Affect Neurosci*. (2018) 13:192–202. doi: 10.1093/scan/nsx140
263. Wong S, Irish M, Savage G, Hodges JR, Piguet O, Hornberger M. Strategic value-directed learning and memory in Alzheimer's disease and behavioural-variant frontotemporal dementia. *J Neuropsychol*. (2018) 2018:12152. doi: 10.1111/jnp.12152
264. Strenziok M, Pulaski S, Krueger F, Zamboni G, Clawson D, Grafman J. Regional brain atrophy and impaired decision making on the balloon analog risk task in behavioral variant frontotemporal dementia. *Cogn Behav Neurol*. (2011) 24:59–67. doi: 10.1097/WNN.0b013e3182255a7c
265. Perry DC, Sturm VE, Wood KA, Miller BL, Kramer JH. Divergent processing of monetary and social reward in behavioral variant frontotemporal dementia and Alzheimer disease. *Alzheimer Dis Assoc Disord*. (2015) 29:161–4. doi: 10.1097/WAD.0000000000000012
266. Perry DC, Datta S, Sturm VE, Wood KA, Zakrzewski J, Seeley WW, et al. Reward deficits in behavioural variant frontotemporal dementia include insensitivity to negative stimuli. *Brain*. (2017) 140:3346–56. doi: 10.1093/brain/awx259
267. Bertoux M, de Souza LC, Zamith P, Dubois B, Bourgeois-Gironde S. Discounting of future rewards in behavioural variant frontotemporal dementia and Alzheimer's disease. *Neuropsychology*. (2015) 29:933–9. doi: 10.1037/neu0000197
268. Bertoux M, Cova F, Pessiglione M, Hsu M, Dubois B, Bourgeois-Gironde S. Behavioral variant frontotemporal dementia patients do not succumb to the Allais paradox. *Front Neurosci*. (2014) 8:1–10. doi: 10.3389/fnins.2014.00287
269. Woolley J, Gorno-Tempini M, Seeley W, Rankin K, Lee S, Matthews B, et al. Binge eating is associated with right orbitofrontal-insular-striatal atrophy in frontotemporal dementia. *Neurology*. (2007) 69:1424–33. doi: 10.1212/01.wnl.0000277461.06713.23
270. Rahman S, Sahakian BJ, Hodges JR, Rogers RD, Robbins TW. Specific cognitive deficits in mild frontal variant frontotemporal dementia. *Brain*. (1999) 122(Pt 8):1469–93. doi: 10.1093/brain/122.8.1469
271. Kloeters S, Bertoux M, O'Callaghan C, Hodges JR, Hornberger M. Money for nothing - Atrophy correlates of gambling decision making in behavioural variant frontotemporal dementia and Alzheimer's disease. *NeuroImage Clin*. (2013) 2:263–72. doi: 10.1016/j.nicl.2013.01.011
272. Mendez MF. The unique predisposition to criminal violations in frontotemporal dementia. *J Am Acad Psychiatry Law*. (2010) 38:318–23.
273. Sturm VE, Perry DC, Wood K, Hua AY, Alcantar O, Datta S, et al. Prosocial deficits in behavioral variant frontotemporal dementia relate to reward network atrophy. *Brain Behav*. (2017) 7:e00807. doi: 10.1002/brb3.807
274. Radakovic R, Stephenson L, Newton J, Crockford C, Swingler R, Chandran S, et al. Multidimensional apathy and executive dysfunction in amyotrophic lateral sclerosis. *Cortex*. (2017) 94:142–51. doi: 10.1016/j.cortex.2017.06.023
275. Kumfor F, Zhen A, Hodges JR, Piguet O, Irish M. Apathy in Alzheimer's disease and frontotemporal dementia: distinct clinical profiles and neural correlates. *Cortex*. (2018) 103:350–9. doi: 10.1016/j.cortex.2018.03.019
276. American Psychiatric Association. *Diagnostic and Statistical Manual of Mental Disorders (DSM-5®)*. Washington DC: American Psychiatric Association (2013). doi: 10.1176/appi.books.9780890425596
277. Panchal H, Paholpak P, Lee G, Carr A, Barsuglia JP, Mather M, et al. Neuropsychological and neuroanatomical correlates of the social norms questionnaire in frontotemporal dementia versus alzheimer's disease. *Am J Alzheimers Dis Other Demen*. (2015) 31:326–32. doi: 10.1177/1533317515617722
278. Ekman P, Friesen WV. *Pictures of Facial Affect*. Palo Alto: Consulting Psychologists Press (1976).
279. McDonald S, Flanagan S, Rollins J, Kinch J. TASIT: a new clinical tool for assessing social perception after traumatic brain injury. *J Head Trauma Rehabil*. (2003) 18:219–38. doi: 10.1097/00001199-200305000-00001
280. Bora E, Velakoulis D, Walterfang M. Meta-analysis of facial emotion recognition in behavioral variant frontotemporal dementia. *J Geriatr Psychiatry Neurol*. (2016) 29:205–11. doi: 10.1177/0891988716640375

281. Chiu I, Piguet O, Diehl-Schmid J, Riedl L, Beck J, Leyhe T, et al. Dissociation in rating negative facial emotions between behavioral variant frontotemporal dementia and major depressive disorder. *Am J Geriatr Psychiatry*. (2016) 24:1017–27. doi: 10.1016/j.jagp.2016.06.011
282. Kandalaft MR, Didehbani N, Cullum CM, Krawczyk DC, Allen TT, Tamminga CA, et al. The wechsler ACS social perception subtest: a preliminary comparison with other measures of social cognition. *J Psychoeduc Assess*. (2012) 30:455–65. doi: 10.1177/0734282912436411
283. Baksh RA, Abrahams S, Auyeung B, MacPherson SE. The Edinburgh Social Cognition Test (ESCoT): examining the effects of age on a new measure of theory of mind and social norm understanding. *PLoS ONE*. (2018) 13:e0195818. doi: 10.1371/journal.pone.0195818
284. Bland AR, Roiser JP, Mehta MA, Schei T, Boland H, Campbell-Meiklejohn DK, et al. EMOTICOM: a neuropsychological test battery to evaluate emotion, motivation, impulsivity, and social cognition. *Front Behav Neurosci*. (2016) 10:25. doi: 10.3389/fnbeh.2016.00025
285. Gonzalez Rothi LJ, Ochipa C, Heilman KM. A cognitive neuropsychological model of limb praxis. *Cogn Neuropsychol*. (1991) 8:443–58. doi: 10.1080/02643299108253382
286. Goldenberg G. *Apraxia - The Cognitive Side of Motor Control*. New York, NY; Oxford: Elsevier Ltd (2013). doi: 10.1016/j.cortex.2013.07.016
287. Poeck K. The clinical examination for motor apraxia. *Neuropsychologia*. (1986) 24:129–34. doi: 10.1016/0028-3932(86)90046-1
288. Koski L, Iacoboni M, Mazziotta JC. Deconstructing apraxia: understanding disorders of intentional movement after stroke. *Curr Opin Neurol*. (2002) 15:71–7. doi: 10.1097/00019052-200202000-00011
289. Niessen E, Fink GR, Weiss PH. Apraxia, pantomime and the parietal cortex. *NeuroImage Clin*. (2014) 5:42–52. doi: 10.1016/j.nicl.2014.05.017
290. Lesourd M, Le Gall D, Baumard J, Croisile B, Jarry C, Osiurak F. Apraxia and alzheimer's disease: review and perspectives. *Neuropsychol Rev*. (2013) 23:234–56. doi: 10.1007/s11065-013-9235-4
291. Ozkan S, Ozbabalik Adapinar D, Tuncer Elmaci N, Arslantas D. Apraxia for differentiating Alzheimer's disease from subcortical vascular dementia and mild cognitive impairment. *Neuropsychiatr Dis Treat*. (2013) 9:947–51. doi: 10.2147/NDT.S47879
292. Della Sala S, Lucchelli F, Spinnler H. Ideomotor apraxia in patients with dementia of Alzheimer type. *J Neurol*. (1987) 234:91–3. doi: 10.1007/BF00314108
293. Crutch SJ, Rossor MN, Warrington EK. The quantitative assessment of apraxic deficits in Alzheimer's disease. *Cortex*. (2007) 43:976–86. doi: 10.1016/S0010-9452(08)70695-6
294. Parakh R, Roy E, Koo E, Black S. Pantomime and imitation of limb gestures in relation to the severity of Alzheimer's disease. *Brain Cogn*. (2004) 55:272–4. doi: 10.1016/j.bandc.2004.02.049
295. Nagahama Y, Okina T, Suzuki N. Impaired imitation of gestures in mild dementia: comparison of dementia with Lewy bodies, Alzheimer's disease and vascular dementia. *J Neurol Neurosurg Psychiatry*. (2015) 86:1248–52. doi: 10.1136/jnnp-2014-309436
296. Costa A, Bak T, Caffarra P, Caltagirone C, Ceccaldi M, Collette F, et al. The need for harmonisation and innovation of neuropsychological assessment in neurodegenerative dementias in Europe: consensus document of the Joint Program for Neurodegenerative Diseases Working Group. *Alzheimers Res Ther*. (2017) 9:27. doi: 10.1186/s13195-017-0254-x
297. Ahmed S, Baker I, Thompson S, Husain M, Butler CR. Utility of testing for apraxia and associated features in dementia. *J Neurol Neurosurg Psychiatry*. (2016) 87:1158–62. doi: 10.1136/jnnp-2015-312945
298. Chandra SR, Issac TG, Abbas MM. Apraxias in neurodegenerative dementias. *Indian J Psychol Med*. (2015) 37:42–7. doi: 10.4103/0253-7176.150817
299. Johnen A, Tokaj A, Kirschner A, Wiendl H, Lueg G, Duning T, et al. Apraxia profile differentiates behavioural variant frontotemporal from Alzheimer's dementia in mild disease stages. *J Neurol Neurosurg Psychiatry*. (2015) 86:809–15. doi: 10.1136/jnnp-2014-308773
300. Chare L, Hodges JR, Leyton CE, McGinley C, Tan RH, Kril JJ, et al. New criteria for frontotemporal dementia syndromes: clinical and pathological diagnostic implications. *J Neurol Neurosurg Psychiatry*. (2014) 85:865–70. doi: 10.1136/jnnp-2013-306948
301. Johnen A, Reul S, Wiendl H, Meuth SG, Duning T. Apraxia profiles—A single cognitive marker to discriminate all variants of frontotemporal lobar degeneration and Alzheimer's disease. *Alzheimer's Dement Diagn Assess Dis Monit*. (2018) 10:363–71. doi: 10.1016/j.dadm.2018.04.002
302. Johnen A, Frommeyer J, Modes F, Wiendl H, Duning T, Lohmann H. Dementia Apraxia Test (DATE): a brief tool to differentiate behavioral variant frontotemporal dementia from alzheimer's dementia based on apraxia profiles. *J Alzheimer's Dis*. (2015) 49:593–605. doi: 10.3233/JAD-150447
303. Lobo PP, Pinto S, Rocha L, Reimão S, de Carvalho M. Orofacial apraxia in motor neuron disease. *Case Rep Neurol*. (2013) 5:47–51. doi: 10.1159/000349895
304. Pawlowski M, Joksch V, Wiendl H, Meuth SG, Duning T, Johnen A. Apraxia screening predicts Alzheimer pathology in frontotemporal dementia. *J Neurol Neurosurg Psychiatry*. (2018) 2018:1–8. doi: 10.1136/jnnp-2018-318470
305. Buxbaum LJ, Shapiro AD, Coslett HB. Critical brain regions for tool-related and imitative actions: a componential analysis. *Brain*. (2014) 137:1971–85. doi: 10.1093/brain/awu111
306. Hoeren M, Kümmerer D, Bormann T, Beume L, Ludwig VM, Vry M-S, et al. Neural bases of imitation and pantomime in acute stroke patients: distinct streams for praxis. *Brain*. (2014) 137:2796–810. doi: 10.1093/brain/awu203
307. Martin M, Beume L, Kümmerer D, Schmidt CSM, Bormann T, Dressing A, et al. Differential roles of ventral and dorsal streams for conceptual and production-related components of tool use in acute stroke patients. *Cereb Cortex*. (2016) 26:3754–71. doi: 10.1093/cercor/bhv179
308. Manuel AL, Radman N, Mesot D, Chouiter L, Clarke S, Annoni J-M, et al. Inter- and intrahemispheric dissociations in ideomotor apraxia: a large-scale lesion-symptom mapping study in subacute brain-damaged patients. *Cereb Cortex*. (2013) 23:2781–9. doi: 10.1093/cercor/bhs280
309. Binkofski F, Buxbaum LJ. Two action systems in the human brain. *Brain Lang*. (2013) 127:222–9. doi: 10.1016/j.bandl.2012.07.007
310. Johnen A, Brandstetter L, Kärgel C, Wiendl H, Lohmann H, Duning T. Shared neural correlates of limb apraxia in early stages of Alzheimer's dementia and behavioural variant frontotemporal dementia. *Cortex*. (2016) 84:1–14. doi: 10.1016/j.cortex.2016.08.009
311. Leslie KR, Johnson-Frey SH, Grafton ST. Functional imaging of face and hand imitation: towards a motor theory of empathy. *Neuroimage*. (2004) 21:601–7. doi: 10.1016/j.neuroimage.2003.09.038
312. Goldenberg G, Karnath H-O. The neural basis of imitation is body part specific. *J Neurosci*. (2006) 26:6282–7. doi: 10.1523/JNEUROSCI.0638-06.2006
313. Raade A, Ginzalez Rothi L, Heilman K. The relationship between buccofacial and limb apraxia. *Brain Cogn*. (1991) 16:130–46. doi: 10.1016/0278-2626(91)90002-P
314. Weiss P, Kalbe E, Kessler J, Fink G, Binder E, Hesse M, et al. *Kölner Apraxie Screening*. Göttingen: Hogrefe Verlag (2013).
315. Vanbellingen T, Kersten B, Van de Winckel A, Bellion M, Baronti F, Muri R, et al. A new bedside test of gestures in stroke: the apraxia screen of TULIA (AST). *J Neurol Neurosurg Psychiatry*. (2011) 82:389–92. doi: 10.1136/jnnp.2010.213371
316. Cameron OG. Interoception: the inside story - a model for psychosomatic processes. *Psychosom Med*. (2001) 63:697–710. doi: 10.1097/00006842-200109000-00001
317. Kleckner IR, Zhang J, Touroutoglou A, Chanes L, Simmons WK, Quigley KS, et al. Evidence for a large-scale brain system supporting allostasis and interoception in humans. *Nat Hum Behav*. (2017) 1:1–37. doi: 10.1038/s41562-017-0069
318. García-Cordero I, Sedeño L, de la Fuente L, Slachevsky A, Forno G, Klein F, et al. Feeling, learning from and being aware of inner states: interoceptive dimensions in neurodegeneration and stroke. *Philos Trans R Soc B Biol Sci*. (2016) 371:0006. doi: 10.1098/rstb.2016.0006
319. Zhou J, Greicius MD, Gennatas ED, Growdon ME, Jang JY, Rabinovici GD, et al. Divergent network connectivity changes in behavioural variant frontotemporal dementia and Alzheimer's disease. *Brain*. (2010) 133:1352–67. doi: 10.1093/brain/awq075

320. Marshall CR, Hardy CJD, Russell LL, Clark CN, Bond RL, Dick KM, et al. Motor signatures of emotional reactivity in frontotemporal dementia. *Nat Sci Rep*. (2018) 8:1–13. doi: 10.1038/s41598-018-19528-2
321. Fletcher PD, Downey LE, Golden HL, Clark CN, Slattery CF, Paterson RW, et al. Pain and temperature processing in dementia: a clinical and neuroanatomical analysis. *Brain*. (2015) 138:3360–72. doi: 10.1093/brain/awv276
322. Ondobaka S, Kilner J, Friston K. The role of interoceptive inference in theory of mind. *Brain Cogn*. (2017) 112:64–8. doi: 10.1016/j.bandc.2015.08.002
323. Shah P, Catmur C, Bird G. From heart to mind: linking interoception, emotion, and theory of mind. *Cortex*. (2017) 93:220–3. doi: 10.1016/j.cortex.2017.02.010
324. Adolfi F, Couto B, Richter F, Decety J, Lopez J, Sigman M, et al. Convergence of interoception, emotion, and social cognition: a twofold fMRI meta-analysis and lesion approach. *Cortex*. (2017) 88:124–42. doi: 10.1016/j.cortex.2016.12.019
325. Joshi A, Mendez MF, Kaiser N, Jimenez E, Mather M, Shapira JS. Skin conductance levels may reflect emotional blunting in behavioral variant frontotemporal dementia. *J Neuropsychiatry Clin Neurosci*. (2014) 26:227–32. doi: 10.1176/appi.neuropsych.12110332
326. Balconi M, Cotelli M, Brambilla M, Manenti R, Cosseddu M, Premi E, et al. Understanding emotions in frontotemporal dementia: the explicit and implicit emotional cue mismatch. *J Alzheimers Dis*. (2015) 46:211–25. doi: 10.3233/JAD-142826
327. Marshall CR, Hardy CJD, Russell LL, Clark CN, Dick KM, Brotherhood E V., et al. Impaired interoceptive accuracy in semantic variant primary progressive aphasia. *Front Neurol*. (2017) 8:610. doi: 10.3389/fneur.2017.00610
328. Woolley JD. Buccofacial apraxia and the expression of emotion. *Ann N Y Acad Sci*. (2006) 1000:395–401. doi: 10.1196/annals.1280.039
329. Ptak R, Schnider A, Fellrath J. The dorsal frontoparietal network: a core system for emulated action. *Trends Cogn Sci*. (2017) 21:589–99. doi: 10.1016/j.tics.2017.05.002
330. Conson M, Trojano L, Vitale C, Mazzarella E, Allocca R, Barone P, et al. The role of embodied simulation in mental transformation of whole-body images: evidence from Parkinson's disease. *Hum Mov Sci*. (2014) 33:343–53. doi: 10.1016/j.humov.2013.10.006
331. Schwoebel J, Buxbaum LJ, Coslett HB. Representations of the human body in the production and imitation of complex movements. *Cogn Neuropsychol*. (2004) 21:285–98. doi: 10.1080/02643290342000348
332. Buxbaum LJ, Kyle KM, Menon R. On beyond mirror neurons: internal representations subserving imitation and recognition of skilled object-related actions in humans. *Brain Res Cogn Brain Res*. (2005) 25:226–39. doi: 10.1016/j.cogbrainres.2005.05.014
333. Buxbaum LJ, Kalénine S. Action knowledge, visuomotor activation, and embodiment in the two action systems. *Ann N Y Acad Sci*. (2010) 1191:201–18. doi: 10.1111/j.1749-6632.2010.05447.x
334. Rumiati RI, Carmo JC, Corradi-Dell'Acqua C. Neuropsychological perspectives on the mechanisms of imitation. *Philos Trans R Soc Lond B Biol Sci*. (2009) 364:2337–47. doi: 10.1098/rstb.2009.0063
335. Berg E. A simple objective technique for measuring flexibility in thinking. *J Gen Psychol*. (1948) 39:15–22. doi: 10.1080/00221309.1948.9918159
336. Nyhus E, Barcelo F. The wisconsin card sorting test and the cognitive assessment of prefrontal executive functions: a critical update. *Brain Cogn*. (2009) 71:437–51. doi: 10.1016/j.bandc.2009.03.005
337. Kohli A, Kaur M. Wisconsin card sorting test: normative data and experience. *Indian J Psychiatry*. (2006) 48:181–4. doi: 10.4103/0019-5545.31582
338. Ameller A, Picard A, D'Hondt F, Vaiva G, Thomas P, Pins D. Implicit recognition of familiar and unfamiliar faces in schizophrenia: a study of the skin conductance response in familiarity disorders. *Front Psychiatry*. (2017) 8:1–11. doi: 10.3389/fpsyt.2017.00181
339. Coughlan G, Coutrot A, Khondoker M, Minihane A-M, Spiers H, Hornberger M. Toward personalized cognitive diagnostics of at-genetic-risk Alzheimer's disease. *Proc Natl Acad Sci USA*. (2019) 116:9285–92. doi: 10.1073/pnas.1901600116
340. Artiola i Fortuny L, Heaton RK, Hermosillo D. Neuropsychological comparisons of Spanish-speaking participants from the U.S.-Mexico border region versus Spain. *J Int Neuropsychol Soc*. (1998) 4:363–79.
341. Gasquoine PG. Variables moderating cultural and ethnic differences in neuropsychological assessment: the case of Hispanic Americans. *Clin Neuropsychol*. (1999) 13:376–83. doi: 10.1076/clin.13.3.376.1735

Conflict of Interest Statement: MB would like to disclose that he is the main author of the mini-SEA.

The remaining author declares that the research was conducted in the absence of any commercial or financial relationships that could be construed as a potential conflict of interest.

The reviewer MI declared a past co-authorship with one of the authors MB to the handling editor.

Copyright © 2019 Johnen and Bertoux. This is an open-access article distributed under the terms of the Creative Commons Attribution License (CC BY). The use, distribution or reproduction in other forums is permitted, provided the original author(s) and the copyright owner(s) are credited and that the original publication in this journal is cited, in accordance with accepted academic practice. No use, distribution or reproduction is permitted which does not comply with these terms.

frontiers in Neurology

ORIGINAL RESEARCH
published: 14 June 2019
doi: 10.3389/fneur.2019.00562

Identification of Cellular Pathogenicity Markers for SIL1 Mutations Linked to Marinesco-Sjögren Syndrome

*Christian Gatz[1], Denisa Hathazi[2,3], Ute Münchberg[2], Stephan Buchkremer[1], Thomas Labisch[1], Ben Munro[3], Rita Horvath[3], Ana Töpf[4], Joachim Weis[1] and Andreas Roos[1,2,5]**

[1] Institute of Neuropathology, RWTH Aachen University Hospital, Aachen, Germany, [2] Leibniz-Institut für Analytische Wissenschaften—ISAS—e.V., Dortmund, Germany, [3] Department of Clinical Neuroscience, University of Cambridge, Cambridge, United Kingdom, [4] International Centre for Life, Institute of Genetic Medicine, Newcastle upon Tyne, United Kingdom, [5] Pediatric Neurology, Faculty of Medicine, University Childrens Hospital, University of Duisburg-Essen, Essen, Germany

OPEN ACCESS

Edited by:
Tobias Ruck,
University of Münster, Germany

Reviewed by:
Manabu Funayama,
Juntendo University, Japan
Kenya Nishioka,
Juntendo University, Japan

***Correspondence:**
Andreas Roos
andreas.roos@uk-essen.de;
andreas.roos@isas.de

Specialty section:
This article was submitted to Neurogenetics, a section of the journal Frontiers in Neurology

Received: 18 December 2018
Accepted: 10 May 2019
Published: 14 June 2019

Citation:
Gatz C, Hathazi D, Münchberg U, Buchkremer S, Labisch T, Munro B, Horvath R, Töpf A, Weis J and Roos A (2019) Identification of Cellular Pathogenicity Markers for SIL1 Mutations Linked to Marinesco-Sjögren Syndrome. Front. Neurol. 10:562. doi: 10.3389/fneur.2019.00562

Background and objective: Recessive mutations in the *SIL1* gene cause Marinesco-Sjögren syndrome (MSS), a rare neuropediatric disorder. MSS-patients typically present with congenital cataracts, intellectual disability, cerebellar ataxia and progressive vacuolar myopathy. However, atypical clinical presentations associated with *SIL1* mutations have been described over the last years; compound heterozygosity of SIL1 missense mutations even resulted in a phenotype not fulfilling the clinical diagnostic criteria of MSS. Thus, a read-out system to evaluate reliably the pathogenicity of amino acid changes in *SIL1* is needed. Here, we aim to provide suitable cellular biomarkers enabling the robust evaluation of pathogenicity of SIL1 mutations.

Methods: Five *SIL1* variants including one polymorphism (p.K132Q), three known pathogenic mutations (p.V231_I232del, p.G312R, and p.L457P) and one ambiguous missense variant (p.R92W) were studied along with the wild-type proteins in Hek293 *in vitro* models by cell biological assays, immunoprecipitation, immunoblotting, and immunofluorescence as well as electron microscopy. Moreover, the SIL1-interactomes were interrogated by tandem-affinity-purification and subsequent mass spectrometry.

Results: Our combined studies confirmed the pathogenicity of p.V231_I232del, p.G312R, and p.L457P by showing instability of the proteins as well as tendency to form aggregates. This observation is in line with altered structure of the ER-Golgi system and vacuole formation upon expression of these pathogenic SIL1-mutants as well as the presence of oxidative or ER-stress. Reduced cellular fitness along with abnormal mitochondrial architecture could also be observed. Notably, both the polymorphic p.K132Q and the ambiguous p.R92W variants did not elicit such alterations. Study of the SIL1-interactome identified POC1A as a novel binding partner of wild-type SIL1; the interaction is disrupted upon the presence of pathogenic mutants but not influenced by the presence of benign variants. Disrupted SIL1-POC1A interaction is associated with centrosome disintegration.

Conclusions: We developed a combination of cellular outcome measures to evaluate the pathogenicity of *SIL1* variants in suitable *in vitro* models and demonstrated that the p. R92W missense variant is a polymorphism rather than a pathogenic mutation leading to MSS.

Keywords: SIL1-interactome, Marinesco-Sjögren syndrome biomarkers, SIL1 missense mutation, POC1A, FAM134B, centrosome

INTRODUCTION

Marinesco-Sjögren syndrome (MSS) was established as an entity by the Romanian neurologist Georges Marinesco in 1931 based on the description of four individuals from a single family presenting with ataxia, cataracts, intellectual disability, and myopathy. This was followed by Torsten Sjögren who further defined the original four cases as well as 10 additional patients. Afterwards, cerebellar atrophy was described as part of the phenotypic spectrum (1). In 2005, two groups independently reported recessive mutations in the *SIL1* gene as the major genetic cause for MSS (2, 3). *SIL1* encodes a co-chaperone for the major Endoplasmic Reticulum (ER)-resident chaperone BiP and thus controls a variety of BiP-dependent functions such as protein folding (4). Hereby, SIL1 acts as a N-linked glycoprotein equipped with an N-terminal ER targeting sequence and a C-terminal ER retention signal. SIL1 dimerises at the N-terminus into a clamp-like configuration that interacts with the BiP ATPase domain and causes substrate release of BiP via the release of ADP (5).

The "clinical triad" of MSS is defined by presence of bilateral cataracts, ataxia, and myopathy whereas intellectual disability can manifest with very varying degree or can even be absent (6). So far, a clear genotype-phenotype correlation does not exist, and the phenotypical presentation becomes even more complex by the description of additional features: pectus carinatum and bilateral clinodactyly in a patient with a homozygous large indel in the 5′UTR (7), Dandy-Walker malformations in a Chinese family with a non-stop mutation (8) and associated motor neuronopathy with a bradykinetic movement disorder in a 5-year-old child, suggesting an intriguing continuum between neurodevelopmental and neurodegenerative multisystem disorders intricately linked in the same cellular pathways (9). Moreover, the phenotypical variation has become even more complex by the first report of compound heterozygous *SIL1* missense mutations causing a neurological phenotype without signs of myopathy or cataracts but including spastic paraplegia, thus not fulfilling the clinical diagnostic criteria for MSS (10). Interestingly, the number of detected *SIL1* variants ($n = 488$; ExAC http://exac.broadinstitute.org/) as of 11/2018 includes 147 missense and 7 non-sense variants with various effects on the phenotype. Notably, these missense mutations also include the p.R92W variant of SIL1, described as segregating with the phenotype in a consanguineous family from Pakistan (11) but reported in ExAC with an allele frequency of nearly 4% in south Asian countries suggesting a polymorphic character. Given that *(i)* the MSS phenotype can present with prominent additional clinical features or characteristic features of the "clinical triad" can be absent, *(ii)* missense mutations may have a detrimental effect (10) and *(iii)* the detection of new *SIL1* sequence variants ever increasing in number, the need to classify the pathogenicity is indicated. Here we introduce an *in vitro* system designed to examine the consequences of *SIL1* mutations at the protein level, focussing on the stability of the variant SIL1 proteins, the morphology of cellular organelles, the build-up of aggregated proteins, the activation of proteolysis and on the SIL1-interactome. This procedure has allowed to differentiate between benign and pathogenic variants (mostly due to amino acid changes).

MATERIALS AND METHODS

Generation of SIL1-TAP and SIL1-HA Expression Constructs

Using the SIL1-TAP expression construct (pcDNA5/FRT/TO vector) (12) missense variants (listed below) as well as one deletion variant of recombinant human *SIL1* were generated by site-directed mutagenesis. To this end, the QuikChange Site-Directed Mutagenesis kit (Stratagene) was used according to the manufacturer's instructions. Primer sequences are available on request. All constructs were verified by sequencing the entire coding region of the inserts.

The ORF of the human *SIL1* cDNA was cloned in-frame into the carboxy-terminal hemagglutinin (HA) tag containing pRC/CMV expression vector. The same missense changes as for the pcDNA5/FRT/TO vector systems were introduced by site-directed mutagenesis using the QuikChange Site-Directed Mutagenesis kit (Stratagene). Primer sequences are available on request. All constructs were verified by sequencing the entire coding region of the inserts.

The following *SIL1* variants were selected and generated as expression systems based on the following reasons:

p.R92W

A missense variant of ambiguous pathogenic character: reported to cause MSS in a consanguineous Pakistani family (11) but present in ExAC with an allele frequency of nearly 4% and hereby also found to be homozygous in south Asian populations. Evaluation of its pathogenicity was one aim of the present study to address the suitability of our introduced *in vitro* system along with different tests.

p.K132Q

A missense variant of benign character (polymorphism) serving as a control. which should give the same results as the wild-type form of the SIL1 protein.

p.V231_I232del

A deletion variant with well-known pathogenicity based on stability of the protein as described previously by immunoblot and proteomics-based studies of MSS-patient-derived immortalized lymphoblastoid cells (6, 13).

p.G312R

A missense variant of well-known pathogenicity based on stability of the protein as described previously by immunoblot- and proteomics-based studies of MSS-patient derived immortalized lymphoblastoid cells (6, 13).

p.L457P

A missense variant with well-known pathogenicity *in vitro* tested in COS7 cells and associated with clinical presentation of MSS (14).

Cell Culture and Treatments:

Using the six pcDNA/FRT/TO-based expression constructs for SIL1-TAP (wild-type and five variants), stable inducible Hek293-TRex cell lines were generated as described previously (12). Cells were cultured in Dulbecco's Modified Eagle's medium (DMEM; Sigma-D5546) supplemented with 10 fetal calf serum (FCS; Sigma- F2442). Transient transfection of pRC/CMV-based constructs for SIL1-HA wildtype and variants was performed utilizing Lipofectamine 2000 (Thermo Fisher Scientific) according to the manufacturer's instructions.

Immunoprecipitation of the SIL1 Variants:

As SIL1 can act as a dimer (5), the ability to form protein dimers was addressed for the five protein variants of SIL1. Dimerization of the wildtype-protein was examined as a positive control to demonstrate functionality of the assay. The generated stable inducible Hek293-TRex cell lines (grown on 10 cm dishes) were additionally transfected with pRC/CMV-based constructs for SIL1-HA wildtype and variants and were collected 8 h post-transfection. Afterwards, cells were lysed in 500 µl of a buffer containing 1 mM EDTA (Sigma-Aldrich), 10% (v/v) glycerol (Roth), 20 mm HEPES (pH 7.5; Sigma-Aldrich), 150 mM NaCl (Sigma-Aldrich) and 0.8% (v/v) NP-40 (Roth) as well as 1 × Complete Protease Inhibitor Cocktail (Roche) for 1 h on ice. Next, centrifugation (1.500 rpm) of the lysates was performed at 4°C for 10 min to separate the protein extracts from cell debris. Protein concentrations were determined using the Pierce BCA protein assay kit (Thermo Fisher) according to manufacturer's instructions. Immunoprecipitation of the different HA-tagged forms of the SIL1 proteins via the TAP-tagged forms was carried out as described previously (12) using 100 µg of total protein extract.

For each experiment, cells overexpressing the solely the C-terminal TAP-Tag were included to exclude unspecific binding of the HA-Tagged versions of the SIL1 protein to the TAP-tag. All co-immunoprecipitation experiments were carried out three times.

Tandem-Affinity Purification of SIL1-Interactome and LC-MS/MS-Based Identification of Binding Partners

Interaction screening [tandem-affinity-purification (15) and subsequent mass spectrometry] of SIL1 wildtype protein as well as the five variant forms was carried out as described previously (6, 12) For each experiment, three independent biological replicates were analyzed.

Investigation of Cellular Fitness

Cellular fitness of Hek293-TRex cell lines overexpressing the wildtype SIL1 protein as well as of cells overexpressing the five variants was addressed by utilizing the WST-1 assay (Roche), according to the manufacturer's instructions. Cells treated with H_2O_2 were included as a positive control of decreased cellular fitness to demonstrate functionality of the assay. Moreover, cells overexpressing the TAP-Tag only were included to demonstrate that the presence/expression of the TAP-tag has no effect on cellular fitness. The relative absorption in cells overexpressing the SIL1 wildtype protein was considered as 100% of cellular fitness.

Native-PAGE, SDS-PAGE and Western Blotting:

Native-PAGE was carried out as described in a protocol available online (http://www.assay-protocol.com/molecular-biology/electrophoresis/native-page) and the immunoblot studies were performed as described previously (16). The following antibodies were used:

Immunofluorescence:

Distribution of SIL1 wildtype protein as well as of the five different variants was addressed in the stable inducible Hek293-TRex cell lines: the respective cell lines (2×10^5 cells) were plated onto 24-well plates on coverslips 12 h prior to induction of expression with doxycycline as described before (12). Beforehand, coverslips were coated with poly-L-lysine (Sigma-Aldrich) for 1 h at room and afterwards washed twice with ultra-pure water. Cells were fixed with 4% paraformaldehyde in PBS pH 7.4 for 20 min at room temperature. Afterwards, cells were washed 3 times with ice-cold PBS. For permeabilization, coverslips were incubated for 10 min in PBS containing 0.25% Triton X-100 (Roth). In the following step, cells were washed in PBS 3 times for 5 min. For blocking and immunostaining, coverslips were incubated in 1% BSA (in PBS+ 0.1% Tween 20) for 45 min and afterwards exposed to the anti-TAP antibody (Sigma-Aldrich) 1:100 diluted in 1% BSA in PBST in a humidified chamber overnight at 4°C. Afterwards, coverslips were washed 3 times in PBS (5 min each washing step) and then incubated with the secondary antibody (goat anti-rabbit Alexa Fluor® 568, Abcam) diluted 1:5,000 in 1% BSA-PBS for 1 h at room temperature in the dark. Next, three washing steps times in PBS (5 min each washing step) were carried out. Finally, cells were mounted with a drop of mounting medium (Thermo Fisher)

and coverslips were sealed with nail polish to prevent drying and movement under microscope. For analysis of immunoreactivity, the Axiovert 200 M microscope from Zeiss (240525) was used. For each SIL1 variant as well as for the wildtype proteins 50 different cells were analyzed with more than 70% of cells giving similar results, respectively.

For co-localization studies of SIL1, Hek293 cells were permeabilized by incubation with 200 µL PBS buffer containing 0.1% Triton X-100 for 10 min and subsequently washed with PBS buffer. For blocking cells were incubated with 200 µL of PBS containing 0.1% TWEEN20 and 1% BSA for 30 min. Afterwards, cells were covered with 200 µL of blocking solution containing the respective combinations of both primary antibodies [α-CASQ1 (Sigma: C0618-200UL), α-FAM134B (Genetex: GTX46621), α-POC1A (Thermo Fisher Scientific: PA5-49028), α-SIL1 (Abcam: ab5639) dilution 1:300 each], incubated for 90 min and then washed with PBS. Secondary antibodies were diluted in 1% BSA (dilution 1:500 for Alexa488 probe, 1:300 for Alexa555 probe). Cells were covered with 200 µl of this antibody-solutions and incubated for 1 h in the dark. Next, antibody solution was removed, and samples were washed with BSA before the coverslips were directly mounted with fluorescent mounting medium ("Prolong Gold antifade reagent with DAPI" Invitrogen) and allowed to dry overnight (at 6°C). Fluorescence measurements were carried out with a modified Leica TCS SP8 CARS laser scanning Microscope using either a 20x objective (HC PL APO CS2 20x/0.75 DRY) or a 63x objective (HC PL APO CS2 63x/1.20 WATER). Images were acquired with a resolution of 2048 × 2048 pixel with a step size of 286 nm for 20x magnification and of 91 nm for 63x magnification. Fluorescence measurements on each position were performed sequentially using laser excitation at 488 nm and detection at 500–540 nm with a hybrid detector (LeicaHyD), excitation at 561 nm and detection at 566–620 nm with a HyD and excitation at 405 nm with detection at 425–500 nm using a PMT. All data processing was carried out using Matlab R2015a. Due to variations in fluorescence intensity between the samples as well as between the different dyes data were preprocessed for better comparability. To reduce background, noise data points having < 2% of intensity were set to this lower threshold value. To account for cosmic spikes, the upper threshold was set so that a maximum of 0.1% of all data points above background showed fluorescence intensity above this limit. Intensities above the upper threshold were set to this value. Images were then rescaled to full range (8bit). For calculation of co-localization values in each channel, all data points exceeding an intensity value of 20% were determined. Data points that are above this value in both channels were considered to be co-localizing. The ratio of co-localization is calculated from the number of co-localizing points divided.

Electron Microscopy

Preparation of Hek293-TRex cell lines and subsequent transmission electron microscopic studies were carried out as described previously (12, 16). For each SIL1 variant as well as for the wildtype protein, at least 50 cells were analyzed showing similar (patho)morphology of subcellular organelles/structures.

RESULTS

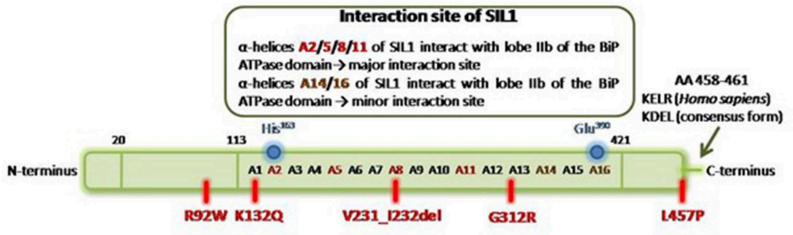
Literature and *in silico*-Based Evaluation of the Pathogenicity of Selected SIL1-Variants

We chose one known polymorphism (p.K132Q), three notoriously pathogenic mutations (p.V231_I232del, p.G312R, and p.L457P) and p.R92W, a variant that was previously described as a pathogenic missense mutation (11). Notably, the two missense variants pR92W and p.K132Q are present in the control population with minor allele frequencies (MAF) of 0.5 and 0.7%, respectively, and in 29 and 72 healthy individuals in homozygous state. On the other hand, p.G312R is absent from a control population of >125,000 individuals (ExaC, http://exac.broadinstitute.org) and p.L457P is found in one allele count (MAF: 0.0004%) (http://gnomad.broadinstitute.org). The sites of the different variants/ mutations are depicted in **Figure 1A**. By affecting α-helix A8 of the SIL1-protein, the p.V231_I232del mutation directly impacts on the physiological SIL1-BiP interaction lobe IIb of the BiP-ATPase domain (major interaction site). Although the polymorphic variant p.K132Q and the reported pathogenic missense mutant p.G312R are also localized within the SIL1-BiP-binding domain, they do not directly affect α-helices mediating the physical interaction with BiP. The ambiguous missense variant, p.R92W, localizes within the N-terminal domain of the 461 amino acid SIL1 protein and p.L457P, another known pathogenic missense mutant of SIL1 affects one amino acid localized before the known ER-retention motif KDEL/KELR (17) (**Figure 1A**). Interestingly, *in silico* testing of pathogenicity with different platforms revealed controversial results including a probably damaging effect for all amino acid substitutions addressed in this study (**Figure 1B**). This result is in contrast with the observed allele frequencies in the control population and by the same token emphasizes the need to define biomarkers that can be used to evaluate the pathogenicity of *SIL1* mutations—in particular of amino acid substitutions.

Molecular Characteristics of Selected SIL1-Variants in a Non-reducing PAGE

First, molecular characteristics of the selected SIL1-variants were addressed in a non-reducing PAGE (and concomitant blotting to a PVDF-membrane) utilizing whole protein extracts. Detection of the different variant forms of the recombinant SIL1-protein utilizing an anti-SIL1 antibody (see **Table 1**) revealed no major differences in the detected molecular weight of wildtype SIL1-TAP in comparison to the ambiguous p.R92W and the benign p.K132Q variants of SIL1. In contrast, no band was detectable for p.V231_I232del-mutant SIL1 (16 h of induced overexpression) suggesting instability of the aberrant protein, a finding which is in line with our previous studies on patient derived cells (6, 12). However, absence of this mutant form of the protein might also arise from a changed antigenicity of this variant product. Immunoblots of the two well-known pathogenic mutant forms, p.G312R and p.L457P, did not only show protein bands of the predicted size of the recombinant fusion-protein (SIL1-TAP) but also additional bands corresponding to a higher molecular weight

A



B

Nucleotide change	Location	Predicted aminoacid change	Family/ origin	ClinVar	In silico prediction	CADD score	Population frequency (homozygos)	Reference
c.274C>T	Exon 4	p.R92W	60078/ Pakistan	Likely benign	D;D;D;B	27,6	0,5% (14)	Riazuddin et al., 2009
c.394A>C	Exon 5	p.K132Q	n/a n/a	Likely benign/ benign	D;D;D;B	25,7	0,7% (29)	n/a
c.691_696del GTGATC	Exon 7	p.V231_ 232del	MSS24.1 Turkey	-	n/a	n/a	absent	Krieger et al., 2013
c.934G>A	Exon 9	p.G312R	MSS32.1 USA	-	D;D;D;B	27,8	absent	Krieger et al., 2013
c.1370T>C	Exon 10	p.L457P	M21 Japan	Patho-genic	D;P;D;P	24,2	absent	Anttonen et al., 2008

FIGURE 1 | Overview of investigated amino acid changes of SIL1. **(A)** Localization of SIL1 amino acid changes in the entire SIL1 protein. Schematic figure is modified from Yan et al. (5). **(B)** Table summarizing the *SIL1* variants by providing information regarding the corresponding nucleotide change/ deletion in different exons within the *SIL1* gene as well as origin of the respective MSS-patient and results of *in silico*-based testing of pathogenicity by "CADD score" and "ClinVar" as well as by "SIFT", "PluPhen2", "MutationTaster" and "FATHMM" (summarized as in silico prediction). D, damagingl; P, pathogenic; B, benign; T, tolerated.

which appear to be more pronounced for p.G312R (**Figure 2A**). The experiment was performed 6 times with similar results.

Influence of Amino Acid Substitutions/Deletions on SIL1-SIL1-Interactions:

Given that SIL1 can act as a dimer (6), we addressed the effect of the various amino acid changes and of the deletion of two amino acids (p.V231_I232del) on the formation of SIL1-protein homomers by immunoprecipitation and subsequent immunoblot analyses. As a proof-of-principle, the well-known homomerization of SIL1 wild-type proteins was confirmed (**Figure 2B**). Both, the ambiguous p.R92W and the benign p.K132Q variants showed a homomerization similar to the one observed for the wild-type SIL1-TAP-SIL1-HA complex (**Figures 2C,D**). Analyses of the well-known pathogenic p.V231_I232del mutation revealed no interaction of the resulting degradation products in terms of the formation of toxic (proteolytic) protein complexes (**Figure 2E**). Study of the two-known pathogenic SIL1-proteins, p.G312R and p.L457P, showed that they can form homomeric complexes along with their degradation products (**Figures 2F,G**). Immunoblot-based analyses of whole protein extracts/ straight lysates confirmed the expression of the respective recombinant SIL1-variants tagged with HA or TAP in each of the respective experiments. All immunoprecipitation and immunoblot experiments were performed three times with similar results.

Influence of Amino Acid Substitutions/ Deletions on the Fitness of the *in vitro* Models

Mitochondrial vulnerability has been repeatedly reported in MSS and woozy mouse tissues (13, 18–20), and in *in vitro* models of the disease (13, 16). As mitochondrial function is essential for cellular fitness, we examined metabolic activity of our *in vitro* models by focussing on processes related to mitochondrial activity as well as on mitochondrial morphology. The WST-1 assay (Roche) was used; in this assay the stable tetrazolium salt, WST-1, is cleaved to a soluble formazan. This conversion depends on the cellular availability of succinate-tetrazolium reductase system that belongs to the respiratory chain of the mitochondria (only active in metabolically intact cells). Thus, the amount of formazan dye formed directly correlates to the number of metabolically intact cells in the culture. Metabolic activity in WT-SIL1 cells was defined as 100% of cellular fitness. The WST-1 assay revealed no reduction in metabolic activity upon overexpression of the ambiguous p.R92W or of the benign p.K231Q variant of SIL1 (**Figure 3A**). Overexpression of the p.V231_I232del mutant form of the SIL1-protein (which displayed instability in our previous experiment, see above) resulted in a minor but significant decrease of the fitness (**Figure 3A**). In contrast, overexpression of the known pathogenic mutants p.G312R and p.L457P led to a 15–20% reduction in cellular viability compared to cells overexpressing the WT-SIL1 (or solely the TAP-Tag) suggesting an effect of

TABLE 1 | All immunoblot studies were carried out at least three times.

Antibody	Company	Dilution
α-Beclin	Novus Biologicals: NB110-87318	1:1000
α-CBP	Thermo Fisher Scientific: PA1-847	1:1000
α-CHOP	Novus Biologicals: NB600-1335SS	1:500
α-DJ-1	Santa Cruz: sc-55572	1:750
α-DNAJB6	Genetex: GTX33160	1:500
α-ERj3	Novus Biologicals: NBP1-68477	1:500
α-FAM134B	Genetex: GTX46621	1:500
α-GAPDH	Genetex: GTX627408	1:1000
α-GRP94	Genetex: GTX103203	1:1000
α-GRP170	Genetex: GTX102255	1:1000
α-HA	Sigma Aldrich: H3663-100UL	1:500
α-IRE1	Genetex: GTX130387	1:500
α-pEif2α (Ser52)	Thermo Fisher Scientific: 44-728G	1:1000
α-PERK	Abcam: ab65142	1:500
α-POC1A	Thermo Fisher Scientific: PA5-49028	1:500
α-SIL1	Abcam: ab5639	1:100
α-SOD1	Genetex: GTX100554	1:1000
α-VCP	Genetex: GTX101089	1:1000

List of antibodies used in the study.

their pathogenicity on cellular metabolism (**Figure 3A**). H_2O_2-treated Hek293 cells were included as a positive control for perturbed mitochondrial function based on massive oxidative stress burden (**Figure 3A**). The assay was carried out 4 times with similar results. Given that mitochondrial vulnerability might be connected to oxidative stress, a well-known epiphenomenon of ER-stress, levels of DJ1 and SOD1 (two proteins known to be modulated by oxidative stress burden) were studied by immunoblotting. Hek293 cells overexpressing the pathogenic missense variants of SIL1, p.G312R, and p.L457P, showed an increase in DJ1 (lower band), with a more pronounced effect in cells overexpressing p.G312R mutant SIL1. Cells overexpressing p.G312R mutant SIL1 showed a considerable increase in SOD1 protein, whereas there was no difference between the cells overexpressing the wildtype protein and those overexpressing the pathogenic p.L457P variant (**Figure 3B**). However, the increase of SOD1 in Hek293 cells overexpressing p.V231_I232del mutant form was comparable to the SOD1 increase in cells overexpressing the benign p.K132Q variant (**Figure 3B**. Notably, a parallel "trend" of abundances of DJ1 and SOD1 expression changes modulated by SIL1 variants can be observed. Prompted by the results of the WST-1 assay and by the immunoblot studies, mitochondrial-morphology was examined by electron microscopy. EM revealed normal ultrastructure of Hek293 cells overexpressing wild-type SIL1 as well as p.R92W- and p.K132Q variant forms of the SIL1 protein (**Figure 3C**). In contrast, Hek293 cells overexpressing the known pathogenic SIL1-missense mutations, p.G312R and p.L457P, presented with perturbed mitochondrial architecture including break-down of cristae and accumulation of electron-dense membranous material in the mitochondrial matrix most likely indicative of incipient mitophagy/ mitoptosis (21) (**Figure 3C**). Overexpression of the pathogenic but instable p.V231_I232del mutant form did not result in such a profound mitochondrial pathology. This might actually be due to the higher stability of the pathogenic missense mutant forms of SIL1 resulting in persistent mitochondrial stress. Pathomorphological mitochondria could be detected in 41 of 50 cells (82%) expressing the p.L457P and in 38 of 50 cells (76%) expressing the p.G312R mutant form whereas in cells expressing wildtype SIL1 or the variants p.R92W and p.K132Q, pathomorphological mitochondria were found in 10%, 18% and 14%, respectively (50 cells were analyzed for each *in vitro* model). Only 12% of Hek293 cells overexpressing the pathogenic but instable p.V231_I232del mutant displayed morphological aberrant mitochondria.

Pattern of Cellular SIL1 Staining—Polymorphic vs. Pathogenic Forms of the Protein:

Immunofluorescence studies of our Hek293 *in vitro* models overexpressing the different forms of the SIL1 protein in an inducible fashion were performed to address the question if the pattern of SIL1-TAP-immunoreactivity allows to differentiate between polymorphic variants and pathogenic mutations. Indeed, cells overexpressing WT-SIL1 in comparison to those overexpressing the two known pathogenic missense forms (p.G312R and p.L457P) showed significant differences regarding the pattern of immunoreactivity. WT-SIL1 was distributed in a reticular network in accordance with a regular ER-localization, whereas p.G312R- and p.L457P mutant SIL1 showed an altered non-reticular immunoreactivity pattern (**Figure 4A**). In contrast, p.V231_I232del mutant SIL1 (after 6 h of induced overexpression) showed a reticular distribution comparable to WT-SIL1 and the polymorphic p.K132Q form but with some focal accumulations (**Figure 4A**). Notably, immunoreactivity of p.R92W variant SIL1 does not show the same subcellular distribution as the p.G312R and p.L457P mutants and rather presents as a reticular network as observed for WT-SIL1 and p.K132Q but with some minor focal accumulations.

Influence of Amino Acid Substitutions/Deletions on ER-Morphology and Function in our *in vitro* Models

To follow up on the immunofluorescence studies described above, EM was performed. ER in Hek293 cells overexpressing WT-, p.R92W and p.K132Q versions of SIL1 showed a regular tubular structure. In cells overexpressing p.G312R and p.L457P mutant SIL1, the ER showed focal widening, occasionally associated with accumulation of electron dense material most likely corresponding to protein aggregates within the widened ER (black arrows in **Figure 4B**). In addition, cells overexpressing these two known-pathogenic mutants exhibited autophagic vacuoles that were often filled with membranous and granular osmophilic material (**Figure 4B**). Deposits of osmophilic material (mostly localized to autophagic vacuoles) were also detected in Hek293 cells with short-term (6 h) overexpression of p.V231_I232del mutant SIL1 (**Figure 4B**).

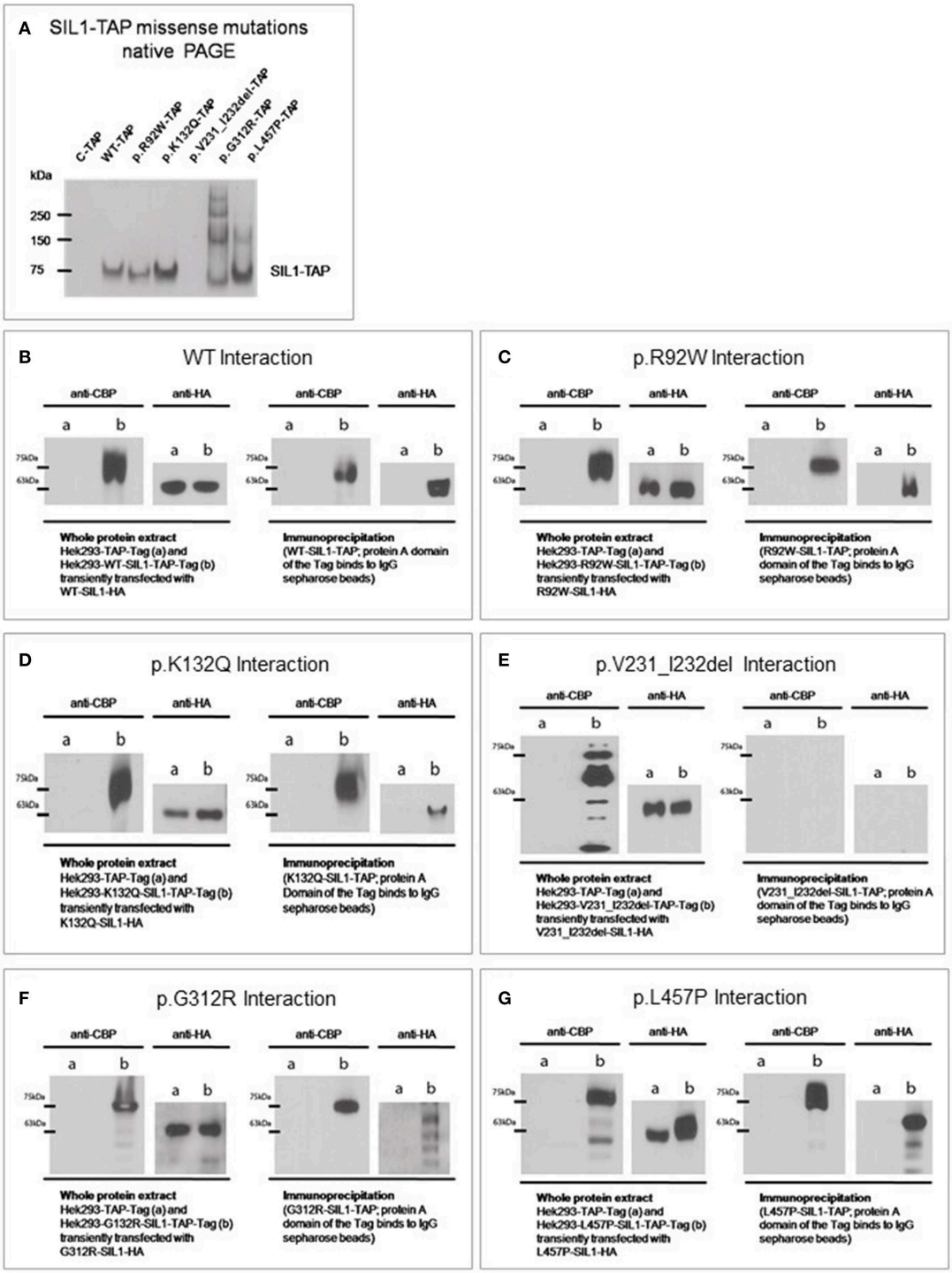


FIGURE 2 | Impact of amino acid substitutions and deletions on the molecular characteristics of SIL1. **(A)** Native-PAGE of SIL1 variants reveals absence of p.V231_I232del mutant SIL1 (16 h of induced overexpression) but no differences in the migration pattern of the different missense variants of SIL1. The two known pathogenic variants p.G312R- and p.L457P present additional bands of a higher molecular weight. **(B–G)** Immunoprecipitation and subsequent immunoblot analysis toward the study of SIL1-homomerization confirmed the known SIL1-SIL1 interaction of the wildtype form of the protein **(B)** and showed no effect of the p.R92W- or p.K132Q-amino acid substitutions on this interaction **(C,D)**. Study of p.V231_I232del mutant SIL1 (6 h of induced overexpression) did not show a physical interaction of the degradation products of this known pathogenic and instable form of SIL1 **(E)**. Analysis of the two known missense mutants p.G312R- and p.L457P revealed in both cases a homomerization of the full-length mutant proteins but also an interaction of the mutant full-length protein with the respective degradation products **(F,G)**.

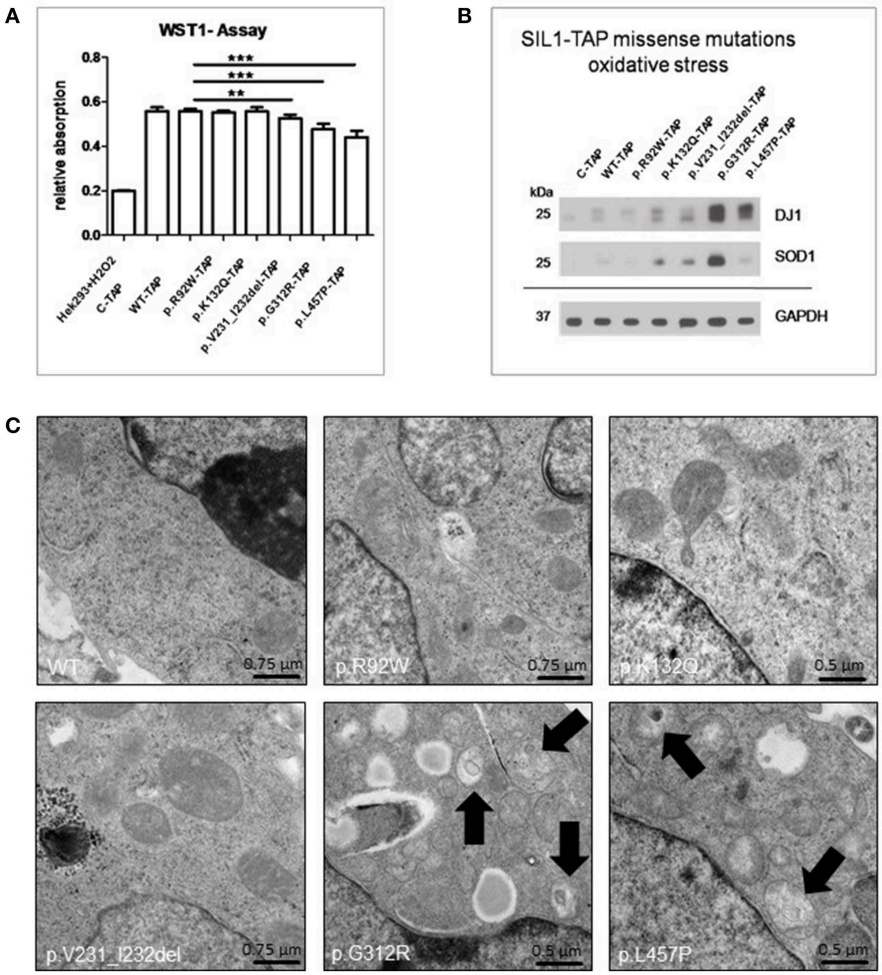


FIGURE 3 | Study of fitness of Hek293 cells overexpressing SIL1 or its variant forms in the context of mitochondrial vulnerability. **(A)** ELISA-based WST-1 assay showed a statistically significant reduction in the fitness of cells overexpressing the known pathogenic variants p.V231_I232del (6 h of induced overexpression), p.G312R and p.L457P, respectively. In accordance with the instability of p.V231_I232del mutant SIL1, the fitness is more reduced in Hek293 cells overexpressing p.G312R and p.L457P mutant forms of SIL1. Hek293 cells treated with H_2O_2 were included as positive control showing the functionality of the assay. **(B)** Immunoblot-based studies of DJ1 (lower band) and SOD1 as two representative marker proteins for oxidative stress (related to mitochondria) showed a considerable increase of DJ1 in cells overexpressing p.G312R or p.L457P mutant SIL1. Surprisingly, SOD1 was only markedly increased in cells overexpressing p.G312R mutant SIL1, but not in cells overexpressing p.L457P mutant SIL1. GAPDH was used to demonstrate equal protein loading. **(C)** EM revealed normal mitochondrial architecture in Hek293 cells overexpressing WT-SIL1, p.R92W and p.K132Q variant SIL1 as well as p.V231_I232del mutant SIL1 but disintegration of cristae and presence of membranous electron-dense material within the mitochondrial matrix (black arrows) in cells overexpressing the two known pathogenic missense variants p.G312R and p.L457P. **Statistically very significant; ***Statistically extremely significant.

Prompted by our ultra-structural findings, we next investigated the presence of ER-stress upon overexpression of wildtype SIL1 as well as the 5 different variants at the molecular level by immunoblotting by focussing on the abundances of 10 proteins modulating the unfolded protein response (UPR) and the ER-associated degradation pathway (ERAD). In accordance with our previous published data (12), overexpression of wildtype SIL1 results in the increased expression of these factors compared to cells overexpressing solely the TAP-Tag (**Figure 4C**). This in turn also explains the altered expression of these factors in Hek293 cells with long-term overexpression of the instable p.V231_I232del mutant form. However, overexpression of neither the polymorphic p.K132Q nor of the ambiguous p.R92W variant led to a sustained increase of the UPR-/ ERAD-related proteins compared to cells overexpressing the wildtype form of SIL1 (**Figure 4C**). Overexpression of p.G312R resulted in an increased expression of GRP170 and Beclin-1 as well as forced phosphorylation of eIF2α compared to cells overexpressing the TAP-tag only, the wildtype variant of SIL1 or the p.R29W and p.K132Q variants, respectively (**Figure 4C**). The overexpression of p.L457P mutant SIL1 even resulted in elevated abundance of all investigated UPR-/ ERAD-proteins except HSP40/ ERj3 (**Figure 4C**).

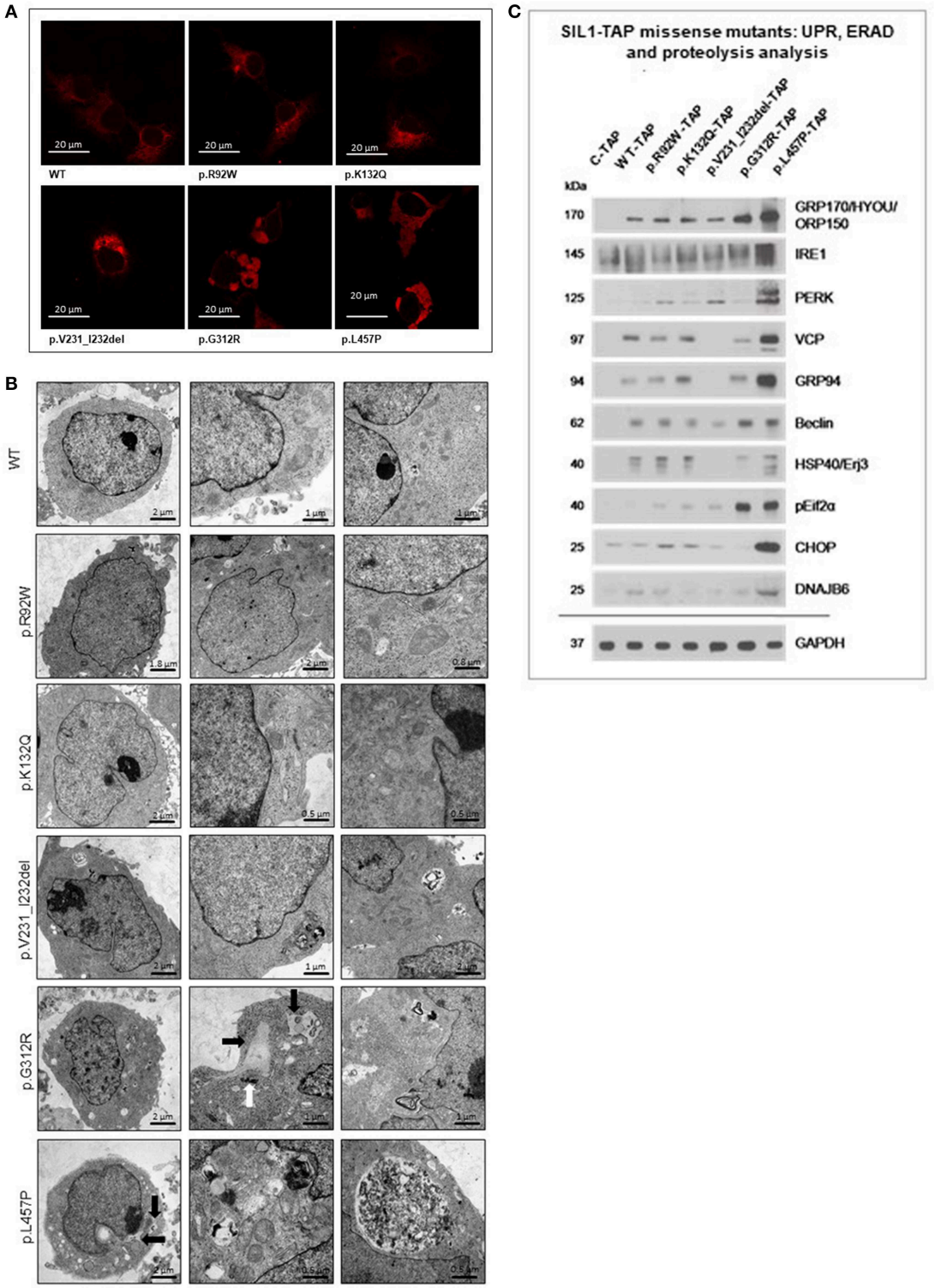


FIGURE 4 | Study of cellular SIL1 immunoreactivity and presence of ER-stress in Hek293 cells overexpressing SIL1 or its variant forms. **(A)** Immunofluorescence-based investigation of the SIL1-immunoreactivity pattern in Hek293 cell revealed a reticular distribution for WT-SIL1, p.R92W and p.K132Q variant forms of SIL1 but a non-reticular rather "clumpy" immunoreactivity for p.G312R and p.L457P mutant forms of SIL1. For p.V231_I232del mutant SIL1, a reticular distribution with focal accumulations was observed. **(B)** EM revealed widened and proliferated ER in cells overexpressing the mutant forms p.G312R and p.L457P, but not in cells overexpressing WT-SIL1, p.R92W, p.K132Q, and p.V231_I232del (6 h of induced overexpression) forms of the proteins. In addition, accumulation of electron dense material could occasionally be seen in cells overexpressing p.G312R and p.L457P muatnt SIL1 (black arrows). Along this line,

(Continued)

FIGURE 4 | overexpression of these two known missense mutants of SIL1 resulted in the build-up of electron dense material (most likely corresponding to aggregated protein) in the cytoplasm as well as in (autophagic) vacuoles. The white arrow highlights an abnormal centrosome in a Hek293 cell overexpressing p.G312R mutant SIL1. **(C)** Immunoblot-based studies aimed to investigate the presence of ER-Stress by focussing on marker proteins for activation of the unfolded protein response (GRP170, IRE1, PERK, GRP94, ERj3 & pEif2α), the ER-associated degradation pathway (VCP, DNAJB6) and proteolysis (Beclin). Results revealed a considerable presence of ER-stress in Hek293 cells overexpressing p.L457P mutant SIL1 than in cells overexpressing p.G312R mutant SIL1 where solely pEif2α and Beclin are increased compared to cells overexpressing WT-SIL1. p.R92W, p.K132Q variant SIL1, and p.V231_I232del mutant SIL1 (6 h of induced overexpression) do not show remarkable changes in abundances of the stress markers compared to cells overexpressing WT-SIL1. GAPDH was investigated to demonstrate equal protein loading. The differences in expression of these markers between C-TAP and WT-SIL1 overexpressing Hek293 cells have been described previously (12).

Influence of Amino Acid Substitutions/Deletions on SIL1-Protein-Binding and Subsequent Morphological Effects in our *in vitro* Models

To define another read-out measure enabling the robust evaluation of the pathogenicity of amino acid changes and deletions in *SIL1*, tandem-affinity-purification followed by mass spectrometric analysis of the different TAP-tagged variants of the SIL1 protein was performed. Overexpression of p.V231_I232del mutant SIL1 was induced by doxycycline treatment for 6 h to study binding partners prior degradation of this instable pathogenic SIL1 protein. Results of this screening approach are presented in **Figure 5A** and show that all variants of the SIL1-protein bind to BiP, Mortalin and the small subunit of Calpain-1. Moreover, our protein-interaction studies revealed a precipitation of ERj3 along with the two pathogenic mutants of SIL1, p.G312R, and p.L457P, but not with the two variants p.R92W and p.K132Q or the wildtype form of SIL1. Remarkably, our unbiased studies focusing on interaction of different forms of SIL1 to other proteins revealed that the wildtype protein as well as the p.R92W and p.K132Q variants are precipitating with POC1A whereas immunoprecipitation of p.G312R and p.L457P mutant SIL1 along with their interactors and subsequent mass spectrometry studies did not result in the identification of POC1A as a binding partner. Given that mutations in *POC1A* are causative for SOFT (short stature, onychodysplasia, facial dysmorphism, and hypotrichosis) syndrome (22) and short stature is also a clinical finding in MSS patients, a regulatory effect of abundances of the SIL1-wildtype protein on level of POC1A was confirmed by immunoblot studies. Our findings highlight an effect of cellular SIL1 level on POC1A protein abundance (**Figure 5B**, left). *POC1A* encodes for a protein linking centrosomes to Golgi assembly and function, and recessive mutations affecting this gene result in perturbed Golgi structures and cytosolic vesicle accumulations, in addition to abnormal multipolar spindles *in vitro* (22, 23). This known POC1A function along the mentioned pathological findings resulting from mutations in the corresponding gene prompted us to also study the level of FAM134B, a newly identified cis-Golgi protein with a pivotal role in neuronal function and survival (24) in relation to the expression of SIL1 wildtype protein as well as the morphology of Golgi and centrosomes. Indeed, immunoblot studies of FAM134B showed a beneficial effect of SIL1 expression on the abundance of this Golgi-protein (**Figure 5B**, left). Results of expression studies in Hek293 cells expressing different mutant forms of the protein show a clear influence of the pathogenicity of SIL1-mutations on the abundance of the FAM134B and POC1A proteins (**Figure 5B**, right).

Prompted by our SIL1-protein interaction findings suggestive for a localization of SIL1 also to the Golgi-apparatus, further immunofluorescence studies have been performed and revealed an expected co-localization of SIL1 with calsequestrin (CASQ1; a known ER-marker protein) and additionally co-localizations with golgin-97 (a known marker protein of the Golgi apparatus) as well as with FAM134B and POC1A. Quantification of these co-localizations revealed that the excessive proportion of the SIL1 protein localizes to the ER but almost equal co-localization with golgin-97, FAM134B and POC1A indicates a minor localization of SIL1 also within the Golgi apparatus (**Figure 5C**).

Results of further ultra-morphological studies focussing on the integrity of Golgi and centrosomes revealed proliferated and dispersed Golgi cisternae in Hek293 cells overexpressing p.G312R or p.L457P but not in cells overexpressing the wildtype form of the protein (**Figure 5D**). Whereas, neither the polymorphic p.K132Q nor the ambiguous p.R92W variant of SIL1 presented with changes in Golgi architecture compared to cells overexpressing WT-SIL1 (data not shown), Hek293 cells with short-term overexpression of p.V231_I232del showed only a very mild widening of Golgi cisternae (**Figure 5D**). Interestingly, altered Golgi structures could frequently be detected adjacent to abnormal centrosomes as exemplified for p.V231_I232del and p.G312R in **Figure 5D** (black arrows). Along this line, overexpression of the pathogenic forms of the SIL1 protein in Hek293 cells repeatedly resulted in disintegration of centrosome architecture including centriole-multiplications and -proliferations as well as mis-localization of centrioles to lysosomes and vacuoles (**Figure 5E**).

DISCUSSION

On a general note, the need of suitable *in vitro* systems allowing a reliable testing of ambiguous gene mutations potentially affecting stability and localization of the corresponding protein is crucial in the cases that patient-derived tissue is not available to perform verification studies. Here, using MSS as a paradigmatic rare neurogenetic disease, we demonstrate that Hek293 cells overexpressing different mutant forms of the SIL1 protein are suitable to evaluate the pathogenicity of SIL1 mutations such as missense variants and in-frame-amino acid deletions. MSS has been selected for our studies as:

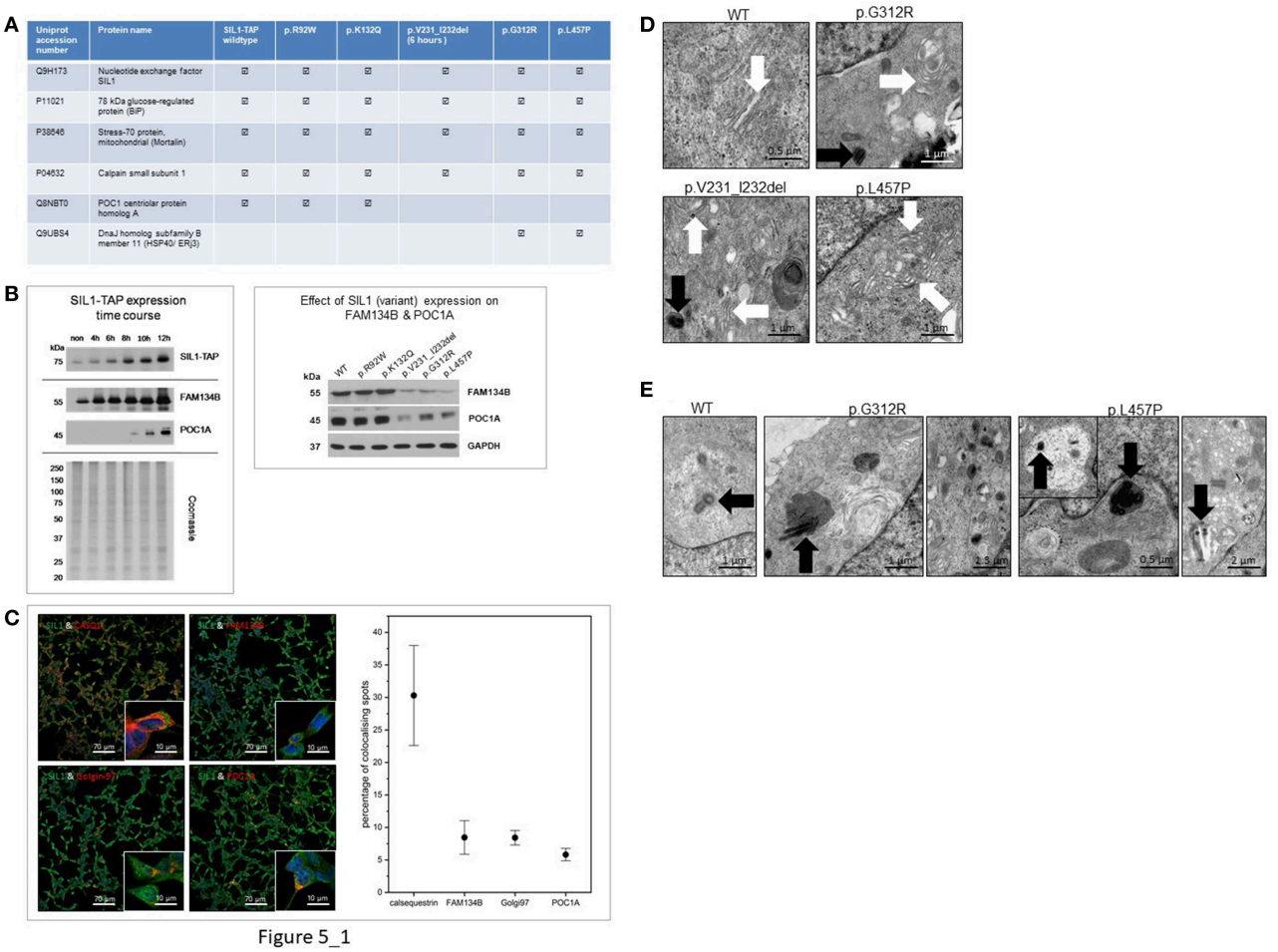


Figure 5_1

FIGURE 5 | Study of SIL1-interactome and impact of interaction on subcellular morphologies. **(A)** Table presenting SIL1-protein interactions identified by tandem-affinity-purification and subsequent mass spectrometry in an unbiased fashion: whereas WT-SIL1 and its (polymorphic and pathogenic) variants interact with BiP, Mortalin and the small subunit of Calpain-1, solely WT-SIL1, p.R92W and p.K132Q variant forms of SIL1 precipitated POC1A. In contrast, solely p.G312R and p.L457P mutant SIL1 precipitated ERj3, a known BiP-binding protein controlled by ER-stress. the detection of SIL1—as shown in the table presented—refers to the identification/ detection of tryptic peptides unique for the SIL1 protein in the mass spectrometric analysis. The peptides identified for the respective SIL1-variant arise from the overexpression of same ones and show the reliability of the combined IP-LC-MS/MS data. **(B)** Immunoblot-based study of FAM134B and POC1A revealed increased expression of both proteins upon elevation of the cellular SIL1 level. Coomassie-staining was carried out to demonstrate equal protein loading (left panel). Results of expression studies in Hek293 cells expressing different mutant forms of the protein show a clear influence of the pathogenicity of SIL1-mutations on the abundance of the FAM134B and POC1A proteins (right panel). **(C)** Results of our co-immunofluorescence studies focussing on SIL1 localizations revealed co-localizations of SIL1 with CASQ1 (calsequestrin), golgin-97, FAM134B, and POC1A. Representative overviews of cells are shown for each respective co-localization study which have also been used for the quantifications of co-localizations (right diagram). **(D)** EM of Golgi morphology revealed a regular architecture in Hek293 cells overexpressing WT-SIL1, but proliferated and dispersed Golgi with widened terminal cisternae (white arrows) and vesicle accumulations in cells overexpressing p.G312R or p.L457P mutant SIL1. In cells overexpressing p.V231_I232del mutant SIL1, solely a mild pathology of the Golgi apparatus (widened cisternae indicated by white arrows) could be observed. **(E)** EM of centrosome morphology revealed a regular architecture in Hek293 cells overexpressing WT-SIL1, but proliferated, multiplicated and dispersed centrosomes in cells overexpressing the pathogenic missense mutant pG312R or p.L457P (black arrows). Remarkably, in cells overexpressing these two known pathogenic forms of SIL1, a mis-localization of abnormal centrosomes to lysosomes (black arrows in pictures 2 and 4) or to vacuoles (black arrow in the inset of picture for as well as in picture 5) was observed.

- The phenotype can present with prominent additional clinical features or characteristic features of the "clinical triad" can be absent thus complicating the evaluation of detected variants in terms of phenotype-causative mutations
- Missense mutations may have a detrimental effect on the clinical presentation (10)
- Detection of new *SIL1* sequence variants is ever increasing in number thus indicating the need to classify their pathogenicity.

Indeed, the combination of different biochemical, morphological and functional studies utilizing Hek293 cells overexpressing different variants of SIL1 of known and ambiguous pathogenicity allowed to introduce a system enabling the *in vitro*-based evaluation of *SIL1* variants leading to amino acid substitutions or deletions: results of our SIL1-protein studies in a non-reducing PAGE suggest that although the pathogenic variants do not cause essential changes in the behavior of the main SIL1 band, bands of higher molecular weight occur which

most likely correspond to aberrant SIL1 protein complexes. The absence of these bands under reducing conditions (data not shown) indicates that these aberrant complexes are soluble. Hence, the presence of additional (higher molecular weight) SIL1 bands in a non-reducing PAGE might serve as a read-out measure to evaluate the pathogenicity of amino acid substitutions in SIL1. The absence of these bands in immunoblots of WT-SIL1, p.K132Q and p.R92W variants of SIL1 suggest that p.R92W is a benign variant rather than a pathogenic mutation.

In addition, studies focussing on the influence of amino acid substitutions/ deletions on SIL1-SIL1-interactions provided a new outcome measure toward the evaluation of the pathogenicity of SIL1 variants: given that degradation products of the p.V231_I232del, the p.G312R and the p.L457P mutant forms of SIL1 can be identified utilizing the straight protein lysates of the SIL1-SIL1 interaction experiment and anti-HA/TAP antibodies (detecting the respective Tags at the C-terminus of the recombinant proteins) a N-terminal initiated degradation of these mutant forms of the protein is suggested. The presence of degradation products for p.G312R and p.L457P mutant SIL1 (**Figures 2F,G**) in combination with the detected higher molecular weight bands for these forms as presented in **Figure 2A** suggests formation of protein aggregates and breakdown. A comparison of the degradation of the variant forms of SIL1 with known pathogenic character suggests a much higher instability of SIL1 exhibiting deletion of two amino acids compared to the two forms with C-terminal substitutions. Taken together, this assay shows that precipitation of degradation products might be indicative for a pathogenic character of amino acid changes in SIL1.

Given that mitochondria display a considerable vulnerability in the etiology of MSS (13, 18–20), WST-1 assay has been performed to investigate mitochondrial activity in our MSS *in vitro* models and results suggest a benign character of the p.R92W and p.K132Q amino acid changes in SIL1 whereas the pathogenic character of the p.G312R and p.L457P missense mutants could be confirmed. The mild reduction of the cellular fitness in cells overexpressing the instable p.V231_I232del mutant form of SIL1 (while cells still also express the endogenous SIL1 protein) might arise from impairment of cellular processes until degradation of the mutant recombinant protein is fully achieved. Findings of this assay suggest a reduced metabolic activity as a cellular biomarker or read-out measure of pathogenicity of *SIL1* mutations. As the expression of pathogenic SIL1 variants also impacts on morphological integrity of mitochondria, presence of oxidative stress and perturbed mitochondrial architecture might represent further useful read-out measures for the *in vitro* evaluation of pathogenicity of overexpressed *SIL1* mutations that are associated with a loss of function rather than a loss of protein. However, the less pronounced oxidative stress burden in the case of overexpression of p.L457P mutant SIL1 (**Figure 3B**) suggests that analysis of oxidative stress should not serve as a mere measure to evaluate the pathogenic character of SIL1 missense variants.

To address cellular SIL1 immunoreactivity and distribution as a further measure to evaluate pathogenicity of SIL1 amino acid substitutions and deletions immunofluorescence studies have been carried out and -in comparison to the Hek293 cells over expressing the SIL1 wildtype protein—altered immunoreactivity could be observed for p.G312R and p.L457P and to a minor degree for p.V231_I232del overexpressing cells but not for cells overexpressing p.R92W or p.K132Q variants of SIL1. As a pathomorphological immunoreactivity-pattern has already been demonstrated for p.L457P mutant SIL1 in COS7 cells (14), the recapitulation in Hek293 cells confirms the suitability of these cells to investigate pathogenicity of *SIL1* mutations. Moreover, a similar pattern of immunoreactivity has been shown *in vitro* upon overexpression of a pathogenic form of *SIL1* caused by a deletion of thymidine at base-pair position 1366 of the corresponding gene (17). Consequently, our immunofluorescence findings confirm the pathogenicity of p.G312R mutant SIL1. One might speculate that the small focal accumulations of the p.V231_I232del mutant form of SIL1 represent early stages of degradation of the mutant protein, an assumption that is in line with the detection of degradation bands upon short-term overexpression (**Figure 2B**) and the absence of the protein upon long-term overexpression (**Figure 2A**). As immunofluorescence studies of p.R29W did not reveal pathological changes compared to the cells overexpressing the wildtype or the p.K132Q variant form of SIL1, the combined results support the notion that p.R92W is a polymorphic variant rather than a pathogenic mutation and also indicate that the pattern of SIL1 immunoreactivity might serve as another cellular biomarker or read-out measure allowing the evaluation of pathogenicity of SIL1 amino acid substitutions.

The altered distribution and aggregation of p.G312R and p.L457P mutant forms of SIL1 prompted us to focus on subcellular ultrastructural alterations suggestive for protein aggregation and proteolysis. Indeed, electron microscopic studies revealed the presence of vacuoles in Hek293 cells overexpressing these two pathogenic missense variants of SIL1. One might assume that these vacuoles result from impaired ER-function and thus protein processing resulting in accumulation of osmophilic material which could also be observed in the cytoplasm (not localized within vacuoles; white arrows in **Figure 4B**). As the p.V231_I232del pathogenic mutation is instable, protein aggregates and vacuoles identified by electron microscopy might correlate to the degradation of the mutant SIL1 protein. Importantly, build-up of electron-dense aggregates and altered ER morphology have also been described in immortalized lymphoblastoid cells from patients [including heterozygosity for p.V231_I232del and p.G312R, (6, 13)] as well as in Hek293 cells with depleted SIL1 expression (16) but also in MSS-patient derived fibroblasts (25). This in turn confirms the suitability of our generated *in vitro* overexpression models to evaluate the pathogenicity of SIL1 mutations on the ultra-structural level. However, results of our immunoblot-studies focussing on ER-stress and activation of proteolysis suggested a more profound ER-vulnerability and proteolytic activation in Hek293 cells overexpressing the p.L457P-mutant form of SIL1 and furthermore again suggest that the p.R92W is in fact a polymorphic missense variant of SIL1. Based on the relatively low effect of the overexpression of p.G312R (showing a detrimental effect on oxidative homeostasis; see above) on ER-homeostasis

and proteolysis compared to overexpression of p.L457P, the necessity of parallel investigations of different read-out measures to draw a meaningful conclusion regarding the pathogenicity of *SIL1* variants is indicated.

SIL1-interactome has been addressed as a potential further measure to evaluate the pathogenicity of amino acid changes in SIL1 and results showed that all variants of the SIL1-protein investigated in this study bind to BiP, Mortalin and the small subunit of Calpain-1. In this context it is important to note that an ER localization of Mortalin which shows a high homology to BiP has already been described (26). Given that Calpain-1 acts as a non-lysosomal thiol-protease catalyzing proteolytic cleavage of substrate proteins, its binding to all five variants of SIL1 as well as to WT-SIL1 might result from protein overexpression and serves toward the elimination of excessive level, an assumption supported by our previous findings in Hek293 cells with WT-SIL1 overexpression (12). As BiP represents a well-known binding partner of SIL1 but also acts as a major chaperone in the UPR facilitating the re-folding of misshaped proteins, it is difficult to evaluate whether the interaction of BiP with the different variants of SIL1 is physiological or a result of an attempt to warrant a native folding of the protein in case of the binding to the pathogenic forms of SIL1. Notably, localization of p.V231_I232del- and p.G312R-amino acid changes in the BiP-binding domain of SIL1 (**Figure 1A**) are suggestive for a binding of BiP to these SIL1-forms (or degradation products) toward re-folding and antagonization of build-up of (toxic) protein aggregates. This hypothesis is further supported by the fact that DNAJB11/ERj3 serves as another BiP co-chaperone (stimulating ATPase activity) by direct binding to both unfolded ERAD-substrates and nascent unfolded peptides, but dissociates from the BiP-unfolded protein complex before folding is completed (27) and our molecular observation of ERj3 binding to p.G312R and p.L457P mutant SIL1 but not to WT-SIL1, and the p.R92W and p.K132Q variants. Thus, it seems plausible that the functional ERj3-BiP complex is recruited to the pathogenic missense variants based on pathophysiological circumstances. On a general note, this finding moreover suggests that ERj3 binding to SIL1 or rather the SIL1-BiP complex might serve as a molecular measure/ biomarker to evaluate the pathogenicity of stable SIL1 missense variants. However, results of our immunoblot studies of ER-stress related proteins did not show elevated ERj3 level in Hek293 cells overexpressing p.G312R and p.L457P mutant SIL1 compared cells overexpressing the wildtype SIL1 protein (**Figure 4C**) indicating that cellular available ERj3 pools are re-located to the two pathogenic mutant forms of SIL1. Mass spectrometry-based analysis of SIL1-interacotme moreover revealed that the wildtype protein as well as the p.R92W and p.K132Q variants bind to POC1A. Interestingly, immunoprecipitation of the p.G312R and p.L457P forms of SIL1 along with their interactors did not result in the identification of the binding to POC1A. This finding defines the interaction of POC1A with SIL1 variants as further read-out measure to evaluate the pathogenicity of amino acid substitutions and deletions in *SIL1* and by the same token underlines our previous findings suggesting that the p.R92W variant form of SIL1 is in fact a polymorphic variant rather than a pathogenic mutant of the BiP co-chaperone. On a more general note, our immunoprecipitation data support the previous description of an interaction of POC1A with the SIL1-BiP machinery as identified by BioPlex 2.0 [Biophysical Interactions of ORFEOME-derived complexes; (28)].

TABLE 2 | Overview of cellular markers and respective analytical approaches toward evaluation of pathogenicity of SIL1-mutants.

Test	Cellular marker of pathogenicity
Native and reducing PAGE with subsequent Western-Blot of SIL1 protein	Higher and lower molecular weight bands as signs of protein aggregates (in native PAGE) and degradation products
WST-1 viability assay	Reduced viability
Immunofluorescence of SIL1-protein	Non-reticular pattern of immunoreactivity
Electron microscopy	Abnormal mitochondria, vacuoles & protein aggregates, dispersed Golgi, disintegrated centrosomes
SIL1-interactome	Loss of interaction with POC1A and binding to DNAJB11/ ERj3
Immunoblot analysis of cellular stress markers	Oxidative- and/ or ER-stress burden
SIL1-SIL1 homomerization	Occurrence of degradation products of pathogenic mutant SIL1-protein which do not present rapid degradation

Prompted by the fact POC1A mutations are causative for a phenotype defined by short stature, onychodysplasia, facial dysmorphism, and hypotrichosis (SOFT syndrome; 22) and short stature is also a recurrent clinical finding in MSS patients, effect of SIL1 expression (wildtype and variant forms) has been studied and highlighted an increasing effect of elevated SIL1 protein level on POC1A protein abundance (**Figure 5B**). Same effect could be observed for p.R92W and p.K132Q but not p.G312R, p.L457P or p.V231_I232del mutant forms of SIL1. This effect indicates that the molecular interaction between the two proteins might also be of relevance for the clinical manifestation of MSS upon loss of (functional) SIL1. Given that POC1A links centrosomes to Golgi assembly and function we further studied level of FAM134B, a newly identified cis-Golgi protein with a pivotal role in neuronal function and survival (24) in relation to the expression of SIL1 wildtype protein. Here same results as for POC1 could be obtained (**Figure 5B**) suggesting an impact of SIL1 expression on the Golgi apparatus, an assumption which accords with the newly identified SIL1-POC1A interaction and the results of our further immunofluorescence studies not only showing a co-localization of SIL1 with POC1A and FAM134B but also with golgin-97, a known Golgi-marker protein (**Figure 5C**). Results of these immunofluorescence-based localization studies in combination with our immunoprecipitation findings also suggest that SIL1 localizes (although to a minor degree) to subcellular compartments beyond the ER. However, to follow the hypothesis that pathogenic SIL1 variant significantly impact on function and structure of centrosome and the Golgi apparatus, ultra-structural studies focussing on their integrity have been carried out and revealed proliferated and

dispersed Golgi cisternae as well as centriole-multiplications and -proliferations in Hek293 cells overexpressing the known pathogenic forms of SIL1 but not in cells overexpressing the wildtype or the p.R92W or p.K132Q forms of the protein (**Figures 5D,E**). These pathomorphological findings in turn further support the concept of an impact of SIL1 on Golgi and centrosome function and integrity and by the same token define changes in Golgi and centrosome structures as further read-out measures enabling the evaluation of the pathogenicity of *SIL1* mutations. In this context, it is important to note that depletion of SIL1 expression in Hek293 cells could be linked to vulnerability of the Golgi apparatus on both the structural and the biochemical level (16).

CONCLUSIONS

Generation and subsequent functional, biochemical and morphological phenotyping of our *in vitro* models overexpressing different (benign and pathogenic) forms of the SIL1 protein allowed to define cellular markers to evaluate the pathogenicity of SIL1-mutations, an aspect of significant importance for genetic counseling and genotype-phenotype correlations. Suitable assays and respective read-out measures (in terms of cellular biomarkers for pathogenicity of changes in SIL1 amino acid composition) are summarized in **Table 2**.

AUTHOR CONTRIBUTIONS

AR and JW conceptualized and designed the study, corrected the manuscript and supervised the experimental work. SB generated the different expression constructs used in this study. TL assisted CG in the generation of the stable-inducible cell Hek293 cell lines. DH performed the mass spectrometric analysis of the SIL1-interactome. AT performed the *in silico*-based analysis of pathogenicity of selected variants. UM performed the immunofluorescence-based co-localization studies of SIL1. CG performed all other experiments and drafted the first version of the manuscript. RH and BM gave expert opinion regarding the mitochondrial findings.

FUNDING

This work was supported by a grant from the French Muscular Dystrophy Association (AFM-Téléthon; #21644; grant to AR). Financial support was moreover obtained from the Ministerium für Kultur und Wissenschaft des Landes Nordrhein-Westfalen and the Bundesministerium für Bildung und Forschung (031A360E) as well as from the Senatsverwaltung für Wirtschaft, Technologie und Forschung des Landes Berlin.

REFERENCES

1. Georgy BA, Snow RD, Brogdon BG, Wertelecki W. Neuroradiologic findings in Marinesco-Sjogren syndrome. *AJNR Am J Neuroradiol.* (1998) 19:281–3.
2. Senderek J, Krieger M, Stendel C, Bergmann C, Moser M, Breitbach-Faller N, et al. Mutations in SIL1 cause Marinesco-Sjogren syndrome, a cerebellar ataxia with cataract and myopathy. *Nat Genet.* (2005) 37:1312–4. doi: 10.1038/ng1678
3. Zhao L, Longo-Guess C, Harris BS, Lee JW, Ackerman SL. Protein accumulation and neurodegeneration in the woozy mutant mouse is caused by disruption of SIL1, a cochaperone of BiP. *Nat Genet.* (2005) 37:974–9. doi: 10.1038/ng1620
4. Dudek J, Benedix J, Cappel S, Greiner M, Jalal C, Muller L, et al. Functions and pathologies of BiP and its interaction partners. *Cell Mol Life Sci.* (2009) 66:1556–69. doi: 10.1007/s00018-009-8745-y
5. Yan M, Li J, Sha B. Structural analysis of the Sil1-Bip complex reveals the mechanism for SIL1 to function as a nucleotide-exchange factor. *Biochem J.* (2011) 438:447–55. doi: 10.1042/BJ20110500
6. Krieger M, Roos A, Stendel C, Claeys KG, Sonmez FM, Baudis M, et al. SIL1 mutations and clinical spectrum in patients with Marinesco-Sjogren syndrome. *Brain.* (2013) 136:3634–44. doi: 10.1093/brain/awt283
7. Nair P, Hamzeh AR, Mohamed M, Tawfiq N, Al-Ali MT, Bastaki F. Marinesco-Sjogren syndrome in an emirati child with a novel mutation in SIL1 affecting the 5' untranslated region. *Med Princ Pract.* (2016) 25:580–2. doi: 10.1159/000449225
8. Gai N, Jiang C, Zou YY, Zheng Y, Liang DS, Wu LQ. Novel SIL1 nonstop mutation in a Chinese consanguineous family with Marinesco-Sjogren syndrome and Dandy-Walker syndrome. *Clin Chim Acta.* (2016) 458:1–4. doi: 10.1016/j.cca.2016.04.018
9. Byrne S, Dlamini N, Lumsden D, Pitt M, Zaharieva I, Muntoni F, et al. SIL1-related Marinesco-Sjoegren syndrome (MSS) with associated motor neuronopathy and bradykinetic movement disorder. *Neuromuscul Disord.* (2015) 25:585–8. doi: 10.1016/j.nmd.2015.04.003
10. Noreau A, La Piana R, Marcoux C, Canada F, Dion PA, Brais B, et al. Novel SIL1 mutations cause cerebellar ataxia and atrophy in a French-Canadian family. *Neurogenetics.* (2015) 16:315–8. doi: 10.1007/s10048-015-0455-z
11. Riazuddin SA, Amiri-Kordestani L, Kaul H, Butt T, Jiao X, Riazuddin S, et al. Novel SIL1 mutations in consanguineous Pakistani families mapping to chromosomes 5q31. *Mol Vis.* (2009) 15:1050–6.
12. Labisch T, Buchkremer S, Phan V, Kollipara L, Gatz C, Lentz C, et al. Tracking effects of SIL1 increase: taking a closer look beyond the consequences of elevated expression level. *Mol Neurobiol.* (2018) 55:2524–46. doi: 10.1007/s12035-017-0494-6
13. Kollipara L, Buchkremer S, Coraspe JAG, Hathazi D, Senderek J, Weis J, et al. (2017). In-depth phenotyping of lymphoblastoid cells suggests selective cellular vulnerability in Marinesco-Sjogren syndrome. *Oncotarget.* 8, 68493–68516. doi: 10.18632/oncotarget.19663
14. Anttonen AK, Siintola E, Tranebjaerg L, Iwata NK, Bijlsma EK, Meguro H, et al. Novel SIL1 mutations and exclusion of functional candidate genes in Marinesco-Sjogren syndrome. *Eur J Hum Genet.* (2008) 16:961–9. doi: 10.1038/ejhg.2008.22
15. Puig O, Caspary F, Rigaut G, Rutz B, Bouveret E, Bragado-Nilsson E, et al. The tandem affinity purification (TAP) method: a general procedure of protein complex purification. *Methods.* (2001) 24:218–29. doi: 10.1006/meth.2001.1183
16. Roos A, Kollipara L, Buchkremer S, Labisch T, Brauers E, Gatz C, et al. Cellular signature of SIL1 depletion: disease pathogenesis due to alterations in protein composition beyond the ER machinery. *Mol Neurobiol.* (2016) 53:5527–41. doi: 10.1007/s12035-015-9456-z
17. Howes J, Shimizu Y, Feige MJ, Hendershot LM. C-terminal mutations destabilize SIL1/BAP and can cause Marinesco-Sjogren syndrome. *J Biol Chem.* (2012) 287:8552–60. doi: 10.1074/jbc.M111.333286
18. Sewry CA, Voit T, Dubowitz V. Myopathy with unique ultrastructural feature in Marinesco-Sjogren syndrome. *Ann Neurol.* (1988) 24:576–80. doi: 10.1002/ana.410240416
19. Roos A, Buchkremer S, Kollipara L, Labisch T, Gatz C, Zitzelsberger M, et al. Myopathy in Marinesco-Sjogren syndrome links endoplasmic reticulum

chaperone dysfunction to nuclear envelope pathology. *Acta Neuropathol.* (2014) 127:761–77. doi: 10.1007/s00401-013-1224-4
20. Buchkremer S, Gonzalez Coraspe JA, Weis J, Roos A. Sil1-mutant mice elucidate chaperone function in neurological disorders. *J Neuromuscul Dis.* (2016) 3:169–81. doi: 10.3233/JND-160152
21. Mijaljica D, Prescott M, Devenish RJ. Mitophagy and mitoptosis in disease processes. *Methods Mol Biol.* (2010) 648:93–106. doi: 10.1007/978-1-60761-756-3_6
22. Sarig O, Nahum S, Rapaport D, Ishida-Yamamoto A, Fuchs-Telem D, Qiaoli L, et al. Short stature, onychodysplasia, facial dysmorphism, and hypotrichosis syndrome is caused by a POC1A mutation. *Am J Hum Genet.* (2012) 91:337–42. doi: 10.1016/j.ajhg.2012.06.003
23. Shaheen R, Faqeih E, Shamseldin HE, Noche RR, Sunker A, Alshammari MJ, et al. POC1A truncation mutation causes a ciliopathy in humans characterized by primordial dwarfism. *Am J Hum Genet.* (2012) 91:330–6. doi: 10.1016/j.ajhg.2012.05.025
24. Kurth I, Pamminger T, Hennings JC, Soehendra D, Huebner AK, Rotthier A, et al. Mutations in FAM134B, encoding a newly identified Golgi protein, cause severe sensory and autonomic neuropathy. *Nat Genet.* (2009) 41:1179–81. doi: 10.1038/ng.464
25. Ezgu F, Krejci P, Li S, De Sousa C, Graham JM Jr, Hansmann I, et al. Phenotype-genotype correlations in patients with Marinesco-Sjogren syndrome. *Clin Genet.* (2014) 86:74–84. doi: 10.1111/cge.12230
26. Ran Q, Wadhwa R, Kawai R, Kaul SC, Sifers RN, Bick RJ, et al. Extramitochondrial localization of mortalin/mthsp70/PBP74/GRP75. *Biochem Biophys Res Commun.* (2000) 275:174–9. doi: 10.1006/bbrc.2000.3237
27. Shen Y, Hendershot LM. ERdj3, a stress-inducible endoplasmic reticulum DnaJ homologue, serves as a cofactor for BiP's interactions with unfolded substrates. *Mol Biol Cell.* (2005) 16:40–50. doi: 10.1091/mbc.e04-05-0434
28. Huttlin EL, Bruckner RJ, Paulo JA, Cannon JR, Ting L, Baltier K, et al. Architecture of the human interactome defines protein communities and disease networks. *Nature.* (2017) 545:505–9. doi: 10.1038/nature 22366

Conflict of Interest Statement: The authors declare that the research was conducted in the absence of any commercial or financial relationships that could be construed as a potential conflict of interest.

Copyright © 2019 Gatz, Hathazi, Münchberg, Buchkremer, Labisch, Munro, Horvath, Töpf, Weis and Roos. This is an open-access article distributed under the terms of the Creative Commons Attribution License (CC BY). The use, distribution or reproduction in other forums is permitted, provided the original author(s) and the copyright owner(s) are credited and that the original publication in this journal is cited, in accordance with accepted academic practice. No use, distribution or reproduction is permitted which does not comply with these terms.

frontiers in Immunology

ORIGINAL RESEARCH
published: 14 June 2019
doi: 10.3389/fimmu.2019.01343

Lymphocyte Count and Body Mass Index as Biomarkers of Early Treatment Response in a Multiple Sclerosis Dimethyl Fumarate-Treated Cohort

*Alessia Manni[1], Antonio Iaffaldano[1], Giuseppe Lucisano[1,2], Mariangela D'Onghia[3], Domenico Maria Mezzapesa[1], Vincenzo Felica[1], Pietro Iaffaldano[1], Maria Trojano[1] and Damiano Paolicelli[1]**

[1] Department of Basic Medical Sciences, Neurosciences and Sense Organs, University of Bari "Aldo Moro", Bari, Italy, [2] Center for Outcomes Research and Clinical Epidemiology, Pescara, Italy, [3] Operative Unit of Neurology, "Dimiccoli" General Hospital, Barletta, Italy

OPEN ACCESS

Edited by:
Marcello Moccia,
University College London,
United Kingdom

Reviewed by:
Rosa Cortese,
University College London,
United Kingdom
Martin Diebold,
University Hospital of
Basel, Switzerland

***Correspondence:**
Damiano Paolicelli
damiano.paolicelli@uniba.it

Specialty section:
This article was submitted to
Multiple Sclerosis and
Neuroimmunology,
a section of the journal
Frontiers in Immunology

Received: 08 January 2019
Accepted: 28 May 2019
Published: 14 June 2019

Citation:
Manni A, Iaffaldano A, Lucisano G, D'Onghia M, Mezzapesa DM, Felica V, Iaffaldano P, Trojano M and Paolicelli D (2019) Lymphocyte Count and Body Mass Index as Biomarkers of Early Treatment Response in a Multiple Sclerosis Dimethyl Fumarate-Treated Cohort. Front. Immunol. 10:1343. doi: 10.3389/fimmu.2019.01343

Introduction: In relapsing Multiple Sclerosis (RMS) patients treated with disease modifying drugs (DMDs), few data are available regarding the biomarkers of treatment response. We aimed to assess the predictive value of lymphocyte count (LC) and Body Mass Index (BMI) for treatment response in a real life setting of dimethyl fumarate (DMF) treated patients.

Materials and Methods: We included in our observational analysis 338 patients who were prescribed DMF in an Italian MS Center. We collected clinical and demographic data at the beginning of DMF (T0), and assessed White Blood Cells (WBC) and LC at T0 and at 3 (T3), 6 (T6), 9 (T9), and 12 (T12) months. Gadolinium enhancing (Gd+), new T2 lesions and relapses within the first year of treatment (T12) were recorded in order to evaluate clinical activity at 12 months. Analysis of correlation was performed to correlate WBC, LC and BMI with clinical and radiological responses. We evaluated whether BMI or LC can predict treatment response by using multivariate logistic regression models at each follow-up.

Results: Our cohort was followed up for a mean period of 19.8 ± 6.8 months. The mean BMI at baseline was 24.19 ± 4.48. The multivariate models gave as predictive factors for Gd+ lesions at T12, LC at T3 (OR = 1.003, 95% CI = 1.00-1.07; $p = 0.046$) and baseline BMI (OR = 0.71, 95% CI = 0.52–0.98; $p = 0.037$). Predictive factors for new T2 lesions at T12 were LC at T3 (OR = 1.01 95%CI = 1.00–1.95; $p = 0.005$) and baseline BMI (OR = 0.99, 95% CI = 0.98–1.00; $p = 0.026$).

Conclusions: In our real life-experience, BMI and LC may be early biomarkers to predict treatment response during DMF.

Keywords: dimethyl fumarate, lymphocyte count, body mass index, biomarkers, treatment response

INTRODUCTION

Multiple Sclerosis (MS) is a chronic immune-mediated disease of the central nervous system mainly affecting young adults (1). The development of disease modifying drugs (DMDs) has made an important contribution to MS treatment, allowing a reduction in the frequency of relapses and delaying disease progression. In recent decades there has been a constant increase in the availability of DMDs with different mechanisms of action, routes of administration and safety profiles. Interferon-β (IFN-β) and glatiramer acetate (GA) are well-established MS therapies which have well-characterized safety profiles and have shown a reduction of relapse rate by approximately one third. However, these DMDs are administered through weekly or daily injections and patients may experience breakthrough disease activity and tolerability may be suboptimal (2, 3). These drawbacks have prompted the search for drugs that could reduce the burden of medication administration and be somehow more efficacious. All newer DMDs have the aim of regulating or suppressing the immune system through specific pathways, and in many cases this has resulted in foreseeable adverse effects (lymphopenia).

Dimethyl fumarate (DMF) is a DMD that was approved for the treatment of relapsing–remitting MS (RRMS) in 2013 in the USA and in 2014 in the European Union. Two Phase III studies and their ongoing long-term extensions have proved that DMF reduces Annualized Relapse Rate (ARR) by ∼50% and also reduces the number of new or enlarging T2 hyperintense lesions, new T1 hypointense lesions, and gadolinium-enhancing (Gd+) lesions (4–6). Although its exact mechanism of action has not been fully explained, DMF has proven capable of reducing white blood cell (WBC) counts and absolute lymphocyte counts (LC) by ∼30% from the baseline within the first year of treatment (7). Of the patients treated for at least 6 months, 2.2% experienced LC <500 mm^3 [grade 3 lymphopenia, according to Common Terminology Criteria for Adverse Events –CTCAE- vs. 4.0 (8)] persisting for at least 6 months (5). However, the clinical implications of DMF-induced leukopenia and lymphopenia on treatment response are not yet fully understood. Nevertheless, the need for a careful surveillance is strong given the cases of progressive multifocal leukoencephalopathy (PML) occurring in DMF treated patients with sustained lymphopenia (grade 3 lymphopenia for >6 months) (9).

In addition to acting via the immunomodulation of various cells, DMF also appears to act through neuroprotection since it induces the nuclear factor erythroid 2–related factor 2 (Nrf2) pathway (10). It has been demonstrated that Nrf2 activity is lessened in diabetes and that body weight could modify its activity (11). In recent years, several studies have investigated the role of the Body Mass Index (BMI) in the pathogenesis of autoimmune diseases, such as MS. It has been shown that obesity may worsen the disease course in several autoimmune diseases (12) and studies have reported a positive association between BMI and disability among MS patients (13). Although this evidence supports the role of obesity as a risk factor for MS and its progression, the potential effects of BMI on treatment response have not yet been fully understood. Our work attempted to assess the predictive value of LC and BMI for treatment response in a real-life cohort of DMF-treated relapsing Multiple Sclerosis (RMS) patients. For this purpose, we evaluated the temporal profile of WBC and LC during the first year of treatment and also correlated clinical and Magnetic Resonance Imaging (MRI) (T1 Gd+ lesions, new or enlarging T2 lesions) variables with BMI and with WBC and LC variation in order to identify potential biomarkers of treatment response.

METHODS

Study Design, Study Population, and Follow-Up

This is an observational, retrospectively acquired cohort study, approved by the Local Ethics Committee. At the beginning of DMF all patients provided their written informed consent to authorize the use of their clinical and MRI data. A total number of 456 patients started DMF-treatment at the Center for Multiple Sclerosis of the University of Bari between 2014 and 2016; we studied a cohort of 338 patients with RMS according to McDonald and Polman criteria (14, 15), who had reached at least 1-year follow up (**Figure 1**). Three patients (0.5%) had an unscheduled MRI before the sixth month of treatment (mean time of MRI acquisition $= 2.8 \pm 0.2$ months), showing, according to their treating physician, a high MRI disease activity compared with the baseline MRI; therefore they interrupted the treatment before reaching the sixth month follow up, underwent a high-dose intravenous glucocorticoids, and were then switched to second line DMDs. Five patients (1.1%) experienced a disabling relapse within the third month of treatment and were therefore treated with high dose steroids. Three of these patients were also treated with plasma exchange. All five interrupted DMF treatment. These eight patients were not included in the study cohort.

At the beginning of the treatment (baseline), the following demographic, clinical and MRI data were collected from all patients using the electronic iMed database: age and gender, weight, height, BMI, disease duration, number of relapses, previous DMDs, presence/absence of new/enlarging T2 lesions, and presence/absence of Gd+ lesions. To avoid the slight weight gain (16), possibly caused by a steroid cycle, patients weight and BMI were recorded at least 30 days after the last day of steroids intake. Patients were assessed for neurological disability using the Expanded Disability Status Scale (EDSS) (17) at baseline and at 3-month intervals, and an additional neurological assessment was performed in the event of a relapse. Relapses were defined as episodes of neurological symptoms occurring at least 30 days after the onset of any previous episode, lasting at least 24 h, not attributable to any other causes, occurring in the absence of an infection or fever, and accompanied either by new clinical signs, i.e., changes in the neurological examination, or by an increased EDSS score (1). Peripheral blood (PB) samples were collected in order to monitor WBC and LC at baseline (T0), and then at 3-month intervals. To avoid any possible confounders due to the effect of steroid treatment in the case of relapses/MRI activity, PB samples were collected at least 30 days after the last day of corticosteroids intake. WBC count and LC were evaluated using

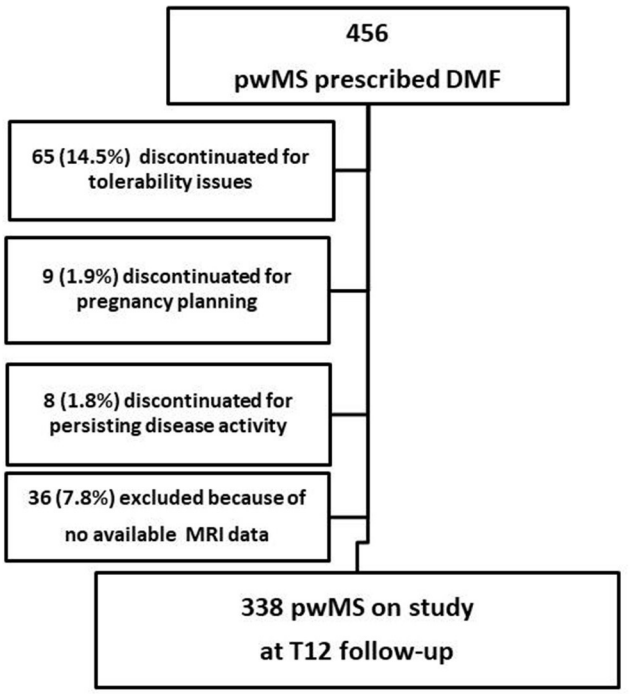


FIGURE 1 | Flow diagram of the study. pwMS, people with Multiple Sclerosis; DMF, dimethyl fumarate; MRI, Magnetic Resonance Imaging; T12, 1 year follow-up.

the quality reference of the same laboratory at the Center for Multiple Sclerosis of the University of Bari.

MRI scans were performed on a 1.5 T Achieva scanner (Philips Healthcare, Best, Netherlands) and 8-channel head coil. Dual-echo sequences (to obtain T2 weighted images; TR 2,800 ms, TE 21/120 ms, flip angle: 90°) and fluid attenuated inversion recovery (FLAIR; TR/TE/TI, 8,900/190/2,500 ms, flip angle: 90°) were acquired in axial orientation (50 slices, 3-mm thick, 1-mm gap, FOV 256 x 256, matrix 400 x 400). Before and after gadolinium administration, T1 weighted images (TR /TE 1,000/12.5 ms, flip angle: 69°) were acquired in axial orientation (22 slices, 5-mm thick, 1-mm gap, FOV 230 × 230, matrix 320 × 320). Spinal cord MRI protocol included T2-weighted (TR/TE 3,500/120 ms) and T1-weighted (before and after gadolinium administration; TR/TE 400/7.5 ms), acquired in sagittal orientation (13 slices, 3.5-mm thick, 0.35-mm gap, FOV 522 × 522, matrix 1,024 × 1,024). Baseline MRI scans were performed no more than 6 months before the start of DMF treatment (mean time of MRI acquisition = 3.8 ± 1.4 months), and then at 6-month intervals (±30 days). MRI outcomes were defined as follows: presence/absence of new/enlarging T2 lesions; presence/absence of Gd+ lesions. Trained neuro-radiologists performed the lesion count by visual analysis of two successive MRI images.

Clinical Variables

The quantitative variation in WBC and LC, considered both in terms of absolute value and of the "delta" (Δ = the difference between the absolute values of WBC and LC between two consecutive time-points), were analyzed. The baseline (T0) was compared with four different periods of treatment: T3 (3rd month ± 30 days), T6 (6th month ± 30 days), T9 (9th month ± 30 days), and T12 (12th month ± 30 days). Moreover, in order to investigate the impact of the DMF-induced lymphopenia (DIL) on the risk of clinical and MRI activity, the median of the absolute LC was calculated at each observation time, and patients were divided into two groups: those with a high DIL (DIHL, above the median) and those with a low DIL (DILL, below the median). We used this statistical (not clinical) classification to divide the study population into two equal-sized groups (50% of the LC distribution for each group).

Outcomes

- Presence/absence of new T2 lesions at the T12 MRI follow-up;
- Presence/absence of Gd+ lesions at the T12 MRI follow-up;
- Presence/absence of relapses within the first year of DMF treatment;
- Variation in WBC and LC over time.

Statistical Analysis

Baseline characteristics were reported for continuous variables as mean ± standard deviation (SD) and for categorical variables as percentages. Characteristics were compared in subjects with and without an event (presence/absence of Gd+ lesions, presence/absence of new T2 lesions, presence/absence of relapses) using the *T*-test for continuous variables and the chi-squared test for categorical variables. For the comparison over time, we used the Wilcoxon matched pair test, and analysis of Pearson correlation was performed to correlate WBC and BMI.

We used multivariate analysis testing the following covariates: sex, age at the start of DMF, presence/absence of T2 lesions at the baseline MRI, presence/absence of Gd+ lesions at the baseline MRI, presence/absence of relapses in the year before starting DMF, previous DMD exposure (naïve patients vs. patients treated with a first-line DMD vs. those treated with a second-line DMD), variation in WBC from T0 to T3, LC at T3, baseline BMI, DIHL at T3 and at T6. Multivariate logistic regression models always considered as covariates the baseline clinical and demographic characteristics of the cohort, and those covariates significant at the univariate analysis, and were used to evaluate whether BMI or LC can predict the outcome. We used a multivariate logistic regression approach for each follow-up because there were no exact dates for follow-up evaluation. Results were expressed as odds ratio (OR) and 95% confidence intervals (95% CI). A 2-sided $p<0.05$ was considered significant. All analyses were performed using the SPSS version 19.0 (SPSS Inc., Chicago, Illinois).

RESULTS

The mean ± standard deviation (SD) follow-up of our cohort was 19.8 ± 6.8 months. The baseline demographic and clinical characteristics of the study population are shown in **Table 1**. Our cohort consisted of 197 (58.3%) female patients and 141 (41.8%) male patients. The mean age at DMF initiation was

TABLE 1 | Baseline demographic, anthropometric, and clinical characteristics of the study population.

Number of patients	**338**
Sex: n (F/M)	197/141
Age at DMF beginning (years, mean± SD)	38 ± 10.7
Disease duration (years, mean± SD)	12.5±7.3
EDSS at DMF initiation (mean± SD)	3.0 ± 1.5
Patients with comorbidities (%)	118 (34.9%)
BMI at DMF beginning (kg/m^2, mean± SD)	24.19 ± 4.48
LC (cells/mm^3 mean± SD)	1,940 ± 667.60
WBC (cells/mm^3 mean± SD)	6380.8 ± 2051.93
Previous DMDs	
-Naïve: *n* (%)	50 (14.8%)
-Only first line treatments: *n* (%)	257 (76%)
-First and second line treatments; *n* (%)	31 (9.2%)

DMF, Dimethyl fumarate; SD, standard deviation; EDSS, Expanded Disability Status Scale; BMI, Body Mass Index; LC, lymphocyte count; WBC, white blood cells; DMDs, Disease modifying drugs.

38 ± 10.7 years, and the mean disease duration was 12.5 ± 7.3 years. The mean EDSS at DMF initiation was 3.0 ± 1.5 and the ARR in the previous year was 0.5. The mean BMI at baseline was 24.19 ± 4.48. Fifty patients were treatment-naïve (14.8%), while 257 switched to DMF from a first-line DMD, and 31 from second-line treatments. The latter 31 patients (2 with Mitoxantrone, 2 with Azathioprine, 21 patients with Fingolimod and 4 patients with Natalizumab), because of a possible overlap of immunosuppressive effects, observed a washout period sufficient to restore immune function and bring LC and WBC back within normal ranges. For patients switching from a first-line DMD, a wash-out period of at least 4 weeks was observed (longer if specifically reported by Summary of Product Characteristics or in accordance with treating-physicians' decisions).

Temporal Profile of WBC and LC

Figure 2 shows WBC and LC values at the beginning of DMF and at 3-month intervals during the first year of treatment. We compared the LC and WBC between T0 and T3, and we observed a reduction of 15.4% in LC (from 1,940 ± 667.60 to 1642.18 ± 184.75; $p < 0.0001$) and a reduction of 5.9% in WBC (from 6380.80 ± 2051.93 to 6010.29 ± 1601.30; $p = 0.124$). In T0–T6, a reduction of 33.2% was observed in LC (from 1,940 ± 667.60 to 1296.06 ± 584.03; $p < 0.001$) and a reduction of 14.9% in WBC (from 6380.80 ± 2051.93 to 5,436 ± 1585.63; $p < 0.001$). In T0–T9, a reduction of 39.1% was observed in LC (from 1,940 ± 667.60 to 1181.86 ± 480.80; $p < 0.001$), and a reduction of 19.9% in WBC (from 6380.80 ± 2051.93 to 5119.28 ± 1252.66; $p < 0.001$). Finally, in T0–T12, a reduction of 37.14% was observed in LC (from 1,940 ± 667.60 to 1213.01 ± 577.6; $p < 0.001$) and a reduction of 15.7% in WBC (from 6380.80 ± 2051.93 to 5383.33 ± 1313.82; $p < 0.001$). From T3, 29 patients presented GRADE I CTCAE lymphopenia (<LLN-800 u/mm^3), and 24 presented GRADE II lymphopenia (<800–500 u/mm^3). The nadir of reduction was observed at T9, both for WBC ($p <$ 0.0001) and LC ($p < 0.0001$), with a reduction, respectively, of 19.8 and 39.1% from T0.

Correlation Between WBC and LC Variation and Disease Activity

During the first year of treatment, in our cohort, the ARR was significantly lower than ARR as recorded in our clinical database for the previous year (0.25 vs. 0.51, $p = 0.001$). We evaluated the correlation between WBC and LC variation and outcomes of disease activity during DMF-treatment (**Table 2**).

In the univariate analysis, patients who experienced relapses within the first year of treatment had a higher WBC count at T3 (6,031 ± 1,687/μl vs. 5,660 ± 1,110/μl, $p = 0.05$) as well as a lower variation in WBC between T0 and T3 (−59.53 ± 1006.33 vs. 167.79 ± 1660.78, $p = 0.05$) than patients who experienced no relapse (**Table 2**). However, multivariate analysis confirmed the reduction in WBC as a predictive factor for relapses occurring during the entire first year of treatment (OR = 1.054, 95% CI = 1.03–2.65; $p = 0.043$, **Table 3**).

We observed no differences in the absolute value or the delta of WBC between patients presenting new Gd+/T2 lesions and patients who did not. On the other hand, LC was higher at T3 in patients who experienced new Gd+ lesions at T6 (1,845 ± 455 vs. 1,486 ± 556, $p = 0.043$), in patients who experienced new T2 lesions at T12 (1,952 ± 317 vs. 1,495 ± 592; $p = 0.040$), and in patients experiencing a relapse during the first year of treatment (1,761 ± 465 vs. 1,386 ± 402; $p = 0.033$) (**Table 2**). Multivariate analysis showed that LC at T3 was a predictive factor for Gd+ lesions at T12 (OR = 1.003, 95% CI = 1.00–1.07; $p = 0.046$) (**Table 3**) and new T2 lesions at T12 (OR = 1.01; 95% CI = 1.00–1.95; $p = 0.005$) (**Table 3**).

In order to investigate the impact of the lymphocytes on the risk of relapses and on worsening MRI, the median values of LC at T3, T6 and T9 were calculated, and the population was divided into two groups:

- Patients with LC below the median calculated (with low number of DMF-induced lymphocytes -DILL-),
- Patients with LC above the median calculated (with high number of DMF-induced lymphocytes -DIHL-).

In the univariate analysis, during the first and second semesters of treatment, no differences were found between the clinical activity of patients with DIHL and patients with DILL (**Table 2**). However, considering MRI activity at T12, patients with DIHL at T3 (OR = 1.31, 95% CI = 1.12–5.34, $p = 0.043$) and at T6 (OR = 1.14, 95% CI = 1.13–6.33; $p = 0.05$) had a higher risk of Gd+ lesions (**Table 3**). Patients with DIHL at T3 (OR = 1.26, 95% CI = 1.07–1.96; $p = 0.04$) and at T6 (OR = 1.48, 95% CI = 1.15–2.59; $p = 0.035$) also had a higher risk of new T2 lesions at T12, compared to patients with DILL (**Table 3**).

Role of BMI

Patients experiencing a relapse during the first year of treatment presented a lower baseline BMI (20.9 ± 2.4 vs. 24.7 ± 4.4; $p =$ 0.001) (**Table 2**). Multivariate analysis, confirmed baseline BMI as a predictive factor for GD+ lesions at T12 (OR = 0.71; CI = 0.52–0.98; $p = 0.037$) (**Table 3**) and also for new T2 lesions at T12

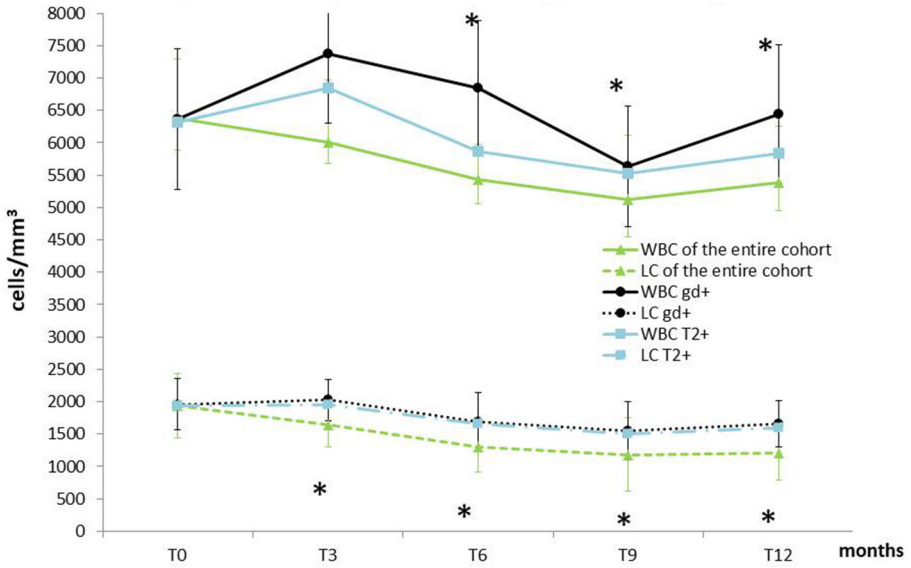


FIGURE 2 | Temporal profile of WBC and LC of the entire cohort compared with patients showing MRI activity at T12. Data are presented as mean ± SD. WBC, white blood cell; LC, lymphocyte count; MRI, Magnetic Resonance Imaging; Gd+, Gadolinium enhancing; T2+, new hyperintense lesions; T0, baseline; T3, 3 months follow up; T6, 6 months follow-up; T9, 9 months follow up; T12, one year follow-up.*Indicates Wilcoxon matched pair test $P < 0.05$ (vs. T0) in the entire sample size.

(OR = 0.99, 95% CI = 0.98–1.00; $p = 0.026$) (**Table 3**). **Figure 3** graphically represents the BMI in patients with and without new T2 lesions at T12.

At T0 we observed a direct correlation between the WBC count and BMI ($r = 0.42$; $p = 0.001$; **Figure 4**); we had also expected a correlation between BMI and LC, as often found in other diseases, but we did not observe this. No other correlations were found between baseline WBC and LC values and any clinical-demographic variable (baseline age and gender, disease duration, number of relapses within the previous year, previous DMDs, presence/absence of new/enlarging T2 lesions, and presence/absence of Gd+ lesions). We further investigated whether any comorbidities, presented by 34.9% of our population (118 patients), could influence BMI at baseline, but we found no difference between BMI in patients with and without comorbidities (24.7 ± 3.8 vs. 23.9 ± 5.4; $p = 0.117$). We also observed a direct correlation between BMI and WBC at T3 ($r = 0.23$; $p = 0.016$); no other correlations were found between baseline BMI and variations in WBC and LC values.

DISCUSSIONS AND CONCLUSIONS

Several DMDs used to treat MS can reduce the occurrence of relapses and slow the progression of neurological disability, thus improving patients' quality of life. However, variability in response to DMDs in patients with MS represents a significant clinical challenge. Potentially, treatment delays may occur in suboptimal responder patients, exposing them to adverse effects without significant benefit. Therefore, biomarkers of treatment response are urgently needed. In our cohort, after 1 year of therapy, DMF was effective in reducing both clinical and MRI disease activity, as shown by the multivariate models used that take into account the absence of exact date of both clinical and MRI relapses. We tried to identify some possible factors that could influence DMF effectiveness, avoiding potential confounders such as baseline disease activity and other patient specific characteristics that were considered in our analysis. Building our hypothesis we also considered the drug effects that involve immunomodulatory action as well as neuroprotection (10, 18). DMF, in fact, reduces cytokine production (19), down-regulates the migratory activity of immune cells at the blood–brain barrier (20) and activates the antioxidant nuclear factor NRF2 transcriptional pathway (10, 21). Considering that the Nrf2 pathway plays an important role in energy metabolism (11, 22) and that recent data demonstrate that DMF is a negative regulator of preadipocyte differentiation mediated by STAT3 inhibition (23), we tried to link patients' BMI with both clinical (relapses) and MRI outcomes. There have been studies indicating that overweight and obese patients have a lesser chance of obtaining complete remission and Non-Evidence of disease Activity (NEDA)-status during IFN-β-treatment, although it remains to be determined whether this is due to a suboptimal treatment response or to a generally more aggressive disease (24). Moreover, Krupp et al. have argued that a higher BMI in US adolescents could be a relevant explanation for their worse outcomes during IFN-ß therapy (25). Obesity, however, is known to effect serum inflammatory markers, promoting a chronic low-grade inflammatory state (26), also through the activation of the nuclear factor (NF) κB pathway (27), and DMF has been shown to prevent the induction of NFκB dependent transcription (28). In our cohort, a lower BMI was

TABLE 2 | LC and WBC of the patients stratified for Gd+ lesions, new T2 lesions and relapses.

	GD+ lesions at baseline MRI (YES) *N* = 95 (28%)	**GD+ lesions at baseline MRI (NO) *N* = 243 (72%)**	**Gd+ lesions at T6 (YES) *N* = 48 (14.2%)**	**Gd+ lesions at T6 (NO) *N* = 290 (85.8%)**	**Gd+ lesions at T12 (YES) *N* = 30 (8.9%)**	**Gd+ lesions at T12 (NO) *N* = 308 (91.1%)**
Baseline LC (cells/mm^3)	1,846 ± 554	1,986 ± 720	1,857 ± 584.4	2,102 ± 912.4	1,903 ± 503	1,967 ± 498
Baseline WBC (cells/mm^3)	6,300 ± 1,636	6,466 ± 2,222	6,630 ± 2,033	6,228 ± 1,995	6,630 ± 917	6,204 ± 1,649
LC at T3 (cells/mm^3)	1,925 ± 1,281	1,588 ± 583	*1,845 ± 455**	*1,486 ± 556**	2,024 ± 337	1,518 ± 581
WBC at T3 (cells/mm^3)	6,208 ± 1,326	6,006 ± 1680	5,875 ± 1,277	5,788 ± 1624	7,376 ± 1165	5,962 ± 1,575
	New T2 lesions at baseline MRI (YES) *N* = 125 (37%)	**New T2 lesions at baseline MRI (NO) *N* = 213 (63%)**	**New T2 lesions at T6 (YES) *N* = 91(26.9%)**	**New T2 lesions at T6 (NO) *N* = 247 (73.1%)**	**New T2 lesions at T12 (YES) *N* = 50 (14.8%)**	**New T2 lesions at T12 (NO) *N* = 288 (85.2%)**
Baseline LC (cells/mm^3)	2,069 ± 740	1,880 ± 642	1,855 ± 546.1	2021.63 ± 837.5	1903.8 ± 614	1,941 ± 393
Baseline WBC (cells/mm^3)	6,344 ± 2,244	6,478 ± 2,000	6,001 ± 2,024	6,419 ± 1,986	6,312 ± 1,090	6,234 ± 1,678
LC at T3 (cells/mm^3)	1,811 ± 1,826	1,518 ± 570	1,739 ± 571	1,461 ± 653	*1,952 ± 317**	*1,495 ± 592**
WBC at T3 (cells/mm^3)	6,247 ± 1,539	5,936 ± 1,357	5,969 ± 1,392	5,729 ± 1,641	6,840 ± 1,073	5,963 ± 1,940
	Relapse before DMF (YES) *N* = 152 (45%)	**Relapse before DMF (NO) *N* = 186 (55%)**	**Relapse within T6 (YES) *N* = 41 (12%)**	**Relapse within T6 (NO) *N* = 297 (88%)**	**Relapse within T12 (YES) *N* = 63 (18.6%)**	**Relapse within T12 (NO) *N* = 275 (81.4%)**
Baseline LC (cells/mm^3)	1,837 ± 622	2,027 ± 696	2054.18 ± 956	1,858.15 ± 561	1,702 ± 549	1,868 ± 858
Baseline WBC (cells/mm^3)	6,194 ± 2,073	6,553 ± 2,033	6,324 ± 2,126	6,216 ± 1,972	6,165 ± 1,045	5,600 ± 1,275
LC at T3 (cells/mm^3)	1,551 ± 574	1,725 ± 1,548	1,687 ± 353	1,597 ± 537	*1,761 ± 465**	*1,386 ± 402**
WBC at T3 (cells/mm^3)	6,193 ± 1,662	5,841 ± 1,537	6,243 ± 1,398	5,850 ± 1,688	*6,031 ± 1,687**	*5,660 ± 1,110**

Values expressed as mean (±SD).

*LC, lymphocyte count; WBC, white blood cells; T3, 3 months follow-up; T6, 6-months follow up; T12, 1 year follow up. * underlines $p < 0.05$.*

TABLE 3 | Predictors of relapses and MRI disease outcomes at T12: multivariate logistic regression analysis.

	OR (95% CI); *p*-value		
Variable	**Relapse within T12**	**New T2 lesions at T12**	**Gd+ lesions at T12**
Gender (F)	0.635 (0.09–4.13); 0.630	0.313 (0.06–15.14); 0.557	0.095 (0.001–5.23); 0.566
Age	0.851 (0.697–1.04); 0.060	0.63 (0.56–11.25); 0.991	0.411 (0.062–2.73); 0.358
Baseline Gd+ (YES)	0.045 (0.005–0.44); 0.080	0.032 (0.001–1.23); 0.994	0.011 (0.001–1.96); 0.088
Baseline T2 (YES)	1.99 (0.25–16.07); 0.510	1.22 (0.28–2.21); 0.198	0.31 (0.074–1.29); 0.109
Relapses pre-DMF (YES)	0.73 (0.61-1.60); 0.060	1.016 (0.175–14.5); 0.993	1.76 (0.175–15.32); 0.998
1st line DMD vs. naive	1.002 (0.045–3.47); 0.990	6.37 (0.19–7.52); 0.988	0.15 (0.001–69.9); 0.545
2nd line DMD vs. naive	0.236 (0.008–6.74); 0.380	2.25 (0.03–2.29); 0.862	0.31 (0.07–1.3); 0.109
Variation in WBC	*1.054 (1.03-2.65); 0.043*	–	–
LC at T3	1.08 (0.98–2.80); 0.090	*1.01 (1.00–1.95); 0.005*	*1.003 (1.00–1.07); 0.046*
Baseline BMI	0.828 (0.61–1.15); 0.213	*0.99 (0.98–1.00); 0.026*	*0.71 (0.52–0.98); 0.037*
DIHL at T3	2.5 (0.77–8.05); 0.125	*1.26(1.07–1.96); 0.040*	*1.31(1.12–5.34); 0.043*
DIHL at T6	0.62 (0.16–2.42); 0.493	*1.48 (1.15–2.59); 0.035*	*1.14 (1.133–6.33); 0.050*

*WBC, white blood cells; BMI, Body Mass Index; LC, lymphocyte count; DIHL, high number of DMF-induced lymphocytes; T3, 3 months follow-up; T6, 6-months follow up; T12, 1 year follow up. * Models always considered as covariates baseline clinical and demographic characteristics of the cohort, and those covariates significant at the univariate analysis. Underlined values are those statistically significant ($p<0.05$).*

a predictive factor for MRI activity at T12, and we tried to explain this finding with the differences in DMF action according to the amount of adipose tissue; we may hypothesize that the higher the amount of adipocytes, the greater the action that DMF can exert on the inflammatory aspect of the disease. Nowadays, in fact, adipocytes are attributed a metabolically

active role in biochemical mechanisms that may contribute to a chronic low-grade inflammatory status (29), increasing ROS oxidative stress. Reactive oxygen and nitrogen species have been described to induce damage to biological macromolecules in MS lesions (30, 31). Moreover, in RR and also in progressive MS, active lesions are associated with inflammation (32), although not always present in the latter form of the disease.

We also found that LC at T3 was a predictive factor for clinical and MRI activity. DMF suppresses lymphocytes and induces T-cell apoptosis. DMF-induced lymphopenia could theoretically be linked to disease control. However, in DEFINE and CONFIRM, the reduction in ARR at 2 years in patients treated with DMF 240 mg bid vs. placebo was not substantially different in patients with lymphopenia (≥1LC < lower limit of normal) compared to those without lymphopenia (all LCs ≥lower limit of normal) (7). However, real-life data are sometimes discordant on this point; for example, data from a Dallas Multiple Sclerosis Center (33) have shown a greater risk of relapses in patients with higher LC at 3 months [$p < 0.001$, hazard ratio [HR]: 1.82], just as we found in our cohort. Moreover, the Dallas examiners stratified LC by tertile, and found a reduced risk in patients with lower LC values: 1,200 cells/mL compared with mid-tier (1,210–1,800 cells/mL) and the highest tertile (>1,810 cells/mL) ($p < 0.01$). We obtained comparable results by stratifying patients according to the LC median during the follow-up, and found that patients with DIHL at T3, T6, and T12 had a higher risk of MRI activity than those with DILL. Conversely, in another cohort from the MS Center of Washington (34), DMF-induced lymphopenia did not predict a good clinical response to therapy. In this Washington study, the authors examined predictive factors of lymphopenia including recent natalizumab exposure as risk factors of developing moderate to severe lymphopenia during treatment with DMF. In our cohort, the previous treatment was not associated with a different incidence in reduction of WBC or LC, and we found no significant correlation between the previous DMD and the disease activity. However, we observed a direct correlation between the WBC count and BMI ($r = 0.32$; $p = 0.001$) at T0; since fat tissue releases inflammatory cytokines, this may explain why in our cohort we found a direct correlation between WBC (which can be considered a non-specific marker of inflammation) and BMI. Moreover, while BMI and LC are independently linked to DMF effectiveness, the association test performed on these did not prove to be a statistically significant effect of either clinical or MRI activity. The reason for this may be that our cohort contained few underweight or obese patients. Another possible explanation could be that the two variables did not change to the same extent: BMI remained constant during the observation period, while there was a reduction (15.36%) in LC which was statistically significant from the third month and tended to stabilize around the ninth month. This finding differs from what has been observed in an integrated analysis of long-term extension studies on DMF (7), which demonstrated that LC decreased by 30% during the first year and then plateaued, remaining above the lower limit of normal (LLN).

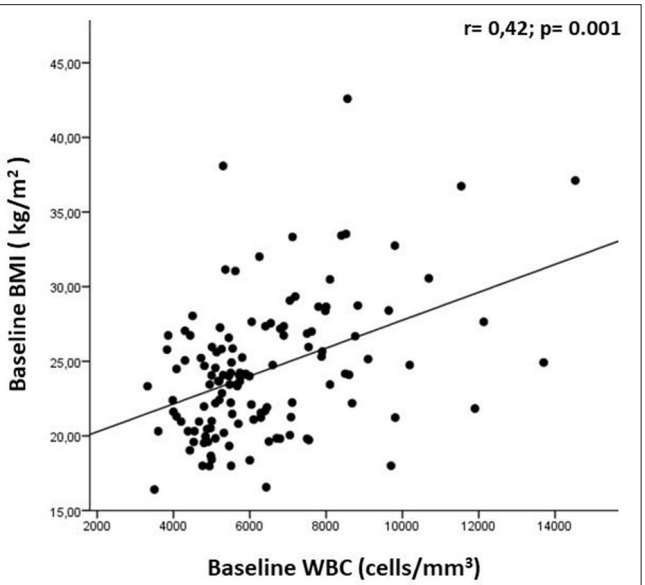


FIGURE 3 | Correlation between baseline BMI and WBC. WBC, white blood cell; BMI, Body Mass Index.

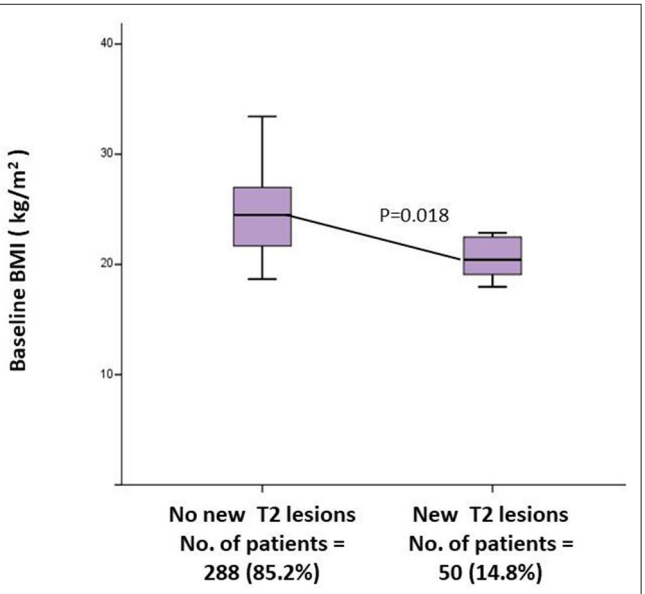


FIGURE 4 | Univariate between baseline BMI and MRI activity at T12. BMI, Body Mass Index; MRI, Magnetic Resonance Imaging; T12, 1 Year follow up.

Our analysis did not investigate the influence of different lymphocytes subsets (LS) on disease activity during DMF. A recent study demonstrated that patients under DMF therapy who remained stable (with no radiological or clinical evidence of disease activity) tended to exhibit greater reductions of CD3+, CD4+, CD8+, and CD19+ cells compared to active MS patients, and they also presented significantly higher CD4/CD8 ratios (35). However, since the monitoring of the immune system re-modulation in DMF relapsing MS patients

is not required during the routine clinical practice, we did not perform, in this real life setting, analyses on specific LS variations and this is one of the limitations of our study. Other limitations may be the lack of a control group treated with a different DMD, as well as the lack of details regarding metabolic parameters of patients (blood glucose levels and urine tests), the metabolic state of immune cells, and patients' consumption behavior. Further studies will be performed that will include these details in order to have a more in-depth analysis of the role of BMI in predicting DMF effectiveness. Another limitation is that, given the oral administration of the drug, we did not check patients' adherence. Finally, the most important limitation may be the observational design of our study: our findings may only reflect a unique sample population and, thus, may not be generalized to other groups.

In conclusion, elucidating the significance of DMF-induced lymphopenia could be important for clinical decisions, including the frequency of monitoring and the possibility of predicting both clinical or MRI activity. This becomes an even more appealing prospect when it is considered that changes in LC can be detected from the third month of treatment, and might therefore offer the possibility of formulating an early prediction of a possible suboptimal response. Moreover, the use of an easily detectable baseline characteristic (BMI), could allow better profiling of patients for a tailored treatment. However, given the observational nature of our work, there is a need for further studies on larger cohorts in order to support the clinical importance of our results.

ETHICS STATEMENT

This study was carried out in accordance with the recommendations of name of guidelines, name of committee with written informed consent from all subjects. All subjects gave written informed consent in accordance with the Declaration of Helsinki. The protocol was approved by the Ethical Committee of the University of Bari.

AUTHOR CONTRIBUTIONS

AM participated in the design of the study, collected the data, and drafted the manuscript. AI collected the data and revised the manuscript, helped to give final approval. GL participated in the design of study, performed statistical analysis and helped to given final approval. MD participated in the design of study and revised the manuscript. DM revised the manuscript and helped to give final approval. VF revised the manuscript. PI helped to draft the manuscript. MT revised the manuscript and helped to give final approval. DP conceived of the study, and participated in its design, revised the manuscript and helped to give final approval of the version to be published.

ACKNOWLEDGMENTS

Preliminary data regarding this topic were presented at the 4th Congress of the European Academy of Neurology - Lisbon 2018 (EPO3067 - Lymphocyte count and Body Mass Index as biomarkers of treatment response in a Multiple Sclerosis Dimethyl-Fumarate-treated cohort).

REFERENCES

1. Olsson T, Barcellos LF, Alfredsson L. Interactions between genetic, lifestyle and environmental risk factors for multiple sclerosis. *Nat Rev Neurol*. (2017) 13:25–36. doi: 10.1038/nrneurol.2016.187
2. Goodin DS. Disease-modifying therapy in MS: a critical review of the literature. Part II: assessing efficacy and dose-response. *J Neurol*. (2004) 251(Suppl. 5):v50–6. doi: 10.1007/s00415-004-1508-7
3. Rudick RA, Polman CH. Current approaches to the identification and management of breakthrough disease in patients with multiple sclerosis. *Lancet Neurol*. (2009) 8:545–59. doi: 10.1016/S1474-4422(09)70082-1
4. Gold R, Kappos L, Arnold DL, Bar-Or A, Giovannoni G, Selmaj K, et al. DEFINE Study Investigators. Placebo-controlled phase 3 study of oral BG-12 for relapsing multiple sclerosis. *N Engl J Med*. (2012) 367:1098–107. doi: 10.1056/NEJMoa1114287
5. Fox RJ, Miller DH, Phillips JT, Hutchinson M, Havrdova E, Kita M, et al. CONFIRM Study Investigators. Placebo-controlled phase 3 study of oral BG-12 or glatiramer in multiple sclerosis. *New Engl J Med*. (2012) 367:1087–97. doi: 10.1056/NEJMoa1206328
6. Gold R, Arnold DL, Bar-Or A, Hutchinson M, Kappos L, Havrdova E, et al. Long-term effects of delayed-release dimethyl fumarate in multiple sclerosis: interim analysis of ENDORSE, a randomized extension study. *Mult Scler*. (2017) 23:253–65. doi: 10.1177/1352458516649037
7. Fox RJ, Chan A, Gold R, Phillips JT, Selmaj K, Chang I, et al. Characterizing absolute lymphocyte count profiles in dimethyl fumarate-treated patients with MS: patient management considerations. *Neurol Clin Pract*. (2016) 6:220–9. doi: 10.1212/CPJ.0000000000000238
8. National Cancer Institute. *Common Terminology Criteria for Adverse Events v4.0, NCI, NIH, DHHS*. Bethesda, MD: NIH publication (2009).
9. European Medicines Agency. *Updated Recommendations to Minimise the Risk of the Rare Brain Infection PML With Tecfidera*. (2015). Available online at: https://www.ema.europa.eu/en/news/updated-recommendations-minimise-risk-rare-brain-infection-pml-tecfidera (accessed May 20, 2019).
10. Linker RA, Lee DH, Ryan S, van Dam AM, Conrad R, Bista P, et al. Fumaric acid esters exert neuroprotective effects in neuroinflammation via activation of the Nrf2 antioxidant pathway. *Brain*. (2011) 134(Pt 3):678–92. doi: 10.1093/brain/awq386
11. Pi J, Leung L, Xue P, Wang W, Hou Y, Liu D, et al. Deficiency in the nuclear factor E2-related factor-2 transcription factor results in impaired adipogenesis and protects against diet-induced obesity. *J Biol Chem*. (2010) 285:9292–300. doi: 10.1074/jbc.M109.093955
12. Versini M, Jeandel PY, Rosenthal E, Shoenfeld Y. Obesity in autoimmune diseases: not a passive bystander. *Autoimmun. Rev*. (2014) 13:981–1000. doi: 10.1016/j.autrev.2014.07.001
13. Oliveira SR, Simão AN, Kallaur AP, de Almeida ER, Morimoto HK, Lopes J, et al. Disability in patients with multiple sclerosis: influence of insulin resistance, adiposity, and oxidative stress. *Nutrition*. (2014) 30:268–73. doi: 10.1016/j.nut.2013.08.001
14. McDonald WI, Compston A, Edan G, Goodkin D, Hartung HP, Lublin FD, et al. Recommended diagnostic criteria for multiple sclerosis: guidelines from the International Panel on the diagnosis of multiple sclerosis. *Ann Neurol*. (2001) 50:121–7. doi: 10.1002/ana.1032
15. Polman CH, Reingold SC, Banwell B, Clanet M, Cohen JA, Filippi M, et al. Diagnostic criteria for multiple sclerosis: 2010 revisions to the "McDonald criteria". *Ann Neurol*. (2011) 69:292–302. doi: 10.1002/ana.22366
16. Durelli L, Cocito D, Riccio A, Barile C, Bergamasco B, Baggio GF, et al. High-dose intravenous methylprednisolone in the treatment of multiple

sclerosis: clinical-immunologic correlations. *Neurology*. (1986) 36:238–43 doi: 10.1212/WNL.36.2.238
17. Kurtzke JF. Rating neurologic impairment in multiple sclerosis: an expanded disability status scale (EDSS). *Neurology*. (1983) 33:1444–52. doi: 10.1212/WNL.33.11.1444
18. Scannevin RH, Chollate S, Jung MY, Shackett M, Patel H, Bista P, et al. Fumarates promote cytoprotection of central nervous system cells against oxidative stress via the nuclear factor (Erythroid-Derived 2)-like 2 pathway. *J Pharmacol Exp Ther*. (2012) 341:274–84. doi: 10.1124/jpet.111.190132
19. McGuire VA, Ruiz-Zorrilla Diez T, Emmerich CH, Strickson S, Ritorto MS, Sutavani RV, et al. Dimethyl fumarate blocks pro-inflammatory cytokine production via inhibition of TLR induced M1 and K63 ubiquitin chain formation. *Sci Rep*. (2016) 6:31159. doi: 10.1038/srep31159
20. Loewe R, Holnthoner W, Gröger M, Pillinger M, Gruber F, Mechtcheriakova D, et al. Dimethylfumarate Inhibits TNF-induced nuclear entry of NF-jB/p65 in human endothelial cells. *J Immunol*. (2002) 168:4781–7. doi: 10.4049/jimmunol.168.9.4781
21. Wang Q, Chuikov S, Taitano S, Wu Q, Rastogi A, Tuck SJ. et al. Dimethyl fumarate protects neural stem/progenitor cells and neurons from oxidative damage through Nrf2-ERK1/2 MAPK Pathway. *Int J Mol Sci*. (2015) 16:13885–907. doi: 10.3390/ijms160613885
22. Hou Y, Xue P, Bai Y, Liu D, Woods CG, Yarborough K, et al. Nuclear factor erythroid-derived factor 2-related factor 2 regulates transcription of CCAAT/enhancer-binding protein β during adipogenesis. *Free Radic Biol Med*. (2012) 52:462–72. doi: 10.1016/j.freeradbiomed.2011.10.453
23. Kang HJ, Seo HA, Go Y, Oh CJ, Jeoung NH, Park KG, et al. Dimethylfumarate suppresses adipogenic differentiation in 3T3-L1 preadipocytes through inhibition of STAT3 activity. *PLoS ONE*. (2013) 8:e61411. doi: 10.1371/journal.pone.0061411
24. Kvistad SS, Myhr KM, Holmøy T, Šaltytė Benth J, Wergeland S, Beiske AG, et al. Body mass index influence interferon-beta treatment response in multiple sclerosis. *J Neuroimmunol*. (2015) 288:92–7. doi: 10.1016/j.jneuroim.2015.09.008
25. Krupp LB, Pohl D, Ghezzi A, Boyko A, Tenembaum S, Chen L, et al. REPLAY Study Group, Subcutaneous interferon β-1a in pediatric patients with multiple sclerosis: regional differences in clinical features, disease management, and treatment outcomes in an international retrospective study, *J Neurol Sci*. (2016) 363:33–8 doi: 10.1016/j.jns.2016.01.023
26. Cao H. Adipocytokines in obesity and metabolic disease. *J Endocrinol*. (2014) 220:T47–59. doi: 10.1530/JOE-13-0339
27. Yuan M, Konstantopoulos N, Lee J, Hansen L, Li ZW, Karin M, et al. Reversal of obesity- and diet-induced insulin resistance with salicylates or targeted disruption of Ikkbeta. *Science*. (2001) 293:1673–7. doi: 10.1126/science.1061620
28. Loewe R, Pillinger M, de Martin R, Mrowietz U, Gröger M, Holnthoner W, et al. Dimethylfumarate inhibits tumor-necrosis-factor-induced CD62E expression in an NF-kappa B-dependent manner. *J Invest Dermatol*. (2001) 117:1363–8. doi: 10.1046/j.0022-202x.2001.01576.x
29. Palavra F, Almeida L, Ambrósio AF, Reis F. Obesity and brain inflammation: a focus on multiple sclerosis. *Obes Rev*. (2016) 17:211–24. doi: 10.1111/obr.12363
30. van Horssen J, Schreibelt G, Drexhage J, Hazes T, Dijkstra CD, van der Valk P, et al. Severe oxidative damage in multiple sclerosis lesions coincides with enhanced antioxidant enzyme expression. *Free Radic Biol Med*. (2008) 45:1729–37. doi: 10.1016/j.freeradbiomed.2008.09.023
31. Haider L, Fischer MT, Frischer JM, Bauer J, Höftberger R, Botond G, et al. Oxidative damage in multiple sclerosis lesions. *Brain*. (2011) 134(Pt 7):1914–24. doi: 10.1093/brain/awr128
32. Frischer JM, Bramow S, Dal-Bianco A, Lucchinetti CF, Rauschka H, Schmidbauer M, et al. The relation between inflammation and neurodegeneration in multiple sclerosis brains. *Brain*. (2009) 132(Pt 5):1175–89. doi: 10.1093/brain/awp070
33. Wright K, Winkler MD, Newton BD, Sormani MP, Okuda DT. Patient outcomes influenced by reduced lymphocyte counts after dimethyl fumarate initiation. *Neurol Neuroimmunol Neuroinflamm*. (2017) 4:e397 doi: 10.1212/NXI.0000000000000397
34. Longbrake EE, Naismith RT, Parks BJ, Wu GF, Cross AH. Dimethyl fumarate-associated lymphopenia: risk factors and clinical significance. *MSJ Exp Transl Clin*. (2015) 1:1–8. doi: 10.1177/2055217315596994
35. Fleischer V, Friedrich M, Rezk A, Bühler U, Witsch E, Uphaus T, et al. Treatment response to dimethyl fumarate is characterized by disproportionate CD8+ T cell reduction in MS. *Mult Scler*. (2018) 24:632–41. doi: 10.1177/1352458517703799

Conflict of Interest Statement: DP received honoraria for consultancy and/or speaking from Biogen Idec, Merck-Serono, Almirall, Sanofi-Aventis, TEVA, Novartis and Genzyme. PI has served on scientific advisory boards for Biogen Idec and Bayer, and has received funding for travel and/or speaker honoraria from Genzyme, Sanofi-Aventis, Biogen Idec, Teva and Novartis. MT received honoraria for consultancy or speaking from Biogen, Sanofi Aventis, Merck Serono, Novartis, Genzyme, TEVA, and Bayer-Schering and research grants from Merck Serono, Biogen, and Novartis.

The remaining authors declare that the research was conducted in the absence of any commercial or financial relationships that could be construed as a potential conflict of interest.

Copyright © 2019 Manni, Iaffaldano, Lucisano, D'Onghia, Mezzapesa, Felica, Iaffaldano, Trojano and Paolicelli. This is an open-access article distributed under the terms of the Creative Commons Attribution License (CC BY). The use, distribution or reproduction in other forums is permitted, provided the original author(s) and the copyright owner(s) are credited and that the original publication in this journal is cited, in accordance with accepted academic practice. No use, distribution or reproduction is permitted which does not comply with these terms.

frontiers in Neurology

CASE REPORT
published: 09 July 2019
doi: 10.3389/fneur.2019.00739

Dysphagia as Isolated Manifestation of Jo-1 Associated Myositis?

Bendix Labeit, Paul Muhle, Sonja Suntrup-Krueger, Sigrid Ahring, Tobias Ruck, Rainer Dziewas and Tobias Warnecke*

Department of Neurology, University Hospital Muenster, Muenster, Germany

Dysphagia can be predominant or sole symptom of myositis. However, diagnostic evaluation is difficult in such cases. Here, we present evidence for dysphagia as sole manifestation of Jo-1 associated myositis. A 77-year-old patient suffering from isolated dysphagia was assessed by flexible endoscopic evaluation of swallowing, videofluoroscopy, high resolution esophageal manometry, whole body muscle MRI, electroneurographic and electromyographic examination, cerebrospinal fluid analysis, screening for autoantibodies, and body plethysmography. We detected isolated oropharyngeal dysphagia including a decreased pressure of the upper esophageal sphincter leading to cachexia in an anti-Jo-1 positive patient without any abnormalities in the other diagnostics. Immunosuppressive therapy with cortisone and azathioprine led to long-term improvement of dysphagia. This is the first report of isolated dysphagia as manifestation of Jo-1 associated myositis. Therefore, Jo-1 associated myositis should be considered as a possible differential diagnosis for isolated dysphagia. Typical signs for myositis in instrumental dysphagia assessment are presented.

Keywords: dysphagia, myositis, antisynthetase syndrome, antisynthetase antibody, Jo-1, Jo-1 autoantibody, diagnostic algorithm, idiopathic inflamed myopathy

OPEN ACCESS

Edited by:
Fabienne Brilot, University of Sydney, Australia

Reviewed by:
Neil John McHugh, University of Bath, United Kingdom
Guochun Wang, China-Japan Friendship Hospital, China
Federica Montagnese, Klinikum der Universität München, Germany

****Correspondence:***
Bendix Labeit
benlabeit@wwu.de

Specialty section:
This article was submitted to Multiple Sclerosis and Neuroimmunology, a section of the journal Frontiers in Neurology

Received: *24 April 2019*
Accepted: *24 June 2019*
Published: *09 July 2019*

Citation:
Labeit B, Muhle P, Suntrup-Krueger S, Ahring S, Ruck T, Dziewas R and Warnecke T (2019) Dysphagia as Isolated Manifestation of Jo-1 Associated Myositis? Front. Neurol. 10:739. doi: 10.3389/fneur.2019.00739

INTRODUCTION

Dysphagia is frequently reported in patients with myositis (1–6) with prevalence rates ranging from 30 to 72% (5, 6). Typical symptoms of myositis related dysphagia are coughing, choking, bolus-sticking in the pharynx and swallowing problems with dry and solid food consistencies (1, 5). Early diagnosis and specific therapeutic management of dysphagia is crucial as it can lead to aspiration pneumonia with respiratory failure, which is the leading cause of mortality in patients with myositis (1, 7). Dysphagia can occur as predominant or sole symptom of myositis: Oh et al. described dysphagia as the only manifestation of inclusion body myositis (8). Shapiro et al. reported 3 cases of isolated pharyngeal dysphagia with biopsies of the omohyoid and cricopharyngeus muscles showing inflammatory myopathy (9). In such cases, diagnostic evaluation is particularly difficult, as myositis-related dysphagia may also be present if laboratory or electrophysiological diagnostics remain unremarkable (10). The role of autoantibodies in the diagnosis of myositis is steadily increasing. Jo-1 antibodies are now part of the current EULAR diagnostic criteria alongside clinical criteria, CK blood level, and histological signs (11). Further, autoantibodies can be helpful in the classification of myositis (12). This biomarker driven development might also be beneficial in patients with unclear dysphagia. In this case-report we present evidence for dysphagia as isolated manifestation of Jo-1 associated myositis, which to the best of our knowledge has not been reported so far. In addition, we give an overview of the literature on the pathophysiology of dysphagia in myositis.

CASE REPORT

Patient History

A 77-year-old patient was presented to our outpatient clinic due to progressive dysphagia. About 10 years ago, he noticed taste disturbances and discomfort in the mouth region, hindering his speech. During the last 3 years, he predominantly suffered from swallowing impairment. He reported of choking and hiccups in particular when eating solid food. In addition, he needed increasingly longer to finish a normal meal and had to extraordinarily concentrate on the eating process. As a consequence, he avoided eating in public. Recently, he was hospitalized due to an aspiration pneumonia. The patient did not take any medication. The detailed clinical examination revealed no fasciculations, muscle weakness, double vision, raynaud's phenomenon, mechanic's hands, skin rash or dyspnea, only a cachectic nutritional status due to dysphagia (size 1.8 m, weight 53 kg, BMI 16.4) was remarkable. There were no relevant pre-existing diseases. Cerebral MRI that had been performed before the presentation in our department showed no pathological findings.

Diagnostic Procedures

Flexible endoscopic evaluation of swallowing (FEES) revealed severe oropharyngeal dysphagia with intradeglutitive aspiration and postdeglutitive residue in the vallecula und pyriform sinus (graded as severe for semisolid and solid consistencies according to the Yale Pharyngeal Residue Severity Scale (13) as a sign of weak pharyngeal constriction (**Figure 1**). The FEES tensilon test (14, 15) showed no improvement of dysphagia upon application of edrophonium. Videoflouroscopy of swallowing (VFSS) confirmed severe pharyngeal dysphagia with markedly restricted pharyngeal contraction and consecutive nasopharyngeal reflux as well as postdeglutitive aspiration due to considerable retention. Furthermore, there was a markedly delayed triggering of swallowing reflex with reduced hyolaryngeal elevation and predeglutitive aspiration, Rosenbek grade 7 (16, 17). High resolution esophageal manometry (HRM) showed a markedly reduced pressure of the upper esophageal sphincter with extended relaxation and recovery time and an amotile tubular esophagus. Functional dysphagia severity according to the FOIS-Score was 1 (18). Basic laboratory and CSF diagnostics were normal (no cytalbuminary dissociation, normal CK-blood level). CSF-screening for ganglioside antibodies was negative (Ganglioside Profile 2 IgG and IgM Euroline, Euroimmun; Lübeck, Germany). Whole body muscle MRI was unremarkable without edema or atrophy. The electroneurographic examination detected a length-dependent, axonal, sensitive polyneuropathy as incidental finding. Repetitive stimulation of the n. facialis on both sides with recording from the m. nasalis revealed no decrement. Repetitive stimulation of the n. ulnaris on the left side with recording from the m. abductor digiti minimi before and after 1-min maximum arbitrary innervation revealed no increment. In the electromyographic examination, isolated chronic neurological changes of the right hand muscles, but otherwise inconspicuous findings were observed (m. deltoideus on both sides: no pathological spontaneous activity, motor unit potential normally configurated, regular recruitment, dense interference; m. abductor pollicis brevis on both sides: no pathological spontaneous activity, motor unit potential on the right side partly with high amplitude, recruitment and interference on the right side slightly reduced; m. abductor digiti minimi on both sides: no pathological spontaneous activity, motor unit potential on the right side partly with high amplitude, recruitment and interference on the right side slightly reduced; m. vastus on both sides: no pathological spontaneous activity, motor unit potential normally configurated, regular recruitment, dense interference; m. tibialis anterior on both sides: no pathological spontaneous activity, motor unit potential normally configurated, regular recruitment, dense interference; paravertebral T8 on both sides: no pathological spontaneous activity; m. glossus on the left side: no pathological spontaneous activity). The antibody screening was positive for Jo-1 IgG (++) and negative for the other screened autoantibodies (ANA, Mi-2a, Mi-2b, TIF1g, MDA5, NXP2, SAE1, Ku, PM100, PM75, SRP, PL-7, PL-12, EJ, OJ, Ro52, Euroline, Euroimmun, Lübeck, Germany, and anti-HMG-CoA, MVZ Labor Volkmann, Karlsruhe, Germany). Also, no myasthenia antibodies could be detected (negative for AChR, titin, MuSK, and VGCC, Euroline, Euroimmun, Lübeck, Germany). Although the role of Jo-1-IgG in the pathophysiology of myositis is poorly understood, it is a highly reliable marker for idiopathic inflammatory myopathies (19). In the absence of signs for other diseases, this led to the diagnosis of Jo-1 associated myositis as underlying disease. Body plethysmography and x-ray-chest revealed no indication of pulmonary involvement.

Therapy

A PEG tube was placed to ensure sufficient enteral nutrition. In addition, an intravenous cortisone therapy with 1 g methylprednisolone per day for 5 days followed by oral therapy with prednisolone and azathioprine was performed. After 4 months of therapy the swallowing function improved, and FEES showed a reduction in penetration and aspiration frequency and severity, lower levels of penetration and aspiration volume, and a more effective bolus clearance. The FOIS-scale had improved from 1 on admission to 3, so that a reinstitution of oral feeding parallel to the PEG nutrition was recommended (18). This improvement sustained in the long term (currently 12 months after beginning of therapy).

DISCUSSION

There are only few studies that investigated the pathophysiological characteristics of myositis related dysphagia. Ebert et al. claimed that myositis mainly affects the proximal esophageal skeletal muscle. They reported decreased upper sphincter pressure and absent pharyngeal contractions in manometry (3). Casal-Dominguez et al. also reported decreased upper esophageal sphincter pressure and failed waves in patients with polymyositis (20). Ertekin et al. showed that myositis mainly leads to pharyngeal dysphagia with prolonged phase of pharyngeal swallowing and weakness of the striated oropharyngeal muscles. Contrary to other manometry studies, they found that the cricopharyngeal sphincter was affected less frequently and showed both

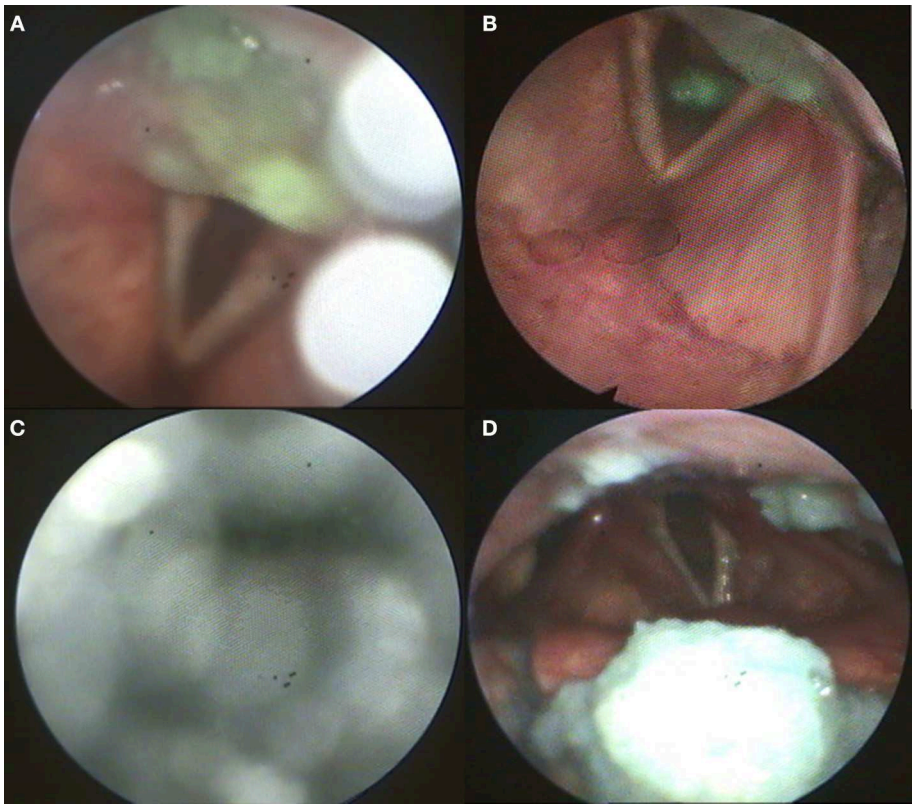


FIGURE 1 | (A) Postdeglutitive residue of pudding; **(B)** Aspiration of pudding; **(C)** Weak white-out as sign for reduced pharyngeal contractility; **(D)** Postdeglutitive residue of bread.

hyporeflexic and hyperreflexic states in myositis (2). In a study using VFSS, Langdon et al. reported delayed swallowing initiation, decreased hyolaryngeal excursion, pyriform residue and penetration (5). Consistent with these findings, Oh et al. also described impaired laryngeal elevation, pharyngeal pooling, disturbed tongue retraction and abnormal cricopharyngeal function (1).

Whether inflammatory myopathies constitute a homogeneous pathophysiological pathophysiological dysphagia entity or specific sub forms e.g., inclusion body myositis, dermatomyositis, and antisynthetase syndrome show their own specific pathophysiological characteristics largely remains an open question. Oh et al. did not find differences between inclusion body myositis, dermatomyositis, and polymyositis in VFSS findings (1). Casal-Dominguez et al. report that antisynthetase syndrome is associated with decreased and hypotonic lower esophageal sphincter pressure and conclude that the autoimmune reaction of this specific myositis entity may affect the smooth muscle of the esophageal body in particular and cause impairment in the lower esophageal sphincter (20). Inclusion body myositis seems to be rather associated with an increased pressure of the upper esophagus sphincter due to a relaxation deficit (21, 22) which manifests as pharyngeal muscle propulsion between C3 and C7 in VFSS (21). Typical findings of instrumental dysphagia assessment that may indicate myositis are shown in **Table 1**.

TABLE 1 | Typical signs for myositis in instrumental dysphagia assessment.

Flexible Endoscopic Evaluation of Swallowing:
• *Reduced pharyngeal contractility (pharyngeal squeeze maneuver)*
• *Weak white-out*
• Pharyngeal residue
• Postdeglutitive penetration/aspiration
Videofluoroscopy:
• *Decreased hyolaryngeal elevation*
• *Pharyngeal muscle propulsions at C3-C7*
• Impairment of the upper or lower esophagus sphincter
• Pharyngeal residue
• Postdeglutitive penetration/aspiration
High Resolution Manometry:
• Impairment of the upper or lower esophagus sphincter

Signs that are specific to one diagnostic procedure are printed in italics.

Here, to our knowledge we present the first ever reported case of isolated dysphagia due to Jo-1 associated myositis: we found pharyngeal dysphagia with impairment of the upper esophagus similar to the impairment pattern commonly described in myositis. This case demonstrates that not only the smooth esophageal muscle (20) but also the striated muscle of the pharynx and upper esophagus can

be affected by the Jo-1 associated autoimmune reaction. Based on our case report, we therefore recommend that myositis focused diagnostics including an autoantibody panel should be done in patients with unclear dysphagia that show typical sings for myositis in the instrumental dysphagia assessment.

LIMITATIONS

There are only few studies that investigated the pathophysiological characteristics of myositis related dysphagia. The pathophysiological conclusions in this study must therefore be considered cautiously. According to the EULAR criteria, the probability of myositis in a patient with dysphagia and detection of Jo-1 antibodies is 80% (11). Myositis is therefore only the probable underlying disease. Since no muscle biopsy was performed, other diseases e.g., atypical IBM cannot be ruled out with certainty.

DATA AVAILABILITY

The raw data supporting the conclusions of this manuscript will be made available by the authors, without undue reservation, to any qualified researcher.

ETHICS STATEMENT

Written and informed consent for this case report and the related data and images was obtained by the patient prior to publication.

AUTHOR CONTRIBUTIONS

BL and TW were responsible for the preparation and conceptual design of the manuscript. TR was responsible for advising on antibody diagnostics. SA was responsible for the coordination and realization of the FEES examination. All other authors (PM, SS-K, and RD) were involved in the preparation and editing of the manuscript.

FUNDING

We acknowledge support from the Open Access Publication Fund of the University of Muenster.

ACKNOWLEDGMENTS

We are very grateful to the patient for giving his consent to the publication of this case report.

REFERENCES

1. Oh TH, Brumfield KA, Hoskin TL, Stolp KA, Murray JA, Bassford JR. Dysphagia in inflammatory myopathy: Clinical characteristics, treatment strategies, and outcome in 62 patients. *Mayo Clin Proc.* (2007) 82:441–7. doi: 10.4065/82.4.441
2. Ertekin C, Secil Y, Yuceyar N, Aydogdu I. Oropharyngeal dysphagia in polymyositis/dermatomyositis. *Clin Neurol Neurosurg.* (2004) 107:32–7. doi: 10.1016/j.clineuro.2004.02.024
3. Ebert EC. Review article: the gastrointestinal complications of myositis. *Aliment Pharmacol Ther.* (2010) 31:359–65. doi: 10.1111/j.1365-2036.2009.04190.x
4. Marie I, Hatron PY, Levesque H, Hachulla E, Hellot MF, Michon-Pasturel U, et al. Influence of age on characteristics of polymyositis and dermatomyositis in adults. *Medicine.* (1999) 78:139–47.
5. Langdon PC, Mulcahy K, Shepherd KL, Low VH, Mastaglia FL. Pharyngeal dysphagia in inflammatory muscle diseases resulting from impaired suprahyoid musculature. *Dysphagia.* (2012) 27:408–17. doi: 10.1007/s00455-011-9384-7
6. Mulcahy KP, Langdon PC, Mastaglia F. *Dysphagia* in inflammatory myopathy: self-report, incidence, and prevalence. *Dysphagia.* (2012) 27:64–9. doi: 10.1007/s00455-011-9338-0
7. Lynn SJ, Sawyers SM, Moller PW, O'Donnell JL, Chapman PT. Adult-onset inflammatory myopathy: North Canterbury experience 1989-2001. *Intern Med J.* (2005) 35:170–3. doi: 10.1111/j.1445-5994.2004.00764.x
8. Olive M, Villanueva P, Ferrer I, Montero J, Martinez-Matos JA. Dysphagia as the only manifestation of inclusion body myositis. *Neurologia.* (1994) 9:202–3.
9. Shapiro J, Martin S, DeGirolami U, Goyal R. Inflammatory myopathy causing pharyngeal dysphagia: a new entity. *Ann Otol Rhinol Laryngol.* (1996) 105:331–5. doi: 10.1177/000348949610500501
10. Williams RB, Grehan MJ, Hersch M, Andre J, Cook IJ. Biomechanics, diagnosis, and treatment outcome in inflammatory myopathy presenting as oropharyngeal dysphagia. *Gut.* (2003) 52:471–8. doi: 10.1136/gut.52.4.471
11. Lundberg IE, Tjarnlund A, Bottai M, Werth VP, Pilkington C, Visser M, et al. 2017 European League Against Rheumatism/American College of Rheumatology classification criteria for adult and juvenile idiopathic inflammatory myopathies and their major subgroups. *Ann Rheumat Dis.* (2017) 76:1955–64. doi: 10.1136/annrheumdis-2017-211468
12. Mariampillai K, Granger B, Amelin D, Guiguet M, Hachulla E, Maurier F, et al. Development of a new classification system for idiopathic inflammatory myopathies based on clinical manifestations and myositis-specific autoantibodies. *JAMA Neurol.* (2018) 75:1528–37. doi: 10.1001/jamaneurol.2018.2598
13. Neubauer PD, Rademaker AW, Leder SB. The yale pharyngeal residue severity rating scale: an anatomically defined and image-based tool. *Dysphagia.* (2015) 30:521–8. doi: 10.1007/s00455-015-9631-4
14. Warnecke T, Teismann I, Zimmermann J, Oelenberg S, Ringelstein EB, Dziewas R. Fiberoptic endoscopic evaluation of swallowing with simultaneous Tensilon application in diagnosis and therapy of myasthenia gravis. *J Neurol.* (2008) 255:224–30. doi: 10.1007/s00415-008-0664-6
15. Im S, Suntrup-Krueger S, Colbow S, Sauer S, Claus I, Meuth SG, et al. Reliability and main findings of the flexible endoscopic evaluation of swallowing-Tensilon test in patients with myasthenia gravis and dysphagia. *Eur J Neurol.* (2018) 25:1235–42. doi: 10.1111/ene.13688
16. Hey C, Pluschinski P, Zaretsky Y, Almahameed A, Hirth D, Vaerst B, et al. Penetration-Aspiration Scale according to Rosenbek. Validation of the German version for endoscopic dysphagia diagnostics. *HNO.* (2014) 62:276–81. doi: 10.1007/s00106-013-2815-z
17. Rosenbek JC, Robbins JA, Roecker EB, Coyle JL, Wood JL. A penetration-aspiration scale. *Dysphagia.* (1996) 11:93–8.
18. Crary MA, Mann GDC, Groher ME. Initial psychometric assessment of a functional oral intake scale for dysphagia in stroke patients. *Arch Phys Med Rehabil.* (2005) 86:1516–20. doi: 10.1016/j.apmr.2004.11.049
19. Zampieri S, Ghirardello A, Iaccarino L, Tarricone E, Gambari PF, Doria A. Anti-Jo-1 antibodies. *Autoimmunity.* (2005) 38:73–8. doi: 10.1080/08916930400022640

20. Casal-Dominguez M, Pinal-Fernandez I, Mego M, Accarino A, Jubany L, Azpiroz F, et al. High-resolution manometry in patients with idiopathic inflammatory myopathy: elevated prevalence of esophageal involvement and differences according to autoantibody status and clinical subset. *Muscle Nerve.* (2017) 56:386–92. doi: 10.1002/mus.25507
21. Murata K-Y, Kouda K, Tajima F, Kondo T. A dysphagia study in patients with sporadic inclusion body myositis (s-IBM). *Neurol Sci.* (2012) 33:765–70. doi: 10.1007/s10072-011-0814-y
22. Riminton DS, Chambers ST, Parkin PJ, Pollock M, Donaldson IM. Inclusion body myositis presenting solely as dysphagia. *Neurology.* (1993) 43:1241–3.

Conflict of Interest Statement: The authors declare that the research was conducted in the absence of any commercial or financial relationships that could be construed as a potential conflict of interest.

Copyright © 2019 Labeit, Muhle, Suntrup-Krueger, Ahring, Ruck, Dziewas and Warnecke. This is an open-access article distributed under the terms of the Creative Commons Attribution License (CC BY). The use, distribution or reproduction in other forums is permitted, provided the original author(s) and the copyright owner(s) are credited and that the original publication in this journal is cited, in accordance with accepted academic practice. No use, distribution or reproduction is permitted which does not comply with these terms.

frontiers in Immunology

ORIGINAL RESEARCH
published: 11 July 2019
doi: 10.3389/fimmu.2019.01600

Neuro-Sjögren: Peripheral Neuropathy With Limb Weakness in Sjögren's Syndrome

*Tabea Seeliger[1], Nils K. Prenzler[2], Stefan Gingele[1], Benjamin Seeliger[3], Sonja Körner[1], Thea Thiele[4], Lena Bönig[1], Kurt-Wolfram Sühs[1], Torsten Witte[4], Martin Stangel[1] and Thomas Skripuletz[1]**

[1] Department of Neurology, Hanover Medical School, Hanover, Germany, [2] Department of Otolaryngology, Hanover Medical School, Hanover, Germany, [3] Department of Respiratory Medicine, Hanover Medical School, Hanover, Germany, [4] Department of Clinical Immunology and Rheumatology, Hanover Medical School, Hanover, Germany

Objective: Sjögren's syndrome is a heterogeneous inflammatory disorder frequently involving peripheral nerves with a wide spectrum of sensory modalities and distribution patterns. The objective of this cross-sectional study was to determine characteristics of Sjögren's syndrome as a cause for severe neuropathy with limb weakness.

Methods: One hundred and eighty four patients with polyneuropathy associated with limb weakness underwent routine diagnostics including investigations for Sjögren's syndrome. Forty-four patients with Sjögren's syndrome (ACR-EULAR classification criteria) and severe neuropathy were identified.

Results: Sjögren's syndrome was found at a median age of 63 years and the gender distribution showed a balanced female-male ratio of 1:1. Anti-SSA(Ro) antibodies were detected in 48% while seronegative patients were diagnosed with Sjögren's syndrome based on sialadenitis on minor salivary gland biopsy with a focus score ≥1. The majority of patients (93%) were diagnosed with Sjögren's syndrome after neurological symptoms appeared. Limbs were symmetrically involved in 84% of patients (57% tetraparesis, 27% paraparesis). Sensory function was not affected in 11% of patients indicating that Sjögren's syndrome associated neuropathy can present as a pure motor syndrome. Electrophysiological measurements did not reveal pathognomonic findings (23% demyelinating pattern, 36% axonal pattern, 41% both demyelinating and axonal damage signs). More than half of our patients fulfilled the European Federation of Neurological Societies (EFNS) diagnostic criteria for CIDP indicating that distinction between Neuro-Sjögren and other causes of neuropathy such as CIDP is challenging.

Interpretation: Our findings show that severe neuropathy with limb weakness is often associated with Sjögren's syndrome. This is of great importance in identifying and understanding the causes of immune mediated polyneuropathy.

Keywords: Sjögren's syndrome, Neuro-Sjögren, neuropathy, chronic inflammatory demyelinating polyneuropathy, motoneuron disease

OPEN ACCESS

Edited by:
Tobias Ruck,
University of Münster, Germany

Reviewed by:
André Huss,
University of Ulm, Germany
Ernestina Santos,
Centro Hospitalar do Porto, Portugal

****Correspondence:***
Thomas Skripuletz
skripuletz.thomas@mh-hannover.de

Specialty section:
This article was submitted to Multiple Sclerosis and Neuroimmunology, a section of the journal Frontiers in Immunology

Received: *02 January 2019*
Accepted: *26 June 2019*
Published: *11 July 2019*

Citation:
Seeliger T, Prenzler NK, Gingele S, Seeliger B, Körner S, Thiele T, Bönig L, Sühs K-W, Witte T, Stangel M and Skripuletz T (2019) Neuro-Sjögren: Peripheral Neuropathy With Limb Weakness in Sjögren's Syndrome. Front. Immunol. 10:1600. doi: 10.3389/fimmu.2019.01600

INTRODUCTION

Sjögren's syndrome has been described as an inflammatory disease of salivary and lacrimal glands characterized by typical sicca symptoms of dry mouth and eyes and lymphocytic infiltration of glandular tissues (1). Extraglandular manifestations are common and include inflammation of joints, skin, kidney, heart, lung, and intestines (2). Inflammation of the nervous system represents another complication of Sjögren's syndrome. Involvement of peripheral nerves predominantly presents with sensory neuropathy and a wide spectrum of sensory modalities and distribution patterns (3). Motor impairment due to neuropathy has not been widely recognized until now in patients with Sjögren's syndrome (3, 4). However, this severe complication of Sjögren's syndrome with fulminant development of limb weakness but favorable outcome after immunosuppressive therapy was described in several case reports (5–9). Since the prevalence of peripheral neuropathy associated with Sjögren's syndrome increases with age (10), underestimation of paralysis as a neurologic complication of Sjögren's syndrome is a great risk. Patients presenting with limb weakness as a main complaint of polyneuropathy are predominantly treated in neurological departments, where a potentially causal Sjögren's syndrome may not be routinely investigated. Since Sjögren's syndrome is usually diagnosed in immunological departments, rheumatologists are more familiar with this rare autoimmune disease than neurologists. In order to define this entity in detail, we assessed the clinical picture of Sjögren's syndrome patients with neuropathy and motor dysfunction to facilitate diagnostic approaches and treatment eligibility.

METHODS

Patient Selection and Disability Scoring

Analyses were performed from patients treated as inpatients at the Department of Neurology of the Hannover Medical School between 10/2015 and 02/2018. Patients were included when there were symptoms and signs of a severe progressive symmetric or asymmetric peripheral neuropathy. This was defined by obligatory objective limb weakness and electrophysiological impairment (demyelination and/or axonal damage) of more than one peripheral nerve. Patients with isolated sensory deficits and patients with confirmed or highly suspected additional central nervous system manifestation were excluded from the analysis. Patients with suggested infectious, toxic, metabolic, amyloid, or paraneoplastic neuropathy were excluded. In case of paraproteinemia investigation for hematologic malignancy was performed. Overall, 184 patients with severe polyneuropathy associated with limb weakness underwent routine diagnostics including investigation for Sjögren's syndrome as a possible cause, and 44 of these 184 patients fulfilled the ACR-EULAR-classification criteria for Sjögren's syndrome. Patients with a marked bilateral difference of upper or lower extremities in strength (two or more Medical Research Council grades) or sensory function were defined as having an asymmetric form of peripheral neuropathy. Patients' disability was graded by the overall disability sum score [ODSS], ranging from 0 (no signs of disability) to 12 (maximum disability comprising severe symptoms in both arms preventing all purposeful movements and implying restriction to wheelchair or bed most of the day) (11, 12).

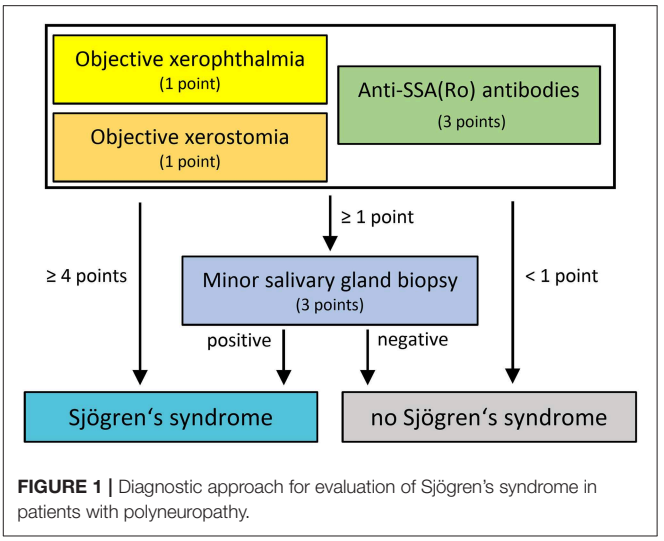


FIGURE 1 | Diagnostic approach for evaluation of Sjögren's syndrome in patients with polyneuropathy.

Sjögren's Syndrome Classification Criteria

The ACR-EULAR classification criteria for Sjögren's syndrome (13) were reappraised for every patient. As suggested, patients were only eligible to classification if they stated at least one symptom of ocular or oral dryness (defined as recurrent sensation of dry eyes for at least 3 months, use of tear substitute >3 times daily, daily experience of a dry mouth and the need of liquids while swallowing). Classification of Sjögren's syndrome was performed when summing up the weights of the following items resulted in a score of ≥4: labial minor salivary gland biopsy with focal lymphocytic sialadenitis and focus score ≥1 (3, 14), positive anti-SSA(Ro) antibodies (3), Schirmer test ≤5 mm/5 min on at least one eye (1), ocular staining score ≥5 on at least one eye (1), and unstimulated whole saliva flow rate ≤ 0.1 ml/min (1). According to the recommendations, a history of head and neck radiation treatment, active hepatitis C infection, acquired immunodeficiency syndrome, sarcoidosis, amyloidosis, graft vs. host disease, and IgG4-related diseases were ruled out.

All patients underwent laboratory testing for anti-SSA(Ro)-antibodies. Tear production was investigated by the Schirmer test, while saliva production was examined by the Saxon test (15). Minor salivary gland biopsy was performed in 41/44 patients. The other 3 patients refused minor salivary gland biopsy. The diagnostic work-up is illustrated in **Figure 1**.

Cerebrospinal Fluid (CSF) and Laboratory Data

CSF and serum were analyzed by routine methods (4, 16). CSF leukocytes were counted manually with a Fuchs-Rosenthal chamber and >4 cells/μl were designated as elevated. CSF total protein (cut off = 500 mg/L) was determined by a Bradford

dye-binding procedure. Albumin, IgG, IgA, and IgM were examined in serum and CSF in the same assay by kinetic nephelometry (Beckman Coulter IMMAGE). The blood-CSF barrier dysfunction was defined as CSF/serum albumin quotients (Qalbumin) higher than the age-adjusted upper reference limit of Qalbumin which was calculated [Qalbumin = (age in years/15) + 4] (17). CSF specific oligoclonal bands were determined by isoelectric focusing in polyacrylamide gels with consecutive silver staining. Anti-Ro antibodies were measured by EliA (ThermoScientific), Rheumatoid Factor was measured by laser nephelometry (Siemens BN ProSpec), and α-Fodrin IgA and IgG were measured by enzyme-linked immunosorbent assay (ELISA, Aesku.Diagnostics).

Nerve Conduction Studies

Standardized electrophysiological diagnostics were performed by using superficial stimulators and recording electrodes according to the recommendations of the International Federation of Clinical Neurophysiology (18). Nerve conduction studies were performed on median, ulnar, peroneal, tibial, and sural nerves depending on the clinical manifestation. Evident polyneuropathy was classified as primarily axonal, primarily demyelinating, or mixed axonal and demyelinating. Classification was assigned depending on signs of the respective damage mechanism in the majority of nerves (**Supplementary Table 1**). The first available neurographic analyses were considered in order to identify the primary damage mechanism. In addition, diagnostic criteria for chronic inflammatory demyelinating polyneuropathy (CIDP) were reappraised for every patient (19).

Statistical Analysis and Data Collection

Descriptive statistics were assessed using (SPSS V24, IBM, USA). Data was analyzed for normal distribution by Shapiro Wilk test. Where normal distribution was not present, non-parametric data were stated as median and range. Data were collected and documented anonymously. Missing values were descriptively handled.

Ethical Approval

The investigation was approved by the local ethics committee of the Hannover Medical School (8172_BO_K_2018). This is a retrospective study and only data were included that were evaluated for patient's treatment.

RESULTS

Patient's Characteristics

Forty-four patients (50% women) were included in the analysis with a median age of 63 years (range: 31–84 years) at confirmation of Sjögren's syndrome. Detailed information about the baseline criteria are displayed in **Table 1**. Female patients presented with a median age of 60 years (range: 45–81 years), and male patients with a median age of 72 years (range: 31–84 years). The median duration between onset of neurological symptoms suggesting peripheral neuropathy and diagnosis of Sjögren's syndrome was 59 months (range 1–231 months).

TABLE 1 | Baseline characteristics, ACR/EULAR classification criteria and patient history data.

	Sjögren's syndrome (included patients)	No Sjögren's syndrome (excluded patients)
Females, *n* (%)	22/44 (50%)	40/140 (59%)
Age (median) at time of Sjögren's syndrome diagnosis		
All patients, years (range)	63 (31–84)	–
Females, years (range)	60 (45–81)	–
Males, years (range)	72 (31–84)	–
ACR/EULAR classification criteria for Sjögren' syndrome		
Evident xerophthalmia, *n* (%)	40/44 (91%)	59/140 (42%)
Evident xerostomia, *n* (%)	18/44 (41%)	31/140 (22%)
Ro-antibody positive, *n* (%)	21/44 (48%)	0/140 (0%)
Sialadenitis with a focus score ≥1, *n* (%)	31/41 (76%)	0/69 (0%)

Diagnosis of Sjögren's Syndrome

Objective xerophthalmia was identified in all but 4 patients (91%), while 18 patients (41%) showed objective xerostomia. Anti-SSA(Ro) antibodies were present in 21 patients (48%). Minor salivary gland biopsy was performed in all but 3 patients. Sialadenitis with a focus score ≥1 was found in 31/41 patients (76%). The ACR sum score was calculated as 4 in 25/44 patients (57%), as 5 in 11/44 patients (25%), as 7 in 5/44 patients (11%), and as 8 in 3/44 patients (7%).

Serological analysis of parameters outside the ACR-EULAR classification criteria for Sjögren's syndrome (13) revealed an elevated ANA titer (≥1:320) in 23 patients (52%). Rheumatoid factor was found in 7 patients (16%)—in 4 patients combined with anti-SSA(Ro) antibodies. Positive α-Fodrin antibodies occurred in 11 patients (25%)—in 8 combined with antibodies against SSA(Ro). In total, 34 patients (77%) showed either antibodies against anti-SSA(Ro) and/or α-Fodrin, ANA with a titer ≥1:320, or positive rheumatoid factor.

Antibodies against SSA(Ro) were not found in patients who were not diagnosed with Sjögren's syndrome and therefore excluded from further detailed analyses ($n = 140$). Positive α-Fodrin antibodies occurred in 19% of these patients while 4% of patients without Sjögren's syndrome showed positive rheumatoid factor. Additional basic immunological results are shown in **Supplementary Table 2**.

Patient's Diagnoses Preceding Diagnosis of Sjögren's Syndrome

Sjögren's syndrome was mostly (41/44; 93%) diagnosed after neurological symptoms had developed. At presentation to our department, 5 patients (11%) received primary workup leading to the diagnosis of peripheral neuropathy and Sjögren's syndrome. The other 39 patients (89%) had previously been diagnosed with neuropathy not associated with Sjögren's syndrome. Preceding diagnoses were polyneuropathy of unknown origin in 14 cases (36%), primary CIDP in 11 cases

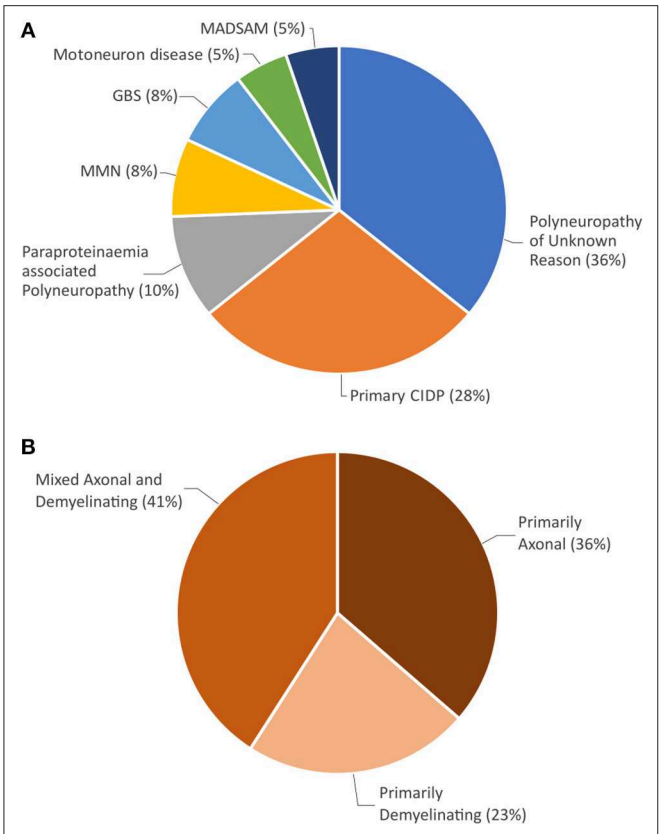


FIGURE 2 | (A) Neuropathy diagnoses prior to Sjögren's syndrome diagnosis. **(B)** Distribution of electrophysiological damage pattern at initial neurographic analysis.

(28%), paraproteinaemia associated polyneuropathy in 4 cases (10%), multifocal motor neuropathy (MMN) in 3 cases (8%), Guillain Barré Syndrome in 3 cases (8%), motoneuron disease in 2 cases (5%), and multifocal acquired demyelinating sensory and motor neuropathy (MADSAM) in 2 cases (5%) (**Figure 2A**). Motoneuron disease had been suspected in 5 cases throughout patient's history.

Patient's Initial Symptoms and Disease Course

Initial symptoms were reported mainly as paraesthesia (17 cases, 39%), weakness (11 cases, 25%), combination of both (6 cases, 14%), and unspecified gait disturbance (5 cases, 11%). Two patients initially presented with muscle cramps (5%) and the remaining 3 patients initially complained about bladder dysfunction, dyspnoea and facial palsy (each $n = 1$). The findings are specified in **Table 2**. All patients developed weakness of extremities throughout disease course. In addition, cranial nerve involvement occurred in 18 patients (41%) with detailed symptoms described in **Table 3**. Involuntary muscle contractions were reported in 17 cases (32%). Persistent bladder dysfunction was found in 9 cases (20%).

Five patients (11%) showed an acute disease course and developed weakness of extremities within days. In those cases, Guillain Barré Syndrome was actively evaluated as initial diagnosis. The remaining patients showed a chronic progressive course of neurological symptoms, while weakness was present at symptom onset in 39% of patients (median 1 month, range 1–130 months).

TABLE 2 | Initial symptoms of Sjögren's syndrome.

Paraesthesia (isolated), *n* (%)	17 (39%)
Pareasthesia with paresis, *n* (%)	6 (14%)
Paresis (isolated), *n* (%)	11 (25%)
Gait disturbance, *n* (%)	5 (11%)
Muscle cramps, *n* (%)	2 (5%)
Bladder dysfunction, *n* (%)	1 (2%)
Dyspnoea, *n* (%)	1 (2%)
Facial palsy, *n* (%)	1 (2%)

TABLE 3 | Cranial and phrenic nerve impairment.

Cranial and phrenic nerves affected	***n* (%)**
Cranial nerve II (anosmia)	1/44 (2.3%)
Cranial nerves III, IV, VI (oculomotor disturbance with diplopia)	2/44 (4.5%)
Cranial nerve V (trigeminal affection with sensory disturbance and neuralgia)	6/44 (13.6%)
Cranial nerve VII (facial nerve palsy)	3/44 (6.8%)
Cranial nerve VIII (hypacusis)	8/44 (18.2%)
Cranial nerves IX, X (dysphagia, hoarseness)	6/44 (13.6%)
Phrenic nerve palsy (dyspnoea, raised diaphragm)	2/44 (4.5%)

Neurological Manifestations at the Time of Worst Documented Clinical Status (Judged by Overall Disability Sum Score)

Weakness of extremities was present in all patients. The most prominent muscle weakness was documented with a median of 3 (by Medical Research Council, range 0–4). Paralysis was distributed symmetrically in 37 patients (84%).

Tetraparesis was the predominant pattern of affected muscles and was found in 25 cases (57%), while 12 patients (27%) suffered from paraparesis. In patients with asymmetric peripheral neuropathy monoparesis occurred in 4 cases (9%) and affection of three extremities was found in 3 cases (7%).

The neurologic examination showed a functional impairment as determined by the overall disability sum score [ODSS] of 3.5 (range 0–12).

Sensory dysfunction was reported by 39 patients (89%). Sensory symptoms occurred symmetrically and showed a stocking- and/ or glove-like distribution in 34 patients (87%). Sensations were reported as pain in 12 cases (31%), numbness or tingle paraesthesia in 35 cases (90%), and dysfunctional proprioception in 32 cases (82%). The full workup is detailed in **Table 4**.

TABLE 4 | Neurologic findings in worst examination (judged by ODSS).

Sensory dysfunction, *n* (%)	39/44 (89%)
Distribution	
Symmetrical, *n* (%)	34/39 (87%)
Stocking-/glove like, *n* (%)	34/39 (87%)
Quality	
Numbness or prickling, *n* (%)	35/39 (90%)
Dysfunctional proprioception, *n* (%)	32/39 (82%)
Pain, *n* (%)	12/39 (31%)
Weakness, *n* (%)	44/44 (100%)
Distribution	
Tetraparesis, *n* (%)	25/44 (57%)
Paraparesis, *n* (%)	12/44 (27%)
Affection of 3 extremities, *n* (%)	3/44 (7%)
Monoparesis, *n* (%)	4/44 (9%)
Most prominent muscle weakness (MRC), median (range)	3 (0–4)
ODSS, median (range)	3.5 (0–12)

Electrophysiological Findings

Nerve conduction examinations demonstrated impairment of motor nerves in all patients and impairment of sensory nerves in 39 patients (89%) with Sjögren's syndrome.

Nerve damage was classified as predominantly axonal in 16 cases (36%), predominantly demyelinating in 10 cases (23%), and mixed axonal and demyelinating in 18 patients (41%) (**Figure 2B**).

Evaluation of the electrodiagnostic criteria for a hypothetical diagnosis of CIDP as suggested by the EFNS classification criteria revealed definite CIDP in 23 patients (52%) and probable CIDP in 4 patients (9%) with Sjögren's syndrome.

In addition, patients who were not diagnosed with Sjögren's syndrome and therefore excluded from further analyses ($n = 140$) were evaluated for a hypothetical CIDP. The EFNS criteria suggested definite CIDP in 73 of these patients (52%), probable CIDP in 6 patients (4%), and possible CIDP in 4 patients (3%).

Cerebrospinal Fluid Findings

Inflammatory CSF findings were only rarely found in patients with peripheral neuropathy associated with Sjögren's syndrome. Four patients (9%) showed a slightly elevated cell count of 8, 10, 13, and 21 cells/μl (**Figure 3**). Total CSF protein was increased in 20 patients (51%). Blood-CSF barrier dysfunction (Qalbumin) was evident in 18 patients (46%). Barrier dysfunction was severe in 3 cases and mild to moderate in 15 cases. All but one patient had normal lactate concentrations. Quantitative intrathecal synthesis of IgG (Reiber graphs) was found in 2 patients (5%). IgM or IgA synthesis did not occur. Oligoclonal bands restricted to the CSF (type 2 and 3) indicating intrathecal IgG synthesis were found in 3 patients (7%).

Therapeutic Profiles in Patients With Peripheral Neuropathy and Sjögren's Syndrome

Immunomodulatory therapy led to clinical benefit in 97% (32/33) of patients that attended follow-up evaluation ($n = 33$). The remaining 11 patients were lost to follow-up. All patients received multiple therapeutic regimes throughout disease course, resulting in a total of 113 treatment regimes with follow-up evaluation in 81 cases (72%). Changes in therapeutic regime (0–4 changes per patient) were made due to disease progression in 21 cases (31%) and adverse events in 12 cases (18%). Riluzol medication was terminated in 4 cases (6%), after motoneuron disease was no longer suspected. Definite clinical benefit with documented improvement of motor function or stabilization of status quo after previous deterioration was considered a favorable response. Analysis of all therapeutic regimens revealed a favorable response in 66 treatment regimens (81%) (**Table 5**).

DISCUSSION

This study facilitates the recognition of Sjögren's syndrome as a cause for severe neuropathy with limb weakness, which favorably responds to immunosuppressive therapy. We propose to further refer to Sjögren's associated neuropathy as "Neuro-Sjögren."

Severe Neuropathy as an Underestimated Complication of Sjögren's Syndrome

The incidence of neuropathy with fulminant development of limb weakness in Sjögren's syndrome is still unknown. Despite the fact, that several cases have been reported (6, 8, 20), studies including high numbers of patients are not available. In a previous analysis of patients with Neuro-Sjögren presenting to our department between 2004 and 2015, 27 patients with polyneuropathy were described (4). However, 5 patients suffered from neuropathy with limb weakness while the remaining 22 patients complained about sensory deficits only. We therefore systematically investigated all patients presenting with severe polyneuropathy and limb weakness for a possible underlying Sjögren's syndrome. During a time period of 2 years and 5 months 184 eligible patients received tests for xeropthalmia and xerostomia and blood analysis for SSA(Ro) antibodies. In the case of one pathological sign a minor salivary gland biopsy was performed. Sjögren's syndrome could be diagnosed in 44/184 patients (24%). This striking rise of the incidence is explained by the implementation of routine screening for Sjögren's syndrome in our department and suggests that this severe complication is frequently unrecognized.

All 44 patients featured neuropathy with limb weakness in which motor impairment manifested symmetrically in 84% and as tetraparesis in 57%. Sensory function was not affected in 11% of patients indicating that Sjögren's syndrome associated neuropathy can involve solely motor functions. Sensory peripheral neuropathy has been recognized among patients with Sjögren's syndrome with reported rates of peripheral neuropathy between 1.6 and 31% when analyzing patients with Sjögren's syndrome in general (21–25). However, patients

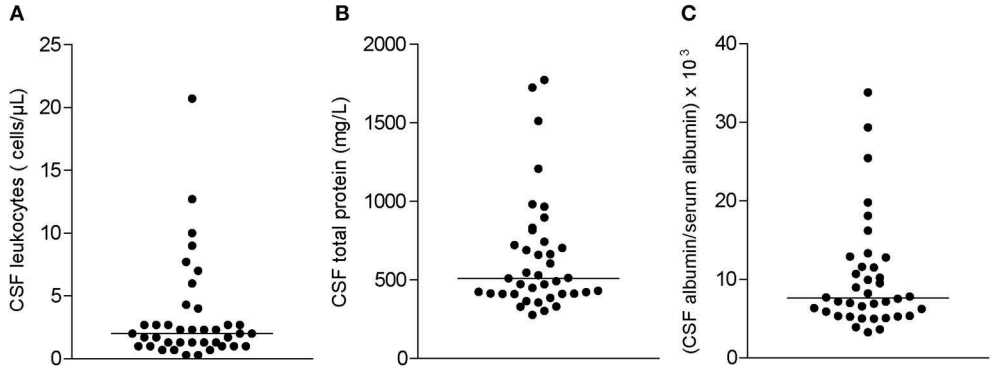


FIGURE 3 | Distribution of cerebrospinal fluid (CSF) parameters in all study patients: **(A)** CSF cell counts, **(B)** CSF total protein, and **(C)** albumin quotient (CSF albumin/serum albumin × 10^3). Horizontal bars indicate median values.

TABLE 5 | Therapeutic profiles administered in at least 3 patients.

Treatments	Favorable response
Treatment regimens with follow up evaluation	66/81
Steroids	
Methylprednisolone (intravenous)	7/8
Prednisolone (oral)	5/10
Primary non-steroid therapy	
Azathioprine	6/6
Azathioprine + intravenous immunoglobulins	2/3
Mycophenolate mofetil	1/3
Intravenous immunoglobulins	22/23
Intensified therapy	
Plasmapheresis	3/3
Cyclophosphamide	3/5
Rituximab	4/4
Rituximab + intravenous immunoglobulins	4/4

with limb weakness were not included or characterization of neuropathy was not performed in these previous cohorts. This might be explained by the fact, that Sjögren's syndrome is not an established diagnosis as a cause of motor impairment in severe polyneuropathy. Patients with sicca symptoms and suspected Sjögren's syndrome are usually referred to rheumatological departments, where diagnosis is reappraised and associated neuropathic complaints are further evaluated. Neuropathy, however, often precedes the development of sicca syndrome (26), rendering the recognition of Sjögren's syndrome during early stages of the disease course nearly impossible. Furthermore, patients presenting with limb weakness as a chief complaint of neuropathy are rather treated in neurological departments, where a potentially causal Sjögren's syndrome is not routinely investigated.

Another contributing factor to the underestimation of Neuro-Sjögren might be the proposition of other causes of neuropathy in neglect of Neuro-Sjögren's diagnosis. Most of our patients had been diagnosed with other entities for a long time, without re-evaluating the validity of the diagnosis in the course of time. Many had received perpetual treatment mainly with intravenous immunoglobulins with short-term clinical benefit and long-term deterioration of symptoms. Some of these patients were thought to suffer from an atypical CIDP. Five patients had even been diagnosed with motoneuron disease until the atypical course prompted re-evaluation of diagnoses.

Clinical Characteristics of Neuro-Sjögren or "Who to Look Out For?"

The gender distribution showed a balanced male-female ratio of 1:1 in our cohort, whereas Sjögren's syndrome in general has a female predominance between 6:1 and 20:1 (27–29). The discrepancy in gender distribution might result from different patient cohorts analyzed. Most previous studies described patients with Sjögren's syndrome in general and predominantly patients with rheumatic symptoms while our cohort included patients with neuropathy with limb weakness only. However, there are already tendencies in previous reports that show a shift of the gender distribution toward male patients: Sivadasan and colleagues described a cohort of 54 patients with Sjögren's syndrome and neuropathy consisting of only 68.5% females (30), and data from the French ASSESS cohort revealed 88% females in the group with nervous system involvement compared to 95% females in the group without nervous system involvement (31). Other possible reasons for the gender discrepancy might be different pathomechanisms in patients with Sjögren's syndrome and associated organ involvement. Furthermore, progressive paralysis is a major cause for disability and directly affects the quality of life. Thus, the majority of such patients, independent if male or female, undergo a diagnostic work-up, which might be a reason for the balanced male-female distribution. However, additional investigations including larger cohorts of patients are needed to confirm our results. The onset of symptoms was reported at a median age of 63 years and limb weakness was among the initial symptoms in most cases. Limbs were symmetrically involved in 84% of patients and led to a median ODSS of 3.5. Additional sensory symptoms matched the typical signs of polyneuropathy with a mostly stocking- or glove-like-distribution. Symptoms developed rarely within days

(11% of patients). In these cases, Guillain Barré syndrome was considered the most likely differential diagnosis and treatment with immunoglobulins was initiated. Intravenous application of immunoglobulins led to temporary improvement of all symptoms, but longterm clinical benefit could not be achieved as symptoms relapsed, and deteriorated over time. In the majority of patients, limb paralysis developed over months indicating a predominantly chronic nature of this disease. Some patients with a pure motor dysfunction were initially misdiagnosed as having a motoneuron disease which aligns with recent case reports about the clinical mimicry of those two entities (6, 32, 33). Those patients responded to immunomodulatory treatment, and thus, the previously suspected diagnosis of motoneuron disease was rejected.

Diagnostic Tools for Evaluation of Neuro-Sjögren

The ACR-EULAR classification criteria were applied for all patients. Still, not all items were equally represented in our cohort. Objective xerophthalmia was detected in most patients (91%), while objective xerostomia was found in less than half of our cohort (41%). Anti-SSA(Ro)-antibodies were present in only 48% of our patients. The other 52% of patients were diagnosed with Sjögren's syndrome based on sufficient sialadenitis on minor salivary gland biopsy. Antibody status alone is therefore no criterion to rule out Sjögren's syndrome. Furthermore, as some patients frequently received treatments with immunoglobulins before evaluation of antibody status, minor salivary gland biopsy resembles the more reliable diagnostic tool, and should be performed liberally.

Inflammatory CSF findings were rarely found and were therefore not specific for Sjögren-associated polyneuropathy which is in accordance with previous studies (4, 33). Nevertheless, lumbar puncture should be performed to rule out other autoimmune and infectious diseases.

Furthermore, electrophysiological measurements did not reveal pathognomonic findings for Neuro-Sjögren. Every third patient presented with a predominantly axonal damage while every fourth patient showed a predominantly demyelinating damage. The remaining patients revealed signs of both demyelinating and axonal damage. Since many of these patients were investigated in an advanced disease stage the primary pattern remains unclear. Notably, more than half of our patients retrospectively fulfilled the EFNS diagnostic criteria for CIDP. However, similar results concerning a hypothetical CIDP were found in the other 140 patients who did not fulfill the diagnostic criteria for Sjögren's syndrome. These results show that the EFNS criteria are not an appropriate tool for differentiation between CIDP and other immunologically mediated neuropathies such as Neuro-Sjögren. Furthermore, Lozeron et al. recently described patients with transthyretin familial amyloid polyneuropathy who fulfilled the EFNS criteria for a CIDP although these patients did not suffer from an immunologically mediated neuropathy (34).

Therapeutic Approaches

In our cohort, immunomodulatory therapy led to a clinical benefit with documented improvement of motor function or stabilization of status quo after previous progression in most patients who visited for follow up. Consistent with previous reports we conclude that immunomodulatory therapy is recommendable to ensure clinical benefit for patients with Sjögren-associated polyneuropathy. However, no therapeutic recommendations can be made based on these data due to a low number of patients and since treatment decisions were very heterogeneous. Still there is a vast insecurity concerning the choice of appropriate therapy in the absence of clinical trials focusing on therapy of Sjögren's syndrome associated neuropathy.

Limitations

All data were collected from patients treated at a university hospital resulting in a selection bias. This is not unusual because most of these patients were treated in other neurological clinics before and were discharged without a sufficient diagnosis and specific treatment. However, the high number of newly diagnosed Sjögren's syndrome in every fourth patient with severe neuropathy with limb weakness might be therefore overestimated. Multicenter studies are required to reach appropriate cohort sizes and minimize selection bias.

Outlook

During preparation of this manuscript 14 further patients with severe neuropathy with limb weakness have been diagnosed with Sjögren's syndrome indicating that this disorder is more frequent than previously assumed. Raising awareness of Neuro-Sjögren is therefore crucial—especially in patients with severe peripheral neuropathy.

Defining a stereotype patient for Neuro-Sjögren is challenging as patient characteristics in terms of comorbidities and severity of symptoms were heterogenous in our cohort. Some patients had been treated with intravenous immunoglobulins and had improved temporarily. Hence, further diagnostic steps were neglected, even when symptoms relapsed, and instead the diagnosis of an atypical CIDP was suggested. In this scenario, the dosage of immunoglobulins was often increased which again improved patients' symptoms temporarily. Some of the older patients were not treated with immunomodulatory substances as age-associated and therefore unchangeable causes for evident neuropathy were implied. In severe progressive motor dysfunction with permanent dependence to wheelchair or confinement to bed phrenic nerve paralysis and dysphagia occurred in some patients, and thus, a motoneuron disease was suspected. These patients improved after implementation of immunomodulatory/immunosuppressive treatment. It is therefore crucial to evaluate a wide variety of patients for Neuro-Sjögren even if symptoms seem to be of fatal dimension.

CONCLUSION

Our data indicate that severe neuropathy with limb weakness is often associated with Sjögren's syndrome. However, there are no pathognomonic clinical signs or electrophysiological findings and therefore distinction between Sjögren' syndrome and other causes of neuropathy such as CIDP can be challenging,

especially in early disease stages. We thus suggest performing screening tests for Sjögren's syndrome in all patients with polyneuropathy and especially in those with motor dysfunction. As neurologic manifestations frequently precede sicca symptoms and laboratory findings (i.e., anti-SSA(Ro)-antibodies), perpetual re-evaluation for objective xerophthalmia or xerostomia should be performed. In case of pathological tear or saliva production, minor salivary gland biopsy should be performed in order to diagnose a potential Sjögren's syndrome in time.

ETHICS STATEMENT

This study was approved by the institutional ethics committee of the Hannover Medical School (8172_BO_K_2018). This is a retrospective study and only data were included that were evaluated for patient's treatment. Thus, the local ethics committee waived the need for written informed consent from the participants.

AUTHOR CONTRIBUTIONS

Recruitment of patients and processing of patient history data were accomplished by TaS, LB, TT, SG, and K-WS. NP contributed in testing for xerophthalmia and significantly drafting the manuscript. BS drafted a substantial portion of the manuscript. Nerve conduction studies and their interpretation were obtained by SK. TW, MS, and ThS provided expertise for conception and design of the study. All authors contributed to manuscript revision, read, and approved the submitted version.

ACKNOWLEDGMENTS

The authors thank Karin Fricke, Kathrin Scheiwe, Sabine Lang, Katharina Dorsch, and Ilona Cierpka-Leja for excellent technical assistance.

SUPPLEMENTARY MATERIAL

The Supplementary Material for this article can be found online at: https://www.frontiersin.org/articles/10.3389/fimmu.2019.01600/full#supplementary-material

Supplementary Table 1 | Applied electrophysiological classification criteria for nerve damage patterns.

Supplementary Table 2 | Extended immunological serologic parameters.

REFERENCES

1. Sjögren H. Zur kenntnis der keratoconjunctivitis sicca. *Acta Ophthalmol.* (1933) 13:1–39. doi: 10.1111/j.1755-3768.1935.tb04186.x
2. Fox RI. Sjögren' s syndrome. *Lancet.* (2004) 321–31. doi: 10.1016/S0140-6736(05)66990-5
3. Mori K, Iijima M, Koike H, Hattori N, Tanaka F, Watanabe H, et al. The wide spectrum of clinical manifestations in Sjögren's syndrome-associated neuropathy. *Brain.* (2005) 128:2518–34. doi: 10.1093/brain/awh605
4. Pars K, Pul R, Schwenkenbecher P, Sühs K-W, Wurster U, Witte T, et al. Cerebrospinal fluid findings in neurological diseases associated with Sjögren's syndrome. *Eur Neurol.* (2017) 77:91–102. doi: 10.1159/000454765
5. Garza-Alpirez A, Arana-Guajardo AC, Esquivel-Valerio JA, Villarreal-Alarcón MA, Galarza-Delgado DA. Hypokalemic paralysis due to primary Sjögren syndrome: case report and review of the literature. *Case Rep Rheumatol.* (2017) 2017:7509238. doi: 10.1155/2017/7509238
6. Lin Y-K, Yang F-C, Liu F-C, Lee J-T, Sung Y-F. Co-occurrence of guillain-barre syndrome and primary sjogren syndrome in an elderly woman. *Acta Neurol Taiwan.* (2016) 25:83–87. Available online at: http://www.ant-tnsjournal.com/Mag_Files/25-3/003.pdf
7. Horai Y, Nishino A, Nakashima Y, Suzuki T, Okada A, Kawashiri S-Y, et al. A case of Sjögren's syndrome presenting as trigeminal nerve palsy. *JPN J Clin Immunol.* (2012) 35:199–202. doi: 10.2177/jsci.35.199
8. Vernant J-C, Buisson G, Magdeleine J, De Thore J, Jouannelle A, Neisson-Vernant C, et al. T-lymphocyte alveolitis, tropical spastic paresis, and sjögren syndrome. *Lancet.* (1988) 331:177. doi: 10.1016/S0140-6736(88)92744-4
9. Pereira PR, Viala K, Maisonobe T, Haroche J, Mathian A, Hié M, et al. Sjögren sensory neuronopathy (Sjögren Ganglionopathy): long-term outcome and treatment response in a series of 13 cases. *Medicine.* (2016) 95:e3632. doi: 10.1097/MD.0000000000003632
10. Gemignani F, Marbini A, Pavesi G, Di Vittorio S, Manganelli P, Cenacchi G, et al. Peripheral neuropathy associated with primary Sjogren's syndrome. *Neurol Neurosurg Psychiatry.* (1994) 57:983–6. doi: 10.1136/jnnp.57.8.983
11. Merkies ISJ, Schmitz PIM, van der Meché FGA, Samijn JPA, van Doorn PA. Inflammatory Neuropathy Cause and Treatment (INCAT) group. Clinimetric evaluation of a new overall disability scale in immune mediated polyneuropathies. *J Neurol Neurosurg Psychiatry.* (2002) 72:596–601. doi: 10.1136/jnnp.72.5.596
12. Merkies ISJ, Schmitz PIM. Getting closer to patients: the INCAT Overall Disability Sum Score relates better to patients' own clinical judgement in immune-mediated polyneuropathies. *J Neurol Neurosurg Psychiatry.* (2006) 77:970–2. doi: 10.1136/jnnp.2005.076174
13. Shiboski CH, Shiboski SC, Seror R, Criswell LA, Labetoulle M, Lietman TM, et al. 2016 American College of Rheumatology/European League Against Rheumatism classification criteria for primary Sjögren's syndrome. *Ann Rheum Dis.* (2017) 76:9–16. doi: 10.1136/annrheumdis-2016-210571
14. Daniels TE, Cox D, Shiboski CH, Schiødt M, Wu A, Lanfranchi H, et al. Associations between salivary gland histopathologic diagnoses and phenotypic features of Sjögren's Syndrome (SS) among 1726 registry participants NIH Public Access. *Arthritis Rheum.* (2011) 63:2021–30. doi: 10.1002/art.30381
15. Kohler PF, Winter ME. A quantitative test for xerostomia. The Saxon test, an oral equivalent of the Schirmer test. *Arthritis Rheum.* (1985) 28:1128–32. doi: 10.1002/art.1780281008
16. Schwenkenbecher P, Sarikidi A, Wurster U, Bronzlik P, Sühs K-W, Raab P, et al. McDonald criteria 2010 and 2005 compared: persistence of high oligoclonal band prevalence despite almost doubled diagnostic sensitivity. *Int J Mol Sci.* (2016) 17:1592. doi: 10.3390/ijms17091592
17. Reiber H. Cerebrospinal fluid–physiology, analysis and interpretation of protein patterns for diagnosis of neurological diseases. *Mult Scler.* (1998) 4:99–107. doi: 10.1177/135245859800400302
18. Stålberg E, Falck B, Gilai A, Jabre J, Sonoo M, Todnem K. Standards for quantification of EMG and neurography. The international federation of clinical neurophysiology. *Electroencephalogr Clin Neurophysiol Suppl.* (1999) 52:213–20.
19. Van den Bergh PYK, Hadden RDM, Bouche P, Cornblath DR, Hahn A, Illa I, et al. European federation of neurological societies/peripheral nerve society guideline on management of chronic inflammatory demyelinating polyradiculoneuropathy: report of a joint task force of the European Federation of Neurological Societies and the Peripheral Nerve Society - first revision. *Eur J Neurol.* (2010) 17:356–63. doi: 10.1111/j.1468-1331.2009.02930.x

20. Paliwal VK, Rai AS, Kumar S, Verma R, Agarwal V. Proximal muscle weakness with overlying hypokalemic periodic paralysis in Sjögren syndrome. *JCR J Clin Rheumatol*. (2018) 1. doi: 10.1097/RHU.0000000000000776
21. Sène D, Jallouli M, Lefaucheur J-P, Saadoun D, Costedoat-Chalumeau N, Maisonobe T, et al. Peripheral neuropathies associated with primary Sjögren syndrome. *Medicine*. (2011) 90:133–8. doi: 10.1097/MD.0b013e31820fd2d1
22. Scofield AK, Radfar L, Ice JA, Vista E, Anaya J-M, Houston G, et al. Relation of sensory peripheral neuropathy in Sjögren syndrome to anti-ro/SSA. *J Clin Rheumatol*. (2012) 18:290–3. doi: 10.1097/RHU.0b013e3182675e4f
23. Brito-Zerón P, Acar-Denizli N, Ng W-F, Zeher M, Rasmussen A, Mandl T, et al. How immunological profile drives clinical phenotype of primary Sjögren's syndrome at diagnosis: analysis of 10,500 patients (Sjögren Big Data Project). *Clin Exp Rheumatol*. (2018) 112 (36 Suppl):102–12. Available online at: https://www.clinexprheumatol.org/abstract.asp?a=12899
24. Ramos-Casals M, Solans R, Rosas J, Camps MT, Gil A, del Pino-Montes J, et al. Primary Sjögren syndrome in Spain. *Medicine*. (2008) 87:210–9. doi: 10.1097/MD.0b013e318181e6af
25. Pavlakis PP, Alexopoulos H, Kosmidis ML, Mamali I, Moutsopoulos HM, Tzioufas AG, et al. Peripheral neuropathies in Sjögren's syndrome: a critical update on clinical features and pathogenetic mechanisms. *J Autoimmun*. (2012) 39:27–33. doi: 10.1016/j.jaut.2012.01.003
26. Delalande S, de Seze J, Fauchais A-L, Hachulla E, Stojkovic T, Ferriby D, et al. Neurologic manifestations in primary Sjögren syndrome: a study of 82 patients. *Medicine*. (2004) 83:280–91. doi: 10.1097/01.md.0000141099.53742.16
27. Beeson PB. Age and sex associations of 40 autoimmune diseases. *Am J Med*. (1994) 96:457–62. doi: 10.1016/0002-9343(94)90173-2
28. Alamanos Y, Tsifetaki N, Voulgari PV, Venetsanopoulou AI, Siozos C, Drosos AA. Epidemiology of primary Sjögren's syndrome in north-west Greece, 1982–2003. *Rheumatology*. (2006) 45:187–91. doi: 10.1093/rheumatology/kei107
29. Izmirly PM, Buyon JP, Wan I, Belmont HM, Sahl S, Salmon JE, et al. The incidence and prevalence of adult primary Sjögren's syndrome in New York County. *Arthr Care Res*. (2019) 71:949–60. doi: 10.1002/acr.23707
30. Sivadasan A, Muthusamy K, Patel B, Benjamin RN, Prabhakar AT, Mathew V, et al. Clinical spectrum, therapeutic outcomes, and prognostic predictors in Sjogren's syndrome-associated neuropathy. *Ann Indian Acad Neurol*. (2017) 20:278–83. doi: 10.4103/aian.AIAN_116_17
31. Carvajal Alegria G, Guellec D, Mariette X, Gottenberg J-E, Dernis E, Dubost J-J, et al. Epidemiology of neurological manifestations in Sjögren's syndrome: data from the French ASSESS Cohort. *RMD Open*. (2016) 2:e000179. doi: 10.1136/rmdopen-2015-000179
32. Zahlane S, Louhab N, El Mellakh M, Kissani N. Anterior horn syndrome: a rare manifestation of primary Sjögren's syndrome. *Jt Bone Spine*. (2016) 83:448–50. doi: 10.1016/j.jbspin.2016.02.018
33. Lafitte C, Amoura Z, Cacoub P, Pradat-Diehl P, Picq C, Salachas F, et al. Neurological complications of primary Sjögren's syndrome. *J Neurol*. (2001) 248:577–84. doi: 10.1007/s004150170135
34. Lozeron P, Mariani L-L, Dodet P, Beaudonnet G, Théaudin M, Adam C, et al. Transthyretin amyloid polyneuropathies mimicking a demyelinating polyneuropathy. *Neurology*. (2018) 91:e143–52. doi: 10.1212/WNL.0000000000005777

Conflict of Interest Statement: The authors declare that the research was conducted in the absence of any commercial or financial relationships that could be construed as a potential conflict of interest.

Copyright © 2019 Seeliger, Prenzler, Gingele, Seeliger, Körner, Thiele, Bönig, Sühs, Witte, Stangel and Skripuletz. This is an open-access article distributed under the terms of the Creative Commons Attribution License (CC BY). The use, distribution or reproduction in other forums is permitted, provided the original author(s) and the copyright owner(s) are credited and that the original publication in this journal is cited, in accordance with accepted academic practice. No use, distribution or reproduction is permitted which does not comply with these terms.

Advantages of publishing in Frontiers

OPEN ACCESS
Articles are free to read for greatest visibility and readership

FAST PUBLICATION
Around 90 days from submission to decision

HIGH QUALITY PEER-REVIEW
Rigorous, collaborative, and constructive peer-review

TRANSPARENT PEER-REVIEW
Editors and reviewers acknowledged by name on published articles

Frontiers
Avenue du Tribunal-Fédéral 34
1005 Lausanne | Switzerland

Visit us: www.frontiersin.org
Contact us: info@frontiersin.org | +41 21 510 17 00

REPRODUCIBILITY OF RESEARCH
Support open data and methods to enhance research reproducibility

DIGITAL PUBLISHING
Articles designed for optimal readership across devices

FOLLOW US
@frontiersin

IMPACT METRICS
Advanced article metrics track visibility across digital media

EXTENSIVE PROMOTION
Marketing and promotion of impactful research

LOOP RESEARCH NETWORK
Our network increases your article's readership